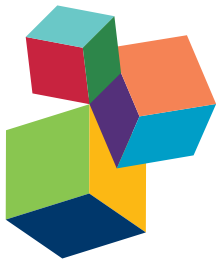


# HYDROTHERMAL MICROBIAL ECOSYSTEMS

EDITED BY: Andreas Teske and Anna-Louise Reysenbach

PUBLISHED IN: *Frontiers in Microbiology*



## **Frontiers Copyright Statement**

© Copyright 2007-2015 Frontiers Media SA. All rights reserved.

All content included on this site, such as text, graphics, logos, button icons, images, video/audio clips, downloads, data compilations and software, is the property of or is licensed to Frontiers Media SA ("Frontiers") or its licensees and/or subcontractors. The copyright in the text of individual articles is the property of their respective authors, subject to a license granted to Frontiers.

The compilation of articles constituting this e-book, wherever published, as well as the compilation of all other content on this site, is the exclusive property of Frontiers. For the conditions for downloading and copying of e-books from Frontiers' website, please see the Terms for Website Use. If purchasing Frontiers e-books from other websites or sources, the conditions of the website concerned apply.

Images and graphics not forming part of user-contributed materials may not be downloaded or copied without permission.

Individual articles may be downloaded and reproduced in accordance with the principles of the CC-BY licence subject to any copyright or other notices. They may not be re-sold as an e-book.

As author or other contributor you grant a CC-BY licence to others to reproduce your articles, including any graphics and third-party materials supplied by you, in accordance with the Conditions for Website Use and subject to any copyright notices which you include in connection with your articles and materials.

All copyright, and all rights therein, are protected by national and international copyright laws.

The above represents a summary only. For the full conditions see the Conditions for Authors and the Conditions for Website Use.

**ISSN 1664-8714**

**ISBN 978-2-88919-682-1**

**DOI 10.3389/978-2-88919-682-1**

## **About Frontiers**

Frontiers is more than just an open-access publisher of scholarly articles: it is a pioneering approach to the world of academia, radically improving the way scholarly research is managed. The grand vision of Frontiers is a world where all people have an equal opportunity to seek, share and generate knowledge. Frontiers provides immediate and permanent online open access to all its publications, but this alone is not enough to realize our grand goals.

## **Frontiers Journal Series**

The Frontiers Journal Series is a multi-tier and interdisciplinary set of open-access, online journals, promising a paradigm shift from the current review, selection and dissemination processes in academic publishing. All Frontiers journals are driven by researchers for researchers; therefore, they constitute a service to the scholarly community. At the same time, the Frontiers Journal Series operates on a revolutionary invention, the tiered publishing system, initially addressing specific communities of scholars, and gradually climbing up to broader public understanding, thus serving the interests of the lay society, too.

## **Dedication to Quality**

Each Frontiers article is a landmark of the highest quality, thanks to genuinely collaborative interactions between authors and review editors, who include some of the world's best academicians. Research must be certified by peers before entering a stream of knowledge that may eventually reach the public - and shape society; therefore, Frontiers only applies the most rigorous and unbiased reviews.

Frontiers revolutionizes research publishing by freely delivering the most outstanding research, evaluated with no bias from both the academic and social point of view.

By applying the most advanced information technologies, Frontiers is catapulting scholarly publishing into a new generation.

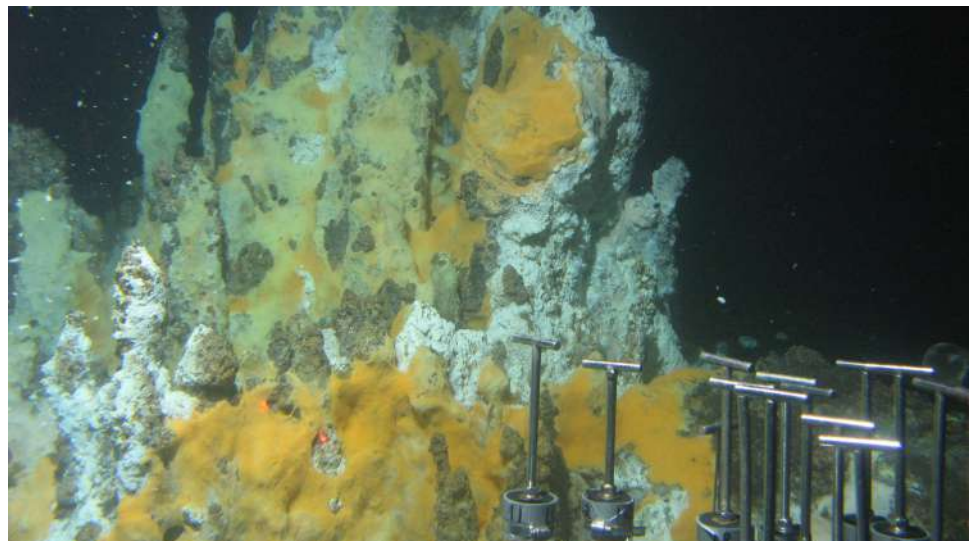
## **What are Frontiers Research Topics?**

Frontiers Research Topics are very popular trademarks of the Frontiers Journals Series: they are collections of at least ten articles, all centered on a particular subject. With their unique mix of varied contributions from Original Research to Review Articles, Frontiers Research Topics unify the most influential researchers, the latest key findings and historical advances in a hot research area! Find out more on how to host your own Frontiers Research Topic or contribute to one as an author by contacting the Frontiers Editorial Office: [researchtopics@frontiersin.org](mailto:researchtopics@frontiersin.org)

# HYDROTHERMAL MICROBIAL ECOSYSTEMS

Topic Editors:

**Andreas Teske**, University of North Carolina at Chapel Hill, USA  
**Anna-Louise Reysenbach**, Portland State University, USA



Hydrothermal Chimneys with Microbial Mats in Guaymas Basin, a sedimented spreading center in the Gulf of California. The yellow and orange-colored bacterial mats overgrowing the chimneys are sulfur-oxidizing, filamentous Beggiatoaceae, which form luxuriant microbial mats on hydrothermal hot spots. Image by: Woods Hole Oceanographic Institution, Woods Hole, MA, USA, used with permission.

The papers in the “Hydrothermal Vent” e-book cover a range of microbiological research in deep and shallow hydrothermal environments, from high temperature “black smokers,” to diffuse flow habitats and episodically discharging subsurface fluids, to the hydrothermal plumes. Together they provide a snapshot of current research interests in a field that has evolved rapidly since the discovery of hydrothermal vents in 1977. Hydrothermally influenced microbial habitats and communities represent a wide spectrum of geological setting, chemical in-situ regimes, and biotic communities; the classical examples of basalt-hosted black smoker chimneys at active mid-ocean spreading centers have been augmented by hydrothermally heated and chemically altered sediments, microbiota fueled by serpentinization reactions, and low-temperature vents with unusual menus of electron donors. Environmental gradients and niches provide habitats for unusual or unprecedented microorganisms and microbial ecosystems. The discovery of novel extremophiles underscores untapped microbial diversity in hydrothermal vent microbial communities. Different stages of hydrothermal activity, from early onset to peak activity, gradual decline, and persistence

of cold and fossil vent sites, correspond to different colonization waves by microorganisms as well as megafauna. Perhaps no other field in microbiology is so intertwined with the geological and geochemical evolution of the oceans, and promises so many biochemical and physiological discoveries still to be made within the unexhausted richness of extreme microbial life.

**Citation:** Teske, A., Reysenbach, A-L., eds. (2015). Hydrothermal Microbial Ecosystems. Lausanne: Frontiers Media. doi: 10.3389/978-2-88919-682-1

# Table of Contents

- 06 Editorial: Hydrothermal microbial ecosystems**  
Andreas Teske and Anna-Louise Reysenbach
- 09 Anaerobic oxidation of short-chain alkanes in hydrothermal sediments: potential influences on sulfur cycling and microbial diversity**  
Melissa M. Adams, Adrienne L. Hoarfrost, Arpita Bose, Samantha B. Joye and Peter R. Girguis
- 20 Phylogenetic diversity and functional gene patterns of sulfur-oxidizing subseafloor Epsilonproteobacteria in diffuse hydrothermal vent fluids**  
Nancy H. Akerman, David A. Butterfield and Julie A. Huber
- 34 The pH and pCO<sub>2</sub> dependence of sulfate reduction in shallow-sea hydrothermal CO<sub>2</sub> – venting sediments (Milos Island, Greece)**  
Elisa Bayraktarov, Roy E. Price, Timothy G. Ferdinand and Kai Finster
- 44 Microbial colonization of basaltic glasses in hydrothermal organic-rich sediments at Guaymas Basin**  
Nolwenn Callac, Céline Rommevaux-Jestin, Olivier Rouxel, Françoise Lesongeur, Céline Liorzou, Claire Bollinger, Antony Ferrant and Anne Godfroy
- 64 Diffuse flow environments within basalt- and sediment-based hydrothermal vent ecosystems harbor specialized microbial communities**  
Barbara J. Campbell, Shawn W. Polson, Lisa Zeigler Allen, Shannon J. Williamson, Charles K. Lee, K. Eric Wommack and S. Craig Cary
- 79 The microbiology of deep-sea hydrothermal vent plumes: ecological and biogeographic linkages to seafloor and water column habitats**  
Gregory J. Dick, Karthik Anantharaman, Brett J. Baker, Meng Li, Daniel C. Reed and Cody S. Sheik
- 95 Diversity and phylogenetic analyses of bacteria from a shallow-water hydrothermal vent in Milos island (Greece)**  
Donato Giovannelli, Giuseppe d'Errico, Elena Manini, Michail Yakimov and Costantino Vetriani
- 108 Biogeochemical implications of the ubiquitous colonization of marine habitats and redox gradients by Marinobacter species**  
Kim M. Handley and Jonathan R. Lloyd
- 118 Metagenome reveals potential microbial degradation of hydrocarbon coupled with sulfate reduction in an oil-immersed chimney from Guaymas Basin**  
Ying He, Xiang Xiao and Fengping Wang
- 131 A comparative study of microbial diversity and community structure in marine sediments using poly(A) tailing and reverse transcription-PCR**  
Tatsuhiko Hoshino and Fumio Inagaki

- 139 Characteristics of microbial communities in crustal fluids in a deep-sea hydrothermal field of the Suiyo Seamount**  
Shingo Kato, Michiyuki Nakawake, Junko Kita, Toshiro Yamanaka, Motoo Utsumi, Kei Okamura, Jun-ichiro Ishibashi, Moriya Ohkuma and Akihiko Yamagishi
- 150 Microbiological characterization of post-eruption "snowblower" vents at Axial Seamount, Juan de Fuca Ridge**  
Julie L. Meyer, Nancy H. Akerman, Giora Proskurowski and Julie A. Huber
- 163 Microbial habitat connectivity across spatial scales and hydrothermal temperature gradients at Guaymas Basin**  
Stefanie Meyer, Gunter Wegener, Karen G. Lloyd, Andreas Teske, Antje Boetius and Alban Ramette,
- 174 Biogeography of Persephonella in deep-sea hydrothermal vents of the Western Pacific**  
Sayaka Mino, Hiroko Makita, Tomohiro Toki, Junichi Miyazaki, Shingo Kato, Hiromi Watanabe, Hiroyuki Imachi, Tomo-o Watsuji, Takuro Nunoura, Shigeaki Kojima, Tomoo Sawabe, Ken Takai and Satoshi Nakagawa
- 186 Archaeal and bacterial diversity in an arsenic-rich shallow-sea hydrothermal system undergoing phase separation**  
Roy E. Price, Ryan Lesniewski, Katja S. Nitzsche, Anke Meyer-Dierks, Chad Saltikov, Thomas Pichler and Jan P. Amend
- 205 Microbial diversity in the deep-subsurface hydrothermal aquifer feeding the giant gypsum crystal-bearing Naica Mine, Mexico**  
Marie Ragon, Alexander E. S. Van Driessche, Juan M. García-Ruiz, David Moreira and Purificación López-García
- 217 Presence and diversity of anammox bacteria in cold hydrocarbon-rich seeps and hydrothermal vent sediments of the Guaymas Basin**  
Lina Russ, Boran Kartal, Huub J. M. op den Camp, Martina Sollai, Julie Le Bruchec, Jean-Claude Caprais, Anne Godfroy, Jaap S. Sinninghe Damsté and Mike S. M. Jetten
- 227 Metagenomic insights into the dominant Fe(II) oxidizing Zetaproteobacteria from an iron mat at Lō‘īhi, Hawai‘i**  
Esther Singer, John F. Heidelberg, Ashita Dhillon and Katrina J. Edwards
- 236 Low temperature geomicrobiology follows host rock composition along a geochemical gradient in Lau Basin**  
Jason B. Sylvan, Tiffany Y. Sia, Amanda G. Haddad, Lindsey J. Briscoe, Brandy M. Toner, Peter R. Girguis and Katrina J. Edwards,
- 254 Widespread occurrence of two carbon fixation pathways in tubeworm endosymbionts: lessons from hydrothermal vent associated tubeworms from the Mediterranean Sea**  
Vera Thiel, Michael Hügler, Martina Blümel, Heike I. Baumann, Andrea Gärtner, Rolf Schmaljohann, Harald Strauss, Dieter Garbe-Schönberg, Sven Petersen, Dominique A. Cowart, Charles R. Fisher and Johannes F. Imhoff
- 274 Multilocus sequence analysis of Thermoanaerobacter isolates reveals recombining, but differentiated, populations from geothermal springs of the Uzon Caldera, Kamchatka, Russia**  
Isaac D. Wagner, Litty B. Varghese, Christopher L. Hemme and Juergen Wiegel



# Editorial: Hydrothermal microbial ecosystems

Andreas Teske<sup>1\*</sup> and Anna-Louise Reysenbach<sup>2</sup>

<sup>1</sup> Department of Marine Sciences, University of North Carolina, Chapel Hill, NC, USA, <sup>2</sup> Biology Department, Portland State University, Portland, OR, USA

**Keywords:** hydrothermal vent, extremophiles, biogeography, chemosynthesis, archaea, bacteria, Guaymas basin

The papers in the “Hydrothermal Vent” research topic cover a range of microbiological research in deep and shallow hydrothermal environments, from high temperature “black smokers,” to diffuse flow habitats and episodically discharging subsurface fluids, to the hydrothermal plumes. Together they provide a snapshot of current research interests in a field that has evolved rapidly since the discovery of hydrothermal vents in 1977.

The topic opens with a review by Dick et al. (2013) on hydrothermal plumes and their microbial communities in the deep sea. The review synthesizes recent advances in the microbial ecology, physiology, and genomics of the mostly chemosynthetic bacteria that have adapted to the supply of carbon and energy sources in the turbulently mixed vent plume. These pelagic communities are distinct from those in hydrothermal chimneys, sediments and the subsurface, yet they show some taxonomic and physiological linkages. This review is followed by four papers that shed new light on microbial ecosystems in mixed vent fluids. The high-flow example is represented by sulfide-rich subsurface vent fluids discharging in “snow blower” bursts dominated by sulfur-oxidizing, microaerobic, and often moderately thermophilic Epsilonproteobacteria (Meyer et al., 2013a). Similar epsilonproteobacterial communities, dominated by the chemosynthetic, sulfur-oxidizing genera *Sulfurimonas* and *Sulfurovum*, were also found in cool, diffusive flow at the same location, Axial Seamount on the Juan de Fuca Ridge (Akerman et al., 2013). The authors proposed that both diffuse flow and episodic high-flow events tap into the same subsurface community of microaerobic sulfur oxidizers. Epsilonproteobacteria accounted again for most of the microbial taxa found in diffuse flow samples from the basalt-hosted vent sites of 9°N East Pacific Rise, but not in similar habitats in the organic-rich hydrothermal sediments of Guaymas Basin in the Gulf of California, where other bacterial groups and hyperthermophilic archaea predominated (Campbell et al., 2013). Changing flow paths and reservoirs for subseafloor mixed fluids and their microbiota can also change the composition of venting microbial communities over time as reported by Kato and colleagues. At Suiyo Seamount in the Izu-Bonin Arc within the Western Pacific, a hot and reducing subsurface reservoir accessed by drilling underwent increasing seawater in-mixing over several years. Consequently, the crustal fluid community of sulfur-oxidizing chemolithotrophs changed to a mixed assemblage harboring abundant marine heterotrophic bacteria (Kato et al., 2013).

While deep-sea hydrothermal vent sites are difficult to access and to sample, shallow water hydrothermal vents that can be reached by scuba divers provide an accessible alternative environment to study. Perhaps the best-investigated of these shallow-water vents are found on the coast of the Greek island Milos in the Aegean Sea, where hot, briny, reducing, CO<sub>2</sub>-rich vent fluids permeate the sandy seafloor sediments of Paleochori Bay. Giovannelli et al. (2013) show that in the surficial sediments the microbial community is dominated by Epsilonproteobacteria (genus *Sulfurovum*) similar to those seen in deep-sea vents; however proteobacterial lineages that are distinct from those of deep-sea vents were also detected. In contrast, in the deeper sediment layers of this sample vent field, Price et al. (2013) find Epsilonproteobacteria, but also Firmicutes, Planctomycetes, and Bacteroidetes coexisting with thermophilic archaea. In addition, arsenite-oxidizing bacteria were identified by

## OPEN ACCESS

### Edited by:

Virginia P Edgcomb,  
Woods Hole Oceanographic  
Institution, USA

### Reviewed by:

Maria Pachiaudiaki,  
Woods Hole Oceanographic  
Institution, USA

### \*Correspondence:

Andreas Teske,  
teske@email.unc.edu

### Specialty section:

This article was submitted to  
Extreme Microbiology,  
a section of the journal  
*Frontiers in Microbiology*

Received: 12 June 2015

Accepted: 12 August 2015

Published: 01 September 2015

### Citation:

Teske A and Reysenbach A-L (2015)  
Editorial: Hydrothermal microbial  
ecosystems. *Front. Microbiol.* 6:884.  
doi: 10.3389/fmicb.2015.00884

functional gene analysis in these arsenite-rich sediments. Site-specific adaptations of vent communities are also the focus of Bayraktarov et al. (2013), as they examine the pH preferences of sulfate-reducing microbial communities in the Milos vent sediments. In the proximity of CO<sub>2</sub>-rich, low-pH fluids, the sulfate-reducing microbial communities show maximal activities at a distinctly lower pH range than at less acidic control sites not impacted by CO<sub>2</sub>-rich vent fluids.

Among deep-sea vent sites, the sediment-covered Guaymas Basin hydrothermal vents in the central Gulf of California is unusual; the buried organic matter in these sediments are hydrothermally processed to petroleum compounds, low-molecular weight organic acids, short-chain alkanes, methane and ammonia. These substrates sustain a unique microbial ecosystem that combines the characteristics of communities from hydrocarbon seeps and mid-ocean ridge hydrothermal vents. Meyer and colleagues demonstrate that the microbial populations in Guaymas sediments show a high degree of microbial connectivity and population overlap within an area of a few 100 m—a consequence of vigorous venting, rapid dispersal via bottom currents, and closely spaced hydrothermal features (Meyer et al., 2013b). Abundant aromatic and aliphatic hydrocarbons in Guaymas Basin sediments and chimneys enrich for microbial specialists—especially sulfate-reducing bacteria—that utilize hydrocarbons, remineralize them to CO<sub>2</sub>, or assimilate them into microbial biomass; these communities feature prominently in metagenomic analyses of hydrocarbon-rich Guaymas chimneys (He et al., 2013). The ammonia-rich and methane-rich hydrothermal fluids at Guaymas sustain ammonia-oxidizing bacteria (anammox) and methane- oxidizing archaea (ANME) in the surficial sediments. The anammox bacteria combine ammonia and nitrite to N<sub>2</sub>, and are usually better known from marine oxygen minimum zones and stratified water columns (Russ et al., 2013). A recently identified, high-temperature tolerant clade of the cosmopolitan seep methane-oxidizing archaeal lineage ANME-1 is widespread at Guaymas Basin. The “ANME\_1Guaymas” have been enriched using *in-situ* colonization chambers that were placed into surficial hydrothermal sediments on the seafloor (Callac et al., 2013). One of the relatively few analogous environments to Guaymas Basin, the alkane-rich hydrothermal sediments of the Middle Valley vent field on the northern Juan de Fuca ridge, provide the opportunity to study similar microbial communities and processes. In anaerobic batch reaction incubations, short alkanes (ethane, propane, butane) were consumed within a mesophilic to thermophilic temperature range, probably by sulfate-reducing bacteria (Adams et al., 2013).

Hydrothermal vents are suitable model systems to explore microbial biogeography because they are island habitats in the deep sea; their thermophilic, chemosynthetic or special substrate-adapted microbial inhabitants likely cannot survive, and certainly cannot thrive in the cold, oxidized sediments and bottom waters of the deep sea that separate hydrothermal hot spots. In this volume several papers evaluate the controls of microbial community structure, geographic distance vs. environmental selection pressures in different habitats such as tubeworm trophosomes, sulfides, and ferric iron hydroxides. Sulfur-oxidizing endosymbionts of vestimentiferan tubeworms,

which thrive in seep and vent habitats, showed a clear separation into different Gulf of Mexico and Mediterranean genotypes by 16S rRNA gene, mitochondrial cytochrome C oxidase, and functional genes of the two coexisting CO<sub>2</sub> assimilation pathways that coexist in the endosymbiont, the Calvin-Benson-Bassham and the reverse TCA cycle (Thiel et al., 2012). Mino et al. (2013) use multi-locus sequence analysis to show that isolates of the chemosynthetic thermophilic genus *Persephonella* from different vent sites in the Okinawa Trough and in the distant Southern Mariana Trench in the western Pacific undergo sympatric speciation. Similarly, Wagner et al. (2013) use multi-locus sequence analysis to demonstrate genetic differentiation among strains of the thermophilic fermenting Firmicute, *Thermoanaerobacter uzonensis*, from different terrestrial hot spring locations within the Uzon Caldera in Kamtchatka. In this case, genetic divergence did not correlate with geographic separation on these short distances of mostly a few 100 m. Sylvan et al. (2013) describe how the biogeographical boundary of the north-south transition from basalt-hosted to andesite-hosted vents on the Eastern Lau Spreading Center and Valu Fa ridge, appears to select for distinct bacterial taxa on silicate rocks, whereas inactive sulfides show major differences in bacterial community structure between the surface and the interior sulfide mineral matrix. Members of the Zetaproteobacteria, including the microaerobic and chemolithotrophic iron oxidizer *Mariprofundus ferrooxidans*, fall into different 16S rRNA phylotypes of Zetaproteobacteria from the Southern Mariana Arc, the Hawaiian hot spot, and from the Vai'lulu/Tonga Arc/East Lau Spreading Center/Kermadec Arc. This study shows that the Zetaproteobacteria from these sites form mutually intertwined microclusters on the 16S rRNA gene level, suggesting more detailed genomic analyses to explore their biogeography in fine resolution (Singer et al., 2013).

This research topic includes methodological assessments. Molecular surveys of biogeographic patterns and dominant microbial populations depend critically on the molecular tools used. To document inherent methodological biases, Hoshino and Inagaki (2013) perform a comparative molecular analysis of bacterial populations in hydrothermal sediments of Yonaguni Knoll in the Southern Okinawa Trough. By comparing the phylotypes recovered by conventional reverse-transcription PCR with domain-specific primers and by previous poly-A tailing of the extracted rRNA, they find different clades of Deltaproteobacteria and detect unusual archaea in the poly-A tailing assay that may escape detection by conventional PCR or RT-PCR using domain-specific primers.

The last two contributions to this research topic discuss microbial groups that are not commonly considered as components of hydrothermal microbiota, marine heterotrophic bacteria and pelagic marine archaea. When cosmopolitan, heterotrophic marine bacteria appear in molecular diversity surveys of hydrothermal vents or other extreme habitats, they are regarded as “hitchhikers” or potentially contaminants from entrainment of seawater. Handley and Lloyd (2013) examine the cosmopolitan marine genus *Marinobacter* and find that these versatile bacteria—commonly regarded as aerobes or fermenters—include nitrate-reducing and metal-reducing representatives from low-temperature vents, marine sediments

and mid-ocean ridge basalts. This genus is therefore well-suited to colonize aerobic- to anoxic gradients in most marine environments, including hydrothermal vents. Likewise, the Thaumarchaeota—marine archaea that are ubiquitous in the cold and oxic marine water column—have been found in surficial marine sediments, hydrothermal plumes, and hot spring sediments. Ragon et al. (2013) report a new phylotype within the terrestrial hot spring branch of the Thaumarchaeota, detected in deep hot ( $60^{\circ}\text{C}$ ) spring waters in Naica Mine, Chihuahua, Mexico. Thus, the Thaumarchaeota emerge as one of the most adaptable archaeal lineages that inhabit marine and terrestrial, oxic and anoxic, cold, and hydrothermal habitats.

These papers represent a sampler of ongoing microbiological research in hydrothermal environments, and demonstrate the wide multidisciplinary context of this field. Hydrothermal

vents are not disconnected in time and space from the wider deep-sea ecosystem, without geological and biogeographical context. The research papers assembled here integrate geology, biogeochemistry, microbial physiology, microbial genomics and systematics across spatial scales that zoom in and out depending on the research question at hand. Perhaps no other field is so intertwined with the geological and geochemical evolution of the oceans, and promises so many biochemical and physiological discoveries still to be made within the unexhausted richness of extreme microbial life.

## Acknowledgments

The editors' hydrothermal vent research and their efforts to develop this research topic were supported by NSF grants OCE-0647633 and 1334371 (AT) and OCE-1235432 (AR).

## References

- Adams, M. M., Hoar frost, A. L., Bose, A., Joye, S. B., and Girguis, P. R. (2013). Anaerobic oxidation of short-chain alkanes in hydrothermal sediments: potential influences on sulfur cycling and microbial diversity. *Front. Microbiol.* 4:110. doi: 10.3389/fmicb.2013.00110
- Akerman, N. H., Butterfield, D. A., and Huber, J. A. (2013). Phylogenetic diversity and functional gene patterns of sulfur-oxidizing subseafloor *Epsilonproteobacteria* in diffuse hydrothermal fluids. *Front. Microbiol.* 4:185. doi: 10.3389/fmicb.2013.00185
- Bayraktarov, E., Price, R. E., Ferdinand, T. G., and Finster, K. (2013). The pH and pCO<sub>2</sub> dependence of sulfate reduction in shallow-sea hydrothermal CO<sub>2</sub>-venting sediments (Milos Island, Greece). *Front. Microbiol.* 4:111. doi: 10.3389/fmicb.2013.00111
- Callac, N., Rommevaux-Jestin, C., Rouxel, O., Lesongeur, F., Liorzou, C., Bollinger, C., et al. (2013). Microbial colonization of basaltic glasses in hydrothermal organic-rich sediments at Guaymas Basin. *Front. Microbiol.* 4:250. doi: 10.3389/fmicb.2013.00250
- Campbell, B. J., Polson, S. W., Allen, L. Z., Williamson, S. J., Lee, C. K., Wommack, K. E., et al. (2013). Diffuse flow environments within basalt- and sediment-hosted hydrothermal vent ecosystems harbor specialized microbial communities. *Front. Microbiol.* 4:182. doi: 10.3389/fmicb.2013.00182
- Dick, G. J., Anantharaman, K., Baker, B. J., Li, M., Reed, D. C., and Sheik, C. S. (2013). The microbiology of deep-sea hydrothermal vent plumes: ecological and biogeographical linkages to seafloor and water column habitats. *Front. Microbiol.* 4:124. doi: 10.3389/fmicb.2013.00124
- Giovannelli, D., d'Errico, G., Manini, E., Yakimov, M., and Vetriani, C. (2013). Diversity and phylogenetic analyses of bacteria from a shallow-water hydrothermal vent in Milos Island (Greece). *Front. Microbiol.* 4:184. doi: 10.3389/fmicb.2013.00184
- Handley, K. M., and Lloyd, J. R. (2013). Biogeochemical implications of the ubiquitous colonization of marine habitat and redox gradients by *Marinobacter* species. *Front. Microbiol.* 4:136. doi: 10.3389/fmicb.2013.00136
- He, Y., Xiao, X., and Wang, F. (2013). Metagenome reveals potential microbial degradation of hydrocarbon coupled with sulfate reduction in an oil-immersed chimney from Guaymas Basin. *Front. Microbiol.* 4:148. doi: 10.3389/fmicb.2013.00148
- Hoshino, T., and Inagaki, F. (2013). A comparative study of microbial diversity and community structure in marine sediments using poly(A) tailing and reverse transcription PCR. *Front. Microbiol.* 4:160. doi: 10.3389/fmicb.2013.00160
- Kato, S., Nakawake, M., Kita, J., Yamanaka, T., Utsumi, M., Okamura, K., et al. (2013). Characteristics of microbial communities in crustal fluids in a deep-sea hydrothermal field of the Suiyo Seamount. *Front. Microbiol.* 4:85. doi: 10.3389/fmicb.2013.00085
- Meyer, J. L., Akerman, N. H., Proskurowski, G., and Huber, J. A. (2013a). Microbiological characterization of post-eruption “snowblower” vents at Axial Seamount, Juan de Fuca Ridge. *Front. Microbiol.* 4:153. doi: 10.3389/fmicb.2013.00153
- Meyer, S., Wegener, G., Lloyd, K. G., Teske, A., Boetius, A., and Ramette, A. (2013b). Microbial habitat connectivity across spatial scales and hydrothermal temperature gradients at Guaymas Basin. *Front. Microbiol.* 4:207. doi: 10.3389/fmicb.2013.00207
- Mino, S., Makita, H., Toki, T., Miyazaki, J., Kato, S., Watanabe, H., et al. (2013). Biogeography of *Persephonella* in deep-sea hydrothermal vents of the Western Pacific. *Front. Microbiol.* 4:107. doi: 10.3389/fmicb.2013.00107
- Price, R. E., Lesniewski, R., Nitzsche, K. S., Meyerderk, A., Saltikov, C., Pichler, T., et al. (2013). Archaeal and bacterial diversity in an arsenic-rich shallow-sea hydrothermal system undergoing phase separation. *Front. Microbiol.* 4:158. doi: 10.3389/fmicb.2013.00158
- Ragon, M., Van Driessche, A. E. S., García-Ruiz, J. M., Moreira, D., and López-García, P. (2013). Microbial diversity in the deep-subsurface hydrothermal aquifer feeding the giant gypsum crystal-bearing Naica Mine, Mexico. *Front. Microbiol.* 4:37. doi: 10.3389/fmicb.2013.00037
- Russ, L., Kartal, B., op den Camp, H. J., Sollai, M., Le Bruchec, J., Caprais, C. J., et al. (2013). Presence and diversity of anammox bacteria in cold hydrocarbon-rich seeps and hydrothermal vent sediments of the Guaymas Basin. *Front. Microbiol.* 4:219. doi: 10.3389/fmicb.2013.00219
- Singer, E., Heidelberg, J. F., Dhillon, A., and Edwards, K. J. (2013). Metagenomic insights into the dominant Fe(II) oxidizing Zetaproteobacteria from an iron mat at Lo'ihi, Hawai'i. *Front. Microbiol.* 4:52. doi: 10.3389/fmicb.2013.00052
- Sylvan, J. B., Sia, T. Y., Haddad, A. G., Briscoe, L. J., Toner, B. M., Girguis, P. R., et al. (2013). Low temperature geomicrobiology follows host rock composition along a geochemical gradient in Lau Basin. *Front. Microbiol.* 4:61. doi: 10.3389/fmicb.2013.00061
- Thiel, V., Hügler, M., Blümel, M., Baumann, H. I., Gärtner, A., Schmaljohann, R., et al. (2012). Widespread occurrence of two carbon fixation pathways in tubeworm endosymbionts: lessons from hydrothermal vent associated tubeworms from the Mediterranean Sea. *Front. Microbiol.* 3:423. doi: 10.3389/fmicb.2012.00423
- Wagner, I. D., Varghese, J. B., Hemme, C. L., and Wiegel, J. (2013). Multilocus sequence analysis of *Thermoanaerobacter* isolates reveals recombining, but differentiated, populations from geothermal springs of the Uzon Caldera, Kamtchatka, Russia. *Front. Microbiol.* 4:169. doi: 10.3389/fmicb.2012.00169

**Conflict of Interest Statement:** The authors declare that the research was conducted in the absence of any commercial or financial relationships that could be construed as a potential conflict of interest.

Copyright © 2015 Teske and Reysenbach. This is an open-access article distributed under the terms of the Creative Commons Attribution License (CC BY). The use, distribution or reproduction in other forums is permitted, provided the original author(s) or licensor are credited and that the original publication in this journal is cited, in accordance with accepted academic practice. No use, distribution or reproduction is permitted which does not comply with these terms.



# Anaerobic oxidation of short-chain alkanes in hydrothermal sediments: potential influences on sulfur cycling and microbial diversity

Melissa M. Adams<sup>1</sup>, Adrienne L. Hoar frost<sup>2</sup>, Arpita Bose<sup>1</sup>, Samantha B. Joye<sup>3</sup> and Peter R. Girguis<sup>1\*</sup>

<sup>1</sup> Department of Organismic and Evolutionary Biology, Harvard University, Cambridge, MA, USA

<sup>2</sup> Department of Marine Sciences, University of North Carolina at Chapel Hill, Chapel Hill, NC, USA

<sup>3</sup> Department of Marine Sciences, University of Georgia, Athens, GA, USA

## Edited by:

Andreas Teske, University of North Carolina at Chapel Hill, USA

## Reviewed by:

Julie A. Huber, Marine Biological Laboratory, USA

Elizaveta Bonch-Osmolovskaya, Winogradsky Institute of Microbiology Russian Academy of Sciences, Russia

## \*Correspondence:

Peter R. Girguis, Department of Organismic and Evolutionary Biology, Harvard University, Biological Laboratories, Room 3085, 16 Divinity Avenue, Cambridge, MA 02138, USA.  
e-mail: pgirguis@oeb.harvard.edu

Short-chain alkanes play a substantial role in carbon and sulfur cycling at hydrocarbon-rich environments globally, yet few studies have examined the metabolism of ethane ( $C_2$ ), propane ( $C_3$ ), and butane ( $C_4$ ) in anoxic sediments in contrast to methane ( $C_1$ ). In hydrothermal vent systems, short-chain alkanes are formed over relatively short geological time scales via thermogenic processes and often exist at high concentrations. The sediment-covered hydrothermal vent systems at Middle Valley (MV, Juan de Fuca Ridge) are an ideal site for investigating the anaerobic oxidation of  $C_1$ – $C_4$  alkanes, given the elevated temperatures and dissolved hydrocarbon species characteristic of these metalliferous sediments. We examined whether MV microbial communities oxidized  $C_1$ – $C_4$  alkanes under mesophilic to thermophilic sulfate-reducing conditions. Here we present data from discrete temperature (25, 55, and 75°C) anaerobic batch reactor incubations of MV sediments supplemented with individual alkanes. Co-registered alkane consumption and sulfate reduction (SR) measurements provide clear evidence for  $C_1$ – $C_4$  alkane oxidation linked to SR over time and across temperatures. In these anaerobic batch reactor sediments, 16S ribosomal RNA pyrosequencing revealed that *Delta proteobacteria*, particularly a novel sulfate-reducing lineage, were the likely phylotypes mediating the oxidation of  $C_2$ – $C_4$  alkanes. Maximum  $C_1$ – $C_4$  alkane oxidation rates occurred at 55°C, which reflects the mid-core sediment temperature profile and corroborates previous studies of rate maxima for the anaerobic oxidation of methane (AOM). Of the alkanes investigated,  $C_3$  was oxidized at the highest rate over time, then  $C_4$ ,  $C_2$ , and  $C_1$ , respectively. The implications of these results are discussed with respect to the potential competition between the anaerobic oxidation of  $C_2$ – $C_4$  alkanes with AOM for available oxidants and the influence on the fate of  $C_1$  derived from these hydrothermal systems.

**Keywords:** hydrothermal vent, metalliferous sediments, Juan de Fuca Ridge, short-chain alkanes, sulfate reduction

## INTRODUCTION

Hydrocarbon gases, including methane ( $C_1$ ), ethane ( $C_2$ ), propane ( $C_3$ ), and *n*-butane ( $C_4$ ), are produced via thermogenic and biogenic processes in the deep subsurface and are substantial components of the organic carbon pool across marine and terrestrial ecosystems (Joye et al., 2004; Milkov, 2005; Cruse and Seewald, 2006; Hinrichs et al., 2006; Savage et al., 2010). Over the past decade, studies focused on the anaerobic oxidation of methane (AOM) revealed the functional potential, ecological physiology, and diversity of microorganisms mediating this process and the global distribution of AOM as an effective benthic filter that reduces methane emissions into the oceans and atmosphere (for reviews, see Conrad, 2009; Knittel and Boetius, 2009; Valentine, 2011). In contrast, the anaerobic oxidation of long-chain alkanes ( $>C_6$ ) and aromatics has also been studied extensively resulting in the isolation of several bacteria, such as sulfate-reducing bacteria (SRB) that oxidize crude oil anaerobically (Van Hamme et al., 2003). There is a gap in our understanding of the metabolism

and fate of non-methane, short-chain ( $C_2$ – $C_4$ ) alkanes in deep sea sediments. Furthermore, there is growing interest in determining the extent to which microorganisms mediate the anaerobic oxidation of  $C_2$ – $C_4$  alkanes, as many studies have indicated that the degradation of these aliphatic hydrocarbons may be linked to global biogeochemical cycles (Lorenson et al., 2002; Formolo et al., 2004; Sassen et al., 2004; Milkov, 2005; Bowles et al., 2011; Quistad and Valentine, 2011).

Recently, SRB from hydrocarbon seep sediments of the Gulf of Mexico and Guaymas Basin – both of which are environments rich in short-chain alkanes – were documented to oxidize short-chain alkanes to  $CO_2$  anaerobically (Kniemeyer et al., 2007). Different temperature regimens (12, 28, and 60°C) along with multiple substrates were tested and a pure culture (deemed BuS5) was isolated from mesophilic enrichments with  $C_3$  or  $C_4$  as the sole exogenous carbon source. Through comparative sequence analysis, strain BuS5 was determined to cluster with the metabolically diverse *Desulfosarcina/Desulfococcus* (DSS) cluster, which also contains the

SRB found in consortia with anaerobic methanotrophs (ANME) in seep sediments. Enrichments from a terrestrial, low temperature sulfidic hydrocarbon seep corroborated the biodegradation mechanism of complete C<sub>3</sub> oxidation to CO<sub>2</sub> with most bacterial phylotypes surveyed belonging to the *Deltaproteobacteria*, particularly within the family *Desulfobacteraceae* (Savage et al., 2010). Cold adapted C<sub>3</sub> and C<sub>4</sub>, sulfate-reducing cultures have also been obtained from Gulf of Mexico and Hydrate Ridge sediments with maximum rates of SR between 16 and 20°C and dominant phylotypes allied to the DSS cluster including BuS5 (Jaekel et al., 2012). In the study by Kniemeyer et al. (2007) C<sub>4</sub> alkane degradation linked to sulfate reduction (SR) was not quantified at thermophilic temperatures, but a Guaymas Basin sediment enrichment with C<sub>3</sub> at 60°C was dominated by Gram positive bacteria most closely allied to the *Desulfotomaculum*. Moreover, there was no evidence for C<sub>2</sub> degradation in mesophilic (28°C) or thermophilic (60°C) enrichments or C<sub>2</sub>-linked SR (albeit, there was very slow C<sub>2</sub>-dependent SR in Gulf of Mexico enrichments at 12°C after >200 days).

The Middle Valley (MV) hydrothermal vent field – located on the northern Juan de Fuca Ridge – is an ideal environment for investigating mesophilic to thermophilic anaerobic oxidation of C<sub>2</sub>–C<sub>4</sub> alkanes, given the elevated temperatures and dissolved hydrocarbon species characteristic of these sediments (Goodfellow and Blaise, 1988; Davis and Fisher, 1994; Cruse and Seewald, 2006). Deep sea hydrothermal vents are complex and dynamic habitats characterized by steep thermal and chemical gradients, a diverse array of carbon and energy sources, and high concentrations of dissolved volatiles (Butterfield et al., 1990, 1994; Von Damm et al., 1995). In the MV system, hydrothermal vent fluids interact with overlying sediments and the thermal alteration of sedimentary organic matter results in the production and/or release of a number of carbon sources, including short-chain alkanes (Cruse and Seewald, 2006; Cruse et al., 2008; Cruse and Seewald, 2010). These hydrothermally influenced sediments also contain high concentrations of reduced compounds, such as H<sub>2</sub> and hydrogen sulfide (H<sub>2</sub>S; Ames et al., 1993; Rushdl and Simonelt, 2002), and metals and metal sulfides at various reduced and oxidized states (Goodfellow and Blaise, 1988; Ames et al., 1993; Wankel et al., 2012). In contrast to the extremely organic-rich sediments of other sedimented hydrothermal systems, e.g., the Guaymas Basin hydrothermal vent fields in the Gulf of California (% OC = 2–4), MV represents a system that is more typical of mid-ocean ridge hydrothermal vents worldwide (% OC = 0.3–0.5; Wankel et al., 2012). Such environments could support the coupling of C<sub>1</sub>–C<sub>4</sub> alkane degradation to SR in addition to alternative electron acceptors, such as metal oxides, particularly when the organic carbon load and associated SR rates are low (Wankel et al., 2012).

We studied the anaerobic oxidation of C<sub>1</sub>–C<sub>4</sub> alkanes in metalliferous, organic-poor MV hydrothermal sediments across environmentally relevant temperature gradients. This biogeochemical investigation aimed to determine: (i) the temperature range over which hydrothermal sediment communities oxidize C<sub>1</sub>–C<sub>4</sub> alkanes, (ii) the degree to which the anaerobic oxidation of these alkanes is coupled to SR, and (iii) the putative microbial phylotypes mediating C<sub>1</sub>–C<sub>4</sub> alkane oxidation. To address these aims,

a series of incubations were conducted using slurries of sediments collected from the MV system. These anaerobic batch reactors enabled the quantification and direct comparison of C<sub>1</sub>–C<sub>4</sub> alkane oxidation and SR rates in a closed system across a broad range of discrete temperatures (25, 55, and 75°C). Archaeal and bacterial community dynamics were investigated via pyrotag sequencing in select batch reactor sediments that exhibited the greatest alkane oxidation activity over the incubation time course. The overall objective of this study was to advance our understanding of the nature and extent of the anaerobic oxidation of short-chain alkanes in hydrothermal systems and to ascertain the potential influence of these processes on other biogeochemical cycles. The data presented herein shed light on the relative contribution of the anaerobic oxidation of C<sub>2</sub>–C<sub>4</sub> alkanes at different temperature regimes, the potential influence on AOM and the sulfur cycle, and the phylotypes most likely allied to the observed metabolisms.

## MATERIALS AND METHODS

### STUDY SITE AND SAMPLE COLLECTION

Sediments were collected during an expedition with the *DSV Alvin* and *R/V Atlantis* in July 2010 from the Chowder Hill hydrothermal vent field in MV (48°27.44 N, 128°42.51 W) at 2413 m depth. Intact sediment cores were recovered with polyvinylchloride core sleeves (20–30 cm height, 6.35 cm ID, 0.32 cm sleeve thickness). Sediment sampling sites were selected based on *in situ* temperature depth profiles collected with *DSV Alvin*, the presence of chemoautotrophic microbial mats atop the sediments, and shimmering water from the diffuse flow sediments. At all sites, sediment temperature profiles were collected using the RTD probe, while dissolved alkanes and other gases were quantified using an *in situ* mass spectrometer (or ISMS; data not shown; Wankel et al., 2011). Pushcores were collected from areas where sediments temperatures ranged from 5–55°C in the upper 15 cm and 57–75°C at 30 cm sediment depth. Upon retrieval, cores were sealed and refrigerated for transport to the laboratory. Upon return to the lab, the overlying water in the sediment cores was replaced weekly with fresh, filter-sterilized anoxic seawater prior to initiation of the experiments.

### ANAEROBIC BATCH REACTORS WITH C<sub>1</sub>–C<sub>4</sub> ALKANES

In an anaerobic chamber (Coy Laboratory Products), 50 ml of homogenized whole core sediment and 50 ml of sterile, anaerobic artificial “diffuse vent fluid” were aliquoted into 200 ml glass autoclaved serum vials for each treatment. The artificial vent fluid was modified from Widdel and Bak (1992) to include 1 mM Na<sub>2</sub>S to ensure that sediments remained at reducing conditions, 50 mM Na<sub>2</sub>SO<sub>4</sub><sup>2-</sup> to reduce the possibility of sulfate limitation, and the pH adjusted to 6 to mimic the diffuse vent fluids. For each incubation temperature, the headspace was pressurized to slightly above 1 atm with the respective alkane (C<sub>1</sub>–C<sub>4</sub>) or nitrogen (N<sub>2</sub>) gas in duplicate batch reactors to avoid alkane limitation in the aqueous phase during the incubation time series. The reactors were incubated at temperatures reflecting the sea water-sediment interface (25°C), the mid-depth average temperature (55°C), and the highest temperatures measured at the deepest depth

(75°C). Flasks were shaken daily to ensure homogeneity in the slurry.

### GEOCHEMICAL MEASUREMENTS

Concentrations of the dissolved C<sub>1</sub>, C<sub>2</sub>, C<sub>3</sub>, and C<sub>4</sub> alkanes were determined after allowing the incubations to reach room temperature and by vigorously shaking samples to transfer gas from the anaerobic seawater media to the batch reactor headspace. Then, a 0.5 ml sample of the headspace was injected into a gas chromatograph equipped with a flame ionization detector (Hewlett Packard 5890 Series II) and a packed column (RestekRt-XL) to quantify all alkanes. Injections of chemically pure alkanes (Airgas East, >99% purity) were used to generate standard curves.

Sulfate reduction rates were determined by quantifying changes in sulfate and sulfide concentrations via ion chromatography and colorimetric assays, respectively (Cline, 1969; Joye et al., 2004). After shaking and allowing the sediment to settle, a 1 ml fluid sub-sample was collected with a syringe from each reactor, filter-sterilized (0.2 μm) and transferred into a vial, preserved with 10 μl HNO<sub>3</sub>, and stored at 7°C until analysis. Concentrations of sulfate were determined using a Dionex ion chromatography system (Dionex Corp. Sunnyvale, CA, USA) at the University of Georgia, and NaBr, a conservation tracer in the batch reactors, was measured simultaneously. A 1 ml headspace sub-sample was collected and mixed with an equal volume of 20% zinc acetate to quantify gaseous H<sub>2</sub>S. Concentrations of H<sub>2</sub>S were then determined colorimetrically as per Cline (1969). The reported values were corrected for HS<sup>-</sup> dissolved in the aqueous phase and reflect both sulfide species in the serum vial headspace and sediment slurry.

### DNA EXTRACTION, MASSIVELY PARALLEL SEQUENCING, AND PHYLOGENETIC ANALYSIS

At the conclusion of each incubation, sediments were sub-sampled in an anaerobic chamber, and ~15 g of sediment slurry from each batch reactor was transferred directly into a 15 ml cryovial, flash frozen in liquid nitrogen and stored at -80°C until further molecular analyses. A time zero T<sub>0</sub> sub-sample was collected at the start of the incubations to represent the initial community after homogenization, but prior to inoculation of the batch reactors. Total genomic DNA was extracted using phenol-chloroform (Barns et al., 1994; Dojka et al., 1998; Elshahed et al., 2004) modified to prevent nucleic acid loss and eliminate potential inhibitors of downstream PCR (as described in Webster et al. (2003)). Briefly, 0.5 g of sediment per batch reactor was washed with 5% HCl and then DNA was extracted with addition of 200 μg of poly adenylic acid (poly A) during the lysis step followed by incubation with lysozyme and proteinase K, multiple freeze-thaw cycles with 5% SDS, addition of hot phenol, extraction with phenol-chloroform, and elution in 50 μl TE buffer (10 mM Tris hydrochloride, 1 mM EDTA, pH 8.0). The concentration of extracts was determined using the Quant-iT<sup>TM</sup> dsDNA high sensitivity Assay (Invitrogen, Carlsbad, CA, USA).

DNA extracted from the 55°C incubations, which represented the highest rates of activity, was subjected to massively parallel sequencing of the 16S ribosomal RNA (rRNA) gene using the primer pairs 27F/519R and 340F/806R for the bacterial V1 – V3

and archaeal V3 – V4 regions, respectively (Dowd et al., 2008; Acosta-Martínez et al., 2010). All pyrosequence data were submitted to the NCBI Sequence Read Archive under accession number SRA066151. The resulting reads were checked for sequence quality, trimmed, filtered, and analyzed in the software MOTHUR (Version 1.28.0; Schloss et al., 2009). Sequences were first filtered by the presence of sequence ambiguities, long homopolymers, and quality scores. The PyroNoise algorithm was then implemented in MOTHUR (i.e., shhh.flows) to remove sequences likely generated by pyrosequencing error (Quince et al., 2009). After selection of unique sequences, chimeras were identified and removed using UCHIME (<http://www.drive5.com/uchime/>). The resulting archaeal and bacterial reads were then aligned to the SILVA SEED Bacterial and Archaeal databases, containing 14,956 and 2,297 sequences, respectively.

For sequence classification, bootstrap values were set to nodes that had >80% support in a bootstrap analysis of 100 replicates, and operational taxonomic units (OTUs) were defined as sequences sharing 97% nucleotide sequence identity for further community analyses. A phylogenetic tree of representative *Delta*proteobacteria (50 unique sequences selected in Mothur, i.e., sub.sample) was then generated with FastTree 2.0.0 (Price et al., 2010) using minimum-evolution subtree-pruning-refranging and maximum-likelihood nearest-neighbor interchanges. Local support values shown are based on the Shimodaira-Hasegawa (SH) test with 1,000 resamples. Only values >80% are shown on the branches as black circles. The tree was rooted to the 16S rRNA sequence of *Archaeoglobus profundus* DSM 5631 (NR\_074522).

## RESULTS

### C<sub>1</sub>–C<sub>4</sub> ALKANE OXIDATION AS A FUNCTION OF TEMPERATURE IN BATCH REACTORS

Batch reactor incubations were conducted using MV sediment slurries with one alkane gas (C<sub>1</sub>, C<sub>2</sub>, C<sub>3</sub>, or C<sub>4</sub>) as the sole exogenous hydrocarbon, and incubated in the laboratory at 25, 55, and 75°C to reflect the range of temperatures measured *in situ*. Temperature affected the time required to detect alkane consumption, the percent of available substrate consumed, and the absolute rates of the anaerobic oxidation of C<sub>1</sub>–C<sub>4</sub>. In batch reactors at 55°C, alkane consumption, defined as 10% of pool consumption, was evident after 71 days of incubation (Figure 1, top). In contrast, alkane consumption was detectable in 25°C batch reactors after 105 days for C<sub>1</sub>–C<sub>4</sub>. In 75°C batch reactors, substantial C<sub>2</sub>–C<sub>4</sub> consumption was apparent after 105 days; however, C<sub>1</sub> consumption was evident after a much shorter time period (30 days) at 75°C.

Examining the fraction of available alkane consumed during the entire experiment (169 days), the greatest total consumption of C<sub>1</sub>–C<sub>4</sub> occurred in the 55°C batch reactors (~93, 75, 93, and 77% of C<sub>1</sub>, C<sub>2</sub>, C<sub>3</sub>, and C<sub>4</sub>, respectively). In addition, C<sub>1</sub> was nearly depleted in the 75°C batch reactors by the end of the time series (with >90% substrate consumed). With the exception of C<sub>1</sub> at 75°C, less than half of the available short-chain alkane pool was consumed during the incubation time course in 25 and 75°C batch reactors (32, 44, 37, and 46% of C<sub>1</sub>, C<sub>2</sub>, C<sub>3</sub>, and C<sub>4</sub> at

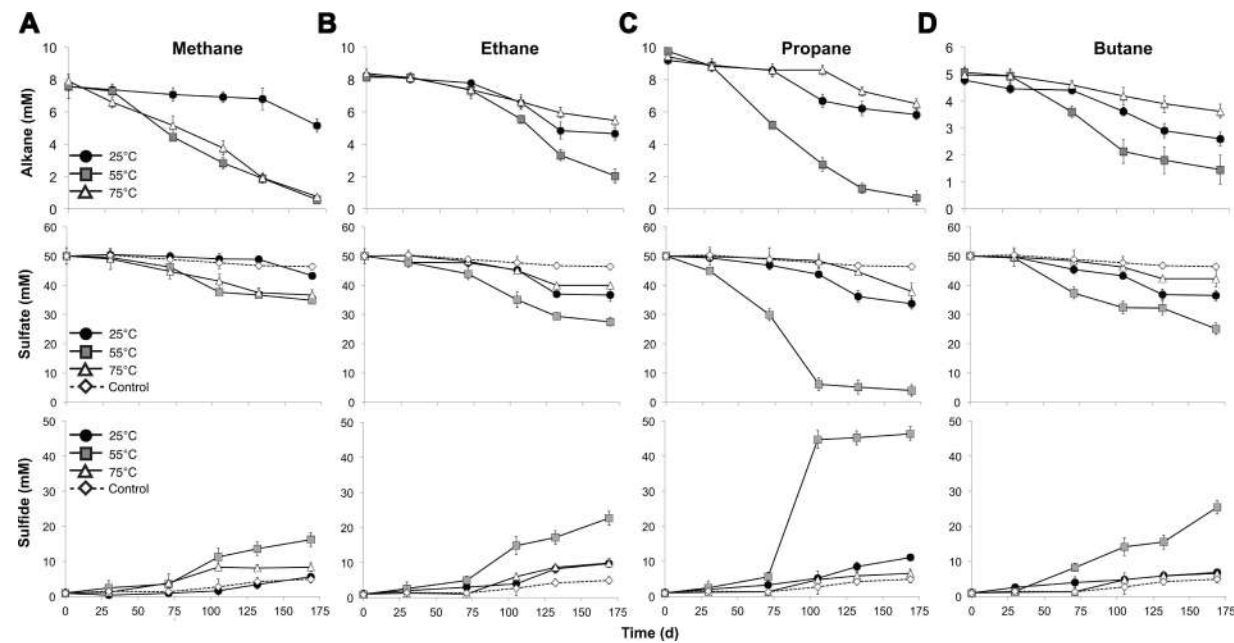


**FIGURE 1 |** Time course of the anaerobic oxidation of short-chain alkanes (top), consumption of sulfate (middle), and production of sulfide (bottom) in anaerobic batch reactors of Middle Valley hydrothermal sediments incubated with methane (A), ethane (B), propane (C), and butane (D) at three discrete temperatures (25, 55, and 75°C). Each time

point represents the average of duplicate reactors with bars indicating the data range. For sulfate and sulfide measurements, the control in each panel represents the average sulfate consumption and sulfide production in the batch reactors with nitrogen for each incubation temperature as described in the text.

25°C, respectively, and 35, 31, and 27% of C<sub>2</sub>, C<sub>3</sub>, and C<sub>4</sub> at 75°C, respectively).

Absolute rate measurements of the batch reactor sediments revealed that maximum C<sub>1</sub>–C<sub>4</sub> oxidation occurred at 55°C (~42, 36, 54, and 23 nmol cm<sup>-3</sup> day<sup>-1</sup> for C<sub>1</sub>, C<sub>2</sub>, C<sub>3</sub>, and C<sub>4</sub>, respectively, *n* = 2; Table 1). Substantially lower rates of the anaerobic oxidation of C<sub>2</sub>–C<sub>4</sub> were observed in all 25 and 75°C batch reactors (~21, 16, and 8 nmol cm<sup>-3</sup> day<sup>-1</sup> for C<sub>2</sub>, C<sub>3</sub>, and C<sub>4</sub> at 25°C, respectively, *n* = 2, and ~17, 17, and 8 nmol cm<sup>-3</sup> day<sup>-1</sup> for C<sub>2</sub>, C<sub>3</sub>, and C<sub>4</sub> at 75°C, respectively, *n* = 2). In contrast to the other short-chain alkanes, maximal rates of AOM were also observed at 75°C (~42 nmol cm<sup>-3</sup> day<sup>-1</sup>, *n* = 2), while rates decreased to less than half of these AOM maxima at 25°C (14 nmol cm<sup>-3</sup> day<sup>-1</sup>, *n* = 2).

#### SULFATE REDUCTION COUPLED TO C<sub>1</sub>–C<sub>4</sub> ALKANE OXIDATION ACROSS TEMPERATURE REGIMES

In addition to a dependence on short-chain alkane length, temperature constrained SR in the anaerobic batch reactors, influencing quantified changes in porewater sulfate and total sulfide. Decreases in sulfate concentration were observed in all batch reactors across time and temperature regimes, consistent with trends for the anaerobic oxidation of C<sub>1</sub>–C<sub>4</sub> alkanes. Analogous to alkane consumption dynamics, sulfate consumption was appreciable (defined as >10% substrate consumption) after 71 days of incubation in C<sub>1</sub>–C<sub>4</sub> batch reactors at 55°C (Figure 1, middle). In contrast, there was a lag of ~105 days in C<sub>2</sub>, C<sub>3</sub>, and C<sub>4</sub> batch reactors prior to substantial sulfate consumption at both the lowest (25°C) and highest (75°C) incubation temperature. Over the span

**Table 1 |** Volume-specific rate measurements of the anaerobic oxidation of methane, ethane, propane, and butane and sulfate reduction in batch reactors incubated at 25, 55, and 75°C.

|                | Anaerobic oxidation<br>nmol cm <sup>-3</sup> day <sup>-1</sup> | Sulfate reduction<br>nmol cm <sup>-3</sup> day <sup>-1</sup> |
|----------------|--|--|
| Methane – 25°C | 14.33 ± 2.88   | 15.01 ± 2.31   |
| Methane – 55°C | 41.45 ± 1.17   | 55.83 ± 4.91   |
| Methane – 75°C | 42.22 ± 1.91   | 68.03 ± 5.01   |
| Ethane – 25°C  | 21.39 ± 4.77   | 53.61 ± 6.53   |
| Ethane – 55°C  | 36.03 ± 4.46   | 99.30 ± 8.48   |
| Ethane – 75°C  | 17.22 ± 3.59   | 47.94 ± 3.65   |
| Propane – 25°C | 19.93 ± 2.81   | 71.96 ± 7.25   |
| Propane – 55°C | 53.66 ± 2.52   | 238.36 ± 10.77   |
| Propane – 75°C | 17.26 ± 1.26   | 60.37 ± 6.18   |
| Butane – 25°C  | 12.84 ± 2.81   | 55.27 ± 8.68   |
| Butane – 55°C  | 23.07 ± 5.13   | 113.46 ± 15.37   |
| Butane – 75°C  | 8.01 ± 1.13  | 34.22 ± 2.39   |

Rates were determined from the consumption of alkanes and sulfate over the incubation time course. Each point represents the average of duplicate reactors with the standard error. To account for background sulfate reduction (due to autochthonous carbon, etc.), the rates measured in the alkane treatments have been corrected via subtraction of those measured in the control (nitrogen) batch reactors.

of the incubation time series (169 days), the greatest reduction in sulfate concentration was at 55°C (~30, 45, 92, and 49% of total sulfate consumed in the C<sub>1</sub>, C<sub>2</sub>, C<sub>3</sub>, and C<sub>4</sub> reactors, respectively). Sulfate consumption was also observed in the N<sub>2</sub>-control batch reactors, albeit to a much smaller extent (~8, 11, and 2% at 25, 55, and 75°C, respectively). SR was also assessed by quantifying the production of gaseous and dissolved sulfide in the batch incubations (**Figure 1**, bottom). In all reactors, sulfide concentrations at the end of each incubation time period accounted for greater than 90% of the initial total sulfate plus sulfide concentration; therefore, these mass balance estimates were within 10% of the total sulfur species observed initially.

Concomitant with the anaerobic oxidation of C<sub>2</sub>–C<sub>4</sub> rates, maximum SR rates were observed at 55°C for the non-methane short-chain alkanes (~99, 238, and 113 nmol cm<sup>-3</sup> day<sup>-1</sup> for C<sub>2</sub>, C<sub>3</sub>, and C<sub>4</sub>, respectively, *n* = 2) (**Table 1**). However, maximum SR rates associated with AOM occurred at 75°C (~68 nmol cm<sup>-3</sup> day<sup>-1</sup>), with lower rates at 55°C (~55 nmol cm<sup>-3</sup> day<sup>-1</sup>, *n* = 2) and even more modest rates at 25°C (~15 nmol cm<sup>-3</sup> day<sup>-1</sup>, *n* = 2). In comparison to maximal SR rates at 55°C, SR rates linked to C<sub>2</sub>–C<sub>4</sub> oxidation were lower at both 25 and 75°C (~54, 72, and 55 nmol cm<sup>-3</sup> day<sup>-1</sup> for C<sub>2</sub>, C<sub>3</sub>, and C<sub>4</sub> at 25°C, respectively, *n* = 2, and ~48, 60, and 34 nmol cm<sup>-3</sup> day<sup>-1</sup> for C<sub>2</sub>, C<sub>3</sub>, and C<sub>4</sub> at 75°C, respectively, *n* = 2).

The observed ratio (mol/mol) of C<sub>1</sub>–C<sub>4</sub> oxidation to SR in the batch reactors was then compared to the predicted stoichiometric ratio assuming the sulfate-dependent complete oxidation of C<sub>1</sub>–C<sub>4</sub> alkanes to CO<sub>2</sub> (from Kniemeyer et al., 2007). These ratios are corrected for the consumption of sulfate in the control (N<sub>2</sub>) batch reactors as an estimate for SR linked to non-alkane organic carbon donors present in the sediment. The ratio of mol alkane consumed per mol sulfate reduced was 1.42, 1.11, and 0.93 mmol of C<sub>1</sub> mmol<sup>-1</sup> sulfate; 0.59, 0.54, and 0.54 mmol of C<sub>2</sub> mmol<sup>-1</sup> sulfate; 0.42, 0.34, and 0.43 mmol of C<sub>3</sub> mmol<sup>-1</sup> sulfate; and 0.35, 0.31, and 0.35 mmol of C<sub>4</sub> mmol<sup>-1</sup> sulfate at 25, 55, and 75°C, respectively (**Table 2**). These ratios closely mirror the predicted stoichiometric ratios of 1, 0.5, 0.4, and 0.3 for C<sub>1</sub>–C<sub>4</sub>, respectively.

## PHYLOGENETIC DIVERSITY AND DISTRIBUTION IN SEDIMENTS FROM BATCH C<sub>1</sub>–C<sub>4</sub> REACTORS

After sequence processing and denoising as previously described, a total of 5783, 6562, 5307, 6985, and 8796 bacterial sequences were analyzed from sediments incubated with N<sub>2</sub>, C<sub>1</sub>, C<sub>2</sub>, C<sub>3</sub>, and C<sub>4</sub> alkane, respectively, and 7965 bacterial sequences from the T<sub>0</sub> sediment. There were substantial shifts at the phyla level between the communities incubated with different alkane substrates in comparison to the control batch reactor and T<sub>0</sub> sediment community (**Figure 2**). From the initial sediment community, sequences allied to the *Bacteroidetes* and *Fusobacteria* decreased from ~9 and 40% of T<sub>0</sub> sequences respectively, to less than 0.5% of sequences in all batch reactor libraries. In turn, sequences allied to the *Proteobacteria*, *Firmicutes*, Candidate Division OP8, *Chloroflexi*, and *Actinobacteria* increased in batch reactor libraries compared to T<sub>0</sub> sequences. Notably, the *Proteobacteria*, which comprised ~36% of T<sub>0</sub> sequences, increased in representation in the N<sub>2</sub>, C<sub>1</sub>, C<sub>2</sub>, and

**Table 2 | The predicted and calculated stoichiometric ratios for the anaerobic oxidation of methane, ethane, propane, and butane coupled to the reduction of sulfate to sulfide.**

|                | Stoichiometric Ratio (mol/mol) | Observed Ratio (mol/mol) |
|----------------|--------------------------------|--------------------------|
| Methane – 25°C | 1                              | 1.42                     |
| Methane – 55°C | 1                              | 1.11                     |
| Methane – 75°C | 1                              | 0.93                     |
| Ethane – 25°C  | 0.5                            | 0.59                     |
| Ethane – 55°C  | 0.5                            | 0.54                     |
| Ethane – 75°C  | 0.5                            | 0.54                     |
| Propane – 25°C | 0.4                            | 0.42                     |
| Propane – 55°C | 0.4                            | 0.34                     |
| Propane – 75°C | 0.4                            | 0.43                     |
| Butane – 25°C  | 0.31                           | 0.35                     |
| Butane – 55°C  | 0.31                           | 0.31                     |
| Butane – 75°C  | 0.31                           | 0.35                     |

From closed system batch reactors, the mol alkane lost was calculated per mol sulfate reduced at 25, 55, and 75°C, respectively. To account for background sulfate reduction (due to autochthonous carbon, etc.), ratios have been corrected via subtraction of those measured in the control (nitrogen) batch reactors.

C<sub>3</sub> sequence libraries (~49, 58, 41, and 46%, respectively). The *Firmicutes* also increased substantially from the T<sub>0</sub> composition (~4%) in N<sub>2</sub>, C<sub>1</sub>, C<sub>2</sub>, and C<sub>4</sub> sequences (~11, 12, 12, and 59%, respectively).

Among the *Proteobacterial* sequences allied to known sulfate-reducing *Deltaproteobacteria*, there was a substantial increase from T<sub>0</sub> sequences (~15%) in the N<sub>2</sub>, C<sub>1</sub>, C<sub>2</sub>, C<sub>3</sub>, and C<sub>4</sub> sequence libraries (~39, 87, 70, 88, and 86%, respectively). Concurrently, there was a substantial decrease in the representation of *Epsilonproteobacteria* in the N<sub>2</sub>, C<sub>1</sub>, C<sub>2</sub>, C<sub>3</sub>, and C<sub>4</sub> sequence libraries (~39, 3, 17, 7, and 9%, respectively). Within the putative sulfate-reducing phylotypes, the C<sub>1</sub> library was comprised primarily (>92%) of sequences allied to *Desulfobulbus*, as shown in a previous study of MV sediment communities associated with AOM (Wankel et al., 2012). Analysis of 16S rRNA gene libraries revealed that a distinct lineage of SRB are the predominant *Deltaproteobacterial* phylotypes in the C<sub>2</sub>–C<sub>4</sub> reactor communities, comprising ~93, 91, and 95% of C<sub>2</sub>, C<sub>3</sub>, and C<sub>4</sub> sequences, respectively (**Figure 4**). The most closely related phylotypes (93–99% nucleotide sequence identity) were previously recovered in two 16S rRNA-based surveys of sulfate-reducing anaerobic enrichments of Guaymas Basin sediments with C<sub>4</sub> at 60°C (Butane60-GuB, accession no. EF077228) and with C<sub>1</sub> at 37°C (Guaymas\_Bac9 clone, accession no. FR682643; Kniemeyer et al., 2007; Kellermann et al., 2012).

A total of 1290, 1724, 1540, 1916, 1780, and 2846 Eurarchaeotal sequences were further analyzed from the N<sub>2</sub>, C<sub>1</sub>, C<sub>2</sub>, C<sub>3</sub>, and C<sub>4</sub> batch reactors and T<sub>0</sub> sediments, respectively (**Figure 3**). There were notable shifts in the sequences allied to

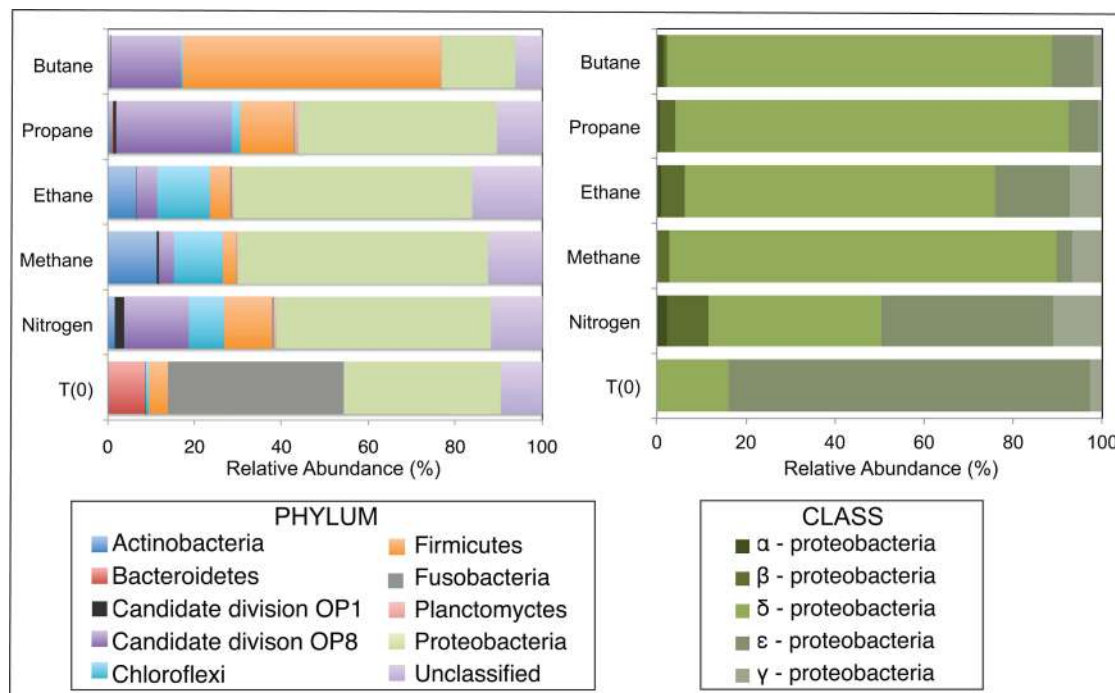


**FIGURE 2 |** Relative abundance (percentage) of bacteria determined from massively parallel sequencing of DNA recovered from anaerobic batch reactor sediments incubated with methane, ethane, propane, butane, and nitrogen at 55°C and pre-incubation (T<sub>0</sub>) sediments. Left and right

side panels show the taxonomic breakdown of sequences at the phylum and class level, respectively. Legend indicates operational taxonomic units (OTUs), defined as sequences sharing 97% nucleotide sequence identity.

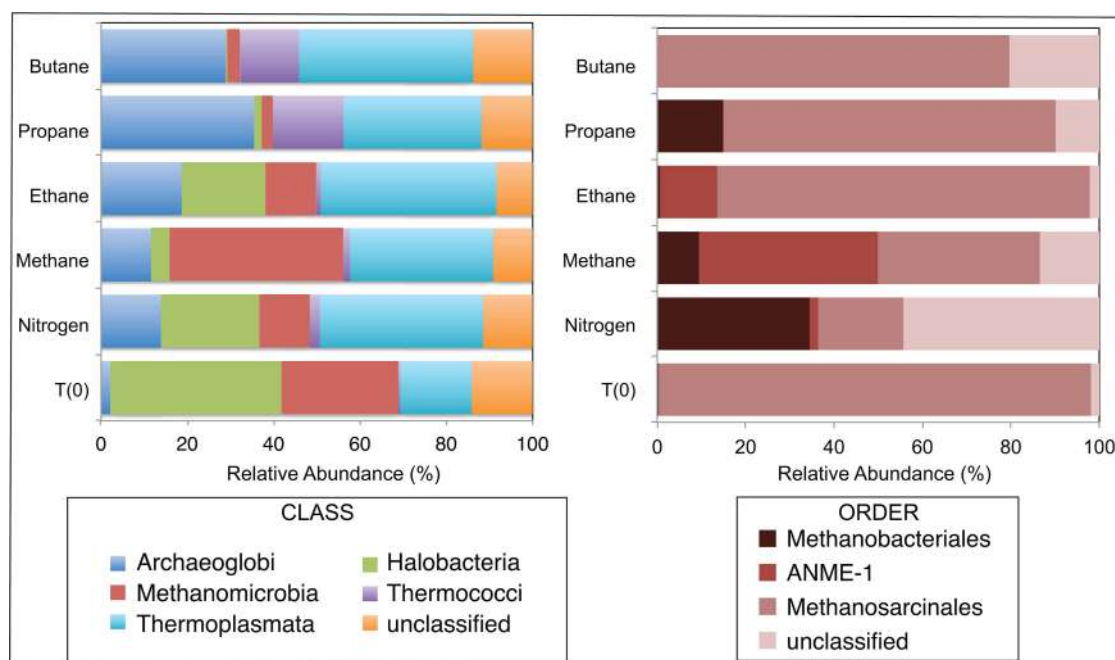


**FIGURE 3 |** Relative abundance (percentage) of archaea determined from massively parallel sequencing of DNA recovered from anaerobic batch reactor sediments incubated with methane, ethane, propane, butane, and nitrogen at 55°C and pre-incubation (T<sub>0</sub>) sediments.

Left and right side panels show the taxonomic breakdown of sequences at the class and order level, respectively. Legend indicates operational taxonomic units (OTUs), defined as sequences sharing 97% nucleotide sequence identity.

the predominant Euryarchaeotal phyla – *Archaeoglobi*, *Halobacteria*, *Methanomicrobia*, *Thermococci*, and *Thermoplasmata* – from the initial sediment community and across the different alkane batch incubations. Over 40% of sequences were allied to the *Halobacteria* in T<sub>0</sub> sediments, decreasing to comprise <0.5–29% of batch reactor sequences. In contrast, *Archaeoglobi* sequences increased from ~2% of T<sub>0</sub> sequences to ~14, 12, 19, 36, and 29% of N<sub>2</sub>, C<sub>1</sub>, C<sub>2</sub>, C<sub>3</sub>, and C<sub>4</sub> sequences, respectively. Other trends in Euryarchaeotal community structure included an increase in *Methanomicrobia* from 27% of T<sub>0</sub> sequences to 40% of C<sub>1</sub> sequences.

Within the *Methanomicrobia*, there were also substantial changes in sequences allied to known methanogens and methane-oxidizing phylotypes. *Methanoscincales* comprised >97% of T<sub>0</sub> sequences and ~19, 36, 84, 75, and 80% of N<sub>2</sub>, C<sub>1</sub>, C<sub>2</sub>, C<sub>3</sub>, and C<sub>4</sub> sequences, respectively. In contrast, *Methanobacteriales* increased from <0.5% of T<sub>0</sub> sequences to ~35, 9, and 26% of N<sub>2</sub>, C<sub>1</sub>, and C<sub>3</sub> sequences (there was no substantial increase in C<sub>2</sub> or C<sub>4</sub> sequences). For the putative methane-oxidizing communities, over 40 and 12% of C<sub>1</sub> and C<sub>2</sub> sequences were allied to ANME-1 ribotypes.

## DISCUSSION

The microbial degradation of short-chain alkanes under oxic conditions and the anaerobic oxidation of methane and other heavier hydrocarbons have been extensively studied in diverse terrestrial and marine environments. Despite studies indicating short-chain alkane degradation in anoxic deep sea sediments (Sassen et al., 2004; Mastalerz et al., 2009; Quistad and Valentine, 2011) and the abundance of short-chain alkanes in hydrocarbon-rich ecosystems (Milkov, 2005; Cruse and Seewald, 2006), relatively little is known about the biogeochemical importance of these processes or the diversity of anaerobic short-chain alkane degrading microorganisms in marine hydrothermal sediments. The data here provide a deeper glimpse into the anaerobic oxidation of C<sub>2</sub>–C<sub>4</sub> in metalliferous hydrothermal sediments and reveal that rates of the anaerobic oxidation of C<sub>2</sub>–C<sub>4</sub> alkanes in hydrothermal vent sediment are heavily influenced by temperature and coupled to SR, though the rates presented herein are derived from conditions not likely to be present *in situ*, and as such care should be taken when extrapolating these rates to natural processes. In batch reactor sediments that exhibited the most substantial activity, changes in the representation of phylotypes in libraries generated via high throughput sequencing implicate *Deltaproteobacteria* in C<sub>2</sub>–C<sub>4</sub> alkane degradation, and shifts in microbial community composition indicate that other members of the community respond to the presence of short-chain alkanes (though the mechanisms underlying this response remain unknown).

These data revealed a preferential consumption of C<sub>2</sub>–C<sub>4</sub> at 55°C, suggesting that the active alkane degraders in these hydrothermal vent sediments are thermophilic. Furthermore, these *ex situ* calculated rates for the anaerobic oxidation of C<sub>2</sub>–C<sub>4</sub> were in the same range (nmolcm<sup>-3</sup>day<sup>-1</sup>) as the recently reported anaerobic oxidation of C<sub>3</sub> in marine hydrocarbon seep sediments and as AOM rates measured in organic-rich coastal sediments at the sulfate-methane transition zone (Alperin et al., 1988; Hoehler et al., 1994; Girguis et al., 2003; Wegener et al., 2008;

Quistad and Valentine, 2011). Based on lag time and total alkane degraded over time, C<sub>3</sub> appeared to be the preferred substrate in the 55°C incubations, followed by C<sub>1</sub>, C<sub>4</sub>, and C<sub>2</sub>, respectively. Similar trends in the biodegradation of short-chain alkanes have been found in stable isotopic studies of hydrocarbon reservoirs at temperatures below 60°C with a preference for C<sub>3</sub> followed by C<sub>4</sub> and then C<sub>2</sub> (Boreham et al., 2001; Wenger et al., 2002; Larter et al., 2005).

Various physicochemical and biotic parameters may impact the degree of C<sub>2</sub>–C<sub>4</sub> consumption in *ex situ* studies and in the natural environment. Notably, the gaseous alkanes were maintained at above saturation conditions for the liquid phase of the batch incubations until the end of the time series to ensure substrate availability (dissolved concentrations of ~1.42, 1.89, 0.91, and 1.05 mM for C<sub>1</sub>, C<sub>2</sub>, C<sub>3</sub>, and C<sub>4</sub>, respectively). Under elevated hydrostatic pressure in the deep sea, hydrothermal vent fluids at MV reach C<sub>1</sub> concentrations of ~20 mM, while the other short-chain alkanes are an order of magnitude lower (~220, 55, and 6 μM for C<sub>2</sub>, C<sub>3</sub>, and C<sub>4</sub>, respectively; Cruse and Seewald, 2006). Although C<sub>1</sub> is most likely more abundant than C<sub>3</sub> in MV hydrothermal sediments, the *in situ* rates of C<sub>3</sub> degradation may be appreciable due to the inherent reactivity of secondary C–H bonds (Schink and Friedrich, 1994; Rabus et al., 2001; Van Hamme et al., 2003).

Our results also suggest that, at the highest incubation temperatures, AOM in MV sediments occurs at higher rates than the anaerobic oxidation of C<sub>2</sub>–C<sub>4</sub> alkanes. In the higher temperature (75°C) incubations, C<sub>1</sub> consumption was evident after 30 days and reached near deplete concentrations (90% substrate consumed), while there was a much longer lag period until C<sub>2</sub>–C<sub>4</sub> degradation (105 days) and much less of the substrates were consumed by the completion of the time series (27–35%; Figure 1, top). In contrast, a greater proportion of C<sub>2</sub> and C<sub>4</sub> (44 and 46%, respectively) were consumed than C<sub>1</sub> and C<sub>3</sub> (32 and 37%, respectively) in the lower temperature incubations (25°C). The increased AOM activity at the higher end of the temperature range in MV sediments is consistent with our previous observations of AOM in these metalliferous sediments (Wankel et al., 2012), and is also consistent with the growth temperatures of archaeal communities (such as ANME phylotypes) from hydrothermal vents, which indicate that many archaea live at their maximum growth temperature *in situ* (Kimura et al., 2013). Another line of evidence for thermophilic AOM was also provided in a recent 16S rRNA based-study identifying a putatively high temperature-adapted ANME subgroup in both hydrothermal sediments from Guaymas Basin and diffuse vent fluids from Axial Volcano and the Endeavor Segment of Juan de Fuca Ridge (Merkel et al., 2013).

Notably, the anaerobic oxidation of C<sub>1</sub>–C<sub>4</sub> was coupled to SR across temperature gradients in MV sediment batch reactors. Sulfate loss (~2–6 mM) was also observed over the time series in alkane-free control batch reactors (Figure 1, middle). In comparison to SR linked to the oxidation of short-chain alkanes, this modest sulfate consumption relates to the oxidation of endogenous substrates, particularly organic carbon, by the sediment communities (Gieg et al., 1999). The sediment organic carbon pool of MV sediments (% OC = ~0.5

in this study) is low in comparison to the high amounts of organic matter that characterize other deep sea environments with known short-chain alkane degraders, such as the organic-rich Guaymas Basin hydrothermal sediments (Jorgensen et al., 1992; Kniemeyer et al., 2007). The observed SR rates in C<sub>1</sub>–C<sub>4</sub> batch reactors of MV sediments demonstrate the potential for organic carbon-poor, high temperature mid-ocean ridge systems to support the anaerobic oxidation of short-chain alkanes coupled to SR.

Our results further indicate that short-chain alkane degradation linked to SR might considerably influence sulfate cycling at these sedimented hydrothermal vents. In accordance with the observed stoichiometries, SR coupled to the anaerobic oxidation of C<sub>2</sub>, C<sub>3</sub>, and C<sub>4</sub> proceeded at a faster rate than AOM at mesophilic and thermophilic temperatures (25 and 55°C, respectively). However, the SR rates in anaerobic batch reactors were observed under sulfate-replete conditions, while the sulfate pool *in situ* depends on the downward advection of seawater and the activity of sulfide-oxidizing microbial communities (Bowles et al., 2011). Sulfate availability will become limiting at greater sediment depths from the seawater surface. Therefore, the C<sub>2</sub>, C<sub>3</sub>, and C<sub>4</sub>-degrading, sulfate-reducing microbial communities likely compete for available sulfate and might indirectly limit AOM in the temperature range from ~25–55°C. As previously discussed, the anaerobic oxidation of these aliphatic hydrocarbons coupled to the reduction of sulfate to sulfide yields greater energy per unit substrate than AOM. Such processes could constrain methane release from the deep-sea with a critical impact on the global carbon cycle and climate. Furthermore, if AOM activity peaks at greater sediment depths and higher temperatures *in situ* as predicted by rate measurements, then sulfate will most likely have been depleted in these sediment horizons. Sulfate limitation may thus result in the coupling of AOM to alternative electron acceptors (i.e., iron oxides), as indicated in previous studies of MV high temperature sediment incubations (Wankel et al., 2012).

Comparison of bacterial communities in batch reactor sediments with maximum rates of C<sub>1</sub>–C<sub>4</sub> degradation, via massively parallel pyrosequencing, suggests that members of the sulfate-reducing *Deltaproteobacteria* mediate the anaerobic oxidation of short-chain alkanes in MV hydrothermal vent sediments (Figure 2). As these sequence data are based on PCR amplification of 16S rRNA genes and are semi-quantitative, an order of magnitude difference in phyla should represent shifts in community composition. Within the *Proteobacteria*, there was a substantial increase of *Deltaproteobacteria* in C<sub>1</sub>–C<sub>4</sub> sequences compared to the initial T<sub>0</sub> bacterial composition dominated by *Epsilonproteobacteria*. Phylogenetic analyses revealed a novel subgroup of SRB that comprised >90% of these *Deltaproteobacteria* in C<sub>2</sub>–C<sub>4</sub> batch reactor sequences (Figure 4). This lineage of *Deltaproteobacteria* is most closely related to C<sub>4</sub>-degrading SRB from Guaymas Basin, and therefore, may be a thermophilic short-chain alkane degrader group (Kniemeyer et al., 2007). Intriguingly, the predominant phylum in C<sub>4</sub> batch reactor sequences is the *Firmicutes*, which contains sulfate-reducing members of previous enrichments with C<sub>3</sub> and C<sub>4</sub> (Kniemeyer et al., 2007; Savage et al., 2010). However, the majority of *Firmicutes* sequences were most closely

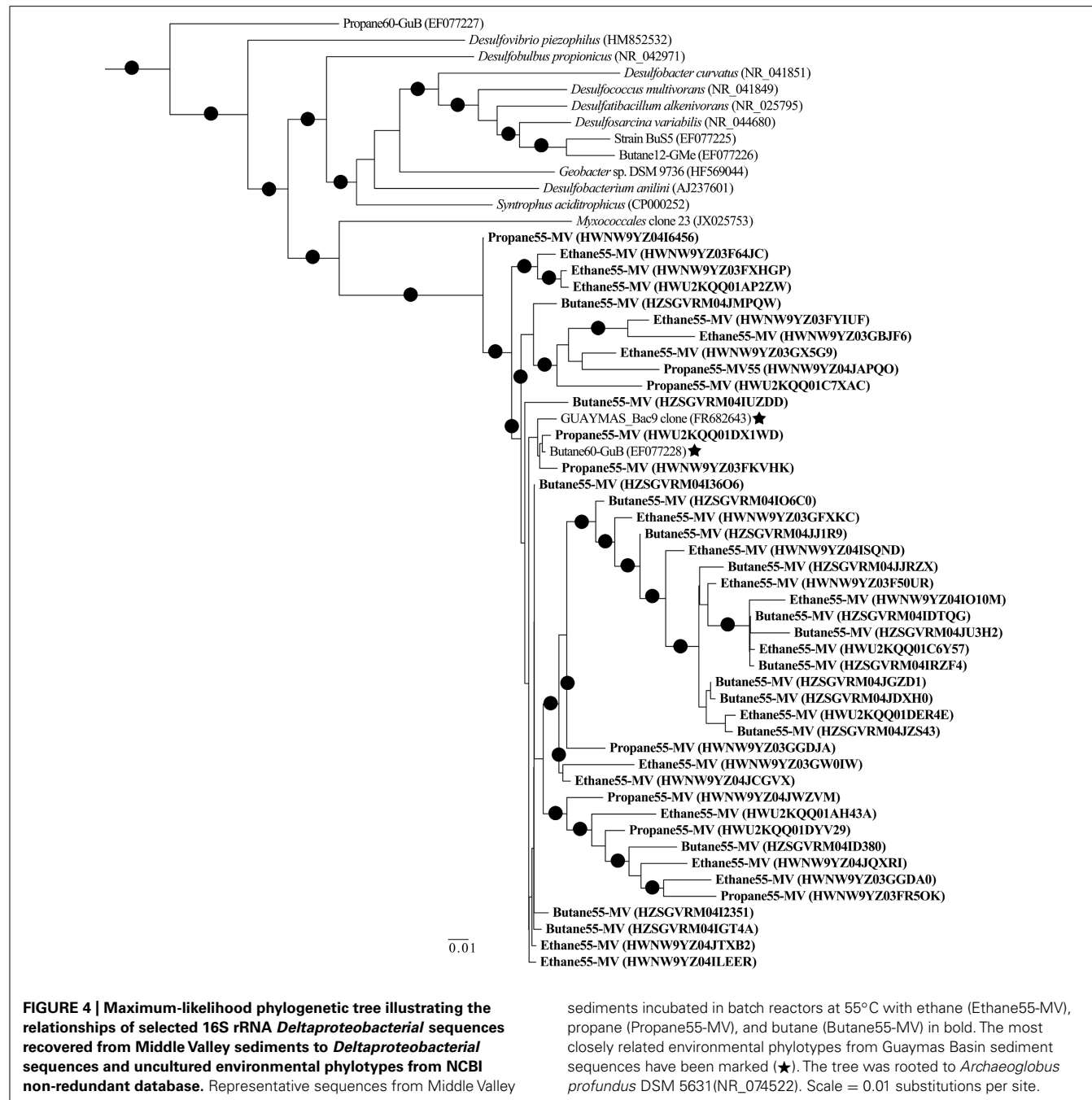
related (98–99%) to uncultured *Bacillus* clones from hydrocarbon-contaminated soils (Wang et al., 2011). The greater proportion of this uncharacterized *Bacillus* group in comparison to SRB may have also affected the lower rates of the anaerobic oxidation of C<sub>4</sub> in comparison to C<sub>2</sub> or C<sub>3</sub> in batch incubations. Future studies should determine if this putative thermophilic short-chain alkane degrader group of SRB is widespread in other hydrothermally influenced environments.

Amongst the batch reactor sediment communities, shifts in archaeal phylogenetic composition were also revealed via 16S rRNA pyrosequencing. There was a substantial increase of *Methanomicrobia* sequences in C<sub>1</sub>-incubated sediments compared to the initial community and C<sub>2</sub>–C<sub>4</sub> batch reactor sediments, with an order of magnitude enrichment of ANME-1 phylotypes within the *Methanomicrobia* (Figure 3). The microbes known to catalyze AOM form three phylogenetically distinct Euryarchaeota clusters (ANME-1, ANME-2, and ANME-3) that often appear to live in consortia with SRB (Hoehler et al., 1994; Boetius et al., 2000; Orphan et al., 2001). However, ANME-1 phylotypes are also found as single cells in sediments, and recent studies have shown that AOM can occur in the absence of SR and that some ANME are not directly dependent on SRB activity (Beal et al., 2009; Milucka et al., 2012; Wankel et al., 2012). There was also a notable increase in *Archaeoglobus* sequences in C<sub>1</sub> – C<sub>4</sub> batch reactors from the initial community composition (Figure 3), which contain hyperthermophilic species known to mediate SR (Shen and Buick, 2004). Based on microbial isolates and enrichments from both deep sea and terrestrial ecosystems, no evidence to date indicates that non-methane short-chain alkanes are anaerobically oxidized by microbial consortia or sulfate-reducing archaea (Kniemeyer et al., 2007; Savage et al., 2010; Jaekel et al., 2012). The data presented herein lack the resolution to conclusively address whether archaeal phylotypes directly mediate or are members of consortia that perform the anaerobic oxidation of short-chain alkanes other than AOM.

The collective results presented here shed light on the potential anaerobic metabolism of short-chain alkanes linked to SR in the hydrothermal vent sediments of MV, Juan de Fuca Ridge. Substantial oxidation of C<sub>1</sub>–C<sub>4</sub> occurs up to 75°C. The coupling of C<sub>2</sub>–C<sub>4</sub> with SR over the *in situ* temperature range may impact AOM and the oxidation of other hydrocarbons, as highlighted by the preferential degradation of C<sub>3</sub> at 55°C. Such microbial communities may play a substantial role in carbon and sulfur cycling at hydrothermal systems on a global-scale. Future studies should expand upon other environmental conditions that may regulate the anaerobic oxidation of C<sub>2</sub>–C<sub>4</sub> alkanes in hydrothermal sediments and should further characterize the *in situ* abundance and activity of the putative thermophilic alkane-degrader SRB lineage.

## CONTRIBUTIONS

Melissa M. Adams, Peter R. Girguis, and Arpita Bose designed the research. Melissa M. Adams, Peter R. Girguis, and Adrienne L. Hoarfrost directed the *in situ* collections and measurements. Melissa M. Adams, Adrienne L. Hoarfrost, and Arpita Bose conducted the batch reactor incubations and geochemical analyses. Samantha B. Joye performed the sulfate consumption measurements. Melissa M. Adams directed and analyzed the



alkane consumption, sulfide production, and all rate calculations. Melissa M. Adams performed the molecular analyses. Melissa M. Adams and Peter R. Girguis wrote the manuscript with input from Samantha B. Joye, Arpita Bose, and Adrienne L. Hoar frost.

## ACKNOWLEDGMENTS

We acknowledge the expert assistance of the R/V *Atlantis* crews and the pilots and team of the DSV *Alvin* for enabling both the collection of temperature data and sediments used in our experiments. We thank Jennifer Delaney, Kimberly Hunter, Johanna Schweers, Ryan Sibert, and Charles Vidoudez for providing assistance with

various aspects of the experiments, sample processing, and/or data interpretation. We also thank David Johnston and Andrew Knoll for constructive input during the preparation of this manuscript. This project was supported by grants from the National Science Foundation (NSF MCB 0702504 to Peter R. Girguis), the National Aeronautics and Space Administration (NASA ASTEP grant 0910169 to C. Scholin and Peter R. Girguis), NASA ASTEP grant NNX07AV51G to A. Knoll and Peter R. Girguis, the Advanced Research Projects Agency – Energy (ARPA-E), U.S. Department of Energy (DoE) (DE-AR 0000079 to Peter R. Girguis), and NSF MCB 0702080 to Samantha B. Joye.

## REFERENCES

- Acosta-Martínez, V., Dowd, S. E., Bell, C. W., Lascano, R., Booker, J. D., Zobeck, T. M., et al. (2010). Microbial community composition as affected by dryland cropping systems and tillage in a semiarid sandy soil. *Diversity* 2, 910–931.
- Alperin, M. J., Reeburgh, W. S., and Whiticar, M. J. (1988). Carbon and hydrogen isotope fractionation resulting from anaerobic methane oxidation. *Global Biogeochem. Cycles* 2, 279–288.
- Ames, D. E., Franklin, J. M., and Hannington, M. H. (1993). Mineralogy and geochemistry of active and inactive chimneys and massive sulfide, Middle Valley, northern Juan de Fuca Ridge: an evolving hydrothermal system. *Can. Mineral.* 31, 997–1024.
- Barns, S. M., Fundyga, R. E., Jeffries, M. W., and Pace, N. R. (1994). Remarkable archaeal diversity detected in a Yellowstone National Park hot spring environment. *Proc. Natl. Acad. Sci. U.S.A.* 91, 1609–1613.
- Beal, E. J., House, C. H., and Orphan, V. J. (2009). Manganese- and iron-dependent marine methane oxidation. *Science* 325, 184–187.
- Boetius, A., Ravenschlag, K., Schubert, C. J., Rickert, D., Widdel, F., Gieseke, A., et al. (2000). A marine microbial consortium apparently mediating anaerobic oxidation of methane. *Nature* 407, 623–626.
- Boreham, C. J., Hope, J. M., and Hartung-Kagi, B. (2001). Understanding source, distribution and preservation of Australian natural gas: a geochemical perspective. *Aust. Prod. Pet. Explor. Assoc. J.* 41, 523–547.
- Bowles, M. W., Samarkin, A., Bowles, K. M., and Joye, S. B. (2011). Weak coupling between sulfate reduction and the anaerobic oxidation of methane in methane-rich seafloor sediments during ex situ incubation. *Geochim. Cosmochim. Acta* 75, 500–519.
- Butterfield, D. A., Massoth, G. J., McDuff, R. E., Lupton, J. E., and Lilley, M. D. (1990). Geochemistry of hydrothermal fluids from Axial Seamount hydrothermal emissions study vent field, Juan-de-Fuca Ridge – Subseafloor boiling and subsequent fluid-rock interaction. *J. Geophys. Res. Solid Earth* 95, 12895–12921.
- Butterfield, D. A., McDuff, R. E., Motz, J., Lilley, M. D., Lupton, J. E., and Massoth, G. J. (1994). Gradients in the composition of hydrothermal fluids from the Endeavour segment vent field: phase separation and brine loss. *J. Geophys. Res.* 99, 9561–9583.
- Cline, J. D. (1969). Spectrophotometric determination of hydrogen sulfide in natural waters. *Limnol. Oceanogr.* 14, 454–458.
- Cruse, A. M., and Seewald, J. S. (2006). Geochemistry of low-molecular weight hydrocarbons in hydrothermal fluids from Middle Valley, northern Juan de Fuca Ridge. *Geochim. Cosmochim. Acta* 70, 2073–2092.
- Cruse, A. M., Seewald, J. S., Saccoccia, P. J., and Zierenberg, R. A. (2008). “Geochemistry of hydrothermal fluids from Middle Valley, northern Juan de Fuca Ridge: temporal variability, subsurface conditions and equilibration during upflow,” in *Magma to Microbe: Modeling Hydrothermal Processes at Oceanic Spreading Ridge*, eds R. Lowell and J. S. Seewald (Washington: AGU Monograph Series), 178, 145–166.
- Cruse, A. M., and Seewald, J. S. (2010). Low-molecular weight hydrocarbons in vent fluids from the Main Endeavour Field, northern Juan de Fuca Ridge. *Geochim. Cosmochim. Acta* 74, 6126–6140.
- Conrad, R. (2009). The global methane cycle: recent advances in understanding the microbial processes involved. *Environ. Microbiol. Rep.* 1, 285–292.
- Davis, E. E., and Fisher, A. T. (1994). “On the nature and consequences of hydrothermal circulation in the Middle Valley sedimented rift: inferences from geophysical and geochemical observations, Leg 139,” in *Proceedings of the Ocean Drilling Program Scientific Results*, Vol. 139, eds M. J. Mottl, E. E. Davis, A. T. Fisher, and J. F. Slack. (College Station: Ocean Drilling Program), 695–717.
- Dojka, M. A., Hugenholtz, P., Haack, S. K., and Pace, N. R. (1998). Microbial diversity in a hydrocarbon- and chlorinated-solvent-contaminated aquifer undergoing intrinsic bioremediation. *Appl. Environ. Microbiol.* 64, 3869–3877.
- Dowd, S. E., Callaway, T. R., Wolcott, R. D., Sun, Y., McKeehan, T., Hagevoort, R. G., et al. (2008). Evaluation of the bacterial diversity in the feces of cattle using 16S rDNA bacterial tag-encoded FLX amplicon pyrosequencing (bTEFAP). *BMC Microbiol.* 8:125. doi: 10.1186/1471-2180-8-125
- Elshahed, M. S., Najar, F. Z., Roe, B. A., Oren, A., Dewers, T. A., and Krumholz, L. R. (2004). Survey of archaeal diversity reveals an abundance of halophilic archaea in a low-salt, sulfide- and sulfur-rich spring. *Appl. Environ. Microbiol.* 70, 2230–2239.
- Formolo, M. J., Lyons, T. W., Zhang, C., Kelley, C., Sassen, R., Horita, J., et al. (2004). Quantifying carbon sources in the formation of authigenic carbonates at gas hydrate sites in the Gulf of Mexico. *Chem. Geol.* 205, 253–264.
- Gieg, L. M., Kolhatkar, R. V., McInerney, M. J., Tanner, R. S., Harris, S. H., Sublette, K. L., et al. (1999). Intrinsic bioremediation of petroleum hydrocarbons in a gas condensate-contaminated aquifer. *Environ. Sci. Technol.* 33, 2550–2560.
- Girguis, P. R., Orphan, V. J., Hallam, S. J., and DeLong, E. F. (2003). Growth and methane oxidation rates of anaerobic methanotrophic archaea in a continuous flow reactor bioreactor. *Appl. Environ. Microbiol.* 69, 5492–5502.
- Goodfellow, W. D., and Blaise, B. (1988). Sulfide formation and hydrothermal alteration of hemipelagic sediment in Middle Valley, northern Juan de Fuca Ridge. *Can. Mineral.* 26, 675–696.
- Hinrichs, K., Hayes, J., Bach, W., Spivack, A., Hmelo, L., Holm, N., et al. (2006). Biological formation of ethane and propane in the deep marine subsurface. *Proc. Natl. Acad. Sci. U.S.A.* 103, 14684–14689.
- Hoehler, T., Alperin, M., and Albert, D. (1994). Field and laboratory studies of methane oxidation in anoxic marine sediment: evidence for a methanogen-sulfate reducer consortium. *Global Biogeochem. Cycles* 8, 451–463.
- Merkel, A. Y., Huber, J. A., Chernyh, N. A., Bonch-Osmolovskaya, E. A., and Lebedinsky, A. V. (2013). Detection of putatively thermophilic anaerobic methanotrophs in diffuse hydrothermal vent fluids. *Appl. Environ. Microbiol.* 79, 915–923.
- Milucka, J., Ferdelman, T. G., Polerecky, L., Franzke, D., Wegener, G., Schmid, M., et al. (2012). Zero-valent sulphur is a key intermediate in marine methane oxidation. *Nature* 491, 541–546.
- Jaekel, U., Musat, N., Adam, B., Kuypers, M., Grundmann, O., and Musat, F. (2012). Anaerobic degradation of propane and butane by sulfate-reducing bacteria enriched from marine hydrocarbon cold seeps. *ISME J.* 1–11.
- Joye, S. B., Boetius, A., Orcutt, B., Montoya, J., Schulz, H., Erickson, M., et al. (2004). The anaerobic oxidation of methane and sulfate reduction in sediments from Gulf of Mexico cold seeps. *Chem. Geol.* 205, 219–238.
- Jorgensen, B. B., Isaksen, M. F., and Janasch, H. W. (1992). Bacterial sulfate reduction above 100°C in deepsea hydrothermal vent sediments. *Science* 258, 1756–1757.
- Kellermann, M. Y., Wegener, G., Elvert, M., Yoshinaga, M. Y., Lin, Y. S., Holler, T., et al. (2012). Autotrophy as a predominant mode of carbon fixation in anaerobic methane-oxidizing microbial communities. *Proc. Natl. Acad. Sci. U.S.A.* 109, 19321–19326.
- Kimura, H., Mori, K., Yamanaka, T., and Ishibashi, J. I. (2013). Growth temperatures of archaeal communities can be estimated from the guanine-plus-cytosine contents of 16S rRNA gene fragments. *Environ. Microbiol. Rep.* 5, 468–474.
- Kniemeyer, O., Musat, F., Sievert, S. M., Knittel, K., Wilkes, H., Blumenberg, M., et al. (2007). Anaerobic oxidation of short-chain hydrocarbons by marine sulphate-reducing bacteria. *Nature* 449, 898–901.
- Knittel, K., and Boetius, A. (2009). The anaerobic oxidation of methane – progress with an unknown process. *Annu. Rev. Microbiol.* 63, 311–334.
- Larter, S. R., Head, I. M., Huang, H., Bennett, B., Jones, M., Aplin, A. C., et al. (2005). Biodegradation, gas destruction and methane generation in deep subsurface petroleum reservoirs: an overview. *Q. J. Geol. Soc. Lond.* 6, 633–639.
- Lorenson, T. D., Kvenvolden, K. A., Hostettler, F. D., Rosenbauer, R. J., Orange, D. L., and Martin, J. B. (2002). Hydrocarbon geochemistry of cold seeps in the Monterey Bay National Marine Sanctuary. *Mar. Geol.* 181, 285–304.
- Mastalerz, V., de Lange, G. J., and Dahlmann, A. (2009). Differential aerobic and anaerobic oxidation of hydrocarbon gases discharged at mud volcanoes in the Nile deep-sea fan. *Geochim. Cosmochim. Acta* 73, 3849–3863.
- Milkov, A. V. (2005). Molecular and stable isotope compositions of natural gas hydrates: a revised global dataset and basic interpretations in the context of geological settings. *Org. Geochem.* 36, 681–702.
- Orphan, V., House, C., and Hinrichs, K. (2001). Methane-consuming archaea revealed by directly coupled isotopic and phylogenetic analysis. *Science* 293, 484–487.
- Price, M. N., Dehal, P. S., and Arkin, A. P. (2010). FastTree 2 – approximately maximum-likelihood trees for large alignments. *PLoS ONE* 5:e9490. doi: 10.1371/journal.pone.0009490
- Quince, C., Lanzén, A., Curtis, T. P., Davenport, R. J., Hall, N., Head, I. M., et al. (2009). Accurate determination of microbial diversity from 454 pyrosequencing data. *Nat. Methods* 6, 639–641.

- Quistad, S. D., and Valentine D. L. (2011). Anaerobic propane oxidation in marine hydrocarbon seep sediments. *Geochim. Cosmochim. Acta* 75, 2159–2169.
- Rabus, R., Wilkes, H., Behrends, A., and Armstroff, A. (2001). Anaerobic initial reaction of n-alkanes in a denitrifying bacterium: evidence for (1-methylpentyl)succinate as initial product and for involvement of an organic radical in n-hexane metabolism. *J. Bacteriol.* 183, 1707–1715.
- Rushd, A. I., and Simonelt, B. R. T. (2002). Hydrothermal alteration of organic matter in sediments of the Northeastern Pacific Ocean: Part 1. Middle Valley, Juan de Fuca Ridge. *Appl. Geochem.* 17, 1401–1428.
- Sassen, R., Roberts, H. H., Carney, R., Milkov, A. V., DeFreitas, D. A., Lanoil, B., et al. (2004). Free hydrocarbon gas, gas hydrate, and authigenic minerals in chemosynthetic communities of the northern Gulf of Mexico continental slope: relation to microbial processes. *Chem. Geol.* 205, 195–217.
- Savage, K. N., Krumholz, L. R., Gieg, L. M., Parisi, V. A., Sulfita, J. M., Allen, J., et al. (2010). Biodegradation of low-molecular-weight alkanes under mesophilic, sulfate-reducing conditions: metabolic intermediates and community patterns. *FEMS Microbiol. Ecol.* 72, 485–495.
- Schink, B., and Friedrich, M. (1994). Energetics of syntrophic fatty acid oxidation. *FEMS Microbiol. Rev.* 15, 85–94.
- Schlloss, P. D., Westcott, S. L., Ryabin, T., Hall, J. R., Hartmann, M., Hollister, E. B., et al. (2009). Introducing mothur: open-source, platform-independent, community-supported software for describing and comparing microbial communities. *Appl. Environ. Microbiol.* 75, 7537–7541.
- Shen, Y., and Buick, R. (2004). The antiquity of microbial sulfate reduction. *Earth Sci. Rev.* 64, 243–272.
- Valentine, D. L. (2011). Fates of methane in the Ocean. *Ann. Rev. Mar. Sci.* 3, 147–171.
- Van Hamme, J., Singh, A., and Ward, O. (2003). Recent advances in petroleum microbiology. *Microbiol. Mol. Biol. Rev.* 67, 503–509.
- Von Damm, K. L., Oosting, S. E., Kozlowski, R., Buttermore, L. G., Colodner, D. C., Edmonds, H. N., et al. (1995). Evolution of East Pacific Rise hydrothermal vent fluids following a volcanic eruption. *Nature* 375, 47–50.
- Wang, Z., Xu, Y., Zhao, J., Li, F., Gao, D., and Xing, B. (2011). Remediation of petroleum contaminated soils through composting and rhizosphere degradation. *J. Hazard. Mater.* 190, 677–685.
- Wankel, S. D., Adams, M. M., Johnston, D. T., Hansel, C. M., Joye, S. B., and Girguis, P. R. (2012). Anaerobic methane oxidation in metalliferous hydrothermal sediments: influence on carbon flux and decoupling from sulfate reduction. *Environ. Microbiol.* 14, 2762–2740.
- Wankel, S. D., Germanovich, L. N., Lilley, M. D., Genc, G., DiPerna, C. J., Bradley, A. S., et al. (2011). Influence of subsurface biosphere on geochemical fluxes from diffuse hydrothermal fluids. *Nat. Geosci.* 4, 461–468.
- Webster, G., Newberry, C. J., Fry, J. C., and Weightman, A. J. (2003). Assessment of bacterial community structure in the deep sub-seafloor biosphere by 16S rDNA-based techniques: a cautionary tale. *J. Microbiol. Methods* 55, 155–164.
- Wegener, G., Niemann, H., Elvert, M., Hinrichs, K. U., and Boetius, A. (2008). Assimilation of methane and inorganic carbon by microbial communities mediating the anaerobic oxidation of methane. *Environ. Microbiol.* 10, 2287–2298.
- Wenger, L. M., Davis, C. L., and Isaksen, G. H. (2002). Multiple controls on petroleum biodegradation and impact on oil quality. *Soc. Petrol. Eng. Reserv. Eval. Eng.* 5, 375–383.

**Conflict of Interest Statement:** The authors declare that the research was conducted in the absence of any commercial or financial relationships that could be construed as a potential conflict of interest.

Received: 15 February 2013; paper pending published: 26 March 2013; accepted: 17 April 2013; published online: 14 May 2013.

Citation: Adams MM, Hoarfrost AL, Bose A, Joye SB and Girguis PR (2013) Anaerobic oxidation of short-chain alkanes in hydrothermal sediments: potential influences on sulfur cycling and microbial diversity. *Front. Microbiol.* 4:110. doi: 10.3389/fmicb.2013.00110

This article was submitted to Frontiers in Extreme Microbiology, a specialty of Frontiers in Microbiology.

Copyright © 2013 Adams, Hoarfrost, Bose, Joye and Girguis. This is an open-access article distributed under the terms of the Creative Commons Attribution License, which permits use, distribution and reproduction in other forums, provided the original authors and source are credited and subject to any copyright notices concerning any third-party graphics etc.



# Phylogenetic diversity and functional gene patterns of sulfur-oxidizing subseafloor *Epsilonproteobacteria* in diffuse hydrothermal vent fluids

Nancy H. Akerman<sup>1†</sup>, David A. Butterfield<sup>2</sup> and Julie A. Huber<sup>1\*</sup>

<sup>1</sup> Josephine Bay Paul Center for Comparative Molecular Biology and Evolution, Marine Biological Laboratory, Woods Hole, MA, USA

<sup>2</sup> Joint Institute for the Study of the Atmosphere and Ocean, University of Washington and NOAA Pacific Marine Environmental Lab, Seattle, WA, USA

**Edited by:**

Andreas Teske, University of North Carolina at Chapel Hill, USA

**Reviewed by:**

Casey R. J. Hubert, Newcastle University, UK

Gordon Webster, Cardiff University, UK

**\*Correspondence:**

Julie A. Huber, Josephine Bay Paul Center for Comparative Molecular Biology and Evolution, Marine Biological Laboratory, 7 MBL Street, Woods Hole, MA 02543, USA  
e-mail: jhuber@mbl.edu

**†Present address:**

Nancy H. Akerman, US Environmental Protection Agency, Washington, DC USA

Microorganisms throughout the dark ocean use reduced sulfur compounds for chemolithoautotrophy. In many deep-sea hydrothermal vents, sulfide oxidation is quantitatively the most important chemical energy source for microbial metabolism both at and beneath the seafloor. In this study, the presence and activity of vent endemic *Epsilonproteobacteria* was examined in six low-temperature diffuse vents over a range of geochemical gradients from Axial Seamount, a deep-sea volcano in the Northeast Pacific. PCR primers were developed and applied to target the sulfur oxidation *soxB* gene of *Epsilonproteobacteria*. *soxB* genes belonging to the genera *Sulfurimonas* and *Sulfurovum* are both present and expressed at most diffuse vent sites, but not in background seawater. Although *Sulfurovum*-like *soxB* genes were detected in all fluid samples, the RNA profiles were nearly identical among the vents and suggest that *Sulfurimonas*-like species are the primary *Epsilonproteobacteria* responsible for actively oxidizing sulfur via the Sox pathway at each vent. Community patterns of subseafloor *Epsilonproteobacteria* 16S rRNA genes were best matched to methane concentrations in vent fluids, as well as individual vent locations, indicating that both geochemistry and geographical isolation play a role in structuring subseafloor microbial populations. The data show that in the subseafloor at Axial Seamount, *Epsilonproteobacteria* are expressing the *soxB* gene and that microbial patterns in community distribution are linked to both vent location and chemistry.

**Keywords:** sulfur oxidation, hydrothermal vent microbiology, 16S rRNA, functional genes, subseafloor, *Epsilonproteobacteria*

## INTRODUCTION

Sulfur is an abundant, multi-valent element in deep-sea hydrothermal vent systems. Large metal sulfide chimneys and biofilms containing filamentous sulfur are often present, and hydrogen sulfide concentrations are typically in the millimolar range (Sievert et al., 2008a). The high concentrations of hydrogen sulfide ( $H_2S$ ) at deep-sea vents are produced mainly via high-temperature seawater-rock interactions in the subseafloor hydrothermal reaction zone (Jannasch and Mottl, 1985). Other partially reduced sulfur compounds, such as thiosulfate, polysulfide, and elemental sulfur, are generated when hydrothermal vent fluids mix with oxygenated seawater (Yamamoto and Takai, 2011). At deep-sea hydrothermal vent systems, the microbially-mediated oxidation of reduced sulfur compounds is a key chemolithotrophic process that provides a substantial primary energy source for higher organisms (Jannasch and Mottl, 1985; Sievert et al., 2008a). Thermodynamic modeling studies show that sulfide oxidation is the major energy source at most non-peridotite, basalt-hosted deep-sea hydrothermal vent systems (Amend et al., 2011), including Axial Seamount on the Juan de Fuca Ridge (Butterfield et al., 2004). Microbial sulfate reduction also occurs across a range of temperatures in hydrothermal discharge areas (Bonch-Osmolovskaya et al., 2011). Even away

from hydrothermal vents, it is clear that reduced inorganic sulfur compounds play an important role in chemolithoautotrophic metabolism throughout the dark ocean (Walsh et al., 2009; Orcutt et al., 2011; Swan et al., 2011).

Many bacteria and some archaea have the capability of oxidizing sulfur or sulfide to sulfate. In bacteria, there are two different sulfur oxidation pathways: the reverse sulfate reduction pathway, which uses the Dsr, Apr, or Sat enzymes (Kappler and Dahl, 2001), and the sulfur oxidation Sox multienzyme system (Friedrich et al., 2001, 2005). The Sox system contains four protein components, SoxYZ, SoxXA, SoxB, and SoxCD, for the complete oxidation of sulfide and thiosulfate to sulfate (Friedrich et al., 2005). The SoxB protein, encoded by the *soxB* single copy gene, has been identified as the sulfate thiol esterase in the Sox system, and the *soxB* gene is used as a marker gene to survey sulfur oxidizing bacteria (Friedrich et al., 2005). Homologous proteins to SoxB have not been found in the domain Archaea (Friedrich et al., 2001). Polymerase chain reaction (PCR) primers targeting the *soxB* gene have previously been developed; these sets are based on *Chlorobia* and *Alphaproteobacteria* sequences and were refined using additional *Alphaproteobacteria* and *Aquificales* sequences (Petri et al., 2001). The primers have been extensively tested and found to amplify the *soxB* gene from mostly

photo- and chemotrophic sulfur oxidizing species, including the *Gammaproteobacteria* (Meyer et al., 2007), with additional examples from the *Epsilonproteobacteria* (Hügler et al., 2010). However, some of the primer sets developed by Petri et al. (2001) are degenerate primers that result in multiple PCR amplicons of approximately the same size, which can give ambiguous sequencing results, and some key phylogenetic groups may also be missed when applied to diverse habitats (Petri et al., 2001; Meyer et al., 2007; Headd and Engel, 2013).

The purpose of this study was to design and test *soxB* PCR primers specific to the *Epsilonproteobacteria* to evaluate the presence, diversity, and gene expression of sulfur-oxidizing *Epsilonproteobacteria* at deep-sea hydrothermal vent systems. Chemolithoautotrophic *Epsilonproteobacteria* are often the most abundant group of bacteria detected in both the free-living and symbiotic microbial communities at deep-sea vents (e.g., Huber et al., 2003; Nakagawa et al., 2007; Nakagawa and Takai, 2008; Sievert et al., 2008a). Epsilonproteobacterial isolates from vents include *Sulfurimonas autotrophica* DSM16294, *Sulfurovum* sp. NBC37-1, and *Nitratiruptor* sp. SB155-2. All recently had their genomes sequenced (Nakagawa et al., 2007; Sikorski et al., 2010), along with a closely related coastal wetland isolate *S. denitrificans* DSM1251 (Sievert et al., 2008b), and all have the capability of oxidizing reduced sulfur compounds using the sulfur oxidation Sox multienzyme system (Yamamoto and Takai, 2011). This new genomic information was used to develop and test *soxB* gene PCR primers specific to the *Epsilonproteobacteria* at diffuse vents from Axial Seamount, where *Epsilonproteobacteria* are known to dominate many low-temperature vent fluids (Huber et al., 2003; Sogin et al., 2006; Huber et al., 2007; Opatkiewicz et al., 2009). After primer optimization and testing, six low-temperature diffuse hydrothermal vent samples that span a range

of temperature, pH, sulfide, and geological settings were screened using both 16S rRNA 454 pyrosequencing and the new *soxB* gene primers to evaluate the presence, diversity, and gene expression of sulfur-oxidizing *Epsilonproteobacteria* at deep-sea hydrothermal vent systems.

## EXPERIMENTAL PROCEDURES

### SAMPLE SITE

Axial Seamount ( $46^{\circ}55' N$ ;  $130^{\circ}00' W$ ) is an active underwater volcano located approximately 250 nautical miles west of the Oregon/Washington coast at the intersection of the Juan de Fuca Ridge and the Cobb-Eickelberg Seamount Chain. The caldera of Axial Seamount is oriented northwest-to-southeast and is  $3 \times 8$  km, with hydrothermal vent fields associated with the north and south rift zones and near the caldera boundary fault in the southern half of the caldera (Embley et al., 1990; Butterfield et al., 2004). All samples in this study were collected from hydrothermal sites along the southern caldera boundary fault.

### SAMPLE COLLECTION

Hydrothermal fluid samples were collected in August and September 2010 using the ROV *Jason II* and the Hydrothermal Fluid and Particulate Sampler (HFPS) (Butterfield et al., 2004). The titanium intake nozzle with in-line temperature probe was inserted into the vents, with the tip generally penetrating into the seafloor. Filtered and unfiltered fluids were sampled after a steady in-line temperature was found and the sampling pump was then turned on to collect fluids at the rate of  $\sim 150$  ml/min. Temperature was monitored and recorded throughout sampling and the maximum and average temperatures for the samples are reported (Table 1). Three liters of fluid was filtered onto

**Table 1 | Characteristics of vent fluid and seawater samples.**

|                                    | Gollum            | Marker 33         | Marker 113        | Pompeii           | Escargot          | 9 m               | Seawater          |
|------------------------------------|-------------------|-------------------|-------------------|-------------------|-------------------|-------------------|-------------------|
| Vent type                          | Basalt            | Basalt            | Basalt            | Sulfide           | Sulfide           | Sulfide           |                   |
| Cells/ml                           | $5.1 \times 10^5$ | $6.3 \times 10^4$ | $6.7 \times 10^5$ | $4.8 \times 10^5$ | $3.8 \times 10^5$ | $3.6 \times 10^5$ | $1.8 \times 10^4$ |
| T <sub>max</sub> , °C              | 22.3              | 39.0              | 29.1              | 33.8              | 22.7              | 51.3              | 2                 |
| T <sub>avg</sub> , °C              | 21.4              | 38.3              | 27.9              | 31.1              | 20.6              | 49.7              | 2                 |
| pH                                 | 5.7               | 5.5               | 6.0               | 5.4               | 5.0               | 4.8               | 7.8               |
| Avg Alk, Meq/kg                    | 2.77              | 1.62              | 2.46              | 2.21              | 2.32              | 2.03              | 2.43              |
| Avg Si, $\mu\text{mol}/\text{kg}$  | 815               | 2857              | 326               | 1568              | 1575              | 2169              | 155               |
| Mg, mmol/kg                        | 50.7              | 41.8              | 50.4              | 46.7              | 48.1              | 44.4              | 52.9              |
| % Seawater <sup>a</sup>            | 96                | 79                | 95                | 88                | 91                | 84                | 100               |
| H <sub>2</sub> S, $\mu\text{M}$    | 84                | 929               | 748               | 452               | 554               | 1626              | 0                 |
| NH <sub>3</sub> , $\mu\text{M}$    | 5.19              | 6.05              | 4.68              | 3.74              | 4.95              | 10.64             | <0.6              |
| H <sub>2</sub> S/Heat <sup>b</sup> | 1                 | 6.3               | 6.9               | 4                 | 6.6               | 8.6               | 0                 |
| H <sub>2</sub> /Heat <sup>b</sup>  | 0.00              | 0.12              | 0.00              | 0.17              | 0.10              | 0.29              | 0                 |
| CH <sub>4</sub> /Heat <sup>b</sup> | 0.09              | 0.13              | 0.38              | 0.05              | 0.11              | 0.06              | 0                 |
| Fe/Heat <sup>b</sup>               | 0.01              | 0.02              | 0.01              | 0.03              | 0.07              | 0.36              | 0                 |
| Fe/Mn                              | 0.03              | 0.03              | 1.52              | 0.17              | 0.35              | 1.36              | 0                 |
| Mn/Heat <sup>b</sup>               | 0.21              | 0.59              | 0.01              | 0.18              | 0.21              | 0.26              | 0                 |

<sup>a</sup> % Seawater calculated as  $Mg_{vf}/Mg_{sw} \times 100$ . Subscripts: vf, vent fluid; sw, seawater.

<sup>b</sup> Ratios to heat, reported in nmol/J, calculated as  $[C_{vf} - C_{sw}] / [(T_{vf} - T_{sw}) \times C_p]$  where  $C_p$  is the heat capacity of water ( $4.15 \text{ J g}^{-1} \text{ }^{\circ}\text{C}^{-1}$  for the temperature and pressure in this study).

Sterivex filters (Millipore) or 47-mm flat filters (Millipore) for DNA analysis and RNA analysis, respectively. For the 47 mm filters, a McLane “pancake” style filter assembly was used and filled with RNALater (Life Technologies), so that immediately after filtration, RNALater diffused over the filter surface and remained until ROV recovery (Cowen et al., 2012). A background seawater sample outside of the Axial Seamount caldera was collected via CTD at ~1500 m depth, and ~3 L of seawater was filtered onto a flat filter on board the ship. Sterivex filters were flooded with RNALater, sealed with Male/Female Luer Caps, and stored in 50-mL sterile Falcon tubes, while flat filters were stored in 5-mL sterile plastic tubes filled with RNALater. All filters were stored at 4°C for 24 h before being stored at -80°C until nucleic acid extraction in the laboratory. Fluid samples for chemistry were analyzed shipboard for pH, alkalinity, hydrogen sulfide, ammonia, methane and hydrogen following the methods of Butterfield et al. (2004). Major cations and anions were analyzed by ion chromatography and iron and manganese were analyzed by atomic absorption and/or ICP-MS on shore. Fluid samples were preserved in formaldehyde for cell enumeration using epifluorescence microscopy with DAPI as described previously (Huber et al., 2002).

#### DNA EXTRACTION

Genomic DNA was extracted from Sterivex filters following the procedure outlined in Sogin et al. (2006) and Huber et al. (2002), with the following minor modifications. RNALater was removed from the filter via pushing the liquid out with a 3 ml syringe. 1.85 mL of DNA extraction buffer (0.1 M Tris-HCl [pH 8], 0.1 M Na<sub>2</sub>-EDTA [pH 8], 0.1 M NaH<sub>2</sub>PO<sub>4</sub> [pH 8], 1.5 M NaCl, and 1% cetyltrimethylammonium bromide) was then added to the filter. Sterivex filters were then re-capped and the extraction method of Huber et al. (2002) with modifications in Sogin et al. (2006) followed. Successful DNA extraction was verified via PCR using bacterial 16S primers 8F (5'-AGA GTT TGA TCC TGG CTC AG-3') and 1492R (5'-GGT TAC CTT GTT ACG ACT T-3') and visualized under UV light on a 1% agarose gel stained with ethidium bromide.

#### RNA EXTRACTION AND REVERSE TRANSCRIPTION PCR

RNA filters were allowed to thaw at room temperature in their 5-mL storage tubes. Total RNA was extracted using the RNAqueous-4PCR kit (Ambion), with the following adaptations. First, RNALater was discarded from the 5-mL tube, and 500 µl of lysis/binding solution was added directly to the tube. Tubes were vortexed at high speed for ~2 min. The lysis/binding solution was removed from the tube and placed in a 2-mL collection tube. An additional 500 µl of lysis/binding solution was added to the 5-mL tube, and the vortex and collection steps were repeated. The protocol was then followed per manufacturer's instructions, including the DNase 1 treatment step. The final elution volume was 120 µl. RNA was quantified using the Quant-iT RiboGreen RNA Reagent and Kit (Invitrogen) and a Turner Biosystems Spectrophotometer. Approximately 30 ng of total RNA was reverse transcribed using the High Capacity RNA-to-cDNA Kit (Applied Biosystems) according to the manufacturer's instructions.

#### soxB GENE PRIMER DESIGN AND PCR OPTIMIZATION USING SULFURIMONAS DENITRIFICANS

Primers were designed using multiple alignments of *soxB* genes from Epsilonproteobacterial species *Nitratiruptor* sp. SB155-2, *Sulfurovum* sp. NBC-37, and *Sulfurimonas denitrificans* DSM 1225 (Table 2). Initial primer sequences were created using the *soxB* nucleotide sequences in Primaclade (Gadberry et al., 2005) and PriFi (Fredslund et al., 2005), and the amino acid sequences in iCODEHOP (Boyce et al., 2009). Sequences were then manually adjusted based on the initial bacterial sequences. CODEHOPs are hybrid primers that consist of a 5' nondegenerate clamp, followed by a 3' degenerate core sequence (indicated in lowercase nucleotides) that stabilizes hybridization (Rose, 2003). Primers were manufactured by Invitrogen (Carlsbad, CA).

#### *Sulfurimonas denitrificans*

DSM 1251 was obtained from the DSMZ culture collection and grown using DSMZ Medium 113, with an additional 10 g/L NaCl and substituting trace element solution 141 (from DSMZ Medium 141) for trace element solution SL-4. DNA was extracted from *S. denitrificans* using the UltraClean Microbial DNA Isolation Kit (MoBio Laboratories, Inc.), using 3 mL of culture and an initial extended centrifugation time (8 min).

Optimal annealing conditions for the primers were determined via gradient PCR using *S. denitrificans* DNA as template. Primers were tested in the following pairs (Table 2): sox190F/sox1198R, sox527F/sox1198R, sox523F/sox1210R, sox523F/sox1292R, and sox523F/F-34R. Gradients were 42–51°C for sox190F/sox1198R, and 52–60°C for all other primer sets. Annealing temperatures of 45°C for sox190F/sox1198R, 46°C for sox527F/sox1198R, and 52°C for sox523F/sox1210R and sox523F/sox1292R were chosen based on visual inspection of the gradient PCR results on a 1% agarose gel stained with ethidium bromide and photographed under UV light. The

**Table 2 | soxB primers designed and PCR settings used in this study.**

| Primer           | Sequence                          | Target nucleotide position <sup>a</sup> |
|------------------|-----------------------------------|---|
| sox190F          | 5'-TGGAGRGAGCCWTCAAC-3'           | 190–206                                 |
| sox527F          | 5'-TGGTWGGWCAYTGGGAATTAA-3'       | 527–547                                 |
| sox523F          | 5'-GTGATGGTGGACAtgggartwya-3'     | 523–547                                 |
| sox1198R         | 5'-AGAANGTATCTCKYTTATAAAG-3'      | 1198–1177                               |
| sox1210R         | 5'-CGAAGGTGGAGTAGAAngtrtctckyt-3' | 1210–1183                               |
| sox1292R         | 5'-GTCGTTCCCCATckrtancncngg-3'    | 1292–1270                               |
| F-34R            | 5'-CTCAAAGGTGTAAACGtyngatakgt-3'  |   |
| Primer           | Annealing combinations            | Amplicon length (bp)                    |
| sox190F/sox1198R | 45                                | 1009                                    |
| sox527F/sox1198R | 46                                | 672                                     |
| sox523F/sox1210R | 52                                | 688                                     |
| sox523F/sox1292R | 52                                | 770                                     |

<sup>a</sup>Using *S. denitrificans* numbering.

PCR reaction mixture consisted of 1X buffer (Promega), 4 mM MgCl<sub>2</sub>, 0.2 mM of each deoxynucleoside triphosphate (dNTP), 0.6 μM of each primer, 1U GoTaq polymerase (Promega), 1 μL DNA template, and DEPC H<sub>2</sub>O to 25 μL. Thermocycling conditions on an Eppendorf thermal cycler consisted of an initial denaturation step at 94°C for 3 min, followed by 35 cycles at 94°C for 30 s, applicable annealing temperature for 45 s, and 72°C for 1 min, followed by a final extension at 72°C for 5 min. Using these PCR conditions, all primer sets yielded a single band amplicon of the predicted size, which ranged from ~670 to 1000 bp depending on the primer set. PCR products were verified to be the correct size on a 1% agarose gel stained with ethidium bromide and photographed under UV light. PCR products were cleaned using the MinElute PCR Purification Kit (Qiagen) following the manufacturer's instructions and directly sequenced on an Applied Biosystems 3730XL sequencer. DNA sequences were compared to sequences in the NCBI database via BLAST and in all cases were the *soxB* gene of *S. denitrificans* DSM 1251.

#### **soxB GENE CLONING, SEQUENCING, AND ANALYSIS**

Each of the 4 primer sets were used with appropriate PCR settings as outlined above on DNA and cDNA from all fluid samples. PCR was visualized by UV light on ethidium bromide-stained 1% agarose gels. While multiple primer sets were tested on each sample, only amplicons from primer pair sox527F/1198R were cloned and sequenced. For the background seawater sample, only primer pair sox 523F/1292R amplified, thus it was cloned and sequenced. PCR products were purified using the MinElute PCR Purification Kit (Qiagen) and the products analyzed on 0.8% agarose gel. Products were gel excised, purified, cloned, and sequenced bidirectionally as described in Huber et al. (2009). Primer sequences were trimmed from nucleotide sequences and translated into amino acids using EMBOSS Transeq (Rice et al., 2000). A protein distance matrix was calculated in ProtDist (Felsenstein, 1989) and operational taxonomic units (OTUs) constructed in mothur (Schloss et al., 2009). Phylogenetic relationships of representative 85% amino acid identity OTUs to other *soxB* genes were determined using MEGA5 (Tamura et al., 2007). Sequences are deposited in GenBank under the following Accession Numbers: KC793341-KC793868.

#### **454 PYROSEQUENCING AND ANALYSIS**

Amplicons targeting the V4V6 rRNA hypervariable region were generated for each DNA and cDNA sample following Filkins et al. (2012). A custom bioinformatic pipeline was used to remove low quality reads according to Filkins et al. (2012). The algorithm GAST assigned taxonomy to each unique read (Huse et al., 2008). All high quality reads that passed initial processing were further analyzed and trimmed to the V5 region based on high error rates at the V4 end, resulting in ~350 bp reads, and UCLUST (Edgar, 2010) identified operational taxonomic units (OTUs) with 96% sequence identity. Singletons were removed from all subsequent reported analyses. The resulting matrix of OTUs shared between samples was used to construct taxonomic summaries and compare background seawater and vent samples. The OTU matrices were normalized to total and transformed via square root and used to calculate a distance matrix

with the Morisita–Horn measure (Horn, 1966). Distance matrices were imported into PRIMER-E (Clarke and Gorley, 2006) for a variety of analyses, including hierarchical cluster analysis, principal component analysis (PCO), analysis of similarity (ANOSIM), and nonmetric multidimensional scaling (MDS) analysis. The entire chemical dataset was also included for PCA and Spearman correlation analyses. To predict which OTUs were active or inactive, the top OTUs that occurred greater than 0.1% of the total sequences in either the RNA or DNA fraction for both the *Epsilon*- and *Gammaproteobacteria* were examined. Each OTU was scored as active or inactive based on its recovery in DNA and RNA samples (Jones and Lennon, 2010). Data is accessible via vamps.mbl.edu under project name JAH\_AXV\_Bv6v4.

## **RESULTS**

### **AXIAL SEAMOUNT FLUID SAMPLES**

Fluid samples were collected from basalt- or sulfide-hosted diffuse flow venting sites with varying physical and chemical parameters, as well as from background seawater (**Table 1**). Gollum, Marker 33, and Marker 113 sites discharge vent fluids directly from basalt, while Pompeii, Escargot, and 9 m sites discharge vent fluids from the sides of metal-sulfide chimneys. Fluids at Pompeii were emanating from a large clump of tubeworms. These samples span a range of sulfide to heat ratios (calculated using the measured H<sub>2</sub>S concentration and the average in-line temperature of individual samples, **Table 1**), reflecting different concentrations of hydrogen sulfide in end-member hydrothermal fluids and variable sulfide oxidation (Butterfield et al., 2004). The site with the lowest sulfide/heat ratio of 1.0 nmol/J was Gollum, the mid-range site Pompeii had a ratio of 4, and the other four sample sites had ratios between 6 and 9. Average temperatures ranged from 20.6 to 49.7°C. The measured temperatures and magnesium content of the collected samples indicate that the fluids are 79–96% seawater (4–21% hot hydrothermal end-member) overall, but this percentage does not tell us their mixing history or subseafloor residence time.

#### **soxB GENE DATA**

Primers that specifically target the *Epsilonproteobacteria* *soxB* gene were designed by comparing conserved regions of the *Sulfurimonas denitrificans* DSM 1225, *Sulfurovum* sp. NBC37-1, and *Nitratiruptor* sp. SB155-2 *soxB* genes (Nakagawa et al., 2007; Sievert et al., 2008b). The primers are not capable of identifying *Arcobacter*-like sequences. The *Arcobacter* *soxB* sequences cluster in a different clade (Hüglér et al., 2010), and homologous regions for primer annealing could not be identified across all *Epsilonproteobacteria* genera, while excluding other groups. The primers were tested and PCR settings were optimized using DNA extracted from a pure culture of *S. denitrificans*. Three forward and three reverse primers were used in four combinations (**Table 2**). The sequences were translated to amino acid residues and checked via BLASTP and alignment to verify amplification of the *soxB* gene. The four different primer sets amplified *soxB* gene fragments ranging in size from 672 to 1009 bp. The primer sets were additionally tested on environmental DNA samples and were shown to be capable of amplifying *Sulfurovum*-, *Sulfurimonas*-, and *Nitratiruptor*-like *soxB* sequences (Meyer et al., 2013).

The four *soxB* primer sets were used to amplify *soxB* from the DNA and RNA fractions of the six Axial Seamount hydrothermal vent fluid samples and the background seawater sample. Positive amplicons were obtained from six of the seven DNA fractions, with the exception of Pompeii. In the RNA fractions, amplicons were not obtained from Pompeii, 9 m, and the background seawater sample. A total of 480 clones were sequenced across the nine DNA and RNA vent fluid samples and the one DNA background seawater sample (**Table 3**).

All hydrothermal vent *soxB* clones were most closely related to the *Sulfurimonas* (Slms) and *Sulfurovum* (Sfvm) genera in the *Epsilonproteobacteria* and represented 10 different phylotypes at an 85% amino acid identity level (**Figures 1, 2**). Of the 405 clones from the nine hydrothermal libraries, all but 37 fell into 3 main OTUs. The most common OTU, Slms-1, represented ~80% of all the clones and was detected at all positively amplified hydrothermal samples in both the DNA and RNA fractions. The other two most common clone sequences were *Sulfurovum*-like phylotypes Sfvm-A and Sfvm-B, which represented 6 and 4%, respectively, of all hydrothermal clones. Sfvm-A was detected in the DNA fraction of all sites, but only in the RNA fraction at Gollum. Sfvm-B was only detected in the DNA fractions at Gollum and Marker 33 and in none of the RNA fractions (**Figure 2**).

Overall, only one *Sulfurovum*-like *soxB* gene was found in the RNA fraction (Gollum). Instead, Slms-1 was the only *soxB* gene detected in all of the RNA fractions (**Figure 2**) and was also the most abundant *soxB* gene in all DNA fractions, except for Gollum. At Gollum, the composition of the DNA and RNA libraries differed, with the DNA library dominated by *Sulfurovum*-like *soxB* gene sequences and the RNA fraction almost completely composed of Slms-1. No comparisons could be made between the

DNA and RNA fractions of the 9 m site since *soxB* was not amplified from the RNA fraction.

In the background seawater sample, a total of five phylotypes were found, with the two most dominant OTUs representing 94% of the background clones. All phylotypes were most closely related to *Alphaproteobacteria*, although these BLASTP matches were made at approximately 67% identity rather than the 90–99% identity of the *Epsilonproteobacteria* BLASTP hits in the libraries from the venting fluids (**Figure 1**). These *Alphaproteobacteria*-like sequences were not found in the vent samples.

#### 16S rRNA GENE 454 PYROSEQUENCING

454 pyrosequencing of the bacterial 16S rRNA gene from both the DNA and cDNA from all samples resulted in 262,325 high-quality non-singleton tag sequences across the hydrothermal and background seawater sites (a DNA library only was constructed for the background seawater sample, **Table 3**). *Epsilonproteobacteria* (58,058 sequences) were present in all 12 hydrothermal vent fluid libraries (**Table 3, Figure 3**). Epsilonproteobacterial sequences were not detected in background seawater, even before singletons were removed (**Table 3, Figure 3**). The background seawater sample was mostly composed of *Alpha-* and *Gammaproteobacteria* (**Figure 3**). Within the *Epsilonproteobacteria*, sequences of the genera *Sulfurimonas* and *Sulfurovum* dominated most libraries (**Figure 4**), although at Pompeii, Escargot, and 9 m, numerous *Caminibacter* sequences were also detected (**Figure 4**). The only other major group within the *Epsilonproteobacteria* was *Arcobacter*, which comprised almost 9% of the DNA fraction at Marker 33. In all cases, *Epsilonproteobacteria* sequences were more abundant in DNA fractions than RNA fractions for each individual vent (**Figure 4**). Comparison of rRNA profiles of the most abundant OTUs for *Epsilonproteobacteria* shows most *Epsilonproteobacteria* were inactive in the sampled vent fluids. Out of 164 *Epsilonproteobacteria* OTUs considered, only 22 were scored as active (**Table 4**).

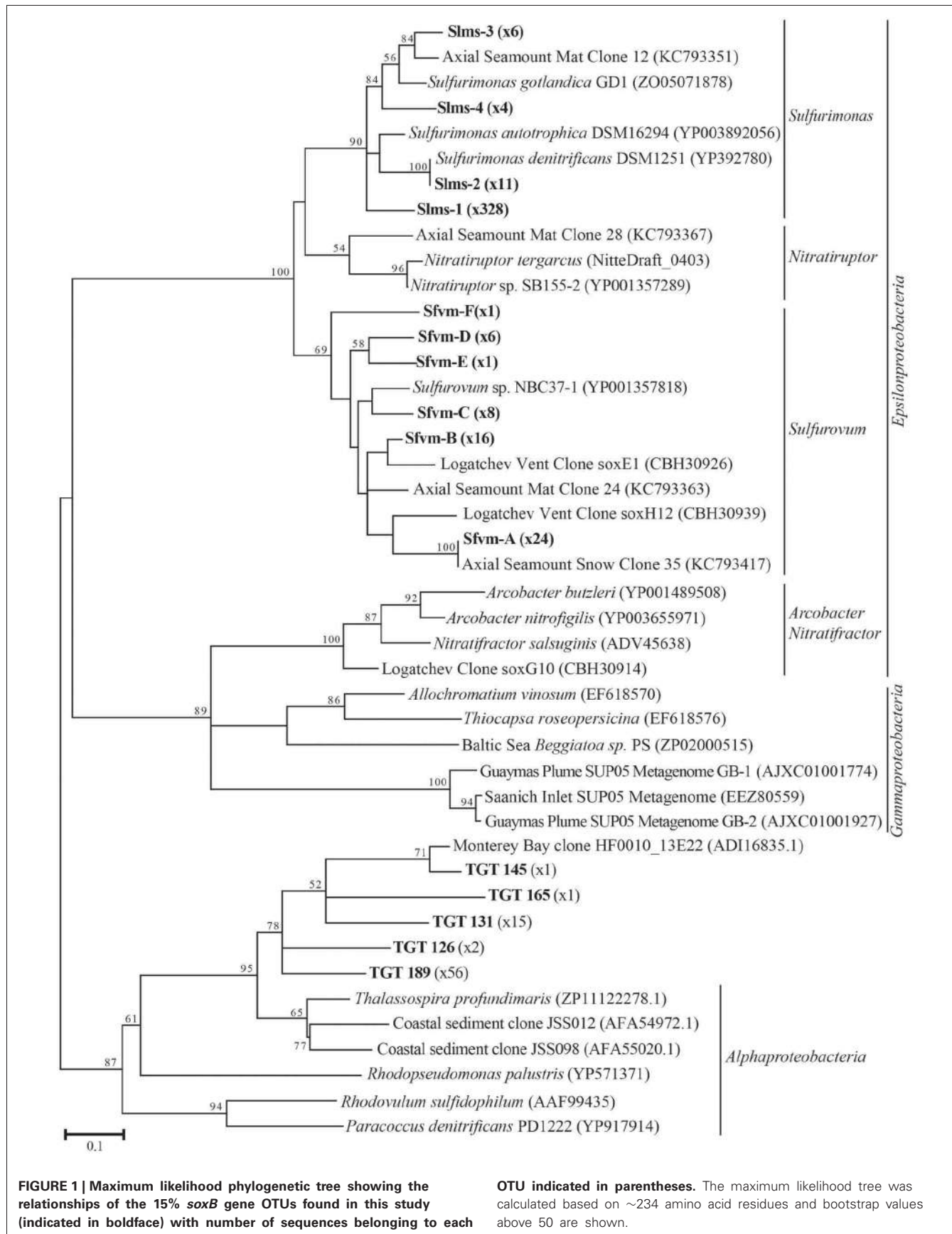
To distinguish vent-specific microbial communities from background seawater communities that mix with venting fluids at the seafloor, all 16S rRNA gene OTUs as well as only Epsilonproteobacterial 16S rRNA gene OTUs were analyzed separately. SIMPROF tests of all OTU datasets indicated there is significant community structure among the individual samples ( $\pi = 6.48$ ,  $P$  value < 0.001 for all OTUs.  $\pi = 8.46$ ,  $P$  value < 0.001 for *Epsilonproteobacterial* OTUs). One-Way ANOSIM (analysis of similarity) tests with a variety of factors resulted in significant global R values for individual vent sampled and type of vent (basalt or sulfide) for both all OTUs and only Epsilonproteobacterial OTUs; values were higher for *Epsilonproteobacteria* ( $R = 0.84$ ,  $P$  value < 0.001 for *Epsilonproteobacteria* and individual vent;  $R = 0.55$ ,  $P$  value = 0.004 for *Epsilonproteobacteria* and type of vent). The type of nucleic acid analyzed (RNA or DNA) was significant only when all OTUs were considered ( $R = 0.39$ ,  $P$  value = 0.006). Principal coordinates analysis of all OTUs showed a clear distinction between DNA and RNA fractions (**Figure 5**) that was not seen when only Epsilonproteobacterial OTUs were analyzed in the same manner (**Figure 6**). BEST analysis [Biota and/or

**Table 3 | Sequencing statistics for 16S rRNA and *soxB* gene sequences.**

|            | Nucleic acid | Total tag sequences <sup>a</sup> | Total epsilon tag sequences | % Epsilon | Total <i>soxB</i> sequences <sup>b</sup> |
|------------|--------------|----------------------------------|-----------------------------|-----------|--|
| Gollum     | DNA          | 14866                            | 7000                        | 47.1      | 47                                       |
|            | RNA          | 11128                            | 157                         | 1.4       | 48                                       |
| Marker 33  | DNA          | 15773                            | 8117                        | 51.5      | 45                                       |
|            | RNA          | 11166                            | 248                         | 2.2       | 45                                       |
| Marker 113 | DNA          | 14820                            | 3998                        | 27.0      | 38                                       |
|            | RNA          | 14451                            | 2870                        | 19.9      | 46                                       |
| Pompeii    | DNA          | 16538                            | 6699                        | 40.5      | –  |
|            | RNA          | 10475                            | 694                         | 6.6       | –  |
| Escargot   | DNA          | 15457                            | 6174                        | 39.9      | 46                                       |
|            | RNA          | 98143                            | 18453                       | 18.8      | 46                                       |
| 9 m        | DNA          | 17570                            | 3241                        | 18.4      | 44                                       |
|            | RNA          | 10256                            | 407                         | 4.0       | –  |
| Seawater   | DNA          | 11682                            | 0                           | 0         | 75                                       |
| Total      | –            | 262325                           | 58058                       | –         | 480                                      |

<sup>a</sup> No singletons.

<sup>b</sup> Primer set 527F/1198R was used for all vent samples; 523F/1292 for seawater.



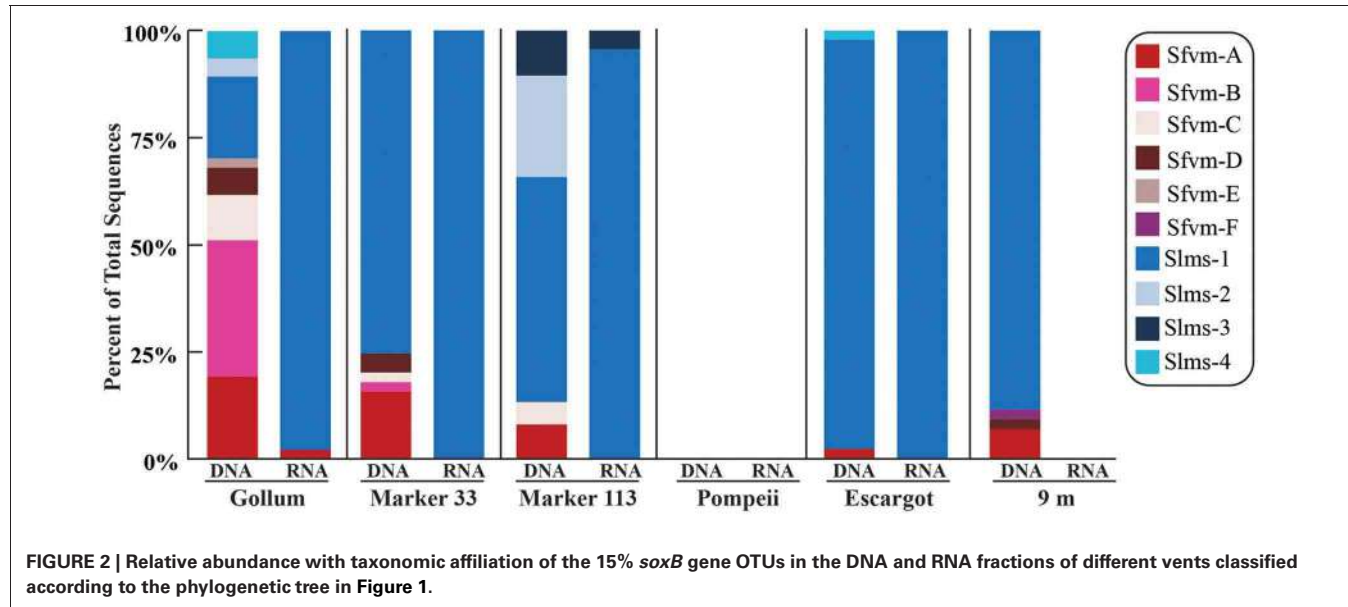


**FIGURE 2 |** Relative abundance with taxonomic affiliation of the 15% *soxB* gene OTUs in the DNA and RNA fractions of different vents classified according to the phylogenetic tree in Figure 1.

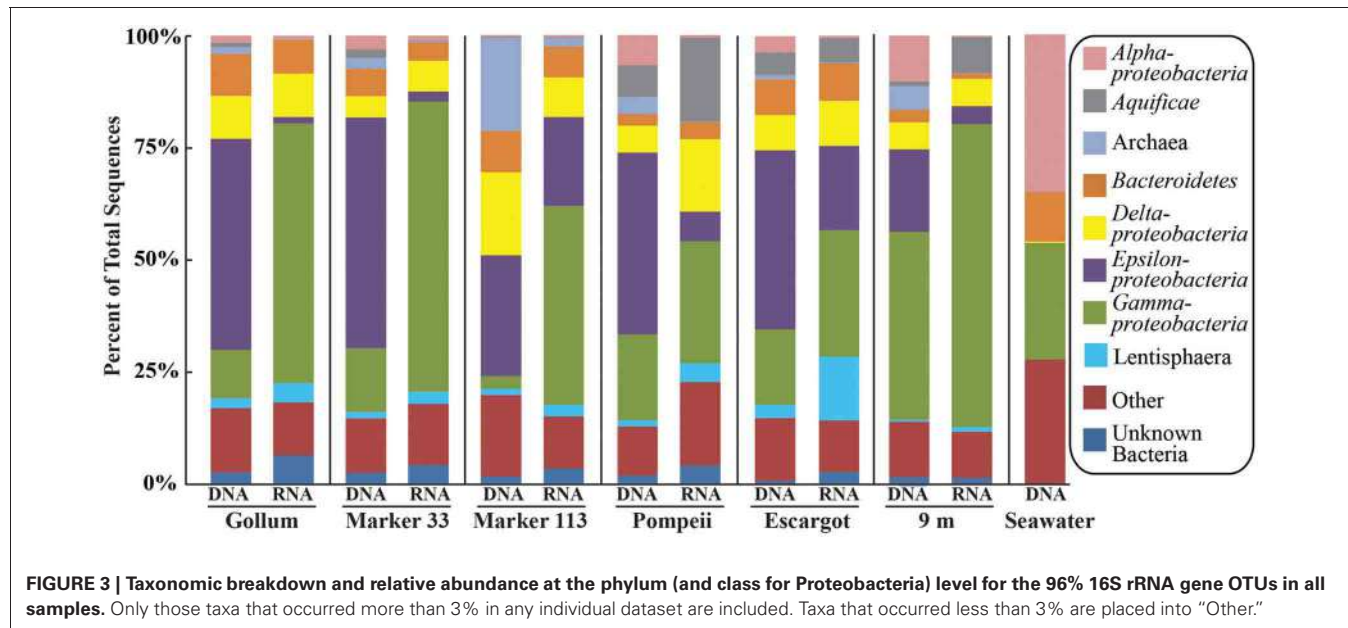


**FIGURE 3 |** Taxonomic breakdown and relative abundance at the phylum (and class for Proteobacteria) level for the 96% 16S rRNA gene OTUs in all samples. Only those taxa that occurred more than 3% in any individual dataset are included. Taxa that occurred less than 3% are placed into "Other."

Environmental matching (Clarke and Gorley, 2006)] was used to match multivariate patterns of OTUs to chemical variables measured in the vent fluids (Table 1). For both all OTUs and only Epsilonproteobacterial OTUs, the most significant R value was with CH<sub>4</sub>/Heat ( $R = 0.69$ ,  $P$  value = 0.003, Figure 6).

Gamma-proteobacterial sequences were also treated separately due to their relatively high abundance in all RNA fractions (Figure 3). They were detected in all 12 hydrothermal vent fluid libraries, as well as background seawater. Within the *Gamma-proteobacteria*, sequences belonging to the SUP05 clade were most frequently recovered, as well as those sequences related to animal endo- and ecto-symbionts (Figure 7, labeled “Unknown γ 2”). Principal coordinates analysis of

all *Gamma-proteobacteria* OTUs showed a clear distinction between DNA and RNA fractions (data not shown), similar to that seen for all OTUs. *Gamma-proteobacterial* sequences were more abundant in RNA fractions than DNA fractions (Figure 7). Comparison of RNA and DNA profiles of the most abundant OTUs for *Gamma-proteobacteria* shows high activity of *Gamma-proteobacteria* in most vent fluids. Out of 67 *Gamma-proteobacteria* OTUs considered, 56 were scored as active (Table 4).

## DISCUSSION

Low-temperature diffuse vent samples represent combined hot hydrothermal vent fluid and deep seawater that mix and react

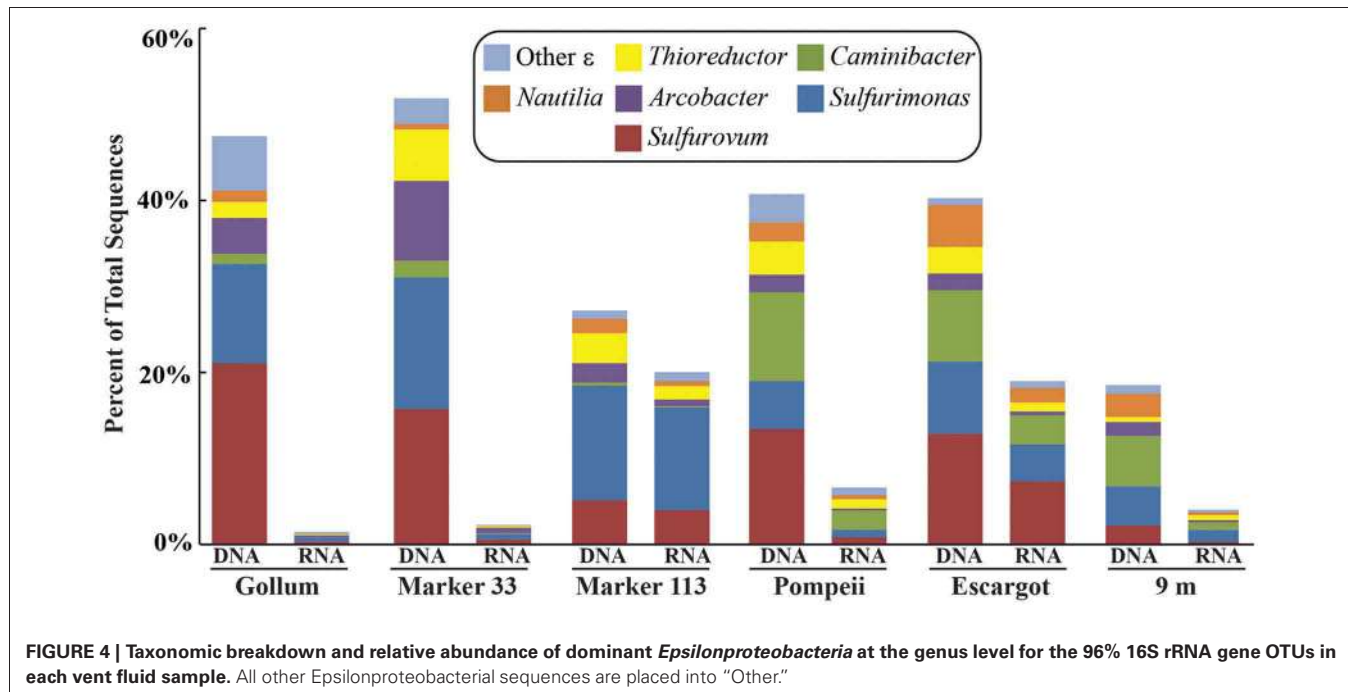


**FIGURE 4 | Taxonomic breakdown and relative abundance of dominant *Epsilonproteobacteria* at the genus level for the 96% 16S rRNA gene OTUs in each vent fluid sample.** All other *Epsilonproteobacterial* sequences are placed into “Other.”

**Table 4 | Predicted percent activity based on 16S rRNA gene data.**

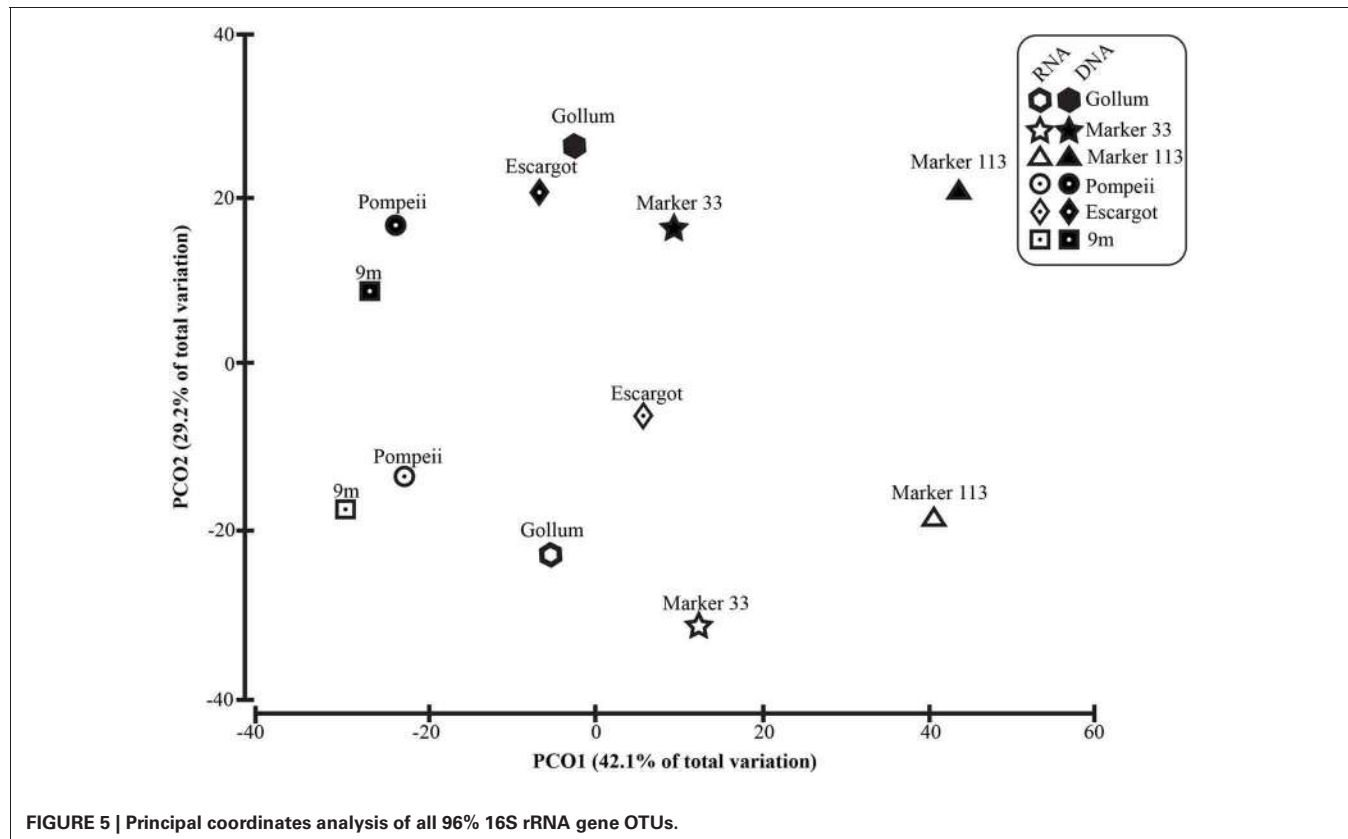
| Site       | <i>Epsilonproteobacteria</i> |                          |          | <i>Gammaproteobacteria</i> |                          |          |
|------------|------------------------------|--------------------------|----------|----------------------------|--------------------------|----------|
|            | Total OTUs <sup>a</sup>      | Active OTUs <sup>b</sup> | % Active | Total OTUs <sup>a</sup>    | Active OTUs <sup>b</sup> | % Active |
| Gollum     | 94                           | 0                        | 0        | 25                         | 18                       | 72       |
| Marker 33  | 79                           | 0                        | 0        | 39                         | 35                       | 89.7     |
| Marker 113 | 41                           | 17                       | 41.5     | 13                         | 13                       | 100      |
| Pompeii    | 47                           | 0                        | 0        | 14                         | 10                       | 71.4     |
| Escargot   | 61                           | 2                        | 3.3      | 18                         | 11                       | 61.1     |
| 9m         | 37                           | 3                        | 8.1      | 19                         | 9                        | 47.4     |

<sup>a</sup>Number of OTUs that occur >0.1% of all sequences in either RNA or DNA fraction.

<sup>b</sup>Number of OTUs that were scored as active if the RNA relative recovery was greater than its recovery from DNA.

beneath the seafloor. Mixing begins beneath the seafloor and continues as fluids vent and are diluted by ambient seawater as they rise up into the water column. By controlled pumping of fluids into a sampler intake that is inserted into the vents, the mixing that occurs with ambient seawater is controlled. However, even if dilution of the vent fluids with ambient seawater during sampling is not completely avoided, it is both possible and likely that seawater is entrained into the fluid along shallow mixing pathways in the subseafloor. Similarly, the microbial composition of the fluids reflects both seawater and subseafloor communities, which means that detection of vent-specific microbial processes can be challenging. By removing sequences from seawater organisms detected in background seawater from the vent fluid sample sequences, the analysis can focus on the diversity, distribution, and gene expression of vent-endemic subseafloor microbes. For this study, *Epsilonproteobacteria* that were not detected in background seawater were targeted to analyze their diversity, distribution, and sulfur-oxidizing gene patterns in the subseafloor.

The *soxB* gene primers were designed to screen for the hydrothermal vent sulfur-oxidizing *Epsilonproteobacteria* belonging to the genera *Sulfurimonas*, *Sulfurovum*, and *Nitratiruptor*. In particular, *Sulfurimonas* and *Sulfurimonas* are frequently detected at high abundances in diverse marine environments where strong gradients of oxygen and sulfide exist, including cold seep sediments (Roalvam et al., 2011), waters of redoxclines (Grote et al., 2007), coastal marine sediments (Hoor, 1975), and both shallow and deep hydrothermal vents (Huber et al., 2010; Zhang et al., 2012). The primers do not detect *Arcobacter*, a genus within the *Epsilonproteobacteria* that also uses the Sox pathway. The 454 16S rRNA gene data in this study suggests *Arcobacter* are not dominant in most hydrothermal vent fluids at Axial Seamount, and while they are sometimes seen in high abundance (Huber et al., 2007), a single primer set to capture all *Epsilonproteobacteria* that use the Sox pathway was not possible to design due to the distant relationship in the *soxB* gene between the different genera (Meyer and Kuever, 2007; Headd and Engel, 2013).



The *soxB* gene OTUs observed as *Sulfurovum*-like in this study generally shared the most identity with *Sulfurovum* sp. NBC37-1, which was isolated from a deep-sea hydrothermal vent and is capable of both hydrogen and sulfur oxidation, as well as denitrification (Nakagawa et al., 2007; Yamamoto et al., 2010). Two other members of this genus have been isolated; one from a hydrothermal vent (*S. lithotrophicum*) and one from marine sediments (*Candidatus S. sediminum*). Both are also described as sulfur oxidizers, although neither has been shown to be capable of hydrogen utilization like NBC37-1 (Inagaki et al., 2004; Park et al., 2012). The *soxB* gene OTUs observed as *Sulfurimonas*-like in this study were closely related to cultivated species of *Sulfurimonas*. *Sulfurimonas autotrophica* was originally isolated from hydrothermal sediments (Inagaki et al., 2003), and other members of the genus have been identified associated with vent animals (Takai et al., 2006), in the redoxcline of the Baltic Sea (Grote et al., 2012), and in coastal marine sediments (Hoor, 1975; Sievert et al., 2008b). Genomic sequencing of some of these isolates shows multiple functional genes for different metabolic pathways such as sulfur oxidation, nitrate reduction, and hydrogen oxidation, highlighting their metabolic flexibility and similarity to members of the *Sulfurovum* (Sievert et al., 2008a; Grote et al., 2012). A key trait of all known isolates of both genera is that they cannot grow at 100% oxygen saturation; they are all described as facultative anaerobes (Inagaki et al., 2004; Takai et al., 2006). These two closely-related genera of *Epsilonproteobacteria* are likely occupying the same subseafloor habitat, but the *soxB*

gene data suggests dominance of *Sulfurimonas* in active sulfur oxidation via the Sox pathway.

The *soxB* gene was not successfully amplified from either the DNA or RNA fraction of the Pompeii site. 16S rRNA profiles show *Sulfurimonas* and *Sulfurovum* are present at this site (Figure 4), and the geochemical conditions are within the range of growth of these organisms, therefore it is not clear why *soxB* did not amplify from these samples. In addition, the examination of *Sulfurimonas* and *Sulfurovum* 16S rRNA gene OTUs did not reveal any patterns specific to these populations at Pompeii and the reason for the lack of *soxB* detection at this site remains unknown.

At 9 m, the *soxB* gene was not amplified from the RNA fraction, although *soxB* was detected in the DNA library. This is likely attributed to the high temperature (maximum 51.3°C) of this metal-sulfide chimney site. Above ~40°C, sulfur oxidation is not favored due to severe oxygen limitation (McCollom and Shock, 1997; Butterfield et al., 2004), and known growth optima of all known cultures within *Sulfurimonas* and *Sulfurovum* are below 40°C (Inagaki et al., 2004; Takai et al., 2006). This site also had the lowest pH (4.8), which is still within the range of growth for *Sulfurovum lithotrophicum* (Inagaki et al., 2004), but outside of the range of growth for *Sulfurimonas paralvinellae* (Takai et al., 2006). A combination of low pH and high temperature likely contributes to the lack of *soxB* gene transcripts detected at this site.

At Gollum, the *soxB* genes and gene transcripts from the DNA and RNA fractions had very different signatures, with diverse

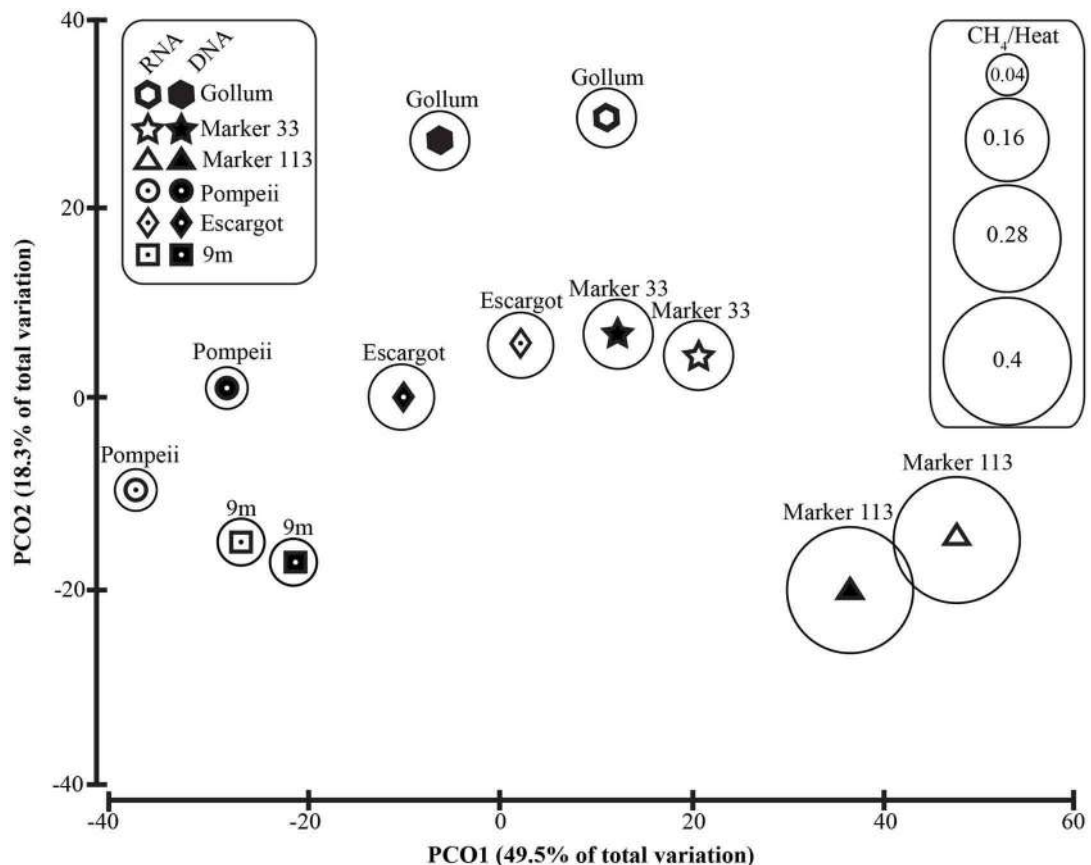


**FIGURE 6 |** Principal coordinates analysis of all 96% Epsilonproteobacterial 16S rRNA gene OTUs with CH<sub>4</sub>/Heat ratios shown in bubbles surrounding symbols.

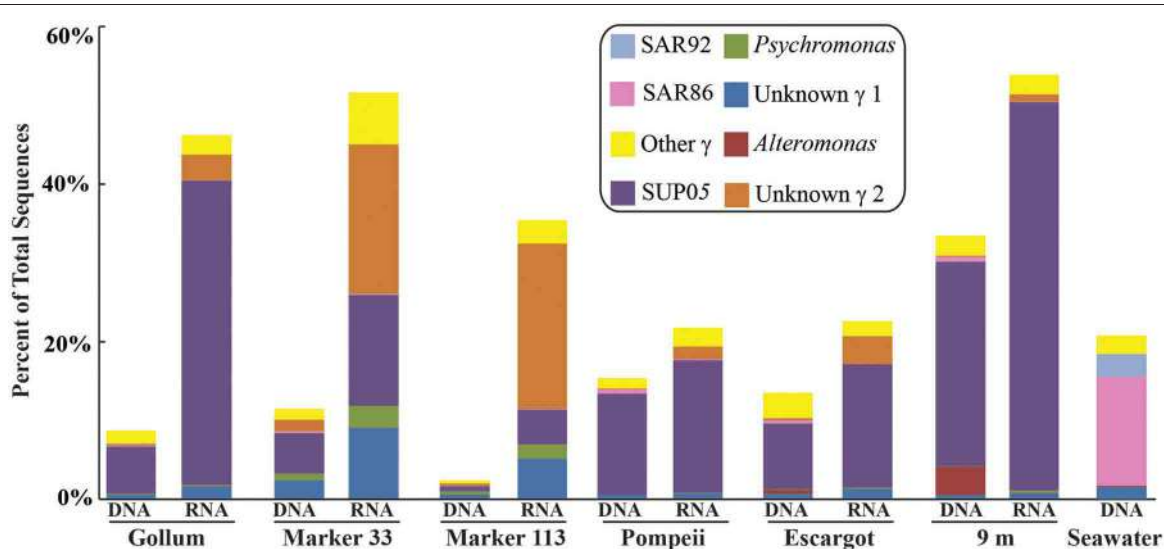


**FIGURE 7 |** Taxonomic breakdown and relative abundance of dominant *Gammaproteobacteria* at the genus level for 96% 16S rRNA gene OTUs in each sample. All other *Gammaproteobacteria* sequences are lumped into "Other."

*Sulfurovum*-like OTUs dominating the DNA fraction and a single *Sulfurimonas*-like OTU comprising almost the entire RNA fraction. In fact, the RNA profiles of *soxB* gene transcripts were nearly identical among the four vent fluid samples where *soxB* amplified and suggest that *Sulfurimonas*-like species are out-competing *Sulfurovum* in actively oxidizing sulfur via the Sox pathway in the subseafloor beneath each vent (**Figure 2**). Significant correlation between sulfide and proportions of *Sulfurovum* has previously been seen in diffuse fluids based on 16S rRNA gene sequencing (Perner et al., 2013), but here there were no statistically significant correlations in this genus with chemistry from either the 454 16S rRNA or *soxB* gene data. However, Gollum has the lowest concentration of hydrogen sulfide (84 μM, **Table 1**), as well as the lowest H<sub>2</sub>S/Heat ratio, suggesting low sulfide levels may favor the presence of *Sulfurovum* carrying the *soxB* gene. But given that all RNA profiles are dominated by Slms-1, there does not appear to be any correlation with respect to expression of *soxB* genes and sulfide to heat ratios or any other chemical variables.

Unlike recent work in terrestrial springs on sulfur oxidation genes (Headd and Engel, 2013), there is no evidence of niche partitioning in the active communities of *Epsilonproteobacteria* expressing the *soxB* gene. However, when examining all of the *Epsilonproteobacteria* 16S rRNA gene sequences (**Figure 6**), there was significant groupings related to the individual vent sampled and the type of vent (basalt or sulfide), highlighting the importance of physical isolation in helping to maintain stable microbial communities in the subseafloor (Huber et al., 2006, 2010; Opatkiewicz et al., 2009). There were also significant groupings of samples that correlated with chemical variables. The most significant correlation was with methane. Those vents high in methane are often conversely low in hydrogen (**Figure 6, Table 1**), suggesting hydrogen is being drawn down and methane generated by hydrogen-utilizing methanogens (Butterfield et al., 2004; Ver Eecke et al., 2012). At Marker 113, where the highest methane concentrations were seen, methanogenic archaea belonging to the genera *Methanocaldococcus*, *Methanococcus*, and *Methanothermococcus* were detected with the universal bacterial primer set, consistent with previous work at Marker 113 that showed hydrogenotrophic methanogens are abundant and active at this site (Ver Eecke et al., 2012).

There are no known *Epsilonproteobacteria* that use or generate methane, but many use hydrogen as an electron donor, including *Caminibacter* and *Nautilia* within the *Nautiliaceae* (Campbell et al., 2006). A higher relative abundance of tag sequences corresponding to these two genera were detected at Pompeii, Escargot, and 9 m, and these samples were all collected from the sides of sulfide chimneys that had among the highest hydrogen concentrations (**Table 1, Figure 4**), suggesting the combination of geological structure and chemistry may favor these thermophilic, hydrogen-utilizing, sulfur-reducing *Epsilonproteobacteria*. This probably reflects the different niches these organisms occupy. *Sulfurimonas* and *Sulfurovum* are likely living in the more shallow, cool subseafloor where microaerobic niches exist, whereas members of the *Nautiliaceae* are likely residing further beneath the seafloor or in walls of sulfide chimneys in warm, anaerobic niches with enriched hydrogen. However, despite the overall structuring of the *Epsilonproteobacterial* microbial community

revealed by 16S rRNA gene sequencing, no patterns of the functional *soxB* gene were seen, suggesting that different lineages at each vent may be carrying out similar metabolic functions.

In addition to examining community patterns and gene expression of subseafloor *Epsilonproteobacteria*, the side-by-side comparison of 16S rRNA gene patterns from DNA and RNA revealed that *Gammaproteobacteria* were present and active at all Axial Seamount vent sites (**Table 4**). The most abundant and active OTU belonged to the SUP05 clade, a ubiquitous group of bacteria frequently found in symbiotic association with hydrothermal vent animals (Newton et al., 2007) as well as in hydrothermal plumes, non-plume deep-sea water (Sunamura et al., 2004; Anantharaman et al., 2013; Dick et al., 2013), and oxygen minimum zones (Lavik et al., 2009; Walsh et al., 2009). Recent quantitative PCR data in low-temperature diffuse vents from Axial Seamount and Endeavour Segment also indicates SUP05 constitute up to 38% of all bacteria in some vent fluids (Bourbonnais et al., 2012; Anderson et al., 2013). There are no SUP05 from the deep sea in culture, but metagenomic and metatranscriptomic datasets indicate they are obligate autotrophs capable of sulfur and hydrogen oxidation, nitrate reduction, as well as storage of sulfur in globules (Walsh et al., 2009; Wright et al., 2012; Anantharaman et al., 2013). Active transcripts of multiple sulfur oxidation genes have even been detected in background seawater (Anantharaman et al., 2013), and while one metagenomic study suggests they are facultative anaerobes or strict anaerobes (Walsh et al., 2009), another suggests they can use oxygen in both fully aerobic and microaerobic conditions (Anantharaman et al., 2013).

There were a small number of sequences belonging to the SUP05 clade in the background seawater sample, and they were highly enriched in vent fluid samples, particularly the RNA fractions. However, when the Gammaproteobacterial 16S rRNA gene OTUs were analyzed, there were similar patterns to those seen when all OTUs were considered (**Figure 5**). This suggests that SUP05 are not vent-endemic or living in the subseafloor, but instead originate from background seawater and are enriched where the oxygen-rich deep seawater mixes with hydrogen sulfide-rich vent fluids in the very shallow subseafloor or as they exit the seafloor at the point of sampling. In contrast, the *Epsilonproteobacteria* sampled are being entrained into vent fluids from beneath the seafloor, where microaerobic and anaerobic pockets exist. Because the samples are being fixed immediately after filtration, those organisms active closer to the point of sampling will be over-represented in the RNA fraction. Organisms abundant within the seafloor will also be captured, but their activity will likely not be as representative of their *in situ* activity, given the unknown length of time for fluids and their resident microbes to travel from their particular subseafloor niche to the seafloor.

Many challenges remain in elucidating the subseafloor microbial ecosystem, but the coupled phylogenetic and functional gene analysis of DNA and RNA from low temperature diffuse vent fluids allows for a fuller picture of what may be occurring both at and within the seafloor at deep-sea hydrothermal vents. The detection of *soxB* gene transcripts shows there are active sulfur-oxidizing *Epsilonproteobacteria* within the subseafloor at Axial Seamount,

mostly belonging to the genus *Sulfurimonas*. The 16S rRNA data suggests SUP05 are extremely active in the shallow subseafloor or at the seafloor where fluids are exiting from the crust and mixing with background seawater, the likely habitat of these organisms. Within the seafloor, it is predicted that *Epsilonproteobacteria* are the main sulfur oxidizers, given their ability to tolerate very low oxygen concentrations and use sulfur compounds as both electron acceptors and donors (Inagaki et al., 2004; Yamamoto and Takai, 2011). These results are consistent with previous work by Yamamoto and Takai (2011) and Anderson et al. (2013) suggesting that *Gammaproteobacteria* dominate when both oxygen and reduced sulfur compounds are steadily supplied but once oxygen begins to disappear, *Epsilonproteobacteria* have greater physiological and metabolic flexibility and potential to occupy diverse vent niches, especially in the subseafloor. Targeted functional approaches that focus on activity and expression of particular metabolic pathways, such as the primers developed here

combined with incubation experiments or *in situ* studies, will help elucidate how these organisms differentiate into their respective niches and contribute to the biogeochemical cycling of sulfur and carbon both in the deep sea and subseafloor.

## ACKNOWLEDGMENTS

We thank the crews of the R/V *Thomas G. Thompson* and ROV *Jason II* for their assistance with fieldwork, and Kevin K. Roe, Hoang-My Christensen, Marvin Lilley, and Eric Olson for chemical analyses. This work was supported by a NASA Astrobiology Postdoctoral Program Fellowship to Nancy H. Akerman and grants from the NSF Division of Ocean Sciences to Julie A. Huber (OCE-0929167) and David A. Butterfield (OCE-0731947 and OCE-0926199), and by the Joint Institute for the Study of the Atmosphere and Ocean (JISAO contribution #2073, PMEL contribution #3984) under NOAA Cooperative Agreement No. NA17RJ1232.

## REFERENCES

- Amend, J. P., McCollom, T. M., Hentscher, M., and Bach, W. (2011). Catabolic and anabolic energy for chemolithoautotrophs in deep-sea hydrothermal systems hosted in different rock types. *Geochim. Cosmochim. Acta* 75, 5736–5748. doi: 10.1016/j.gca.2011.07.041
- Anantharaman, K., Breier, J. A., Sheik, C. S., and Dick, G. J. (2013). Evidence for hydrogen oxidation and metabolic plasticity in widespread deep-sea sulfur-oxidizing bacteria. *Proc. Natl. Acad. Sci. U.S.A.* 110, 330–335. doi: 10.1073/pnas.1215340110
- Anderson, R. E., Beltrán, M. T., Hallam, S. J., and Baross, J. A. (2013). Microbial community structure across fluid gradients in the Juan de Fuca Ridge hydrothermal system. *FEMS Microbiol. Ecol.* 83, 324–339. doi: 10.1111/j.1574-6941.2012.01478.x
- Bonch-Osmolovskaya, E. A., Perevalova, A. A., Kolganova, T. V., Rusanov, I. I., Jeanthon, C., and Pimenov, N. V. (2011). Activity and distribution of thermophilic prokaryotes in hydrothermal fluid, sulfidic structures, and sheaths of Alvinellids (East Pacific Rise, 13N). *Appl. Environ. Microbiol.* 77, 2803–2806. doi: 10.1128/AEM.02266-10
- Bourbonnais, A., Juniper, S. K., Butterfield, D. A., Devol, A. H., Kuypers, M. M. M., Lavik, G., et al. (2012). Activity and abundance of denitrifying bacteria in the subsurface biosphere of diffuse hydrothermal vents of the Juan de Fuca Ridge. *Biogeosciences* 9, 4661–4678. doi: 10.5194/bg-9-4661-2012
- Boyce, R., Chilana, P., and Rose, T. M. (2009). iCODEHOP: a new interactive program for designing COnsensus-DEgenerate hybrid oligonucleotide primers from multiply aligned protein sequences. *Nucleic Acids Res.* 37, W222–W228. doi: 10.1093/nar/gkp379
- Butterfield, D. A., Roe, K. K., Lilley, M. D., Huber, J. A., Baross, J. A., Embley, R. W., et al. (2004). “Mixing, reaction, and microbial activity in the sub-seafloor revealed by temporal and spatial variation in diffuse flow vents at Axial Volcano,” in *The Subseafloor Biosphere at Mid-Ocean Ridges*, eds W. S. D. Wilcock, E. F. DeLong, D. S. Kelley, J. A. Baross, and S. C. Cary (Washington, DC: American Geophysical Union), 269–289. doi: 10.1029/144GM17
- Campbell, B. J., Engel, A. S., Porter, M. L., and Takai, K. (2006). The versatile ε-proteobacteria: key players in sulphidic habitats. *Nat. Rev. Microbiol.* 4, 458–468. doi: 10.1038/nrmicro1414
- Clarke, K. R., and Gorley, R. N. (2006). PRIMER v6: user manual/tutorial. *PRIMER-E*.
- Cowen, J. P., Copson, D. A., Jolly, J., Hsieh, C.-C., Lin, H.-T. T., Glazer, B. T., et al. (2012). Advanced instrument system for real-time and time-series microbial geochemical sampling of the deep (basaltic) crustal biosphere. *Deep Sea Res. Part I* 61, 43–56. doi: 10.1016/j.dsr.2011.11.004
- Dick, G. J., Anantharaman, K., Baker, B. J., Li, M., Reed, D. C., and Sheik, C. S. (2013). Hydrothermal vent plume microbiology: ecological and biogeographic linkages to seafloor and water column habitats. *Front. Microbiol.* 4:124. doi: 10.3389/fmicb.2013.00124
- Edgar, R. C. (2010). Search and clustering orders of magnitude faster than BLAST. *Bioinformatics* 26, 2460–2461. doi: 10.1093/bioinformatics/btq461
- Embley, R. W., Murphy, K. M., and Fox, C. G. (1990). High-resolution studies of the summit of Axial Volcano. *J. Geophys. Res.* 95, 12785–12812. doi: 10.1029/JB095iB08p12785
- Felsenstein, J. (1989). PHYLIP – Phylogeny inference package. *Cladistics* 5, 164–166.
- Filkins, L. M., Hampton, T. H., Gifford, A. H., Gross, M. J., Hogan, D. A., Sogin, M. L., et al. (2012). The prevalence of *Streptococci* and increased polymicrobial diversity associated with cystic fibrosis patient stability. *J. Bacteriol.* 194, 4709–4717. doi: 10.1128/JB.00566-12
- Fredslund, J., Schauser, L., Madsen, L. H., Sandal, N., and Stougaard, J. (2005). PriFi: using a multiple alignment of related sequences to find primers for amplification of homologs. *Nucleic Acids Res.* 33, W516–W520. doi: 10.1093/nar/gki425
- Friedrich, C. G., Bardishevsky, F., Rother, D., Quentmeier, A., and Fischer, J. (2005). Prokaryotic sulfur oxidation. *Curr. Opin. Microbiol.* 8, 253–259. doi: 10.1016/j.mib.2005.04.005
- Friedrich, C. G., Rother, D., Quentmeier, A., Fischer, J., and Bardishevsky, F. (2001). Oxidation of reduced inorganic sulfur compounds by bacteria: emergence of a common mechanism? *Appl. Environ. Microbiol.* 67, 2873–2880. doi: 10.1128/AEM.67.7.2873-2880.2001
- Gadberry, M. D., Malcomber, S. T., Doust, A. N., and Kellogg, E. A. (2005). Primaclade—a flexible tool to find conserved PCR primers across multiple species. *Bioinformatics* 21, 1263–1264. doi: 10.1093/bioinformatics/bti134
- Grote, J., Labrenz, M., Pfeiffer, B., Jost, G., and Jurgens, K. (2007). Quantitative distributions of *Epsilonproteobacteria* and a *Sulfurimonas* subgroup in pelagic redoxclines of the Central Baltic Sea. *Appl. Environ. Microbiol.* 73, 7155–7161. doi: 10.1128/AEM.00466-07
- Grote, J., Schott, T., Bruckner, C. G., Oliver, F., Jost, G., and Teeling, H. (2012). Genome and physiology of a model *Epsilonproteobacterium* responsible for sulfide detoxification in marine oxygen depletion zones. *Proc. Natl. Acad. Sci. U.S.A.* 109, 506–510. doi: 10.1073/pnas.1111262109
- Headd, B., and Engel, A. S. (2013). Evidence for niche partitioning revealed by the distribution of sulfur oxidation genes collected from areas of a terrestrial sulfidic spring with differing geochemical conditions. *Appl. Environ. Microbiol.* 79, 1171–1182. doi: 10.1128/AEM.02812-12
- Hoor, A. T.-T. (1975). A new type of thiosulphate oxidizing, nitrate reducing microorganism: *Thiomicrospira denitrificans* sp. Nov. *Neth. J. Sea Res.* 9, 344–346. doi: 10.1016/0077-7579(75)90008-3
- Horn, H. S. (1966). Measurement of “overlap” in comparative ecological studies. *Am. Nat.* 100, 419–424. doi: 10.1086/282436
- Huber, J. A., Butterfield, D. A., and Baross, J. A. (2002). Temporal

- changes in archaeal diversity and chemistry in a mid-ocean ridge subseafloor habitat. *Appl. Environ. Microbiol.* 68, 1585–1594. doi: 10.1128/AEM.68.4.1585-1594.2002
- Huber, J. A., Butterfield, D. A., and Baross, J. A. (2003). Bacterial diversity in a subseafloor habitat following a deep-sea volcanic eruption. *FEMS Microbiol. Ecol.* 43, 393–409. doi: 10.1111/j.1574-6941.2003.tb01080.x
- Huber, J. A., Butterfield, D. A., and Baross, J. A. (2006). Diversity and distribution of subseafloor Thermococcales populations in diffuse hydrothermal vents at an active deep-sea volcano in the northeast Pacific Ocean. *J. Geophys. Res.* 111, 1–13. doi: 10.1029/2005JC000097
- Huber, J. A., Morrison, H. G., Huse, S. M., Neal, P. R., Sogin, M. L., and Mark Welch, D. B. (2009). Effect of PCR amplicon size on assessments of clone library microbial diversity and community structure. *Environ. Microbiol.* 11, 1292–1302. doi: 10.1111/j.1462-2920.2008.01857.x
- Huber, J. A., Cantin, H. V., Huse, S. M., Welch, D. B. M., Sogin, M. L., Butterfield, D. A., et al. (2010). Isolated communities of *Epsilonproteobacteria* in hydrothermal vent fluids of the Mariana Arc seamounts. *FEMS Microbiol. Ecol.* 73, 538–549.
- Huber, J. A., Mark Welch, D. B., Morrison, H. G., Huse, S. M., Neal, P. R., Butterfield, D. A., et al. (2007). Microbial population structures in the deep marine biosphere. *Science* 318, 97–100. doi: 10.1126/science.1146689
- Hügler, M., Gärtner, A., Imhoff, F. J., and Imhoff, J. F. (2010). Functional genes as markers for sulfur cycling and CO<sub>2</sub> fixation in microbial communities of hydrothermal vents of the Logatchev field. *FEMS Microbiol. Ecol.* 73, 526–537.
- Huse, S. M., Dethlefsen, L., Huber, J. A., Welch, D. M., Relman, D. A., and Sogin, M. L. (2008). Exploring microbial diversity and taxonomy using SSU rRNA hypervariable tag sequencing. *PLoS Genet.* 4:e1000255. doi: 10.1371/journal.pgen.1000255
- Inagaki, F., Takai, K., Kobayashi, H., Nealson, K. H., and Horikoshi, K. (2003). *Sulfurimonas autotrophica* gen. nov., sp. nov., a novel sulfur-oxidizing epsilon-proteobacterium isolated from hydrothermal sediments in the Mid-Okinawa Trough. *Int. J. Syst. Evol. Microbiol.* 53, 1801–1805. doi: 10.1099/ijss.0.02682-0
- Inagaki, F., Takai, K., Nealson, K. H., and Horikoshi, K. (2004). *Sulfurovum lithotrophicum* gen. nov., sp. nov., a novel sulfur-oxidizing chemolithoautotroph within the e-Proteobacteria isolated from Okinawa Trough hydrothermal sediments. *Int. J. Syst. Evol. Microbiol.* 54, 1477–1482. doi: 10.1099/ijss.0.03042-0
- Jannasch, H. W., and Mottl, M. J. (1985). Geomicrobiology of deep-sea hydrothermal vents. *Science* 229, 717–725. doi: 10.1126/science.229.4715.717
- Jones, S. E., and Lennon, J. T. (2010). Dormancy contributes to the maintenance of microbial diversity. *Proc. Natl. Acad. Sci. U.S.A.* 107, 5881–5886. doi: 10.1073/pnas.0912765107
- Kappler, U., and Dahl, C. (2001). Enzymology and molecular biology of prokaryotic sulfite oxidation. *FEMS Microbiol. Lett.* 203, 1–9.
- Lavik, G., Stuurmann, T., Bruchert, V., Van der Plas, A., Mohrholz, V., Lam, P., et al. (2009). Detoxification of sulphidic African shelf waters by blooming chemolithotrophs. *Nature* 457, 581–585. doi: 10.1038/nature07588
- McCormick, T. M., and Shock, E. L. (1997). Geochemical constraints on chemolithoautotrophic metabolism by microorganisms in seafloor hydrothermal systems. *Geochim. Cosmochim. Acta* 61, 4375–4391. doi: 10.1016/S0016-7037(97)00241-X
- Meyer, B., and Kuever, J. (2007). Molecular analysis of the diversity of sulfate-reducing and sulfur-oxidizing prokaryotes in the environment, using aprA as functional marker gene. *Appl. Environ. Microbiol.* 73, 7664–7679. doi: 10.1128/AEM.01272-07
- Meyer, B., Imhoff, J. F., and Kuever, J. (2007). Molecular analysis of the distribution and phylogeny of the soxB gene among sulfur-oxidizing bacteria-evolution of the Sox sulfur oxidation enzyme system. *Environ. Microbiol.* 9, 2957–2977. doi: 10.1111/j.1462-2920.2007.01407.x
- Meyer, J. L., Akerman, N. H., Proskurowski, G., and Huber, J. A. (2013). Microbiological characterization of post-eruption “snowblower” vents at Axial Seamount, Juan de Fuca Ridge. *Front. Microbiol.* 4:153. doi: 10.3389/fmicb.2013.00153
- Nakagawa, S., and Takai, K. (2008). Deep-sea vent chemoautotrophs: diversity, biochemistry and ecological significance. *FEMS Microbiol. Ecol.* 65, 1–14. doi: 10.1111/j.1574-6941.2008.00502.x
- Nakagawa, S., Takaki, Y., Shimamura, S., Reysenbach, A., and Takai, K. (2007). Deep-sea vent epsilonproteobacterial genomes provide insights into emergence of pathogens. *Proc. Natl. Acad. Sci. U.S.A.* 104, 12,146–12,150. doi: 10.1073/pnas.0700687104
- Newton, I. L. G., Woyke, T., Achtung, T. A., Dilly, G. F., Dutton, R. J., Fisher, M. C., et al. (2007). The *Calyptogena magnifica* chemoautotrophic symbiont genome. *Science* 315, 998–1000. doi: 10.1126/science.1138438
- Opatakiewicz, A. D., Butterfield, D. A., and Baross, J. A. (2009). Individual hydrothermal vents at Axial Seamount harbor distinct subseafloor microbial communities. *FEMS Microbiol. Ecol.* 70, 413–424. doi: 10.1111/j.1574-6941.2009.00747.x
- Orcutt, B. N., Sylvan, J. B., Knab, N. J., and Edwards, K. J. (2011). Microbial ecology of the dark ocean above, at, and below the seafloor. *Microbiol. Mol. Biol. Rev.* 75, 361–422. doi: 10.1128/MMBR.00039-10
- Park, S.-J., Ghai, R., Martin-Cuadrado, A.-B., Rodriguez-Valera, F., Jung, M.-Y., Kim, J.-G., et al. (2012). Draft genome sequence of the sulfur-oxidizing bacterium “*Candidatus Sulfurovum sediminum*” AR, which belongs to the *Epsilonproteobacteria*. *J. Bacteriol.* 194, 4128–4129. doi: 10.1128/JB.00741-12
- Perner, M., Gonnella, G., Hourdez, S., Böhnke, S., Kurtz, S., and Girguis, P. (2013). In situ chemistry and microbial community compositions in five deep-sea hydrothermal fluid samples from Irina II in the Logatchev field. *Environ. Microbiol.* 15, 1551–1560. doi: 10.1111/1462-2920.12038
- Petri, R., Lilijana, P., and Johannes, F. I. (2001). Phylogeny and distribution of the soxB gene among thiosulfate-oxidizing bacteria. *FEMS Microbiol. Lett.* 197, 171–178. doi: 10.1111/j.1574-6968.2001.tb10600.x
- Rice, P., Longden, I., and Bleasby, A. (2000). EMBOSS: the European molecular biology open software suite. *Trends Genet.* 16, 276–277. doi: 10.1016/S0168-9525(00)02042-2
- Roalkvam, I., Jørgensen, S. L., Chen, Y., Stokke, R., Dahle, H., Hocking, W. P., et al. (2011). New insight into stratification of anaerobic methanotrophs in cold seep sediments. *FEMS Microbiol. Ecol.* 78, 233–243. doi: 10.1111/j.1574-6941.2011.01153.x
- Rose, T. (2003). CODEHOP (COnsensus-D Eggerate hybrid oligonucleotide primer) PCR primer design. *Nucleic Acids Res.* 31, 3763–3766. doi: 10.1093/nar/gkg524
- Schloss, P. D., Westcott, S. L., Ryabin, T., Hall, J. R., Hartmann, M., Hollister, E. B., et al. (2009). Introducing mothur: open-source, platform-independent, community-supported software for describing and comparing microbial communities. *Appl. Environ. Microbiol.* 75, 7537–7541. doi: 10.1128/AEM.01541-09
- Sievert, S. M., Hugler, M., Taylor, C. D., and Wirsén, C. O. (2008a). “Sulfur oxidation at deep-sea hydrothermal vents,” in *Microbial Sulfur Metabolism*, eds C. Dahl and C. G. Friedrich (New York, NY: Springer), 238–258. doi: 10.1007/978-3-540-72682-1\_19
- Sievert, S. M., Scott, K. M., Klotz, M. G., Chain, P. S. G., Hauser, L. J., Hemp, J., et al. (2008b). Genome of the epsilonproteobacterial chemolithoautotroph *Sulfurimonas denitrificans*. *Appl. Environ. Microbiol.* 74, 1145–1156. doi: 10.1128/AEM.01844-07
- Sikorski, J., Christine, M., Alla, L., Olivier Ngatchou, D., Susan, L., Tijana Glavina Del, R., et al. (2010). Complete genome sequence of *Sulfurimonas autotrophica* type strain (OK10T). *Stand. Genom. Sci.* 3, 194–202.
- Sogin, M. L., Morrison, H. G., Huber, J. A., Mark Welch, D. Huse, S. M., Neal, P. R., et al. (2006). Microbial diversity in the deep sea and the underexplored “rare biosphere”. *Proc. Natl. Acad. Sci. U.S.A.* 103, 12115–12120. doi: 10.1073/pnas.0605127103
- Sunamura, M., Higashi, Y., Miyako, C., Ishibashi, J., and Maruyama, A. (2004). Two bacteria phylotypes are predominant in the Suiyo Seamount hydrothermal plume. *Appl. Environ. Microbiol.* 70, 1190–1198. doi: 10.1128/AEM.70.2.1190-1198.2004
- Swan, B. K., Martinez-Garcia, M., Preston, C. M., Sczyrba, A., Woyke, T., Lamy, D., et al. (2011). Potential for chemolithoautotrophy among ubiquitous bacteria lineages in the dark ocean. *Science* 333, 1296–1300. doi: 10.1126/science.1203690
- Takai, K., Suzuki, M., Nakagawa, S., Miyazaki, M., Suzuki, Y., Inagaki, F., et al. (2006). *Sulfurimonas paralvinellae* sp. nov., a novel mesophilic,

- hydrogen- and sulfur-oxidizing chemolithoautotroph within the Epsilonproteobacteria isolated from a deep-sea hydrothermal vent polychaete nest, reclassification of *Thiomicrospira denitrificans* as *Sulfurimonas denitrificans* comb. nov. and emended description of the genus *Sulfurimonas*. *Int. J. Syst. Evol. Microbiol.* 56, 1725–1733. doi: 10.1099/ijts.0.64255-0
- Tamura, K., Dudley, J., Nei, M., and Kumar, S. (2007). MEGA4: molecular evolutionary genetics analysis (MEGA) software version 4.0. *Mole. Biol. Evol.* 24, 1596–1599. doi: 10.1093/molbev/msm092
- Ver Eecke, H. C., Butterfield, D. A., Huber, J. A., Lilley, M. D., Olson, E. J., Roe, K. K., et al. (2012). Hydrogen-limited growth of hyperthermophilic methanogens at deep-sea hydrothermal vents. *Proc. Natl. Acad. Sci. U.S.A.* 109, 13674–13679. doi: 10.1073/pnas.1206632109
- Walsh, D. A., Zaikova, E., Howes, C. G., Song, Y. C., Wright, J. J., Tringe, S. G., et al. (2009). Metagenome of a versatile chemolithoautotroph from expanding oceanic dead zones. *Science* 326, 578–582. doi: 10.1126/science.1175309
- Wright, J. J., Konwar, K. M., and Hallam, S. J. (2012). Microbial ecology of expanding oxygen minimum zones. *Nat. Rev. Microbiol.* 10, 381–394.
- Yamamoto, M., Satoshi, N., Shigeru, S., Takai, K., and Horikoshi, K. (2010). Molecular characterization of inorganic sulfur-compound metabolism in the deep-sea epsilonproteobacterium *Sulfurovum* sp. NBC37-1. *Environ. Microbiol.* 12, 1144–1153. doi: 10.1111/j.1462-2920.2010.02155.x
- Yamamoto, M., and Takai, K. (2011). Sulfur metabolism in epsilon- and gamma-proteobacteria in deep-sea hydrothermal fields. *Front. Microbiol.* 2:192. doi: 10.3389/fmicb.2011.00192
- Zhang, Y., Zhao, Z., Chen, C.-T. A., Tang, K., Su, J., and Jiao, N. (2012). Sulfur metabolizing microbes dominate microbial communities in andesite-hosted shallow-sea hydrothermal systems. *PLoS ONE* 7:e44593. doi: 10.1371/journal.pone.0044593
- Conflict of Interest Statement:** The authors declare that the research was conducted in the absence of any commercial or financial relationships that could be construed as a potential conflict of interest.

Received: 16 February 2013; accepted: 18 June 2013; published online: 08 July 2013.

Citation: Akerman NH, Butterfield DA and Huber JA (2013) Phylogenetic diversity and functional gene patterns of sulfur-oxidizing subseafloor Epsilonproteobacteria in diffuse hydrothermal vent fluids. *Front. Microbiol.* 4:185. doi: 10.3389/fmicb.2013.00185

This article was submitted to Frontiers in Extreme Microbiology, a specialty of Frontiers in Microbiology.

Copyright © 2013 Akerman, Butterfield and Huber. This is an open-access article distributed under the terms of the Creative Commons Attribution License, which permits use, distribution and reproduction in other forums, provided the original authors and source are credited and subject to any copyright notices concerning any third-party graphics etc.



# The pH and pCO<sub>2</sub> dependence of sulfate reduction in shallow-sea hydrothermal CO<sub>2</sub> – venting sediments (Milos Island, Greece)

Elisa Bayraktarov<sup>1\*</sup>, Roy E. Price<sup>2†</sup>, Timothy G. Ferdelman<sup>1,2</sup> and Kai Finster<sup>3,4</sup>

<sup>1</sup> Department of Biogeochemistry, Max Planck Institute for Marine Microbiology, Bremen, Germany

<sup>2</sup> Center for Marine Environmental Sciences, Bremen, Germany

<sup>3</sup> Department of Biosciences, Section for Microbiology, University of Aarhus, Aarhus C, Denmark

<sup>4</sup> Department of Physics and Astronomy, Stellar Astrophysics Centre, University of Aarhus, Aarhus C, Denmark

## Edited by:

Andreas Teske, University of North Carolina at Chapel Hill, USA

## Reviewed by:

Tim Magnuson, Idaho State University, USA

Julia Maresca, University of Delaware, USA

## \*Correspondence:

Elisa Bayraktarov, Department of Ecology, Leibniz Center for Tropical Marine Ecology, Fahrenheitstraße 6, 28359 Bremen, Germany.  
e-mail: elisa.bayraktarov@zmt-bremen.de

## †Present address:

Elisa Bayraktarov, Department of Ecology, Leibniz Center for Tropical Marine Ecology, Fahrenheitstraße 6, 28359 Bremen, Germany;

Roy E. Price, Department of Earth Sciences, University of Southern California, Los Angeles, CA, USA.

Microbial sulfate reduction (SR) is a dominant process of organic matter mineralization in sulfate-rich anoxic environments at neutral pH. Recent studies have demonstrated SR in low pH environments, but investigations on the microbial activity at variable pH and CO<sub>2</sub> partial pressure are still lacking. In this study, the effect of pH and pCO<sub>2</sub> on microbial activity was investigated by incubation experiments with radioactive <sup>35</sup>S targeting SR in sediments from the shallow-sea hydrothermal vent system of Milos, Greece, where pH is naturally decreased by CO<sub>2</sub> release. Sediments differed in their physicochemical characteristics with distance from the main site of fluid discharge. Adjacent to the vent site ( $T \sim 40-75^\circ\text{C}$ , pH ~5), maximal sulfate reduction rates (SRR) were observed between pH 5 and 6. SR in hydrothermally influenced sediments decreased at neutral pH. Sediments unaffected by hydrothermal venting ( $T \sim 26^\circ\text{C}$ , pH ~8) expressed the highest SRR between pH 6 and 7. Further experiments investigating the effect of pCO<sub>2</sub> on SR revealed a steep decrease in activity when the partial pressure increased from 2 to 3 bar. Findings suggest that sulfate reducing microbial communities associated with hydrothermal vent system are adapted to low pH and high CO<sub>2</sub>, while communities at control sites required a higher pH for optimal activity.

**Keywords:** sulfate reduction, sulfate reduction rate, shallow-sea hydrothermal vents, pH effect, pCO<sub>2</sub> effect, microbial activity, extreme environment

## INTRODUCTION

Microbial sulfate reduction (SR) is a dominant process for the anaerobic degradation of organic material in marine sediments where organic carbon or hydrogen gas serve as the electron donors and are oxidized to CO<sub>2</sub> and water, while sulfate is reduced to hydrogen sulfide (Jørgensen, 1982). SR also plays an important role in deep-sea hydrothermal vent microbial processes, and has a significant impact on sulfur biogeochemistry at high temperatures (Jørgensen et al., 1992). The influence of temperature on SR is well documented (Isaksen et al., 1994; Knoblauch and Jørgensen, 1999; Finke and Jørgensen, 2008; Hubert et al., 2009). However, our understanding of the effects of pH and CO<sub>2</sub>, two important parameters that significantly impact microbial community structure and function is limited.

Submarine hydrothermal vents are well known for the extreme geochemical conditions that they impose on their inhabiting microbiota. Important selecting factors are low pH, high temperatures and high metal and sulfide concentrations in the hydrothermal fluids (Jannasch and Mottl, 1985; Frank et al., 2013). Furthermore, steep temperature gradients demand adaptations to variable temperature regimes. Cultivation-based studies have shown that sulfur compounds are important substrates for

microbes in hydrothermal vent systems (Jannasch and Mottl, 1985).

Most studies of sulfate reducing bacteria (SRB) have focused on environments at circumneutral pH including marine and freshwater sediments (Widdel, 1988; Hao et al., 1996). However, there is now increasing evidence for SR to occur also in low pH habitats, such as acidic lakes and rivers, acidic soils, peat lands, acid rock, or mine tailings (Koschorreck, 2008 and references therein). SR was also observed in hydrothermal systems where the pH is lowered due to CO<sub>2</sub> venting (Amend et al., 2004) but further knowledge on the activity of these microbial communities is limited. SR has a low yield of metabolic energy (Widdel, 1988). However, surprisingly SRB are active under acidic conditions where additional energy requirements to keep an elevated intracellular pH (Martin, 1990; Lowe et al., 1993), the toxicity of metabolic products (e.g., H<sub>2</sub>S or protonated fatty acids, Hao et al., 1996) and competition with other more resistant microbes (e.g., iron reducing bacteria or methanogens) may inhibit SR to occur (Koschorreck, 2008). Below a pH of 5, the metabolic product of SR is exclusively present in its undissociated form H<sub>2</sub>S which is considered as the most toxic form of sulfide (Moosa and Harrison, 2006). As uncharged gas, H<sub>2</sub>S permeates the cell membrane where it

can react with free metal ions and metal containing functional groups of the electron carrier system of the cell (Hao et al., 1996), amino acids and metabolic coenzymes inhibiting the functionality of the microbial cell (Koschorreck, 2008). Volatile fatty acids (VFA) are fermentation products of organic carbon and represent typical substrates of sulfate reducers. VFA exist as protonated organic acids under low pH. In their protonated form they can diffuse through the cytoplasmic membrane and act as “uncouplers” (Bruun et al., 2010) leading to a collapse of the membrane potential (Baronofsky et al., 1984). In addition, protonated organic acids decrease the pH of the cytoplasm upon entering by diffusion. Free intracellular protons can impair processes such as DNA transcription, protein synthesis, and enzyme activities (Baker-Austin and Dopson, 2007). In nature, intermediates of fermentation, e.g., VFA and H<sub>2</sub>, are generally maintained at low concentrations, showing a close coupling of terminal oxidation to fermentation (Finke and Jørgensen, 2008) counteracting an accumulation of acid and a subsequent decrease in pH.

In addition, SR at low pH is of special interest because this process can be applied for biogenic neutralization of acid rock drainage environments and for bioremediation (Kaksanen and Puhakka, 2007). The investigation of CO<sub>2</sub> venting hydrothermal sediments is of particular interest, as they represent a system in which the degassing-effects of previously sequestered CO<sub>2</sub> can be investigated (Shitashima et al., 2008). Based on all these implications further knowledge is necessary to understand the biological and chemical dynamics in acidified sediments.

This study was conducted on sediments collected from a shallow submarine hydrothermal vent system in the Aegean Sea near the island of Milos (Greece), and focuses on the effect of pH and pCO<sub>2</sub> on the activity of SRB. By incubation experiments involving the addition of electron donors and at different pH and pCO<sub>2</sub>, SR activities of hydrothermally influenced sediments were compared to activities in control sediments with higher pH and no CO<sub>2</sub> venting.

## MATERIALS AND METHODS

### STUDY SITE

The study site (36° 40' 25N, 24° 30' 58E; **Figure 1A**) was located ~1 m from an active gaseous hydrothermal vent system at 4.5 m water depth in Paleochori Bay, Milos Island, Greece. The bay is situated at the southeastern coast of Milos in the Aegean Sea (**Figure 1B**). Free gases sampled from the site (collected in 2011) had a mean gas composition of 92.5% CO<sub>2</sub>, 0.13% O<sub>2</sub>, 0.67% N<sub>2</sub>, 7 ppm He, 11450 ppm H<sub>2</sub>, 0.7 ppm CO, and 916 ppm CH<sub>4</sub> (Price et al., 2013, this issue). These free gas values can be used as an approximation for the discharged gases of the seep. The vent sites displayed a characteristic zonation of colored surface deposits surrounding the gas outlets (**Figure 2**). The sediment next to the vent was covered by a layer of bright yellow-orange deposits containing the arsenic sulfide minerals similar to orpiment (Price et al., 2012). A zone covered by white flocculent material on top of black sediment termed “white zone” surrounded this area. The white precipitate consists of a mixture of amorphous silica and native S (Fitzsimons et al., 1997). It is assumed that this precipitate is associated with microbial mat communities (Dando et al., 1995; Fitzsimons et al., 1997). The white zone was surrounded by an area

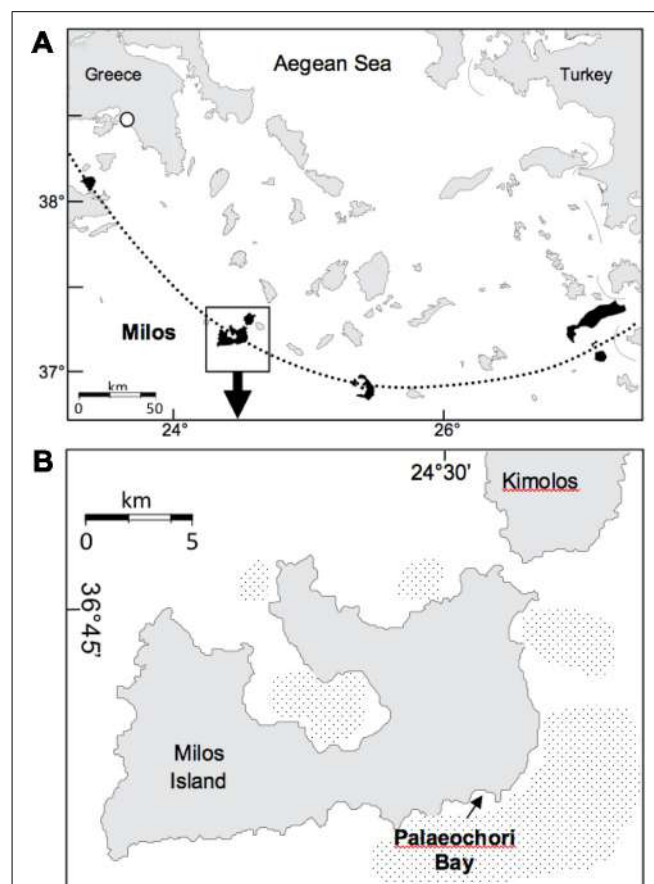


**FIGURE 1 | (A)** Location of Milos Island and other calc-alkaline volcanoes (shaded) along the Aegean Island Arc (dotted line). **(B)** Milos Island and the location of Palaeochori Bay. Stippled offshore areas around the island are mapped gas emissions by echo sounding (Dando et al., 1995). Maps modified from Price et al., 2012.

of gray sediment referred to as the “transition zone” and a brown background zone called the “brown zone” with hydrothermally unaffected sediment characteristics such as ambient temperature and pH. Sediments from the brown zone were used as a control.

### SAMPLING

Sampling was carried out along a transect through different sediment zones by SCUBA diving in August 2010. Sediments at increasing distance (ca. 1, 2, and 5 m) from the gas emission zone were sampled underwater with 1 L preserving jars (**Figure 2**; J. WECK GmbH & Co. KG, Wehr, Germany) containing a butyl rubber stopper which prevented the contamination of the sample with oxygen. Samples were maintained dark and cold during shipping. Temperature measurements were conducted *in situ* at a sediment depth of ~10 cm with a digital thermometer in a custom underwater housing (Fisher Scientific, Germany). The pH measurements integrated over 60 mL of sediment pore water. Measurements were performed ~1 h after sampling from a 10 cm sediment depth at the main sampling locations using 60 mL syringes elongated by tubing connected to long perforated pipette tips. Pore water from the white zone was sampled down

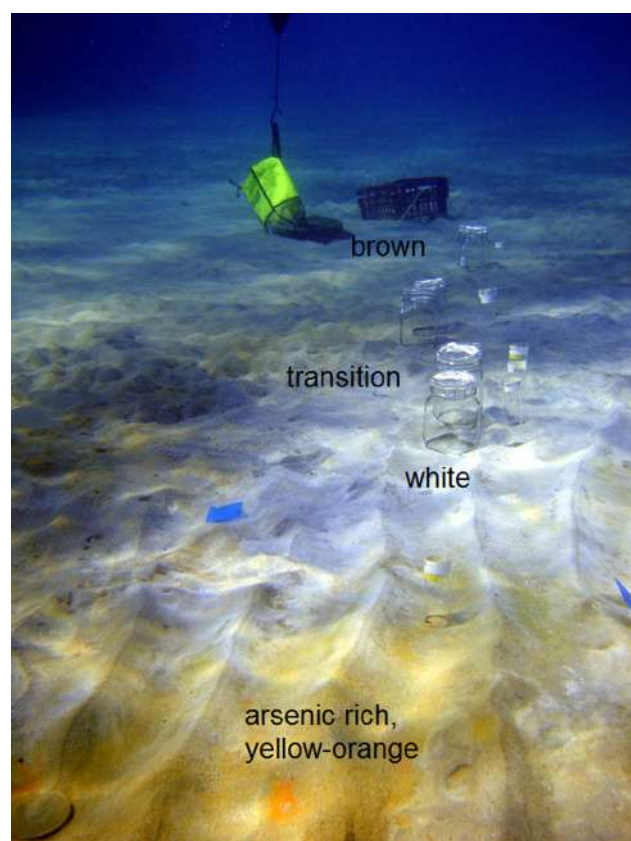


**FIGURE 2 |** Transect through the different zones of Paleochori Bay marked with sample bottles. Zones were divided in yellow-orange, white, transition, and brown. The yellow-orange zone was located adjacent to the venting site.

to 12 cm sediment depth at 2 cm resolution for analysis of sulfide, sulfate, alkalinity and pH using rhizone soil moisture samplers (5 and 10 cm rhizones, pore size: 0.1 m, Rhizon core solution sampler (CSS), Rhizosphere Research Products, The Netherlands). For sulfide analysis, pore water samples were fixed with an equal volume of 50 mmol L<sup>-1</sup> zinc acetate (ZnAc) solution.

#### PHYSICOCHEMICAL MEASUREMENTS

Pore water sulfide fixed with ZnAc was analyzed spectrophotometrically according to Cline (1969). Concentrations of SO<sub>4</sub><sup>2-</sup> were measured on a Metrohm Compact 761 ion chromatograph equipped with a Metrohm Metrosep A column. The eluent was a 3.2 mmol L<sup>-1</sup> Na<sub>2</sub>CO<sub>3</sub>/1 mmol L<sup>-1</sup> NaHCO<sub>3</sub> solution and the flow rate was 0.7 mL min<sup>-1</sup>. The standard deviation of repeated measurements was always below 2% of the measured concentration. Prior to measurement, samples were diluted 100-fold with distilled water. Blanks were used for background corrections.

#### MEDIUM

Artificial seawater medium for SRB (modified from Widdel, 1988) contained (mmol per liter): KBr (0.756), KCl (8.05); CaCl<sub>2</sub>\*2 H<sub>2</sub>O (10); MgCl<sub>2</sub>\*6 H<sub>2</sub>O (27.89); MgSO<sub>4</sub>\*7 H<sub>2</sub>O (11); NaCl (451);

NH<sub>4</sub>Cl (4.67) and KH<sub>2</sub>PO<sub>4</sub> (1.47) and was prepared without the addition of NaHCO<sub>3</sub> as buffering solution to allow for easier pH adjustment. For incubation experiments the pH was adjusted to values of 3, 4, 5, 6, and 7 with sterile 1 mmol L<sup>-1</sup> phosphoric acid (H<sub>3</sub>PO<sub>4</sub>) or NaHCO<sub>3</sub> (Widdel, 1988) before sterilization for 25 min at 121°C and re-adjusted if necessary. Prior to sterilization, needles were inserted into the butyl stoppers of each medium bottle to allow escape of oxygen from the liquid at high temperature. The 75°C hot medium was allowed to cool down under constant stirring and flushing the headspace of the bottle with a mixture of N<sub>2</sub>/CO<sub>2</sub> at a 9/1 ratio(v/v). The salinity of the SRB-media was 33.

#### SULFATE REDUCTION RATE MEASUREMENTS

To determine sulfate reduction rates (SRR) for the different incubation experiments, 20 µL of <sup>35</sup>S-sulfate tracer containing 100 kBq were injected into 15 mL Hungate tubes containing 2 mL homogenized sediment and 3 mL of SRB medium in 1:1.5 (v/v). Samples were incubated at 40 or 75°C. Per experiment, three killed controls were prepared by transferring the sediment and the medium directly to Hungate tubes containing 5 mL of 20% (w/v) ZnAc solution in centrifuge tubes. The tubes were shaken and tracer was added to the killed slurries. Every sample was prepared in triplicate. Incubations were stopped by transferring the sediment slurries into centrifuge tubes containing 5 mL of a 20% (w/v) ZnAc solution.

Reduced inorganic sulfur compounds were removed from the fixed samples by single step cold acidic chromium distillation method as described by Fossing and Jørgensen (1989) and further modified by Kallmeyer et al. (2004). The <sup>35</sup>S incorporated into the pool of total reduced inorganic sulfur was recovered as zinc sulfide in traps containing 7 mL of a 5% (w/v) ZnAc solution and finally counted in a scintillation counter (Packard Tri-Carb Liquid Scintillation Counter, MA, USA). SRR were determined as described in Kallmeyer et al. (2004). The porosity of each sediment type was determined by differential weighting of wet and dry sediment after drying for 2 days at 80°C to constant weight.

#### INCUBATIONS

All collected sediment samples were used for experiments on residual sulfate reducing activity 52 days after sampling as this was the time required for shipping of sampled material and installation of experimental setup. A pre-incubation for 18 h without tracer was followed by tracer incubation for 35 h. Incubations were performed either at 40 or 75°C. A SRB medium with 11 mmol L<sup>-1</sup> of sulfate and pH 5.3 was used to mimic the *in situ* characteristics of the white zone sediment.

A device for anaerobic slurry preparation and simultaneous pH measurement was constructed of sterilized material (15 min at 121°C). Slurry of 1:4 (v/v) ratio of sediment to medium was prepared and the pH was adjusted with phosphoric acid or NaHCO<sub>3</sub>. After pH adjustment, 5 mL of slurry were transferred into pre-flushed oxygen-free Hungate tubes. The headspace of each tube was flushed with a mixture of N<sub>2</sub> and CO<sub>2</sub> at a 9/1 ratio (v/v) and the tube was sealed with a butyl rubber stopper and kept in place by a screw cap.

For experiments on stimulated SR, a mix of VFA (Widdel, 1988) was supplied to the sediment samples as additional electron

donors. It contained formate, acetate, propionate, butyrate and succinate in equal-molar amounts providing a total fatty acid concentration of 1 mol L<sup>-1</sup>. The mixture of VFA was added with a N<sub>2</sub>/CO<sub>2</sub>-flushed 1 mL syringe through the butyl stopper of the slurry bottles to produce a final slurry concentration of 1 mmol L<sup>-1</sup> VFA. The pH was re-adjusted for each slurry bottle after fatty acid addition. For each experiment with VFA-supplemented slurries, three incubations were prepared as killed controls. All experiments were carried out in triplicates.

For pH experiments, samples were incubated for 16–18 h at 40°C after a short pre-incubation. Pre-incubation time was calculated as the time required for pH adjustment and the distribution of slurry into Hungate tubes prior to incubation with radioactive tracer. Sample preparation was conducted at room temperature and was completed in less than 4 h. For all incubation experiments, the surface sediment fractions (0–5 cm) of white and transition zone sediments and a deeper fraction (5–10 cm) of the brown zone sediment were used. For incubation experiments at pH of 3, 4, 5, 6, and 7, the phosphate buffering system, with pKa values 2.15, 6.87, and 12.33 (Perrin, 1972) was appropriate. Before and after each incubation experiment, the pH of each tube was measured after gentle mixing. For pH measurement prior to incubation, 200 µL of the liquid were removed with a needle and a N<sub>2</sub>/CO<sub>2</sub>-flushed 1 mL syringe through the butyl stopper of the tube. The pH was measured after the incubation by inserting the pH electrode into each tube after gentle shaking. All pH values were determined in triplicates. The pH changed during the incubation between ± 0.1 and ± 0.5 pH units (horizontal error bars in Figure 4).

Additionally, incubation experiments were conducted to investigate the combined effects of pH and pCO<sub>2</sub> on SR. Therefore, different CO<sub>2</sub> partial pressures in the range of 0, 1, 2, and 3 bar were applied after a pre-incubation for 12 h at 40°C. Prior to incubation experiments, CO<sub>2</sub> partial pressures were adjusted to the gas phase of tubes (10 mL headspace in a total volume of 15 mL) using a pressure reducer.

## STATISTICAL ANALYSES

Arithmetic means and standard errors were calculated for each triplicate set of experiments and are represented by vertical error bars in the activity diagrams (Figures 4 and 5). Statistical analysis was performed with SigmaPlot, 12.0, Copyright © 2011 Systat Software, Inc. A One-Way-ANOVA was used to test for statistically significant differences between the groups considering a triplicate at a certain pH value (3, 4, 5, 6, and 7) or CO<sub>2</sub> partial pressure (0, 1, 2, and 3 bar) as a group. The dependent variable was SRR. Only values above the reported detection limit of 0.04 nmol SO<sub>4</sub><sup>2-</sup> cm<sup>-3</sup> d<sup>-1</sup> were taken into account and values below this limit were set to 0. Degree of freedom df, F factor, and P-value (df, F, and P) are given. A Two-Way ANOVA was applied to test for differences between groups and treatment (untreated or supplemented sediment).

## RESULTS

### GEOCHEMICAL CHARACTERIZATION

*In situ* measurements of temperature and *ex situ* determination of pH demonstrated that the shallow-sea hydrothermal vent site

constituted an extreme environment. The pH decreased with increasing proximity to the gas vent reaching values of 5.3 in the white and 7.6 in the pore water of brown zone sediment (zonation displayed in Figure 2). Temperatures measured at 10 cm sediment depth were 75°C in the white and 26°C in the brown zone sediment. Temperature and pH measurements were not conducted in the transition zone sediment. The pore water concentration of hydrogen sulfide increased from 553 µM at a sediment depth of 2 cm to 608 µM at 4 cm; concomitantly, the sulfate concentration decreased from 11.3 to 10.5 mmol L<sup>-1</sup> at the same depth.

The bulk seawater pH was 8.0 and the alkalinity 3.6 mmol kg<sup>-1</sup>. The pH in the white zone depth profile was between 5.2 and 5.3. Alkalinity decreased with depth from 2.1 to 1.1 mmol kg<sup>-1</sup> in white sediment pore water (Price et al., 2012).

## SULFATE REDUCTION RATE MEASUREMENTS

Sulfate reduction rates determined at 40°C in sediments that were collected close to the main venting site (white zone) were below 1 nmol SO<sub>4</sub><sup>2-</sup> cm<sup>-3</sup> d<sup>-1</sup>. At this temperature, SRR increased with distance from the gas discharge zone, reaching 24 nmol SO<sub>4</sub><sup>2-</sup> cm<sup>-3</sup> d<sup>-1</sup> in surface sediment of the transition zone (Figure 3A). The highest activity at 40°C was found within the brown zone sediment (control) with 35 nmol SO<sub>4</sub><sup>2-</sup> cm<sup>-3</sup> d<sup>-1</sup>. SR was mostly inhibited at 75°C (Figure 3B). However, SR was measurable in brown zone sediment at 75°C, with a SRR of 2.4 nmol SO<sub>4</sub><sup>2-</sup> cm<sup>-3</sup> d<sup>-1</sup>, which is approximately 15 times less than the rate measured at 40°C. As SRR were below the detection limit of our method at 75°C, all further incubation experiments were conducted at an intermediate temperature of 40°C, which represents approximately the average found in hydrothermally influenced sediments.

## THE pH EFFECT ON SULFATE REDUCTION

The SRR increased with pH until they reached a pH optimum (pH<sub>opt</sub>) defined as the pH at which the highest SRR was measured (Figures 4A–C). The different sediment types of Paleochori Bay varied in the level of SR activity, its pH dependence and pH<sub>opt</sub>.

Among all tested sediments, the white zone sediment showed the lowest SR activity. The rates were statistically different for pH values between 3 and 7 (df = 4, F = 17.47, P < 0.001). Highest rates were measured at pH 6.3 with an arithmetic average of 0.2 nmol SO<sub>4</sub><sup>2-</sup> cm<sup>-3</sup> d<sup>-1</sup> (Figure 4A). At pH 7 SRR were below the detection limit. This was also the case at pH < 4. At pH of 4.7 the rates were close to detection limit. The addition of 1 mmol L<sup>-1</sup> of VFA to white zone sediment samples decreased SRR to below the detection limit at pH values < 4.5. The pH<sub>opt</sub> remained at pH 6.4 but the corresponding SRR showed an increasing trend from 0.2 to 0.3 nmol SO<sub>4</sub><sup>2-</sup> cm<sup>-3</sup> d<sup>-1</sup> after VFA addition. SR activity could also be detected at pH 7.3 with a rate of 0.1 nmol SO<sub>4</sub><sup>2-</sup> cm<sup>-3</sup> d<sup>-1</sup> after VFA addition. In summary, the white zone sediment showed the highest SRR at pH values between 6.3 and 6.4 in treatments, both with and without VFA-amendment.

The transition zone sediments showed significantly different SRR for all pH values (df = 4, F = 19.89, P < 0.001; Figure 4B). The highest rate was measured between pH 5.5 and 6.3 with rates of 6.5 nmol SO<sub>4</sub><sup>2-</sup> cm<sup>-3</sup> d<sup>-1</sup>. The SRR measured at pH<sub>opt</sub> were

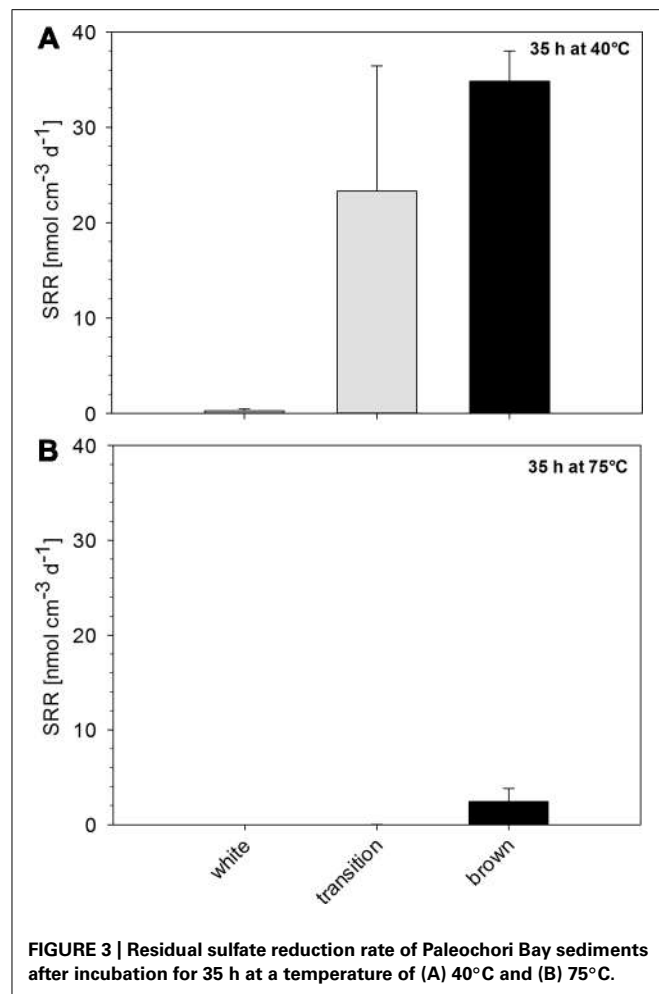


**FIGURE 3 |** Residual sulfate reduction rate of Paleochori Bay sediments after incubation for 35 h at a temperature of (A) 40°C and (B) 75°C.

40 times higher in the transition zone as compared to the highest rates in white zone sediments. Furthermore, measurable rates at pH < 5 were found with 1.9 nmol SO<sub>4</sub><sup>2-</sup> cm<sup>-3</sup> d<sup>-1</sup> at a pH 4.6. At a pH < 4 the rates were below the detection limit. At pH 7.3 SRR were four times lower than at pH<sub>opt</sub>. After VFA-addition an increase in SRR could be identified as compared to the untreated slurries ( $df = 1, F = 5.02, P = 0.037$ ) and the highest rates increased significantly from 6.5 nmol SO<sub>4</sub><sup>2-</sup> cm<sup>-3</sup> d<sup>-1</sup> (-VFA) to 9.0 nmol SO<sub>4</sub><sup>2-</sup> cm<sup>-3</sup> d<sup>-1</sup> (+VFA) at pH<sub>opt</sub> of 6.1. The SRR at pH ≤ 5.5 was slightly increased from 6.5 nmol SO<sub>4</sub><sup>2-</sup> cm<sup>-3</sup> d<sup>-1</sup> at a pH of 5.5 to a rate of 7.6 nmol SO<sub>4</sub><sup>2-</sup> cm<sup>-3</sup> d<sup>-1</sup> at pH 5.2 after amendment. At pH < 4, SR could no longer be detected. At pH > 7 the SRR were only increased from 1.6 nmol SO<sub>4</sub><sup>2-</sup> cm<sup>-3</sup> d<sup>-1</sup> without amendment to 2.4 nmol SO<sub>4</sub><sup>2-</sup> cm<sup>-3</sup> d<sup>-1</sup> after addition of VFA.

Sulfate reduction rates in the brown zone sediment were 2.3 nmol SO<sub>4</sub><sup>2-</sup> cm<sup>-3</sup> d<sup>-1</sup> at pH<sub>opt</sub> of 6.0 (Figure 4C). Rates were significantly different between the tested pH values ( $df = 4, F = 213.73, P < 0.001$ ). At pH 7.2 SRR showed a decrease from 2.4 to 1.6 nmol SO<sub>4</sub><sup>2-</sup> cm<sup>-3</sup> d<sup>-1</sup>. In these sediment samples a steep decrease in SRR was observed at pH values < 6, reaching 0.7 nmol SO<sub>4</sub><sup>2-</sup> cm<sup>-3</sup> d<sup>-1</sup> at pH 5.5 and 0.1 nmol SO<sub>4</sub><sup>2-</sup> cm<sup>-3</sup> d<sup>-1</sup> at pH 5.0.

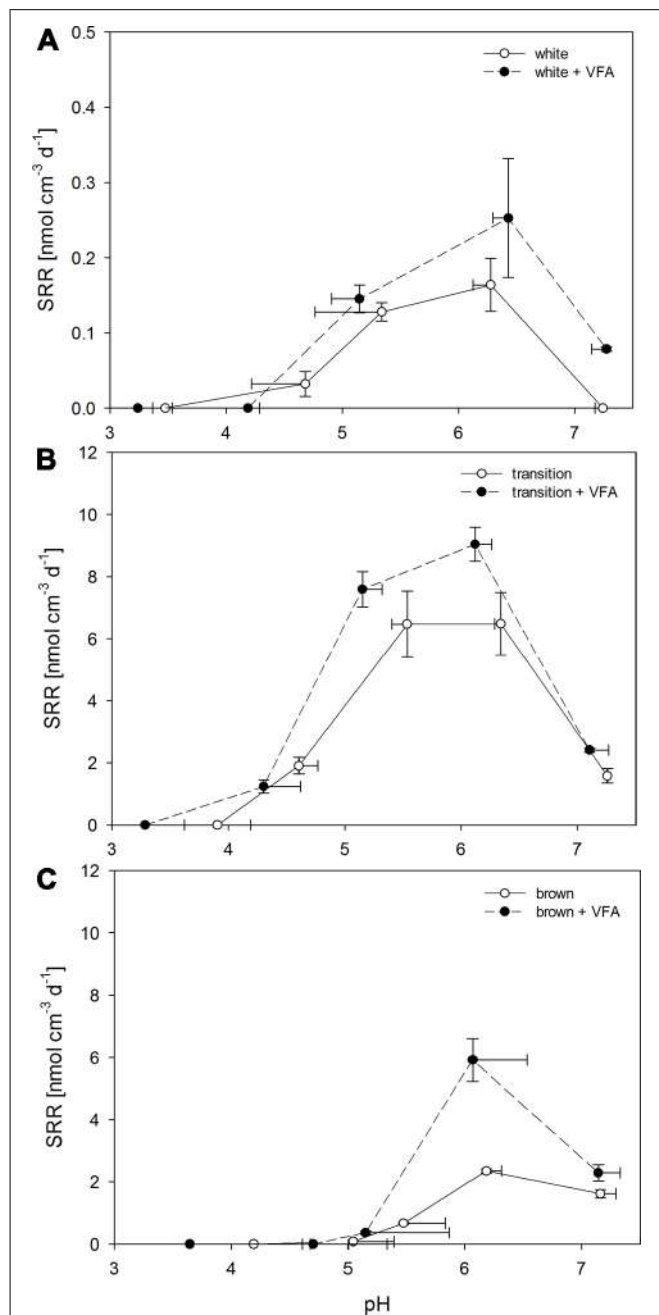


**FIGURE 4 |** Sulfate reduction rates after incubations for 16 h of Paleochori Bay, white, transition, and brown zone sediment incubated in not amended and VFA-supplemented media as a function of pH. Incubation temperature was 40°C. Horizontal error bars show development of pH value over time of incubation. Vertical error bars show the standard errors of rates ( $n = 3$ ). (A) White zone sediment. (B) Transition zone sediment. (C) Brown zone sediment.

At pH < 5, SRR were below the detection limit. VFA amendment resulted in a significant increase ( $df = 1, F = 26.06, P < 0.001$ ) and a different response as compared to the other sediments. The pH<sub>opt</sub> was 6.1 as was the case in the non-amended samples and the SRR increased from 2.3 nmol SO<sub>4</sub><sup>2-</sup> cm<sup>-3</sup> d<sup>-1</sup> with no amendment

to 5.9 nmol SO<sub>4</sub><sup>2-</sup> cm<sup>-3</sup> d<sup>-1</sup> after VFA-addition. At pH 7 only a slight increase in SRR from 1.6 nmol SO<sub>4</sub><sup>2-</sup> cm<sup>-3</sup> d<sup>-1</sup> without amendment to 2.3 nmol SO<sub>4</sub><sup>2-</sup> cm<sup>-3</sup> d<sup>-1</sup> at after amendment was observed.

### THE pCO<sub>2</sub> EFFECT ON SULFATE REDUCTION

The different pCO<sub>2</sub> partial pressures resulted in different pore water pH values in sediment samples obtained from the Paleochori Bay sites. In all sediment types a decreasing trend in SRR was observed with increasing pCO<sub>2</sub> (Figures 5A–C). A stimulation of SRR upon VFA amendment was observed for all sediment types at a pCO<sub>2</sub> of 1 bar. However, the rates decreased with increasing pCO<sub>2</sub> after VFA addition and were significantly different for the transition ( $df = 2, F = 31.51, P < 0.001$ ) and the brown zone sediment ( $df = 2, F = 19.68, P = 0.002$ ). We observed a steep decrease of SRR in all samples after the CO<sub>2</sub> gas pressure was increased from 2 to 3 bar even though the pH only decreased slightly, from 4.8 to 4.7 for the white zone sediment, from 4.7 to 4.6 for transition zone sediment and from 5.5 to 5.4 for the brown zone sediment (Figures 5A–C).

The sediment samples showed different buffering capacities, which were expressed as the relation between pCO<sub>2</sub> and subsequent pH decrease (Figure 6). The pore water of white zone sediment had an intermediate buffering capacity expressed by a pH decrease from 5.6 to 4.7 after addition of 3 bar of pCO<sub>2</sub>. The pore water of transition zone sediment had the lowest buffering capacity since the pH decreased from 5.5 to 4.4 after addition of 3 bar pCO<sub>2</sub>. The highest pH value and buffering capacity was found in samples from the brown zone sediment which decreased from 6.1 to 5.2 after pCO<sub>2</sub> adjustment (Figure 6).

### DISCUSSION

In this study, the highest SRR without VFA amendment were measured in the brown zone sediment with 35 nmol SO<sub>4</sub><sup>2-</sup> cm<sup>-3</sup> d<sup>-1</sup>. SRR determined in these control sediment samples were close to rates reported from temperate regions. For example, Jørgensen and Bak (1991) reported SRR between 5 and 20 nmol SO<sub>4</sub><sup>2-</sup> cm<sup>-3</sup> d<sup>-1</sup> from marine sediments of Kattegat, Denmark. Dando et al. (1995) studied a neighboring hydrothermal vent site in Paleochori Bay at a water depth of 10 m and determined SRR of between 5 and 80 nmol SO<sub>4</sub><sup>2-</sup> cm<sup>-3</sup> d<sup>-1</sup> applying a radio-tracer method (Dando et al., 1991) immediately after sampling. SRR peaked at 2 cm sediment depth with maximal rates of up to 80 nmol SO<sub>4</sub><sup>2-</sup> cm<sup>-3</sup> d<sup>-1</sup>, which were probably supported by residual organic carbon (Dando et al., 1995) and/or hydrogen gas from the vent fluids. The overall lowered rates in our sediment samples were most likely a consequence of electron donor limitation as the experiments could not be performed immediately after sampling. Intermediate activity was found in surface samples of transition zone sediment with a SRR of 24 nmol SO<sub>4</sub><sup>2-</sup> cm<sup>-3</sup> d<sup>-1</sup>. SRR in brown and transition zone sediment were in the range of SR determined in deep-sea hydrothermal vent sediments (19–61 nmol SO<sub>4</sub><sup>2-</sup> cm<sup>-3</sup> d<sup>-1</sup>) with *in situ* temperatures > 100°C (Jørgensen et al., 1992) but below the rates measured for the Logatchev hydrothermal field at the Mid Atlantic Ridge with 122–136 nmol SO<sub>4</sub><sup>2-</sup> cm<sup>-3</sup> d<sup>-1</sup> at temperatures between 65 and 100°C (Schauer et al., 2011). The lowest SRR was measured in the white zone sediment. There, SRR were below 1 nmol SO<sub>4</sub><sup>2-</sup> cm<sup>-3</sup> d<sup>-1</sup> after incubation at 40°C and below detection limit when the samples were incubated at 75°C, which is the *in situ* temperature at 10 cm sediment depth. The low SRR in the white zone may be due

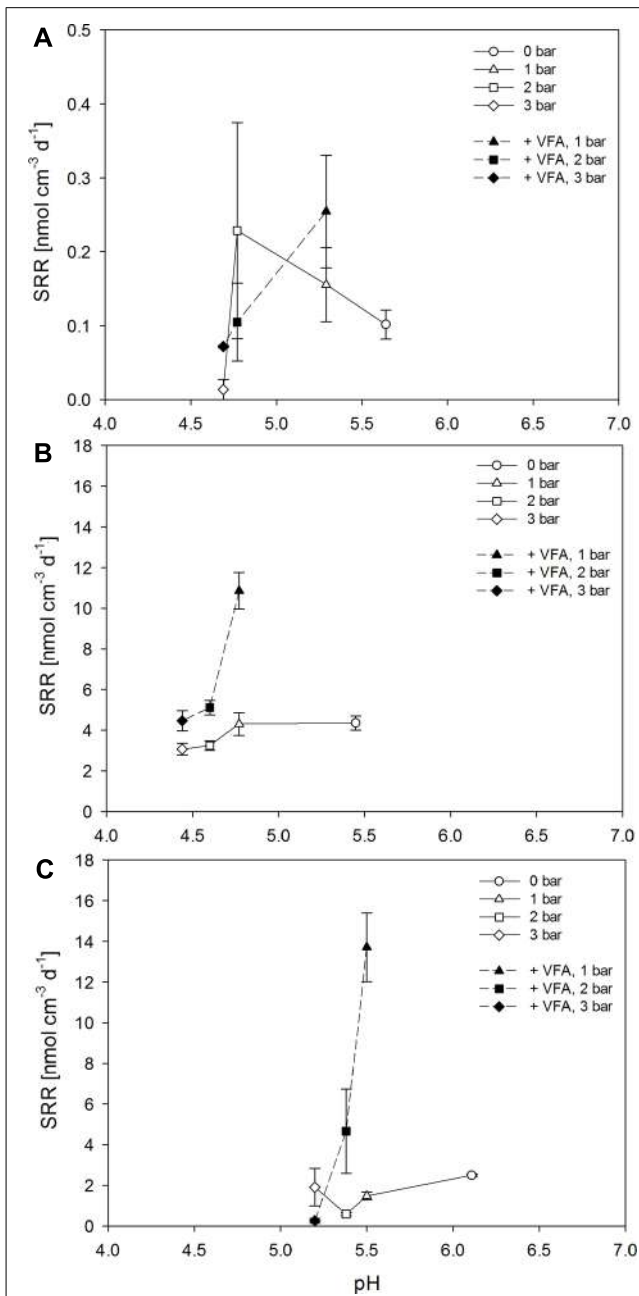
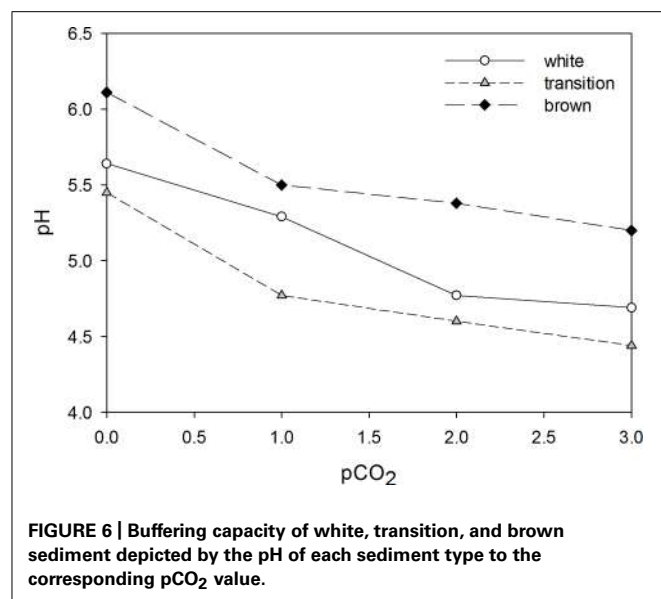


**FIGURE 5 |** Sulfate reduction rates after incubations for 16 h of Paleochori Bay, white (A), transition (B), and brown zone sediment (C) incubated in not amended and VFA-supplemented media as a function of changing pCO<sub>2</sub>. Incubation temperature was 40°C. Vertical error bars show the standard errors of rates ( $n = 3$ ). Symbols represent different pCO<sub>2</sub> conditions, starting with circles for no pCO<sub>2</sub>, triangles for 1 bar, squares for 2 bar, and diamonds for 3 bar.



to substrate limitation, in particular lack of hydrogen gas from venting fluids.

The SRB are found in several phylogenetic groups, but mostly belong to the Deltaproteobacteria (e.g., 23 out of 60 genera), followed by the Firmicutes (Muyzer and Stams, 2008; Barton and Fauque, 2009). It is possible that the low SRR, especially in the white zone sediments, may be due to a smaller population size of SRB, at least relative to our other sediment types. Sievert et al. (1999) found mainly Cyanobacteria and sulfur oxidizing *Thiomicrospira* spp in a hydrothermal vent system that is located close to our study site. Our sediments were collected from a slightly higher temperature, 75°C at 10 cm depth, whereas the white zone temperatures for Sievert et al. (1999) study reached only 50°C at 5 cm sediment depth. Even if polymerase chain reaction (PCR) biases cannot be excluded, the elevated numbers of 16S rRNA sequences affiliated with the Deltaproteobacteria, to which most SRB belong, found in the transition and brown zone sediments (Sievert et al., 1999) are in agreement with our results as we found the highest SRR in these sediments.

In a more quantitative study, 16S rRNA clone libraries and phylogenetic data were obtained for samples collected in the same area and temperature as this study (Price et al., 2013, this issue). In the white zone with equivalent temperatures to our study, 7 out of 51 clones were obtained for the Deltaproteobacteria in a 0–1.5 cm sediment depth, whereas none were found in the deeper 3–4.5 and 9–10.5 cm layers. Four out of those seven clones were affiliated with the order Desulfobacterales, one of the major groups known for SR (Muyzer and Stams, 2008). Price et al. (2013, this issue) also reported that members of the Firmicutes phylum became dominant in the deeper sediments, but were exclusively associated with *Bacillus* sp (at ~100% ID). In a pooled 0–6 cm sample from a lower temperature (~45°C) white zone at the same site as this study, 24 out of 119 clones were affiliated with Deltaproteobacteria, 12 of which were associated with the Desulfobacterales order. In pooled 0–6 cm sample from a nearby background brown area, 10 out of 97 clones were affiliated with Desulfobacterales. Thus, in

pooled samples of brown zone sediment, about 10 % of the clones in the clone libraries affiliate with groups with the most potential for SO<sub>4</sub><sup>2-</sup> reduction, while 10% affiliated with SRBs in white zone sediments. In the 0–1.5 cm sediment sample, the contribution of 16S rDNA affiliated with SRB was 8%. Due to the small size of the libraries we do not consider the ratios to significantly different among sites. In future studies the microbial diversity in general and that of sulfate reducers should be addressed with next generation sequencing methods (Frank et al., 2013).

A possible explanation for the low SRR in white zone sediment could also be its high spatial instability due to transport of gas, venting and mixing in combination with oxygenation of the sediment layers which could lead to a removal of microorganisms. Mixing might also disturb the coupling between fermenters and sulfate reducers, which thrive on oxidizing fermentation products such as VFA and H<sub>2</sub>. Finke and Jørgensen (2008) observed that temperature had an effect on the coupling between fermentation and SR in sediment samples from Svalbard and Wadden Sea as fermentation products accumulated in incubations above a critical temperature of 40°C. The authors concluded that temperature is a factor that might disturb the metabolic link between both process types because sulfate reducers were inhibited at a lower critical temperature than fermenters (Finke and Jørgensen, 2008). In our study, a higher threshold for negative temperature effects is expected as the natural temperatures of the hydrothermal vent system ranged from 26 to 75°C. Effects that reduce SRR can most likely be attributed to low pH leading to a protonation of acid anions, which short-cuts proton gradients in the cells and disrupts adenosine triphosphate (ATP) synthesis (Baronofsky et al., 1984).

#### THE pH EFFECT ON SULFATE REDUCTION

Based on cell culture studies, it was suggested that SR may preferentially occur at pH between 6 and 8 (Widdel, 1988; Hao et al., 1996). However, Dando et al. (1995) have documented that SR can take place at high rates in shallow submarine hydrothermal vent systems with low pH. Our results are in line with those reported by Dando et al. (1995), and demonstrate that hydrothermal sediments with lower pH and increased temperature harbor populations of SRB that respond distinctly to different pH conditions. In addition, our data indicate that hydrothermal sediments had different pH optima than SR populations of sediments with low temperature and neutral to slightly alkaline pH characteristics. We observed SR at pH < 5 in hydrothermally influenced, CO<sub>2</sub>-vented sediments. However, optimal pH of SR was found between pH 5 and 6 for the hydrothermally influenced white and transition zone sediments but between pH 6–7 for brown zone sediment that served as control.

Sulfate reducing activity under low pH conditions is often explained by the existence of microenvironments with more reduced and alkaline conditions than the acidic surroundings (Fortin, 1996). Koschorreck (2008) argued against the existence of neutral microniches formed by the alkalinity produced during SR. He calculated that a SRR of  $1.8 \times 10^8$  nmol SO<sub>4</sub><sup>2-</sup> cm<sup>-3</sup> d<sup>-1</sup> is required to maintain circumneutral pH in a sphere with 100 μm diameter while the pH in the surrounding is 3. Applying this calculation to the hydrothermal vent sediments of Paleochori Bay,

a SRR of  $1.6 \times 10^6$  nmol SO<sub>4</sub><sup>2-</sup> cm<sup>-3</sup> d<sup>-1</sup> would be needed to maintain the center of the sphere at pH 6 when the pH of the surrounding pore water was 5. This rate exceeds the SRR in the hydrothermal vent system of Paleochori Bay by five to six orders of magnitude and supports our argument that SRB populations are adapted to low pH rather than the presence of neutral microsites.

In previous studies, it was suggested that sulfate reducers are more susceptible to high VFA concentrations than methanogens (James et al., 1998), which might result in a shift from SR to methanogenesis at low pH (Koschorreck, 2008). A study on methanogenesis in a bioreactor at pH of 4.5 showed a 30% increase of methane yield as compared to neutral conditions, after a slow acclimation of the methanogens to lowered pH (Taconi et al., 2008). A competition between sulfate reducers and methanogens due to diluted sulfate concentrations by the vent outflow and higher susceptibility of the sulfate reducing community to low pH, can be excluded as the abundance of Archaea as well as their diversity was low in white and brown zone sediments (Nitzsche, 2010; Price et al., 2013, this issue).

#### THE EFFECT OF VOLATILE FATTY ACIDS ON SULFATE REDUCTION AT LOW pH

Protonated short-chained fatty acids diffuse through the cell membrane and consequently act as protonophores and as uncoupling agents (Kell et al., 1981). This is not the case for their conjugate anions, which are excluded by their physical properties and charged head groups of lipids from the biological bilayer. Small fatty acids turn lipophilic under acidic conditions depending on their dissociation constant pKa, pass through membranes by passive diffusion and destruct the gradients (pH gradient, ΔpH and membrane potential ΔΨ) necessary for ATP synthesis and transport function. In addition, they acidify the intrinsic circumneutral cytoplasm of the cell by dissociation and proton release. The reduced cytoplasmic pH inhibits cellular reactions and energy conservation triggered by proton-motive force (Baronofsky et al., 1984). With the formula:

$$[\text{Ac}] / [\text{HAc}] = 10^{\text{pH} - \text{pKa}}$$

where [Ac] equals the total acid concentration and [HAc] the amount of protonated acid at a certain pH and the pKa values of a total concentration of 1 mmol L<sup>-1</sup> VFA (formate, acetate, propionate, butyrate, and succinate) with pKa values of 3.75; 4.76; 4.87; 4.81; 4.16 (Perrin, 1972) in the slurry we can calculate the concentration of protonated fatty acids (Bruun et al., 2010) at pH values from 3 to 7. The total concentration of protonated organic acids of the VFA in the slurry is 43.3 mmol L<sup>-1</sup> at pH of 3; 4.3 mmol L<sup>-1</sup> at pH 4, 0.4 mmol L<sup>-1</sup> at pH 5; 0.01 mmol L<sup>-1</sup> at pH 6 and negligible for a pH 7 (0.004 mmol L<sup>-1</sup>). In this study, only the protonated fatty acid concentration at pH values of 3 and 4 might become harmful to SRB (Baronofsky et al., 1984). This is consistent with our pH-experiment data in which the SRR of the VFA-amended slurry is lower than the rate measured in unamended sediment of white and transition zone sediment at pH < 5. At pH 6.4, the SRR measured after VFA addition to white zone sediment (0.3 nmol SO<sub>4</sub><sup>2-</sup> cm<sup>-3</sup> d<sup>-1</sup>) exceeded

the SRR (0.2 nmol SO<sub>4</sub><sup>2-</sup> cm<sup>-3</sup> d<sup>-1</sup>) at a similar pH (pH 6.3) without addition. In brown zone sediment slurries, the limit for VFA stimulation was equal to unamended sediment at pH 5.5. The SRR at pH 6.2 of 2.3 nmol SO<sub>4</sub><sup>2-</sup> cm<sup>-3</sup> d<sup>-1</sup> was stimulated by VFA amendment to a rate of 5.9 nmol SO<sub>4</sub><sup>2-</sup> cm<sup>-3</sup> d<sup>-1</sup>. A SRR increase was also observed at neutral pH for brown zone sediments: here SRR increased from 1.6 nmol SO<sub>4</sub><sup>2-</sup> cm<sup>-3</sup> d<sup>-1</sup> without amendment to 2.3 nmol SO<sub>4</sub><sup>2-</sup> cm<sup>-3</sup> d<sup>-1</sup> in amended slurries. Since VFA were added as a mixture to the slurries, no further differentiation between the individual fatty acids on SRR was possible. The presented results are consistent with studies on activity inhibition caused by organic acids at artificially lowered pH (Ottosen et al., 2009) and fresh water seep systems (Bruun et al., 2010).

#### THE EFFECT OF pCO<sub>2</sub> ON SULFATE REDUCTION

The content of CO<sub>2</sub> correlates with pH. Dissolved CO<sub>2</sub> reacts with water to form carbonic acid (H<sub>2</sub>CO<sub>3</sub>), which immediately dissociates to bicarbonate (HCO<sub>3</sub><sup>-</sup>) and protons (H<sup>+</sup>). HCO<sub>3</sub><sup>-</sup> and H<sup>+</sup> can further dissociate to CO<sub>3</sub><sup>2-</sup> and H<sup>+</sup> decreasing the pH in the solution. In this context, “carbonic acid” encompasses the species CO<sub>2</sub>, H<sub>2</sub>CO<sub>3</sub>, HCO<sub>3</sub><sup>-</sup>, and CO<sub>3</sub><sup>2-</sup> (Zeebe and Wolf-Gladrow, 2001). The existence of the different carbonic acid species depends on their concentrations, dissociation constants and pH as described by the Bjerrum plot (Zeebe and Wolf-Gladrow, 2001).

In this study, the relation between pH and SRR relative to different pCO<sub>2</sub> was examined. This is of particular interest in order to understand microbial functioning in CO<sub>2</sub> – venting sediments which are perfect natural laboratories for studies focused on CO<sub>2</sub> sequestration in which carbon dioxide is removed from the atmosphere and stored in sediments that should serve as long-term reservoirs (Shitashima et al., 2008). After adjustment of the CO<sub>2</sub> partial pressure to 0, 1, 2, and 3 bar, we found that a pCO<sub>2</sub> increase resulted in different pH values among the sediment types. This may be a consequence of different chemical and biological buffering capacities of the sediment (Heijmans et al., 1999). The mineral characteristics of the sediment (e.g., silicate, carbonate) and the bicarbonate content of the seawater dictate chemical buffering capacity of the sediment. The addition of CO<sub>2</sub> results in a decrease in pH (Zeebe and Wolf-Gladrow, 2001). SR produces bicarbonate alkalinity and consequently counteracts a decrease of pH. The data obtained from pCO<sub>2</sub> incubation experiments provide a rough indication of the buffering capacity of the Paleochori Bay sediments: the brown zone sediment has the highest buffering capacity followed by white and finally transition zone sediments. This was also obvious from the amounts of phosphoric acid needed to decrease the pH in the pH experiments (data not shown).

Sulfate reduction rates responded to increase in pCO<sub>2</sub> with a decrease in activity in nearly all experiments although effect of an increase in pCO<sub>2</sub> from 2 to 3 bar on pH was negligible. A pCO<sub>2</sub> increase from 1 to 2 bar reduced SRR from 0.2 to 0.1 nmol SO<sub>4</sub><sup>2-</sup> cm<sup>-3</sup> d<sup>-1</sup> in the white zone sediment slurries, from 4.3 to 3.2 nmol SO<sub>4</sub><sup>2-</sup> cm<sup>-3</sup> d<sup>-1</sup> in transition zone slurries and from 1.5 to 0.6 nmol SO<sub>4</sub><sup>2-</sup> cm<sup>-3</sup> d<sup>-1</sup> for the brown zone sediment

slurries. The increase in pCO<sub>2</sub> was accompanied by pH changes from 4.8 to 4.7, 4.8 to 4.6 and 5.5 to 5.4 in the three sediments, respectively. The effect of SRR reduction upon pCO<sub>2</sub> increase was even stronger after VFA were added to the slurries (Figure 5). In our experiments we observed similar effects as in Debs-Louka et al. (1999) concluding that the reduction in pH due to increasing pCO<sub>2</sub> was not sufficient to account for antimicrobial activity. In this study microbial inactivation depended strongly on CO<sub>2</sub> partial pressure (tested for 15–55 bar), exposure time, the decompression time and water content of the sample. A sudden increase in pCO<sub>2</sub> was observed to provoke cell ruptures and lead to reduced bacterial numbers (Debs-Louka et al., 1999). Additionally, it can be suggested that the content of CO<sub>2</sub> in the form of carbonic acid has a negative effect on the cell as it can permeate the membrane and dissociate in CO<sub>3</sub><sup>2-</sup> and H<sup>+</sup> in the circumneutral cytoplasm, decreasing the intrinsic pH of the cell.

## CONCLUSION

We observed a significant difference between SR in hydrothermally influenced and background sediments suggesting that microbial communities are adapted to low pH in the hydrothermal sediments of Milos. Sulfate reducing communities in hydrothermal sediments showed pH activity optima between 5 and 6. In contrast, SR in sediments with no hydrothermal influence exhibited

pH optima between 6 and 7. The shallow-sea hydrothermal vent of Paleochori Bay, Milos (Greece) with pH between 5 and 7, temperature range of 26–90°C and a high content of dissolved arsenic and sulfide in the sediment pore water, represents an extreme environment in which SR may play an important role in the degradation of organic material. This study suggests that marine microbial SR communities that are specifically adapted to a life at high pCO<sub>2</sub> and low pH do exist.

## ACKNOWLEDGMENTS

This was an International Max Planck Research School of Marine Microbiology (MarMic) project with funding provided by the Max Planck Society. Partial funding for logistics and geochemical analyses was also provided by a University of Bremen MARUM Postdoc Fellowship (to Roy E. Price) and MARUM Incentive Funding (to Roy E. Price and S. Bühring). Thanks to MARUM for providing the possibility to join the Milos Expedition in October 2009 and C.I. Huang for the kind collaboration. We are grateful to the expedition team M.J. Ruiz Chancho, M. Sollich, M. Bausch. Special thanks to A. Godelitsas, A. Vichos, the Artemis Bungalows, and the Sirocco Restaurant for logistical support in Athens and Milos. Thanks to K. Imhoff for the assistance in sulfate measurements and A. Meyerdierks for revision of the manuscript. The manuscript has been greatly improved by the valuable comments of the reviewers.

## REFERENCES

- Amend, J., Rogers, K., and Meyer-Dombard, D. (2004). Microbially mediated sulfur -redox: energetics in marine hydrothermal vent systems. *Geol. Soc. Am.* 379, 17–34.
- Baker-Austin, C., and Dopson, M. (2007). Life in acid: pH homeostasis in acidophiles. *Trends Microbiol.* 15, 165–171.
- Baronofsky, J. J., Schreurs, W. J., and Kashket, E. R. (1984). Uncoupling by acetic acid limits growth of and acetogenesis by *Clostridium thermoaceticum*. *Appl. Environ. Microbiol.* 48, 1134–1139.
- Barton, L. L., and Fauque, G. D. (2009). Biochemistry, physiology and biotechnology of sulfate-reducing bacteria. *Adv. Appl. Microbiol.* 68, 41–98.
- Bruun, A. M., Finster, K., Gunnlaugsson, H. P., Nürnberg, P., and Friedrich, M. W. (2010). A comprehensive investigation on iron cycling in a freshwater seep including microscopy, cultivation and molecular community analysis. *Geomicrobiol. J.* 27, 15–34.
- Cline, J. D. (1969). Spectrophotometric determination of hydrogen sulfide in natural waters. *Limnol. Oceanogr.* 14, 454–458.
- Dando, P. R., Austen, M. C., Burke, R. A., Kendall, M. A., Kennicutt, M. C. II., Judd, A. G., et al. (1991). Ecology of a North Sea pockmark with an active methane seep. *Mar. Ecol. Prog. Ser.* 70, 49–63.
- Dando, P. R., Hughes, J. A., Leahy, Y., Niven, S. J., Taylor, L. J., and Smith, C. (1995). Gas venting rates from submarine hydrothermal areas around the island of Milos, Hellenic Volcanic Arc. *Cont. Shelf Res.* 15, 913–929.
- Debs-Louka, E., Louka, N., Abraham, G., Chabot, V., and Allaf, K. (1999). Effect of compressed carbon dioxide on microbial cell viability. *Appl. Environ. Microbiol.* 65, 626–631.
- Finke, N., and Jørgensen, B. B. (2008). Response of fermentation and sulfate reduction to experimental temperature changes in temperate and Arctic marine sediments. *ISME J.* 2, 815–829.
- Fitzsimons, M. F., Dando, P. R., Hughes, J. A., Thiermann, F., Akoumianaki, I., and Pratt, S. M. (1997). Submarine hydrothermal brine seeps off Milos, Greece. Observations and geochemistry. *Mar. Chem.* 57, 325–340.
- Fortin, D. (1996). Role of Thiobacillus and sulfate-reducing bacteria in iron biocycling in oxic and acidic mine tailings. *FEMS Microbiol. Ecol.* 21, 11–24.
- Fossing, H., and Jørgensen, B. B. (1989). Measurement of bacterial sulfate reduction in sediments: evaluation of a single-step chromium reduction method. *Biogeochemistry* 8, 205–222.
- Frank, K. L., Rogers, D. R., Ollins, H. C., Vidoudez, C., and Girguis, P. R. (2013). Characterizing the distribution and rates of microbial sulfate reduction at Middle Valley hydrothermal vents. *ISME J.* doi: 10.1038/ismej.2013.17 [Epub ahead of print].
- Hao, O. J., Chen, J. M., Huang, L., and Buglass, R. L. (1996). Sulfate-reducing bacteria. *Crit. Rev. Environ. Sci. Technol.* 26, 155–187.
- Heijls, S. K., Jonkers, H. M., van Gemerden, H., Schaub, B. E. M., and Stal, L. J. (1999). The buffering capacity towards free sulphide in sediments of a coastal lagoon (Bassin d'Arcachon, France)—the relative importance of chemical and biological processes. *Estuar. Coast. Shelf Sci.* 49, 21–35.
- Hubert, C., Loy, A., Nickel, M., Arnosti, C., Baranyi, C., Brüchert, V., et al. (2009). A constant flux of diverse thermophilic bacteria into the cold Arctic seabed. *Science* 325, 1541–1544.
- Isaksen, M. F., Bak, F., and Jørgensen, B. B. (1994). Thermophilic sulfate-reducing bacteria in cold marine sediment. *FEMS Microbiol. Ecol.* 14, 1–8.
- James, A. G., Watson-Craik, I. A., and Senior, E. (1998). The effects of organic acids on the methanogenic degradation of the landfill leachate molecules butyrate and valerate. *Water Res.* 32, 792–800.
- Jannasch, H. W., and Mottl, M. J. (1985). Geomicrobiology of deep-sea hydrothermal vents. *Science* 239, 717–725.
- Jørgensen, B. B. (1982). Mineralization of organic matter in the sea bed—the role of sulphate reduction. *Nature* 296, 643–645.
- Jørgensen, B. B., and Bak, F. (1991). Pathways and microbiology of thiosulfate transformations and sulfate reduction in a marine sediment (Kattegat, Denmark). *Appl. Environ. Microbiol.* 57, 847–856.
- Jørgensen, B. B., Isaksen, M. F., and Jannasch, H. W. (1992). Bacterial sulfate reduction above 100°C in deep-sea hydrothermal vent sediments. *Science* 258, 1756–1757.
- Kaksonen, A. H., and Puhakka, J. A. (2007). Sulfate reduction based bioprocesses for the treatment of acid mine drainage and the recovery of metals. *Eng. Life Sci.* 7, 541–564.
- Kallmeyer, J., Ferdelman, T. G., Weber, A., Fossing, H., and Jørgensen, B. B. (2004). A cold chromium distillation procedure for radiolabeled sulfide applied to sulfate reduction measurements. *Limnol. Oceanogr.* 2, 171–180.
- Kell, D. B., Peck, M. W., Rodger, G., and Morris, J. G. (1981). On the permeability to weak acids and bases of the cytoplasmic membrane of *Clostridium pasteurianum*. *Biochem. Biophys. Res. Commun.* 99, 81–88.
- Knoblauch, C., and Jørgensen, B. B. (1999). Effect of temperature on sulphate reduction, growth rate and growth yield in five psychrophilic

- sulphate-reducing bacteria from Arctic sediments. *Environ. Microbiol.* 1, 457–467.
- Koschorreck, M. (2008). Microbial sulphate reduction at a low pH. *FEMS Microbiol. Ecol.* 64, 329–342.
- Lowe, S. E., Jain, M. K., and Zeikus, J. G. (1993). Biology, ecology, and biotechnological applications of anaerobic bacteria adapted to environmental stresses in temperature, pH, salinity, or substrates. *Microbiol. Rev.* 57, 451–509.
- Martin, A. (1990). Bioenergetic parameters and transport in obligate acidophiles. *Biochim. Biophys. Acta* 1018, 267–270.
- Moosa, S., and Harrison, S. T. L. (2006). Product inhibition by sulfide species on biological sulphate reduction for the treatment of acid mine drainage. *Hydrometallurgy* 83, 214–222.
- Muyzer, G., and Stams, A. J. (2008). The ecology and biotechnology of sulphate-reducing bacteria. *Nat. Rev. Microbiol.* 6, 441–454.
- Nitzsche, K. (2010). *Microbial Diversity of Hydrothermally Influenced Arsenic-Rich Sediments off the Coast of Milos Island, Greece.* thesis, TU Bergakademie, Freiberg, Germany.
- Ottosen, L. D. M., Poulsen, H. V., Nielsen, D. A., Finster, K., Nielsen, L. P., and Revsbech, N. P. (2009). Observations on microbial activity in acidified pig slurry. *Biosyst. Eng.* 102, 291–297.
- Perrin, D. D. (1972). *Dissociation Constants of Organic Bases in Aqueous Solution*. London: Franklin Book Co.
- Price, R. E., Savov, I., Planer-Friedrich, B., Bühring, S., Amend, J., and Pichler, T. (2012). Processes influencing extreme enrichment in shallow-sea hydrothermal fluids of Milos Island, Greece. *Chem. Geol.* doi: 10.1016/j.chemgeo.2012.06.007
- Price, R. P., Nitzsche, K., Lesniewski, R., Meyerderiks, A., Saltikov, C., Edwards, K., et al. (2013, this issue). Microbial diversity and arsenic metabolism in depth profiles from a shallow-sea hydrothermal vent system undergoing phase separation; Milos Island (Greece). (this issue).
- Schauer, R., Røy, H., Augustin, N., Gennerich, H. H., Peters, M., Wenzhoefer, F., et al. (2011). Bacterial sulfur cycling shapes microbial communities in surface sediments of an ultramafic hydrothermal vent field. *Environ. Microbiol.* 13, 2633–2648.
- Shitashima, K., Maeda, Y., Koike, Y., and Ohsumi, T. (2008). Natural analogue of the rise and dissolution of liquid CO<sub>2</sub> in the ocean. *Int. J. Greenh. Gas Con.* 2, 95–104.
- Sievert, S. M., Brinkhoff, T., Muyzer, G., Ziebis, W., and Kuever, J. (1999). Spatial heterogeneity of bacterial populations along an environmental gradient at a shallow submarine hydrothermal vent near Milos Island (Greece). *Appl. Environ. Microbiol.* 65, 3834–3842.
- Taconi, K. A., Zappi, M. E., French, W. T., and Brown, L. R. (2008). Methanogenesis under acidic pH conditions in a semi-continuous reactor system. *Bioresour. Technol.* 99, 8075–8081.
- Widdel, F. (1988). “Microbiology and ecology of sulfate and sulfur-reducing bacteria,” in *Biology of Anaerobic Microorganisms* ed. A. J. B. Zehnder (New York: John Wiley), 469–586.
- Zeebe, R. E., and Wolf-Gladrow, D. (2001). *CO<sub>2</sub> in Seawater: Equilibrium, Kinetics, Isotopes*. Amsterdam: Elsevier Oceanography Book Series.
- Conflict of Interest Statement:** The authors declare that the research was conducted in the absence of any commercial or financial relationships that could be construed as a potential conflict of interest.
- Received: 28 January 2013; accepted: 17 April 2013; published online: 08 May 2013.*
- Citation: Bayraktarov E, Price RE, Ferdelman TG and Finster K (2013) The pH and pCO<sub>2</sub> dependence of sulfate reduction in shallow-sea hydrothermal CO<sub>2</sub> – venting sediments (Milos Island, Greece). *Front. Microbiol.* 4:111. doi: 10.3389/fmicb.2013.00111*
- This article was submitted to Frontiers in Extreme Microbiology, a specialty of Frontiers in Microbiology.*
- Copyright © 2013 Bayraktarov, Price, Ferdelman and Finster. This is an open-access article distributed under the terms of the Creative Commons Attribution License, which permits use, distribution and reproduction in other forums, provided the original authors and source are credited and subject to any copyright notices concerning any third-party graphics etc.*



# Microbial colonization of basaltic glasses in hydrothermal organic-rich sediments at Guaymas Basin

Nolwenn Callac<sup>1,2,3,4</sup>, Céline Rommevaux-Jestin<sup>5</sup>, Olivier Rouxel<sup>4,6</sup>, Françoise Lesongeur<sup>1,2,3</sup>, Céline Liorzou<sup>4</sup>, Claire Bollinger<sup>7</sup>, Antony Ferrant<sup>8</sup> and Anne Godfroy<sup>1,2,3\*</sup>

<sup>1</sup> Laboratoire de Microbiologie des Environnements Extrêmes UMR 6197, Université de Bretagne Occidentale, UEB, IUEM, Plouzané, France

<sup>2</sup> Laboratoire de Microbiologie des Environnements Extrêmes UMR 6197, Ifremer, Plouzané, France

<sup>3</sup> Laboratoire de Microbiologie des Environnements Extrêmes UMR 6197, CNRS, Plouzané, France

<sup>4</sup> Domaines Océaniques UMR6538, IUEM, Université de Bretagne Occidentale, Plouzané, France

<sup>5</sup> Laboratoire Géobiosphère Actuelle et Primitive, CNRS, IPGP, Sorbonne Paris Cité, Univ Paris Diderot, UMR 7154, Paris, France

<sup>6</sup> Laboratoire de Géochimie et de Métalllogénie, Ifremer, Plouzané, France

<sup>7</sup> IUEM, Université de Bretagne Occidentale, UMS 3113, Plouzané, France

<sup>8</sup> Unité Recherches et Développements Technologiques, Ifremer, Plouzané, France

## Edited by:

Andreas Teske, University of North Carolina at Chapel Hill, USA

## Reviewed by:

Jinjun Kan, Stroud Water Research Center, USA

Tatiana A. Vishnivetskaya, University of Tennessee, USA

## \*Correspondence:

Anne Godfroy, Laboratoire de Microbiologie des Environnements Extrêmes - UMR 6197, IFREMER - Centre de Brest, BP70, 29280 Plouzané, France  
e-mail: anne.godfroy@ifremer.fr

Oceanic basalts host diverse microbial communities with various metabolisms involved in C, N, S, and Fe biogeochemical cycles which may contribute to mineral and glass alteration processes at, and below the seafloor. In order to study the microbial colonization on basaltic glasses and their potential biotic/abiotic weathering products, two colonization modules called AISICS ("Autonomous *in situ* Instrumented Colonization System") were deployed in hydrothermal deep-sea sediments at the Guaymas Basin for 8 days and 22 days. Each AISICS module contained 18 colonizers (including sterile controls) filled with basaltic glasses of contrasting composition. Chemical analyses of ambient fluids sampled through the colonizers showed a greater contribution of hydrothermal fluids (maximum temperature 57.6°C) for the module deployed during the longer time period. For each colonizer, the phylogenetic diversity and metabolic function of bacterial and archaeal communities were explored using a molecular approach by cloning and sequencing. Results showed large microbial diversity in all colonizers. The bacterial distribution was primarily linked to the deployment duration, as well as the depth for the short deployment time module. Some 16s rRNA sequences formed a new cluster of *Epsilonproteobacteria*. Within the Archaea the retrieved diversity could not be linked to either duration, depth or substrata. However, *mcrA* gene sequences belonging to the ANME-1 *mcrA*-guaymas cluster were found sometimes associated with their putative sulfate-reducers syntrophs depending on the colonizers. Although no specific glass alteration texture was identified, nano-crystals of barite and pyrite were observed in close association with organic matter, suggesting a possible biological mediation. This study gives new insights into the colonization steps of volcanic rock substrates and the capability of microbial communities to exploit new environmental conditions.

**Keywords:** colonization module, basalt alteration, Guaymas basin, organic-rich sediment, hydrothermal systems

## INTRODUCTION

Alteration of the oceanic crust by seawater is one of the most important processes controlling the global fluxes of many elements at mid-oceanic ridges and ridge flanks (e.g., Staudigel and Hart, 1983; Wheat and Mottl, 2000) and the mineralogical and chemical composition of the aging oceanic crust (Alt, 1995). Since sub-seafloor basaltic crust represents the largest habitable zone by volume on Earth, microbes may play a significant role in the alteration process (Bach and Edwards, 2003). Microorganisms exploiting these reactions are known from basalt exposed at the seafloor, where the oxidation of reduced sulfur (S) and iron (Fe) compounds from basalt with dissolved oxygen and nitrate from seawater supports high microbial biomass and diversity (Mason et al., 2008; Santelli et al., 2008a; Orcutt et al., 2011b). It has been

also demonstrated that seafloor basalts harbor diverse microbial communities either on the rock surfaces (epilithic microorganisms) or inside the rocks (endolithic microorganisms; Mason et al., 2007; Santelli et al., 2009).

Seafloor hydrothermal systems are also complex environments with highly diverse and active microbial communities (Schrenk et al., 2003; Edwards et al., 2005; Nakagawa et al., 2006; Page et al., 2008; Flores et al., 2011) fueled by steep physical and chemical gradients in the mixing zone between oxygenated cold seawater and reduced metal-rich high temperature hydrothermal fluid. Likewise, seafloor hydrothermal chimneys and hydrothermally-affected sediments provide specific habitats hosting a wide range of microorganisms involved in key biogeochemical reactions related to carbon, sulfur, nitrogen, and iron cycles (Burggraf

et al., 1990; Kashefi et al., 2002; Teske et al., 2002; Dhillon et al., 2003; Francis et al., 2007; Byrne et al., 2009; Biddle et al., 2012; Bowles et al., 2012). Hence, microorganisms interact with their environment in many ways, and, in turn, could affect fluid composition, and promote mineral dissolution or precipitation (Edwards et al., 2003a, 2005; Houghton and Seyfried Jr, 2010). Evidence for microbial alteration of basaltic glasses is also increasing, and includes the alteration textures of volcanic glass (Furnes et al., 2001; Einen et al., 2006) as well as putative presence of DNA revealed by high C, N, and P contents in altered glass (Thorseth et al., 1992). The light isotopic composition of C and S in altered basalts also demonstrates potential organic C cycling and sulfate reduction within volcanic basement (Furnes et al., 2001; Rouxel et al., 2008b).

Hydrothermally heated sediments covering oceanic basalts are present in the Guaymas Basin, one of the semi-closed basins of the Gulf of California (Mexico). The Guaymas Basin is covered by a thick layer of organic and diatomaceous-rich sediments (100–500 m) due to a high sedimentation rate (up to 2 mm per year) and biological productivity in the upper ocean (Simoneit and Lonsdale, 1982; Von Damm et al., 1985b; De La Lanza-Espino and Soto, 1999; Dean et al., 2004). In the Southern Trough area, where crustal accretion takes place (Lonsdale and Becker, 1985), the seafloor is exposed to high-temperature hydrothermal activity. The circulation of hydrothermal fluids results in both the formation of sulfide and carbonate-rich chimneys and profoundly affects sediment geochemistry. Diagenetic interactions between the ascending hydrothermal fluids and sediments result in the pyrolysis of organic matter and precipitation of metal-sulfide minerals in subsurface (e.g., pyrrhotite FeS). Products of pyrolysis include light hydrocarbons, short-chain organic acids, particulate organic matter, ammonia and methane (Welhan, 1988; Martens, 1990) which provide unique conditions for sustaining uncommon and diverse microbial life (Teske et al., 2002). Likewise, microbial communities within microbial mats at Guaymas Basin have been extensively studied in term of their physiological and phylogenetical diversity, using both cultural and molecular approaches (Teske et al., 2002; Dhillon et al., 2005; Holler et al., 2011; Biddle et al., 2012; Bowles et al., 2012; McKay et al., 2012).

The colonization of mineral substrates in hydrothermal environments or their vicinity has been already studied using diverse approaches in order to assess both prokaryotic and micro-eukaryotic diversity. Many microbial colonization systems (e.g., vent caps, TRAC, ISCS, vent catheters, growth chamber, thermocouples) were previously deployed on various hydrothermal areas (Reysenbach et al., 2000; Corre et al., 2001; Takai et al., 2003; Alain et al., 2004; Higashi et al., 2004; Page et al., 2008; Rassa et al., 2009). Those studies generally showed that the *Epsilonproteobacteria* were dominant, and that the microbial diversity can vary both in terms of structure and size, depending on environmental conditions, mineral substrate composition, and deployment duration. More recently, rock substrates were deployed directly in boreholes (Orcutt et al., 2010, 2011a; Edwards et al., 2011) using the FLOCSS (Flow-Trough Osmo Colonization Systems). So far, microbial or/and abiotic alteration of basaltic glasses were investigated at low (i.e., 3–4°C; Mason et al., 2007; Santelli et al., 2009) to medium temperatures (i.e.,

40 and 60°C; Orcutt et al., 2010, 2011a) in organic-matter poor volcanic environments. However, little is known about microbial colonization processes and basaltic glass alteration under hydrothermal conditions and in an organic-matter rich system, especially in term of the carbon and energy sources for microbial life and impact on basaltic glass alteration. Here, the AISICS “Autonomous *in situ* Instrumented Colonization System” containing basaltic substrata was deployed for 8 and 22 days into the sediments underlying microbial mats and exposed to hydrothermal conditions in the Guaymas Basin. Since basaltic glass substrates exposed to *in situ* conditions may be affected by both biological and inorganic (i.e., fluid/rock) interactions, colonization experiments were systematically performed in the presence of abiotic controls. The microbial diversity of the samples was analyzed using 16S rRNA and functional gene sequencing, and fluids were recovered to determine their chemical composition. Moreover, glass alteration and secondary mineral precipitation were investigated under both biotic and abiotic conditions.

## MATERIALS AND METHODS

### SITE DESCRIPTION

Deployments were conducted by the research submersible *Nautile* (Ifremer) during the BIG (Biodiversité et Interactions à Guaymas) oceanographic cruise (RV *L'Atalante*) that took place in the Guaymas Basin in June 2010. AISICS deployments were performed at the Mat Mound site (N27°00.388, W111°25.471; 2004 m depth, BIG1 Marker) on the Southern Trough (Figure 1). This site consists of a small sulfide- and carbonate-rich active hydrothermal mound emerging above the sediment at the seafloor. The mound and surrounding sediments are covered by thick, white and orange microbial mats. The macrofauna is dominated by dense *Riftia* worm bushes at the top of the mound, and *Alvinellids* and *Polynoids* around the mound (Figure 1). The choice of this site was guided by the occurrence of abundant white and orange microbial mat. The colonizers were deployed within a 20 cm<sup>2</sup> area located on the edge of a white microbial mat at the base of the mound. Temperatures of 36.5, 68, 84.5, and 103°C were measured at 10, 20, 30, and 40 cm depth below seafloor, respectively. The deployment and recovery of the AISICS module were carried out one after the other, in order to minimize sediment and fluid flow disturbance.

### DESCRIPTION OF THE AUTONOMOUS *in situ* INSTRUMENTED COLONIZATION SYSTEM

The AISICS system is an autonomous instrumented microbial colonizer. It consists of the incubator itself and the instrumented module (Figure 1) (Sarrazin et al., 2006). The incubator is a titanium cylindrical chamber, perforated by numerous apertures 0.5 cm in diameter. A central titanium sheath, also perforated with 0.5 cm holes, hosts a Micrel™ temperature sensor and a titanium sampling pipe (0.5 cm diameter) both connected to the instrumented module by a 1 m long sampling tube. The AISICS instrumented module contains the electronic control card and battery for the pumping system encased in a watertight cylinder. The temperature probe electronics and four 100 mL sampling bags (PVC pouch, Baxter Clinic) are connected to a four-ways pump device for fluid collection (Sarrazin et al., 2006). The

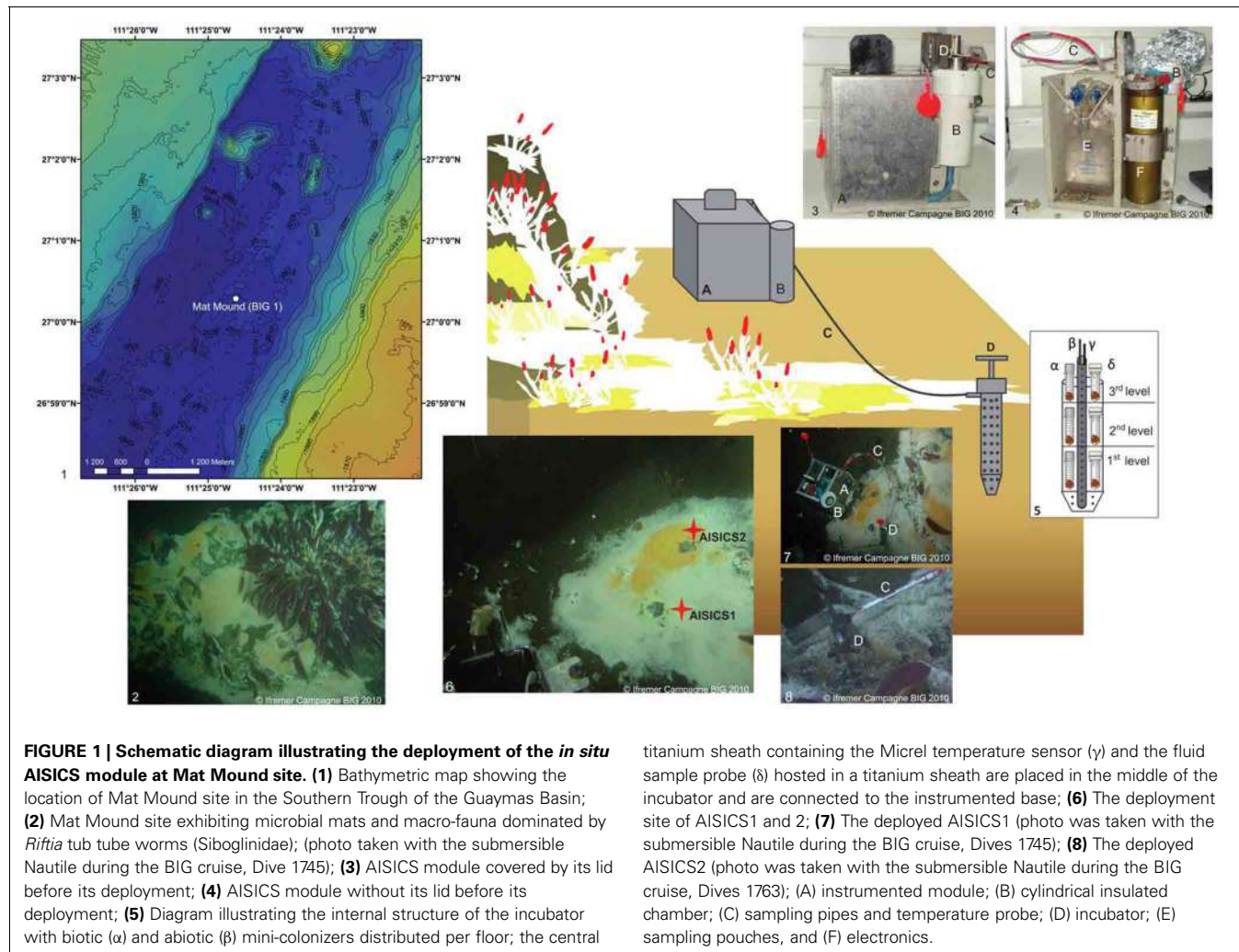


**FIGURE 1 | Schematic diagram illustrating the deployment of the *in situ* AISICS module at Mat Mound site. (1)** Bathymetric map showing the location of Mat Mound site in the Southern Trough of the Guaymas Basin; **(2)** Mat Mound site exhibiting microbial mats and macro-fauna dominated by *Riftia* tub tube worms (Siboglinidae); (photo taken with the submersible Nautilus during the BIG cruise, Dive 1745); **(3)** AISICS module covered by its lid before its deployment; **(4)** AISICS module without its lid before its deployment; **(5)** Diagram illustrating the internal structure of the incubator with biotic ( $\alpha$ ) and abiotic ( $\beta$ ) mini-colonizers distributed per floor; the central

titanium sheath containing the Micrel temperature sensor ( $\gamma$ ) and the fluid sample probe ( $\delta$ ) hosted in a titanium sheath are placed in the middle of the incubator and are connected to the instrumented base; **(6)** The deployment site of AISICS1 and 2; **(7)** The deployed AISICS1 (photo was taken with the submersible Nautilus during the BIG cruise, Dives 1745); **(8)** The deployed AISICS2 (photo was taken with the submersible Nautilus during the BIG cruise, Dives 1763); (A) instrumented module; (B) cylindrical insulated chamber; (C) sampling pipes and temperature probe; (D) incubator; (E) sampling pouches, and (F) electronics.

pump speed was set to a low flow rate ( $3.3 \text{ mL min}^{-1}$ ) in order to minimize environmental perturbation. The insulated chamber was designed for aseptic transportation of the incubator by the means of o-rings at the top and bottom. The temperature probe was computer-encoded before deployment to record the temperature at regular time intervals. The four-way valve and fluid pumping device was also programmed on board to set the trigger time for fluid sampling. Within each AISICS module, a total of 18 mini-colonizers were placed around the central sheath, and stacked over three layers (i.e., six per floor; 4 biotic, 2 abiotic). A perforated Teflon disk separated each layer from the other and allowed fluid circulation through the colonizers, (Figure 1). For the biotic experiments, the mini-colonizers consisted of a set of 2 mL polypropylene microtubes with caps (SX-8G IP-Star® Compact), both perforated with 1 mm holes (Figure 1). For abiotic controls, the mini-colonizers also consist of a set of 2 mL polypropylene microtubes (SX-8G IP-Star® Compact) with the cap replaced by a  $0.22 \mu\text{m}$  filter cellulose membrane (Millipore; Figure 1). The apertures of the incubator, Teflon disk and mini-colonizer tubes and caps, ensure fluid exchange throughout the different compartment of the mini-colonizers.

## SUBSTRATA, INSTRUMENTAL SETTING, AND DEPLOYMENT

Synthetic basaltic glasses were prepared using a mixture of pure element oxide and carbonate powder leading after synthesis to typical composition of tholeiitic basalt (with proportion in weight %:  $\text{SiO}_2$ , 48.68;  $\text{Al}_2\text{O}_3$ , 15.7;  $\text{CaO}$ , 11.2;  $\text{MgO}$ , 7.7;  $\text{FeO}$ , 12.5;  $\text{Na}_2\text{O}$ , 2.7;  $\text{K}_2\text{O}$ , 0.2;  $\text{TiO}_2$ , 1.39). One batch of synthetic basaltic glass was prepared using  $^{57}\text{Fe}$ -enriched  $\text{Fe}_2\text{O}_3$  powder obtained from Oak Ridge National Laboratory. Before mixing in agate mortar, powders were dried at  $150^\circ\text{C}$  for at least 24 h. Two different furnaces were used to prepare glass beads: a Carbolite™ 1700 muffle furnace with a maximum temperature of  $1600^\circ\text{C}$  with manual quenching under ambient atmosphere conditions, and a vertical furnace, mounted at Geomaterials laboratory (Univ. Marne La Vallée, France), with automatic quench system under controlled atmosphere ( $\text{H}_2$  or  $\text{O}_2$ ). The glass beads were prepared according to the following scheme: a temperature ramp up to  $600^\circ\text{C}$  for 30 min to 2 h, decarbonation at  $600^\circ\text{C}$  for 45 min to 1 h, another temperature increase up to  $1600^\circ\text{C}$  from 45 min to 3 h, followed by 60 min at  $1600^\circ\text{C}$  and immediate quenching.

A sample of natural basaltic glass was obtained by separating the chilled margin of a pillow basalt (sample Bat09-ROC22) from the Mid-Atlantic Ridge recovered during the Bathyluck cruise

(2009) at Lucky Strike hydrothermal field. Glass composition (wt%) has been determined: SiO<sub>2</sub>, 51.74; Al<sub>2</sub>O<sub>3</sub>, 14.96; CaO, 12.18; MgO, 8.1; Fe<sub>2</sub>O<sub>3</sub>, 9.95; Na<sub>2</sub>O, 2.28; K<sub>2</sub>O, 0.16; TiO<sub>2</sub>, 1.05; MnO, 0.18; P<sub>2</sub>O<sub>5</sub>, 0.12. All natural and synthetic glasses were crushed in an agate mortar to obtain fragments of less than 2 mm in size. Chips were subsequently cleaned in an ultrasonic bath in ethanol and then air-dried.

Each mini-colonizer was filled with about 0.6 mL of glass fragments, and sterilized by autoclaving during 30 min at 121°C, then by UV for at least 1 h. All titanium parts (i.e., incubator and the central titanium sheath) and Teflon-disks were rinsed five times with deionized water (MilliQ™ 18 mΩ), cleaned up using Desibac HPC® solution, rinsed again with deionized water then with Ethanol 96% and finally UV-treated for at least 1 h. The cylindrical insulated chamber was also cleaned using Desibac HPC®, deionized water, and Ethanol 96% then filled with sterilized seawater prior to deployment.

## AISICS1 AND 2

The AISICS1 module was deployed in the sediment at 40 cm depth below a thick white microbial mat (**Figure 1**). The maximum temperature reached at this depth was measured at 57.6°C over the 22 days of deployment. The AISICS1 mini-colonizers were filled with three different basaltic glass types: two synthetic glasses including one doped with <sup>57</sup>Fe (noted, respectively, βsyn and βsyn\*), and the basaltic glass (noted βnat). Each of the three layers contained 1 biotic mini-colonizer with βsyn, 1 biotic mini-colonizer with βsyn, 2 biotic mini-colonizers with βnat, 1 abiotic mini-colonizer with βsyn and 1 abiotic mini-colonizer with βnat. The temperature measurement frequency was fixed every 30 s. The fluid pumping system was programmed to collect three fluid samples at 48 h intervals.

The AISICS2 module was deployed for 8 days, at the junction between a white and orange microbial mat, at a distance of 5–10 cm from the location of AISICS1 module (**Figure 1**). Each of the three layers contained two biotic mini-colonizers filled with βnat and two others with βsyn\* and one abiotic tube for each substrate. Because of the short duration of deployment of this module, the temperature measurement frequency was set for every second and the fluid pumping system was programmed to collect fluids every 48 h after deployment.

## SAMPLE PROCESSING

Immediately after on board recovery, each glass sample from the mini-colonizers was aseptically split into five fractions. Two fractions were stored for molecular diversity analysis by freezing one at -80°C and storing the other at -20°C in 96% ethanol. One fraction was stored directly at -20°C for Scanning Electron Microscopy (SEM) and RAMAN spectroscopy analysis; one fraction was fixed for 2 h in 2% formaldehyde (prepared with sterile seawater), rinsed 3 times with sterile seawater and stored in 96% ethanol at -20°C for further Fluorescent *in situ* Hybridization (FISH) experiments and SEM analysis, as the last fraction directly stored in 50% ethanol—phosphate-buffered saline pH 7.2 (PBS) 1× solution (1:1) at -20°C. During processing of the mini-colonizers located in the 3rd level of the AISICS1 module, biotic

βnat and βsyn\* samples were accidentally mixed but nevertheless treated, and referred as βmix.

## DNA EXTRACTION

Total genomic DNA was extracted from the two fractions of basaltic glasses for molecular diversity analysis, using the FastDNA® Spin Kit for Soil (Bio101 Systems, MP Biomedicals), following the protocol modified by Webster et al. (2003). The DNA extractions of each sample were done independently for each type of storage and the extraction products were then pooled prior to PCR amplification.

## 16S rRNA GENE AMPLIFICATION

The 16S rRNA gene was amplified using the specific archaeal or bacterial domain primer combinations of A8F and ARC915R (Casamayor et al., 2000; Kolganova et al., 2002) and E8F and U907R (Lane et al., 1985; Lane, 1991), respectively (**Table 1**). Both archaeal and bacterial 16S rRNA gene amplification reactions were performed in 50 μl reaction mixtures containing: 10 μl of 5× GO Taq® DNA polymerase buffer (Promega), 5 μl of 25 mM MgCl<sub>2</sub> solution (Promega), 1 μl of 10 mM dNTPs (Eurogentec), 0.2 μl of each primers at 100 μM and 0.24 μl of 5 U·μl<sup>-1</sup> GO Taq® DNA polymerase (Promega). All amplifications were conducted in 30 cycles of denaturation at 94°C for 1 min, annealing for 1 min 30 s at 58°C or 52°C for the archaeal or bacterial 16S rRNA gene, respectively, and extension at 72°C for 7 min. All PCR reactions were carried out using a GeneAmp® PCR system 9700 (Applied Biosystems) thermal cycler, and PCR products were visualized using gel electrophoresis.

## PCR AMPLIFICATION OF FUNCTIONAL GENES

The presence of sulfate-reducers was highlighted with the amplification of *dsrAB* gene targets [coding for the (di)sulfite reductase], with a DSR1F and DSR4R primer combination (Wagner et al., 1998) (**Table 1**). The presence of methanogens was investigated with the amplification of *mcrA* gene (coding for the alpha subunit of the methyl-coenzyme M-reductase) using ME1 and ME2 as coupled primers (Hales et al., 1996) (**Table 1**). Each amplification reaction was performed in 50 μl reaction mix containing: 10 μl of 5× GO Taq® DNA polymerase buffer (Promega), 5 μl of 25 mM MgCl<sub>2</sub> solution (Promega), 1 μl of 10 mM dNTPs (Eurogentec), 0.2 μl of each primer at 100 μM and 0.24 μl of 5 U·μl<sup>-1</sup> GO Taq® DNA polymerase (Promega). All amplifications were conducted in 30 cycles of denaturation at 94°C for 1 min, annealing for 1 min 30 s and extension at 72°C for 7 min. The annealing temperature was set at 55 and 50°C for *dsrAB* gene and *mcrA* gene, respectively.

## CLONING, SEQUENCING OF 16S rRNA AND FUNCTIONAL GENES, PHYLOGENETIC AND STATISTICAL ANALYSIS

Prior to cloning, positively amplified PCR products were purified using NucleoSpin® Gel and PCR Clean-up kit (Macherey Nagel) according the manufacturer's instructions.

All of the 16S rRNA clone libraries were carried out with the TOPO XL cloning kit (Invitrogen) and functional gene clone libraries with the pGEM®-T cloning kit (Promega), both following the manufacturer's recommendations. Positive clones were processed for sequencing at GATC Biotech (Konstanz, Germany) using M13F primers. Sequences were imported into the BLAST

**Table 1 | List of the PCR primers used during the study.**

| Primers        | Target             | Sequence (5'-3')  | Tm°C | References                                       |
|----------------|--------------------|---|------|--|
| A8F<br>ARC915R | Archaeal 16S rRNA  | CGG-TTG-ATC-CTG-CCG-GA<br>CTG-CTC-CCC-CGC-CAA-TTC-CT      | 58   | Kolganova et al., 2002<br>Casamayor et al., 2000 |
| E8F<br>U907R   | Bacterial 16S rRNA | AGA-GTT-TGA-TCA-TGG-CTC-AG<br>CCG-TCA-ATT-CMT-TTG-AGT-TT  | 52   | Lane, 1991<br>Lane et al., 1985                  |
| DSR1F<br>DSR4R | <i>dsrAB</i> gene  | AC[C/G]-CAC-TGG-AAG-CAC-G<br>GTG-TAG-CAG-TTA-CCG-CA       | 55   | Wagner et al., 1998                              |
| ME1<br>ME2     | <i>mcrA</i> gene   | GCM-ATG-CAR-ATH-GGW-ATG-TC<br>TCA-TKG-CRT-AGT-TDG-GRT-AGT | 50   | Hales et al., 1996                               |

nucleotide search program through the National Center for Biotechnology Information (NCBI website: <http://www.ncbi.nlm.nih.gov/BLAST>) to find closely related sequences within the GenBank database. The clone library 16S rRNA sequences were aligned, edited and analyzed using Bioedit version 7.1.3 software. Phylogenetic trees were constructed using the MEGA 5 program (Kumar et al., 2008). The robustness of the inferred topologies was tested using 1000 bootstrap resampling of the trees calculated on the basis of neighbor-joining algorithm (Saitou and Nei, 1987) using the Kimura two-parameter correction matrix (Kimura, 1980). All sequences more than 97% similar were considered to belong to the same phylotype (OTU) and were clustered together in the alignment (Schloss and Handelsman, 2004).

The sequence data reported in this study have been submitted to GenBank nucleotide sequence databases under accession numbers KC901750 to KC901834 and KC901560 to KC901725 for the *Archaea* and *Bacteria* gene sequences, respectively, and KC901726 to KC901749 for the *mcrA* gene sequences and KC901835 to KC901870 for the *dsrAB* gene sequences.

To examine the influence of the deployment time, depth or substrata type on both archaeal and bacterial diversity, we used the UniFrac computational tool (Lozupone et al., 2006). The habitats (defined by: the duration of incubation, the depth of incubation and the type of substrata) were clustered using the jackknife environment clusters analysis tool with 100 permutations.

## GEOCHEMICAL ANALYSIS

Interstitial fluids from the colonization modules and deep seawater above the Mat Mound site (Dive 1770) were sub-sampled and stored as follows: 10 mL of fluid was used to measure pH at room temperature. For the analysis of dissolved major and trace elements, 30 mL of sample was filtered through 0.22 µm (Sterivex™, Millipore) membrane and stored at 4°C. For hydrogen sulfide analysis, 10 mL was filtered through a 0.45 µm (Sterivex™, Millipore) membrane and precipitated as ZnS in 25 mL evacuated septum vials containing 0.1g of Zinc Acetate (Sigma-Aldrich) and stored at 4°C. In the AISICS1 module pouch number 1, two immiscible fluids were recovered: a small amount of a buoyant liquid (about 5 mL) overlying a saline, seawater-like liquid (around 60 mL). Only the denser phase was treated as described above while the lighter phase, likely composed of hydrocarbons,

was not processed further. Concentration of major elements was measured using Inductively Coupled Plasma-Atomic Emission Spectrophotometry (ICP-AES, Ultima 2, Horiba JobinYvon) while the concentration of trace elements was measured using High-Resolution ICP Mass Spectrometer (HR-ICP-MS, Element 2, ThermoFisher), both operated at the Pole Spectrometry Ocean Brest (PSO, Brest). Prior to elemental analysis, samples were acidified at least 1 month in advance to 0.28 mol.L⁻¹ HNO₃ prepared from ultra-pure reagent grades. Solutions for ICP-AES and ICP-MS analysis were diluted 100-fold with 0.28 mol.L⁻¹ HNO₃. Three water solution standards (Slew 3, Cass 4 and Nass 5 from the National Research Council of Canada) were also prepared along with the samples. For both ICP-AES and ICP-MS analysis, two sets of calibrating standards were used by adding multi-elemental standard solutions either with pure Milli-Q™ water or with 100-fold diluted Cass 4 in 0.28 mol.L⁻¹ HNO₃. Dissolved hydrogen sulfide was measured using spectrophotometric method using the protocol described by (Cline, 1969).

## SCANNING ELECTRON MICROSCOPY: SEM

Scanning electron microscopy (SEM) was carried out at the “Service Commun de Microscopie Electronique à Balayage” (UPMC, Paris, France) using a Zeiss SUPRA® 55 VP Field Emission Scanning Electron Microscope (FE-SEM). The variable chamber pressure capability (2–133 Pa) permits the examination of both uncoated and Au- or C-coated samples. Three secondary electron detectors (Everhart-Thornley for high voltage mode, VPSE used for variable pressure mode and InLens for low voltage mode) and a backscattered electron detector enable the acquisition of high-spatial resolution images using analytical conditions that varied from 3–30 kV, 10 pA-1 nA, and 30–133 Pa with a 3.3–7.2 mm working distance. We also performed elemental microanalysis using an Energy Dispersive X-ray spectrometer (PGT Sahara).

## CONFOCAL RAMAN SPECTROSCOPY

RAMAN spectra were obtained at IPGP (Paris, France) on resin free samples using a Renishaw InVia spectrometer. A 514 nm argon laser (20 mW) was focused through an Olympus BX61 microscope equipped with an x50 objective (numerical aperture 0.75). This configuration yields a planar resolution of about 1 µm, with a power delivered at the sample surface of 0.5 mW.

An integration time of 100 s was used to ensure that the delivered radiation didn't damage the organic matter. The signal was dispersed using a holographic grating with 1800 grooves.mm<sup>-1</sup> coupled for the detection with a RENCAM CCD (charge-coupled device) detector. The acquired RAMAN spectra were then processed using the WiRE 3.3 Renishaw software and compared to the RRUFF database (<http://rruff.info/>).

## RESULTS

### FLUID GEOCHEMISTRY

About 60 mL of fluids were successfully recovered in each pouch of AISICS1, whereas very low quantities of fluid were pumped in AISICS2, probably due to clogging of the inlet. Hence, H<sub>2</sub>S and pH determinations were not performed for AISICS2.

During the AISICS1 deployment, the average fluid temperature was 44.3°C with minimum and maximum values of 36 and 57.6°C, respectively. The fluid exhibited a near neutral pH (7.6) and low dissolved H<sub>2</sub>S concentrations (below 5 µM). For AISICS2, the average temperature was 42.9°C with a minimum at 36.9°C and a maximum at 46.3°C (Table 2). In general, the concentrations of major cations (Ca, K), trace metals (Mn, Fe), and Si were higher in AISICS1 compared to AISICS2 (Table 2), reflecting a higher contribution of hydrothermal fluids in the AISICS1 colonization module. This is consistent with the lower concentration of Mg in the AISICS1, which is typically depleted in hydrothermal vent fluids (Von Damm et al., 1985a,b). In general, fluids recovered from AISICS2 had chemical compositions quite similar to the overlying seawater (Table 2).

Sulfate concentrations, determined as total dissolved sulfur on acidified and filtered sample (i.e., devoid of H<sub>2</sub>S) in AISICS1 and AISICS2 were close to seawater values, albeit slightly lower for AISICS1, consistent with the higher contribution of sulfate-depleted hydrothermal fluid. Additional evidence that the AISICS2 incubator was deployed under seawater dominated conditions comes from Mo concentrations (Table 2). Under anoxic conditions, where [H<sub>2</sub>S] ≥ 11 µM and [O<sub>2</sub>] ≈ 0 µM, seawater-derived molybdate ion will be reduced to the reactive tetrathiomolybdate species (Erickson and Helz, 2000) and readily precipitated. Hence, the complete removal of Mo observed in AISICS1 suggests predominantly anoxic, and probably

sulfidic conditions while seawater-like Mo concentrations in AISICS2 provide evidence for rather oxic or micro-aerophilic conditions.

### MICROBIAL DIVERSITY ACCORDING TO 16S rRNA GENES SEQUENCES

The 16S rRNA gene was analyzed for 24–50 clones for each sample. High bacterial and archaeal diversity was generally observed in both colonizers with a slight difference in relation to the position of the mini-colonizers within the incubator (i.e., top or bottom). This translated into an increase in phylogenetic diversity with increasing depth in the sediment (Figures 2, 3) and Table 3).

In general, the main groups retrieved in all samples were the *Epsilonproteobacteria*, *Deltaproteobacteria*, and *Thermococcus* sp. In addition, *Gammaproteobacteria*, *Caldithrix* sp., *Thermotogales*, and *Spirochaetes* were observed in lesser proportions, and the DHVE2 (Deep-sea Hydrothermal Vent *Euryarchaeota* group 2) were also detected (Figures 2, 3 and Table 3). Sequences belonging to *Siboglinidae* as *Osedax* sp. or *Siboglinum* sp. endosymbiont and sequences close to the uncultured WS3 candidate division were retrieved in AISICS 1, the sampler that experienced a higher contribution of hydrothermal fluids and longer exposure time. In contrast, a new clade of *Epsilonproteobacteria*, named Guaymas *Epsilonproteobacteria* group (Figure 4), DHVE-1 (Deep-sea Hydrothermal Vent *Euryarchaeota* group 1) as well as ANME 2 sequences were found only in AISICS2 (Figure 2 and Table 3).

The cluster tree obtained with the Archaeal sequences (Figure 2) using the statistical jackknife environment clusters did not show any correlation between the archaeal diversity and deployment duration, the depth, or substrata composition. This contrasts with the cluster tree obtained for the Bacteria, where there was a correlation between bacterial diversity and deployment time and hydrothermal contribution (samples from AISICS1 and from AISICS2 were clustered together, respectively) and with depth in the sediment and the temperature for AISICS2 only (Figure 3).

### *mcrA* AND *dsrAB* GENE DIVERSITY

The *mcrA* gene sequences were detected in AISICS1, in particular in the deepest mini-colonizers (Table 3). In AISICS2, the

**Table 2 | Geochemical composition and pH measured in the sampling pouches and bottom seawater (Dive 1770).**

|                             | Mean T°C<br>(max-min) | Pouch<br>number | pH  | H <sub>2</sub> S<br>µM | Mg<br>mM | Na<br>mM | K<br>mM | Ca<br>mM | Sr<br>mM | S<br>mM | Si<br>mM | Ba<br>µM | Fe<br>µM | Mn<br>µM | Mo<br>µM |
|-----------------------------|-----------------------|-----------------|-----|------------------------|----------|----------|---------|----------|----------|---------|----------|----------|----------|----------|----------|
| AISICS 1                    | 44.3 (57.6-36)        | SX1-A           | 7.5 | <5                     | 42.0     | 434.0    | 13.8    | 13.8     | 0.13     | 29.66   | 1.88     | 0.96     | 0.88     | 17.83    | <0.01    |
|                             |                       | SX1-B           | 7.6 | <5                     | 45.0     | 468.2    | 15.3    | 15.1     | 0.14     | 31.91   | 1.94     | 1.03     | 0.83     | 19.34    | <0.01    |
|                             |                       | SX1-C           | 7.6 | <5                     | 44.5     | 466.2    | 15.1    | 15.0     | 0.14     | 31.21   | 1.82     | 1.02     | 1.06     | 18.46    | <0.01    |
|                             |                       | SX1-D           | 7.6 | <5                     | 45.2     | 472.1    | 15.3    | 15.1     | 0.13     | 30.62   | 1.87     | 0.99     | 1.21     | 17.88    | <0.01    |
| AISICS 2                    | 42.9 (46.3-36.9)      | SX2-A           | nd  | nd                     | 53.5     | 485.3    | 10.3    | 10.0     | 0.10     | 32.52   | 0.10     | 0.07     | 0.03     | 0.07     | 0.10     |
|                             |                       | SX2-B           | nd  | nd                     | 53.6     | 482.7    | 10.5    | 9.8      | 0.10     | 33.16   | 0.11     | 0.07     | <0.02    | 0.07     | 0.11     |
|                             |                       | SX2-C           | nd  | nd                     | 55.1     | 492.9    | 10.9    | 10.2     | 0.10     | 32.58   | 0.18     | 0.11     | <0.02    | 0.23     | 0.10     |
|                             |                       | SX2-D           | nd  | nd                     | 53.2     | 481.1    | 10.4    | 9.8      | 0.10     | 32.75   | 0.16     | 0.10     | <0.02    | 0.13     | 0.10     |
| Bottom seawater (Dive 1770) |                       |                 | nd  | nd                     | 54.6     | 489.3    | 10.6    | 10.1     | 0.11     | 34.08   | 0.20     | 0.15     | <0.02    | 0.17     | 0.12     |

nd for not determined.

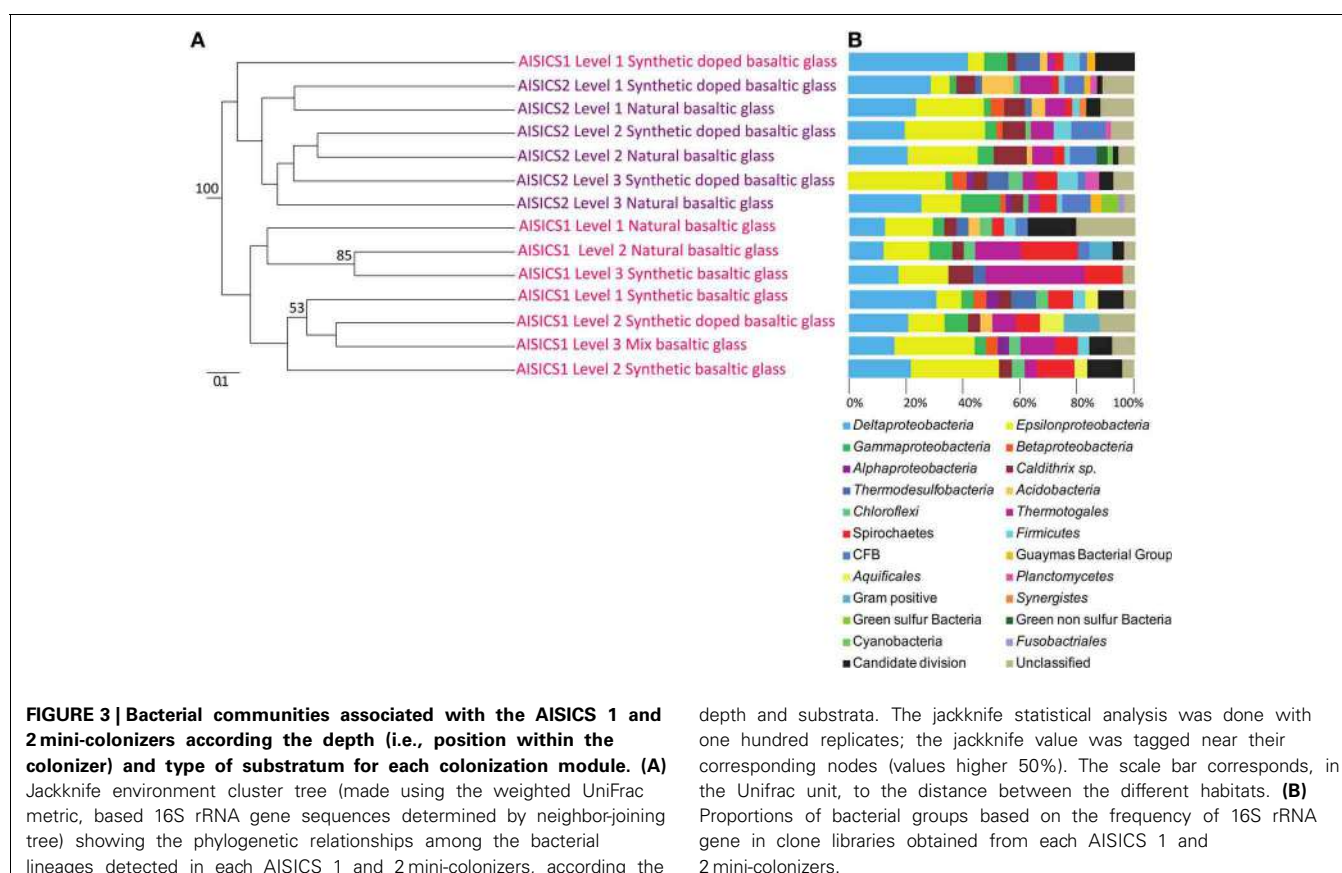
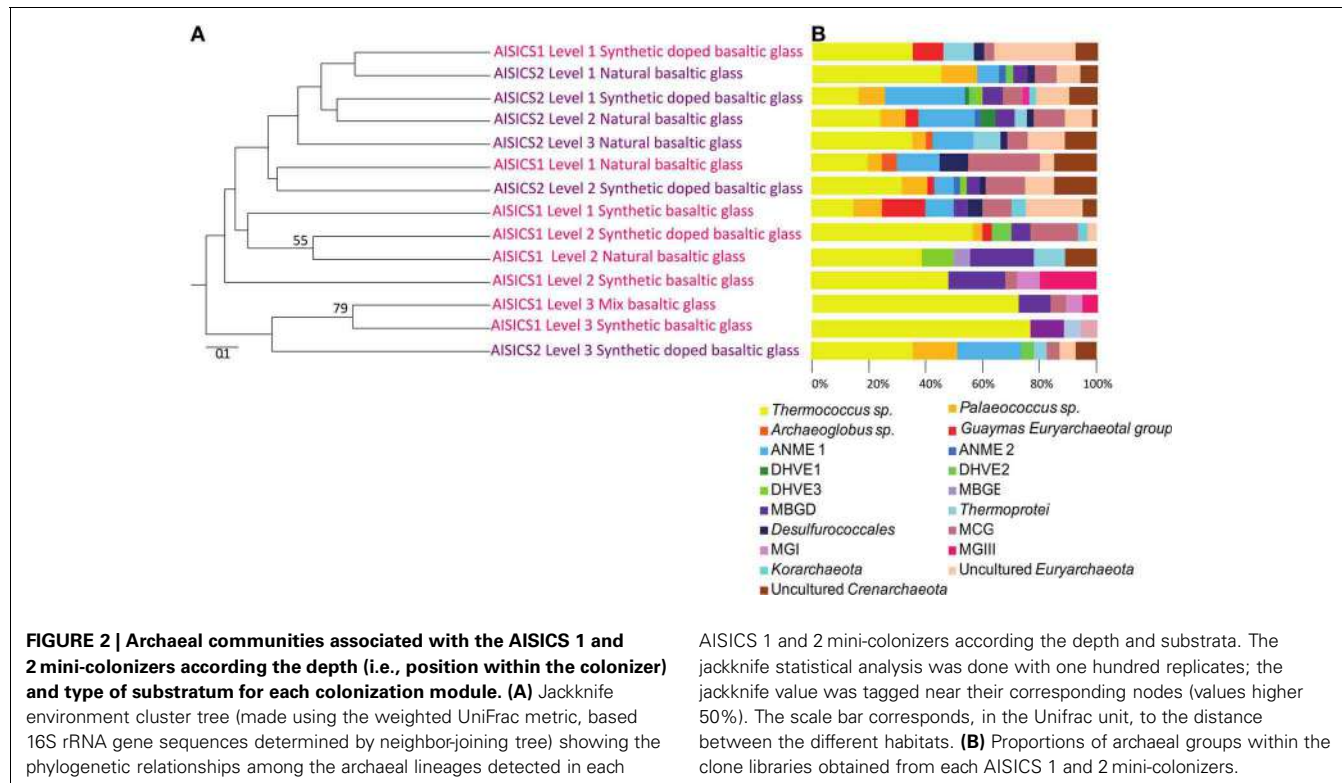


**Table 3 | Microbial composition determined per level, substratum and module.**

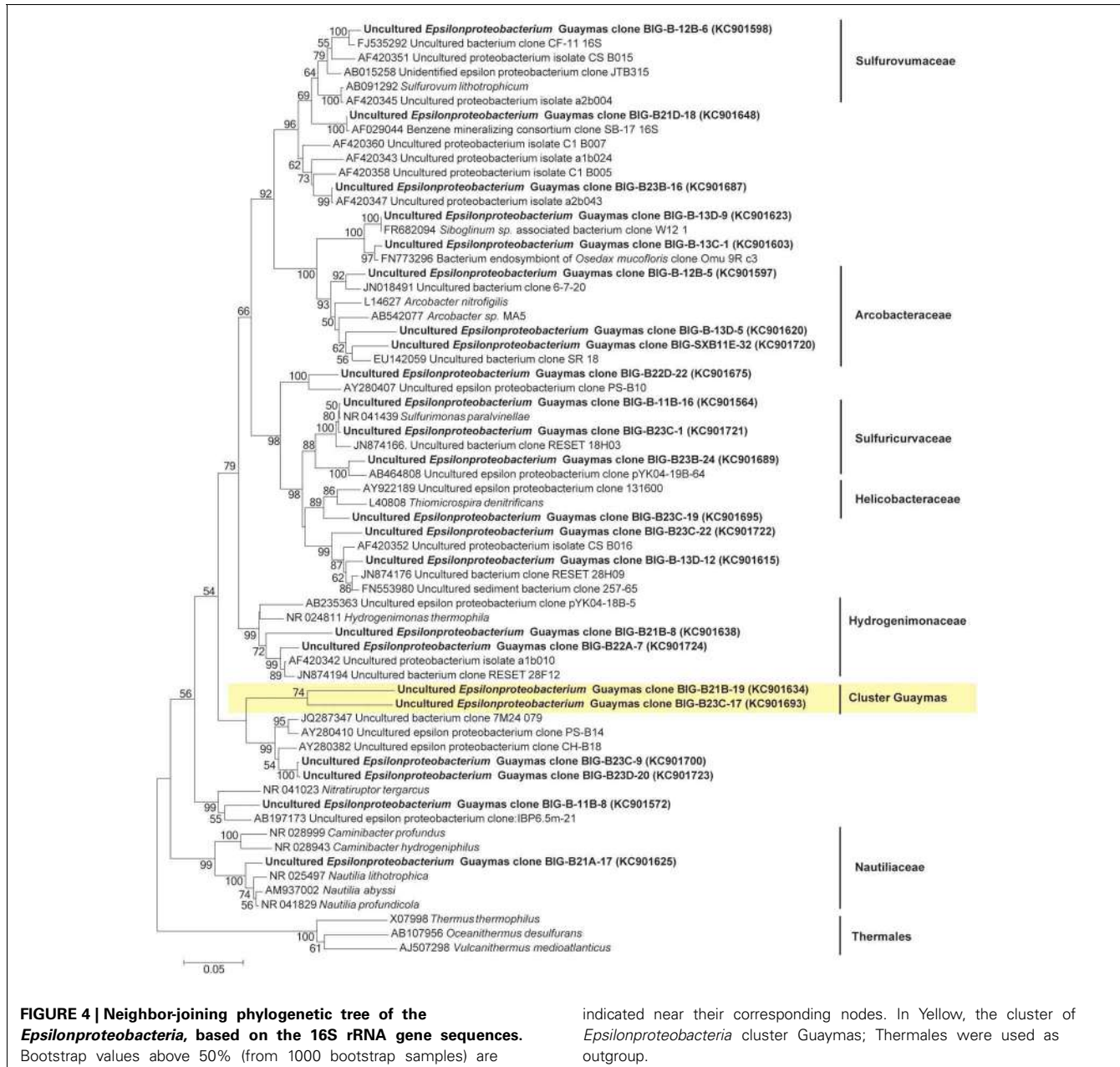
| Deployment location             | AISICS1                                   |      |       |      |         |      |      |      | AISICS2  |      |      |      |         |      |         |      |
|---------------------------------|---|------|-------|------|---------|------|------|------|--|------|------|------|---------|------|---------|------|
|                                 | Sediment covered by a white microbial mat |      |       |      |         |      |      |      | Sediment covered by a white and orange microbial mat |      |      |      |         |      |         |      |
| Deployment time                 | 22 days                                   |      |       |      |         |      |      |      | 8 days   |      |      |      |         |      |         |      |
|                                 | Level 1                                   |      |       |      | Level 2 |      |      |      | Level 3  |      |      |      | Level 1 |      | Level 2 |      |
| Substratum                      | βnat                                      | βsyn | βsyn* | βnat | βsyn*   | βsyn | βnat | βmix | βnat   | βsyn | βnat | βsyn | βnat    | βsyn | βnat    | βsyn |
| <b>BACTERIA</b>                 |   |      |       |      |         |      |      |      |  |      |      |      |         |      |         |      |
| <i>Deltaproteobacteria</i>      | +   | +    | +     | +    | +       | +    | +    | +    | +  | +    | +    | +    | +       | +    | +       | +    |
| <i>Epsilonproteobacteria</i>    | +   | +    | +     | +    | +       | +    | +    | +    | +  | +    | +    | +    | +       | +    | +       | +    |
| <i>Gammaproteobacteria</i>      | +   | +    | +     | +    | +       | -    | -    | +    | +  | +    | +    | +    | +       | +    | +       | +    |
| <i>Betaproteobacteria</i>       | -   | +    | -     | -    | -       | -    | -    | +    | +  | -    | -    | +    | +       | +    | +       | +    |
| <i>Caldithrix</i> sp.           | +   | +    | +     | +    | +       | +    | +    | -    | +  | +    | +    | +    | +       | +    | +       | +    |
| <i>Thermodesulfobacteria</i>    | +   | +    | +     | -    | -       | -    | +    | -    | +  | +    | -    | -    | -       | -    | -       | +    |
| <i>Acidobacteria</i>            | +   | -    | +     | -    | +       | -    | -    | -    | +  | +    | +    | +    | -       | -    | -       | -    |
| <i>Chloroflexi</i>              | +   | +    | -     | +    | -       | +    | -    | +    | -  | +    | -    | +    | -       | +    | +       | +    |
| <i>Thermotogales</i>            | -   | -    | +     | +    | +       | +    | +    | +    | +  | +    | +    | +    | +       | +    | +       | +    |
| <i>Spirochaetes</i>             | +   | +    | +     | +    | +       | +    | +    | +    | +  | +    | +    | +    | +       | -    | +       | +    |
| <i>Firmicutes</i>               | +   | +    | +     | -    | -       | -    | -    | +    | +  | +    | +    | +    | +       | +    | +       | +    |
| CFB                             | +   | -    | +     | +    | -       | -    | -    | -    | -  | +    | +    | +    | +       | +    | +       | +    |
| Guaymas bacterial group         | -   | -    | +     | -    | -       | -    | -    | -    | -  | +    | -    | -    | -       | +    | -       | -    |
| <i>Aquificales</i>              | -   | +    | -     | -    | +       | +    | -    | -    | -  | -    | -    | -    | -       | -    | -       | -    |
| <i>Planctomycetes</i>           | -   | -    | -     | -    | -       | -    | -    | -    | -  | +    | -    | +    | -       | -    | -       | +    |
| <b>ARCHAEA</b>                  |   |      |       |      |         |      |      |      |  |      |      |      |         |      |         |      |
| <i>Thermococcus</i> sp.         | +   | +    | +     | +    | +       | +    | +    | +    | +  | +    | +    | +    | +       | +    | +       | +    |
| <i>Palaeococcus</i> sp.         | +   | +    | -     | -    | -       | -    | -    | -    | -  | +    | +    | +    | +       | +    | +       | +    |
| <i>Archaeoglobus</i> sp.        | +   | -    | -     | -    | -       | -    | -    | -    | -  | -    | -    | -    | -       | -    | +       | -    |
| Guaymas euryarchaeotal group    | -   | +    | +     | -    | -       | -    | -    | -    | -  | -    | -    | -    | +       | +    | -       | -    |
| ANME 1                          | +   | +    | -     | -    | -       | -    | -    | -    | -  | +    | +    | +    | +       | +    | +       | +    |
| ANME 2                          | -   | -    | -     | -    | -       | -    | -    | -    | -  | +    | -    | +    | +       | -    | -       | -    |
| DHVE2                           | -   | -    | -     | -    | +       | -    | +    | -    | +  | +    | +    | -    | -       | -    | -       | +    |
| DHVE3                           | -   | -    | -     | +    | -       | -    | -    | -    | -  | -    | +    | -    | -       | +    | -       | -    |
| MBGB                            | -   | -    | -     | +    | -       | -    | -    | -    | -  | -    | -    | -    | -       | -    | -       | -    |
| MBGD                            | -   | +    | -     | +    | +       | +    | -    | +    | +  | +    | -    | +    | +       | -    | -       | -    |
| <i>Thermoprotei</i>             | -   | -    | +     | +    | -       | -    | -    | -    | -  | -    | -    | +    | -       | -    | +       | +    |
| <i>Desulfurococcales</i>        | +   | +    | +     | -    | -       | -    | -    | -    | -  | +    | -    | +    | +       | +    | +       | -    |
| MCG                             | +   | +    | +     | -    | +       | +    | -    | +    | +  | +    | +    | +    | +       | +    | +       | +    |
| MGI                             | -   | -    | -     | -    | -       | +    | -    | +    | -  | -    | -    | -    | -       | -    | -       | -    |
| MGIII                           | -   | -    | -     | -    | -       | +    | -    | +    | -  | -    | +    | -    | -       | -    | -       | -    |
| Korarchaeota                    | -   | +    | -     | -    | +       | -    | -    | -    | -  | -    | +    | -    | -       | -    | -       | -    |
| Uncultured                      | +   | +    | +     | -    | +       | -    | -    | -    | -  | +    | +    | +    | +       | +    | +       | +    |
| <i>Euryarchaeota</i>            |   |      |       |      |         |      |      |      |  |      |      |      |         |      |         |      |
| Uncultured                      | +   | +    | +     | +    | -       | -    | +    | -    | -  | +    | +    | +    | +       | +    | +       | +    |
| Crenarchaeota                   |   |      |       |      |         |      |      |      |  |      |      |      |         |      |         |      |
| <b>FUNCTIONAL GENE</b>          |   |      |       |      |         |      |      |      |  |      |      |      |         |      |         |      |
| <i>mcrA</i> gene amplification  | +   | +    | +     | +    | -       | +    | -    | -    | +  | +    | +    | +    | +       | +    | +       | +    |
| <i>dsrAB</i> gene amplification | +   | +    | +     | +    | +       | +    | +    | +    | -  | -    | -    | -    | -       | -    | -       | -    |

Only groups with more than 3 clones per samples are presented. + presence; - absence.

In dark orange, microbial group retrieved in all samples; in light orange microbial group retrieved in almost all sample.

In dark blue, microbial group retrieved only in all and/or mainly in AISICS1 samples; in light blue microbial group retrieved only in almost all and/or mainly in AISICS1 samples.

In dark green, microbial group retrieved only in all and/or mainly in AISICS2 samples; in light green microbial group retrieved only in almost all and/or mainly in AISICS2 samples.



*mcrA* gene was amplified in almost all mini-colonizers irrespective of deployment depth. With the exception of one methanogen sequence detected in a mini-colonizer containing  $\beta$ nat substrate, all *mcrA* sequences were affiliated to ANME 1 related to the Guaymas *mcrA* cluster (Holler et al., 2011; Biddle et al., 2012) or to the deeply branching Guaymas *mcrA* cluster (Biddle et al., 2012) (Figure 5).

Using *dsrAB* gene sequencing, sulfate-reducers were detected in all mini-colonizers of AISICS1 (Table 3) but none in AISICS2. The majority of *dsrAB* (Figure 6) sequences were related to *Deltaproteobacteria*, especially the *Syntrophobacteraceae*, and some were close to *Desulfoarculaceae*, *Desulfovibrionaceae*, and *Desulfobacteriaceae*.

*anilini* group and to group IV (Dhillon et al., 2003). In addition few *Archaeoglobus* sequences were found in most samples.

#### MICROSCOPY AND RAMAN SPECTROSCOPY ANALYSES

Irrespective of their composition (i.e., natural or synthetic) or exposure conditions (i.e., biotic or abiotic), microscopy analyses show that glass surfaces are covered by salt crystals ( $\text{NaCl}$  or  $\text{MgCl}_2$ ), and sulfate minerals ( $\text{CaSO}_4 \cdot 2\text{H}_2\text{O}$  gypsum or  $\text{BaSO}_4$  barite) due to direct precipitation from seawater after sample recovery. Glass surfaces from both AISICS modules did not present any clear alteration textures or replacement by secondary minerals. All natural glass fragments ( $\beta$ nat) and

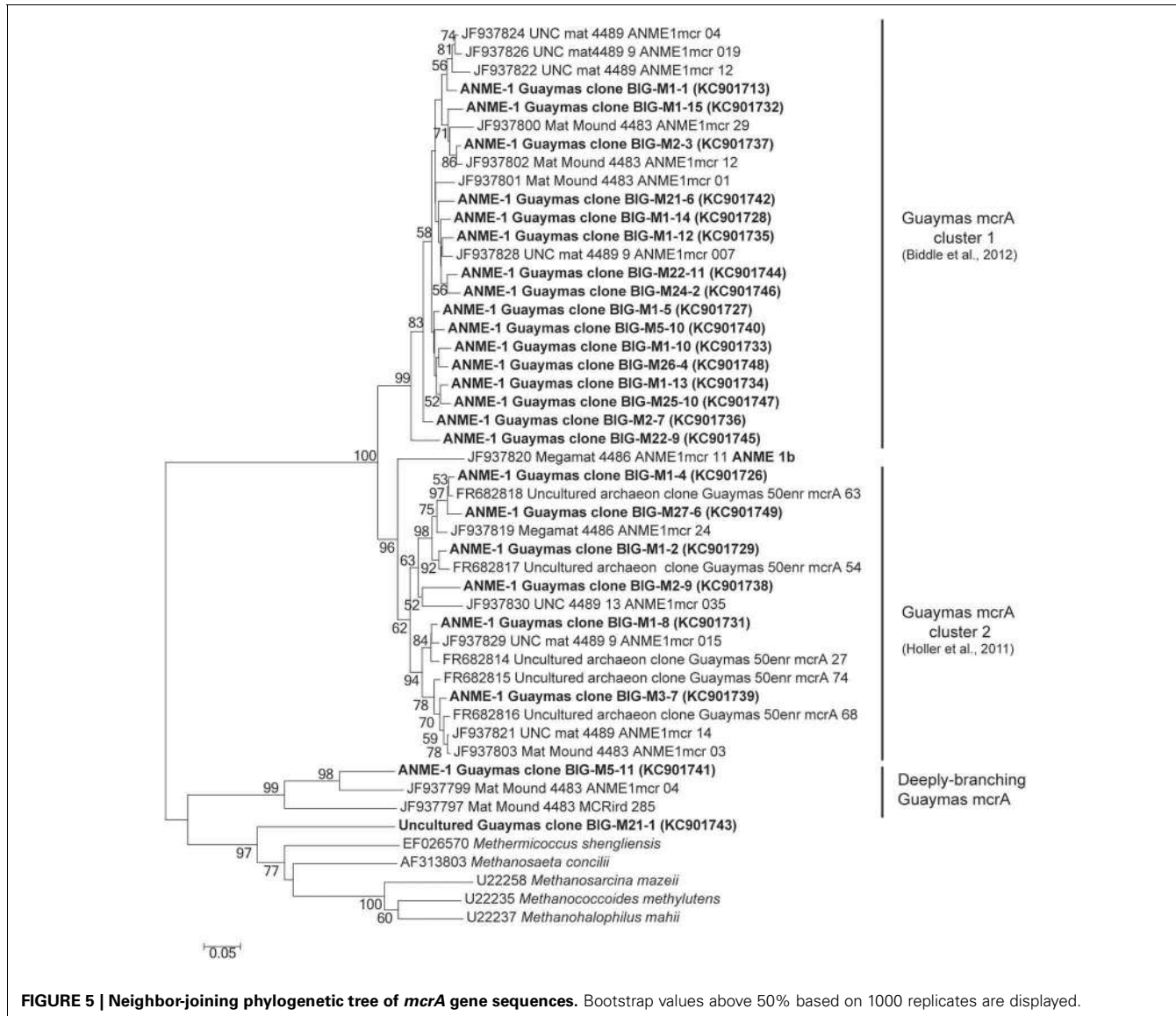


**FIGURE 5 |** Neighbor-joining phylogenetic tree of *mcrA* gene sequences. Bootstrap values above 50% based on 1000 replicates are displayed.

several artificial glass fragments ( $\beta$ syn or  $\beta$ syn\*) have exhibited small rounded vesicles whose diameters vary between 10 and 100  $\mu\text{m}$  (Figure 7). Those cavities were filled with sparse crystals of pyrite (Figure 7). In some cases, vesicles could be completely filled with nano-pyrite (Figure 7A). Since vesicles were present in  $\beta$ nat before deployment, they represent original features of submarine basalts that formed during magma degassing and were preserved during quenching. Interestingly, vesicles were not observed on the  $\beta$ syn and  $\beta$ syn\* before deployment. In addition to halite and pyrite crystals, vesicles of biotic samples also contain filaments and microbial cells-like structures. The biotic samples also exhibited an enrichment in organic matter forming small aggregates or film covering the glass surface (Figures 7, 8). In some cases, accumulations of organic matter with remnants of diatoms were observed together with frambooidal pyrite or nano-crystals of barite (Figures 7, 8).

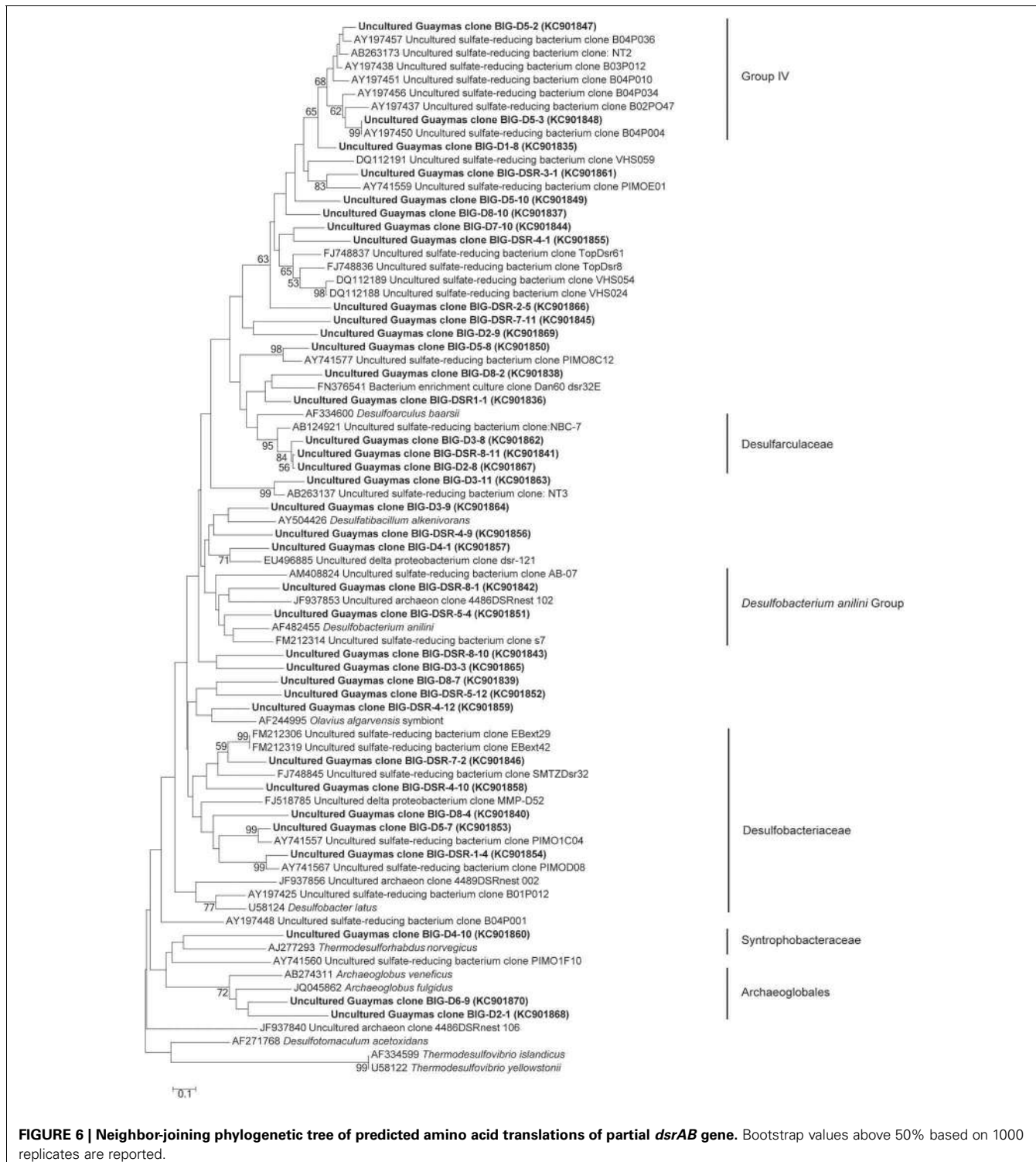
In the associated Raman spectra, we observed broad and overlapping bands, designated as D and G bands (at 1360 and 1580  $\text{cm}^{-1}$ , respectively), along with the aliphatic and aromatic C-H vibrational bands between 2800–3000  $\text{cm}^{-1}$ , that are characteristic of disordered carbonaceous matter with a weak structural organization (Figure 9) (Spötl et al., 1998). This likely corresponds to degraded microbial mat as organic aggregates and microbial cells (mainly rods) were observed in both vesicles and on glass surfaces (Figures 7, 9) (Maquelin et al., 2002).

## DISCUSSION

### MICROBIAL COLONIZATION OF BASALTIC GLASS

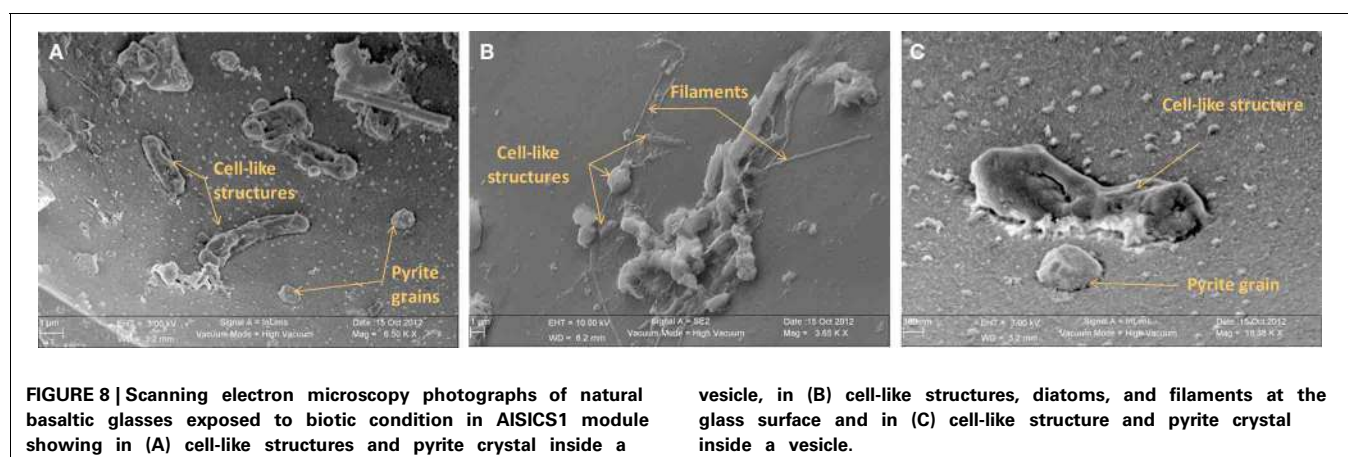
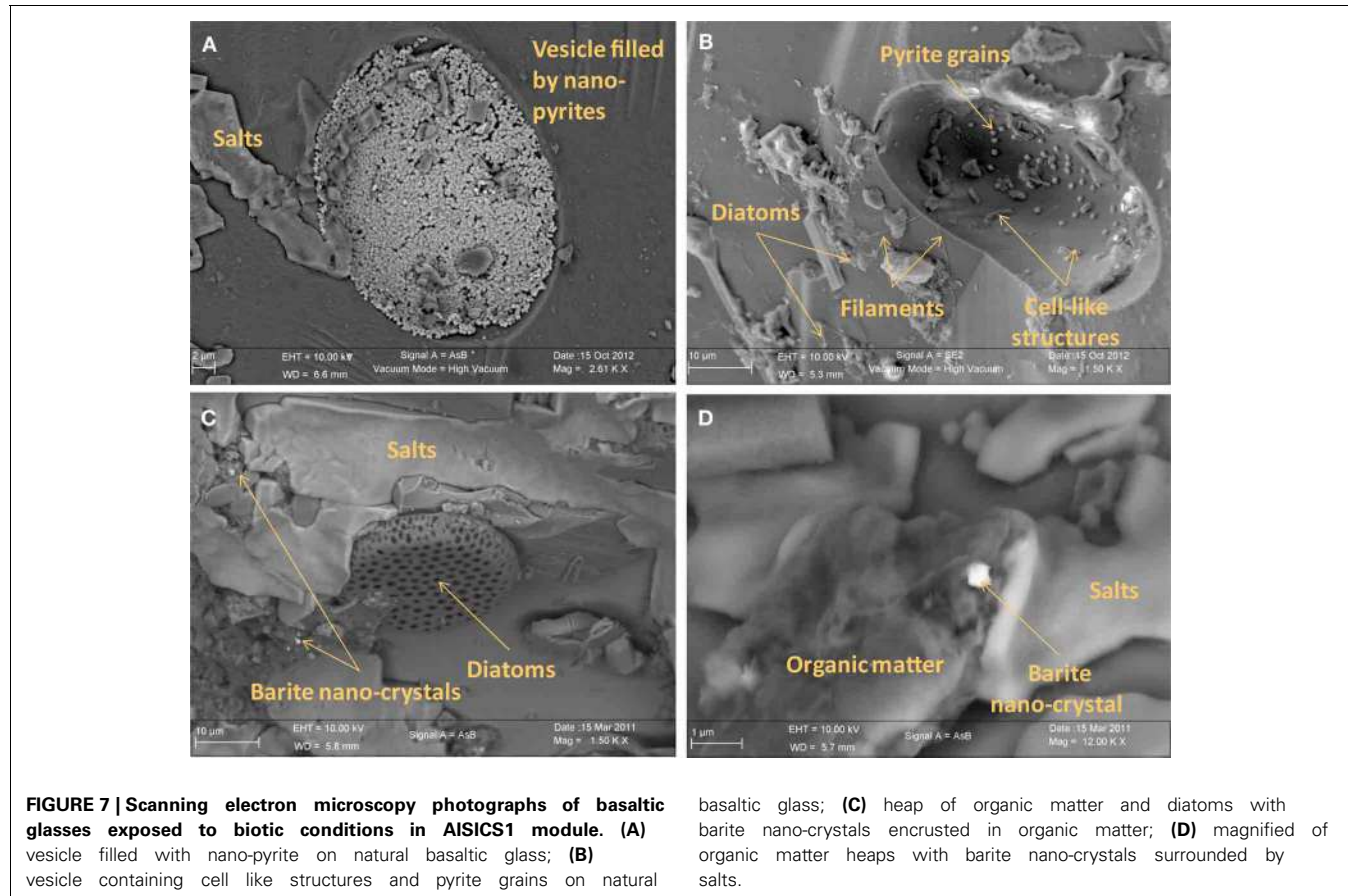
#### *Microbial diversity and putative metabolisms*

Miscellaneous groups of *Archaea* or *Bacteria* were detected in both short- and long-term deployments. According to the recorded temperature during incubation, all of the colonizing microbes



should be mesophiles to thermophiles (Table 3), and exposed to mainly anaerobic conditions. In both colonization modules, archaeal and bacterial diversity generally increased with burial depth in the sediment (Figures 2, 3); this observation was more evident in the longer-term deployment module (AISICS1). The detected microorganisms could have several metabolism

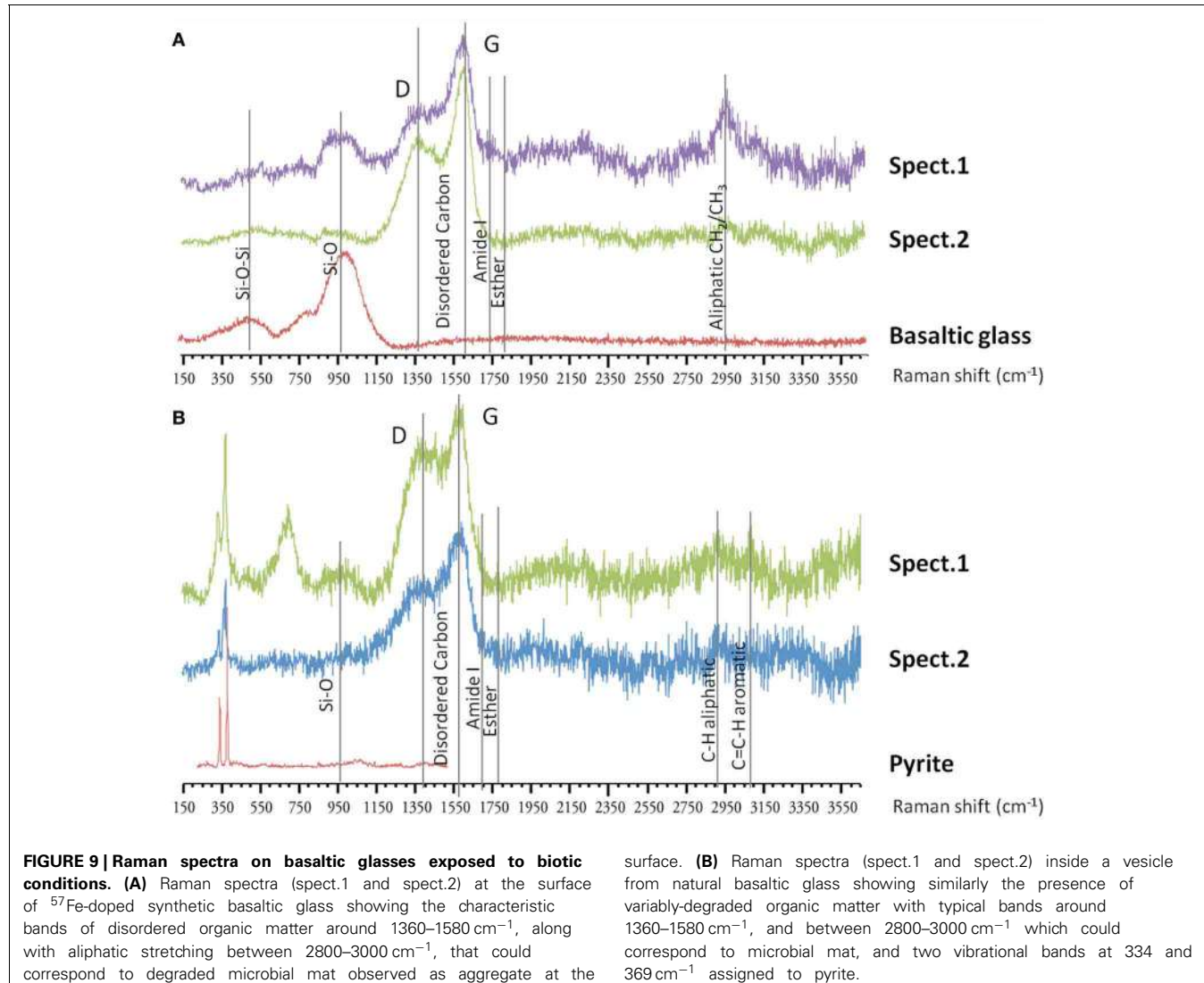
including those involved in carbon, sulfur, iron, or nitrogen biogeochemical cycles. Although phylogenetic affiliation may not be necessarily linked to specific metabolic or physiological properties, we cautiously inferred metabolic and physiological trends for clusters of microorganisms sharing similar properties. The implications of the observed microbial diversity for sulfur, iron,



carbon, and nitrogen cycles are detailed below, with the aim to highlight potential biogeochemical reactions that may govern fluid-basalt interactions at high temperatures and in organic-rich environments:

**Carbon cycle.** Due to the enrichment of organic matter at Guaymas basin, carbon cycling is likely a major metabolic driver in our colonizers. At Guaymas basin, the sediments accumulated a wide variety of organic compounds including light hydrocarbons, short-chain organic acids, particulate organic matter

and ammonia (Welhan, 1988; Martens, 1990). These compounds were derived from diagenetic reactions between high temperature hydrothermal fluids and sediments, resulting in the pyrolysis of organic matter and precipitation of metal-sulfide in the subsurface. In biotic colonizers, organic compounds occur as small particle deposits or aggregates, droplets or mats, and result in characteristic RAMAN spectra (Figure 9). This organic matter, likely derived from the surrounding sediments, could directly support chemoorganotrophic microbial life associated with basalt substrata. We observed evidence for fermentative



microorganisms (e.g., *Thermococcales*) that are likely involved in the degradation of complex organic substrates into smaller molecules such as short organic acids as acetate, amines, alcohol,  $\text{H}_2$ , and  $\text{CO}_2$  (Orcutt et al., 2011b). Organic end products of fermentation, together with compounds resulting from pyrolysis processes, could be used by heterotrophic microorganisms detected in the AISICS1 and 2, such as those from CFB division, *Proteobacteria* or *Spirochaetes*. Organic acids could also be used as energy sources by a wide range of organotrophic microorganisms, including sulfate-reducing *Deltaproteobacteria*. In all cases, produced  $\text{CO}_2$  will be available for autotrophic microorganisms such as *Aquificales*, *Thermodesulfobacteria*, *Planctomycetes*, or some *Epsilonproteobacteria* that were detected in the modules. Methanogenesis may also occur, however, only one methanogen sequence was detected in the modules. In contrast, ANME phylogenotypes, which mediate anaerobic methane oxidation (AOM), were retrieved in almost all mini-colonizers from both AISICS modules. ANMEs involved in AOM in deep marine sediment are frequently associated with syntrophic sulfate-reducers, although

nitrate, ferric iron, and manganese oxides may also serve as electron acceptors (Raghoebarsing et al., 2006; Beal et al., 2009). This issue is discussed in more detail in the following section.

In both colonizer modules, our microbial diversity surveys revealed the presence of both heterotrophic, autotrophic, and organotrophic microorganisms. These results suggest that anaerobic carbon cycling occurs in the colonizers in the same way as in the surrounding sediments. This finding is similar to studies of the microbial diversity of seafloor lava (Santelli et al., 2009) and Guaymas Basin sediments (Teske et al., 2009) but contrasts with ultramafic rock-hosted hydrothermal systems (Roussel et al., 2011) and pillow basalts (Mason et al., 2008; Santelli et al., 2008b), that are dominated by autotrophic organisms.

**Sulfur cycle.** The data obtained from the 16S rRNA and *dsrAB* gene sequences both suggest that sulfate-reduction occurs, particularly due to the presence of members of the *Deltaproteobacteria*, *Firmicutes*, *Thermodesulfobacteria*, and *Archaeoglobales* (Figure 2;

**Table 3)** (Widdel et al., 1992). Sequences of *Deltaproteobacteria* are found in all mini-colonizers, while dsrAB gene amplification was successful only in the long-term deployment (AISICS1), suggesting that in AISICS2 *Deltaproteobacteria* were not all sulfate-reducing bacteria. Indeed, strains belonging to the *Deltaproteobacteria* and the *Firmicutes* phyla are associated with numerous metabolisms in addition to sulfur metabolisms (Orcutt et al., 2011a,b). Microbial sulfate reduction has also been previously reported in Guaymas sediments (Dhillon et al., 2003; Teske et al., 2003; Biddle et al., 2012) and may occur in the colonizers using dissolved organic substrates and seawater sulfate. As discussed below, *in situ* sulfate reduction may also explain the occurrence of pyrite observed in basalt vesicles.

Sulfur-reduction is also inferred from the occurrence of *Epsilonproteobacteria*, *Desulfuroccales*, *Thermotogales*, *Thermococcales* as well as *Deltaproteobacteria* and *Planctomycetes* that were retrieved in all samples. Indeed, some isolated strains of these groups are able to reduce diverse sulfur compounds (Bertoldo and Antranikian, 2006; Campbell et al., 2006; Elshahed et al., 2007).

Based on the physiology of the isolate *Caldisericum exile*, which is a thermophilic, anaerobic, thiosulfate-reducing bacterium and affiliated with OP5 clones (Mori et al., 2008, 2009), and based upon the OP5 occurrence in sediments and sulfur-rich environments (Hugenholtz et al., 1998; Teske et al., 2002), it can be assumed that OP5 members could be also involved in sulfur cycle. A metagenomic study of OP3 division members suggested that they share similar metabolic properties with *Deltaproteobacteria* (Glöckner et al., 2010) and single-cell analyses revealed that SKK-01 strain harbors sulfur-containing intracellular inclusions (Kolinko et al., 2012). The physiological properties of *Aciduliprofundum boonei*, and the environmental niches of other DHVE2 members, demonstrate that this clade is highly involved in the sulfur cycle (Nercessian et al., 2003; Reysenbach et al., 2006; Flores et al., 2012). Thus, even if the physiological properties of these microorganisms still remain unclear, OP5, OP3, and DHVE-2 members could have played a role in sulfur cycle. Therefore, we suggest that an active anaerobic sulfur cycle took place within the mini-colonizers where both sulfate and sulfide coexist.

**Iron cycle.** Considering the abundance of iron in volcanic glass and its potential importance for supporting endolithic microbial growth [e.g., (Bach and Edwards, 2003)], it is crucial to evaluate the role of microorganisms in iron biogeochemical cycling. Among the groups identified in our experiments, *Beta-* and *Alpha-proteobacteria*, *Thermotogales*, DHVE2, and OP3 members could all be involved in iron cycling. For example, within the *Thermotogales* (Vargas et al., 1998), and within the DHVE2 [*Aciduliprofundum boonei* (Reysenbach et al., 2006)], some species are able to grow as dissimilatory iron reducers using poorly crystalline ferric iron [Fe(III)] as an electron acceptor. In addition, *Betaproteobacteria* and some *Alphaproteobacteria* are able to oxidize Fe(II) (Edwards et al., 2003b; Nakagawa and Takai, 2008). Moreover, despite the lack of any cultivated OP3 members, the SKK-01 strain is a magnetotactic bacteria harboring Fe-containing magnetosomes (Kolinko et al., 2012). In addition,

the OP3 group frequently occurs in anoxic deep-sea hydrothermal system and in heavy metal contaminated sediments (Teske et al., 2002; Rastogi et al., 2011), which may implicate OP3 in iron cycling.

The high concentration of dissolved Fe in AISICS1 may have multiple sources, including a direct contribution from hydrothermal fluids and dissimilatory iron reduction (DIR). High concentrations of other elements typically enriched in hydrothermal fluids (e.g., Si and Mn) argue for the former hypothesis and preclude identifying geochemical evidence for active DIR in the colonizers. In turn, both the prevailing anoxic conditions and our diversity surveys suggest the predominance of iron-reduction over Fe-oxidation pathways.

**Nitrogen cycle.** The chemical analysis of the ambient fluid sampled through the colonizers (Table 2) showed an important seawater contribution of nitrate and nitrogen compounds which could have supported the growth of microorganisms in the colonizers. Our diversity survey corroborates previous studies demonstrating that denitrification took place in deep-sea sediments affected by hydrothermal circulation in the Guaymas Basin (Bowles et al., 2012). Nitrate is a common electron acceptor used by a number of microorganisms under anaerobic conditions (Brandes et al., 2007; Jetten, 2008). Among all the microorganisms known to be able to use nitrates as final electron acceptor, *Aquificales* (Gotz et al., 2002; Huber et al., 2002), *Firmicutes* (L'Haridon et al., 2006), *Caldithrix* (Miroshnichenko et al., 2003), and *Epsilonproteobacteria* (Bowles et al., 2012) were detected in both AISICS modules.

In addition, it appears that ANAMMOX bacteria may also be active in our colonizers. Sequences closely related to *Planctomycetes* were found in AISICS2 colonizers (short exposure time). Within the *Planctomycetes*, the ANAMMOX bacteria are the sole group known to be able to perform anaerobic oxidation of ammonium, (Jetten et al., 2005; Francis et al., 2007) where nitrite, one of the product of denitrification, serves as electron acceptor to form dinitrogen (gas) (Strous et al., 1999; Francis et al., 2007). Although the presence of sequences affiliated to *Planctomycetes* does not allow us to infer their function, ANAMMOX bacteria were known to be active in hydrothermal systems (Byrne et al., 2009) and were already detected in Guaymas basin sediment samples (Russ et al., 2013). Hence, all together, these results suggest that the anaerobic nitrogen cycle, denitrification, and ANAMMOX processes might all occur in our colonizer modules, and by extension, in the surrounding sediments. This finding suggests that the anaerobic part of the nitrogen cycle is one of major processes in hydrothermal sediments, as well as previously noted for basaltic substrates (Mason et al., 2008; Santelli et al., 2009).

**Uncultivated lineage and under-represented groups.** Many sequences belonging to uncultivated lineages were detected. The lack of information about their putative physiology did not allow us to infer their role in the colonization process or their ecological importance. Members of the Guaymas Bacterial Group (Teske et al., 2002) and Guaymas *Euryarchaeotal* Group (Teske

et al., 2002; Dhillon et al., 2005) were found in the two modules. These groups were previously detected in hydrothermally-affected deep-sea sediments and active chimneys of the Guaymas Basin (Teske et al., 2002; Callac et al., submitted). Since their distribution is restricted to hydrothermal environments, it can be assumed that these microorganisms are anaerobes and probably involved in organic matter and hydrocarbon compound degradation.

A new cluster of *Epsilonproteobacteria*, named Guaymas *Epsilonproteobacteria* group, was identified in AISCS 2; this group is only 91% similar to any known environmental clones or cultivated representatives (Figure 4). Like other members of the *Epsilonproteobacteria* from hydrothermal ecosystems, these microorganisms could be mesophilic or moderately thermophilic and involved in organic matter degradation and sulfur cycling in organic matter-rich hydrothermally affected sediments.

#### **AOM: ANMEs, potential syntrophs, and other members**

ANME-1 and more specifically “ANME-1 Guaymas *mcrA* cluster” sequences (Holler et al., 2011; Biddle et al., 2012), as well as “deeply-branching Guaymas *mcrA*” sequences, were retrieved in both modules (Figure 5; Table 3). Most of them are affiliated to sequences previously found in Guaymas hydrothermal sediments with a range of temperature regime (Biddle et al., 2012; Merkel et al., 2013).

Interestingly, no *dsrAB* genes could be amplified from the AISCS2 module (short-term deployment) where ANME sequences were retrieved (Table 3). In contrast, both ANME and *dsrAB* sequences were detected in the long-term AISCS1 deployment that experienced a greater hydrothermal fluid contribution (Table 2). In addition to *Desulfobacteriaceae*, sulfate-reducers such as *Deltaproteobacteria* are known to be ANME syntrophs. However, none of those groups could be detected using either *dsrAB* (Figure 6), or 16S rRNA sequencing. This suggests that detected ANME might have other syntrophs. For example, sulfate-reducers identified in AISCS 1 such as *Syntrophobacterales*, *Desulfobacterium anilini* group, group IV or archaea *Archaeoglobus* could play this role. Another hypothesis is that the syntrophs are not sulfate-reducers but rather are denitrifiers or iron-reducers (Raghoebarsing et al., 2006; Beal et al., 2009). Potential syntrophs identified in most mini-colonizers could be *Thermotogales* involved in iron-reduction, or *Epsilonproteobacteria* and/or *Caldithrix* involved in nitrate-reduction. It is also possible that sulfate-reducers involved in AOM colonize AISCS modules after ANME, or that sulfate-reducers progressively replace other syntrophs (e.g., nitrates and/or iron-reducers) to create new consortia with ANME. Alternatively, we cannot exclude that the ANME, especially the AISCS2 ANME-1, are able utilize carbon, energy sources, and electron acceptor needed for their growth without syntrophs, as previously shown (Knittel et al., 2005), or by doing AOM alone (Milucka et al., 2012). In addition, within the *Archaea*, MCG sequences were detected. The MCG are well-represented in the deep subsurface biosphere (Sorensen and Teske, 2006; Teske and Sorensen, 2007; Kubo et al., 2012). In previous works, it was largely hypothesized that MCG are anaerobes and heterotrophs able to use organic substrates (Biddle et al.,

2006). It has also been suggested that they are able to oxidize methane without the assimilation of methane-derived carbon, using dissimilatory methane metabolism (Biddle et al., 2006). They could also benefit from AOM, directly or not (Sorensen and Teske, 2006). In our colonization modules, MCG could play a direct or indirect role in the methane cycle in association with methanogens and ANMEs. These data support the idea that anaerobic methane cycling is common in hydrothermal systems (Teske et al., 2002).

#### **Sediments: a nest for free-living symbionts?**

Sequences of endosymbionts of *Siboglinidae* (*Osedax sp.* and *Siboglinum sp.*, Figure 3) were retrieved in the AISCS1 module. Previous studies have reported free-living symbionts in bottom seawater overlying seafloor hydrothermal fields (Harmer et al., 2008), or in microbial mats (Crépeau et al., 2011). At Mat Mound site, vent fauna include *Riftia* worms, an unidentified *Siboglinidae*, polychaetes *Paralvinella sp.* and *Ampharetidae* in association with microbial mat (Figure 1; Decker et al., pers. commun.). To date, symbionts of *Riftia* sp. and *Paralvinella* sp epibionts were never reported in their free-living form. However, it has been suggested that vent fauna may gain their endosymbionts locally, leading to an opportunistic environmental acquisition of the best adapted microorganisms (Rodrigues et al., 2011). The presence of free-living symbionts in hydrothermally-affected sediment (e.g., average temperature around 44.3°C) suggest they are able to live in such conditions, which highlights the role of sediment substrate for the dispersion and horizontal transmission of vent fauna symbionts.

#### **MICROBIAL DIVERSITY AND POTENTIAL CONTROL OF GEOCHEMISTRY, SUBSTRATA TYPE, TEMPERATURE, AND/OR DEPLOYMENT TIME**

A large microbial diversity was evident in the colonization modules, and some phylotypes were common among both modules. Archaeal diversity was not correlated with deployment duration, fluid chemistry, sediment depth, or substrata (Figure 2). In contrast, bacterial colonization patterns are driven by a number of factors, such as the duration of deployment and fluid chemistry (Figure 3). In AISCS 2, the bacterial diversity is also influenced by the burial depth in the sediments (Figure 3). This is supported by the statistical analyses of the 16S rRNA sequences for AISCS2, where the diversity clusters according to burial depth (Figure 3). In addition, the bacterial diversity tends to increase with depth (Figure 3), suggesting that the bacterial distribution could be linked to the thermal gradient and the availability of hydrothermally-derived compounds. A recent study at Guaymas Basin has shown that the thermal regime and geochemistry of hydrothermally-affected sediments are highly heterogeneous (McKay et al., 2012). AISCS1 was deployed in a white mat and AISCS2 at the junction between white and orange mats, and while the *in situ* temperature at 20 cm depth was almost the same for both modules (average of 44.3 and 42.9°C, respectively), the geochemistry of recovered pore water was drastically different. Indeed, the long-term deployment module (AISCS1) experienced a much higher hydrothermal contribution than AISCS2 (Table 2).

This suggests that AISICS1 micro-colonizers encountered significant concentration of  $H_2S$  (although  $<5\ \mu M$ ) while fluids sampled in AISICS2 correspond mainly to heated seawater (Table 2). Hence, the geochemical differences between AISICS1 and 2 could explain the differences in bacterial colonization patterns. From the statistical jackknife environment clusters trees (Figures 2, 3), it is clear that microbial colonization is not related to other parameters such as substrata composition.

Given the high concentration of organic matter in the sediment (between 2 and 4% of organic carbon (Kastner, 1982), and the ubiquitous deposition of organic matter on basaltic glass surfaces, as observed by RAMAN spectroscopy and SEM, it is likely that heterotrophic strains could have been pioneers. Fermentative strains can hydrolyze organic matter into small compounds, e.g., small organic acids, amines, or alcohol. These metabolic products could have fueled other heterotrophs and organotrophs, as well as lithoautotrophs.

### GEOMICROBIOLOGICAL INTERACTIONS

Both biotic and abiotic mini-colonizers were filled with identical substratum and exposed to the same environmental conditions allowing a direct comparison between chemical (abiotic) and biological processes taking place on the surface of basaltic glasses. To our knowledge, the systematic use of a sterile control for *in situ* basalt and/or mineral alteration experiments has never been attempted. Micro- and nano-crystals were observed, thus, it is important to note the difference between the micro- and the nano-crystal formation (both pyrite and barite). Micro-crystals of pyrite and barite were observed on basaltic glass surfaces incubated under both biotic and abiotic conditions (Figures 7, 8) suggesting that they result solely from inorganic processes. Similar to our results, laboratory microcosm experiments of

basalt alteration have failed to reveal differences of alteration textures and secondary mineral precipitation between biotic and abiotic conditions (Einen et al., 2006). Nano-crystals of pyrite were only observed in basalts exposed to biotic conditions, which suggests a role of biological process in pyrite formation (Figures 7, 8). Although pyrite can precipitate abiotically from  $H_2S$  and  $Fe^{2+}$  enriched in the hydrothermal fluid, microbial sulfate, and sulfur reduction could have promoted nano-crystalline pyrite precipitation instead of micro-crystalline pyrite (Figure 10). In addition, SEM observations of glass vesicles on biotic samples show a dense mineralization of nano-crystals of pyrite lining the cavity, and wrapped in a film of organic material. The vesicles likely provide a favorable microenvironment for pyrite precipitation, for example through local build up of microbially produced hydrogen sulfide, leading to supersaturation with regard to pyrite (or its FeS mono-sulfide precursors, Berner, 1984). Framboidal pyrite mineralization was also observed on biotic glass surfaces. Although initially attributed to microbial process, this type of pyrite may form without microbial activity (Butler and Rickard, 2000). Ongoing study of sulfur isotopes of pyrite should help in distinguishing between those two models [e.g., Canfield, 2001; Rouxel et al., 2008a,b].

Nano-crystals of barite were also observed in close association with organic matter, suggesting similarly a possible biological mediation for nano-barite crystallization. Barite is known to form bio-aggregates in association with decaying organic matter (Bishop, 1988). However, a direct precipitation of barite from hydrothermal fluid is also possible due to the enrichment of Ba in hydrothermal fluids (Von Damm et al., 1985b).

Small rounded to slightly elongated vesicles ( $10\text{--}100\ \mu m$  diameter; Figure 7) were observed in all glass samples. The occurrence of vesicles in synthetic glass implies that they existed before

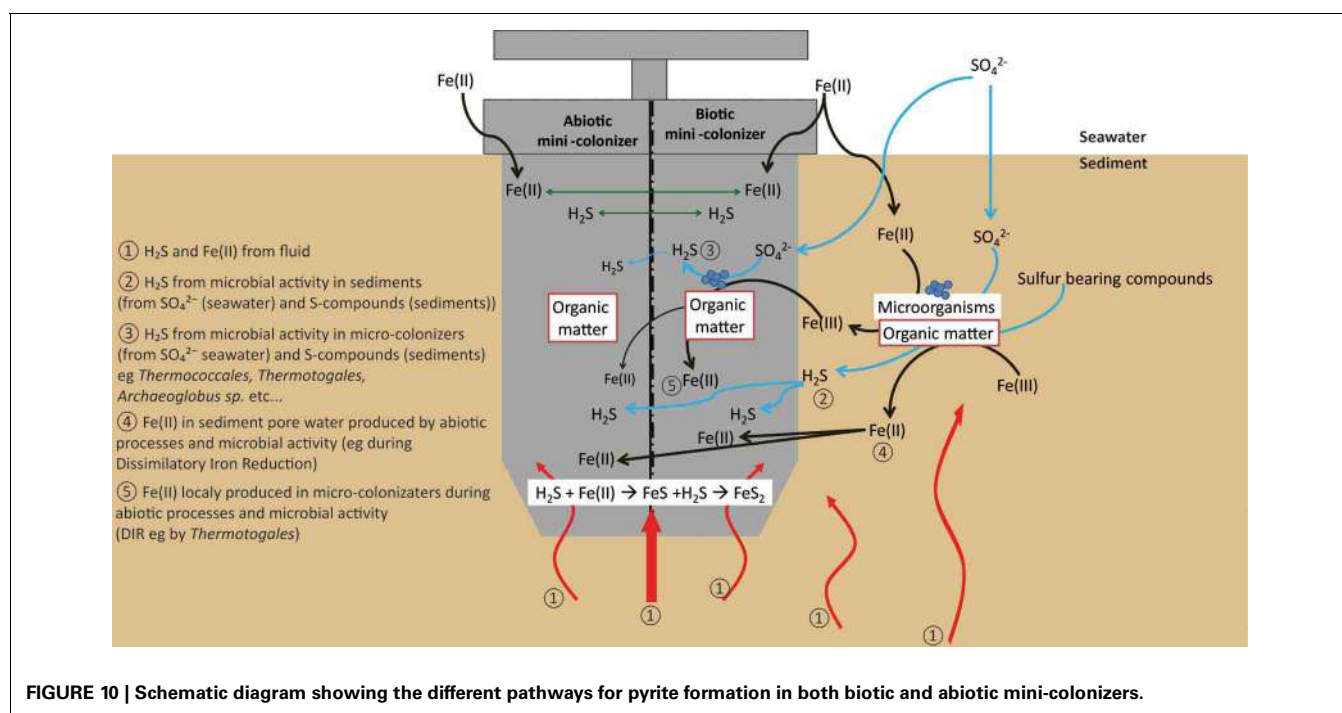


**FIGURE 10 |** Schematic diagram showing the different pathways for pyrite formation in both biotic and abiotic mini-colonizers.

incubation, although they were not detected macroscopically due to their small size of less than 50 µm. As for natural basaltic glass, vesicles formation is likely due to gas micro-bubbles in silicate melt, trapped, and preserved as vesicles during quenching.

Accumulations of diatom debris and carbon-rich aggregates were frequently observed on biotic samples (**Figures 7, 8**) but carbon-rich aggregates were also identified on abiotic samples due to the quantity of organic matter present in the neighboring sediments. The presence of microbial cells has been nonetheless observed using SEM imaging only on biotic samples. Finally, in comparison with studies done on long time (1 year; Einen et al., 2006) or on natural samples (Thorseth et al., 1992; Furnes et al., 2001) the lack of glass alteration evidence is certainly due to the relatively short deployment time (less than 22 days), precluding formation of even incipient alteration rims.

## CONCLUSION

By deploying *in-situ* colonization modules this study showed that diverse microbial communities involved in carbon, nitrogen, sulfur, and iron cycles are able to colonize the surface of basaltic glasses in hydrothermal and organic matter-rich conditions.

While the archaeal colonization pattern is not dependent upon deployment duration, fluid chemistry, sediment depth, or substrata composition, the diverse bacterial colonization patterns are driven by deployment time and fluid chemistry. In all cases, the nature of basalt does not seem to influence microbial colonization.

The presence of a new cluster of *Epsilonproteobacteria*, the Guaymas *Epsilonproteobacteria* group, which is distantly related to any known environmental clones and cultivated representatives expand our current view of microbial diversity in hydrothermal systems.

In some cases, we detected anaerobic methane oxidizers related to ANME 1 and 2, which were not associated with their usual sulfate-reducer syntrophs. This suggests that the ANME groups detected in this study are able to live without syntrophs or may have other sulfate-reducer, denitrifier (some *Epsilonproteobacteria* and/or *Caldithrix*), or iron-reducer (*Thermotogales*) syntrophs.

## REFERENCES

- Alain, K., Zbinden, M., Le Bris, N., Lesongeur, F., Gaill, F., and Cambon-Bonavita, M.-A. (2004). Early steps of microbial colonization process at deep-sea hydrothermal vents. *Environ. Microbiol.* 6, 227–241. doi: 10.1111/j.1462-2920.2003.00557.x
- Alt, J. C. (1995). Sulfur isotopic profile through the oceanic crust: sulfur mobility and seawater-crustal sulfur exchange during hydrothermal alteration. *Geology* 23, 585–588.
- Bach, W., and Edwards, K. J. (2003). Iron and sulfide oxidation within the basaltic ocean crust: implications for chemolithoautotrophic microbial biomass production. *Geochim. Cosmochim. Acta* 67, 3871–3887. doi: 10.1016/S0016-7037(03)00304-1
- Beal, E. J., House, C. H., and Orphan, V. J. (2009). Manganese- and iron-dependent marine methane oxidation. *Science* 325, 184–187. doi: 10.1126/science.1169984
- Berner, R. A. (1984). Sedimentary pyrite formation: An update. *Geochim. Cosmochim. Acta* 48, 605–615. doi: 10.1016/0016-7037(84)90089-9
- Bertoldo, C., and Antranikian, G. (2006). “The order thermococcales,” in *The Prokaryotes*, eds M. Dworkin, S. Falkow, E. Rosenberg, K.-H. Schleifer, and E. Stackebrandt (New York, NY: Springer), 69–81.
- Biddle, J. F., Cardman, Z., Mendlovitz, H., Albert, D. B., Lloyd, K. G., Boetius, A., et al. (2012). Anaerobic oxidation of methane at different temperature regimes in Guaymas Basin hydrothermal sediments. *ISME J.* 6, 1018–1031. doi: 10.1038/ismej.2011.164
- Biddle, J. F., Lipp, J. S., Lever, M. A., Lloyd, K. G., Sørensen, K. B., Anderson, R., et al. (2006). Heterotrophic Archaea dominate sedimentary subsurface ecosystems off Peru. *Proc. Natl. Acad. Sci. U.S.A.* 103, 3846–3851. doi: 10.1073/pnas.0600035103
- Bishop, J. K. B. (1988). The barite-opal-organic carbon association in oceanic particulate matter. *Nature* 332, 24. doi: 10.1038/332341a0
- Bowles, M. W., Nigro, L. M., Teske, A. P., and Joye, S. (2012). Denitrification and environmental factors influencing nitrate removal in Guaymas Basin hydrothermally-altered sediments. *Front. Microbiol.* 3:377. doi: 10.3389/fmicb.2012.00377
- Brandes, J. A., Devol, A. H., and Deutsch, C. (2007). New developments in the marine nitrogen cycle. *Chem. Rev.* 107, 577–589. doi: 10.1021/cr050377t
- Burggraf, S., Jannasch, H. W., Nicolaus, B., and Stetter, K. O. (1990).

Despite the lack of specific glass alteration textures, the formation of secondary minerals was observed on glass surface for both biotic and abiotic experiments. Micro- and nanocrystalline pyrite was generally detected within basalt vesicles associated with organic matter aggregates. Further work, for example applying sulfur isotope systematic, is required to discriminate between biotic and abiotic processes involved in pyrite formation. Applying a similar experimental approach in future studies, providing that deployment duration is sufficient, should provide new insights into the capability of microbial communities to exploit new environmental conditions, colonize new niches, and promote mineral and rock substrate alteration.

## ACKNOWLEDGMENTS

The authors acknowledge the BIG shipboard cruise party for their work and support during the BIG cruise: officers, crew, and technicians of the *R/V L'Atalante*, the DSV *Nautilus* team and scientific team, in particular Philippe Noel, Philippe Rodier, Christian Le Gall, and Pierre-Marie Sarradin for their precious help during the AISICS preparation, as well as Mathilde Le Roy for her help during the AISICS samples conditioning. The “Recherches et Développements Technologiques” unit (Ifremer) is thanked for the AISICS design and manufacturing. The authors thank Stéphanie Rossano (Lab. Géomatériaux et Environnement, Univ. de Marne La Vallée, France), who has allowed us to use her lab equipments and has shared with us her experience in the synthesis of MORB-type basaltic glasses. The authors want to thank Carole Decker, Florence Pradillon, and Josée Sarazin for the fauna identification, their helps and discussion about the host-symbiont interaction. We are indebted to Alexis Templeton for her helpful comments and corrections. We also thank the anonymous reviewers, Bénédicte Menez and Karine Alain for their constructive suggestions and comments. This cruise was funded by Ifremer (France) and has benefited from a work permit in Mexican waters (DAPA/2/281009/3803, October 28th, 2009). This work was supported by Ifremer, the GIS Europôle Mer, UEB, CNRS, and has benefited from state aid managed by the Agence Nationale de la Recherche under the program “Investments for the Future” with the reference ANR-10-LabX-19-01.

- Archaeoglobus profundus* sp. nov., represents a new species within the sulfate-reducing archaeabacteria. *Syst. Appl. Microbiol.* 13, 24–28. doi: 10.1016/S0723-2020(11)80176-1
- Butler, I. B., and Rickard, D. (2000). Framboidal pyrite formation via the oxidation of iron (II) monosulfide by hydrogen sulphide. *Geochim. Cosmochim. Acta* 64, 2665–2672. doi: 10.1016/S0016-7037(00)00387-2
- Byrne, N., Strous, M., Crépeau, V., Kartal, B., Jean-Louis, B., Schmid, M. C., et al. (2009). Presence and activity of anaerobic ammonium-oxidizing bacteria at deep-sea hydrothermal vents. *ISME J.* 3, 117–123. doi: 10.1038/ismej.2008.72
- Campbell, B. J., Engel, A. S., Porter, M. L., and Takai, K. (2006). The versatile e-proteobacteria: key players in sulphidic habitats. *Nat. Rev. Microbiol.* 4, 458–468. doi: 10.1038/nrmicro1414
- Canfield, D. E. (2001). Isotope fractionation by natural populations of sulfate-reducing bacteria. *Geochim. Cosmochim. Acta* 65, 1117–1124. doi: 10.1016/S0016-7037(00)00584-6
- Casamayor, E. O., Schafer, H., Baneras, L., Pedros-Alio, C., and Muyzer, G. (2000). Identification of and spatio-temporal differences between microbial assemblages from two neighboring sulfuriferous lakes: comparison by microscopy and denaturing gradient gel electrophoresis. *Appl. Environ. Microbiol.* 66, 499–508. doi: 10.1128/AEM.66.2.499-508.2000
- Cline, J. D. (1969). Spectrophotometric determination of hydrogen sulfide in natural waters. *Limnol. Oceanogr.* 14, 454–458. doi: 10.4319/lo.1969.14.3.0454
- Corre, E., Reysenbach, A.-L., and Prieur, D. (2001). e-Proteobacterial diversity from a deep-sea hydrothermal vent on the Mid-Atlantic Ridge. *FEMS Microbiol. Lett.* 205, 329–335.
- Crépeau, V., Cambon Bonavita, M.-A., Lesongeur, F., Randrianaivelio, H., Sarradin, P.-M., Sarrazin, J., and Godfroy, A. (2011). Diversity and function in microbial mats from the Lucky Strike hydrothermal vent field. *FEMS Microbiol. Ecol.* 76, 524–540. doi: 10.1111/j.1574-6941.2011.01070.x
- Dean, W., Pride, C., and Thunell, R. (2004). Geochemical cycles in sediments deposited on the slopes of the Guaymas and Carmen Basins of the Gulf of California over the last 180 years. *Quat. Sci. Rev.* 23, 1817–1833. doi: 10.1016/j.quascirev.2004.03.010
- De La Lanza-Espino, G., and Soto, L. A. (1999). Sedimentary geochemistry of hydrothermal vents in Guaymas Basin, Gulf of California, Mexico. *Appl. Geochim.* 14, 499–510. doi: 10.1016/S0883-2927(98)00064-X
- Dhillon, A., Lever, M., Lloyd, K. G., Albert, D. B., Sogin, M. L., and Teske, A. (2005). Methanogen diversity evidenced by molecular characterization of methyl coenzyme M reductase A (mcra) genes in hydrothermal sediments of the Guaymas Basin. *Appl. Environ. Microbiol.* 71, 4592–4601. doi: 10.1128/AEM.71.8.4592-4601.2005
- Dhillon, A., Teske, A., Dillon, J., Stahl, D. A., and Sogin, M. L. (2003). Molecular characterization of sulfate-reducing bacteria in the Guaymas Basin. *Appl. Environ. Microbiol.* 69, 2765–2772. doi: 10.1128/AEM.69.5.2765-2772.2003
- Edwards, K. J., Bach, W., and McCollom, T. M. (2005). Geomicrobiology in oceanography: microbe-mineral interactions at and below the seafloor. *Trends Microbiol.* 13, 449–456. doi: 10.1016/j.tim.2005.07.005
- Edwards, K. J., McCollom, T. M., Konishi, H., and Buseck, P. R. (2003a). Seafloor bioalteration of sulfide minerals: results from *in situ* incubation studies. *Geochim. Cosmochim. Acta* 67, 2843–2856. doi: 10.1016/S0016-7037(03)00089-9
- Edwards, K. J., Rogers, D. R., Wirsen, C. O., and McCollom, T. M. (2003b). Isolation and characterization of novel psychrophilic, neutrophilic, Fe-oxidizing, chemolithoautotrophic α- and γ-proteobacteria from the deep sea. *Appl. Environ. Microbiol.* 69, 2906–2913. doi: 10.1128/AEM.69.5.2906-2913.2003
- Edwards, K. J., Wheat, C. G., and Sylvan, J. B. (2011). Under the sea: microbial life in volcanic oceanic crust. *Nat. Rev. Microbiol.* 9, 703–712. doi: 10.1038/nrmicro2647
- Einen, J., Kruber, C., Øvreås, L., Thorseth, I. H., and Torsvik, T. (2006). Microbial colonization and alteration of basaltic glass. *Biogeosci. Discuss.* 3, 273–307. doi: 10.5194/bgd-3-273-2006
- Elshahed, M. S., Youssef, N. H., Luo, Q., Najar, F. Z., Roe, B. A., Sisk, T. M., et al. (2007). Phylogenetic and metabolic diversity of Planctomyces from anaerobic, sulfide- and sulfur-rich Zodolite Spring, Oklahoma. *Appl. Environ. Microbiol.* 73, 4707–4716. doi: 10.1128/AEM.00591-07
- Erickson, B. E., and Helz, G. R. (2000). Molybdenum(VI) speciation in sulfidic waters: stability and lability of thiomolybdates. *Geochim. Cosmochim. Acta* 64, 1149–1158. doi: 10.1016/S0016-7037(99)00423-8
- Flores, G. E., Campbell, J. H., Kirshtein, J. D., Meneghin, J., Podar, M., Steinberg, J. I., et al. (2011). Microbial community structure of hydrothermal deposits from geochemically different vent fields along the Mid-Atlantic Ridge. *Environ. Microbiol.* 13, 2158–2171. doi: 10.1111/j.1462-2920.2011.02463.x
- Flores, G. E., Wagner, I., Liu, Y., and Reysenbach, A.-L. (2012). Distribution, abundance, and diversity patterns of the thermoacidophilic “Deep-sea Hydrothermal Vent Euryarchaeota 2” (DHVE2). *Front. Microbiol.* 3:47. doi: 10.3389/fmicb.2012.00047
- Francis, C. A., Beman, J. M., and Kuyper, M. M. M. (2007). New processes and players in the nitrogen cycle: the microbial ecology of anaerobic and archaeal ammonia oxidation. *ISME J.* 1, 19–27. doi: 10.1038/ismej.2007.8
- Furnes, H., Staudigel, H., Thorseth, I. H., Torsvik, T., Muehlenbachs, K., and Tumyr, O. (2001). Bioalteration of basaltic glass in the oceanic crust. *Geochim. Geophys. Geosyst.* 2, 1049–1079. doi: 10.1029/2000GC000150
- Glöckner, J., Kube, M., Shrestha, P. M., Weber, M., Glöckner, F. O., Reinhardt, R., and Liesack, W. (2010). Phylogenetic diversity and metagenomics of candidate division OP3. *Environ. Microbiol.* 12, 1218–1229. doi: 10.1111/j.1462-2920.2010.02164.x
- Gotz, D., Banta, A., Beveridge, T. J., Rushdi, A. I., Simoneit, B., and Reysenbach, A. L. (2002). *Persephonella marina* gen. nov., sp. nov. and *Persephonella guaymasensis* sp. nov., two novel, thermophilic, hydrogen-oxidizing microaerophiles from deep-sea hydrothermal vents. *Int. J. Syst. Evol. Microbiol.* 52, 1349–1359. doi: 10.1099/ijss.0.02126-0
- Hales, B., Edwards, C., Ritchie, D., Hall, G., Pickup, R., and Saunders, J. (1996). Isolation and identification of methanogen-specific DNA from blanket bog peat by PCR amplification and sequence analysis. *Appl. Environ. Microbiol.* 62, 668–675.
- Harmer, T. L., Rotjan, R. D., Nussbaumer, A. D., Bright, M., Ng, A. W., Dechaine, E. G., et al. (2008). Free-living tube worm endosymbionts found at deep-sea vents. *Appl. Environ. Microbiol.* 74, 3895–3898. doi: 10.1128/AEM.02470-07
- Higashi, Y., Sunamura, M., Kitamura, K., Nakamura, K.-I., Kurusu, Y., Ishibashi, J.-I., et al. (2004). Microbial diversity in hydrothermal surface to subsurface environments of Suiyo Seamount, Izu-Bonin Arc, using a catheter-type *in situ* growth chamber. *FEMS Microbiol. Ecol.* 47, 327–336. doi: 10.1016/S0168-6496(04)00004-2
- Holler, T., Widdel, F., Knittel, K., Amann, R., Kellermann, M. Y., Hinrichs, K.-U., et al. (2011). Thermophilic anaerobic oxidation of methane by marine microbial consortia. *ISME J.* 5, 1946–1956. doi: 10.1038/ismej.2011.77
- Houghton, J. L., and Seyfried, W. E. Jr. (2010). An experimental and theoretical approach to determining linkages between geochemical variability and microbial biodiversity in seafloor hydrothermal chimneys. *Geobiology* 8, 457–470. doi: 10.1111/j.1472-4669.2010.00255.x
- Huber, H., Diller, S., Horn, C., and Rachel, R. (2002). *Thermovibrio ruber* gen. nov., sp. nov., an extremely thermophilic, chemolithoautotrophic, nitrate-reducing bacterium that forms a deep branch within the phylum Aquificae. *Int. J. Syst. Evol. Microbiol.* 52, 1859–1865. doi: 10.1099/ijs.0.02235-0
- Hugenholz, P., Pitulle, C., Hershberger, K. L., and Pace, N. R. (1998). Novel division level bacterial diversity in a Yellowstone hot spring. *J. Bacteriol.* 180, 366–376.
- Jetten, M. S. M. (2008). The microbial nitrogen cycle. *Environ. Microbiol.* 10, 2903–2909. doi: 10.1111/j.1462-2920.2008.01786.x
- Jetten, M. S. M., Schmid, M. C., Van De Pas-Schoonen, K., Sinnigha Damsté, J., and Strous, M. (2005). Anammox organisms: enrichment, cultivation, and environmental analysis. *Methods Enzymol.* 397, 34–57. doi: 10.1016/S0076-6879(05)97003-1
- Kashefi, K., Tor, J. M., Holmes, D. E., Gaw Van Praagh, C. V., Reysenbach, A. L., and Lovley, D. R. (2002). *Geoglobus ahangari* gen. nov., sp. nov., a novel hyperthermophilic archaeon capable of oxidizing organic acids and growing autotrophically on hydrogen with Fe(III) serving as the sole electron acceptor. *Int. J. Syst. Evol. Microbiol.* 52, 719–728. doi: 10.1099/ijss.0.01953-0

- Kastner, M. (1982). "Evidence of two distinct hydrothermal systems in the Guaymas Basin," in *Initial reports of the Deep Sea Drilling Project*, ed J. R. Curray (Washington, DC: Leg 64. U.S. Government Printing Office), 64. doi: 10.2973/dsdp.proc.64.154.1982
- Kimura, M. (1980). A simple method for estimating evolutionary rates of base substitutions through comparative studies of nucleotide sequences. *J. Mol. Evol.* 16, 111–120. doi: 10.1007/BF01731581
- Knittel, K., Losekann, T., Boetius, A., Kort, R., and Amann, R. (2005). Diversity and Distribution of methanotrophic archaea at cold seeps. *Appl. Environ. Microbiol.* 71, 467–479. doi: 10.1128/AEM.71.1.467-479.2005
- Kolganova, T. V., Kuznetsov, B. B., and Tourova, T. P. (2002). Designing and testing oligonucleotide primers for amplification and sequencing of archaeal 16S rRNA genes. *Microbiology* 71, 243–246. doi: 10.1023/A:1015122926687
- Kolinko, S., Jogler, C., Katzmüller, E., Wanner, G., Peplies, J., and Schüller, D. (2012). Single-cell analysis reveals a novel uncultivated magnetotactic bacterium within the candidate division OP3. *Environ. Microbiol.* 14, 1709–1721. doi: 10.1111/j.1462-2920.2011.02609.x
- Kubo, K., Lloyd, K. G., F Biddle, J., Amann, R., Teske, A., and Knittel, K. (2012). Archaea of the Miscellaneous Crenarchaeotal Group are abundant, diverse and widespread in marine sediments. *ISME J.* 6, 1949–1965. doi: 10.1038/ismej.2012.37
- Kumar, S., Nei, M., Dudley, J., and Tamura, K. (2008). MEGA: a biologist-centric software for evolutionary analysis of DNA and protein sequences. *Brief. Bioinform.* 9, 299–306. doi: 10.1093/bib/bbn017
- Lane, D. J. (1991). 16S/23S rRNA sequencing. *Nucleic Acid Tech. Bact. Syst.* 1, 115–176.
- Lane, D. J., Pace, B., Olsen, G. J., Stahl, D. A., Sogin, M. L., and Pace, N. R. (1985). Rapid determination of 16S ribosomal RNA sequences for phylogenetic analyses. *Proc. Natl. Acad. Sci. U.S.A.* 82, 6955–6959. doi: 10.1073/pnas.82.20.6955
- L'Haridon, S., Miroshnichenko, M. L., Kostrikina, N. A., Tindall, B. J., Spring, S., Schumann, P., et al. (2006). *Vulcanibacillus modestaldus* gen. nov., sp. nov., a strictly anaerobic, nitrate-reducing bacterium from deep-sea hydrothermal vents. *Int. J. Syst. Evol. Microbiol.* 56, 1047–1053. doi: 10.1099/ijm.0.64012-0
- Lonsdale, P., and Becker, K. (1985). Hydrothermal plumes, hot springs, and conductive heat flow in the Southern Trough of Guaymas Basin. *Earth Planet. Sci. Lett.* 73, 211–225. doi: 10.1016/0012-821X(85)90070-6
- Lozupone, C., Hamady, M., and Knight, R. (2006). UniFrac—an online tool for comparing microbial community diversity in a phylogenetic context. *BMC Bioinform.* 7:371. doi: 10.1186/1471-2105-7-371
- Maquelin, K., Kirschner, C., Choo-Smith, L. P., Van Den Braak, N., Endtz, H. P., Naumann, D., et al. (2002). Identification of medically relevant microorganisms by vibrational spectroscopy. *J. Microbiol. Methods* 51, 255–271. doi: 10.1016/S0167-7012(02)00127-6
- Martens, C. S. (1990). Generation of short chain acid anions in hydrothermally altered sediments of the Guaymas Basin, Gulf of California. *Appl. Geochem.* 5, 71–76. doi: 10.1016/0883-2927(90)90037-6
- Mason, O. U., Di Meo-Savoie, C. A., Van Nostrand, J. D., Zhou, J., Fisk, M. R., and Giovannoni, S. J. (2008). Prokaryotic diversity, distribution, and insights into their role in biogeochemical cycling in marine basalts. *ISME J.* 3, 231–242. doi: 10.1038/ismej.2008.92
- Mason, O. U., Stingl, U., Wilhelm, L. J., Moeseneder, M. M., Di Meo-Savoie, C. A., Fisk, M. R., et al. (2007). The phylogeny of endolithic microbes associated with marine basalts. *Environ. Microbiol.* 9, 2539–2550. doi: 10.1111/j.1462-2920.2007.01372.x
- Mckay, L. J., Macgregor, B. J., Biddle, J. F., Albert, D. B., Mendlovitz, H. P., Hoer, D. R., et al. (2012). Spatial heterogeneity and underlying geochemistry of phylogenetically diverse orange and white Beggiatoa mats in Guaymas Basin hydrothermal sediments. *Deep Sea Res. Oceanogr. Res. Pap.* 67, 21–31. doi: 10.1016/j.dsr.2012.04.011
- Merkel, A. Y., Huber, J. A., Chernyh, N. A., Bonch-Osmolovskaya, E. A., and Lebedinsky, A. V. (2013). Detection of putatively thermophilic anaerobic methanotrophs in diffuse hydrothermal vent fluids. *Appl. Environ. Microbiol.* 79, 915–923. doi: 10.1128/AEM.03034-12
- Milucka, J., Ferdelman, T. G., Polerecky, L., Franzke, D., Wegener, G., Schmid, M., et al. (2012). Zero-valent sulphur is a key intermediate in marine methane oxidation. *Nature* 491, 541–546. doi: 10.1038/nature11656
- Miroshnichenko, M. L., Kostrikina, N. A., Chernyh, N. A., Pimenov, N. V., Tourova, T. P., Antipov, A. N., et al. (2003). *Caldithrix abyssi* gen. nov., sp. nov., a nitrate-reducing, thermophilic, anaerobic bacterium isolated from a Mid-Atlantic Ridge hydrothermal vent, represents a novel bacterial lineage. *Int. J. Syst. Evol. Microbiol.* 53, 323–329. doi: 10.1099/ijm.0.02390-0
- Mori, K., Sunamura, M., Yanagawa, K., Ishibashi, J.-I., Miyoshi, Y., Iino, T., et al. (2008). First cultivation and ecological investigation of a bacterium affiliated with the candidate phylum OP5 from hot springs. *Appl. Environ. Microbiol.* 74, 6223–6229. doi: 10.1128/AEM.01351-08
- Mori, K., Yamaguchi, K., Sakiyama, Y., Urabe, T., and Suzuki, K.-I. (2009). *Caldisericum exile* gen. nov., sp. nov., an anaerobic, thermophilic, filamentous bacterium of a novel bacterial phylum, Caldiserica phyl. nov., originally called the candidate phylum OP5, and description of Caldisericaceae fam. nov., Caldisericales ord. nov. and Caldiserica classis nov. *Int. J. Syst. Evol. Microbiol.* 59, 2894–2898. doi: 10.1099/ijm.0.010033-0
- Nakagawa, S., and Takai, K. (2008). Deep-sea vent chemoautotrophs: diversity, biochemistry and ecological significance. *FEMS Microbiol. Ecol.* 65, 1–14. doi: 10.1111/j.1574-6941.2008.00502.x
- Nakagawa, T., Takai, K., Suzuki, Y., Hirayama, H., Konno, U., Tsunogai, U., et al. (2006). Geomicrobiological exploration and characterization of a novel deep-sea hydrothermal system at the TOTO caldera in the Mariana Volcanic Arc. *Environ. Microbiol.* 8, 37–49. doi: 10.1111/j.1462-2920.2005.00884.x
- Nercessian, O., Reysenbach, A.-L., Priour, D., and Jeanthon, C. (2003). Archaeal diversity associated with *in situ* samplers deployed on hydrothermal vents on the East Pacific Rise (13°N). *Environ. Microbiol.* 5, 492–502. doi: 10.1046/j.1462-2920.2003.00437.x
- Orcutt, B., Wheat, C. G., and Edwards, K. J. (2010). Subseafloor ocean crust microbial observatories: development of FLOCS (FLow-through Osmo Colonization System) and evaluation of borehole construction materials. *Geomicrobiol. J.* 27, 143–157. doi: 10.1080/01490450903456772
- Orcutt, B. N., Bach, W., Becker, K., Fisher, A. T., Hentscher, M., Toner, B. M., et al. (2011a). Colonization of subsurface microbial observatories deployed in young ocean crust. *ISME J.* 5, 692–703. doi: 10.1038/ismej.2010.157
- Orcutt, B. N., Sylvan, J. B., Knab, N. J., and Edwards, K. J. (2011b). Microbial ecology of the dark ocean above, at, and below the seafloor. *Microbiol. Mol. Biol. Rev.* 75, 361–422. doi: 10.1128/MMBR.00039-10
- Page, A., Tivey, M. K., Stakes, D. S., and Reysenbach, A.-L. (2008). Temporal and spatial archaeal colonization of hydrothermal vent deposits. *Environ. Microbiol.* 10, 874–884. doi: 10.1111/j.1462-2920.2007.01505.x
- Raghoebarsing, A. A., Pol, A., Van De Pas-Schoonen, K. T., Smolders, A. J. P., Ettwig, K. F., Rijpstra, W. I. C., et al. (2006). A microbial consortium couples anaerobic methane oxidation to denitrification. *Nature* 440, 918–921. doi: 10.1038/nature04617
- Rassa, A. C., Mcallister, S. M., Safran, S. A., and Moyer, C. L. (2009). Zeta-Proteobacteria dominate the colonization and formation of microbial mats in low-temperature hydrothermal vents at Loihi Seamount, Hawaii. *Geomicrobiol. J.* 26, 623–638. doi: 10.1080/01490450903263350
- Rastogi, G., Barua, S., Sani, R., and Peyton, B. (2011). Investigation of microbial populations in the extremely metal-contaminated coeur d'Alene River sediments. *Microb. Ecol.* 62, 1–13. doi: 10.1007/s00248-011-9810-2
- Reysenbach, A.-L., Liu, Y., Banta, A. B., Beveridge, T. J., Kirshtein, J. D., Schouten, S., et al. (2006). A ubiquitous thermoacidophilic archaeon from deep-sea hydrothermal vents. *Nature* 442, 444–447. doi: 10.1038/nature04921
- Reysenbach, A. L., Longnecker, K., and Kirshtein, J. (2000). Novel bacterial and archaeal lineages from an *in situ* growth chamber deployed at a Mid-Atlantic Ridge hydrothermal vent. *Appl. Environ. Microbiol.* 66, 3798–3806. doi: 10.1128/AEM.66.9.3798-3806.2000
- Rodrigues, C., Hilário, A., Cunha, M., Weightman, A., and Webster, G. (2011). Microbial diversity in Frenulata (Siboglinidae, Polychaeta) species from mud volcanoes in the Gulf of Cadiz (NE Atlantic). *Antonie Van Leeuwenhoek* 100, 83–98. doi: 10.1007/s10482-011-9567-0
- Roussel, E. G., Konn, C., Charlou, J.-L., Donval, J.-P., Fouquet, Y., Querellou, J., et al. (2011).

- Comparison of microbial communities associated with three Atlantic ultramafic hydrothermal systems. *FEMS Microbiol. Ecol.* 77, 647–665. doi: 10.1111/j.1574-6941.2011.01161.x
- Rouxel, O., Ono, S., Alt, J., Rumble, D., and Ludden, J. (2008a). Sulfur isotopes as tracers for the subsurface biosphere in altered oceanic basalts. *Earth Planet. Sci. Lett.* 268, 110–123. doi: 10.1016/j.epsl.2008.01.010
- Rouxel, O., Shanks III, W. C., Bach, W., and Edwards, K. J. (2008b). Integrated Fe- and S-isotope study of seafloor hydrothermal vents at East Pacific Rise 9–10°N. *Chem. Geol.* 252, 214–227. doi: 10.1016/j.chemgeo.2008.03.009
- Russ, L., Kartal, B., Op Den Camp, H. J., Sollai, M., Le Bruchec, J., Caprais, J.-C., et al. (2013). Presence and diversity of anammox bacteria in cold hydrocarbon-rich seeps and hydrothermal vent sediments of the Guaymas Basin. *Front. Microbiol.* 4:219. doi: 10.3389/fmicb.2013.00219
- Saitou, N., and Nei, M. (1987). The neighbor-joining method: a new method for reconstructing phylogenetic trees. *Mol. Biol. Evol.* 4, 406–425.
- Santelli, C. M., Edgcomb, V. P., Bach, W., and Edwards, K. J. (2009). The diversity and abundance of bacteria inhabiting seafloor lavas positively correlate with rock alteration. *Environ. Microbiol.* 11, 86–98. doi: 10.1111/j.1462-2920.2008.01743.x
- Santelli, C. M., Orcutt, B. N., Banning, E., Bach, W., Moyer, C. L., Sogin, M. L., et al. (2008a). Abundance and diversity of microbial life in ocean crust. *Nature* 453, 653–657. doi: 10.1038/nature06899
- Santelli, C. M., Orcutt, B. N., Banning, E., Bach, W., Moyer, C. L., Sogin, M. L., et al. (2008b). Abundance and diversity of microbial life in ocean crust. *Nature* 453, 653–656. doi: 10.1038/nature06899
- Sarrazin, J., Sarradin, P.-M., and Participants, A. T. M. C. (2006). MoMARETO: a cruise dedicated to the spatio-temporal dynamics and the adaptations of hydrothermal vent fauna on the Mid-Atlantic Ridge. *InterRidge News* 15, 24–33.
- Schloss, P. D., and Handelsman, J. (2004). Status of the microbial census. *Microbiol. Mol. Biol. Rev.* 68, 686–691. doi: 10.1128/MMBR.68.4.686-691.2004
- Schrenk, M. O., Kelley, D. S., Delaney, J. R., and Baross, J. A. (2003). Incidence and diversity of microorganisms within the walls of an active deep-sea sulfide chimney. *Appl. Environ. Microbiol.* 69, 3580–3592. doi: 10.1128/AEM.69.6.3580-3592.2003
- Simoneit, B. R. T., and Lonsdale, P. F. (1982). Hydrothermal petroleum in mineralized mounds at the seabed of Guaymas Basin. *Nature* 295, 198–202. doi: 10.1038/295198a0
- Sorensen, K. B., and Teske, A. (2006). Stratified communities of active archaea in deep marine subsurface sediments. *Appl. Environ. Microbiol.* 72, 4596–4603. doi: 10.1128/AEM.00562-06
- Spötl, C., W. Houseknecht, D., and Jaques, R. C. (1998). Kerogen maturation and incipient graphitization of hydrocarbon source rocks in the Arkoma Basin, Oklahoma and Arkansas: a combined petrographic and Raman spectrometric study. *Org. Geochem.* 28, 535–542. doi: 10.1016/S0146-6380(98)00021-7
- Staudigel, H., and Hart, S. R. (1983). Alteration of basaltic glass: mechanisms and significance for the oceanic crust-seawater budget. *Geochim. Cosmochim. Acta* 47, 337–350. doi: 10.1016/0016-7037(83)90257-0
- Strous, M., Kuenen, J. G., and Jetten, M. S. M. (1999). Key physiology of anaerobic ammonium oxidation. *Appl. Environ. Microbiol.* 65, 3248–3250.
- Takai, K., Inagaki, F., Nakagawa, S., Hirayama, H., Nunoura, T., Sako, Y., et al. (2003). Isolation and phylogenetic diversity of members of previously uncultivated ε-Proteobacteria in deep-sea hydrothermal fields. *FEMS Microbiol. Lett.* 218, 167–174.
- Teske, A., Dhillon, A., and Sogin, M. L. (2003). Genomic markers of ancient anaerobic microbial pathways: sulfate reduction, methanogenesis, and methane oxidation. *Biol. Bull.* 204, 186–191. doi: 10.2307/1543556
- Teske, A., Edgcomb, V., Rivers, A., Thompson, J., De Vera Gomez, A., Molyneaux, S., et al. (2009). A molecular and physiological survey of a diverse collection of hydrothermal vent Thermococcus and Pyrococcus isolates. *Extremophiles* 13, 905–915. doi: 10.1007/s00792-009-0278-7
- Teske, A., Hinrichs, K.-U., Edgcomb, V., De Vera Gomez, A., Kysela, D., Sylva, S. P., et al. (2002). Microbial diversity of hydrothermal sediments in the guaymas basin: evidence for anaerobic methanotrophic communities. *Appl. Environ. Microbiol.* 68, 1994–2007. doi: 10.1128/AEM.68.4.1994-2007.2002
- Teske, A., and Sorensen, K. B. (2007). Uncultured archaea in deep marine subsurface sediments: have we caught them all? *ISME J.* 2, 3–18. doi: 10.1038/ismej.2007.90
- Thorseth, I. H., Furnes, H., and Heldal, M. (1992). The importance of microbiological activity in the alteration of natural basaltic glass. *Geochim. Cosmochim. Acta* 56, 845–850. doi: 10.1016/0016-7037(92)90104-Q
- Vargas, M., Kashefi, K., Bluntharris, E. L., and Lovley, D. R. (1998). Microbiological evidence for Fe(III) reduction on early Earth. *Nature* 395, 65–67. doi: 10.1038/25720
- Von Damm, K. L., Edmond, J. M., Grant, B., Measures, C. I., Walden, B., and Weiss, R. F. (1985a). Chemistry of submarine hydrothermal solutions at 21°N, East Pacific Rise. *Geochim. Cosmochim. Acta* 49, 2197–2220. doi: 10.1016/0016-7037(85)90222-4
- Von Damm, K. L., Edmond, J. M., Measures, C. I., and Grant, B. (1985b). Chemistry of submarine hydrothermal solutions at Guaymas Basin, Gulf of California. *Geochim. Cosmochim. Acta* 49, 2221–2237. doi: 10.1016/0016-7037(85)90223-6
- Wagner, M., Roger, A. J., Flax, J. L., Brusseau, G. A., and Stahl, D. A. (1998). Phylogeny of dissimilatory sulfite reductases supports an early origin of sulfate respiration. *J. Bacteriol.* 180, 2975–2982.
- Webster, G., Newberry, C. J., Fry, J. C., and Weightman, A. J. (2003). Assessment of bacterial community structure in the deep sub-seafloor biosphere by 16S rDNA-based techniques: a cautionary tale. *J. Microbiol. Methods* 55, 155–164. doi: 10.1016/S0167-7012(03)00140-4
- Welhan, J. A. (1988). Origins of methane in hydrothermal systems. *Chem. Geol.* 71, 183–198. doi: 10.1016/0009-2541(88)90114-3
- Wheat, C. G., and Mottl, M. J. (2000). Composition of pore and spring waters from Baby Bare: global implications of geochemical fluxes from a ridge flank hydrothermal system. *Geochim. Cosmochim. Acta* 64, 629–642. doi: 10.1016/S0016-7037(99)00347-6
- Widdel, F., Hansen, T., Balows, A., Truper, H., Dworkin, M., Harder, W., et al. (1992). “The dissimilatory sulfate-and sulfur-reducing bacteria,” in *The Prokaryotes: A Handbook on the Biology of Bacteria: Ecophysiology, Isolation, Identification, Applications*, Vol. 1, eds A. Balows, H. G. Truper, M. Dworkin, W. Harder, and K. H. Schleifer (New York, NY: Springer-Verlag), 582–624.

**Conflict of Interest Statement:** The authors declare that the research was conducted in the absence of any commercial or financial relationships that could be construed as a potential conflict of interest.

Received: 15 February 2013; accepted: 07 August 2013; published online: 27 August 2013.

Citation: Callac N, Rommevaux-Jestin C, Rouxel O, Lesongeur F, Liorzou C, Bollinger C, Ferrant A and Godfroy A (2013) Microbial colonization of basaltic glasses in hydrothermal organic-rich sediments at Guaymas Basin. *Front. Microbiol.* 4:250. doi: 10.3389/fmicb.2013.00250

This article was submitted to Extreme Microbiology, a section of the journal *Frontiers in Microbiology*.

Copyright © 2013 Callac, Rommevaux-Jestin, Rouxel, Lesongeur, Liorzou, Bollinger, Ferrant and Godfroy. This is an open-access article distributed under the terms of the Creative Commons Attribution License (CC BY). The use, distribution or reproduction in other forums is permitted, provided the original author(s) or licensor are credited and that the original publication in this journal is cited, in accordance with accepted academic practice. No use, distribution or reproduction is permitted which does not comply with these terms.



# Diffuse flow environments within basalt- and sediment-based hydrothermal vent ecosystems harbor specialized microbial communities

Barbara J. Campbell<sup>1</sup>, Shawn W. Polson<sup>2</sup>, Lisa Zeigler Allen<sup>3</sup>, Shannon J. Williamson<sup>4</sup>, Charles K. Lee<sup>5</sup>, K. Eric Wommack<sup>2</sup> and S. Craig Cary<sup>2,5\*</sup>

<sup>1</sup> Department of Biological Sciences, Life Science Facility, Clemson University, Clemson, SC, USA

<sup>2</sup> Delaware Biotechnology Institute, University of Delaware, Newark, DE, USA

<sup>3</sup> J. Craig Venter Institute, San Diego, CA, USA

<sup>4</sup> Lake Pend Oreille Waterkeeper, Sandpoint, ID, USA

<sup>5</sup> Department of Biological Sciences, University of Waikato, Hamilton, New Zealand

**Edited by:**

Anna-Louise Reysenbach, Portland State University, USA

**Reviewed by:**

Kasthuri Venkateswaran, NASA-Jet Propulsion Laboratory, USA

Takuro Nunoura, Japan Agency for Marine-Earth Science & Technology, Japan

**\*Correspondence:**

S. Craig Cary, Department of Biological Sciences, University of Waikato, Gate 1 Knighton Road, Private Bag 3105, Hamilton 3240, New Zealand  
e-mail: c.cary@waikato.ac.nz

Hydrothermal vents differ both in surface input and subsurface geochemistry. The effects of these differences on their microbial communities are not clear. Here, we investigated both alpha and beta diversity of diffuse flow-associated microbial communities emanating from vents at a basalt-based hydrothermal system along the East Pacific Rise (EPR) and a sediment-based hydrothermal system, Guaymas Basin. Both Bacteria and Archaea were targeted using high throughput 16S rRNA gene pyrosequencing analyses. A unique aspect of this study was the use of a universal set of 16S rRNA gene primers to characterize total and diffuse flow-specific microbial communities from varied deep-sea hydrothermal environments. Both surrounding seawater and diffuse flow water samples contained large numbers of Marine Group I (MGI) *Thaumarchaea* and *Gammaproteobacteria* taxa previously observed in deep-sea systems. However, these taxa were geographically distinct and segregated according to type of spreading center. Diffuse flow microbial community profiles were highly differentiated. In particular, EPR dominant diffuse flow taxa were most closely associated with chemolithoautotrophs, and off axis water was dominated by heterotrophic-related taxa, whereas the opposite was true for Guaymas Basin. The diversity and richness of diffuse flow-specific microbial communities were strongly correlated to the relative abundance of *Epsilonproteobacteria*, proximity to macrofauna, and hydrothermal system type. Archaeal diversity was higher than or equivalent to bacterial diversity in about one third of the samples. Most diffuse flow-specific communities were dominated by OTUs associated with *Epsilonproteobacteria*, but many of the Guaymas Basin diffuse flow samples were dominated by either OTUs within the *Planctomycetes* or hyperthermophilic Archaea. This study emphasizes the unique microbial communities associated with geochemically and geographically distinct hydrothermal diffuse flow environments.

**Keywords:** diffuse flow, microbial diversity, 16S rRNA, pyrosequencing, hydrothermal vents

## INTRODUCTION

A defining characteristic of deep-sea hydrothermal environments is that microbial chemosynthetic processes are the primary driver of ecosystem productivity. Thus, a better comprehension of the factors influencing the composition and diversity of vent microbial communities has direct implications for understanding the resilience and productivity of these extreme environments. Previous investigations have found that the taxonomic diversity of hydrothermal vent microbial communities is extensive, particularly when assessed by high throughput sequencing (HTS) approaches (Huber et al., 2007, 2010). There is substantial evidence from standard 16S rRNA gene library and functional gene analyses, as well as metagenomic data that support this conclusion, especially within the *Epsilonproteobacteria* class (Moyer

et al., 1995; Lopez-Garcia et al., 2002; Campbell and Cary, 2004; Grzymski et al., 2008; Robidart et al., 2008; Campbell et al., 2009; Nunoura et al., 2010). Archaeal communities at hydrothermal vents are generally thought to be less diverse than coexisting bacterial communities (Huber et al., 2002, 2010; Opatkiewicz et al., 2009; Nunoura et al., 2010). However, these assessments of microbial diversity relied upon PCR primers specific for each domain and are therefore difficult to compare.

The composition of hydrothermal vent-associated microbial communities tends to segregate by vent and distance from actively venting structures (Huber et al., 2007; Opatkiewicz et al., 2009; Dick and Tebo, 2010; Kato et al., 2010; Nunoura et al., 2010). While most of these studies examined either plume water or bottom water, few specifically looked at diffuse flow waters (Huber

et al., 2003; Sogin et al., 2006). The factors shaping microbial community diversity and composition are not well understood in these environments. Segregation according to differences in geochemistry is especially prevalent among members of the typically dominant vent bacterial class, *Epsilonproteobacteria* (Nakagawa et al., 2005; Nakagawa and Takai, 2008; Opatkiewicz et al., 2009; Kato et al., 2010). Yet, location seemed to dictate microbial community structure more than geochemistry in other studies (Opatkiewicz et al., 2009; Huber et al., 2010). In fact, recent work showed that endemism was a major factor shaping vent microbial communities even though geochemistry had changed during the 6-year study of the Axial Seamount caldera (Opatkiewicz et al., 2009).

*Epsilonproteobacteria* are a diverse class of mesophilic to moderately thermophilic bacteria that dominate culture-independent surveys of most moderate to high temperature marine hydrothermal vent surfaces. The presence of this class seems to be restricted to associations with macrofauna and the outer surfaces of active vents (Campbell et al., 2006). They are also found in high abundance in some diffuse flow water and plume environments, but were shown to be in low abundance within Guaymas Basin plume 16S rRNA gene libraries (Sunamura et al., 2004; Nakagawa et al., 2005; Dick and Tebo, 2010; Huber et al., 2010). The success of *Epsilonproteobacteria* at hydrothermal vents is likely due to their chemoautotrophic strategy via the reductive tricarboxylic acid (rTCA) cycle along with a moderately versatile metabolism (Campbell et al., 2006). Most vent *Epsilonproteobacteria* are microaerophilic to facultative anaerobes and have the ability to use many sulfur species or hydrogen for energy (Campbell et al., 2006), electron donors found in large quantities at most active deep-sea hydrothermal systems (Von Damm, 1990).

Many other thermophilic Bacteria and Archaea are found less frequently at hydrothermal vents in culture-independent 16S rRNA gene surveys or by quantitative PCR analyses (Gotz et al., 2002; Wery et al., 2002; Huber et al., 2010; Nunoura et al., 2010). Most of these thermophiles and hyperthermophiles appear to also segregate to specific vents, to higher temperature sediments, or internal chimney habitats (Schrenk et al., 2003; Vetriani et al., 2008; Nunoura et al., 2010). One group of mesophilic Archaea, the Thaumarchaeota (formally known as mesophilic Crenarchaeota) Marine Group I (MGI) clade, are found in high abundance in deep marine waters and in non-diffuse flow hydrothermal vents (Takai et al., 2004; Agogue et al., 2008; Brochier-Armanet et al., 2008; Dick and Tebo, 2010). Although cultured members of MGI are chemoautotrophic ammonium-oxidizers, some uncultured members may be heterotrophic, especially those found in deep water (Konneke et al., 2005; Agogue et al., 2008).

The primary goal of this study was to examine biogeographic and geochemical effects on microbial community composition at vents within the 9°N East Pacific Rise (EPR) and Guaymas Basin vent fields, two widely divergent deep-sea hydrothermal vent environments. Bacterial and archaeal communities within diffuse flow vent fluids and background seawater were examined using a combination of HTS and universal primers for the 16S rRNA gene. While there have been limited studies on symbiotic

microbial communities and microcolonizers at these sites, and one study of a Guaymas Basin vent plume, we know of no microbial community surveys from 9°N EPR or Guaymas Basin diffuse flow samples (Haddad et al., 1995; Reysenbach et al., 2000; McCliment et al., 2006; Dick and Tebo, 2010). Because microbial communities within background deep-sea water were also examined, it was possible to identify microbial taxa specific to the unique diffuse flow environments.

## MATERIALS AND METHODS

### SITE DESCRIPTIONS AND SAMPLE COLLECTION

Diffuse flow samples were taken with a large volume water sampler (LVWS, Wommack et al., 2004) from various hydrothermal vent and sediment locations at 9°N, EPR, and the Guaymas Basin (Table 1). The LVWS platform was positioned, and its operation was commenced by the DSV Alvin submersible. Temperature was measured at the mouth of the funnel at the start of each collection using Alvin's high temperature probe and therefore indicated the general temperature of the diffuse flow area collected. In addition, small discrete water (SIPPER) samples were taken for chemical analyses (Di Meo et al., 1999). After the LVWS system was purged of surface seawater, diffuse flow water, entrained with bottom seawater, was pumped (~2000L) *in situ* through a 200 µm Nytex net pre-filter, then serially filtered across a 3.0 µm 293 mm filter then two parallel 0.2 µm 293 mm filters (Supor membrane disc filters, Pall Life Sciences) for ~14–16 h. The first ~120L of 0.2 µm filtrate was collected in three Tedlar gas-impermeable plastic bags housed within Nalgene HDPE boxes during each deployment. The LVWS was allowed to surface after an acoustically triggered removal of dive weights, and sample processing occurred immediately upon platform retrieval (within 2 h of triggering).

Two off-axis water samples were taken at least 200 m off the vent axis (one adjacent to Tica –9°N 50.417, 104°W 17.540—at EPR; one near Southern Site—27°N 01.21, 111°W 24.04—at Guaymas) were collected in 30L Niskin bottles on a Carousel Water Sampler/CTD (SBE32; Sea-Bird Electronics) remotely triggered at a depth of 5–15 m above ocean bottom. Samples were immediately filtered and processed on deck using an identical setup as LVWS samples.

### SAMPLE PROCESSING AND CHEMICAL ANALYSES

Ten ml of unprocessed water collected via the SIPPER apparatus was used for all chemical analyses. Aliquots of the sample were separated for dissolved Fe(II) and Fe(total) [defined as Fe(total) = dissolved Fe(III) + dissolved Fe(II)] and analyzed by colorimetry with a Spectronic 601 (Milton Roy) following the ferrozine method (Stookey, 1970). Total sulfide was measured using a standard methylene blue spectrometric method as described previously (Grasshoff et al., 1999). Trace element samples (3 mL) were filtered (0.2 mm cellulose nitrate membrane filters) into acid washed glass vials, acidified with 50 µL of concentrated ultra-pure HNO<sub>3</sub> acid and stored at 4°C until analysis. These samples were prepared for analysis by diluting 50-fold with ultra-pure 2% HNO<sub>3</sub> and analyzed using a Perkin Elmer Elan SCIEX DRC II inductively coupled plasma mass spectrometer (ICP-MS). To correct for mass bias and instrument

**Table 1 | Site descriptions of 9°N East Pacific Rise (EPR) and Guaymas Basin hydrothermal vent samples.**

| Site name                  | Date     | Dive # | Location                       | Depth (m) | Temp. (°C) | Near macrofauna | Notes  |
|----------------------------|----------|--------|--------------------------------|-----------|------------|-----------------|--|
| <b>EPR</b>                 |          |        |                                |           |            |                 |  |
| Tica                       | 11/12/08 | 4470   | 9°N 50.414<br>104°W 17.499     | 2515      | 14–19      | Y               | Located near Riftia and a Tevnia colony.   |
| Bio-9/P-Vent               | 11/14/08 | 4472   | 9°N 50.17367<br>104°W 17.46176 | 2511      | 17–27      | Y               | Placed near shimmering water, near a Riftia patch.   |
| Marker 28 (Trick or Treat) | 11/15/08 | 4473   | 9°N 50.17367<br>104°W 17.46176 | 2505      | 30–50      | Y               | Placed near crabs, next to shimmering water (370 C) black smoker, placed on top of Tevnia patch behind shimmering water.             |
| V-Vent                     | 11/16/08 | 4474   | 9°N 50.169<br>104°W 17.457     | 2513      | 22         | N               | Placed near a crack at the floor of V-Vent.  |
| <b>GUAYMAS</b>             |          |        |                                |           |            |                 |  |
| Rebecca's Roost            | 11/23/08 | 4476   | 27°N 0.6763<br>111°W 24.4168   | 1987      | 30         | Y               | Placed near a Riftia patch near top, scale worms nearby, shimmering water.   |
| Mark's Crack/Pagoda site   | 11/24/08 | 4477   | 27°N 0.4608<br>111°W 24.5353   | 2010      | 26         | N               | Located near the diffuse flow through crack in vent, white bacterial mat nearby. Hydrocarbon rich.                                   |
| Rebecca's Roost            | 11/25/08 | 4478   | 27°N 0.6763<br>111°W 24.4168   | 1988      | 27–35      | Y               | Same location as Dive 4476.  |
| Southern Site/Area         | 11/26/08 | 4479   | 27°N 0.455<br>111°W 24.573     | 1999      | 36         | N               | Semi-hard bottom, sort of crust on top of sediment; bacterial mat covering; diffuse flow venting out of a crack.                     |
| Theme Park                 | 11/27/08 | 4480   | 27°N 0.7039<br>111°W 24.3176   | 2014      | 15–22      | N               | Orange mat, scraped away to reveal bare sediment, white mat around the orange mat, with yellow splotches on the order of ~10 meters. |
| Southern Site/Area         | 11/28/08 | 4481   | 27°N 0.455<br>111°W 24.573     | 1998      | 35         | N               | Directly above a hole in an orange mat. The hole has an outpouring of diffuse flow water. Same location as Dive 4479.                |

Samples collected at the same site on separate dates are indicated.

drift, a 2% HNO<sub>3</sub> blank solution and Marek standards were run periodically. pH was measured on each sample using a Orion D2 meter.

#### DNA EXTRACTION, AMPLICON GENERATION AND SEQUENCING

Immediately upon reaching the surface, the 0.22 μm membranes were aseptically removed from the filter apparatus, placed into sterile plastic bags, and immersed in DNA extraction buffer containing 1× TE, 50 mM EDTA, and 50 mM EGTA. Filters were flash-frozen in liquid nitrogen, held at -80°C while at sea, and returned on dry ice to the J. Craig Venter Institute, San Diego for DNA extraction and library preparation. Methods for DNA extraction from filters can be found elsewhere (Rusch et al., 2007). Briefly, after thawing, the cells were lysed using SDS/Proteinase K and the lysate purified using one phenol extraction and one phenol/chloroform extraction. The supernatant was precipitated using ethanol and eluted in TE buffer. Environmental DNA (eDNA) was then used as template in the

PCR targeting 16S rDNA (2 μl). The primers used to isolate the 16S were TX-9, 5'-GGATTAGAWACCBGGTAGTC-3' and 1391R, 5'-GACGGGCRGTGWGTRCA-3' (Ashby et al., 2007; Walker and Pace, 2007), and the following reaction used for gene amplification: 94°C for 3 min, 35 cycles of 94°C for 30 s, 55°C for 30 s, 72°C for 90 s, and 72°C for 10 min. Libraries were barcoded and sequenced using 454-pyrosequencing. The PCR primers were determined to be universal. The 1391R primer has been utilized in the past as a universal primer (Loy et al., 2007) and calculations with Silva testprobe (<http://www.arb-silva.de/search/testprobe>) estimate the coverage of Bacteria at 88% and Archaea at 76% with one mismatch allowed. The TX-9 primer is not currently present in probeBase, so we calculated an estimated coverage in RDPII (<http://rdp.cme.msu.edu/probematch/search.jsp>) using the Probe Match tool (Cole et al., 2007). Based on sequences >1200 nucleotides long and of good quality (a total of 1195961 sequences), with one mismatch, the estimated coverage of Bacteria is 99% and Archaea is 98%.

## SEQUENCE ANALYSES

Approximately one million (932,657) sequences were screened for quality by AmpliconNoise as described in detail elsewhere (Quince et al., 2011). A total of 457,209 sequences (average length of 381 bp) passed initial quality filtering. Sequences were then further screened and analyzed in mothur by dereplication, alignment, filtering, preclustering, and average neighbor clustering analyses, with the remaining 456,943 sequences used in clustering, diversity, and taxonomic analyses (Schloss et al., 2009). SFF files were assigned GenBank SRA Bioproject number PRJNA193540.

Ocean floor seawater is often entrained with the vent diffuse flow water during sampling. To calculate which OTUs were significantly enhanced in vent vs. off-axis water, we used statistical tests as described previously (Campbell et al., 2010, 2011). Briefly, significant shifts in OTU abundance between samples were determined in a pairwise fashion by an independent implementation of the statistics used by the RDP LibCompare tool (Wang et al., 2007) using the methods described by Audic and Claverie (1997) and the standard two-population proportions test (Christensen, 1992). Statistically significant results were considered to have a *P*-value less than 0.01 (*P*-values for two-population proportions test were inferred from the *Z* critical value). In addition, to be included in the pool of sequences belonging to OTUs enhanced in the vent samples, differences in OTU frequency between vent and off axis waters had to be greater than 2-fold. Individual comparisons were between the EPR vent samples and EPR off-axis water or between Guaymas vent samples and Guaymas off-axis water.

Both alpha and beta diversity estimates from the total and vent-specific sequences were calculated in mothur (Schloss et al., 2009). Briefly, the *Sobs* (observed richness), Chao I (non-parametric estimator of richness), Good's coverage, *inv Simpson* (Inverse Simpson, richness estimator not affected by sampling effort) and *np Shannon* (non-parametric Shannon index) calculators were implemented to estimate alpha diversity of each sample. Additionally, phylogenetic distances of the samples based on a phylogenetic tree of the vent specific sequences were calculated with the Clearcut program in mothur (Schloss et al., 2009). The beta diversity, similarities between samples from the entire dataset or just the vent-specific OTUs were calculated based on the theta (Yue and Clayton) similarity coefficient ( $\theta_{YC}$ ) (Schloss et al., 2009) at a distance of 0.03.

A representative sequence from each OTU was classified by multiple methods, including: Silva, RDPII and greengenes web alignment and classification tools as well as by BLAST analyses (Desantis et al., 2006; Pruesse et al., 2007; Johnson et al., 2008; Cole et al., 2009). In general, the results from all classification schemes were consistent with each other (data not shown).

## STATISTICAL METHODS

Nonmetric multidimensional scaling (NMDS) was used to examine the relationship between samples based on a  $\theta_{YC}$  similarity matrix calculated in mothur (Schloss et al., 2009). Only the vent-specific OTUs were used in the analyses. Individual OTUs, which best correlated with NMDS sample distribution by the method of Pearson were overlaid with a biplot, based on vectors calculated in mothur. Only OTUs that were represented by at least 200

sequences and had *r* values of at least 0.6 were plotted. In addition, correlations between the sample distributions and relative abundances of OTUs were also measured in mothur. Only factors which had *r* values of at least 0.2 were plotted. NMDS ordinations were also verified in the vegan package in R, using a Bray-Curtis distance calculation. Environmental factors that best correlated to the OTU data were calculated with the bioenv function in R and mothur after log transformation (Schloss et al., 2009) (<http://www.r-project.org/>).

## HEAT MAP METHODS

Relative abundance of each OTU served as input for the R PhyloTemp function (a phylogenetically enabled adaptation of the heatmap.2 function; R gplots package; <http://phylotemp.microeco.org>) (Polson, 2007). The resulting heat map displays relative abundance of each OTU across the individual libraries, with neighbor joining phylogenetic clustering of OTU representative sequences displayed along the y-axis and hierarchical clustering (Bray-Curtis) of taxonomic relative abundance on the x-axis.

## RESULTS

### PHYSICAL AND CHEMICAL DESCRIPTION OF THE SAMPLES

A variety of diffuse flow samples were collected from both hard basalt-based EPR and hydrocarbon-rich, sediment-based Guaymas Basin hydrothermal vent habitats (Table 1) using a modified large volume water sampler deployed on an elevator platform (Wommack et al., 2004). Half of the samples were collected near macrofaunal communities, while the other half were collected near hydrothermal diffuse flow vents or sediment surfaces, many with prominent bacterial mats. There were two sets of similar samples collected from the same site but on different dates: Rebecca's Roost and Southern site, both from Guaymas Basin (Table 1).

In general, most chemical and physical features, including temperature, were either very similar among the vents or no discernable patterns were observed within or between spreading center types (Table 2). However, cobalt, nickel and iron levels were significantly different between the spreading centers (*t*-test, Co and Ni, *p* < 0.05; Fe, *p* < 0.08). Cobalt and iron levels were 10 or 30 times higher in the EPR than Guaymas samples and nickel was 2.5 times higher in the Guaymas than the EPR samples.

### MICROBIAL COMMUNITY DIVERSITY

Between 15,000 and 48,000 16S rRNA gene sequences were analyzed from each sample after quality control processing. From the resulting 456,943 sequences, diversity estimates were calculated in mothur (Schloss et al., 2009) and after average neighbor clustering at a 0.03 distance level, 6277 OTUs were produced. The resulting dataset included all archaeal and bacterial sequences because a single set of primers encompassing both domains were used for amplification prior to sequencing (Ashby et al., 2007; Walker and Pace, 2007). The calculated level of Good's coverage from all sequences within each sample was high, between 0.97 and 1 (Table 3). Overall richness estimates (Chao I and *Sobs*) of the Guaymas Basin sites were much lower than the EPR sites.

**Table 2 |** Chemical characterizations of discrete diffuse flow aquatic water samples.

| Dive   | Li    | B      | 10    | Mg   | 24    | Al    | 27   | K    | 39   | Ca    | 43   | Cr   | 52    | Mn  | 55    | Co   | 59   | Ni   | 60    | Cu   | 65    | As    | 75    | Se    | 82 | Sr | 88 | Ba | 137 | Pb | 207 | T | pH | S | Fe | NH <sub>4</sub> | NO <sub>2</sub> | NO <sub>3</sub> | PO <sub>4</sub> |
|--------|-------|--------|-------|------|-------|-------|------|------|------|-------|------|------|-------|-----|-------|------|------|------|-------|------|-------|-------|-------|-------|----|----|----|----|-----|----|-----|---|----|---|----|-----------------|-----------------|-----------------|-----------------|
| 4470-3 | 8.88  | 213.76 | 56886 | 0.68 | 18294 | 13532 | 0.69 | 13.8 | 0.23 | 5.24  | 0.72 | 4.45 | 19.23 | 433 | 1.89  | 0.06 | 15.1 | 6.46 | 3.37  | 0.27 | 0.01  | 0.000 | 0.376 | 0.075 |    |    |    |    |     |    |     |   |    |   |    |                 |                 |                 |                 |
| 4472-3 | 7.78  | 186.78 | 52500 | 1.06 | 17649 | 12561 | 0.45 | 2.02 | 0.09 | 1.48  | 0.41 | 4.03 | 17.55 | 374 | 1.12  | 0.07 | 15   | 7.34 | 0.01  | 2.19 | 0.002 | 0.002 | 0.493 | 0.169 |    |    |    |    |     |    |     |   |    |   |    |                 |                 |                 |                 |
| 4473-3 | 7.83  | 195.63 | 53211 | 0.5  | 18207 | 13018 | 0.53 | 0.14 | 0.3  | 4.9   | 3    | 4.86 | 19.1  | 418 | 1.32  | 0.26 | 30   | 7.55 | 2.68  | 1.82 | 0.236 | 0.001 | 0.480 | 0.056 |    |    |    |    |     |    |     |   |    |   |    |                 |                 |                 |                 |
| 4474-1 | 8.23  | 204.65 | 54809 | 0.2  | 19149 | 13449 | 0.64 | 0.13 | 0.04 | 5.52  | 3.85 | 5.36 | 22.86 | 406 | 0.95  | 0.76 | 20.6 | 6.55 | 0.19  | 0.01 | 0.000 | 0.000 | 0.460 | 0.010 |    |    |    |    |     |    |     |   |    |   |    |                 |                 |                 |                 |
| 4476-1 | 13.22 | 211.6  | 51587 | 0.58 | 19594 | 13363 | 0.4  | 6.81 | 0    | 3.73  | 0.37 | 4.76 | 19.92 | 439 | 16.86 | 0.02 | 29   | 6.33 | 19.85 | 0.16 | 3.295 | 0.003 | 0.164 | 0.084 |    |    |    |    |     |    |     |   |    |   |    |                 |                 |                 |                 |
| 4477-1 | 8.54  | 212.19 | 52734 | 1.67 | 18618 | 13245 | 0.46 | 1.32 | 0.1  | 5.51  | 0.51 | 4.43 | 17.74 | 425 | 2.43  | 0.02 | 4.3  | 7.08 | 0.97  | 0.01 | 0.284 | 0.001 | 0.494 | 0.087 |    |    |    |    |     |    |     |   |    |   |    |                 |                 |                 |                 |
| 4478-1 | 7.97  | 186.28 | 58475 | 0.46 | 18318 | 13602 | 0.64 | 0.31 | 0    | 15.14 | 2.02 | 4.7  | 18.95 | 410 | 0.98  | 0.14 | 31.4 | 7.15 | 0.01  | 0.01 | 0.039 | 0.001 | 0.468 | 0.101 |    |    |    |    |     |    |     |   |    |   |    |                 |                 |                 |                 |
| 4479-1 | 12.34 | 190.56 | 61679 | 3.28 | 20802 | 14464 | 0.54 | 5.03 | 0    | 15.79 | 0.54 | 5.17 | 21.32 | 451 | 2.45  | 0.02 | 20.9 | 6.65 | 33.4  | 0.01 | 0.672 | 0.001 | 0.461 | 0.004 |    |    |    |    |     |    |     |   |    |   |    |                 |                 |                 |                 |
| 4480-1 | 7.42  | 184.07 | 46381 | 0.12 | 17339 | 12372 | 0.46 | 0.73 | 0    | 14.02 | 0.52 | 5.57 | 21.19 | 429 | 1.13  | 0.02 | 2.5  | 7.26 | 0.19  | 0.01 | 0.088 | 0.001 | 0.438 | 0.079 |    |    |    |    |     |    |     |   |    |   |    |                 |                 |                 |                 |
| 4481-1 | 8.35  | 170.77 | 58467 | 0.26 | 17753 | 12933 | 0.41 | 0.77 | 0    | 6.21  | 0.46 | 4.89 | 19.32 | 392 | 1.48  | 0.02 | 16.5 | 7.43 | 0.01  | 0.01 | 0.067 | 0.002 | 0.428 | 0.091 |    |    |    |    |     |    |     |   |    |   |    |                 |                 |                 |                 |

Gray boxed columns are those found to be significantly correlated with microbial community structure. Values listed for Li/Pb are in micromolar, T in °C, S/Po4 in mg/L.

Conversely, the diversity of the total individual communities as measured by the inverse Simpson or np Shannon calculations did not segregate by geographic location.

To examine the diversity and structure of microbial communities specific to diffuse flow waters, OTUs that were not statistically different between vent and off-axis water were removed from the dataset using previously described statistical methods (Wang et al., 2007; Campbell et al., 2010, 2011). 826 OTUs (at a 0.03 distance) were significantly enriched in vent vs. off-axis water, for a total of 33,001 sequences (about 7% of the total). The number of vent-specific sequences per sample ranged from 0.5 to 25.3% of the total number of sequences per sample (between 167 and 9516 vent specific sequences, **Table 4**). There were 396 and 90 OTUs that were significantly enriched in the EPR and Guaymas vent samples compared to off axis water, respectively. Of those, about 4% of the EPR and 28% of the Guaymas OTUs were also present in off-axis waters. Generally, vent-specific Guaymas communities displayed lower diversity than EPR communities (**Figure 1**) even after normalization for differences in sequencing effort (data not shown). Good's coverage estimates were about the same for the EPR communities (0.96–0.99) and only slightly lower for the Guaymas communities (0.85–0.98). Both richness estimates were lower in the vent-specific communities (**Table 4**), but paralleled the total community richness estimates (**Table 3**).

A direct assessment of differences between bacterial and archaeal diversity from individual samples showed that, in most samples, richness and diversity was higher in Bacteria than Archaea (**Table 5**, **Figures 2, 3**). However, in two of the samples (4470 and 4472), archaeal diversity was higher than bacterial diversity and in another sample (4480), they were not statistically different. Archaeal and bacterial evenness was more similar among the vent sites, where three of the samples (4476, 4478, and 4480) had roughly equivalent evenness estimates (**Table 3**, **Figure 2**). Interestingly, the two samples with the highest archaeal diversity and richness also had the highest archaeal evenness (4470 and 4472) (**Table 5**, **Figure 2B**). Phylogenetic diversity was not correlated with the percentage of Archaea or Bacteria, but the highest indices were found in the communities with roughly equal frequencies of archaeal and bacterial sequences (EPR—4474, Guaymas—4477; **Figure 4**). Neither sample was located near a macrofaunal community. Samples with low phylogenetic diversity either contained high levels of archaeal sequences and were from non-macrofaunal associated sites, or contained high levels of bacterial sequences and were from macrofaunal associated sites (**Figure 4**).

## COMMUNITY COMPOSITION

Microbial community composition of the various samples was assessed by phylogenetic analysis of 16S rRNA gene OTUs present in the entire sample and after subtraction of off-axis OTUs. Overall, the two most abundant OTUs (OTUs 1563 and 40) belonged to the Marine Group 1 (MGI) *Thaumarchaeota*, and their abundance segregated by geographic location where they made up about 60% of the community in either the EPR or Guaymas locations (**Figure 5**). The closest related sequences to the EPR MGI OTU (0.002 phylogenetic distance) were from

**Table 3 | Diversity estimates from 16S rRNA amplicon libraries of diffuse flow vent samples collected at 9°N East Pacific Rise (EPR) and Guaymas Basin (Guay) hydrothermal vent sites.**

| Sample              | # seqs <sup>b</sup> | Good's coverage | S <sup>c</sup> <sub>obs</sub> | Chao I richness | Simpson evenness | Inverse simpson | np shannon |
|---------------------|---------------------|-----------------|-------------------------------|-----------------|------------------|-----------------|------------|
| EPR-4470            | 41,992              | 0.97            | 2224                          | 4193            | 0.0011           | 2.29            | 2.68       |
| EPR-4472            | 42,092              | 0.98            | 1696                          | 3319            | 0.0011           | 1.92            | 2.13       |
| EPR-4473            | 37,602              | 0.98            | 1216                          | 2468            | 0.0032           | 3.82            | 3.06       |
| EPR-4474            | 44,487              | 0.98            | 1141                          | 2535            | 0.0017           | 1.96            | 1.85       |
| Guay-4476           | 48,670              | 0.99            | 512                           | 1194            | 0.0033           | 1.65            | 1.12       |
| Guay-4477           | 29,886              | 0.99            | 312                           | 744             | 0.0069           | 2.17            | 1.65       |
| Guay-4478           | 34,086              | 0.99            | 732                           | 1519            | 0.0028           | 2.03            | 1.66       |
| Guay-4479           | 23,965              | 0.99            | 588                           | 1325            | 0.0054           | 3.12            | 2.31       |
| Guay-4480           | 15,196              | 0.99            | 291                           | 690             | 0.0076           | 2.19            | 1.70       |
| Guay-4481           | 17,152              | 0.99            | 336                           | 1102            | 0.0061           | 2.03            | 1.55       |
| EPR OA <sup>a</sup> | 76,838              | 1.00            | 507                           | 1073            | 0.0036           | 1.83            | 1.40       |
| GUAY OA             | 44,977              | 1.00            | 289                           | 663             | 0.0114           | 3.28            | 2.08       |

<sup>a</sup>OA, off-axis.<sup>b</sup>#seqs, number of 16S rDNA amplicon sequences.<sup>c</sup>Sobs, number of observed species.**Table 4 | Diversity estimates from vent-specific 16S rDNA amplicons of diffuse flow vent samples collected at 9°N East Pacific Rise (EPR) and Guaymas Basin (Guay) hydrothermal vent sites.**

| Sample    | No of seqs | % of total <sup>a</sup> | Good's coverage | Sobs | Chao I | Simpson even | Inv Simpson | np shannon | Phylo diversity <sup>b</sup> |
|-----------|------------|-------------------------|-----------------|------|--------|--------------|-------------|------------|------------------------------|
| EPR-4470  | 8582       | 20.4                    | 0.99            | 538  | 574    | 0.0733       | 39.41       | 4.93       | 3.75                         |
| EPR-4472  | 7187       | 17.1                    | 0.99            | 452  | 5084   | 0.0649       | 29.32       | 4.49       | 3.60                         |
| EPR-4473  | 9516       | 25.3                    | 0.99            | 390  | 484    | 0.0729       | 28.42       | 4.35       | 2.68                         |
| EPR-4474  | 1667       | 3.7                     | 0.96            | 240  | 315    | 0.1339       | 32.14       | 4.65       | 5.08                         |
| Guay-4476 | 757        | 1.6                     | 0.94            | 114  | 166    | 0.1773       | 20.21       | 3.84       | 4.44                         |
| Guay-4477 | 163        | 0.5                     | 0.87            | 44   | 70     | 0.2195       | 9.66        | 3.25       | 4.60                         |
| Guay-4478 | 2024       | 5.9                     | 0.98            | 164  | 213    | 0.1683       | 27.60       | 4.06       | 3.47                         |
| Guay-4479 | 1888       | 7.9                     | 0.98            | 108  | 137    | 0.0328       | 3.55        | 2.60       | 2.96                         |
| Guay-4480 | 164        | 1.1                     | 0.85            | 57   | 80     | 0.5678       | 32.36       | 3.93       | 5.12                         |
| Guay-4481 | 965        | 5.6                     | 0.98            | 59   | 73     | 0.0324       | 1.91        | 1.65       | 2.29                         |

<sup>a</sup>Percentage of total library that were considered as vent-specific sequences.<sup>b</sup>Based on phylogenetic distances of 200 sequences (rarefied).

North Atlantic deep water and the Sea of Marmara. The Guaymas MG1 OTU was more closely related to *Nitrosopumilus* sp. (0.011 distance). The second most abundant OTU belonged to the *Oceanospirillales* (SUP05) within the *Gammaproteobacteria* and comprised about 7 and 13% in the EPR and Guaymas off-axis bacterioplankton, respectively; and between 0.1 and 3% in some of the diffuse flow samples (EPR-4470, 4472, Guay-4476, 4478) (Walsh et al., 2009).

Other phylotypes that were present at 0.5% or greater abundance in both EPR and Guaymas vent and off axis water included members of the Marine Groups II and III (MGII, MGIII) *Euryarchaeota*, as well as *Deltaproteobacteria* and *Deferribacteres* SAR406 (Marine Group A) bacterial clades. OTUs more abundant at Guaymas than EPR included members of the *Methylococcales* and *Thiotrichales* (*Gammaproteobacteria*), *Methylophilales* (*Betaproteobacteria*), and *Desulfobacterales* (*Deltaproteobacteria*) and ranged from about 20- to more than 200-fold more abundant

in Guaymas than EPR off-axis waters. Prevalence of many of these taxa, especially the *Methylococcales* and *Methylophilales*, are likely related to the high methane and hydrocarbon concentrations of the Guaymas spreading center (Edmond et al., 1982; Von Damm et al., 1985).

Among OTUs that were significantly enriched or specific to diffuse flow samples, three were found in every diffuse flow sample (Figure 6). The first, an OTU within the *Planctomycetales* (OTU-2438), with a range of frequency between 0.01 and 15%, was more prevalent in the Guaymas than EPR diffuse flow samples. The second, a member of the Deep Sea Hydrothermal Vent Group 6 archaeal clade (OTU-3227), ranged in abundance from 0.01 to about 10% and did not segregate by geographic location. The last OTU present in all vent samples, an *Archaeoglobales* (OTU-5145), comprised 0.07–4.3% of the community and was not found at all in off-axis waters. Seven OTUs were found in at least 80% of diffuse flow samples, two of which were within

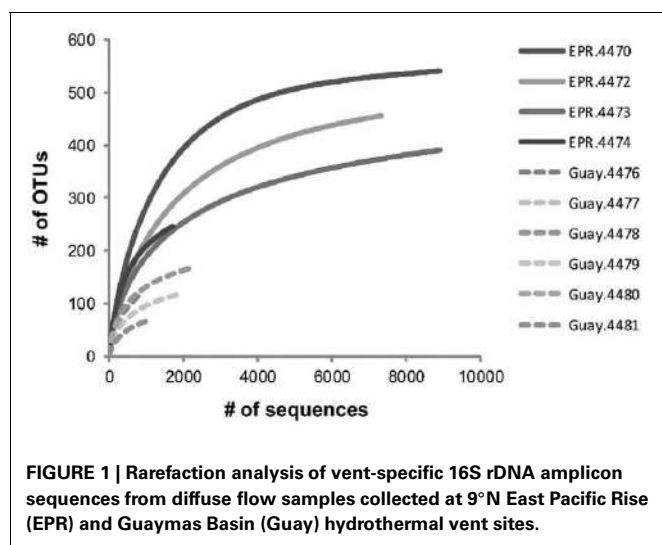


**FIGURE 1 |** Rarefaction analysis of vent-specific 16S rDNA amplicon sequences from diffuse flow samples collected at 9°N East Pacific Rise (EPR) and Guaymas Basin (Guay) hydrothermal vent sites.

the *Planctomycetes* phylum (OTU-2438 and 2918) and were more prevalent in Guaymas Basin samples than EPR samples. The closest BLAST hits to these *Planctomycetes* were uncultured members of the phylum; all cultured *Planctomycetes* and members of the annamox clade were at least 15% divergent within the amplified region, illustrating the diversity of this group according to 16S rRNA gene sequence (data not shown). One OTU (29), belonging to the *Thermococcales* family, was found in high abundance (3–76% of vent specific sequences) in EPR-4473 and four Guaymas samples (4477, 4478, 4479, and 4481). The other four OTUs (537, 3491, 3534, 4223) belonged to the *Epsilonproteobacteria* and each OTU comprised up to 7% of the vent-specific OTUs in at least 80% of the samples. Of the most abundant vent-specific OTUs, there were eight that were unique to one or two of the diffuse flow samples, but comprised up to 16% of the vent-specific OTUs. One of these was a member of MGII and was not found in off-axis water but only in EPR-4474 (OTU-8). Two other OTUs (144 and 3489) were found in one or two

**Table 5 |** Diversity estimates from 16S rRNA amplicon libraries of diffuse flow vent samples collected at 9°N East Pacific Rise (EPR) and Guaymas Basin (Guay) hydrothermal vent sites.

| Group   | #seqs <sup>a</sup> | Sobs <sup>b</sup> | Chao<br>I | Chao<br>I hci <sup>c</sup> | Chao<br>I hci <sup>d</sup> | np<br>shannon           | Inverse<br>simpson | Invsimpson<br>Ici | Invsimpson<br>hci | simpson<br>evenness |
|---|--------------------|-------------------|-----------|----------------------------|----------------------------|-------------------------|--------------------|-------------------|-------------------|---------------------|
| <b>BACTERIA DIFFUSE FLOW VENT SPECIFIC OTUs</b> |                    |                   |           |                            |                            |                         |                    |                   |                   |                     |
| EPR.4470  | 6810               | 305               | 334       | 317                        | 377                        | 4.24                    | 25.19              | 24.05             | 26.44             | 0.083               |
| EPR.4472  | 6380               | 275               | 301       | 287                        | 328                        | 4.00                    | 23.05              | 22.03             | 24.16             | 0.084               |
| EPR.4473  | 8080               | 303               | 356       | 330                        | 408                        | 4.17                    | 24.39              | 23.27             | 25.63             | 0.081               |
| EPR.4474  | 867                | 145               | 188       | 165                        | 239                        | 4.55                    | 59.60              | 52.58             | 68.78             | 0.411               |
| Guay.4476                                       | 653                | 77                | 104       | 88                         | 145                        | 3.33                    | 13.17              | 11.74             | 14.99             | 0.171               |
| Guay.4477                                       | 72                 | 25                | 41        | 29                         | 83                         | 3.07                    | 13.24              | 9.58              | 21.47             | 0.530               |
| Guay.4478                                       | 1697               | 105               | 120       | 111                        | 148                        | 3.57                    | 18.38              | 17.06             | 19.92             | 0.175               |
| Guay.4479                                       | 387                | 57                | 78        | 64                         | 117                        | 3.45                    | 20.03              | 17.68             | 23.11             | 0.351               |
| Guay.4480                                       | 143                | 32                | 38        | 34                         | 59                         | 3.18                    | 16.95              | 13.78             | 22.02             | 0.530               |
| Guay.4481                                       | 23                 | 13                | 18        | 14                         | 41                         | 2.89                    | 16.87              | 10.26             | 47.45             | 1.297               |
| Group   | #seqs              | Sobs              | Chao<br>I | Chao<br>I hci              | Chao<br>I hci              | np<br>shannon           | Inverse<br>simpson | Invsimpson<br>Ici | Invsimpson<br>hci | simpson<br>evenness |
| <b>ARCHAEA DIFFUSE FLOW VENT SPECIFIC OTUs</b>  |                    |                   |           |                            |                            |                         |                    |                   |                   |                     |
| EPR.4470  | 2043               | 220               | 224       | 221                        | 236                        | <b>4.79<sup>e</sup></b> | <b>41.14</b>       | 35.74             | 48.45             | 0.187               |
| EPR.4472  | 908                | 168               | 198       | 181                        | 236                        | <b>4.77</b>             | <b>76.26</b>       | 67.78             | 87.15             | 0.454               |
| EPR.4473  | 1289               | 68                | 118       | 86                         | 204                        | 2.19                    | 3.27               | 3.00              | 3.58              | 0.048               |
| EPR.4474  | 767                | 86                | 105       | 93                         | 136                        | 3.21                    | 8.04               | 7.02              | 9.41              | 0.094               |
| Guay.4476                                       | 183                | 31                | 51        | 37                         | 97                         | 2.54                    | 5.73               | 4.74              | 7.24              | 0.185               |
| Guay.4477                                       | 102                | 19                | 31        | 22                         | 73                         | 2.21                    | 4.18               | 3.19              | 6.06              | 0.220               |
| Guay.4478                                       | 416                | 49                | 73        | 57                         | 124                        | 3.04                    | 11.23              | 9.81              | 13.15             | 0.229               |
| Guay.4479                                       | 1553               | 55                | 63        | 57                         | 86                         | 1.85                    | 2.42               | 2.26              | 2.60              | 0.044               |
| Guay.4480                                       | 60                 | 20                | 38        | 24                         | 95                         | 2.80                    | 9.37               | 6.62              | 15.97             | 0.468               |
| Guay.4481                                       | 953                | 49                | 56        | 51                         | 75                         | 1.55                    | 1.87               | 1.74              | 2.02              | 0.038               |

Sequences derived after subtraction of off-axis OTUs.

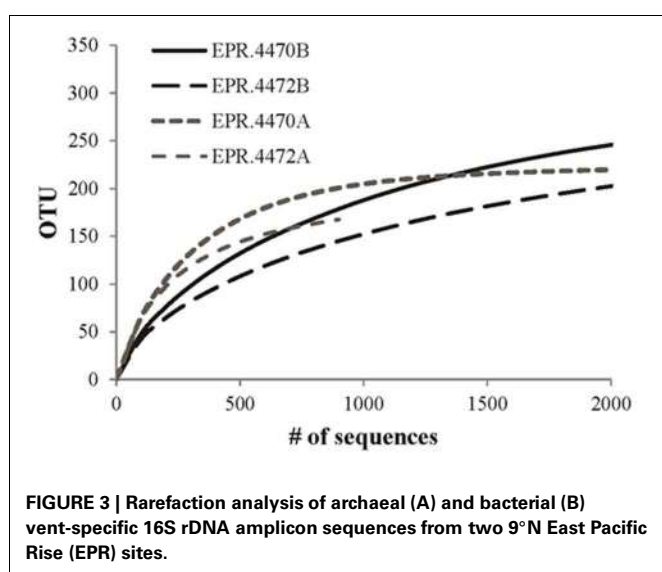
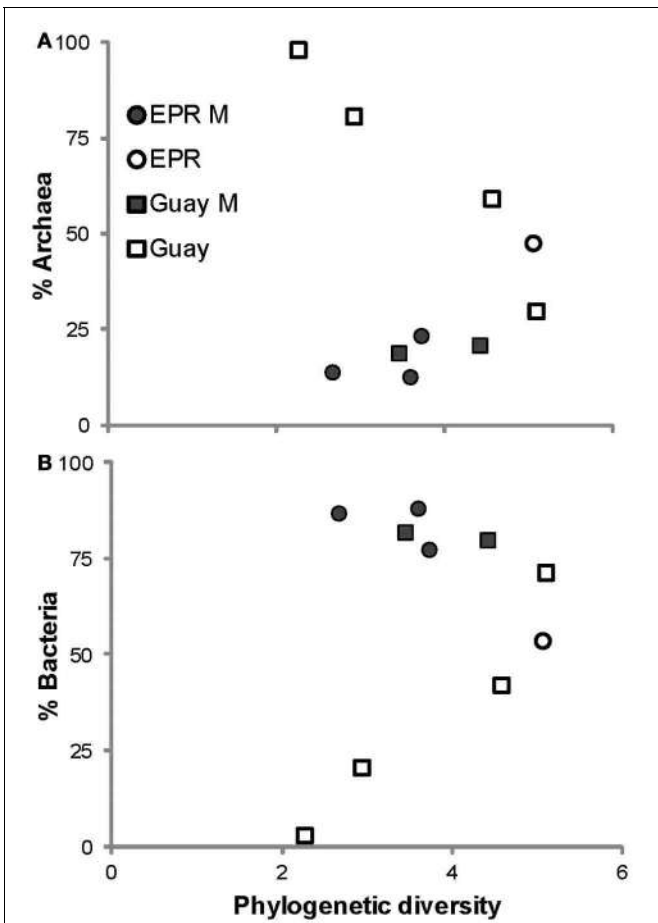
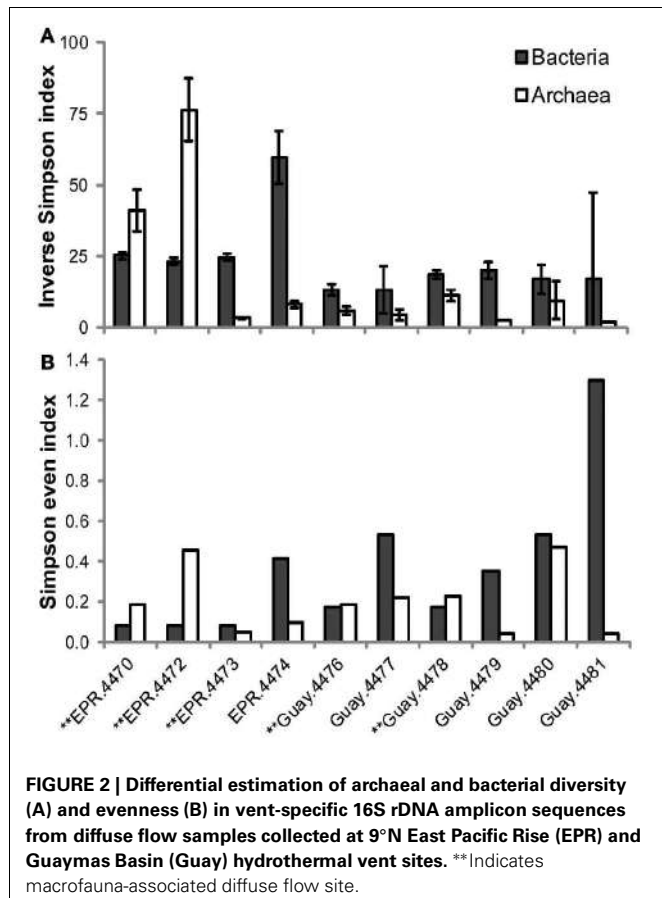
<sup>a</sup>#seqs, number of 16S rDNA amplicon sequences.

<sup>b</sup>Sobs, number of observed species.

<sup>c</sup>Low confidence interval.

<sup>d</sup>High confidence interval.

<sup>e</sup>Bold values indicate sites where estimated diversity of Archaea exceed that of Bacteria.



EPR diffuse flow samples respectively and were members of the *Epsilonproteobacteria*. Another OTU (1998), classified as a member of the ANME-1 group, was found only in Guaymas 4479 and 4481. Other Guaymas Basin-specific OTUs (196, 1042) include members of the *Flavobacteriales* and *Alteromonadales* families, as well as an unclassified bacterial phylotype (OTU-12).

Half of the sample locations (three of four sites at EPR and two of six sites at Guaymas) were adjacent to significant concentrations/colonies of macrofauna (e.g., Riftia, Tevnia, crabs; Table 1). The diffuse flow samples collected near macrofaunal communities had significantly higher percentages of Bacteria and *Epsilonproteobacteria* than the other samples ( $t$ -test,  $p < 0.05$ ), mainly driven by *Sulfurovum* (average frequency of 21 vs. 3%). Samples not collected near macrofaunal communities had significantly higher percentages of Archaea than the other samples ( $t$ -test,  $p < 0.05$ ), with increased frequencies of *Thermococcus* (30 vs. 3%). Despite this, there were no OTUs that were specific to diffuse flow water collected near macrofaunal communities.

We next looked at the archaeal composition of the two samples where the archaeal diversity was significantly higher than the bacterial diversity, EPR-4470 and 4472. EPR-4470 contained 220 different archaeal OTUs, whereas EPR-4472 contained 168. These were much higher than the rest of the samples, where the number of OTUs ranged from 19 to 86 (data not shown). There were 46 OTUs from EPR-4470 that contained 10 or more sequences in

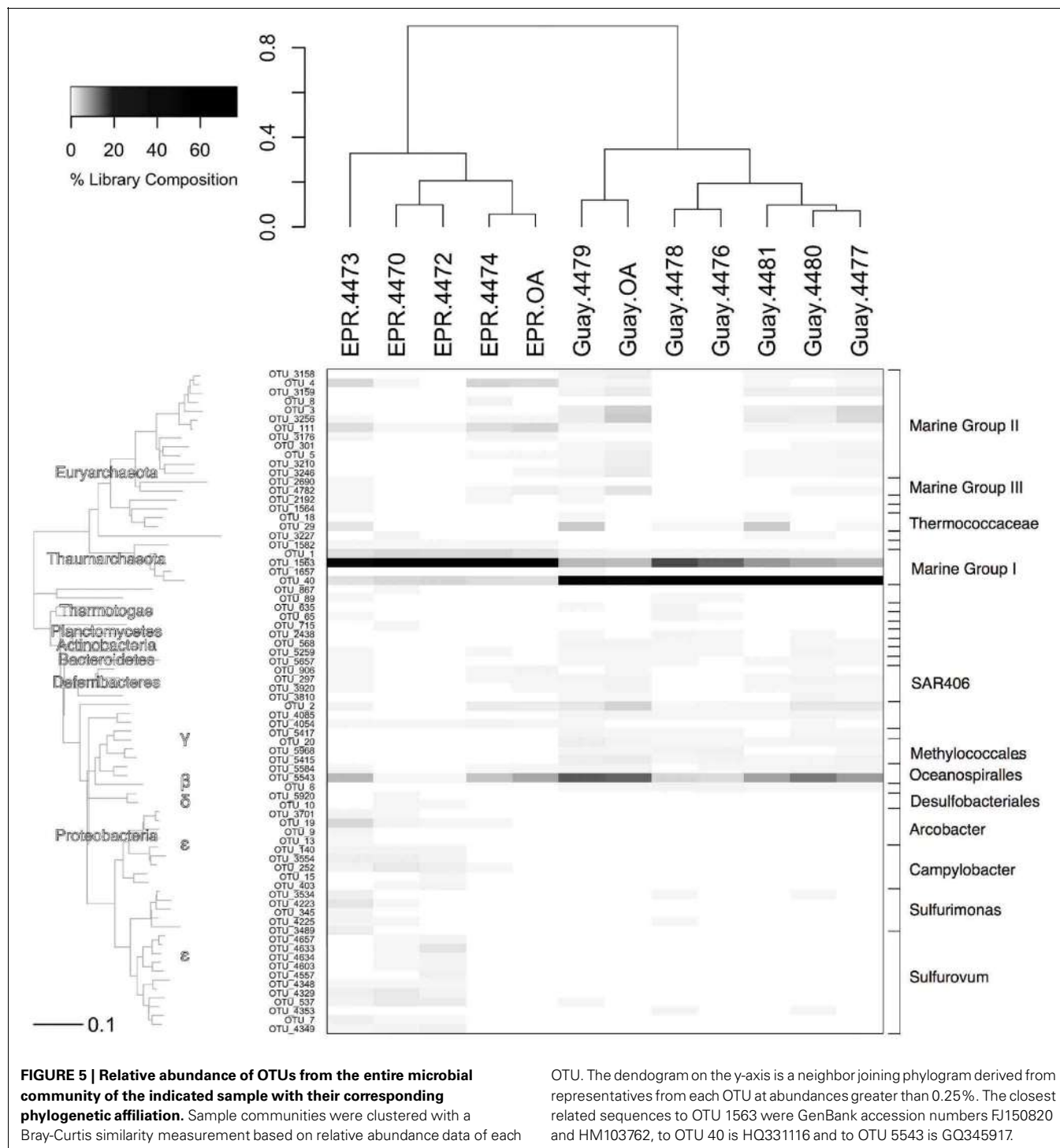


**FIGURE 5 | Relative abundance of OTUs from the entire microbial community of the indicated sample with their corresponding phylogenetic affiliation.** Sample communities were clustered with a Bray-Curtis similarity measurement based on relative abundance data of each

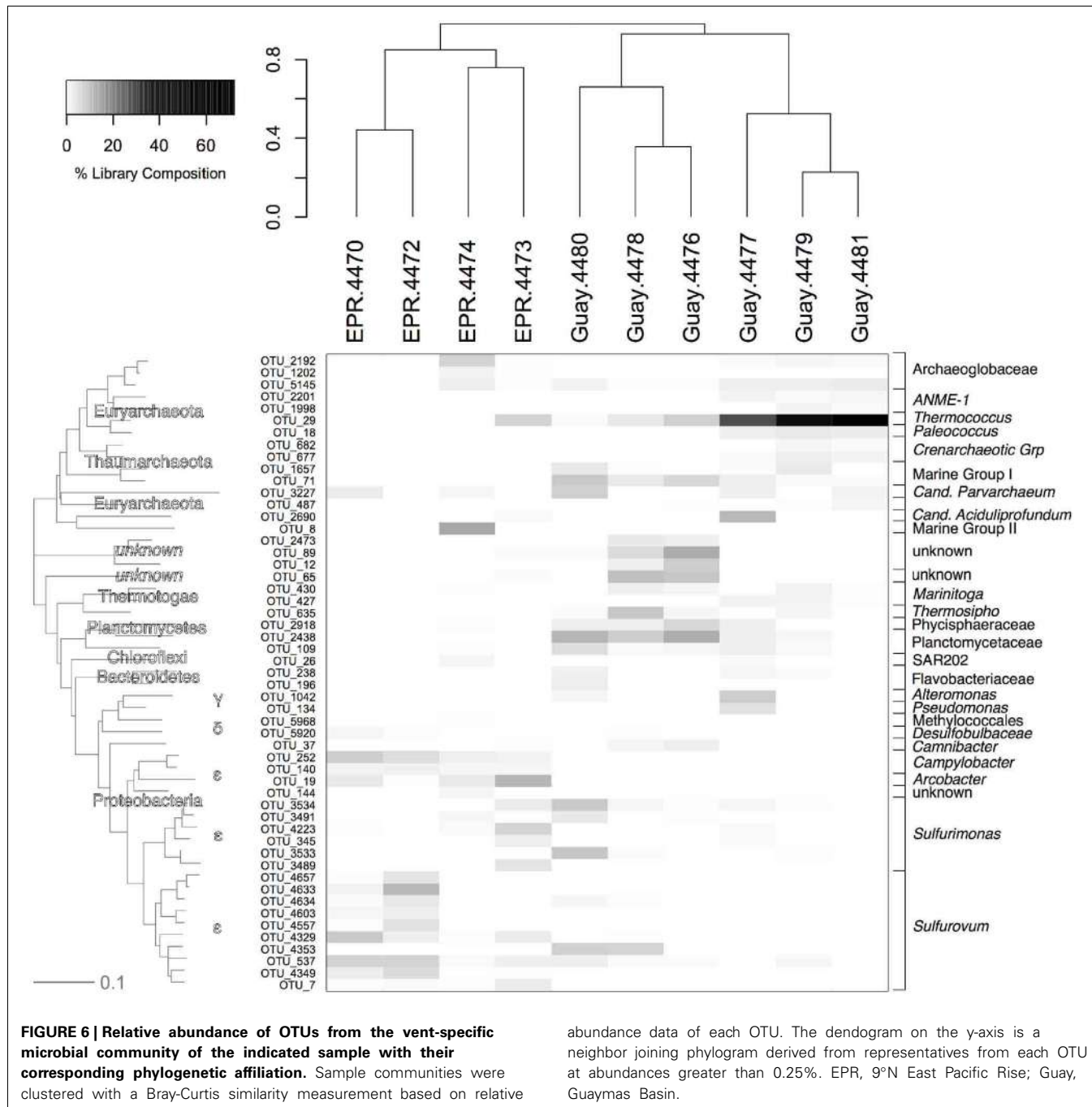
OTU. The dendrogram on the y-axis is a neighbor joining phylogram derived from representatives from each OTU at abundances greater than 0.25%. The closest related sequences to OTU 1563 were GenBank accession numbers FJ150820 and HM103762, to OTU 40 is HQ331116 and to OTU 5543 is GQ345917.

each OTU. Less than half that number (19) was in the EPR-4472 sample. There were no dominant OTUs in either sample except for an unclassified Archaea, most likely in the *Methanospaera* group, found in the EPR-4470 sample. There were more OTUs within the *Euryarchaeota* (54 and 42%, respectively for the EPR-4470 and 4472 samples) than *Crenarchaeota* (20 and 42%) or unclassified Archaea (26 and 16%). In contrast, the samples with the lowest archaeal diversity (Guay-4477 and Guay-4480) were

composed of 19 and 20 OTUs, respectively, and were dominated by *Thermococcus* and unclassified Archaea (data not shown).

#### COMPARATIVE ANALYSIS OF DIFFUSE FLOW MICROBIAL COMMUNITIES

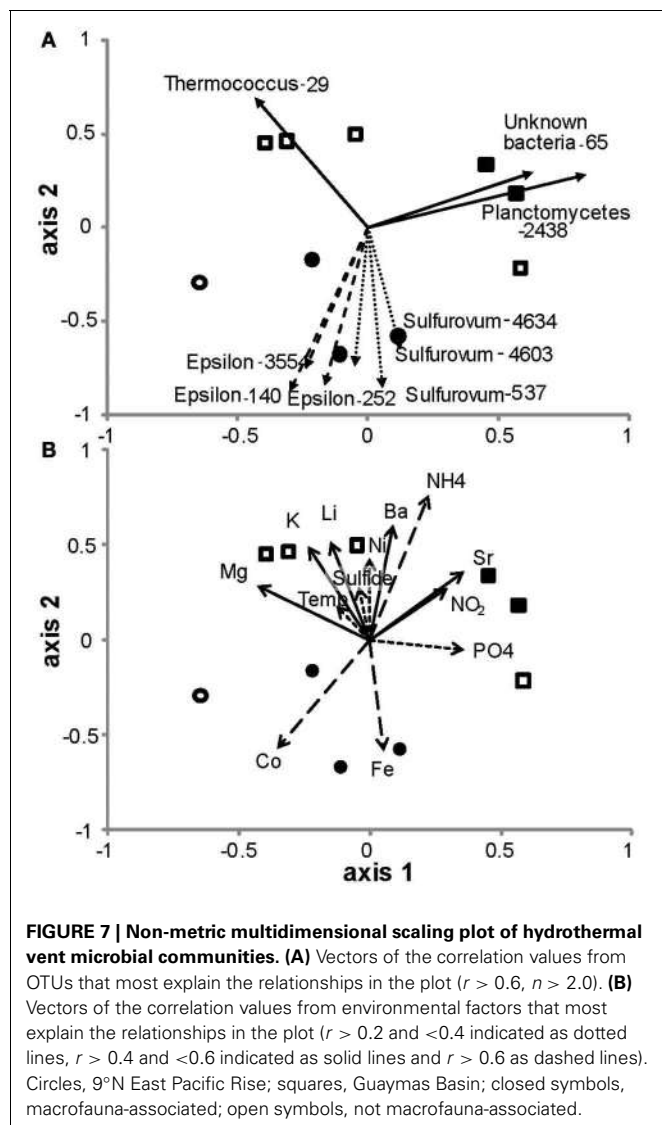
Analysis of diffuse flow communities separated EPR from the Guaymas sites according to both Bray-Curtis similarity (Figure 6) and nonmetric dimensional scaling (NMDS) of the



nonparametric Theta – Yue and Clayton ( $\theta_{YC}$ ) similarity coefficients (Schloss and Handelsman, 2005; Schloss et al., 2009) (Figure 7). To explain the grouping of the samples along the axes, the correlation of the relative abundance of individual OTUs in the NMDS dataset was calculated. The vector values of the most abundant OTUs were overlaid on the NMDS plot (Figure 7A). The OTUs that most contributed to the spatial distribution of the samples were within the *Epsilonproteobacteria*. About half of these were within the *Sulfurovum* genera, the others did not classify at genera level. Three other OTUs within the *Sulfurovum* genera also

were correlated but were left off the plot because of their similarity to the vectors of the other *Sulfurovum* genera (data not shown). A *Thermococcus* (OTU-29) that was found in very high abundance in three Guaymas samples (4477, 4479, 4481), and a *Planctomycetes* (OTU-2918 & 2438) and an unclassified bacteria (OTU-65) found in high abundance in Guaymas 4476, 4478, or 4480 also significantly contributed to the observed distribution (Figure 7A).

Out of 24 constituent geochemical features (Table 2), iron, cobalt and ammonium concentrations correlated best to the



community similarity plot ( $r > 0.6$ , confirmed with function `bioenv` in `R` where  $r = 0.6$ ) (Figure 7B). Ammonium was correlated more with the distribution of microbial communities in the Guaymas Basin samples, while iron and cobalt were better correlated with communities in the EPR samples. Also included on the plots were constituents whose  $r$  values were between 0.2 and 0.6 (Figure 7B). These included temperature, sulfide, nickel, and phosphate (between 0.2 and 0.4) and magnesium, potassium, lithium, barium, strontium, and nitrite (between 0.4 and 0.6).

## DISCUSSION

Our experimental approach allowed us to deeply sample microbial diversity and community composition between two geochemically and geographically distinct hydrothermal vent diffuse flow environments. Using statistical subtraction of taxa found in surrounding deep-sea water, it was possible to directly compare vent-specific taxa and further partition this diversity

by taxonomic domain. As with other microbial diversity studies of hydrothermal vent microbial communities (Huber et al., 2007, 2010), *Epsilonproteobacteria* dominated the vent specific taxa in most samples. Samples collected near macrofaunal communities had a higher abundance of bacteria, specifically *Epsilonproteobacteria*, than those collected near sediments or vents not populated by macrofauna. Unexpectedly, we found that some diffuse flow environments contained archaeal communities that were of higher diversity and evenness than co-existing bacterial communities. Additionally, one of the dominant taxa groups found in the off axis water, Thaumarchaeota (formerly marine Crenarchaeota) MGI (Delong, 1992; Brochier-Armanet et al., 2008), was differentially present between the two geographic locations. The second, SUP05, is found in many oxygen minimum zones, including hydrothermal vent plumes (Sunamura et al., 2004; Walsh et al., 2009). Nevertheless, distinct patterns in microbial community composition between sites were apparent after statistical subtraction of taxa present in background seawater. These patterns were correlated both to specific taxa (e.g., *Epsilonproteobacteria*, *Planctomycetes*) and to environmental factors (e.g., iron, ammonium).

## DISTINCTIONS IN MICROBIAL DIVERSITY BETWEEN DIFFUSE FLOW SAMPLES

The diversity of hydrothermal vent microbial communities is extensive, especially when measured with HTS techniques (Huber et al., 2007, 2010). In this study, total microbial diversity in both locations was positively correlated with the prevalence of Bacteria, especially *Epsilonproteobacteria*, within the vent-specific component of the community. Additionally, epsilonproteobacterial abundance as measured by frequency analyses was also significantly correlated with overall microbial richness. Other studies have noted high levels of epsilonproteobacterial diversity in hydrothermal vent environments (Huber et al., 2007, 2010; Opatkiewicz et al., 2009).

Collection near macrofaunal communities was correlated with increased overall diversity but decreased phylum-level diversity. These communities were dominated by *Sulfurovum* spp. within the *Epsilonproteobacteria*. This class of Proteobacteria may be more diverse than other groups due to their genetic makeup, where much of the group lacks standard DNA repair gene pathways seen in other bacterial groups (Miller et al., 2007; Campbell et al., 2009). We also observed higher levels of archaeal than microbial diversity or evenness in three out of five of the macrofauna-associated sites. This finding contrasts with prior reports, where the diversity of archaeal populations was lower than bacterial diversity when different sets of primers and different library constructs are used (Huber et al., 2002, 2003, 2010; Opatkiewicz et al., 2009). The resolution afforded by using a single set of domain-independent primers, as well as sampling of macrofauna-associated and non-macrofauna sites, likely contributed to our discovery of high levels of archaeal diversity at the vent sites.

While diversity estimates were not significantly different for vent-specific microbial communities between geographic locations, which agrees with our Good's coverage estimates, richness estimates were significantly different, even when corrected for

sequencing effort. Several location-specific factors may account for the decreased richness observed in the Guaymas samples. Historically, Guaymas Basin hydrothermal fluids are depleted in sulfides and enriched in ammonium, nickel, methane and hydrocarbons as compared to the EPR spreading center (Edmond et al., 1982; Von Damm et al., 1985). Extreme or disturbed conditions often result in less richness (Campbell et al., 2010; Fierer and Lennon, 2011), and these features of the Guaymas site may act to decrease richness. Additional properties not investigated here, such as diffuse flow rates or numbers of particles may also be different between the sites and affect microbial richness. Nevertheless, even at the gross level of richness estimates, there were clear biogeographic effects on deep-sea hydrothermal vent communities.

### MICROBIAL COMPOSITION ANALYSES OF DIFFUSE FLOW SAMPLES

Off-axis microbial communities from each region, EPR and Guaymas, were significantly different from one another. Our analyses revealed that archaeal phylotypes, specifically within the MGI clade, were the most abundant phylotypes in the seawater surrounding hydrothermal vents and differentiated the two regions. The MGI clade has been reported to dominate seawater microbial communities adjacent to hydrothermal vents and plumes, in some cases up to 46% of the entire community (Huber et al., 2002; Takai et al., 2004; Dick and Tebo, 2010). The dominant MGI Thaumarchaeota OTU at the EPR site grouped with other MGI species within the sub-tropical and equatorial deep water cluster; whereas the dominant MGI OTU at the Guaymas Basin grouped with North Atlantic clones within the *amoA* archaeal isolates cluster. It is likely that most MGI found in deep waters, including the major MGI at the basalt-dominated EPR are different than the MGI at Guaymas in terms of their metabolic properties (Agogue et al., 2008; Bouskill et al., 2012). Despite the low latitude location of the Guaymas site, the occurrence of a taxon related to *amoA* Archaea from North Atlantic suggests that the most abundant MGI species in Guaymas sedimentary-dominated deep-sea water is an autotrophic archaeal ammonium oxidizer. The generally higher ammonium concentrations in the Guaymas samples support this hypothesis. Therefore, our data indicate that the dominant deep-sea taxa from the EPR are most likely heterotrophs or mixotrophs and the dominant taxa from Guaymas are most likely autotrophs. This could be driven mostly by environmental conditions, where Guaymas Basin sites have high levels of ammonium resulting from high temperature breakdown of photosynthetic organisms sinking from the productive surface waters of the Gulf of California (Von Damm et al., 1985). Recent metagenomic and metatranscriptomic studies of both background and plume waters indicated high levels of chemolithoautotrophic processes from Guaymas Basin environment, supporting this findings (Baker et al., 2012; Lesniewski et al., 2012).

After statistical subtraction of OTUs within background deep-sea water, detailed patterns in microbial community structure emerged between the samples from various diffuse flow environments. In general, bacterial species distributions between the EPR and Guaymas indicated a trend toward dominance of autotrophic-associated taxa

(*Epsilonproteobacteria*) at the EPR sites and heterotrophic-associated taxa (*Planctomycetes*, *Alteromonas*, *Thermosiphon*, *Thermococcus*) at the Guaymas sites. At some of the sites (4472, 4478, 4480), the *Epsilonproteobacteria* were dominated by OTUs related to the *Sulfurovum*, *Sulfurocurvum*, and *Sulfuromonas* genera. Members of these genera are autotrophs and generally mesophilic and microaerophilic, but may respire nitrate, and use various sulfur species as electron donors (Campbell et al., 2006). These sites generally had higher pH and lower sulfide concentrations than others, perhaps indicating that these bacterial groups were actively oxidizing the sulfide. The epsilonproteobacterial communities at the other EPR sites (4470, 4473, 4474) were more evenly distributed between OTUs within the *Sulfurocurvum*, *Sulfuromonas*, and *Sulfurovum* genera and *Arcobacter/Sulfurospirillum* genera. While isolates within the *Sulfurospirillum* are heterotrophic, members of the *Arcobacter* can be autotrophic as well, and both can use sulfur as an electron donor (Campbell et al., 2006). Two of the samples taken at the same site (4476 and 4478) had relatively high levels of OTUs within the *Nautiliaceae*. Members of this family are thermophilic anaerobic autotrophs who obtain energy from hydrogen and may respire nitrate (Alain et al., 2002; Voordeckers et al., 2005; Campbell et al., 2006, 2009). Differential dominance of epsilonproteobacterial genera at vents has been previously observed at the Axial and Mariana Arc seamounts (Huber et al., 2007, 2010; Opatkiewicz et al., 2009) but not in the EPR or Guaymas Basin spreading centers.

At most of the Guaymas sites, member genera within the *Planctomycetes* were particularly frequent in the vent-specific samples. The *Planctomycetes* have been described in multiple habitats and include some genera that perform anaerobic ammonium oxidation (Neef et al., 1998; Jetten et al., 2001; Chistoserdova et al., 2004). This is the first study to demonstrate that members of the *Planctomycetes* occur at high abundance (>5% in the vent-specific community) within hydrothermal vent environments, although they have been found in terrestrial thermal springs (Kanokratana et al., 2004; Elshahed et al., 2007). *Planctomycetes* are generally considered heterotrophic, and isolates from low temperature sulfide springs are able to reduce sulfur species, therefore this group may be important in the heterotrophic cycling of sulfur in marine hydrothermal environments as well (Elshahed et al., 2007).

The two Guaymas samples taken from the Southern Site (4479 and 4481), as well as one other Guaymas sample from Pagoda and one of the EPR samples (V-vent) had more than 25% archaeal phylotypes. The high percentage of Archaea in the Guaymas samples was driven by a single OTU belonging to the *Thermococcales* order. Members of the *Thermococcales*, frequently isolated from hydrothermal vents, are generally considered anaerobic heterotrophic hyperthermophiles (Holden et al., 2001; Slobodkin et al., 2001; Jolivet et al., 2004; Teske et al., 2009; Perevalova et al., 2011). V-vent contained a large percentage of members of the *Archaeoglobales* and unclassified Euryarchaeota, many of which may be heterotrophic (Kletzin et al., 2004; Rusch and Amend, 2008). The sulfate-reducing *Archaeoglobales*, *Theromococcales*, and other Euryarchaeota are most likely hyperthermophiles as well (Stetter, 1996) and thus, diffuse flow from these sites are

enriched with microbes originating from very high temperature environments.

While we base our discussion on the known thermal and metabolic properties of cultured Bacteria and Archaea, we did find some interesting trends in the data that suggest that, after subtraction of off-axis microbes, some sites are dominated by thermophilic to hyperthermophilic heterotrophs and others by mesophilic autotrophs. This indicates that not all diffuse flow environments are equally represented by microbes across all thermal regimes. It could also be the result of a lack of complete diversity and compositional coverage of all the samples. However, Good's estimates of coverage were quite high, even with subtraction of OTUs specific to off-axis bottom water.

## CONCLUSIONS

This study underscores the utility of using HTS techniques combined with simultaneous amplification of the 16S rRNA gene from both Bacteria and Archaea to statistically separate off axis from vent-specific taxa. We found that overall diversity was significantly lower in the sedimentary Guaymas vent environments than in the basaltic EPR deep-sea hydrothermal vent environments, which has implications for understanding environmental controls of microbial diversity in these extreme habitats (Huber et al., 2007; Quince et al., 2008). Our study also suggests that environment-specific factors such as proximity to macrofaunal communities can have a dramatic effect on microbial community richness, diversity and composition. Furthermore, we observed unique microbial sub-communities that were specialized to the

diffuse flow environment and were different between spreading centers. Regrettably, we can only speculate as to the physiological features of member populations within diffuse flow communities as these observations are based on 16S rRNA gene homologies to known microbes. Deeper understanding of connections between phylogeny and physiology in these diffuse flow specialized microbial phyla can only come through genome level studies (Baker et al., 2012; Lesniewski et al., 2012).

## ACKNOWLEDGMENTS

We thank the captain and crew of the R/V Atlantis and especially the pilots and technicians of the DSV Alvin for their essential roles in the collection of specimens used in this study. We would also like to acknowledge the support from JCVI Joint Technology Center for their assistance with next-gen sequencing. This research was supported by grants from the National Science Foundation to K. Eric Wommack, Shannon J. Williamson and S. Craig Cary (MCB-0731916), to S. Craig Cary (OCE-0550491) and to Barbara J. Campbell (OCE-0825468). Computational infrastructure support from the University of Delaware Center for Bioinformatics and Computational Biology Core Facility and Delaware Biotechnology Institute was made possible through funding from Delaware INBRE (National Center for Research Resources 2 P20 RR016472-09; National Institute of General Medical Sciences 8 P20 GM103446-12); and Delaware EPSCoR (National Science Foundation EPS-081425). The New Zealand Marsden Fund provided financial support for S. Craig Cary (UOW0802), and Charles K. Lee (UOW1003).

## REFERENCES

- Agogue, H., Brink, M., Dinasquet, J., and Herndl, G. J. (2008). Major gradients in putatively nitrifying and non-nitrifying Archaea in the deep North Atlantic. *Nature* 456, 788–791. doi: 10.1038/nature07535
- Alain, K., Querellou, J., Lesongeur, F., Pignet, P., Crassous, P., Raguenes, G., et al. (2002). *Cannibibacter hydrogenophilus* gen. nov., sp nov., a novel thermophilic, hydrogen-oxidizing bacterium isolated from an East Pacific Rise hydrothermal vent. *Int. J. Syst. Evol. Microbiol.* 52, 1317–1323. doi: 10.1099/ijs.0.02195-0
- Ashby, M. N., Rine, J., Mongodin, E. F., Nelson, K. E., and Dimster-Denk, D. (2007). Serial analysis of rRNA genes and the unexpected dominance of rare members of microbial communities. *Appl. Environ. Microbiol.* 73, 4532–4542. doi: 10.1128/AEM.02956-06
- Audic, S., and Claverie, J. M. (1997). The significance of digital gene expression profiles. *Genome Res.* 7, 986–995.
- Baker, B. J., Lesniewski, R. A., and Dick, G. J. (2012). Genome-enabled transcriptomics reveals archaeal populations that drive nitrification in a deep-sea hydrothermal plume. *ISME J.* 6, 2269–2279. doi: 10.1038/ismej.2012.64
- Bouskill, N. J., Eveillard, D., Chien, D., Jayakumar, A., and Ward, B. B. (2012). Environmental factors determining ammonia-oxidizing organism distribution and diversity in marine environments. *Environ. Microbiol.* 14, 714–729. doi: 10.1111/j.1462-2920.2011.02623.x
- Brochier-Armanet, C., Boussau, B., Gribaldo, S., and Forterre, P. (2008). Mesophilic crenarchaeota: proposal for a third archaeal phylum, the Thaumarchaeota. *Nat. Rev. Microbiol.* 6, 245–252. doi: 10.1371/journal.pgen.1000362
- Campbell, B. J., and Cary, S. C. (2004). Abundance of reverse tricarboxylic acid cycle genes in free-living microorganisms at deep-sea hydrothermal vents. *Appl. Environ. Microbiol.* 70, 6282–6289. doi: 10.1128/AEM.70.10.6282-6289.2004
- Campbell, B. J., Engel, A. S., Porter, M. L., and Takai, K. (2006). The versatile epsilon-proteobacteria: key players in sulphidic habitats. *Nat. Rev. Microbiol.* 4, 458–468. doi: 10.1038/nrmicro1414
- Campbell, B. J., Polson, S. W., Hanson, T. E., Mack, M. C., and Schuur, E.a.G. (2010). The effect of nutrient deposition on bacterial communities in Arctic tundra soil. *Environ. Microbiol.* 12, 1842–1854. doi: 10.1111/j.1462-2920.2010.02189.x
- Campbell, B. J., Smith, J. L., Hanson, T. E., Klotz, M. G., Stein, L. Y., Lee, C. K., et al. (2009). Adaptations to submarine hydrothermal environments exemplified by the genome of *Nautilia profundicola*. *PLoS Genet.* 5:e1000362. doi: 10.1371/journal.pgen.1000362
- Campbell, B. J., Yu, L., Heidelberg, J. F., and Kirchman, D. L. (2011). Activity of abundant and rare bacteria in a coastal ocean. *Proc. Natl. Acad. Sci. U.S.A.* 108, 12776–12781. doi: 10.1073/pnas.1101405108
- Chistoserdova, L., Jenkins, C., Kalyuzhnaya, M. G., Marx, C. J., Lapidus, A., Vorholt, J. A., et al. (2004). The enigmatic Planctomycetes may hold a key to the origins of methanogenesis and methylotrophy. *Mol. Biol. Evol.* 21, 1234–1241. doi: 10.1093/molbev/msh113
- Christensen, H. B. (1992). *Introduction to Statistics: a Calculus-Based Approach*. 1st Edn. Orlando, FL: Harcourt Brace Jovanovich, Inc., 510–512.
- Cole, J. R., Chai, B., Farris, R. J., Wang, Q., Kulam-Syed-Mohideen, A. S., McGarrell, D. M., et al. (2007). The ribosomal database project (RDP-II): introducing myRDP space and quality controlled public data. *Nucleic Acids Res.* 35, D169–D172. doi: 10.1093/nar/gkl889
- Cole, J. R., Wang, Q., Cardenas, E., Fish, J., Chai, B., Farris, R. J., et al. (2009). The Ribosomal Database Project: improved alignments and new tools for rRNA analysis. *Nucleic Acids Res.* 37, D141–D145. doi: 10.1093/nar/gkn879
- Delong, E. F. (1992). Archaea in coastal marine environments. *Proc. Natl. Acad. Sci. U.S.A.* 89, 5685–5689. doi: 10.1073/pnas.89.12.5685
- Desantis, T. Z., Hugenholtz, P., Larsen, N., Rojas, M., Brodie, E. L., Keller, K., et al. (2006). Greengenes, a chimeric-checked 16S rRNA gene database and workbench compatible with ARB. *Appl. Environ. Microbiol.* 72, 5069–5072. doi: 10.1128/AEM.03006-05
- Dick, G. J., and Tebo, B. M. (2010). Microbial diversity and biogeochemistry of the Guaymas Basin deep-sea

- hydrothermal plume. *Environ. Microbiol.* 12, 1334–1347. doi: 10.1111/j.1462-2920.2010.02177.x
- Di Meo, C. A., Wakefield, J. R., and Cary, S. C. (1999). A new device for sampling small volumes of water from marine micro-environments. *Deep Sea Res. (Pt I)* 46, 1279–1287. doi: 10.1016/S0967-0637(99)0002-3
- Edmond, J. M., Von Damm, K. L., McDuff, R. E., and Measures, C. I. (1982). Chemistry of hot springs on the East Pacific Rise and their effluent dispersal. *Nature* 297, 187–191. doi: 10.1038/297187a0
- Elshahed, M. S., Youssef, N. H., Luo, Q. W., Najar, F. Z., Roe, B. A., Sisk, T. M., et al. (2007). Phylogenetic and metabolic diversity of *Planctomycetes* from anaerobic, sulfide- and sulfur-rich Zodletoe Spring, Oklahoma. *Appl. Environ. Microbiol.* 73, 4707–4716. doi: 10.1128/AEM.00591-07
- Fierer, N., and Lennon, J. T. (2011). The generation and maintenance of diversity in microbial communities. *Am. J. Bot.* 98, 439–448. doi: 10.3732/ajb.1000498
- Gotz, D., Banta, A., Beveridge, T. J., Rushdi, A. I., Simoneit, B. R. T., and Reysenbach, A. (2002). *Persephonella marina* gen. nov., sp nov and *Persephonella guaymasensis* sp nov, two novel, thermophilic, hydrogen- oxidizing microaerophiles from deep-sea hydrothermal vents. *Int. J. Syst. Evol. Microbiol.* 52, 1349–1359. doi: 10.1099/ijss.0.02126-0
- Grasshoff, K., Kremling, K., and Ehrhardt, M. (1999). *Methods of Seawater Analysis*. Weinheim: Wiley, V. H. C. doi: 10.1002/9783527613984
- Grzymski, J. J., Murray, A. E., Campbell, B. J., Kaplarevic, M., Gao, G., Lee, C. K., et al. (2008). Metagenome analysis of an extreme microbial symbiosis reveals eurythermal adaptation and metabolic flexibility. *Proc. Natl. Acad. Sci. U.S.A.* 105, 17516–17521. doi: 10.1073/pnas.0802782105
- Haddad, A., Camacho, F., Durand, P., and Cary, S. (1995). Phylogenetic characterization of the epibiotic bacteria associated with the hydrothermal vent polychaete *Alvinella pompejana*. *Appl. Environ. Microbiol.* 61, 1679–1687.
- Holden, J. F., Takai, K., Summit, M., Bolton, S., Zyskowski, J., and Baross, J. A. (2001). Diversity among three novel groups of hyperthermophilic deep-sea *Thermococcus* species from three sites in the northeastern Pacific Ocean. *FEMS Microbiol. Ecol.* 36, 51–60. doi: 10.1111/j.1574-6941.2001.tb00825.x
- Huber, J. A., Butterfield, D. A., and Baross, J. A. (2002). Temporal changes in archaeal diversity and chemistry in a mid-ocean ridge subseafloor habitat. *Appl. Environ. Microbiol.* 68, 1585–1594. doi: 10.1128/AEM.68.4.1585-1594.2002
- Huber, J. A., Butterfield, D. A., and Baross, J. A. (2003). Bacterial diversity in a subseafloor habitat following a deep-sea volcanic eruption. *FEMS Microbiol. Ecol.* 43, 393–409. doi: 10.1111/j.1574-6941.2003.tb01080.x
- Huber, J. A., Cantin, H. V., Huse, S. M., Welch, D. B. M., Sogin, M. L., and Butterfield, D. A. (2010). Isolated communities of Epsilonproteobacteria in hydrothermal vent fluids of the Mariana Arc seamounts. *FEMS Microbiol. Ecol.* 73, 538–549.
- Huber, J. A., Welch, D. B. M., Morrison, H. G., Huse, S. M., Neal, P. R., Butterfield, D. A., et al. (2007). Microbial population structures in the deep marine biosphere. *Science* 318, 97–100. doi: 10.1126/science.1146689
- Jetten, M. S. M., Wagner, M., Fuerst, J., van Loosdrecht, M., Kuenen, G., and Strous, M. (2001). Microbiology and application of the anaerobic ammonium oxidation ('anammox') process. *Curr. Opin. Biotechnol.* 12, 283–288. doi: 10.1016/S0958-1669(00)00211-1
- Johnson, M., Zaretskaya, I., Raytselis, Y., Merezhuk, Y., McGinnis, S., and Madden, T. L. (2008). NCBI BLAST: a better web interface. *Nucleic Acids Res.* 36, W5–W9. doi: 10.1093/nar/gkn201
- Jolivet, E., Corre, E., L'Haridon, S., Forterre, P., and Prieur, D. (2004). *Thermococcus marinus* sp. nov. and *Thermococcus radiotolerans* sp. nov., two hyperthermophilic archaea from deep-sea hydrothermal vents that resist ionizing radiation. *Extremophiles* 8, 219–227. doi: 10.1007/s00792-004-0380-9
- Kanokratana, P., Chanapan, S., Pootanakit, K., and Eurwilaichitr, L. (2004). Diversity and abundance of Bacteria and Archaea in the Bor Klueng hot spring in Thailand. *J. Basic Microbiol.* 44, 430–444. doi: 10.1002/jobm.200410388
- Kato, S., Takano, Y., Kakegawa, T., Oba, H., Inoue, K., Kobayashi, C., et al. (2010). Biogeography and biodiversity in sulfide structures of active and inactive vents at deep-sea hydrothermal fields of the southern mariana trough. *Appl. Environ. Microbiol.* 76, 2968–2979. doi: 10.1128/AEM.00478-10
- Kletzin, A., Urich, T., Muller, F., Bandeiras, T. M., and Gomes, C. M. (2004). Dissimilatory oxidation and reduction of elemental sulfur in thermophilic archaea. *J. Bioenerg. Biomembr.* 36, 77–91. doi: 10.1023/B:JOBB.0000019600.36757.8c
- Konneke, M., Bernhard, A. E., de la Torre, J. R., Walker, C. B., Waterbury, J. B., and Stahl, D. A. (2005). Isolation of an autotrophic ammonia-oxidizing marine archaeon. *Nature* 437, 543–546. doi: 10.1038/nature03911
- Lesniewski, R. A., Jain, S., Anantharaman, K., Schloss, P. D., and Dick, G. J. (2012). The metatranscriptome of a deep-sea hydrothermal plume is dominated by water column methanotrophs and lithotrophs. *ISME J.* 6, 2257–2268. doi: 10.1038/ismej.2012.63
- Lopez-Garcia, P., Gaill, F., and Moreira, D. (2002). Wide bacterial diversity associated with tubes of the vent worm *Riftia pachyptila*. *Environ. Microbiol.* 4, 204–215. doi: 10.1046/j.1462-2920.2002.00286.x
- Loy, A., Maixner, F., Wagner, M., and Horn, M. (2007). probeBase – an online resource for rRNA-targeted oligonucleotide probes: new features 2007. *Nucleic Acids Res.* 35, D800–D804. doi: 10.1093/nar/gkl856
- McCliment, E. A., Voglesonger, K. M., O'Day, P. A., Dunn, E. E., Holloway, J. R., and Cary, S. C. (2006). Colonization of nascent, deep-sea hydrothermal vents by a novel Archaeal and Nanoarchaeal assemblage. *Environ. Microbiol.* 8, 114–125. doi: 10.1111/j.1462-2920.2005.00874.x
- Miller, W. G., Parker, C. T., Rubenfield, M., Mendz, G. L., Wosten, M. M., Ussery, D. W., et al. (2007). The complete genome sequence and analysis of the epsilonproteobacterium *Arcobacter butzleri*. *PLoS ONE* 2:e1358. doi: 10.1371/journal.pone.00001358
- Moyer, C. L., Dobbs, F. C., and Karl, D. M. (1995). Phylogenetic diversity of the bacterial community from a microbial mat at an active, hydrothermal vent system, Loihi Seamount, Hawaii. *Appl. Environ. Microbiol.* 61, 1555–1562.
- Nakagawa, S., and Takai, K. (2008). Deep-sea vent chemoautotrophs: diversity, biochemistry and ecological significance. *FEMS Microbiol. Ecol.* 65, 1–14. doi: 10.1111/j.1574-6941.2008.00502.x
- Nakagawa, S., Takai, K., Inagaki, F., Hirayama, H., Nunoura, T., Horikoshi, K., et al. (2005). Distribution, phylogenetic diversity and physiological characteristics of epsilon-Proteobacteria in a deep-sea hydrothermal field. *Environ. Microbiol.* 7, 1619–1632. doi: 10.1111/j.1462-2920.2005.00856.x
- Neef, A., Amann, R., Schlesner, H., and Schleifer, K. H. (1998). Monitoring a widespread bacterial group: *in situ* detection of *Planctomycetes* with 16S rRNA-targeted probes. *Microbiology* 144, 3257–3266.
- Nunoura, T., Oida, H., Nakaseama, M., Kosaka, A., Ohkubo, S. B., Kikuchi, T., et al. (2010). Archaeal diversity and distribution along thermal and geochemical gradients in hydrothermal sediments at the Yonaguni Knoll IV hydrothermal field in the Southern Okinawa trough. *Appl. Environ. Microbiol.* 76, 1198–1211. doi: 10.1128/AEM.00924-09
- Opatkiewicz, A. D., Butterfield, D. A., and Baross, J. A. (2009). Individual hydrothermal vents at Axial Seamount harbor distinct subseafloor microbial communities. *FEMS Microbiol. Ecol.* 70, 413–424. doi: 10.1111/j.1574-6941.2009.00747.x
- Perevalova, A. A., Bonch-Osmolovskaya, E. A., Kolganova, T. V., Rusanov, I. I., Jeanthon, C., and Pimenov, N. V. (2011). Activity and distribution of thermophilic prokaryotes in hydrothermal fluid, sulfidic structures, and sheaths of alvinellids (east pacific rise, 13 degrees N). *Appl. Environ. Microbiol.* 77, 2803–2806. doi: 10.1128/AEM.02266-10
- Polson, S. W. (2007). *Comparative Analysis of Microbial Community Structure Associated with Acroporid Corals during a Disease Outbreak in the Florida reef tract*. Charleston, SC: Medical University of South Carolina.
- Pruesse, E., Quast, C., Knittel, K., Fuchs, B. M., Ludwig, W., Peplies, J., et al. (2007). SILVA: a comprehensive online resource for quality checked and aligned ribosomal RNA sequence data compatible with ARB. *Nucleic Acids Res.* 35, 7188–7196. doi: 10.1093/nar/gkm864
- Quince, C., Curtis, T. P., and Sloan, W. T. (2008). The rational exploration of microbial diversity. *ISME J.* 2, 997–1006. doi: 10.1038/ismej.2008.69
- Quince, C., Lanzen, A., Davenport, R. J., and Turnbaugh, P. J. (2011). Removing noise from

- pyrosequenced amplicons. *BMC Bioinformatics* 12:38. doi: 10.1186/1471-2105-12-38
- Reysenbach, A. L., Longnecker, K., and Kirshstein, J. (2000). Novel bacterial and archaeal lineages from an *in situ* growth chamber deployed at a Mid-Atlantic Ridge hydrothermal vent. *Appl. Environ. Microbiol.* 66, 3798–3806. doi: 10.1128/AEM.66.9.3798-3806.2000
- Robidart, J. C., Bench, S. R., Feldman, R. A., Novoradovsky, A., Podell, S. B., Gaasterland, T., et al. (2008). Metabolic versatility of the *Riftia pachyptila* endosymbiont revealed through metagenomics. *Environ. Microbiol.* 10, 727–737. doi: 10.1111/j.1462-2920.2007.01496.x
- Rusch, A., and Amend, J. P. (2008). Functional characterization of the microbial community in geothermally heated marine sediments. *Microbiol. Ecol.* 55, 723–736. doi: 10.1007/s00248-007-9315-1
- Rusch, D. B., Halpern, A. L., Sutton, G., Heidelberg, K. B., Williamson, S., Yooseph, S., et al. (2007). The Sorcerer II global ocean sampling expedition: northwest Atlantic through eastern tropical Pacific. *PLoS Biol.* 5:e77. doi: 10.1371/journal.pbio.0050077
- Schloss, P. D., and Handelsman, J. (2005). Introducing DOTUR, a computer program for defining operational taxonomic units and estimating species richness. *Appl. Environ. Microbiol.* 71, 1501–1506. doi: 10.1128/AEM.71.3.1501-1506.2005
- Schloss, P. D., Westcott, S. L., Ryabin, T., Hall, J. R., Hartmann, M., Hollister, E. B., et al. (2009). Introducing mothur: open-source, platform-independent, community-supported software for describing and comparing microbial communities. *Appl. Environ. Microbiol.* 75, 7537–7541. doi: 10.1128/AEM.01541-09
- Schrenk, M. O., Kelley, D. S., Delaney, J. R., and Baross, J. A. (2003). Incidence and diversity of microorganisms within the walls of an active deep-sea sulfide chimney. *Appl. Environ. Microbiol.* 69, 3580–3592. doi: 10.1128/AEM.69.6.3580-3592.2003
- Slobodkin, A., Campbell, B., Cary, S. C., Bonch-Osmolovskaya, E., and Jeanthon, C. (2001). Evidence for the presence of thermophilic Fe(III)-reducing microorganisms in deep-sea hydrothermal vents at 13 degrees N (East Pacific Rise). *FEMS Microbiol. Ecol.* 36, 235–243.
- Sogin, M. L., Morrison, H. G., Huber, J. A., Welch, D. M., Huse, S. M., Neal, P. R., et al. (2006). Microbial diversity in the deep sea and the underexplored “rare biosphere”. *Proc. Natl. Acad. Sci. U.S.A.* 103, 12115–12120. doi: 10.1073/pnas.0605127103
- Stetter, K. O. (1996). Hyperthermophilic prokaryotes. *FEMS Microbiol. Rev.* 18, 149–158. doi: 10.1111/j.1574-6976.1996.tb00233.x
- Stookey, L. L. (1970). Ferrozine-A new spectrophotometric reagent for iron. *Anal. Chem.* 42, 779–781. doi: 10.1021/ac60289a016
- Sunamura, M., Higashi, Y., Miyako, C., Ishibashi, J., and Maruyama, A. (2004). Two bactetia phylotypes are predominant in the Suiyo Seamount hydrothermal plume. *Appl. Environ. Microbiol.* 70, 1190–1198. doi: 10.1128/AEM.70.2.1190-1198.2004
- Takai, K., Oida, H., Suzuki, Y., Hirayama, H., Nakagawa, S., Nunoura, T., et al. (2004). Spatial distribution of marine crenarchaeota group I in the vicinity of deep-sea hydrothermal systems. *Appl. Environ. Microbiol.* 70, 2404–2413. doi: 10.1128/AEM.70.4.2404-2413.2004
- Teske, A., Edgcomb, V., Rivers, A. R., Thompson, J. R., Gomez, A. D., Molyneaux, S. J., et al. (2009). A molecular and physiological survey of a diverse collection of hydrothermal vent Thermococcus and Pyrococcus isolates. *Extremophiles* 13, 905–915. doi: 10.1007/s00792-009-0278-7
- Vetriani, C., Voordeckers, J. W., Do, M. H., Hugler, M., Ko, V., and Sievert, S. M. (2008). Culture dependent and independent analyses of 16S rRNA and ATP citrate lyase genes: a comparison of microbial communities from different black smoker chimneys on the Mid-Atlantic Ridge. *Extremophiles* 12, 627–640. doi: 10.1007/s00792-008-0167-5
- Von Damm, K. L. (1990). Seafloor hydrothermal activity - black smoker chemistry and chimneys. *Annu. Rev. Earth Planet. Sci.* 18, 173–204. doi: 10.1146/annurev.ea.18.050190.001133
- Von Damm, K. L., Edmond, J. M., Measures, C. I., and Grant, B. (1985). Chemistry of submarine hydrothermal solutions at guaymas basin, gulf of california. *Geochim. Cosmochim. Acta* 49, 2221–2237. doi: 10.1016/0016-7037(85)90223-6
- Voordeckers, J. W., Starovoytov, V., and Vetriani, C. (2005). *Caminibacter mediatlanticus* sp nov., a thermophilic, chemolithoautotrophic, nitrate-ammonifying bacterium isolated from a deep-sea hydrothermal vent on the Mid-Atlantic Ridge. *Int. J. Syst. Evol. Microbiol.* 55, 773–779. doi: 10.1099/ijns.0.63430-0
- Walker, J. J., and Pace, N. R. (2007). Phylogenetic composition of Rocky Mountain endolithic microbial ecosystems. *Appl. Environ. Microbiol.* 73, 3497–3504. doi: 10.1128/AEM.02656-06
- Walsh, D. A., Zaikova, E., Howes, C. G., Song, Y. C., Wright, J. J., Tringe, S. G., et al. (2009). Metagenome of a versatile chemolithoautotroph from expanding oceanic dead zones. *Science* 326, 578–582. doi: 10.1126/science.1175309
- Wang, Q., Garrity, G. M., Tiedje, J. M., and Cole, J. R. (2007). Naive Bayesian classifier for rapid assignment of rRNA sequences into the new bacterial taxonomy. *Appl. Environ. Microbiol.* 73, 5261–5267. doi: 10.1128/AEM.00062-07
- Wery, N., Cambon-Bonavita, M. A., Lesongeur, F., and Barbier, G. (2002). Diversity of anaerobic heterotrophic thermophiles isolated from deep-sea hydrothermal vents of the Mid-Atlantic Ridge. *FEMS Microbiol. Ecol.* 41, 105–114. doi: 10.1111/j.1574-6941.2002.tb00971.x
- Wommack, K. E., Williamson, S. J., Sundbergh, A., Helton, R. R., Glazer, B. T., Portune, K., et al. (2004). An instrument for collecting discrete large-volume water samples suitable for ecological studies of microorganisms. *Deep Sea Res. (Pt I)* 51, 1781–1792.
- Conflict of Interest Statement:** The authors declare that the research was conducted in the absence of any commercial or financial relationships that could be construed as a potential conflict of interest.
- Received:** 14 February 2013; **accepted:** 17 June 2013; **published online:** 24 July 2013.
- Citation:** Campbell BJ, Polson SW, Zeigler Allen L, Williamson SJ, Lee CK, Wommack KE and Cary SC (2013) Diffuse flow environments within basalt- and sediment-based hydrothermal vent ecosystems harbor specialized microbial communities. *Front. Microbiol.* 4:182. doi: 10.3389/fmicb.2013.00182
- This article was submitted to Frontiers in Extreme Microbiology, a specialty of Frontiers in Microbiology.
- Copyright © 2013 Campbell, Polson, Zeigler Allen, Williamson, Lee, Wommack and Cary. This is an open-access article distributed under the terms of the Creative Commons Attribution License, which permits use, distribution and reproduction in other forums, provided the original authors and source are credited and subject to any copyright notices concerning any third-party graphics etc.



# The microbiology of deep-sea hydrothermal vent plumes: ecological and biogeographic linkages to seafloor and water column habitats

Gregory J. Dick<sup>1,2,3\*</sup>, Karthik Anantharaman<sup>1</sup>, Brett J. Baker<sup>1</sup>, Meng Li<sup>1</sup>, Daniel C. Reed<sup>1</sup> and Cody S. Sheik<sup>1</sup>

<sup>1</sup> Department of Earth and Environmental Sciences, University of Michigan, Ann Arbor, MI, USA

<sup>2</sup> Department of Ecology and Evolutionary Biology, University of Michigan, Ann Arbor, MI, USA

<sup>3</sup> Center for Computational Medicine and Bioinformatics, University of Michigan, Ann Arbor, MI, USA

**Edited by:**

Andreas Teske, University of North Carolina at Chapel Hill, USA

**Reviewed by:**

James F. Holden, University of Massachusetts Amherst, USA  
Victoria Jean Bertics, Harvard University, USA

**\*Correspondence:**

Gregory J. Dick, Department of Earth and Environmental Sciences, University of Michigan, 2534 CC Little Building, Ann Arbor, MI 48109-1005, USA.  
e-mail: gdick@umich.edu

Hydrothermal plumes are an important yet understudied component of deep-sea vent microbial ecosystems. The significance of plume microbial processes can be appreciated from three perspectives: (1) mediation of plume biogeochemistry, (2) dispersal of seafloor hydrothermal vent microbes between vents sites, (3) as natural laboratories for understanding the ecology, physiology, and function of microbial groups that are distributed throughout the pelagic deep sea. Plume microbiology has been largely neglected in recent years, especially relative to the extensive research conducted on seafloor and subseafloor systems. Rapidly advancing technologies for investigating microbial communities provide new motivation and opportunities to characterize this important microbial habitat. Here we briefly highlight microbial contributions to plume and broader ocean (bio)geochemistry and review recent work to illustrate the ecological and biogeographic linkages between plumes, seafloor vent habitats, and other marine habitats such as oxygen minimum zones (OMZs), cold seeps, and oil spills. 16S rRNA gene surveys and metagenomic/transcriptomic data from plumes point to dominant microbial populations, genes, and functions that are also operative in OMZs (SUP05, ammonia-oxidizing Archaea, and SAR324 *Deltaproteobacteria*) and hydrocarbon-rich environments (methanotrophs). Plume microbial communities are distinct from those on the seafloor or in the subsurface but contain some signatures of these habitats, consistent with the notion that plumes are potential vectors for dispersal of microorganisms between seafloor vent sites. Finally, we put forward three pressing questions for the future of deep-sea hydrothermal plume research and consider interactions between vents and oceans on global scales.

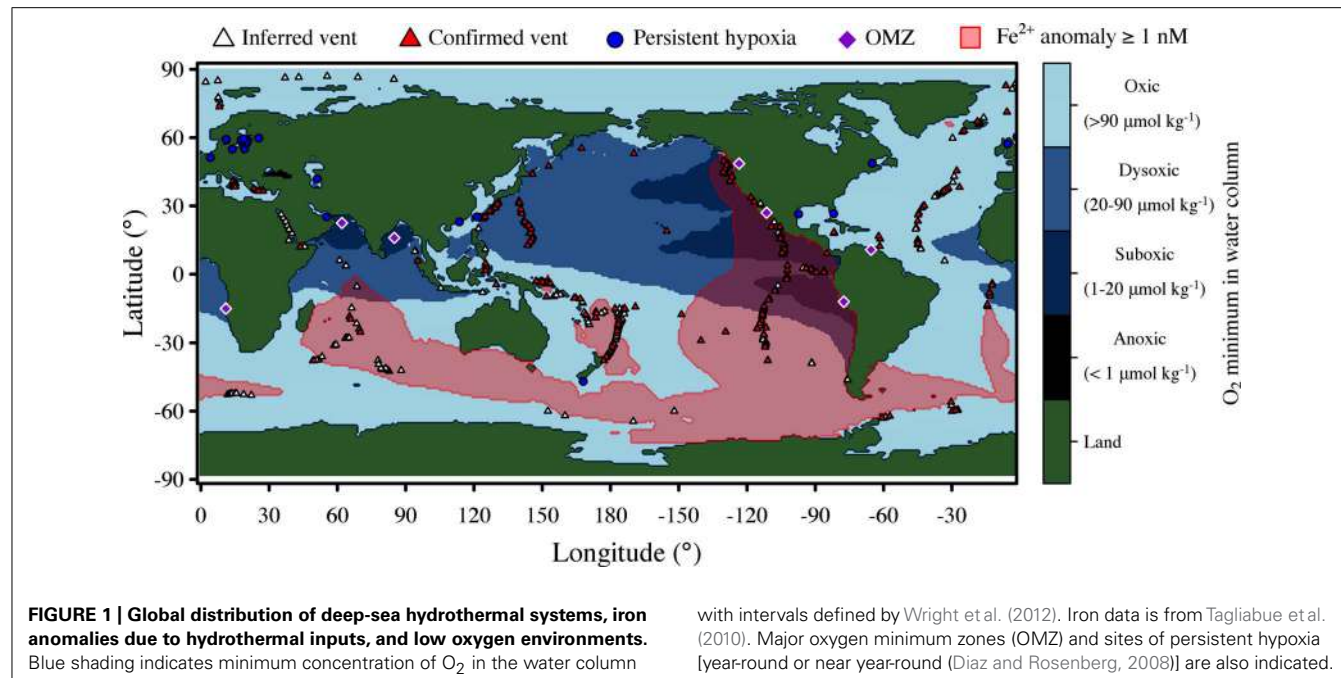
**Keywords:** chemosynthesis, chemoautotroph, deep-sea, biogeochemistry, hydrothermal, vent, biogeography

## INTRODUCTION

Deep-sea hydrothermal plumes occur where seafloor vents inject hydrothermal fluids replete with potential microbial energy sources such as H<sub>2</sub>S, Fe, Mn, CH<sub>4</sub>, and H<sub>2</sub> into the deep oceans. These hot, chemically reduced fluids rapidly mix with cold, oxidizing seawater, forming hydrothermal plumes that rise hundreds of meters off the seafloor and disperse hundreds of kilometers away from their source. Because of their extensive spatial coverage and easily detectable hydrothermal signals (Fe, Mn, turbidity, Helium-3), plumes played an important role in the history of deep-sea hydrothermal vent research (Lupton and Craig, 1981) and continue to be utilized for discovery of new seafloor hydrothermal systems (German et al., 2010). Hydrothermal plumes are highly variable in terms of scale and chemical and physical properties, and can be detected by a variety of methods (chemical, physical, optical), thus the definition of a plume depends on the parameter being measured (Lupton, 1995). For many of the geochemical and microbiological processes of interest here, “plume” often refers to hydrothermal fluid that has been heavily diluted by seawater (e.g., ~1:10,000), but some work has addressed microbial processes in

the rising portion of the plume where hydrothermal constituents are more concentrated.

Hydrothermal plumes are found at vents sites distributed globally along the mid-ocean ridge system (Figure 1) at a frequency correlated to seafloor spreading rate (Beaulieu et al., 2012). Deep-sea vent systems continue to be discovered at a rapid pace; over 500 vent fields are now known, nearly double the number known before the year 2000 (Beaulieu et al., 2012). Yet much of the mid-ocean ridge system remains unexplored, especially at ultra-slow spreading ridges, which have only recently been recognized to host hydrothermal activity (German et al., 2010) and are particularly abundant in the Arctic and Southern oceans. Hydrothermal venting in shallow waters is also widespread (Prol-Ledesma et al., 2005), but here we focus only on deep-sea systems. Given the global distribution and extent of hydrothermal venting, it is clear that deep-sea vents exert significant influence on the chemistry of the global oceans (Elderfield and Schultz, 1996). A recent modeling study of hydrothermal contributions to the marine iron inventory (Tagliabue et al., 2010) highlights the global impacts of vents (Figure 1).



## MICROBIAL MEDIATION OF PLUME BIOGEOCHEMISTRY: TRACE ELEMENTS, PHOSPHORUS AND CARBON

The impact of deep-sea hydrothermal vents on ocean chemistry involves several processes that are influenced by microbial activities in hydrothermal plumes. First, vents are thought to be a significant source of Fe and Mn to the oceans because their concentrations in hydrothermal fluids are up to 10<sup>6</sup> times that of background seawater (Elderfield and Schultz, 1996; Tagliabue et al., 2010; Sander and Koschinsky, 2011). The oceanic fate of these metals is influenced by scavenging and oxidation, which are promoted by microorganisms (Cowen and Bruland, 1985; Cowen et al., 1986; Mandernack and Tebo, 1993; Dick et al., 2009), and by binding with organic matter, which is presumably derived from microbial activity (Bennett et al., 2008; Toner et al., 2009; Breier et al., 2012; Holden et al., 2012). Second, the iron and manganese oxides produced by microbial oxidation are extraordinarily reactive (Goldberg, 1954; Tebo et al., 2004) and thus remove phosphorous and trace elements (rare earth elements, potassium, vanadium, arsenic, chromium, uranium) from seawater via scavenging and co-precipitation reactions (Feely et al., 1998; German and Von Damm, 2004). Because of the rapid mixing of seawater with hydrothermal fluids and the large volumes of plumes, the entire volume of the global oceans cycles through hydrothermal plumes and is scavenged of reactive elements on relatively short times scales ( $2.4 \times 10^5$  y; Kadko, 1993). Thus plumes essentially act as a filter for the global oceans, scavenging them of phosphorous, rare earth elements, and trace metals, and acting as a chemical sink for these elements (Kadko, 1993). As these Fe and Mn oxides and their scavenged elements are deposited to the seafloor, they form metalliferous sediments that potentially preserve a record of seawater nutrient status and chemistry that is valuable from paleoceanographic perspectives (Feely et al., 1998). Similarly, banded iron formations, which are likely sourced from

hydrothermal activity, provide a Precambrian record of ocean chemistry (Konhauser et al., 2009; Planavsky et al., 2011). Thus, microbially mediated metal oxide formation and the properties of the resulting biogenic minerals in plumes influence scavenging reactions and outcomes in terms of ocean chemistry, and understanding these processes is critical for interpretation of the sedimentary record for paleoceanographic purposes.

The third process by which plume microorganisms mediate broader ocean biogeochemistry is chemosynthetic fixation of carbon. Chemosynthetic activity at vents was recognized upon the initial discovery of deep-sea hydrothermal vent ecosystems (Jannasch and Wirsen, 1979) and in early plume studies (Winn et al., 1986) yet the magnitude of chemosynthesis in plumes remains poorly constrained. Based on extrapolation of data from the Southern East Pacific Rise to the global oceans, Maruyama et al. (1998) estimated that net primary production in plumes represents 0.1–1% of total marine photosynthetic net primary production. Because only a small fraction of surface organic carbon reaches the deep oceans, the hydrothermal contribution could represent up to 25% of the global deep ocean organic carbon inventory (Maruyama et al., 1998). Thermodynamic models support the idea that plumes are a significant source of chemosynthetically derived organic carbon to the deep oceans (McCollum, 2000), and several observational studies confirm an important contribution of plumes to deep-sea organic carbon on regional scales (De Angelis et al., 1993; Cowen and German, 2003; Lam et al., 2004, Lam et al., 2008). Indeed, plumes are enriched with organic carbon, some of which is labile, and are responsible for dispersing it kilometers away from vent sites (Roth and Dymond, 1989; Cowen et al., 2001; Shackelford and Cowen, 2006; Lam et al., 2008; Bennett et al., 2011a,b). More recently, transcriptomic evidence confirms that autotrophy is a prevalent process in plumes (Baker et al., 2012; Lesniewski et al., 2012; Anantharaman et al., 2013).

Two recent developments provide fresh motivation for re-examining the global impact of hydrothermal vents on the chemistry and biology of the oceans. First, hydrothermal activity along the mid-ocean ridges is more common than previously recognized, especially at slow-spreading systems (German et al., 2010; Beaulieu et al., 2012). Slow-spreading ridges represent a large but poorly explored portion of the global mid-ocean system and host high-energy, H<sub>2</sub>-rich systems that are potential hotspots for chemosynthesis (Amend et al., 2011). Second, the discovery of cryptic biogeochemical cycling of sulfur (Canfield et al., 2010) and widespread chemolithoautotrophy in the broader pelagic oceans (Aristegui et al., 2009; Swan et al., 2011) suggests that current models underestimate chemosynthesis and raise questions regarding ecological connections between plume and other pelagic environments, which we consider below.

## MICROBIAL COMMUNITIES IN DEEP-SEA HYDROTHERMAL PLUMES

Despite the well-recognized importance of microorganisms in the biogeochemistry of hydrothermal plumes, few studies have characterized microbial communities that inhabit them. Thus the physical source, taxonomic composition, and ecological nature of these organisms remain poorly understood. Potential sources of microbes for deep-sea hydrothermal plumes can be divided into three broad categories: (i) seafloor (or sub-seafloor) communities, (ii) background deep seawater communities, or (iii) growth *within* the plume (Figure 2). The traditional view is that plume microbes are likely sourced from highly productive biological communities that inhabit vent chimneys and surrounding areas (Winn et al., 1986). Such sources could also include bottom water that is heavily influenced by low-temperature diffuse flow (Kadko et al., 1990), which may be responsible for geochemical flux comparable to focused hydrothermal venting and contains microbes from the subsurface biosphere (Wankel et al., 2011; Akerman et al., submitted). Indeed, tracer studies indicate that diffuse flow and larvae of vent fauna can be entrained into plumes (Jackson et al., 2010). Alternatively, plume microbes could be derived primarily from ambient background seawater, which seems feasible given that plumes are a mix of >99% seawater and ~0.01% hydrothermal fluid (Lupton et al., 1985) and that benthic and pelagic habitats differ greatly (Zinger et al., 2011). Regardless of the original source of microbes, it is likely that plume communities are dynamic in time and space. Shifts in microbial community structure are to be expected as the geochemical environment of hydrothermal fluids evolves with plume age (i.e., become more dilute and oxidized). Consistent with this notion are observations of progressive removal of electron donors (Kadko et al., 1990) and morphological evidence of changes in microbial communities with plumes age (Cowen and Li, 1991). However, only recently has plume microbial diversity been sampled and analyzed with molecular tools in a spatially resolved manner.

Many studies have reported elevated microbial biomass and activity in plumes relative to background, suggesting that plume microbes are distinct from those in the ambient water column (Winn et al., 1986; Naganuma et al., 1989; Juniper et al., 1998; Maruyama et al., 1998; O'Brien et al., 1998; Lam et al., 2004; Lam et al., 2008; Dick et al., 2009). In one of the first applications of

molecular tools to deep-sea hydrothermal plumes, Sunamura et al. (2004) showed that the Suiyo Seamount hydrothermal plume is dominated by just two phylotypes, one group of *Gammaproteobacteria* and one group of *Epsilonproteobacteria*. Interestingly, both of these phylotypes were most closely related (at the time) to symbionts of hydrothermal vent animals – the *Gammaproteobacteria* to bivalve gill symbionts and the *Epsilonproteobacteria* to ectosymbionts of the tubeworm *Riftia pachyptila* and shrimp *Rimicaris exoculata* (Sunamura et al., 2004). The *Gammaproteobacteria*, designated “SUP05,” were also found to dominate low-temperature diffuse flow emanating from a bivalve-colonized mound (99% of cells; Sunamura et al., 2004), raising the possibility that microbial communities in the subsurface or animal symbioses are sources of plume microbes (see further discussion of links between plumes and symbionts below). Indeed, SUP05-like sequences have also been retrieved from diffuse hydrothermal fluids on the seafloor at the Juan de Fuca ridge (Huber et al., 2003; Bourbonnais et al., 2012; Anderson et al., 2013). However, recent rRNA gene surveys show that SUP05 are also widely distributed in pelagic environments, raising the question of whether the connection between plumes and subsurface is physical (i.e., transport only) or ecological (i.e., actively operating in similar niches in both environments) in nature. An extreme example of the physical transport of seafloor and/or subsurface material to the water column is “snowblower” vents that discharge elemental sulfur and bacterial filaments (Haymon et al., 1993; Crowell et al., 2008). Thermophilic microbes derived from the subsurface have also been observed in eruptive event plumes (Summit and Baross, 1998). *Epsilonproteobacteria* are also commonly encountered in vent seafloor environments (Nakagawa et al., 2005; Campbell et al., 2006; Zinger et al., 2011), again highlighting potential connections between the seafloor and plumes. Clear signals of *Epsilonproteobacteria* and other seafloor hydrothermal microbes have been observed in plumes at the Mid-Cayman Rise (German et al., 2010), in the Iheya hydrothermal field (Nakagawa et al., 2005), the Logatchev hydrothermal plume (Perner et al., 2013), and in descending particles from plumes at the East Pacific Rise, which are genetically distinct from surrounding seawater (Sylvan et al., 2012). Recent studies employing fine-scale phylogenetic approaches and coupled DNA and RNA approaches hold great promise for elucidating the niche space and distribution of sulfur-oxidizing *Gammaproteobacteria* and *Epsilonproteobacteria* in subsurface, seafloor, plume, and background environments. Anderson et al. (2013) noted partitioning of distinct clades of sulfur-oxidizing *Gammaproteobacteria* in vent environments (SUP05 in plumes and animal symbioses) versus others [Arctic96BD-19 in background and oxygen minimum zones (OMZs)] and noted that sulfide concentration likely controls the balance of *Gammaproteobacteria* versus *Epsilonproteobacteria*. Consistent with that view, coupled RNA and DNA analyses revealed showed that *Epsilonproteobacteria* are more active in the reducing environment of the subseafloor, whereas *Gammaproteobacteria* are more active at the seafloor where mixing with seawater is more prevalent (Akerman et al., submitted).

In contrast with the hypothesis that seafloor environments are the major source of plume biota, microbial communities in hydrothermal plumes at Guaymas Basin in the Gulf of California are distinct from those of the underlying seafloor habitats such

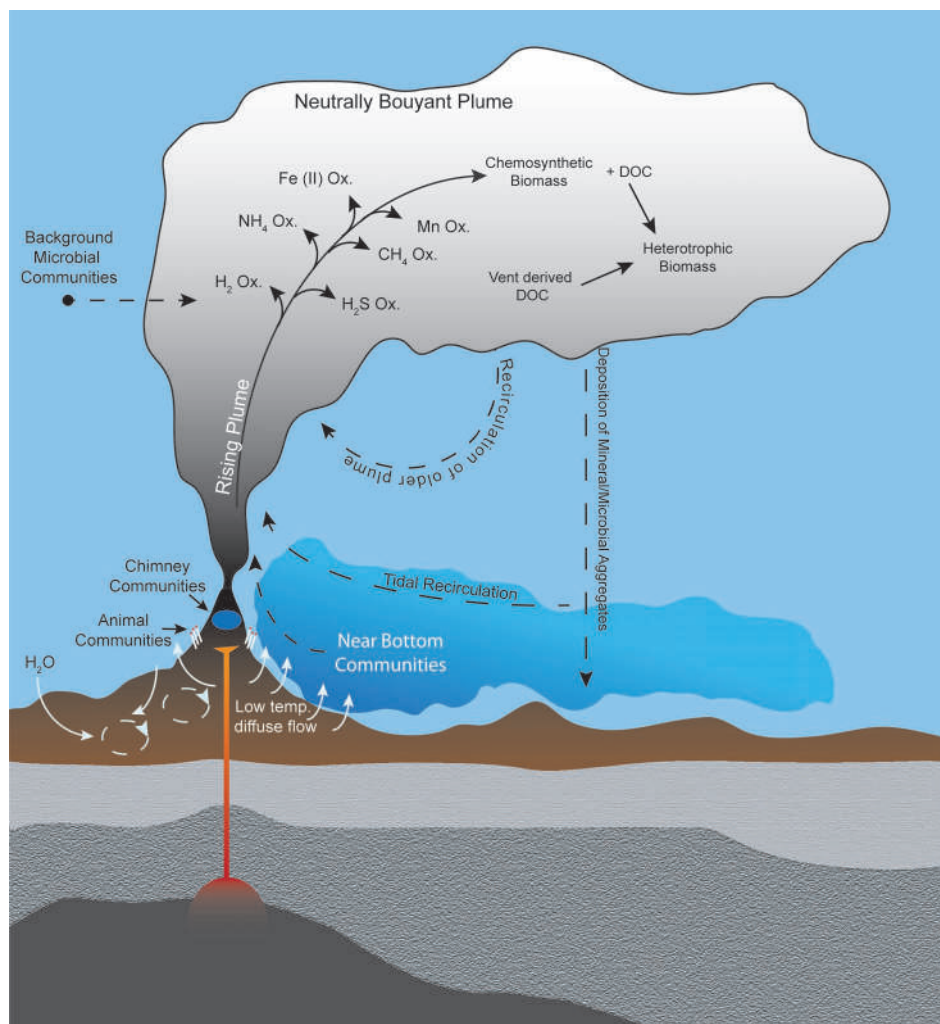


**FIGURE 2 | Potential sources of plume microorganisms include microbial communities in background seawater, vent chimneys, near-vent animal symbioses, subsurface environments, near-bottom waters, and recirculation of aged plumes.** Microbial growth within the plume also shapes the plume community, including utilization of hydrothermally sourced

electron donors for chemosynthesis as well as heterotrophic consumption of organic carbon produced chemosynthetically or hydrothermally. Hydrothermal plumes contain distinct regions (e.g., the rising plume and neutrally buoyant plume) with steep gradients of physical and chemical properties that likely hold distinct microbial communities.

as hydrothermal sediments or chimneys (Dick and Tebo, 2010). Rather, Guaymas Basin plume communities closely resemble those from background seawater samples taken just above the plume or in the neighboring Carmen Basin, which is 100 km away and does not host hydrothermal activity. Metagenomic and metatranscriptomic data further reinforces the plume–water column connection, showing that the metabolically active microbes in Guaymas plumes are pelagic rather than benthic in nature, and suggesting an ecological boundary between seafloor and plume (Lesniewski et al., 2012). These studies interpreted the above-plume and Carmen Basin samples as true background communities, and this is supported by the absence of detectable physical and chemical tracers of hydrothermal activity in those samples. However, another possibility is that this deep seawater surrounding Guaymas Basin is impacted by microbes that are exported from the highly productive chemoautotrophic plumes. Processes that could

facilitate export include ascending and descending particles and migratory zooplankton (Cowen et al., 2001), buoyant transparent exopolymeric substances (Shackelford and Cowen, 2006; Prieto and Cowen, 2007), and large scale advection such as mesoscale eddies (Adams et al., 2011). Regional influence of vents on deep-sea microbial communities may be particularly important in the Gulf of California, where restricted basins could limit dispersal of plumes and mixing with true non-hydrothermally-impacted seawater. We will re-visit the potential impact of hydrothermal plumes on the broader deep oceans below.

## ECOLOGICAL AND BIOGEOGRAPHIC LINKAGES BETWEEN HYDROTHERMAL PLUMES AND OTHER MARINE HABITATS

There is growing recognition that chemical species that fuel microbial growth in hydrothermal plumes ( $H_2$ , various sulfur species, ammonium, and iron) also support microbial growth in

marine environments well beyond hydrothermal systems, including OMZs, oil spills, and cold seeps (Paull et al., 1984; Lösekann et al., 2007; Tavormina et al., 2008, 2010; Redmond et al., 2010), whale falls (Baco and Smith, 2003; Tringe et al., 2005; Gofredi and Orphan, 2010), and within microenvironments of organic-rich particles in the oxic water column (Karl et al., 1984; **Figure 3**). Indeed, recent molecular surveys show that microorganisms that are abundant in deep-sea hydrothermal plumes are also abundant in these other marine habitats. SUP05 and another group of uncultivated putative sulfur-oxidizing bacteria, SAR324 *Deltaproteobacteria*, are abundant in OMZs, where they play important roles in linking the sulfur and nitrogen cycles (Lavik et al., 2009; Walsh et al., 2009; Canfield et al., 2010; Stewart et al., 2012; Wright et al., 2012). These two groups have also been identified in the dark pelagic oceans (e.g., Swan et al., 2011; Ghiglione et al., 2012). In addition, methanotrophic populations and functional genes for methane oxidation (particulate methane monooxygenase; *pMMO*) that are prevalent in the Guaymas Basin hydrothermal plume are closely related to those in plumes of the Deepwater Horizon oil spill (Lesniewski et al., 2012; Li et al., unpublished). Cultures also support connections between plumes and other marine environments; close relatives of the Mn(II)-oxidizing alphaproteobacterium SI85-9A1 (>99% 16S rRNA gene sequence identity), which was originally isolated from the Saanich Inlet oxic/anoxic interface (Dick et al., 2008), have been isolated from the surface of *Alvinella pompejana* tubeworms at 9°N East Pacific Rise (Anderson et al., 2009), and from plumes of the Lau

Basin. Finally, *Halomonas* and *Marinobacter* species detected in hydrothermal plumes are present throughout the oceans (Kaye and Baross, 2000, 2004; Kaye et al., 2011). Hence, plume ecological niches and the microorganisms that fill them appear to be widespread in the oceans, and understanding their distribution is paramount for understanding the dispersal of plume microorganisms, the “inoculation” of plumes with microbes from background seawater, and ultimately for understanding the distribution and abundance of chemoautotrophy throughout the global oceans. Below we focus on comparisons of plumes to OMZs and seafloor environments.

### CONNECTIONS TO OXYGEN MINIMUM ZONES

Oxygen minimum zones are widely distributed in the oceans and are expanding due to anthropogenic global change (Wyrtki, 1962; Stramma et al., 2008; Wright et al., 2012). Reduced O<sub>2</sub> concentrations favor alternative terminal electron acceptors, the products of which drive chemoautotrophic metabolisms. Hence, microbial metabolisms that take advantage of redox gradients mediate OMZ biogeochemistry and contribute significantly to the global cycling of nitrogen and greenhouse gasses (Wright et al., 2012). OMZs in which the concentration of O<sub>2</sub> falls below 20 μM, a threshold below which some anaerobic metabolisms operate (Kalvelage et al., 2011; Ulloa et al., 2012), overlap geographically with the mid-ocean ridge system, especially in the Eastern Pacific (**Figure 1**). Although OMZs and deep-sea hydrothermal vent plumes are typically separated vertically by 1500 m or more, communication

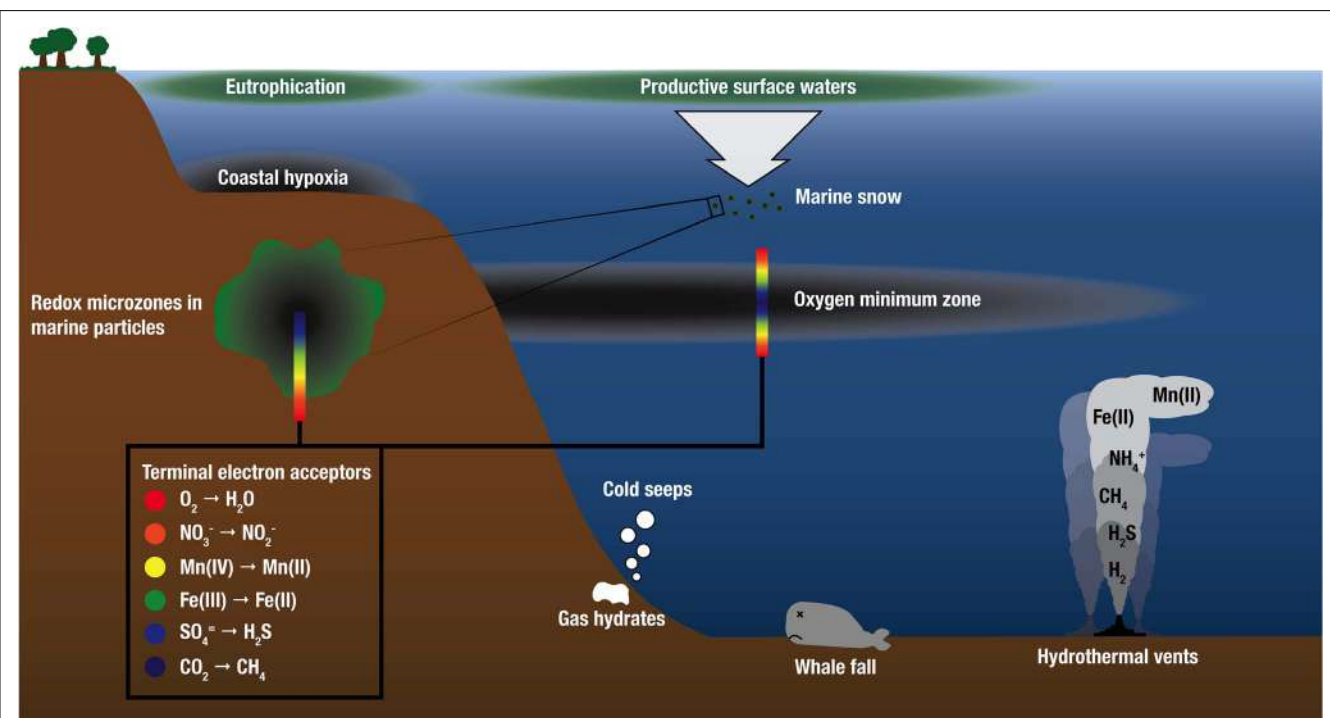


**FIGURE 3 |** Schematic water column profile showing selected marine habitats that are sources of electron donors for chemosynthetic growth and support microbial communities similar to those found in deep-sea hydrothermal plumes. Electron donors for

microbial growth are supplied by geothermal sources at deep-sea vents and as the products of anaerobic microbial respiration in low-O<sub>2</sub> environments. OMZ and redox schematics after Wright et al. (2012).

between these habitats likely occurs via sinking particles. Whereas nitrogen cycling was classically thought to dominate the microbial ecology and metabolism of OMZs, cryptic sulfur cycling has also been recently demonstrated in the Eastern Tropical South Pacific OMZ (Canfield et al., 2010). Such cryptic sulfur cycling occurs when sulfide produced by sulfate reduction is rapidly oxidized back to sulfate. Though easily overlooked by chemical methods, numerous reports of abundant sulfur-oxidizing autotrophs in OMZs (Stevens and Ulloa, 2008; Lavik et al., 2009; Walsh et al., 2009) and even in oxic waters (Swan et al., 2011) suggest that this process may be widespread in the broader oceans.

To evaluate potential connections between the microbial ecology of deep-sea hydrothermal plumes and other marine environments, we compared the most abundant microbial groups across a variety of pelagic and benthic habitats including both oxic and anoxic as well as hydrothermal and non-hydrothermal environments (Figure 4). Although there are obviously a variety of environmental and biogeographic factors that shape microbial community structure in these diverse habitats, there are some striking similarities in terms of the organisms that dominate. SUP05 are among the most abundant microbial groups in the Guaymas Basin and Suiyo Seamount hydrothermal plumes, Saanich Inlet and ETSP OMZs, and in coastal waters of the Benguela upwelling zone off Namibia (Lavik et al., 2009). SUP05 are also found at appreciable abundance in the OMZ of Guaymas Basin (Anantharaman et al., 2013) and in the Black Sea redoxcline (Fuchsman et al., 2011). The SAR324 group of *Deltaproteobacteria*

(also known as the Marine Group B), which has recently been implicated in hydrocarbon and sulfur metabolism and autotrophy (Swan et al., 2011; Li et al., unpublished; Sheik et al., unpublished), is also abundant in widespread environments (Figure 4). It should be noted there is considerable diversity within these important groups, which likely reflects specific ecological adaptations. For example, there are clades of SAR324 that appear to be specific to Saanich Inlet (Wright et al., 2012), and there is plasticity of electron donors and acceptors within the SUP05 (Anantharaman et al., 2013). Enigmatic groups such as SAR406, SAR86, and Arctic97B-4 also exhibit similar distributions to those of SAR324 and SUP05 and further highlight the links between deep-ocean and pelagic environments.

#### PLUMES AS DISPERSAL VECTORS FOR VENT MICROBES, SYMBIOTS, AND LARVAE

Hydrothermal plumes entrain both focused and diffuse hydrothermal fluids and thus are potential dispersants of vent-associated organisms (Jackson et al., 2010). Indeed, vent-associated larvae have been observed in plumes (Mullineaux et al., 1995), where they are likely transported great distances to colonize vent sites (Mullineaux et al., 2010). As discussed previously (Dick and Tebo, 2010; Lesniewski et al., 2012), the microbial community of the Guaymas Basin hydrothermal plume is clearly distinct from seafloor communities (Figure 4). Despite this ecological boundary between hydrothermal seafloor and plume habitats, hydrothermal plumes could play a key role in the dispersal of seafloor

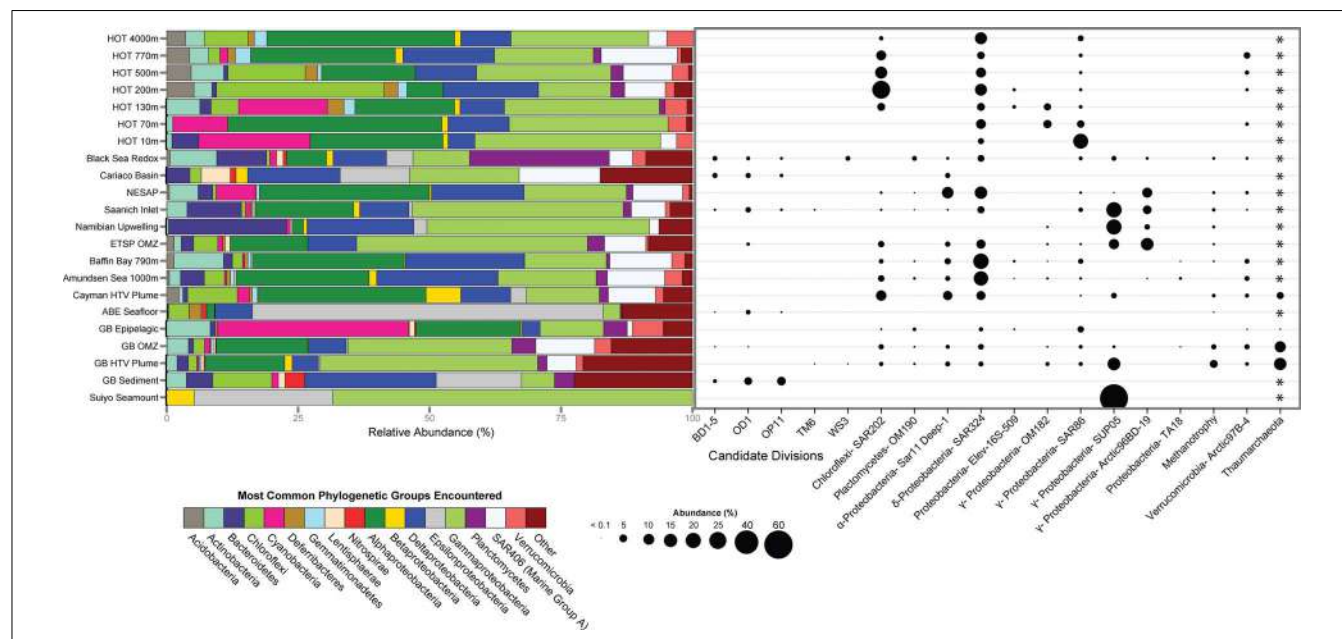


**FIGURE 4 | Microbial community structure and abundance of key populations in plumes and other marine habitats.** 16S rRNA gene clone and pyrosequencing reads were downloaded from Genbank or VAMPS ([vamps.mbl.edu](http://vamps.mbl.edu)) repositories and classified to the Silva v. 111 database (Quast et al., 2013) using the Mothur software package (Schloss et al., 2009). Sequences were taken from: Hawaii Ocean Time Series (HOT; Pham et al., 2008), Black Sea (Fuchsman et al., 2011), Cariaco Basin (Madrid et al., 2001), Northeast Subarctic Pacific (Wright et al., 2012), Saanich Inlet (Walsh et al.,

2009), Namibian upwelling zone (Lavik et al., 2009), Eastern Tropical South Pacific OMZ (ETSP; Stevens and Ulloa, 2008), Baffin Bay and Amundsen Sea (Ghiglione et al., 2012), Mid-Cayman Rise hydrothermal vent plume (German et al., 2010), ABE hydrothermal vent seafloor at Lau Basin (Flores et al., 2012), Guaymas Basin (Anantharaman et al., 2013), Guaymas Basin Sediment (Teske et al., 2002), and Suiyo Seamount (Sunamura et al., 2004). \*Primer sets used were bacterial specific and did not allow for comparison of Archaea.

hydrothermal organisms such as hydrothermal sediment and chimney-associated microbes. Consistent with this notion, deep sequencing of 16S rRNA genes from Guaymas Basin (Anantharaman et al., 2013) revealed the presence, albeit at low abundance, of candidate division bacteria that are common in seafloor hydrothermal environments (**Figure 4**). To our knowledge, this represents the first evidence of seafloor microbes in the rare portion of the plume microbial community at a chronic vent site [they have been detected previously in eruptive event plumes (Summit and Baross, 1998)], and suggests that plumes could indeed be an important mechanism of dispersal of deep-sea vent organisms.

Potential connections between free-living microbes in plumes and symbionts of hydrothermal vent animals have long been recognized, but views on the nature of this relationship are evolving. The similarity of free-living SUP05 in plumes to symbionts was noted with the original discovery of SUP05 (Sunamura et al., 2004). More recently, plume SUP05 were found to have and express genes for H<sub>2</sub> oxidation (Anantharaman et al., 2013) that are highly similar to those of bathymodiolin mussel symbionts at deep-sea vents (Petersen et al., 2011), and symbiont-like methanotrophs were detected in the Guaymas Basin hydrothermal plume (Li et al., unpublished). The traditional view of these microbial symbionts is that they evolved from free-living ancestors to form a few distinct symbiont clades. However, recent analysis shows that symbionts are phylogenetically interspersed with free-living forms of the bacteria, suggesting numerous evolutionary transitions between symbiotic and free-living forms (Petersen et al., 2012). Furthermore, horizontal gene transfer has been implicated as a significant mechanism of metabolic evolution of the symbionts (Kleiner et al., 2012). Bathymodiolin symbionts are thought to be transmitted horizontally and acquired by each generation from the environment (Petersen et al., 2012), and the relatively low diversity of symbionts within animal populations suggests that the animals carefully select symbionts from the pool of diversity present within free-living communities. However, the mechanisms by which this selection takes place, the degree to which symbionts and free-living populations are genetically and ecologically distinct, and the time scales over which transitions between free-living and symbiotic lifestyles occur all remain intriguing frontiers for understanding the relationship between animal symbionts and free-living plume microorganisms.

### THE INFLUENCE OF BENTHIC AND PELAGIC HABITATS ON PLUME MICROBIAL COMMUNITIES

What controls the relative contribution of benthic versus pelagic microbes to plume microbial communities? Although the limited data on microbial communities in plumes provides few answers, there are some preliminary clues. Both physical and biological factors likely play a role in determining the balance of seafloor versus water column microbes in plumes. Physical factors include (i) the fluid flux and entrainment rate of the rising plume, (ii) the properties and habitability of the near-vent environment that could potentially be entrained, such as temperature and material properties (e.g., hard substrate versus easily transported sediments or biological material such as biofilms or dense animal communities), (iii) bathymetry of the seafloor surrounding the vent environment [e.g., bathymetric highs lead to rapid dilution

and dispersal whereas restricted volumes such as Guaymas Basin or the Suiyo Seamount caldera tend to accumulate hydrothermal chemistry and biota (German and Von Damm, 2004)], and (iv) the bioenergetic potential of plume geochemistry (i.e., high concentration of energy-rich electron donors is more likely to support a seafloor-derived community in the plume). Biological factors that influence the balance of seafloor versus water column microbes likely hinge on the properties of the water mass in which venting takes place, including the cell density and the structure of the community with regard to metabolic potential. Denser microbial communities and those that hold a large portion of organisms able to utilize inorganic electron donors for lithotrophic growth will promote a greater water column contribution to plume microbial communities. Finally, the microbial growth response to temperature likely influences the degree to which seafloor microbes are metabolically active in hydrothermal plumes. Thermophiles or hyperthermophiles are unlikely to be metabolically active in cold hydrothermal plumes, whereas mesophiles or psychrophiles from lower-temperature seafloor habitats may indeed remain active at plume temperatures.

### METABOLIC AND FUNCTIONAL LINKAGES BETWEEN PLUMES AND OTHER MARINE HABITATS

Recent reports of genomic and metabolic plasticity within microbial groups such as SUP05 (Anantharaman et al., 2013) underscore the need to use caution when inferring microbial metabolism and function from 16S rRNA genes of plume populations, even at fine phylogenetic scales. On the other hand, the emergence of random shotgun metagenomic and metatranscriptomic approaches, driven by rapidly increasing throughput and decreasing costs of DNA sequencing, provides new opportunities to directly assess microbial metabolism and its effect on biogeochemistry in deep-sea hydrothermal plumes. Lesniewski et al. (2012) used a parallel metagenomic and metatranscriptomic approach to show that ammonium, methane, and sulfur are the primary energy sources in the Guaymas Basin hydrothermal plume. Genomes and transcriptomes of abundant microbial groups were subsequently reconstructed to reveal the genetic potential and expression of specific microbial populations (Baker et al., 2012; Anantharaman et al., 2013; Li et al., unpublished; Sheik et al., unpublished). Comparison of these large 'omics datasets to those from other marine environments provides a view of the dynamics of both community-wide functions and specific microbial groups across distinct settings, and potentially provides powerful insights into the factors that govern microbial and ecosystem functions in the deep sea.

We analyzed the abundance of key functional genes in shotgun sequencing datasets from recent studies of the Guaymas Basin hydrothermal plume (Lesniewski et al., 2012), the Deepwater Horizon oil spill (Goldstamp Gm00382, IMG TaxonID 2149837026), the Eastern Tropical Pacific OMZ (Stewart et al., 2012), and the North Pacific subtropical gyre (DeLong et al., 2006; **Figure 5**). This data shows that functional genes for oxidation of nitrogen, sulfur, hydrogen, and hydrocarbons that are highly expressed in the Guaymas Basin hydrothermal plume are also widely present and expressed in these other disparate marine habitats (**Figure 5**). Genes for ammonia oxidation are abundant

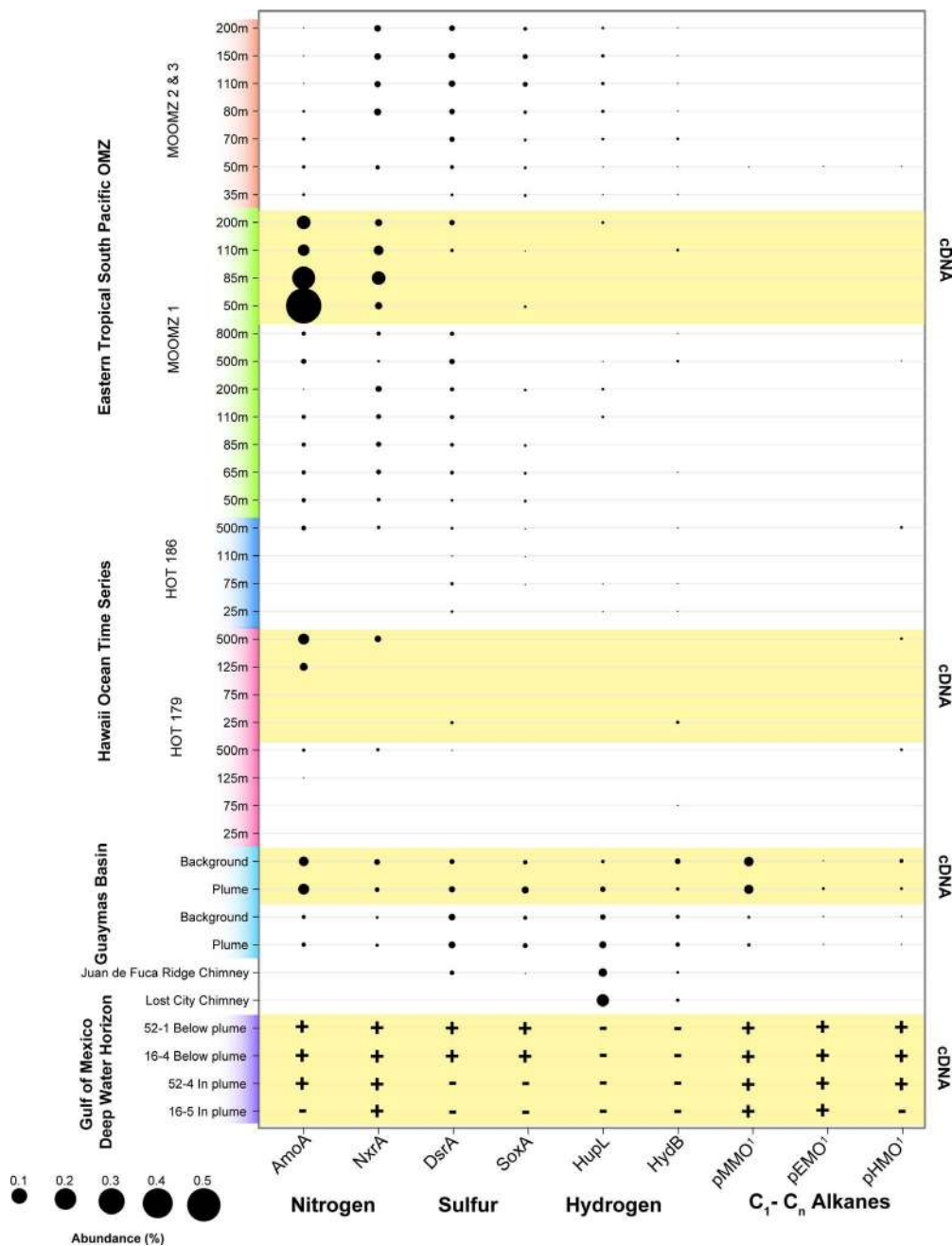


**FIGURE 5 | Abundance of functional genes and transcripts for oxidation of selected nitrogen, sulfur, hydrogen, and hydrocarbon species in the following samples and studies: Eastern Tropical South Pacific OMZ (Stewart et al., 2012), Hawaii Ocean Time Series (DeLong et al., 2006), Guaymas Basin plumes and background (Lesniewski et al., 2012), and Deepwater Horizon oil spill (Goldstamp Gm00382, IMG TaxonID 2149837026).** Metagenomic sequences from these studies were used as queries with BLASTX against databases containing the following sequences: AMO – ammonia monooxygenase subunit A (from both ammonia-oxidizing archaea and bacteria); Nxr – nitrite oxidoreductase subunit A; DsrA – dissimilatory sulfite reductase subunit A; SoxA – sulfur oxidation protein subunit A; HupL and HydB – group 1 membrane-bound Ni,Fe hydrogenase, large subunit; pMMO – particulate methane monooxygenase subunit A; pEMO – putative particulate ethane monooxygenase subunit A, includes sequences from Methylococcaceae

bacterium species ET-HIRO (AB453962 and AB453963) and ET-SHO (AB453960 and AB453961), and environmental sequences (Redmond et al., 2010; Li et al., unpublished; SAR324\_pHMO: putative C<sub>2</sub>-C<sub>4</sub> alkane oxidizing monooxygenase subunit A, contains sequences from SAR324\_J09 (Swan et al., 2011) and Guaymas Basin SAR324 (Li et al., unpublished; Sheik et al., unpublished). BLASTX bit scores >50 were considered positive matches. Abundance of sequence reads recruiting to each functional gene is shown as a percentage of total (putative) mRNA-containing cDNAs. rRNA were identified using Ribopicker [Version 0.4.3 (Schmieder et al., 2012)] with the comprehensive Ribopicker database “rnadb” and removed from all datasets. The absence of data for samples simply indicates that it was not identified at the sequencing depth and does not necessarily imply the absence of genes/transcripts. Note that due to novelty of sequences, in some cases the pathway and substrate specificity are uncertain.

and highly expressed in nearly all datasets analyzed here except for surface waters of the ALOHA station, consistent with the widespread abundance of ammonia-oxidizing Archaea (Karner et al., 2001; Francis et al., 2005), specific populations of which are stimulated in the ammonium-rich hydrothermal plumes of Guaymas Basin (Baker et al., 2012). NXR (nitrite oxidoreductase) genes for nitrite oxidation (Lucker et al., 2010; Baker et al., 2013) were recovered from many of the datasets, especially OMZs. However, this result should be interpreted with caution given the novelty of NXR genes; it is difficult to distinguish the forms utilized by nitrite-oxidizing bacteria versus anaerobic ammonia oxidation (anammox) bacteria (Strous et al., 2006). Thus, we suspect that a significant fraction of NXR hits in the OMZ are from genes involved in anammox. Sulfur oxidation systems (*sox* and *dsr* genes) are most prevalent in the Guaymas Basin hydrothermal plume and in the OMZ cores, but they are also detectable in Guaymas Basin background and in some samples in the oxic water column at HOT (Hawaii Ocean Time Series). These sulfur oxidation genes are present in all metatranscriptomes of the Guaymas Basin, but only in a subset of those from the Gulf of Mexico, HOT, and ETSP OMZ. These results, especially expression of sulfur oxidation genes in oxic waters (HOT), are consistent with widespread cryptic geochemical cycling of sulfur (Canfield et al., 2010), perhaps in association with organic-rich particles (Karl et al., 1984; Wright et al., 2012). H<sub>2</sub> oxidation genes are less widely distributed, but are most prevalent in ultramafic vent chimney samples (Brazelton et al., 2012) and in the Guaymas Basin hydrothermal plume, consistent with H<sub>2</sub> being sourced primarily from hydrothermal fluids and being rapidly utilized in plumes (Kadko et al., 1990). However, H<sub>2</sub> oxidation genes were also detected in some OMZ, ALOHA, and background Guaymas samples (Anantharaman et al., 2013), consistent with H<sub>2</sub> production in association with organic-rich particles in the oxic water column also being a substantial source of H<sub>2</sub> as predicted decades ago (Karl et al., 1984).

Utilization of methane and other hydrocarbons as an energy source represents another potential connection between hydrothermal plumes and other marine microbial habitats. The capability of naturally occurring marine microbes to consume hydrocarbons has recently been highlighted by the Deepwater Horizon disaster (Mason et al., 2012). While the connections need further investigation, natural sources of hydrocarbons in the deep sea (Jorgensen and Boetius, 2007) such as hydrocarbon seeps, hydrothermal vents, or *in situ* water column production (Karl et al., 2008) may prime deep ocean microbial communities for hydrocarbon degradation. Guaymas Basin hydrothermal fluids have unusually high concentrations of methane due to interaction with sediments that overlay the ridge. High methane concentrations are also found at the Endeavour Segment of the Juan de Fuca ridge (De Angelis et al., 1993), and ultramafic systems on the Mid-Atlantic Ridge (Charlou et al., 1998) and the Mid-Cayman Rise (German et al., 2010). The imprint of methane is clearly apparent in microbial communities of the Guaymas Basin hydrothermal plume; genes for pMMO are among the most abundant mRNAs represented in the metatranscriptome (Lesniewski et al., 2012). Recent work shows that there is extensive diversity of pMMOs and related Cu membrane monooxygenases at Guaymas, and that they affiliate phylogenetically with enzymes involved

in C<sub>2</sub>–C<sub>4</sub> alkane oxidation (Li et al., unpublished). We refer to these methane, ethane, and butane monooxygenases collectively as particulate hydrocarbon monooxygenases (pHMOs). pHMOs are also present in the metatranscriptome of the Deepwater Horizon oil spill (Mason et al., 2012; Li et al., unpublished) and in a few samples from station ALOHA (Figure 5). pHMOs were only detected at low levels in a few of the shotgun sequencing datasets, but they have been reported to be abundant in OMZs off Costa Rica (Tavormina et al., 2013).

## COMPARATIVE METATRANSCRIPTOMICS OF POPULATIONS IN PLUME AND BACKGROUND: SUP05 AND Thaumarchaeota

One of the remarkable conclusions emerging from comparison of different interfacial redox environments in the oceans is that the same microbial groups often dominate disparate environmental settings. For example, despite marked environmental differences between deep-sea hydrothermal plumes and OMZs (e.g., depth, temperature, pressure, nutrient availability, water mass history, quantity, and quality of DOC and POC), they share several of the most abundant microbial populations, including SUP05, SAR324, and *Thaumarchaea* (Figure 4). The nature of these two oxic/anoxic interfaces is quite different: in plumes, reduced chemicals are injected into an oxic water column, whereas in OMZs, reduced chemical species are produced through anaerobic microbial respiration of organic carbon. However, many of the microbial players appear to be the same, indicating that these organisms thrive at redox interfaces regardless of differences in other environmental parameters described above.

Recent metatranscriptomic studies (Baker et al., 2012; Lesniewski et al., 2012; Stewart et al., 2012; Anantharaman et al., 2013) permit detailed views of the gene expression patterns of these microbial groups and their roles in biogeochemistry. Comparison of transcripts from OMZ and Guaymas Basin plume/background samples recruited to SUP05 and *Thaumarchaea* genomes shows that the overall patterns of transcript abundance are quite similar between the two environments (Figure 6). Indeed, the differences between samples *within* each environment (plume versus background at Guaymas, different depths of the OMZ) appear to be as significant if not greater than differences between environments. For *Thaumarchaea*, acquisition of ammonium and oxidation of ammonia dominate the metatranscriptome in both environments. Conserved hypothetical proteins of unknown function are similarly highly expressed in both environments, highlighting large gaps in our knowledge of what are likely critical functions for these organisms. In addition to obtaining ammonia directly from the environment, uptake of urea also appears to be an important source of ammonia for both populations (Figure 6). Utilization of urea has now been noted for *Thaumarchaeota* in diverse settings such as sponge symbionts (Hallam et al., 2006), soil (Tourna et al., 2011), polar waters (Alonso-Saez et al., 2012), and surface waters of the Gulf of Maine (Tully et al., 2012).

Like *Thaumarchaea*, transcript abundance profiles of SUP05 show striking similarities in the genes that are most highly expressed in plumes and OMZs (Figure 6B). Many of the highly expressed genes are involved in cell maintenance and growth (e.g., translation and DNA replication), which is expected in any

environment. However, similarly high transcript abundance of other genes likely reflects common interactions between SUP05 and the two different environments. Ammonium transporters were the most highly expressed genes in all OMZ and plume samples except the 200 m depth of the OMZ. A predicted ABC (ATP-binding cassette) transporter for amino acids is expressed in all samples, but it appears to be most abundant in the deep sea.

SUP05 potentially plays an important role in linking the sulfur and nitrogen cycles by coupling the oxidation of reduced sulfur species to the reduction of nitrate or nitrite (Walsh et al., 2009; Canfield et al., 2010). Perhaps the most intriguing difference between plume and OMZ transcript profiles is that the

*soxA* gene for sulfur oxidation is highly expressed in plumes but not in deep background waters or the OMZ. This suggests a difference in the form of sulfur used by SUP05 in plumes versus OMZs; abundant *soxA* transcripts point to thiosulfate oxidation in plumes, whereas free sulfide may be the preferred substrate in OMZs, as hypothesized by Walsh et al. (2009). Additional differences between populations of SUP05 include diversity in terms of electron donors and acceptors. SUP05 at the Saanich Inlet oxic/anoxic interface were described as anaerobes (Walsh et al., 2009), but SUP05-related symbionts appear to be aerobic (Kuwahara et al., 2007; Newton et al., 2007), and those in the Guaymas Basin plume are primarily aerobic (Anantharaman et al., 2013). Guaymas Basin SUP05 also have genes for H<sub>2</sub> oxidation that do

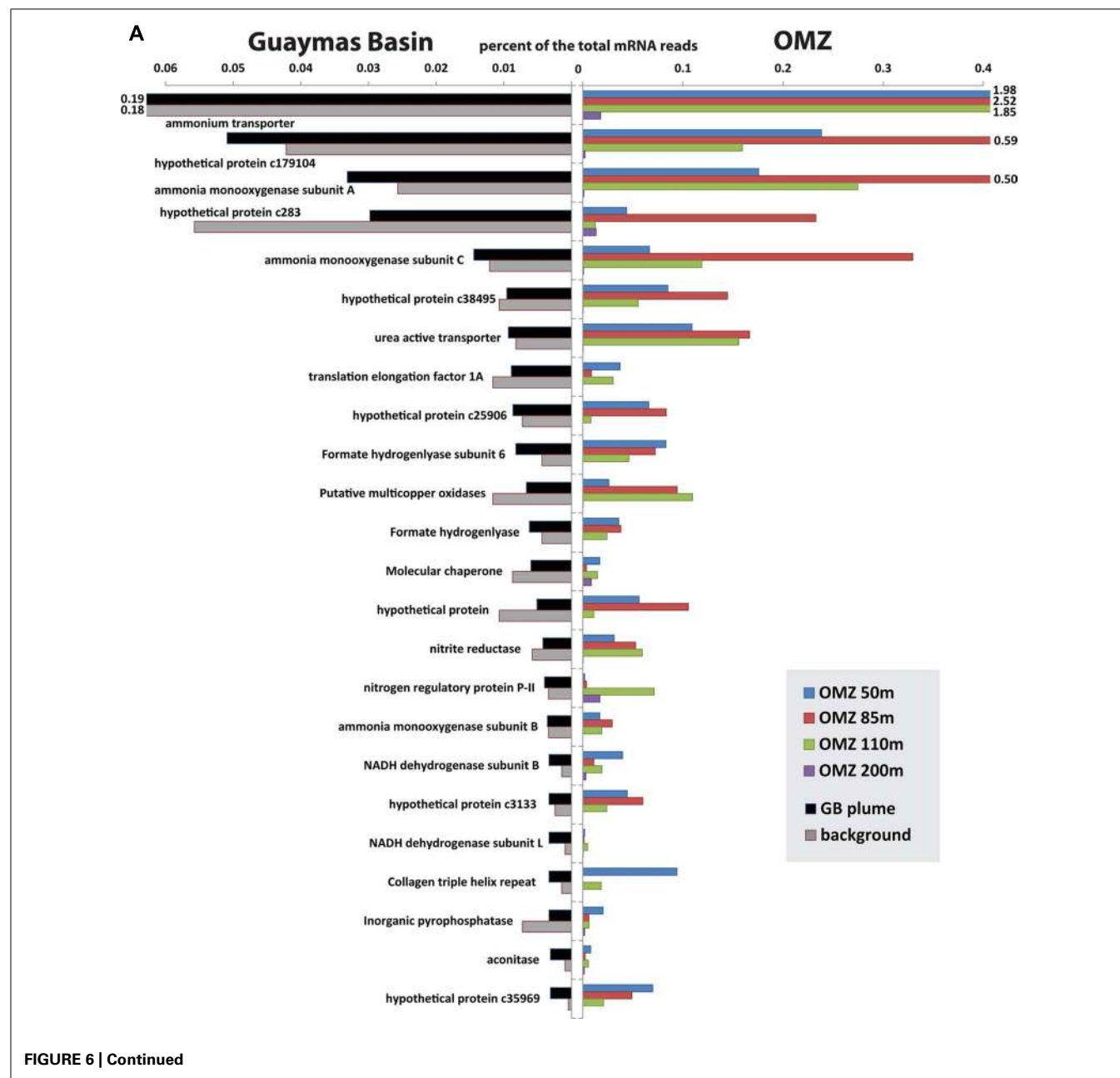
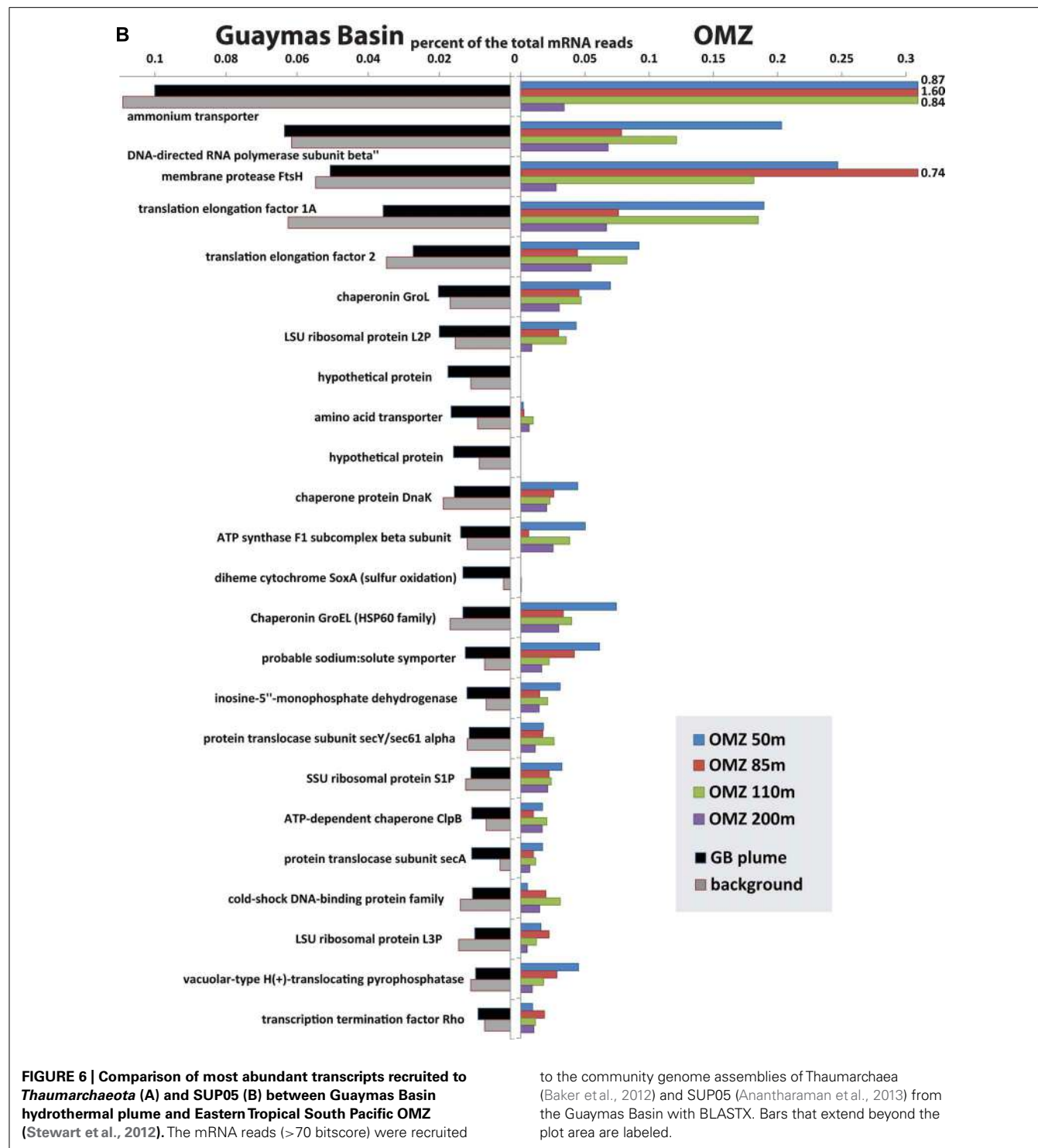


FIGURE 6 | Continued



**FIGURE 6 | Comparison of most abundant transcripts recruited to Thaumarchaeota (A) and SUP05 (B) between Guaymas Basin hydrothermal plume and Eastern Tropical South Pacific OMZ (Stewart et al., 2012). The mRNA reads (>70 bitscore) were recruited**

to the community genome assemblies of Thaumarchaeota (Baker et al., 2012) and SUP05 (Anantharaman et al., 2013) from the Guaymas Basin with BLASTX. Bars that extend beyond the plot area are labeled.

not appear to be present in other populations (Anantharaman et al., 2013).

### THREE BIG QUESTIONS FOR THE FUTURE OF DEEP-SEA HYDROTHERMAL PLUME MICROBIOLOGY

The recent explosion of new data on deep-sea microbial communities has revealed connections between deep-sea hydrothermal

plumes and other marine habitats. These insights raise intriguing new questions regarding the roles of deep-sea hydrothermal systems in the chemistry and biology of the broader oceans. At the same time, revolutionary technological advances provide new opportunities to address these questions. One exciting future goal is to define how the interplay between microbiology and geochemistry in hydrothermal plumes extends to global-scale interactions

between mid-ocean ridges and deep-sea microbiology. The global mid-ocean ridge hosts geochemically diverse hydrothermal systems. This geochemical diversity is tied to geological differences in the underlying host rock of hydrothermal systems, which shapes the quantity and types of metabolic energy available for chemoautotrophic growth in hydrothermal plumes (Amend et al., 2011). Indeed, vents show the highest variability in biodiversity of all marine systems (Zinger et al., 2011). Although microbial growth in plumes is predicted to be significant for carbon budgets in the deep oceans (McCollum, 2000), several first-order questions remain poorly constrained and need to be addressed.

### WHAT SHAPES THE STRUCTURE OF MICROBIAL COMMUNITIES IN DEEP-SEA HYDROTHERMAL PLUMES?

As we have seen, hydrothermal plume communities are composed of microbes from both seafloor and pelagic environments, and while data is scarce, the balance between these two sources appears to be variable and depends on both physical and biological factors. In addition to external contributions, chemoautotrophic growth *within* plumes likely contributes to the plume microbial community. Hence, the structure of communities in deep-sea hydrothermal plumes is shaped by both the geochemistry of the seafloor hydrothermal system (which shapes seafloor microbial communities and the energy available for growth in plumes) and the composition of communities in the surrounding water column. Microbial biogeography in the deep oceans is largely controlled by deep-sea circulation (Ghiglione et al., 2012) and hydrography (Galand et al., 2010), thus if the contributions from surrounding seawater are significant, then the geographic location of vents along the global deep conveyor belt of circulation could be an important determinant of plume community composition. Determining the relative importance of vent geochemistry and geography in shaping the community structure of plumes should be possible by tracking microbial diversity along local gradients of vent geochemistry in locations such as the Eastern Lau Spreading Center (Tivey et al., 2012). Expanded sampling and characterization of microbial communities in geographically widespread plumes in the broader deep sea will also be critical to evaluate biogeographic characteristics of deep-sea hydrothermal plumes.

### DO HYDROTHERMAL PLUMES INFLUENCE THE DIVERSITY OF DEEP-SEA MICROBIAL COMMUNITIES ON A GLOBAL SCALE?

So far we have focused on the contribution of background deep-sea microbes to plumes, but the interaction between communities in these two environments may in fact be bi-directional. Cell count data and thermodynamic modeling indicate that deep-sea hydrothermal plumes are productive environments compared to surrounding deep waters, and several studies have suggested that vents influence deep-sea microbial communities in their vicinity (Moyer et al., 1998; Takai et al., 2004). Active venting occurs in every ocean basin at over 1000 vent fields globally (Beaulieu et al., 2012), and surface-generated mesoscale eddies potentially transport hydrothermal plumes long distances (Adams et al., 2011). Although dispersion of plumes may be largely constrained by the ridge axis (Speer et al., 2003) or confined to a narrow corridor 10 km to either side of the ridge axis (German and Von

Damm, 2004), deep-sea microbial communities are relatively stable (Ghiglione et al., 2012), so microbes exported from plumes could persist for long periods of time. Clearly there is potential, but to what extent does chemoautotrophic growth in plumes influence the broader deep oceans? The answer is poorly constrained, but given recent insights into cryptic chemoautotrophy throughout the oceans, the nature of potential influence takes on new meaning. Rather than being unique oases of chemoautotrophy in the oceans, perhaps vents should be viewed as one of many potential sources of electron donors that collectively maintain widespread chemoautotrophy in the oceans. Advances in thermodynamic-bioenergetic modeling of plumes on a global scale, incorporation of this data into ecological models, and evaluation of the results with experiments and observations provides great promise for addressing this question. Finally, even if the answer is that plumes do not influence broader deep-sea microbial communities, the value of deep-sea hydrothermal plumes as natural laboratories to examine the response of deep-sea microorganisms to diverse geochemical perturbations should not be ignored.

### HOW DOES MICROBIAL ACTIVITY IN DEEP-SEA HYDROTHERMAL PLUMES IMPACT CARBON BUDGETS OF THE DEEP OCEANS?

The deep oceans hold the largest reservoir of rapidly exchangeable inorganic carbon on the Earth's surface. Microbial autotrophy potentially converts dissolved inorganic carbon into the organic phase within the biota. Subsequent grazing and viral predation transfer this carbon through the food chain or into the dissolved organic carbon pool. Although plume autotrophy likely has a negligible impact on the dissolved inorganic carbon inventories over global and short-term scales, its impact on organic carbon in the deep sea, especially on regional spatial scales, is potentially significant. In particular, the possibility that microbial autotrophy, heterotrophy, and/or lysis in hydrothermal plumes contribute to a significant conversion of inorganic matter to refractory organic matter, and thus sequestration of carbon as a component of the "microbial carbon pump" (Jiao et al., 2010), has not been explored in any detail. Improved measurements of plume microbial carbon fixation rates and studies of the fate of that carbon are required to evaluate this possibility. Another important but understudied aspect of microorganisms in deep-sea hydrothermal plumes is their role in modulating the flux of hydrocarbons from the seafloor through the water column and into the atmosphere (Orcutt et al., 2011). Future investigation on the interrelationship between plume microbial activity and hydrocarbon degradation will provide a better understanding of the impact of hydrothermal plume microbial activity on deep ocean carbon cycling.

Although this review has focused on hydrothermal plumes from high-temperature venting along the mid-ocean ridges, it should also be noted that low-temperature venting, including ridge-flank circulation, also likely contributes significantly to the processes described here. In fact, some estimates suggest that low-temperature ridge flank systems drive fluxes of fluid, heat, and solutes that are larger than those from high-temperature hydrothermal systems (Wheat and Mottl, 2000; Fisher and Harris, 2010). The microbial biogeochemistry of such systems is poorly known, but (McCarthy et al., 2011) showed that chemosynthesis

by crustal microbial communities is a major source of dissolved organic carbon in ridge-flank and on-axis hydrothermal fluids sampled from the Juan de Fuca Ridge. Thus ridge-flank systems likely amplify the contributions of hydrothermal/subsurface circulation to the biology and geochemistry of the oceans and strengthen ecological and biogeographic connections between these systems.

## REFERENCES

- Adams, D. K., Mcgillicuddy, D. J., Zamudio, L., Thurnherr, A. M., Liang, X. F., Rouxel, O., et al. (2011). Surface-generated mesoscale eddies transport deep-sea products from hydrothermal vents. *Science* 332, 580–583.
- Alonso-Saez, L., Waller, A. S., Mende, D. R., Bakker, K., Farnelid, H., Yager, P. L., et al. (2012). Role for urea in nitrification by polar marine Archaea. *Proc. Natl. Acad. Sci. U.S.A.* 109, 17989–17994.
- Amend, J. P., Mccollom, T. M., Hentscher, M., and Bach, W. (2011). Catabolic and anabolic energy for chemolithoautotrophs in deep-sea hydrothermal systems hosted in different rock types. *Geochim. Cosmochim. Acta* 75, 5736–5748.
- Anantharaman, K., Breier, J. A., Sheik, C. S., and Dick, G. J. (2013). Evidence for hydrogen oxidation and metabolic plasticity in widespread deep-sea sulfur-oxidizing bacteria. *Proc. Natl. Acad. Sci. U.S.A.* 110, 330–335.
- Anderson, R. E., Beltran, M. T., Hallam, S. J., and Baross, J. A. (2013). Microbial community structure across fluid gradients in the Juan de Fuca Ridge hydrothermal system. *FEMS Microbiol. Ecol.* 83, 324–339.
- Anderson, C. R., Dick, G. J., Chu, M. L., Cho, J. C., Davis, R. E., Brauer, S. L., et al. (2009). *Aurantimonas manganoxydans*, sp. nov. and *Aurantimonas litoralis*, sp. nov.: Mn(II) oxidizing representatives of a globally distributed clade of alpha-Proteobacteria from the Order Rhizobiales. *Geomicrobiol. J.* 26, 189–198.
- Aristegui, J., Gasol, J. M., Duarte, C. M., and Herndl, G. J. (2009). Microbial oceanography of the dark ocean's pelagic realm. *Limnol. Oceanogr.* 54, 1501–1529.
- Baco, A. R., and Smith, C. R. (2003). High species richness in deep-sea chemoautotrophic whale skeleton communities. *Mar. Ecol. Prog. Ser.* 260, 109–114.
- Baker, B. J., Lesniewski, R. A., and Dick, G. J. (2012). Genome-enabled transcriptomics reveals archaeal populations that drive nitrification in a deep-sea hydrothermal plume. *ISME J.* 6, 2269–2279.
- Baker, B. J., Sheik, C. S., Taylor, C. A., Jain, S., Bhasi, A., Cavalcoli, J. D., et al. (2013). Community transcriptomic assembly reveals microbes that contribute to deep-sea carbon and nitrogen cycling. *ISME J.* (in press).
- Beaulieu, S. E., Baker, E. T., and German, C. R. (2012). On the Global Distribution of Hydrothermal Vent Fields: One Decade Later, Abstract OS22B-01. *American Geophysical Union Fall Meeting, presented at 2012 Fall Meeting*. AGU, San Francisco.
- Bennett, S. A., Achterberg, E. P., Connelly, D. P., Statham, P. J., Fones, G. R., and German, C. R. (2008). The distribution and stabilisation of dissolved Fe in deep-sea hydrothermal plumes. *Earth Planet. Sci. Lett.* 270, 157–167.
- Bennett, S. A., Hansman, R. L., Sessions, A. L., Nakamura, K., and Edwards, K. J. (2011a). Tracing iron-fueled microbial carbon production within the hydrothermal plume at the Loihi seamount. *Geochem. Cosmochim. Acta* 75, 5526–5539.
- Bennett, S. A., Statham, P. J., Green, D. R. H., Bris, N. L., McDermott, J. M., Prado, F., et al. (2011b). Dissolved and particulate organic carbon in hydrothermal plumes from the East Pacific Rise, 9°50'N. *Deep Sea Res. Part A* 58, 922–931.
- Bourbonnais, A., Juniper, S. K., Butterfield, D. A., Devol, A. H., Kuypers, M. M. M., Lavik, G., et al. (2012). Activity and abundance of denitrifying bacteria in the subsurface biosphere of diffuse hydrothermal vents of the Juan de Fuca Ridge. *Biogeosciences* 9, 4661–4678.
- Brazelton, W. J., Nelson, B., and Schrenk, M. O. (2012). Metagenomic evidence for H<sub>2</sub> oxidation and H<sub>2</sub> production by serpentine-hosted subsurface microbial communities. *Front. Microbiol.* 2:268. doi: 10.3389/fmicb.2011.00268
- Breier, J. A., Toner, B. M., Fakra, S. C., Marcus, M. A., White, S. N., Thurnherr, A. M., et al. (2012). Sulfur, sulfides, oxides and organic matter aggregated in submarine hydrothermal plumes at 9 degrees 50' N East Pacific Rise. *Geochim. Cosmochim. Acta* 88, 216–236.
- Campbell, B. J., Summers Engel, A., Porter, M. L., and Takai, K. (2006). The versatile ε-proteobacteria. *Nat. Rev. Microbiol.* 4, 458–468.
- Canfield, D. E., Stewart, F. J., Thamdrup, B., De Brabandere, L., Dalsgaard, T., Delong, E. F., et al. (2010). A cryptic sulfur cycle in oxygen-minimum-zone waters off the Chilean coast. *Science* 330, 1375–1378.
- Charlou, J. L., Fouquet, Y., Bougault, H., Donval, J. P., Etoubleau, J., Jean-Baptiste, P., et al. (1998). Intense CH<sub>4</sub> plumes generated by serpentinization of ultramafic rocks at the intersection of the 15 degrees 20' N fracture zone and the Mid-Atlantic Ridge. *Geochim. Cosmochim. Acta* 62, 2323–2333.
- Cowen, J. P., Bertram, M. A., Wakeham, S. G., Thomson, R. E., Lavelle, J. W., Baker, E. T., et al. (2001). Ascending and descending particle flux from hydrothermal plumes at Endeavour Segment, Juan de Fuca Ridge. *Deep Sea Res. Part I Oceanogr. Res. Pap.* 48, 1093–1120.
- Cowen, J. P., and Bruland, K. W. (1985). Metal deposits associated with bacteria: implications for Fe and Mn marine biogeochemistry. *Deep Sea Res. Part A* 32, 253–272.
- Cowen, J. P., and German, C. R. (2003). “Biogeochemical cycling in hydrothermal plumes,” in *Energy and Mass Transfer in Marine Hydrothermal Systems*, eds P. Halbach, V. Tunnicliffe, and J. Hein (Berlin: Dahlem University Press), 303–316.
- Cowen, J. P., and Li, Y. H. (1991). The influence of a changing bacterial community on trace-metal scavenging in a deep-sea particle plume. *J. Mar. Res.* 49, 517–542.
- Cowen, J. P., Massoth, G. J., and Baker, E. T. (1986). Bacterial scavenging of Mn and Fe in a mid- to far-field hydrothermal particle plume. *Nature* 322, 169–171.
- Crowell, B. W., Lowell, R. P., and Von Damm, K. L. (2008). A model for the production of sulfur floc and “snowblower” events at mid-ocean ridges. *Geochemistry Geophysics Geosystems* 9:Q10T02. doi: 10.1029/2008GC002103
- De Angelis, M. A., Lilley, M. D., Olson, E. J., and Baross, J. A. (1993). Methane oxidation in deep-sea hydrothermal plumes of the Endeavour Segment of the Juan de Fuca Ridge. *Deep Sea Res.* 40, 1169–1186.
- DeLong, E. F., Preston, C. M., Mincer, T., Rich, V., Hallam, S. J., Frigaard, N.-U., et al. (2006). Community genomics among stratified microbial assemblages in the ocean's interior. *Science* 311, 496–503.
- Diaz, R. J., and Rosenberg, R. (2008). Spreading dead zones and consequences for marine ecosystems. *Science* 321, 926–929.
- Dick, G. J., Clement, B. G., Fodrie, F. J., Webb, S. M., Bargar, J. R., and Tebo, B. M. (2009). Enzymatic microbial Mn(II) oxidation and Mn biooxide production in the Guaymas Basin hydrothermal plume. *Geochim. Cosmochim. Acta* 73, 6517–6530.
- Dick, G. J., Podell, S., Johnson, H. A., Rivera-Espinoza, Y., Bernier-Latmani, R., McCarthy, J. K., et al. (2008). Genomic insights into Mn(II) oxidation by the marine alphaproteobacterium *Aurantimonas* sp. strain SI85-9A1. *Appl. Environ. Microbiol.* 74, 2646–2658.
- Dick, G. J., and Tebo, B. M. (2010). Microbial diversity and biogeochemistry of the Guaymas Basin deep-sea hydrothermal plume. *Environ. Microbiol.* 12, 1334–1347.
- Elderfield, H., and Schultz, A. (1996). Mid-ocean ridge hydrothermal fluxes and the chemical composition of the ocean. *Annu. Rev. Earth Planet. Sci.* 24, 191–224.
- Feely, R. A., Trefry, J. H., Lebon, G. T., and German, C. R. (1998). The relationship between P/Fe and V/Fe ratios in hydrothermal precipitates and dissolved phosphate in seawater. *Geophys. Res. Lett.* 25, 2253–2256.
- Fisher, A. T., and Harris, R. N. (2010). Using seafloor heat flow as a tracer to map subseafloor fluid flow in the ocean crust. *Geofluids* 10, 142–160.
- Flores, G. E., Shakya, M., Meneghin, J., Yang, Z. K., Seewald, J. S., Wheat, C. G., et al. (2012). Inter-field variability in the microbial communities of hydrothermal vent deposits from a back-arc basin. *Geobiology* 10, 333–346.
- Francis, C. A., Roberts, K. J., Beman, J. M., Santoro, A. E., and Oakley, B.

## ACKNOWLEDGMENTS

We are grateful to Anna-Louise Reysenbach for providing Lau Basin seafloor microbial data and to Alessandro Tagliabue for providing modeled iron distributions. This project is funded by the Gordon and Betty Moore Foundation through Grant GBMF 2609 to Dr. Gregory J. Dick and by National Science Foundation grants OCE 1029242 and OCE 1038006 to Dr. Gregory J. Dick.

- B. (2005). Ubiquity and diversity of ammonia-oxidizing archaea in water columns and sediments of the ocean. *Proc. Natl. Acad. Sci. U.S.A.* 102, 14683–14688.
- Fuchsman, C. A., Kirkpatrick, J. B., Brazelton, W. J., Murray, J. W., and Staley, J. T. (2011). Metabolic strategies of free-living and aggregate-associated bacterial communities inferred from biologic and chemical profiles in the Black Sea suboxic zone. *FEMS Microbiol. Ecol.* 78, 586–603.
- Galand, P. E., Potvin, M., Casamayor, E. O., and Lovejoy, C. (2010). Hydrography shapes bacterial biogeography of the deep Arctic Ocean. *ISME J.* 4, 564–576.
- German, C. R., and Von Damm, K. L. (2004). “Hydrothermal processes,” in *Treatise on Geochemistry*, eds H. D. Holland and K. K. Turekian (Oxford: Elsevier), 181–222.
- German, C. R., Bowen, A., Coleman, M. L., Honig, D. L., Huber, J. A., Jakuba, M. V., et al. (2010). Diverse styles of submarine venting on the ultra-slow spreading Mid-Cayman Rise. *Proc. Natl. Acad. Sci. U.S.A.* 107, 14020–14025.
- Ghiglione, J. F., Galand, P. E., Pommier, T., Pedros-Alio, C., Maas, E. W., Balkker, K., et al. (2012). Pole-to-pole biogeography of surface and deep marine bacterial communities. *Proc. Natl. Acad. Sci. U.S.A.* 109, 17633–17638.
- Goffredi, S. K., and Orphan, V. J. (2010). Bacterial community shifts in taxa and diversity in response to localized organic loading in the deep sea. *Environ. Microbiol.* 12, 344–363.
- Goldberg, E. D. (1954). Marine geochemistry I. Chemical scavengers of the sea. *J. Geol.* 62, 249–265.
- Hallam, S. J., Konstantinidis, K. T., Putnam, N., Schleper, C., Watanabe, Y., Sugahara, J., et al. (2006). Genomic analysis of the uncultivated marine crenarchaeote Cenarchaeum symbiosum. *Proc. Natl. Acad. Sci. U.S.A.* 103, 18296–18301.
- Haymon, R. M., Fornari, D. J., Von Damm, K. L., Lilley, M. D., Perfitt, M. R., Edmond, J. M., et al. (1993). Volcanic eruption of the mid-ocean ridge along the East Pacific Rise crest at 9°45–52°N: direct submersible observations of seafloor phenomena associated with an eruption event in April, 1991. *Earth Planet. Sci. Lett.* 199, 85–101.
- Holden, J. F., Breier, J. A., Rogers, K. L., Schulte, M. D., and Toner, B. M. (2012). Biogeochemical processes at hydrothermal vents: Microbes and minerals, bioenergetics, and carbon fluxes. *Oceanography* 25, 196–208.
- Huber, J. A., Butterfield, D. A., and Baross, J. A. (2003). Bacterial diversity in a subseafloor habitat following a deep-sea volcanic eruption. *FEMS Microbiol. Ecol.* 475, 1–17.
- Jackson, P. R., Ledwell, J. R., and Thurnherr, A. M. (2010). Dispersion of a tracer on the East Pacific Rise (9 degrees N to 10 degrees N), including the influence of hydrothermal plumes. *Deep Sea Res. Part I Oceanogr. Res. Pap.* 57, 37–52.
- Jannasch, H. W., and Wirsen, C. O. (1979). Chemosynthetic primary production at East Pacific sea floor spreading centers. *BioScience* 29, 592–598.
- Jiao, N., Herndl, G. J., Hansell, D. A., Benner, R., Kattner, G., Wilhelm, S. W., et al. (2010). Microbial production of recalcitrant dissolved organic matter: long-term carbon storage in the global ocean. *Nat. Rev. Microbiol.* 8, 593–599.
- Jorgensen, B. B., and Boetius, A. (2007). Feast and famine – microbial life in the deep-sea bed. *Nat. Rev. Microbiol.* 5, 770–781.
- Juniper, S. K., Bird, D. F., Summit, M., Vong, M. P., and Baker, E. T. (1998). Bacterial and viral abundances in hydrothermal vent plumes over northern Gorda Ridge. *Deep Sea Res. Part I Top. Stud. Oceanogr.* 45, 2739–2749.
- Kadko, D. (1993). An assessment of the effect of chemical scavenging within submarine hydrothermal plumes upon ocean geochemistry. *Earth Planet. Sci. Lett.* 120, 361–374.
- Kadko, D. C., Rosenberg, N. D., Lupton, J. E., Collier, R. W., and Lilley, M. D. (1990). Chemical-reaction rates and entrainment within the Endeavor Ridge hydrothermal plume. *Earth Planet. Sci. Lett.* 99, 315–335.
- Kalvelage, T., Jensen, M. M., Contreras, S., Revsbech, N. P., Lam, P., Gunter, M., et al. (2011). Oxygen sensitivity of anammox and coupled N-cycle processes in oxygen minimum zones. *PLoS ONE* 6:e29299. doi: 10.1371/journal.pone.0029299
- Karl, D. M., Beversdorf, L., Bjorkman, K. M., Church, M. J., Martinez, A., and Delong, E. F. (2008). Aerobic production of methane in the sea. *Nat. Geosci.* 1, 473–478.
- Karl, D. M., Knauer, G. A., Martin, J. H., and Ward, B. B. (1984). Bacterial chemolithotrophy in the ocean is associated with sinking particles. *Nature* 309, 54–56.
- Karner, M. B., Delong, E. F., and Karl, D. M. (2001). Archaeal dominance in the mesopelagic zone of the Pacific Ocean. *Nature* 409, 507–510.
- Kaye, J. Z., and Baross, J. A. (2000). High incidence of halotolerant bacteria in Pacific hydrothermal vent and pelagic environments. *FEMS Microbiol. Ecol.* 32, 249–260.
- Kaye, J. Z., and Baross, J. A. (2004). Synchronous effects of temperature, hydrostatic pressure, and salinity on growth, phospholipid profiles, and protein patterns of four *Halomonas* species isolated from deep-sea hydrothermal vent and sea surface environments. *Appl. Environ. Microbiol.* 70, 6220–6229.
- Kaye, J. Z., Sylvan, J. B., Edwards, K. J., and Baross, J. A. (2011). Halomonas and Marinobacter ecotypes from hydrothermal vent, subseafloor and deep-sea environments. *FEMS Microbiol. Ecol.* 75, 123–133.
- Kleiner, M., Petersen, J. M., and Dubilier, N. (2012). Convergent and divergent evolution of metabolism in sulfur-oxidizing symbionts and the role of horizontal gene transfer. *Curr. Opin. Microbiol.* 15, 621–631.
- Konhauser, K. O., Pecoits, E., Lalonde, S. V., Papineau, D., Nisbet, E. G., Barley, M. E., et al. (2009). Oceanic nickel depletion and a methanogen famine before the Great Oxidation Event. *Nature* 458, U750–U785.
- Kuwahara, H., Yoshida, T., Takaki, Y., Shimamura, S., Nishi, S., Harada, M., et al. (2007). Reduced genome of the thioautotrophic intracellular symbiont in a deep-sea clam, *Calyptogena okutanii*. *Curr. Biol.* 17, 881–886.
- Lam, P., Cowen, J. P., and Jones, R. D. (2004). Autotrophic ammonia oxidation in a deep-sea hydrothermal plume. *FEMS Microbiol. Ecol.* 47, 191–206.
- Lam, P., Cowen, J. P., Popp, B. N., and Jones, R. D. (2008). Microbial ammonia oxidation and enhanced nitrogen cycling in the Endeavour hydrothermal plume. *Geochim. Cosmochim. Acta* 72, 2268–2286.
- Lavik, G., Stuurmann, T., Bruchert, V., Van Der Plas, A., Mohrholz, V., Lam, P., et al. (2009). Detoxification of sulphidic African shelf waters by blooming chemolithotrophs. *Nature* 457, 581–584.
- Lesniewski, R. A., Jain, S., Anantharaman, K., Schloss, P. D., and Dick, G. J. (2012). The metatranscriptome of a deep-sea hydrothermal plume is dominated by water column methanotrophs and lithotrophs. *ISME J.* 6, 2257–2268.
- Lösekann, T., Knittel, K., Nadalig, T., Fuchs, B., Niemann, H., Boetius, A., et al. (2007). Diversity and abundance of aerobic and anaerobic methane oxidizers at the Haakon Mosby Mud Volcano, Barents Sea. *Appl. Environ. Microbiol.* 73, 3348–3362.
- Lucker, S., Wagner, M., Maixner, F., Pelletier, E., Koch, H., Vacherie, B., et al. (2010). A *Nitrospira* metagenome illuminates the physiology and evolution of globally important nitrite-oxidizing bacteria. *Proc. Natl. Acad. Sci. U.S.A.* 107, 13479–13484.
- Lupton, J. E. (1995). “Hydrothermal plumes: near and far field,” in *Seafloor Hydrothermal Systems*, eds S. E. Humphris, R. A. Zierenberg, L. S. Mullineaux, and R. E. Thomson (Washington: American Geophysical Union), 317–346.
- Lupton, J. E., and Craig, H. (1981). A Major Helium-3 Source at 15S on the East Pacific Rise. *Science* 214, 13–18.
- Lupton, J. E., Delaney, J. R., Johnson, H. P., and Tivey, M. K. (1985). Entrainment and vertical transport of deep-ocean water by buoyant hydrothermal plumes. *Nature* 316, 621–623.
- Madrid, V. M., Taylor, G. T., Scranton, M. I., and Chistoserdov, A. Y. (2001). Phylogenetic diversity of bacterial and archaeal communities in the anoxic zone of the Cariaco Basin. *Appl. Environ. Microbiol.* 67, 1663–1674.
- Manderack, K. W., and Tebo, B. M. (1993). Manganese scavenging and oxidation at hydrothermal vents and in vent plumes. *Geochim. Cosmochim. Acta* 57, 3907–3923.
- Maruyama, A., Urabe, T., Ishibashi, J., Feely, R. A., and Baker, E. T. (1998). Global hydrothermal primary production rate estimated from the southern East Pacific Rise. *Cah. Biol. Mar.* 39, 249–252.
- Mason, O. U., Hazen, T. C., Borglin, S., Chain, P. S. G., Dubinsky, E. A., Fortney, J. L., et al. (2012). Metagenome, metatranscriptome and single-cell sequencing reveal microbial response to Deepwater Horizon oil spill. *ISME J.* 6, 1715–1727.
- McCarthy, M. D., Beaupre, S. R., Walker, B. D., Voparil, I., Guilderston, T. P., and Druffel, E. R. M. (2011). Chemosynthetic origin of C-14-depleted dissolved organic matter

- in a ridge-flank hydrothermal system. *Nat. Geosci.* 4, 32–36.
- McCollum, T. M. (2000). Geochemical constraints on primary productivity in submarine hydrothermal vent plumes. *Deep Sea Res.* 47, 85–101.
- Moyer, C. L., Tiedje, J. M., Dobbs, F. C., and Karl, D. M. (1998). Diversity of deep-sea hydrothermal vent Archaea from Loihi seamount, Hawaii. *Deep Sea Res. Part II Top. Stud. Oceanogr.* 45, 303–317.
- Mullineaux, L. S., Adams, D. K., Mills, S. W., and Beaulieu, S. E. (2010). Larvae from afar colonize deep-sea hydrothermal vents after a catastrophic eruption. *Proc. Natl. Acad. Sci. U.S.A.* 107, 7829–7834.
- Mullineaux, L. S., Wiebe, P. H., and Baker, E. T. (1995). Larvae of benthic invertebrates in hydrothermal vent plumes over Juan-De-Fuca Ridge. *Mar. Biol.* 122, 585–596.
- Naganuma, T., Otsuki, A., and Seki, H. (1989). Abundance and growth-rate of bacterioplankton community in hydrothermal vent plumes of the North Fiji Basin. *Deep Sea Res. Part A Oceanogr. Res. Pap.* 36, 1379–1390.
- Nakagawa, S., Takai, K., Inagaki, F., Hirayama, H., Nunoura, T., Horikoshi, K., et al. (2005). Distribution, phylogenetic diversity and physiological characteristics of epsilon-Proteobacteria in a deep-sea hydrothermal field. *Environ. Microbiol.* 7, 1619–1632.
- Newton, I. L., Woyke, T., Achtung, T. A., Dilly, G. F., Dutton, R. J., Fisher, M. C., et al. (2007). The *Calystogena magnifica* chemoautotrophic symbiont genome. *Science* 315, 998–1000.
- O'Brien, D., Carton, M., Eardly, D., and Patching, J. W. (1998). In situ filtration and preliminary molecular analysis of microbial biomass from the Rainbow hydrothermal plume at 36 degrees 15' N on the Mid-Atlantic Ridge. *Earth Planet. Sci. Lett.* 157, 223–231.
- Orcutt, B. N., Sylvan, J. B., Knab, N. J., and Edwards, K. J. (2011). Microbial ecology of the dark ocean above, at, and below the seafloor. *Microbiol. Mol. Biol. Rev.* 75, 361.
- Paull, C. K., Hecker, B., Commeau, R., Freemanlynde, R. P., Neumann, C., Corso, W. P., et al. (1984). Biological Communities at the Florida Escarpment Resemble Hydrothermal Vent Taxa. *Science* 226, 965–967.
- Perner, M., Gonnella, G., Hourdez, S., Böhnke, S., Kurtz, S., and Girguis, P. (2013). In situ chemistry and microbial community compositions in five deep-sea hydrothermal fluid samples from Irina II in the Logatchev field. *Environ. Microbiol.* 15, 1551–1560.
- Petersen, J. M., Wentrup, C., Verna, C., Knittel, K., and Dubilier, N. (2012). Origins and evolutionary flexibility of chemosynthetic symbionts from deep-sea animals. *Biol. Bull.* 223, 123–137.
- Petersen, J. M., Zielinski, F. U., Pape, T., Seifert, R., Moraru, C., Amann, R., et al. (2011). Hydrogen is an energy source for hydrothermal vent symbioses. *Nature* 476, 176–180.
- Pham, V. D., Konstantinidis, K. T., Palden, T., and Delong, E. F. (2008). Phylogenetic analyses of ribosomal DNA-containing bacterioplankton genome fragments from a 4000 m vertical profile in the North Pacific Subtropical Gyre. *Environ. Microbiol.* 10, 2313–2330.
- Planavsky, N. J., McGoldrick, P., Scott, C. T., Li, C., Reinhard, C. T., Kelly, A. E., et al. (2011). Widespread iron-rich conditions in the mid-Proterozoic ocean. *Nature* 477, 448–451.
- Prieto, L., and Cowen, J. P. (2007). Transparent exopolymer particles in a deep-sea hydrothermal system: Guaymas Basin, Gulf of California. *Mar. Biol.* 150, 1093–1101.
- Prol-Ledesma, R. M., Dando, P. R., and De Ronde, C. E. J. (2005). Special issue on “shallow-water hydrothermal venting.” *Chem. Geol.* 224, 1–4.
- Quast, C., Pruesse, E., Yilmaz, P., Gerken, J., Schweer, T., Yarza, P., et al. (2013). The SILVA ribosomal RNA gene database project: improved data processing and web-based tools. *Nucleic Acids Res.* 41, D590–D596.
- Redmond, M. C., Valentine, D. L., and Sessions, A. L. (2010). Identification of novel methane-, ethane-, and propane-oxidizing bacteria at marine hydrocarbon seeps by stable isotope probing. *Appl. Environ. Microbiol.* 76, 6412–6422.
- Roth, S. E., and Dymond, J. (1989). Transport and settling of organic material in a deep-sea hydrothermal plume – evidence from particle-flux measurements. *Deep Sea Res. A* 36, 1237–1254.
- Sander, S. G., and Koschinsky, A. (2011). Metal flux from hydrothermal vents increased by organic complexation. *Nat. Geosci.* 4, 145–150.
- Schloss, P. D., Westcott, S. L., Ryabin, T., Hall, J. R., Hartmann, M., Hollister, E. B., et al. (2009). Introducing mothur: open-source, platform-independent, community-supported software for describing and comparing microbial communities. *Appl. Environ. Microbiol.* 75, 7537–7541.
- Schmieder, R., Lim, Y. W., and Edwards, R. (2012). Identification and removal of ribosomal RNA sequences from metatranscriptomes. *Bioinformatics* 28, 433–435.
- Shackelford, R., and Cowen, J. P. (2006). Transparent exopolymer particles (TEP) as a component of hydrothermal plume particle dynamics. *Deep Sea Res. Part I Oceanogr. Res. Pap.* 53, 1677–1694.
- Speer, K. G., Maltrud, M., and Thurnherr, A. (2003). “A global view of dispersion on the mid-oceanic ridge,” in *Energy and Mass Transfer in Marine Hydrothermal Systems*, eds P. Halbach, B. Tunnicliffe, and J. Hein (Berlin: DUP), 287–302.
- Stevens, H., and Ulloa, O. (2008). Bacterial diversity in the oxygen minimum zone of the eastern tropical South Pacific. *Environ. Microbiol.* 10, 1244–1259.
- Stewart, F. J., Ulloa, O., and Delong, E. F. (2012). Microbial metatranscriptomics in a permanent marine oxygen minimum zone. *Environ. Microbiol.* 14, 23–40.
- Stramma, L., Johnson, G. C., Sprintall, J., and Mohrholz, V. (2008). Expanding oxygen-minimum zones in the tropical oceans. *Science* 320, 655–658.
- Strous, M., Pelletier, E., Mangenot, S., Rattei, T., Lehner, A., Taylor, M. W., et al. (2006). Deciphering the evolution and metabolism of an annamox bacterium from a community genome. *Nature* 440, 790–794.
- Summit, M., and Baross, J. A. (1998). Thermophilic subseafloor microorganisms from the 1996 north Gorda Ridge eruption. *Deep Sea Res. Part I Top. Stud. Oceanogr.* 45, 2751–2766.
- Sunamura, M., Higashi, Y., Miyako, C., Ishibashi, J., and Maruyama, A. (2004). Two Bacteria phylotypes are predominant in the Suiyo Seamount hydrothermal plume. *Appl. Environ. Microbiol.* 70, 1190–1198.
- Swan, B. K., Martinez-Garcia, M., Preston, C. M., Sczyrba, A., Woyke, T., Lamy, D., et al. (2011). Potential for chemolithoautotrophy among ubiquitous bacteria lineages in the dark ocean. *Science* 333, 1296–12300.
- Sylvan, J. B., Pyenson, B. C., Rouxel, O., German, C. R., and Edwards, K. J. (2012). Time-series analysis of two hydrothermal plumes at 9 degrees 50'N East Pacific Rise reveals distinct, heterogeneous bacterial populations. *Geobiology* 10, 178–192.
- Taglibaue, A., Bopp, L., Dutay, J. C., Bowie, A. R., Chever, F., Jean-Baptiste, P., et al. (2010). Hydrothermal contribution to the oceanic dissolved iron inventory. *Nat. Geosci.* 3, 252–256.
- Takai, K., Oida, H., Suzuki, Y., Hirayama, H., Nakagawa, S., Nunoura, T., et al. (2004). Spatial distribution of marine crenarchaeota group I in the vicinity of deep-sea hydrothermal systems. *Appl. Environ. Microbiol.* 70, 2404–2413.
- Tavormina, P. L., Ussler, W., Joye, S. B., Harrison, B. K., and Orphan, V. J. (2010). Distributions of putative aerobic methanotrophs in diverse pelagic marine environments. *ISME J.* 4, 700–710.
- Tavormina, P. L., Ussler III, W., Steele, J. A., Connon, S. A., Klotz, M. G., and Orphan, V. J. (2013). Abundance and distribution of diverse membrane-bound monooxygenase (Cu-MMO) genes within the Costa Rica oxygen minimum zone. *Environ. Microbiol. Rep.* 5, 414–424.
- Tavormina, P. L., Ussler, W., and Orphan, V. J. (2008). Planktonic and sediment-associated aerobic methanotrophs in two seep systems along the North American margin. *Appl. Environ. Microbiol.* 74, 3985–3995.
- Tebo, B. M., Bargar, J. R., Clement, B. G., Dick, G. J., Murray, K. J., Parker, D., et al. (2004). Biogenic manganese oxides: properties and mechanisms of formation. *Annu. Rev. Earth Planet. Sci.* 32, 287–328.
- Teske, A., Hinrichs, K.-U., Edgcomb, V., Gomez, A., Kysela, D., Sylva, S. P., et al. (2002). Microbial diversity of hydrothermal sediments in the Guaymas Basin: evidence for anaerobic methanotrophic communities. *Appl. Environ. Microbiol.* 68, 1994–2007.
- Tivey, M. K., Becker, E., Beinart, R., Fisher, C. R., Girguis, P. R., Langmuir, C. H., et al. (2012). Links from mantle to microbe at the Lau Integrated Study Site: Insights from a back-arc spreading center. *Oceanography* 25, 62–77.
- Toner, B. M., Fakra, S. C., Manganini, S. J., Santelli, C. M., Marcus, M. A., Moffett, J. W., et al. (2009). Preservation of iron(II) by carbon-rich matrices in a hydrothermal plume. *Nat. Geosci.* 2, 197–201.
- Tourna, M., Stieglmeier, M., Spang, A., Konneke, M., Schintlmeister, A., Urich, T., et al. (2011). *Nitrososphaera viennensis*, an ammonia oxidizing archaeon from soil. *Proc. Natl. Acad. Sci. U.S.A.* 108, 8420–8425.
- Tringe, S. G., Mering, C. V., Kobayashi, A., Salamov, A. A., Chen, K.,

- Chang, H. W., et al. (2005). Comparative metagenomics of microbial communities. *Science* 308, 554–557.
- Tully, B. J., Nelson, W. C., and Heidelberg, J. F. (2012). Metagenomic analysis of a complex marine planktonic thaumarchaeal community from the Gulf of Maine. *Environ. Microbiol.* 14, 254–267.
- Ulloa, O., Canfield, D. E., Delong, E. F., Letelier, R. M., and Stewart, F. J. (2012). Microbial oceanography of anoxic oxygen minimum zones. *Proc. Natl. Acad. Sci. U.S.A.* 109, 15996–16003.
- Walsh, D. A., Zaikova, E., Howes, C. G., Song, Y. C., Wright, J. J., Tringe, S. G., et al. (2009). Metagenome of a versatile chemolithoautotroph from expanding oceanic dead zones. *Science* 326, 578–582.
- Wankel, S. D., Germanovich, L. N., Lilley, M. D., Genc, G., Diperna, C. J., Bradley, A. S., et al. (2011). Influence of subsurface biosphere on geochemical fluxes from diffuse hydrothermal fluids. *Nat. Geosci.* 4, 461–468.
- Wheat, C. G., and Mottl, M. J. (2000). Composition of pore and spring waters from Baby Bare: global implications of geochemical fluxes from a ridge flank hydrothermal system. *Geochim. Cosmochim. Acta* 64, 629–642.
- Winn, C. D., Karl, D. M., and Massoth, G. J. (1986). Microorganisms in deep-sea hydrothermal plumes. *Nature* 320, 744–746.
- Wright, J. J., Konwar, K. M., and Hallam, S. J. (2012). Microbial ecology of expanding oxygen minimum zones. *Nat. Rev. Microbiol.* 10, 381–394.
- Wyrtki, K. (1962). The Oxygen Minima in Relation to Ocean Circulation. *Deep Sea Research A* 9, 11–23.
- Zinger, L., Amaral-Zettler, L. A., Fuhrman, J. A., Horner-Devine, M. C., Huse, S. M., Welch, D. B. M., et al. (2011). Global patterns of bacterial beta-diversity in seafloor and seawater ecosystems. *PLoS ONE* 6:e24570. doi: 10.1371/journal.pone.0024570
- 30 April 2013; published online: 21 May 2013.
- Citation: Dick GJ, Anantharaman K, Baker BJ, Li M, Reed DC and Sheik CS (2013) The microbiology of deep-sea hydrothermal vent plumes: ecological and biogeographic linkages to seafloor and water column habitats. *Front. Microbiol.* 4:124. doi: 10.3389/fmicb.2013.00124
- This article was submitted to Frontiers in Extreme Microbiology, a specialty of Frontiers in Microbiology.
- Copyright © 2013 Dick, Anantharaman, Baker, Li, Reed and Sheik. This is an open-access article distributed under the terms of the Creative Commons Attribution License, which permits use, distribution and reproduction in other forums, provided the original authors and source are credited and subject to any copyright notices concerning any third-party graphics etc.



# Diversity and phylogenetic analyses of bacteria from a shallow-water hydrothermal vent in Milos island (Greece)

**Donato Giovannelli<sup>1,2,3\*</sup>, Giuseppe d'Errico<sup>3</sup>, Elena Manini<sup>3</sup>, Michail Yakimov<sup>4</sup> and Costantino Vetriani<sup>1,2\*</sup>**

<sup>1</sup> Department of Biochemistry and Microbiology, Rutgers University, New Brunswick, NJ, USA

<sup>2</sup> Institute of Marine and Coastal Sciences, Rutgers University, New Brunswick, NJ, USA

<sup>3</sup> Institute for Marine Science - ISMAR, National Research Council of Italy - CNR, Ancona, Italy

<sup>4</sup> Institute Coastal Marine Environment - IAMC, National Research Council of Italy - CNR, Messina, Italy

**Edited by:**

Anna-Louise Reysenbach, Portland State University, USA

**Reviewed by:**

Karine Alain, Centre National de la Recherche Scientifique, France

Casey R. J. Hubert, Newcastle University, UK

**\*Correspondence:**

Donato Giovannelli, Institute for Marine Science - ISMAR, National Research Council of Italy - CNR, Largo Fiera della Pesca 60125, Ancona, Italy  
e-mail: d.giovannelli@an.ismar.cnr.it;

Costantino Vetriani, Institute of Marine and Coastal Sciences, Rutgers University, 71 Dudley Road, New Brunswick, NJ 08901, USA  
e-mail: vetriani@marine.rutgers.edu

Studies of shallow-water hydrothermal vents have been lagging behind their deep-sea counterparts. Hence, the importance of these systems and their contribution to the local and regional diversity and biogeochemistry is unclear. This study analyzes the bacterial community along a transect at the shallow-water hydrothermal vent system of Milos island, Greece. The abundance and biomass of the prokaryotic community is comparable to areas not affected by hydrothermal activity and was, on average,  $1.34 \times 10^8$  cells g<sup>-1</sup>. The abundance, biomass and diversity of the prokaryotic community increased with the distance from the center of the vent and appeared to be controlled by the temperature gradient rather than the trophic conditions. The retrieved 16S rRNA gene fragments matched sequences from a variety of geothermal environments, although the average similarity was low (94%), revealing previously undiscovered taxa. *Epsilonproteobacteria* constituted the majority of the population along the transect, with an average contribution to the total diversity of 60%. The larger cluster of 16S rRNA gene sequences was related to chemolithoautotrophic *Sulfurovum* spp., an *Epsilonproteobacterium* so far detected only at deep-sea hydrothermal vents. The presence of previously unknown lineages of *Epsilonproteobacteria* could be related to the abundance of organic matter in these systems, which may support alternative metabolic strategies to chemolithoautotrophy. The relative contribution of *Gammaproteobacteria* to the Milos microbial community increased along the transect as the distance from the center of the vent increased. Further attempts to isolate key species from these ecosystems will be critical to shed light on their evolution and ecology.

**Keywords:** bacteria, *Epsilonproteobacteria*, shallow-water hydrothermal vent, Milos, geothermal

## INTRODUCTION

Microbes are one of the most abundant life forms on Earth, they are ubiquitous, possess a great metabolic plasticity and drive major biogeochemical cycles (Staley and Reysenbach, 2002). Studies carried out in geothermal and extreme environments have shown that life on Earth is far more diverse, widespread, and resistant to extreme conditions than previously thought. Despite the crucial roles of prokaryotes in extreme ecosystems, our understanding of their diversity and ecological relevance in these environments is limited.

Deep-sea hydrothermal vent ecosystems are largely based on chemolithoautotrophic primary production (Jannasch, 1985; Bach et al., 2006; Nakagawa and Takai, 2008). Photoautotrophic contribution to these ecosystems is limited to the sinking of low-quality particulate material from the photic zone (Comita et al., 1984). In contrast, shallow-water hydrothermal vent systems (located at depth <200 m) are largely influenced by photosynthesis (Tarasov et al., 2005). In these environments, chemolithoautotrophy and photoautotrophy occur simultaneously and spatial separation is often influenced by

steep thermal and geochemical gradients (Wenzhöfer et al., 2000).

Shallow-water hydrothermal vents are widespread ecosystems that have been previously understudied compared to their deep-sea counterparts (InterRidge vents database, <http://www.interridge.org/>), despite the fact that these systems were known long before the discovery of the deep-sea vents on the Galapagos Rift in 1977 (Lonsdale, 1977). Because of their proximity to the surface, shallow-water hydrothermal systems are influenced both by geothermally generated reducing power and by light, and can be described as "high energy" environments, where microbial metabolism is fueled by different energy sources (Baross and Hoffman, 1985). According to Dando et al. (1995, 2000), the emission of carbon dioxide from the Milos venting area alone ( $35 \text{ km}^2$ ) could account for 10% of the carbon dioxide emission caused by the venting associated with the Mid-Oceanic Ridges. It has been suggested that the conditions found in shallow-water hydrothermal systems could resemble those in which life originated and where metabolic divergence began (Nisbet and Fowler, 1996; Nisbet and Sleep, 2001; Martin et al., 2008).

Understanding the microbiology of shallow-water hydrothermal vents is necessary to evaluate how microorganisms influence biogeochemical cycles. The geology and chemistry of the hydrothermal system located in Paleochori Bay, a sandy bay off the South East coast of the island of Milos, was previously investigated by Dando et al. (2000) and Valsami-Jones et al. (2005). In Paleochori Bay, the vents are located in shallow waters, with temperatures ranging from 25 to 119°C (Botz et al., 1996) and extensive gas and fluid seepage. Early microbiological studies based on fingerprinting approaches showed the presence of bacteria associated to the *Cytophaga-Flavobacteria-Bacteroides* as well as *Arcobacter* spp. (*Epsilonproteobacteria*) and *Thiomicrospira* spp. (*Gammaproteobacteria*) (Brinkhoff et al., 1999; Sievert et al., 1999a, 2000a,b).

In this study, we carried out an environmental survey of a shallow-water hydrothermal vent located in Paleochori bay, Milos island, Greece. The site was sampled to investigate the structure and diversity of the bacterial community along a 1.5 m transect starting at the center of one of the vents.

## MATERIALS AND METHODS

### SITE DESCRIPTION AND SAMPLE COLLECTION

The Milos hydrothermal system is one of the largest in the Mediterranean Sea. It is part of the Hellenic Arc, whose eastern section reaches the Turkish coast and the island of Kos, and

Methana to the west. Extensive submarine venting occurs offshore, from the intertidal zone to depths of more than 100 m, with an approximate extension of 34 km<sup>2</sup> of seabed (Dando et al., 2000).

Inside the Paleochori bay (Figure 1), the venting area is characterized by strong degassing activities coupled with fluid seepage (Valsami-Jones et al., 2005). The entire shallow venting area is surrounded by patches of the seagrass *Posidonia oceanica*, and the vents occur as areas of high temperature and degassing on the sandy bottom (referred to hereafter as the center of the vent) that gradually decrease to ambient conditions as the distance from the vent increases. Steep thermal and redox gradients occur vertically, with temperature increasing with the depth of the sediment, while more gradual temperature and redox changes occur horizontally as the distance from the center of the vent increases (Sievert et al., 1999a, 2000a; Dando et al., 2000; Wenzhöfer et al., 2000). Temperatures of up to 119°C at a vent site in 10 m water depth have been reported (Botz et al., 1996). Venting fluids are enriched with freshwater with varying salinity. The composition of CO<sub>2</sub> released with the fluids ranged between 54.9 and 91.9%, while the concentrations of H<sub>2</sub>S, CH<sub>4</sub> and H<sub>2</sub> were ≤8.1, ≤9.7, and ≤3%, respectively (Botz et al., 1996; Dando et al., 2000). In addition, the hydrothermal fluids have been shown to contain elevated concentrations of reduced inorganic chemicals, such as NH<sub>4</sub><sup>+</sup> (up to 1 mM), H<sub>2</sub>S (up to 1 mM) and Mn<sup>2+</sup> (up to 0.4 mM)

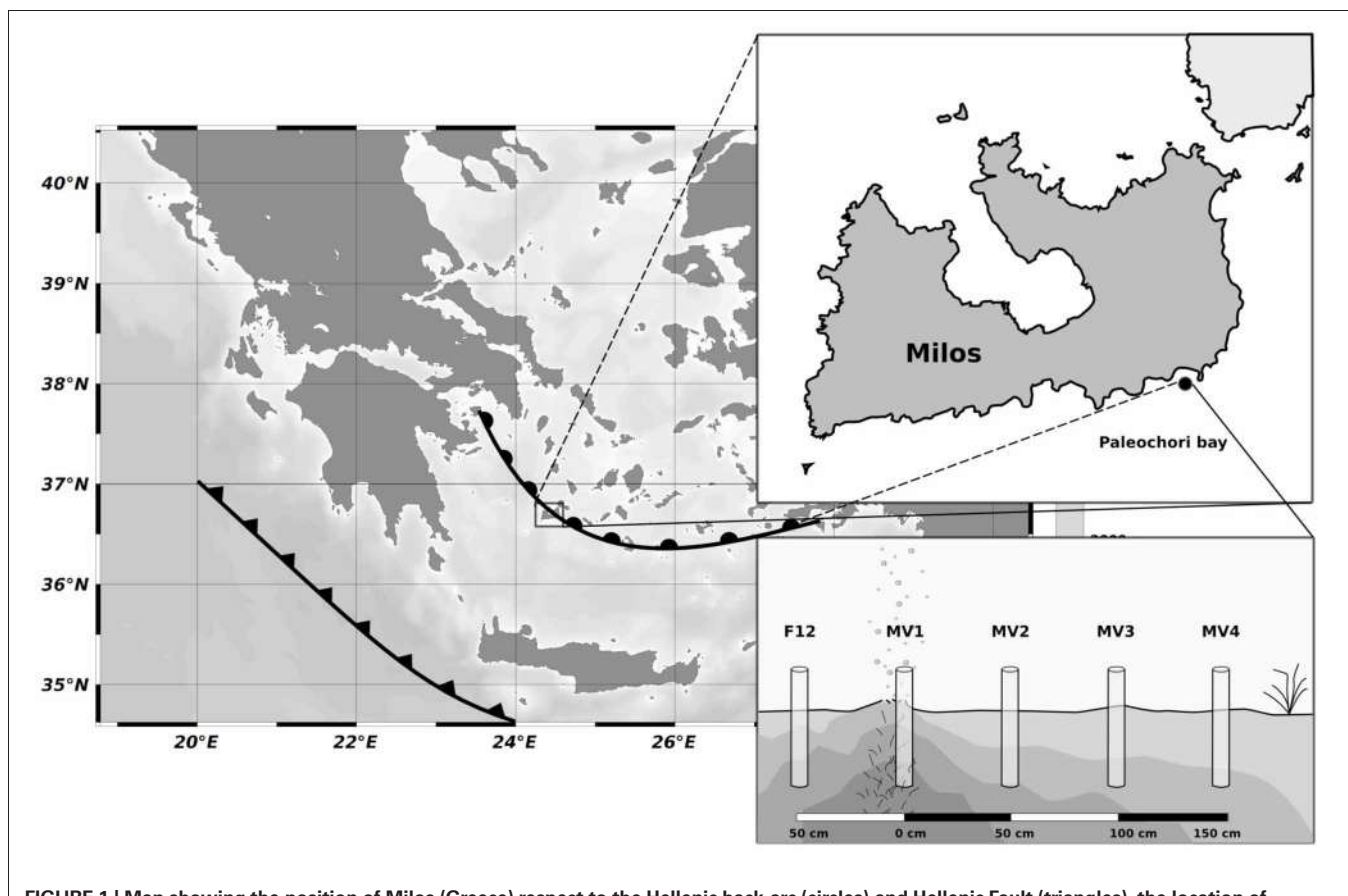


**FIGURE 1 |** Map showing the position of Milos (Greece) respect to the Hellenic back-arc (circles) and Hellenic Fault (triangles), the location of Paleochori Bay and the sampling strategy along the transect. Cores were placed at interval of 50 cm moving away from the vent orifice.

(Fitzsimons et al., 1997). Arsenic and sulfur precipitates are common in proximity to vent orifices, and dense brines can be found in sediment depressions (Dando et al., 2000).

SCUBA divers collected sediment samples using push-cores during the MAMBA cruise in 2010. Starting from the center of a vent located at a depth of 12 m (designated as MV1; 36° 40.351' N, 24° 31.108' E), a horizontal transect consisting of four stations located 50 cm apart from each other was sampled (MV1, 0 cm distance from the center of the vent; MV2, 50 cm distance; MV3, 100 cm distance; MV4, 150 cm distance; **Figure 1** and **Table 1**). Additionally, a single station was sampled at ca. 50 cm from the center of the vent in a yellow sediment patch (F12). The transect was characterized by a 20°C thermal gradient (45 and 25°C at stations MV1 and MV4, respectively) and differences in sediment color were observed. Station MV4 appeared only marginally influenced by hydrothermal activity as the temperature of its surface sediments was close to ambient and *P. oceanica* was observed in close proximity (**Table 1**).

Cores were retrieved on board, sediment horizons separated (0–1, 3–5, and 10–15 cm) and processed according to the analytical procedure described in following paragraphs.

### ORGANIC MATTER COMPOSITION

Aliquots of sediments were immediately frozen at –20°C for determination of organic matter quantity and composition. Total protein concentrations were determined on sediment sub-samples according to Hartree (1972). Total carbohydrates were analyzed according to Gerchakov and Hatcher (1972) and expressed as glucose equivalents. Total lipids were extracted from the sediment by direct elution with chloroform:methanol (1:1 v/v) according to Bligh and Dyer (1959) and then determined according to Marsh and Weinstein (1966). All readings were performed spectrophotometrically. Carbohydrate, protein and lipid concentrations were converted into carbon equivalents using the

conversion factors 0.40 and 0.49 and 0.75 mgC mg<sup>−1</sup>, respectively, and normalized to sediment dry weight (Fabiano et al., 1995). Biopolymeric organic carbon was calculated as the sum of the C equivalents of protein, lipid and carbohydrate.

Chlorophyll-a and phaeopigments were extracted from sediment sub-samples according to Plante-Cuny (1974). Briefly, a few mg of MgCO<sub>3</sub> were added to 1 g of wet sediment to avoid chlorophyll-a degradation. Samples were supplemented with 90% acetone, sonicated and incubated in the dark at 4°C for 12 h. Following incubation, the samples were centrifuged to remove the sediment and the concentration of the pigments in the supernatant were determined spectrofluorimetrically (ex. 430 nm, em. 665 nm) before and after acidification with HCl 0.1 N. Concentrations were calculated against a standard curve and normalized to sediment dry weight. Total phytopigments (CPE) were obtained from the sum of chlorophyll-a and phaeopigments.

### PROKARYOTIC ABUNDANCE AND BIOMASS

Total prokaryotic abundance was determined by direct counts after staining with acridine orange (Danovaro et al., 2002). Briefly, 0.5 g of each sample was supplemented with 5 mM tetrasodium pyrophosphate and incubated for 15 min before sonication. The samples were then stained with 0.025% (wt/vol) acridine orange and filtered on 0.2 mm pore-size Nucleopore black polycarbonate filters, under low vacuum (<100 mm Hg). The filters were analyzed as described by Fry (1990), using epifluorescence microscopy (Zeiss Axioskop 2; 1000 × magnification). The total prokaryotic abundance was normalized to sediment dry weight after desiccation.

Prokaryotic biovolume was estimated using the image analysis software ImageJ (Schneider et al., 2012). Average carbon content was assumed to be 310 fg C μm<sup>3</sup> (Fry, 1990). The prokaryotic biomass (PBM) was normalized to sediment dry weight.

**Table 1 | Sampled stations, temperature, organic matter content and main characteristic of the area.**

| Station    | Sediment depth cm | Surface temperature °C | Protein mg g <sup>−1</sup> | Carbohydrate mg g <sup>−1</sup> | Lipids mg g <sup>−1</sup> | BPC mg C g <sup>−1</sup> | CPE μg g <sup>−1</sup> | Notes                           |
|------------|-------------------|------------------------|----------------------------|---------------------------------|---------------------------|--------------------------|------------------------|---------------------------------|
| <b>MV1</b> | 0–1               | 45                     | 0.70 ± 0.05                | 0.07 ± 0.00                     | 0.18 ± 0.02               | 0.45 ± 0.03              | 11.84 ± 1.35           | Vent orifice–dark gray sediment |
|            | 3–5               |                        | 0.27 ± 0.20                | 0.06 ± 0.01                     | 0.07 ± 0.00               | 0.19 ± 0.08              | 6.17 ± 3.29            |                                 |
|            | 10–15             |                        | 0.39 ± 0.00                | 0.12 ± 0.02                     | 0.10 ± 0.03               | 0.29 ± 0.03              | 6.12 ± 0.64            |                                 |
| <b>MV2</b> | 0–1               | 32                     | 0.53 ± 0.15                | 0.03 ± 0.01                     | 0.10 ± 0.01               | 0.30 ± 0.06              | 9.31 ± 0.94            |                                 |
|            | 3–5               |                        | 0.21 ± 0.03                | 0.02 ± 0.00                     | 0.07 ± 0.04               | 0.15 ± 0.05              | 12.97 ± 0.64           |                                 |
|            | 10–15             |                        | 0.88 ± 0.63                | 0.01 ± 0.00                     | 0.14 ± 0.01               | 0.46 ± 0.25              | 2.14 ± 0.51            |                                 |
| <b>MV3</b> | 0–1               | 28                     | 0.42 ± 0.17                | 0.05 ± 0.01                     | 0.21 ± 0.02               | 0.34 ± 0.09              | 25.69 ± 2.24           | Presence of white precipitate   |
|            | 3–5               |                        | 0.10 ± 0.05                | 0.02 ± 0.00                     | 0.09 ± 0.02               | 0.12 ± 0.01              | 11.37 ± 0.38           |                                 |
| <b>MV4</b> | 0–1               | 25                     | 0.20 ± 0.03                | 0.08 ± 0.03                     | 0.15 ± 0.15               | 0.23 ± 0.08              | 154.6 ± 3.89           | Proximity to <i>P. oceanica</i> |
|            | 3–5               |                        | 0.21 ± 0.04                | 0.08 ± 0.02                     | 0.24 ± 0.11               | 0.30 ± 0.11              | 72.21 ± 4.45           |                                 |
|            | 10–15             |                        | 0.32 ± 0.03                | 0.05 ± 0.01                     | 0.17 ± 0.08               | 0.28 ± 0.05              | 12.67 ± 0.63           |                                 |
| <b>F12</b> | 0–1               | 34                     | 3.62 ± 0.23                | 0.03 ± 0.00                     | 0.06 ± 0.01               | 1.51 ± 0.08              | 7.6 ± 1.1              | Yellow sediments                |

Means are reported with standard deviation. BPC, Biopolymeric organic carbon; CPE, total phytopigments.

## GENOMIC DNA EXTRACTION AND PCR AMPLIFICATION

Genomic DNA was extracted from sediment biomass by the phenol:chloroform method (Maniatis, 1989). Briefly, aliquots of frozen sediments (ca. 0.5 g) were resuspended in extraction buffer (100 mM Tris-HCl, 100 mM EDTA, 1.5 M NaCl pH 8.0), supplemented with 10 mg ml<sup>-1</sup> lysozyme and incubated for 30' at 37°C. Subsequently, 20% SDS was added and each sample was incubated with agitation for 1 h at 60°C. Sediments were removed by centrifugation (5 min at 14,000 × g) and supernatants were collected and extracted with 1 volume of phenol:chloroform:isoamyl alcohol (25:24:1) followed by one extraction with chloroform:isolamyl alcohol (24:1). DNA was then precipitated overnight with 0.1 volumes of sodium acetate and 0.7 volumes isopropanol, washed with 70% ice-cold ethanol, resuspended in PCR grade water and visualized on 1% agarose gel.

The bacterial 16S rRNA gene was amplified by polymerase chain reaction (PCR) using universal bacterial primer 8F (5'-AGA GTT TGA TCC TGG CTC AG-3') and 1517R (5'-ACG GCT ACC TTG TTA CGA CTT-3') (Weisburg et al., 1991). Aliquots of 5 µl of PCR products were visualized by staining with ethidium bromide on 1.5% agarose gel.

## DENATURING GRADIENT GEL ELECTROPHORESIS

A preliminary assessment of the diversity of the sediment bacterial communities was carried out by Denaturing Gradient Gel Electrophoresis (DGGE) analysis of the bacterial 16S rRNA gene. The full-length 16S rRNA gene was obtained as described above, gel-purified and used as a template for nested PCR to amplify the V3 region using the GC-clamp primer 338F-(GC) (5'-CGC CCG CCG CGC GCG GCG GGC GGG GCG GGG GCA CGG GGG GAC TCC TAC GGG AGG CAG CAG-3') and 519R (5'-GWA TTA CCG CGG CKG CTG-3'). DGGE was performed with a D Gene system (Bio-Rad Laboratories, Hercules, CA). PCR products (15 µl) were applied directly onto 6% (wt/vol) polyacrylamide gels in 1 × TAE (0.04 M Tris base, 0.02 M sodium acetate, 1 mM EDTA pH 7.4), with denaturant gradient from 40 to 60% (where 100% denaturant contains 7 M urea and 40% formamide). Electrophoresis was performed at a constant voltage of 45 V for 14 h. After electrophoresis, the gels were incubated for 15 min in 0.5 mg l<sup>-1</sup> ethidium bromide, rinsed for 10 min in distilled water, and photographed with a UV Foto Analyst system (Fotodyne, Inc., Hartland, WI).

## LIBRARY CONSTRUCTION AND RFLP ANALYSIS

Amplified 16S rRNA gene fragments were excised from agarose gels, purified, and cloned into the pCR2-TOPO vector using the TOPO-TA Cloning Kit (Invitrogen, Inc., Carlsbad, California) following the manufacturer's instructions. The resulting ligation products were used to transform competent *Escherichia coli* TOP10 cells. Recombinant *E. coli* clones were grown on Luria-Broth media supplemented with 100 µg ml<sup>-1</sup> ampicillin. Sixty to ninety clones for each library were randomly chosen and analyzed for insert-containing plasmids by direct PCR followed by gel electrophoresis of the amplified products. Insert 16S rRNA gene fragments were digested with HaeIII and MspI (Promega, Inc., Madison, Wis.) restriction endonucleases for 3 h at 37°C and

subjected to Restriction Fragment Length Polymorphism (RFLP) analysis on 3% low-melting agarose gel. Clones were grouped into operational taxonomic units (OTUs) based on their RFLP profiles, and sequences (about 900 bases) were obtained from representative clones of each OTU.

## STATISTICAL AND PHYLOGENETIC ANALYSES

Analysis of variance (ANOVA) using the statistical R-Software (R-Cran project, <http://cran.r-project.org/>) was carried out to identify significantly different samples, which were subjected to the Tukey HSD *post-hoc* test. Where ANOVA assumptions were rejected, a more conservative level of *p* was chosen (Underwood, 1991). DGGE profiles were analyzed with ImageJ (Schneider et al., 2012) and R-software for cluster analysis to identify significant differences in the composition of bacterial communities. Briefly, the position of each DGGE band was recorded using the ImageJ Gel plugin and the resulting matrix was fed to R for the determination of the distance matrix based on Jaccard dissimilarity and used for cluster analysis.

Sequences obtained from libraries were manually checked for quality, primers were removed and the resulting sequences were aligned using ClustalW (Larkin et al., 2007) and SeaView (Gouy et al., 2010). The software Bellerophon (Huber et al., 2004) was used to identify chimeric sequences, which were removed from the dataset (2.2 % of total sequences were identified as chimeric). Neighbor-Joining trees were constructed using the Jukes-Cantor correction and tree topologies were tested using 1000 bootstraps replications (Perriere and Gouy, 1996). Sequences of cultured bacteria retrieved as top blast hits against our sequences were included as references in the alignment. Phylogenetic designation of the sequences to a specific group was obtained by integrating blastn and EzTaxon results with phylogenetic analyses (Chun et al., 2007). Chao1 non-parametric diversity estimator and rarefaction curves were computed using Rarefaction software (<http://www2.biology.ualberta.ca/jbrzusto/rarefact.php>).

The sequences from this study are available through GenBank under accession numbers from KC463698 to KC463741.

## RESULTS

### SEDIMENTARY ORGANIC MATTER CONTENT

Biopolymeric organic carbon (BPC) in the surface sediments decreased along the transect from the center of the vent (MV1) toward the background station (MV4) with values ranging from  $0.45 \pm 0.03$  to  $0.23 \pm 0.08$  mg C g<sup>-1</sup> at station MV1 and station MV4, respectively (Table 1). At station F12, BPC was highest ( $1.51 \pm 0.08$  mg C g<sup>-1</sup>). The observed horizontal gradients were significant (ANOVA *p* < 0.001), and a BPC minimum at a depth of 3–5 cm was observed at all stations. Proteins dominated the carbon pool at all stations with an average contribution to BPC of 55%, followed by lipids and carbohydrates. Protein contribution to the carbon pool decreased along the transect from MV1 to MV4 (Table 1). In contrast, total phytopigment (CPE) concentration increased along the transect from MV1 to MV4 (ANOVA *p* < 0.001). Chlorophyll-a concentrations were extremely low, and phaeopigments were the most abundant class. The quantity and composition of the organic matter of the yellow surface

sediments at station F12 differed from that of the other stations with proteins contributing nearly 95% of the BPC (**Table 1**).

### PROKARYOTIC ABUNDANCE AND BIOMASS

In general, total prokaryotic abundance decreased as the depth of the sediment increased at all stations, despite their proximity to vent orifice (**Figure 2A**; ANOVA  $p < 0.001$ ). Values ranged from  $0.8 \pm 0.4 \times 10^8$  to  $2.7 \pm 1.1 \times 10^8$  cells  $\text{g}^{-1}$  in the surficial sediments for MV1 and MV4, respectively, indicating higher abundances in the surface sediment layers and an increasing trend along the transect from MV1 to MV4. These trends were statistically significant (ANOVA  $p < 0.001$ ). Prokaryotic biomass in surficial sediments ranged from  $1.61 \pm 1.06$  to  $11.95 \pm 6.3 \mu\text{g C g}^{-1}$  in station MV2 and MV4, respectively (**Figure 2B**). Again, a trend of decreasing biomass with increasing sediment depth and increasing biomass along the transect toward the periphery of the vent was observed (**Figure 2B**; ANOVA  $p < 0.01$ ).

Prokaryotic abundance in station F12 was comparable to station MV1, while prokaryotic biomass was significantly higher. The decreasing trend along the vertical sediment profile was more evident at stations located further away from the center of the vent. Inter-replicate variability was also higher at those stations.

### PROKARYOTIC DIVERSITY

DGGE was used to investigate the diversity of the sediment bacteria from the 0–1, 5–10 and 10–15 cm layers along the transect stations, and that from the 0–1 cm layer of station F12 (**Figure 3**). Similar DGGE profiles were obtained from stations MV1, MV3 and MV4 and F12 (data were not obtained for station MV2). Cluster analysis based on the DGGE profiles indicated that the bacterial communities from the same sediment layers tend to group together (**Figure 3**). A relevant group included communities from the 0–1 cm sediments from the transect stations and from F12, while the 3–5 and 10–15 cm layers from MV1 and MV4

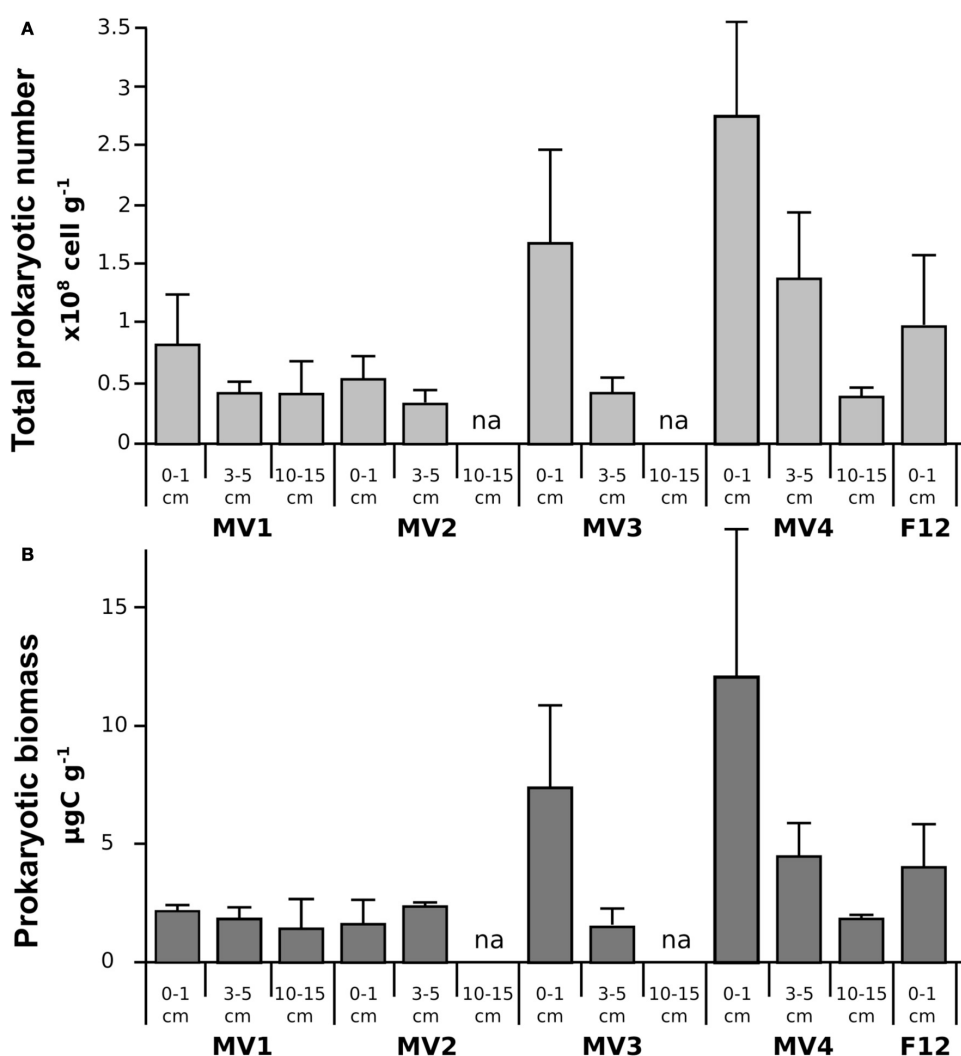
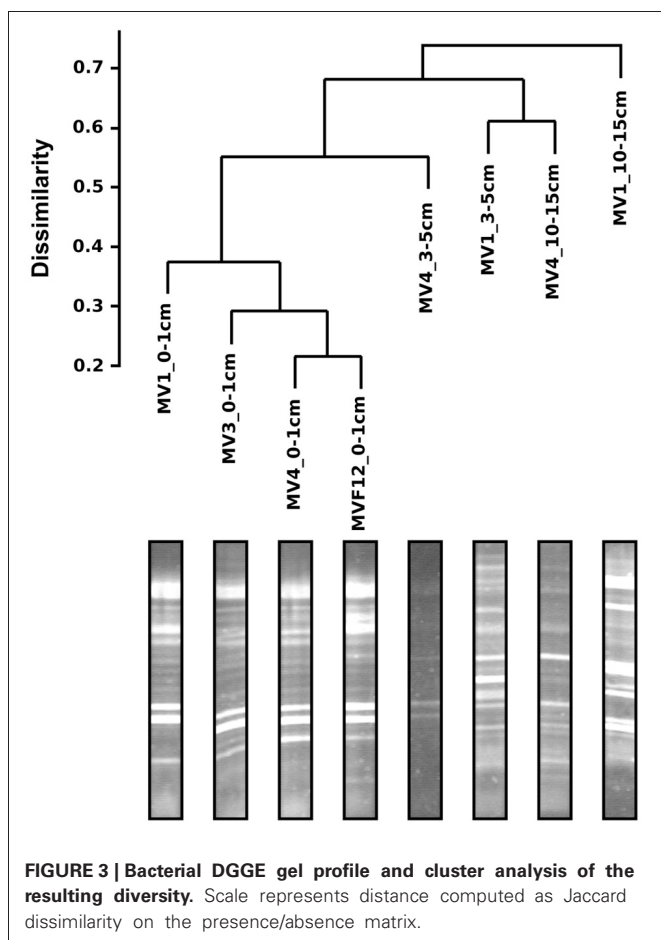


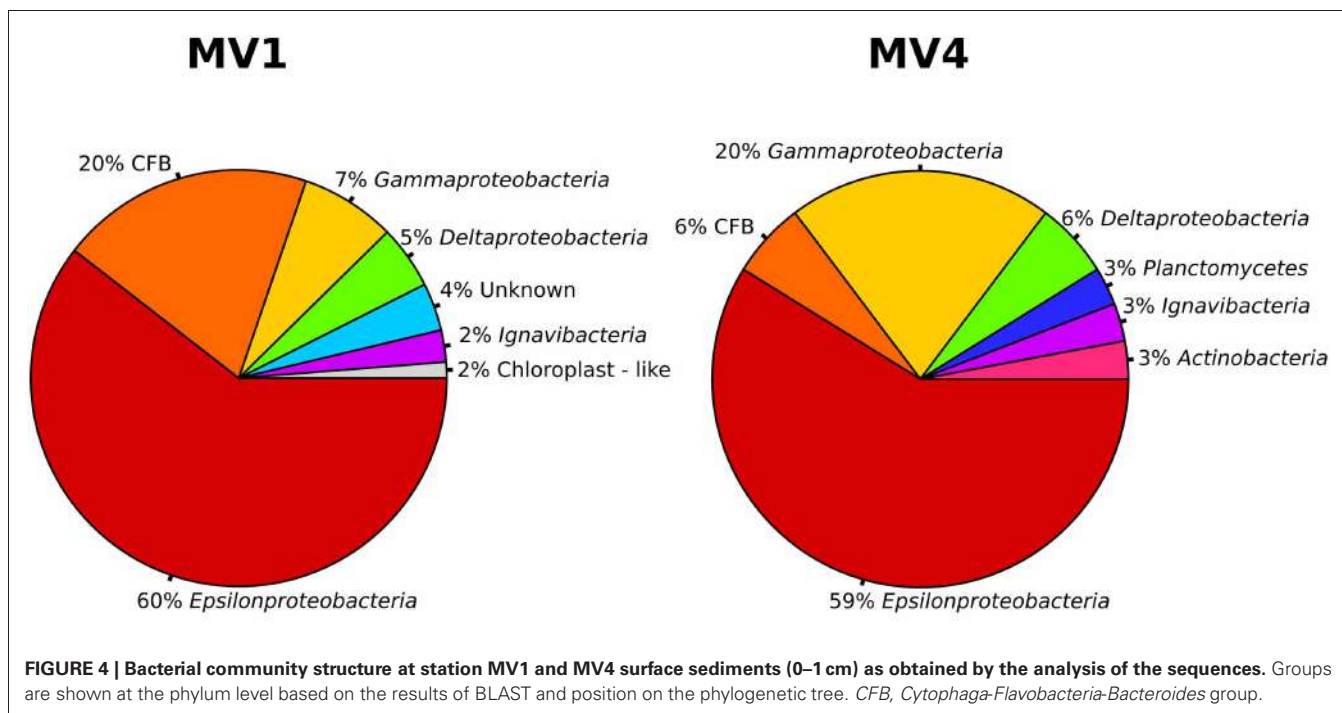
**FIGURE 2 |** Prokaryotic abundance (TPN; A) and biomass (PBM; B) along the sampled stations. Mean values are reported with standard deviation. na = data not available.



formed a second group (**Figure 3**). The bacterial communities from the 0–1 cm layer of stations MV1 (center of the vent) and MV4 (periphery of the vent) were selected to construct 16S rRNA gene libraries.

Both the MV1 and MV4 libraries were dominated by sequences that could be assigned to the *Epsilonproteobacteria* (60 and 59% for MV1 and MV4, respectively; **Figure 4**). Other common phyla in both libraries were sequences belonging to the CFB (20 and 6% for MV1 and MV4, respectively; **Figure 4**) and *Gammaproteobacteria* (7 and 20% for MV1 and MV4, respectively; **Figure 4**). The number of gammaproteobacterial clones increased at the periphery of the vent and the ratio of *Epsilon*-to *Gammaproteobacteria* was 8.2 and 2.9 at stations MV1 and MV4, respectively. Sequences related to the *Deltaproteobacteria*, Planctomycetes, *Actinobacteria* and *Ignavibacteria* were also found. Four percent of the sequences retrieved from station MV1 could not be assigned to any known lineage (**Figure 4**).

The sequences were further analyzed by aligning them against closest cultured relatives and a neighbor-joining tree was constructed (**Figure 5**). Both libraries are well represented in the tree, with numerous sequences clustering together despite their different origins. A large number of sequences obtained from the libraries were related to *Sulfurovum lithotrophicum* (Inagaki et al., 2004), and clustered around this sequence on the tree (average similarity of 93%; **Figure 5** and **Table 2**). The *Sulfurovum*-related sequences were organized in two discrete clusters, each containing clones from both libraries, and represented 44% of the clones in each library. The same clusters had best hits in the non-redundant database to sequences identified during environmental surveys in a variety of submarine geothermal



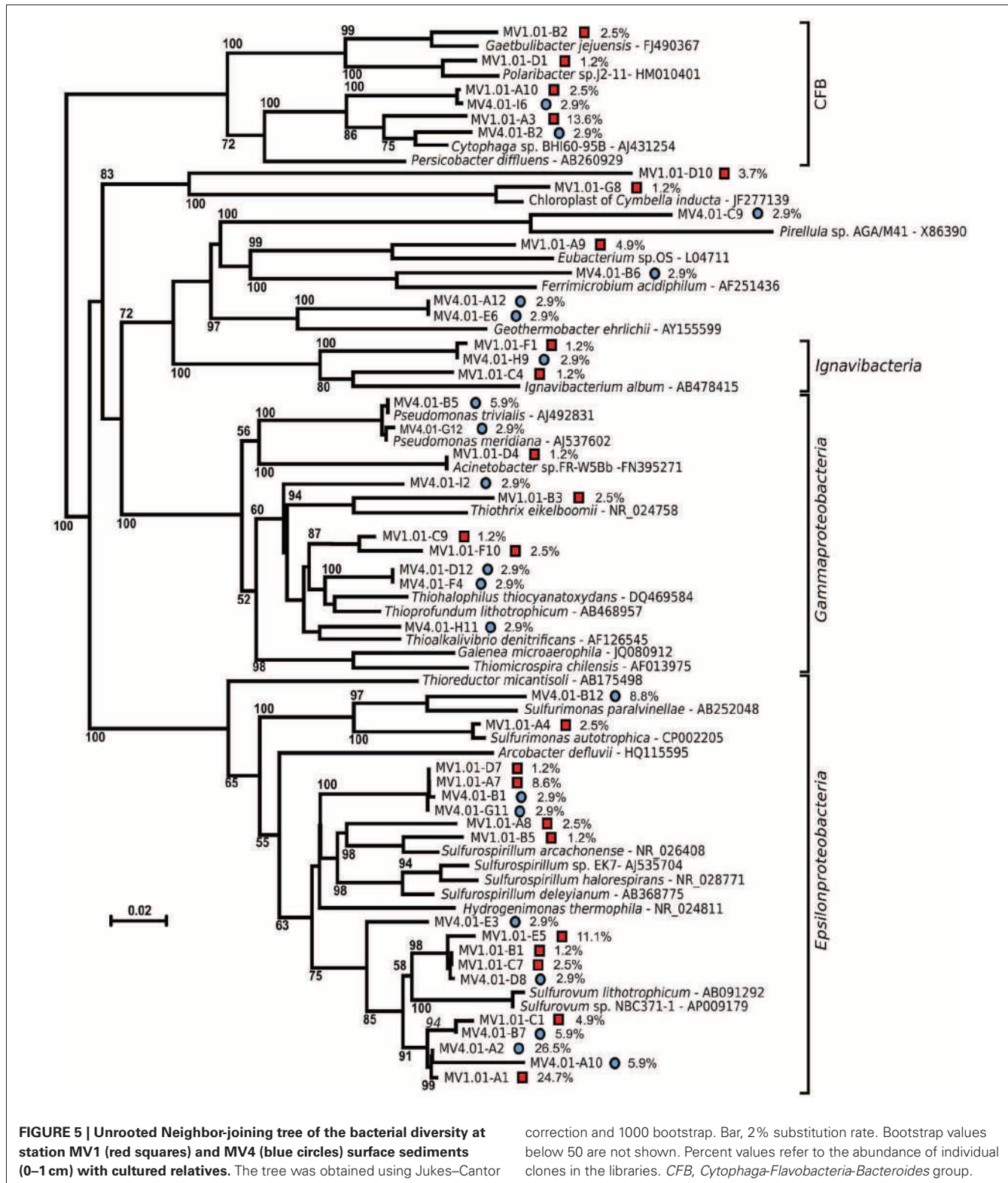


**FIGURE 5 | Unrooted Neighbor-joining tree of the bacterial diversity at station MV1 (red squares) and MV4 (blue circles) surface sediments (0–1 cm) with cultured relatives.** The tree was obtained using Jukes–Cantor

correction and 1000 bootstrap. Bar, 2% substitution rate. Bootstrap values below 50 are not shown. Percent values refer to the abundance of individual clones in the libraries. CFB, Cytophaga-Flavobacter-Bacteroides group.

environments such as the Logatchev field on the Mid-Atlantic Ridge (Nakagawa et al., 2005; Hügler et al., 2010), Vailulu seamount in the Samoa and submarine volcanoes on the Kermadec Arc (Hodges and Olson, 2009).

A second major group of epsilonproteobacterial sequences was related to *Sulfurospirillum* spp. (90.8% average similarity), and clustered outside of the *Sulfurospirillum* group, constituting 13.6 and 5.8% of the two libraries respectively (Figure 5

**Table 2 | Sequenced clones, top blast hits to the non-redundant database (closest relative) and best hit among cultured bacteria (closest cultured relative).**

| Clone Group | Accession no. | % in library | Closest relative (top blast hit)                           | % similarity | Closest cultured relative                              | % similarity |
|-------------|---------------|--------------|--|--------------|--|--------------|
| MV1.01-A1   | KC463698      | 24.7         | Uncultured <i>Epsilonproteobacterium</i> FN562857          | 92           | <i>Sulfurovum lithotrophicum</i> 42BKT AB091292        | 94           |
| MV1.01-A3   | KC463699      | 13.6         | Uncultured bacterium clone VS_CL-76 16S FJ497327           | 93           | <i>Cytophaga</i> sp. BHI60-95B AJ431254                | 91           |
| MV1.01-A4   | KC463700      | 2.5          | Uncultured bacterium clone VS_CL-308 16S FJ497560          | 95           | <i>Sulfurimonas autotrophica</i> DSM 16294 CP002205    | 98           |
| MV1.01-A7   | KC463701      | 8.6          | Uncultured <i>Epsilonproteobacterium</i> AB175533          | 90           | <i>Sulfurospirillum</i> sp. EK7 AJ535704               | 92           |
| MV1.01-A8   | KC463702      | 2.5          | Uncultured <i>Epsilonproteobacterium</i> AB247847          | 96           | <i>Sulfurospirillum halorespirans</i> PCE-M2 NR_028771 | 90           |
| MV1.01-A9   | KC463703      | 4.9          | Uncultured bacterium clone C13S-4 16S EU617730             | 95           | <i>Eubacterium</i> sp. (OS type K) L04711              | 84           |
| MV1.01-A10  | KC463704      | 2.5          | Uncultured bacterium partial 16S rRNA gene, SZB56 AM176864 | 93           | <i>Cytophaga</i> sp. BHI60-95B AJ431254                | 90           |
| MV1.01-B1   | KC463705      | 1.2          | Uncultured bacterium partial 16S rRNA gene AF449240        | 95           | <i>Sulfurovum lithotrophicum</i> 42BKT AB091292        | 93           |
| MV1.01-B2   | KC463706      | 2.5          | Uncultured bacterium partial 16S rRNA gene FM179896        | 93           | <i>Gaetbulibacter jejuensis</i> CNURIC014 FJ490367     | 93           |
| MV1.01-B3   | KC463707      | 2.5          | Uncultured bacterium clone MF-Oct-95 16S HQ225056          | 95           | <i>Thiothrix eikelboomii</i> AP3 NR_024758             | 90           |
| MV1.01-B5   | KC463708      | 1.2          | Uncultured <i>Epsilonproteobacterium</i> AJ969489          | 92           | <i>Sulfurospirillum arcachonense</i> F1F6 NR_026408    | 95           |
| MV1.01-C1   | KC463709      | 4.9          | Uncultured epsilon clone AT-co11 AY225616                  | 95           | <i>Sulfurovum lithotrophicum</i> 42BKT AB091292        | 93           |
| MV1.01-C4   | KC463710      | 1.2          | Uncultured bacterium clone SIMO-2441 AY711807              | 92           | <i>Ignavibacterium album</i> Mat9-16 AB478415          | 87           |
| MV1.01-C7   | KC463711      | 2.5          | Uncultured <i>Epsilonproteobacterium</i> AB197179          | 93           | <i>Sulfurovum lithotrophicum</i> 42BKT AB091292        | 94           |
| MV1.01-C9   | KC463712      | 1.2          | Uncultured Gammaproteobacterium clone ARTE12_226 GU230337  | 95           | <i>Thioalkalivibrio denitrificans</i> ALJD AF126545    | 91           |
| MV1.01-D1   | KC463713      | 1.2          | Uncultured marine bacterium clone B-SW120 HM437670         | 91           | <i>Polaribacter</i> sp. J2-11 HM010401                 | 91           |
| MV1.01-D4   | KC463714      | 1.2          | Uncultured bacterium clone ncd2696f09c JF221689            | 98           | <i>Acinetobacter</i> sp. FR-W5Bb FN395271              | 98           |
| MV1.01-D7   | KC463715      | 1.2          | Uncultured <i>Epsilonproteobacterium</i> AB175533          | 91           | <i>Sulfurospirillum deleyianum</i> AB368775            | 88           |
| MV1.01-D10  | KC463716      | 3.7          | Uncultured bacterium clone TF-33 16S FJ535257              | 94           | <i>Thioreductor micantisoli</i> BKB25Ts-Y AB175498     | 78           |
| MV1.01-E5   | KC463717      | 11.1         | Uncultured <i>Epsilonproteobacterium</i> AB197179          | 94           | <i>Sulfurovum lithotrophicum</i> 42BKT AB091292        | 93           |
| MV1.01-F1   | KC463718      | 1.2          | Uncultured bacterium clone TS-31 16S FJ535328              | 95           | <i>Ignavibacterium album</i> Mat9-16 AB478415          | 88           |
| MV1.01-F10  | KC463719      | 2.5          | Uncultured bacterium clone D13S-50 EU617758                | 94           | <i>Thioalkalivibrio denitrificans</i> ALJD AF126545    | 89           |
| MV1.01-G8   | KC463720      | 1.2          | Uncultured bacterium clone GUP5D05 16S HQ178788            | 94           | <i>Cymbella inducta</i> NJCI77 chloroplast JF277139    | 94           |
| MV4.01-A2   | KC463721      | 26.5         | Uncultured <i>Epsilonproteobacterium</i> BH8 FN562857      | 96           | <i>Sulfurovum lithotrophicum</i> 42BKT AB091292        | 94           |
| MV4.01-A10  | KC463722      | 5.9          | Epsilon ectosymbiont of <i>Symmetromphalus</i> GU253366    | 94           | <i>Sulfurovum lithotrophicum</i> 42BKT AB091292        | 90           |
| MV4.01-A12  | KC463723      | 2.9          | Uncultured bacterium clone SMI1-GC205-Bac66                | 98           | <i>Geothermobacter ehrlichii</i> SS015 AY155599        | 88           |

(Continued)

**Table 2 | Continued**

| Clone Group | Accession no. | % in library | Closest relative (top blast hit)  | % similarity | Closest cultured relative                             | % similarity |
|-------------|---------------|--------------|---|--------------|---|--------------|
| MV4.01-B1   | KC463724      | 2.9          | Uncultured <i>Epsilonproteobacterium</i> AB175533                       | 94           | <i>Sulfurospirillum deleyianum</i> AB368775           | 91           |
| MV4.01-B2   | KC463725      | 2.9          | Uncultured <i>Bacteroidetes</i> bacterium clone VS_CL-132 FJ497383      | 97           | <i>Persicobacter diffluens</i> NBRC 15940 AB260929    | 84           |
| MV4.01-B5   | KC463726      | 5.9          | Pseudomonas sp. VS05_25 FJ662886  | 99           | <i>Pseudomonas trivialis</i> DSM 14937 AJ492831       | 99           |
| MV4.01-B6   | KC463727      | 2.9          | Uncultured <i>Actinobacterium</i> AB099989                              | 97           | <i>Ferrimicrobium acidiphilum</i> T23 AF251436.2      | 87           |
| MV4.01-B7   | KC463728      | 5.9          | Uncultured <i>Epsilonproteobacterium</i> FN562857                       | 97           | <i>Sulfurovum</i> sp. NBC37-1 AP009179                | 93           |
| MV4.01-B12  | KC463729      | 8.8          | Uncultured bacterium clone KM51 AY216438                                | 98           | <i>Sulfurimonas paralvinellae</i> GO25 AB252048       | 93           |
| MV4.01-C9   | KC463730      | 2.9          | Uncultured bacterium clone NT2_C15 HM630159                             | 97           | <i>Pirellula</i> sp. AGA/M41 X86390                   | 87           |
| MV4.01-D8   | KC463731      | 2.9          | Uncultured <i>Epsilonproteobacterium</i> clone R103-B76 AF449240        | 97           | <i>Sulfurovum lithotrophicum</i> 42BKT AB091292       | 93           |
| MV4.01-D12  | KC463732      | 2.9          | Uncultured sediment bacterium clone JSS S04 514 HQ191081                | 97           | <i>Thiohalophilus thiocyanatoxydans</i> HRhD DQ469584 | 92           |
| MV4.01-E3   | KC463733      | 2.9          | Uncultured <i>Epsilonproteobacterium</i> clone BSC2_c21 DQ295546        | 93           | <i>Hydrogenimonas thermophila</i> EP1-55 NR_024811    | 88           |
| MV4.01-E6   | KC463734      | 2.9          | Uncultured bacterium clone SMI1-GC205-Bac66 DQ521800                    | 98           | <i>Geothermobacter ehrlichii</i> SS015 AY155599       | 87           |
| MV4.01-F4   | KC463735      | 2.9          | Uncultured sediment bacterium clone JSS S04 HQ191081                    | 97           | <i>Thiohalophilus thiocyanatoxydans</i> HRhD DQ469584 | 92           |
| MV4.01-G11  | KC463736      | 2.9          | Uncultured <i>Epsilonproteobacterium</i> AB175533                       | 95           | <i>Sulfurospirillum deleyianum</i> DSM 6946 CP001816  | 89           |
| MV4.01-G12  | KC463737      | 2.9          | Uncultured bacterium clone nbw124b GQ024593                             | 99           | <i>Pseudomonas meridiana</i> CMS 38 AJ537602          | 98           |
| MV4.01-H9   | KC463738      | 2.9          | Uncultured bacterium clone TS-31 FJ535328                               | 98           | <i>Ignavibacterium album</i> Mat9-16 AB478415         | 88           |
| MV4.01-H11  | KC463739      | 2.9          | Uncultured <i>Gammaproteobacterium</i> clone TRAN-099 JF344515          | 99           | <i>Thiohalophilus thiocyanatoxydans</i> HRhD DQ469584 | 91           |
| MV4.01-I2   | KC463740      | 2.9          | Uncultured bacterium clone SSW84Ap EU592359                             | 97           | <i>Thiopropfundum lithotrophicum</i> 108 AB468957     | 92           |
| MV4.01-I6   | KC463741      | 2.9          | Uncultured <i>Bacteroidetes</i> bacterium clone Belgica2005/10 DQ351801 | 94           | <i>Cytophaga</i> sp. BHI60-95B AJ431254               | 90           |

and **Table 2**). Clones closely related to the *Epsilonproteobacterium Sulfurimonas authotrophica* were found exclusively in library MV1 (2.5% of the library sequences), while sequences related to *Sulfurimonas paralvinellae* constituted 8.8% of the MV4 library (93% similarity).

Sequences related to the *Gammaproteobacteria* constituted the second largest group in the MV4 library and were mainly related to *Pseudomonas* spp. and members of the *Thiohalophilus/Thiopropfundum* cluster (98.5 and 91.7% average similarity, respectively) constituting 20.6% of the clones sequenced from this library. In the library from MV1, the *Gammaproteobacteria*-related sequences were related to *Thioalkalivibrio denitrificans* and *Thiothrix eikelboomii* (average similarity 90%), constituting only 6.2% of the library. The

remaining gammaproteobacterial clones were associated with *Acinetobacter* sp. FR-W5Bb (98% similarity, 1.2% of the library) and a cluster that included clones MV1.01-C9 and MV1.01-F10, related to *Thioalkalivibrio denitrificans* (90% average similarity, 3.7% of the library, **Figure 5** and **Table 2**).

Sequences related to the *Flavobacteria-Bacteroides-Cytophaga* cluster were the second major group in library MV1, with an average similarity of 90% to *Cytophaga* sp. BHI60-95B (constituting 16% of the clones in the library). Sequences related to the same species were also found in library MV4 (5.9% of the library). Unique sequences related to the *Flavobacterium Gaetbulibacter jejuensis* and *Polaribacter* sp. j2-11 were present at station MV1 (93 and 91% similarity, respectively). *Deltaproteobacteria* were represented in library MV4

by sequences related to *Geothermobacter ehrlichii* (87.5% similarity, 5.8% of the clones in the library). MV1 sequences related to the *Deltaproteobacteria* represented 5% of the clones in this library and were associated to *Eubacterium* sp. OS (84% similarity).

Clones related to the *Ignavibacterium album* (87.7% similarity on average) were retrieved from both libraries, MV1 and MV4.

Despite the lower number of clone sequenced at station MV4, computed Chao1 diversity estimate indicated that diversity at MV4 was higher than MV1 (Chao1,  $63.7 \pm 22$  and  $28.8 \pm 4.2$  respectively). This can be also inferred from the slope visible on the rarefaction curves computed for both libraries (**Figure 6**).

## DISCUSSION

Shallow-water hydrothermal vents are distributed worldwide and, while understudied relative to their deep-sea counterparts, they represent unique ecosystems where primary productivity is supported both by chemosynthesis and photosynthesis (Tarasov et al., 2005). In this study, we investigated the abundance, biomass, community structure and diversity of the prokaryotic community at a shallow-water hydrothermal vent in Paleochori Bay, Milos island, Greece (**Figure 1**).

Prokaryotic abundance was as high as  $2.7 \pm 1.1 \times 10^8$  cells  $\text{g}^{-1}$ , with average values comparable to those reported in previous studies of the same area and other shallow-water hydrothermal systems, as well as at deep-sea vents (**Figure 2A**; Sievert et al., 1999b, 2000a,b; Nakagawa et al., 2005; Manini et al., 2008; Williamson et al., 2008; Maugeri et al., 2009, 2010). Prokaryotic abundance decreased with depth in the sediments at all stations, a general trend previously reported for shallow-water marine sediments (Molari et al., 2012). In contrast, prokaryotic abundance increased toward the periphery of the vent (**Figure 2A**). Prokaryotic biomass followed similar spatial patterns, with higher values at the surface (0–1 cm) and at station MV4 (**Figure 2B**). A previous report of the Milos vents indicated that deeper sediments tend to be hotter (Sievert et al., 2000b), while we

observed that surface sediments along the transect became gradually cooler at the periphery of the vent (**Table 1**). Hence, it appears that temperature and prokaryotic biomass are inversely correlated (**Figure 2**, Pearson moment correlation  $r = 0.617$ ,  $p < 0.05$ ).

Biopolymeric organic carbon (BPC), as well as proteins, decreased along the transect from the center (MV1) to the periphery of the vent (MV4), while carbohydrates and lipids remained fairly stable (**Table 1**). In contrast, phytopigments (CPE) followed an opposite pattern, increasing along the transect from MV1 to MV4 (**Table 1**). The highest concentrations of proteins and lowest concentration of CPE were measured at station F12 (yellow sediments, temperature  $34^\circ\text{C}$ ; **Table 1**). The increasing concentration of CPE as the sediment temperature decreases implies an increase of phototrophic organisms in the lower temperature regions of the vent system, probably due by the presence of previously described diatoms and cyanobacteria mats in the outer rings of similar vents (Thiermann et al., 1997). This is consistent with the general notion that photoautotrophs are less tolerant to elevated temperatures than chemoautotrophic or chemoheterotrophic microorganisms (Madigan et al., 2012). These findings suggest a gradual enrichment of phototrophic organisms along the decreasing thermal gradient. While BPC and proteins decreased along the transect from MV1 to MV4, prokaryotic abundance and biomass increased (**Table 1** and **Figures 2A,B**) and no significant correlation was found among the two parameters (Pearson moment correlation  $r = -0.214$ ,  $p > 0.05$ ). Since the transect was relatively short and all sampling stations were at the same depth, it is safe to assume that the input of organic matter from the water column and lateral advection was constant for all stations. We hypothesize that the decreasing prokaryotic biomass in the hottest section of the vent may lead to a decrease in carbon consumption, which is reflected in the higher concentration of measurable proteins and BPC. This hypothesis implies that temperature, rather than trophic resources, mainly controls the distribution of prokaryotes in this system.

Bacterial diversity, investigated by DGGE profiles, showed that the main DGGE banding pattern was highly conserved, while the highest number of unique bands was obtained from the 3–5 and 10–15 cm depth profiles at station MV1 (**Figure 3**). In total, 30 unique bands with distinct electrophoretic mobility were obtained. As expected, the DGGE analysis highlights the presence of distinct bacterial populations in surface and deeper sediments, which likely reflect different thermal and redox regimes (**Figure 3**). Similar findings have been reported for a variety of environments, including shallow-water and deep-sea hydrothermal vents (Moyer et al., 1995; Sievert et al., 1999b, 2000a; Manini et al., 2008).

Previous studies of the Paleochori Bay vents based on DGGE and fingerprinting analyses reported a population dominated by the *Cytophaga-Flavobacteria-Bacteroides* cluster, *Gamma proteobacteria* of the genus *Thiomicrospira* and *Epsilonproteobacteria* of the genus *Arcobacter* (Brinkhoff et al., 1999; Sievert et al., 1999a, 2000a). Here, we integrated fingerprinting, sequencing and phylogenetic analyses to assess the bacterial diversity of the shallow-water vent ecosystems of Milos

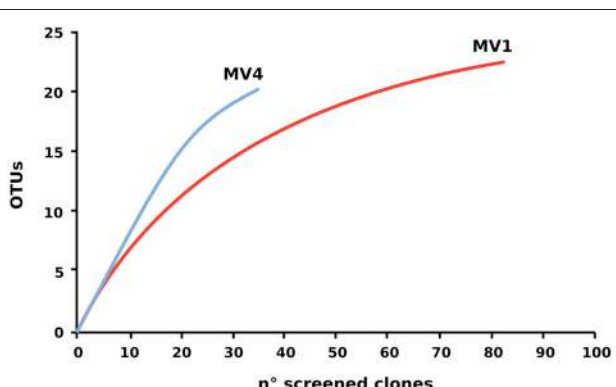


**FIGURE 6 |** Rarefaction curve of the 16S rRNA gene libraries.

Rarefaction curves were computed using Rarefaction software (<http://www2.biology.ualberta.ca/jbrusto/rarefact.php>).

island. Our survey of the bacterial 16S rRNA gene sequences of the surface sediments of stations MV1 and MV4 showed that *Epsilonproteobacteria* were the most represented class in both libraries. *Epsilonproteobacteria* are well adapted to sulfidic conditions and are commonly detected in environmental surveys of geothermal environments, as well as isolated as pure cultures from deep-sea hydrothermal vents (Campbell et al., 2006; Sievert and Vetriani, 2012). In contrast, *Gammaproteobacteria* constituted only 7 and 20% of the MV1 and MV4 clone libraries, respectively. It is worth noting that the relative abundance of gammaproteobacterial clones increased from the center to the periphery of the vent (**Figure 4**). The *Epsilon-* to *Gammaproteobacteria* ratio decreased accordingly, from 8.8 at station MV1 to 2.9 at station MV4. Overall, the expected diversity, calculated as Chao1 and rarefaction analyses (**Figure 6**), appeared to be higher at MV4. Sievert et al. (1999a) reached a similar conclusion, as they found that the microbial diversity based on DGGE profiles was higher at the periphery of the vent. Despite this, the beta-diversity within the transect appeared to be relatively low as cloned sequences retrieved from both MV1 and MV4 were closely related (**Figure 5**).

Phylogenetic analysis showed a large number of the sequences retrieved from both libraries were placed in the *Sulfurovum* cluster, although the average similarity of the clones generated in this study to the type strain, *Sulfurovum lithotrophicum*, was only 93% (**Figure 5**). *S. lithotrophicum* is a sulfur-oxidizing *Epsilonproteobacterium* isolated from deep-sea hydrothermal sediments of the Okinawa trough (Inagaki et al., 2004) and it has since been identified in deep-sea vent communities worldwide (Campbell et al., 2006; Huber et al., 2007; Tokuda et al., 2007; Huber et al., 2010). The identification of *Sulfurovum*-related clones in the Milos vents extended the distribution of this group of *Epsilonproteobacteria* to shallow-water hydrothermal systems. Currently, all the cultured *Epsilonproteobacteria* isolated from geothermal environments are chemolithoautotrophs, although some of these bacteria have the ability to use one-carbon compounds (and in some rare cases complex organic carbon compounds; Campbell et al., 2006; Sievert and Vetriani, 2012). Given the phylogenetic distance between the *Epsilonproteobacteria* identified in this study and both cultured and uncultured relatives, it is possible that the shallow-water hydrothermal vents of Milos harbor members of the *Epsilonproteobacteria* with novel metabolic characteristics. One interesting hypothesis is that such *Epsilonproteobacteria* might be mixotrophic or facultatively heterotrophic. Herrmann et al. (2010) and Hubert et al. (2012) formulated similar hypotheses after detecting *Epsilonproteobacteria* in a benzene-degrading enrichment culture and in discharge waters collected from an oil sands reservoir, respectively. An effort to use alternative strategies to culture and isolate key members of the epsilonproteobacterial community is needed to understand their physiology and metabolism, and ultimately elucidate their role in these ecosystems.

A large number of the sequences retrieved in this study have low similarity to currently cultured bacterial strains (on average 90.1% similarity), while only four sequences (two for each

library, 12.5% of the total investigated sequences) had similarities over 97%, a value considered as cut-off for closely related species/strains (Rossello-Mora and Amann, 2001). The non-redundant database indicated that the closest relatives to the Milos sequences were clones retrieved in the course of microbial diversity surveys of deep-sea hydrothermal vents (Lopez-Garcia et al., 2003; Nakagawa et al., 2005; Hügler et al., 2010), cold-seeps (Wegener et al., 2008) and seamounts (Hodges and Olson, 2009). However, the average similarity with those sequences was rather low (93.6 and 96.7% for MV1 and MV4, respectively). This was particularly true for station MV1, where the average similarity between cultured and uncultured relatives was comparable (**Table 2**). This suggests that the Milos shallow-water hydrothermal vents harbor previously undiscovered taxa, and raises questions about the physiology and metabolism of the *Bacteria* at this site. Aside from temperature, the quantity and quality of organic matter found at the Milos vent (**Table 1**) are likely a key factor in selecting for heterotrophic or facultative heterotrophic bacteria. This observation is supported by the abundance of members of the *Cytophaga-Flavobacteria-Bacteroides* (CFB) cluster in the libraries (**Figure 4**). Since all cultured members of the CFB are heterotrophs, it is reasonable to speculate that the Milos CFB have a similar metabolism.

None of the 16S rRNA gene sequences identified in this study were related to the newly described genus *Galenea*, isolated from the same sediment samples (Giovannelli et al., 2012). In contrast to previous studies, none of the gammaproteobacterial 16S rRNA gene sequences were related to the genus *Thiomicrospira*, and none of the epsilonproteobacterial sequences were related to the genus *Arcobacter*, both of which were previously reported to be abundant in the Milos vents (Brinkhoff et al., 1999; Sievert et al., 1999b, 2000a). This suggests that spatial and/or temporal differences in the composition of the microbial communities of these vents could be enormous. Shallow-water hydrothermal vents are characterized by fluctuating conditions with elevated temporal and spatial variability of oxygen, salinity, composition of fluids, and venting regimes (Wenzhöfer et al., 2000), and they are furthermore affected by weather conditions, swell, tides and currents. Such variability creates micro-niches and high spatial and temporal heterogeneity, possibly leading to an increase of the overall community variability and gamma-diversity.

In conclusion, we showed that prokaryotic abundances at the shallow-water vents of Milos island are comparable to those reported in other shallow-water and deep-sea hydrothermal systems. Temperature appears to be the main driving factor in controlling prokaryotic distribution in proximity of the vent and photoautotrophy seems to increase in the lower temperature regions of the vent system. For the first time, *Sulfurovum*-related sequences were found in shallow-water hydrothermal sediments, which underscores their possible relevance in the microbial communities of both shallow-water and deep-sea hydrothermal vents. The Milos shallow-water hydrothermal vent investigated in this study harbors previously undescribed and unexpected diversity, as most of the sequences retrieved had a very low similarity to previously reported ones.

This may be due to the abundance of organic matter in these systems, which may support *Epsilonproteobacteria* with novel metabolic characteristics. Further attempts to isolate key species in those ecosystems will be important to shed light on their ecology and evolution and to better understand these environments.

## REFERENCES

- Bach, W., Edwards, K., Hayes, J., Huber, J., Sievert, S., and Sogin, M. (2006). Energy in the dark: fuel for life in the deep ocean and beyond. *Eos* 87, 73–78. doi: 10.1029/2006EO070002
- Baross, J. A., and Hoffman, S. E. (1985). Submarine hydrothermal vents and associated gradient environments as sites for the origin and evolution of life. *Orig. Life Evol. B.* 15, 327–345. doi: 10.1007/BF01808177
- Bligh, E. G., and Dyer, W. J. (1959). A rapid method of total lipid extraction and purification. *Can. J. Biochem. Physiol.* 37, 911–917. doi: 10.1139/o59-099
- Botz, R., Stoben, D., Winckler, G., Bayer, R., Schmitt, M., and Faber, E. (1996). Hydrothermal gases offshore Milos Island, Greece. *Chem. Geol.* 130, 161–173. doi: 10.1016/0009-2541(96)00023-X
- Brinkhoff, T., Sievert, S. M., Kuever, J., and Muyzer, G. (1999). Distribution and diversity of sulfur-oxidizing Thiomicrospira spp. at a shallow-water hydrothermal vent in the Aegean Sea (Milos, Greece). *Appl. Environ. Microbiol.* 65, 3843–3849.
- Campbell, B. J., Engel, A. S., Porter, M. L., and Takai, K. (2006). The versatile epsilon-proteobacteria: key players in sulphidic habitats. *Nat. Rev. Microbiol.* 4, 458–468. doi: 10.1038/nrmicro1414
- Chun, J., Lee, J. H., Jung, Y., Kim, M., Kim, S., Kim, B. K., et al. (2007). EzTaxon: a web-based tool for the identification of prokaryotes based on 16S ribosomal RNA gene sequences. *Int. J. Syst. Evol. Micr.* 57, 2259–2261. doi: 10.1099/ijst.0.64915-0
- Comita, P. B., Gagosian, R. B., and Williams, P. M. (1984). Suspended particulate organic material from hydrothermal vent waters at 21 N. *Nature* 307, 450–453. doi: 10.1038/307450a0
- Dando, P., Aliani, S., Arab, H., Bianchi, C., Brehmer, M., Cocito, S., et al. (2000). Hydrothermal studies in the Aegean Sea. *Phys. Chem. Earth B. Hydrol. Oceans Atmos.* 25, 1–8. doi: 10.1016/S1464-1909(99)00112-4
- Dando, P., Hughes, J., Leahy, Y., Niven, S., Taylor, L., and Smith, C. (1995). Gas venting rates from submarine hydrothermal areas around the island of Milos, Hellenic Volcanic Arc. *Cont. Shelf Res.* 15, 913–929. doi: 10.1016/0278-4343(95)80002-U
- Danovaro, R., Manini, E., and Dell'anno, A. (2002). Higher abundance of bacteria than of viruses in deep Mediterranean sediments. *Appl. Environ. Microbiol.* 68, 1468–1472. doi: 10.1128/AEM.68.3.1468-1472.2002
- Fabiano, M., Danovaro, R., and Fraschetti, S. (1995). A three-year time series of elemental and biochemical composition of organic matter in subtidal sandy sediments of the Ligurian Sea (northwestern Mediterranean). *Cont. Shelf Res.* 15, 1453–1469. doi: 10.1016/0278-4343(94)00088-5
- Fitzsimons, M., Dando, P., Hughes, J., Thiermann, F., Akoumianaki, I., and Pratt, S. (1997). Submarine hydrothermal brine seeps off Milos, Greece. Observations and geochemistry. *Mar. Chem.* 57, 325–340. doi: 10.1016/S0304-4203(97)00021-2
- Fry, J. C. (1990). 2 Direct Methods and Biomass Estimation. *Methods Microbiol.* 22, 41–85. doi: 10.1016/S0580-9517(08)70239-3
- Gerchakov, S. M., and Hatcher, P. G. (1972). Improved technique for analysis of carbohydrates in sediments. *Limnol. Oceanogr.* 17, 938–943. doi: 10.4319/lo.1972.17.6.0938
- Giovannelli, D., Grosche, A., Starovoitov, V., Yakimov, M., Manini, E., and Vetriani, C. (2012). Galenea microaerophila gen. nov., sp. nov., a mesophilic, microaerophilic, chemosynthetic, thiosulfate-oxidizing bacterium isolated from a shallow water hydrothermal vent. *Int. J. Syst. Evol. Microbiol.* 62, 3060–3066. doi: 10.1099/ijst.0.040808-0
- Gouy, M., Guindon, S., and Gascuel, O. (2010). SeaView version 4: a multiplatform graphical user interface for sequence alignment and phylogenetic tree building. *Mol. Biol. Evol.* 27, 221–224. doi: 10.1093/molbev/msp259
- Hartree, E. (1972). Determination of protein: a modification of the Lowry method that gives a linear photometric response. *Anal. Biochem.* 48, 422–427. doi: 10.1016/0003-2697(72)90094-2
- Herrmann, S., Kleinstuber, S., Chatzinotas, A., Kuppardt, S., Lueders, T., Richnow, H.-H., et al. (2010). Functional characterization of an anaerobic benzene-degrading enrichment culture by DNA stable isotope probing. *Environ. Microbiol.* 12, 401–411. doi: 10.1111/j.1462-2920.2009.02077.x
- Hodges, T. W., and Olson, J. B. (2009). Molecular comparison of bacterial communities within iron-containing flocculent mats associated with submarine volcanoes along the Kermadec Arc. *Appl. Environ. Microbiol.* 75, 1650–1657. doi: 10.1128/AEM.01835-08
- Huber, J. A., Cantin, H. V., Huse, S. M., Mark Welch, D. B., Sogin, M. L., and Butterfield, D. A. (2010). Isolated communities of Epsilonproteobacteria in hydrothermal vent fluids of the Mariana Arc seamounts. *FEMS Microbiol. Ecol.* 73, 538–549.
- Huber, J. A., Welch, D. B. M., Morrison, H. G., Huse, S. M., Neal, P. R., Butterfield, D. A., et al. (2007). Microbial population structures in the deep marine biosphere. *Science* 318, 97–100. doi: 10.1126/science.1146689
- Huber, T., Faulkner, G., and Hugenholtz, P. (2004). Bellerophon: a program to detect chimeric sequences in multiple sequence alignments. *Bioinformatics* 20, 2317–2319. doi: 10.1093/bioinformatics/bth226
- Hubert, C. R., Oldenburg, T. B. P., Fustic, M., Gray, N. D., Larter, S. R., Penn, K., et al. (2012). Massive dominance of Epsilonproteobacteria in formation waters from a Canadian oil sands reservoir containing severely biodegraded oil. *Environ. Microbiol.* 14, 387–404. doi: 10.1111/j.1462-2920.2011.02521.x
- Hügler, M., Gartner, A., and Imhoff, J. F. (2010). Functional genes as markers for sulfur cycling and CO<sub>2</sub> fixation in microbial communities of hydrothermal vents of the Logatchev field. *FEMS Microbiol. Ecol.* 73, 526–537.
- Inagaki, F., Takai, K., Nealson, K. H., and Horikoshi, K. (2004). *Sulfurovum lithotrophicum* gen. nov., sp. nov., a novel sulfur-oxidizing chemolithoautotroph within the epsilon-Proteobacteria isolated from Okinawa Trough hydrothermal sediments. *Int. J. Syst. Evol. Microbiol.* 54, 1477–1482. doi: 10.1099/ijst.0.03042-0
- Jannasch, H. (1985). Review lecture: the chemosynthetic support of life and the microbial diversity at deep-sea hydrothermal vents. *Proc. Royal Soc. Lond. B* 225, 277–297. doi: 10.1098/rspb.1985.0062
- Larkin, M., Blackshields, G., Brown, N., Chenna, R., Mcgettigan, P., Mcwilliam, H., et al. (2007). Clustal W and Clustal X version 2.0. *Bioinformatics* 23, 2947–2948. doi: 10.1093/bioinformatics/btm404
- Lonsdale, P. (1977). Clustering of suspension-feeding macrobenthos near abyssal hydrothermal vents at oceanic spreading centers. *Deep Sea Res.* 24, 857–863. doi: 10.1016/0146-6291(77)90478-7
- Lopez-Garcia, P., Duperron, S., Philippot, P., Foriel, J., Susini, J., and Moreira, D. (2003). Bacterial diversity in hydrothermal sediment and epsilonproteobacterial dominance in experimental microcolonizers at the Mid-Atlantic Ridge. *Environ. Microbiol.* 5, 961–976. doi: 10.1046/j.1462-2920.2003.00495.x
- Madigan, M. T., Martinko, J. M., Stahl, D. A., and Clark, D. P. (2012). in *Brock Biology of Microorganisms*, 13th Edn. (Pearson Education Inc.), 138–139.
- Maniatis, T. (1989). *Molecular Cloning: A Laboratory Manual/J. Sambrook, EF Fritsch, T. Maniatis*. New York, NY: Cold Spring Harbor Laboratory Press.
- Manini, E., Luna, G., Corinaldesi, C., Zeppilli, D., Bortoluzzi, G., Caramanna, G., et al. (2008). Prokaryote diversity and virus abundance in shallow hydrothermal vents of the Mediterranean Sea (Panarea Island) and the Pacific Ocean (North Sulawesi-Indonesia). *Microb. Ecol.* 55, 626–639. doi: 10.1007/s00248-007-9306-2
- Marsh, J. B., and Weinstein, D. B. (1966). Simple charring method for

## ACKNOWLEDGMENTS

The authors wish to thank the Captain and Crew of R/V Urania for their assistance in sampling operation. This work has been supported by the InterRidge Student and Postdoctoral Fellowships 2011 to Donato Giovannelli and NSF grants MCB 08-43678 and OCE 11-24141 to Costantino Vetriani.

- determination of lipids. *J. Lipid Res.* 7, 574–576.
- Martin, W., Baross, J., Kelley, D., and Russell, M. J. (2008). Hydrothermal vents and the origin of life. *Nat. Rev. Microbiol.* 6, 805–814.
- Maugeri, T. L., Lentini, V., Gugliandolo, C., Cousin, S., and Stackebrandt, E. (2010). Microbial Diversity at a Hot, Shallow-Sea Hydrothermal Vent in the Southern Tyrrhenian Sea (Italy). *Geomicrobiol. J.* 27, 380–390. doi: 10.1080/01490450903451518
- Maugeri, T. L., Lentini, V., Gugliandolo, C., Italiano, F., Cousin, S., and Stackebrandt, E. (2009). Bacterial and archaeal populations at two shallow hydrothermal vents off Panarea Island (Eolian Islands, Italy). *Extremophiles* 13, 199–212. doi: 10.1007/s00792-008-0210-6
- Molari, M., Giovannelli, D., D'errico, G., and Manini, E. (2012). Factors influencing prokaryotic community structure composition in subsurface coastal sediments. *Estuar. Coast. Shelf Sci.* 97, 141–148. doi: 10.1016/j.ecss.2011.11.036
- Moyer, C. L., Dobbs, F. C., and Karl, D. M. (1995). Phylogenetic diversity of the bacterial community from a microbial mat at an active, hydrothermal vent system, Loihi Seamount, Hawaii. *Appl. Environ. Microbiol.* 61, 1555–1562.
- Nakagawa, S., and Takai, K. (2008). Deep-sea vent chemoautotrophs: diversity, biochemistry and ecological significance. *FEMS Microbiol. Ecol.* 65, 1–14. doi: 10.1111/j.1574-6941.2008.00502.x
- Nakagawa, S., Takai, K., Inagaki, F., Hirayama, H., Nunoura, T., Horikoshi, K., et al. (2005). Distribution, phylogenetic diversity and physiological characteristics of epsilon-Proteobacteria in a deep-sea hydrothermal field. *Environ. Microbiol.* 7, 1619–1632. doi: 10.1111/j.1462-2920.2005.00856.x
- Nisbet, E., and Fowler, C. (1996). The hydrothermal imprint on life: did heat-shock proteins, metallocproteins and photosynthesis begin around hydrothermal vents? *Geol. Soc. Lond. Spec. Publ.* 118, 239–251. doi: 10.1144/GSL.SP.1996.118.01.15
- Nisbet, E., and Sleep, N. (2001). The habitat and nature of early life. *Nature* 409, 1083–1091. doi: 10.1038/35059210
- Perriere, G., and Gouy, M. (1996). WWW-query: an on-line retrieval system for biological sequence banks. *Biochimie* 78, 364–369. doi: 10.1016/0300-9084(96)84768-7
- Plante-Cuny, M. R. (1974). *Evaluation par spectrophotométrie des teneurs en chlorophylle a fonctionnelle et en phéopigments des substrats meubles marins*. (Nosy-Bé : ORSTOM).
- Rossello-Mora, R., and Amann, R. (2001). The species concept for prokaryotes. *FEMS Microbiol. Rev.* 25, 39–67. doi: 10.1016/S0168-6445(00)00040-1
- Schneider, C. A., Rasband, W. S., and Eliceiri, K. W. (2012). NIH Image to ImageJ: 25 years of image analysis. *Nat. Methods* 9, 671–675. doi: 10.1038/nmeth.2089
- Sievert, S. M., Brinkhoff, T., Muyzer, G., Ziebis, W., and Kuever, J. (1999a). Spatial heterogeneity of bacterial populations along an environmental gradient at a shallow submarine hydrothermal vent near Milos Island (Greece). *Appl. Environ. Microbiol.* 65, 3834–3842.
- Sievert, S. M., Brinkhoff, T., Muyzer, G., Ziebis, W., and Kuever, J. (1999b). Spatial heterogeneity of bacterial populations along an environmental gradient at a shallow submarine hydrothermal vent near Milos Island (Greece). *Appl. Environ. Microbiol.* 65, 3834–3842.
- Sievert, S. M., Kuever, J., and Muyzer, G. (2000a). Identification of 16S ribosomal DNA-defined bacterial populations at a shallow submarine hydrothermal vent near Milos Island (Greece). *Appl. Environ. Microbiol.* 66, 3102–3109. doi: 10.1128/AEM.66.7.3102-3109.2000
- Sievert, S. M., Ziebis, W., Kuever, J., and Sahm, K. (2000b). Relative abundance of Archaea and Bacteria along a thermal gradient of a shallow-water hydrothermal vent quantified by rRNA slot-blot hybridization. *Microbiology* 146, 1287–1293.
- Sievert, S. M., and Vetriani, C. (2012). Chemoautotrophy at deep-sea vents: past, present, and future. *Oceanography* 25, 218–233. doi: 10.5670/oceanog.2012.21
- Staley, J. T., and Reysenbach, A. L. (2002). *Biodiversity of Microbial Life: Foundation of Earth's Biosphere*. New York, NY: Wiley-Liss.
- Tarasov, V., Gebruk, A., Mironov, A., and Moskalev, L. (2005). Deep-sea and shallow-water hydrothermal vent communities: two different phenomena? *Chem. Geol.* 224, 5–39. doi: 10.1016/j.chemgeo.2005.07.021
- Thiermann, F., Akoumianaki, I., Hughes, J., and Giere, O. (1997). Benthic fauna of a shallow-water gaseohydrothermal vent area in the Aegean Sea (Milos, Greece). *Mar. Biol.* 128, 149–159. doi: 10.1007/s002270050078
- Tokuda, G., Yamada, A., Nakano, K., Arita, N. O., and Yamasaki, H. (2007). Colonization of Sulfovorum sp. on the gill surfaces of Alvinocaris longirostris, a deep-sea hydrothermal vent shrimp. *Mar. Ecol.* 29, 106–114. doi: 10.1111/j.1439-0485.2007.00211.x
- Underwood, A. (1991). Beyond BACI: experimental designs for detecting human environmental impacts on temporal variations in natural populations. *Mar. Freshw. Res.* 42, 569–587. doi: 10.1071/MF9910569
- Valsami-Jones, E., Baltatzis, E., Bailey, E., Boyce, A., Alexander, J., Magganas, A., et al. (2005). The geochemistry of fluids from an active shallow submarine hydrothermal system: Milos island, Hellenic Volcanic Arc. *J. Volcanol. Geother. Res.* 148, 130–151. doi: 10.1016/j.jvolgeores.2005.03.018
- Wegener, G., Niemann, H., Elvert, M., Hinrichs, K. U., and Boetius, A. (2008). Assimilation of methane and inorganic carbon by microbial communities mediating the anaerobic oxidation of methane. *Environ. Microbiol.* 10, 2287–2298. doi: 10.1111/j.1462-2920.2008.01653.x
- Weisburg, W. G., Barns, S. M., Pelletier, D. A., and Lane, D. J. (1991). 16S ribosomal DNA amplification for phylogenetic study. *J. Bacteriol.* 173, 697–703.
- Wenzhöfer, F., Holby, O., Glud, R. N., Nielsen, H. K., and Gundersen, J. K. (2000). *In situ* microsensor studies of a shallow water hydrothermal vent at Milos, Greece. *Mar. Chem.* 69, 43–54. doi: 10.1016/S0304-4203(99)00091-2
- Williamson, S. J., Cary, S. C., Williamson, K. E., Helton, R. R., Bench, S. R., Winget, D., et al. (2008). Lysogenic virus-host interactions predominate at deep-sea diffuse-flow hydrothermal vents. *Isme. J.* 2, 1112–1121. doi: 10.1038/ismej.2008.73
- Conflict of Interest Statement:** The authors declare that the research was conducted in the absence of any commercial or financial relationships that could be construed as a potential conflict of interest.
- Received:** 11 January 2013; **accepted:** 18 June 2013; **published online:** 08 July 2013.
- Citation:** Giovannelli D, d'Errico G, Manini E, Yakimov M and Vetriani C (2013) Diversity and phylogenetic analyses of bacteria from a shallow-water hydrothermal vent in Milos island (Greece). *Front. Microbiol.* 4:184. doi: 10.3389/fmicb.2013.00184
- This article was submitted to Frontiers in Extreme Microbiology, a specialty of Frontiers in Microbiology.
- Copyright © 2013 Giovannelli, d'Errico, Manini, Yakimov and Vetriani. This is an open-access article distributed under the terms of the Creative Commons Attribution License, which permits use, distribution and reproduction in other forums, provided the original authors and source are credited and subject to any copyright notices concerning any third-party graphics etc.



# Biogeochemical implications of the ubiquitous colonization of marine habitats and redox gradients by *Marinobacter* species

Kim M. Handley<sup>1,2\*</sup> and Jonathan R. Lloyd<sup>3</sup>

<sup>1</sup> Searle Chemistry Laboratory, Computation Institute, University of Chicago, Chicago, IL, USA

<sup>2</sup> Computing, Environment and Life Sciences, Argonne National Laboratory, Chicago, IL, USA

<sup>3</sup> School of Earth, Atmospheric, and Environmental Sciences, University of Manchester, Manchester, UK

**Edited by:**

Andreas Teske, University of North Carolina at Chapel Hill, USA

**Reviewed by:**

Purificacion Lopez-Garcia, Centre National de la Recherche Scientifique, France

Juergen Wiegel, University of Georgia, USA

**\*Correspondence:**

Kim M. Handley, Searle Chemistry Laboratory, Computation Institute, University of Chicago, 5735 South Ellis Avenue, Chicago, IL 60637, USA.

e-mail: kmhandley@uchicago.edu

The *Marinobacter* genus comprises widespread marine bacteria, found in localities as diverse as the deep ocean, coastal seawater and sediment, hydrothermal settings, oceanic basalt, sea-ice, sand, solar salterns, and oil fields. Terrestrial sources include saline soil and wine-barrel-decalcification wastewater. The genus was designated in 1992 for the Gram-negative, hydrocarbon-degrading bacterium *Marinobacter hydrocarbonoclasticus*. Since then, a further 31 type strains have been designated. Nonetheless, the metabolic range of many *Marinobacter* species remains largely unexplored. Most species have been classified as aerobic heterotrophs, and assessed for limited anaerobic pathways (fermentation or nitrate reduction), whereas studies of low-temperature hydrothermal sediments, basalt at oceanic spreading centers, and phytoplankton have identified species that possess a respiratory repertoire with significant biogeochemical implications. Notable physiological traits include nitrate-dependent Fe(II)-oxidation, arsenic and fumarate redox cycling, and Mn(II) oxidation. There is also evidence for Fe(III) reduction, and metal(lloid) detoxification. Considering the ubiquity and metabolic capabilities of the genus, *Marinobacter* species may perform an important and underestimated role in the biogeochemical cycling of organics and metals in varied marine habitats, and spanning aerobic-to-anoxic redox gradients.

**Keywords:** *Marinobacter*, marine, hydrothermal, biogeochemical cycling, hydrocarbon, iron, arsenic, opportunistic

## INTRODUCTION

Marine habitats are host to a diverse range of substrates and physicochemical regimes. Among these, hydrothermal features attract particular interest owing to ore-grade concentrations of metals, physicochemical extremes, and the presence of chemolithoautotrophic macrofauna and microbiota. Bacteria and Archaea occupying marine habitats have a substantial physical presence. There are an estimated  $3.9 \times 10^{30}$  prokaryotic cells in the open ocean and unconsolidated marine sediments, comprising  $\sim 3.1 \times 10^{11}$  tonnes of carbon (Whitman et al., 1998). This is slightly more than the estimated carbon content of terrestrial prokaryotes, and just under half of that in all plant life. Prokaryotes can contribute significantly to marine ecosystem functioning and biogeochemical cycles (Jørgensen, 2006), owing to their prevalence and enormous capacity for transforming their environments through metabolism of organic and inorganic matter (Gadd, 2010). Yet much of the marine microbial biomass remains unexplored, and there is still much to learn about heterotrophic and autotrophic bacterial functioning in the ocean (e.g., Moran et al., 2004; Emerson et al., 2010; Holden et al., 2012).

*Marinobacter* is a heterotrophic, and in some instances mixotrophic (Dhillon et al., 2005; Handley et al., 2009a,b), metabolically flexible genus found in an exceptionally wide range of marine and saline terrestrial settings, including various

low-temperature hydrothermal environments (Table 1). The genus comprises Gram-negative *Gammaproteobacteria* within the *Alteromonadales* order. All known species are motile with polar flagella (excluding *M. goseongensis*, Roh et al., 2008), slightly to moderately halophilic (cf. DasSarma and Arora, 2012), aerobic heterotrophs (Table 2). However, few are confirmed strict aerobes, and several are facultative anaerobes (Table 1). All are rod-shaped, with the exception of the ellipsoidal *M. Segnicrescens* (Guo et al., 2007), and most are neutrophilic, except the slightly alkaliphilic *M. alkaliphilus*, which grows optimally at pH 8.5–9.0 (Takai et al., 2005; also see Al-Awadhi et al., 2007; Table 2). Although most species are mesophilic, many are psychrotolerant (also known as psychrotrophic) and capable of growth down to  $\sim 4^{\circ}\text{C}$  (Table 2; Moyer and Morita, 2007). A couple of other species are either psychrophilic (with a growth optimum near  $15^{\circ}\text{C}$ ) or thermotolerant (with growth up to  $50^{\circ}\text{C}$  and an optimum of  $45^{\circ}\text{C}$ ). This phenotypic versatility contributes to the ubiquity of this genus, and its ability to occupy diverse physicochemical regimes.

## MARINOBACTER HYDROCARBONOCLASTICUS, DENITRIFICATION AND HYDROCARBONS

The genus was created for *M. hydrocarbonoclasticus*, which was isolated from hydrocarbon-polluted sediment, collected from the

**Table 1 | Marinobacter species metabolism and isolation source.**

| <i>Marinobacter</i> species                           | HC | CH <sup>b</sup> | NO <sub>3</sub> <sup>-</sup> | Gluc ferm | AA | Anaer  | Env       | Isolation source  |
|---|----|-----------------|------------------------------|-----------|----|--------|-----------|---|
| <i>hydrocarbonoclasticus</i> <sup>1,a</sup>           | Y  | N               | resp                         | N         | Y  | Y      | –         | Oil-polluted sediment; Gulf of Fos; Mediterranean coast; France                   |
| <i>aquaeolei</i> <sup>2</sup>                         | Y  | N               | resp                         | N         | Y  | Y      | –         | Oil-producing well-head; offshore platform; Vietnam                               |
| <i>excellens</i> <sup>3,a</sup>                       | –  | Y               | resp                         | Y         | Y  | Y      | 12°C      | Radionuclide-polluted sediment; 0.5 m depth; Chazhma Bay; Sea of Japan; Russia    |
| <i>lipolyticus</i> <sup>4,a</sup>                     | –  | Y               | N                            | –         | N  | st-aer | –         | Saline soil; seaside city of Cádiz; Spain   |
| <i>squalenivorans</i> <sup>5</sup>                    | Y  | –               | resp                         | N         | Y  | Y      | –         | Oil-contaminated coastal sediment; Carteau Cove; Gulf of Fos; France              |
| <i>lutaoensis</i> <sup>6,a</sup>                      | –  | Y               | N                            | N         | Y  | st-aer | 43°C      | Coastal hot spring water; Lutao; Taiwan   |
| <i>litoralis</i> <sup>7,a</sup>                       | –  | –               | Y                            | N         | N  | N      | –         | Sea water; Jungdongjin beach; East Sea; Korea                                     |
| <i>flavimaris</i> <sup>8,a</sup>                      | –  | Y               | Y                            | –         | N  | Y      | –         | Sea water; Daepo Beach; Yellow Sea; Korea   |
| <i>daepoensis</i> <sup>8,a</sup>                      | –  | –               | N                            | –         | N  | Y      | –         | Sea water; Daepo Beach; Yellow Sea; Korea   |
| <i>bryozoorum</i> <sup>9,a</sup>                      | –  | Y               | Y                            | –         | Y  | Y      | –         | Sediment; Bearing Sea; Russia   |
| <i>sediminum</i> <sup>9,a</sup>                       | –  | Y               | –                            | –         | Y  | –      | –         | Sediment; Peter the Great Bay; Sea of Japan; Russia                               |
| <i>maritimus</i> <sup>10,a</sup>                      | Y  | Y               | –                            | –         | Y  | –      | –         | Sea water; 110 km SW of subantarctic Kerguelen islands                            |
| <i>alkaliphilus</i> <sup>11</sup>                     | Y  | Y               | Y                            | –         | Y  | Y      | 1.7–1.9°C | Subseafloor alkaline serpentine mud; South Chamorro Seamount; Mariana Forearc     |
| <i>algicola</i> <sup>12,a</sup>                       | Y  | Y               | resp                         | –         | Y  | Y      | –         | Dinoflagellate <i>Gymnodinium catenatum</i> ; Yellow Sea; Korea                   |
| <i>koreensis</i> <sup>13,a</sup>                      | –  | N               | Y                            | N         | Y  | Y      | –         | Sea-shore sand at Homi Cape; Pohang; Korea  |
| <i>vinifirmus</i> <sup>14,a</sup>                     | –  | N               | N                            | N         | N  | st-aer | –         | Wine tank decalcification wastewater-evaporation pond. Location?                  |
| <i>salsuginis</i> <sup>15,a</sup>                     | Y  | Y               | resp                         | Y         | Y  | Y      | –         | Brine-seawater interface; Shaban Deep (a brine-filled deep); Red Sea              |
| <i>gudaonensis</i> <sup>16,17,a</sup>                 | Y  | Y               | Y                            | –         | Y  | Y      | –         | Oil-polluted soil underlying wastewater from the coastal Shengli Oil field; China |
| <i>segnicrescens</i> <sup>17,a</sup>                  | N  | Y               | Y                            | –         | N  | Y      | –         | Benthic sediment; 1161 m depth; South China Sea                                   |
| <i>salicampi</i> <sup>18,a</sup>                      | –  | N               | Y                            | –         | –  | Y      | –         | Sediment; marine solar saltern; Yellow Sea; Korea                                 |
| <i>pelagius</i> <sup>19,a</sup>                       | –  | N               | Y                            | –         | Y  | –      | –         | Coastal seawater; Zhoushan Archipelago; China                                     |
| <i>guineae</i> <sup>20,a</sup>                        | –  | Y               | resp                         | N         | –  | Y      | –         | Marine sediment; Deception Island; Antarctica                                     |
| <i>psychrophilus</i> <sup>21,a</sup>                  | –  | Y               | Y                            | –         | Y  | –      | Freezing  | Sea-ice; Canadian Basin; Arctic Ocean   |
| <i>mobilis</i> ; <i>zhejiangensis</i> <sup>22,a</sup> | –  | N               | Y                            | –         | Y  | –      | –         | Sediment; Dayu Bay; East China Sea (Lat. 27.33, Long. 120.57)                     |
| <i>goseongensis</i> <sup>23,a</sup>                   | –  | N               | –                            | –         | N  | –      | –         | Coastal seawater; 100 m depth; East Sea of Korea                                  |
| <i>santoriniensis</i> <sup>24,a</sup>                 | G  | N               | resp                         | N         | –  | Y      | 25°C      | Ferruginous hydrothermal marine sediment; Santorini; Greece                       |
| <i>szutsaonensis</i> <sup>25,a</sup>                  | –  | Y               | Y                            | –         | Y  | –      | 16–17°C   | Soil; Szutsao solar saltern; southern Taiwan                                      |
| <i>lacisalsi</i> <sup>26,a</sup>                      | –  | N               | Y                            | –         | N  | –      | –         | Water; hypersaline lake; ~50 km inland; saline-wetland; Fuente de Piedra; Spain   |
| <i>zhanjiangensis</i> <sup>27,a</sup>                 | –  | Y               | Y                            | –         | N  | –      | –         | Sea water; tidal flat, Naozhou Island; South China Sea                            |
| <i>oulmenensis</i> <sup>28,a</sup>                    | –  | Y               | N                            | N         | Y  | –      | –         | Brine; salt concentrator (input material?); ~60 km inland; Ain Oulmene; Algeria.  |
| <i>daqiaonensis</i> <sup>29,a</sup>                   | –  | Y               | N                            | N         | –  | –      | –         | Sediment; Daqiao salt pond; Yellow Sea; east coast of China                       |
| <i>adhaerens</i> <sup>30,a</sup>                      | –  | Y               | N                            | –         | Y  | –      | –         | <i>Thalassiosira weissflogii</i> diatom aggregates; Wadden sea surface; Germany   |
| <i>antarcticus</i> <sup>31,a</sup>                    | –  | Y               | Y                            | –         | Y  | –      | –         | Intertidal sandy sediment; Larsemann Hills; Antarctica                            |

(Continued)

**Table 1 | Continued**

| <i>Marinobacter</i> species                        | HC | CH <sup>b</sup> | NO <sub>3</sub> <sup>-</sup> | Gluc ferm | AA | Anaer | Env        | Isolation source   |
|--|----|-----------------|------------------------------|-----------|----|-------|------------|--|
| <i>xestospongiae</i> <sup>32,a</sup>               | –  | Y               | Y                            | Y         | Y  | –     | –          | Coastal marine sponge; 8 m depth; Obhor Sharm; Red Sea; Saudi Arabia                 |
| Terrestrial strain MB <sup>33</sup>                | –  | –               | –                            | –         | –  | Y     | –          | Cyanobacterial mat; saline lake; near the Red Sea                                    |
| <i>manganoxydans</i> <sup>34</sup>                 | G  | –               | –                            | –         | –  | –     | –          | Heavy metal-rich sediment; hydrothermal vent; Indian Ocean (Lat. 25.32, Long. 70.04) |
| <i>Marinobacter</i> -like isolates <sup>35,c</sup> | –  | N               | –                            | –         | –  | Y     | ~4°C       | Weathering metal sulfide rock and sediment; Main Endeavour/Middle Valley; JdFR       |
| <i>Marinobacter</i> -like clones <sup>36,d</sup>   | –  | –               | –                            | –         | –  | –     | ≥4°C       | Metal sulfides rock and sediment; Main Endeavour/Middle Valley; JdFR                 |
| <i>Marinobacter</i> clones <sup>37,e</sup>         | –  | –               | –                            | –         | –  | –     | 4°C        | Relict 50 ka metal sulfide sediment; Alvin mound; TAG; Mid-Atlantic Ridge            |
| <i>Marinobacter</i> isolates <sup>38,f</sup>       | –  | –               | –                            | –         | –  | –     | ~2°C       | Lateral hydrothermal plumes; Mothra vent field and Axial Seamount; JdFR              |
| <i>Marinobacter</i> env/enrich <sup>39,g</sup>     | –  | –               | –                            | –         | –  | –     | –0.4–0.8°C | Fresh basalt; Arctic oceanic spreading ridges; Norwegian-Greenland Sea               |

<sup>a</sup>Validly published species names as of April 2013.<sup>b</sup>Carbohydrates used by species are glucose, glycerol, fructose, maltose, mannitol, sucrose, cellobiose, galactose, dextrin, sorbitol, trehalose, xylose, ribose, sorbose, erythritol, inositol, dulcitol, arabinose, and N-acetyl-D-glucosamine.<sup>c–g</sup>87–94%, 89–97%, 96–99%, 99%, 96–98% 16S rRNA gene sequence similarity to *Marinobacter* species, respectively.

Abbreviations: HC, hydrocarbon utilization; CH, carbohydrate utilization; NO<sub>3</sub><sup>-</sup>, nitrate reduction; gluc ferm, glucose fermentation; AA, amino acid metabolism; Env, environment; Y, yes; N, no; –, unknown; G, genomic evidence; resp, respiratory; st-aer, strict aerobe; env/enrich, environmental/enrichment; JdFR, Juan de Fuca Ridge; TAG, Trans-Atlantic Geotransverse hydrothermal field.

1–39 References: <sup>1</sup>Gauthier et al., 1992; <sup>2</sup>Huu et al., 1999 and Márquez and Ventosa, 2005; <sup>3</sup>Gorshkova et al., 2003; <sup>4</sup>Martín et al., 2003; <sup>5</sup>Rontani et al., 2003; <sup>6</sup>Shieh et al., 2003 and Validation List no. 94., 2003; <sup>7</sup>Yoon et al., 2003; <sup>8</sup>Yoon et al., 2004; <sup>9</sup>Romanenko et al., 2005; <sup>10</sup>Shivaji et al., 2005; <sup>11</sup>Takai et al., 2005; <sup>12</sup>Green et al., 2006; <sup>13</sup>Kim et al., 2006; <sup>14</sup>Liebgott et al., 2006; <sup>15</sup>Antunes et al., 2007; <sup>16</sup>Gu et al., 2007; <sup>17</sup>Guo et al., 2007; <sup>18</sup>Yoon et al., 2007; <sup>19</sup>Xu et al., 2008; <sup>20</sup>Montes et al., 2008; <sup>21</sup>Zhang et al., 2008; <sup>22</sup>Huo et al., 2008; <sup>23</sup>Roh et al., 2008; <sup>24</sup>Handley et al., 2009a, 2010; <sup>25</sup>Wang et al., 2007, 2009; <sup>26</sup>Aguilera et al., 2009; <sup>27</sup>Zhuang et al., 2009 and Validation List no. 148., 2012; <sup>28</sup>Kharroub et al., 2011; <sup>29</sup>Qu et al., 2011; <sup>30</sup>Kaeppele et al., 2012; <sup>31</sup>Liu et al., 2012; <sup>32</sup>Lee et al., 2012; <sup>33</sup>Sigalevich et al., 2000; <sup>34</sup>Wang et al., 2012; <sup>35</sup>Edwards et al., 2003; <sup>36</sup>Rogers et al., 2003; <sup>37</sup>Müller et al., 2010; <sup>38</sup>Kaye and Baross, 2000; <sup>39</sup>Lysnes et al., 2004.

mouth of an oil refinery outlet along the French Mediterranean coast (Gauthier et al., 1992), and includes the later heterotypic synonym, *M. aquaeolei* (Huu et al., 1999; Márquez and Ventosa, 2005). The species has an obligate requirement for sodium. It grows readily on complex organic media containing yeast extract and peptone, and aerobically on a range of organic acids (acetate, butyrate, caproate, fumarate, adipate, lactate, citrate), and the amino acids L-glutamate, L-glutamine, and L-proline. Under anaerobic conditions *M. hydrocarbonoclasticus* can perform denitrification using a membrane-bound respiratory NarGHI complex to reduce nitrate (Correia et al., 2008). The nitrite formed is reduced to N<sub>2</sub> via nitrite reductase cytochrome cd1 (Besson et al., 1995), nitric oxide reductase NorBC (EMBL-EBI ABM20188.1, ABM20189.1), and nitrous oxide reductase (Prudêncio et al., 2000). *M. hydrocarbonoclasticus* is most notable, however, for its ability to aerobically degrade liquid and solid, aliphatic (pristane, heneicosane, eicosane, hexadecane, tetradecane) and aromatic (phenanthrene, phenyldecane) hydrocarbons. It uses each hydrocarbon as a sole energy source, and produces large quantities of bioemulsifier. Bioemulsifiers (biosurfactants), are thought to aid in bacterial adhesion to hydrophobic surfaces, water-immiscible material breakdown, and competitor inhibition, and are attracting increasing interest for various industrial applications

(Banat et al., 2000; Nerurkar et al., 2009; Williams, 2009; Soberón-Chávez and Maier, 2011).

Of the 34 species named since the genus was created, several exhibit hydrocarbonoclastic activity, while others remain untested (Table 1). Additional hydrocarbons utilized by *Marinobacter* species include squalene, which is metabolized under denitrifying conditions (Rontani et al., 2003), polycyclic aromatic hydrocarbons (PAHs) (Cui et al., 2008), hexane, heptane, petroleum ether (Shivaji et al., 2005; Antunes et al., 2007), n-pentadecane, n-tridecane, n-undecane, n-decane, n-nonane, butane, and kerosene (Takai et al., 2005).

This hydrocarbonoclastic capacity in *Marinobacter* has attracted attention owing to the potential for these bacteria to remediate crude oil contamination in environments as diverse as the Arabian Gulf (Al-Awadhi et al., 2007) and Artic sea ice (Gerdes et al., 2005). Nitrate reduction by *Marinobacter* species has also been exploited for potential use in oilfield maintenance. Dunsmore et al. (2006) showed reduction of added nitrate prevented deleterious growth of sulfate-reducing bacteria in produced water from a North Sea oilfield oil reservoir, controlling microbial souring reactions. The beneficial reduction of nitrate was largely attributed to indigenous *Marinobacter* species.

**Table 2 | Marinobacter species attributes.**

| <i>Marinobacter</i> species                 | Halophilic | Optimum salinity (%) | Salinity range (%) | Mesophilic | Optimum temp (°C) | Temp range (°C) | Optimum pH | Major resp. quinone (ubiquinone) | G + C (%) <sup>a</sup> | Motility mechanism <sup>b</sup> |
|---|------------|----------------------|--------------------|------------|-------------------|-----------------|------------|----------------------------------|------------------------|---------------------------------|
| <i>hydrocarbonoclasticus</i> <sup>1,2</sup> | s-mod      | 3–6                  | 0.5–20             | Y          | 32                | 10–45           | 7.0–7.5    | Q9                               | (52.7) 57.3            | Polar flagellum <sup>c</sup>    |
| <i>aquaeolei</i> <sup>2</sup>               | slightly   | 5                    | 0–20               | Y          | 30                | 13–50           | –          | Q9                               | 55.7                   | Polar flagellum                 |
| <i>excellens</i> <sup>3</sup>               | –          | –                    | 1–15               | Y          | 28                | 10–41           | 7.5        | Q9                               | 56                     | Polarly flagellated             |
| <i>lipolyticus</i> <sup>4</sup>             | mod        | 7.5                  | 1–15               | Y          | 37                | 15–40           | 7.5        | –                                | 57                     | –                               |
| <i>squalenivorans</i> <sup>5</sup>          | –          | –                    | >0                 | Y          | 32                | –               | –          | –                                | 54.3                   | Polar flagellum                 |
| <i>lutaoensis</i> <sup>6</sup>              | slightly   | 3–5                  | 0.5–12             | therm      | 45                | 25–50           | 7.0        | Q8                               | 63.5                   | One–several flagella            |
| <i>litoralis</i> <sup>7</sup>               | s-mod      | 2–7                  | 0.5–18             | psyt       | 30–37             | 4–46            | 7.0–8.5    | Q9                               | 55                     | Polar flagellum                 |
| <i>flavimaris</i> <sup>8</sup>              | s-mod      | 2–6                  | >0–20              | psyt       | 37                | ≤4–45           | 7.0–8.0    | Q9                               | 58                     | Polar flagellum                 |
| <i>daepoensis</i> <sup>5</sup>              | s-mod      | 2–6                  | >0–18              | psyt       | 30–37             | >4–45           | 7.0–8.0    | Q9                               | 57                     | Polar flagellum                 |
| <i>bryozoorum</i> <sup>9</sup>              | –          | –                    | 1.0–18             | Y          | –                 | 7–42            | –          | –                                | 59.6                   | –                               |
| <i>sediminum</i> <sup>9</sup>               | –          | –                    | 0.5–18             | psyt       | –                 | 4–42            | –          | –                                | 56.5                   | –                               |
| <i>maritimus</i> <sup>10</sup>              | slightly   | 4                    | 1–13               | psyt       | 22                | 4–37            | 8.5        | Q9                               | 58                     | –                               |
| <i>alkaliphilus</i> <sup>11</sup>           | slightly   | 2.5–3.5              | 0–21               | Y          | 30–35             | 10–45           | 8.5–9.0    | –                                | 57.5                   | Polar flagellum                 |
| <i>algicola</i> <sup>12</sup>               | s-mod      | 3–6                  | 1.0–12             | psyt       | 25–30             | 5–40            | 7.5        | Q9                               | 54–55                  | Polar flagellum <sup>c</sup>    |
| <i>koreensis</i> <sup>13</sup>              | s-mod      | 3–8                  | 0.5–20             | Y          | 28                | 10–45           | 6.0–8.0    | Q9                               | 54.1                   | Polar flagellum                 |
| <i>vinifirmus</i> <sup>14</sup>             | s-mod      | 3–6                  | 0–20               | Y          | 20–30             | 15–45           | 6.5–8.4    | –                                | 58.7                   | –                               |
| <i>salsuginis</i> <sup>15</sup>             | slightly   | 5                    | 1–20               | Y          | 35–37             | 10–45           | 7.5–8.0    | Q9                               | 55.9                   | Polar flagellum                 |
| <i>gudaonensis</i> <sup>16</sup>            | slightly   | 2.0–3.0              | 0–15               | Y          | –                 | 10–45           | 7.5–8.0    | Q9                               | 57.9                   | Polar flagellum                 |
| <i>segnicrescens</i> <sup>17</sup>          | s-mod      | 4–8                  | 1–15               | Y          | 30–37             | 15–45           | 7.5–8.0    | Q9                               | 62.2                   | Polar flagellum                 |
| <i>salicampi</i> <sup>18</sup>              | s-mod      | 8                    | >0–15              | psyt       | 30                | 4–39            | 7.0–8.0    | Q9                               | 58.1                   | Polar flagellum                 |
| <i>pelagius</i> <sup>19</sup>               | slightly   | 5.0                  | 0.5–15             | psyt       | 35–30             | 4–48            | 7.0–8.0    | –                                | 59.0                   | –                               |
| <i>guineae</i> <sup>20</sup>                | –          | –                    | 1–15               | psyt       | –                 | 4–42            | –          | Q9                               | 57.1                   | Polar flagella                  |
| <i>psychrophilus</i> <sup>21</sup>          | –          | –                    | 2–8                | psyph      | 16–18             | 0–22            | 6.0–9.0    | Q9                               | 55.4                   | –                               |
| <i>mobilis</i> <sup>22</sup>                | slightly   | 3.0–5.0              | 0.5–10.0           | Y          | 30–35             | 15–42           | 7.0–7.5    | –                                | 58.0–58.9              | Polar flagellum                 |
| <i>zhejiangensis</i> <sup>22</sup>          | slightly   | 1.0–3.0              | 0.5–10.0           | Y          | 30–35             | 15–42           | 7.0–7.5    | –                                | 58.4                   | Polar flagellum                 |
| <i>goseongensis</i> <sup>23</sup>           | slightly   | 4–5                  | 1–25               | Y          | 25–30             | 10–37           | 7.5        | –                                | –                      | –                               |
| <i>santoriniensis</i> <sup>24</sup>         | mod        | 5–10                 | 0.5–16             | Y          | 35–40             | 15–45           | 7–8        | Q9                               | 58.1                   | Polar flagellum                 |
| <i>szutsaonensis</i> <sup>25</sup>          | slightly   | 5                    | 0–20               | Y          | 35–40             | 10–50           | 7.5–8.0    | Q9                               | 56.5                   | Polar flagellum                 |
| <i>lacisalsi</i> <sup>26</sup>              | mod        | 7.5                  | 3–15               | Y          | 30–35             | 20–40           | 7.0        | –                                | 58.6                   | Polar flagellum                 |
| <i>zhanjiangensis</i> <sup>27</sup>         | slightly   | 2–4                  | 1–15               | psyt       | 25–30             | 4–35            | 7.5        | Q9                               | 60.6                   | Polar flagellum                 |
| <i>oulmenensis</i> <sup>28</sup>            | mod        | 5–7.5                | 1–15               | Y          | 37–40             | 30–47           | 6.5–7.0    | Q9                               | 57.4                   | –                               |
| <i>daqiaonensis</i> <sup>29</sup>           | mod        | 5–10                 | 1–15               | Y          | 30                | 10–45           | 7.5        | Q9                               | 60.8                   | Polar flagellum                 |
| <i>adhaerens</i> <sup>30</sup>              | s-mod      | 2–6                  | 0.5–20             | Y          | 34–38             | 4–45            | 7.0–8.5    | Q9                               | 56.9                   | Polar flagellum                 |
| <i>antarcticus</i> <sup>31</sup>            | slightly   | 3.0–4.0              | 0–25               | psyt       | 25                | 4–35            | 7.0        | –                                | 55.8                   | Polar flagellum                 |
| <i>xestospongiae</i> <sup>32</sup>          | slightly   | 2.0                  | 0.5–6.0            | Y          | 28–36             | 15–42           | 7.0–8.0    | Q9                               | 57.1                   | Polar flagellum                 |

<sup>a</sup>GC contents range from 54.0–63.5% (average, 57.6%), using the Márquez and Ventosa (2005) value for *hydrocarbonoclasticus*.<sup>b</sup>All species are motile, excluding *M. goseongensis*. *M. lutaoensis* also has bipolar pili. The number of flagella on *M. guineae* cells is unknown.<sup>c</sup>Unsheathed flagellum.

Abbreviations: Haloph, halophile; Mesoph, mesophile; temp, temperature; resp, respiratory; Y, yes; N, no; –, unknown; s-mod, slightly-moderately; psyt, psychrotolerant; psyph, psychrophile; therm, thermotolerant.

1–32 References: refer to **Table 1**.

## EXPANDED FUNCTIONAL TRAITS OF THE GENUS

Following the characterization of *M. hydrocarbonoclasticus*, the functional range of the genus has been further expanded to include (non-exhaustively) fermentation; the ability to respire at least 19 different carbohydrates (**Table 1**) and several extra amino (e.g., L-alanine, D-glutamate, L-phenylalanine; Antunes et al., 2007 and Green et al., 2006) and organic acids [e.g., malonate, formate, pyruvate, alpha-ketoglutarate; Kim et al. (2006) and Kharroub et al. (2011)]; degradation of the isoprenoid ketone 6,10,14-trimethylpentadecan-2-one (Rontani et al., 1997);

growth on ethanol (Gu et al., 2007; Huo et al., 2008), phenol (Liebgott et al., 2006), and various Tweens (e.g., Takai et al., 2005; Green et al., 2006) following enzymatic evidence in *M. hydrocarbonoclasticus*; utilization of fumarate as an electron acceptor (Takai et al., 2005; Handley et al., 2009a); and oxidation/reduction of arsenic, iron or manganese (Handley et al., 2009a,b; Wang et al., 2012).

As for *M. hydrocarbonoclasticus*, all subsequently described species are able to grow aerobically on complex organic matter, and oxidize organic acids. Many, but not all are enzymatically able

to reduce nitrate (**Table 1**). Lack of fermentation by *M. hydrocarbonoclasticus* was initially proposed as a distinctive feature of the genus; however, a number of subsequently isolated type strains exhibit both fermentative and respiratory metabolisms, owing to their ability to ferment glucose (**Table 1**), lactate (Handley et al., 2009a) and other substrates (Lee et al., 2012). Evaluation of recently available genome sequences also suggests certain *Marinobacter* species may exhibit enzymatic resistance to arsenic and heavy metals (e.g., Wang et al., 2012).

## BIOGEOGRAPHY AND PHYLOGENY

*Marinobacter* colonize diverse saline habitats, e.g., sea ice and hydrothermal sediments, facilitated by psychrophilic to thermotolerant physiologies, and an ability to metabolize an array of (in)organic compounds under aerobic or anaerobic conditions. However, evaluation of phylogenetic trees, constructed using 16S rRNA gene sequences, suggest the genus is monophyletic, forming a single clade distinct from other closely related epsilonproteobacterial lineages (**Figure 1**).

Despite the physiological versatility of the genus, and the ability of some strains to grow (non-optimally) without salt (e.g., Huu et al., 1999; Sigalevich et al., 2000; Liebgott et al., 2006), *Marinobacter* appear to be geographically restricted to marine or terrestrial environments rich in sodium salts. This observation is consistent with the hypothesis that microorganisms exhibit non-random biogeographical differentiation and distribution, due in part to environmental selection (Martiny et al., 2006).

In marine environments, dispersal does not appear to be a limiting factor for *Marinobacter*. Strains have been isolated from, and phylogenetically detected in, oceans (Pacific, Atlantic, Indian, Arctic, and Antarctic) and seas, spanning the globe from pole to equator (**Table 1**; Kaye et al., 2011). They display both attached and planktonic lifestyles, and the distribution of the genus extends from deep-ocean (hydrothermal) benthic sediment and exposed basalt to surface water, or coastal (hydrothermal) sediment, hot spring water and sand (**Table 1**; **Figure 1**).

In many instances, terrestrial isolation sources can be clearly linked to the ocean (e.g., coastal solar salterns and hot springs, and polluted soil from a coastal oil field; **Table 1**). Isolation of species from terrestrial sources, up to 50–60 km inland, implies a greater degree of terrestrial dispersal (**Table 1**; **Figure 1** and Table S2 in Kaye et al., 2011). However, there is insufficient information regarding the nature of terrestrial isolation sources, and too few isolate and phylogenetic data, to judge how well-dispersed this genus is on land, or whether terrestrial sources are strictly independent from marine influences.

## LIFESYLES

In many respects *Marinobacter* species are generalists like their marine and terrestrial *Alteromonadales* cousins in the *Shewanella* genus. *Shewanella* species are respiratory generalists (e.g., Heidelberg et al., 2002), and at least one species (*S. baltica*) has been described as “very close to the ultimate [marine] *r*-strategist,” starkly contrasting with genetically streamlined *K*-strategist (or oligotrophic) marine bacteria like *Prochlorococcus* (Caro-Quintero et al., 2011). In the presence of surplus organic

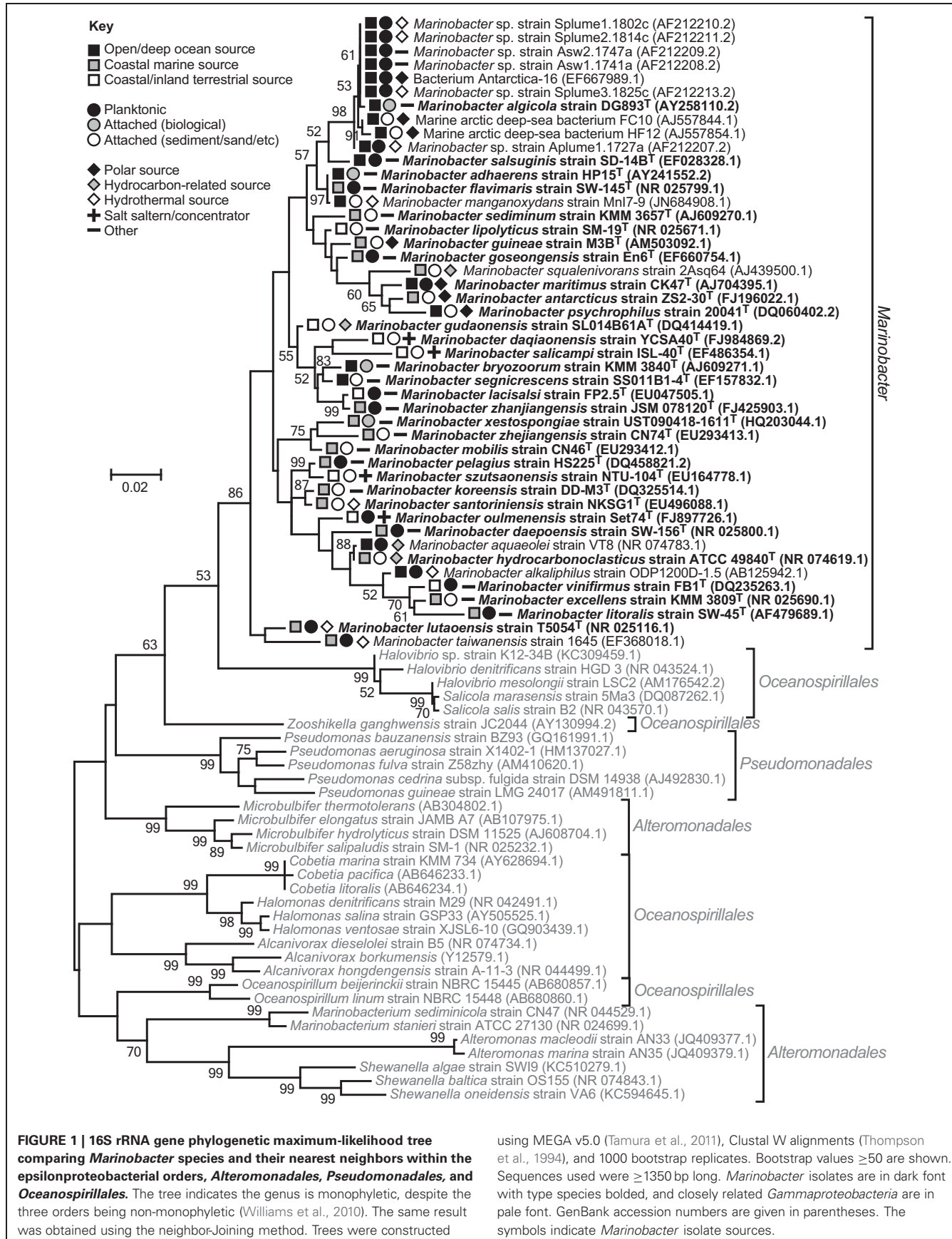
carbon, *Marinobacter* can grow rapidly, out-competing other bacteria in enrichment cultures (e.g., Handley et al., 2010). This *r*-strategist (or copiotrophic) behavior renders them weed-like and relatively easy to cultivate, even compared with other heterotrophic marine bacteria (Kaye and Baross, 2000). *Marinobacter* can also excel under aerobic-to-anaerobic conditions with no added substrate, while in the presence of Fe(II) (Edwards et al., 2003; Handley et al., 2013a).

This type of lifestyle exhibited by *Marinobacter* strains has been described as opportunistic or “opportunitrophic” (Singer et al., 2011), following the definition given by Moran et al. (2004) in describing the ability of the marine bacterium *Silicibacter pomeroyi* to switch rapid between lithoheterotrophy to heterotrophy in response to nutrient pulses. Use of “-troph” in this context describes the mode of obtaining nourishment (as for the term “psychrotroph”) rather than the source of the nourishment (as in “organotroph”), and as such may be considered a misnomer. The term was applied in order to differentiate between types of fast growing and nominally *r*-strategist bacteria, specifically between specialists (e.g., *Geobacter*, Mahadevan and Lovley, 2008), and generalists like *Marinobacter*, *Shewanella*, *Pseudomonas*, *Vibrio* and *Roseobacter* (Singer et al., 2011)—with the latter two genera already having been deemed opportunistic based on their versatile lifestyles (“opportunitrophs”; Polz et al., 2006). Singer et al. (2011) also identified other potential commonalities shared among the genomes of opportunistic bacteria and *M. aquaeolei* VT8, including a large genomic toolkit for responding to environmental stimuli and for defense (cf. Polz et al., 2006).

There are few phylogenetic studies of the environments from which *Marinobacter* species have been isolated that evaluate their *in situ* relative abundance. Nevertheless, the studies that have been published show two different scenarios for *Marinobacter*. Strains may be characterized as *r*-strategists or opportunistic (Polz et al., 2006; Singer et al., 2011), and dominate communities sporadically when stimulated by high nutrient loads, encountered, for example, in marine aggregates or enrichment cultures (Balzano et al., 2009; Handley et al., 2010). In contrast, relatively high *in situ* abundances of *Marinobacter* (Müller et al., 2010) and uncultured organisms closely related to *Marinobacter* (Rogers et al., 2003; Edwards et al., 2004) have been observed in some hydrothermal systems, implying these organisms may play an important and sustained role in post-depositional mineral alteration.

## HYDROTHERMAL SETTINGS

Marine hydrothermal systems are dispersed throughout the world’s oceans (Martin et al., 2008), and support abundant psychrophilic-to-mesophilic life even in close proximity to high-temperature venting (Reysenbach and Cady, 2001; Edwards et al., 2003). A number of studies suggest *Marinobacter* may be significant in ‘low-temperature’ hydrothermal systems, defined by low-temperature hydrothermalism (e.g., ~8 to ~40°C, McCollom and Shock, 1997) or ambient seawater temperatures (e.g., ~2° in the deep ocean). This is due to their documented association with several different hydrothermal features (**Table 1**), and to their ability to heterotrophically or mixotrophically respire inorganic compounds abundant in hydrothermal systems.



A common hydrothermal feature found at plate boundaries, and with which *Marinobacter* or near-relatives have been associated (Edwards et al., 2003; Rogers et al., 2003; Müller et al., 2010), are massive sulfides, which comprise an estimated  $6 \times 10^8$  tonnes of material globally (Hannington et al., 2011), and adjunct metalliferous sediments. While much of the material for massive sulfides originates from high-temperature hydrothermal fluids ( $>350^{\circ}\text{C}$ ) emanating from black smoker chimneys (Hannington et al., 2011), particulates distributed locally by plumes and talus from mound and chimney collapse can equilibrate with ambient temperatures (Edwards et al., 2003), or entire mounds can be inactive (Müller et al., 2010). Adjacent to massive sulfide deposits are low-temperature iron- and manganese-rich metalliferous sediments, derived from distal plume fallout with contributions from mound mass wasting (Jannasch and Mottl, 1985; Mills et al., 1993; Hannington et al., 1998)—possibly of the type from which *M. manganoxydans* was isolated (Wang et al., 2012).

Deposits consisting of iron oxyhydroxides, nontronite (a ferric iron-rich clay) and iron-manganese crusts can form independently at plate boundaries or at places of intra-plate volcanism (e.g., Alt, 1988; Karl et al., 1988; Boyd and Scott, 2001; Kennedy et al., 2004; Edwards et al., 2011). They form from diffuse low-temperature venting (Karl et al., 1988; Edwards et al., 2011), and can span areas  $>100\text{ m}^2$  (Boyd and Scott, 2001). Similar deposits exist in shallow marine settings, such as the ferruginous arsenic-rich sediments found in Papua New Guinea and Santorini (Smith and Cronan, 1983; Pichler and Veizer, 1999). *M. santoriniensis* was isolated from the Santorini sediment (Handley et al., 2009a).

Further examples of low-temperature hydrothermal habitats, with which *Marinobacter* or near relatives are associated, include those created by sharp temperature gradients that form across high-temperature chimney walls (Rogers et al., 2003), or buoyant plumes (Kaye and Baross, 2000) that rise 200–300 m up from these vents and spread laterally (German et al., 1991). Exposed, iron-rich basalt, delivered by oceanic spreading centers, provides another environment associated with many deep-sea hydrothermal systems (Lysnes et al., 2004), whereas *M. alkaliphilus* was isolated from alkaline serpentine mud (Takai et al., 2005) from a setting peculiar to mud volcanoes on the non-accretionary Mariana forearc (Fryer et al., 1999).

## FUNCTION, BIOGEOCHEMISTRY AND HYDROTHERMAL SYSTEMS

The various low-temperature hydrothermal settings *Marinobacter*(-like) species inhabit are rich in metals/metalloids, such as iron, manganese, arsenic, copper and zinc (Smith and Cronan, 1983; Hannington et al., 1998) that certain *Marinobacter* strains can transform enzymatically. Moreover, oxygen gradients established in these sediments may be exploited by *Marinobacter* species able to grow heterotrophically under anaerobic/aerobic conditions and mixotrophically under aerobic conditions.

Among the functions *Marinobacter* may perform in these environments is ferrous iron oxidation. The potential for *Marinobacter* Fe(II) oxidation was first suggested by Edwards et al. (2003) after isolating iron-oxidizing bacteria, phylogenetically resembling *M. aquaeolei*, from low-temperature

hydrothermal metal sulfides. The isolates were able to grow chemoautotrophically on pyrite, basalt glass and siderite under micro-aerobic conditions. This promoted subsequent study of *M. aquaeolei*, including genome sequencing, and identification of its ability to anaerobically oxidize Fe(II) under mixotrophic conditions (Dhillon et al., 2005; Edwards et al., 2006; Singer et al., 2011). Subsequently, *M. santoriniensis*, which was isolated from iron-rich hydrothermal sediment, was also shown to perform nitrate-dependent Fe(II) oxidation when supplemented with a small amount of organic carbon (Handley et al., 2009a).

Interestingly, *M. santoriniensis* was isolated from sediment rife with stalk-like cells and bacteria phylogenetically resembling iron-oxidizing *Zetaproteobacteria* (Handley et al., 2010). Other *Marinobacter* (or near relatives) were also cultivated from environments containing stalks (Edwards et al., 2003; Lysnes et al., 2004) that speculatively belong to this increasingly characteristic phylum of marine iron-oxidizers—the *Zetaproteobacteria* (Emerson et al., 2007, 2010; Edwards et al., 2011).

As *Marinobacter* are reputedly more versatile than *Mariprofundus ferrooxydans* strains (the sole representatives of the *Zetaproteobacteria*) it is possible they perform other functions in these environments instead of, or in addition to, Fe(II) oxidation. For instance, *Marinobacter* and *Marinobacter*-like isolates have been implicated in Fe(III) reduction, but only in complex or simple co-cultures with other bacteria (Lysnes et al., 2004; Balzano et al., 2009; Handley et al., 2010). This metabolic trait remains to be demonstrated in definitively anoxic cultures. *M. santoriniensis* has the genetic potential to reductively detoxify arsenate and mercury using proteins encoded by an *Escherichia coli*-like *arsC* and *merRTA* genes (Handley et al., 2013c), in addition to being able to conserve energy for growth via arsenate [As(V)] respiration using an unidentified mechanism, and mixotrophically oxidize arsenite [As(III)] using the *aro* gene cluster—making it one of a handful of bacteria currently known to completely redox-cycle arsenic (Handley et al., 2009b). This is particularly relevant given that the bacterium was isolated from sediment containing  $\sim 400$  ppm of arsenic.

It remains to be explored whether other *Marinobacter* species share this ability to respire arsenic. However, there is cursory evidence for non-respiratory arsenate reductase (plus/minus putative respiratory arsenite oxidase) genes in several publicly available *Marinobacter* genomes (namely, *M. hydrocarbonoclasticus* ATCC49840, GenBank FO203363.1, Grimaud et al., 2012; *M. aquaeolei* VT8, GenBank CP000514.1, Singer et al., 2011; *M. adhaerens* HP15, GenBank CP001978.1, Gärdes et al., 2010; *M. algicola* DG893, GenBank ABCP00000000.1; *Marinobacter* spp. BSs20148 and ELB17, GenBank CP003735.1 and AAXY00000000.1). Likewise, in a recent genome announcement Wang et al. (2012) described a *Marinobacter* candidate, *M. manganoxydans* MnI7-9 that has not only a putative *arsC* gene for arsenic detoxification (GenBank YP\_005884959.1), but also a host of other genes that may be used for nickel, mercury, copper, chromate, zinc, cobalt, and cadmium resistance. This bacterium adsorbs and tolerates high levels of metals/metalloids, alongside a demonstrated ability to oxidize manganese, Mn(II), to a mixed-valency Mn(III)/Mn(IV) product via an

unidentified genetic mechanism. Bacterial manganese oxidation is not thought to be an energy conserving process, but it is considered significant in environmental Mn(IV) oxide formation (Geszvain et al., 2012).

## CONCLUSIONS AND FUTURE DIRECTIONS

Although the genus is widespread in marine settings, and dozens of cultivated representatives and several sequenced genomes exist, the functional breadth of *Marinobacter* species remains largely unexplored. The ability to metabolize hydrocarbons and inorganic elements (e.g., iron, arsenic, manganese) has been tested in relatively few species. Information, based on cultures and isolation source characteristics, suggests species within the genus are able to contribute, for example, to the degradation of hydrocarbons in oil-polluted sediment, and the oxidation of Fe(II) in ferruginous sediment or basalt. However, we know little about the nature and magnitude of their actual function in the environment. High-throughput omics (genomics, transcriptomics,

proteomics) techniques promise to expand our knowledge into the uncultivated black box that encompasses much of the microbiome, and to facilitate *in situ* investigations of communities (e.g., Ram et al., 2005; Lo et al., 2007; Baker et al., 2012; Handley et al., 2013b), but are limited in part by the large number of genes of unknown function. Much can still be achieved from cultivation experiments. In moving forward, a combination of omics, functional gene expression studies, isotope tracer and cultivation techniques will provide a powerful complement of tools for characterizing both the real and potential function of microorganisms in marine settings and elsewhere, and elucidating the (opportunistic?) role of *Marinobacter* species in environmental biogeochemical cycles.

## ACKNOWLEDGMENTS

We acknowledge funding support from the European Union through the BIOTRANSFORMATIONS of TRace elements in Aquatic Systems (BIOTRACS) EST programme, Marie Curie Actions.

## REFERENCES

- Aguilera, M., Jiménez-Pranteda, M. L., Kharroub, K., González-Paredes, A., Durban, J. J., Russell, N. J., et al. (2009). *Marinobacter lacisalisp* sp. nov., a moderately halophilic bacterium isolated from the saline-wetland wildfowl reserve Fuente de Piedra in southern Spain. *Int. J. Syst. Evol. Microbiol.* 59, 1691–1695.
- Al-Awadhi, H., Sulaiman, R. H., Mahmoud, H. M., and Radwan, S. S. (2007). Alkaliphilic and halophilic hydrocarbon-utilizing bacteria from Kuwaiti coasts of the Arabian Gulf. *Appl. Microbiol. Biotechnol.* 77, 183–186.
- Alt, J. C. (1988). Hydrothermal oxide and nontronite deposits on seamounts in the eastern Pacific. *Mar. Geol.* 81, 227–239.
- Antunes, A., Franca, L., Rainey, F. A., Huber, R., Nobre, M. F., Edwards, K. J., et al. (2007). *Marinobacter salsuginis* sp. nov., isolated from the brine-seawater interface of the Shaban Deep, Red Sea. *Int. J. Syst. Evol. Microbiol.* 57, 1035–1040.
- Baker, B. J., Lesniewski, R. A., and Dick, G. J. (2012). Genome-enabled transcriptomics reveals archaeal populations that drive nitrification in a deep-sea hydrothermal plume. *ISME J.* 6, 2269–2279.
- Balzano, S., Statham, P. J., Pancost, R. D., and Lloyd, J. R. (2009). Role of microbial populations in the release of reduced iron to the water column from marine aggregates. *Aquat. Microb. Ecol.* 54, 291–303.
- Banat, I. M., Makkar, R. S., and Cameotra, S. S. (2000). Potential commercial applications of microbial surfactants. *Appl. Microbiol. Biotechnol.* 53, 495–508.
- Besson, S., Carneiro, C., Moura, J. J., Moura, I., and Fauque, G. (1995). A cytochrome cd1-type nitrite reductase isolated from the marine denitrifier *Pseudomonas nautica* 617: purification and characterization. *Anaerobe* 1, 219–226.
- Boyd, T. D., and Scott, S. D. (2001). Microbial and hydrothermal aspects of ferric oxyhydroxides and ferrosic hydroxides: the example of Franklin Seamount, Western Woodlark Basin, Papua New Guinea. *Geochem. Trans.* 2, 45.
- Caro-Quintero, A., Deng, J., Auchtung, J., Brettar, I., Höfle, M. G., Klappenbach, J., et al. (2011). Unprecedented levels of horizontal gene transfer among spatially co-occurring *Shewanella* bacteria from the Baltic Sea. *ISME J.* 5, 131–140.
- Correia, C., Besson, S., Brondino, C. D., Gonzalez, P. J., Fauque, G., Lampreia, J., et al. (2008). Biochemical and spectroscopic characterization of the membrane-bound nitrate reductase from *Marinobacter hydrocarbonoclasticus* 617. *J. Biol. Inorg. Chem.* 13, 1321–1333.
- Cui, Z., Lai, Q., Dong, C., and Shao, Z. (2008). Biodiversity of polycyclic aromatic hydrocarbon-degrading bacteria from deep sea sediments of the Middle Atlantic Ridge. *Environ. Microbiol.* 10, 2138–2149.
- DasSarma, S., and Arora, P. (2012). “Halophiles,” in *eLS*. Chichester: John Wiley and Sons, Ltd. doi: 10.1002/9780470015902.a0000394. pub3
- Dhillon, A., Edwards, K. J., Webb, E., Rogers, D., and Sogin, M. L. (2005). “Marinobacter aquaeolei gene expression studies for clues to neutrophilic iron oxidation,” in *NASA Astrobiology Institute biennial meeting, Abstract 829* (University of Colorado, Boulder, CO).
- Dunsmore, B., Youldon, J., Thrasher, D. R., and Vance, I. (2006). Effects of nitrate treatment on a mixed species, oil field microbial biofilm. *J. Ind. Microbiol. Biotechnol.* 33, 454–462.
- Edwards, K., Sogin, M., and Dhillon, A. (2006). Why Sequence *Marinobacter aquaeolei*? DOE Joint Genome Institute, Available online at: <http://www.jgi.doe.gov/sequencing/why/marinobacter.html>
- Edwards, K. J., Bach, W., McCollom, T. M., and Rogers, D. R. (2004). Neutrophilic iron-oxidizing bacteria in the ocean: their habitats, diversity, and roles in mineral deposition, rock alteration, and biomass production in the deep-sea. *Geomicrobiol. J.* 21, 393–404.
- Edwards, K. J., Glazer, B. T., Rouxel, O. J., Bach, W., Emerson, D., Davis, R. E., et al. (2011). Ultra-diffuse hydrothermal venting supports Fe-oxidizing bacteria and massive umber deposition at 5000 m off Hawaii. *ISME J.* 5, 1748–1758.
- Edwards, K. J., Rogers, D. R., Wirsen, C. O., and McCollom, T. M. (2003). Isolation and characterization of novel psychrophilic, neutrophilic, Fe-oxidizing, chemolithoautotrophic alpha- and gamma-proteobacteria from the deep sea. *Appl. Environ. Microbiol.* 69, 2906–2913.
- Emerson, D., Fleming, E. J., and McBeth, J. M. (2010). Iron-oxidizing bacteria: an environmental and genomic perspective. *Annu. Rev. Microbiol.* 64, 561–583.
- Emerson, D., Rentz, J. A., Lilburn, T. G., Davis, R. E., Aldrich, H., Chan, C., et al. (2007). A novel lineage of proteobacteria involved in formation of marine Fe-oxidizing microbial mat communities. *PLoS ONE* 2:e667. doi: 10.1371/journal.pone.0000667
- Fryer, P., Wheat, C. G., and Mottl, M. J. (1999). Mariana blueschist mud volcanism: implications for conditions within the subduction zone. *Geology* 27, 103–106.
- Gadd, G. M. (2010). Metals, minerals and microbes: geomicrobiology and bioremediation. *Microbiology* 156, 609–643.
- Gärdes, A., Kaeppler, E., Shehzad, A., Seebah, S., Teeling, H., Yarza, P., et al. (2010). Complete genome sequence of *Marinobacter adhaerens* type strain (HP15), a diatom-interacting marine microorganism. *Stand. Genomic. Sci.* 3, 97–107.
- Gauthier, M. J., Lafay, B., Christen, R., Fernandez, L., Acquaviva, M., Bonin, P., et al. (1992). *Marinobacter hydrocarbonoclasticus* gen. nov., sp. nov., a new, extremely halotolerant, hydrocarbon-degrading marine bacterium. *Int. J. Syst. Bacteriol.* 42, 568–576.
- Gerdes, B., Brinkmeyer, R., Dieckmann, G., and Helmke, E. (2005). Influence of crude oil on changes of bacterial communities in Arctic sea-ice. *FEMS Microbiol. Ecol.* 53, 129–139.
- German, C. R., Campbell, A. C., and Edmond, J. M. (1991). Hydrothermal scavenging at the Mid-Atlantic Ridge: modification of trace element dissolved

- fluxes. *Earth Planet. Sc. Lett.* 107, 101–114.
- Geszvain, K., Butterfield, C., Davis, R. E., Madison, A. S., Lee, S. W., Parker, D. L., et al. (2012). The molecular biogeochemistry of manganese(II) oxidation. *Biochem. Soc. Trans.* 40, 1244–1248.
- Gorshkova, N. M., Ivanova, E. P., Sergeev, A. F., Zhukova, N. V., Alexeeva, Y., Wright, J. P., et al. (2003). *Marinobacter excellens* sp. nov., isolated from sediments of the Sea of Japan. *Int. J. Syst. Evol. Microbiol.* 53, 2073–2078.
- Green, D. H., Bowman, J. P., Smith, E. A., Gutierrez, T., and Bolch, C. J. (2006). *Marinobacter algicola* sp. nov., isolated from laboratory cultures of paralytic shellfish toxin-producing dinoflagellates. *Int. J. Syst. Evol. Microbiol.* 56, 523–527.
- Grimaud, R., Ghiglione, J. F., Cagnon, C., Lauga, B., Vaysse, P. J., Rodriguez-Blanco, A., et al. (2012). Genome sequence of the marine bacterium *Marinobacter hydrocarbonoclasticus* SP17, which forms biofilms on hydrophobic organic compounds. *J. Bacteriol.* 194, 3539–3540.
- Gu, J., Cai, H., Yu, S. L., Qu, R., Yin, B., Guo, Y. F., et al. (2007). *Marinobacter gudaonensis* sp. nov., isolated from an oil-polluted saline soil in a Chinese oilfield. *Int. J. Syst. Evol. Microbiol.* 57, 250–254.
- Guo, B., Gu, J., Ye, Y. G., Tang, Y. Q., Kida, K., and Wu, X. L. (2007). *Marinobacter segnircrescens* sp. nov., a moderate halophile isolated from benthic sediment of the South China Sea. *Int. J. Syst. Evol. Microbiol.* 57, 1970–1974.
- Handley, K. M., Boothman, C., McBeth, J., Charnock, J. M., Wincott, P. L., Vaughan, D. J., et al. (2013a). Effect of microbially mediated iron redox transformations on arsenic solid-phase associations in a high-iron, arsenic-rich hydrothermal sediment. *Geochim. Cosmochim. Acta* 102, 124–142.
- Handley, K. M., Verberkmoes, N. C., Steefel, C. I., Williams, K. H., Sharon, I., Miller, C. S., et al. (2013b). Biostimulation induces syntrophic interactions that impact C, S and N cycling in a sediment microbial community. *ISME J.* 7, 800–816.
- Handley, K. M., Upton, M., Beatson, S. A., Héry, M., and Lloyd, J. R. (2013c). Genome sequence of hydrothermal arsenic-respiring bacterium *Marinobacter santoriniensis* strain NKSG1T. *Genome Announc.* 1:e00231-13. doi: 10.1128/genomeA.00231-13
- Handley, K. M., Boothman, C., Mills, R. A., Pancost, R. D., and Lloyd, J. R. (2010). Functional diversity of bacteria in a ferruginous hydrothermal sediment. *ISME J.* 4, 1193–1205.
- Handley, K. M., Héry, M., and Lloyd, J. R. (2009a). *Marinobacter santoriniensis* sp. nov., an arsenate-respiring and arsenite-oxidizing bacterium isolated from hydrothermal sediment. *Int. J. Syst. Evol. Microbiol.* 59, 886–892.
- Handley, K. M., Héry, M., and Lloyd, J. R. (2009b). Redox cycling of arsenic by the hydrothermal marine bacterium *Marinobacter santoriniensis*. *Environ. Microbiol.* 11, 1601–1611.
- Hannington, M., Jamieson, J., Monecke, T., Petersen, S., and Beaulieu, S. (2011). The abundance of seafloor massive sulfide deposits. *Geology* 39, 1155–1158.
- Hannington, M. D., Galley, A. G., Herzig, P. M., and Petersen, S. (1998). “Comparison of the TAG mound and stockwork complex with Cyprus type massive sulfide deposits,” in *Proceedings of the Ocean Drilling Program, Scientific Results*, Vol. 158 (College Station, TX), 380–415.
- Heidelberg, J. F., Paulsen, I. T., Nelson, K. E., Gaidos, E. J., Nelson, W. C., Read, T. D., et al. (2002). Genome sequence of the dissimilatory metal ion-reducing bacterium *Shewanella oneidensis*. *Nat. Biotechnol.* 20, 1118–1123.
- Holden, J. F., Breier, J. A., Rogers, K. L., Schulte, M. D., and Toner, B. M. (2012). Biogeochemical processes at hydrothermal vents: microbes and minerals, bioenergetics, and carbon fluxes. *Oceanography* 25, 196–208.
- Huo, Y. Y., Wang, C. S., Yang, J. Y., Wu, M., and Xu, X. W. (2008). *Marinobacter mobilis* sp. nov. and *Marinobacter zhejiangensis* sp. nov., halophilic bacteria isolated from the East China Sea. *Int. J. Syst. Evol. Microbiol.* 58, 2885–2889.
- Huu, N. B., Denner, E. B., Ha, D. T., Wanner, G., and Stan-Lotter, H. (1999). *Marinobacter aquaeolei* sp. nov., a halophilic bacterium isolated from a Vietnamese oil-producing well. *Int. J. Syst. Bacteriol.* 49(Pt 2), 367–375.
- Jannasch, H. W., and Mottl, M. J. (1985). Geomicrobiology of deep-sea hydrothermal vents. *Science* 229, 717–725.
- Jørgensen, B. B. (2006). “Bacteria and marine biogeochemistry,” in *Marine Geochemistry*, eds. H. D. Schultz and M. Zabel (Berlin: Springer), 169–206.
- Kaeppele, E. C., Gardes, A., Seebah, S., Grossart, H. P., and Ullrich, M. S. (2012). *Marinobacter adhaerens* sp. nov., isolated from marine aggregates formed with the diatom *Thalassiosira weissflogii*. *Int. J. Syst. Evol. Microbiol.* 62, 124–128.
- Karl, D. M., McMurtry, G. M., Malahoff, A., and Garcia, M. O. (1988). Loihi Seamount, Hawaii: a mid-plate volcano with a distinctive hydrothermal system. *Nature* 335, 532–535.
- Kaye, J. Z., and Baross, J. A. (2000). High incidence of halotolerant bacteria in Pacific hydrothermal-vent and pelagic environments. *FEMS Microbiol. Ecol.* 32, 249–260.
- Kaye, J. Z., Sylvan, J. B., Edwards, K. J., and Baross, J. A. (2011). *Halomonas* and *Marinobacter* ecotypes from hydrothermal vent, subseafloor and deep-sea environments. *FEMS Microbiol. Ecol.* 75, 123–133.
- Kennedy, C. B., Scott, S. D., and Ferris, F. G. (2004). Hydrothermal phase stabilization of 2-line ferrihydrite by bacteria. *Chem. Geol.* 212, 269–277.
- Kharroub, K., Aguilera, M., Luján, M., Jiménez-Pranteda, M. L., González-Paredes, A., Ramos-Cormenzana, A., et al. (2011). *Marinobacter oulmenensis* sp. nov., a moderately halophilic bacterium isolated from brine of a salt concentrator. *Int. J. Syst. Evol. Microbiol.* 61, 2210–2214.
- Kim, B. Y., Weon, H. Y., Yoo, S. H., Kim, J. S., Kwon, S. W., Stackebrandt, E., et al. (2006). *Marinobacter koreensis* sp. nov., isolated from sea sand in Korea. *Int. J. Syst. Evol. Microbiol.* 56, 2653–2656.
- Lee, O. O., Lai, P. Y., Wu, H. X., Zhou, X. J., Miao, L., Wang, H., and Qian, P. Y. (2012). *Marinobacter xestospongiae* sp. nov., isolated from the marine sponge *Xestospongia testudinaria* collected from the Red Sea. *Int. J. Syst. Evol. Microbiol.* 62, 1980–1985.
- Liebgott, P. P., Casalot, L., Paillard, S., Lorquin, J., and Labat, M. (2006). *Marinobacter vinifirmus* sp. nov., a moderately halophilic bacterium isolated from a wine-barrel-decalcification wastewater. *Int. J. Syst. Evol. Microbiol.* 56, 2511–2516.
- Liu, C., Chen, C. X., Zhang, X. Y., Yu, Y., Liu, A., Li, G. W., et al. (2012). *Marinobacter antarcticus* sp. nov., a halotolerant bacterium isolated from Antarctic intertidal sandy sediment. *Int. J. Syst. Evol. Microbiol.* 62, 1838–1844.
- Lo, I., Denef, V. J., Verberkmoes, N. C., Shah, M. B., Goltsman, D., DiBartolo, G., et al. (2007). Strain-resolved community proteomics reveals recombining genomes of acidophilic bacteria. *Nature* 446, 537–541.
- Lysnes, K., Thorseth, I. H., Steinsbu, B. O., Ovreas, L., Torsvik, T., and Pedersen, R. B. (2004). Microbial community diversity in seafloor basalt from the Arctic spreading ridges. *FEMS Microbiol. Ecol.* 50, 213–230.
- Mahadevan, R., and Lovley, D. R. (2008). The degree of redundancy in metabolic genes is linked to mode of metabolism. *Biophys. J.* 94, 1216–1220.
- Márquez, M. C., and Ventosa, A. (2005). *Marinobacter hydrocarbonoclasticus* Gauthier et al. 1992 and *Marinobacter aquaeolei* Nguyen et al. 1999 are heterotypic synonyms. *Int. J. Syst. Evol. Microbiol.* 55, 1349–1351.
- Martin, S., Márquez, M. C., Sánchez-Porro, C., Mellado, E., Arahal, D. R., and Ventosa, A. (2003). *Marinobacter lipolyticus* sp. nov., a novel moderate halophile with lipolytic activity. *Int. J. Syst. Evol. Microbiol.* 53, 1383–1387.
- Martin, W., Baross, J., Kelley, D., and Russell, M. J. (2008). Hydrothermal vents and the origin of life. *Nat. Rev. Microbiol.* 6, 805–814.
- Martiny, J. B., Bohannan, B. J., Brown, J. H., Colwell, R. K., Fuhrman, J. A., Green, J. L., et al. (2006). Microbial biogeography: putting microorganisms on the map. *Nat. Rev. Microbiol.* 4, 102–112.
- McCollom, T. M., and Shock, E. L. (1997). Geochemical constraints on chemolithoautotrophic metabolism by microorganisms in seafloor hydrothermal systems. *Geochim. Cosmochim. Acta* 61, 4375–4391.
- Mills, R., Elderfield, H., and Thomson, J. (1993). A dual origin for the hydrothermal component in a metalliferous sediment core from the Mid-Atlantic Ridge. *J. Geophys. Res.* 98, 9671–9681.
- Montes, M. J., Bozal, N., and Mercade, E. (2008). *Marinobacter guineae* sp. nov., a novel moderately halophilic bacterium from an Antarctic environment. *Int. J. Syst. Evol. Microbiol.* 58, 1346–1349.
- Moran, M. A., Buchan, A., Gonzalez, J. M., Heidelberg, J. F., Whitman, W. B., Kiene, R. P., et al. (2004). Genome sequence of *Silicibacter pomeroyi* reveals adaptations to the marine environment. *Nature* 432, 910–913.
- Moyer, C. L., and Morita, R. Y. (2007). “Psychrophiles and psychrotrophs,” In *eLS*. Chichester: John Wiley and Sons Ltd. doi: 10.1002/9780470015902.a0000402.pub2

- Müller, M., Handley, K. M., Lloyd, J., Pancost, R. D., and Mills, R. A. (2010). Biogeochemical controls on microbial diversity in seafloor sulphidic sediments. *Geobiology* 8, 309–326.
- Nerurkar, A. S., Hingurao, K. S., and Suthar, H. G. (2009). Bioemulsifiers from marine microorganisms. *J. Sci. Ind. Res.* 68, 273–277.
- Pichler, T., and Veizer, J. (1999). Precipitation of Fe(III) oxyhydroxide deposits from shallow-water hydrothermal fluids in Tutum Bay, Ambitle Island, Papua New Guinea. *Chem. Geol.* 162, 15–31.
- Polz, M. F., Hunt, D. E., Preheim, S. P., and Weinreich, D. M. (2006). Patterns and mechanisms of genetic and phenotypic differentiation in marine microbes. *Philos. Trans. R. Soc. Lond. B Biol. Sci.* 361, 2009–2021.
- Prudêncio, M., Pereira, A. S., Tavares, P., Besson, S., Cabrito, I., Brown, K., et al. (2000). Purification, characterization, and preliminary crystallographic study of copper-containing nitrous oxide reductase from *Pseudomonas nautica* 617. *Biochemistry* 39, 3899–3907.
- Qu, L., Zhu, F., Zhang, J., Gao, C., and Sun, X. (2011). *Marinobacter daqiaonensis* sp. nov., a moderate halophile isolated from a Yellow Sea salt pond. *Int. J. Syst. Evol. Microbiol.* 61, 3003–3008.
- Ram, R. J., Verberkmoes, N. C., Thelen, M. P., Tyson, G. W., Baker, B. J., Blake, R. C. I. I., et al. (2005). Community proteomics of a natural microbial biofilm. *Science* 308, 1915–1920.
- Reysenbach, A. L., and Cady, S. L. (2001). Microbiology of ancient and modern hydrothermal systems. *Trends Microbiol.* 9, 79–86.
- Rogers, D. R., Santelli, C. M., and Edwards, K. J. (2003). Geomicrobiology of deep-sea deposits: estimating community diversity from low-temperature seafloor rocks and minerals. *Geobiology* 1, 109–117.
- Roh, S. W., Quan, Z. X., Nam, Y. D., Chang, H. W., Kim, K. H., Rhee, S. K., et al. (2008). *Marinobacter goseongensis* sp. nov., from seawater. *Int. J. Syst. Evol. Microbiol.* 58, 2866–2870.
- Romanenko, L. A., Schumann, P., Rohde, M., Zhukova, N. V., Mikhailov, V. V., and Stachebrandt, E. (2005). *Marinobacter bryozorum* sp. nov. and *Marinobacter sediminum* sp. nov., novel bacteria from the marine environment. *Int. J. Syst. Evol. Microbiol.* 55, 143–148.
- Rontani, J. F., Gilewicz, M. J., Michotey, V. D., Zheng, T. L., Bonin, P. C., and Bertrand, J. C. (1997). Aerobic and anaerobic metabolism of 6, 10, 14-trimethylpentadecan-2-one by a denitrifying bacterium isolated from marine sediments. *Appl. Environ. Microbiol.* 63, 636–643.
- Rontani, J. F., Mouzdahir, A., Michotey, V., Caumette, P., and Bonin, P. (2003). Production of a polyunsaturated isoprenoid wax ester during aerobic metabolism of squalene by *Marinobacter squalenivorans* sp. nov. *Appl. Environ. Microbiol.* 69, 4167–4176.
- Shieh, W. Y., Jean, W. D., Lin, Y. T., and Tseng, M. (2003). *Marinobacter lutaensis* sp. nov., a thermotolerant marine bacterium isolated from a coastal hot spring in Lutao, Taiwan. *Can. J. Microbiol.* 49, 244–252.
- Shivaji, S., Gupta, P., Chaturvedi, P., Suresh, K., and Delille, D. (2005). *Marinobacter maritimus* sp. nov., a psychrotolerant strain isolated from sea water off the subantarctic Kerguelan islands. *Int. J. Syst. Evol. Microbiol.* 55, 1453–1456.
- Sigalevich, P., Baev, M. V., Teske, A., and Cohen, Y. (2000). Sulfate reduction and possible aerobic metabolism of the sulfate-reducing bacterium *Desulfovibrio oxydclineae* in a chemostat coculture with *Marinobacter* sp. Strain MB under exposure to increasing oxygen concentrations. *Appl. Environ. Microbiol.* 66, 5013–5018.
- Singer, E., Webb, E. A., Nelson, W. C., Heidelberg, J. F., Ivanova, N., Pati, A., et al. (2011). Genomic potential of *Marinobacter aquaeolei*, a biogeochemical “opportunist”. *Appl. Environ. Microbiol.* 77, 2763–2771.
- Smith, P. A., and Cronan, D. S. (1983). The geochemistry of metalliferous sediments and waters associated with shallow submarine hydrothermal activity (Santorini, Aegean Sea). *Chem. Geol.* 39, 241–262.
- Soberón-Chávez, G., and Maier, R. M. (2011). “Biosurfactants: a general overview,” in *Biosurfactants*, Vol. 20, ed G. Soberón-Chávez (Berlin: Springer), 1–11.
- Takai, K., Moyer, C. L., Miyazaki, M., Nogi, Y., Hirayama, H., Nealson, K. H., et al. (2005). *Marinobacter alkaliphilus* sp. nov., a novel alkaliphilic bacterium isolated from seafloor alkaline serpentinite mud from Ocean Drilling Program Site 1200 at South Chamorro Seamount, Mariana Forearc. *Extremophiles* 9, 17–27.
- Tamura, K., Peterson, D., Peterson, N., Stecher, G., Nei, M., and Kumar, S. (2011). MEGA5: molecular evolutionary genetics analysis using maximum likelihood, evolutionary distance, and maximum parsimony methods. *Mol. Biol. Evol.* 28, 2731–2739.
- Thompson, J. D., Higgins, D. G., and Gibson, T. J. (1994). CLUSTAL W: improving the sensitivity of progressive multiple sequence alignment through sequence weighting, position-specific gap penalties and weight matrix choice. *Nucleic Acids Res.* 22, 4673–4680.
- Validation List no. 94. (2003). Validation of publication of new names and new combinations previously effectively published outside the IJSEM. *Int. J. Syst. Evol. Microbiol.* 53, 1701–1702.
- Validation List no. 148. (2012). List of new names and new combinations previously effectively, but not validly, published. *Int. J. Syst. Evol. Microbiol.* 62, 2549–2554.
- Wang, C. Y., Ng, C. C., Chen, T. W., Wu, S. J., and Shyu, Y. T. (2007). Microbial diversity analysis of former salterns in southern Taiwan by 16S rRNA-based methods. *J. Basic Microbiol.* 47, 525–533.
- Wang, C. Y., Ng, C. C., Tzeng, W. S., and Shyu, Y. T. (2009). *Marinobacter szutsaonensis* sp. nov., isolated from a solar saltern. *Int. J. Syst. Evol. Microbiol.* 59, 2605–2609.
- Wang, H., Li, H., Shao, Z., Liao, S., Johnstone, L., Rensing, C., et al. (2012). Genome sequence of deep-sea manganese-oxidizing bacterium *Marinobacter manganoxydans* MnI7–9. *J. Bacteriol.* 194, 899–900.
- Whitman, W. B., Coleman, D. C., and Wiebe, W. J. (1998). Prokaryotes: the unseen majority. *Proc. Natl. Acad. Sci. U.S.A.* 95, 6578–6583.
- Williams, K. (2009). Biosurfactants for cosmetic applications: overcoming production challenges. *Basic Biotech.* 5, 78–83.
- Williams, K. P., Gillespie, J. J., Sobral, B. W., Nordberg, E. K., Snyder, E. E., Shallom, J. M., et al. (2010). Phylogeny of *Gammaproteobacteria*. *J. Bacteriol.* 192, 2305–2314.
- Xu, X. W., Wu, Y. H., Wang, C. S., Yang, J. Y., Oren, A., and Wu, M. (2008). *Marinobacter pelagi* sp. nov., a moderately halophilic bacterium. *Int. J. Syst. Evol. Microbiol.* 58, 637–640.
- Yoon, J. H., Lee, M. H., Kang, S. J., and Oh, T. K. (2007). *Marinobacter salicampi* sp. nov., isolated from a marine solar saltern in Korea. *Int. J. Syst. Evol. Microbiol.* 57, 2102–2105.
- Yoon, J. H., Shin, D. Y., Kim, I. G., Kang, K. H., and Park, Y. H. (2003). *Marinobacter litoralis* sp. nov., a moderately halophilic bacterium isolated from sea water from the East Sea in Korea. *Int. J. Syst. Evol. Microbiol.* 53, 563–568.
- Yoon, J. H., Yeo, S. H., Kim, I. G., and Oh, T. K. (2004). *Marinobacter flavimaris* sp. nov. and *Marinobacter daeponensis* sp. nov., slightly halophilic organisms isolated from sea water of the Yellow Sea in Korea. *Int. J. Syst. Evol. Microbiol.* 54, 1799–1803.
- Zhuang, D. C., Chen, Y. G., Zhang, Y. Q., Tang, S. K., Wu, X. L., Tan, Z. C., et al. (2009). *Marinobacter zhanjiangensis* sp. nov., a marine bacterium isolated from sea water of a tidal flat of the South China Sea. *Antonie Van Leeuwenhoek* 96, 295–301.
- Zhang, D. C., Li, H. R., Xin, Y. H., Chi, Z. M., Zhou, P. J., and Yu, Y. (2008). *Marinobacter psychrophilus* sp. nov., a psychrophilic bacterium isolated from the Arctic. *Int. J. Syst. Evol. Microbiol.* 58, 1463–1466.

**Conflict of Interest Statement:** The authors declare that the research was conducted in the absence of any commercial or financial relationships that could be construed as a potential conflict of interest.

**Received:** 15 February 2013; **accepted:** 07 May 2013; **published online:** 22 May 2013.

**Citation:** Handley KM and Lloyd JR (2013) Biogeochemical implications of the ubiquitous colonization of marine habitats and redox gradients by *Marinobacter* species. *Front. Microbiol.* 4:136. doi: 10.3389/fmicb.2013.00136

This article was submitted to Frontiers in Extreme Microbiology, a specialty of Frontiers in Microbiology.

Copyright © 2013 Handley and Lloyd. This is an open-access article distributed under the terms of the Creative Commons Attribution License, which permits use, distribution and reproduction in other forums, provided the original authors and source are credited and subject to any copyright notices concerning any third-party graphics etc.



# Metagenome reveals potential microbial degradation of hydrocarbon coupled with sulfate reduction in an oil-immersed chimney from Guaymas Basin

**Ying He<sup>1,2</sup>, Xiang Xiao<sup>1,2</sup> and Fengping Wang<sup>1,2\*</sup>**

<sup>1</sup> State Key Laboratory of Microbial Metabolism, School of Life Sciences and Biotechnology, Shanghai, China

<sup>2</sup> State Key Laboratory of Ocean Engineering, Shanghai Jiao Tong University, Shanghai, China

**Edited by:**

Andreas Teske, University of North Carolina at Chapel Hill, USA

**Reviewed by:**

Melanie R. Mormile, Missouri University of Science and Technology, USA

Jinjun Kan, Stroud Water Research Center, USA

**\*Correspondence:**

Fengping Wang, Laboratory of Microbial Oceanography, School of Life Sciences and Biotechnology, Shanghai Jiao Tong University, 800 Dongchuan Road, Shanghai 200240, China  
e-mail: fengpingw@sjtu.edu.cn

Deep-sea hydrothermal vent chimneys contain a high diversity of microorganisms, yet the metabolic activity and the ecological functions of the microbial communities remain largely unexplored. In this study, a metagenomic approach was applied to characterize the metabolic potential in a Guaymas hydrothermal vent chimney and to conduct comparative genomic analysis among a variety of environments with sequenced metagenomes. Complete clustering of functional gene categories with a comparative metagenomic approach showed that this Guaymas chimney metagenome was clustered most closely with a chimney metagenome from Juan de Fuca. All chimney samples were enriched with genes involved in recombination and repair, chemotaxis and flagellar assembly, highlighting their roles in coping with the fluctuating extreme deep-sea environments. A high proportion of transposases was observed in all the metagenomes from deep-sea chimneys, supporting the previous hypothesis that horizontal gene transfer may be common in the deep-sea vent chimney biosphere. In the Guaymas chimney metagenome, thermophilic sulfate reducing microorganisms including bacteria and archaea were found predominant, and genes coding for the degradation of refractory organic compounds such as cellulose, lipid, pullulan, as well as a few hydrocarbons including toluene, ethylbenzene and o-xylene were identified. Therefore, this oil-immersed chimney supported a thermophilic microbial community capable of oxidizing a range of hydrocarbons that served as electron donors for sulphate reduction under anaerobic conditions.

**Keywords:** metagenome, deep sea, hydrothermal vent, chimney, Guaymas, biodegradation, hydrocarbon, sulfate reduction

## INTRODUCTION

Deep-sea hydrothermal vents characterized by steep physico-chemical gradients harbor a wide range of microorganisms in different ecological niches, including the high-temperature chimney matrix (Reysenbach and Shock, 2002). Deep-sea hydrothermal vent chimneys are the product of hydrothermal circulation and alteration of seawater entrained through geothermally heated subseafloor basalt, and subsequent precipitation of metal sulfides when hot vent fluids emerge into cold sea water (Von Damm, 1990). The geochemical disequilibria within and surrounding chimneys provide rich energy sources for microorganisms, as various reduced chemicals (such as sulfur, methane, and H<sub>2</sub>) are utilized as potential electron donors (Jannasch and Mottl, 1985; Distel et al., 1988; Lam et al., 2004; Petersen et al., 2011). The structures of these microbial communities are shaped primarily by variation of hydrothermal fluid composition, in particular H<sub>2</sub> concentrations (Flores et al., 2011). Thanks to advances in sequencing technologies, molecular microbial diversity studies of deep-sea hydrothermal environments have made significant progress in understanding the geographic distributions of these microbial communities (Teske et al., 2002; Huber et al., 2007,

2010; Brazelton et al., 2010; Dick and Tebo, 2010; Roussel et al., 2011).

Despite the increased knowledge of the microbial diversity of deep-sea hydrothermal vents, much less was known about the metabolic potential and ecological functions of these communities, especially when considering that less than 1% of environmental microorganisms could be cultured under laboratory conditions (Amann et al., 1995). Metagenomic-based methods have provided unique opportunities to explore the features of microbial communities from diverse deep-sea hydrothermal vent environments. So far, metagenomes from two deep-sea hydrothermal vent chimneys have been published, from a carbonate white chimney at Lost City with relatively low temperature and high pH (<90°C, pH 9–11) (Brazelton and Baross, 2009), and from a chimney sample collected from Juan de Fuca (Xie et al., 2011) characterized by high temperature and low pH fluids (>300°C, pH 2–3). Both metagenomes were found enriched in transposases, implying that horizontal gene transfer may be a common feature of hydrothermal vent chimney biosphere. Comparative metagenomic studies with more chimney samples from different deep-sea hydrothermal vents should be performed

to reveal common features of the chimney-originated microbial communities.

The Guaymas Basin (Gulf of California) is a unique hydrothermal vent site, where emitted high-temperature fluids are influenced by the presence of a thick layer (100–500 m) of sediments (with 2–4% organic matter, OM). These sediments were formed by precipitation from the highly productive surface waters and terrigenous input (Von Damm et al., 1985). The venting fluids are characterized by an increase of pH (around 6.0), and a decrease in the highest temperature of fluids emitted on the seafloor (270–325°C) (Von Damm et al., 1985). Therefore, the chimney sample from the Guaymas site would be an ideal sample for comparative metagenomic analysis together with the two published ones. In addition, Guaymas Basin is unique due to the fact that under high-temperature conditions, the OM in its rapidly accumulating sediments is pyrolyzed to petroleum-like hydrocarbon products, such as aliphatic and aromatic hydrocarbons, short-chain fatty acids, ammonia, and methane (Bazylinski et al., 1988; Welhan, 1988; Martens, 1990; Kawka and Simoneit, 1994). The hydrothermally active sediments of the Guaymas Basin were reported with intensive methane oxidizing and sulfate reducing activities (Jørgensen et al., 1990, 1992; Elsgaard et al., 1994; Weber and Jørgensen, 2002; Kallmeyer and Boetius, 2004). Various hydrocarbon degrading microorganisms which are using sulfate as the electron acceptor have been isolated from Guaymas Basin sites and similar marine habitats (Rüter et al., 1994; Galushko et al., 1999; Musat and Widdel, 2008; Kleindienst et al., 2012). Nevertheless, the metabolic potential, in particular for hydrocarbon degradation, of the whole microbial community from Guaymas vent chimneys has never been investigated. Therefore, comprehensive studies on biodegradation, in particular under anaerobic conditions, still remain to be conducted to characterize the structure and metabolic potential of microbial ecosystems with capability for hydrocarbon biodegradation.

In this study, the metagenome of an oil-immersed chimney in Guaymas Basin was analyzed to demonstrate the metabolic potential and ecological functions of the inhabited microbial community. Additionally, questions related to anaerobic biodegradation of hydrocarbons are addressed: do the microorganisms from this chimney community have anaerobic hydrocarbon degradation activities? If so, what kinds of hydrocarbons could be potentially degraded? Which groups of microorganisms are responsible for carrying out the degradations? Which processes are coupled/closely related to the degradation for electron transfer? Are there any features shared among different chimney-originated samples?

## MATERIALS AND METHODS

### DNA EXTRACTION AND SEQUENCING

The sample 4558-6 under investigation represented the outer layer of a black-smoker chimney with preliminary venting fluid temperature 190°C (measured above the chimney prior to sampling), and was collected in Guaymas Basin (27°0.9'N, 111°24.6'W, depth = 2013 m) by the R/V Alvin (supported by the R/V Atlantis) in November, 2009. The chimney (**Figure A1**) was kept at –20°C immediately after sample collection, and stored with dry ice during transportation and stored at –80°C

in laboratory until further analyses. The genomic DNA was extracted from outer sections of all collected samples where highest DNA quantity was found. Isolation of DNA was conducted as described in a previous study (Wang et al., 2009). Metagenome pyrosequencing was performed according to company protocol on the 454 Life Sciences GS FLX system with a practical limit of 400 bp. All the sequences were deposited in the MG-RAST server.

### METAGENOMIC ANALYSIS AND ASSEMBLY

Low quality sequencing reads were trimmed in Geneious 6.04 (Biomatters Ltd.) with default parameters. Technical replicates (Gomez-Alvarez et al., 2009) were removed with cd-hit (at 96% sequence identity) (Niu et al., 2010). Shorter reads (<100 bp) were then excluded, and the remaining reads were assembled with Velvet (Zerbino and Birney, 2008). This metagenome from Guaymas Basin chimney was uploaded (MG-RAST ID: 4510962.3) and analyzed using MG-RAST (Meyer et al., 2008).

### METAGENOMIC SEQUENCE ANALYSIS

Coding regions within the metagenome were predicted using FragGeneScan (Rho et al., 2010), and the predicted sequence features were then annotated (e-value <1e-5) against M5NR protein database. 16S rRNA genes were predicted with HMM and BLASTN (e-value <1e-5) in webMGA (Wu et al., 2011), respectively. To analyze the taxonomic contents, all predicted gene features were subject to blastx (Altschul et al., 1997) searches against NCBI non-redundant (NR) database (e-value <1e-5, word size = 3, multi hit window size = 40 and low complexity filter on) and visualized in MEGAN (Huson et al., 2007). Each predicted sequence feature in the metagenome was assigned to a certain taxon when at least 75% of the BLAST hits of this query were from that specific taxon. Sequences with matches to the eggNOG (Powell et al., 2012), COG (Tatusov et al., 2003) and KEGG (Ogata et al., 1999) database were retrieved to build functional categories and reconstruct metabolic pathways.

### ANNOTATION OF SEQUENCES WITH DEGRADATION/METABOLIC ACTIVITIES

Sequences that were annotated as enzymes in the degradation of cellulose and fatty acids were extracted and subject to manual examination. Annotated KEGG pathways in this metagenome were visualized in MEGAN to demonstrate the metabolic potential in the microbial community. Enzymes involved in the degradation of a few organic chemicals (such as benzene, toluene, ethylbenzene, and xylenes) were collected from the Biocatalysis/Biodegradation Database (BBD) of the University of Minnesota (Gao et al., 2010), an online web service that listed known degradation pathways for hundreds of chemicals/contaminants. Within this chimney metagenome, a sequence-similarity based search against BBD was conducted to identify candidate genes that were involved in the biodegradation of certain hydrocarbons. Sequences of previously reported anaerobic alkane degradation genes (Callaghan et al., 2010), benzylsuccinate synthase (*bss*) and alkylsuccinate synthase (*ass*), were retrieved from GenBank (accession no.: DQ826035, DQ826036, AJ001848, AB066263, AY032676, and AF113168) and searched against our Guaymas metagenome.

## CLUSTERING ANALYSIS OF FUNCTIONAL CATEGORIES

Clustering of functional categories (with KEGG annotation, e-value < 1e-5, min. identity of 30% and min. align. length of 15 a.a.) was conducted in MG-RAST (using ward with canberra distance metric based on normalized values) among metagenomes as following: Guaymas Basin chimney 4558-6 (MG-RAST ID: 4510962.3), Juan de Fuca chimney (MG-RAST ID: 4510965.3) (Xie et al., 2011), Lost City hydrothermal vent field (MG-RAST ID: 4461585.3) (Brazelton and Baross, 2009), two biofilm samples from acid mine drainage (UBA and 5way, with MG-RAST ID 4441137.3 and 4441138.3, respectively) (Tyson et al., 2004), a gutless worm (MG-RAST ID: 4441115.3) (Woyke et al., 2006), the North Pacific Subtropical Gyre microbial communities (the HOT project with depth of 10, 70, 130, 200, 500, 770 and 4000 m, and with MG-RAST ID: 4441051.3, 4441057.4, 4441055.3, 4441041.3, 4441057.3, 4441062.3, and 4441056.3, respectively) (Delong et al., 2006) and a deeply buried sediments from Peru Margin (for sample original, am1mbsf, am16mbsf, am32mbsf and am50mbsf, and with MG-RAST ID: 4440960.3, 4440961.3, 4440973.3, 4459940.3, and 4459941.3, respectively) (Biddle et al., 2008). All metagenomes were stored in MG-RAST database.

## RESULTS

### SEQUENCING SUMMARY AND COVERAGE

Initially, as shown in **Table 1**, a total amount of 512,830 reads and 196,377,880 bp of sequence data were generated by 454 pyrosequencing. After removing low-quality reads and technical duplicates, the remaining 504,915 reads (with an average length 383 bp) were assembled into 49,055 contigs (totaling 26,241,624 bp, with an average length of 543 bp). 187,308 singletons with an average length of 367 bp could not be assembled. From this assembly, 52,366 gene features were predicted, 37,372 of which (71.4%) were with known annotations. A rarefaction analysis of the final assembly was conducted based on the taxonomic information retrieved from annotation results in MG-RAST (**Figure 1**), which indicated that a reasonable number of individual genomes were sampled and covered in the metagenome.

### TAXONOMIC DIVERSITY BASED ON 16S rRNA GENE PREDICTION

70 and 90 16S rRNA sequences were predicted from webMGA (Wu et al., 2011), with the use of HMM and BLASTN, respectively (**Table 2**). In both of the results, around 3/4 (72.9 and 76.7%,

respectively) of all identified 16S rRNA sequences were from bacteria. Deltaproteobacteria and Euryarchaeota had dominated the bacteria and archaea, respectively.

## PHYLOGENY FROM 454 PYROSEQUENCING DATA

A total number of 37,372 predicted gene features were utilized to extract taxonomic information by BLASTing against the NCBI NR database. In total, 21,792 (58.3%) and 11,249 (30.1%) hits were assigned to bacteria and archaea (rules for taxonomic assignment were stated in “Materials and Methods”), respectively (**Table A1**). At the phylum level, Proteobacteria (9558, 25.6%), Euryarchaeota (9078, 24.3%), Crenarchaeota (1354, 3.6%), Firmicutes (786, 2.1%), Thermotogae (725, 1.9%), and Bacteroidetes (607, 1.6%) had the top matches (**Figure 2**). Taxa with most hits assigned were listed in **Table 3**. Notably, the majority of sequences in this chimney metagenome originated from the families *Archaeoglobaceae*, *Thermococcaceae*, and *Desulfobacteraceae*, and a high proportion (>21.2%) of sequences potentially originated from sulfate reducing prokaryotes (SRP). Moreover, thermophilic sulfate reducing microorganisms, including bacteria (*Thermodesulfobacteriaceae*) and archaea (*Archaeoglobaceae*) were found predominant, highlighting their roles in reducing sulfates and/or sulfites to sulfides during energy metabolism under anaerobic conditions.

## FUNCTIONAL CATEGORY HITS DISTRIBUTION

Major KEGG function categories were listed (**Table 4**) and ordered by the number of unique hits assigned to each category. Similar to a previous study on the chimney from hydrothermal vents (Xie et al., 2011), genes involved in Recombination and Repair were among the abundant categories (**Table 4**). In addition, transposases were found to be highly enriched in this sample (**Table A3**), and genes participated in Chemotaxis and Flagellar Assembly was all identified with high abundance in this metagenome.

## DEGRADATION OF REFRACTORY OM AND PETROLEUM HYDROCARBONS

Sequences coding for the complete degradation pathway of cellulose and fatty acids, as well as key enzymes involved in breakdown of lipid and pullulan were all identified in this metagenome (**Table A2**). Many of these identified enzymes were with thermophilic-origin best hits (as marked with asterisk in **Table A2**). Peptidases were found to be of low abundance in this metagenome (data not shown). For anaerobic hydrocarbon degradation, sequences coding for benzylsuccinate synthase (*bss*) and alkylsuccinate synthase (*ass*), key enzymes in the fumarate addition pathway for the anaerobic oxidation of hydrocarbons (Callaghan et al., 2010), were identified (**Table 5**). In particular, gene candidates involved in BTEX (benzene, toluene, ethylbenzene, and xylenes) degradation were identified by searching against the BBD of the University of Minnesota (Gao et al., 2010) (**Table 5**). Additionally, to show the metabolic potential of this Guaymas sample in the degradation and remediation of organic contaminants (He et al., 2010), genes involved in the degradation of aromatic carboxylic acid (benzoate, phenylpropionate and phthalate), chlorinated aromatics (2- and 4-chlorobenzoate,

**Table 1 | Summary of sequences from the chimney sample 4558-6.**

| Properties                              | Value       |
|---|-------------|
| Clean reads                             | 504,915     |
| Base pairs                              | 193,336,182 |
| GC content                              | 42%         |
| Average read length                     | 383         |
| Singletons                              | 187,308     |
| Contigs                                 | 49,055      |
| Average contig length                   | 543         |
| Best hit gene features with NR database | 37372       |

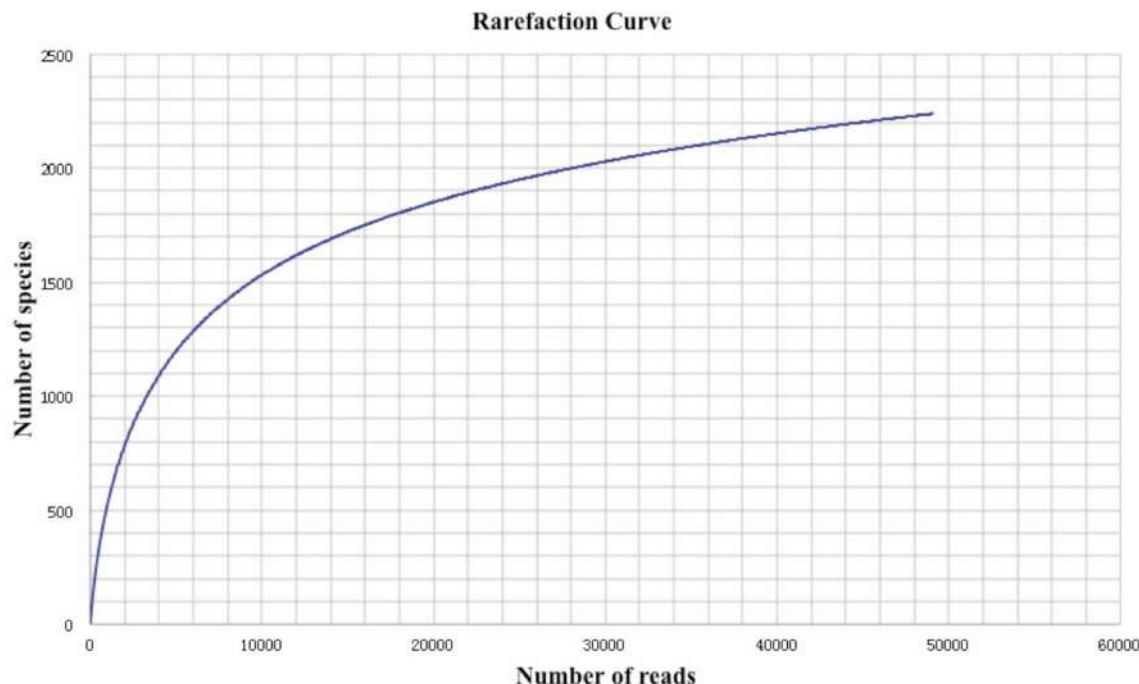


**FIGURE 1 |** Rarefaction plot of the total number of distinct taxon annotations (MG-RAST) as a function of the number of sequences from the assembly.

**Table 2 |** Taxonomic diversity based on 16S rRNA gene prediction from the metagenome.

| Methods | Domain [total no. of sequences (%)] | Diversity (% in domain)  |
|---------|-------------------------------------|--|
| HMM     | Bacteria (51, 72.9)                 | Deltaproteobacteria (25.4)<br>Gammaproteobacteria (21.6)<br>Epsilonproteobacteria (13.7)<br>Deferribacteres (7.8)                        |
|         | Archaea (19, 27.1)                  | Euryarchaeota (63.2)<br>Crenarchaeota/Thermoprotei (36.8)  |
| BLASTN  | Bacteria (69, 76.7)                 | Deltaproteobacteria (23.4)<br>Gammaproteobacteria (18.8)<br>Epsilonproteobacteria (12.5)<br>Acidobacteria (9.4)<br>Deferribacteres (7.8) |
|         | Archaea (21, 23.3)                  | Euryarchaeota (52.4)<br>Crenarchaeota/Thermoprotei (47.6)  |

2,4,5-trichlorophenoxyacetic acid), heterocyclic aromatics (carbazole and dibenzothiophene), nitroaromatics (nitrobenzene and nitrophenol) as well as a few of other hydrocarbons (cyclohexane and tetrahydrofuran) were searched within the Guaymas metagenome. Notably, this chimney sample seemed to have the potential to degrade toluene, ethylbenzene and o-xylene (**Table 5**), yet no such evidence for benzene or the rest has been detected.

#### COMPARATIVE METAGENOMIC ANALYSIS

Clustering on (KEGG) functional gene categories was conducted among different environmental samples (**Figure 3**). Guaymas chimney sample 4558-6 (4510962.3) was clustered most closely with chimney sample from Juan de Fuca (4510965.3). Both of these two metagenomes were almost depleted in categories of RNA family and folding, sorting and degradation, while they showed higher abundance in the categories of signaling molecules, and interaction and cell communication. These features might be highly related to the specific environmental conditions where these two chimney samples were collected. The metagenome of the Lost City chimney sample (4461585.3) was not grouped with the above two chimney samples. The two biofilm samples from acid mine drainage (4441137.3 and 4441138.3) shared similar functional profiles in the heatmap, adjacent to the chimney sample from Lost City and the gutless worm sample (4441115.3). Samples from the North Pacific Subtropical Gyre microbial communities (4441051.3, 4441057.4, 4441055.3, 4441041.3, 4441057.3, 4441062.3, and 4441056.3) were grouped next to each other in the functional heatmap, and a similar pattern was observed for Peru Margin sediments samples (4440960.3, 4440961.3, 4440973.3, 4459940.3, and 4459941.3). Enzymes involved in hydrocarbon biodegradation in metagenomes from different environments were listed in **Table A3**. When compared to metagenomes from different environments, 4458-6 from Guaymas hydrothermal vent chimney was the only one with enzymes for biodegradation of toluene, ethylbenzene, and o-xylene (**Table A3**), highlighting its metabolic

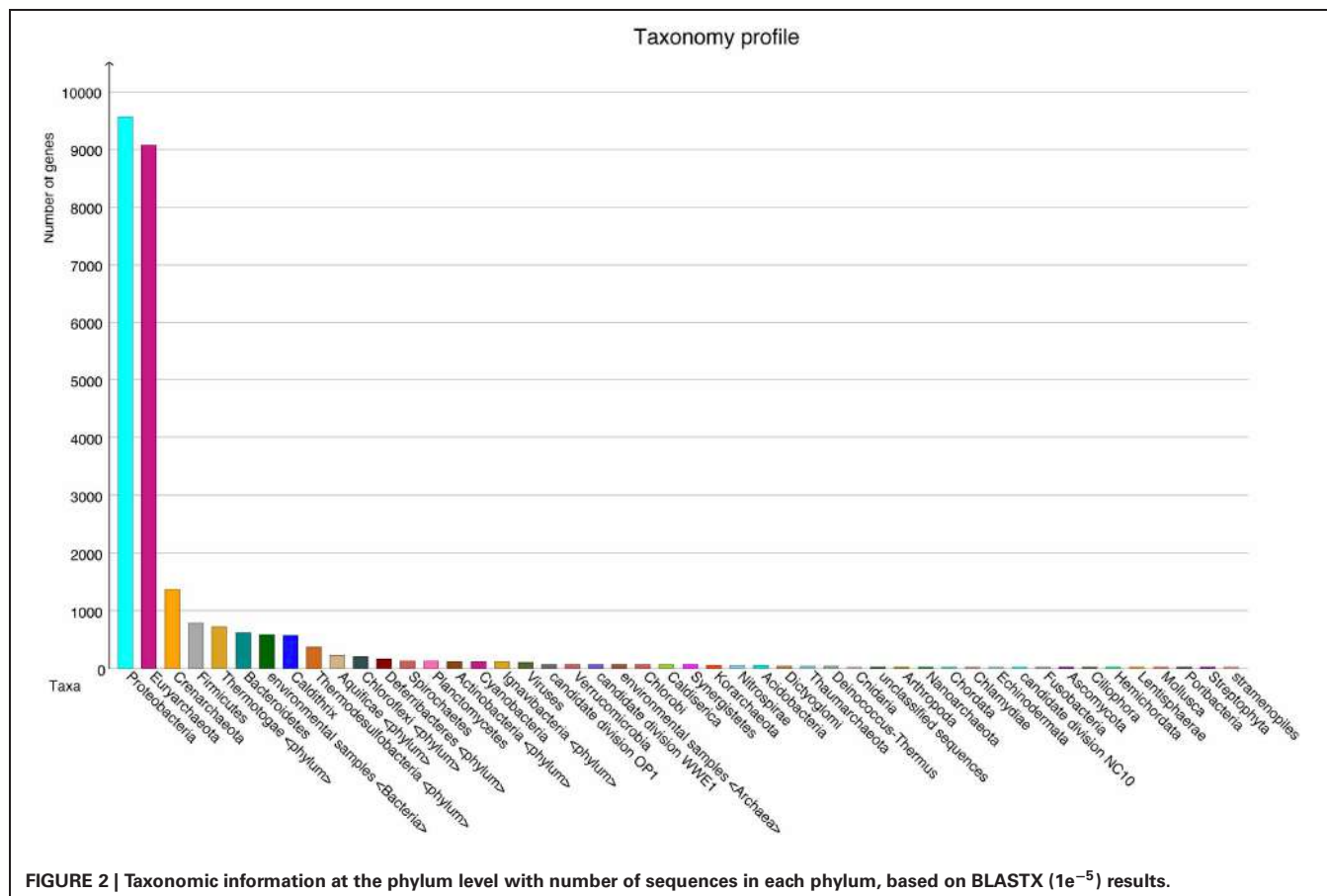


**FIGURE 2 | Taxonomic information at the phylum level with number of sequences in each phylum, based on BLASTX ( $1e^{-5}$ ) results.**

**Table 3 | Top families with the most hits assigned.**

| Family                       | No. of hits assigned (%) | Phylum                   |
|------------------------------|--------------------------|--------------------------|
| Archaeoglobaceae             | 4777 (12.78)             | Euryarchaeota            |
| Thermococcaceae              | 2365 (6.33)              | Euryarchaeota            |
| Desulfobacteraceae           | 2117 (5.66)              | (Delta) Proteobacteria   |
| Thermotogaceae               | 723 (1.93)               | Proteobacteria           |
| Desulfurococcaceae           | 672 (1.80)               | Crenarchaeota            |
| Helicobacteraceae            | 375 (1.00)               | (Epsilon) Proteobacteria |
| Thermodesulfobacteriaceae    | 355 (0.95)               | Proteobacteria           |
| Colwelliaceae                | 344 (0.92)               | (Gamma) Proteobacteria   |
| Thiotrichaceae               | 214 (0.57)               | (Gamma) Proteobacteria   |
| Desulfovibrionaceae          | 208 (0.56)               | (Delta) Proteobacteria   |
| Sulfate reducing prokaryotes | 7921* (21.2)             | –                        |

The exact number of blast hits was listed for each family, with the percentages (out of total hits) listed in the parentheses.

\*The number of hits for SRP was generated by summing all the hits from Archaeoglobaceae, Desulfobacteraceae, Desulfurococcaceae, Desulfovibrionaceae, and Thermodesulfobacteriaceae.

potential in degrading hydrocarbons in the native oil-immersed condition.

## DISCUSSION

Advances in sequencing technologies have made microbial diversity studies easier and more accurate. However, biases were

introduced during sequencing and analyzing of environmental sequences. For instance, biases were generated when multiple reads were produced for a unique DNA fragment in a random manner. Such biases might result in an inaccurate representation of the fragments and lead to misleading conclusions. Therefore, strict quality control of the sequenced reads should be done. In this study, a decent sequencing coverage has been reached (Figure 1) and we are in the position to investigate the taxonomic diversity as well as the metabolic potential of this Guaymas chimney sample.

## DIVERSITY AT DIFFERENT TAXONOMIC LEVELS

Estimated from both 16S rRNA sequences as well as taxonomic classifications based on blast hits, the proportion of bacteria in the community was about 60–75%, and 25–30% for archaea. Bacteria were dominated by Proteobacteria, while Euryarchaeota were most abundant among the archaea. So far, sulfate-reducing bacteria and archaea have been isolated in vent chimneys, with either high or low growth temperature (30–90°C) (Burggraf et al., 1990; Audiffren et al., 2003; Moussard et al., 2004). Sulfate reduction may occur at temperatures up to 110°C in hot sediments from Guaymas hydrothermal field (Jørgensen et al., 1992). In this study, a high proportion (at least 21.2%) of sequences from this chimney metagenome was potentially originated from SRP (Table 3), a large and extremely diverse physiological group of anaerobic microorganisms. Sulfate-reducing bacteria and archaea

were capable of degrading a wide range of organic substrates (Widdel and Bak, 1992; Widdel and Rabus, 2001), including petroleum-based products that were discussed in this study. The presence of large numbers of SRP in the oil-immersed chimney suggested that the microbial community had the potential of hydrocarbon biodegradation, which were likely to be coupled with sulfate reduction. Besides, most of the retrieved sequences were estimated to originate from thermophile microorganisms such as *Archaeoglobus*, heterotrophic *Thermococcales* and *Thermodesulfobacteriaceae*, reflecting the influence of the high temperature on the structure of the microbial community.

**Table 4 | List of major KEGG families.**

| KEGG (level 2) annotation            | Avg. % ident | Avg. aligned len. | No. of hits |
|--------------------------------------|--------------|-------------------|-------------|
| Amino acid metabolism                | 69.68        | 80.99             | 1756        |
| Carbohydrate metabolism              | 69.96        | 75.17             | 1365        |
| Translation                          | 71.01        | 66.33             | 1301        |
| Membrane transport                   | 68.01        | 70.23             | 836         |
| Metabolism of cofactors and vitamins | 68.73        | 71.72             | 723         |
| Energy metabolism                    | 72.02        | 73.84             | 689         |
| Nucleotide metabolism                | 68.99        | 68.01             | 550         |
| Replication and repair               | 67.7         | 71.41             | 515         |
| Folding, sorting and degradation     | 71.9         | 71.82             | 386         |
| Signal transduction                  | 67.86        | 62.85             | 375         |
| Cell motility                        | 70.33        | 57.04             | 258         |
| Glycan biosynthesis and metabolism   | 67           | 65.77             | 240         |
| Transcription                        | 73.36        | 75.02             | 213         |
| Cell growth and death                | 68.78        | 64.14             | 209         |
| Lipid metabolism                     | 70.28        | 64.61             | 184         |

Average sequence identity (Avg % ident) and aligned sequence length (Avg aligned len) were presented. No. of Hits represented the number of unique hits within each functional protein category. Uncharacterized proteins were excluded.

## METABOLIC POTENTIAL FOR HYDROCARBON DEGRADATION

Deep-sea environments have been characterized by the lack of easily biodegradable OM, thus genes related to the degradation of refractory OM have been extensively recovered from the metagenomes of deep oceans (Martin-Cuadrado et al., 2007). Moreover, bacteria isolated from the deep sea have been shown to be capable of degrading refractory OM such as chitin and cellulose (Hedges et al., 2000; Vezzi et al., 2005; Wang et al., 2008). Here, the potential of a chimney microbial community for refractory OM degradation was evaluated. Genes coding for chitin degradation were not found in the metagenome, while all the genes involved in the degradation of cellulose and fatty acids, as well as a few key enzymes in the breakdown of lipid and pullulan were identified, which probably reflected in part the input of terrestrial OM circulating in this Guaymas vent field. As most of the identified enzymes had a presumably thermophilic origin (Table 5 and Table A2), and thermophilic microorganisms were predominant in the chimney sample (Table 3), it was likely that these enzymes had some degree of heat tolerance. Additionally, microorganisms of this Guaymas chimney were predicted to have the potential to degrade toluene, ethylbenzene, and o-xylene. Notably, anaerobic hydrocarbon degrading microorganisms have been successfully enriched and most extensively studied with the benzene-toluene-ethylbenzene-xylanes (BTEX) group of petroleum hydrocarbons (Stockton et al., 2009). For example, pure culture strain EbS7 was isolated from the sediments of Guaymas Basin which was reported with the ethylbenzene-dependent sulfate reduction (Kniemeyer et al., 2003). This Guaymas chimney sample was oil immersed, thus it was not surprising to see the presence of genes involved in the degradations of petroleum hydrocarbons (Table 5). Our data further highlighted the potential of this microbial community using the fumarate addition pathway for the degradation of aromatic and aliphatic hydrocarbons. Identification of genes coding for hydrocarbon degradation would advance characterizations of the potential source of electrons and energy, as well as the roles of this chimney microbial community had played in its native environment. Notably, this Guaymas chimney

**Table 5 | List of annotated gene features involved in degradation of hydrocarbons, absence of gene was marked with “-”.**

| Substrate             | Enzyme (EC)                | Best hit contig | Metagenome best hit organism                | Similarity % (e-value) |
|-----------------------|----------------------------|-----------------|---|------------------------|
| n-Alkanes             | assA1                      | Contig00511     | <i>Desulfoglaeba alkanexedens</i> AK-01     | 78 (5.2e-27)           |
|                       | assA2                      | Contig45077     | <i>Desulfoglaeba alkanexedens</i> AK-01     | 95 (9e-10)             |
| Aromatic hydrocarbons | bssA                       | Contig28667     | <i>Desulfotomaculum</i> sp. Ox39            | 76 (1.7e-6)            |
|                       | bssB                       | -               | -   | -                      |
|                       | bssC                       | Contig46590     | <i>Desulfatibacillus alkenivorans</i> AK-01 | 35 (2e-7)              |
|                       | bssD                       | Contig29655     | <i>Desulfatibacillus alkenivorans</i> AK-01 | 67 (1e-35)             |
|                       | bssE                       | Contig46456     | <i>Azoarcus</i> sp.                         | 72 (1e-6)              |
|                       | bssG                       | Contig46590     | <i>Desulfatibacillus alkenivorans</i> AK-01 | 79 (1e-6)              |
| Toluene               | toluene 4-monooxygenase    | Contig31764     | <i>Dechloromonas aromatica</i> (strain RCB) | 77 (1.6e-64)           |
| Ethylbenzene          | ethylbenzene dehydrogenase | Contig32722     | <i>Desulfococcus oleovorans</i> Hxd3        | 86 (3.4e-145)          |
| o-Xylene              | o-xylene monooxygenase     | Contig31764     | <i>Dechloromonas aromatica</i> (strain RCB) | 77 (1.6e-64)           |

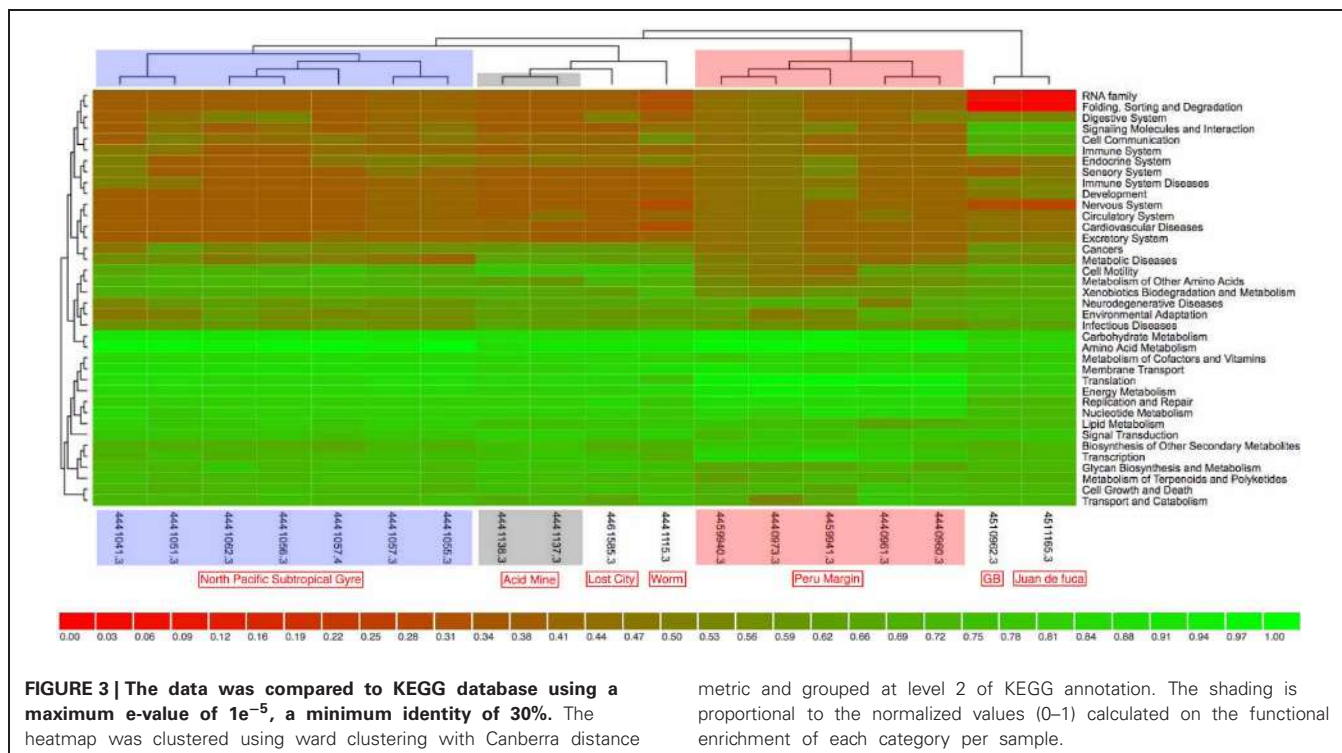


**FIGURE 3 |**The data was compared to KEGG database using a maximum e-value of  $1e^{-5}$ , a minimum identity of 30%. The heatmap was clustered using ward clustering with Canberra distance

metagenome seemed to be the only one (among all the samples included in the comparative metagenomic analysis) with metabolic potential for hydrocarbons biodegradation (**Table A3**). Enzymes activated by oxygen (namely active under aerobic conditions) were not identified in our metagenome, consistent with the strict anaerobic condition where this chimney sample was collected. Metagenomic analysis suggested that degradation of a variety of petroleum hydrocarbons by SRP might play an important role in the energy metabolism of this chimney microbial community.

#### COMPARISON AMONG DIFFERENT SAMPLES

For the moment, only three metagenomes from hydrothermal vent chimney are available, one from Juan de Fuca (Xie et al., 2011), one from Lost City (Brazelton and Baross, 2009) and the last one was our chimney sample 4458-6 from Guaymas Basin. The whole metagenome-based comparison (**Figure 3**) showed that Lost City was not clustered next to the other two chimney samples, which could be due to the fact that the Lost City sample was collected from a white carbonate chimney (CC) rather than a black sulfide chimney (SC) as the other two samples were. When considering the fact that the dominant energy sources for SC and CC were significant different (i.e., metal sulfides in SC and reduced volatiles such as hydrogen, methane in CC, respectively), the genomic differences between the two types of chimneys become clear as different energy metabolisms were promoted accordingly. Moreover, the venting fluid of Lost City had a pH of 9–11 and temperatures lower than 90°C, whereas that of Juan de Fuca sample was acidic and hot (temperature around 310°C); the vent fluid of our Guaymas chimney

metric and grouped at level 2 of KEGG annotation. The shading is proportional to the normalized values (0–1) calculated on the functional enrichment of each category per sample.

sample represented an intermediate temperature regime (190°C). Differences in environmental factors (such as temperature, pH, and physico-chemical gradients) between white and black chimneys could also have a significant influence on the distribution of functional gene categories, and as a result the three chimney samples were not clustered next to each other. On the other hand, when looking at specific gene categories, metagenomes from hydrothermal vent chimneys (Guaymas Basin, Juan de Fuca and Lost City) kept a larger collection of genes involved in recombination and repair, chemotaxis and flagellar assembly, as well as transposases. This could be a chimney-specific feature, reflecting adaptations of microorganisms and the microbial community to the extreme fluctuating chemical and physical conditions that characterize deep-sea hydrothermal vent chimneys.

#### ACKNOWLEDGMENTS

We thank Anna-Louise Reysenbach for providing the chance to attend the expedition, and all the crew members from R/V Atlantis/DSV Alvin on the Guaymas Basin Expedition 2009 for collecting the samples. This research was supported by the National High Technology Research and Development Program of China (Grant No. 2012AA092103-2), China Ocean Mineral Resources R & D Association (Grant No.DYXY-125-8-YP-2), National Basic Research Program of China (Grant No.2011CB808800), National Science Foundation of China (Grant No. 91228201 and 31290232), “ShuGuang” Project supported by Shanghai Municipal Education Commission and Shanghai Education Development Foundation, and the US-NSF (OCE-0728391) to Anna-Louise Reysenbach.

## REFERENCES

- Altschul, S. F., Madden, T. L., Schaffer, A. A., Zhang, J., Zhang, Z., Miller, W., et al. (1997). Gapped BLAST and PSI-BLAST: a new generation of protein database search programs. *Nucleic Acids Res.* 25, 3389–3402. doi: 10.1093/nar/25.17.3389
- Amann, R. I., Ludwig, W., and Schleifer, K. H. (1995). Phylogenetic identification and *in situ* detection of individual microbial cells without cultivation. *Microbiol. Rev.* 59, 143–169.
- Audiffrin, C., Cayol, J. L., Joulian, C., Casalot, L., Thomas, P., García, J. L., et al. (2003). *Desulfonautilus submarinus* gen. nov., sp. nov., a novel sulfate-reducing bacterium isolated from a deep-sea hydrothermal vent. *Int. J. Syst. Evol. Microbiol.* 53, 1585–1590.
- Bazylinski, D. A., Farrington, J. W., and Jannasch, H. W. (1988). Hydrocarbons in surface sediments from a Guaymas Basin hydrothermal vent site. *Org. Geochem.* 12, 547–559. doi: 10.1016/S0146-6380(88)90146-5
- Biddle, J. F., Fitz-Gibbon, S., Schuster, S. C., Brenchley, J. E., and House, C. H. (2008). Metagenomic signatures of the Peru Margin subseafloor biosphere show a genetically distinct environment. *Proc. Natl. Acad. Sci. U.S.A.* 105, 10583–10588. doi: 10.1073/pnas.0709942105
- Brazelton, W. J., and Baross, J. A. (2009). Abundant transposases encoded by the metagenome of a hydrothermal chimney biofilm. *ISME J.* 3, 1420–1424. doi: 10.1038/ismej.2009.79
- Brazelton, W. J., Ludwig, K. A., Sogin, M. L., Andreishcheva, E. N., Kelley, D. S., Shen, C. C., et al. (2010). Archaea and bacteria with surprising microdiversity show shifts in dominance over 1,000-year time scales in hydrothermal chimneys. *Proc. Natl. Acad. Sci. U.S.A.* 107, 1612–1617. doi: 10.1073/pnas.0905369107
- Burggraf, S., Jannasch, H. W., Nicolaus, B., and Stetter, K. O. (1990). *Archaeoglobus profundus* sp. nov., represents a new species within the sulfate-reducing Archaeabacteria. *Syst. Appl. Microbiol.* 13, 24–28. doi: 10.1016/S0723-2020(11)80176-1
- Callaghan, A. V., Davidova, I. A., Savage-Ashlock, K., Parisi, V. A., Gieg, L. M., Suflita, J. M., et al. (2010). Diversity of benzyl- and alkylsuccinate synthase genes in hydrocarbon-impacted environments and enrichment cultures. *Environ. Sci. Technol.* 44, 7287–7294. doi: 10.1021/es1002023
- Delong, E. F., Preston, C. M., Mincer, T., Rich, V., Hallam, S. J., Frigaard, N. U., et al. (2006). Community genomics among stratified microbial assemblages in the ocean's interior. *Science* 311, 496–503. doi: 10.1126/science.1120250
- Dick, G. J., and Tebo, B. M. (2010). Microbial diversity and biogeochemistry of the Guaymas Basin deep-sea hydrothermal plume. *Environ. Microbiol.* 12, 1334–1347.
- Distel, D. L., Lane, D. J., Olsen, G. J., Giovannoni, S. J., Pace, B., Pace, N. R., et al. (1988). Sulfur-oxidizing bacterial endosymbionts: analysis of phylogeny and specificity by 16S rRNA sequences. *J. Bacteriol.* 170, 2506–2510.
- Elsgaard, L., Isaksen, M. F., Jørgensen, B. B., Alyase, A. M., and Jannasch, H. W. (1994). Microbial sulfate reduction in deep-sea sediments at the Guaymas Basin hydrothermal vent area: influence of temperature and substrates. *Geochim. Cosmochim. Acta* 58, 3335–3343. doi: 10.1016/0016-7037(94)90089-2
- Flores, G. E., Campbell, J. H., Kirshtein, J. D., Meneghin, J., Podar, M., Steinberg, J. I., et al. (2011). Microbial community structure of hydrothermal deposits from geochemically different vent fields along the Mid-Atlantic Ridge. *Environ. Microbiol.* 13, 2158–2171. doi: 10.1126/science.229.4715.717
- Jørgensen, B. B., Isaksen, M. F., and Jannasch, H. W. (1992). Bacterial sulfate reduction above 100°C in deep-sea hydrothermal vent sediments. *Science* 258, 1756–1757. doi: 10.1126/science.258.5089.1756
- Jørgensen, B. B., Zawacki, L. X., and Jannasch, H. W. (1990). Thermophilic bacterial sulfate reduction in deep-sea sediments at the Guaymas Basin hydrothermal vents (Gulf of California). *Deep-Sea Res. I* 37, 695–710. doi: 10.1016/0198-0149(90)90099-H
- Kallmeyer, J., and Boetius, A. (2004). Effects of temperature and pressure on sulfate reduction and anaerobic oxidation of methane in hydrothermal sediments of Guaymas Basin. *Appl. Environ. Microbiol.* 70, 1231–1233. doi: 10.1128/AEM.70.2.1231-1233.2004
- Kawka, O. E., and Simoneit, B. R. T. (1994). Hydrothermal pyrolysis of organic matter in Guaymas Basin. I. Comparison of hydrocarbon distributions in subsurface sediments and seabed petroleums. *Org. Geochem.* 22, 947–978. doi: 10.1016/0146-6380(94)90031-0
- Kleindienst, S., Ramette, A., Amann, R., and Knittel, K. (2012). Distribution and *in situ* abundance of sulfate-reducing bacteria in diverse marine hydrocarbon seep sediments. *Environ. Microbiol.* 14, 2689–2710. doi: 10.1111/j.1462-2920.2012.02832.x
- Kniemeyer, O., Fischer, T., Wilkes, H., Glockner, F. O., and Widdel, F. (2003). Anaerobic degradation of ethylbenzene by a new type of marine sulfate-reducing bacterium. *Appl. Environ. Microbiol.* 69, 760–768. doi: 10.1128/AEM.69.2.760-768.2003
- Lam, P., Cowen, J. P., and Jones, R. D. (2004). Autotrophic ammonia oxidation in a deep-sea hydrothermal plume. *FEMS Microbiol. Ecol.* 47, 191–206. doi: 10.1016/S0168-6496(03)00256-3
- Martens, C. S. (1990). Generation of short chain organic acid anions in hydrothermally altered sediments of the Guaymas Basin, Gulf of California. *Appl. Geochem.* 5, 71–76. doi: 10.1016/0883-2927(90)90037-6
- Martin-Cuadrado, A. B., Lopez-Garcia, P., Alba, J. C., Moreira, D., Monticelli, L., Strittmatter, A., et al. (2007). Metagenomics of the deep Mediterranean, a warm bathypelagic habitat. *PLoS ONE* 2:e914. doi: 10.1371/journal.pone.0000914
- Meyer, F., Paarmann, D., D'Souza, M., Olson, R., Glass, E. M., Kubal, M., et al. (2008). The metagenomics RAST server - a public resource for the automatic phylogenetic and functional analysis of metagenomes. *BMC Bioinformatics* 9:386. doi: 10.1186/1471-2105-9-386
- Moussard, H., L'Haridon, S., Tindall, B. J., Banta, A., Schumann, P., Stackebrandt, E., et al. (2004). *Thermodesulfatator indicus* gen. nov., sp. nov., a novel thermophilic chemolithoautotrophic sulfate-reducing bacterium isolated from the Central Indian Ridge. *Int. J. Syst. Evol. Microbiol.* 54, 227–233. doi: 10.1099/ijns.0.02669-0
- Musat, F., and Widdel, F. (2008). Anaerobic degradation of benzene by a marine sulfate-reducing enrichment culture, and cell hybridization of the dominant phylotype. *Environ. Microbiol.* 10, 10–19. doi: 10.1111/j.1462-2920.2007.01425.x
- Niu, B., Fu, L., Sun, S., and Li, W. (2010). Artificial and natural duplicates in pyrosequencing reads of metagenomic data. *BMC Bioinformatics* 11:187. doi: 10.1186/1471-2105-11-187
- Ogata, H., Goto, S., Sato, K., Fujibuchi, W., Bono, H., and Kanehisa, M. (1999). KEGG: kyotoencyclopedia of genes and genomes. *Nucleic Acids Res.* 27, 29–34. doi: 10.1093/nar/27.1.29
- Petersen, J. M., Zielinski, F. U., Pape, T., Seifert, R., Moraru, C., Amann, R., et al. (2013). Metagenome of a Guaymas chimney sample. *Frontiers in Microbiology* | Extreme Microbiology

- et al. (2011). Hydrogen is an energy source for hydrothermal vent symbioses. *Nature* 476, 176–180. doi: 10.1038/nature10325
- Powell, S., Szklarczyk, D., Trachana, K., Roth, A., Kuhn, M., Muller, J., et al. (2012). eggNOG v3.0: orthologous groups covering 1133 organisms at 41 different taxonomic ranges. *Nucleic Acids Res.* 40, D284–D289. doi: 10.1093/nar/gkr1060
- Reysenbach, A. L., and Shock, E. (2002). Merging genomes with geochemistry in hydrothermal ecosystems. *Science* 296, 1077–1082. doi: 10.1126/science.1072483
- Rho, M., Tang, H., and Ye, Y. (2010). FragGeneScan: predicting genes in short and error-prone reads. *Nucleic Acids Res.* 38:e191. doi: 10.1093/nar/gkq747
- Roussel, E. G., Konn, C., Charlou, J. L., Donval, J. P., Fouquet, Y., Querellou, J., et al. (2011). Comparison of microbial communities associated with three Atlantic ultramafic hydrothermal systems. *FEMS Microbiol. Ecol.* 77, 647–665. doi: 10.1111/j.1574-6941.2011.01161.x
- Rüter, P., Rabus, R., Wilkes, H., Aeckersberg, F., Rainey, F. A., Jannasch, H. W., et al. (1994). Anaerobic oxidation of hydrocarbons in crude oil by new types of sulphate-reducing bacteria. *Nature* 372, 455–458. doi: 10.1038/372455a0
- Stockton, A. M., Chiesl, T. N., Scherer, J. R., and Mathies, R. A. (2009). Polycyclic aromatic hydrocarbon analysis with the Mars organic analyzer microchip capillary electrophoresis system. *Anal. Chem.* 81, 790–796. doi: 10.1021/ac802033u
- Tatusov, R. L., Fedorova, N. D., Jackson, J. D., Jacobs, A. R., Kiryutin, B., Koonin, E. V., et al. (2003). The COG database: an updated version includes eukaryotes. *BMC Bioinformatics* 4:41. doi: 10.1186/1471-2105-4-41
- Teske, A., Hinrichs, K. U., Edgcomb, V., De Vera Gomez, A., Kysela, D., Sylva, S. P., et al. (2002). Microbial diversity of hydrothermal sediments in the Guaymas Basin: evidence for anaerobic methanotrophic communities. *Appl. Environ. Microbiol.* 68, 1994–2007.
- Tyson, G. W., Chapman, J., Hugenholtz, P., Allen, E. E., Ram, R. J., Richardson, P. M., et al. (2004). Community structure and metabolism through reconstruction of microbial genomes from the environment. *Nature* 428, 37–43. doi: 10.1038/nature02340
- Vezzi, A., Campanaro, S., D'Angelo, M., Simonato, F., Vitulo, N., Lauro, F. M., et al. (2005). Life at depth: photobacterium profundum genome sequence and expression analysis. *Science* 307, 1459–1461. doi: 10.1126/science.1103341
- Von Damm, K. L. (1990). Seafloor hydrothermal activity: black smoker chemistry and chimneys. *Annu. Rev. Earth Planet Sci.* 18, 173–204. doi: 10.1146/annurev.ea.18.050190.001133
- Von Damm, K. L., Edmond, J. M., Measures, C. I., and Grant, B. (1985). Chemistry of submarine hydrothermal solutions at Guaymas Basin, Gulf of California *Geochimica et Cosmochimica Acta* 49, 2221–2237. doi: 10.1016/0016-7037(85)90223-6
- Wang, F., Wang, J., Jian, H., Zhang, B., Li, S., Wang, F., et al. (2008). Environmental adaptation: genomic analysis of the piezotolerant and psychrotolerant deep-sea iron reducing bacterium Shewanella piezotolerans WP3. *PLoS ONE* 3:e1937. doi: 10.1371/journal.pone.0001937
- Wang, F., Zhou, H., Meng, J., Peng, X., Jiang, L., Sun, P., et al. (2009). GeoChip-based analysis of metabolic diversity of microbial communities at the Juan de Fuca Ridge hydrothermal vent. *Proc. Natl. Acad. Sci. U.S.A.* 106, 4840–4845. doi: 10.1073/pnas.0810418106
- Weber, A., and Jørgensen, B. B. (2002). Bacterial sulfate reduction in hydrothermal sediments of the Guaymas Basin, Gulf of California, Mexico. *Deep Sea Res. I* 49, 827–841.
- Welhan, J. A. (1988). Origins of methane in hydrothermal systems. *Chem. Geol.* 71, 183–198.
- Widdel, F., and Bak, F. (1992). “Gram-negative mesophilic sulfate-reducing bacteria,” in *The Prokaryotes*, eds A. Balows, H. G. Trüper, M. Dworkin, W. Harder, and K.H. Schleifer (New York, NY: Springer-Verlag), 3352–3378.
- Widdel, F., and Rabus, R. (2001). Anaerobic biodegradation of saturated and aromatic hydrocarbons. *Curr. Opin. Biotechnol.* 12, 259–276.
- Woyke, T., Teeling, H., Ivanova, N. N., Huntemann, M., Richter, M., Gloeckner, F. O., et al. (2006). Symbiosis insights through metagenomic analysis of a microbial consortium. *Nature* 443, 950–955. doi: 10.1038/nature05192
- Wu, S., Zhu, Z., Fu, L., Niu, B., and Li, W. (2011). WebMGA: a customizable web server for fast metagenomic sequence analysis. *BMC Genomics* 12:444. doi: 10.1186/1471-2164-12-444
- Xie, W., Wang, F., Guo, L., Chen, Z., Sievert, S. M., Meng, J., et al. (2011). Comparative metagenomics of microbial communities inhabiting deep-sea hydrothermal vent chimneys with contrasting chemistries. *ISME J.* 5, 414–426. doi: 10.1038/ismej.2010.144
- Zerbino, D. R., and Birney, E. (2008). Velvet: algorithms for de novo short read assembly using de Bruijn graphs. *Genome Res.* 18, 821–829. doi: 10.1101/gr.074492.107
- Conflict of Interest Statement:** The authors declare that the research was conducted in the absence of any commercial or financial relationships that could be construed as a potential conflict of interest.
- Received:** 30 January 2013; **accepted:** 27 May 2013; **published online:** 14 June 2013.
- Citation:** He Y, Xiao X and Wang F (2013) Metagenome reveals potential microbial degradation of hydrocarbon coupled with sulfate reduction in an oil-immersed chimney from Guaymas Basin. *Front. Microbiol.* 4:148. doi: 10.3389/fmicb.2013.00148
- This article was submitted to Frontiers in Extreme Microbiology, a specialty of Frontiers in Microbiology.
- Copyright © 2013 He, Xiao and Wang. This is an open-access article distributed under the terms of the Creative Commons Attribution License, which permits use, distribution and reproduction in other forums, provided the original authors and source are credited and subject to any copyright notices concerning any third-party graphics etc.

**APPENDIX**

**FIGURE A1 |** The photo of a black-smoker chimney sample (4558-6), collected in Guaymas Basin ( $27^{\circ}0.9'N$ ,  $111^{\circ}24.6'W$ , depth = 2013 m).

**Table A1 | Taxonomic information based on assigned blastx results to each domain.**

| Domain     | No. of hits assigned | % of hits assigned |
|------------|----------------------|--------------------|
| Bacteria   | 21792                | 58.3               |
| Archaea    | 11249                | 30.1               |
| Eukaryota  | 224                  | 0.6                |
| Virus      | 88                   | 0.2                |
| Unassigned | 4019                 | 10.8               |

**Table A2 | List of annotated protein features involved in degradation processes.**

| <b>Substrate: step enzyme</b>                                      | <b>Best BLAST hit organism</b>  |
|--|---|
| <b>STEP [CELLULOSE]: → CELLULOSE CELLOBIOSIDE</b>                  |   |
| Endo-1,4-beta-glucanase  | <i>Thermotoga neapolitana</i> *   |
| Cellulase  | <i>Thermosiphon melanesiensis</i> Bl429*<br><i>Methanococcoides burtonii</i> DSM 6242   |
| Endoglucanase  | <i>Archaeoglobus fulgidus</i> DSM 4304*   |
| Celllobiose → beta-D-Glucose                                       |   |
| Beta-glucosidase   | <i>Dictyoglomus thermophilum</i> H-6-12 (2)   |
| <b>STEP [FATTY ACIDS]: FATTY ACIDS → HEXA-DECANOYL-COA</b>         |   |
| Long chain fatty acid CoA ligase                                   | <i>Bacillus thuringiensis</i> serovar <i>huazhongensis</i> BGSC 4BD1<br><i>Bacteroides</i> sp.2_1_7<br><i>Bacillus cereus</i> BDRD-ST196<br><i>Desulfobacterium autotrophicum</i> HRM2(2)<br><i>Carboxydothermus hydrogenoformans</i> Z-2901*<br><i>Archaeoglobus fulgidus</i> DSM 4304 (16)*   |
| Acy-CoA synthetase   | <i>Picrophilus torridus</i> DSM 9790*<br><i>Syntrophus aciditrophicus</i> SB<br><i>Desulfatibacillum alkenivorans</i> AK-01<br><i>Archaeoglobus fulgidus</i> DSM 4304 (6)*  |
| <b>Hexa-decanoyl-CoA → Trans-hexadec-2-enoyl-CoA</b>               |   |
| Acyl-CoA dehydrogenase   | <i>Pseudomonas aeruginosa</i> PA7<br><i>Marinobacter algicola</i> DG893<br><i>Colwellia psychrerythraea</i> 34H<br><i>Oceanobacter</i> sp. RED65<br><i>Oceanospirillum</i> sp. MED92<br><i>Gamma proteobacterium</i> NOR51-B<br><i>Brucella abortus</i> bv. 1 str. 9-941<br><i>Labrenzia alexandrii</i> DFL-11<br><i>Brucella suis</i> bv. 5 str. 513<br><i>Cytophaga hutchinsonii</i> ATCC 33406<br><i>Candidatus Cloacamonas acidaminovorans</i><br><i>Bacillus clausii</i> KSM-K16<br><i>Archaeoglobus fulgidus</i> DSM 4304 (16)* |
| <b>Trans-hexadec-2-enoyl-CoA → (S)-3-Hydroxy-hexa-decanoyl-CoA</b> |   |
| Beta-hydroxyacyl-CoA dehydrase                                     | <i>Desulfuromonas acetoxidans</i> DSM 684<br><i>Desulfococcus oleovorans</i> Hxd3 (4)   |
| Enoyl-CoA hydratase  | <i>Burkholderia multivorans</i> CGD2M<br><i>Acidaminococcus</i> sp. D21<br><i>Thermosinus carboxydovorans</i> Nor1<br><i>Desulfococcus oleovorans</i> Hxd3 (4)<br><i>Desulfatibacillum alkenivorans</i> AK-01<br><i>Geobacter bemandiensis</i> Bem<br><i>Candidatus Koribacter versatilis</i> Ellin345<br><i>Marinomonas</i> sp. MWYL1<br><i>Colwellia psychrerythraea</i> 34H<br><i>Carboxydothermus hydrogenoformans</i> Z-2901*<br><i>Archaeoglobus fulgidus</i> DSM 4304*<br><i>Rubrobacter xylanophilus</i> DSM 9941 (2)*        |

(Continued)

**Table A2 | Continued**

| <b>Substrate: step enzyme</b>                                    | <b>Best BLAST hit organism</b>  |
|--|---|
| <b>(S)-3-Hydroxy-hexa-decanoyl-CoA → 3-Oxo-hexa-decanoyl-CoA</b> |   |
| 3-Hydroxyacyl-CoA dehydrogenase                                  | <i>Gallionella ferruginea</i> ES-2<br><i>Desulfococcus oleovorans</i> Hxd3<br><i>Xanthobacter autotrophicus</i> Py2<br><i>Rhodospirillum centenum</i> SW<br><i>Geobacter uraniireducens</i> Rf4<br><i>Archaeoglobus fulgidus</i> DSM 4304 (12)*                         |
| Beta-hydroxyacyl dehydrogenase                                   | <i>Desulfococcus oleovorans</i> Hxd3 (4)<br><i>Desulfuromonas acetoxidans</i> DSM 684   |
| 3-Ketoacyl-CoA thiolase  | <i>Colwellia psychrerythraea</i> 34H<br><i>Halobacterium</i> sp. NRC-1<br><i>Anaeromyxobacter dehalogenans</i> 2CP-C<br><i>Archaeoglobus fulgidus</i> DSM 4304 (6)*   |
| Thiolase   | <i>Geobacter metallireducens</i> GS-15<br><i>Polaromonas</i> sp. JS666  |
| <b>STEP [PULLULAN]: PULLULAN → PANOSE</b>                        |   |
| Pullulanase  | <i>Thermococcus onnurineus</i> NA1(3)*<br><i>Thermococcus hydrothermalis</i> *<br><i>Thermotoga</i> sp. EMP   |
| Amylopullulanase   | <i>Thermococcus</i> sp. AM4*  |
| <b>STEP [LIPID]: LIPID → GLYCEROL</b>                            |   |
| Glycerate kinase   | <i>Thermoanaerobacter</i> sp. X513*   |
| Aldehyde dehydrogenase   | <i>Desulfitobacterium dichloroeliminans</i> LMG P-21439<br><i>Rhodothermus marinus</i> SG0.5JP17-172<br><i>Melioribacter roseus</i> P3M<br><i>Thermoplasma volcanium</i> GSS1*<br><i>Calditerrivibrio nitroreducens</i> DSM 19672<br>Uncultured Acidobacteria bacterium |
| Glycerol dehydrogenase   | <i>Archaeoglobus fulgidus</i> DSM 4304*   |

Thermalphilic species were marked with an asterisk.

**Table A3 | List of enzymes involved in hydrocarbon biodegradation in metagenomes from different environments, presence was marked with “+,” while absence with “–.”**

|                    | Transposase |      | Toluene  | Ethylbenzene | <i>o</i> -Xylene |
|--------------------|-------------|------|----------|--------------|------------------|
|                    | No. of hits | %    | Presence | Presence     | Presence         |
| 4558-6             | 313         | 1.32 | +        | +            | +                |
| Juan de Fuca       | 158         | 1.10 | –        | –            | –                |
| Lost City          | 1387        | 9.64 | –        | –            | –                |
| Acid mine drainage | 119         | 2.27 | –        | –            | –                |
| 5way acid mine     |             |      | –        | –            | –                |
| Worm               | 200         | 2.80 | –        | –            | –                |
| Peru_ori1          | 36          | 0.49 | –        | –            | –                |
| Peru_amp1          | 10          | 0.18 | –        | –            | –                |
| Peru_amp16         | 6           | 0.10 | –        | –            | –                |
| Peru_amp32         | 12          | 0.11 | –        | –            | –                |
| Peru_amp50*        | 6           | 0.08 | –        | +            | –                |
| HOT_10             | 1           | 0.03 | –        | –            | –                |
| HOT_70             | 3           | 0.08 | –        | –            | –                |
| HOT_130            | 2           | 0.08 | –        | –            | –                |
| HOT_200            | 3           | 0.09 | –        | –            | –                |
| HOT_500            | 13          | 0.32 | –        | –            | –                |
| HOT_770            | 15          | 0.31 | –        | –            | –                |
| HOT_4000           | 49          | 1.03 | –        | –            | –                |

\*Hit property: e-value 4.0e-12, similarity 50%, ethylbenzene dehydrogenase alpha subunit.



# A comparative study of microbial diversity and community structure in marine sediments using poly(A) tailing and reverse transcription-PCR

Tatsuhiko Hoshino<sup>1,2\*</sup> and Fumio Inagaki<sup>1,2</sup>

<sup>1</sup> Geomicrobiology Group, Kochi Institute for Core Sample Research, Japan Agency for Marine-Earth Science and Technology, Nankoku, Kochi, Japan

<sup>2</sup> Geobio-Engineering and Technology Group, Submarine Resources Research Project, Japan Agency for Marine-Earth Science and Technology, Nankoku, Kochi, Japan

**Edited by:**

Anna-Louise Reysenbach, Portland State University, USA

**Reviewed by:**

Gordon Webster, Cardiff University, UK

Jinjun Kan, Stroud Water Research Center, USA

**\*Correspondence:**

Tatsuhiko Hoshino, Geomicrobiology Group, Kochi Institute for Core Sample Research, Japan Agency for Marine-Earth Science and Technology, Monobe B200, Nankoku, Kochi 783-8502, Japan  
e-mail: hoshinot@jamstec.go.jp

To obtain a better understanding of metabolically active microbial communities, we tested a molecular ecological approach using poly(A) tailing of environmental 16S rRNA, followed by full-length complementary DNA (cDNA) synthesis and sequencing to eliminate potential biases caused by mismatching of polymerase chain reaction (PCR) primer sequences. The RNA pool tested was extracted from marine sediments of the Yonaguni Knoll IV hydrothermal field in the southern Okinawa Trough. The sequences obtained using the poly(A) tailing method were compared statistically and phylogenetically with those obtained using conventional reverse transcription-PCR (RT-PCR) with published domain-specific primers. Both methods indicated that Deltaproteobacteria are predominant in sediment (>85% of the total sequence read). The poly(A) tailing method indicated that Desulfobacterales were the predominant Deltaproteobacteria, while most of the sequences in libraries constructed using RT-PCR were derived from Desulfuromonadales. This discrepancy may have been due to low coverage of Desulfobacterales by the primers used. A comparison of library diversity indices indicated that the poly(A) tailing method retrieves more phylogenetically diverse sequences from the environment. The four archaeal 16S rRNA sequences that were obtained using the poly(A) tailing method formed deeply branching lineages that were related to *Candidatus "Parvarchaeum"* and the ancient archaeal group. These results clearly demonstrate that poly(A) tailing followed by cDNA sequencing is a powerful and less biased molecular ecological approach for the study of metabolically active microbial communities.

**Keywords:** 16S rRNA, less biased diversity analysis, hydrothermal sediment

## INTRODUCTION

Numerous studies on natural microbial communities from a variety of environments have been undertaken using 16S rRNA gene sequencing mediated by polymerase chain reaction (PCR) with oligonucleotide primers. In the past decade, high-throughput next-generation sequencing (NGS) technologies have facilitated the identification of a diverse array of organisms that are rare in terms of biomass and could not be examined using previous molecular assays such as Sanger sequencing analysis of clone libraries (Sogin et al., 2006; Webster et al., 2010). Despite the fact that the latest NGS technologies enable reading only of relatively short sequence fragments (~500 bp), these so-called “deep sequencing” methods are still powerful tools that ultimately may enable researchers to obtain a more holistic understanding of microbial communities in their natural environments (Fuhrman, 2009). Considering the current limitations of NGS technology, full-length 16S rRNA gene sequences are better suited to downstream analytical methods such as fluorescence *in situ* hybridization.

The original designs of most of the PCR primers used for the analysis of 16S rRNA genes were based on known sequences

deposited in public databases. Researchers have since cautioned that these primer sequences contain mismatches with respect to environmental 16S rRNA genes (Baker et al., 2003, 2006; Teske and Sørensen, 2008), which may lead to considerable bias in interpreting results (Hong et al., 2009). In addition, primer sequence mismatches may have a negative impact on the amplification efficiency of PCR analyses (Acinas et al., 2005; Sipos et al., 2007; Bru et al., 2008). Regardless of the presence of sequence mismatches, the use of PCR with primers may introduce biases associated with the next base adjacent to annealed oligonucleotide primers (Ben-Dov et al., 2012).

One way to avoid these bias issues is to employ PCR-independent metagenomic approaches. For example, a complete 16S rRNA gene sequence can be obtained by analyzing the sequences of genomes or large genome fragments, providing taxonomic information along with information on other functional genes. However, metagenomic approaches may not be well-suited to focused studies of microbial diversity and community structure that involve a large number of samples. In fact, it has been reported that only a small portion of inserts in fosmid libraries contain 16S rRNA genes (Vergin et al., 1998; Takami et al., 2012).

Another method that can avoid the possibility of bias caused by primer mismatching is the addition of a poly(A) tail to the 3' end of fractionated 16S rRNA prior to synthesis of the full-length complementary DNA (cDNA; Botero et al., 2005). Since the technique does not involve the use of published primers, we anticipate that this method will enable recovery of full-length environmental 16S rRNAs, potentially illuminating as yet unknown microbial community constituents that have otherwise been difficult or impossible to detect using conventional PCR-dependent molecular approaches (Inagaki et al., 2002). In the present study, we tested this hypothesis using poly(A) tailing of full-length 16S rRNA and reverse transcription-PCR (RT-PCR) with domain-specific primers, and compared sequence libraries prepared from a marine sediment sample collected from the Yonaguni Knoll IV hydrothermal field.

## MATERIALS AND METHODS

### SAMPLING OF MARINE SEDIMENTS

The sediment samples used in this study were obtained from the Yonaguni Knoll IV hydrothermal field in the southern Okinawa Trough ( $24^{\circ}50.544'N$ ,  $122^{\circ}42.878'E$ , water depth: 1,371 m) using a push corer, and were collected during the JAMSTEC NT10-06 cruise involving *RV Natsushima* and *ROV Hyper-Dolphin* (Dive #1111, April 17, 2010). Sediment samples were anaerobically placed in autoclaved 250-ml glass bottles using a nitrogen flush and the bottles were sealed with a rubber cap and stored at  $4^{\circ}C$  until analysis.

### RNA EXTRACTION AND PURIFICATION

Bulk environmental RNA was extracted from 8 g of sediment using an RNA PowerSoil® Total RNA Isolation Kit (MO BIO Laboratories, Inc., Solana Beach, CA, USA) according to the manufacturer's instructions. The extracted RNA was electrophoresed on a 2% agarose gel for 30 min in 1× TAE [Tris-acetate-ethylenediaminetetraacetic acid (EDTA)] buffer, and the gel was stained with 1× SYBR Green II (Life Technologies Japan, Tokyo, Japan) to visualize 16S and 23S rRNA. The rRNA was recovered from the gel using a Recochip (Takara Bio, Japan), and then further purified using a PureLink RNA Mini Kit (Life Technologies Japan) according to the manufacturer's instructions. The quality of the recovered 16S rRNA was verified by electrophoresis using an automated capillary electrophoresis system (Experion; Bio-Rad Laboratories, Tokyo, Japan) and an Experion RNA HighSens Analysis Kit.

### POLY(A) TAILING AND COMPLEMENTARY DNA SYNTHESIS

We compared two molecular approaches [poly(A) tailing and RT-PCR] for examining metabolically active microbial communities. The approaches are summarized in **Figure 1**. Since the reaction buffer composition and source of poly(A) polymerase can reportedly affect the efficiency of the poly(A) tailing reaction (Raynal and Carposnis, 1999; Sillero et al., 2001), we used two commercially available poly(A) polymerases: *Escherichia coli* poly(A) polymerase (New England Biolabs, hereafter denoted as NEB) and Takara Bio poly(A) polymerase. Each poly(A) tailing reaction was conducted in 20  $\mu$ l of reaction mixture containing 10  $\mu$ l of

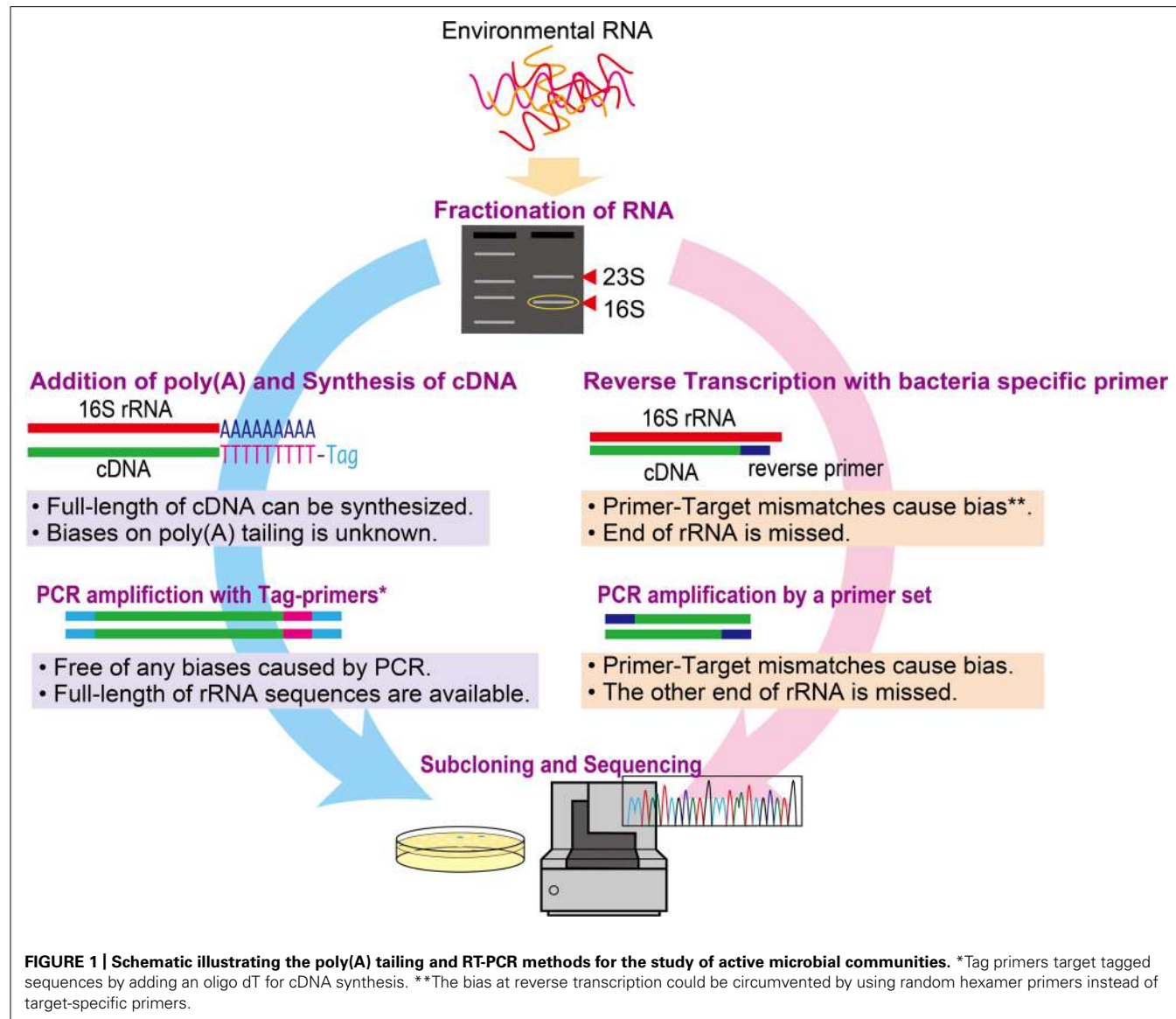
purified 16S rRNA solution. The other components of the reaction mixture were as follows: for NEB polymerase, 1× reaction buffer (50 mM Tris-HCl, 250 mM NaCl, and 10 mM MgCl<sub>2</sub>), 1 mM ATP, and 0.25 U/ $\mu$ l of poly(A) polymerase; for Takara Bio, 1× reaction buffer [50 mM Tris-HCl, 10 mM MgCl<sub>2</sub>, 2.5 mM MnCl<sub>2</sub>, 250 mM NaCl, and 1 mM dithiothreitol (DTT)], 0.5 mg/ml of bovine serum albumin, 0.5 mM ATP, and 0.1 U/ $\mu$ l of poly(A) polymerase. After incubation at  $37^{\circ}C$  for 30 min, the reaction was stopped by adding 2  $\mu$ l of 250 mM EDTA. The poly(A)-tailed 16S rRNA was subsequently purified using a NucleoSpin® RNA XS Kit (Takara Bio). The cDNA of full-length 16S rRNA was synthesized and amplified by PCR using a SMARTer™ Pico PCR cDNA Synthesis Kit (Takara Bio) according to the manufacturer's instructions.

### REVERSE TRANSCRIPTION-PCR

Reverse transcription-PCR was performed to obtain nearly full-length rRNA gene sequences from the purified 16S rRNA without poly(A) tailing using a One-Step PrimeScript RT-PCR Kit (Takara Bio). The bacterial domain-specific primers 26F (AGAGTTTGATCTGGCTCA; Hicks et al., 1992) and 1492R (GGYTACCTTGTACGACTT; Loy et al., 2002) were used for RT-PCR. The reaction mixture consisted of 1× PrimeScript buffer, 300 nM of each primer, 0.8  $\mu$ l of PrimeScript Enzyme mix, 1  $\mu$ l of 16S rRNA (diluted 1,000-fold), and water to 20  $\mu$ l. First, reverse transcription was performed at  $50^{\circ}C$  for 30 min followed by inactivation of the reverse transcriptase at  $94^{\circ}C$  for 2.5 min. Next, synthesized cDNA was amplified by PCR under the following condition: 20 cycles of  $94^{\circ}C$  for 30 s,  $54^{\circ}C$  for 30 s, and  $72^{\circ}C$  for 90 s. The number of PCR cycles used in this study was determined by selecting a cycle number in the log-linear phase of the real-time PCR amplification curve (i.e., before the plateau phase). The PCR products were purified using NucleoSpin Extract II Columns (Takara Bio) and stored at  $-20^{\circ}C$  until further analysis.

### CLONING AND SEQUENCING

The PCR products obtained using poly(A) tailing and RT-PCR were cloned into the pCR®2.1-TOPO® vector and transformed into competent *E. coli* DH5 $\alpha$  (Life Technologies Japan, Tokyo, Japan). For RT-PCR, the cloned inserts were sequenced using an ABI 3130xl genetic analyzer (Life Technologies Japan) with the primers M13M4, M13rev, 926R/F (Liu et al., 1997), and 1390R (Zheng et al., 1996). For the poly(A) tailing method, sequencing was first performed using the M13 primers followed by screening of the 16S rRNA sequence using a hidden Markov model implemented in version 3.0 of the HMMER software package (Eddy, 1998), as described elsewhere (Lagesen et al., 2007; Huang et al., 2009). The screened 16S rRNA inserts were sequenced using primers 338R/F (Amann et al., 1990), 515R/F (Walters et al., 2011), 926R/F, and 1390R to assemble full-length 16S rRNA sequences. A primer walking approach was employed for inserts that could not be sequenced using the primers described above. The sequences were trimmed and assembled to obtain consensus sequences using Sequencher software (Hitachi Software, Tokyo, Japan). Chimeric sequences were removed using the UCHIME program (Edgar et al., 2011) implemented in the Mothur Utility package (Schloss et al., 2009).



## DATA ANALYSIS

Alignment of all 16S rRNA sequences was performed using the ARB software package (Ludwig et al., 2004). Since some of the 16S rRNA sequences were fragmented after poly(A) tailing, a 600-bp fragment (corresponding to *E. coli* 16S rRNA positions 287–886) was used for comparisons of microbial diversity and community structure. Taxonomic assignments were made using Silva taxonomy and the Bayesian classifier. Clustering sequences, calculation of diversity indices (i.e., Shannon and Simpson indices) and Libshuff test (Singleton et al., 2001; Schloss et al., 2004) were performed using the Mothur software package (Schloss et al., 2009; Hoshino et al., 2011). Phylogenetic tree was constructed by ARB software (Ludwig et al., 2004) using the neighbor-joining method (Saitou and Nei, 1987) with an Olsen correction. The coverage rate of the used primer set (26F-1492R) at the genus level was evaluated using TestPrime 1.0 program (Klindworth et al., 2013) using SILVA database SSU r114 with RefNR.

## NUCLEOTIDE SEQUENCE ACCESSION NUMBERS

All 16S rRNA sequences obtained in this study were deposited in the DDBJ/EMBL/GenBank nucleotide sequence databases under the accession numbers KC470861–KC471309.

## RESULTS AND DISCUSSION

### HMMER SCREENING OF 16S rRNA

HMMER screening of 16S rRNA sequences obtained using the poly(A) tailing method resulted in the detection of 115 and 144 bacterial 16S rRNA sequences for the NEB and Takara poly(A) polymerase reactions, respectively. Approximately a half number of the total cDNA sequences (i.e., 107 and 92 sequences in the NEB and Takara cDNA libraries, respectively) were found to be 23S rRNA fragments according to the HMMER analysis. Interestingly, few cDNAs from mRNA were detected. The fragmented 23S rRNA sequences were excluded from the downstream analysis. Some fragmented 16S rRNA sequences were also

observed in the poly(A) tailing libraries, suggesting that part of the 16S rRNA pool was damaged during the fractionation step by excision of the band and extraction of 16S rRNA from agarose gel.

Only one and three of the 16S rRNA sequences obtained using the NEB and Takara polymerases, respectively, were identified as archaeal 16S rRNA. This result was consistent with results from previous analyses of samples from the same location, which indicated that the archaeal population is generally smaller than the bacterial population (Yanagawa et al., 2012). In addition, a previous study of geothermally heated soil from Yellowstone National Park in the United States recovered no archaeal RNA sequences using the poly(A) tailing method, despite the fact that numerous archaeal 16S rRNA sequences were obtained using the PCR-based clone library method (Botero et al., 2005). Therefore, poly(A) tailing might have bias which underestimate archaeal population although it is unknown whether the low abundance of archaeal sequences in the poly(A) tailing libraries is from the native archaeal abundance or due to this bias. It is important to note here that RNA-based methods depend on the recovery of intracellular RNA; therefore, the results cannot be correlated with the cellular biomass or DNA copy number of the genomic pool.

### COMPARISON OF MICROBIAL DIVERSITY

More than 85% of the total 16S rRNA sequences obtained using the poly(A) tailing and conventional RT-PCR methods were found to be derived from the Deltaproteobacteria, indicating that sulfate-reducing bacteria are predominant members of sedimentary habitats (**Figure 2**, pie charts on the left). Conventional RT-PCR analysis identified 94% (169/179) of the sequences obtained as Deltaproteobacteria, whereas 85% (98/115) and 88% (127/144) of the bacterial 16S rRNA sequences obtained using the NEB and Takara polymerase poly(A) tailing methods, respectively, were identified as Deltaproteobacteria (**Figure 2**, pie charts on the left). Overall, these results are consistent with those of a previous RNA-based study of the same hydrothermal field (Yanagawa et al., 2012).

The Deltaproteobacteria orders Desulfuromonadales and Desulfobacterales, both of which contain sulfur- and/or sulfate-reducing bacteria, consistently appeared as predominant phylogenotypes in the clone libraries. However, there was a clear difference in the clonal frequency between libraries constructed using the two methods; the RT-PCR method indicated the predominance of Desulfuromonadales, while the poly(A)-tailing method indicated that Desulfobacterales predominate (**Figure 2**).

The detected sequences affiliated with Desulfuromonadales were mainly composed by the genera *Pelobacter*, *Geoalkalibacter*, and *Geopsychrobacter* (**Figure 3**). Almost half of the sequences from RT-PCR (84/179) and more than 25 sequences from both poly(A) libraries were classified to be *Pelobacter*, indicating predominance of this genus in the environment. TestPrime analysis (Klindworth et al., 2013) indicated that the coverage rates of the 26F and 1492R primers with perfect match for *Pelobacter*, *Geoalkalibacter*, and *Geopsychrobacter* are 50.0, 75.0, and 100%, respectively. On the other hand, the detected sequences of Desulfobacterales mainly consist of the genera *Desulfopila*, *Desulfovaba*, and *Desulforhopalus* (**Figure 3**), for which the coverage rates are 40,

100, and 41.7%, respectively. Among those three genera, the *Desulfopila*-related sequences were predominant in both poly(A) tailing clone libraries. The coverage rates of the detected genera within the Desulfobacterales were lower than those of Desulfuromonadales, resulting in lower abundance of Desulfobacterales in the RT-PCR libraries. Therefore, we infer that primer-dependent RT-PCR assay overestimated Desulfuromonadales but underestimated Desulfobacterales due to the primer bias.

Representatives of the Gammaproteobacteria and Sphingobacteria were relatively minor components of all three libraries we examined. Although some sequences derived from Lentisphaerae and Holophagae were only detected by RT-PCR, the poly(A) tailing libraries constructed using the two different polymerases revealed more diverse lineages than did the RT-PCR library. The clone libraries obtained from poly(A) tailing included some classes that were not detected by RT-PCR, such as *Nitrospira*, *Alphaproteobacteria*, and *Caldilineae*.

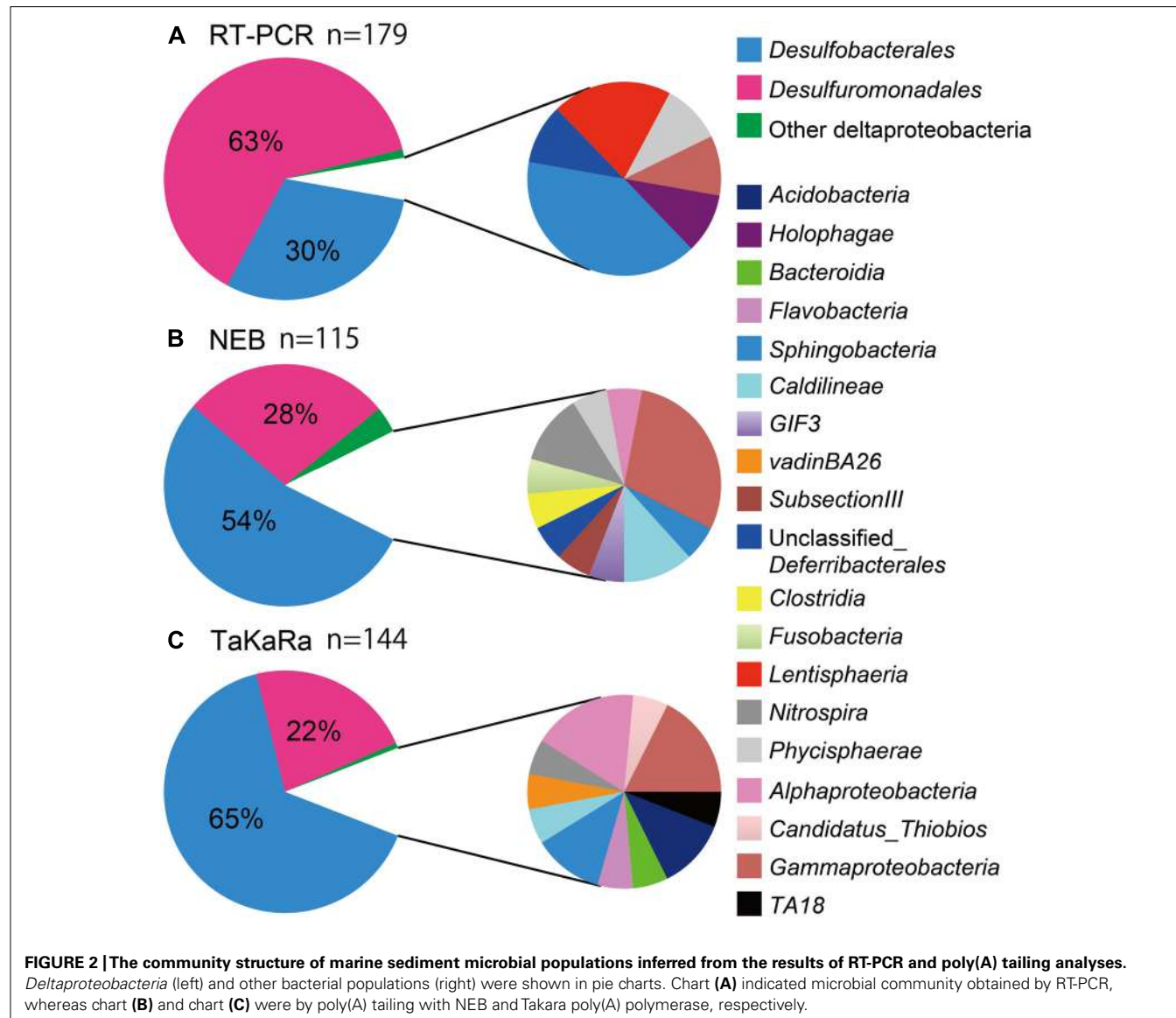
In theory, poly(A) tailing methods could also be used to obtain archaeal 16S rRNA, although a previous study failed to retrieve any archaeal 16S rRNA from geothermally heated soils from Yellowstone National Park (Botero et al., 2005). In this study, a total of four archaeal 16S rRNA sequences were obtained using the poly(A) tailing method.

Two of these sequences were derived from *Candidatus "Parvarchaeum"* (Baker et al., 2010), which belonged to Deep-sea Hydrothermal Vent Euryarchaeotic Group (DHVEG-6; Takai and Horikoshi, 1999), while the other two sequences formed a new branch distinct from the ancient archaeal group (AAG; Takai and Horikoshi, 1999; **Figure 4**). Organisms belonging to DHVEG-6 are primarily associated with deep-sea hydrothermal vent systems (Takai and Horikoshi, 1999; Teske and Sørensen, 2008; Nunoura et al., 2012), but have also been found in marine sediment and anoxic soil. The AAG were first described as a hydrothermal vent lineage, and, consistent with the results of this study, were later found in the cold organic-rich subsurface environment (Sørensen and Teske, 2006). Due to primer mismatching, there have been few reports to date of the use of conventional PCR with published primer sets to detect the four archaeal 16S rRNA sequences we detected in this study. For example, all four sequences have one mismatch to A806F (Wang and Qian, 2009), while Arch958R (DeLong, 1992) has six mismatches to T\_34 and N\_100, and two mismatches to T\_35 and T\_36.

In addition, we retrieved 23S rRNA by poly(A) tailing with Takara polymerase: a total of 78 partial 23S rRNA sequences (~600 bp in length) were obtained. Although classification of the 23S rRNA sequences might be insufficient for the genus-level classification due to the limited number of 23S rRNA in the database, we found predominance of Deltaproteobacteria (60/78) containing Desulfobacterales (19/78), Desulfuromonadales (20/78), and unclassified sequences (19/78), consistently supporting our observation of 16S rRNA gene sequences.

### COMPARISON OF MICROBIAL COMMUNITY STRUCTURES

To compare the microbial community structures indicated by the poly(A) tailing and RT-PCR approaches, we calculated Shannon ( $H'$ ) and Simpson diversity ( $1/D$ ) indices for the 16S rRNA libraries. The highest diversity value was for the poly(A)-tailed



sequences obtained using the NEB polymerase (**Table 1**). For the unique poly(A)-tailed sequences (i.e., singletons), the highest diversity indices were obtained using the Takara polymerase. In contrast, the RT-PCR method was associated with the lowest diversity indices, regardless of the similarity cutoff used or not (**Table 1**). The results of Libshuff analysis indicate that the two poly(A) clone libraries are statistically different from that of RT-PCR whereas poly(A) libraries are not significantly different (**Table 2**). Overall, these results indicate that the poly(A) tailing methods retrieve more diverse 16S rRNA sequences from the environment than does the conventional RT-PCR approach. In other words, it is important to recognize that primer-dependent molecular ecological approaches carry a risk of bias that could result in underestimation of microbial diversity. The bias effect may be more significant for microbial communities in rare and/or extreme habitats that have never been explored because we do not know exactly what organisms reside there.

## CONCLUSION AND PERSPECTIVES

For decades, PCR-mediated molecular ecological approaches have been used to investigate the diversity of microbial communities in a variety of natural habitats. The primer sequences for amplifying 16S rRNA (or its gene fragments) are based on known sequences contained in databases, targeting conserved regions that cover specific taxonomic groups. In this context, a critical issue in microbial ecology is the possibility of bias caused by mismatches between the published primers and the target sequences, especially for unidentified constituents of microbial communities in natural habitats. Bias of this sort has caused significant differences in estimates of microbial diversity and community structure, and also increases the difficulty of detecting previously unidentified organisms in the environment.

The poly(A) tailing of environmental 16S rRNA is totally independent of published PCR primers. In this study, we clearly showed that the poly(A) tailing approach holds potential for

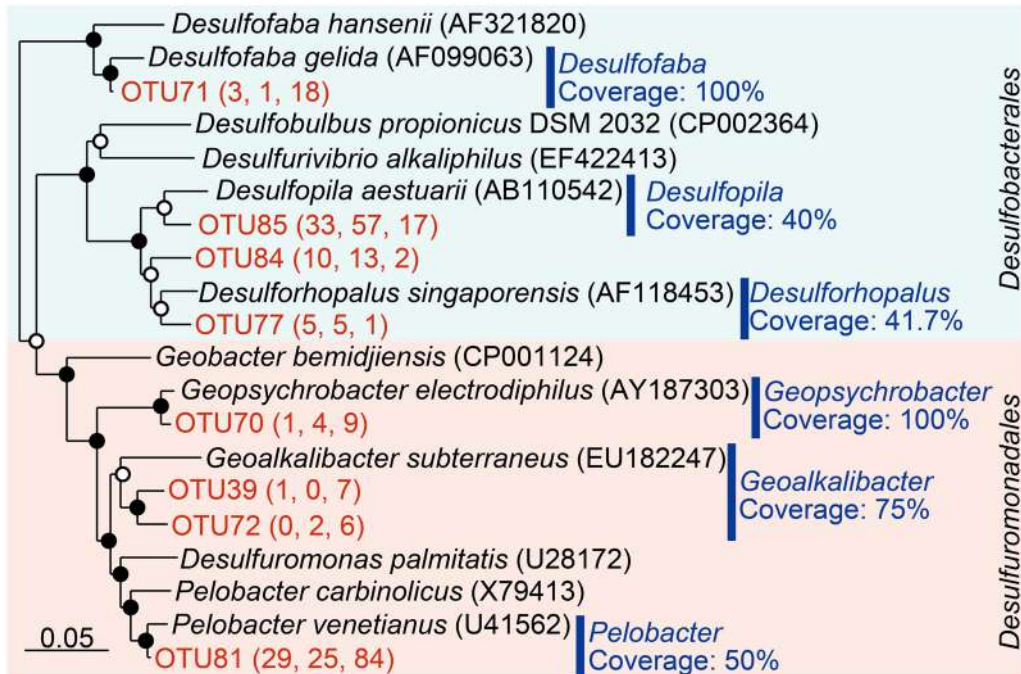


**FIGURE 3 | Phylogenetic classification of *Deltaproteobacteria* sequences obtained in this study.** The tree was constructed by neighbor-joining analysis with an Olsen correction. Operational taxonomic units (OTUs) were defined as the clusters at 97% sequence identity and only OTUs containing more than five sequences were shown in the tree. The numbers in parenthesis indicate the number of clones obtained by NEB poly(A) polymerase, Takara

poly(A) polymerase, and conventional RT-PCR, respectively (from left to right). Coverage of the primer set (26F-1492R) determined by TestPrime (<http://www.arb-silva.de/search/testprime/>) is shown for each genus. Bootstrap values are shown at branch nodes by closed circles (>80%) and open circles (<80%) as percentages of 1,000 replicates. Scale bar indicates 5% sequence divergence.

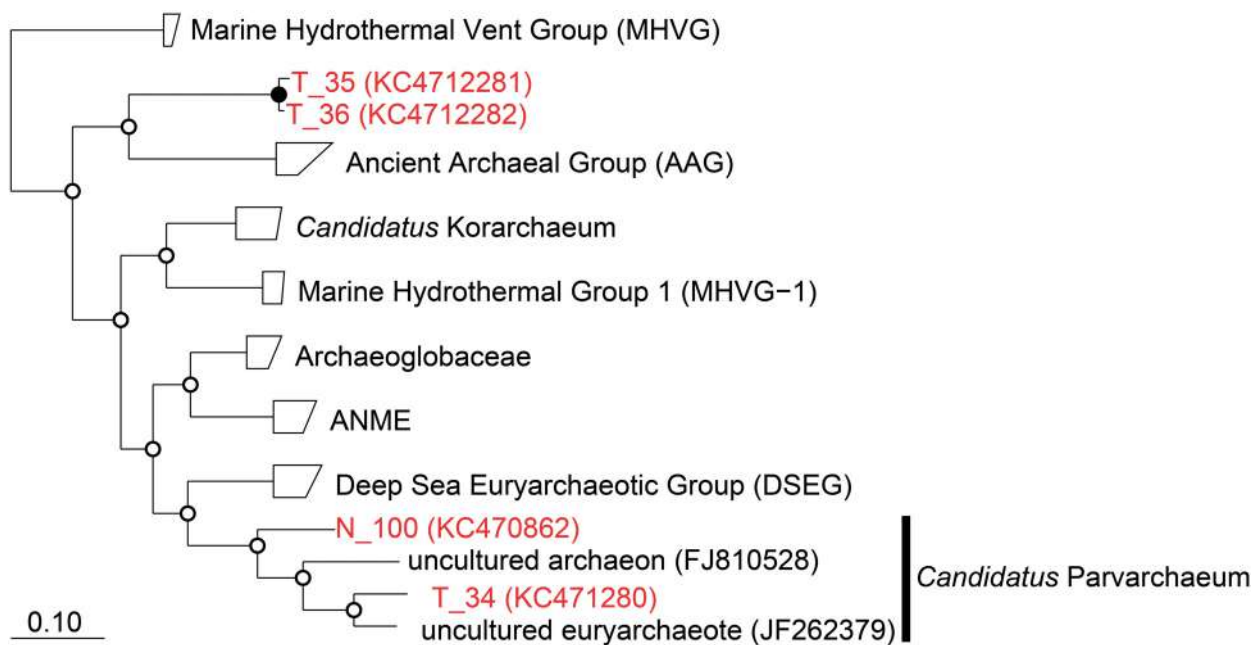


**FIGURE 4 | Phylogenetic classification of archaeal 16S rRNA sequences obtained in this study.** The tree was constructed by neighbor-joining analysis with an Olsen correction. Bootstrap values were shown at branch point as

percentages of 1,000 replicates. Bootstrap values are shown at branch nodes by closed circles (>80%) and open circles (<80%) as percentages of 1,000 replicates. Scale bar indicated 10% sequence divergence.

**Table 1 | Diversity indices.**

| Similarity cutoff (%) | Shannon diversity index ( $H'$ ) |             |                | Simpson diversity index (1/D) |             |                |
|-----------------------|----------------------------------|-------------|----------------|-------------------------------|-------------|----------------|
|                       | RT-PCR                           | Poly(A) NEB | Poly(A) Takara | RT-PCR                        | Poly(A) NEB | Poly(A) Takara |
| 0 (unique)            | 4.41                             | 4.22        | 4.54           | 49.17                         | 64.90       | 70.52          |
| 3                     | 2.23                             | 2.48        | 2.41           | 4.13                          | 6.53        | 5.16           |

NEB: New England BioLabs *Escherichia coli* poly(A) polymerase. Takara: Takara poly(A) polymerase.

**Table 2 | P-values\* estimating similarity among each treatment generated using Libshuff (10,000 randomizations) among the three clone libraries.**

| P-value comparison of library (Y) with Xa |                   |               |                |
|---|-------------------|---------------|----------------|
| Library (X)                               | RT-PCR            | NEB poly(A)   | Takara poly(A) |
| RT-PCR                                    | /                 | <b>0.0001</b> | <b>0.0003</b>  |
| NEB poly(A)                               | <b>&lt;0.0001</b> | /             | 0.4009         |
| Takara poly(A)                            | <b>0.0051</b>     | 0.2407        | /              |

\*P-values comparing either X to Y or Y to X indicate that the two communities are significantly different bold face values indicated significant difference ( $P < 0.0085$ , employing the Bonferroni correction).

understanding of naturally occurring active microbial communities. This approach also has great potential for facilitating the

## REFERENCES

- Acinas, S. G., Sarma-Rupavtarm, R., Klepac-Ceraj, V., and Polz, M. F. (2005). PCR-induced sequence artifacts and bias: insights from comparison of two 16S rRNA clone libraries constructed from the same sample. *Appl. Environ. Microbiol.* 71, 8966–8969. doi: 10.1128/AEM.71.12.8966–8969.2005
- Amann, R. I., Binder, B. J., Olson, R. J., Chisholm, S. W., Devereux, R., and Stahl, D. A. (1990). Combination of 16S rRNA-targeted oligonucleotide probes with flow cytometry for analyzing mixed microbial populations. *Appl. Environ. Microbiol.* 56, 1919–1925.
- Baker, B. J., Comolli, L. R., Dick, G. J., Hauser, L. J., Hyatt, D., Dill, B. D., et al. (2010). Enigmatic, ultra-small, uncultivated archaea. *Proc. Natl. Acad. Sci. U.S.A.* 107, 8806–8811. doi: 10.1073/pnas.0914470107
- Baker, B. J., Tyson, G. W., Webb, R. I., Flanagan, J., Hugenholtz, P., Allen, E. E., et al. (2006). Lineages of acidiophilic archaea revealed by community genomic analysis. *Science* 314, 1933–1935. doi: 10.1126/science.1132690
- Baker, G. C., Smith, J. J., and Cowan, D. A. (2003). Review and re-analysis of domain-specific 16S primers. *J. Microbiol. Methods* 55, 541–555. doi: 10.1016/j.mimet.2003.08.009
- Ben-Dov, E., Shapiro, O. H., and Kushmaro, A. (2012). ‘Next-base’ effect on PCR amplification. *Environ. Microbiol. Rep.* 4, 183–188. doi: 10.1111/j.1758-2229.2011.00318.x
- Botero, L. M., D’Imperio, S., Burr, M., Mcdermott, T. R., Young, M., and Hassett, D. J. (2005). Poly(A) polymerase modification and reverse transcriptase PCR amplification of environmental RNA. *Appl. Environ. Microbiol.* 71, 1267–1275. doi: 10.1128/AEM.71.3.1267–1275.2005
- Bru, D., Martin-Laurent, F., and Philippot, L. (2008). Quantification of the detrimental effect of a single primer-template mismatch by real-time PCR using the 16S rRNA gene as an example. *Appl. Environ. Microbiol.* 74, 1660–1663. doi: 10.1128/AEM.02403-07
- DeLong, E. F. (1992). Archaea in coastal marine environments. *Proc. Natl. Acad. Sci. U.S.A.* 89, 5685–5689. doi: 10.1073/pnas.89.12.5685
- Eddy, S. R. (1998). Profile hidden Markov models. *Bioinformatics* 14, 755–763. doi: 10.1093/bioinformatics/14.9.755
- Edgar, R. C., Haas, B. J., Clemente, J. C., Quince, C., and Knight, R. (2011). UCHIME improves sensitivity and speed of chimeral detection. *Bioinformatics* 27, 2194–2200. doi: 10.1093/bioinformatics/btr381
- Fuhrman, J. A. (2009). Microbial community structure and its functional implications. *Nature* 459, 193–199. doi: 10.1038/nature08058
- Hicks, R. E., Amann, R. I., and Stahl, D. A. (1992). Dual staining of natural bacterioplankton with 4',6-diamidino-2-phenylindole and fluorescent oligonucleotide probes targeting kingdom-level 16S rRNA sequences. *Appl. Environ. Microbiol.* 58, 2158–2163.
- Hong, S., Bunge, J., Leslin, C., Jeon, S., and Epstein, S. S. (2009). Polymerase chain reaction primers miss half of rRNA microbial diversity. *ISME J.* 3, 1365–1373. doi: 10.1038/ismej.2009.89
- Hoshino, T., Morono, Y., Terada, T., Imachi, H., Ferdelman, T. G., and Inagaki, F. (2011). Comparative study of subseafloor microbial community structures in deeply buried coral fossils and sediment matrices from the challenger mound in the porcupine seafight. *Front. Microbiol.* 2:231. doi: 10.3389/fmicb.2011.00231
- Huang, Y., Gilna, P., and Li, W. (2009). Identification of ribosomal RNA genes in metagenomic fragments. *Bioinformatics* 25, 1338–1340. doi: 10.1093/bioinformatics/btp161
- Inagaki, F., Sakihama, Y., Inoue, A., Kato, C., and Horikoshi, K. (2002). Molecular phylogenetic analyses of reverse-transcribed bacterial rRNA obtained from deep-sea cold seep sediments. *Environ. Microbiol.* 4, 277–286. doi: 10.1046/j.1462-2920.2002.00294.x
- Klindworth, A., Pruesse, E., Schweer, T., Peplies, J., Quast, C., Horn, M., et al. (2013). Evaluation of general 16S ribosomal RNA gene PCR primers for classical and next-generation sequencing-based diversity studies. *Nucleic Acids Res.* 41, e1. doi: 10.1093/nar/gks808
- Lagesen, K., Hallin, P., Rodland, E. A., Staerfeldt, H. H., Rognes, T., and Ussery, D. W. (2007). RNAmmer: consistent and rapid annotation of ribosomal RNA genes. *Nucleic Acids Res.* 35, 3100–3108. doi: 10.1093/nar/gkm160
- Liu, W. T., Marsh, T. L., Cheng, H., and Forney, L. J. (1997). Characterization of microbial diversity by determining

discovery of as yet unknown microbes for which their 16S rRNA gene sequence do not match published primer sequences, although the potential bias of poly(A) tailing to rRNA genes needs to be studied further. By combining this approach with “deep sequencing” NGS technologies that allow for sequencing full-length 16S rRNAs, it may be possible in the future to obtain a detailed view of the true structure of microbial communities in natural habitats.

## ACKNOWLEDGMENTS

The authors thank Ms. Sayo Hashimoto for technical assistance. This work was supported in part by the JSPS Strategic Fund for Strengthening Leading-edge Research and Development (to JAMSTEC), by a Sasakawa Scientific Research Grant from the Japan Science Society (to Tatsuhiko Hoshino), and by the JSPS Funding Program for Next Generation World-leading Researchers (NEXT Program, to Fumio Inagaki).

- terminal restriction fragment length polymorphisms of genes encoding 16S rRNA. *Appl. Environ. Microbiol.* 63, 4516–4522.
- Loy, A., Lehner, A., Lee, N., Adamczyk, J., Meier, H., Ernst, J., et al. (2002). Oligonucleotide microarray for 16S rRNA gene-based detection of all recognized lineages of sulfate-reducing prokaryotes in the environment. *Appl. Environ. Microbiol.* 68, 5064–5081. doi: 10.1128/AEM.68.10.5064-5081.2002
- Ludwig, W., Strunk, O., Westram, R., Richter, L., Meier, H., Yadhukumar, et al. (2004). ARB: a software environment for sequence data. *Nucleic Acids Res.* 32, 1363–1371. doi: 10.1093/nar/gkh293
- Nunoura, T., Takaki, Y., Kazama, H., Hirai, M., Ashi, J., Imachi, H., et al. (2012). Microbial diversity in deep-sea methane seep sediments presented by SSU rRNA gene tag sequencing. *Microbes Environ.* 27, 382–390. doi: 10.1264/jsmc2. ME12032
- Raynal, L. C., and Carpousis, A. J. (1999). Poly(A) polymerase I of *Escherichia coli*: characterization of the catalytic domain, an RNA binding site and regions for the interaction with proteins involved in mRNA degradation. *Mol. Microbiol.* 32, 765–775. doi: 10.1046/j.1365-2958.1999.01394.x
- Saitou, N., and Nei, M. (1987). The neighbor-joining method: a new method for reconstructing phylogenetic trees. *Mol. Biol. Evol.* 4, 406–425.
- Schloss, P. D., Larget, B. R., and Handelsman, J. (2004). Integration of microbial ecology and statistics: a test to compare gene libraries. *Appl. Environ. Microbiol.* 70, 5485–5492. doi: 10.1128/AEM.70.9.5485-5492.2004
- Schloss, P. D., Westcott, S. L., Ryabin, T., Hall, J. R., Hartmann, M., Hollister, E. B., et al. (2009). Introducing mothur: open-source, platform-independent, community-supported software for describing and comparing microbial communities. *Appl. Environ. Microbiol.* 75, 7537–7541. doi: 10.1128/AEM.01541-09
- Sillero, M. A., Socorro, S., Baptista, M. J., Del Valle, M., De Diego, A., and Sillero, A. (2001). Poly(A) polymerase from *Escherichia coli* adenylates the 3'-hydroxyl residue of nucleosides, nucleoside 5'-phosphates and nucleoside(5')oligophospho(5')nucleosides (NpnN). *Eur. J. Biochem.* 268, 3605–3611. doi: 10.1046/j.1432-1327.2001.02271.x
- Singleton, D. R., Furlong, M. A., Rathbun, S. L., and Whitman, W. B. (2001). Quantitative comparisons of 16S rRNA gene sequence libraries from environmental samples. *Appl. Environ. Microbiol.* 67, 4374–4376. doi: 10.1128/AEM.67.9.4374-4376.2001
- Sipos, R., Szekely, A. J., Palatinuszky, M., Revesz, S., Mariáligeti, K., and Nikolausz, M. (2007). Effect of primer mismatch, annealing temperature and PCR cycle number on 16S rRNA gene-targetting bacterial community analysis. *FEMS Microbiol. Ecol.* 60, 341–350. doi: 10.1111/j.1574-6941.2007.00283.x
- Sogin, M. L., Morrison, H. G., Huber, J. A., Welch, D. M., Huse, S. M., Neal, P. R., et al. (2006). Microbial diversity in the deep sea and the underexplored “rare biosphere”. *Proc. Natl. Acad. Sci. U.S.A.* 103, 12115–12120. doi: 10.1073/pnas.0605127103
- Sørensen, K. B., and Teske, A. (2006). Stratified communities of active Archaea in deep marine subsurface sediments. *Appl. Environ. Microbiol.* 72, 4596–4603. doi: 10.1128/AEM.00562-06
- Takai, K., and Horikoshi, K. (1999). Genetic diversity of archaea in deep-sea hydrothermal vent environments. *Genetics* 152, 1285–1297.
- Takami, H., Noguchi, H., Takaki, Y., Uchiyama, I., Toyoda, A., Nishi, S., et al. (2012). A deeply branching thermophilic bacterium with an ancient acetyl-CoA pathway dominates a subsurface ecosystem. *PLoS ONE* 7:e30559. doi: 10.1371/journal.pone.0030559
- Teske, A., and Sørensen, K. B. (2008). Uncultured archaea in deep marine subsurface sediments: have we caught them all? *ISME J.* 2, 3–18.
- Vergin, K. L., Urbach, E., Stein, J. L., Delong, E. F., Lanoil, B. D., and Giovannoni, S. J. (1998). Screening of a fosmid library of marine environmental genomic DNA fragments reveals four clones related to members of the order Planctomycetales. *Appl. Environ. Microbiol.* 64, 3075–3078.
- Walters, W. A., Caporaso, J. G., Lauber, C. L., Berg-Lyons, D., Fierer, N., and Knight, R. (2011). PrimerProspector: de novo design and taxonomic analysis of barcoded polymerase chain reaction primers. *Bioinformatics* 27, 1159–1161. doi: 10.1093/bioinformatics/btr087
- Wang, Y., and Qian, P. Y. (2009). Conservative fragments in bacterial 16S rRNA genes and primer design for 16S ribosomal DNA amplicons in metagenomic studies. *PLoS ONE* 4:e7401. doi: 10.1371/journal.pone.0007401
- Webster, N. S., Taylor, M. W., Behnam, F., Luckner, S., Rattei, T., Whalan, S., et al. (2010). Deep sequencing reveals exceptional diversity and modes of transmission for bacterial sponge symbionts. *Environ. Microbiol.* 12, 2070–2082.
- Yanagawa, K., Morono, Y., De Beer, D., Haeckel, M., Sunamura, M., Futagami, T., et al. (2012). Metabolically active microbial communities in marine sediment under high-CO<sub>2</sub> and low-pH extremes. *ISME J.* 7, 555–567. doi: 10.1038/ismej.2012.124
- Zheng, D., Alm, E. W., Stahl, D. A., and Raskin, L. (1996). Characterization of universal small-subunit rRNA hybridization probes for quantitative molecular microbial ecology studies. *Appl. Environ. Microbiol.* 62, 4504–4513.

**Conflict of Interest Statement:** The authors declare that the research was conducted in the absence of any commercial or financial relationships that could be construed as a potential conflict of interest.

Received: 05 March 2013; accepted: 31 May 2013; published online: 18 June 2013.

Citation: Hoshino T and Inagaki F (2013) A comparative study of microbial diversity and community structure in marine sediments using poly(A) tailing and reverse transcription-PCR. *Front. Microbiol.* 4:160. doi: 10.3389/fmicb.2013.00160

This article was submitted to Frontiers in Extreme Microbiology, a specialty of *Frontiers in Microbiology*.

Copyright © 2013 Hoshino and Inagaki. This is an open-access article distributed under the terms of the Creative Commons Attribution License, which permits use, distribution and reproduction in other forums, provided the original authors and source are credited and subject to any copyright notices concerning any third-party graphics etc.



# Characteristics of microbial communities in crustal fluids in a deep-sea hydrothermal field of the Suiyo Seamount

Shingo Kato<sup>1,2</sup>, Michiyuki Nakawake<sup>2</sup>, Junko Kita<sup>2</sup>, Toshiro Yamanaka<sup>3</sup>, Motoo Utsumi<sup>4</sup>, Kei Okamura<sup>5</sup>, Jun-ichiro Ishibashi<sup>6</sup>, Moriya Ohkuma<sup>1</sup> and Akihiko Yamagishi<sup>2\*</sup>

<sup>1</sup> Japan Collection of Microorganisms, RIKEN BioResource Center, Wako-shi, Saitama, Japan

<sup>2</sup> Department of Molecular Biology, Tokyo University of Pharmacy and Life Science, Hachioji, Tokyo, Japan

<sup>3</sup> Graduate School of Natural Science and Technology, Okayama University, Tsushima, Okayama, Japan

<sup>4</sup> Graduate School of Life and Environmental Sciences, University of Tsukuba, Tsukuba, Ibaraki, Japan

<sup>5</sup> Center for Advanced Marine Core Research, Kochi University, Nankoku, Kochi, Japan

<sup>6</sup> Department of Earth and Planetary Science, Faculty of Science, Kyushu University, Higashi-ku, Fukuoka-shi, Fukuoka, Japan

**Edited by:**

Anna-Louise Reysenbach, Portland State University, USA

**Reviewed by:**

Karen G. Lloyd, Aarhus University, Denmark

Timothy Ferdelman, Max Planck Institute for Marine Microbiology, Germany

**\*Correspondence:**

Akihiko Yamagishi, Department of Molecular Biology, Tokyo University of Pharmacy and Life Science, 1432-1 Horinouchi, Hachioji, Tokyo 192-0392, Japan.

e-mail: [yamagish@toyaku.ac.jp](mailto:yamagish@toyaku.ac.jp)

To directly access the sub-seafloor microbial communities, seafloor drilling has been done in a deep-sea hydrothermal field of the Suiyo Seamount, Izu-Bonin Arc, Western Pacific. In the present study, crustal fluids were collected from the boreholes, and the bacterial and archaeal communities in the fluids were investigated by culture-independent molecular analysis based on 16S rRNA gene sequences. Bottom seawater, sands, rocks, sulfide mound, and chimneys were also collected around the boreholes and analyzed for comparisons. Comprehensive analysis revealed the characteristics of the microbial community composition in the crustal fluids. Phylotypes closely related to cultured species, e.g., *Alteromonas*, *Halomonas*, *Marinobacter*, were relatively abundant in some crustal fluid samples, whereas the phylotypes related to *Pelagibacter* and the SUP05-group were relatively abundant in the seawater samples. Phylotypes related to other uncultured environmental clones in *Alphaproteobacteria* and *Gammaproteobacteria* were relatively abundant in the sand, rock, sulfide mound, and chimney samples. Furthermore, comparative analysis with previous studies of the Suiyo Seamount crustal fluids indicates the change in the microbial community composition for 3 years. Our results provide novel insights into the characteristics of the microbial communities in crustal fluids beneath a deep-sea hydrothermal field.

**Keywords:** bacteria, archaea, 16S rRNA gene, crustal fluids, deep-sea hydrothermal vent, sub-seafloor biosphere, Island-Arc, Western Pacific

## INTRODUCTION

Microbes are expected to be widely distributed within oceanic crusts. However, little is known about the sub-seafloor biosphere because of the technical difficulties in directly sampling their habitats: what kinds of microbes are there, what function do they have, to what extent are they distributed, how abundant and how productive are they? The presence of microbial communities in aged (thousands-years-old) crustal fluids directly collected from the deep borehole have been shown by *in situ* colonization experiments and direct culture-independent molecular analysis (Cowen et al., 2003; Orcutt et al., 2011a). Considering the vast extent of the seafloor on Earth (~70% of the total surface area), the microbes within the crusts potentially play an important role in global geochemical cycling between crusts and oceans (Schrenk et al., 2009; Orcutt et al., 2011b).

Microbial communities in crustal fluids, which were directly collected from shallow sub-seafloor environments (~10 m depth below the seafloor) by drilling or pipe-insertion approach, have been investigated for three areas with different tectonic backgrounds, i.e., ridge flank, back-arc spreading center, and island-arc. Results from the Baby Bare seamount in the flank of the Juan de

Fuca Ridge (JdFR) suggest that diverse bacteria and archaea are present in the crustal fluids (~20°C) collected by pipe-insertion, and the microbial communities have been interpreted to be the mixture of those in the fluids, overlying seawater and sediments (Huber et al., 2006). In the Southern Mariana Trough (SMT) of a back-arc spreading center, microbial communities in the crustal fluids were different from those of the other habitats, as shown by comparative analysis of crustal fluids (6–40°C) collected from boreholes drilled by the benthic multi-coring system (BMS), bottom seawater, vent fluids, microbial mats, and sulfide chimneys (Kato et al., 2009b,c, 2010). The distinct difference found in different habitats can be explained by energy availability of each inorganic redox reaction for chemolithoautotrophs thriving there (Kato et al., 2012a). In the Suiyo Seamount of the Izu-Bonin Arc, several researchers have collected crustal fluids from BMS boreholes and characterized microbial communities in the fluids (4–112°C) by culture-independent molecular analysis (Higashi et al., 2004; Nakagawa et al., 2004; Hara et al., 2005; Kato et al., 2009a). These results have implied that the phylotypes in the crustal fluids were distinct from those in the surrounding seawater. However, uniqueness of the microbial communities for the crustal fluids

has not been evaluated because no data of surrounding sediments, rocks or chimneys in the Suiyo Seamount hydrothermal field are available.

The Suiyo Seamount is an active deep-sea volcano, which lies on the Izu-Bonin Arc, Western Pacific. The seafloor in the caldera of the Suiyo Seamount is covered with sandy pumice and hydrothermal deposits. The temperature within the pumices at 10–40 cm depth ranged from 10 to 40°C in non-hydrothermal areas, while those within ~10 m of active vents ranged from 5 to 80°C (Kinoshita et al., 2006). Heat flow measurement have indicated that local heat flow and fluid circulation occurs around active vents (Kinoshita et al., 2006). Seven boreholes (called APSK01 to APSK07) were drilled on the seafloor using BMS in June 2001, and three boreholes (APSK08 to APSK10) were added in July 2002. The analysis of core samples obtained from the boreholes have indicated that there is an impermeable layer, which consists of clay and anhydrite, at 1–3 m depth below the seafloor, and that over 300°C hydrothermal fluids are trapped below the layer (Urabe et al., 2002; Marumo et al., 2008).

Previously researchers have revisited the Suiyo Seamount hydrothermal field in July, August and September 2001, August and September 2002, and December 2003. The temperatures of fluids discharged from the boreholes ranged from 9 to 308°C when the boreholes were drilled, and fluctuated over time (Higashi et al., 2004; Nakagawa et al., 2004; Hara et al., 2005; Kinoshita et al., 2006; Marumo et al., 2008; Kato et al., 2009a). The microbial communities in the crustal fluids collected from these boreholes in 2001 and 2002 have been previously reported (Higashi et al., 2004; Nakagawa et al., 2004; Hara et al., 2005; Kato et al., 2009a). We hypothesize that the microbial communities in crustal fluids change temporally by physicochemical fluctuation of the fluids. In 2005, we revisited the seamount and collected crustal fluids from the boreholes APSK07, APSK08, APSK09, and APSK10, in addition to the overlying bottom seawater, sandy sediments, rocks, and sulfide deposits. The locations of the sampling points are shown in Figure 1. Comprehensive analysis using these samples enables us to evaluate the characteristics of the microbial communities of the crustal fluids in this field. Furthermore, comparative analysis of the previous and present data of the Suiyo Seamount will provide information for a better understanding of temporal change of the microbial communities within the crustal aquifers caused by physicochemical fluctuation.

## MATERIALS AND METHODS

### SAMPLE COLLECTION

Fluid samples from boreholes, a natural vent and overlying seawater, and solid samples of sands, sulfide deposits, and rocks were collected in the deep-sea hydrothermal field of the Suiyo Seamount during the NT05-16 cruise (22 September to 7 October 2005) of R/V *Natsushima* (JAMSTEC, Japan) with the remotely operated vehicle *Hyper-Dolphin* (JAMSTEC, Japan). The sample IDs and other information of the collected samples are shown in Table 1. We collected the fluids from boreholes APSK07 (1,383 m water depth), APSK08 (1,386 m), APSK09 (1,387 m), APSK10 (1,380 m), and the vent AP04 (1,376 m) using fluid samplers as described previously (Kato et al., 2009c). To avoid cross-contamination from seawater, the sampling nozzle was inserted

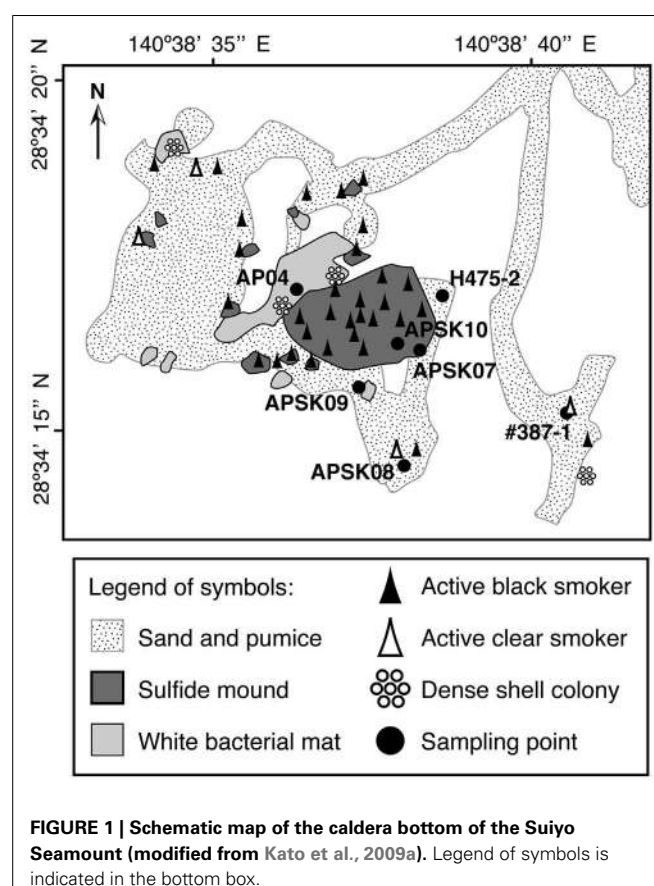


**FIGURE 1 | Schematic map of the caldera bottom of the Suiyo Seamount (modified from Kato et al., 2009a).** Legend of symbols is indicated in the bottom box.

deeply into the boreholes, and the fluids were collected carefully and slowly (100 mL/min) using a peristaltic pump. Detailed information about APSK07, APSK09, and APSK10 has been described previously (Kato et al., 2009a). Titanium pipes were inserted into the boreholes APSK08, APSK09, and APSK10, except APSK07. To trap particles in the collected liquid samples, 1 l of the bottom seawater, and 0.3 l of the borehole and vent fluids were filtered through 0.2-μm-pore-size polycarbonate membranes (Advantec, Tokyo, Japan) using a vacuum pump on board. The filters were stored at -80°C for DNA analysis. For microscopy, aliquots of the liquid samples were fixed, filtered and stored at -20°C as described previously (Kato et al., 2009c). The rock and sulfide deposits collected by a manipulator on the vehicle were crushed into pieces using an autoclaved hammer and chisel in a clean box on board. The sands were collected using a sediment sampler that can be capped immediately after a sampling like a Niskin bottle. The solid samples were stored in DNA/RNA-free plastic tubes at -80°C until DNA extraction.

### GEOCHEMICAL ANALYSIS

The geochemical characteristics were determined as previously described (Nakagawa et al., 2004). In brief, the temperature of fluid was determined *in situ* using a thermometer equipped with the vehicle. The pH was determined onboard using a pH electrode. The pH meter was standardized using NBS standards (pH = 6.86 and 4.01). The electrode was soaked in surface seawater for

**Table 1 | List of the samples used in this study and their characteristics.**

| Sample type        | Sample ID | Sampling site | Sampling date/Dive# | Geochemical characteristics <sup>a</sup> |      |         |                       |         |                         | Cell density (cells/ml) <sup>c</sup> | Bac/Arc <sup>d</sup> |
|--------------------|-----------|---------------|---------------------|--|------|---------|-----------------------|---------|-------------------------|--------------------------------------|----------------------|
|                    |           |               |                     | Temp. (°C)                               | pH   | Si (µM) | H <sub>2</sub> S (mM) | Mg (mM) | Seawater % <sup>b</sup> |                                      |                      |
| Borehole fluid     | Sm7cp     | APSK07        | 2005.10.1/HD476     | 115–165 <sup>g</sup>                     | 4.72 | 8291    | 2.58                  | 19.6    | 36.1                    | 3.56 (0.16) × 10 <sup>5</sup>        | 99.9                 |
|                    | Sm8cp     | APSK08        | 2005.9.28/HD473     | 4.5                                      | 7.74 | 132     | n.d. <sup>e</sup>     | 49.6    | 99.6                    | 1.22 (0.04) × 10 <sup>5</sup>        | 99.2                 |
|                    | Sm9cp     | APSK09        | 2005.10.1/HD476     | 4.7                                      | 7.63 | 153     | n.d.                  | 50.3    | 98.2                    | 1.19 (0.05) × 10 <sup>5</sup>        | >99.9                |
|                    | Sm10cp    | APSK10        | 2005.9.28/HD474     | 4.8                                      | 7.60 | 140     | n.d.                  | 50.0    | 98.5                    | 0.78 (0.04) × 10 <sup>5</sup>        | 99.9                 |
| Ambient seawater   | Sm7sw     | APSK07        | 2005.10.1/HD476     | 4.2                                      | 7.62 | 132     | n.d.                  | 54.3    | — <sup>f</sup>          | 0.52 (0.04) × 10 <sup>5</sup>        | 99.3                 |
|                    | Sm8sw     | APSK08        | 2005.9.28/HD473     | 4.2                                      | 7.72 | 140     | n.d.                  | 49.8    | —                       | 1.05 (0.07) × 10 <sup>5</sup>        | 99.6                 |
|                    | Sm10sw    | APSK10        | 2005.9.28/HD474     | 4.7                                      | 7.56 | 156     | n.d.                  | 50.8    | —                       | 0.95 (0.04) × 10 <sup>5</sup>        | 99.4                 |
|                    | Sm4sw     | AP04          | 2005.9.29/HD475     | 4.2                                      | 7.67 | 133     | n.d.                  | 50.2    | —                       | 0.83 (0.07) × 10 <sup>5</sup>        | 99.6                 |
| Natural vent fluid | Sm4hw     | AP04          | 2005.9.29/HD475     | 6.3–27 <sup>g</sup>                      | 7.08 | 659     | 0.06                  | 45.7    | 91.0                    | 2.86 (0.13) × 10 <sup>5</sup>        | >99.9                |
| Sulfide mound      | Sm4sm     | AP04          | 2005.9.29/HD475     | (6.3–27) <sup>h</sup>                    | —    | —       | —                     | —       | —                       | n.d.                                 | 98.5                 |
| Rock               | Sm4rk     | near A04      | 2005.10.1/HD476     | —  | —    | —       | —                     | —       | —                       | n.d.                                 | >99.9                |
| Sand               | Smhsd     | Marker H475-2 | 2005.9.29/HD475     | —  | —    | —       | —                     | —       | —                       | n.d.                                 | >99.9                |
| Active chimney     | Smmcs     | Marker #387-1 | 2005.10.1/HD476     | (22–49) <sup>h</sup>                     | —    | —       | —                     | —       | —                       | n.d.                                 | 91.4                 |

<sup>a</sup>Geochemical characteristics were determined as previously described (Nakagawa et al., 2004). <sup>b</sup>Calculation based on the Mg concentration of the fluid and ambient seawater samples. <sup>c</sup>Cell numbers in fluids were counted by microscopy. Numbers in parentheses indicate standard deviations of the means. <sup>d</sup>Determined by Q-PCR.

<sup>e</sup>No data. <sup>f</sup>Unapplicable. <sup>g</sup>The temperature of the fluids fluctuated during the sampling. <sup>h</sup>The temperature of the venting fluid.

conditioning, for more than an hour till the sample measurements. The H<sub>2</sub>S and Si concentrations were determined onboard by colorimetry. The Mg concentration was determined using inductively coupled plasma atomic emission spectroscopy in an onshore laboratory.

#### DIRECT CELL COUNTING

Cells on the filters were stained with SYBR Green I for 5 min. Microscopic images were collected using a fluorescence microscope BX60 (Olympus, Tokyo, Japan). To estimate the cell density, cells in at least 40 microscopic images were counted for each sample. The filtration volume of each sample was adjusted to at least 10 cells per view.

#### PCR-BASED PHYLOGENETIC ANALYSIS

PCR-based analysis for the liquid and solid samples was performed as previously described (Kato et al., 2009b,c) with minor modifications. In brief, genomic DNA was extracted from the samples by FastDNA SPIN Kit for Soil (Qbiogene, Carlsbad, CA, USA). Partial 16S rRNA gene sequences of the whole prokaryote and *Archaea* were amplified by PCR with a prokaryote-universal primer set, Uni515F and Uni1406R (Kato et al., 2009b), and with an *Archaea*-specific primer set, Arc21F and Arc958R (DeLong, 1992). PCR amplification of *cbbM* genes using the primer set, cbbM343F and cbbM1126R, was performed as previously described (Kato et al., 2012b). The PCR products were cloned, and the nucleotide sequences of randomly selected clones were determined. The archaeal clones in the libraries from the PCR with the prokaryote-universal primer set were excluded from the analyses. The 16S rRNA gene sequences were aligned using Infernal build in Ribosomal Database Project (Cole et al., 2009). Clones having 97% sequence similarity or higher were sorted using

mothur (Schloss et al., 2009) and treated as the same phylotype. Maximum likelihood (ML) trees were constructed using PHYLML (Guindon and Gascuel, 2003). The taxonomic distribution of the clones was shown using VITCOMIC (Mori et al., 2010). Rarefaction analysis, Shannon diversity index and Chao1 richness estimators for each clone library, and the numbers of shared phylogenotypes among clone libraries were calculated using mothur. The principal coordinates analysis (PCoA) were performed using Fast UniFrac (Hamady et al., 2009).

#### QUANTITATIVE PCR

Bacterial and archaeal rRNA gene copy numbers in the DNA extracts were determined by quantitative PCR (Q-PCR) as previously described (Kato et al., 2009b). Regression coefficient (*r*<sup>2</sup>) values of the standard curve were 0.996 and 0.992 for bacterial and archaeal analyses, respectively. Relative abundance of bacterial and archaeal cells in each sample was estimated based on their average copy numbers of 16S rRNA gene per cell, 4.13 and 1.77, respectively (Lee et al., 2009). All assays were performed in triplicate.

#### ACCESSION NUMBER

The nucleotide sequences of the phylotypes reported in this paper have been deposited in the DDBJ database under the following accession numbers: AB629061–AB629489 for bacterial 16S rRNA genes and AB629490–AB629623 for archaeal 16S rRNA genes, respectively.

## RESULTS

#### GEOCHEMICAL CHARACTERISTICS

The temperature, pH, concentrations of Si, H<sub>2</sub>S, and Mg, seawater fraction of fluid samples, the cell densities and the ratio of bacteria and archaea are shown in Table 1. The borehole and vent fluid

samples contained a large amount of seawater ranging from 91.0 to 99.6% by volume, except APSK07 borehole fluids (**Table 1**), estimated from measured Mg concentration. It should be noted that the seawater fraction in **Table 1** does not simply refer to the amount of cross-contamination by seawater during sampling, but contain a certain amount of not hydrothermally altered seawater as discussed below. The fluids discharging from the APSK07 bore-hole and the AP04 vent obviously contained hydrothermal fluids as shown by geochemical differences such as high temperature, low pH and high concentrations of Si and H<sub>2</sub>S. The temperatures of the fluids from the APSK08, APSK09 and APSK10 boreholes were slightly higher (0.1 to 0.3°C) than that of the surrounding seawater.

### MICROBIAL ABUNDANCE

Relative abundance of bacteria and archaea determined by Q-PCR (**Table 1**) indicated that bacteria dominated in all the samples (**Table 1**). The cell densities of the fluid samples of the boreholes (except sm10cp) and the vent were relatively higher than that of the surrounding seawater near each borehole (**Table 1**).

### DIVERSITY OF 16S rRNA GENE SEQUENCES

Shannon diversity indices of the microbial communities of the samples are shown in **Figure 2** (see also Table S1 in Supplementary Material in details). When the diversity indices were compared between bacterial and archaeal communities within single samples, the archaeal communities for all the seawater samples (Sm4sw, Sm7sw, Sm8sw, and Sm10sw) showed higher diversity than the bacterial communities (1.1–2.0 times; **Figure 2**). The bacterial communities in the borehole fluids (Sm7cp, Sm8cp, Sm9cp, and Sm10cp), rock (Sm4rk), sand (Smhsd), and sulfide chimney (Smmcs) samples showed higher diversity (1.6–3.8 times; **Figure 2**) than the archaeal communities. The bacterial communities in the vent fluid (Sm4hw) and sulfide mound (Sm4sm) samples were more diverse than the archaeal communities (1.2 times; **Figure 2**). When the diversity indices of the bacterial communities were compared among the samples, Sm4rk and Smmcs had the highest diversity (Shannon diversity index, 4.3–4.5) and Sm8sw had the lowest diversity (<1.0) (**Figure 2**; Table S1 in Supplementary Material). The bacterial communities of the borehole fluid samples, except Sm10cp, showed higher diversity than those of the seawater samples (**Figure 2**). When the diversity indices of the archaeal communities were compared among the samples, Smmcs, Sm4sm, and Sm4hw had high diversity (Shannon diversity index, >2.1) and the seawater samples (Sm4sw, Sm7sw, Sm8sw, and Sm10sw) had moderate diversity (1.7–2.0). The borehole fluid samples, except Sm9cp, had low archaeal diversity (Shannon diversity index, <1.0) (**Figure 2**). Chao1 species richness estimates (Table S1 in Supplementary Material) and rarefaction curves (Figure S1 in Supplementary Material) showed the similar patterns.

### BACTERIAL COMMUNITY STRUCTURES

To grasp the overview of the common and unique phylotypes among the samples, the microbial community structures (both archaea and bacteria) are displayed on a VITCOMIC image in **Figure 3** (see also Figure S2 in Supplementary Material for

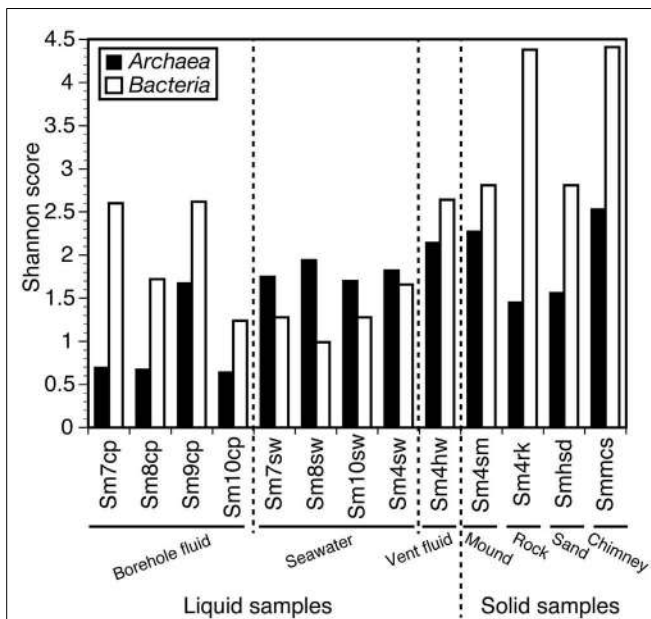


**FIGURE 2 |** Shannon diversity index for archaeal and bacterial 16S rRNA gene clone libraries. Values in details are shown in Table S1 in Supplementary Material.

enlarge views of *Alpha*-, *Beta*-, *Gamma*-, and *Epsilonproteobacteria* and *Archaea*). The image of VITCOMIC displays the taxonomic composition for not only major but also minor phylotypes in each library without loss of similarity information (Mori et al., 2010). This enables us to visually compare the microbial community structures. The taxonomic affiliation of the phylotypes related to cultured species and their relative abundance as shown in the VITCOMIC image well corresponded to that resulted from the phylogenetic tree (Figures S3 and S4 in Supplementary Material).

The recovered bacterial phylotypes were affiliated to taxonomic groups (the details are shown in Table S2 in Supplementary Material). Most phylotypes recovered from the liquid samples (i.e., the borehole fluids, vent fluid, and seawater samples) and from the sand sample were affiliated to *Proteobacteria* (82.5–100% of the total clone numbers; Table S2 in Supplementary Material). In contrast, the proportion of the proteobacterial phylotypes was relatively low (56.0–62.0%) for the rock, sulfide mound and chimney samples. Other bacterial phyla (i.e., the *Acidobacteria*, *Actinobacteria*, *Aquificae*, *Bacteroidetes*, “*Caldithrix*” *Chlamydiae*, *Chlorobi*, *Chloroflexi*, *Cyanobacteria*, *Firmicutes*, *Gemmatimonadetes*, *Lentisphaerae*, *Nitrospirae*, *Planctomycetes*, “*Poribacteria*,” *Spirochetes*, *Thermotogae*, and *Verrucomicrobia*) and uncultured clone groups (GN02, GN06, JS1, KSB1, Marine group A, OD1, OP1, OP3, TM6, TM7, WS3) were also detected (Table S2 and Figure S3 in Supplementary Material).

The relative abundance of the phylotypes in several taxonomic groups is summarized in **Figure 4**. Many bacterial phylotypes (57.4–78.7% of the total clone numbers) recovered from Sm8cp, Sm10cp, Sm4hw, and all the seawater samples were affiliated to SUP05-related group in the *Gammaproteobacteria* (see also Table S2 and Figure S3E in Supplementary Material), which have been

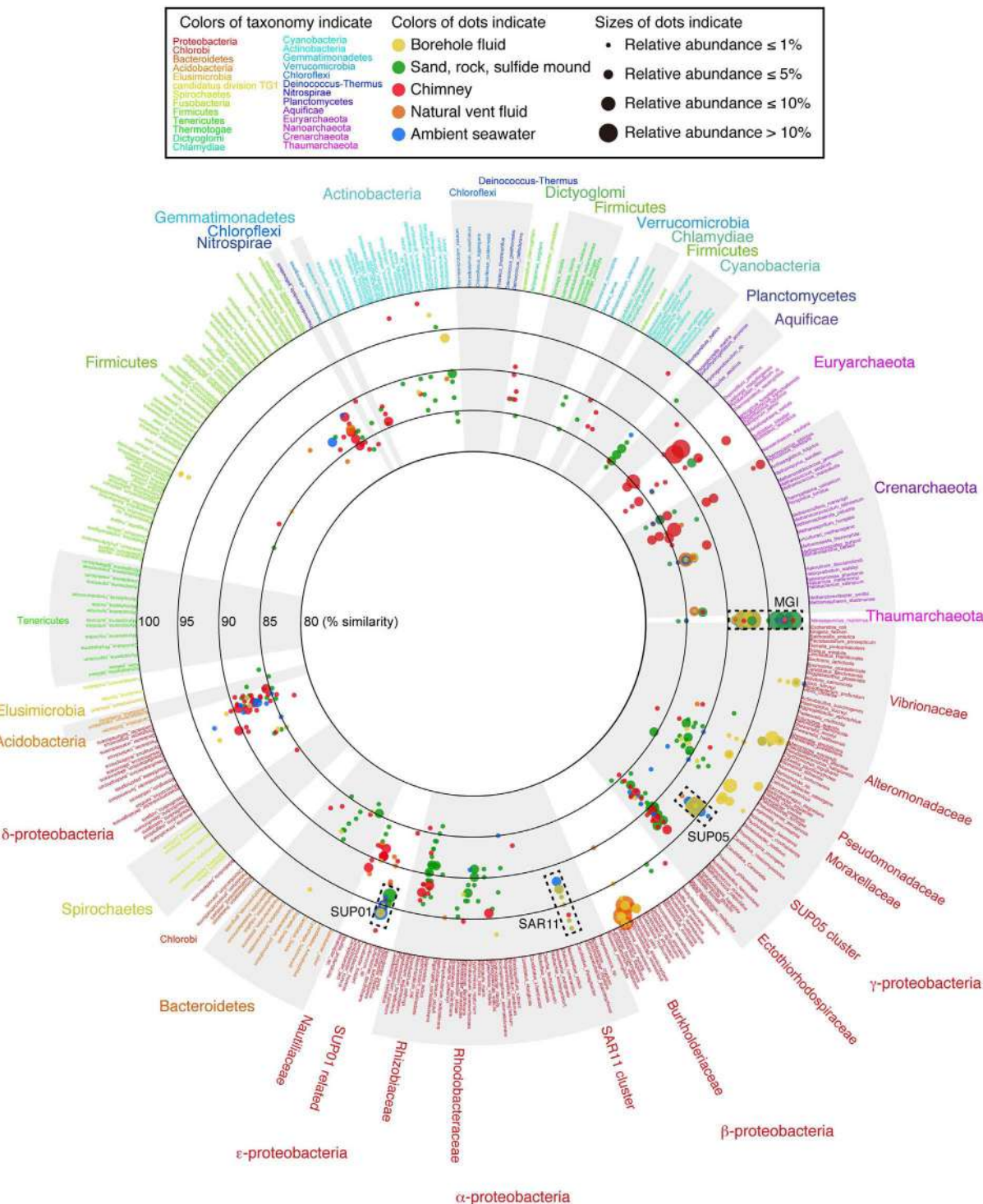
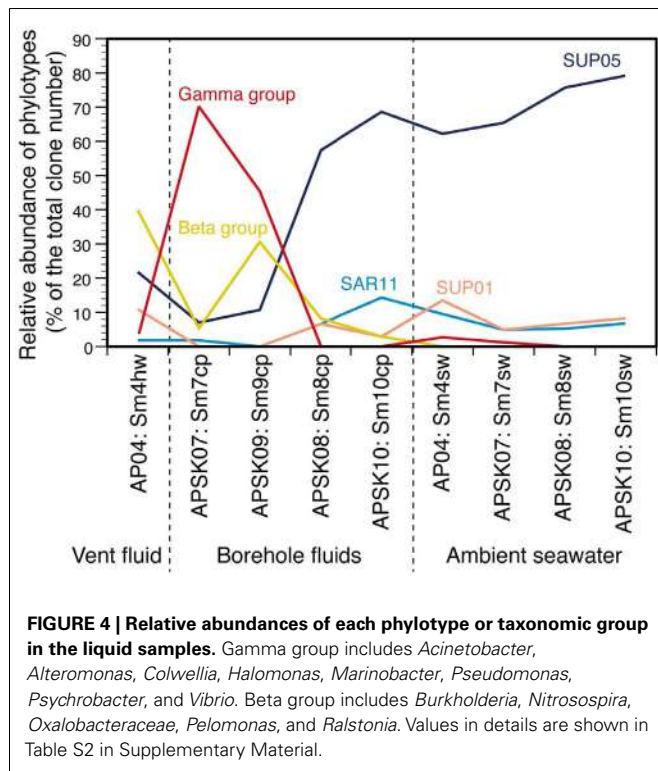


**FIGURE 3 | The overview of the microbial community structures for the whole prokaryote based on 16S rRNA gene sequences visualized by VITCOMIC.** Scientific names of prokaryotic species in the reference database of VITCOMIC are shown outside of the circle. The font color for each name indicates its phylum name as shown in the box and outside of the circle. The large circles indicate boundaries of similarities (80, 85, 90, 95, and 100% similarities to the database sequence). The location of colored dots represents average similarity of full-length sequence of amplicon of each

phylotype against the nearest relative species. The color of the dots indicates the sample type as shown in the box. The VITCOMIC analysis for archaeal or bacterial communities was performed separately. The total number of archaeal or bacterial sequences in the all samples is 1,011 or 1,025, respectively. The size of the dots indicates relative abundance of the phylotypes in the archaeal or bacterial clone library integrated by the sample type (smallest dot < 1%, second smallest dot < 5%, third smallest dot < 10%, and the largest dot > 10%).



reported as the most abundant members in the hydrothermal plume in the Suiyo Seamount (Sunamura et al., 2004). This group has been found at other hydrothermal vent fields (Kato et al., 2009c) and oxygen minimum zone in oceans (Walsh et al., 2009), and may contain chemolithoautotrophic sulfur-oxidizing bacteria suggested by whole-genome analysis (Walsh et al., 2009). These samples also contained phylotypes related to SAR11 cluster that is a common bacterial member in oceans (Morris et al., 2002) and those related to SUP01 in the *Thiovulgaceae* that is the second abundant member in the hydrothermal plume in the Suiyo Seamount (Sunamura et al., 2004) (Figures S3A,D in Supplementary Material).

In contrast, phylotypes recovered from the other two bore-hole fluid samples, Sm7cp and Sm9cp, were phylogenetically close to cultured species (e.g., *Acinetobacter*, *Alteromonas*, *Halomonas*, *Marinobacter*, *Pseudomonas*, and *Vibrio* in the *Gammaproteobacteria*, and *Ralstonia* in the *Betaproteobacteria*) (Figure 3; figures S3B,E in Supplementary Material), which account for >10% of the total clone number of each library (Table S2 in Supplementary Material). The phylotypes related to *Ralstonia* and also the *Oxalobacteraceae* in the *Betaproteobacteria* were relatively abundant in the clone library from Sm4hw (21.8% of the total clone number). The SUP24-24 clone recovered from the Suiyo seamount hydrothermal plume (Sunamura et al., 2004) belongs to the *Oxalobacteraceae* (Figure S3B in Supplementary Material).

Phylotypes recovered from the solid samples, i.e., Sm4sm, Sm4rk, Smhsd, and Smmcs, had low similarity to cultured species (<95%, a general genus-level definition; Figure 3). In particular, unclassified gammaproteobacterial phylotypes were recovered from all solid samples (Table S2 in Supplementary Material;

Figure 3; see also Figure S2A in Supplementary Material). These phylotypes were related to environmental clones recovered from seafloor habitats (sediment and rocks, and symbionts) in various areas and were also relatively close to chemolithoautotrophic members of *Thioprofundum* and the *Ectothiorhodospiraceae*, including sulfide-, arsenite-, and nitrite-oxidizers (Takai et al., 2009), in the phylogenetic tree (Figure S3E in Supplementary Material).

## ARCHAEAL COMMUNITY STRUCTURES

The recovered archaeal phylotypes were affiliated with taxonomic groups as shown in Table S3 in Supplementary Material. All phylotypes recovered from Sm7cp, Sm8cp, Sm10cp, and Sm4rk were affiliated with Marine Group I (MGI) (Figure 3; see also Figures S2C and S4 in Supplementary Material), which is one of the most abundant archaeal members in oceans (Fuhrman and Davis, 1997; Karner et al., 2001) and contain an ammonia-oxidizing isolate “*Nitrosopumilus maritimus*” (Könneke et al., 2005). In addition to MGI, phylotypes related to pSL12-related group, Marine Group II and III (MGII and MGIII) or Marine Benthic Group E (MBGE) in the *Euryarchaeota* were recovered from Sm9cp, Smhsd, and all the seawater samples (Table S3 and Figure S4 in Supplementary Material). The libraries from Sm4sm and Smmcs contained phylotypes related to (hyper)thermophilic members of *Archaeoglobi* and *Thermoprotei*. Furthermore, phylotypes related to “*Aciduliprofundum*,” *Thermococci*, and Marine Benthic Group D (MBGD) in *Euryarchaeota*, *Korarchaeota*, and ambiguous groups, i.e., Hot Water Crenarchaeota Group (HWCG), Marine Benthic Group B (MBGB), Marine Hydrothermal Vent Group I (MHVG-I), and Terrestrial Hot Spring Crenarchaeota (THSC), which did not clearly clustered in above archaeal phyla in the phylogenetic tree (Figure S4B in Supplementary Material), were recovered only from Smmcs (Table S3 in Supplementary Material).

## COMPARISON OF BACTERIAL AND ARCHAEOAL COMMUNITY STRUCTURES

The communities were divided into four groups each in archaeal and bacterial communities in PCoA (Figures 5A,B). The bacterial four groups are: GroupB1 consisted of all the seawater samples (Sm4sw to Sm10sw), vent fluid sample (Sm4hw) and two bore-hole samples (Sm8cp and Sm10cp); GroupB2 consisted of the other borehole samples (Sm7cp and Sm9cp); GroupB3 consisted of the sand (Smhsd), rock (Sm4rk), and sulfide mound (Sm4sm) samples; and GroupB4 consisted of the chimney sample (Smmcs). The archaeal four groups are: GroupA1 consisted of all the seawater samples, Sm4hw and Sm9cp; GroupA2 consisted of Sm7cp, Sm8cp, and Sm10cp; and GroupA3 and GroupA4 consisted of the same samples as in the case of GroupB3 and GroupB4 for bacterial communities.

The shared phylotype numbers among the groups are shown in Venn diagrams (Figures 5C,D). Over half of the bacterial phylotypes in GroupB3 (92.9% of the total phylotype number) and GroupB4 (95.5%) and archaeal phylotypes in GroupA3 (57.9%) and GroupA4 (86.2%) were unique. These groups were all derived from the communities in the solid samples. In addition, many bacterial phylotypes (70.4–95.6%) were unique among each solid sample (Figure S5A in Supplementary Material). In contrast,

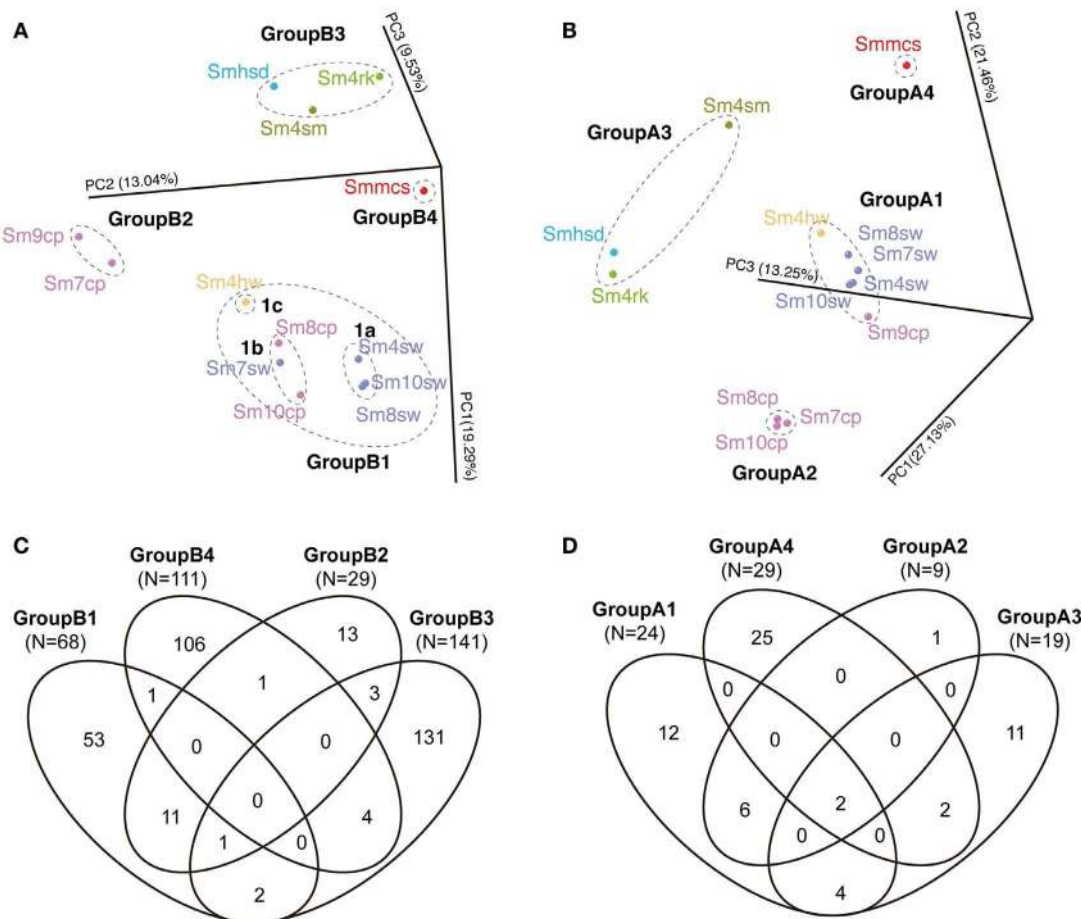


**FIGURE 5 | Comparison of bacterial and archaeal community structures of the Suiyo Seamount.** The results of (A,B) PCoA and (C,D) Venn diagrams indicating the shared phylotype numbers among the groups defined in the PCoA are shown. The results of the comparative analyses for (A,C) bacterial and (B,D) archaeal communities are shown.

(A,B) The percentages in the axis labels represent the percentages of variation explained by the principal coordinates. (A,B) The color of the sample name indicates each sample type: purple, borehole fluid; orange, natural vent fluid; ultramarine, seawater; green, rock; sky blue, sand; olive, sulfide mound; red, active chimney.

relatively small numbers of the phylotypes in GroupB2 (37.9% of the total phylotype number) were shared with GroupB1 (16.2%) and those in GroupA2 (66.7%) were shared with GroupA1 (25.0%); these groups were derived from the communities in the liquid samples (**Figure 5**). Furthermore, GroupB1 was divided into three subgroups, GroupB1a, b and c (**Figure 5A**). The shared phylotype numbers among GroupB1a, b, c, and GroupB2 are shown in Figure S5B in Supplementary Material. Although these (sub)groups were similar each other in the PCoA result (**Figure 5A**), unique phylotypes constituted a half or more of the total phylotype numbers (Figure S5B in Supplementary Material).

### CHANGE IN MICROBIAL COMMUNITIES IN CRUSTAL FLUIDS FOR 3 YEARS

The microbial community structures in the crustal fluids collected from the boreholes in the Suiyo Seamount in 2001 and 2002 have already been reported (Higashi et al., 2004; Nakagawa et al., 2004; Kato et al., 2009a). Comparative analysis between the data in 2001–2002 and 2005 samples provide a unique opportunity to

address the change of microbial communities in crustal fluids. The difference in the community compositions in the crustal fluids of the Suiyo Seamount is shown in Figure S6A in Supplementary Material by VITCOMIC. Remarkably, the phylotype related to *Thiomicrospira* was detected in the borehole fluids in 2001 and 2002 (Higashi et al., 2004; Nakagawa et al., 2004; Kato et al., 2009a); however no or few phylotypes related to these members were detected in 2005. In contrast, in 2005, the phylotypes related to gammaproteobacterial genera such as *Alteromonas*, *Pseudomonas*, and *Marinobacter* accounted for relatively high percentages in the clone libraries from the borehole fluids (Sm7cp and Sm9cp; Table S2 in Supplementary Material).

Likewise, such change in microbial communities has been observed in the borehole fluids in the SMT between 2004 and 2005 (Kato et al., 2009c) (Figure S6B in Supplementary Material). The analytical processes, such as the seafloor drilling, collecting fluids, and DNA analysis, has been performed by almost the same methods, so that we could compare the results of the Suiyo Seamount with those of the SMT in minimized methodological bias. The

results of PCoA including the data of the Suiyo Seamount and SMT indicated that the community of the SMT borehole fluid collected in 2005 (as F2apm1 in **Figure 6**) was clustered within the GroupB2 (**Figure 6**). These communities in GroupB2 include phylotypes related to cultured *Beta-* and *Gammaproteobacteria* (**Figure 6** in Supplementary Material). This grouping suggested that the characteristics of bacterial community structures in crustal fluids might converge for at least 1 year after drilling despite the difference in geographical (spatial distance) and geological settings (island-arc vs. back-arc spreading center). The communities of the SMT vent and borehole fluids collected in 2004 were clustered within GroupBm that is defined in **Figure 6**, which represents phylotypes related to *Thiomicrospira* and *Mariprofundus* (sulfide- and iron-oxidizing bacteria, respectively) (Kato et al., 2009c). The Suiyo Seamount borehole fluid collected in 2002 may be clustered in the GroupBm because of the representative phylotypes related to *Thiomicrospira* (**Figure S6A** in Supplementary Material; Kato et al., 2009a); however, we could not include these 2002 data into PCoA because only partial sequences were determined.

## DISCUSSION

Although microbes within the crustal aquifers potentially play a role in global geochemical cycling, knowledge of these sub-seafloor microbes, i.e., their abundance, diversity, function, activity, and productivity, is still extremely limited because of the technical difficulties in directly access their habitats. Seafloor drilling provides a unique opportunity to approach microbes within crustal aquifers. Our comprehensive analysis of the 16S rRNA gene sequences (especially for bacteria) picks up the difference and commonality of the characteristics of microbial communities in each habitat-type (i.e., borehole fluid, vent fluid, ambient seawater, sand, rock, sulfide mound, and chimney) in the Suiyo Seamount, a model

of the island-arc hydrothermal fields. Furthermore, comparative analysis including the previous results of the Suiyo Seamount in 2002 (Kato et al., 2009a) and of the SMT in 2004 and 2005 (Kato et al., 2009c) allows us to discuss the difference in microbial communities in the crustal fluids.

## CHARACTERISTICS OF MICROBIAL COMMUNITIES IN CRUSTAL FLUIDS

The crustal fluid communities are likely to be distinguished from the communities in the seawater and solid habitats, such as rocks. Our comparative analysis shed light on the characteristics of the crustal fluid communities in 2005. The cell densities in the borehole fluids are comparable to or slightly higher than those in ambient seawater (**Table 1**). The cell densities in the overlying seawater and borehole fluids is comparable to the previous reports of the JdFR flank (0.23–0.85 and  $0.38\text{--}1.30 \times 10^5$  cells/mL, respectively) (Cowen et al., 2003; Huber et al., 2006) and to those of the SMT ( $0.17\text{--}0.18$  and  $0.66\text{--}1.03 \times 10^5$  cells/mL, respectively) (Kato et al., 2009c).

A characteristic of the crustal fluid communities of Sm7cp and Sm9cp samples is the relatively high abundance of phylotypes closely related to cultured species in *Gammaproteobacteria* (e.g., *Alteromonas*, *Halomonas*, *Marinobacter*, *Pseudomonas*, and *Vibrio*). This characteristic is one of the reasons for the separation between the crustal fluid communities (Sm7cp and Sm9cp) and the others in PCoA (**Figure 5A**). *Halomonas* and *Marinobacter* are widely distributed in low temperature hydrothermal vent fields (Kaye et al., 2011). These facts support that the gammaproteobacterial members in Sm7cp and Sm9cp may be present there and adapt to the low temperature crustal fluid environments. The temperature of APSK07 borehole fluids dramatically increased for 3 years (55–165°C). Despite the high temperature of the fluid sample Sm7cp, no phylotypes related to known thermophilic members were observed in the Sm7cp library. We interpret that the detected phylotypes in the Sm7cp may be transported from low temperature sub-seafloor environments. Organic carbon for the above-mentioned heterotrophic bacteria, e.g., *Alteromonas* and *Halomonas*, might be produced by chemolithoautotrophs (e.g., *Thiomicrospira*) during the first year after the drilling (Kato et al., 2009a) and/or by those (e.g., *Archaeoglobus*) in hot deeper sub-seafloor environments (Higashi et al., 2004; Hara et al., 2005). It should be noted that we have shown the presence of a variety of putative chemolithoautotrophs in the solid samples (i.e., Sm4rk, Smhsd, and Smmcs), the seawater and vent fluid samples (i.e., Sm8sw, Sm10sw, Sm4sw, and Sm4hw) (Kato et al., 2012b) used in the present study by PCR-based analysis of *cbbM* gene encoding form II of ribulose-1,5-bisphosphate carboxylase/oxygenase (RubisCO), a key enzyme in the Calvin–Benson–Basham cycle. However, *cbbM* and other genes related to carbon fixation (i.e., *cbbL* and *aclB*) have not been detected in the borehole fluid samples.

Archaeal communities seem to be different between the borehole fluid samples (except Sm9cp) and the seawater samples (**Figure 5B**). This likely results from the absence of MGI α-cluster and MGII in these borehole fluids (Table S3 and Figure S4 in Supplementary Material), although most of the archaeal phylotypes in the borehole fluids were also found in the seawater (**Figure 5D**). In contrast, the archaeal communities were clearly different

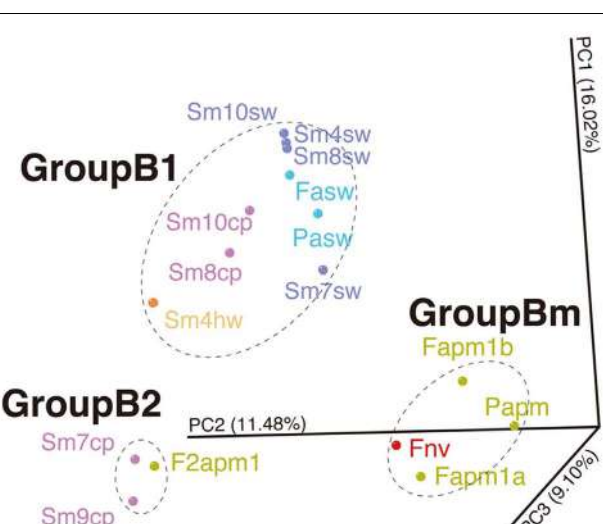


**FIGURE 6 | Comparison of bacterial communities between the Suiyo Seamount and Southern Mariana Trough.** The results of PCoA are shown. Data from the previous reports of the Southern Mariana Trough (Kato et al., 2009c) are included in this analysis: Fapm1a, Fapm1b, Papm, F2apm1, Fnv, Faws, and Pasw. The percentages in the axis labels represent the percentages of variation explained by the principal coordinates.

between the liquid samples (representing Group A1 and 2) and the solid samples (representing Group A3 and 4) (Figures 5B,D). This difference is likely caused by the presence/absence of MGII  $\epsilon - \zeta - \theta$  cluster and of the other archaeal groups (except MGII and pSL12-related) (Table S3 in Supplementary Material). The presence/absence of these archaeal groups may reflect the temperature, pH, and availability of energy sources associated with hydrothermal activity as discussed previously (Kato et al., 2010), as well as their life-style, i.e., free-living or attached to a solid support as reported in other marine environments (Durbin and Teske, 2010; Nitahara et al., 2011).

Our results show the characteristics of the bottom seawater communities: (i) low cell density ( $<1.1 \times 10^5$  cells/mL); (ii) low phylogenetic diversity ( $<2.0$  of Shannon diversity index); (iii) higher diversity of archaea than bacteria (1.1–2.0 times); and (iv) high relative abundance of the phylotypes of the SUP05-related group in *Gammaproteobacteria* (60–80% of the total clone numbers), SUP01 cluster in *Epsilonproteobacteria* (5–15%), and SAR11 cluster in *Alphaproteobacteria* (5–10%). These characteristics are partially consistent with those reported for the bottom seawater of the Suiyo Seamount sampled in 2002 (Kato et al., 2009a) and those of the back-arc spreading center deep-sea hydrothermal fields of the SMT (Kato et al., 2009c), suggesting that these characteristics of the bottom seawater communities are common at deep-sea water around hydrothermal fields in island-arc and back-arc systems. Microbial communities in the habitats of the solid samples are characterized as: (i) moderate or high phylogenetic diversity (Shannon diversity index, 2.8–4.3); (ii) relatively high abundance of the phylotypes related to uncultured bacteria including *Proteobacteria* and other phyla; and (iii) distinct community structures among the habitats (i.e., sands, rocks, sulfide mounds, and chimneys). These characteristics are consistent with those of the SMT (Kato et al., 2009b, 2010). Overall, our results suggest that the characteristics of the microbial communities of overlaying bottom seawater and surrounding solid habitats are different from those of crustal fluids in island-arc and back-arc systems.

#### THE CHANGE IN MICROBIAL COMMUNITY COMPOSITIONS IN CRUSTAL FLUIDS FOR 3 YEARS

The changes in the community compositions in the crustal fluids of the Suiyo Seamount for 3 years are summarized (Figure 7) based on comprehensive data regarding the geological and geochemical characterization as described previously (Marumo et al., 2008; Toki et al., 2008). Although putative sulfide-oxidizing chemolithoautotrophs related to *Thiomicrospira* were relatively abundant in the borehole fluids in 2001 and 2002 (Higashi et al., 2004; Nakagawa et al., 2004; Kato et al., 2009a), putative heterotrophs related to such as *Alteromonas*, *Pseudomonas*, and *Marinobacter* were relatively abundant in the borehole fluids in 2005 (Figure S6A in Supplementary Material). Considering the inferred physiological characteristics of the detected phylotypes, the changes in microbial communities in the crustal fluids for 3 years may be caused by the changes of geochemical characteristics of the crustal fluids. As compared with 2002 data, the increase in pH (6.6–7.6) and decrease in concentrations of H<sub>2</sub>S (0.74 mM to not detected) was observed for

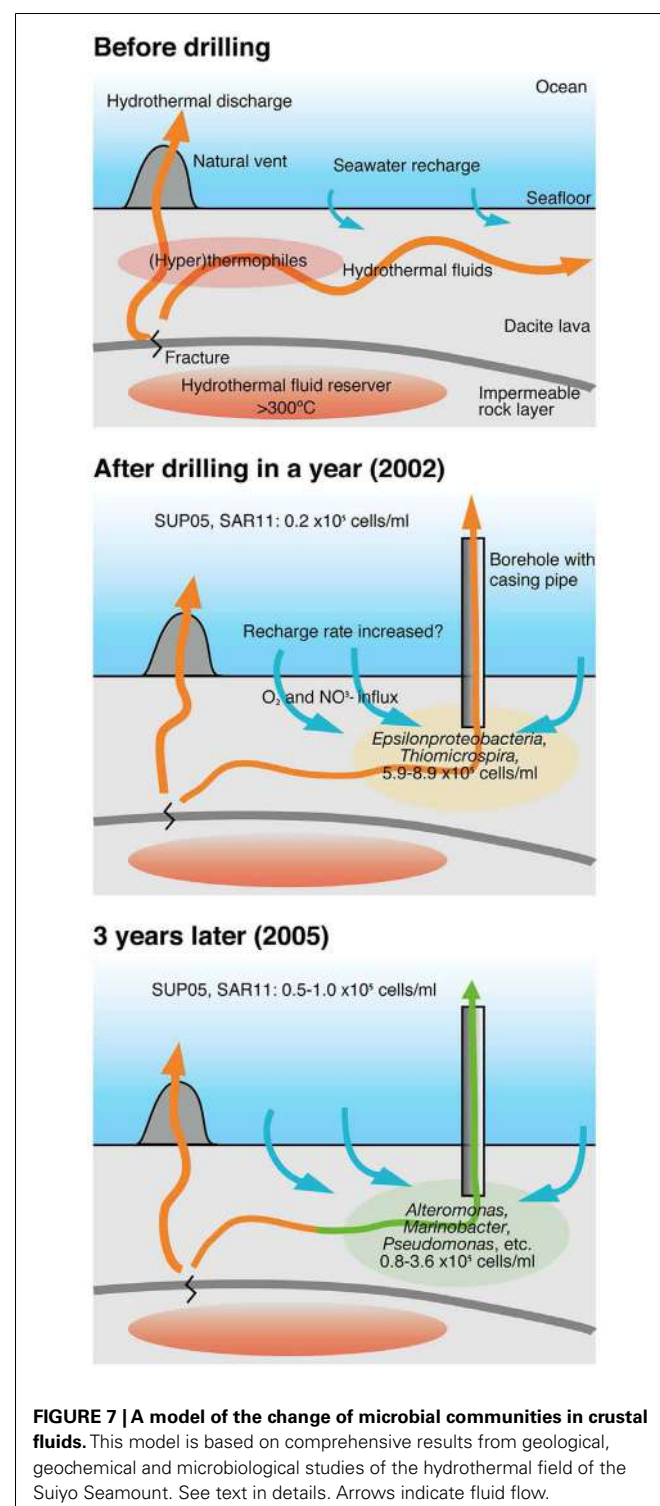


**FIGURE 7 | A model of the change of microbial communities in crustal fluids.** This model is based on comprehensive results from geological, geochemical and microbiological studies of the hydrothermal field of the Suiyo Seamount. See text in details. Arrows indicate fluid flow.

APS09 borehole fluids. The decrease in H<sub>2</sub>S is consisted with the decrease in the relative abundance of the phylotypes related to *Thiomicrospira*.

It is possible that the geochemical changes are caused by the creation of new discharging points using the drilling process. The creation of a discharging point is expected to lead to more

recharge of the seawater and to oxygenation of the sub-seafloor habitats. During the first year after drilling, phylotypes related to *Thiomicrospira* were present in sub-seafloor, and might utilize reduced-sulfides contained in hydrothermal fluids and oxygen and/or nitrate contained in recharged seawater (Figure 7; Kato et al., 2009a). Heat flow measurements indicate that local recharges of seawater into the seafloor occur in the Suiyo Seamount (Kinoshita et al., 2006). After the depletion of these electron donors (i.e., reduced-sulfides) by microbial consumption and/or chemical precipitation, putative heterotrophic bacteria could thrive utilizing organic carbon as described above. Our hypothesis can clearly explain the observed change in the microbial communities in the crustal fluids of the Suiyo Seamount from 2002 to 2005 and also of the SMT from 2004 to 2005 (Figure 6). The change in the microbial communities potentially occurs in global sub-seafloor environments from the opening of a new hydrothermal vent to the ceasing of hydrothermal activity. Further investigations, e.g., physiological characterization of these phylotypes by cultivation and/or metagenomic approaches, *in situ* measurement of the metabolic reaction and detailed geochemical characterization of the crustal fluids over time, are needed to assess this hypothesis.

## REFERENCES

- Cole, J. R., Wang, Q., Cardenas, E., Fish, J., Chai, B., Farris, R. J., et al. (2009). The Ribosomal Database Project: improved alignments and new tools for rRNA analysis. *Nucleic Acids Res.* 37, D141–D145.
- Cowen, J., Giovannoni, S., Kenig, F., Johnson, H., Butterfield, D., Rappé, M., et al. (2003). Fluids from aging ocean crust that support microbial life. *Science* 299, 120–123.
- DeLong, E. (1992). Archaea in coastal marine environments. *Proc. Natl. Acad. Sci. U.S.A.* 89, 5685–5689.
- Durbin, A. M., and Teske, A. (2010). Sediment-associated microdiversity within the marine group I crenarchaeota. *Environ. Microbiol. Rep.* 2, 693–703.
- Fuhrman, J., and Davis, A. (1997). Widespread archaea and novel bacteria from the deep sea as shown by 16S rRNA gene sequences. *Mar. Ecol. Prog. Ser.* 150, 275–285.
- Guindon, S., and Gascuel, O. (2003). A simple, fast, and accurate algorithm to estimate large phylogenies by maximum likelihood. *Syst. Biol.* 52, 696–704.
- Hamady, M., Lozupone, C., and Knight, R. (2009). Fast UniFrac: facilitating high-throughput phylogenetic analyses of microbial communities including analysis of pyrosequencing and phylochip data. *ISME J.* 4, 17–27.
- Hara, K., Kakegawa, T., Yamashiro, K., Maruyama, A., Ishibashi, J., Marumo, K., et al. (2005). Analysis of the archaeal sub-seafloor community at Suiyo Seamount on the Izu-Bonin arc. *Adv. Space Res.* 35, 1634–1642.
- Higashi, Y., Sunamura, M., Kitamura, K., Nakamura, K., Kurusu, Y., Ishibashi, J., et al. (2004). Microbial diversity in hydrothermal surface to subsurface environments of Suiyo Seamount, Izu-Bonin arc, using a catheter-type *in situ* growth chamber. *FEMS Microbiol. Ecol.* 47, 327–336.
- Huber, J. A., Johnson, H. P., Butterfield, D. A., and Baross, J. A. (2006). Microbial life in ridge flank crustal fluids. *Environ. Microbiol.* 8, 88–99.
- Karner, M. B., Delong, E. F., and Karl, D. M. (2001). Archaeal dominance in the mesopelagic zone of the Pacific Ocean. *Nature* 409, 507–510.
- Kato, S., Hara, K., Kasai, H., Teramura, T., Sunamura, M., Ishibashi, J., et al. (2009a). Spatial distribution, diversity and composition of bacterial communities in sub-seafloor fluids at a deep-sea hydrothermal field of the Suiyo Seamount. *Deep Sea Res. Part 1 Oceanogr. Res. Pap.* 56, 1844–1855.
- Kato, S., Kobayashi, C., Kakegawa, T., and Yamagishi, A. (2009b). Microbial communities in iron-silica-rich microbial mats at deep-sea hydrothermal fields of the Southern Mariana Trough. *Environ. Microbiol.* 11, 2094–2111.
- Kato, S., Yanagawa, K., Sunamura, M., Takano, Y., Ishibashi, J., Kakegawa, T., et al. (2009c). Abundance of *Zetaproteobacteria* within crustal fluids in back-arc hydrothermal fields of the Southern Mariana Trough. *Environ. Microbiol.* 11, 3210–3222.
- Kato, S., Nakamura, K., Toki, T., Ishibashi, J., Tsunogai, U., Hirota, A., et al. (2012a). Iron-based microbial ecosystem on and below the seafloor: a case study of hydrothermal fields of the Southern Mariana Trough. *Front. Microbiol.* 3:89. doi:10.3389/fmicb.2012.00089
- Kato, S., Nakawake, M., Ohkuma, M., and Yamagishi, A. (2012b). Distribution and phylogenetic diversity of *cbbM* genes encoding RubisCO form II in a deep-sea hydrothermal field revealed by newly designed PCR primers. *Extremophiles* 16, 277–283.
- Kato, S., Takano, Y., Kakegawa, T., Oba, H., Inoue, K., Kobayashi, C., et al. (2010). Biogeography and biodiversity in sulfide structures of active and inactive vents at deep-sea hydrothermal fields of the Southern Mariana Trough. *Appl. Environ. Microbiol.* 76, 2968–2979.
- Kaye, J. Z., Sylvan, J. B., Edwards, K. J., and Baross, J. A. (2011). *Halomonas* and *Marinobacter* ecotypes from hydrothermal vent, sub-seafloor and deep-sea environments. *FEMS Microbiol. Ecol.* 75, 123–133.
- Kinoshita, M., Kawada, Y., Tanaka, A., and Urabe, T. (2006). Recharge/discharge interface of a secondary hydrothermal circulation in the Suiyo Seamount of the Izu-Bonin arc, identified by submersible-operated heat flow measurements. *Earth Planet. Sci. Lett.* 245, 498–508.
- Könneke, M., Bernhard, A. E., De La Torre, J. R., Walker, C. B., Waterbury, J. B., and Stahl, D. A. (2005). Isolation of an autotrophic ammonia-oxidizing marine archaeon. *Nature* 437, 543–546.
- Lee, Z. M.-P., Bussema, C., and Schmidt, T. M. (2009). rrnDB: documenting the number of rRNA and tRNA genes in bacteria and archaea. *Nucleic Acids Res.* 37, D489–D493.
- Marumo, K., Urabe, T., Goto, A., Takano, Y., and Nakaseama, M. (2008). Mineralogy and isotope geochemistry of active submarine hydrothermal field at Suiyo Seamount, Izu-Bonin arc, West Pacific Ocean. *Resource Geol.* 58, 220–248.
- Mori, H., Maruyama, F., and Kurokawa, K. (2010). VITCOMIC: visualization tool for taxonomic compositions of microbial communities based on 16S rRNA gene sequences. *BMC Bioinformatics* 11:332. doi:10.1186/1471-2105-11-332
- Morris, R. M., Rappé, M. S., Connon, S. A., Vergin, K. L., Siebold, W. A., Carlson, C. A., et al. (2002). SAR11 clade dominates ocean surface bacterioplankton communities. *Nature* 420, 806–810.
- Nakagawa, T., Ishibashi, J., Maruyama, A., Yamanaka, T., Morimoto, Y., Kimura, H., et al. (2004). Analysis of dissimilatory sulfite reductase and 16S rRNA gene fragments from deep-sea hydrothermal sites of the Suiyo Seamount, Izu-Bonin arc, western Pacific. *Appl. Environ. Microbiol.* 70, 393–403.

## ACKNOWLEDGMENTS

We would like to thank the crew of the R/V *Natsushima* and the operation team of the ROV *Hyper-Dolphin* for their cooperation in sample collection. We would like to thank H. Oba and S. Ono for handling the samples on board. We would like to thank the two reviewers for their helpful comments. We are also grateful to the scientists that joined the NT05-16 cruise and members of the Archaean Park Project for providing valuable samples and for helpful discussion. This research was funded by the Ministry of Education, Culture, Science, and Technology (MEXT), Japan, through a special coordination fund (Archaean Park Project: International Research Project on Interaction between Sub-Vent Biosphere and Geo-Environments) and partially a special coordination fund (Project TAIGA: Trans-crustal Advection and *In situ* biogeochemical processes of Global sub-seafloor Aquifer) and the RIKEN Special Postdoctoral Researchers Program.

## SUPPLEMENTARY MATERIAL

The Supplementary Material for this article can be found online at [http://www.frontiersin.org/Extreme\\_Microbiology/10.3389/fmicb.2013.00085/abstract](http://www.frontiersin.org/Extreme_Microbiology/10.3389/fmicb.2013.00085/abstract)

- Nitahara, S., Kato, S., Urabe, T., Usui, A., and Yamagishi, A. (2011). Molecular characterization of the microbial community in hydrogenetic ferromanganese crusts of the Takuyodoigo Seamount, northwest Pacific. *FEMS Microbiol. Lett.* 321, 121–129.
- Orcutt, B. N., Bach, W., Becker, K., Fisher, A. T., Hentscher, M., Toner, B. M., et al. (2011a). Colonization of subsurface microbial observatories deployed in young ocean crust. *ISME J.* 5, 692–703.
- Orcutt, B. N., Sylvan, J. B., Knab, N. J., and Edwards, K. J. (2011b). Microbial ecology of the dark ocean above, at, and below the seafloor. *Microbiol. Mol. Biol. Rev.* 75, 361–422.
- Schloss, P. D., Westcott, S. L., Ryabin, T., Hall, J. R., Hartmann, M., Hollister, E. B., et al. (2009). Introducing mothur: open-source, platform-independent, community-supported software for describing and comparing microbial communities. *Appl. Environ. Microbiol.* 75, 7537–7541.
- Schrenk, M. O., Huber, J. A., and Edwards, K. J. (2009). Microbial provinces in the subseafloor. *Ann. Rev. Mar. Sci.* 2, 279–304.
- Sunamura, M., Higashi, Y., Miyako, C., Ishibashi, J., and Maruyama, A. (2004). Two bacteria phylotypes are predominant in the Suiyo Seamount hydrothermal plume. *Appl. Environ. Microbiol.* 70, 1190–1198.
- Takai, K., Miyazaki, M., Hirayama, H., Nakagawa, S., Querellou, J., and Godfroy, A. (2009). Isolation and physiological characterization of two novel, piezophilic, thermophilic chemolithoautotrophs from a deep-sea hydrothermal vent chimney. *Environ. Microbiol.* 11, 1983–1997.
- Toki, T., Tsunogai, U., Ishibashi, J., Utsumi, M., and Gamo, T. (2008). Methane enrichment in low-temperature hydrothermal fluids from the Suiyo Seamount in the Izu-Bonin arc of the western Pacific Ocean. *J. Geophys. Res.* 113, B08S13.
- Urabe, T., Ishibashi, J., Marumo, K., and Seama, N. (2002). Influence of magmatic volatiles to hydrothermal activity at Suiyo Seamount, Izu-Ogasawara arc, western Pacific. *Eos Trans. American Geophysical Union* 83, Fall Meeting, Abstract V11C-03, San Francisco.
- Walsh, D. A., Zaikova, E., Howes, C. G., Song, Y. C., Wright, J. J., Tringe, S. G., et al. (2009). Metagenome of a versatile chemolithoautotroph from expanding oceanic dead zones. *Science* 326, 578–582.
- Conflict of Interest Statement:** The authors declare that the research was conducted in the absence of any commercial or financial relationships that could be construed as a potential conflict of interest.
- Received: 12 January 2013; accepted: 27 March 2013; published online: 17 April 2013.*
- Citation: Kato S, Nakawake M, Kita J, Yamanaka T, Utsumi M, Okamura K, Ishibashi J, Ohkuma M and Yamagishi A (2013) Characteristics of microbial communities in crustal fluids in a deep-sea hydrothermal field of the Suiyo Seamount. *Front. Microbiol.* 4:85. doi: 10.3389/fmicb.2013.00085*
- This article was submitted to Frontiers in Extreme Microbiology, a specialty of Frontiers in Microbiology.*
- Copyright © 2013 Kato, Nakawake, Kita, Yamanaka, Utsumi, Okamura, Ishibashi, Ohkuma and Yamagishi. This is an open-access article distributed under the terms of the Creative Commons Attribution License, which permits use, distribution and reproduction in other forums, provided the original authors and source are credited and subject to any copyright notices concerning any third-party graphics etc.*



# Microbiological characterization of post-eruption “snowblower” vents at Axial Seamount, Juan de Fuca Ridge

Julie L. Meyer<sup>1</sup>, Nancy H. Akerman<sup>1†</sup>, Giora Proskurowski<sup>2</sup> and Julie A. Huber<sup>1\*</sup>

<sup>1</sup> Josephine Bay Paul Center, Marine Biological Laboratory, Woods Hole, MA, USA

<sup>2</sup> School of Oceanography, University of Washington, Seattle, WA, USA

**Edited by:**

Anna-Louise Reysenbach, Portland State University, USA

**Reviewed by:**

Casey R. J. Hubert, Newcastle University, UK

Victoria J. Bertics, Harvard University, USA

**\*Correspondence:**

Julie A. Huber, Josephine Bay Paul Center, Marine Biological Laboratory, 7 MBL St., Woods Hole, MA 02543, USA

e-mail: jhuber@mbl.edu

**†Present address:**

Nancy H. Akerman, U.S. Environmental Protection Agency, Washington, DC, USA

Microbial processes within the subseafloor can be examined during the ephemeral and uncommonly observed phenomena known as snowblower venting. Snowblowers are characterized by the large quantity of white floc that is expelled from the seafloor following mid-ocean ridge eruptions. During these eruptions, rapidly cooling lava entrains seawater and hydrothermal fluids enriched in geochemical reactants, creating a natural bioreactor that supports a subseafloor microbial “bloom.” Previous studies hypothesized that the eruption-associated floc was made by sulfide-oxidizing bacteria; however, the microbes involved were never identified. Here we present the first molecular analysis combined with microscopy of microbial communities in snowblower vents from samples collected shortly after the 2011 eruption at Axial Seamount, an active volcano on the Juan de Fuca Ridge. We obtained fluid samples and white flocculent material from active snowblower vents as well as orange flocculent material found on top of newly formed lava flows. Both flocculent types revealed diverse cell types and particulates when examined by phase contrast and scanning electron microscopy (SEM). Distinct archaeal and bacterial communities were detected in each sample type through Illumina tag sequencing of 16S rRNA genes and through sequencing of the sulfide oxidation gene, *soxB*. In fluids and white floc, the dominant bacteria were sulfur-oxidizing *Epsilonproteobacteria* and the dominant archaea were thermophilic *Methanococcales*. In contrast, the dominant organisms in the orange floc were *Gammaproteobacteria* and *Thaumarchaeota* Marine Group I. In all samples, bacteria greatly outnumbered archaea. The presence of anaerobic methanogens and microaerobic *Epsilonproteobacteria* in snowblower communities provides evidence that these blooms are seeded by subseafloor microbes, rather than from microbes in bottom seawater. These eruptive events thus provide a unique opportunity to observe subseafloor microbial communities.

**Keywords:** hydrothermal vents, *Epsilonproteobacteria*, snowblowers, eruption, subseafloor

## INTRODUCTION

Most of the volcanic activity on Earth occurs on the seafloor and eruptions at mid-ocean ridges may have profound impacts on global biogeochemical cycles (Baker et al., 2012). During submarine eruptive events, intense changes in the circulation of subseafloor fluids flush both fluids and microbes from within the crust out into the water column, including extremely high concentrations of dissolved gases such as CO<sub>2</sub> and H<sub>2</sub>S that fuel chemolithoautotrophic communities (Delaney, 1998). One remarkable consequence of these changes is the ephemeral phenomenon known as a snowblower vent, first observed at 9°N on the East Pacific Rise in 1991 (Haymon et al., 1993). Haymon et al. found widespread diffuse flow following an eruption, including new venting sites that they termed “snowblower vents” because of the abundant white flocculent material emanating from the seafloor. While the microbial populations creating this bloom were not identified, it was postulated that the white floc

was created by sulfide-oxidizing bacteria taking advantage of an increase in available hydrogen sulfide. The white floc producers were thought to be members of the *Epsilonproteobacterial* genus *Arcobacter* since an isolate of this genus from salt marshes was shown to create similar white flocculent material composed of excreted elemental sulfur in a lab-based bioreactor (Taylor and Wirsén, 1997; Wirsén et al., 2002). Rapid production of white floc was later also observed using *in situ* colonization experiments and in shipboard bioreactors inoculated with filamentous white mat collected at non-eruptive diffuse flow vents at 9°N (Taylor et al., 1999). The white floc producers in both the colonization traps and the shipboard bioreactors were later identified as two different *Arcobacter* groups (Sievert et al., 2008a). Despite the evidence that *Arcobacter* from multiple habitats can produce white floc, there has been no direct evidence that *Arcobacter* are present or produce the white floc in snowblower vents.

In addition to active snowblower vents, orange flocculent material was observed coating the seafloor surrounding diffuse flow sites following multiple seafloor eruptions. Orange floc collected following the 1993 eruption at the CoAxial Segment of the Juan de Fuca Ridge consisted of diverse aggregates of cells that were coated with iron and silica, many of which did not stain with DAPI (Juniper et al., 1995). Carbon fixation through RuBisCo activity and the oxidation of hydrogen sulfide were detected in this orange floc, indicating an active microbial community. In addition, thermophiles and hyperthermophiles were detected by enrichment culture from low-temperature diffuse fluids sampled for several years following the 1993 CoAxial eruption (Holden et al., 1998). Some of these enrichment cultures were capable of producing white flocculent material similar in appearance to the floc emanating from snowblower vents (Holden et al., 1998). The production of floc in cultures from both filamentous white mats and diffuse fluids collected between eruptions suggests that the floc producers responsible for snowblowers are long-term residents of vent habitats that bloom during the surge of geochemical fuels concurrent with eruptions. Taken together, these early examinations of eruptive materials suggest that the flocculent material characterizing snowblower vents is generated by a bloom of sulfide-oxidizing bacteria producing elemental sulfur that may become coated with iron and silica as the bloom ages.

Axial Seamount is an active submarine volcano along the Juan de Fuca Ridge that has been closely monitored for more than a decade and is now part of the networked seafloor observatory being installed as part of the Regional Scale Nodes component of the NSF's Ocean Observatories Initiative. Axial Seamount erupted in 1998 and several post-eruption time series studies were performed to monitor changes in the chemistry and microbiological communities in diffuse fluids from the Marker 33 vent (Huber et al., 2003, 2002; Butterfield et al., 2004). Although snowblower vents were observed following the 1998 eruption, the microbial populations were not sampled from these short-lived diffuse flow sites (Butterfield et al., 2004; Chadwick et al., 2013). Fluids from Marker 33 were very gas-rich in the first year after the 1998 eruption and contained high levels of H<sub>2</sub>S and CO<sub>2</sub>, making sulfide oxidation the dominant source of chemical energy for microbial metabolisms (Butterfield et al., 2004). While the energy available from methanogenesis was much lower than that from sulfide oxidation (Butterfield et al., 2004), both putatively mesophilic and hyperthermophilic methanogens were detected in the three years following the eruption (Huber et al., 2002). Temporal changes in the archaeal communities at Marker 33 corresponded with the changing chemistry of the fluids, including an increase in thermophilic *Methanococcus* and a decrease in the *Thaumarchaeota* Marine Group I common in bottom seawater as fluid temperatures increased (Huber et al., 2002). In a separate study of the bacterial community response following the eruption, lower diffuse fluid temperatures and the corresponding increase in oxygen availability favored *Epsilonproteobacteria*, with an increase in the diversity of *Epsilonproteobacteria* over time (Huber et al., 2003).

Axial Seamount erupted again in April 2011 (Caress et al., 2012; Chadwick et al., 2012; Dziak et al., 2012). Fortunately scheduled research cruises in July and August of 2011 allowed

the sampling of both white and orange flocculent types as well as diffuse fluids from active snowblower vents. Here we present the first direct molecular characterization of microbial communities associated with short-lived snowblower vents to examine the major microbial players in orange and white flocs as well as snowblower diffuse fluids. We address how these ephemeral communities relate to more stable diffuse flow vents and the potential sources of the taxa associated with snowblowers.

## MATERIALS AND METHODS

### SITE DESCRIPTION AND SAMPLE COLLECTION

The April 2011 eruption at Axial Seamount was discovered during a regularly scheduled research expedition in July when seafloor monitoring sites were found buried (Chadwick et al., 2012). Diffuse fluids were collected from newly discovered snowblower vents at Axial Seamount in late July 2011 with the ROV *Jason II* using the hydrothermal fluid and particle sampler (Butterfield et al., 2004). Cells were filtered on the seafloor onto a 0.22 µm Sterivex-GP filter, fixed at 4°C for 24 h with RNA Later immediately upon recovery, then frozen at -80°C until DNA extraction. Whole fluids were fixed with 3.7% formaldehyde for cell counts as previously described (Huber et al., 2002). Basic chemistry for the Snow Globe and Boca snowblower vent fluids was provided by D. Butterfield (personal communication). White and orange flocculent materials were collected on the subsequent University of Washington Visions'11 cruise, in support of the Regional Scale Nodes component of the Ocean Observatories Initiative in August 2011. White flocculent material was collected from the orifice of the Subway snowblower vent (**Figure 1**) on dives R1467 (White Floc 1) and R1472 (White Floc 2) and orange flocculent material was collected on the seafloor distal to Marker 33 during dive R1472 where it coated freshly deposited basalt (**Video S1**). All of the fluid and floc samples analyzed in this study are from a small area in the south rift zone at the southeastern edge of Axial Caldera, with the exception of background seawater which was collected outside of the caldera (**Table 1**).

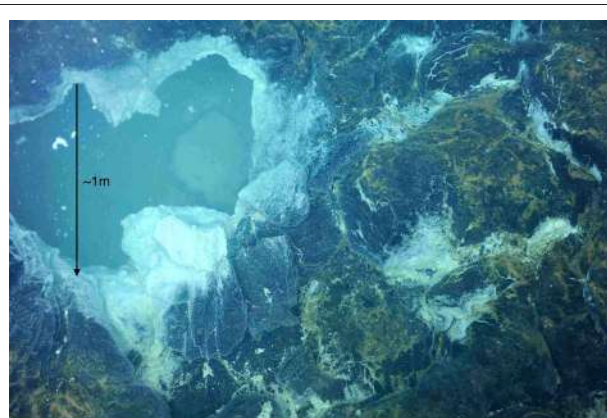


**FIGURE 1 | Seafloor photograph of the "Subway" snowblower vent, Axial Seamount, Juan de Fuca Ridge, showing white flocculent "snow" inside the venting orifice and orange floc coating the surrounding seafloor.** White floc samples 1 and 2 were collected here, while orange floc was collected further away from the venting site.

**Table 1 | Sampling site descriptions.**

| Sample        | Vent       | Latitude/Longitude | Depth (m) | Tmax (°C) | Tavg (°C) | pH  | Cells g <sup>-1</sup> of wet floc* or cells ml <sup>-1</sup> of fluid** ( $\pm$ 95% confidence level) |
|---------------|------------|--------------------|-----------|-----------|-----------|-----|---|
| <b>SOLIDS</b> |            |                    |           |           |           |     |   |
| White Floc 1  | Subway     | 45.942/-129.985    | 1517      | ND        | ND        | ND  | $8.6 \times 10^8 (\pm 2.7 \times 10^7)^*$   |
| White Floc 2  | Subway     | 45.942/-129.985    | 1516      | ND        | ND        | ND  | $9.8 \times 10^8 (\pm 2.0 \times 10^7)^*$   |
| Orange Floc   | Marker 33  | 45.933/-129.982    | 1515      | ND        | ND        | ND  | $3.4 \times 10^7 (\pm 1.2 \times 10^6)^*$   |
| <b>FLUIDS</b> |            |                    |           |           |           |     |   |
| FS825         | Snow globe | 45.946/-129.985    | 1524      | 12        | 11.4      | 5.5 | $3.0 \times 10^5 (\pm 1.5 \times 10^4)^{**}$  |
| FS834         | Boca       | 45.928/-129.985    | 1519      | 17.1      | 16.8      | 5.4 | $3.3 \times 10^5 (\pm 1.1 \times 10^4)^{**}$  |
| Seawater      | —          | 45.947/-129.984    | 1526      | 2.5       | 2.4       | 7.8 | $2.8 \times 10^4 (\pm 9.6 \times 10^2)^{**}$  |

ND, not determined.

## MICROSCOPY

Subsamples of flocculent material were viewed under phase contrast, fixed and stained with DAPI for cell counting via epifluorescent microscopy, or fixed for scanning electron microscopy (SEM) with elemental detection system (EDS) on a Zeiss Supra 40VP. White and orange flocs were fixed with 2.5% glutaldehyde for both cell counts and SEM. Samples were prepared for SEM by dehydration in a series of chilled alcohol washes (50, 70, 85, 95, 100%), dried with a critical point dryer, mounted, and sputter-coated with platinum. Preserved whole fluids were also stained with DAPI for cell counts.

## BULK CARBON, NITROGEN, AND SULFUR MEASUREMENTS

Bulk carbon and nitrogen were measured using a Thermo Scientific CN Analyzer (Model Flash 2000) from subsamples of flocculent material dried at 50–60°C for 2 days. A standard curve for bulk carbon and nitrogen was made using aspartic acid as a standard and acetanilide and apple leaf as standard curve checks. Bulk sulfur was measured using a LECO S632 Sulfur Analyzer from subsamples of flocculent material dried in a dessicator for 4 days and supplemented with sterile sea sand (Fisher) to meet minimum volume requirements. A standard curve for bulk sulfur was made using coal with known sulfur content provided by LECO. Two subsamples were analyzed for each floc sample and replicate readings were averaged for all bulk C, N, and S measurements.

## DNA EXTRACTION AND ILLUMINA TAG SEQUENCING

Total genomic DNA was extracted from Sterivex filters as previously described (Sogin et al., 2006) with the minor modifications described by Akerman et al. (in review). Total genomic DNA was extracted from 20 to 30 mg of wet flocculent material using a MoBio UltraClean® Soil DNA Isolation Kit. The V6 region of 16S rRNA genes were amplified in triplicate for each sample with previously reported primers designed for archaea and bacteria (Huber et al., 2007) that were modified to include indices and barcodes compatible with the Illumina HiSeq1000 platform rather than 454 Life Sciences Adapters (Eren et al., 2013). Triplicate PCR amplifications were pooled for each sample, cleaned with a Qiagen MinElute kit, and quantified by PicoGreen assay on a Turner Biosystems spectrophotometer. Fifty nanograms of each cleaned amplicon library was then size selected with a 2% agarose PippinPrep cassette to produce a narrow range of fragment

sizes from 200 to 300 bp for sequencing and cleaned again to remove agarose. All of the amplicon libraries included in this study were sequenced in the same run and on the same paired-end lane, along with 60 other libraries. Equimolar amounts of pooled amplicon libraries and a metagenomic library were run in the same lane to avoid known difficulties of sequencing low-complexity amplicon libraries with Illumina (Caporaso et al., 2012).

## SEQUENCE ANALYSIS

Paired Illumina sequencing reads were quality filtered to remove any reads containing ambiguous nucleotides and only pairs with perfectly overlapping reads were used for further analysis. Quality-filtered reads are publicly available through the VAMPS database, <http://vamps.mbl.edu> under the project name JAH\_AXV\_Bv6 and JAH\_AXV\_Av6, where orange floc is listed as “eruption mat,” white floc 1 is listed as “snow\_R1467,” and white floc 2 is listed as “snow\_R1472.” Sequences were clustered at 97% similarity with a minimum word length of 30, using usearch (Edgar, 2010). Taxonomy was assigned by global alignment for sequence taxonomy (GAST; Huse et al., 2008) with the SILVA 111 database (Quast et al., 2012). Operational taxonomic units (OTUs) were then analyzed with Qiime 1.5 (Caporaso et al., 2010). Even sequencing depth per sample was established by multiple rarefactions to roughly 75% of the smallest sequencing depth, using a total of 195,000 bacterial reads and 145,000 archaeal reads per sample. To compare bacterial communities in snowblower fluids and flocculent samples to background seawater by dendrogram, we retrieved bacterial V6 454 reads from background seawater collected outside the Axial Caldera from the VAMPS database under the project name KCK\_SMT\_Bv6, fluid sample FS501. To compensate for the fewer number of reads in the background seawater sample, a second set of multiple rarefactions was performed with 7112 reads per sample. Distance matrices were calculated for 10 rarefactions using the Morisita-Horn index (Horn, 1966) and the resulting tree topographies were clustered using UPGMA to create a final jackknifed tree.

## SULFUR OXIDATION GENES

The oxidation of reduced sulfur compounds, including hydrogen sulfide, thiosulfate, elemental sulfur, and sulfite, can be

achieved through the Sox pathway, which is present in several genera of *Epsilonproteobacteria* in hydrothermal vent systems (Yamamoto and Takai, 2011). As the sulfur-oxidizing genera *Sulfurovum* and *Sulfurimonas* are often abundant in 16S rRNA gene libraries from Axial Seamount (Huber et al., 2007), we targeted the amplification of the *soxB* gene in *Epsilonproteobacteria* to assess the diversity of sulfur oxidizers in white floc vs. orange floc samples. The *soxB* gene was amplified in one white flocculent sample (White Floc 2) and in the orange flocculent sample, using the newly designed primers and conditions described by Akerman et al. (in review). The PCR reaction mixture consisted of 1X buffer (Promega), 4 mM MgCl<sub>2</sub>, 0.2 mM of each deoxynucleoside triphosphate (dNTP), 0.6 μM of each primer, 1 U GoTaq polymerase (Promega), 1 μl DNA template, and DEPC H<sub>2</sub>O to 25 μl. Thermocycling conditions on an Eppendorf thermal cycler consisted of an initial denaturation step at 94°C for 3 min, followed by 35 cycles of 94°C for 30 s, 46°C for 45 s, and 72°C for 1 min, followed by a final extension at 72°C for 5 min. The primers used in this study were sox527F (5'-TGGTWGGWCAYGGAAATTAA-3') and sox1198R (5'-AGAANGTATCTKYTTATAAAG-3'). These primers target the genera *Sulfurovum*, *Sulfurimonas*, and *Nitratiruptor*. The *soxB* gene in members of the *Epsilonproteobacterial* genera *Arcobacter* and *Nitratiruptor* are more like sequences in *Gammaproteobacteria* and are not expected to amplify with this primer set. Successfully amplified *soxB* PCR products were cleaned with a Qiagen MinElute PCR purification kit and run on a 0.8% agarose gel. Bands in the expected size range were gel excised, purified with the MinElute kit, cloned, and sequenced as previously described (Huber et al., 2009). Nucleotide sequences were translated into amino acids using EMBOSS Transeq (Rice et al., 2000) and phylogenetic relationships were analyzed using MEGA5 (Tamura et al., 2011). Sequences are deposited in GenBank under Accession numbers KC793341-KC793425.

#### QUANTITATIVE PCR (qPCR)

The relative abundances of bacteria and archaea were determined by qPCR TaqMan assays as previously described (Huber et al., 2010). Briefly, standards were constructed from linearized plasmids of Axial diffuse vent clone libraries. Each 20 μl reaction contained TaqMan Gene Expression Master Mix (Applied Biosystems), forward and reverse primers of 9 μM (bacteria) or 8 μM (archaea), probe concentrations of 1.5 μM (bacteria) or 2 μM (archaea), DEPC-treated water, and 2 μl of DNA template. Triplicate reactions were performed on a StepOne Plus Real Time PCR System (Applied Biosystems) for each sample and for no template controls. Standard curves had  $R^2$  values > 0.997 and efficiencies ranging from 89 to 96%.

## RESULTS

### MICROSCOPY

Freshly prepared slurries of white flocculent material contained very fine particulates, giving an overall milky appearance. Examination of this white floc under phase contrast revealed copious amounts of small bright spheres around 1 μm in diameter and rods up to 20 μm in length, presumably made up of

or coated with elemental sulfur, as well as single rods or large clumps of cells and debris (**Figure 2A**). None of the bright spheres or rods could be stained with DAPI (**Figure 2B**) and were not identified by SEM (**Figures 2C,D**), likely because the elemental sulfur was removed during the dehydration alcohol washes. Only small quantities of sulfur were detected by EDS. Large clumps of filamentous cells as well as debris from eukaryotic cells were visible by SEM (**Figures 2C,D**). Sheet-like structures and other eukaryotic debris were mostly made up of silica and oxygen, with traces of iron, calcium, magnesium, and aluminum. Nitrogen and potassium were detected only in the large clumps of filamentous cells.

Fresh slurries of the orange floc contained much larger particulates that were visible to the naked eye and readily settled out of solution. Examination of orange floc under phase contrast showed that this floc is composed mostly of the same kind of eukaryotic debris in the white floc as well as likely iron oxides, but generally lacking in the bright spheres and rods seen in the white floc (**Figures 2E–H**). Aggregates of debris contained microbial cells that stained with DAPI (**Figures 2E,F**). Sheath-like structures were visible by both phase contrast and SEM in the orange floc (**Figures 2G,H**) but not in white floc.

Cell counts revealed higher numbers of cells in the white floc than in orange floc and higher numbers of cells in the vent fluids compared to background seawater (**Table 1**).

### CHARACTERIZATION OF FLOC AND FLUIDS

Bulk carbon, nitrogen, and sulfur values were obtained for both white and orange flocculent materials (**Table 2**). Total organic carbon ranged from 0.73 to 1.82% and nitrogen ranged from 0.16 to 0.45% of dry weight. Total sulfur ranged from 0.79 to 37.9% of dry weight. Both white floc samples contained much higher proportions of sulfur than the orange floc. Fluid chemistry from both Snow Globe and Boca vents had elevated temperatures and lower pH compared to background seawater (**Table 1**). In addition, dissolved silica in the snowblower fluids was three times higher than in background seawater and hydrogen sulfide concentrations were greater than 100 μM (D. Butterfield, personal communication).

### COMMUNITY COMPOSITION

Genomic DNA was successfully extracted and amplified from all samples. Over three million perfectly overlapping reads were obtained for bacterial and archaeal amplicon libraries (**Table 3**). At the 3% clustering level, a total of 8228 OTUs were obtained for bacteria and a total of 2352 OTUs were obtained for archaea. The smaller subset of reads used for the dendrogram with background seawater had a total of 1508 OTUs at the 3% clustering level. The microbial communities clearly clustered by sample type (**Figure 3**). Using the full set of bacterial and archaeal reads yielded the same topography within the snowblower fluid and flocculent samples (data not shown). White floc and snowblower fluid samples were dominated by *Epsilonproteobacteria*, while orange floc and background seawater were dominated by *Gammaproteobacteria*. All samples were dominated by bacteria, with less than 1% of the community DNA belonging to archaea in the snowblower fluid and floc samples and just under 3% archaea in the background seawater (**Table 3**).

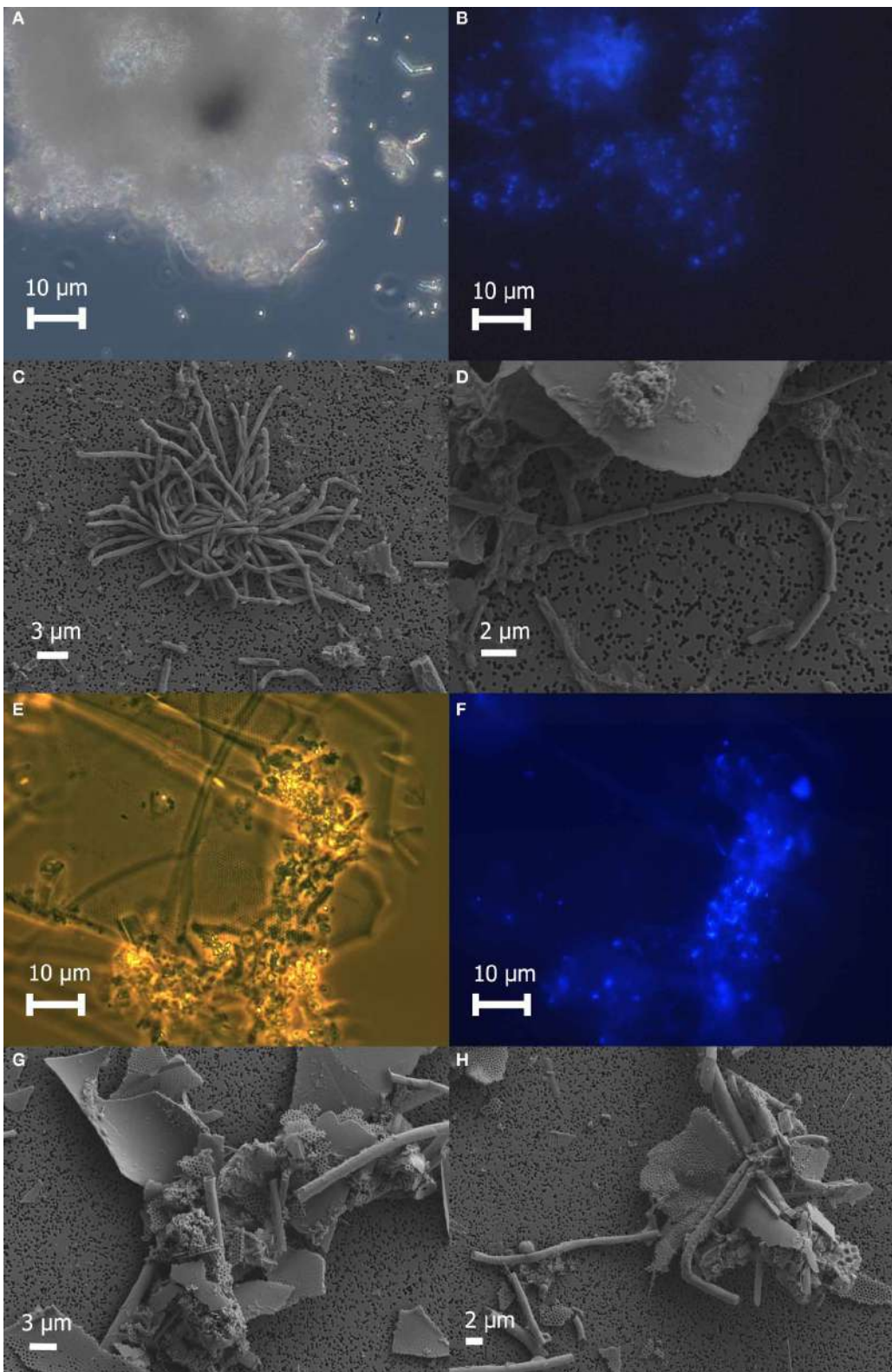


**FIGURE 2 | Microscopic examination of white floc 2 (panels A through D) and orange floc (panels E through H).** Paired phase contrast (A) and epifluorescent (B) images of DAPI-stained cells in white flocculent material from the Subway snowblower vent. SEM images of white floc show

large clumps (C) and filaments (D) of microbial cells. Paired phase contrast (E) and epifluorescent (F) images of DAPI-stained cells in orange flocculent material from the seafloor surrounding Marker 33. SEM images of orange floc showing eukaryotic debris and hollow sheaths (G and H).

### EPSILONPROTEOBACTERIA

The *Epsilonproteobacteria* dominated the bacterial communities from snowblower vents (Figure 4). By far, the two most dominant groups of *Epsilonproteobacteria* were *Sulfurovum* and *Sulfurimonas*, although a total of 20 *Epsilon* genera were detected (Figure 5). In white floc samples, up to 40% of reads were *Sulfurovum* and up to 37% of reads were *Sulfurimonas*. The two snowblower fluid samples were also dominated by *Sulfurovum* and *Sulfurimonas*, but one of the fluid samples had somewhat higher levels of the genera *Arcobacter*, *Campylobacter*, *Nautilia*, and an unclassified genus of *Helicobacteriaceae*. *Sulfurospirillum* was a minor component of all of the samples, but appeared more abundant in white floc than in other samples. In orange floc, far fewer reads were assigned to *Epsilonproteobacteria*, with *Sulfurovum* and *Sulfurimonas* making up 3.5 and 3.7% of the reads, respectively. The only *Epsilonproteobacteria* detected in the background seawater were *Sulfurimonas* and an unclassified genus of the same family (*Helicobacteraceae*), both of which were constituted less than 0.02% of reads.

### GAMMAPROTEOBACTERIA

The *Gammaproteobacteria* dominated the orange floc and were also a major component of the snowblower fluid samples (Figure 4). While 55% of the reads from the orange floc and up to 18% of reads in the fluid samples were assigned to *Gammaproteobacteria*, less than two percent of the white floc samples were *Gammaproteobacteria*. Dominant *Gammaproteobacterial* groups in the orange floc included the uncultured deep-sea sediment BD7-8 Marine Group (10.8% of reads), *Kangiella* (8.7%), an unclassified *Gammaproteobacterial* group (8.6%), *Thiotrichales* (5.3%), and *Methylcoccales* (3.5%) (Figure 6). In contrast, the dominant group of *Gammaproteobacteria* in the fluid samples was the SUP05

cluster of *Oceanospirillales*, which made up 7–11% of the reads from fluid samples. The SUP05 cluster made up less than 1% of reads in the white floc and just 1.2% of the orange floc.

Ninety-seven percent of the reads in background seawater were *Gammaproteobacteria*, most of which were assigned to the genera *Pseudoalteromonas* (76%) and *Pseudomonas* (16%) (Figure 7). *Pseudoalteromonas* was also present in all snowblower floc and fluid samples, making up 2.9% of the reads in fluid sample FS825, 0.1% of reads in FS834 and the orange floc, and 0.3% of reads in each of the white floc samples. *Pseudomonas* was detected in all of the snowblower floc and fluid samples, but constituted less than 0.14% of reads in any single snowblower sample. SUP05 was also detected in the background seawater, making up about 2% of the reads.

### DELAPROTEOBACTERIA AND BETAPROTEOBACTERIA

*Delaproteobacteria* were more prominent in the snowblower fluid samples than in other samples (Figure 4). In fluids, the most dominant genera of *Delaproteobacteria* detected were *Desulfobulbus*, *Desulfobacterium*, and *Desulfocapsa*, all of which belong to the order *Desulfobacterales*. Several groups of *Bdellovibrionales* were also detected, primarily the OM27 clade and *Peredibacter*. In white floc, the most dominant genera were *Delsulfocapsa* and several genera of *Desulfuromonadales*. In contrast, the most dominant groups in the orange floc were *Myxococcales* and the *Bdellovibrionales* OM27 clade. *Myxococcales* made up 1.6% of reads in the orange floc but only 0.2% of reads in all other samples. *Betaproteobacteria* made up only a minor fraction (<1% of reads) of all fluid and floc samples. The most frequently detected *Betaproteobacterial* genus in each snowblower

**Table 2 | Bulk carbon, nitrogen, and sulfur measurements of flocculent material.**

| Sample       | % Carbon | % Nitrogen | % Sulfur |
|--------------|----------|------------|----------|
| White Floc 1 | 1.83     | 0.45       | 37.9     |
| White Floc 2 | 0.71     | 0.16       | 6.66     |
| Orange Floc  | 1.28     | 0.16       | 0.79     |

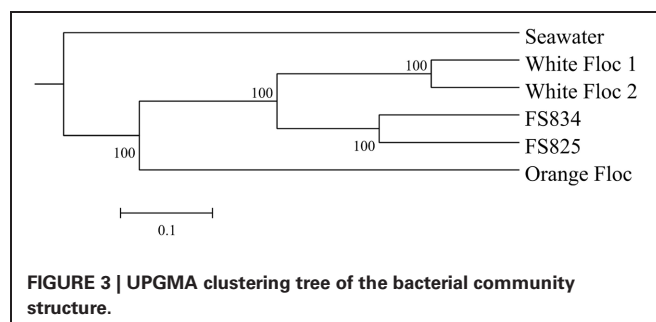
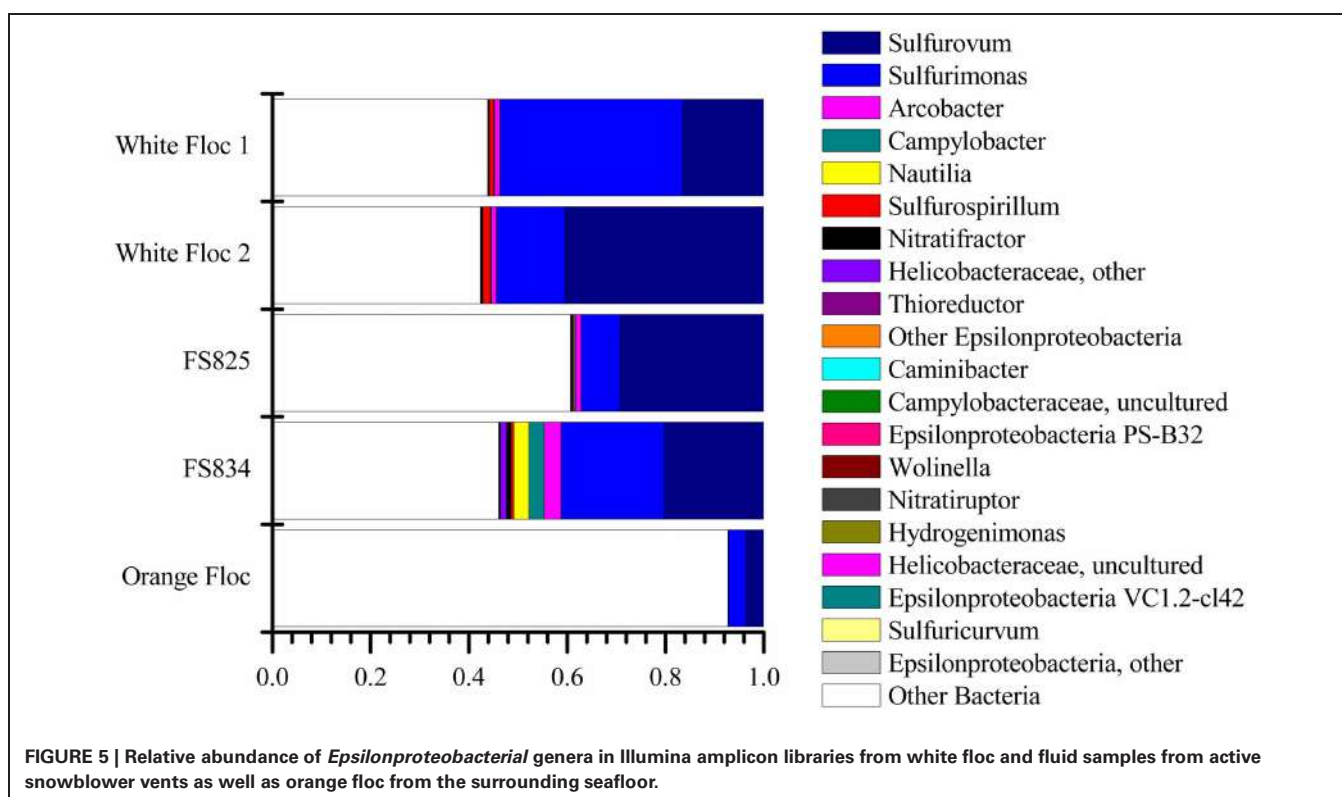
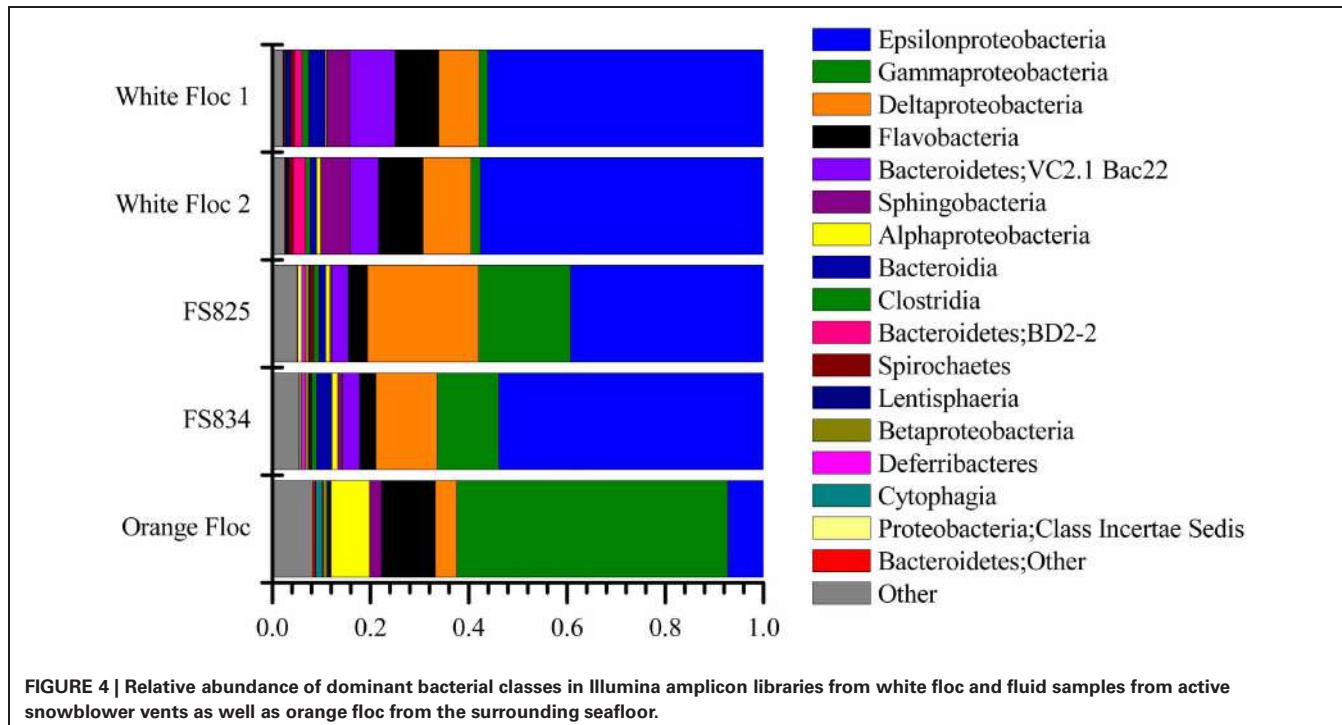


**FIGURE 3 | UPGMA clustering tree of the bacterial community structure.**

**Table 3 | Summary of Illumina sequencing and qPCR results for each sample.**

|              | Bacterial V6 quality-filtered reads | Bacterial V6 unique sequences | Archaeal V6 quality-filtered reads | Archaeal V6 unique sequences | Bacteria (%) <sup>†</sup> | Archaea (%) <sup>†</sup> |
|--------------|-------------------------------------|-------------------------------|------------------------------------|------------------------------|---------------------------|--------------------------|
| White floc 1 | 530,098                             | 20,248                        | 314,342                            | 15,281                       | 99.95                     | 0.05                     |
| White floc 2 | 359,002                             | 17,617                        | 216,716                            | 10,914                       | 99.95                     | 0.05                     |
| FS825        | 295,915                             | 20,242                        | 248,244                            | 10,161                       | 99.89                     | 0.11                     |
| FS834        | 265,443                             | 20,243                        | 252,980                            | 10,382                       | 99.66                     | 0.34                     |
| Orange Floc  | 605,312                             | 41,684                        | 196,620                            | 9,781                        | 99.10                     | 0.90                     |
| Seawater     | —                                   | —                             | —                                  | —                            | 97.15                     | 2.85                     |
| Total        | 2,055,770                           | 120,034                       | 1,228,902                          | 56,519                       |                           |                          |

<sup>†</sup>Based on qPCR as described in Materials and Methods.



fluid or floc sample was *Sideroxydans*, which constituted 0.4% of reads in the orange floc, 0.5% of reads in both snowblower fluid samples, and 0.08–0.1% of reads in the white floc. The genus *Leptothrix* was detected only in the orange floc, where this genus was assigned to 0.05% of reads.

#### BACTEROIDETES

After *Sulfurovum* and *Sulfurimonas*, the third most abundant taxonomic group overall was the uncultured *Bacteroidetes* group defined by the hydrothermal vent clone VC2.1 Bac22 (Reysenbach et al., 2000). This group made up more than 3% of total reads in

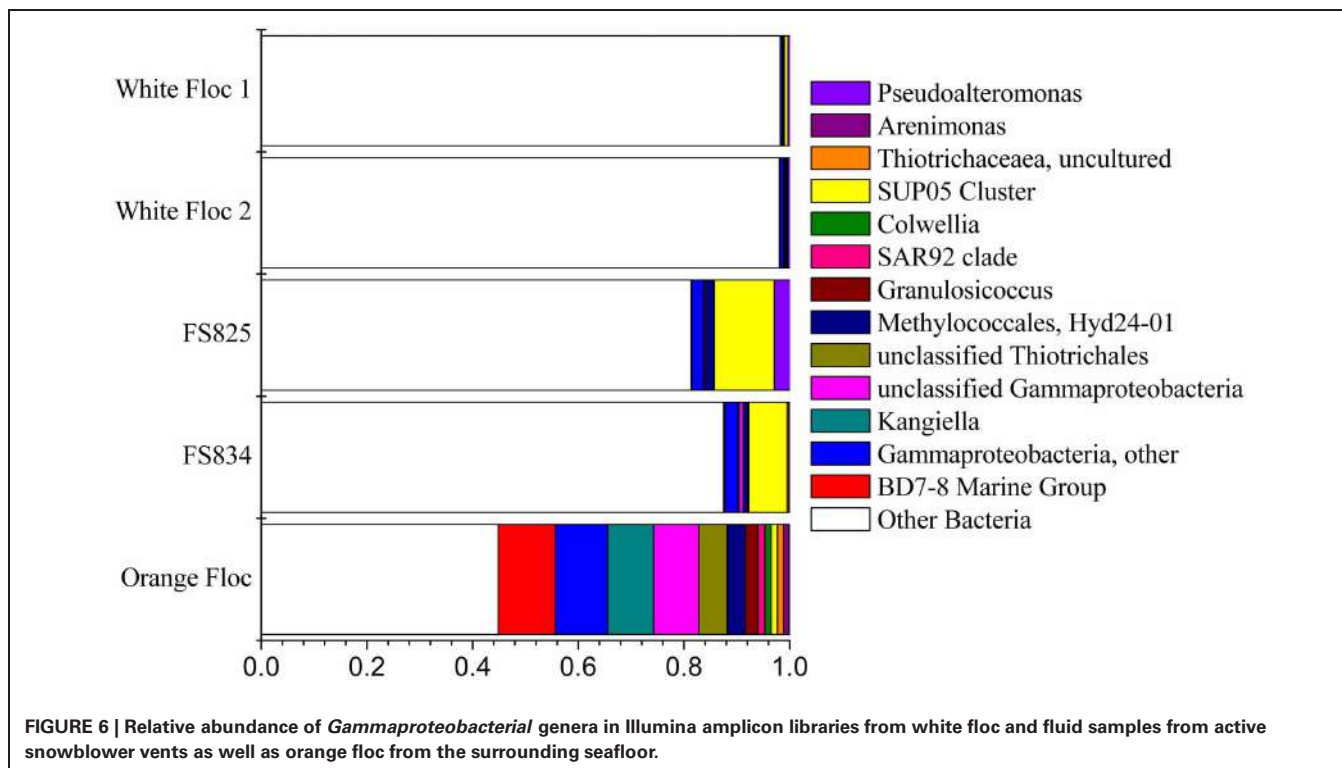


**FIGURE 6 |** Relative abundance of *Gammaproteobacterial* genera in Illumina amplicon libraries from white floc and fluid samples from active snowblower vents as well as orange floc from the surrounding seafloor.

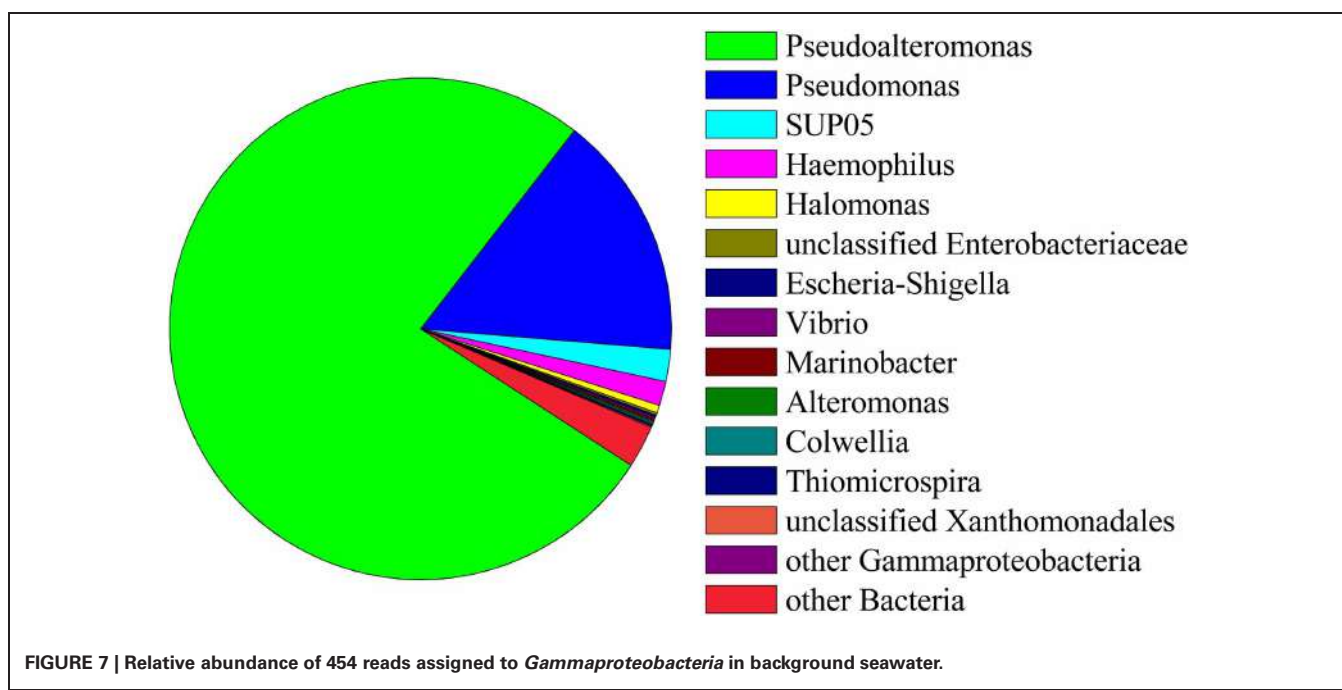


**FIGURE 7 |** Relative abundance of 454 reads assigned to *Gammaproteobacteria* in background seawater.

both fluid samples and in white floc 2 and made up more than 9% of reads in white floc 1. In contrast, less than 0.1% of reads in the orange floc were assigned to *Bacteroidetes* VC2.1 Bac22. Other abundant *Bacteroidetes* groups in fluids and white floc samples included reads that were similar to the *Sphingobacteriales* group WCHB1–69 from a hydrocarbon-contaminated aquifer (Dojka et al., 1998) and an uncultured group of *Marinilabiaceae*. In the

orange floc, two uncultured groups of *Flavobacteriaceae* were the dominant *Bacteroidetes*, making up more than 6% of the total reads for orange floc.

#### ARCHAEA

Although archaea do not make up a large proportion of the microbial communities in these samples, the differences in

composition of the archaeal communities in white floc or fluid samples and the orange floc were striking (**Figure 8**). As in the bacterial community, the archaeal communities in white floc and fluid samples were very similar. The snowblower fluids and white floc were dominated by methanogens, with 42–87% of total archaeal reads assigned to methanogenic groups, while methanogens made up only 4% of archaeal reads in the orange floc. The dominant methanogens in the fluids and white floc were the *Methanococci*, including the genera *Methanococcus*, *Methanothermococcus*, and *Methanocaldococcus*. The *Methanococcales* made up more than 66% of the reads from fluid samples and 39–57% of the reads from white floc. The *Methanosarcinales* GOM Arc I clade within the *Methanomicrobia* made up almost 20% of the reads in fluid sample FS825 from the Snow Globe vent. Other dominant *Euryarchaeota* groups in the fluid samples and white floc include *Archaeoglobi* and the *Thermoplasmata* clades AMOS1A-4113-D04 and Marine Benthic Group D. In contrast, the orange floc was dominated by *Thaumarchaeota* Marine Group I, which made up more than 71% of the archaeal reads. The orange floc also had reads assigned to the *Thermoplasmata*, but these were representatives of the clades Marine Group II and Marine Group III, which each made up more than 5% of the reads.

#### SULFUR OXIDATION THROUGH THE SOX PATHWAY

*Epsilonproteobacterial soxB* genes were successfully amplified, cloned, and sequenced from both white floc 2 and orange floc, yielding 31 sequences from white floc 2 and 40 sequences from orange floc. These sequences clustered with *soxB* from *Sulfurovum*, *Sulfurimonas*, and *Nitratiruptor* (**Figure 9**). A total of four phylotypes were detected at the 90% amino acid similarity level from these 71 clones, none of which were shared between white and orange floc samples. All clones from the white floc (White Floc 2) were most closely related to *soxB* from *Sulfurovum*, the most dominant genus in this sample, which made up 40% of the 16S rRNA gene sequences. The orange floc also had *Sulfurovum*-like *soxB* genes that were 85% similar to the white floc sequences. In addition, the orange floc had *Sulfurimonas*- and *Nitratiruptor*-like *soxB* sequences. The *Sulfurovum* and *Sulfurimonas* *soxB* genes detected here were similar to *soxB* genes from the Irina II hydrothermal vent chimney complex at the Logatchev vent field on the Mid-Atlantic Ridge (Hügler et al., 2010) and to *soxB* in the genomes of *Sulfurovum* sp. NBC37-1 (Nakagawa et al., 2007) and several *Sulfurimonas* isolates (Sievert et al., 2008b; Sikorski et al., 2010; Grote et al., 2011; **Figure 9**).

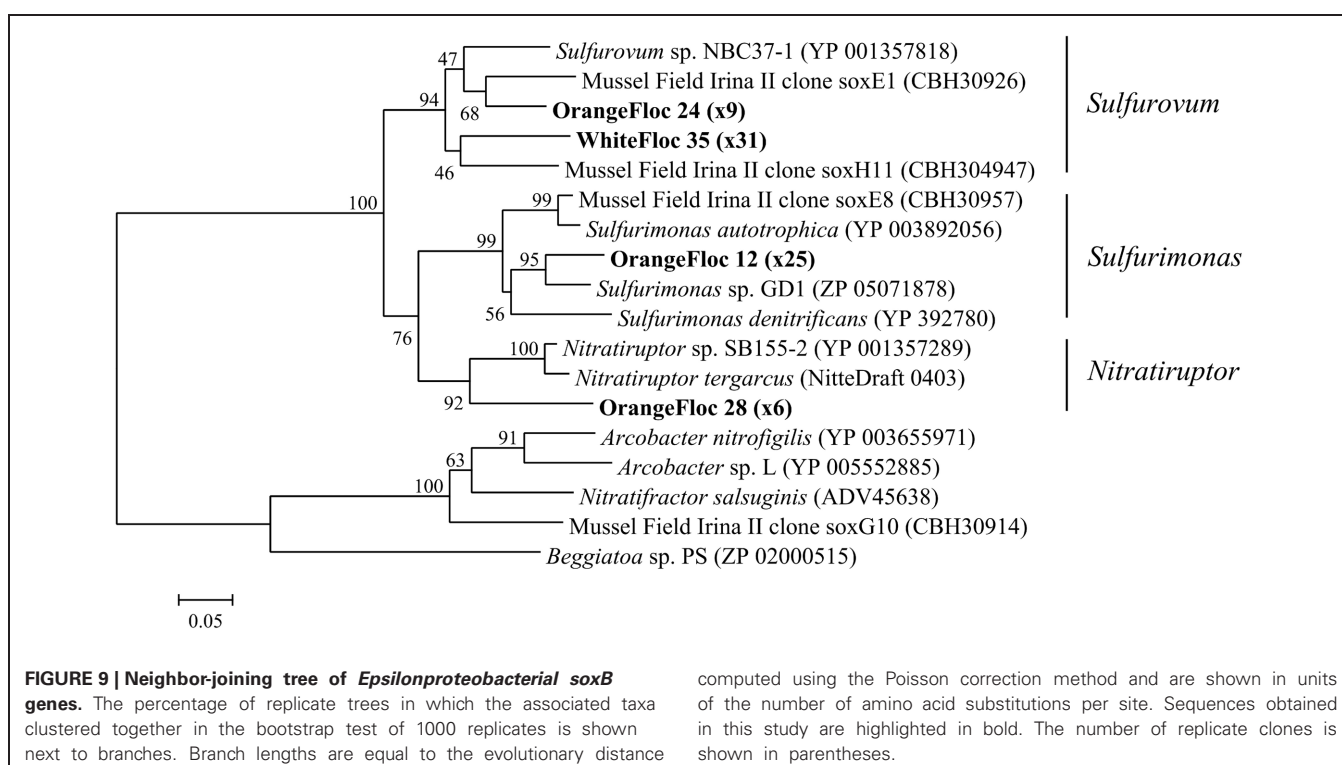
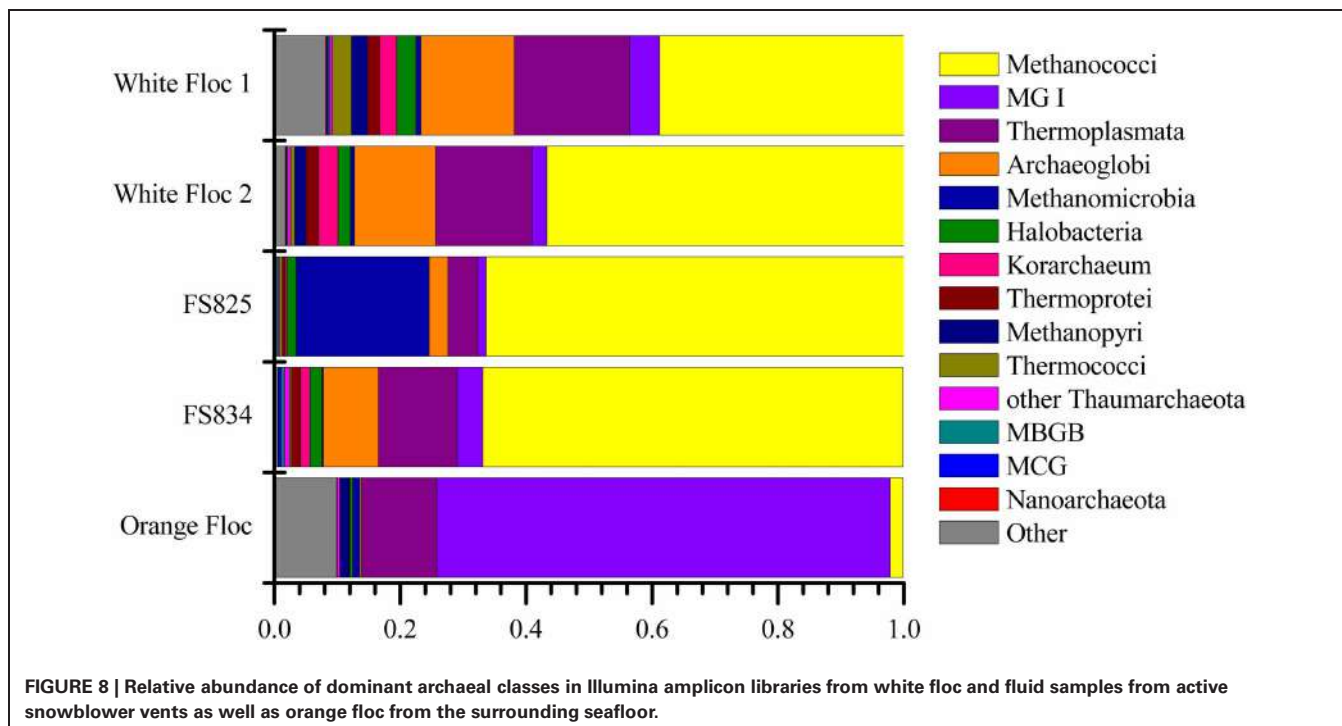
#### DISCUSSION

These results demonstrate that the microbial communities in white floc and fluids from snowblower vents are distinct from those in the orange floc coating fresh basalt following a volcanic eruption. Visual and microscopic evidence suggest the orange floc is made up of larger and heavier particulates than the white floc, especially iron oxides and multi-cellular debris. The orange floc may, in part, be fallout from snowblower vents which becomes colonized by a distinct subset of microbes from the surrounding cold and oxygenated deep seawater, including iron oxidizing

bacteria. Given the observed presence of orange floc on both vertical and overhanging surfaces (Chadwick et al., 2013), it is clear that growth of this eruption mat occurs in place on fresh lava flows. While the most dominant bacterial class in both the orange floc and in background seawater was *Gammaproteobacteria*, the most abundant genera detected in each were different. In the orange floc, no more than 10.8% of reads were assigned to any one genus within the *Gammaproteobacteria*, in contrast to background seawater from outside the Axial Caldera, which was dominated almost entirely by just *Pseudoalteromonas* and *Pseudomonas*. The most dominant bacteria in orange floc was the *Gammaproteobacteria* BD7–8 Marine Group which was first identified from deep sea sediments (Li et al., 1999) and has since also been detected in iron rich mats from both Vailulu'u Seamount near American Samoa (Sudek et al., 2009) and Loihi Seamount, near Hawaii (Fleming et al., 2013). While the iron oxidizer *Sideroxydans* was detected at low levels in all snowblower fluid and floc samples, *Leptothrix* was detected only in the orange mat. Both freshwater and marine strains of the iron oxidizing bacteria *Leptothrix* have demonstrated the ability to form sheaths very similar in appearance by phase contrast and SEM (Fleming et al., 2013) to the sheaths we detected only in the orange mat from Axial Seamount. In addition, the orange floc contained higher numbers of reads assigned to *Myxococcales*, a group which has previously been shown as enriched in the particulate fraction of the deep-sea water column (Eloe et al., 2011). Taken together, these results suggest that the orange mat coating freshly deposited lava flows contains iron oxidizing bacteria and other groups which colonize particulates that fall out of eruption-related hydrothermal plumes.

The orange floc still contained low levels of the *Sulfurovum* and *Sulfurimonas* that dominated the bacterial snowblower community. However, it is likely that these sulfide oxidizers are diminishing in the orange floc as the particulates settle out of the snowblower plume and away from the source of sulfide. Bulk sulfur was much lower in the orange floc than in the white floc, indicating that sulfur is not as readily available as an energy source in the orange floc nor is elemental sulfur being copiously produced by sulfur oxidizing microorganisms. The orange floc contained a higher diversity of *Epsilonproteobacterial soxB* genes and these phylotypes were distinct from white floc phylotypes and from the dominant phylotypes in diffuse fluids collected a year prior to the 2011 eruption at Axial Seamount (Akerman et al., in review). The *soxB* phylotypes in orange floc may therefore represent *Epsilonproteobacteria* that are adapted to cooler, more aerobic habitats than the phylotypes found in the white floc and non-eruptive diffuse fluids.

The white floc appeared to be made up primarily of elemental sulfur and bacterial cells, with far less of the multi-cellular debris. This elemental sulfur is likely the byproduct of sulfide oxidation by the dominant *Epsilonproteobacteria*, *Sulfurovum*, and *Sulfurimonas*, which made up roughly half of all reads in the white floc and fluid samples. Isolates of *Sulfurovum* and *Sulfurimonas* from hydrothermal vent habitats can perform both the oxidation of various sulfur compounds to sulfate using the *sox* system and the oxidation of sulfide to elemental sulfur using sulfide-quinone reductase (*sqr*) (Inagaki et al., 2003; Nakagawa et al.,



2007; Sikorski et al., 2010). These dominant genera likely require a very narrow range of redox conditions between warm, sulfide-rich diffuse flow and cold, oxygenated seawater as vent isolates of *Sulfurovum* and *Sulfurimonas* oxidize sulfide under microaerobic and mesophilic conditions (Inagaki et al., 2003; Nakagawa et al.,

2007). While members of the genus *Arcobacter* may also perform sulfide oxidation with the production of elemental sulfur (Taylor and Wirsén, 1997) and have been detected as dominant members of other diffuse flow vents at Axial (Huber et al., 2007), here they constituted only a small fraction of all samples. *Sulfurovum* and

*Sulfurimonas* have previously been identified as the most abundant and diverse groups in diffuse hydrothermal fluids in the Mid-Atlantic Ridge (Hügler et al., 2010) and in hydrothermal plumes at the East Pacific Rise (Sylvan et al., 2012). It is possible that the *Sulfurovum* and *Sulfurimonas* outcompete *Arcobacter* at snowblower vents during conditions of elevated hydrogen sulfide levels. A recent study of the microbial community in diffuse fluids from the Logatchev hydrothermal field found a significant correlation between sulfide enrichment and the proportions of *Sulfurovum* found (Perner et al., 2013), supporting the idea that *Sulfurovum* flourishes when sulfide levels are high.

It is not clear why only *Sulfurovum* was detected in clone libraries of *Epsilonproteobacterial* *soxB* from white floc. The primer set used in this study was capable of recovering *Sulfurimonas*-like *soxB* from orange floc. It is possible that not all of the *Sulfurimonas* detected in these samples contain the same type of *soxB* that most *Epsilonproteobacteria* have and instead contain a *soxB* more similar to the distantly related *Arcobacter*-like *soxB* that does not amplify with these primers. Alternatively, deeper sequencing of the clone libraries may have revealed some *Sulfurimonas*-like *soxB*.

The snowblower fluid samples contained many of the same dominant taxa as the white floc, however, two groups clearly stood out as elevated in fluids, namely the *Gammaproteobacteria* SUP05 cluster and the *Methanoscincales* GoM Arc 1 clade. Metagenomic and metatranscriptomic analyses have revealed that the uncultured SUP05 group also has the *sqr* gene for sulfide oxidation to elemental sulfur and that it expresses *sqr* as a member of hydrothermal vent plume communities (Anantharaman et al., 2013). SUP05 was also ubiquitous in fluid samples from the Main Endeavour Field on the Juan de Fuca Ridge, including background seawater, hydrothermal plumes, and hydrothermal diffuse flow (Anderson et al., 2012). Of these fluid types, SUP05 was most abundant in plume samples, making up almost a third of the total bacteria (Anderson et al., 2012). The *Methanoscincales* were more abundant only in the Snow Globe fluid, but both fluid samples had higher proportions of total methanogens compared to the flocculent materials. This is likely a reflection that the strictly anaerobic methanogen populations are being flushed out from deeper subsurface layers in diffuse fluids, while the white floc is generated closer to the surface in microaerobic, mesophilic niches just below the seafloor.

Despite the apparent differences in circulation and chemistry between snowblower vents and more stable diffuse flow vents (Butterfield et al., 2004), our results show that the dominant organisms in snowblower fluids and white floc are similar to non-eruptive diffuse flow. Both the bacterial and archaeal communities in the white floc and the fluids were dominated by organisms previously found in diffuse flow at Axial Seamount, including, but not limited to, *Sulfurovum* and *Sulfurimonas* (Huber et al., 2003, 2007) and *Methanococcales* (Huber et al., 2002; Ver Eecke et al., 2012). The presence of mesophilic *Epsilonproteobacteria* and several strictly anaerobic, thermophilic archaeal groups such as *Methanococcus*, *Thermococcus*, and *Archaeoglobus* indicates that snowblower vents are seeded by subseafloor communities. During eruptive events, snowblower microbial communities form through two processes: the flushing of microbes from different

thermal zones in the subsurface and the secondary bloom of microbes near the surface of the seafloor (Delaney, 1998). At Axial snowblower vents, the *Methanococci* and other thermophiles are likely present due to flushing, while the *Sulfurovum* and *Sulfurimonas* are likely residents of shallower subsurface layers and experiencing a secondary bloom just below the seafloor. Modeling of the biogenic production of white floc after the 1991 eruption at 9°N East Pacific Rise suggested that the source of material for snowblower vents may be a combination of microbial bloom and a flushing of accumulated floc within the seafloor (Crowell et al., 2008).

The peak activity of observed snowblower vents lasts from weeks to months, with microbial biomass diminishing as the sulfide levels decrease (Haymon et al., 1993). Snowblowers at Axial Seamount following the 1998 eruption were inactive 18 months post eruption (Butterfield et al., 2004). Though short-lived, snowblower vents provide episodic pulses of energy-rich fluids and chemolithoautotrophic microbial communities to the surface of the seafloor and therefore impact ocean biogeochemistry, especially sulfur and carbon cycling. In particular, snowblower vents may be a significant source of biogenic elemental sulfur through sulfide oxidation by *Epsilonproteobacteria* such as *Sulfurovum*, *Sulfurimonas*, and *Arcobacter*, using either the Sox pathway or the sulfide-quinone reductase (*sqr*) gene. *Gammaproteobacteria*, such as sulfur-oxidizing members of the *Thiotrichales*, may also contribute to biogenic elemental sulfur production. Isolates of the *Gammaproteobacterial* genus *Thiomicrospira* from multiple vent systems in the Atlantic and Pacific are known to oxidize sulfur with the production of elemental sulfur (Wirsén et al., 1998) and the partial genomes of *Beggiatoa* filaments contain both *sox* and *sqr* genes (Mussmann et al., 2007). Members of the order *Thiotrichales* were detected at low levels in all of the fluid and white floc samples and were one of the most dominant groups in the orange floc. Finally, representatives of the *Gammaproteobacteria* clade SUP05 may also perform sulfide oxidation with *sox* and *sqr* genes (Anantharaman et al., 2013) both during eruptive events, as indicated by its presence in snowblower vents, and between eruptive events (Breier et al., 2012).

In summary, our observations of snowblower microbial communities substantiate the model of microbial responses to submarine eruptions described by Delaney (1998) which includes the transportation of subseafloor microbes out into the water column and a microbial population bloom in response to elevated levels of reduced compounds such as sulfide and iron. We saw clear differences between white and orange flocculent materials, with the white floc containing high levels of sulfur and the orange floc containing sheath-like structures similar to those in iron rich microbial mats. While quantitative PCR indicated that bacteria greatly outnumber archaea, the differences in both bacterial and archaeal community composition are informative to distinguish the sample types. We detected both *Epsilon-* and *Gammaproteobacteria* groups that are capable of sulfur oxidation in all microbial communities associated with snowblower vents. In addition, *Beta-* and *Gamma-proteobacteria* groups capable of iron oxidation were detected in the orange floc coating the seafloor around snowblower vents. These sulfur and iron oxidizing groups take advantage of the transient energy sources

provided by deep-sea eruptions and are seeded from both sub-seafloor and bottom seawater communities. Future analyses will include metagenomic and metatranscriptomic work to determine the metabolic potential of the dominant and active members of snowblower communities.

## ACKNOWLEDGMENTS

We thank the NOAA/PMEL Vents Program, John Delaney, Deborah Kelley and the University of Washington Visions'11 Team, ROVs *Jason 2* and *ROPOS*, and Dave Butterfield and Bill Chadwick for sample collection. We thank L. Kerr (Marine Biological Laboratory) for expert guidance on the scanning electron microscope and S. Kelsey, S. Strelbel, and A. Giblin (Marine

Biological Laboratory) for chemical analysis of solid materials. This work was supported by a National Science Foundation Grant OCE-0929167 (to Julie A. Huber), a NASA Astrobiology Postdoctoral Fellowship (to Nancy H. Akerman), and a Center for Dark Energy Biosphere Investigations Postdoctoral Fellowship (to Julie L. Meyer).

## SUPPLEMENTARY MATERIALS

The Supplementary Material for this article can be found online at: [http://www.frontiersin.org/Extreme\\_Microbiology/10.3389/fmicb.2013.00153/abstract](http://www.frontiersin.org/Extreme_Microbiology/10.3389/fmicb.2013.00153/abstract)

**Video S1 | Sample collection of white and orange flocculent materials at Axial Seamount, August 2011.**

## REFERENCES

- Anantharaman, K., Breier, J. A., Sheik, C. S., and Dick, G. J. (2013). Evidence for hydrogen oxidation and metabolic plasticity in widespread deep-sea sulfur-oxidizing bacteria. *Proc. Natl. Acad. Sci. U.S.A.* 110, 330–335. doi: 10.1073/pnas.1215340110
- Anderson, R. E., Beltrán, M. T., Hallam, S. J., and Baross, J. A. (2012). Microbial community structure across fluid gradients in the Juan de Fuca Ridge hydrothermal system. *FEMS Microbiol. Ecol.* 83, 324–339. doi: 10.1111/j.1574-6941.2012.01478.x
- Baker, E. T., Chadwick, W. W., Cowen, J. P., Dziak, R. P., Rubin, K. H., and Fornari, D. J. (2012). Hydrothermal discharge during submarine eruptions: The importance of detection, response, and new technology. *Oceanography* 25, 128–141. doi: 10.5670/oceanog.2012.111
- Breier, J. A., Toner, B. M., Fakra, S. C., Marcus, M. A., White, S. N., Thurnherr, A. M., et al. (2012). Sulfur, sulfides, oxides and organic matter aggregated in submarine hydrothermal plumes at 9°50'N East Pacific Rise. *Geochim. Cosmochim. Acta* 88, 216–236. doi: 10.1016/j.gca.2012.04.003
- Butterfield, D. A., Roe, K. K., Lilley, M. D., Huber, J. A., Baross, J. A., Embley, R. W., et al. (2004). “Mixing, reaction, and microbial activity in the sub-seafloor revealed by temporal and spatial variation in diffuse flow vents at Axial Volcano,” in *The Subseafloor Biosphere at Mid-Ocean Ridges*, eds W. S. D. Wilcock, E. F. DeLong, D. S. Kelley, J. A. Baross, and S. C. Cary (Washington, DC: American Geophysical Union), 269–289. doi: 10.1029/144GM17
- Caporaso, J. G., Kuczynski, J., Stombaugh, J., Bittinger, K., Bushman, F. D., Costello, E. K., et al. (2010). QIIME allows analysis of high-throughput community sequencing data. *Nat. Methods* 7, 335–336. doi: 10.1038/nmeth. f.303
- Caporaso, J. G., Lauber, C. L., Walters, W. A., Berg-Lyons, D., Huntley, J., Fierer, N., et al. (2012). Ultra-high-throughput microbial community analysis on the Illumina HiSeq and MiSeq platforms. *ISME J.* 6, 1621–1624. doi: 10.1038/ismej.2012.8
- Caress, D. W., Clague, D. A., Paduan, J. B., Martin, J., Dreyer, B., Chadwick, W. W., et al. (2012). Repeat bathymetric surveys at 1-metre resolution of lava flows erupted at Axial Seamount in April 2011. *Nat. Geosci.* 5, 483–488. doi: 10.1038/ ngeo1496
- Chadwick, W. W., Clague, D. A., Embley, R. W., Perfitt, M. R., Butterfield, D. A., Caress, D. W., et al. (2013). The 1998 eruption of Axial Seamount: new insights on submarine lava flow emplacement from high-resolution mapping. *Geochem. Geophys. Geosyst.* doi: 10.1029/2013GC004710. (in press).
- Chadwick, W. W., Nooner, S. L., Butterfield, D. A., and Lilley, M. D. (2012). Seafloor deformation and forecasts of the April 2011 eruption at Axial Seamount. *Nat. Geosci.* 5, 449–458. doi: 10.1111/j.1758-2229. 2010.00223.x
- Eren, A. M., Vineis, J. H., Morrison, H. G., and Sogin, M. L. (2013). A filtering method to generate high quality short reads using Illumina paired-end technology. *PLoS ONE*. doi: 10.1371/journal.pone.0066643
- Fleming, E. J., Davis, R. E., McAllister, S. M., Chan, C. S., Moyer, C. L., et al. (2013). Hidden in plain sight: discovery of sheath-forming, iron-oxidizing Zetaproteobacteria at Loihi Seamount, Hawaii, USA. *FEMS Microbiol. Ecol.* 1–12. doi: 10.1111/1574-6941.12104. [Epub ahead of print].
- Grote, J., Schott, T., Bruckner, C. G., Oliver, F., Jost, G., and Teeling, H. (2011). Genome and physiology of a model *Epsilonproteobacterium* responsible for sulfide detoxification in marine oxygen depletion zones. *Proc. Natl. Acad. Sci. U.S.A.* 109, 506–510. doi: 10.1073/pnas.1111262109
- Haymon, R. M., Fornari, D. J., Von Damm, K. L., Lilley, M. D., Perfitt, M. R., Edmond, J. M., et al. (1993). Volcanic eruption of the mid-ocean ridge along the East Pacific Rise crest at 9°45–52'N: direct submersible observations of seafloor phenomena associated with an eruption event in April, 1991. *Earth Planet. Sci. Lett.* 119, 85–101. doi: 10.1016/ 0012-821X(93)90008-W
- Holden, J. F., Summit, M., and Baross, J. A. (1998). Thermophilic and hyperthermophilic microorganisms in 3–30°C hydrothermal fluids following a deep-sea volcanic eruption. *FEMS Microbiol. Ecol.* 25, 33–41.
- Horn, H. S. (1966). Measurement of “Overlap” in comparative ecological studies. *Am. Nat.* 100, 419–424. doi: 10.1086/282436
- Huber, J. A., Butterfield, D. A., and Baross, J. A. (2002). Temporal changes in archaeal diversity and chemistry in a mid-ocean ridge subseafloor habitat. *Appl. Environ. Microbiol.* 68, 1585. doi: 10.1128/AEM.68.4.1585-1594.2002
- Huber, J. A., Butterfield, D. A., and Baross, J. A. (2003). Bacterial diversity in a subseafloor habitat following a deep-sea volcanic eruption. *FEMS Microbiol. Ecol.* 43, 393–409. doi: 10.1111/j.1574-6941. 2003.tb01080.x
- Huber, J. A., Cantin, H. V., Huse, S. M., Welch, D. B. M., Sogin, M. L., and Butterfield, D. A. (2010). Isolated communities of *Epsilonproteobacteria* in hydrothermal vent fluids of the Mariana Arc seamounts. *FEMS Microbiol. Ecol.* 73, 538–549.
- Huber, J. A., Mark Welch, D. B., Morrison, H. G., Huse, S. M., Neal, P. R., Butterfield, D. A.,

- et al. (2007). Microbial population structures in the deep marine biosphere. *Science* 318, 97. doi: 10.1126/science.1146689
- Huber, J. A., Morrison, H. G., Huse, S. M., Neal, P. R., Sogin, M. L., and Mark Welch, D. B. (2009). Effect of PCR amplicon size on assessments of clone library microbial diversity and community structure. *Environ. Microbiol.* 11, 1292–1302. doi: 10.1111/j.1462-2920.2008.01857.x
- Hügler, M., Gärtner, A., and Imhoff, J. F. (2010). Functional genes as markers for sulfur cycling and CO<sub>2</sub> fixation in microbial communities of hydrothermal vents of the Logatchev field. *FEMS Microbiol. Ecol.* 73, 526–537.
- Huse, S. M., Dethlefsen, L., Huber, J. A., Mark Welch, D., Welch, D. M., Relman, D. A., et al. (2008). Exploring microbial diversity and taxonomy using SSU rRNA hyper-variable tag sequencing. *PLoS Genet.* 4:e1000255. doi: 10.1371/journal.pgen.1000255
- Inagaki, F., Takai, K., Kobayashi, H., Nealson, K. H., and Horikoshi, K. (2003). *Sulfurimonas autotrophica* gen. nov., sp. nov., a novel sulfur-oxidizing ε-proteobacterium isolated from hydrothermal sediments in the Mid-Okinawa Trough. *Int. J. Syst. Evol. Microbiol.* 53, 1801–1805. doi: 10.1099/ijst.0.02682-0
- Juniper, S. K., Martineau, P., and Sarrazin, J. (1995). Microbial-mineral flocs associated with nascent hydrothermal activity on CoAxial Segment, Juan de Fuca Ridge. *Geophys. Res. Lett.* 22, 179–182. doi: 10.1029/94GL02436
- Li, L., Kato, C., and Horikoshi, K. (1999). Bacterial diversity in deep-sea sediments from different depths. *Biodivers. Conserv.* 8, 659–677. doi: 10.1023/A:1008848203739
- Mussmann, M., Hu, F. Z., Richter, M., De Beer, D., Preisler, A., Jørgensen, B. B., et al. (2007). Insights into the genome of large sulfur bacteria revealed by analysis of single filaments. *PLoS Biol.* 5:e230. doi: 10.1371/journal.pbio.0050230
- Nakagawa, S., Takaki, Y., Shimamura, S., Reysenbach, A., Takai, K., and Horikoshi, K. (2007). Deep-sea vent ε-proteobacterial genomes provide insights into emergence of pathogens. *Proc. Natl. Acad. Sci. U.S.A.* 104, 12146–12150. doi: 10.1073/pnas.0700687104
- Perner, M., Gonnella, G., Hourdez, S., Böhnke, S., Kurtz, S., and Girguis, P. (2013). *In-situ* chemistry and microbial community compositions in five deep-sea hydrothermal fluid samples from Irina II in the Logatchev field. *Environ. Microbiol.* 15, 1551–1560. doi: 10.1111/1462-2920.12038
- Quast, C., Pruesse, E., Yilmaz, P., Gerken, J., Schweer, T., Yarza, P., Peplies, J., et al. (2012). The SILVA ribosomal RNA gene database project: improved data processing and web-based tools. *Nucleic Acids Res.* 41, D590–D596. doi: 10.1093/nar/gks1219
- Reysenbach, A. L., Longnecker, K., and Kirshtein, J. (2000). Novel bacterial and archaeal lineages from an *in situ* growth chamber deployed at a Mid-Atlantic Ridge hydrothermal vent. *Appl. Environ. Microbiol.* 66, 3798–3806. doi: 10.1128/AEM.66.9.3798-3806.2000
- Rice, P., Longden, I., and Bleasby, A. (2000). EMBOSS: The european molecular biology open software suite. *Trends Genet.* 16, 276–277. doi: 10.1016/S0168-9525(00)02024-2
- Sievert, S. M., Hugler, M., Taylor, C. D., and Wirsén, C. O. (2008a). “Sulfur oxidation at deep-sea hydrothermal vents,” in *Microbial Sulfur Metabolism*, eds. C. Dahl and C. G. Friedrich (Berlin: Springer), 238–258.
- Sievert, S. M., Scott, K. M., Klotz, M. G., Chain, P. S. G., Hauser, L. J., Hemp, J., et al. (2008b). Genome of the epsilonproteobacterial chemolithoautotroph *Sulfurimonas denitrificans*. *Appl. Environ. Microbiol.* 74, 1145–1156.
- Sikorski, J., Munk, C., Lapidus, A., Ngatchou Djao, O. D., Lucas, S., Glavina Del Rio, T., et al. (2010). Complete genome sequence of *Sulfurimonas autotrophica* type strain (OK10). *Stand. Genomic Sci.* 3, 194–202.
- Sogin, M. L., Morrison, H. G., Huber, J. A., Mark Welch, D., Huse, S. M., Neal, P. R., et al. (2006). Microbial diversity in the deep sea and the underexplored “rare biosphere”. *Proc. Natl. Acad. Sci. U.S.A.* 103, 12115–12120. doi: 10.1073/pnas.0605127103
- Sudek, L. A., Templeton, A. S., Tebo, B. M., and Staudigel, H. (2009). Microbial ecology of Fe hydroxide mats and basaltic rock from Vailulu'u Seamount, American Samoa. *Geomicrobiol. J.* 26, 581–596. doi: 10.1080/01490450903263400
- Sylvan, J. B., Pyenson, B. C., Rouxel, O., German, C. R., and Edwards, K. J. (2012). Time-series analysis of two hydrothermal plumes at 9°50'N East Pacific Rise reveals distinct, heterogeneous bacterial populations. *Geobiology* 10, 178–192. doi: 10.1111/j.1472-4669.2011.00315.x
- Tamura, K., Peterson, D., Peterson, N., Stecher, G., Nei, M., and Kumar, S. (2011). MEGA5: molecular evolutionary genetics analysis using maximum likelihood, evolutionary distance, and maximum parsimony methods. *Mol. Biol. Evol.* 28, 2731–2739. doi: 10.1093/molbev/msr121
- Taylor, C. D., and Wirsén, C. O. (1997). Microbiology and ecology of filamentous sulfur formation. *Science* 277, 1483–1485. doi: 10.1126/science.277.5331.1483
- Taylor, C., Wirsén, C., and Gaill, F. (1999). Rapid microbial production of filamentous sulfur mats at hydrothermal vents. *Appl. Environ. Microbiol.* 65, 2253–2255.
- Ver Eecke, H. C., Butterfield, D. A., Huber, J. A., Lilley, M. D., Olson, E. J., Roe, K. K., et al. (2012). Hydrogen-limited growth of hyperthermophilic methanogens at deep-sea hydrothermal vents. *Proc. Natl. Acad. Sci. U.S.A.* 109, 13674–13679. doi: 10.1073/pnas.1206632109
- Wirsén, C. O., Brinkhoff, T., Kuever, J., Muyzer, G., and Jannasch, H. W. (1998). Comparison of a new *Thiomicrospira* strain from the Mid-Atlantic Ridge with known hydrothermal vent isolates. *Appl. Environ. Microbiol.* 64, 4057–4059. doi: 10.1128/AEM.64.1.316-325.2002
- Wirsén, C. O., Sievert, S. M., Cavanaugh, C. M., Molyneaux, S. J., Ahmad, A., Taylor, L. T., et al. (2002). Characterization of an autotrophic sulfide-oxidizing marine *Arcobacter* sp. that produces filamentous sulfur. *Appl. Environ. Microbiol.* 68, 316–325.
- Yamamoto, M., and Takai, K. (2011). Sulfur metabolisms in epsilon- and gamma-Proteobacteria in deep-sea hydrothermal fields. *Front. Microbiol.* 2:192. doi: 10.3389/fmicb.2011.00192

**Conflict of Interest Statement:** The authors declare that the research was conducted in the absence of any commercial or financial relationships that could be construed as a potential conflict of interest.

*Received: 12 February 2013; paper pending published: 27 March 2013; accepted: 29 May 2013; published online: 17 June 2013.*

*Citation: Meyer JL, Akerman NH, Proskurowski G and Huber JA (2013) Microbiological characterization of post-eruption “snowblower” vents at Axial Seamount, Juan de Fuca Ridge. *Front. Microbiol.* 4:153. doi: 10.3389/fmicb.2013.00153*

*This article was submitted to Frontiers in Extreme Microbiology, a specialty of Frontiers in Microbiology.*

*Copyright © 2013 Meyer, Akerman, Proskurowski and Huber. This is an open-access article distributed under the terms of the Creative Commons Attribution License, which permits use, distribution and reproduction in other forums, provided the original authors and source are credited and subject to any copyright notices concerning any third-party graphics etc.*



# Microbial habitat connectivity across spatial scales and hydrothermal temperature gradients at Guaymas Basin

**Stefanie Meyer<sup>1,2</sup>, Gunter Wegener<sup>1,2,3</sup>, Karen G. Lloyd<sup>4</sup>, Andreas Teske<sup>5</sup>, Antje Boetius<sup>1,2</sup> and Alban Ramette<sup>1,2\*</sup>**

<sup>1</sup> HGF-MPG Joint Research Group on Deep Sea Ecology and Technology, Alfred Wegener Institute for Polar and Marine Research, Bremerhaven, Germany

<sup>2</sup> HGF-MPG Joint Research Group on Deep Sea Ecology and Technology, Max Planck Institute for Marine Microbiology, Bremen, Germany

<sup>3</sup> MARUM Center for Marine Environmental Sciences, University of Bremen, Bremen, Germany

<sup>4</sup> Department of Microbiology, University of Tennessee, Knoxville, TN, USA

<sup>5</sup> Department of Marine Sciences, University of North Carolina - Chapel Hill, Chapel Hill, NC, USA

**Edited by:**

Anna-Louise Reysenbach, Portland State University, USA

**Reviewed by:**

Barbara J. Campbell, Clemson University, USA

William D. Orsi, Woods Hole Oceanographic Institution, USA

**\*Correspondence:**

Alban Ramette, HGF-MPG Joint Research Group, Max Planck Institute for Marine Microbiology, Celsiusstr. 1, 28359 Bremen, Germany  
e-mail: aramette@mpi-bremen.de

The Guaymas Basin (Gulf of California) hydrothermal vent area is known as a dynamic and hydrothermally vented sedimentary system, where the advection and production of a variety of different metabolic substrates support a high microbial diversity and activity in the seafloor. The main objective of our study was to explore the role of temperature and other environmental factors on community diversity, such as the presence of microbial mats and seafloor bathymetry within one hydrothermally vented field of 200 × 250 m dimension. In this field, temperature increased strongly with sediment depth reaching the known limit of life within a few decimeters. Potential sulfate reduction rate as a key community activity parameter was strongly affected by *in situ* temperature and sediment depth, declining from high rates of 1–5 µmol ml<sup>-1</sup> d<sup>-1</sup> at the surface to the detection limit below 5 cm sediment depth, despite the presence of sulfate and hydrocarbons. Automated Ribosomal Intergenic Spacer Analysis yielded a high-resolution fingerprint of the dominant members of the bacterial community. Our analyses showed strong temperature and sediment depth effects on bacterial cell abundance and Operational Taxonomic Units (OTUs) number, both declining by more than one order of magnitude below the top 5 cm of the sediment surface. Another fraction of the variation in diversity and community structure was explained by differences in the local bathymetry and spatial position within the vent field. Nevertheless, more than 80% of all detected OTUs were shared among the different temperature realms and sediment depths, after being classified as cold ( $T < 10^{\circ}\text{C}$ ), medium ( $10^{\circ}\text{C} \leq T < 40^{\circ}\text{C}$ ) or hot ( $T \geq 40^{\circ}\text{C}$ ) temperature conditions, with significant OTU overlap with the richer surface communities. Overall, this indicates a high connectivity of benthic bacterial habitats in this dynamic and heterogeneous marine ecosystem influenced by strong hydrothermalism.

**Keywords:** microbial habitat connectivity, bacterial diversity, Guaymas Basin, ARISA

## INTRODUCTION

The Guaymas Basin is located in the central Gulf of California and represents a unique hydrothermal sedimentary basin. High-temperature fluids, which pass through an on average 100-m-thick sedimentary cover, facilitate the pyrolysis of buried organic matter (Simoneit and Lonsdale, 1982) and enrich hydrothermal sediments in petroleum-like compounds, light hydrocarbons (methane, organic acids) and ammonia (Von Damm et al., 1985; Bazylinski et al., 1988; Martens, 1990). The hydrothermal sediments are characterized by a wide range in temperature regimes, generally reaching the known limits of life (>120°C) at 15–40 cm below the sediment surface (McKay et al., 2012). The fluids discharged at Guaymas Basin contain hydrogen, carbon dioxide and hydrogen sulfide (Welhan and Lupton, 1987; Elsgaard et al., 1994; Paull et al., 2007). Supported by this large variety of potential microbial energy sources, Guaymas Basin sediments host diverse anaerobic and aerobic microbial communities (Teske et al., 2002). Among these are the giant sulfide oxidizers *Beggiatoa* that can

form thick white and orange bacterial mats on the seafloor, in habitats characterized by high sulfide fluxes (Jannasch et al., 1989; Nelson et al., 1989; McKay et al., 2012). In benthic ecosystems, these mats are hence often used as visual indicators of biogeochemical hotspots of high hydrocarbon flux and chemosynthetic production (Van Gaever et al., 2006; Lichtschlag et al., 2010; Lloyd et al., 2010). The key microbial processes such as nitrification (Mével et al., 1996; Baker et al., 2012), nitrate reduction (Bowles et al., 2012), sulfate reduction (Elsgaard et al., 1994; Weber and Jørgensen, 2002; Dhillon et al., 2003) and methanogenesis (Dhillon et al., 2005; Teske, 2010), were found to occur across a wide range of temperatures, suggesting a high diversity of the main functional groups of bacteria and archaea. Archaeal-bacterial consortia that mediate the anaerobic oxidation of methane (AOM) with sulfate are an important microbial community component in the Guaymas hydrothermal sediments (Teske et al., 2002, 2003), but *ex-situ* measurements of AOM have shown that this process is limited to temperatures <80°C

(Kallmeyer and Boetius, 2004). Previous studies indicated that different types of methanotrophs are favored by different temperature ranges (Holler et al., 2011; Biddle et al., 2012).

Few studies have investigated in detail spatial distribution patterns of microbial communities at Guaymas Basin (e.g., Guezennec et al., 1996; Edgcomb et al., 2002; Kysela et al., 2005), to understand the main drivers of microbial diversity. Microbes are known to display biogeographic patterns, ranging from cosmopolitanism to provincialism, but the underlying mechanisms that generate and maintain those patterns at a wide range of spatial scales remain largely underexplored (Hughes Martiny et al., 2006; Ramette and Tiedje, 2007a; Zinger et al., 2011; Hanson et al., 2012). Within the conceptual framework of metacommunity dynamics (Leibold et al., 2004), and by statistically disentangling the effects of space and environment on community composition, insights into community assembly mechanisms such as patch dynamics, species sorting, mass effects or neutral processes, or combination thereof, may be obtained and quantified (Cottenie, 2005).

In this study, a high-resolution sampling effort of hydrothermal sediments was conducted, investigating the patchiness of bacterial communities at spatial scales ranging from decimeters to hundreds of meters, and across temperature ranges typical for psychrophilic ( $T < 10^{\circ}\text{C}$ ), mesophilic ( $10^{\circ}\text{C} \leq T < 40^{\circ}\text{C}$ ) and thermophilic ( $T \geq 40^{\circ}\text{C}$ ) communities. Community fingerprinting data were obtained by Automated Ribosomal Intergenic Spacer Analysis (ARISA), which is useful to describe variations in bacterial community structure at a higher genetic resolution than what is provided by 16S rRNA gene sequencing (e.g., Brown et al., 2005; Nocker et al., 2007), because it is based on the amplification of the more variable ITS (Internal Transcribed Spacer) region. It may thus help reveal core communities and community shifts of the dominant bacterial types (Nocker et al., 2007; Fuhrman et al., 2008), but see Ramette (2009) for the possible detection of minor populations. To test for a potential effect of niche differentiation by temperature regimes on Guaymas Basin benthic bacterial communities, the following variables were chosen: *in situ* temperature was assessed during sampling, and vertical profiles of microbial assemblages inhabiting different temperature ranges were compared. Spatial variation was additionally assessed by latitude, longitude and water depth, relating to seafloor landscape features such as hydrothermal mounds. Further environmental parameters included bacterial mat presence/color as potential indicators for habitat heterogeneity, e.g., with regard to sulfide fluxes (Grünke et al., 2012; McKay et al., 2012). To infer potential changes in microbial abundance and function, microbial cell numbers, and potential sulfate reduction rates were included as additional parameters.

## MATERIALS AND METHODS

### SAMPLE COLLECTION

Sediment samples were obtained from a hydrothermally active field of  $0.05\text{ km}^2$  in the Southern Guaymas trench (Gulf of California,  $\sim 2000\text{ m}$  water depth,  $27^{\circ}00.37'\text{N}$  to  $27^{\circ}00.49'\text{N}$  and  $111^{\circ}24.58'\text{W}$  to  $111^{\circ}24.44'\text{W}$ ), by push coring into enclosed plastic tubes with the *Alvin* submersible (operated by Woods Hole Oceanographic Institution, Woods Hole, MA) during R/V

*Atlantis* expedition AT15-40 in December 2008. *In situ* subsurface temperatures were measured before coring ( $<50\text{ cm}$  away from the sampled areas) by using either the external “High Temperature Probe” or the external “Heatflow Probe” on the *Alvin* submersible (operated by WHOI; for probe details see McKay et al., 2012). The temperature values used in this study are reported in Table S1. Replicate sediment cores were collected separately for bacterial community analyses, for sulfate reduction rate measurements and for pore water geochemistry. During ascent of the submersible, all cores were tightly closed and stored upright in a fixed position. Cores with intact layering of mats and sediments were used for further analyses. Subsampling of the cores occurred within 4–12 h after sampling and storage at  $4^{\circ}\text{C}$ . The upper  $10\text{--}30\text{ cm}$  of sediment cores were sectioned into 1-cm and 2-cm horizons and were preserved for subsequent analyses accordingly (see below). Samples for molecular work were immediately frozen at  $-20^{\circ}\text{C}$ .

### DETERMINATION OF SULFATE CONCENTRATIONS AND SULFATE REDUCTION RATES

For a limited number of cores, pore water was extracted by centrifugation of sediment from the respective horizons, and sulfate pore water concentrations were measured as described previously (Biddle et al., 2012; McKay et al., 2012). Additional cores were used to measure sulfate turnover constants *ex situ* using the whole-core injection method (Jørgensen, 1978) with  $5\text{--}10\text{ }\mu\text{l}$  carrier-free  $^{35}\text{SO}_4^{2-}$  (dissolved in water,  $50\text{ kBq}$ ) in the dark, at a fixed temperature of  $20^{\circ}\text{C}$  for all cores. After 8–24 h incubation time, samples were preserved in  $20\text{ ml}$  of  $20\%$  (w/v)  $\text{ZnAc}$  solution. Sulfate turnover constants (Table S2) and average sulfate concentrations (Table S3) determined in adjacent cores of the same dive were used to calculate potential sulfate reduction rates (Kallmeyer et al., 2004; Felsen et al., 2010). Because of the substantial heterogeneity of *in situ* temperature and pore water composition between cores a few centimeters or decimeters apart (McKay et al., 2012), the resulting potential sulfate reduction rates (Table S2) should be regarded as an approximation. To show that sulfate concentrations are variable even over small spatial scales, the measured sulfate turnover constants are plotted alongside sulfate concentrations for nearby cores in Figure S1.

### ACRIDINE ORANGE DIRECT CELL COUNTING (AODC)

Sediment sections ( $2\text{ ml}$ ) for microbial cell counts were fixed onboard in 4% formaldehyde/seawater ( $9\text{ ml}$ ) and stored at  $4^{\circ}\text{C}$ . In the home laboratories, samples were stained with acridine orange according to a modified protocol (Boetius and Lochte, 1996) of Meyer-Reil (1983). For each sample, single cells were counted on at least 2 replicate filters and for a minimum of 30 random grids per filter (dilution factors 2000–4000).

### BACTERIAL COMMUNITY FINGERPRINTING

Sediment sections for DNA analyses were directly transferred to sterile plastic tubes and were kept frozen at  $-20^{\circ}\text{C}$  until further use in the home laboratories. Total community DNA was extracted from  $1\text{ g}$  of sediment by using the Ultra Clean Soil DNA Isolation Kit (MoBio, Carlsbad, CA) and by following the manufacturer’s specifications for maximum yield. DNA was

eluted in 100  $\mu$ l 1  $\times$  TE buffer (Promega Corporation, Madison, WI) and stored at  $-20^{\circ}\text{C}$  until further use. DNA concentration per volume buffer was measured by using a NanoQuant infinite M200 (Tecan, Crailsheim, Germany). Bacterial community analyses are based on profiles generated by Automated Ribosomal Intergenic Spacer Analysis (ARISA). The procedure has been previously published in detail (Ramette, 2009). In this study, a slightly modified version of the protocol was used: Within a 50  $\mu\text{l}$ -reaction, final concentrations of PCR ingredients were 0.4  $\mu\text{M}$  of each primer (Biomers, Ulm, Germany), 250  $\mu\text{M}$  of each dNTP (peqGOLD Kit; Peqlab, Erlangen, Germany), 0.1 mg  $\text{ml}^{-1}$  BSA (Sigma-Aldrich Biochemie GmbH, Hamburg, Germany), 1  $\times$  Buffer S with 1.5 mM MgCl<sub>2</sub> (Peqlab), 1.0 mM extra MgCl<sub>2</sub> (Peqlab) and 2.5 U peqGOLD Taq-DNA-Polymerase (Peqlab). Per reaction, 20–25 ng of extracted DNA were used as template. Primers were ITSf (FAM-5'-GTC GTA ACA AGG TAG CCG TA-3' Cardinale et al., 2004) and ITSReub (5'-GCC AAG GCA TCC ACC-3' Cardinale et al., 2004).

### STATISTICAL ANALYSES

Quality assessment of ARISA profiles and binning were done as described in Ramette (2009). For merging PCR replicate profiles into master profiles, Operational Taxonomic Units (OTUs) consisted of peaks that occurred at least once among the respective PCR triplicates. All numerical analyses were conducted in R (v.2.13.2; The R Foundation for Statistical Computing; [www.R-project.org](http://www.R-project.org)) using the *vegan* library as well as standard packages and custom scripts (available at [www.ecologyresearch.com](http://www.ecologyresearch.com)).

Contextual parameters are summarized in Tables S1 and S4. DNA concentrations and total cell numbers were log-transformed to ensure normal distribution of the data. Presence and absence of mat as well as mat color (i.e., white, orange and yellow vs. no mat) were recoded as dummy variables (Ramette, 2007). Numbers of shared OTUs between different categories of contextual parameters were calculated by first merging all respective profiles of a given category into a single community profile where all peaks present were counted. Non-metric Multidimensional Scaling (NMDS) was used to represent dissimilarity matrices based on Bray-Curtis or Jaccard coefficients into a reduced space (Legendre and Legendre, 1998). Redundancy Analysis (RDA) models were combined with stepwise selection procedure, so as to retain the minimum number of significant variables as indicated by minimal Akaike Information Criterion (AIC) model value. Different sets of explanatory variables were then tested for significance in a variation partitioning framework (Borcard et al., 1992; Ramette, 2007). When negative  $R^2$  values were obtained, as it is the case sometimes for partial regression models (Legendre and Legendre, 1998), they were set to 0, and the total explained variation was recalculated, by adding up only the positive fractions. The heterogeneity of bacterial community structures among and between samples associated to certain environmental categories was quantified by their average variation in bacterial beta-diversity to each category's centroid (e.g., Zinger et al., 2011) and tested for significance by ANOVA followed by Tukey's Honestly Significant Difference tests, as implemented in the R package *vegan*.

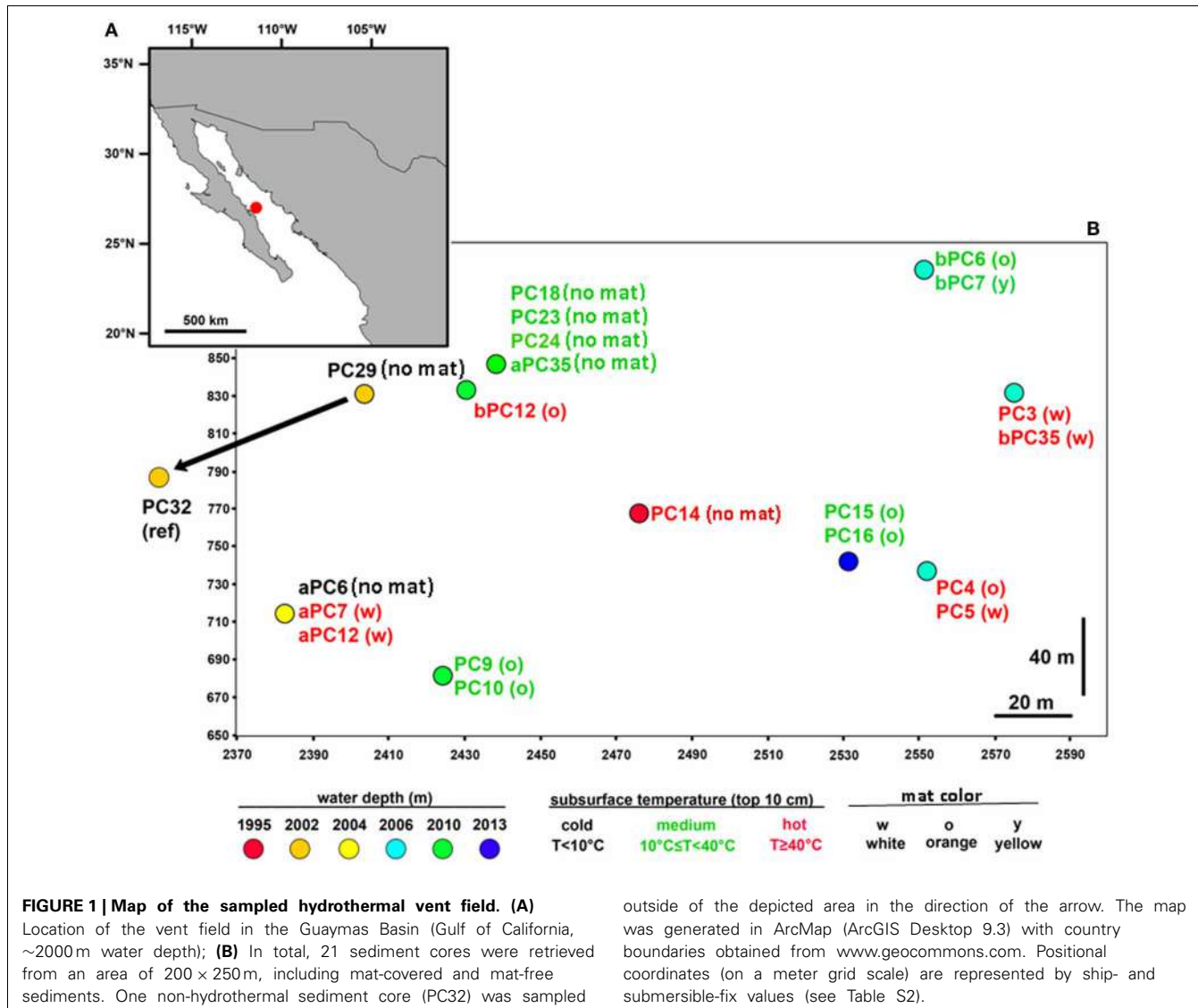
## RESULTS

### SITE DESCRIPTION

To gain insight into the processes generating and maintaining bacterial community structure at Guaymas Basin, 21 sediment cores were obtained across an area of 200  $\times$  250 m, including more or less hydrothermally vented sediments, and one background core was retrieved from outside the vent field (Figure 1; Table 1). The sampling area was located within a hilly area of the Southern Guaymas trench (Gulf of California) covering water depths of 1995–2013 m, and harboring hydrothermal mounds densely populated by *Riftia* tubeworms, sulfide spires and flanges as well as numerous white, orange and yellow *Beggiatoa* mats on the seafloor, some of them growing on mounds. One of these mounds, termed "Mat Mound" ( $N27^{\circ}00.388$ ;  $W111^{\circ}24.560$ ) was surrounded by an apron of hydrothermally active sediments overgrown with microbial mats, and was repeatedly visited for sampling (Figures 2A,B). Sediment pushcores aPC7, aPC12 and aPC6 (Figure 1) and several sulfate reduction cores (Figure S1) were sampled at this location. Bacterial mats growing on sediment surfaces typically had diameters of 1–2 m and could be several cm thick. One large mat-covered hydrothermal sediment area termed "Megamat" of ca. 10–15 m diameter ( $N27^{\circ}00.464$ ;  $W111^{\circ}24.512$ ) was visited and sampled repeatedly (Figures 2C,D); the subsurface temperature field underlying a portion of this extensive hydrothermal area was mapped and reconstructed in 3D (McKay et al., 2012). Pushcores PC18, PC23, PC24, and aPC35 (Figure 1) and several sulfate reduction cores (Figure S1) were sampled on the edge of Megamat. A smaller, orange-colored microbial mat termed UNC Mat ( $N27^{\circ}00.445$ ,  $W111^{\circ}24.530$ ) ca. 20 m southwest of Megamat was sampled (Figures 2E,F). This location showed strong *in situ* evidence for high-temperature sulfate-dependent methane oxidation (Biddle et al., 2012). Here sediment core bPC12 (Figure 1) and several sulfate reduction cores (Figure S1) were sampled. Additional sampling sites were visited, several of them on extensive survey dives (Alvin dives 4492 and 4493) to maximize the geographic range of sediment cores (Figure 1, Table 1).

The distribution of mats across the overall investigated sampling area was patchy, and there was no obvious spatial gradient in the temperature field or in the distribution of bacterial mats recorded. As *Beggiatoa* mats are known to indicate geochemical and biodiversity hotspots (Lloyd et al., 2010; Grünke et al., 2012; McKay et al., 2012), they were repeatedly sampled within this study, resulting in the recovery of 13 mat-covered cores and 8 mat-free cores for comparison. Upon recovery, most cores were found to be rich in methane gas (Biddle et al., 2012; McKay et al., 2012). *In situ* subsurface temperatures varied between 3 and 96°C in the upper 10 cm of sediment (Table S1), and cores were classified into different temperature ranges according to these measurements.

Potential microbial sulfate reduction rates assessed at 20°C reached values as high as 5500 nmol  $\text{ml}^{-1}$   $\text{d}^{-1}$  in the surface layers originating from an *in situ* temperature range of 3–40°C (Table S2), but then decreased abruptly beneath 5 cm sediment depth (*in situ* T approx. 10–40°C), and were almost absent below 10 cm (*in situ* T range 20–96°C) (Figure 3A, Table S1). In most cores sulfate was not depleted within the top 10 cm, indicating



that availability of electron donors or sulfate did not limit sulfate reduction (**Figure 3B**; Table S3). This observed predominance of mesophilic sulfate reduction in surficial sediment layers may partially be explained by the fact that all potential sulfate reduction rate measurements were conducted at 20°C; thus, the contribution of high-temperature sulfate reduction rates to overall sedimentary sulfate-reducing activity was not assessed in this study. However, cell numbers also decreased rapidly with increasing sediment depth (**Figure 3C**; Table S4), varying between 1.0 and  $3.7 \times 10^9$  cells ml<sup>-1</sup> in mat-covered and mat-free surface sediments, and declining to  $< 0.6 \times 10^9$  cells ml<sup>-1</sup> in sediment layers below 5 cm.

#### EVALUATION OF ENVIRONMENTAL FACTORS AFFECTING COMMUNITY STRUCTURE AND FUNCTION

Indicator factors for habitat variation tested within this study included *in situ* seafloor temperature (T), mat color/presence (MC) and sediment depth (SD), as well as bathymetry (measured

as water depth, WD), and coordinates in the local sampling grid in meters (X,Y) as defined by seafloor radiobeacons (pingers) set out by RV *Atlantis* before the start of the sampling campaign (Table S4). Linear (Pearson) and rank-based (Spearman) correlations were used to determine the degree of correlation between all numerical parameters for the most complete subset of the data, which included T (real temperature values with number of samples  $n = 46$ ; Table S1), SD, WD, X and Y. The analyses revealed significant positive correlations between SD and T (Pearson's  $r = 0.653$ ,  $P < 0.001$ ), with the deeper sediment layers representing hotter habitats (Table S1), as well as between X and Y sampling grid coordinates (Pearson's  $r = 0.420$ ,  $P < 0.01$ ), reflecting the fact that most of the sampling took place within a specific area, and not randomly dispersed around the zero origin of the coordinates. All other pairwise comparisons among parameters (i.e., T, SD, WD, X and Y) were not significant. Mat color variation was found to be significantly related to bathymetry (WD; F ratio = 11.003,  $P \leq 0.001$ ; explaining 20% of the variation in

**Table 1 | Cores analyzed in this study by ARISA.**

| Label | Date     | Dive | Water depth (m) | Location              | Core description  |
|-------|----------|------|-----------------|-----------------------|---|
| aPC12 | 06.12.08 | 4483 | 2004            | Mat mound             | Gray sediment with dark green and brown spots in between; white mat   |
| aPC7  | 07.12.08 | 4484 | 2004            | Mat mound             | Gray sediment; white mat  |
| aPC6  | 09.12.08 | 4485 | 2004            | Outside mat mound     | Green-gray sediment, worms; no mat  |
| PC23  | 10.12.08 | 4486 | 2010            | Outside Megamat       | Olive-green sediment, gas holes; no mat   |
| PC18  | 10.12.08 | 4486 | 2010            | Outside Megamat       | Top 5 cm fluffy brown, then olive-green sediment, gas holes; no mat   |
| PC24  | 10.12.08 | 4486 | 2010            | Outside Megamat       | Top dark olive-green, rest olive-green, worm carcasses; no mat  |
| bPC12 | 14.12.08 | 4489 | 2010            | UNC mat, near Megamat | Top 5 cm fluffy, then olive sediment, hole at bottom, sulfidic; orange mat with few white filaments   |
| aPC35 | 15.12.08 | 4490 | 2010            | Megamat               | Top 9–10 cm blackish, then olive-gray, gas holes, oily spots; no mat  |
| PC32  | 16.12.08 | 4491 | 2002            | 100 m from Megamat    | Top 1–3 cm fluffy blackish sediment, then mixed dark-gray with green-brown sediment; no detectable hydrothermal temperature gradient; no mat                                |
| PC29  | 16.12.08 | 4491 | 2002            | 50 m from Megamat     | Top 1–3 cm fluffy brown sediment, then olive-gray sediment; no detectable hydrothermal temperature gradient; no mat   |
| PC3   | 17.12.08 | 4492 | 2006            | Survey site 1         | Bubbling, top 2–4 cm brownish fluffy, then oily layer with oil/gas pockets, then grayish sediment, worm; white mat  |
| PC4   | 17.12.08 | 4492 | 2006            | Survey site 2         | Bubbling, 9 cm organic layer, oily, with gas/oil pockets, then grayish sediment; orange mat   |
| bPC6  | 17.12.08 | 4492 | 2006            | Survey site 3         | Top 2 cm fluffy, then 5 cm blackish, then olive sediment; orange mat with yellow parts  |
| bPC35 | 17.12.08 | 4492 | 2006            | Survey site 1         | Fluffy brownish layer (partly pushed to bottom of the core), then grayish sediment with darker spots in-between, core liner melted at the bottom; white mat                 |
| PC5   | 17.12.08 | 4492 | 2006            | Survey site 2         | Bubbling, 1 cm gray sediment on top, then 4 cm grayish-brownish fluff, then 4 cm olive and oily layer with gas/oil pockets, then grayish sediment (more compact); white mat |
| bPC7  | 17.12.08 | 4492 | 2006            | Survey site 3         | Top 4 cm fluffy, then 4.5 cm darker and then brown-olive sediment; yellow mat   |
| PC9   | 18.12.08 | 4493 | 2010            | Survey site 4         | 8 cm grayish sediment, then mixed layer with red oily droplets, white inclusions towards the bottom; orange mat   |
| PC10  | 18.12.08 | 4493 | 2010            | Survey site 4         | 4 cm fluffy, then mixed sediment, some white inclusions, holes, red oily droplets; orange mat   |
| PC14  | 18.12.08 | 4493 | 1995            | Survey site 5         | Top 6 cm darker, then 12 cm greenish, then 8 cm grayish sediment; no mat  |
| PC15  | 18.12.08 | 4493 | 2013            | Survey site 6         | Olive sediment with blackish spots at top; orange mat   |
| PC16  | 18.12.08 | 4493 | 2013            | Survey site 6         | 3 cm fluffy, then olive-grayish sediment, white deposits, holes; orange mat   |

mat color) and spatial distance ( $X + Y$ ;  $F$  ratio = 8.135,  $P \leq 0.001$ ; 25% of explained variation). There was no significant relationship between MC and T, when using the subset of data for which contextual *in situ* temperatures were obtained ( $n = 46$ ). However, when assigning the full data set including all sediment depths ( $n = 188$ ) into three temperature categories (cold  $T < 10^\circ\text{C}$ , medium  $10^\circ\text{C} \leq T < 40^\circ\text{C}$ , hot  $T \geq 40^\circ\text{C}$ , as measured in the upper 10 cm of sediment),  $T$  was significantly ( $P \leq 0.001$ ) related to MC and explained up to 28% of the observed variation. Within individual mat locations, orange mats were found in the central area (Figure 1) characterized by the steepest geochemical gradients, and inferred hydrothermal fluxes (McKay et al., 2012), and were associated with temperatures ranging from 4 to  $96^\circ\text{C}$  (average  $33 \pm 26.5$  [sd]  $^\circ\text{C}$ ; Table S4).

#### MICROBIAL CELL NUMBERS AND VARIATION IN OTU NUMBER

Cell numbers declined significantly with sediment depth (partial coefficient =  $-0.161$ ,  $P < 0.001$ ). The overall variation in

cell numbers (Figure 4A) was significantly explained by SD and WD (full model: 74%;  $n = 49$ ), with SD alone explaining up to 66% of the observed variation ( $P < 0.001$ ), while WD, respectively, explained 0.5% ( $P < 0.01$ ; partial coefficient = 0.144,  $P < 0.001$ ) of the variation in cell number (see Supplementary text and Figure S2, for analyses of the variation in extracted DNA concentrations).

Furthermore, also OTU number decreased with increasing temperature and sediment depth (Figure 3D). A total pool of 439 different OTUs was detected when considering all 188 samples, with OTU numbers per sample ranging from 1 to 223. OTU numbers were negatively related with SD (Figures S3, S4; Pearson's  $r = -0.567$ ,  $P < 0.001$ ;  $n = 188$ ) and  $T$  (Pearson's  $r = -0.500$ ,  $P < 0.001$ ;  $n = 46$ , real temperature values), representing a substantial loss of bacterial richness with deeper, generally hotter sediments. Higher OTU numbers were obtained on average for the upper sediment layers ( $112 \pm 65$  OTUs; 0–10.5 cm) than for the deeper ones ( $54 \pm 61$  OTUs; 11–24 cm). However, considering sediment

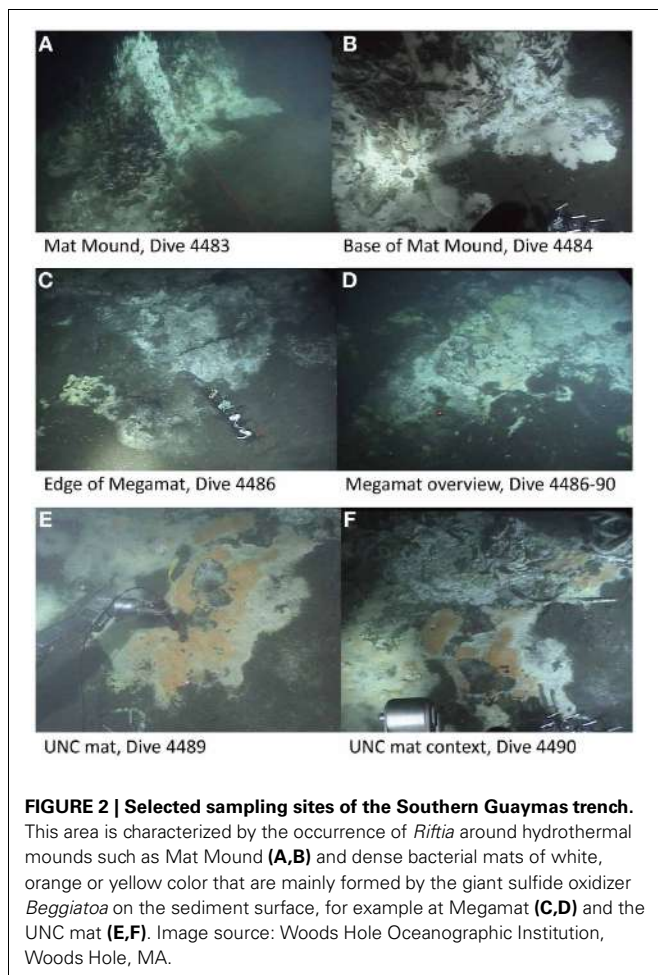


**FIGURE 2 | Selected sampling sites of the Southern Guaymas trench.**

This area is characterized by the occurrence of *Riftia* around hydrothermal mounds such as Mat Mound (**A,B**) and dense bacterial mats of white, orange or yellow color that are mainly formed by the giant sulfide oxidizer *Beggiatoa* on the sediment surface, for example at Megamat (**C,D**) and the UNC mat (**E,F**). Image source: Woods Hole Oceanographic Institution, Woods Hole, MA.

depth alone, maximum and minimum numbers of OTUs fell into a wide range, with 3–223 OTUs for the upper horizons and 1–218 OTUs for the deeper layers. The two depth categories had 90% OTUs in common.

Across all sediment depths, the range of OTU numbers determined for the different *T* categories (cold  $T < 10^{\circ}\text{C}$ , medium  $10^{\circ}\text{C} \leq T < 40^{\circ}\text{C}$ , hot  $T \geq 40^{\circ}\text{C}$ ) also varied widely, i.e., 30–223 OTUs (cold), 2–214 OTUs (medium) and 1–198 OTUs (hot), indicating a large spatial variability as well as potentially also a temporal variability of temperature (**Figure 3D**). The average OTU numbers decreased from cold to hot samples with  $165 \pm 60$ ,  $116 \pm 59$ , and  $90 \pm 63$  OTUs for cold, medium and hot samples, respectively. Cold and medium temperature samples shared 85%, cold and hot samples 86%, and medium and hot cores 90% of their OTUs (0–24 cm sediment depth). The reference core (PC32, cold), taken outside of the hydrothermal vent field, shared between 70 and 77% of its OTUs with any other cores taken within the surveyed area, while the percentages of shared OTUs was higher among samples within the vent field ranging from 83 and 90% (all *T* categories compared). Further OTU partitioning revealed that the number of unique OTUs in cold (3 OTUs) and hot habitats (4 OTUs) was lower than that of intermediate temperatures (18 OTUs) (**Figure 4B**).

Mat presence was generally associated with lower OTU numbers for the upper 10 cm of sediment, with average values of  $93 \pm 58$  for mat-covered sediments vs.  $149 \pm 61$  OTUs for mat-free sites (see also Figure S5), concurring with previous work suggesting that the sulfide- and methane-rich regime selects for a more specialized microbial community than in normal surface sediments (Lloyd et al., 2010). However, when taking all sediment depths into account, no clear difference in total OTU numbers between mat-covered (2–198 OTUs) and mat-free sites (1–223 OTUs) could be detected. The percentage of shared OTUs between mat-free and mat-covered sediments ranged from 63 to 88%. Multivariate analyses with the full data set ( $n = 188$ ) indicated that variation in OTU number could be best explained by variation in SD (32%), space ( $X + Y$ ; 7%) and *T* (4%), altogether explaining 52% of the total variation (**Figure 4A**).

## CHANGES IN BACTERIAL COMMUNITY STRUCTURE

When considering all samples on the NMDS ordination plot (**Figure 5**) a clear separation appeared between samples that contained  $<70$  OTUs and those with a higher richness (as determined by a frequency distribution analysis; Figure S6). Overall, samples with OTU numbers  $<70$  OTUs were less similar to each other (i.e., communities were more heterogeneous) than the ones with OTU numbers higher than 70 OTUs (**Figure 5A**). They were mostly associated with sediment layers deeper than 10 cm and a temperature range of  $20\text{--}96^{\circ}\text{C}$ , depending on core and sampling location (**Figure 5B**; Table S1). Samples with OTU numbers  $\geq 70$  OTUs were mostly associated to cold (19 samples, i.e., 18% of all samples) or medium temperature (73 samples or 70%) conditions and generally originated from the top 10 cm surface layers (81 samples, i.e., 77% of all samples) (**Figure 5C**; Figure S7). No significant pattern was found to be associated with variation in mat color (**Figure 5D**), but within the group of samples with  $\geq 70$  OTUs, mat-free sediment samples were more similar to each other than mat-associated ones (**Figure 5D**).

When taking all contextual parameters analyzed here into account, 24% of the observed variation in bacterial community structure could be explained (**Figure 4A**;  $n = 188$ ). Most of the variation was explained by SD (7%) and MC (4%), followed by spatial distance ( $X + Y$ , 3%), *T* (2%) and WD (2%), when taking the variations of each other parameter into account (partial regression analyses done via variation partitioning). All of these factors had highly significant ( $P \leq 0.001$ ) effects. Beta dispersion analyses revealed that medium temperature cores contained the highest community heterogeneity (average distance to centroid: 0.60), as compared to hot (average distance to centroid: 0.58), and cold cores (average distance to centroid: 0.46). Tukey's HSD tests indicated highly significant differences between cold cores and all other categories ( $P < 0.001$ ), but no significant difference between hot and medium cores ( $P > 0.05$ ).

## DISCUSSION

### IMPACT OF TEMPERATURE ON BENTHIC BACTERIAL COMMUNITIES AT GUAYMAS BASIN

Guaymas Basin hydrothermal sediments are rich in hydrocarbons, methane, hydrogen sulfide, and contain a variety of other potential microbial energy sources, supporting complex

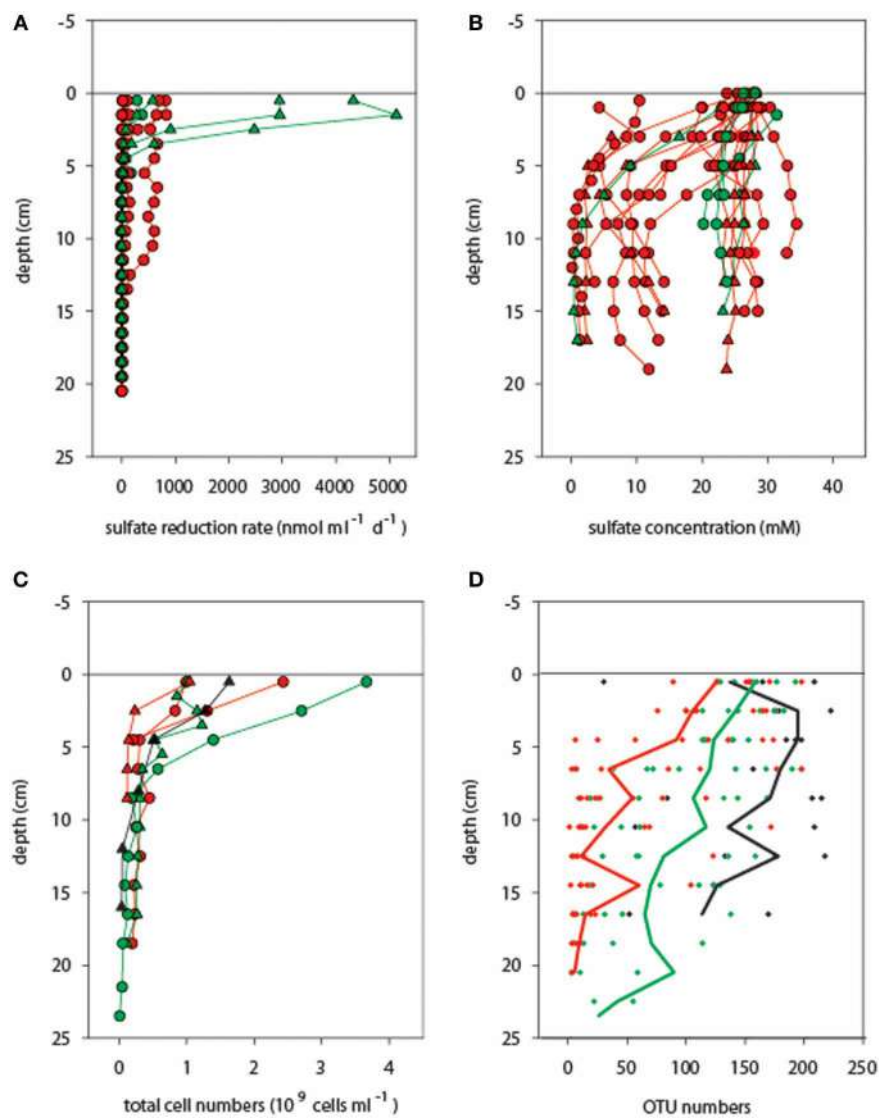


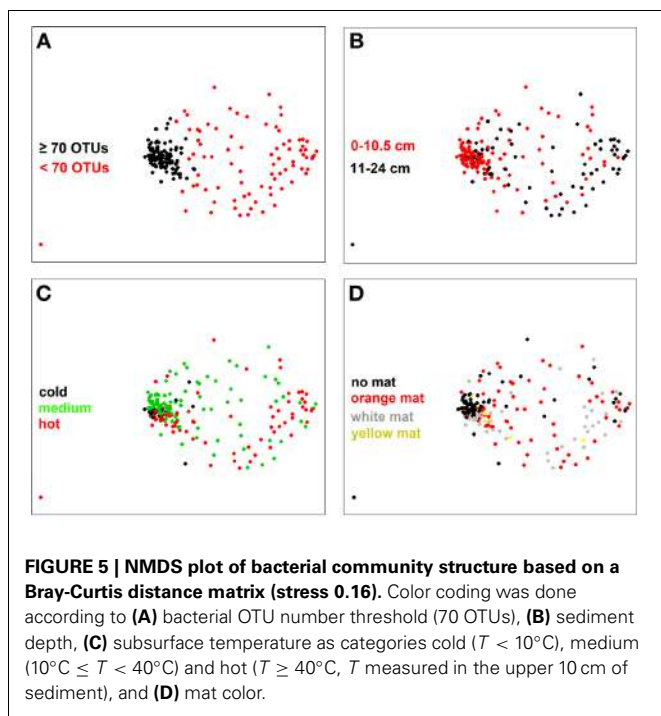
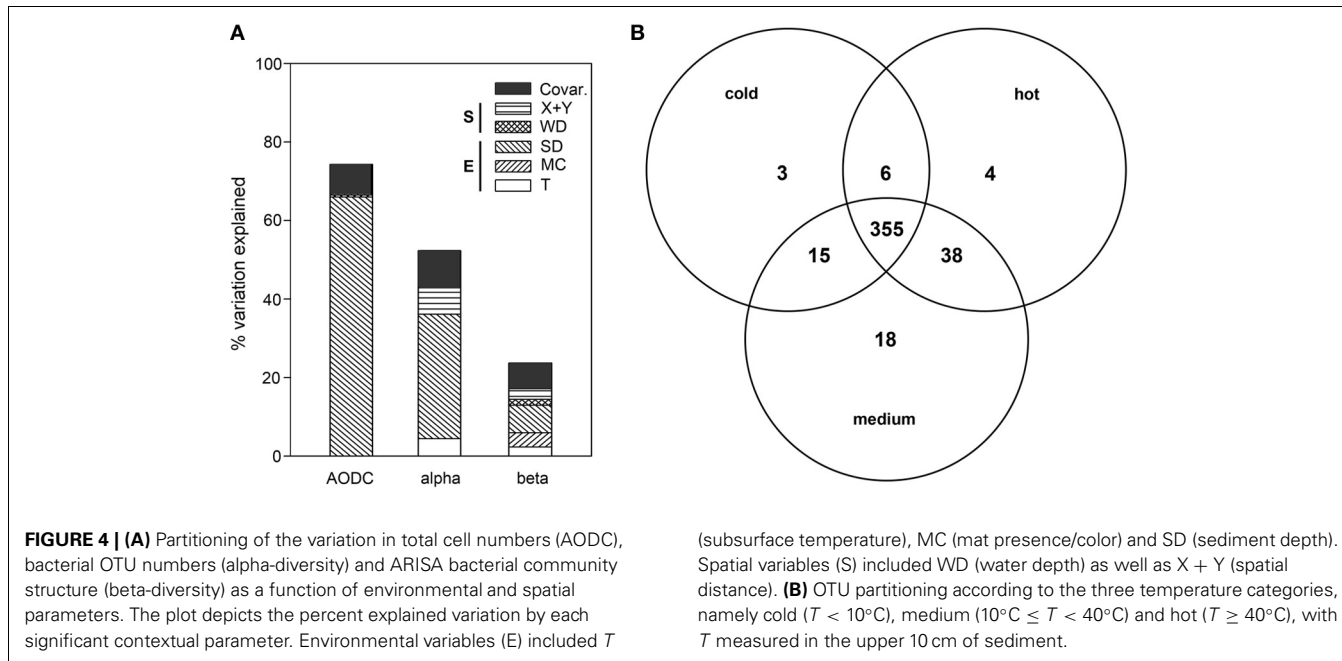
**FIGURE 3 | Activity and biomass of microbial communities associated with different temperature ranges. (A)** Potential sulfate reduction rates and **(B)** sulfate concentrations were determined in adjacent cores (not available for cold cores). Total single cells **(C)** and OTU numbers **(D)** generally decreased with increasing sediment depth [the lines in **(D)** indicate average

OTU numbers across cores]. Temperature categories indicated by color codes are cold ( $T < 10^{\circ}\text{C}$ , black symbols), medium ( $10^{\circ}\text{C} \leq T < 40^{\circ}\text{C}$ , green symbols), and hot ( $T \geq 40^{\circ}\text{C}$ , red symbols), as measured in the upper 10 cm of sediment before coring. Circles and triangles correspond to mat-covered and mat-free sediments, respectively.

anaerobic and aerobic microbial communities (Bazylinski et al., 1988; Martens, 1990; Dhillon et al., 2005; Biddle et al., 2012). Furthermore, the sediments at Guaymas Basin are characterized by a wide range of temperatures (3–200°C), thus crossing the realms of psychrophilic, mesophilic and thermophilic bacterial communities, as well as abiotic zones within small spatial scales (McKay et al., 2012). Temporal dynamics in fluid flow may also be high and can add substantial variation in fluxes of electron donors and acceptors as well as temperature (Gundersen et al., 1992). It is important to note that *in situ* temperatures obtained during sampling could rather be snapshots in time, and a site vented by very hot fluids a few days before may still show substantial disturbance effects after cooling, such as low cell counts and a low richness and sulfate reduction activity.

Guaymas Basin sediments are long known to be an interesting natural laboratory for the study of temperature-dependent oxidation of methane and sulfate reduction, and both processes have been found over a wide range of temperatures (Weber and Jørgensen, 2002; Kallmeyer and Boetius, 2004; Holler et al., 2011; Biddle et al., 2012). In general, at 20°C potential microbial sulfate reduction was strongly repressed below 4–5 cm (Figure 3A), despite the presence of sulfate and methane as well as other electron donors throughout the core, a phenomenon previously observed for Guaymas Basin sediments (Martens, 1990; Elsgaard et al., 1994; Weber and Jørgensen, 2002; Dhillon et al., 2005; Biddle et al., 2012; McKay et al., 2012).

Potentially, episodic heat pulses by upward advecting hot fluids may act as strong disturbances to the microbial assemblages



selected by certain temperature ranges in space and time. Upward advection of very hot fluids  $>100^{\circ}\text{C}$  could even lead to sterilization of the present assemblages, which then will be repopulated by the surface communities. This may explain the reduction or disappearance of biomass and diversity below 5–10 cm sediment depth detected in total cell numbers (Figure 3C), as well as bacterial OTU numbers (Figure S3). A substantial decline in cell numbers within a decimeter of the seafloor has also been observed in other highly fluid-flow advected marine sediments (Lösekann

et al., 2007; Grünke et al., 2011), as well as in disturbed seep environments such as submarine mud volcanoes (Pop Ristova et al., 2012). If such geophysical disturbances can affect microbial abundances, they are also likely to affect community diversity and function. Even though archaeal diversity was not covered by our molecular approach, it is known for instance that archaea isolated from Guaymas Basin have demonstrated susceptibility to heavy metals (Edgcomb et al., 2004) or to the combination of low pH, high sulfide and low temperature typically present in vent fluids (Lloyd et al., 2005).

The rapid loss of OTU number and microbial activity with sediment depth and increasing temperature indicate that from a relatively diverse community, only few members can occupy the niches available in the deep hot sediments at Guaymas (Figures 3–5). Interestingly, most of these OTUs were not unique, but occurred throughout the surface sediments sampled from the vent field. Hence, it seems likely that the prevailing diverse communities of bacteria in the highly reduced surface sediments of Guaymas Basin are functioning as a seed bank to deeper depths, and that many community members are adapted to a relatively wide range of temperature conditions. This is in general accordance with findings on the relatively broad temperature ranges of anaerobic methane oxidizers and sulfate reducers at Guaymas (Elsgaard et al., 1994; Weber and Jørgensen, 2002; Kallmeyer and Boetius, 2004; Holler et al., 2011; Biddle et al., 2012). Furthermore, ANME1-Guaymas archaea were previously found at temperatures between 20 and  $>90^{\circ}\text{C}$ , suggesting their eurythermal nature and adaptation to fluctuations in temperature and heat flow (Biddle et al., 2012). Most likely the small-scale variation in space and time of the upward advective transport of hot hydrothermal fluids, and downward mixing of seawater penetrating surficial sediments (Gundersen et al., 1992) is likely exerting a substantial challenge to the microbial community, leading to substantial losses in diversity with sediment depth, and blurring a

typical temperature-induced zonation of microbial habitats in the sediments.

#### OTHER NICHE EFFECTS ON BACTERIAL COMMUNITY COMPOSITION

*Beggiatoa* mats are generally linked to steep gradients and high fluxes of sulfide, DIC and CH<sub>4</sub>; they can be flushed by oxygenated seawater (Gundersen et al., 1992) and indicate hotspots of CH<sub>4</sub> and sulfur cycling (Lichtschlag et al., 2010; Lloyd et al., 2010; Grünke et al., 2012; McKay et al., 2012). Their distribution across the investigated area at Guaymas Basin was patchy and not directly related to bathymetry or temperature regimes. Thus, we investigated whether the sampled areas may represent hotspots of bacterial diversity, especially via the presence of *Beggiatoa* that have been proposed to be acting as ecosystem engineers at Guaymas Basin by “providing specialized habitats for unique assemblages of species, thereby creating seafloor biodiversity hotspots” (Levin and Dayton, 2009). OTU number was compared across different mat types and mat-free sediments. In the top 2.5 cm sediment layers, mat-covered sediments were associated on average with fewer OTU with 137 OTU ( $n = 30$ ) as compared to 162 OTU ( $n = 14$ ) in mat-free sediments (two-sample Wilcoxon test,  $W = 115$ ,  $P = 0.0172$ ). These numbers are comparable to those found in and around sulfide-oxidizer mats at cold seeps along the Norwegian continental margin (on average 121–166 OTUs in 0–2.5 cm sediment depth; Grünke et al., 2012). The total OTU number of 439 detected in Guaymas Basin sediments was similar to bacterial OTUs from a cold seep site at the West African margin (~3200 m water depth, 450 OTUs; Pop Ristova et al., 2012). The percentage of shared OTUs between mat-covered and mat-free sediments (63–88%, 0–24 cm) was slightly higher than what has previously been found in a study on bacterial sulfide oxidizer mats at the Norwegian margin (41–63%, 0–2.5 cm; Grünke et al., 2012), and for other chemosynthetic communities at the cold seep REGAB of the West African margin (average 74%, 0–10 cm; Pop Ristova et al., 2012). The effects on community diversity of mat presence and color (corresponding to different *Beggiatoa* spp.) (McKay et al., 2012), could not be further disentangled in this study, because of the highly variable temperature regimes within the different mats. Although mat-forming sulfide oxidizers of the family *Beggiatoaceae* have previously been shown to specifically associate with certain types of bacteria (Kojima et al., 2006; Prokopenko et al., 2006; Teske et al., 2009), our results overall did not support the idea that the presence *Beggiatoa* mats was associated with higher bacterial diversity or specificity as compared to neighboring mat-free sediment communities.

#### SPATIAL EFFECTS ON BACTERIAL COMMUNITIES

The investigated hydrothermal field at Guaymas Basin was characterized by various structures typical for vent fields such as chimneys and mounds overgrown with *Beggiatoa* mats (Figure 2A), and dense *Beggiatoa* mats covering surface sediments (Figures 2B,C; Jannasch et al., 1989), vent chimneys and sulfide spires (Figures 2D–F). There was a slightly elevated area in the middle of the investigated area, where the water depth reached only 1995 m as compared to >2000 m in the other areas, however, this feature was not distinctly related to a temperature

gradient. Nevertheless, we explored whether spatial distance and bathymetry (mounds vs. troughs on the landscape level) had an effect on community assemblage.

The complex interplay of environmental and spatial factors on microbial diversity has already been observed in patchy terrestrial environments (e.g., Ramette and Tiedje, 2007b). Our analyses of 0.05 km<sup>2</sup> of the Guaymas hydrothermal field showed that most tested biological variables, i.e., total cell numbers, OTU numbers and beta-diversity, were significantly influenced by spatial factors (X, Y or WD) at the scale of meters to hundreds of meters (Figure 4A). Total cell numbers were positively correlated with bathymetry, so that elevated landscape features showed a lower microbial biomass (based on partial linear regression models), but they were not correlated with latitude and longitude. OTU numbers were correlated to the geographic positions of the samples (both increasing with Y and decreasing with X), but not to the bathymetric features. Changes in overall bacterial community structure could be related to changes in both bathymetry and geographic locations, yet we were unable to determine which environmental variables were explaining these spatial community patterns.

By comparing the effects of each investigated parameter, environmental factors (T, SD, MC) always explained more of biological variation than combined spatial variables (X, Y, WD), in total cell numbers, OTU number, and beta-diversity. This is consistent with a recently published review on the current knowledge about what processes influence the distribution of microbes, and the percentages of total explained variation in our study are comparable to the overall reported mean of 50% across studies (Hanson et al., 2012). It should be noted that, because not all selective environmental variables can be assessed in field studies, and especially their past temporal variation remains unknown, pure spatial effects on community structure may be potentially overestimated (Cottenie, 2005; Hanson et al., 2012). Interpreted within a metacommunity ecology framework (Leibold et al., 2004), our findings overall suggest that Guaymas bacterial communities are subjected to a combination of species sorting (i.e., to dispersal associated with niche differentiation) and of mass effect (i.e., dispersal effects through source-sink relationships).

#### CONCLUSION

Guaymas Basin hydrothermal sediment bacterial communities displayed a high variation in community richness and activity on small spatial scales. Community activity, abundance and richness declined substantially with increasing temperature, indicating that only few microbial types of the core community of the investigated vent field were adapted to populate deep hot sediments at temperatures >10°C and higher (Figure S7). However, community similarity was high across the different temperature regimes and habitat types sampled, and across the entire range of temperature regimes—from normal deep-sea settings to the predicted limits of life >120°C—only few unique microbial types were detected. This is best explained by the scenario of connected bacterial habitats, where temporary disturbances by the upward expulsion of hot fluids can locally decrease cell activity, biomass and diversity, and where a repopulation occurs by a diverse, eurythermic and more stable surface community of the highly

reduced Guaymas sediments. Besides temperature and sediment depth, the presence of microbial mats, local bathymetry and spatial orientation in the vent field also showed significant effects on community richness and composition, but due to the complexity of the vent field, no distinct spatial gradient was detected, indicative of active but chaotic upward venting in space and time. Bacterial habitats seemed highly interconnected across the investigated vent area, which may be a consequence of dynamically fluctuating temperatures and biogeochemical factors.

## ACKNOWLEDGMENTS

For their excellent support at sea we would like to thank the scientific team and crews of R/V *Atlantis* (Expedition AT15-40) and the *Alvin* submersible (operated by Woods Hole Oceanographic

Institution, Woods Hole, MA). We thank Barbara MacGregor for meticulous record keeping on Guaymas sediment cores. Further, we acknowledge the help by Susanne Menger, Rafael Stiens, Daniel Santillano, Erika Weiz and Janine Felden during sampling as well as subsequent analyses. This study has been funded by NSF (Biological Oceanography grant OCE 0647633), as well as by the Leibniz program of the DFG to Antje Boetius, the MARUM Excellence Cluster and the Max Planck Society.

## SUPPLEMENTARY MATERIAL

The Supplementary Material for this article can be found online at: [http://www.frontiersin.org/Extreme\\_Microbiology/10.3389/fmicb.2013.00207/abstract](http://www.frontiersin.org/Extreme_Microbiology/10.3389/fmicb.2013.00207/abstract)

## REFERENCES

- Baker, B. J., Lesniewski, R. A., and Dick, G. J. (2012). Genome-enabled transcriptomics reveals archaeal populations that drive nitrification in a deep-sea hydrothermal plume. *ISME J.* 6, 2269–2279. doi: 10.1038/ismej.2012.64
- Bazylinski, D. A., Farrington, J. W., and Jannasch, H. W. (1988). Hydrocarbons in surface sediments from a Guaymas Basin hydrothermal vent site. *Org. Geochem.* 12, 547–558. doi: 10.1016/0146-6380(88)90146-5
- Biddle, J. F., Cardman, Z., Mendlovitz, H., Albert, D. B., Lloyd, K. G., Boetius, A., et al. (2012). Anaerobic oxidation of methane at different temperature regimes in Guaymas Basin hydrothermal sediments. *ISME J.* 6, 1018–1031. doi: 10.1038/ismej.2011.164
- Boetius, A., and Lohse, K. (1996). Effect of organic enrichments on hydrolytic potentials and growth of bacteria in deep-sea sediments. *Mar. Ecol. Prog. Ser.* 140, 239–250. doi: 10.3354/meps140239
- Bordard, D., Legendre, P., and Drapeau, P. (1992). Partitioning out the spatial component of ecological variation. *Ecology* 73, 1045–1055. doi: 10.2307/1940179
- Bowles, M. W., Nigro, L. M., Teske, A. P., and Joye, S. B. (2012). Denitrification and environmental factors influencing nitrate removal in Guaymas Basin hydrothermally altered sediments. *Front. Microbiol.* 3:377. doi: 10.3389/fmicb.2012.00377
- Brown, M. V., Schwalbach, M. S., Hewson, I., and Fuhrman, J. A. (2005). Coupling 16S-ITS rDNA clone libraries and automated ribosomal intergenic spacer analysis to show marine microbial diversity: development and application to a time series. *Environ. Microbiol.* 7, 1466–1479. doi: 10.1111/j.1462-2920.2005.00835.x
- Cardinale, M., Brusetti, L., Quatrini, P., Borin, S., Puglia, A. M., Rizzi, A., et al. (2004). Comparison of different primer sets for use in automated ribosomal intergenic spacer analysis of complex bacterial communities. *Appl. Environ. Microbiol.* 70, 6147–6156. doi: 10.1128/AEM.70.10.6147-6156.2004
- Cottenie, K. (2005). Integrating environmental and spatial processes in ecological community dynamics. *Ecol. Lett.* 8, 1175–1182. doi: 10.1111/j.1461-0248.2005.00820.x
- Dhillon, A., Lever, M., Lloyd, K. G., Albert, D. B., Sogin, M. L., and Teske, A. (2005). Methanogen diversity evidenced by molecular characterization of Methyl Coenzyme M Reductase A (*mcrA*) genes in hydrothermal sediments of the Guaymas Basin. *Appl. Environ. Microbiol.* 71, 4592–4601. doi: 10.1128/AEM.71.8.4592-4601.2005
- Dhillon, A., Teske, A., Dillon, J., Stahl, D. A., and Sogin, M. L. (2003). Molecular characterization of sulfate-reducing bacteria in the Guaymas Basin. *Appl. Environ. Microbiol.* 69, 2765–2772. doi: 10.1128/AEM.69.5.2765-2772.2003
- Edgcomb, V. P., Kysela, D. T., Teske, A., Gomez, A. D. V., and Sogin, M. L. (2002). Benthic eukaryotic diversity in the Guaymas Basin hydrothermal vent environment. *Proc. Natl. Acad. Sci. U.S.A.* 99, 7658–7662. doi: 10.1073/pnas.062186399
- Edgcomb, V. P., Molyneaux, S. J., Saito, M. A., Lloyd, K., Böer, S., Wirsen, C. O., et al. (2004). Sulfide ameliorates metal toxicity for deep-sea hydrothermal vent Archaea. *Appl. Environ. Microbiol.* 70, 2551–2555. doi: 10.1128/AEM.70.4.2551-2555.2004
- Elsgaard, L., Isaksen, M. F., Jørgensen, B. B., Alayse, A. M., and Jannasch, H. W. (1994). Microbial sulfate reduction in deep-sea sediments at the Guaymas Basin hydrothermal vent area: influence of temperature and substrates. *Geochim. Cosmochim. Acta* 58, 3335–3343. doi: 10.1016/0016-7037(94)90089-2
- Felden, J., Wenzhöfer, F., Feseker, T., and Boetius, A. (2010). Transport and consumption of oxygen and methane in different habitats of the Håkon Mosby Mud Volcano (HMMV). *Limnol. Oceanogr.* 55, 2366–2380. doi: 10.4319/lo.2010.55.6.2366
- Fuhrman, J. A., Steele, J. A., Hewson, I., Schwalbach, M. S., Brown, M. V., Green, J. L., et al. (2008). A latitudinal diversity gradient in planktonic marine bacteria. *Proc. Natl. Acad. Sci. U.S.A.* 105, 7774–7778. doi: 10.1073/pnas.0803070105
- Grönke, S., Felden, J., Lütschlag, A., Girnth, A.-C., De Beer, D., Wenzhöfer, F., et al. (2011). Niche differentiation among mat-forming, sulfide-oxidizing bacteria at cold seeps of the Nile Deep Sea Fan (Eastern Mediterranean Sea). *Geobiology* 9, 330–348. doi: 10.1111/j.1472-4669.2011.00281.x
- Grönke, S., Lütschlag, A., De Beer, D., Felden, J., Salman, V., Ramette, A., et al. (2012). Mats of psychrophilic thiotrophic bacteria associated with cold seeps of the Barents Sea. *Biogeosciences* 9, 2947–2960. doi: 10.5194/bg-9-2947-2012
- Guezennec, J. G., Dussauze, J., Bian, M., Rocchiccioli, F., Ringelberg, D., Hedrick, D. B., et al. (1996). Bacterial community structure in sediments from Guaymas basin, Gulf of California, as determined by analysis of phospholipid ester-linked fatty acids. *J. Mar. Biotechnol.* 4, 165–175.
- Gundersen, J. K., Jørgensen, B. B., Larsen, E., and Jannasch, H. W. (1992). Mats of giant sulphur bacteria on deep-sea sediments due to fluctuating hydrothermal flow. *Nature* 360, 454–456. doi: 10.1038/360454a0
- Hanson, C. A., Fuhrman, J. A., Horner-Devine, M. C., and Martiny, J. B. H. (2012). Beyond biogeographic patterns: processes shaping the microbial landscape. *Nat. Rev. Microbiol.* 10, 497–506.
- Holler, T., Widdel, F., Knittel, K., Amann, R., Kellermann, M. Y., Hinrichs, K.-U., et al. (2011). Thermophilic anaerobic oxidation of methane by marine microbial consortia. *ISME J.* 5, 1946–1956. doi: 10.1038/ismej.2011.77
- Hughes Martiny, J. B., Bohannan, B. J. M., Brown, J. H., Colwell, R. K., Fuhrman, J. A., Green, J. L., et al. (2006). Microbial biogeography: putting microorganisms on the map. *Nat. Rev. Microbiol.* 4, 102–112. doi: 10.1038/nrmicro1341
- Jannasch, H. W., Nelson, D. C., and Wirsen, C. O. (1989). Massive natural occurrence of unusually large bacteria (*Beggiatoa* sp.) at a hydrothermal deep-sea vent site. *Nature* 342, 834–836. doi: 10.1038/342834a0
- Jørgensen, B. B. (1978). A comparison of methods for the quantification of bacterial sulfate reduction in coastal marine sediments. *Geomicrobiol. J.* 1, 29–47. doi: 10.1080/01490457809377722
- Kallmeyer, J., and Boetius, A. (2004). Effects of temperature and pressure on sulfate reduction and anaerobic oxidation of methane in hydrothermal sediments of Guaymas Basin. *Appl. Environ. Microbiol.* 70, 1231–1233. doi: 10.1128/AEM.70.2.1231-1233.2004
- Kallmeyer, J., Ferdelman, T. G., Weber, A., Fossing, H., and Jørgensen, B. B. (2007). Bacterial sulfate reduction in Guaymas Basin hydrothermal sediments. *Geobiology* 5, 330–348. doi: 10.1111/j.1472-4669.2007.00281.x

- B. B. (2004). A cold chromium distillation procedure for radio-labeled sulfide applied to sulfate reduction measurements. *Limnol. Oceanogr. Meth.* 2, 171–180. doi: 10.4319/lom.2004.2.171
- Kojima, H., Koizumi, Y., and Fukui, M. (2006). Community structure of bacteria associated with sheaths of freshwater and brackish *Thioploca* species. *Microb. Ecol.* 52, 765–773. doi: 10.1007/s00248-006-9127-8
- Kysela, D. T., Palacios, C., and Sogin, M. L. (2005). Serial analysis of V6 ribosomal sequence tags (SARST-V6): a method for efficient, high-throughput analysis of microbial community composition. *Environ. Microbiol.* 7, 356–364. doi: 10.1111/j.1462-2920.2004.00712.x
- Legendre, P., and Legendre, L. (1998). *Numerical Ecology*. Amsterdam: Elsevier Science BV.
- Leibold, M. A., Holyoak, M., Mouquet, N., Amarasekare, P., Chase, J. M., Hoopes, M. F., et al. (2004). The metacommunity concept: a framework for multi-scale community ecology. *Ecol. Lett.* 7, 601–613. doi: 10.1111/j.1461-0248.2004.00608.x
- Levin, L. A., and Dayton, P. K. (2009). Ecological theory and continental margins: where shallow meets deep. *Trends Ecol. Evol.* 24, 606–617. doi: 10.1016/j.tree.2009.04.012
- Lichtschlag, A., Felden, J., Brüchert, V., Boetius, A., and De Beer, D. (2010). Geochemical processes and chemosynthetic primary production in different thiotrophic mats of the Håkon Mosby mud volcano (Barents Sea). *Limnol. Oceanogr.* 55, 931–949. doi: 10.4319/lo.2009.55.2.0931
- Lloyd, K. G., Albert, D. B., Biddle, J. F., Chanton, J. P., Pizarro, O., and Teske, A. (2010). Spatial structure and activity of sedimentary microbial communities underlying a *Beggiatoa* spp. mat in a Gulf of Mexico hydrocarbon seep. *PLoS ONE* 5:e8738. doi: 10.1371/journal.pone.0008738
- Lloyd, K. G., Edgcomb, V. P., Molyneaux, S. J., Böer, S., Wirsén, C. O., Atkins, M. S., et al. (2005). Effect of dissolved sulfide, pH, and temperature on the growth and survival of marine hyperthermophilic archaea. *Appl. Environ. Microbiol.* 71, 6383–6387. doi: 10.1128/AEM.71.10.6383-6387.2005
- Lösekann, T., Knittel, K., Nadalig, T., Fuchs, B., Niemann, H., Boetius, A., et al. (2007). Diversity and abundance of aerobic and anaerobic methane oxidizers at the Haakon Mosby Mud Volcano, Barents Sea. *Appl. Environ. Microbiol.* 73, 3348–3362. doi: 10.1128/AEM.00016-07
- Martens, C. S. (1990). Generation of short chain acid anions in hydrothermally altered sediments of the Guaymas Basin, Gulf of California. *Appl. Geochem.* 5, 71–76. doi: 10.1016/0883-2927(90)90037-6
- McKay, L. J., MacGregor, B. J., Biddle, J. F., Albert, D. B., Mendlovitz, H. P., Hoer, D. R., et al. (2012). Spatial heterogeneity and underlying geochemistry of phylogenetically diverse orange and white *Beggiatoa* mats in Guaymas Basin hydrothermal sediments. *Deep-Sea Res. Part I* 67, 21–31. doi: 10.1016/j.dsr.2012.04.011
- Mével, G., Faidy, C., and Prieur, D. (1996). Distribution, activity, and diversity of heterotrophic nitrifiers originating from East Pacific deep-sea hydrothermal vents. *Can. J. Microbiol.* 42, 162–171. doi: 10.1139/m96-024
- Meyer-Reil, L.-A. (1983). Benthic response to sedimentation events during autumn to spring at a shallow water station in the Western Kiel Bight. *Mar. Biol.* 77, 247–256. doi: 10.1007/BF00395813
- Nelson, D. C., Wirsén, C. O., and Jannasch, H. W. (1989). Characterization of large, autotrophic *Beggiatoa* spp. abundant at hydrothermal vents of the Guaymas Basin. *Appl. Environ. Microbiol.* 55, 2909–2917.
- Nocker, A., Burr, M., and Camper, A. K. (2007). Genotypic microbial community profiling: a critical technical review. *Microb. Ecol.* 54, 276–289. doi: 10.1007/s00248-006-9199-5
- Paull, C. K., Ussler III, W., Peltzer, E. T., Brewer, P. G., Keaten, R., Mitts, P. J., et al. (2007). Authigenic carbon entombed in methane-soaked sediments from the northeastern transform margin of the Guaymas Basin, Gulf of California. *Deep-Sea Res. Part II* 54, 1240–1267. doi: 10.1016/j.dsr2.2007.04.009
- Pop Ristova, P., Wenzhöfer, F., Ramette, A., Zabel, M., Fischer, D., Kasten, S., et al. (2012). Bacterial diversity and biogeochemistry of different chemosynthetic habitats of the REGAB cold seep (West African margin, 3160 m water depth). *Biogeosciences* 9, 5031–5048. doi: 10.5194/bg-9-5031-2012
- Prokopenko, M. G., Hammond, D. E., Berelson, W. M., Bernhard, J. M., Stott, L., and Douglas, R. (2006). Nitrogen cycling in the sediments of Santa Barbara basin and Eastern Subtropical North Pacific: nitrogen isotopes, diagenesis and possible chemosymbiosis between two lithotrophs (*Thioploca* and *Anammox*) – “riding on a glider.” *Earth Planet. Sci. Lett.* 242, 186–204. doi: 10.1016/j.epsl.2005.11.044
- Ramette, A. (2007). Multivariate analysis in microbial ecology. *FEMS Microbiol. Ecol.* 62, 142–160. doi: 10.1111/j.1574-6941.2007.00375.x
- Ramette, A. (2009). Quantitative community fingerprinting methods for estimating the abundance of operational taxonomic units in natural microbial communities. *Appl. Environ. Microbiol.* 75, 2495–2505. doi: 10.1128/AEM.02409-08
- Ramette, A., and Tiedje, J. M. (2007a). Biogeography: an emerging cornerstone for understanding prokaryotic diversity, ecology, and evolution. *Microb. Ecol.* 53, 197–207. doi: 10.1007/s00248-005-5010-2
- Ramette, A., and Tiedje, J. M. (2007b). Multiscale responses of microbial life to spatial distance and environmental heterogeneity in a patchy ecosystem. *Proc. Natl. Acad. Sci. U.S.A.* 104, 2761–2766. doi: 10.1073/pnas.0610671104
- Simoneit, B. R. T., and Lonsdale, P. F. (1982). Hydrothermal petroleum in mineralized mounds at the seabed of Guaymas Basin. *Nature* 295, 198–202. doi: 10.1038/295198a0
- Teske, A. (2010). “Sulfate-reducing and methanogenic hydrocarbon-oxidizing microbial communities in the marine environment,” in *Handbook of Hydrocarbon and Lipid Microbiology, Part 21*, ed K. N. Timmis (Berlin, Heidelberg: Springer), 2203–2223. doi: 10.1007/978-3-540-77587-4\_160
- Teske, A., Dhillon, A., and Sogin, M. S. (2003). Genomic Markers of ancient anaerobic microbial pathways: sulfate reduction, methanogenesis, and methane oxidation. *Biol. Bull.* 204, 186–191. doi: 10.2307/1543556
- Teske, A., Hinrichs, K.-U., Edgcomb, V., Gomez, A. D. V., Kysela, D., Sylva, S. P., et al. (2002). Microbial diversity of hydrothermal sediments in the Guaymas Basin: evidence for anaerobic methanotrophic communities. *Appl. Environ. Microbiol.* 68, 1994–2007. doi: 10.1128/AEM.68.4.1994-2007.2002
- Teske, A., Jørgensen, B. B., and Gallardo, V. A. (2009). Filamentous bacteria inhabiting the sheaths of marine *Thioploca* spp. on the Chilean continental shelf. *FEMS Microbiol. Ecol.* 68, 164–172. doi: 10.1111/j.1574-6941.2009.00659.x
- Van Gaever, S., Moodley, L., De Beer, D., and Vanreusel, A. (2006). Meiobenthos at the arctic Håkon Mosby Mud Volcano, with a parental-caring nematode thriving in sulfide-rich sediments. *Mar. Ecol. Prog. Ser.* 321, 143–155. doi: 10.3354/meps321143
- Von Damm, K. L., Edmond, J. M., Measures, C. I., and Grant, B. (1985). Chemistry of submarine hydrothermal solutions at Guaymas Basin, Gulf of California. *Geochim. Cosmochim. Acta* 49, 2221–2237. doi: 10.1016/0016-7037(85)90223-6
- Weber, A., and Jørgensen, B. B. (2002). Bacterial sulfate reduction in hydrothermal sediments of the Guaymas Basin, Gulf of California, Mexico. *Deep-Sea Res. Part I* 49, 827–841. doi: 10.1016/S0967-0637(01)00079-6
- Welhan, J. A., and Lupton, J. E. (1987). Light hydrocarbon gases in Guaymas Basin hydrothermal fluids: thermogenic versus abiogenic origin. *AAPG Bull.* 71, 215–223.
- Zinger, L., Amaral-Zettler, L. A., Fuhrman, J. A., Horner-Devine, M. C., Huse, S. M., Welch, D. B. M., et al. (2011). Global patterns of bacterial beta-diversity in seafloor and seawater ecosystems. *PLoS ONE* 6:e24570. doi: 10.1371/journal.pone.0024570

**Conflict of Interest Statement:** The authors declare that the research was conducted in the absence of any commercial or financial relationships that could be construed as a potential conflict of interest.

**Received:** 25 March 2013; **accepted:** 05 July 2013; **published online:** 25 July 2013. **Citation:** Meyer S, Wegener G, Lloyd KG, Teske A, Boetius A and Ramette A (2013) Microbial habitat connectivity across spatial scales and hydrothermal temperature gradients at Guaymas Basin. *Front. Microbiol.* 4:207. doi: 10.3389/fmicb.2013.00207

This article was submitted to Frontiers in Extreme Microbiology, a specialty of Frontiers in Microbiology.

Copyright © 2013 Meyer, Wegener, Lloyd, Teske, Boetius and Ramette. This is an open-access article distributed under the terms of the Creative Commons Attribution License, which permits use, distribution and reproduction in other forums, provided the original authors and source are credited and subject to any copyright notices concerning any third-party graphics etc.



# Biogeography of *Persephonella* in deep-sea hydrothermal vents of the Western Pacific

Sayaka Mino<sup>1\*</sup>, Hiroko Makita<sup>2</sup>, Tomohiro Toki<sup>3</sup>, Junichi Miyazaki<sup>2</sup>, Shingo Kato<sup>4</sup>, Hiromi Watanabe<sup>5</sup>, Hiroyuki Imachi<sup>2</sup>, Tomo-o Watsujii<sup>2</sup>, Takuro Nunoura<sup>2</sup>, Shigeaki Kojima<sup>6</sup>, Tomoo Sawabe<sup>1</sup>, Ken Takai<sup>2</sup> and Satoshi Nakagawa<sup>1,2</sup>

<sup>1</sup> Laboratory of Microbiology, Faculty of Fisheries Sciences, Hokkaido University, Hakodate, Japan

<sup>2</sup> Subsurface Geobiology Advanced Research Project, Institute of Biogeosciences, Japan Agency for Marine-Earth Science and Technology, Yokosuka, Japan

<sup>3</sup> Department of Chemistry, Biology, and Marine Science, Faculty of Science, University of the Ryukyus, Nishihara, Okinawa, Japan

<sup>4</sup> Japan Collection of Microorganisms, RIKEN BioResource Center, Tsukuba, Japan

<sup>5</sup> Marine Biodiversity Research Program, Japan Agency for Marine-Earth Science and Technology, Yokosuka, Japan

<sup>6</sup> Department of Marine Ecosystem Dynamics, Atmosphere and Ocean Research Institute, The University of Tokyo, Kashiwa, Japan

## Edited by:

Anna-Louise Reysenbach, Portland State University, USA

## Reviewed by:

Barbara J. Campbell, University of Delaware, USA

Elizaveta Bonch-Osmolovskaya, Winogradsky Institute of Microbiology, Russian Academy of Sciences, Russia

## \*Correspondence:

Sayaka Mino, Laboratory of Microbiology, Faculty of Fisheries Sciences, Hokkaido University, 3-1-1, Minato-cho, Hakodate 041-8611, Japan.

e-mail: mino@ec.hokudai.ac.jp

Deep-sea hydrothermal vent fields are areas on the seafloor with high biological productivity fueled by microbial chemosynthesis. Members of the *Aquificales* genus *Persephonella* are obligately chemosynthetic bacteria, and appear to be key players in carbon, sulfur, and nitrogen cycles in high temperature habitats at deep-sea vents. Although this group of bacteria has cosmopolitan distribution in deep-sea hydrothermal ecosystem around the world, little is known about their population structure such as intraspecific genomic diversity, distribution pattern, and phenotypic diversity. We developed the multi-locus sequence analysis (MLSA) scheme for their genomic characterization. Sequence variation was determined in five housekeeping genes and one functional gene of 36 *Persephonella hydrogeniphila* strains originated from the Okinawa Trough and the South Mariana Trough (SNT). Although the strains share >98.7% similarities in 16S rRNA gene sequences, MLSA revealed 35 different sequence types (ST), indicating their extensive genomic diversity. A phylogenetic tree inferred from all concatenated gene sequences revealed the clustering of isolates according to the geographic origin. In addition, the phenotypic clustering pattern inferred from whole-cell matrix-assisted laser desorption ionization-time of flight mass spectrometry (MALDI-TOF/MS) analysis can be correlated to their MLSA clustering pattern. This study represents the first MLSA combined with phenotypic analysis indicative of allopatric speciation of deep-sea hydrothermal vent bacteria.

**Keywords:** population structure, biogeography, deep-sea hydrothermal vent, *Persephonella*, *Aquificales*, MLSA, MALDI-TOF/MS, chemolithoautotroph

## INTRODUCTION

Mixing of hydrothermal fluids and ambient seawater at the seafloor creates physically and chemically dynamic habitats for microorganisms. Vent fluids physicochemistry is variable both spatially and temporally as a result of subsurface geological and geochemical processes (Edmond et al., 1979; Butterfield and Massoth, 1994; Butterfield et al., 2004). Diverse microorganisms including both Archaea and Bacteria have been isolated in pure cultures from various hydrothermal fields (Nakagawa and Takai, 2006). In addition, culture-independent studies revealed the dominance of yet-to-be cultured microorganisms in deep-sea hydrothermal environments (Haddad et al., 1995; Takai and Horikoshi, 1999; Reysenbach et al., 2000; Corre, 2001; Teske et al., 2002), and provided insight into the great heterogeneity of microbial communities between hydrothermal systems. The heterogeneity can be correlated to differences in the geological and chemical properties between different vents (Takai et al., 2004; Nakagawa et al., 2005a,b; Takai and Nakamura, 2011). On the other hand, there are also some cosmopolitan

genera found in deep-sea hydrothermal systems occurring not only in the Mid-Ocean Ridge systems but in the Back-Arc Basin systems and the Volcanic Arc systems (Takai et al., 2006; Nakagawa and Takai, 2008; Kaye et al., 2011). Members of the genus *Persephonella* belonging to the order *Aquificales*, obligately sulfur- and/or hydrogen-oxidizing, chemoautotrophic, thermophilic bacteria, are widely distributed in deep-sea hydrothermal systems (Reysenbach et al., 2000, 2002; Takai et al., 2004; Nakagawa et al., 2005a,b; Ferrera et al., 2007; Takai et al., 2008). Although the widespread occurrence of this group suggests that they may play important role, many questions remained about their physiology, metabolism, and ecology within the environment because of the difficulty in isolating these strains. Some isolates have been characterized (Götz et al., 2002; Nakagawa et al., 2003), and implied their role in carbon, sulfur and nitrogen cycles in high temperature habitats at deep-sea vents (Reysenbach et al., 2002; Ferrera et al., 2007). However, little is known about the spatial or biogeographical pattern of *Persephonella* microdiversity and phenotypic heterogeneity.

Weak biogeographical signals in microbial communities are usually explained by the hypothesis of microbial cosmopolitanism formulated by Bass Becking (Wit and Bouvier, 2006). However, recent studies have explored the effects of dispersal limitation on microbial biogeography. Like macroorganisms, the genetic similarity negatively correlated with geographic distance, i.e., distance-decay relationship, have been reported for cyanobacteria, sulfate-reducing bacteria, marine planktonic bacteria, and hyperthermophilic archaea (Papke et al., 2003; Whitaker et al., 2003; Vergin et al., 2007; Oakley et al., 2010). In addition, the biogeographical diversity pattern was reported in detail for members of the “deep-sea hydrothermal vent euryarchaeota 2” (Flores et al., 2012). Microbial biogeographical studies have been usually based solely on genetic data. Microbial biogeography was recently

studied at the phenotypic level (Rosselló-Mora et al., 2008), however, genetic and phenotypic correlation has not been explored. We investigated the spatial diversity pattern of *Persephonella* population by the combined use of comparative genetic and phenotypic characterizations.

## MATERIALS AND METHODS

### FIELD SITE AND SAMPLING

Samples, i.e., chimney structures, fluids, and sediments, were collected with R/V Natsushima and ROV Hyper-Dolphin or R/V Yokosuka and DSV Shinkai 6500 from the Okinawa Trough (OT) in 2007 and 2009, or the South Mariana Trough (SMT) in 2010 (**Table 1**). Vent fluids from the OT are characteristic in the high contents of methane and carbon dioxide (Kawagucci et al., 2011).

**Table 1 | Information of samples and cultivation temperature.**

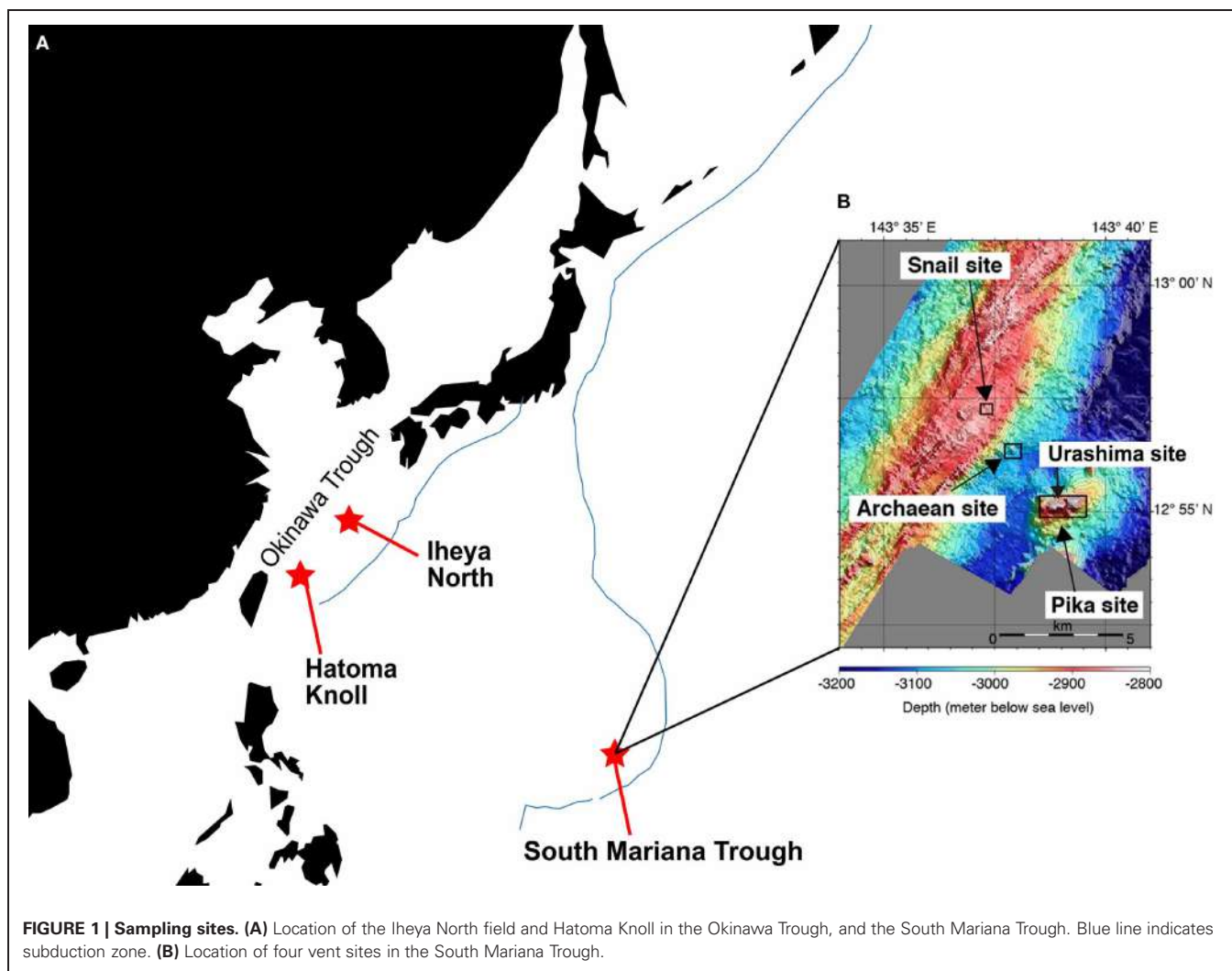
| Strains | Originated samples | Origins          | Sodium sulfide | Isolated temperature (°C) | Sequence similarity to <i>P. hydrogeniphila</i> 29W <sup>T</sup> (%) |
|---------|--------------------|------------------|----------------|---------------------------|--|
| OT-1    | CS                 | Iheya North, OT  | +              | 55                        | 99.7   |
| OT-2    | CS                 | Iheya North, OT  | -              | 55                        | 99.6   |
| OT-3    | CI                 | Iheya North, OT  | +              | 55                        | 98.9   |
| OT-4    | CS                 | Iheya North, OT  | -              | 55                        | 99.6   |
| OT-5    | CS                 | Hatoma Knoll, OT | -              | 55                        | 99.7   |
| MT-6    | CI                 | Urashima, SMT    | -              | 55                        | 99.6   |
| MT-7    | CI                 | Urashima, SMT    | +              | 55                        | 99.5   |
| MT-8    | CS                 | Urashima, SMT    | -              | 55                        | 99.5   |
| MT-9    | CS                 | Urashima, SMT    | +              | 55                        | 99.5   |
| MT-10   | CI                 | Urashima, SMT    | +              | 55                        | 99.7   |
| MT-11   | CA                 | Urashima, SMT    | +              | 55                        | 99.5   |
| MT-12   | CS                 | Urashima, SMT    | +              | 55                        | 99.5   |
| MT-13   | CI                 | Urashima, SMT    | -              | 47                        | 99.6   |
| MT-14   | CS                 | Urashima, SMT    | +              | 47                        | 99.5   |
| MT-15   | CS                 | Urashima, SMT    | +              | 70                        | 99.5   |
| MT-16   | CI                 | Urashima, SMT    | -              | 70                        | 99.6   |
| MT-17   | CS                 | Urashima, SMT    | -              | 55                        | 99.6   |
| MT-18   | CS                 | Urashima, SMT    | +              | 55                        | 99.5   |
| MT-19   | CA                 | Urashima, SMT    | +              | 55                        | 98.7   |
| MT-20   | CA                 | Urashima, SMT    | +              | 47                        | 98.7   |
| MT-21   | CA                 | Urashima, SMT    | +              | 70                        | 99.5   |
| MT-22   | SE                 | Snail, SMT       | -              | 55                        | 99.5   |
| MT-23   | HR                 | Snail, SMT       | -              | 55                        | 99.5   |
| MT-24   | HR                 | Snail, SMT       | +              | 55                        | 99.6   |
| MT-25   | CS                 | Archaean, SMT    | -              | 55                        | 98.7   |
| MT-26   | CI                 | Archaean, SMT    | +              | 55                        | 98.7   |
| MT-27   | CA                 | Archaean, SMT    | -              | 55                        | 99.5   |
| MT-28   | CS                 | Archaean, SMT    | -              | 55                        | 99.7   |
| MT-29   | BS                 | Archaean, SMT    | -              | 55                        | 99.5   |
| MT-30   | FW                 | Archaean, SMT    | -              | 55                        | 99.5   |
| MT-31   | CS                 | Archaean, SMT    | -              | 55                        | 99.5   |
| MT-32   | CS                 | Archaean, SMT    | +              | 55                        | 99.6   |
| MT-33   | CA                 | Archaean, SMT    | -              | 55                        | 99.7   |
| MT-34   | CS                 | Archaean, SMT    | -              | 47                        | 99.5   |
| MT-35   | CS                 | Pika, SMT        | -              | 55                        | 99.5   |
| MT-36   | CI                 | Pika, SMT        | +              | 55                        | 99.5   |

CS, chimney surface; CI, chimney inside parts; CA, all of chimney; SE, sediment sample; HR, rock influenced by vent fluids; FS, fluid sample; BS, biological sample; +, presence of sodium sulfide; -, absence of sodium sulfide. Sequence similarity was based on 16S rRNA gene sequences of each strain.

Among the OT hydrothermal fields, this study focused on the Iheya North and Hatoma Knoll (**Figure 1**). In the SMT, four vent sites were studied (**Figure 1**). The Archaean site is located at a ridge flank, about 2 km apart from the backarc-spreading axis. Discharging fluids ( $T_{\max} = 318^{\circ}\text{C}$ ) was acidic and depleted in  $\text{Cl}^-$  ( $\text{Cl}^- = 401 \text{ mM}$ ) (Ishibashi et al., 2006). Pika site is located on an off-axis knoll, about 5 km from the axis. Fluid chemistry ( $T_{\max} = 330^{\circ}\text{C}$ ) of Pika site showed brine-rich signature ( $\text{Cl}^- = 600 \text{ mM}$ ) (Ishibashi et al., 2006). Urashima site is newly discovered in 2010, and located at the northern foot of the western peak of the same knoll as Pika. Snail site is located on the active backarc-spreading axis. After retrieval on board, each of the chimney structures were sectioned immediately into the exterior surface and the inside parts, and slurried with 25 ml of sterilized seawater in the presence or absence of 0.05% (w/v) neutralized sodium sulfide in 100 ml glass bottles (Schott Glaswerke, Mainz, Germany). Bottles were then tightly sealed with butyl rubber caps under a gas phase of 100%  $\text{N}_2$  (0.2 MPa). Similarly, fluid, sediment, and biological samples were prepared anaerobically in 10 ml glass bottles. Samples were stored at  $4^{\circ}\text{C}$  until use.

#### ENRICHMENT, ISOLATION, AND PHYLOGENETIC ANALYSIS

Serial dilution cultures were performed using the MMJHS medium (Takai et al., 2003) containing a mixture of electron donors and electron acceptors for hydrogen/sulfur-oxidizing chemoautotrophs at 47, 55 and  $70^{\circ}\text{C}$ . MMJHS medium included 1 g each of  $\text{NaHCO}_3$ ,  $\text{Na}_2\text{S}_2\text{O}_3 \cdot 5\text{H}_2\text{O}$ , and  $\text{NaNO}_3$ , 10 g of  $\text{S}^0$  and 10 ml vitamin solution (Balch et al., 1979) per liter of MJ synthetic seawater [gas phase: 80%  $\text{H}_2$  + 20%  $\text{CO}_2$  (0.3 MPa)]. To obtain pure cultures, dilution-to-extinction was repeated at least 2 times (Baross, 1995). The purity was confirmed routinely by microscopic examination and by sequencing of the 16S rRNA gene using several PCR primers. Genomic DNA was extracted from isolates using the UltraClean Microbial DNA isolation Kit (MoBio Laboratories, Inc., Solana Beach, CA, USA) following the manufacturer's protocol. The 16S rRNA gene of each isolate was amplified by PCR using LA Taq polymerase (TaKaRa Bio, Otsu, Japan) as described previously (Takai et al., 2001). The primers used were Eubac 27F and 1492R (Weisburg et al., 1991). These amplicons were bidirectionally determined by the dideoxynucleotide chain-termination method. Almost complete sequences of the 16S rRNA gene were assembled using Sequencher ver 4.8.



(Gene Codes Corporation, Ann Arbor, MI, USA). In order to determine the phylogenetic positions of isolates, the sequences were aligned using Greengenes NAST alignment tool (DeSantis et al., 2006), and compiled using ARB software version 03.08.22 (Ludwig et al., 2004).

#### MULTI-LOCUS SEQUENCE ANALYSIS

Intraspecies diversity among isolates was evaluated using multi-locus sequence analysis [MLSA; formerly called multilocus sequence typing (MLST)] technique (Gevers et al., 2005). MLSA represents a universal and unambiguous method for strain genotyping, population genetics, and molecular evolutionary studies (Whitaker et al., 2005; Mazard et al., 2012). Genes selected for MLSA were *tkt* (transketolase), *atpA* (ATP synthase, A subunit), *dnaK* (Hsp 70 chaperon protein), *napA* (nitrate reductase, large subunit), *metG* (methionyl-tRNA synthetase), and *gyrB* (DNA gyrase, B subunit). Primers (**Table 2**) were designed according to the published complete genome sequences of *Aquificales* members, i.e., *Persephonella marina* EX-H1<sup>T</sup> (NC\_012439) (Reysenbach et al., 2009), *Sulfurihydrogenibium azorense* (NC\_012438) (Reysenbach et al., 2009), *Sulfurihydrogenibium* sp. YO3AOP1 (NC\_010730) (Reysenbach et al., 2009), *Hydrogenobaculum* sp. YO4AAS1 (NC\_011126) (Reysenbach et al., 2009), *Aquifex aeolicus* VF5 (NC\_000918) (Deckert et al., 1998), and *Hydrogenivirga* sp. 128-5-R1-1 (NZ\_ABHJ01000000) (Reysenbach et al., 2009). ClustalX version 2.0 was used for the alignment of nucleotide sequences (Larkin et al., 2007). PCR were performed under the following conditions: 96°C for 1 min, 35–38 cycles of 96°C for 20 s, annealing for 45 s at temperatures shown in **Table 2**, and 72°C for 2 min. The PCR products were confirmed by 1% agarose gel electrophoresis and purified with exonuclease I and shrimp alkaline

phosphatase. If necessary, bands were excised and purified using Wizard® SV Gel and PCR Clean-up System (Promega, Madison, WI, USA). Purified PCR products were used as templates for Sanger sequencing reaction. The sequences were assembled and edited using Sequencher ver 4.8, and aligned with ClustalX. The sequences were translated into amino acid using Transeq program (EMBOSS; European Molecular Biology Open Software Suite).

Z-test, non-synonymous (Ka)/synonymous (Ks) substitution, and Tajima's *D* test were performed as described elsewhere (Vergin et al., 2007). Briefly, values of Ka and Ks were determined using the software program SWAAP ver 1.0.3 (Pride, 2000), set to the Li method with a window size of 90 and step size of 18. Z-test was performed using MEGA ver 5.05 software (Tamura et al., 2011) with the following options: purifying selection, overall average, 1000 bootstrap replicates, pairwise deletion and the Pamilo–Bianchi–Li method. Tajima's *D* based on the total number of mutation were calculated using DnaSP ver 5 (Librado and Rozas, 2009). The combination of allele types for each isolate defined the sequence type (ST). Phylogenetic trees were constructed by the maximum likelihood (ML) method using MEGA ver 5.05. ML bootstrap support was computed after 100 reiterations. Split decomposition trees were constructed with SplitsTree ver 4 using the Neighbor-Net algorithm (Huson, 1998).

The levels of genetic variation within and between populations were calculated with the Arlequin ver 3.5 software (Excoffier and Lischer, 2010). *F<sub>ST</sub>* values were estimated for groups of two or more strains and were tested for significance against 1000 randomized bootstrap resamplings. Average pairwise genetic distance and standard error based on 500 bootstrap resamplings of each population were estimated using MEGA ver 5.05. Mantel test was performed with XLSTAT software ([www.xlstat.com](http://www.xlstat.com)). Sequences obtained in this study have

**Table 2 |** Primers and PCR conditions for MLSA.

| Genes       | Primer name | Primers (5'-3')        | Primer combination and annealing temperature (°C) | Amplicon size (bp) |
|-------------|-------------|------------------------|---|--------------------|
| <i>atpA</i> | atpA101F    | ADGTDGGWGAYGGTGYGC     | 101F-1081R: 55                                    | 980                |
|             | atpA1081R   | CGTTRATAGCWGGCTDATAACC |   |                    |
|             | atpA983R    | ACGTCACCBGCYTKWGTTC    | 101F-983R: 52                                     | 882                |
| <i>dnaK</i> | dnaK464F    | GDCARGCWACMAARGAYGC    | 55  | 741                |
|             | dnaK1118R   | GCMACWACYTCRTCDGG      |   |                    |
| <i>gyrB</i> | gyrB377F    | CTYCAYGGWGTWGGWGC      | 52  | 1186               |
|             | gyrB1563R   | TCWACRTCRGCRTCHGYCAT   |   |                    |
| <i>napA</i> | napA181F    | TTCTGTGGWACDGGWTGYGG   | 181F-1713R: 59                                    | 1532               |
|             | napA690F*   | ATGGCWGARATGCAYCC      |   |                    |
|             | napA1714R   | CKBGCHGCTTRATCCARTG    |   |                    |
|             | napA1347R*  | GRTTVAWWCCATTGTCCA     |   |                    |
| <i>metG</i> | metG145F    | ACRGGWACMGATGARCATGG   | 55  | 686                |
|             | metG831R    | GCDGGCCARTAWACDGYATG   |   |                    |
| <i>tkt</i>  | tkt478F     | AWSGSYGTRGGTATGGC      | 52  | 1063               |
|             | tkt1541R    | TGKGTwGGDCRCYTC        |   |                    |

\*Primers used for sequencing reaction.

been deposited in DDBJ/EMBL/GenBank under Accession No. AB773894-AB774147.

### GEOCHEMICAL ANALYSIS

Chemical compositions listed in **Table 6** were analyzed as previously described (Takai et al., 2008; Toki et al., 2008). End-member fluids compositions were estimated by the conventional method, that is extrapolation to  $Mg = 0$  of linear relationship of concentration of each species to Mg among the obtained samples (Von Damm et al., 1985).

### PREPARATION OF BACTERIAL SAMPLES FOR WHOLE-CELL MALDI-TOF/MS

Samples for whole-cell matrix-assisted laser desorption ionization-time of flight mass spectrometry (MALDI-TOF/MS) were prepared as described in Hazen et al. (2009). Briefly, *Persephonella* strains were cultured in 3 ml of MMJHS medium at their isolated temperatures (**Table 1**). Following incubation,

cells were washed once in 1 ml of 0.85% NaCl and twice in 1 ml of 50% ethanol at 4°C. Cell pellets were weighed and resuspended in 1% trifluoroacetic acid (TFA) to yield a final concentration of 0.2 mg cells/ $\mu$ l of 1% TFA. Equal volumes of the TFA bacterial suspension and the MALDI-TOF/MS matrix solution (10 mg/ml sinapinic acid in 50% acetonitrile, 50% water, and 0.1% TFA) were mixed in a microcentrifuge tube, and then 1.0  $\mu$ l of this mixture was spotted in triplicate on a stainless steel MALDI-TOF/MS sample plate (corresponding to approximately  $1.4 \times 10^8$  cells/spot). Samples were allowed to air dry before being loaded in the mass spectrometer.

### MALDI-TOF/MS AND DATA PROCESSING

All mass spectra were acquired using the MALDI-TOF/MS spectrometer (4700 proteomics analyzer; Applied Biosystems, Foster City, CA, USA) in the linear and positive-ion modes. The laser ( $N_2$ , 337 nm) intensity was set above the ion generation threshold. Mass spectra were recorded in the m/z range of 2000–14,000.

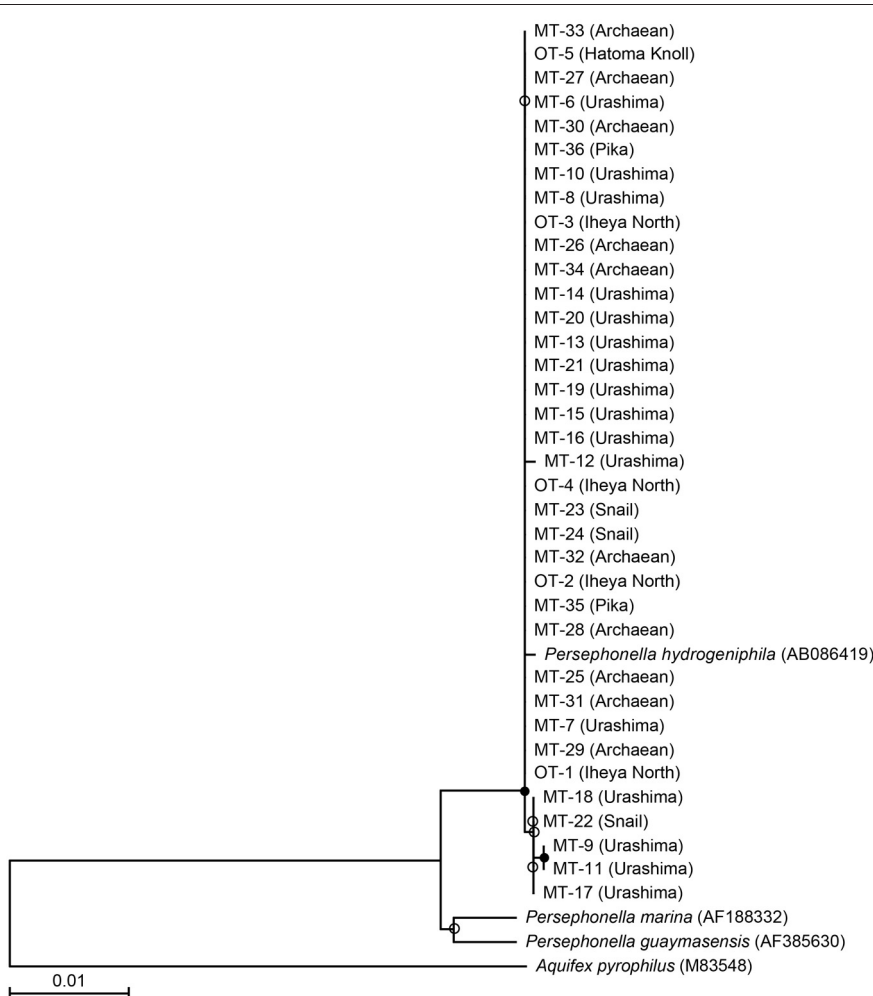


**FIGURE 2 |** Phylogenetic relationship of isolates and representative *Persephonella* species as determined by neighbor-joining analysis of 16S rRNA gene sequences. Tree was constructed by using 1119 sites that could be

unambiguously aligned. Origins of isolates and DDBJ accession numbers are shown in parentheses. Branch points conserved with bootstrap values of >75% (filled circle) and bootstrap value of 50–74% (open circles) are indicated.

**Table 3 | Genetic features at the six MLSA loci.**

| Gene        | Sequence length | Nucleoid identity | Amino acid identity | Ka/Ks           | Theta   | Z   | Tajima's D |
|-------------|-----------------|-------------------|---------------------|-----------------|---------|-----|------------|
| <i>tkt</i>  | 810             | 95.8 (6.5)        | 97.5 (4.12)         | 0.0131 (0.0215) | 0.05286 | 7.4 | -0.77603   |
| <i>atpA</i> | 669             | 96.3 (5.5)        | 99.7 (0.45)         | 0.0062 (0.1535) | 0.04456 | 7.4 | -0.59903   |
| <i>dnaK</i> | 495             | 94.6 (9.1)        | 98.0 (8.04)         | 0.0024 (0.0461) | 0.11838 | 4.8 | -2.05655   |
| <i>napA</i> | 882             | 94.8 (4.3)        | 97.9 (2.75)         | 0.0581 (0.0812) | 0.05326 | 8.9 | -0.06984   |
| <i>metG</i> | 555             | 95.9 (6.0)        | 98.4 (2.48)         | 0.0381 (0.0754) | 0.04858 | 5.3 | -0.61694   |
| <i>gyrB</i> | 843             | 95.6 (6.1)        | 99.5 (0.68)         | 0.0146 (0.0269) | 0.05223 | 7.1 | -0.57104   |

Average nucleotide identities (ANI) and synonymous (Ks) vs. non-synonymous (Ka) substitutions were determined from 36 different *Persephonella* isolates.

**Table 4 | Allelic properties at six loci of *Persephonella* isolates analyzed in this study.**

| Strains  | Sequence type | Allele no. at locus |             |             |             |             | Origin              |
|----------|---------------|---------------------|-------------|-------------|-------------|-------------|---------------------|
|          |               | <i>atpA</i>         | <i>dnaK</i> | <i>gyrB</i> | <i>metG</i> | <i>napA</i> |                     |
| MT-17,18 | 1             | 1                   | 1           | 1           | 1           | 2           | 2 Urashima, SMT     |
| MT-31    | 2             | 1                   | 7           | 6           | 3           | 3           | 3 Archaean, SMT     |
| MT-33    | 3             | 1                   | 2           | 2           | 1           | 4           | 3 Archaean, SMT     |
| MT-22    | 4             | 1                   | 11          | 12          | 11          | 10          | 14 Snail, SMT       |
| MT-11    | 5             | 2                   | 4           | 2           | 4           | 5           | 5 Urashima, SMT     |
| MT-28    | 6             | 2                   | 5           | 3           | 10          | 4           | 12 Archaean, SMT    |
| MT-12    | 7             | 2                   | 10          | 11          | 5           | 5           | 13 Urashima, SMT    |
| MT-25    | 8             | 2                   | 2           | 3           | 6           | 5           | 3 Archaean, SMT     |
| MT-10    | 9             | 2                   | 2           | 19          | 1           | 15          | 2 Urashima, SMT     |
| MT-6     | 10            | 2                   | 13          | 15          | 5           | 5           | 16 Urashima, SMT    |
| MT-9     | 11            | 2                   | 4           | 2           | 4           | 14          | 21 Urashima, SMT    |
| MT-35    | 12            | 3                   | 4           | 3           | 4           | 3           | 4 Pika,SMT          |
| MT-27    | 13            | 3                   | 5           | 3           | 4           | 3           | 8 Archaean, SMT     |
| MT-16    | 14            | 4                   | 6           | 4           | 4           | 13          | 6 Urashima, SMT     |
| MT-13    | 15            | 4                   | 6           | 4           | 4           | 6           | 6 Urashima, SMT     |
| MT-15    | 16            | 4                   | 14          | 4           | 4           | 6           | 19 Urashima, SMT    |
| MT-20    | 17            | 5                   | 3           | 16          | 2           | 2           | 17 Urashima, SMT    |
| MT-21    | 18            | 5                   | 15          | 18          | 2           | 2           | 2 Urashima, SMT     |
| MT-7     | 19            | 6                   | 2           | 3           | 1           | 1           | 4 Urashima, SMT     |
| MT-8     | 20            | 6                   | 2           | 3           | 1           | 1           | 20 Urashima, SMT    |
| MT-29    | 21            | 7                   | 2           | 5           | 7           | 1           | 1 Archaean, SMT     |
| MT-19    | 22            | 8                   | 3           | 1           | 2           | 2           | 2 Urashima, SMT     |
| MT-32    | 23            | 9                   | 8           | 7           | 8           | 4           | 4 Archaean, SMT     |
| MT-23    | 25            | 10                  | 4           | 8           | 1           | 8           | 9 Snail, SMT        |
| MT-24    | 26            | 11                  | 2           | 9           | 9           | 9           | 10 Snail, SMT       |
| MT-36    | 27            | 12                  | 9           | 10          | 1           | 3           | 11 Pika, SMT        |
| MT-30    | 28            | 13                  | 12          | 3           | 1           | 11          | 5 Archaean, SMT     |
| MT-26    | 30            | 14                  | 2           | 13          | 6           | 12          | 1 Archaean, SMT     |
| MT-14    | 31            | 15                  | 4           | 3           | 3           | 3           | 3 Urashima, SMT     |
| MT-34    | 32            | 16                  | 4           | 17          | 1           | 3           | 18 Archaean, SMT    |
| OT-1     | 33            | 17                  | 16          | 20          | 12          | 7           | 22 Iheya North, OT  |
| OT-2     | 34            | 18                  | 17          | 21          | 13          | 16          | 23 Iheya North, OT  |
| OT-4     | 35            | 19                  | 18          | 22          | 14          | 7           | 24 Iheya North, OT  |
| OT-3     | 36            | 20                  | 19          | 23          | 15          | 17          | 7 Iheya North, OT   |
| OT-5     | 37            | 21                  | 20          | 14          | 16          | 18          | 15 Hatoma Knoll, OT |

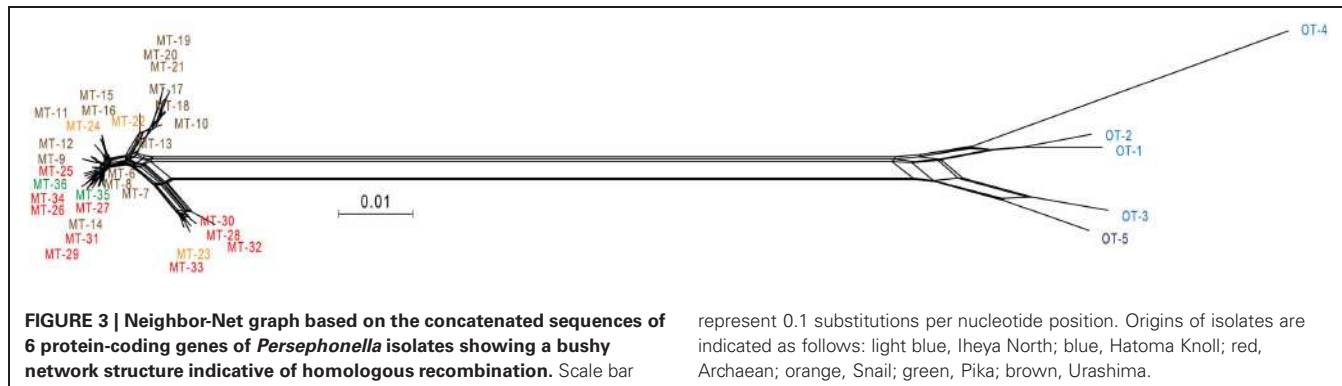


**FIGURE 3 |** Neighbor-Net graph based on the concatenated sequences of 6 protein-coding genes of *Persephonella* isolates showing a bushy network structure indicative of homologous recombination. Scale bar

represent 0.1 substitutions per nucleotide position. Origins of isolates are indicated as follows: light blue, Iheya North; blue, Hatoma Knoll; red, Archaean; orange, Snail; green, Pika; brown, Urashima.

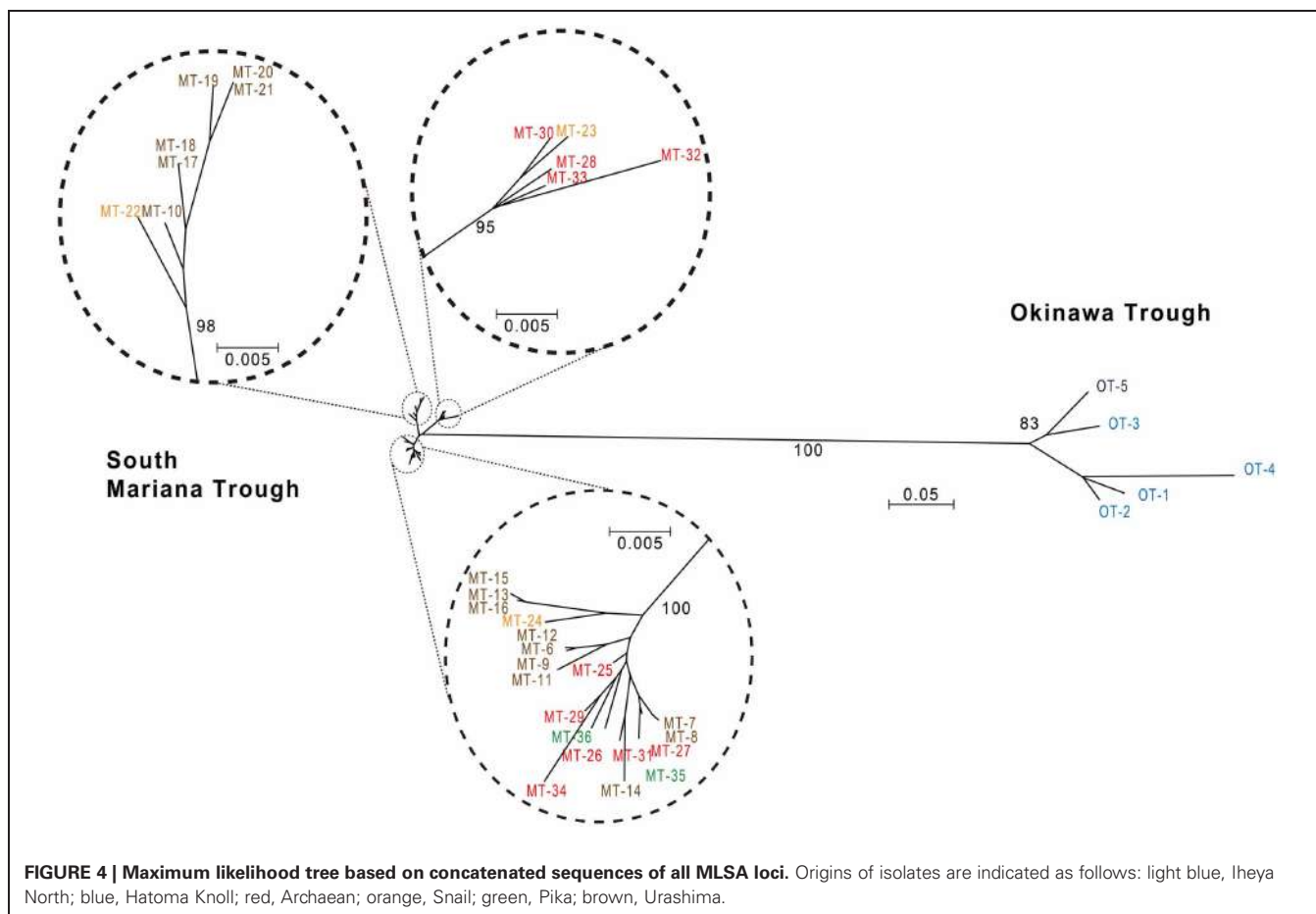


**FIGURE 4 |** Maximum likelihood tree based on concatenated sequences of all MLSA loci. Origins of isolates are indicated as follows: light blue, Iheya North; blue, Hatoma Knoll; red, Archaean; orange, Snail; green, Pika; brown, Urashima.

The acceptance criteria, based on 1000 laser shots per spot, were signal intensities between 2000 and 55,000 counts and a signal/noise ratio of 10 or greater.

Raw mass spectra from three spots were normalized using Data Explorer software (Applied Biosystems, Foster City, CA, USA) by baseline correction and combined to generate an averaged peak list. The peaks around 2000 m/z were excluded as noise.

The peaks were ranked according to their signal intensities, and the top 15 most intense peaks were chosen for further analysis. The relative intensity ratio was calculated for the 15 peaks. Squared distance was estimated based on the presence or absence of peaks by Ward's minimum variance method using MVSP software ver 3.21 (Kovach Computing Services, Wales, UK). The

presence or absence of peaks was determined within a tolerance of 14 Da.

## RESULTS

### ISOLATION OF *Persephonella* STRAINS

We investigated a total of 36 *Persephonella* strains originating from various hydrothermal samples from the OT (4 strains from Iheya North, and 1 strain from Hatoma Knoll) and the SMT (16 strains from Urashima site, 10 strains from Archaean site, 3 strains from Snail site, and 2 strains from Pika site) (Figure 2 and Table 1). All of the 36 strains shared >98.7% 16S rRNA gene similarities with one another and with *P. hydrogeniphila* 29W<sup>T</sup>.

## GENETIC DIVERSITY OF *Persephonella* POPULATION

We developed a MLSA scheme for the *Persephonella* population based on five housekeeping genes and a functional gene. The gene fragments sequenced varied from 501 to 882 bp in length (**Table 1**), and nucleotide sequence similarity at MLSA loci varied from 94.6 to 96.3% (average 95.8%). We obtained concatenated sequences of 4254 bp and identified a total of 702 variable positions. Ratios of non-synonymous to synonymous substitutions ( $K_a/K_s$ ) were much smaller than 1 for all loci (**Table 3**), indicating the genes were subject to purifying selection, conforming to the general requirements for MLSA loci (Maiden, 2006). This was statistically supported by the high values from the  $Z$ -test (**Table 3**).

## POPULATION GENETIC STRUCTURE

Typing based on sequences of six protein-coding gene fragments revealed 35 different STs among 36 isolates, indicating the high genetic diversity of *Persephonella* population (**Table 4**). The number of different alleles per locus varied between 16 for *metG* and 24 for *tkt*. Strains MT-17 and –18 had identical sequences for all MLSA loci. These strains were isolated from the same chimney sample, but the slurries were prepared in the presence (used for strain MT-18) or absence (used for strain MT-17) of 0.05% (w/v) sodium sulfide. In other cases, the presence of sodium sulfide in slurries resulted in the isolation of strains classified into different STs (**Table 1**).

**Table 5 |  $F_{ST}$  values between each population.**

|          | Snail   | Archaeon      | Pika    | Urashima | SMT           | OT     |
|----------|---------|---------------|---------|----------|---------------|--------|
| Snail    | 0.0000  |               |         |          |               |        |
| Archaeon | –0.0173 | 0.0000        |         |          |               |        |
| Pika     | –0.4221 | –0.3450       | 0.0000  |          |               |        |
| Urashima | –0.0130 | <b>0.1200</b> | –0.1909 | 0.0000   |               |        |
| SMT      | –       | –             | –       | –        | 0.0000        |        |
| OT       | –       | –             | –       | –        | <b>0.8711</b> | 0.0000 |

*P*-values <0.05 are bold.

**Table 6 | End-member compositions of vent fluids from the OT and the SMT.**

| Venting sit                     | Sampling | Tmax <sup>*3</sup> | pH <sup>*4</sup> | Cl <sup>–</sup> | Na      | K       | Ca      | Mn                     | NH <sub>4</sub> <sup>+</sup> | SO <sub>4</sub> <sup>2–</sup> | H <sub>2</sub> S |
|---------------------------------|----------|--------------------|------------------|-----------------|---------|---------|---------|------------------------|------------------------------|-------------------------------|------------------|
|                                 | year     | °C                 |                  | mmol/kg         | mmol/kg | mmol/kg | mmol/kg | μmol/kg                | μ mol/kg                     | mmol/kg                       | mmol/kg          |
| Iheya North <sup>*1</sup> (NBC) | 2007     | 309                | 5.0              | 557             | 407     | 72.4    | 21.9    | 6.58 × 10 <sup>2</sup> | 1.71 × 10 <sup>3</sup>       | 0                             | –                |
| Hatoma Knoll <sup>*2</sup>      | 2000     | 240                | 5.2              | 381             | 285     | 54.6    | 17.0    | 4.83 × 10 <sup>2</sup> | 7.20 × 10 <sup>3</sup>       | –                             | –                |
| Urashima                        | 2010     | 280                | 3.0              | 623             | 456     | 37.0    | 31.9    | 2.22 × 10 <sup>3</sup> | <100                         | –4.11                         | 2.4              |
| Snail                           | 2010     | 61                 | 3.5              | 558             | 442     | 28.4    | 28.0    | 1.84 × 10 <sup>3</sup> | <100                         | –0.41                         | 2.0              |
| Archaeon                        | 2010     | 318                | 3.0              | 401             | 312     | 33.0    | 15.8    | 1.28 × 10 <sup>3</sup> | <100                         | –0.24                         | 9.6              |
| Pika                            | 2010     | 322                | 3.0              | 469             | 444     | 31.6    | 37.8    | 1.14 × 10 <sup>3</sup> | <100                         | –2.98                         | 7.0              |

<sup>\*1</sup> Kawagucci et al. (2011).

<sup>\*2</sup> Kishida et al. (2004).

<sup>\*3</sup> Maximum temperature.

<sup>\*4</sup> Measured at 25°C.

–, No data.

The split graph obtained from the concatenated sequence data displayed bushy network structures with complex parallel-ogram formation indicative of extensive homologous recombination (**Figure 3**). The result of PHI test (Bruen et al., 2006) for the concatenated sequences also showed the presence of the past recombination events during the evolution of *Persephonella* ( $p < 0.05$ ).

## POPULATION DIFFERENCE BETWEEN THE OT AND THE SMT

A ML phylogenetic tree derived from the concatenated alignment of six loci showed two different clades with high bootstrap support (**Figure 4**). The two clades corresponded to the two geographic regions, showing that the SMT strains share a common evolutionary history distinct from the OT strains. The  $F_{ST}$  value confirmed that the OT and the SMT populations were significantly different ( $F_{ST} = 0.8711$ ,  $p < 0.05$ ) (**Table 5**).

## CORRELATION BETWEEN CHEMISTRY AND GENETIC DIVERSITY

Geochemical analysis revealed that different vent fluids had distinctive end-member chemical compositions (**Table 6**). Although the vent fluids from Archaeon and Pika were respectively

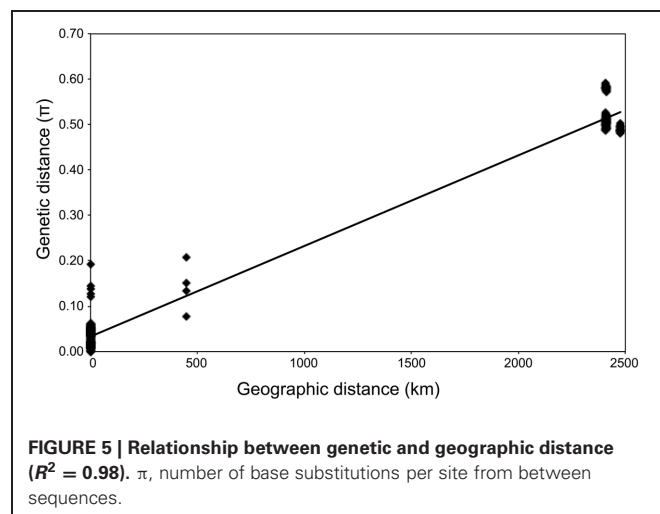


**FIGURE 5 | Relationship between genetic and geographic distance ( $R^2 = 0.98$ ).**  $\pi$ , number of base substitutions per site from between sequences.

$\text{Cl}^-$ -depleted and -enriched in 2004 and 2005 (Ishibashi et al., 2006), no significant difference was found between them in this study. We assessed the relative contributions of environmental factors (such as pH and maximum temperature of vent fluids) and geographic distance to *Persephonella* genetic structure using the Mantel test. The pH of SMT vent fluids (pH 3.0–3.5) were significantly lower than those (pH 5.0–5.2) of OT (Table 6). However, we found no significant correlation between the genetic distance and the absolute difference in vent fluid pH and temperature (Mantel  $r = -0.28, p = 0.4$ ). In contrast, a large, significant correlation coefficient (Mantel  $r = 0.993, p < 0.0001$ ) was found in a Mantel test of all pairwise comparisons of the genetic and the geographic distance between strains (Figure 5).

#### WHOLE-CELL MALDI-TOF/MS ANALYSIS

MALDI-TOF/MS fingerprinting of whole microbial cells was highly reproducible. A peak at  $m/z$  9678 in the MALDI-TOF/MS

spectra was detected in all strains despite their geographical origin (Figure 6). Some peaks were detected in some strains with relatively low intensities. Cluster analysis based on the presence or absence of peaks identified two clusters that would correspond to the geographical regions of isolation (Figure 7). Two *Persephonella* trees, one generated from the whole-cell MALDI-TOF/MS data and a ML tree from concatenated MLSA sequences, show similar topologies (Figure 7).

#### DISCUSSION

Here we investigated the microdiversity and phenotypic heterogeneity of extremely thermophilic chemolithoautotrophic bacteria in deep-sea hydrothermal vents. Genetic and phenotypic differences corresponding to the geographic origins were discovered by the combined use of MLSA and whole-cell MALDI-TOF/MS fingerprinting. The biogeography of hydrothermal vent-associated microbial community has been

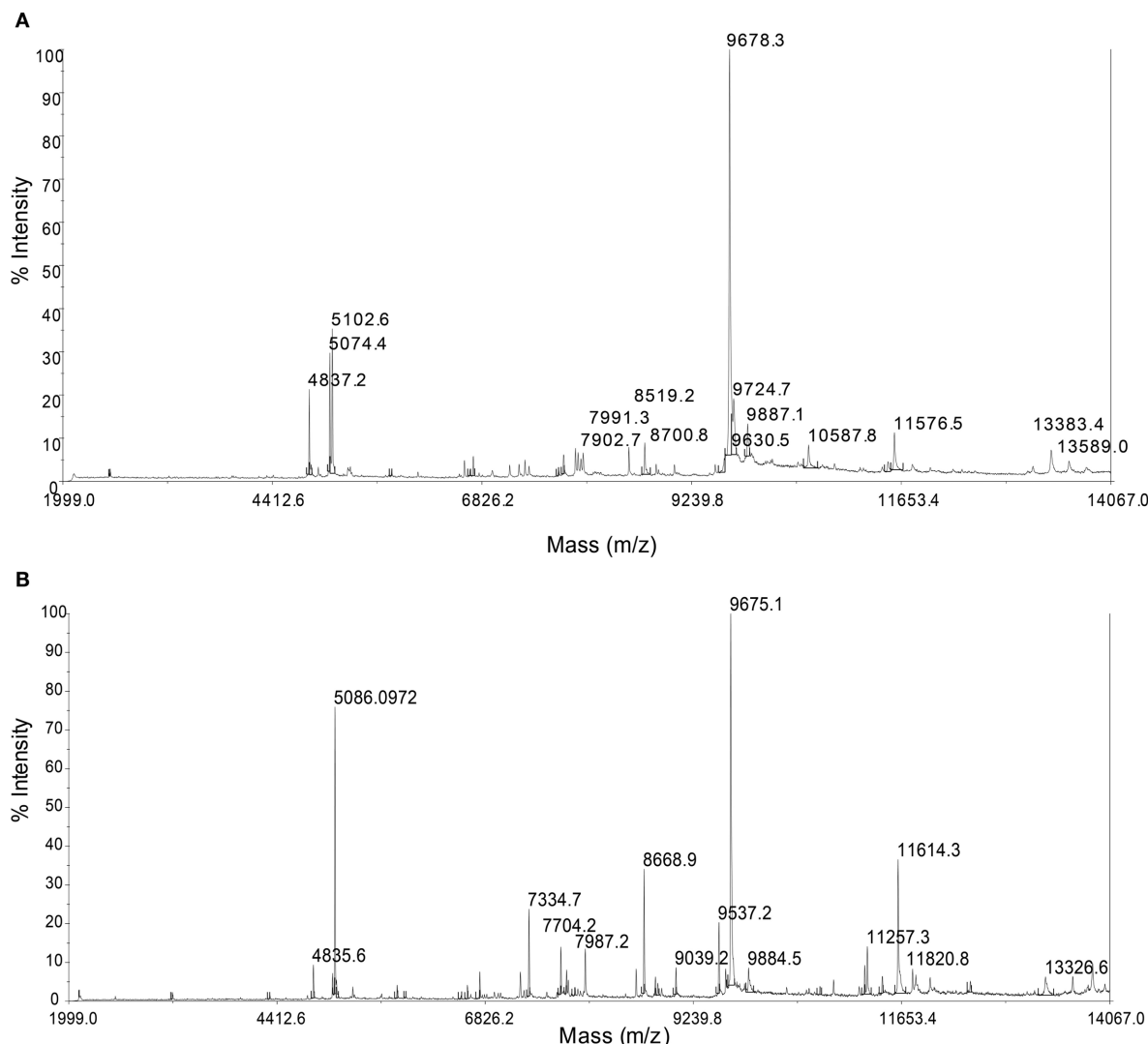
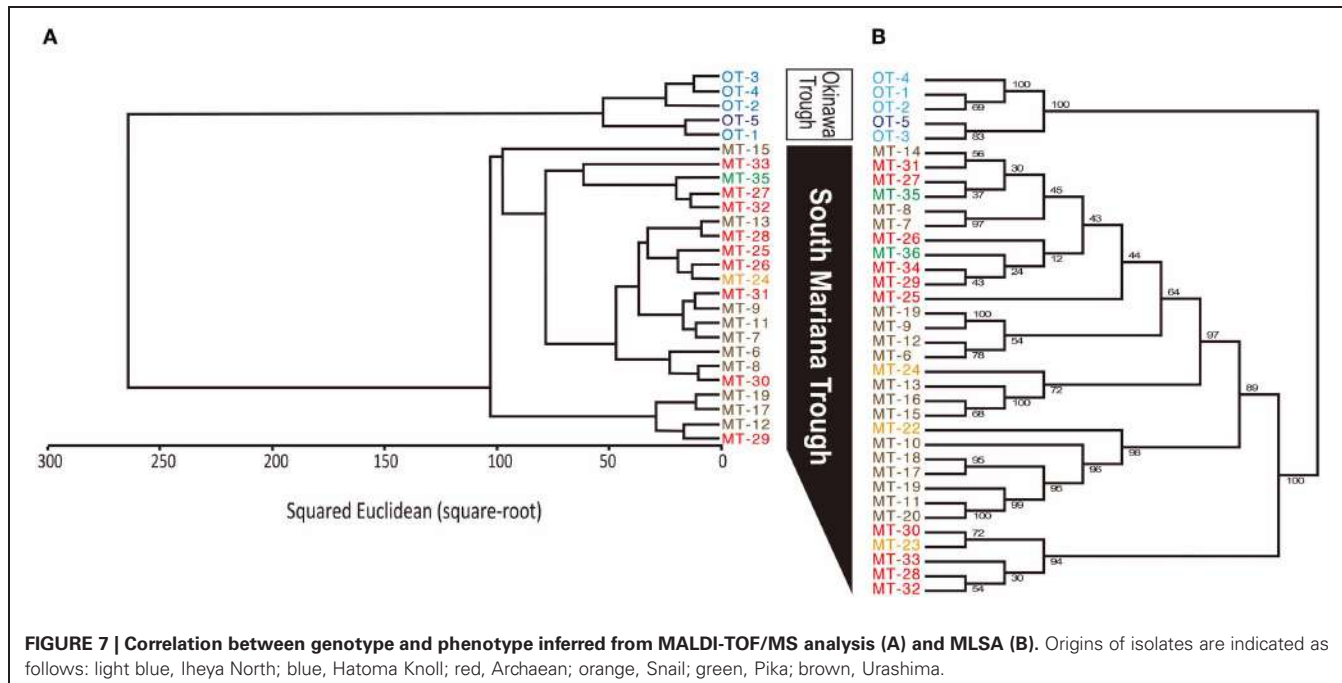


**FIGURE 6 |** Representative whole-cell MALDI-TOF/MS spectra from the OT strain (OT-2, A) and the SMT strain (MT-26, B).



well studied (Takai et al., 2004; Nakagawa et al., 2005a,b; Kato et al., 2010). Members of the genus *Persephonella* have been found in global hydrothermal vent fields, however, their genetic and phenotypic heterogeneities were poorly understood.

#### GENETIC DIFFERENCE BETWEEN OT AND SMT POPULATIONS

We identified 35 STs among 36 *Persephonella* strains by MLSA based on 6 protein-coding genes, indicating high genetic diversity of *Persephonella* population. The same ST is rarely shared among *Persephonella* strains, however, all SMT strains have the same alleles with other SMT strains but not with OT strains in one or more MLSA loci, suggesting that OT and SMT populations are significantly different. Likewise, two OT strains, i.e., OT-1 and -4, have the same allele (no. 7) at *napA* (Table 4), although the number of OT strains obtained in this study is small.

The split decomposition tree showed the evidence of recombination (Figure 3), which might contribute to increased STs. Previous studies showed that recombination generated the large number of unique combinations of alleles in some archaea and bacteria (Suerbaum et al., 2001; Whitaker et al., 2005; Doroghazi and Buckley, 2010).

#### BIOGEOGRAPHY OF *Persephonella*

The phylogenetic analysis based on concatenated gene sequences separated the strains into two clusters according to their geographic origins (Figure 4). The  $F_{ST}$  value supported significant biogeographical isolation between SMT and OT populations. These results indicate that ubiquitous occurrence of *Persephonella* in deep-sea vents has not resulted from widespread contemporary dispersal but is an ancient historical legacy.

The microbial distribution seems to be not only influenced by local environmental conditions (Martiny et al., 2006). In this study, we observed clear correlation between the genetic distance

and the geographic distance of isolates (Figure 5) as described in thermophilic archaea (Whitaker et al., 2003; Flores et al., 2012). On the contrary, genetic distance has no significant correlation with the difference in vent fluid pH and temperature. We cannot rule out the possibility that other factors not determined in this study, including grazing pressure and virus activity, may be correlated with the genetic difference of *Persephonella*. Recently, H<sub>2</sub> concentration in vent fluids was shown to have an impact on the formation of microbial community structures in deep-sea vents (Takai and Nakamura, 2011).

#### CORRELATION BETWEEN GENOTYPIC AND PHENOTYPIC HETEROGENEITY

Some peaks in the MALDI-TOF/MS spectra were shared among some *Persephonella* strains. Major peaks of whole-cell MALDI-TOF/MS analysis are considered to reflect ribosomal proteins (Fenselau and Plamen, 2001; Ryzhov and Fenselau, 2001) and thus are independent of growth conditions (Bernardo et al., 2002). There were also some minor peaks that were specific to SMT or OT strains. Likewise the concatenated nucleotide alignment of MLSA loci, MALDI-TOF/MS data clustered the strains into two distinct groups corresponding to the geographic regions (Figure 7), suggesting that protein expression of *Persephonella* is tuned to function optimally in their original habitats. The genotypic and phenotypic correlation found among *Persephonella* isolates indicates the occurrence of allopatric speciation.

#### CONCLUSION

By using both comparative genetic and phenotypic population characterizations, this study for the first time indicated the *Persephonella* populations were geographically distinct. Since the *Persephonella* members are extremely thermophilic

chemoautotrophs endemic to deep-sea vents, considerable dispersal barriers for the migration to spatially distinct niches should exist. Focal points raised by this study for future research include the effects of cold, oxic deep-sea conditions on the viability of deep-sea vent (hyper) thermophiles during the dispersal, the biogeographical comparison with other ubiquitous thermophiles with different metabolic traits (e.g., heterotrophic fermenters and methanogens), and the comparison with moderately thermophiles or mesophiles with similar

energy/carbon metabolisms (e.g., *Epsilonproteobacteria*) in deep-sea vents.

## ACKNOWLEDGMENTS

We thank the captain and crew of the *R/V Yokosuka* and *R/V Natsushima* and *Shinkai 6500* and *Hyper Dolphin* operation team on cruises JAMSTEC YK10-10, YK10-11, NT07-13, and NT09-11. Sayaka Mino was supported by the Research Fellowship of the Japan Society for the Promotion of Science.

## REFERENCES

- Balch, W. E., Fox, G. E., Magrum, L. J., Woese, C. R., and Wolfe, R. S. (1979). Methanogens: reevaluation of a unique biological group. *Microbiol. Rev.* 43, 260–296.
- Baross, J. A. (1995). “Isolation, growth and maintenance of hyperthermophiles,” in *Archaea: A Laboratory Manual, Thermophiles*, eds F. T. Robb and A. R. Place (New York, NY: Cold Spring Harbor Laboratory), 15–23.
- Bernardo, K., Fleer, S., Pakulat, N., Krut, O., Hünger, F., and Krönke, M. (2002). Identification of *Staphylococcus aureus* exotoxins by combined sodium dodecyl sulfate gel electrophoresis and matrix-assisted laser desorption/ionization-time of flight mass spectrometry. *Proteomics* 2, 740–746.
- Bruen, T. C., Philippe, H., and Bryant, D. (2006). A simple and robust statistical test for detecting the presence of recombination. *Genetics* 172, 2665–2681.
- Butterfield, D. A., and Massoth, G. J. (1994). Geochemistry of north cleft segment vent fluids: temporal changes in chlorinity and their possible relation to recent volcanism. *J. Geophys. Res.* 99, 4951–4968.
- Butterfield, D. A., Roe, K. K., Lilley, M. D., Huber, J., Baross, J. A., Embley, R. W., et al. (2004). “Mixing, reaction and microbial activity in the sub-seafloor revealed by temporal and spatial variation in diffuse flow vents at Axial Volcano,” in *The Subseafloor Biosphere at Mid-Ocean Ridges, Geophysical Monograph Series*. Vol. 144, eds W. S. D. Wilcock, E. F. DeLong, D. S. Kelley, J. A. Baross, and S. C. Cary (Washington, DC: American Geophysical Union), 269–289.
- Corre, E. (2001).  $\epsilon$ -Proteobacterial diversity from a deep-sea hydrothermal vent on the Mid-Atlantic Ridge. *FEMS Microbiol. Lett.* 205, 329–335.
- Deckert, G., Warren, P. V., Gaasterland, T., Young, W. G., Lenox, A. L., and Graham, D. E. (1998). The complete genome of the hyperthermophilic bacterium *Aquifex aeolicus*. *Nature* 392, 353–358.
- DeSantis, T. Z., Hugenholtz, P., Keller, K., Brodie, E. L., Larsen, N., and Piceno, Y. M. (2006). NAST: a multiple sequence alignment server for comparative analysis of 16S rRNA genes. *Nucleic Acids Res.* 34, W394–W399.
- Doroghazi, J. R., and Buckley, D. H. (2010). Widespread homologous recombination within and between *Streptomyces* species. *ISME J.* 4, 1136–1143.
- Edmond, J. M., McDuff, R. E., and Chan, L. H. (1979). Ridge crest hydrothermal activity and the balances of the major and minor elements in the ocean: the Galapagos data. *Earth Planet. Sci. Lett.* 46, 1–18.
- Excoffier, L., and Lischer, H. E. (2010). Arlequin suite ver 3.5: a new series of programs to perform population genetics analyses under Linux and Windows. *Mol. Ecol. Resour.* 10, 564–567.
- Fenselau, C., and Plamen, A. D. (2001). Characterization of intact microorganisms by MALDI mass spectrometry. *Mass Spectrom. Rev.* 20, 157–171.
- Ferrera, I., Longhorn, S., Banta, A. B., Liu, Y., Preston, D., and Reysenbach, A. L. (2007). Diversity of 16S rRNA gene, ITS region and *acb* gene of the *Aquificales*. *Extremophiles* 11, 57–64.
- Flores, G. E., Wagner, I. D., Liu, Y., and Reysenbach, A. L. (2012). Distribution, abundance, and diversity patterns of the thermoacidophilic “deep-sea hydrothermal vent euryarchaeota 2”. *Front. Microbiol.* 3:47. doi: 10.3389/fmicb.2012.00047
- Gevers, D., Cohan, F. M., Lawrence, J. G., Spratt, B. G., Coenye, T., and Feil, E. J. (2005). Re-evaluating prokaryotic species. *Nat. Rev. Microbiol.* 3, 733–739.
- Götz, D., Banta, A., Beveridge, T. J., Rushdi, A. I., Simoneit, B. R., and Reysenbach, A. L. (2002). *Persephonella marina* gen. nov., sp. nov. and *Persephonella guaymasensis* sp. nov., two novel, thermophilic, hydrogen-oxidizing microaerophiles from deep-sea hydrothermal vents. *Int. J. Syst. Evol. Microbiol.* 52, 1349–1359.
- Haddad, A., Camacho, F., Durand, P., and Cary, S. C. (1995). Phylogenetic characterization of the epibiotic bacteria associated with the hydrothermal vent polychaete *Alvinella pompejana*. *Appl. Environ. Microbiol.* 61, 1679–1687.
- Hazen, T. H., Martinez, R. J., Chen, Y., Lafon, C., Garrett, N. M., and Parsons, M. B. (2009). Rapid identification of *Vibrio parahaemolyticus* by whole-cell matrix-assisted laser desorption ionization-time of flight mass spectrometry. *Appl. Environ. Microbiol.* 75, 6745–6756.
- Huson, D. H. (1998). SplitsTree: analyzing and visualizing evolutionary data. *Bioinformatics* 14, 68–73.
- Ishibashi, J., Suzuki, R., Yamanaka, T., Toki, T., Kimura, H., Noguchi, T., et al. (2006). Seafloor hydrothermal activity at off-axial seamounts of backarc spreading in southern Mariana Trough. *Geochim. Cosmochim. Acta* 70, A279.
- Kato, S., Takano, Y., Kakegawa, T., Oba, H., Inoue, K., Kobayashi, C., et al. (2010). Biogeography and biodiversity in sulfide structures of active and inactive vents at deep-sea hydrothermal fields of the southern mariana trough. *Appl. Environ. Microbiol.* 76, 2968–2979.
- Kawagucci, S., Chiba, H., Ishibashi, J., Yamanaka, T., Toki, T., Muramatsu, Y., et al. (2011). Hydrothermal fluid geochemistry at the Iheya North field in the mid-Okinawa Trough: Implication for origin of methane in subseafloor fluid circulation systems. *Geochim. J.* 45, 109–124.
- Kaye, J. Z., Sylvan, J. B., Edwards, K. J., and Baross, J. A. (2011). *Halomonas* and *Marinobacter* ecotypes from hydrothermal vent, subseafloor and deep-sea environments. *FEMS Microbiol. Ecol.* 75, 123–133.
- Kishida, K., Sohrin, Y., Okamura, K., and Ishibachi, J. (2004). Tungsten enriched in submarine hydrothermal fluids. *Earth Planet. Sci. Lett.* 222, 819–827.
- Larkin, M. A., Blackshields, G., Brown, N. P., Chenna, R., McGettigan, P. A., McWilliam, H., et al. (2007). Clustal W and Clustal X version 2.0. *Bioinformatics* 23, 2947–2948.
- Librado, P., and Rozas, J. (2009). DnaSP v5: a software for comprehensive analysis of DNA polymorphism data. *Bioinformatics* 25, 1451–1452.
- Ludwig, W., Strunk, O., Westram, R., Richter, L., Meier, H., Yadukumar, et al. (2004). ARB: a software environment for sequence data. *Nucleic Acids Res.* 32, 1363–1371.
- Maiden, M. C. J. (2006). Multilocus sequence typing of bacteria. *Annu. Rev. Microbiol.* 60, 561–588.
- Martiny, J. B., Bohannan, B. J., Brown, J. H., Colwell, R. K., Fuhrman, J. A., Green, J. L., et al. (2006). Microbial biogeography: putting microorganisms on the map. *Nat. Rev. Microbiol.* 4, 102–112.
- Mazard, S., Ostrowski, M., Partensky, F., and Scanlan, D. J. (2012). Multi-locus sequence analysis, taxonomic resolution and biogeography of marine *Synechococcus*. *Environ. Microbiol.* 14, 372–386.
- Nakagawa, S., and Takai, K. (2006). The isolation of thermophiles from deep-sea hydrothermal environments. *Methods Microbiol.* 35, 55–91.
- Nakagawa, S., and Takai, K. (2008). Deep-sea vent chemoautotrophs: diversity, biochemistry and ecological significance. *FEMS microbiol. Ecol.* 65, 1–14.
- Nakagawa, S., Takai, K., Horikoshi, K., and Sako, Y. (2003). *Persephonella hydrogeniphila* sp. nov., a novel thermophilic, hydrogen-oxidizing bacterium from a deep-sea hydrothermal vent chimney. *Int. J. Syst. Evol. Microbiol.* 53, 863–869.
- Nakagawa, S., Takai, K., Inagaki, F., Hirayama, H., Nunoura, T., Horikoshi, K., et al. (2005a). Distribution, phylogenetic diversity and physiological characteristics of epsilon-Proteobacteria in

- a deep-sea hydrothermal field. *Environ. Microbiol.* 7, 1619–1632.
- Nakagawa, S., Takai, K., Inagaki, F., Chiba, H., Ishibashi, J., Kataoka, S., et al. (2005b). Variability in microbial community and venting chemistry in a sediment-hosted backarc hydrothermal system: impacts of subseafloor phase-separation. *FEMS Microbiol. Ecol.* 54, 141–155.
- Oakley, B. B., Carbonero, F., Van der Gast, C. J., Hawkins, R. J., and Purdy, K. J. (2010). Evolutionary divergence and biogeography of sympatric niche-differentiated bacterial populations. *ISME J.* 4, 488–497.
- Papke, R. T., Ramsing, N. B., Bateson, M. M., and Ward, D. M. (2003). Geographical isolation in hot spring cyanobacteria. *Environ. Microbiol.* 5, 650–659.
- Pride, D. T. (2000). SWAAP Version 1.0.0 - Sliding Windows Alignment Analysis Program: A Tool for Analyzing Patterns of Substitutions and Similarity in Multiple Alignments. Distributed by the author.
- Reysenbach, A. L., Dorothée, G., Banta, A., Jeanthon, C., and Fouquet, Y. (2002). Expanding the distribution of the *Aquificales* to the deep-sea vents on Mid-Atlantic Ridge and Central Indian Ridge. *Cah. Biol. Mar.* 43, 425–428.
- Reysenbach, A. L., Hamamura, N., Podar, M., Griffiths, E., Ferreira, S., Hochstein, R., et al. (2009). Complete and draft genome sequences of six members of the *Aquificales*. *J. Bacteriol.* 191, 1992–1993.
- Reysenbach, A. L., Longnecker, K., and Kirshtein, J. (2000). Novel bacterial and archaeal lineages from an *in situ* growth chamber deployed at a Mid-Atlantic Ridge hydrothermal vent. *Appl. Environ. Microbiol.* 66, 3798–3806.
- Rosselló-Mora, R., Lucio, M., Peña, A., Brito-Echeverría, J., López-López, A., Valens-Vadell, M., et al. (2008). Metabolic evidence for biogeographic isolation of the extremophilic bacterium *Salinibacter ruber*. *ISME J.* 2, 242–253.
- Ryzhov, V., and Fenselau, C. (2001). Characterization of the protein subset desorbed by MALDI from whole bacterial cells. *Anal. Chem.* 73, 746–750.
- Suerbaum, S., Lohrengel, M., Sonneveld, A., Ruberg, F., and Kist, M. (2001). Allelic diversity and recombination in *Campylobacter jejuni*. *J. Bacteriol.* 183, 2553–2559.
- Takai, K., Gamo, T., Tsunogai, U., Nakayama, N., Hirayama, H., Nealson, K. H., et al. (2004). Geochemical and microbiological evidence for a hydrogen-based, hyperthermophilic subsurface lithoautotrophic microbial ecosystem (HyperSLiME) beneath an active deep-sea hydrothermal field. *Extremophiles* 8, 269–282.
- Takai, K., and Horikoshi, K. (1999). Genetic diversity of Archaea in deep-sea hydrothermal vent environments. *Genetics* 152, 1285–1297.
- Takai, K., Inagaki, F., Nakagawa, S., Hirayama, H., Nunoura, T., Sako, Y., et al. (2003). Isolation and phylogenetic diversity of members of previously uncultivated epsilon-Proteobacteria in deep-sea hydrothermal fields. *FEMS Microbiol. Lett.* 218, 167–174.
- Takai, K., Komatsu, T., Inagaki, F., and Horikoshi, K. (2001). Distribution of archaea in a black smoker chimney structure. *Appl. Environ. Microbiol.* 67, 3618–3629.
- Takai, K., Nakagawa, S., Reysenbach, A. L., and Hoek, J. (2006). “Microbial ecology of mid-ocean ridges and back-arc basins,” in *Back-arc Spreading Systems: Geological, Biological, Chemical, and Physical Interactions, Geophysical Monograph Series*. Vol. 166, eds D. M. Christie, C. R. Fisher, S. M. Lee, and S. Givens (Washington, DC: American Geophysical Union), 185–213.
- Takai, K., and Nakamura, K. (2011). Archaeal diversity and community development in deep-sea hydrothermal vents. *Curr. Opin. Microbiol.* 14, 282–291.
- Takai, K., Nunoura, T., Ishibashi, J., Lupton, J., Suzuki, R., Hamasaki, H., et al. (2008). Variability in the microbial communities and hydrothermal fluid chemistry at the newly discovered Mariner hydrothermal field, southern Lau Basin. *J. Geophys. Res.* 113:G02031. doi: 10.1029/2007JG000636
- Tamura, K., Peterson, D., Peterson, N., Stecher, G., Nei, M., and Kumar, S. (2011). MEGA5: molecular evolutionary genetics analysis using maximum likelihood, evolutionary distance, and maximum parsimony methods. *Mol. Biol. Evol.* 28, 2731–2739.
- Teske, A., Hinrichs, K. U., Edgcomb, V., de Vera Gomez, A., Kysela, D., Sylva, S. P., et al. (2002). Microbial diversity of hydrothermal sediments in the Guaymas Basin: evidence for anaerobic methanotrophic communities. *Appl. Environ. Microbiol.* 68, 1994–2007.
- Toki, T., Tsunogai, U., Ishibashi, J., Utsumi, M., and Gamo, T. (2008). Methane enrichment in low-temperature hydrothermal fluids from the Suiyo Seamount in the Izu-Bonin Arc of the western Pacific Ocean. *J. Geophys. Res.* 113:B08S13. doi: 10.1029/2007JB005476
- Vergin, K. L., Tripp, H. J., Wilhelm, L. J., Denver, D. R., Rappé, M. S., and Giovannoni, S. J. (2007). High intraspecific recombination rate in a native population of *Candidatus pelagibacter ubique* (SAR11). *Environ. Microbiol.* 9, 2430–2440.
- Von Damm, K. L. V., Edmond, J. M., and Grant, B. (1985). Chemistry of submarine hydrothermal solutions at 21°N, East Pacific Rise. *Geochim. Cosmochim. Acta* 49, 2197–2220.
- Weisburg, W. G., Barns, S. M., Pelletier, D. A., and Lane, D. J. (1991). 16S ribosomal DNA amplification for phylogenetic study. *J. Bacteriol.* 173, 697–703.
- Whitaker, R. J., Grogan, D. W., and Taylor, J. W. (2003). Geographic barriers isolate endemic populations of hyperthermophilic archaea. *Science* 301, 976–978.
- Whitaker, R. J., Grogan, D. W., and Taylor, J. W. (2005). Recombination shapes the natural population structure of the hyperthermophilic archaeon *Sulfobolus islandicus*. *Mol. Biol. Evol.* 22, 2354–2361.
- Wit, R. D., and Bouvier, T. (2006). Correspondence ‘everything is everywhere, but, the environment selects’; what did Baas Becking and Beijerinck really say? *Environ. Microbiol.* 8, 755–758.

**Conflict of Interest Statement:** The authors declare that the research was conducted in the absence of any commercial or financial relationships that could be construed as a potential conflict of interest.

*Received: 30 December 2012; paper pending published: 28 February 2013; accepted: 13 April 2013; published online: 25 April 2013.*

*Citation: Mino S, Makita H, Toki T, Miyazaki J, Kato S, Watanabe H, Imachi H, Watsuji T, Nunoura T, Kojima S, Sawabe T, Takai K and Nakagawa S (2013) Biogeography of *Persephonella* in deep-sea hydrothermal vents of the Western Pacific. *Front. Microbiol.* 4:107. doi: 10.3389/fmicb.2013.00107*

*This article was submitted to Frontiers in Extreme Microbiology, a specialty of Frontiers in Microbiology.*

*Copyright © 2013 Mino, Makita, Toki, Miyazaki, Kato, Watanabe, Imachi, Watsuji, Nunoura, Kojima, Sawabe, Takai and Nakagawa. This is an open-access article distributed under the terms of the Creative Commons Attribution License, which permits use, distribution and reproduction in other forums, provided the original authors and source are credited and subject to any copyright notices concerning any third-party graphics etc.*



# Archaeal and bacterial diversity in an arsenic-rich shallow-sea hydrothermal system undergoing phase separation

Roy E. Price<sup>1\*</sup>, Ryan Lesniewski<sup>2</sup>, Katja S. Nitzsche<sup>3,4</sup>, Anke Meyer-Dierks<sup>3</sup>, Chad Saltikov<sup>5</sup>, Thomas Pichler<sup>6</sup> and Jan P. Amend<sup>1,2</sup>

<sup>1</sup> Department of Earth Sciences, University of Southern California, Los Angeles, CA, USA

<sup>2</sup> Department of Biological Sciences, University of Southern California, Los Angeles, CA, USA

<sup>3</sup> Department of Molecular Ecology, Max Planck Institute for Marine Microbiology, Bremen, Germany

<sup>4</sup> Geomicrobiology, Center for Applied Geosciences, University of Tübingen, Tübingen, Germany

<sup>5</sup> Department of Microbiology and Environmental Toxicology, University of California, Santa Cruz, Santa Cruz, CA, USA

<sup>6</sup> Department of Geochemistry and Hydrogeology, University of Bremen, Bremen, Germany

**Edited by:**

Anna-Louise Reysenbach, Portland State University, USA

**Reviewed by:**

John Stoltz, Duquesne University, USA

Julie L. Meyer, Marine Biological Laboratory, USA

**\*Correspondence:**

Roy E. Price, Department of Earth Sciences, University of Southern California, 3651 Trousdale Pkwy, Los Angeles, 90089 CA, USA  
e-mail: roypice@usc.edu

Phase separation is a ubiquitous process in seafloor hydrothermal vents, creating a large range of salinities. Toxic elements (e.g., arsenic) partition into the vapor phase, and thus can be enriched in both high and low salinity fluids. However, investigations of microbial diversity at sites associated with phase separation are rare. We evaluated prokaryotic diversity in arsenic-rich shallow-sea vents off Milos Island (Greece) by comparative analysis of 16S rRNA clone sequences from two vent sites with similar pH and temperature but marked differences in salinity. Clone sequences were also obtained for *aioA*-like functional genes (AFGs). *Bacteria* in the surface sediments (0–1.5 cm) at the high salinity site consisted of mainly *Epsilonproteobacteria* (*Arcobacter* sp.), which transitioned to almost exclusively *Firmicutes* (*Bacillus* sp.) at ~10 cm depth. However, the low salinity site consisted of *Bacteroidetes* (*Flavobacteria*) in the surface and *Epsilonproteobacteria* (*Arcobacter* sp.) at ~10 cm depth. *Archaea* in the high salinity surface sediments were dominated by the orders *Archaeoglobales* and *Thermococcales*, transitioning to *Thermoproteales* and *Desulfurococcales* (*Staphylothermus* sp.) in the deeper sediments. In contrast, the low salinity site was dominated by *Thermoplasmatales* in the surface and *Thermoproteales* at depth. Similarities in gas and redox chemistry suggest that salinity and/or arsenic concentrations may select for microbial communities that can tolerate these parameters. Many of the archaeal 16S rRNA sequences contained inserts, possibly introns, including members of the *Euryarchaeota*. Clones containing AFGs affiliated with either *Alpha*- or *Beta*proteobacteria, although most were only distantly related to published representatives. Most clones (89%) originated from the deeper layer of the low salinity, highest arsenic site. This is the only sample with overlap in 16S rRNA data, suggesting arsenotrophy as an important metabolism in similar environments.

**Keywords:** microbial diversity, arsenic, hydrothermal, gradients, milos, phase separation

## INTRODUCTION

Geochemical gradients often dictate microbial community structures, and metabolic processes directly influence these gradients. In hydrothermal systems, steep gradients generate redox disequilibria that can provide the necessary energy for a wide diversity of *Archaea* and *Bacteria*. Since their discovery in the 1970s, deep-sea hydrothermal environments have garnered much attention in this regard, with a number of studies linking geochemical composition, reaction energetics, and metabolic diversity (e.g., Flores et al., 2011; Meyer-Dombard et al., 2011). Their shallow-sea counterparts provide highly complementary research opportunities that are often overlooked. These systems are ubiquitous, readily accessible, and geochemically diverse; many exhibit geological, chemical, and biological characteristics similar to those found at deep-sea vents.

Shallow-sea and deep-sea hydrothermal systems also differ in several key ways (Dando et al., 1999; Pichler, 2005; Tarasov et al., 2005; Price et al., 2012). For example, the evolved discharging hydrothermal fluids in shallow-sea systems may have originally been seawater, meteoric water, or a mixture of the two. They often occur within the photic zone and thus provide the opportunity for both chemosynthetic and photosynthetic microbial metabolisms. They are most often associated with arc volcanism, which provides the heat source that drives hydrothermal circulation. Well known examples of shallow-sea hydrothermal systems are found near the Tabar-Feni (Pichler et al., 1999, 2006), the Aeolian (Italiano and Nuccio, 1991; Amend et al., 2003), the South Aegean (or Hellenic; Varnavas and Cronan, 1988; Dando et al., 1995), the Caribbean (McCarthy et al., 2005), and the Kurile-Kamchatka island arcs (Tarasov et al., 1990).

In addition, some shallow-sea vent systems also occur in other areas related to faulting (e.g., Bahía Concepción; Forrest et al., 2005) or serpentinization reactions (e.g., New Caledonia; Cox et al., 1982). Many of these shallow-sea systems are sediment covered, allowing steep vertical and horizontal geochemical gradients to evolve as reduced, low pH, high temperature fluids mix with overlying seawater (e.g., Price et al., 2007). Across the geochemical gradients, “niches” of potential energy develop that constrain the resident microbial communities. While most shallow-sea hydrothermal fluids seem to be sulfur- and/or iron-rich, they can also be elevated in potentially toxic elements such as As, Sb, Cr, Pb, Cd, Cu, Zn, and Hg (Varnavas and Cronan, 1988; Koski et al., 2001; Pichler et al., 2006; Price et al., 2012).

Many seafloor hydrothermal systems are modified by phase separation (German and Von Damm, 2003; Von Damm et al., 2003), resulting in vent fluids that can vary drastically in salinity, from <6 to ~200% of seawater values (German and Von Damm, 2003). The resultant high and low salinity fluids differ markedly in the concentrations of many solutes, but the relation to microbial community structures has not been adequately considered. Previous investigations indicate that the vapor phase fluids may be enriched in important electron donors, such as H<sub>2</sub>, relative to the high salinity brine phase, and may contribute to stratification of microbial communities (Nakagawa et al., 2005; Nunoura and Takai, 2009). Arsenic is known to partition into the vapor phase (Pokrovski et al., 2002; Price et al., 2012). If the hydrothermal reservoir is enriched in arsenic and undergoing phase separation, this element can therefore be elevated in both high and low salinity discharging hydrothermal fluids. The highest As levels in a marine hydrothermal fluid were reported for the shallow-sea hydrothermal vent system in Palaeochori Bay, Milos Island, Greece (Price et al., 2012). There, high arsenic concentrations were reported for high and low salinity fluids; typically in the range of 30 μM, but as high as 78 μM in the low salinity fluids, suggesting As partitions into the vapor phase in this system.

The purpose of this investigation was to identify the dominant bacterial and archaeal lineages in Palaeochori Bay in an attempt to understand the link between geochemical gradients and microbial groups, including arsenic oxidizers. These relationships were investigated at two sites with similar pH and temperature, but different salinities.

## SITE CHARACTERISTICS

Gas discharge defines an ~35 km<sup>2</sup> area of hydrothermal venting around Milos, making it one of the largest shallow-sea hydrothermal systems described to date (**Figures 1A,B**; Dando et al., 1995). The most intense venting occurs in Palaeochori Bay, where CO<sub>2</sub>-rich gases and hydrothermal fluids discharge through sand (**Figures 1A–C**, 2). Nearby—but little explored—Spathi Bay, to the east, also features abundant hydrothermal venting, although free gas emissions are less abundant. The high salinity hydrothermal fluids in Palaeochori Bay were slightly acidic (pH ~5), sometimes highly sulfidic (up to 3 mM), and warm (ambient to ~110°C; Stüben and Glasby, 1999; Valsami-Jones et al., 2005; Price et al., 2012).

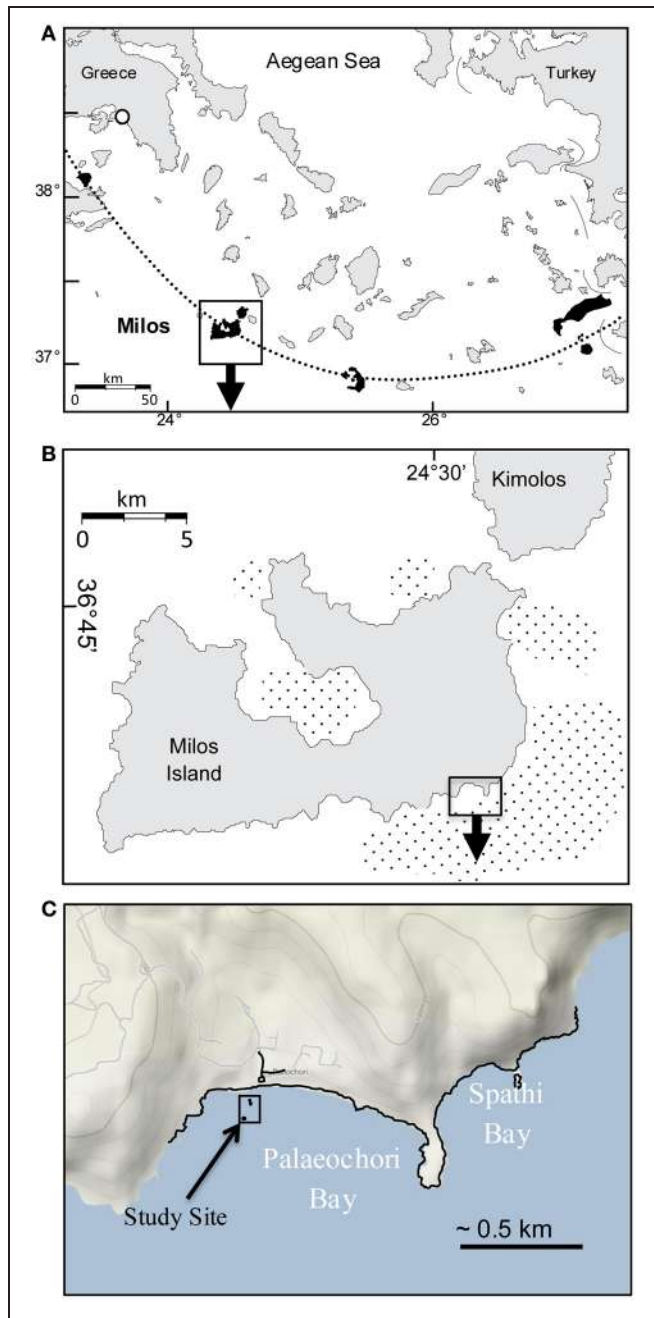


**FIGURE 1 | (A)** Location of Milos Island (box) and other calc-alkaline volcanoes (shaded) along the Aegean island arc (dotted line). **(B)** Milos Island and the location of Palaeochori and Spathi Bays (box). Stippled offshore areas around the island are mapped gas emissions by echo sounding (Dando et al., 1995). **(C)** Location of our study site (box) in Palaeochori Bay.

The occurrence of orange, white, or brown microbial mats and hydrothermal precipitates on the seafloor sediments are a major feature of the hydrothermal system. The different colors correlate to different sediment temperatures, where the hottest areas (>90°C) are typically covered by bright yellow native sulfur or orange-colored arsenic sulfide deposits (**Figure 2A**). White mats

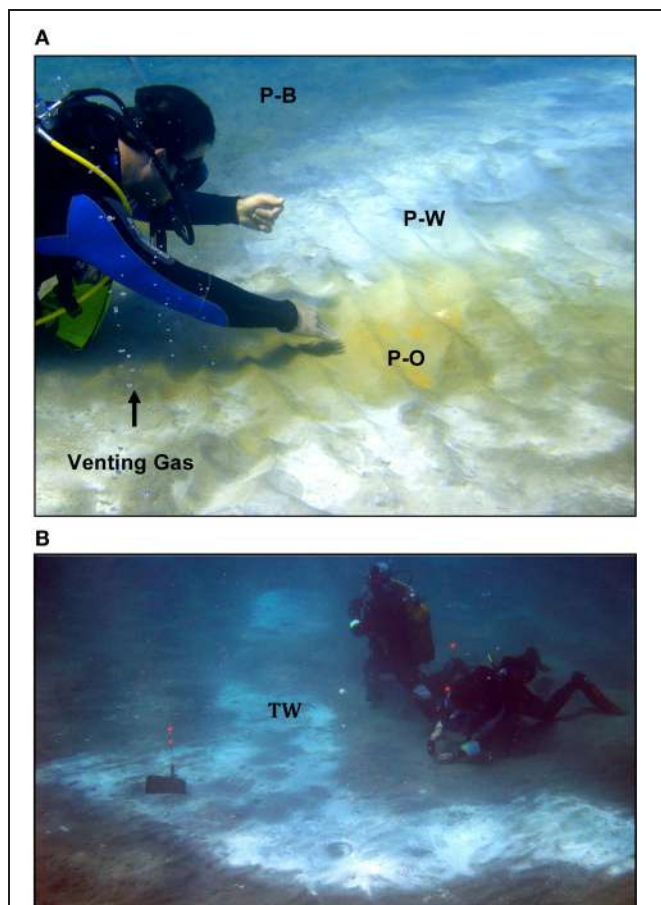


**FIGURE 2 | (A)** Photograph of the RP site investigated in this study. P-O, Palaeochori orange; P-W, Palaeochori white; and P-B, Palaeochori background. Geochemical profiles and sediment cores were sampled at ~P-W. **(B)** Photograph of the TW site. Geochemical and microbiological samples for this study are indicated at the location of TW.

make up the largest areas of hydrothermal venting throughout the bay, and display mid-range temperatures (e.g., ~45–85°C). In the lower temperature areas (~30–35°C), brown colored manganese and/or iron oxide deposits are present (**Figure 2A**).

Several microbiological investigations were carried out for the high salinity sites in Palaeochori Bay, although none to date targeted low salinity environments. They included culture-dependent and molecular-based microbiological studies, as well as the isolation of several new bacterial and archaeal species (Jochimsen et al., 1997; Dando et al., 1998; Brinkhoff et al., 1999; Sievert et al., 1999, 2000a,b; Arab et al., 2000; Sievert and Kuever, 2000; Schlesner et al., 2001; Bayraktarov et al., 2013). One study investigated the microbial ecology and arsenic functional genes in lower temperature 0–6 cm pooled sediments at the same high salinity site investigated here (Nitzsche, 2010). Results indicated a high diversity in the bacterial community sequences of *Gamma*-, *Delta*-, and *Epsilonproteobacteria*, *Bacteroidetes*, and *Cyanobacteria*. Closest cultivated relatives were associated with photo- and chemotrophic lifestyle and seemed

mostly to be involved in sulfur cycling. Archaeal sequences predominantly affiliated with *Thermoplasmatales* or *Thermococcales*. Screening for arsenic functional genes indicated affiliation with either *Alpha*- or *Betaproteobacteria*, although affiliation with *Gammaproteobacteria* was noted. These studies indicated that metabolisms based on sulfur, either oxidation of H<sub>2</sub>S or reduction of SO<sub>4</sub><sup>2-</sup>, may be dominant at the high salinity sites, although dissimilatory iron reducing (DIR) *Bacteria* are abundant in some FeIII-rich sediments. They also suggest that both heterotrophic and chemotrophic metabolisms are possible, with a range from mesophilic to hyperthermophilic functioning, and that arsenite oxidase genes are present at the high-salinity, lower temperature sites. This study expands on these investigations by studying the microbial ecology at greater sediment depth than the previous investigations and for the first time compares community structure between a high salinity and low salinity site.

## MATERIALS AND METHODS

### SITE DESCRIPTION

Two sites in Palaeochori Bay [Rocky Point (RP) and Twinkie (TW)] were investigated in this study; both are ~100 m offshore in ~4.5 m deep water (**Figures 1C, 2A,B**). Preliminary data indicate nearly identical pH and temperature profiles, although the RP site was demonstrably more saline than the TW site. The RP site features concentric rings of colored sediments, with orange in the center, transitioning to white and then brown (**Figure 2A**). The TW site is located ~8 m due east of the RP site and consisted primarily of white mats with some gas bubbles at the north side of the patch. Samples for this study were collected from the white areas from both sites (“P-W” in **Figure 2A** and “TW” in **Figure 2B**).

### Field sampling protocols

Pore fluids and sediments for geochemical and microbiological analyses were collected by SCUBA. Sediments were cored with polycarbonate tubes (Arthur Krüger GmbH) and capped underwater with rubber end caps. Pore fluids were either collected *in situ* into a BD™ (Becton, Dickinson and Company) 60 mL syringe from a tube inserted into the sediments, or extracted through holes in the core tube once onshore using 10 mL syringes attached to rhizons (long filters which can be inserted into the core; Rhizosphere) following Seeberg-Elverfeldt et al. (2005). Sediment cores were sliced for subsequent microbiological analyses. Each core slice was aseptically placed into sterile bags and frozen on dry ice. Samples were then shipped on dry ice back to the laboratory and kept frozen at -80°C.

Samples for free gas geochemistry were obtained by inverting a serum bottle under water and holding it over the streaming gas bubbles. Once the gas had completely filled the bottle, it was capped and crimped underwater with little to no seawater inside the bottle. Pore fluids for dissolved gases were sampled at 10 cm depth in the sediments by inserting a tube into the sediments, and filling a syringe. Subsequently, these pore fluids were put into N<sub>2</sub>-filled 60 mL serum bottles until a reverse meniscus formed, then capped and crimped.

## Geochemistry

Temperatures were measured *in situ* using a temperature probe in a custom-built underwater housing (constructed at the Max Planck Institute for Marine Microbiology, Bremen, Germany). The pH was measured on shore using a WTW pH meter 3210 with Mic-D electrode with temperature compensation. Analytical uncertainties were approximately  $\pm 0.1^{\circ}\text{C}$  for temperature and  $\pm 0.1$  for pH. Pore fluid concentrations of  $\text{Fe}^{2+}$ ,  $\text{NO}_3^-$ ,  $\text{NO}_2^-$ , and  $\text{NH}_3$  were analyzed in the field using a HACH spectrophotometer. Samples for free ( $\text{CO}_2$ ,  $\text{O}_2$ ,  $\text{N}_2$ , He,  $\text{H}_2$ , CO, and  $\text{CH}_4$ ) and dissolved (He,  $\text{H}_2$ ,  $\text{O}_2$ ,  $\text{N}_2$ , CO,  $\text{CH}_4$ , and  $\text{CO}_2$ ) gases were shipped on ice to the Istituto Nazionale di Geofisica e Vulcanologia, Palermo (Italy), for analysis. Pore fluid samples for anion analysis (Br, Cl, and  $\text{SO}_4^{2-}$ ) were filtered in the field (0.2  $\mu\text{m}$ ), placed on dry ice, and kept frozen until measurement in the laboratory. Samples for analysis of major seawater cations (Na, Ca, K, B, Sr), minor elements (Si, Ba, Mn, Fe), and trace elements (Li, Rb, Cs) were preserved in the field by filtering (0.2  $\mu\text{m}$ ) and acidification with 0.1% ultrapure  $\text{HNO}_3$ .

## LABORATORY PROTOCOLS

### Geochemistry

Major anions were analyzed using a Dionex ion chromatography system, whereas major cations were measured by inductively coupled plasma-optical emission spectrometry (ICP-OES; Perkin-Elmer Optima 3300). Lithium, rubidium, and cesium were measured by inductively coupled plasma-mass spectrometry (ICP-MS; High-resolution double-focusing ICP-MS Thermo Finnigan Element 2). Free ( $\text{CO}_2$ ,  $\text{O}_2$ ,  $\text{H}_2$ , CO, and  $\text{CH}_4$ ) and dissolved ( $\text{H}_2$ ,  $\text{O}_2$ , CO,  $\text{CH}_4$ , and  $\text{CO}_2$ ) gases were measured on a Perkin Elmer 8500 gas chromatograph equipped with a double-detector (TCD-FID) using argon as carrier gas (Italiano et al., 2009).

### Microbiology

**DNA extraction, PCR, and Cloning.** Bulk environmental (genomic) DNA was extracted from  $\sim 0.5$  g of sediment according to the protocol outlined in the MPBio FastDNA<sup>®</sup> spin kit, and stored at  $-20^{\circ}\text{C}$ . Amplification of 16S rRNA genes for both *Archaea* and *Bacteria* was performed by polymerase chain reaction (PCR) using primer sets 27F/1492R and 21F/1391R, respectively (Lane, 1991), on a Hybaid PCR express thermocycler. A total reaction volume of 20 or 50  $\mu\text{L}$  was prepared, containing 1× PCR buffer, 0.25 mM each dNTPs, 0.5  $\mu\text{M}$  each forward and reverse primer, 0.5–2  $\mu\text{L}$  DNA template depending on sample concentration, and 5 U Taq DNA polymerase (5 PRIME). DMSO was added to some samples to increase reaction yield. The final volume was adjusted with autoclaved milli-Q water. The amplification was initiated with denaturation at  $95^{\circ}\text{C}$  for 5 min, followed by denaturation (at  $95^{\circ}\text{C}$  for 1 min), annealing (at  $55^{\circ}\text{C}$  for *Archaea*,  $52^{\circ}\text{C}$  for *Bacteria*, for 1 min), and elongation (at  $72^{\circ}\text{C}$  for 1 min) for 30–35 cycles. A final extension step was carried out at  $72^{\circ}\text{C}$  for 10 min. Agarose gel electrophoresis was performed to verify amplification.

Degenerate primer sets used for arsenite oxidase functional gene (*aioA*-like) amplification were AOX-F-A2 (5'-TGC

ATCGTCGGCT GYGGNTAY-3') and AOX-R-E2 (5'-TTCGGAGTTATAG GCCGNCKRTTRTG-3') (Zargar et al., 2012) on a Hybaid PCR express thermocycler. These primers target the *aoxB* gene sequence of the arsenite oxidase operon and typically result in  $\sim 670$  bp product. A total reaction volume of 50  $\mu\text{L}$  was prepared, containing 1× PCR buffer, 0.25 mM each dNTPs, 0.5  $\mu\text{M}$  each forward and reverse primer, 0.5–2  $\mu\text{L}$  DNA template depending on sample concentration, and 5 U Taq DNA polymerase (5 PRIME). DMSO was added for some samples to increase reaction yield, and the final volume was adjusted with autoclaved milli-Q water. The amplification was initiated with denaturation at  $95^{\circ}\text{C}$  for 1 min, followed by denaturation (at  $95^{\circ}\text{C}$  for 0.5 min), annealing (at  $57^{\circ}\text{C}$  for 0.5 min), and elongation (at  $72^{\circ}\text{C}$  for 1 min) for 35 cycles. A final extension step was carried out at  $72^{\circ}\text{C}$  for 5 min. Agarose gel electrophoresis was performed to verify amplification.

PCR products were cloned separately using the pCR4-TOPO<sup>®</sup> Plasmid Vector Kit with One Shot TOP10 chemically competent *Escherichia coli* cells. Volumes of 25, 50, and 100  $\mu\text{L}$  of each transformation reaction were spread on selective LB agar plates containing ampicillin and incubated overnight at  $37^{\circ}\text{C}$ . White colonies were transferred with sterile toothpicks into 2.5 mL, 96 well microtiter plates containing a final volume of 200  $\mu\text{L}$  of LB medium. After an overnight incubation at  $37^{\circ}\text{C}$ , 100  $\mu\text{L}$  aliquots of liquid cultures were pipetted into a 96 well standard microplate with 20 % glycerol and shipped frozen to Beckman Coulter for sanger sequencing.

**16S rRNA gene clone library analysis.** Forward and reverse sequence fragments were trimmed and assembled using Geneious version 5.6.3, created by Biomatters (<http://www.geneious.com/>). Contigs were checked for chimeras using Mothur (Schloss et al., 2009) and Bellerophon (Huber et al., 2004). Sequences were classified using Mothur's Bayesian classifier and the RDP training set version 9 (Wang et al., 2007). Sequences were also aligned, compared, and clustered into operational taxonomic units (OTUs) using the default settings in Mothur. Representative OTUs at the 97 % sequence identity were selected and used to search for similar sequences in NCBI's nr/nt database using nucleotide BLAST (<http://blast.ncbi.nlm.nih.gov/Blast.cgi>). Organisms with complete genomes, closest cultured representatives, or sequences isolated from relevant hydrothermal or arsenic-rich environments were added as references to the 16S rRNA and *aioA*-like phylogenetic trees. The 97% OTU representatives and the database reference sequences were realigned in Mothur, and imported into Geneious. The PHYML plugin (Guindon and Gascuel, 2003) was used to construct a maximum likelihood tree for bacterial and archaeal sequences.

Several richness and evenness calculations were performed using their respective commands in Mothur. These include calculations for rarefaction curve data, Sobs (the observed richness reported, OTU), chao (the Chao1 estimator for richness), and the simpsoneven and shannoneven (both index-based measures of evenness), all at 97% cutoff.

For *aioA*-like gene sequences, assembly and vector trimming was also done in Geneious. Trimmed sequences were searched against Ref\_Seq using BLASTx. Sequences that hit

arsenite oxidase subjects with an *e*-value lower than e-40 were used to build the tree. Selected bacterial *aioA*-like genes were taken from Genbank and also added to the tree for reference. Sequences were aligned and compared in Geneious using both nucleotide and amino acid translation. The *aioA* tree was built using PHYML.

#### SUBMISSION OF NUCLEOTIDE SEQUENCE AND ACCESSION NUMBERS

Sequence data for 16S rRNA bacterial and archaeal clone libraries were submitted to GenBank under accession numbers KF278514-KF278557 and KF278485-KF278513, respectively. Partial nucleotide sequences for the arsenite oxidase genes were submitted under accession numbers KF303544-KF303564.

## RESULTS

### GEOCHEMISTRY

**Table 1** presents the geochemical data, including temperature, pH, Fe<sup>2+</sup>, NO<sub>3</sub><sup>-</sup>, NO<sub>2</sub><sup>-</sup>, NH<sub>3</sub>, and major and minor elements, collected from RP and TW sites. For comparison, seawater values, as well as a depth profile from a control site, were included. Temperature and pH were very similar between sites, but Mg<sup>2+</sup> and SO<sub>4</sub><sup>2-</sup> concentrations were depleted in both RP and TW samples. Furthermore, major cations, such as Na, Ca, K, B, and Sr, were enriched in the RP samples, but depleted in the TW samples, relative to seawater. Major anions, such as Cl and Br, are also enriched in RP samples but depleted in TW samples, relative to seawater. Most minor elements, including Si, Li, Rb, Fe, and Ba, were enriched in both fluids, although only slightly so in the TW fluids. Mn was only enriched in the RP samples. Arsenic concentrations followed a different pattern compared to all other elements. Both sites were highly enriched in this element, but in this case, the TW site was much more so, with a maximum concentration of 31.7 μM compared to 9.4 μM at RP. Depth profiles of temperature, pH, and concentrations of Cl and As are also shown in **Figure 3**. Note that the values of temperature and pH for RP and TW were similar with depth, but values for Cl and As differed markedly between sites (**Figure 3**). **Table 2** presents the dissolved and free gas data collected for this study. Dissolved gases were sampled at 10 cm depths at equivalent temperature and pH. Both RP and TW free gas was mostly CO<sub>2</sub>, followed by N<sub>2</sub>, O<sub>2</sub>, H<sub>2</sub>, CH<sub>4</sub>, He, and CO, although H<sub>2</sub>S concentrations in the free gas phase were not analyzed. Dissolved gases followed a similar trend.

### MICROBIOLOGY

#### Richness and evenness

The total number of clones generated for *Bacteria* per site is as follows: RP 0–1.5 (51), RP 3–4.5 (41), RP 9–10.5 (53), TW 0–1.5 (56), TW 3–4.5 (23), and TW 9–10.5 (27). The total number of clones generated for *Archaea* per site was: RP 0–1.5 (27), RP 3–4.5 (34), RP 9–10.5 (47), TW 0–1.5 (40), TW 3–4.5 (35), and TW 9–10.5 (66). Rarefaction analyses of the 16S rRNA gene sequences for *Bacteria* (**Figure A1A**) and *Archaea* (**Figure A1B**) indicated that the RP 0–1.5 sample displayed the highest diversity, with 22 OTUs out of 51 sequences. The steep slope for the RP 0–1.5 sample indicates that a large fraction of the species diversity remains to be discovered. The same is true for the RP

3–4.5 layer, which had 13 OTUs out of 41 sequences. The RP 9–10.5 sample had the lowest bacterial diversity for all samples analyzed. However, the TW 0–1.5 sample had the lowest bacterial diversity of all TW samples, with 12 OTUs out of 56 sequences. The TW 9–10.5 layer diversity was similar to TW 0–1.5, only slightly more diverse, and a slight development of an asymptotic curve. The TW 3–4.5 layer had the highest bacterial diversity of all TW samples, with a slope similar to the RP 0–1.5 sample. The RP site showed a clear decrease in bacterial diversity vs. depth, although the TW site did not follow this pattern. Hydrothermal environments, compared with many other marine environments, are often dominated by relatively few taxa (Polz and Cavanaugh, 1995; Schrenk et al., 2004). Therefore, in theory, fewer clones may be necessary for adequate sampling and evaluation of diversity. However, it is important to note that these curves may be most useful for assessing relative differences in the diversity of major groups between sites and depths.

For the archaeal OTUs, both sites showed increasing diversity vs. depth (**Figure A1B**). Archaeal OTU diversity for the TW 0–1.5 layer was the lowest, sequences from TW 3–4.5 slightly more so, with the TW 9–10.5 layer having the highest diversity. The RP 0–1.5, RP 3–4.5, and RP 9–10.5 samples followed a similar trend, with increasing archaeal diversity vs. depth. Each of the archaeal rarefaction curves level off to the right of the plot, suggesting the archaeal diversity may have been sampled adequately.

Richness indices for *Bacteria* and *Archaea* for each site vs. depth are presented in **Table 3**. The Chao1 index indicated that generally the bacterial communities were more diverse in the surface layers of the RP site relative to any other sample, and both RP and TW bacterial richness decreased with depth. Both the Shannon index and Simpson index indicated that the most diverse samples were RP 0–1.5 and TW 3–4.5, and that the RP site bacterial richness decreases vs. depth, whereas the TW site has the highest bacterial richness in the 3–4.5 depth sample. Each of these three indices generally indicated that archaeal richness was highest in the deepest samples with overall richness increasing vs. depth.

#### Bacterial affiliations

The diversity and distribution of bacterial 16S rRNA clones at the phylum (**Figure 4A**) and class (**Figure 4B**) levels were investigated for three depths at RP and TW. The RP 0–1.5 cm sediments were dominated by the phylum *Proteobacteria* (40 out of 51 clones), followed by representatives from the *Firmicutes* (6), *Bacteroidetes* (2), *Actinobacteria* (1), *Aquificae* (1), and *Deferribacteres* (1) (**Figure 4A**). Within the *Proteobacteria*, the *Epsilon* class dominated (**Figure 4B**), with nearly all clones identified as *Arcobacter* spp. Minor classes include *Deltaproteobacteria* (7 clones), *Bacilli* (6), and 1–2 clones each affiliated with *Actinobacteria*, *Aquificae*, *Flavobacteria*, and *Deferribacteres* (**Figure 4B**). In the 3–4.5 cm layer, the *Firmicutes* phylum dominated (33/41), followed by *Proteobacteria* (6), and one clone each of *Bacteroidetes* and *Actinobacteria* (**Figure 4A**). The *Firmicutes* consisted almost entirely of *Bacillus* spp. (100% confidence); the *Proteobacteria* were composed of the *Epsilon* (4) and *Gamma* classes (2) (**Figure 4B**). The deepest layer investigated at RP (9–10.5 cm)

**Table 1 | Major physicochemical parameters, major and minor elements in hydrothermal fluids collected from Paleochori Bay hydrothermal system.**

| Site name           | Field data |            |     |                       |                                   |                                   | Major elements       |         |         |         |        |        | Minor elements |         |         |         |         |         |         |         |         |         |      |     |
|---------------------|------------|------------|-----|-----------------------|-----------------------------------|-----------------------------------|----------------------|---------|---------|---------|--------|--------|----------------|---------|---------|---------|---------|---------|---------|---------|---------|---------|------|-----|
|                     | Depth (cm) | Temp. (°C) | pH  | Fe <sup>2+</sup> (mM) | NO <sub>3</sub> <sup>-</sup> (mM) | NO <sub>2</sub> <sup>-</sup> (mM) | NH <sub>3</sub> (mM) | Mg (mM) | Na (mM) | Ca (mM) | K (mM) | B (mM) | Sr (mM)        | Br (mM) | Cl (mM) | Si (mM) | Li (mM) | Rb (uM) | Fe (uM) | Mn (uM) | As (uM) | Ba (uM) |      |     |
| Seawater            | n.a.*      | 22.1       | 7.9 |                       |                                   |                                   |                      | 69.8    | 590.5   | 7.9     | 23.0   | 0.4    | 0.1            | 0.9     | 620.3   | 34.3    | 0.0     | 0.2     | 31.3    | b.d.    | 0.0     | 0.4     | b.d. |     |
| Control pore fluids | 5          | 22.1       | 7.4 |                       | 6                                 |                                   |                      | 66.8    | 581.4   | 7.1     | 21.7   | 0.4    | 0.1            | 0.9     | 638.0   | 32.8    | 0.0     | 0.1     | 30.7    | 0.5     | b.d.    | 0.2     | 0.0  |     |
| Control pore fluids | 15         | 23         | 7.4 | 0.024                 | 0.06                              | n.a.                              | n.a.                 | 42      | 68.6    | 583.3   | 7.5    | 22.8   | 0.4            | 0.1     | 0.9     | 640.1   | 33.0    | 0.1     | 0.1     | 30.8    | 29.5    | b.d.    | 0.3  | 0.1 |
| Rocky Point         | 10         | 67.9       | 5.3 | n.a.                  | 0.28                              | 0.7                               | 0.4                  | 257     | 55.3    | 703.7   | 16.6   | 60.7   | 1.7            | 0.1     | 0.9     | 744.9   | 20.8    | 1.8     | 3.2     | 231.8   | 11.0    | 27.2    | 6.9  | 1.4 |
| Rocky Point         | 20         | 79.4       | 5.3 | n.a.                  | 0.30                              | 0.7                               | 0.5                  | 246     | 56.0    | 696.3   | 16.3   | 59.5   | 1.7            | 0.1     | 0.9     | 731.2   | 20.8    | 1.8     | 3.1     | 227.3   | 8.2     | 25.9    | 9.4  | 1.3 |
| Twinkie             | 5          | 52.8       | 5.3 | 0.014                 | 0.40                              | 1.4                               | 0.2                  | 253     | 612     | 507.0   | 6.5    | 21.8   | 0.5            | 0.1     | 0.8     | 560.5   | 27.5    | 1.1     | 0.3     | 39.7    | 15.8    | b.d.    | 31.7 | 0.6 |
| Twinkie             | 10         | 64.3       |     |                       |                                   |                                   |                      |         |         |         |        |        |                |         |         |         |         |         |         |         |         |         |      |     |
| Twinkie             | 15         | 69.6       | 5.4 | 0.005                 | 0.38                              | 0.8                               | 0.1                  | 286     | 59.8    | 507.6   | 6.2    | 21.2   | 0.5            | 0.1     | 0.8     | 563.4   | 29.9    | 1.1     | 0.3     | 39.2    | 8.3     | b.d.    | 25.0 | 0.6 |
| Twinkie             | 20         | 71.5       |     |                       |                                   |                                   |                      |         |         |         |        |        |                |         |         |         |         |         |         |         |         |         |      |     |

\*n.a. or empty cell, not available; b.d., below detection.

\*\*Note: H<sub>2</sub>S data are from Druschel et al., unpublished data.

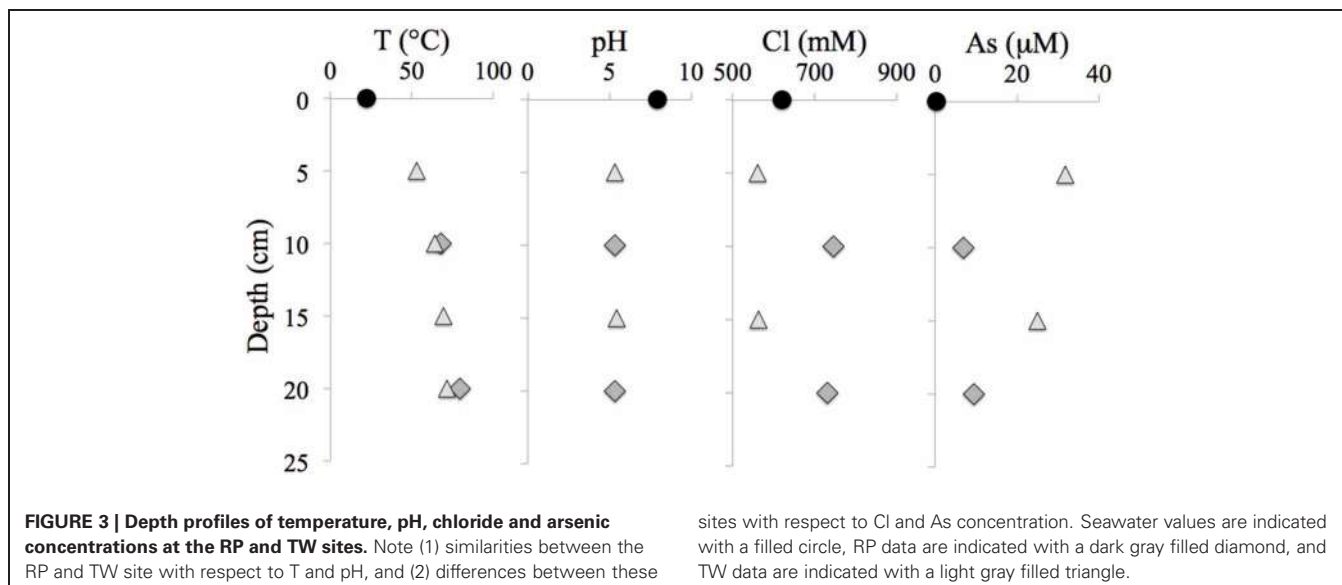


**Table 2 | Free and dissolved gas collected for this study\*.**

| FREE                      | CO <sub>2</sub> (%) | O <sub>2</sub> (%) | N <sub>2</sub> (%) | He (ppm) | H <sub>2</sub> (ppm) | CO (ppm) | CH <sub>4</sub> (ppm) |
|---------------------------|---------------------|--------------------|--------------------|----------|----------------------|----------|-----------------------|
| RP                        | 92.5                | 0.13               | 0.67               | 7.0      | 11450                | 0.7      | 916                   |
| TW                        | 93.5                | 0.39               | 1.2                | 11.7     | 14635                | 2.2      | 1890.0                |
| [mL(STP)/L <sup>#</sup> ] |                     |                    |                    |          |                      |          |                       |
| Dissolved                 | CO <sub>2</sub>     | O <sub>2</sub>     | N <sub>2</sub>     | He       | H <sub>2</sub>       | CO       | CH <sub>4</sub>       |
| RP                        | 50.9                | 0.0256             | 2.4                | **bdl    | 0.0077               | 0.00029  | 0.0058                |
| TW                        | 245.9               | 0.0109             | 3.2                | 0.00027  | 0.0004               | 0.00027  | 0.0303                |

\*Note: TW free and RP and TW dissolved gases are averages ( $n = 3$ ; free gas for RP was only collected once).

\*\*bdl, below detection limit.

<sup>#</sup>Dissolved gas data reported as mL of gas at standard temperature and pressure per liter of water.

was also dominated by the *Firmicutes* phylum (51/53; **Figure 4A**), with 47 clones identified as *Bacilli* (**Figure 4B**), predominantly within the genus *Bacillus*.

At TW in the 0–1.5 cm layer, *Bacteroidetes* dominated (37/56; **Figure 4A**), with 36 of those affiliating with the *Flavobacteria* (**Figure 4B**). The other phyla include *Proteobacteria* (16), *Actinobacteria* (2), and *Thermotogae* (1) (**Figure 4A**). Within the *Proteobacteria*, 14 affiliated with the *Epsilon* class (genus *Arcobacter*), and 2 with the *Gamma* class (**Figure 4B**). The TW 3–4.5 cm layer was dominated by the *Aquificae* (13 of 23 clones; **Figures 4A,B**), especially *Thermosulfidobacter* spp. (often with 100% confidence). The other phyla in this sample included *Actinobacteria*, *Planctomycetes*, *Proteobacteria*, *Thermodesulfobacteria*, and *Thermotogae* (**Figure 4A**). The deepest (9–10.5 cm) sediment sample at TW was dominated by the *Proteobacteria*, followed by *Bacteroidetes*, *Thermotogae*, and *Chloroflexi* (**Figure 4A**). Within the *Proteobacteria*, the *Epsilon* class (*Arcobacter* spp.; 18 of 27) dominated, followed by the *Beta* (3) and *Gamma* classes (2) (**Figure 4B**).

The bacterial 16S rRNA phylogenetic tree (**Figure 5**) includes the OTUs from our 16S rRNA clone libraries and some of their closest relatives, both isolates and other uncultured clones. Three

OTUs represented >5 clones each, which are noted in the **Figure 5** with a green star (173 total clones), and 50 OTUs represented ≤5 clones (78 total clones). OTU 23 represents 80 clones from the RP site (4 in the top layer, 29 in the middle, and 47 in the deepest layer). This OTU closely affiliates with the *Firmicutes* class (*Bacillus* spp.; **Figure 5**). OTU 30 (54 clones) affiliates with the *Epsilonproteobacteria* and was identified in all samples, except RP 9–10.5 cm. OTU 39 (39 clones) affiliated with *Bacteroidetes* and was identified almost exclusively in the TW 0–1.5 cm layer.

#### Archaeal affiliations

The diversity and distribution of archaeal clones at the three depths of RP and TW sediments is shown in **Figures 6A** (phylum) and **B** (class). At both sites, *Euryarchaeota* dominated in the surface layers (**Figure 6A**). At RP, most of the clones affiliated with the *Archaeoglobi* (16/27; specifically the genus *Ferroglobus*) and *Thermococci* (8/27; specifically the genera *Palaeococcus* and *Thermococcus*) (**Figure 6B**). At TW, clones affiliating with *Thermoplasmata* (*Euryarchaeota*) dominated (31 of 40 clones; **Figure 6B**; specifically the genus *Thermogymnomonas*). Two clones affiliated with *Thermoprotei* (*Crenarchaota*). At both sites, with increasing depth, the phyla

**Table 3 | Microbial diversity richness indices for bacterial and archaeal depth profiles from RP and TW sites in Palaeochori Bay.**

| Kingdom  | Site         | $S_{obs}^*$ | Chao | Shannon | Simpson |
|----------|--------------|-------------|------|---------|---------|
| BACTERIA | RP 0–1.5 cm  | 22          | 73   | 2.2     | 0.2     |
|          | RP 3–4.5 cm  | 13          | 79   | 1.3     | 0.5     |
|          | RP 9–10.5 cm | 4           | 5    | 0.5     | 0.8     |
|          | TW 0–1.5 cm  | 12          | 30   | 1.4     | 0.4     |
|          | TW 3–4.5 cm  | 11          | 19   | 2.2     | 0.1     |
|          | TW 9–10.5 cm | 8           | 10   | 1.4     | 0.4     |
| ARCHAEA  | RP 0–1.5 cm  | 9           | 10   | 1.9     | 0.2     |
|          | RP 3–4.5 cm  | 14          | 19   | 2.3     | 0.1     |
|          | RP 9–10.5 cm | 14          | 19   | 2.2     | 0.1     |
|          | TW 0–1.5 cm  | 10          | 12   | 1.3     | 0.5     |
|          | TW 3–4.5 cm  | 11          | 26   | 2.1     | 0.1     |
|          | TW 9–10.5 cm | 20          | 42   | 2.4     | 0.1     |

\*Sobs, number of OTUs identified.

changed from predominantly *Euryarchaeota* to more and mostly *Crenarchaeota*. The middle layer at RP (3–4.5 cm) was dominated by *Archaeoglobi* (*Euryarchaeota*), followed by *Thermoprotei* (*Crenarchaeota*; **Figure 6B**). The *Archaeoglobi* were again affiliated with genus *Ferroglobus*, while the *Thermoprotei* genera included *Staphylothermus*, *Pyrodictium*, and *Thermofilum*. The deepest RP site (9–10.5 cm) was dominated by *Thermoprotei* (*Crenarchaeota*; **Figure 6B**), with 42 of 47 clones affiliating with 5 genera including *Thermofilum* (25) and *Staphylothermus* (10). In the middle TW layer (3–4.5 cm), *Euryarchaeota* affiliated predominantly with *Archaeoglobi* (15; *Ferroglobus* sp.), and *Thermoplasmata* (9; *Thermogymnomonas* sp.), while the *Crenarchaeota* were entirely composed of *Thermoprotei* (5) (**Figure 6B**; specifically the genera *Hyperthermus* and *Thermofilum*). The TW 9–10.5 sequences affiliated with *Thermoprotei* (*Crenarchaeota*; 30 clones; genus *Thermofilum*), *Archaeoglobi* (*Euryarchaeota*; 11 clones; genus *Ferroglobus*) and *Thermoplasmata* (*Euryarchaeota*; 22 clones; genus *Thermogymnomonas*) (**Figure 6B**). Note, only one clone in all the libraries (RP 9–10.5) affiliated with the *Korarchaeota*.

The 16S rRNA archaeal phylogenetic tree (**Figure 7**) includes the OTUs from our 16S rRNA clone libraries and some of their closest relatives, other clones, and related isolates. Twelve OTUs represented >5 clones each, and are indicated by a green star in **Figure 7** (212 total clones), and 20 OTUs represented ≤5 clones (37 total clones). Primary OTUs affiliated with *Thermoprotei* (*Crenarchaeota*), and *Thermococci* (*Euryarchaeota*; **Figure 7**). Many sequences were <90% similar to other archaeal representatives found in public databases and therefore do not cluster with any major group. A considerable fraction of our archaeal sequences (~20%) contained large ~26–80 bp “inserts,” possibly introns (Burggraf et al., 1993). The OTU sequences containing these inserts (OTUs 8, 1, 30, 5, 3, 27, 2, 33, and 4) passed comprehensive quality and chimera checks, and are therefore included in the phylogenetic tree, and indicated with an asterisk, “\*” (**Figure 7**). BLAST hits indicate they are related to the *Euryarchaeota* (*Archaeoglobi* or *Thermoplasmata*), and

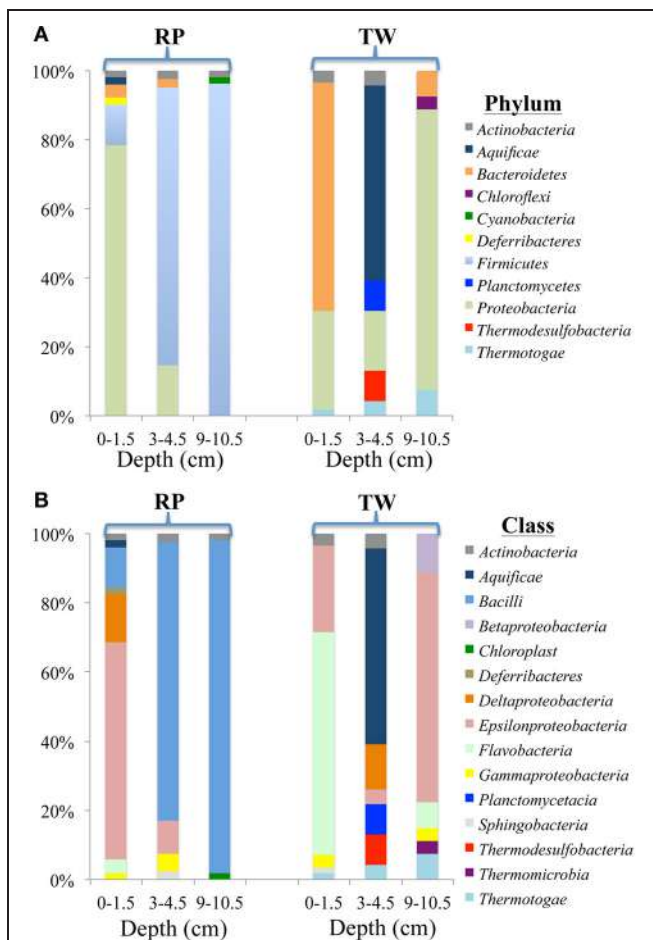
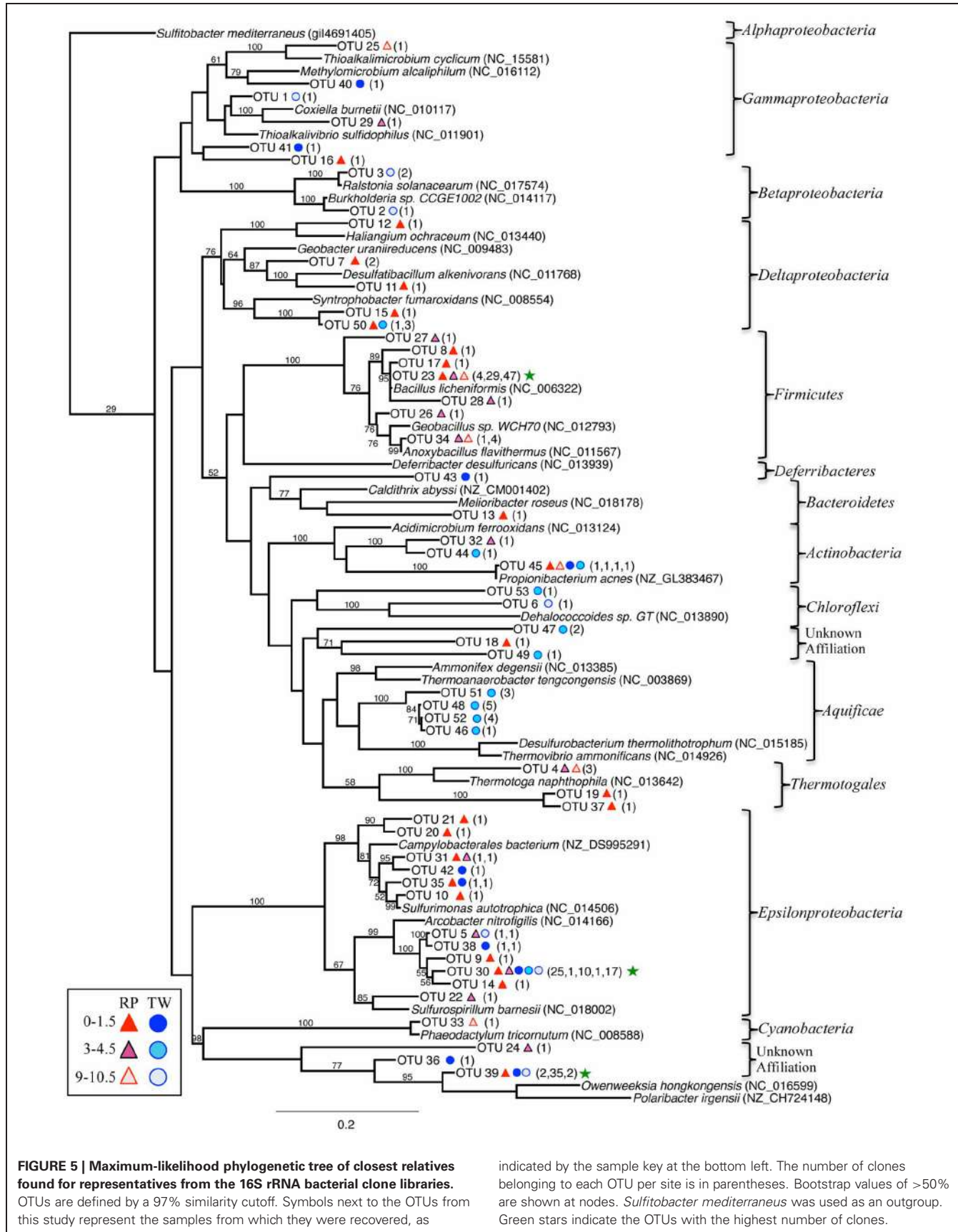


**FIGURE 4 | Diversity and distribution of clones within bacterial phylum (A) and class (B) clone libraries for three depths of RP and TW sediment layers investigated in this study.** Each color represents the percentages of each taxon in the total respective clone library, as determined by screening of full length 16S rRNA gene sequences. Depths are 0–1.5, 3–4.5, and 9–10.5 cm, and indicated at the bottom of site designation.

*Crenarchaeota* (*Thermoproteales* or *Desulfurococcales*). Five of the top six OTUs with the highest number of clones contained these inserts (8, 1, 30, 3, and 27). OTU 27 (39 clones) was found in all samples except RP 0–1.5 (**Figure 7**), and is identifiable to *Thermoprotei* according to the RDP classification. Three OTUs (8, 30, and 1; 38, 38, and 13 clones, respectively) were distantly related to *Archaeoglobi* or *Thermoplasmata*. OTU 12 (25 clones) poorly affiliated with *Archaeoglobi* (38% ID), which results in it being separate from the other groups in the phylogenetic tree (**Figure 7**, top left).

#### Arsenic functional genes

A phylogenetic tree of the *aioA*-like functional genes (AFGs) is shown in **Figure 8**, and includes sequences from our clone library, related isolates and other uncultured clones. Sequences affiliated with those detected in *Beta* (*Ralstonia* and *Burkholderia* genera), and *Alpha* classes of the *Proteobacteria* (*Polymorphum*, *Roseovarius* and *Bradyrhizobium* genera) cluster into two distinct



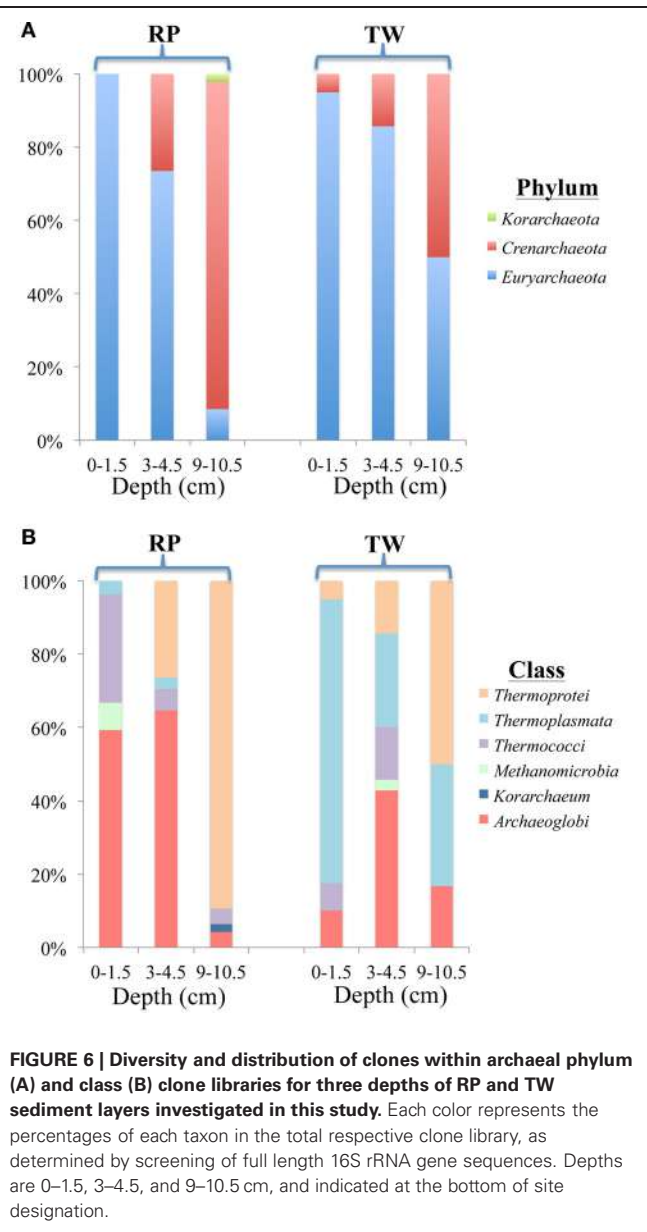


**FIGURE 6 | Diversity and distribution of clones within archaeal phylum (A) and class (B) clone libraries for three depths of RP and TW sediment layers investigated in this study.** Each color represents the percentages of each taxon in the total respective clone library, as determined by screening of full length 16S rRNA gene sequences. Depths are 0–1.5, 3–4.5, and 9–10.5 cm, and indicated at the bottom of site designation.

lineages (**Figure 8**). Most of the AFGs associated with *Beta* class had no closely related cultured representative. A total of 105 clones across 22 taxa contained the AFG. Of these, 93 were from the TW site, with 57, 24, and 12 clones from the surface, middle, and deepest layers, respectively. At the RP site, the AFG was found only in the surface (5 clones) and middle (7 clones) layers.

## DISCUSSION

### MICROBIAL DIVERSITY

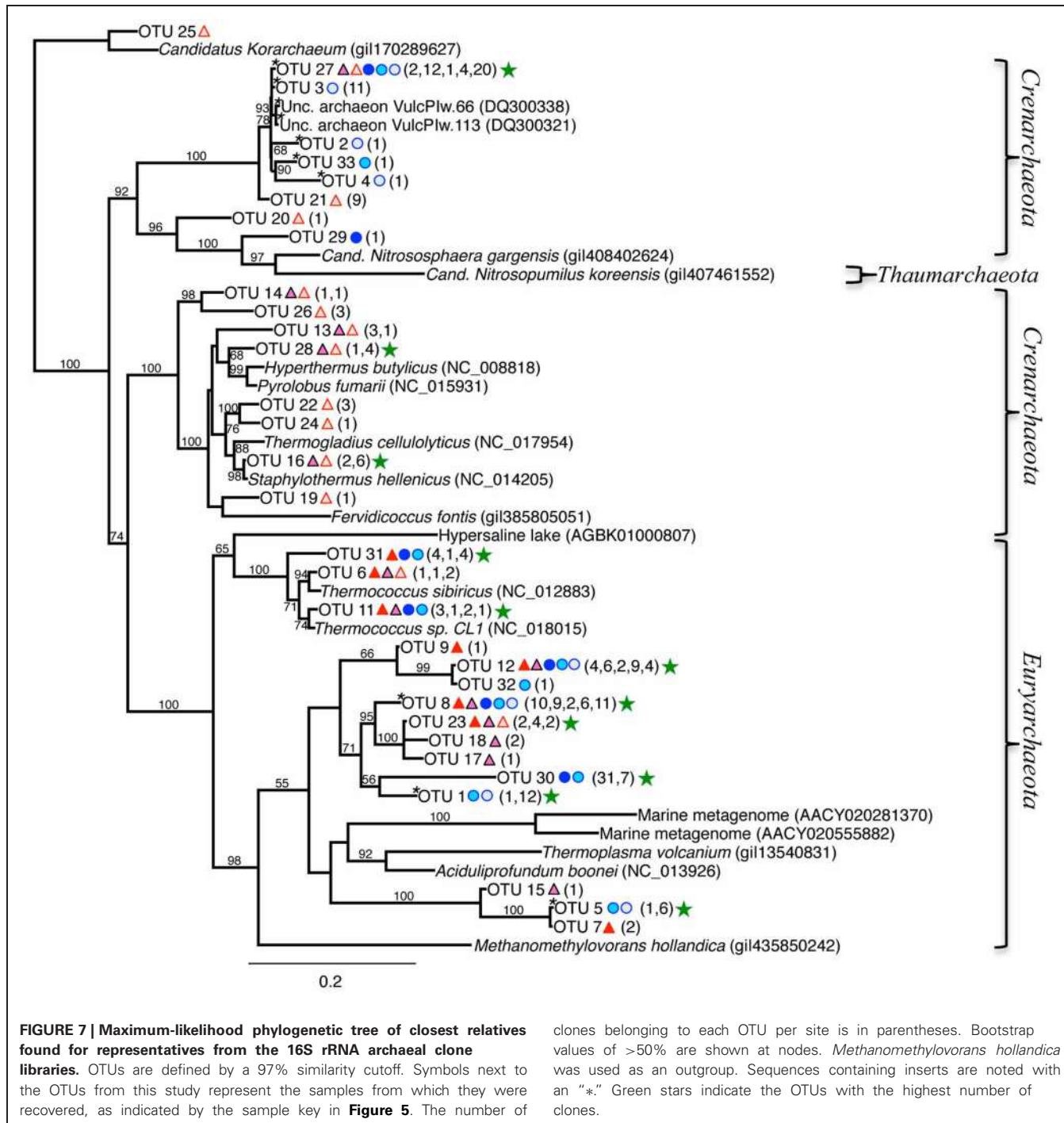
Our 16S rRNA gene sequence data indicate that bacterial and archaeal communities in the hydrothermally influenced sediments of Palaeochori Bay differ significantly when comparing the same depths of the RP high salinity and TW low salinity sites, although they have approximately the same temperature and pH (**Figures 4–8, Table 1**). Archaeal and bacterial class distribution

between each site and vs. depth is shown in **Table 4**, and indicates that several classes were exclusive to either the RP or TW site. For example, comparing the 0–1.5 cm sediment depth, *Aquificae*, *Deferribacteres*, *Bacilli*, and *Deltaproteobacteria* were only present in the RP site, whereas *Sphingobacteriia* and *Thermotogae* were only present in the TW sample (**Table 4; Figures 4A,B**). The same is true for the other sediment horizons, with distinct bacterial affiliations only occurring at one or the other site. Of the major bacterial groups, the *Firmicutes* were only present in the RP samples, while none were present in any of the TW sample depths. The 9–10.5 layer has zero overlapping bacterial classes between RP and TW sites (**Table 4**). *Betaproteobacteria* were identified in the TW sample from this depth, the only time this group was seen in any of the samples.

Differences in the archaeal communities in surface samples are also quite distinct; e.g., *Archaeoglobi* is dominant at the RP site while *Thermoplasmata* was dominant at the TW site (**Figures 6A,B**). As was the case for the *Bacteria*, there exist some groups at RP, which were not found at the TW site, and vice versa (**Table 4**). For example, the RP surface sample did not contain *Thermoprotei*, a dominant archaeal group for the TW site. In the deepest layer, the RP site contained *Thermococci*, but no *Thermoplasmata* (**Table 4**). These results suggest that the major archaeal and bacterial groups in Palaeochori Bay are distinctly different in the high vs. low salinity sites.

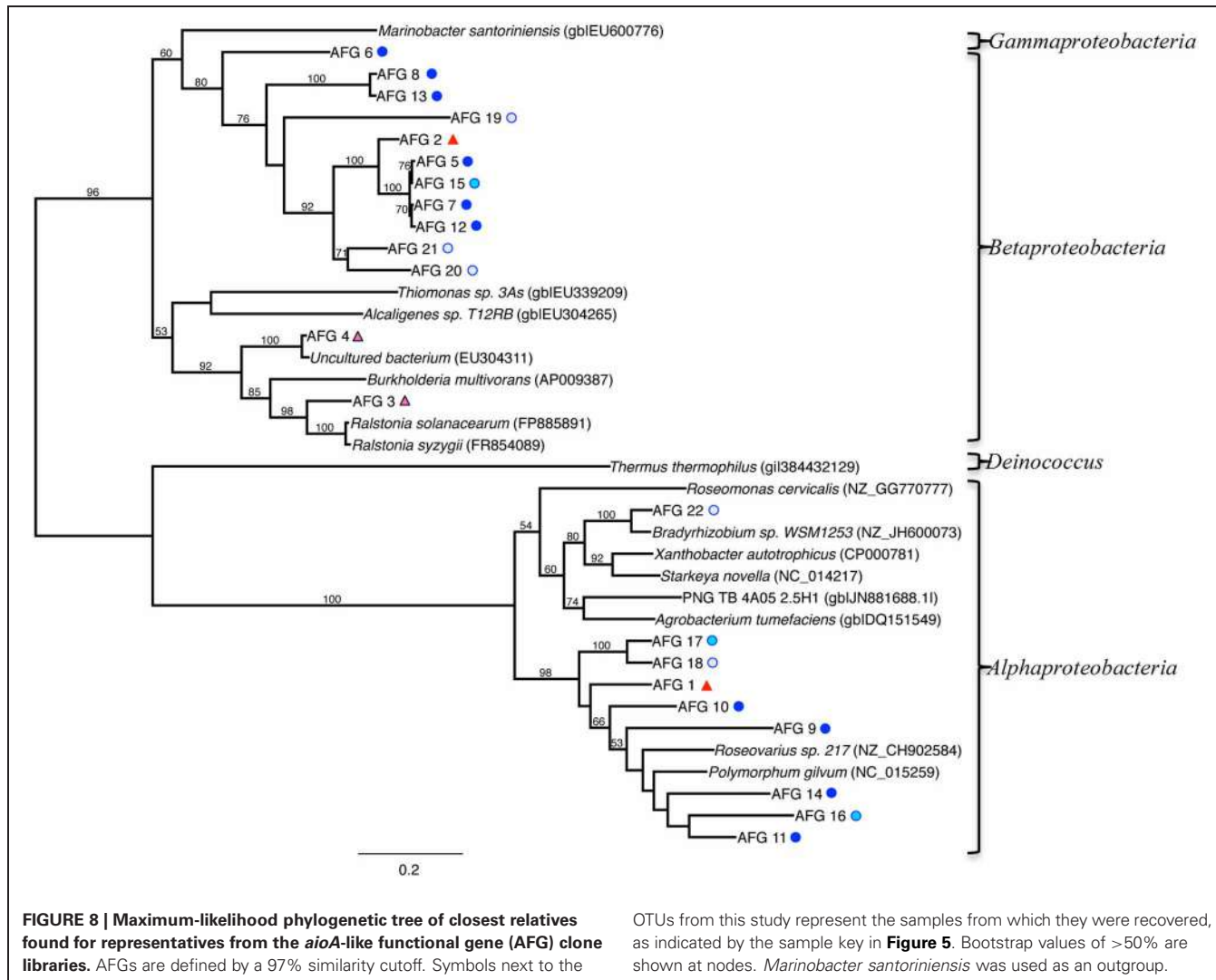
### THE ROLE OF PHASE SEPARATION

Subcritical phase separation is a ubiquitous process in hydrothermal systems, but its effect on microbial communities is rarely evaluated. Investigations of the Iheya North Field back-arc hydrothermal system south of Japan, suggested that subseafloor phase-separation and segregation may influence the supply of energy and carbon to vent-associated chemolithoautotrophs and related microbial communities (Nakagawa et al., 2005). When comparing microbial communities of gas-depleted “normal” fluids (i.e., those related to the remaining fluid phase after phase separation has taken place) to gas-enriched fluids (i.e., those which are related to the vapor phase; German and Von Damm, 2003), chemolithotrophs associated with gas-dependent energy metabolism, such as hydrogenotrophic methanogenesis, were more abundant. Another study investigated differences in microbial communities in phase separated hydrothermal fluids from the Yonaguni Knoll IV hydrothermal field in the southern Okinawa Trough (Nunoura and Takai, 2009). While fluids showed variability in the physical and chemical compositions (e.g., gas content), the microbial communities were relatively similar. There, chemolithotrophic hydrogen oxidation was the primary metabolism, and it was suggested that similarities in microbial communities could have been due to elevated concentrations of hydrogen in both types of fluids. Thus, microbial diversity may be influenced by a change in the concentration of potential electron donors as a result of phase separation (i.e., dissolved gases such as H<sub>2</sub>), not necessarily from salinity differences alone, although halotolerance cannot be ruled out. As we discuss below, metabolisms based on dissolved gases such as H<sub>2</sub> are possible at each site investigated here, but do not seem to play a dominant role in influencing major groups.



Our geochemical results indicate that salinity and arsenic concentrations are among the most variable parameters when comparing RP with TW pore fluid compositions (**Tables 1, 2; Figure 3**). Free gas data indicate that O<sub>2</sub>, N<sub>2</sub>, He, H<sub>2</sub>, CO, and CH<sub>4</sub> were only slightly higher for TW compared to RP (**Table 2**). Dissolved gas data suggest that no significant differences between sites exists for O<sub>2</sub>, CO, and H<sub>2</sub> concentrations; the dissolved CH<sub>4</sub> is slightly higher in the TW pore fluids (**Table 2**). For the redox sensitive species analyzed in this

study, dissolved Fe<sup>2+</sup>, NO<sub>3</sub><sup>-</sup>, and NO<sub>2</sub><sup>-</sup> were slightly higher, while NH<sub>3</sub> was slightly lower, in fluids from the TW site (**Table 1**). Hydrogen sulfide concentrations can be very elevated (up to 3 mM) in high salinity fluids, but were essentially equal (~0.25 mM) in both high- and low-salinity hydrothermal fluids analyzed for this study (Druschel et al., unpublished data; **Table 1**). These geochemical parameters suggest that the phase separation process at Milos may create differences in concentrations of dissolved gases, as well as some other important



redox couples, which could ultimately be contributing to the variability in microbial communities when comparing high- vs. low-salinity sites. However, we suggest that these differences are not significant, and therefore differences in microbial diversity may be influenced more by salinity and/or arsenic concentrations.

#### DOMINANT BACTERIAL METABOLISMS

The genus *Arcobacter*, which dominates the RP 0–1.5 cm sample, can grow at moderately thermophilic and halophilic conditions, utilizing nitrogen or sulfur, including sulfide oxidation (Wirsén, 2004; Donachie et al., 2005; Pati et al., 2010). For example, *A. nitrofigilis*, isolated from the roots of a salt marsh plant, can fix nitrogen (Pati et al., 2010). “*Candidatus Arcobacter sulfidicus*” has been shown to produce large white sulfur mats in hydrothermal environments (Wirsén, 2004), and related organisms may be responsible for the large white mats observed in Palaeochori Bay (Sievert et al., 1999). The white sulfur mats contain elemental sulfur, which may be the end product of sulfide oxidation. However, a comparison of our representative 16S rRNA gene sequence

(OTU 30; Figure 5) against this and other *Arcobacter* species indicated only a 91–93% sequence similarity (BLAST comparison Max ID).

In the deeper RP sediments, *Firmicutes* dominate, in particular, *Bacillus* sp. This group is phenotypically highly diverse, and includes obligate aerobes, facultative anaerobes, chemotrophs, and heterotrophs, halotolerant members, and organisms that tolerate a wide range of temperatures (Graumann, 2012). Our representative sequence (OTU 23) is most closely related to *B. licheniformis* DSM 13 (Figure 5) which, along with many other members of the *Bacilli*, can reduce nitrate to N<sub>2</sub> (Nakano and Zuber, 1998). Other investigations suggest that Mn(II) oxidation (Dick et al., 2006) and arsenate reduction may also be mediated by *Bacillus* spp. (Switzer et al., 1998). Four new strains of *Bacillus* were isolated from shallow-sea hydrothermal vents—two from Panarea and Vulcano Islands (Italy) (Maugeri et al., 2002; Spano et al., 2013), and two from the sediments in Palaeochori Bay (Milos) (Sievert et al., 2000a; Schlesner et al., 2001). The Milos isolates are *Halothiobacillus kellyi*, a mesophilic, obligately autotrophic, strictly aerobic,

**Table 4 | Bacterial and archaeal class distribution arranged by site and by depth.**

| Depth (cm) | Bacterial class              |                              | Archaeal class                |                        |
|------------|------------------------------|------------------------------|-------------------------------|------------------------|
|            | RP                           | TW                           | RP                            | TW                     |
| 0–1.5      | <i>Actinobacteria</i>        | <i>Actinobacteria</i>        | NP                            | <i>Thermoprotei</i>    |
|            | <i>Aquificae</i>             | NP                           | <i>Archaeoglobi</i>           | <i>Archaeoglobi</i>    |
|            | <i>Flavobacteria</i>         | <i>Flavobacteria</i>         | <i>Methanomicrobia</i>        | NP                     |
|            | <i>Deferribacteres</i>       | NP                           | <i>Thermococci</i>            | <i>Thermococci</i>     |
|            | <i>Bacilli</i>               | NP                           | <i>Thermoplasmata</i>         | <i>Thermoplasmata</i>  |
|            | NP*                          | <i>Sphingobacteria</i>       |                               |                        |
|            | <i>Deltaproteobacteria</i>   | NP                           |                               |                        |
|            | <i>Epsilonproteobacteria</i> | <i>Epsilonproteobacteria</i> |                               |                        |
|            | <i>Gammaproteobacteria</i>   | <i>Gammaproteobacteria</i>   |                               |                        |
|            | NP                           | <i>Thermotogae</i>           |                               |                        |
| 3–4.5      | <i>Actinobacteria</i>        | <i>Actinobacteria</i>        | <i>Thermoprotei</i>           | <i>Thermoprotei</i>    |
|            | <i>Sphingobacteria</i>       | NP                           | <i>Archaeoglobi</i>           | <i>Archaeoglobi</i>    |
|            | <i>Bacilli</i>               | NP                           | NP                            | <i>Methanomicrobia</i> |
|            | NP                           | <i>Aquificae</i>             | <i>Thermococci</i>            | <i>Thermococci</i>     |
|            | NP                           | <i>Planctomycetacia</i>      | <i>Thermoplasmata</i>         | <i>Thermoplasmata</i>  |
|            | NP                           | <i>Deltaproteobacteria</i>   |                               |                        |
|            | <i>Epsilonproteobacteria</i> | <i>Epsilonproteobacteria</i> |                               |                        |
|            | <i>Gammaproteobacteria</i>   | NP                           |                               |                        |
|            | NP                           | <i>Thermodesulfobacteria</i> |                               |                        |
|            | NP                           | <i>Thermotogae</i>           |                               |                        |
| 9–10.5     | <i>Actinobacteria</i>        | NP                           | <i>Thermoprotei</i>           | <i>Thermoprotei</i>    |
|            | <i>Chloroflexi</i>           | NP                           | <i>Archaeoglobi</i>           | <i>Archaeoglobi</i>    |
|            | <i>Bacilli</i>               | NP                           | NP                            | <i>Thermoplasmata</i>  |
|            | NP                           | <i>Flavobacteria</i>         | <i>Thermococci</i>            | NP                     |
|            | NP                           | <i>Thermomicrobia</i>        | <i>Candidatus Korarchaeum</i> | NP                     |
|            | NP                           | <i>Betaproteobacteria</i>    |                               |                        |
|            | NP                           | <i>Epsilonproteobacteria</i> |                               |                        |
|            | NP                           | <i>Gammaproteobacteria</i>   |                               |                        |
|            | NP                           | <i>Thermotogae</i>           |                               |                        |

\*NP, not present.

chemolithoautotrophic, sulfur-oxidizing bacterium (Sievert et al., 2000a), and *Filobacillus milensis*, a halophilic, facultatively anaerobic, endospore-forming heterotroph (Schlesner et al., 2001). In addition, 39 of 80 aerobic mesophiles isolated from Milos by Dando et al. (1998) are phenotypically similar to *Bacillus sp.*

The most abundant bacterial group in the surface sample at Twinkie (TW 0–1.5) was *Bacteroidetes*. However, the RDP classification confidence was quite low even at the class level (average 74%), suggesting many possibilities for representatives from this phylum. The representative OTU for these sequences is OTU 39, which had 35 out of 39 clones in the TW 0–1.5 cm sample. Due to the low confidence identification of this group, it is not affiliated with any other main group in the bacterial phylogenetic tree (Figure 5, bottom left). BLAST results most closely identified with uncultured clones, making identification of primary metabolisms difficult. The phylum *Bacteroidetes* contains among the most abundant microbes in coastal marine waters (Alonso et al., 2007). Cultured representatives from this phylum

are typically heterotrophs, non-thermophilic, and use complex organic substrates, either by aerobic respiration or fermentation (Kirchman, 2002). They can also be found in hydrothermal environments. For example, Kormas et al. (2006) detected *Bacteroidetes spp.* on a white smoker chimney at 9° N, East Pacific Rise. Recently, Sylvan et al. (2012) suggested that *Bacteroidetes* replaced “normal” microbial communities once smoker chimneys become inactive. Sievert et al. (2000b) and Nitzsche (2010) both identified *Bacteroidetes* as dominant members in the white areas from Milos sediments, but temperatures were in both cases quite lower than for our study (~20°C less). This suggests the possibility that *Bacteroidetes* activity is limited to lower temperature environments. Temperatures were comparable between the RP and TW sites (i.e., <~40°C), but salinity was quite different, suggesting the lack of *Arcobacter* in place of *Bacteroidetes* at the TW site may also be influenced by halotolerance. However, as discussed, dissolved gases and other redox couple concentrations may play a role, as they are slightly elevated in the TW pore fluids.

The TW 3–4.5 site was dominated by *Thermosulfidibacter* spp., whose closest cultured representative is *Thermosulfidibacter takaii*, a thermophilic, sulfur-reducing chemolithoautotroph from a deep-sea hydrothermal vent at the Yonaguni Knoll IV, Southern Okinawa Trough (Nunoura et al., 2008). Growth was observed within the temperature range of 55–78°C, and 0.5–4.5% NaCl. Temperatures at this sediment depth should be near 50°C, and salinity should be slightly lower than seawater (**Table 1**; **Figure 3**).

The TW 9–10.5 was dominated by *Arcobacter* spp. (*Epsilonproteobacteria*; 18 out of 27 clones). As discussed, the group could be conducting nitrate reduction or sulfide oxidation. Comparing the OTU representative sequence (OTU 5) from TW 9–10.5 to the 16S rRNA gene sequence from *A. nitrofigilus* and “*Ca. A. sulfidicus*” indicates BLAST max ID of 93% and 93%, respectively. Indeed, the representative OTUs from RP 0–1.5 (OTU 14) and TW 9–10.5 (OTU 5) were only 96% max ID when compared to each other. This suggests that the *Arcobacter* species in both the RP 0–1.5 and TW 9–10.5 samples are only distantly related, and it is probable that they are different species or genera with different environmental tolerances.

These data indicate that bacterial communities are stratified by depth, and that sulfur- and nitrogen-based metabolisms may dominate at the RP site, whereas phototrophy, sulfur, and/or nitrogen-based metabolisms may be dominant at the TW site. Temperature may be the dominant parameter which influences microbial community structure as a function of depth at both RP and TW sites, as vertical gradients are more pronounced for this parameter compared to any other (**Table 1**; **Figure 4**). Sunlight may also play a role, particularly for the surface TW site where *Bacteroidetes* is present.

#### DOMINANT ARCHAEOAL METABOLISMS

The dominant archaeal genera for RP 0–1.5 were *Ferroglobus* (*Archaeoglobi*) and *Palaeococcus/Thermococcus* (*Thermococci*). These groups become replaced mostly by the *Thermoprotei* (*Staphylothermus* and *Thermophilum*) at depth. However, poor RDP classification confidence makes identification beyond the phylum level difficult. Further complicating matters, the OTU chosen to represent the sequences associated with the *Archaeoglobi* (OTU 8) contained a 44 bp insert. BLAST analysis of OTU 8 returned no cultured representatives, and identified most closely with uncultured clones from the Logatchev hydrothermal field (LHF) and terrestrial hydrothermal vents on Ambitle Island, PNG. Removing the insert from OTU 8 and conducting a BLAST analysis for the remaining sequence indicates *Aciduliprofundum* spp. as the closest cultured match (100% query coverage; 86% max ID). This organism belongs to the “Deep-sea Hydrothermal Vent Euryarchaeota 2” (DHVE2) lineage (Takai and Horikoshi, 1999), which are widespread at deep-sea hydrothermal vents (Reysenbach et al., 2006; Flores et al., 2012). Unfortunately, relatively little is known about their distribution and phylogenetic diversity (Flores et al., 2012). The only described species from the *Aciduliprofundum* genus is *A. boonei* T469<sup>T</sup>, which is an obligate thermoacidophilic sulfur- or iron-reducing heterotroph capable of growing from pH 3.3–5.8 and between 55 and 75°C

(Reysenbach et al., 2006). This organism is included in the phylogenetic tree, but does not affiliate closely with our sequences (**Figure 7**).

The second most abundant archaeal group in the RP 0–1.5 sample was *Thermococci*, consisting of both *Thermococcus* spp. and *Palaeococcus* spp., with ~100% RDP confidence. Our OTUs for this group (31, 6, and 11) did not contain insertions, and identified most closely with *Thermococcus* spp. (**Figure 7**). There are numerous species related to this genus; most are considered extreme thermophiles, typically identified as organotrophic anaerobes which grow above 70°C, sometimes requiring elemental S, producing H<sub>2</sub>S and CO<sub>2</sub>, and have the ability to use H<sup>+</sup> (Arab et al., 2000).

The RP 9–10.5 sample was dominated by the *Crenarchaeota-Thermoprotei*, was composed of several genera, which were dominated by *Thermofilum* spp., although mostly with very poor confidence, followed by *Staphylothermus* spp., often with 100% confidence, and several others. Our OTUs chosen to represent the *Thermofilum* spp. identified by the RDP classification (21, 26, and 27) most closely affiliated with *Thermoprotei* (**Figure 7**). However, OTU 26 is within a slightly different cluster, and had much higher RDP % confidence than the other two with *Thermofilum* spp. BLAST analysis of this OTU most closely matched with *Thermofilum pendens*, a thermophilic, anaerobic sulfur-respirer. OTU 27 contained an insert, and BLAST analysis indicated the closest representative was the uncultured clone VulcPlw.113, from the shallow-sea hydrothermal vents off Vulcano, Italy. The sequence from this clone, as noted, also contains an insert. Removing the insert from OTU 27 and conducting a BLAST analysis indicates it does not affiliate with any cultured representatives, and is most closely related to various uncultured *Archaea* from the Mariana Trough, East Pacific Rise, and the shallow-sea vents off Ambitle Island, Papua New Guinea (Meyer-Dombard et al., 2011).

The TW 0–1.5 was by far dominated by the *Thermoplasmata* class, *Thermogymnomonas* genus. This genus has one heterotrophic species, *T. acidicola*, and can grow at temperatures in the range 38–68°C (optimally at 60°C), at pH 1.8–4.0 (optimally at around pH 3.0), and is obligately aerobic and heterotrophic, requiring yeast extract for growth (Itoh et al., 2007). These clones are represented by OTU 30, which according to RDP, poorly affiliated with *Thermoprotei*. This OTU contained an insert, and BLAST analysis indicated affiliation to uncultured clones VulcPlw.76, and those from terrestrial vents from Papua New Guinea. The closest cultured representative was *Aciduliprofundum* sp. MAR08-237A. BLAST analysis of this sequence with the insert removed indicates similar results.

In the deeper 9–10.5 sample for TW, dominant members transition to *Thermoprotei* (mostly *Thermofilum* spp.; OTUs 2 and 3), although abundant *Thermoplasmata* (*Thermogymnomonas* spp.; OTUs 1 and 5) were also present. Metabolisms for these organisms have been discussed previously. Each of these OTUs contained inserts. OTUs 2 and 3 identified most closely with VulcPlw.76 uncultured clone and previously obtained clone sequences from Milos, with no affiliation to a cultured representative. OTUs 1 and 5 identified with the isolate *A. boonei*. OTU 4 in this sample identified with *Stetteria* sp., from the *Thermoprotei-Desulfurococcaceae* family, by the RDP classification. BLAST

analysis of this sequenced indicates affiliation with the previously described uncultured clones from the shallow-sea vents off Vulcano and Milos.

These results indicate that archaeal metabolisms in both surface and deeper sediments are dominated by sulfur oxidizers, can be heterotrophic, and may also have the ability to conduct Fe oxidation. These poorly classified groups, particularly those which contain an insert, could represent new genera or new higher order taxa.

Although we cannot say for sure these extra nucleotide sequence insertions are introns, we believe the extra nucleotides in our sequences are real for three main reasons: (1) The quality scores for most of these sequences were very high. (2) Multiple chimera checks suggested they are not chimeras (see Materials and Methods section), (3) They are found not only in our dataset, but also in several other datasets from Milos [Brehmer, 2000 (unpublished data, NCBI database); Nitzsche, 2010], and the near-shore hydrothermal vent system of Vulcano (Italy) (Rogers and Amend, 2005). The other datasets were obtained from completely different laboratories using different methods, making it highly unlikely that there is an error. All of the other introns found in this study, when blasted independently after exons were removed, consistently returned affiliations with clone sequences from these previously reported groups as the closest representatives. An intron is an additional piece of nucleotide sequence found in the genes of most organisms and many viruses, and can be located in a wide range of genes, including those that generate proteins, rRNA, and tRNA (Itoh et al., 2003). Introns in the 16S rRNA gene of *Archaea* are rare, and primarily restricted to the *Crenarchaeota*, within the families *Thermoproteaceae* and *Desulfurococcaceae* (Morinaga et al., 2002; Itoh et al., 2003). Although outside the current scope of this paper, it is important to note that if the extra nucleotide sequence contained within our archaeal sequences for OTU 8, as well as OTUs 1, 30, and 5, are in fact introns, it is a significant finding as introns contained within the 16S rRNA gene sequences of *Euryarchaeota* have not, to our knowledge, been reported.

### ARSENIC FUNCTIONAL GENE SURVEY

Elevated arsenic concentrations may clearly influence microbial community structure and function, since the concentrations encountered can be toxic and may also provide additional redox couples for microbial metabolism (e.g., arsenotrophy). For example, in reducing hydrothermal fluids, arsenic exists most commonly as arsenite, with a +3 oxidation state ( $\text{AsIII}$ ,  $\text{H}_2\text{AsO}_3^-$ ). However, in surface seawater and other oxidizing environments, arsenic is dominantly in the +5 oxidation state (arsenate,  $\text{AsV}$ ,  $\text{HAsO}_4^{2-}$ ). Thus, microorganisms can play an important role in the arsenic cycle as they catalyze the transformation of different arsenic redox species (Handley et al., 2009; Akerman et al., 2011; Meyer-Dombard et al., 2011, 2013). The three main types of arsenotrophs thus far known to occur are heterotrophic arsenite oxidizers (HAOs), chemotrophic arsenite oxidizers (CAOs), and dissimilatory arsenate-reducing prokaryotes (DARPs; Oremland and Stoltz, 2003). Genes involved in these arsenic transformations include detoxification via the ArsC system, and energy gain via the arsenate respiratory reductase (two subunits, ArrA and ArrB) or the arsenite oxidase (two subunits, AioA and AioB, formerly

referred to as AroA and/or AoxB; Oremland and Stoltz, 2003; Zargar et al., 2010). Recently, an alternative AsIII-oxidation gene was discovered (arxa-type; Zargar et al., 2010). To date, most studies of As microbial cycling have focused on various naturally or anthropogenically impacted environments, primarily located in terrestrial (non-marine) settings. Next to nothing is known about As cycling in coastal marine environments.

At the two sites investigated here, analysis of the AFGs revealed affiliation with only two classes within the *Proteobacteria* phylum, although we must keep in mind that lateral gene transfer may have occurred (Figure 8). The *Alphaproteobacteria* containing the arsenite oxidase gene were predominantly affiliated with the genera *Polymorphum*, *Bradyrhizobium* and *Roseovarius*, while the *Betaproteobacteria* were affiliated with the *Burkholderia* or *Ralstonia* genera. The primers used for screening of *aioA*-like genes were based on a range of groups, and therefore should be broadly applicable (i.e., should not be specific to one or two groups). For example, primer design relied on the sequence alignment of 16 arsenite oxidase amino acid sequences consisting of 5 *Alpha*-, 4 *Beta*-, 3 *Gammaproteobacteria*, 2 *Deinococci*, and one *Chloroflexi* (Zargar et al., 2012). Thus, there could be a bias toward *Alpha*- and *Betaproteobacteria*, but many published arsenite oxidizers are in these groups (e.g., the most updated phylogenetic tree for arsenotrophs has many of the *aioA*-like gene containing microbes as *Alpha*- and *Betaproteobacteria*). There are some newer isolates being reported within the *Gammaproteobacteria*, and various genome sequencing projects are also starting to show the presence of *aioA*-like genes (Handley et al., 2009; Cavalca et al., 2013). The primers used here were the best available at the time of their design.

AFG distribution was primarily associated with the TW samples, which is somewhat expected given the higher concentrations of arsenic at this site (Figure 8). Phylogenetic analysis revealed that both the *Beta*- and *Alphaproteobacteria* relationships can be further subdivided into two distinct lineages (Figure 8). While some of the *Betaproteobacteria* were most closely related to *Ralstonia* and *Burkholderia* genera (AFGs 3 and 4), nearly all of the other AFGs associated with *Betaproteobacteria* had no closely related cultured representative (Figure 8). Four main clusters exist for these *Betaproteobacteria*. They consist of (1) AFG 6, (2) AFGs 2, 5, 15, 7, 12, 20, and 21, (3) AFG 19, and (4) AFGs 8 and 13. BLAST analysis of these AFGs indicate they are associated with either *Beta*- or *Alphaproteobacteria*, mostly *Burkholderiales*, but cannot be constrained beyond the *Proteobacteria* phylum. The *Alphaproteobacteria* were most closely related either to *Polymorphum*, *Roseovarius*, or *Bradyrhizobium* spp. AFG 11 was closest to *Polymorphum gilvum* in the phylogenetic analysis (Figure 8). Only *Burkholderiales* occurred in the low salinity 9–10.5 cm depth in the 16S rRNA gene clone libraries. BLAST analysis of these AFG sequences indicates similarity to *aioA*-like genes from various terrestrial arsenic-rich environments.

These species are only distantly related, and therefore discussion of their arsenic oxidation strategy is limited. For example, *Polymorphum gilvum* was isolated from a crude oil-polluted saline soil in Shengli Oilfield, China, and was able to use the crude oil as the sole carbon source, and is not known to conduct arsenic metabolism, although its genome contains genes for both arsenite

oxidation and arsenate reduction (detoxification) (Li et al., 2011). All of the related groups in the AFG analysis can be confirmed to contain an arsenite oxidase, but none of them have been shown to oxidize or reduce arsenic for detoxification or for their metabolism.

Overlap in AFG and 16S rRNA gene sequence data occurred only in the low salinity TW 9–10.5 sediments. For example, two OTUs (2 and 3) from the bacterial 16S rRNA data set were identified most closely with the *Betaproteobacteria*, specifically *Ralstonia* sp. and *Burkholderia* sp. This suggests arsenotrophy may be an important metabolism in deep, low-salinity, As-rich environments similar to those found in the TW 9–10.5 layer.

Other molecular investigations of the genes responsible for As redox transformations have revealed intriguing evidence for As microbial transformations in marine hydrothermal environments. For example, Nitzsche (2010) used arsenic primers for *aioA*-like gene amplification of 0–6 cm pooled sediments from Milos, and obtained similar results to our data (i.e., *Alpha-* and *Betaproteobacteria*). At a marine shallow-water hydrothermal vent off Ambitle Island, Papua New Guinea, microorganisms may be key in the oxidation of As(III) in areas immediately surrounding the vent source (Akerman, 2009; Meyer-Dombard et al., 2011, 2013). Using PCR primers designed to amplify arsenic functional genes, biofilm communities at the site were shown to possess the genetic capacity for the oxidation of As(III). The *aroA*-like (now known as *aioA*-like) clone sequences analyzed belonged to relatives of *Alpha-* and *Betaproteobacteria*, *Thermus*, and *Pyrobaculum*, but were only 71–80% similar to these sequences available in GenBank, suggesting that many of the Ambitle Island As-functional genes are unique. Thus, in marine environments, arsenite oxidation may be limited to the *Alpha-* and *Betaproteobacteria*, but much more research is necessary, particularly cultivation and molecular-based (next generation metagenomic) approaches focusing on arsenotrophy.

## CONCLUSIONS AND OUTLOOK

Our results indicate that differences in archaeal and bacterial community structure exist at the site as a function of not only depth, but also when comparing high vs. low salinity environments with similar redox potential. A wide range of metabolisms seem possible, with affiliated members likely involved in the nitrogen or sulfur cycle. However, it should be noted that rare members of the community can also be very active and function as “keystone species,” yet not be detected

in clone libraries. Differences in bacterial and archaeal communities between the RP high-salinity and TW low-salinity sites suggest geochemical signatures resulting from phase separation may be a controlling factor in hydrothermal vent microbial ecology (e.g., salinity, arsenic). Our screening of AFGs responsible for arsenite oxidation indicate that both the *Alpha-* and *Betaproteobacteria* may be responsible for arsenite oxidation in sediments from both sites, although the most abundant clusters are from the higher-arsenic TW site. These results are similar to previously reported AFG screening in marine environments, suggesting that *Alpha-* and *Betaproteobacteria* are the key players in marine hydrothermal arsenic metabolism. Since these groups are only distantly related to known arsenite oxidizers, novel genera may be present at the site; much more research is necessary including targeted cultivation of arsenotrophs. These results also provide incentive for metagenomic investigation of these sites to identify potential novel shallow vent species, and confirm arsenite metabolism is present primarily in the *Alpha-* and *Betaproteobacteria*. Affiliations from the arsenic gene screening were often not reflected in the 16S rRNA results, suggesting that arsenite may only be an important electron donor in the deeper, low salinity, high arsenic sediments. However, this could also be the result of a lack of sufficient database representation, relatively shallow sequencing depth or potential bias in the AFG primers. Finally, many of the archaeal 16S rRNA sequences contained putative introns, including members of *Euryarchaeota*, which has not been reported previously.

## ACKNOWLEDGMENTS

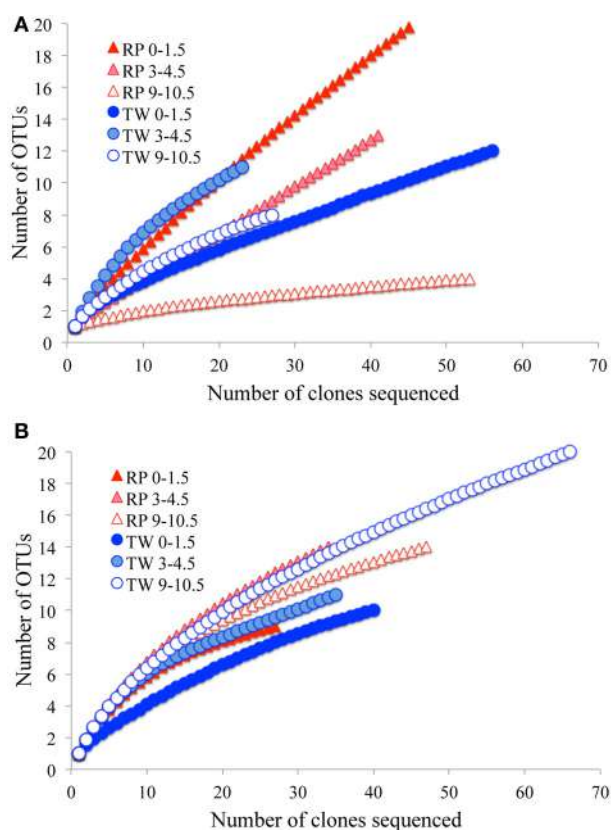
Funding for this project was provided by a University of Bremen MARUM Post-doc Fellowship (to Roy E. Price), MARUM Unforeseen Incentive Funding (to Roy E. Price and Solveig Buehring), NSF-EAR Grant 1222533 and NSFOCE Grant 1061476 (to David Fike, Gregory Druschel, and Jan P. Amend), and NSF-EAR Grant 0951947 (to Chad Saltikov). We thank Paul Dando for his unselfish discussions about the Milos system, Wolfgang Bach and Heike Anders for the ICP-MS analyses. We thank David Fike, William Gilhooley, and Gregory Druschel for help in the field, and Gregory Druschel for providing H<sub>2</sub>S data for this manuscript. Thanks to Katrina Edwards for providing laboratory space. Special thanks to Athanasios Godelitsas, Antonios Vichos and the Artemis Bungalows, and the Sirocco Restaurant for logistical support in Athens and Milos.

## REFERENCES

- Akerman, N. (2009). *Microbial diversity and geochemical energy sources of Tutum Bay, Ambitle Island, Papua New Guinea, an arsenic-rich shallow-sea hydrothermal system*. Ph.D. dissertation, Washington University in St. Louis.
- Akerman, N., Price, R., Pichler, T., and Amend, J. P. (2011). Energy sources for chemolithotrophs in an arsenic- and iron-rich shallow-sea hydrothermal system. *Geobiology* 9, 436–445.
- Alonso, C., Warnecke, F., Amann, R., and Pernthaler, J. (2007). High local and global diversity of *Flavobacteria* in marine plankton. *Environ. Microbiol.* 9, 1253–1266. doi: 10.1111/j.1462-2920.2007.01244.x
- Amend, J. P., Rogers, K. L., Shock, E. L., Gurrieri, S., and Inguaggiato, S. (2003). Energetics of chemolithoautotrophy in the hydrothermal system of Vulcano Island, southern Italy. *Geobiology* 1, 37–58. doi: 10.1046/j.1472-4669.2003.00006.x
- Arab, H., Voelker, H., and Thomm, M. (2000). *Thermococcus aegaeicus* sp. nov. and *Staphylothermus hellenicus* sp. nov., two novel hyperthermophilic archaea isolated from geothermally heated vents off Palaeochori Bay, Milos, Greece. *Int. J. Syst. Evol. Microbiol.* 50, 2101–2108. doi: 10.1099/00207713-50-6-2101
- Bayraktarov, E., Price, R. E., Ferdelman, T. G., and Finster, K. (2013). The pH and pCO<sub>2</sub> dependence of sulfate reduction in shallow-sea hydrothermal CO<sub>2</sub>-venting sediments (Milos Island, Greece). *Front. Microbiol.* 4, 1–10. doi: 10.3389/fmicb.2013.00111
- Brinkhoff, T., Sievert, S., Kuever, J., and Muyzer, G. (1999). Distribution and diversity of sulfur-oxidizing *Thiomicrospira* spp. at a shallow-water hydrothermal vent in the Aegean Sea (Milos, Greece). *Appl. Environ. Microbiol.* 65, 3843–3849.
- Burggraf, S., Larsen, N., Woese, C. R., and Stetter, K. (1993). An intron within the 16S ribosomal RNA

- gene of the archaeon *Pyrobaculum aerophilum*. *Proc. Natl. Acad. Sci. U.S.A.* 90, 2547–2550. doi: 10.1073/pnas.90.6.2547
- Cavalca, L., Corsini, A., Zaccheo, P., Andreoni, V., and Muyzer, G. (2013). Microbial transformations of arsenic: perspectives for biological removal of arsenic from water. *Future Microbiol.* 8, 753–768. doi: 10.2217/fmb.13.38
- Cox, M. E., Launay, J., and Paris, J. P. (1982). “Geochemistry of low temperature geothermal systems in New Caledonia,” in *Pacific Geothermal Conference*, (Auckland: University of Auckland), 453–459.
- Dando, P. R., Thomm, M., Arab, H., Brehmer, M., Hooper, L. E., Jochimsen, B., et al. (1998). Microbiology of shallow hydrothermal sites off Palaeochori Bay, Milos (Hellenic Volcanic Arc). *Cah. Biol. Mar.* 39, 369–372.
- Dando, P. R., Hughes, J. A., Leahy, Y., Niven, S. J., Taylor, L. J., and Smith, C. (1995). Gas venting rates from the submarine hydrothermal areas around the island of Milos, Hellenic volcanic arc. *Cont. Shelf Res.* 15, 913–929. doi: 10.1016/0278-4343(95)80002-U
- Dando, P. R., Stüben, D., and Varnavas, S. P. (1999). Hydrothermalism in the Mediterranean Sea. *Prog. Oceanogr.* 44, 333–367. doi: 10.1016/S0079-6611(99)00032-4
- Dick, G. J., Lee, Y. E., and Tebo, B. M. (2006). Manganese(II)-oxidizing *Bacillus* spores in Guaymas Basin hydrothermal sediments and plumes. *Appl. Environ. Microbiol.* 72, 3184–3190. doi: 10.1128/AEM.72.5.3184–3190.2006
- Donachie, S. P., Bowman, J. P., On, S. L. W., and Alam, M. (2005). *Arcobacter halophilus* sp. nov., the first obligate halophile in the genus *Arcobacter*. *Int. J. Syst. Evol. Microbiol.* 55, 1271–1277. doi: 10.1099/ijjs.0.63581-0
- Flores, G. E., Campbell, J. H., Kirshtein, J. D., Meneghin, J., Podar, M., Steinberg, J. I., et al. (2011). Microbial community structure of hydrothermal deposits from geochemically different vent fields along the Mid-Atlantic Ridge. *Environ. Microbiol.* 13, 2158–2171. doi: 10.1111/j.1462-2920.2011.02463.x
- Flores, G. E., Wagner, I. D., Liu, Y., and Reysenbach, A. L. (2012). Distribution, abundance, and diversity patterns of the thermoacidophilic “deep-sea hydrothermal vent euryarchaeota 2”. *Front. Microbiol.* 3:47. doi: 10.3389/fmicb.2012.00047
- Forrest, M. J., Ledesma-Vazquez, J., Ussler III, W., Kulongoski, J. T., Hilton, D. R., and Greene, H. G. (2005). Gas geochemistry of a shallow submarine hydrothermal vent associated with the El Requeson fault zone, Bahia Concepcion, Baja California Sur, Mexico. *Chem. Geol.* 224, 82–95. doi: 10.1016/j.chemgeo.2005.07.015
- German, C. R., and Von Damm, K. L. (2003). “Hydrothermal processes,” in *Treatise on Geochemistry*, eds H. D. Holland and K. K. Turekian (Amsterdam: Elsevier), 145–180.
- Graumann, P. (2012). *Bacillus: Cellular and Molecular Biology*. (Norfolk: Caister Academic Press).
- Guindon, S., and Gascuel, O. (2003). A simple, fast, and accurate algorithm to estimate large phylogenies by maximum likelihood. *Syst. Biol.* 52, 696–704. doi: 10.1080/10635150390235520
- Handley, K. M., Hery, M., and Lloyd, J. R. (2009). Redox cycling of arsenic by the hydrothermal marine bacterium *Marinobacter santoriniensis*. *Environ. Microbiol.* 11, 1601–1611. doi: 10.1111/j.1462-2920.2009.01890.x
- Huber, T., Faulkner, G., and Hugenholtz, P. (2004). Bellerophon; a program to detect chimeric sequences in multiple sequence alignments. *Bioinformatics* 20, 2317–2319. doi: 10.1093/bioinformatics/bth226
- Italiano, F., Bonfanti, P., Ditta, M., Petrini, R., and Slejko, F. (2009). Helium and carbon isotopes in the dissolved gases of Friuli Region (NE Italy): geochemical evidence of CO<sub>2</sub> production and degassing over a seismically active area. *Chem. Geol.* 266, 76–85. doi: 10.1016/j.chemgeo.2009.05.022
- Italiano, F., and Nuccio, F. (1991). Geochemical investigations of submarine volcanic exhalations to the east of Panarea, Aeolian Islands, Italy. *J. Volcanol. Geother. Res.* 46, 125–141. doi: 10.1016/0377-0273(91)90079-F
- Itoh, T., Nomura, N., and Sako, Y. (2003). Distribution of 16S rRNA introns among the family Thermoproteaceae and their evolutionary implications. *Extremophiles* 7, 229–233.
- Itoh, T., Yoshikawa, N., and Takashina, T. (2007). *Thermogymnomonas acidicola* gen. nov., sp. nov., a novel thermoacidophilic, cell wall-less archaeon in the order Thermoplasmatales, isolated from a solfatitic soil in Hakone, Japan. *Int. J. Syst. Evol. Microbiol.* 57, 2557–2561. doi: 10.1099/ijss.0.65203-0
- Jochimsen, B., Peinemann-Simon, S., Volker, H., Stuben, D., Botz, R., Stoffers, P., et al. (1997). *Stetteria hydrogenophila* gen. nov. and sp. nov., a novel mixotrophic sulfur-dependent crenarchaeote isolated from Milos, Greece. *Extremophiles* 1, 67–73. doi: 10.1007/s007920050016
- Kirchman, D. L. (2002). The ecology of *Cytophaga-Flavobacteria* in aquatic environments. *FEMS Microbiol. Ecol.* 39, 91–100. doi: 10.1016/S0168-6496(01)00206-9
- Kormas, K. A., Tivey, M. K., Von Damm, K. L., and Teske, A. (2006). Bacterial and archaeal phylotypes associated with distinct mineralogical layers of a white smoker spire from a deep-sea hydrothermal vent site (9°N, East Pacific Rise). *Environ. Microbiol.* 8, 909–920. doi: 10.1111/j.1462-2920.2005.00978.x
- Koski, R. A., Pichler, T., and Foster, A. L. (2001). “The fate of arsenic in submarine hydrothermal environments: a summary of recent data,” in *USGS Workshop on Arsenic in the Environment* (Denver, CO).
- Lane, D. J. (1991). “16S/23S rRNA sequencing,” in *Nucleic Acid Techniques in Bacterial Systematics*, eds E. Stackebrandt and M. Goodfellow (Chichester: John Wiley and Sons), 115–175.
- Li, S.-G., Tang, Y.-Q., Nie, Y., Cai, M., and Wu, X.-L. (2011). Complete genome sequence of *Polymorphum gilvum* SL003B-26A1T, a crude oil-degrading bacterium from oil polluted saline soil. *J. Bacteriol.* 193, 2894–2895. doi: 10.1128/JB.00333-11
- Maugeri, T. L., Gugliandolo, C., Caccamo, D., Panico, A., Lama, L., Gambacorta, A., et al. (2002). A halophilic thermotolerant *Bacillus* isolated from a marine hot spring able to produce a new exopolysaccharide. *Biotechnol. Lett.* 24, 515–519. doi: 10.1023/A:1014891431233
- McCarthy, K. T., Pichler, T., and Price, R. E. (2005). Geochemistry of Champagne Hot Springs shallow hydrothermal vent field and associated sediments, Dominica, Lesser Antilles. *Chem. Geol.* 224, 55–68. doi: 10.1016/j.chemgeo.2005.07.014
- Meyer-Dombard, D., Amend, J. P., and Osburn, M. R. (2013). Microbial diversity and potential for arsenic and iron biogeochemical cycling at an arsenic-rich, shallow-sea hydrothermal vent (Tutum Bay, Papua New Guinea). *Chem. Geol.* 348, 37–47. doi: 10.1016/j.chemgeo.2012.02.024
- Meyer-Dombard, D. R., Price, R. E., Pichler, T., and Amend, J. P. (2011). Prokaryotic populations in arsenic-rich shallow-sea hydrothermal sediments of Ambite Island, Papua New Guinea. *Geomicrobiol. J.* 29, 1–17.
- Morinaga, Y., Nomura, N., and Sako, Y. (2002). Population dynamics of archaeal mobile introns in natural environments: a shrewd invasion strategy of the latent parasitic DNA. *Microbes Environ.* 17, 153–163. doi: 10.1264/jsme2.17.153
- Nakagawa, S., Takai, K., Inagaki, F., Chiba, H., Ishibashi, J.-I., Kataoka, S., et al. (2005). Variability in microbial community and venting chemistry in a sediment-hosted backarc hydrothermal system: impacts of subseafloor phase-separation. *FEMS Microbiol. Ecol.* 54, 141–155. doi: 10.1016/j.femsec.2005.03.007
- Nakano, M. M., and Zuber, P. (1998). Anaerobic growth of a “strict aerobe” (*Bacillus subtilis*). *Annu. Rev. Microbiol.* 52, 165–190. doi: 10.1146/annurev.micro.52.1.165
- Nitzsche, K. (2010). *Microbial Diversity of Hydrothermally Influenced Arsenic-Rich Sediments off the Coast of Milos Island, Greece*. Diploma thesis, TU Bergakademie, Freiberg, Germany.
- Nunoura, T., Oida, H., Miyazaki, M., and Suzuki, Y. (2008). *Thermosulfidobacter takaii* gen. nov., sp. nov., a thermophilic, hydrogen-oxidizing, sulfur-reducing chemolithoautotroph isolated from a deep-sea hydrothermal field in the Southern Okinawa Trough. *Int. J. Syst. Evol. Microbiol.* 58, 659–665. doi: 10.1099/ijss.0.64615-0
- Nunoura, T., and Takai, K. (2009). Comparison of microbial communities associated with phase-separation-induced hydrothermal fluids at the Yonaguni Knoll IV hydrothermal field, the Southern Okinawa Trough. *FEMS Microbiol. Ecol.* 67, 351–370. doi: 10.1111/j.1574-6941.2008.00636.x
- Oremland, R. S., and Stolz, J. F. (2003). The ecology of arsenic. *Science* 300, 939–944. doi: 10.1126/science.1081903
- Pati, A., Gronow, S., Lapidus, A., Copeland, A., Glavina Del Rio, T., Nolan, M., et al. (2010). Complete genome sequence of *Arcobacter nitrofigilis* type strain (CI). *Stand. Genomic. Sci.* 2, 300–308. doi: 10.4056/sigs.912121

- Pichler, T. (2005). Stable and radiogenic isotopes as tracers for the origin, mixing and subsurface history of fluids in submarine shallow-water hydrothermal systems. *J. Volcanol. Geother. Res.* 139, 211–226. doi: 10.1016/j.jvolgeores.2004.08.007
- Pichler, T., Amend, J. P., Garey, J., Hallock, P., Hsia, N. P., Karlen, D. J., et al. (2006). A natural laboratory to study arsenic geochemical complexity. *EOS* 87, 221–225. doi: 10.1029/2006EO230002
- Pichler, T., Giggenbach, W. F., McInnes, B. I. A., and Duck, B. (1999). Fe-sulfide formation due to seawater-gas-sediment interaction in a shallow-water hydrothermal system, Lihir Island, Papua New Guinea. *Econ. Geol.* 94, 281–288. doi: 10.2113/gsecongeo.94.2.281
- Pokrovski, G. S., Zakirov, I. V., Roux, J., Testemale, D., Hazemann, J. L., Bychkov, A., et al. (2002). Experimental study of arsenic speciation in vapor phase to 500°C: implications for As transport and fractionation in low-density crustal fluids and volcanic gases. *Geochim. Cosmochim. Acta* 66, 3453–3480. doi: 10.1016/S0016-7037(02)00946-8
- Polz, M. F., and Cavanaugh, C. M. (1995). Dominance of one bacterial phylotype at a Mid-Atlantic ridge hydrothermal vent site. *Proc. Natl. Acad. Sci. U.S.A.* 92, 7232–7236. doi: 10.1073/pnas.92.16.7232
- Price, R. E., Amend, J. P., and Pichler, T. (2007). Enhanced geochemical gradients in a marine shallow-water hydrothermal system: unusual arsenic speciation in horizontal and vertical pore water profiles. *Appl. Geochem.* 22, 2595–2605. doi: 10.1016/j.apgeochem.2007.06.010
- Price, R. E., Savo, I., Planer-Friedrich, B., Bühring, S., Amend, J. P., and Pichler, T. (2012). Processes influencing extreme As enrichment in shallow-sea hydrothermal fluids of Milos Island, Greece. *Chem. Geol.* 348, 15–26. doi: 10.1016/j.chemgeo.2012.06.007
- Reysenbach, A. L., Liu, Y., Banta, A. B., Beveridge, T. J., Kirshtein, J. D., Schouten, S., et al. (2006). A ubiquitous thermoacidophilic archaeon from deep-sea hydrothermal vents. *Nat. Lett.* 442, 444–447. doi: 10.1038/nature04921
- Rogers, K. L., and Amend, J. P. (2005). Archaeal diversity and geochemical energy yields in a geothermal well on Vulcano Island, Italy. *Geobiology* 3, 319–332. doi: 10.1111/j.1472-4669.2006.00064.x
- Schlesner, H., Lawson, P. A., Collins, M. D., Weiss, N., Wehmeyer, U., Voelker, H., et al. (2001). *Filibacillus milensis* gen. nov., sp. nov., a new halophilic spore-forming bacterium with Orn-D-Glu-type peptidoglycan. *Int. J. Syst. Evol. Microbiol.* 51, 425–431.
- Schloss, P. D., Westcott, S. L., Ryabin, T., Hall, J. R., Hartmann, M., Hollister, E. B., et al. (2009). Introducing mothur: open-source, platform-independent, community-supported software for describing and comparing microbial communities. *Appl. Environ. Microbiol.* 75, 7537–7541. doi: 10.1128/AEM.01541-09
- Schrenk, M. O., Kelley, D. S., Bolton, S. A., and Baross, J. A. (2004). Low archaeal diversity linked to seafloor geochemical processes at the Lost City hydrothermal field, Mid-Atlantic Ridge. *Environ. Microbiol.* 6, 1086–1095. doi: 10.1111/j.1462-2920.2004.00650.x
- Seeberg-Elverfeldt, J., Schlüter, M., Feseker, T., and Kölling, M. (2005). Rhizon sampling of pore waters near the sediment/water interface of aquatic systems. *Limnol. Oceanogr. Methods* 3, 361–371. doi: 10.4319/lom.2005.3.361
- Sievert, S. M., Brinkhoff, T., Muyzer, G., Ziebis, W., and Kuever, J. (1999). Spatial heterogeneity of bacterial population along an environmental gradient at a shallow submarine hydrothermal vent field, Mid-Atlantic Ridge. *Environ. Microbiol.* 1, 19–30. doi: 10.1007/s002030050673
- Sylvan, J. B., Toner, B. M., and Edwards, K. J. (2012). Life and death of deep-sea vents: bacterial diversity and ecosystem succession on inactive hydrothermal sulfides. *mBio* 3, 1–10. doi: 10.1128/mBio.00279-11
- Takai, K., and Horikoshi, K. (1999). Genetic diversity of archaea in deep-sea hydrothermal vent environments. *Genetics* 152, 1285–1297.
- Tarasov, V. G., Gebruk, A. V., Mironov, A. N., and Moskalev, L. I. (2005). Deep-sea and shallow-water hydrothermal vent communities: two different phenomena? *Chem. Geol.* 224, 5–39. doi: 10.1016/j.chemgeo.2005.07.021
- Tarasov, V. G., Propp, M. V., Propp, L. N., Zhirmunsky, A. V., Namsaraev, B. B., Gorlenko, V. M., et al. (1990). Shallow-water gasohydrothermal vents of Ushishir Volcano and the ecosystem of Kraternaya Bight (The Kurile Islands). *Mar. Ecol.* 11, 1–23. doi: 10.1111/j.1439-0485.1990.tb00225.x
- Valsami-Jones, E., Baltatzis, E., Bailey, E. H., Boyce, A. J., Alexander, J. L., Magganas, A., et al. (2005). The geochemistry of fluids from an active shallow submarine hydrothermal system: Milos island, Hellenic Volcanic Arc. *J. Volcanol. Geothermal Res.* 148, 130–151. doi: 10.1016/j.jvolgeores.2005.03.018
- Varnavas, S. P., and Cronan, D. S. (1988). Arsenic, antimony and bismuth in sediments and waters from the Santorini hydrothermal field, Greece. *Chem. Geol.* 67, 295–305. doi: 10.1016/0009-2541(88)90135-0
- Von Damm, K. L., Lilley, M. D., Shanks, W. C., Brockington, M., Bray, A. M., O’Grady, K. M., et al. (2003). Extraordinary phase separation and segregation in vent fluids from the southern East Pacific Rise. *Earth Planet. Sci. Lett.* 206, 365–378. doi: 10.1016/S0012-821X(02)01081-6
- Wang, Q., Garrity, G. M., Tiedje, J. M., and Cole, J. R. (2007). Naive Bayesian classifier for rapid assignment of rRNA sequences into the new bacterial taxonomy. *Appl. Environ. Microbiol.* 73, 5261–5267. doi: 10.1128/AEM.00062-07
- Wirsén, C. (2004). Is life thriving deep beneath the seafloor? *Oceanus* 42, 1–6. Available online at: <http://oceausmag.whoi.edu/v42n2/wirsens.html>
- Zargar, K., Conrad, A., Bernick, D. L., Lowe, T. M., Stolc, V., Hoeft, S., et al. (2012). ArxA, a new clade of arsenite oxidase within the DMSO reductase family of molybdenum oxidoreductases. *Environ. Microbiol.* 14, 1635–1645. doi: 10.1111/j.1462-2920.2012.02722.x
- Zargar, K., Hoeft, S. E., Oremland, R. S., and Saltikov, C. (2010). Identification of a novel arsenite oxidase gene, arxA, in the haloalkaliphilic, arsenite-oxidizing bacterium *Alkalilimnicola ehrlichii* strain MLHE-1. *J. Bacteriol.* 192, 3755–3762. doi: 10.1128/JB.00244-10
- Conflict of Interest Statement:** The authors declare that the research was conducted in the absence of any commercial or financial relationships that could be construed as a potential conflict of interest.
- Received:** 15 March 2013; **accepted:** 30 May 2013; **published online:** 09 July 2013.
- Citation:** Price RE, Lesniewski R, Nitzsche KS, Meyerdierks A, Saltikov C, Pichler T and Amend JP (2013) Archaeal and bacterial diversity in an arsenic-rich shallow-sea hydrothermal system undergoing phase separation. *Front. Microbiol.* 4:158. doi: 10.3389/fmicb.2013.00158
- This article was submitted to Frontiers in Extreme Microbiology, a specialty of Frontiers in Microbiology.
- Copyright © 2013 Price, Lesniewski, Nitzsche, Meyerdierks, Saltikov, Pichler and Amend. This is an open-access article distributed under the terms of the Creative Commons Attribution License, which permits use, distribution and reproduction in other forums, provided the original authors and source are credited and subject to any copyright notices concerning any third-party graphics etc.

**APPENDIX**

**FIGURE A1 | Rarefaction curves showing 16S rRNA OTU richness for each of the sampling sites and depths for this study.** Curves were calculated using the furthest neighbor approach with a 97% sequence similarity cutoff. Data shown are for *Bacteria* (A) and *Archaea* (B).



# Microbial diversity in the deep-subsurface hydrothermal aquifer feeding the giant gypsum crystal-bearing Naica Mine, Mexico

**Marie Ragon<sup>1</sup>, Alexander E. S. Van Driessche<sup>2</sup>, Juan M. García-Ruiz<sup>2</sup>, David Moreira<sup>1</sup> and Purificación López-García<sup>1\*</sup>**

<sup>1</sup> Unité d'Ecologie, Systématique et Evolution, CNRS UMR 8079, Université Paris-Sud, Orsay, France

<sup>2</sup> Laboratorio de Estudios Cristalográficos, Instituto Andaluz de Ciencias de la Tierra, Consejo Superior de Investigaciones Científicas, Universidad Granada, Granada, Spain

**Edited by:**

Andreas Teske, University of North Carolina at Chapel Hill, USA

**Reviewed by:**

Kasthuri Venkateswaran, National Aeronautics and Space Administration - Jet Propulsion Laboratory, USA

Mohammad Ali Amoozegar, University of Tehran, Iran

**\*Correspondence:**

Purificación López-García, Unité d'Ecologie, Systématique et Evolution, CNRS UMR 8079, Université Paris-Sud, 91405 Orsay Cedex, France.

e-mail: puri.lopez@u-psud.fr

The Naica Mine in northern Mexico is famous for its giant gypsum crystals, which may reach up to 11 m long and contain fluid inclusions that might have captured microorganisms during their formation. These crystals formed under particularly stable geochemical conditions in cavities filled by low salinity hydrothermal water at 54–58°C. We have explored the microbial diversity associated to these deep, saline hydrothermal waters collected in the deepest (ca. 700–760 m) mineshafts by amplifying, cloning and sequencing small-subunit ribosomal RNA genes using primers specific for archaea, bacteria, and eukaryotes. Eukaryotes were not detectable in the samples and the prokaryotic diversity identified was very low. Two archaeal operational taxonomic units (OTUs) were detected in one sample. They clustered with, respectively, basal Thaumarchaeota lineages and with a large clade of environmental sequences branching at the base of the Thermoplasmatales within the Euryarchaeota. Bacterial sequences belonged to the Candidate Division OP3, Firmicutes and the Alpha- and Beta-proteobacteria. Most of the lineages detected appear autochthonous to the Naica system, since they had as closest representatives environmental sequences retrieved from deep sediments or the deep subsurface. In addition, the high GC content of 16S rRNA gene sequences belonging to the archaea and to some OP3 OTUs suggests that at least these lineages are thermophilic. Attempts to amplify diagnostic functional genes for methanogenesis (*mcrA*) and sulfate reduction (*dsrAB*) were unsuccessful, suggesting that those activities, if present, are not important in the aquifer. By contrast, genes encoding archaeal ammonium monooxygenase (*AamoA*) were amplified, suggesting that Naica Thaumarchaeota are involved in nitrification. These organisms are likely thermophilic chemolithoautotrophs adapted to thrive in an extremely energy-limited environment.

**Keywords:** aerobic ammonium oxidation, Candidate Division OP3, GC content, hydrothermal, Thaumarchaeota, thermophile, Thermoplasmatales

## INTRODUCTION

At the onset of the 1980s, the detection of living microorganisms in deep sediment cores revealed the occurrence of a hitherto unsuspected but vast subsurface ecosystem associated to deep-sea sediments as well as continental and oceanic crusts (Ghiorse and Wilson, 1988; Gold, 1992; White et al., 1998; Whitman et al., 1998; Pedersen, 2000). Since then, the number of microbial diversity surveys on the deep subsurface has multiplied, especially in the subseafloor, benefiting from initiatives such as the International Ocean Drilling Program (IODP<sup>1</sup>). As data accumulate, initial quantitative assessments predicting that over 50% of all prokaryotic cells occur in the subsurface (Whitman et al., 1998) have been seriously challenged (Jorgensen, 2012; Kallmeyer et al., 2012). This illustrates that, despite increasing efforts, the diversity, extent, and function of the deep biosphere remain largely unknown.

This limited knowledge is due to a variety of factors including the inherent difficulty of sampling at progressively higher underground depths, the problem of external microbial contamination, and the refractory nature of many subsurface microbes that are dormant or living at extremely low metabolic rates (White et al., 1998; Teske, 2005). Indeed, although the deep subseafloor constitutes the largest biotope on Earth, it seemingly possesses the lowest metabolic rates. The deep biosphere is also highly heterogeneous. Hot spots of microbial activity occur whenever chemical energy derived from redox reactions involving organic matter or inorganic electron donors (hydrogen, methane, hydrogen sulfide, or iron) are available at sedimentary and/or geochemical interfaces (Chapelle et al., 2002; Parkes et al., 2005; Jorgensen and Boetius, 2007). Subseafloor sediments are rich in organic matter as compared to rocky environments and, thus, sustain relatively diverse microorganisms, some of which degrade aromatic and other recalcitrant compounds (Fredrickson et al., 1995). Nonetheless, the microbial activities that dominate in these

<sup>1</sup><http://www.iodp.org/>

settings are methanogenesis and sulfate reduction, which constitute the terminal steps in the degradation of organics in the biogeochemical carbon cycle (Newberry et al., 2004; Webster et al., 2006; Fry et al., 2008). Active microorganisms have been detected in marine subseafloor sediments down to depths of 1,626 m below the sea floor at the Newfoundland margin, which corresponds to the oldest (111 million years old), and potentially hottest ( $\sim 100^{\circ}\text{C}$ ) marine sediments investigated (Roussel et al., 2008). Deep oil/petroleum reservoirs also sustain active microbial communities and several of their members are able to degrade long hydrocarbon chains and other complex organics (Rueter et al., 1994; Head et al., 2003; Kim and Crowley, 2007).

However, most of the deep subsurface, especially the bed rock, harbors organisms living under extreme energy limitation. Under these conditions, microorganisms are likely inactive or display exceedingly low metabolic activities (Jorgensen and D'Hondt, 2006; Jorgensen and Boetius, 2007). The detection of subsurface microorganisms may be hampered by such low metabolic rates (Teske, 2005) but also by the occurrence of divergent phylogenetic lineages, since general primers used to amplify marker ribosomal RNA genes may fail to amplify genes from such divergent clades, a problem that may typically affect the archaea (Teske and Sorensen, 2008). The volcanic oceanic crust has also been less explored due to the challenging sampling conditions and the needs for specific equipment (Edwards et al., 2011). Nonetheless, microbial communities have been recently studied in subseafloor basement fluids as deep as 2,667 m on the eastern flank of the Juan de Fuca Ridge in the Pacific (Jungbluth et al., 2012). While very deep rock communities in, for instance, granite or basalts, are much poorer than sediment communities due to the extreme nutrient depletion, organisms able to degrade hydrocarbons that might originate from serpentinization have been detected in very deep ocean gabbro (Mason et al., 2010), opening an intriguing new window for life in such ecosystems.

The microbiology of the deep continental crust is even less well explored than that of the oceanic crust. Among the investigated sites, often from an applied perspective, are deep aquifers (Kimura et al., 2005), potential sites for the storage of radioactive waste (Stroes-Gascoyne and West, 1997) or gas (Basso et al., 2009), and deep mines (Onstott et al., 2003; Sahl et al., 2008; Rastogi et al., 2010). One of the deepest sites studied is the Archaean metabasalt at 2.825 km below the land surface in the Mponeng gold mine, South Africa, where sulfate reducers belonging to the Firmicutes appeared to be sustained by geologically produced sulfate and hydrogen (Lin et al., 2006b). Deep mines offer a relatively easy access to the continental subsurface biosphere, and allow for sampling in very different geological settings.

In this work, we have explored the microbial diversity associated to a deep, saline hydrothermal aquifer by sampling water springing at ca.  $60^{\circ}\text{C}$  in the deepest (ca. 700 m) shafts of the Naica Mine, Mexico. Naica, one of the most important lead and silver deposits in the world, is located in a semi-desertic region but, during the raining season, temporary lagoons and flooding zones parallel to the regional fault system may recharge the hydrothermal aquifer (Villasuso, 2002). The Naica area is under a mild thermal anomaly and water springing in the mine galleries has a temperature ranging from 50 to  $60^{\circ}\text{C}$  (Garcia-Ruiz et al.,

2007). The unique geochemical conditions of the mine have led to the formation, at very low calcium-sulfate supersaturation, of giant gypsum crystals (Erwood et al., 1979; Garcia-Ruiz et al., 2007; Van Driessche et al., 2011). Some of these giant crystals contain fluid inclusions that might have captured microorganisms during their formation. The description of current microbial communities associated to the subsurface hydrothermal water where these crystals formed is a pre-requisite to predict the type of microorganisms that may have been trapped in fluid inclusions and a control to distinguish potential contaminants during the analysis of such small fluid inclusions.

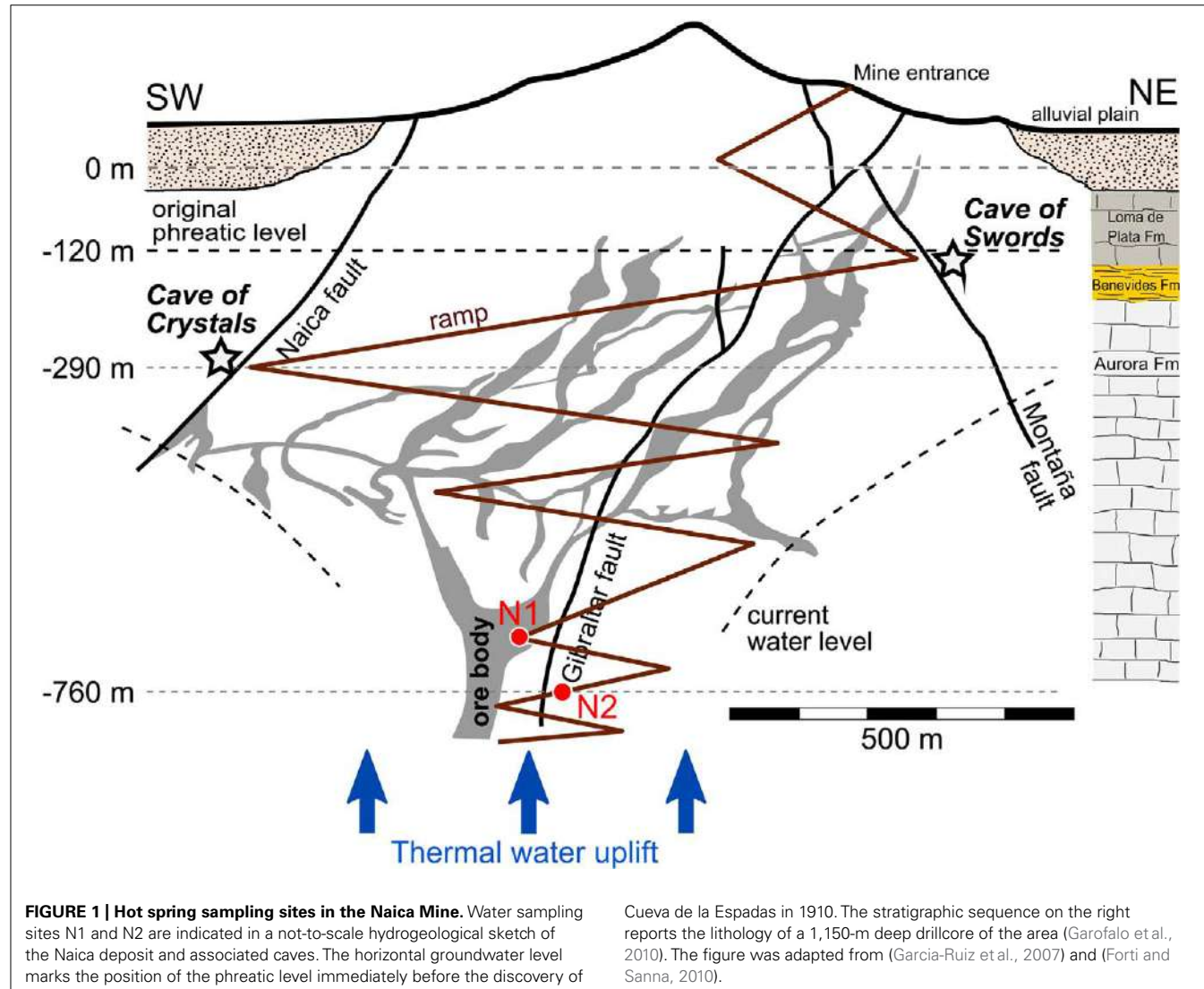
## MATERIALS AND METHODS

### SAMPLING AND DNA PURIFICATION

The Naica Mine is located 112 km southeast of Chihuahua City in northern Mexico ( $27^{\circ}51'3''\text{N}$ ;  $105^{\circ}29'47''\text{W}$ ). A further description of the geological and hydrological setting of the mine is provided as Appendix. Water samples N1 and N2 were collected in the deepest excavated Naica mineshafts at ca. 700 and 760 m depth (Figure 1). Having been abandoned and partially inundated, these sites are seldom visited by miners, which limits potential contamination brought from the exterior or from upper layers of the mine. The air temperature was ca.  $40^{\circ}\text{C}$  and the humidity ca. 90%. The water vigorously sprang from fractures in the rock wall. The water temperature measured *in situ* in N1 and N2 was of ca.  $60^{\circ}\text{C}$  and the pH of 7.5. Chemical analyses of the aquifer water have been carried out from 1976 to 2003, showing a rather stable composition through time. The water is highly enriched in calcium ( $\sim 600 \text{ mg/l}$ ) and sulfate ( $\sim 2 \text{ g/l}$ ) but contains also  $100 \text{ mg/l}$  Na,  $24 \text{ mg/l}$  Cl, and  $120 \text{ mg/l}$  Mg as major components (see Table DR4 in Data Repository Item; Garcia-Ruiz et al., 2007). Two water samples of 20 l each were collected from two different hot springs (N1 and N2) in clean plastic containers thoroughly rinsed with the same hot spring water. The containers were immediately transported to the nearest laboratory and the water filtered directly through GTTP<sup>TM</sup> isopore filters (Millipore, MA, USA) of  $0.22 \mu\text{m}$ -pore diameter. Filters were fixed *in situ* in 96% ethanol and stored at  $-20^{\circ}\text{C}$  until DNA was purified. For DNA extraction, the ethanol was removed from the filters by evaporation. The remaining ethanol was filtered through a small  $0.22 \mu\text{m}$ -pore size filter to retain detached microbial biomass. Filters from each sample were cut in small fragments, which were immediately rehydrated in the initial resuspension buffer of the PowerSoil DNA isolation kit (Mo Bio, Laboratories Inc., CA, USA). DNA was purified then using the PowerSoil DNA isolation kit following the instructions of the manufacturer. DNA was eluted in  $60 \mu\text{l}$  of Tris-HCl, pH 8 and conserved at  $-20^{\circ}\text{C}$ .

### PCR AMPLIFICATION, CLONING, AND SEQUENCING

Small-subunit ribosomal RNA genes were amplified by polymerase chain reaction (PCR) using specific primers for each domain of life. For bacteria, we used the primers 27F (AGAGTT-TGATCCTGGCTCAG) and 23S-1R (GGGTTTCCCCATTG-GAAATC), which also amplify the adjacent internal transcribed spacer (ITS) region. Semi-nested reactions were subsequently carried out with 27F and the reverse prokaryotic primer 1492R (GGTTACCTTGTTACGACTT). Archaeal 16S rRNA genes were



initially amplified using the forward archaea-specific primer 21FQ (GGGCAGGGCTTCCGGTTGATCCTGCCGA) and 1492R. Subsequent semi-nested amplifications were carried out with the internal forward primer Ar109 (AC(G/T)GCTGCTCAGTAACACGT)(N1-4A), W36 (TCCAGGCCCTACGGGG) (N1-5A), and ANMEF (GGCTCAGTAACACGTGGA) (N1-6A). Attempts to amplify eukaryotic 18S rRNA genes were carried out using the specific primers 82F (GAAACTGCGAATGGCTC) and 1520R (CYGCAGGTTCACCTAC) followed by semi-nested PCRs with 1498R (CACCTACGGAACCTTGTAA). PCR reactions were carried out in 25  $\mu$ l of reaction buffer, containing 1.5  $\mu$ l of the eluted DNA, 1.5 mM MgCl<sub>2</sub>, dNTPs (10 nmol each), 20 pmol of each primer, and 0.2 U Taq platinum DNA polymerase (Invitrogen). PCR reactions were performed under the following conditions: 35 cycles (denaturation at 94°C for 15 s, annealing at 55°C for 30 s, extension at 72°C for 2 min) preceded by 2 min denaturation at 94°C, and followed by 7 min extension at 72°C. Negative controls were carried out systematically for each PCR amplification experiment; all were negative. In addition, to

identify and eliminate potential contaminant sequences introduced during the manipulation in the laboratory of samples with extremely low biomass, e.g., contaminants associated to the DNA extraction kit and process, we had previously built a database of potential contaminants (Gerard et al., 2009). Naica sequences were not closely related to them. Attempts to amplify *dsrAB* genes encoding the dissimilatory sulfite reductase diagnostic of sulfate reducers and *mcrA* genes encoding the methyl coenzyme M reductase characteristic of methanogenic archaea were done using, respectively, the specific primers DSR-1F (ACSCACTG-GAAGCACG) + DSR-4R (GTG TAG CAG TTA CCG CA) (Perez-Jimenez et al., 2001) and ME1F (CGMATGCARATHG-GWATGTC) + ME2R (TCATKGCRTAGTTDGGRTAGT) (Inagaki et al., 2004). Archaeal *amoA* genes encoding the ammonium monooxygenase were amplified with primers Arch-*amoAF* (STAATGGTCTGGCTTAGACG) and Arch-*amoAR* (GCGGC-CATCCATCTGTATGT) (Francis et al., 2005). To amplify protein genes an annealing-temperature gradient of 47–55°C was used to maximize the chances of amplification. Clone libraries were

constructed using the TopoTA cloning kit (Invitrogen, Carlsbad, CA, USA) according to the manufacturer's instructions. Clone inserts were PCR-amplified using flanking vector primers, and inserts of expected size were partially sequenced (Beckman Coulter Genomics, Takeley, UK) with 1492R yielding sequences of 800–1,000 bp. A total of 91 archaeal and 266 bacterial high quality sequences were retained for this study. Potential chimeric sequences were identified manually by comparing BLAST (Basic Local Alignment Search Tool) results from several portions of the full-length sequence. Operational taxonomic units (OTUs) were defined as groups of 16S rRNA gene sequences sharing  $\geq 98\%$  identity. Several representative 16S rRNA clones of the different OTUs were nearly fully sequenced by using forward primers. Complete sequences were assembled using Code Aligner (CodonCode Corporation<sup>2</sup>) prior to phylogenetic analyses.

### PHYLOGENETIC ANALYSES

Environmental 16S rRNA gene sequences from the Naica Mine were compared with sequences in the database GenBank<sup>3</sup> by BLAST (Altschul et al., 1997). We retrieved the closest sequences found in the database and included them in an alignment containing also sequences from the closest cultivated members and some representative sequences of the major taxa found. Sequences were aligned using MUSCLE (MULTiple Sequence Comparison by Log-Expectation; Edgar, 2004). Ambiguously aligned positions and gaps were eliminated using Gblocks (Castresana, 2000). A total of 1,079 and 846 unambiguously aligned nucleotide positions were retained for, respectively, archaeal and bacterial sequences in order to carry out subsequent phylogenetic analyses. The resulting sequence alignments were used as input to build phylogenetic trees by approximate maximum likelihood using Fasttree (Price et al., 2010) with a general time reversible (GTR) model of sequence evolution, and taking among-site rate variation into account by using a four-category discrete approximation of a  $\Gamma$  distribution. ML bootstrap proportions were inferred using 1,000 replicates. For protein (amoA) phylogenetic analyses, amino acid alignments were obtained with MUSCLE and trimmed using Gblocks. The ML phylogenetic tree was reconstructed using Treefinder (Jobb et al., 2004) with the WAG- $\Gamma$  model of sequence evolution. Phylogenetic trees were visualized using the program FIGTREE<sup>4</sup>. The sequences reported in this study have been deposited in GenBank with accession numbers KC481372-KC481399.

### RESULTS AND DISCUSSION

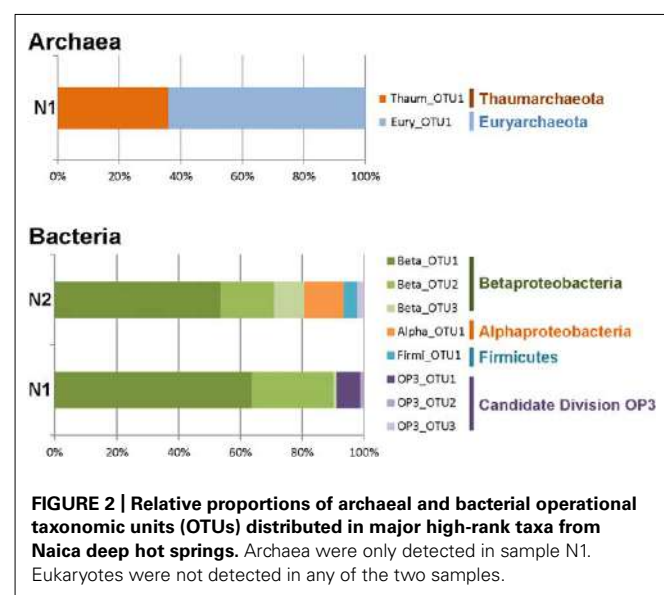
#### MICROBIAL DIVERSITY IN NAICA DEEP HYDROTHERMAL WATER

We tried to amplify archaeal, bacterial, and eukaryotic 16S/18S rRNA genes in the samples collected in two of the deepest accessible fracture-associated springs in the Naica mineshafts at approximately 700 and 760 m below the entrance level (Figure 1). However, despite several attempts, including nested PCR experiments, we failed to amplify eukaryotic 18S rRNA genes. Similarly, we failed to amplify archaea from N2. By contrast, we detected archaea belonging to the Thaumarchaeota and the Euryarchaeota

in N1 (Figure 2). Nested PCR reactions were also required to amplify bacterial 16S rRNA genes, indicating that microbial biomass in this thermal water is very low. Only two high rank-bacterial taxa were detected in both samples, Betaproteobacteria, which represented between 80% (N2) and 90% (N1) of the 16S rRNA gene sequences analyzed, and the Candidate Division OP3, which represented 2% (N2) and 10% (N1) of the clone sequences. N2 displayed a higher bacterial diversity, with a few additional representatives of Firmicutes and Alphaproteobacteria accounting for up to 18% of the sequences (Figure 2).

The low prokaryotic diversity was not only observed at the level of high-rank taxa but also within taxa. Thus, very few OTUs (defined at  $\geq 98\%$  sequence similarity level) were detected. Thaumarchaeota, Euryarchaeota, Alphaproteobacteria, and Firmicutes were represented by a single OTU, while up to three OTUs were detected within the Beta-proteobacteria and the Candidate Division OP3 (Figure 2). Nonetheless, the different OTUs were not singletypes, but encompassed several closely related sequences, sometimes detected in both samples N1 and N2.

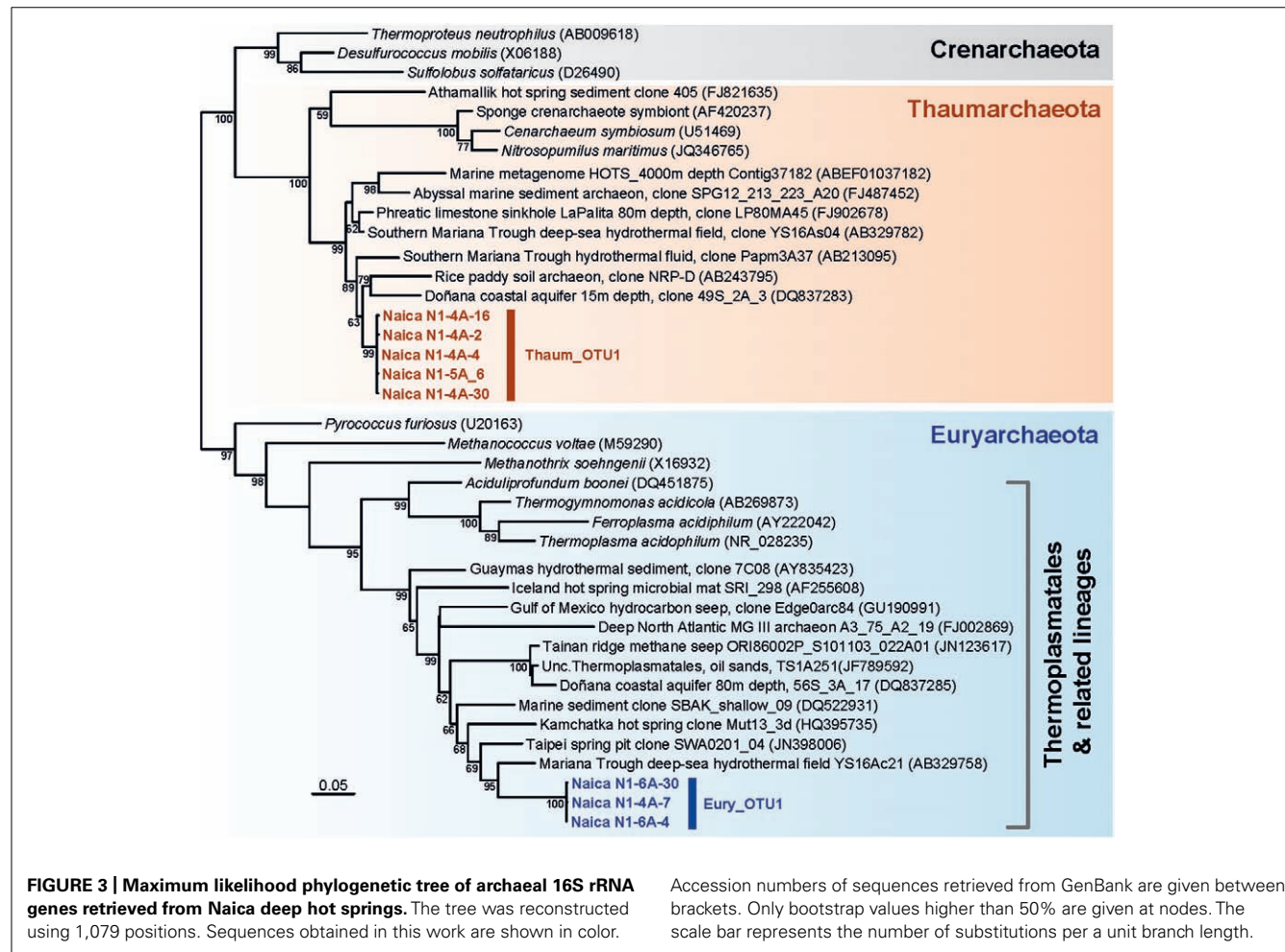
The two detected archaeal OTUs formed clades with other environmental sequences, but were very far from sequences of cultured species. The Thaumarchaeota Thaum\_OTU1 clustered with a group of sequences retrieved mostly from deep-sea waters, sediments, and fluids, including sequences from crustal fluids in back-arc hydrothermal fields of the southern Mariana Trough (Kato et al., 2009; Figure 3). Related sequences came from boreholes in other Mexican regions and from subsurface coastal aquifers (López-Arrolla et al., 2007). Similarly, the Euryarchaeota Eury\_OTU1 belonged to a large clade consisting exclusively of environmental sequences branching as a sister group to the Thermoplasmatales. Again the closest neighbors were sequences retrieved from deep-sea hydrothermal fields, continental hot springs or pits (Figure 3). The Thaumarchaeota or Group I archaea constitute one of the most diversified archaeal phyla, being abundant in deep-sea plankton and soils, but also frequently associated with hot springs and the deep subsurface (Chandler et al., 1998;



<sup>2</sup>[www.codoncode.com](http://www.codoncode.com)

<sup>3</sup><http://www.ncbi.nlm.nih.gov/>

<sup>4</sup><http://tree.bio.ed.ac.uk/software/figtree/>



Rastogi et al., 2009). While many of the marine and soil mesophilic Thaumarchaeota may be nitrifiers, aerobically oxidizing ammonia to nitrite, the metabolism of the deeper Thaumarchaeota branches to which the Naica OTU belongs, remains unknown (Pester et al., 2011). The Thermoplasmatales are moderately thermoacidophilic archaea frequent in hot springs. The related lineages to which the Naica sequences resemble have been identified in deep-sea sediments and also in the deep subsurface (Lin et al., 2006a; Kato et al., 2009; Zhang et al., 2010). This suggests that both archaeal OTUs are autochthonous lineages in the Naica hydrothermal springs.

Bacteria were dominated by the Betaproteobacteria, and in particular by the Beta\_OTU1, which represented between 50 and 65% of the sequences retrieved in N1 and N2. Naica sequences were identical or nearly identical to *Delftia* sp. XYJ6, a strain isolated from wastewater and being able to degrade aniline (Yan et al., 2011) and to an environmental sequence obtained from a coral (Figure 4). By contrast the Beta\_OTU2 is most closely related to *Alcaligenes denitrificans*, which can be an opportunistic pathogen. This OTU might therefore represent an external contaminant.

The remaining bacterial OTUs appear also to be autochthonous to the Naica system. The alphaproteobacterial OTU detected in N2 ascribed to the genus *Paracoccus*, encompassing bacteria

often associated to soils but which can be isolated from the deep seafloor (Kobayashi et al., 2008). Likewise, the Firmicutes sequences (Firmi\_OTU1) were nearly 100% identical to sequences retrieved from a subsurface aquifer at the Hanford Site (USA; Lin et al., 2012) and also to sequences retrieved from deeply buried coral carbonates and sediment at Porcupine Seabight (site U1317 Hole A; Figure 4). Finally, the three OTUs ascribing to the Candidate Division OP3 are most likely indigenous as well. So far, there is no cultured member of this taxon, but their 16S rRNA sequences have been identified in a variety of ecosystems such as marine sediments, hypersaline deep-sea, freshwater lakes, aquifers, flooded paddy soils, and methanogenic bioreactors (Madrid et al., 2001; López-Archilla et al., 2007; Glockner et al., 2010). The fact that many of these environments are anoxic and the identification of OP3 genes potentially involved in anaerobic respiration in metagenomic libraries suggest that many OP3 bacteria are anaerobes (Glockner et al., 2010). Very recently, some OP3 members have been shown to be magnetotactic bacteria (Kolinko et al., 2012). They have been notably detected in fracture-derived groundwater in a deep gold mine of South Africa (Lin et al., 2006a). The Naica OP3 OTUs are divergent and have as closest relatives, although relatively distant, environmental sequences retrieved from deep-sea sediments or the seafloor (Figure 4).

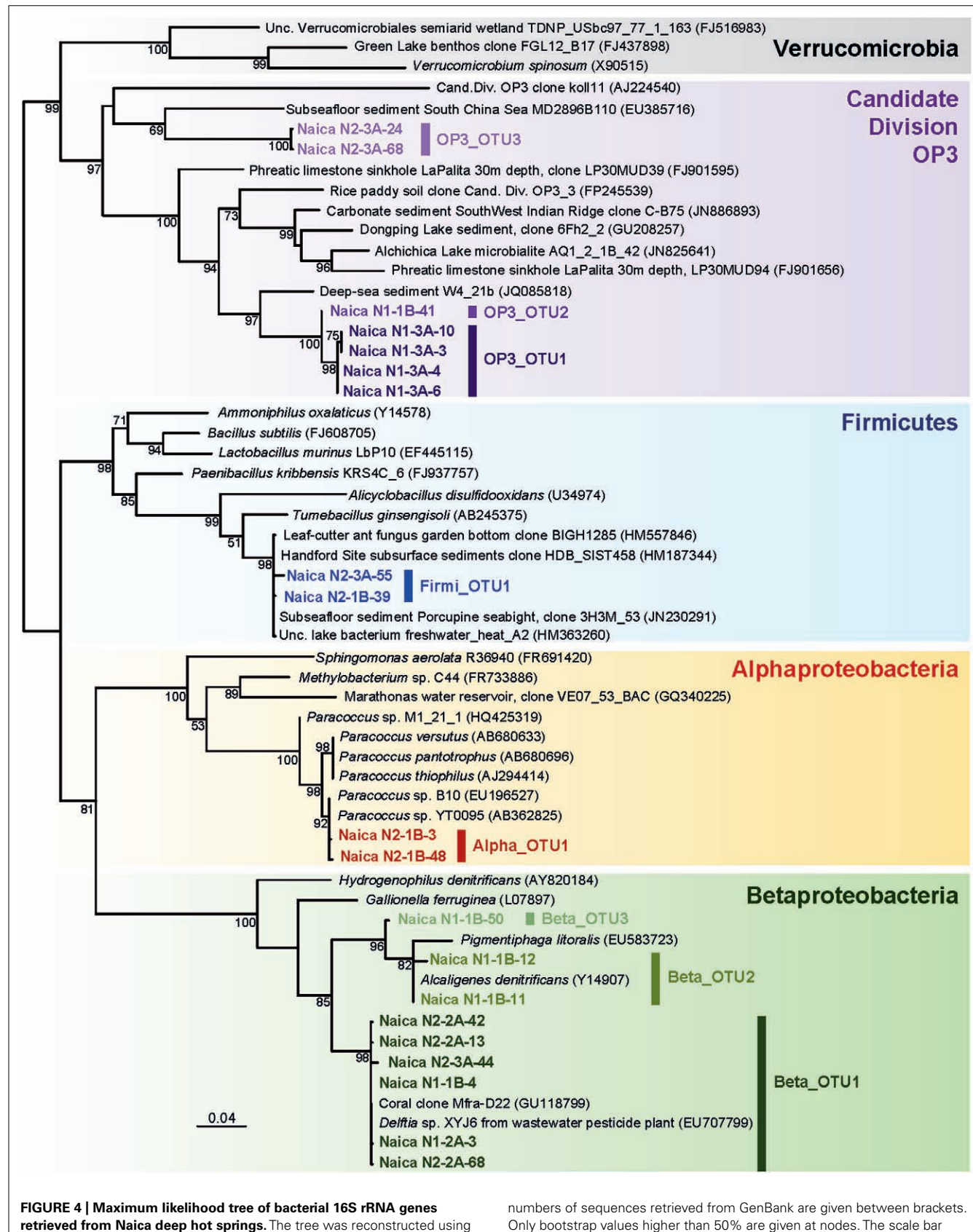


**FIGURE 4 | Maximum likelihood tree of bacterial 16S rRNA genes retrieved from Naica deep hot springs.** The tree was reconstructed using 846 positions. Sequences obtained in this work are shown in color. Accession

numbers of sequences retrieved from GenBank are given between brackets. Only bootstrap values higher than 50% are given at nodes. The scale bar represents the number of substitutions per a unit branch length.

## LIKELY THERMOPHILIC LIFESTYLE UNDER EXTREME ENERGY LIMITATION

The microbial diversity identified in the Naica hydrothermal water samples N1 and N2 was very low, being only comparable to that found in strongly energy-limited areas of the subsurface (Jorgensen and Boetius, 2007). Even samples from other deep-sea mines seemed to host a larger microbial diversity (Onstott et al., 2003; Lin et al., 2006b; Sahl et al., 2008; Rastogi et al., 2010), although the introduction of external contaminants by the mining activity or during the processing of extremely low biomass samples remains a general risk in deep-subsurface studies. In our case, most of the OTUs identified had as closest relatives other environmental sequences coming from deep sediments or subseafloor environments, suggesting that many of the microorganisms detected are indeed autochthonous to the Naica system. This is particularly clear for the archaea and bacteria of the Candidate Division OP3, and possibly for the Firmicutes OTU identified. With the exception of Beta\_OTU2, which may be a human-related contaminant, the remaining Alpha- and Beta-proteobacterial sequences identified in Naica samples may be also indigenous. However, the possibility that they are associated to soil or dust particles that have been introduced in the shaft cannot be completely ruled out. Given the low prokaryotic diversity of the system and its extreme conditions, especially the relatively high temperatures and the high nutrient depletion (oligotrophy), the absence of detectable eukaryotes in the Naica hot springs was not surprising.

The above observations were further confirmed by the GC content of the retrieved sequences, which suggests that the archaeal and at least two OTUs of the Candidate Division OP3 correspond to thermophilic organisms. Although GC content varies along the genome and across phylogenetic lineages, it is well known that thermophiles and, most especially, hyperthermophiles increase the GC content of their rRNA molecules to cope with high temperatures (Groussin and Gouy, 2011). As can be seen in **Figure 5**, the GC content of Naica archaea, OP3 OTUs 1, and 2 and the Firmicutes fall among that of organisms growing optimally at temperatures between 50 and 70°C. This suggests that these organisms are indeed thermophiles. The Thaumarchaeota, with over 60% GC at their 16S rRNA genes might be even extreme thermophiles and be able to grow in even hotter areas of the aquifer (~60–70°C). By contrast, little can be said about the optimal growth temperature of the remaining OTUs that display lower GC content in their rRNA sequences. They could be mesophiles or they might be moderate thermophiles growing well at temperatures around 50–55°C in the Naica system. Intriguingly, the sequences with the lowest GC content were those of the Candidate Division OP3 OTU3 (**Figure 5**), which is most certainly autochthonous to Naica. This might indicate an overall low GC content in the genome of these organisms.

With the exception of the thermophilic character of microorganisms thriving in Naica waters, little can be said about their metabolic potential from their 16S rRNA genes. Therefore, we aimed at providing some metabolic information about the Naica community by amplifying genes involved in specific metabolic pathways. In the case of archaea, many Thaumarchaeota are known to be nitrifiers, oxidizing ammonia aerobically to nitrite, although the presence of archaeal *amo* genes does not necessarily

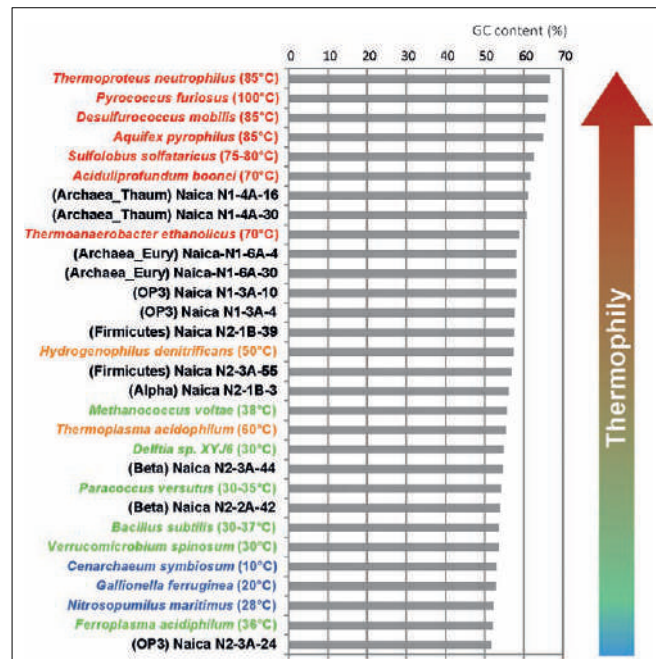
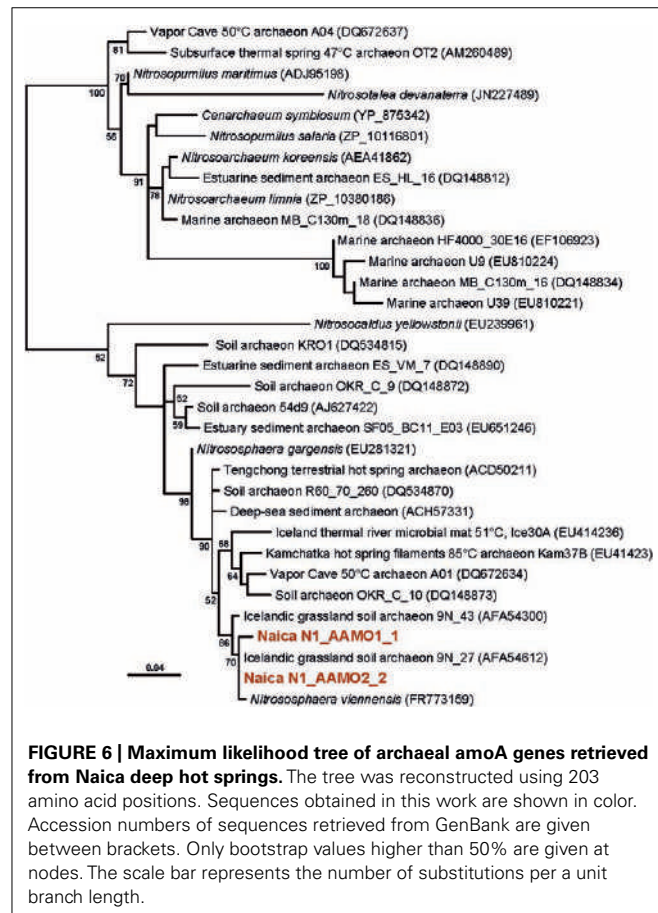


**FIGURE 5 | Comparative histogram showing the GC content of the same 16S rRNA region in Naica clones and in a wide range of microbial species growing at different temperatures.**

correlate with the basal branching groups, leaving the question open for these basal Thaumarchaeota (Pester et al., 2011). We succeeded in amplifying archaeal *amoA* genes, which branched together with *amoA* genes coming from soils and hot springs forming a clade distinct from that of marine planktonic archaea (**Figure 6**). This strongly suggests that these Naica archaea are thermophilic nitrifiers that, given the highly oligotrophic conditions, are likely chemolithoautotrophic, as other members of the group (Pester et al., 2011).

Methanogenic archaea and sulfate-reducing bacteria are often detected in subsurface environments (Jorgensen and Boetius, 2007; Fry et al., 2008; Roussel et al., 2008). However, archaeal sequences belonging to classical methanogenic Euryarchaeota were not observed in Naica. Nonetheless, very recently, the occurrence of methanogenesis has been discovered in organisms branching at the base of the Thermoplasmatales (Paul et al., 2012). Although our Naica sequences are not very closely related to these new “Methanoplasmatales,” they remain related to deep-sea sequences forming a cluster with them (**Figure 3**; Paul et al., 2012). However, we failed to amplify *mcrA* genes, used as a marker for methanogenesis, suggesting that Eury\_OTU2 are not methanogens and gain energy by an unknown mechanism.

In principle, the presence of sulfate-reducing bacteria could be expected in Naica since its hydrothermal waters are highly enriched in sulfate, allowing for the formation of massive gypsum crystals at a delicate super-saturation balance between anhydrite and gypsum (Garcia-Ruiz et al., 2007; Van Driesche et al., 2011; Krueger et al., 2013). However, members of the sulfate-reducing Deltaproteobacteria were not identified. Sulfate reducers are also found within the Firmicutes, but the Naica OTU is not closely related to



known Gram-positive sulfate reducers (**Figure 4**), suggesting that they use another type of metabolism. We failed to amplify *dsrA*

## REFERENCES

- Altschul, S. F., Madden, T. L., Schaffer, A. A., Zhang, J., Zhang, Z., Miller, W., et al. (1997). Gapped BLAST and PSI-BLAST: a new generation of protein database search programs. *Nucleic Acids Res.* 25, 3389–3402.
- Basso, O., Lascurreges, J. F., Le Borgne, F., Le Goff, C., and Magot, M. (2009). Characterization by culture and molecular analysis of the microbial diversity of a deep subsurface gas storage aquifer. *Res. Microbiol.* 160, 107–116.
- Castresana, J. (2000). Selection of conserved blocks from multiple alignments for their use in phylogenetic analysis. *Mol. Biol. Evol.* 17, 540–552.
- Chandler, D. P., Brockman, F. J., Bailey, T. J., and Fredrickson, J. K. (1998). Phylogenetic diversity of Archaea and bacteria in a deep subsurface paleosol. *Microb. Ecol.* 36, 37–50.
- Chapelle, F. H., O'Neill, K., Bradley, P. M., Methé, B. A., Ciufo, S. A., Knobel, L. L., et al. (2002). A hydrogen-based subsurface microbial community dominated by methanogens. *Nature* 415, 312–315.
- Edgar, R. C. (2004). MUSCLE: multiple sequence alignment with high accuracy and high throughput. *Nucleic Acids Res.* 32, 1792–1797.
- Edwards, K. J., Wheat, C. G., and Sylvan, J. B. (2011). Under the sea: microbial life in volcanic oceanic crust. *Nat. Rev. Microbiol.* 9, 703–712.
- Erwood, R. J., Kesler, S. E., and Cloke, P. L. (1979). Compositionally distinct, saline hydrothermal solutions, Naica Mine, Chihuahua, Mexico. *Economic Geology* 74, 95–108.
- Forti, P., and Sanna, L. (2010). The Naica project – A multidisciplinary study of the largest gypsum crystal of the world. *Episodes* 33, 23–32.
- Francis, C. A., Roberts, K. J., Beman, J. M., Santoro, A. E., and Oakley, B. B. (2005). Ubiquity and diversity of ammonia-oxidizing archaea in water columns and sediments of the ocean. *Proc. Natl. Acad. Sci. U.S.A.* 102, 14683–14688.
- Fredrickson, J. K., Balkwill, D. L., Drake, G. R., Romine, M. F., Ringelberg, D. B., and White, D. C. (1995). Aromatic-degrading *Sphingomonas* isolates from the deep subsurface. *Appl. Environ. Microbiol.* 61, 1917–1922.
- Fry, J. C., Parkes, R. J., Cragg, B. A., Weightman, A. J., and Webster, G. (2008). Prokaryotic biodiversity and activity in the deep seafloor biosphere. *FEMS Microbiol. Ecol.* 66, 181–196.
- Garcia-Ruiz, J. M., Villasuso, R., Ayora, C., Canals, A., and Otalora, F. (2007). Formation of natural gypsum megacrystals in Naica, Mexico. *Geology* 35, 327–330.
- Garofalo, P. S., Fricker, M., Günther, D., Mercuri, A. M., Loret, M., Forti, P., et al. (2010). A climatic control on the formation of gigantic gypsum crystals within the hypogenic caves of Naica (Mexico)? *Earth Planet Sci. Lett.* 289, 560–569.
- Gerard, E., Moreira, D., Philippon, P., Van Kranendonk, M. J., and Lopez-Garcia, P. (2009). Modern subsurface bacteria in pristine 2.7 Ga-old fossil stromatolite drillcore samples from the Fortescue Group, Western Australia. *PLoS ONE* 4:e5298. doi: 10.1371/journal.pone.0005298
- Ghiorse, W. C., and Wilson, J. T. (1988). Microbial ecology of the terrestrial subsurface. *Adv. Appl. Microbiol.* 33, 107–172.
- Glockner, J., Kube, M., Shrestha, P. M., Weber, M., Glockner, F. O., Reinhardt, R., et al. (2010). Phylogenetic diversity and metagenomics of candidate division OP3. *Environ. Microbiol.* 12, 1218–1229.
- Gold, T. (1992). The deep, hot biosphere. *Proc. Natl. Acad. Sci. U.S.A.* 89, 6045–6049.
- Groussin, M., and Gouy, M. (2011). Adaptation to environmental temperature is a major determinant of molecular evolutionary rates in archaea. *Mol. Biol. Evol.* 28, 2661–2674.
- Head, I. M., Jones, D. M., and Larter, S. R. (2003). Biological activity genes encoding the dissimilatory sulfite reductase, which further reinforces the idea that Naica-associated microbial communities do not (or not dominantly) carry out sulfate reduction. At any rate, for sulfate reduction to occur, either organic matter or inorganic electron donors, typically H<sub>2</sub>, must be present to fuel the redox reaction. However, both appear to be extremely low in the aquifer. Conversely, appreciable amounts of H<sub>2</sub>S, the resulting product of sulfate reduction, are not detectable in Naica (unpublished observations). All these observations suggest that sulfate reduction, if it exists, is not a dominant metabolism in the microbiota of the Naica hydrothermal water despite an overwhelming availability of sulfate. This highlights the importance of having access to redox interfaces for life and implies that microorganisms thriving in the deep-subsurface thermal waters of the Naica system are among the most oligotrophic and energy-challenged communities explored to date.
- Given the low biomass and diversity associated to the Naica thermal water, the possibility that microorganisms were entrapped in fluid inclusions in the massive crystals that slowly formed in these saline hot waters is small. Nevertheless, the present description offers a list of potential bona-fide candidate lineages to be captured in the fluid inclusions. Whether their macromolecules, especially their DNA, have escaped thermal degradation upon metabolic exhaustion in the fluid entraptments and are still detectable should be the subject of future studies.

## ACKNOWLEDGMENTS

We are grateful to Eng. Roberto Carlos Reyes and Compañía Peñoles for the facilities provided during the field studies. This work was financed by the Spanish MINECO (Consolider-Ingenio 2010 project “Factoría de Cristalización” and project CGL2010-16882) and by the French Agence Nationale de la Recherche (ANR-08-GENM-024-001).

- in the deep subsurface and the origin of heavy oil. *Nature* 426, 344–352.
- Inagaki, F., Tsunogai, U., Suzuki, M., Kosaka, A., Machiyama, H., Takai, K., et al. (2004). Characterization of C1-metabolizing prokaryotic communities in methane seep habitats at the Kuroshima Knoll, southern Ryukyu Arc, by analyzing pmoA, mmoX, mxaF, mcrA, and 16S rRNA genes. *Appl. Environ. Microbiol.* 70, 7445–7455.
- Jobb, G., Von Haeseler, A., and Strimmer, K. (2004). TREEFINDER: a powerful graphical analysis environment for molecular phylogenetics. *BMC Evol. Biol.* 4:18. doi: 10.1186/1471-2148-4-18
- Jorgensen, B. B. (2012). Shrinking majority of the deep biosphere. *Proc. Natl. Acad. Sci. U.S.A.* 109, 15976–15977.
- Jorgensen, B. B., and Boetius, A. (2007). Feast and famine – microbial life in the deep-sea bed. *Nat. Rev. Microbiol.* 5, 770–781.
- Jorgensen, B. B., and D'Hondt, S. (2006). Ecology. A starving majority deep beneath the seafloor. *Science* 314, 932–934.
- Jungbluth, S. P., Grote, J., Lin, H. T., Cowen, J. P., and Rappe, M. S. (2012). Microbial diversity within basement fluids of the sediment-buried Juan de Fuca Ridge flank. *ISME J.* 7, 161–172.
- Kallmeyer, J., Pockalny, R., Adhikari, R. R., Smith, D. C., and D'Hondt, S. (2012). Global distribution of microbial abundance and biomass in subseafloor sediment. *Proc. Natl. Acad. Sci. U.S.A.* 109, 16213–16216.
- Kato, S., Yanagawa, K., Sunamura, M., Takano, Y., Ishibashi, J., Kakegawa, T., et al. (2009). Abundance of Zetaproteobacteria within crustal fluids in back-arc hydrothermal fields of the Southern Mariana Trough. *Environ. Microbiol.* 11, 3210–3222.
- Kim, J. S., and Crowley, D. E. (2007). Microbial diversity in natural asphalts of the Rancho La Brea Tar Pits. *Appl. Environ. Microbiol.* 73, 4579–4591.
- Kimura, H., Sugihara, M., Yamamoto, H., Patel, B. K., Kato, K., and Hanada, S. (2005). Microbial community in a geothermal aquifer associated with the subsurface of the Great Artesian Basin, Australia. *Extremophiles* 9, 407–414.
- Kobayashi, T., Koide, O., Mori, K., Shimamura, S., Matsaura, T., Miura, T., et al. (2008). Phylogenetic and enzymatic diversity of deep subseafloor aerobic microorganisms in organics- and methane-rich sediments off Shimokita Peninsula. *Extremophiles* 12, 519–527.
- Kolinko, S., Jogler, C., Katzenmann, E., Wanner, G., Peplies, J., and Schuler, D. (2012). Single-cell analysis reveals a novel uncultivated magnetotactic bacterium within the candidate division OP3. *Environ. Microbiol.* 14, 1709–1721.
- Krueger, Y., Garcia-Ruiz, J. M., Canals, A., Marti, D., Frenz, M., and Van Driessche, A. E. S. (2013). Determining gypsum growth temperatures using monophase fluid inclusions – application to the giant gypsum crystals of Naica, Mexico. *Geology*. doi: 10.1130/G33581.33581 [Epub ahead of print].
- Lin, L.-H., Hall, J., Onstott, T. C., Gilring, T., Sherwood Lollar, B., Boice, E., et al. (2006a). Planktonic microbial communities associated with fracture-derived groundwater in a deep gold mine of South Africa. *Geomicrobiol. J.* 23, 475–497.
- Lin, L. H., Wang, P. L., Rumble, D., Lippmann-Pipke, J., Boice, E., Pratt, L. M., et al. (2006b). Long-term sustainability of a high-energy, low-diversity crustal biome. *Science* 314, 479–482.
- Lin, X., Kennedy, D., Fredrickson, J., Bjornstad, B., and Konopka, A. (2012). Vertical stratification of sub-surface microbial community composition across geological formations at the Hanford Site. *Environ. Microbiol.* 14, 414–425.
- López-Arrolla, A. I., Moreira, D., Velasco, S., and López-García, P. (2007). Archaeal and bacterial community composition of a pristine coastal aquifer in Doñana National Park, Spain. *Aquatic Microbiol. Ecol.* 47, 123–129.
- Madrid, V. M., Taylor, G. T., Scranton, M. I., and Chistoserdov, A. Y. (2001). Phylogenetic diversity of bacterial and archaeal communities in the anoxic zone of the Cariaco Basin. *Appl. Environ. Microbiol.* 67, 1663–1674.
- Mason, O. U., Nakagawa, T., Rosner, M., Van Nostrand, J. D., Zhou, J., Maruyama, A., et al. (2010). First investigation of the microbiology of the deepest layer of ocean crust. *PLoS ONE* 5:e9490. doi: 10.1371/journal.pone.0009490
- Rastogi, G., Osman, S., Kukkadapu, R., Engelhard, M., Vaishampayan, P. A., Andersen, G. L., et al. (2010). Microbial and mineralogical characterizations of soils collected from the deep biosphere of the former Homestake gold mine, South Dakota. *Microb. Ecol.* 60, 539–550.
- Rastogi, G., Stetler, L. D., Peyton, B. M., and Sani, R. K. (2009). Molecular analysis of prokaryotic diversity in the deep subsurface of the former Homestake gold mine, South Dakota, USA. *J. Microbiol.* 47, 371–384.
- Roussel, E. G., Bonavita, M. A., Querellou, J., Cragg, B. A., Webster, G., Prieur, D., et al. (2008). Extending the sub-sea-floor biosphere. *Science* 320, 1046.
- Rueter, P., Rabus, R., Wilkes, H., Aeckersberg, F., Rainey, F. A., Jannasch, H. W., et al. (1994). Anaerobic oxidation of hydrocarbons in crude oil by new types of sulphate-reducing bacteria. *Nature* 372, 455–458.
- Program Leg 190. *Environ. Microbiol.* 6, 274–287.
- Onstott, T. C., Moser, D. P., Pfiffner, S. M., Fredrickson, J. K., Brockman, F. J., Phelps, T. J., et al. (2003). Indigenous and contaminant microbes in ultradeep mines. *Environ. Microbiol.* 5, 1168–1191.
- Parkes, R. J., Webster, G., Cragg, B. A., Weightman, A. J., Newberry, C. J., Ferdelman, T. G., et al. (2005). Deep sub-seafloor prokaryotes stimulated at interfaces over geological time. *Nature* 436, 390–394.
- Paul, K., Nonoh, J. O., Mikulski, L., and Brune, A. (2012). "Methanoplasmatales," thermoplasmatales-related archaea in termite guts and other environments, are the seventh order of methanogens. *Appl. Environ. Microbiol.* 78, 8245–8253.
- Pedersen, K. (2000). Exploration of deep intraterrestrial microbial life: current perspectives. *FEMS Microbiol. Lett.* 185, 9–16.
- Perez-Jimenez, J. R., Young, L. Y., and Kerkhoff, L. J. (2001). Molecular characterization of sulfate-reducing bacteria in anaerobic hydrocarbon-degrading consortia and pure cultures using the dissimilatory sulfite reductase (dsrAB) genes. *FEMS Microbiol. Ecol.* 35, 145–150.
- Pester, M., Schleper, C., and Wagner, M. (2011). The Thaumarchaeota: an emerging view of their phylogeny and ecophysiology. *Curr. Opin. Microbiol.* 14, 300–306.
- Price, M. N., Dehal, P. S., and Arkin, A. P. (2010). FastTree 2—approximately maximum-likelihood trees for large alignments. *PLoS ONE* 5:e9490. doi: 10.1371/journal.pone.0009490
- Rastogi, G., Osman, S., Kukkadapu, R., Engelhard, M., Vaishampayan, P. A., Andersen, G. L., et al. (2010). Microbial and mineralogical characterizations of soils collected from the deep biosphere of the former Homestake gold mine, South Dakota. *Microb. Ecol.* 60, 539–550.
- Rastogi, G., Stetler, L. D., Peyton, B. M., and Sani, R. K. (2009). Molecular analysis of prokaryotic diversity in the deep subsurface of the former Homestake gold mine, South Dakota, USA. *J. Microbiol.* 47, 371–384.
- Roussel, E. G., Bonavita, M. A., Querellou, J., Cragg, B. A., Webster, G., Prieur, D., et al. (2008). Extending the sub-sea-floor biosphere. *Science* 320, 1046.
- Rueter, P., Rabus, R., Wilkes, H., Aeckersberg, F., Rainey, F. A., Jannasch, H. W., et al. (1994). Anaerobic oxidation of hydrocarbons in crude oil by new types of sulphate-reducing bacteria. *Nature* 372, 455–458.
- Sahl, J. W., Schmidt, R., Swanner, E. D., Mandernack, K. W., Templeton, A. S., Kieft, T. L., et al. (2008). Subsurface microbial diversity in deep-granitic-fracture water in Colorado. *Appl. Environ. Microbiol.* 74, 143–152.
- Stroes-Gascoyne, S., and West, J. M. (1997). Microbial studies in the Canadian nuclear fuel waste management program. *FEMS Microbiol. Rev.* 20, 573–590.
- Teske, A., and Sorensen, K. B. (2008). Uncultured archaea in deep marine subsurface sediments: have we caught them all? *ISME J.* 2, 3–18.
- Teske, A. P. (2005). The deep subsurface biosphere is alive and well. *Trends Microbiol.* 13, 402–404.
- Van Driessche, A. E., Garcia-Ruiz, J. M., Tsukamoto, K., Patino-Lopez, L. D., and Satoh, H. (2011). Ultraslow growth rates of giant gypsum crystals. *Proc. Natl. Acad. Sci. U.S.A.* 108, 15721–15726.
- Villasuso, M. R. (2002). "Descripción del yacimiento de Naica," in *Geología Económica de México*, 2nd Edn, eds K. F. Clark, G. A. Salas Piza, and R. C. Estrada (Pachuca: Servicio Geológico Mexicano), 10.
- Webster, G., Parkes, R. J., Cragg, B. A., Newberry, C. J., Weightman, A. J., and Fry, J. C. (2006). Prokaryotic community composition and biogeochemical processes in deep subseafloor sediments from the Peru Margin. *FEMS Microbiol. Ecol.* 58, 65–85.
- White, D. C., Phelps, T. J., and Onstott, T. C. (1998). What's up down there? *Curr. Opin. Microbiol.* 1, 286–290.
- Whitman, W. B., Coleman, D. C., and Wiebe, W. J. (1998). Prokaryotes: the unseen majority. *Proc. Natl. Acad. Sci. U.S.A.* 95, 6578–6583.
- Yan, H., Yang, X., Chen, J., Yin, C., Xiao, C., and Chen, H. (2011). Synergistic removal of aniline by carbon nanotubes and the enzymes of *Delftia* sp. XYJ6. *J. Environ. Sci.* 23, 1165–1170.
- Zhang, W., Saren, G., Li, T., Yu, X., and Zhang, L. (2010). Diversity and community structure of archaea in deep subsurface sediments from the tropical Western Pacific. *Curr. Microbiol.* 60, 439–445.

**Conflict of Interest Statement:** The authors declare that the research was conducted in the absence of any commercial or financial relationships that could be construed as a potential conflict of interest.

*Received: 13 December 2012; paper pending published: 09 January 2013; accepted: 12 February 2013; published online: 06 March 2013*

Citation: Ragon M, Van Driessche AES, García-Ruiz JM, Moreira D and López-García P (2013) Microbial diversity in the deep-subsurface hydrothermal aquifer feeding the giant gypsum crystal-bearing

Naica Mine, Mexico. *Front. Microbiol.* 4:37. doi: 10.3389/fmicb.2013.00037  
This article was submitted to Frontiers in Extreme Microbiology, a specialty of *Frontiers in Microbiology*.

Copyright © 2013 Ragon, Van Driessche, García-Ruiz, Moreira and López-García. This is an open-access article distributed under the terms of the Creative Commons Attribution License, which permits use,

distribution and reproduction in other forums, provided the original authors and source are credited and subject to any copyright notices concerning any third-party graphics etc.

## APPENDIX

### HYDROLOGICAL AND GEOLOGICAL SETTING OF THE NAICA MINE (CHIHUAHUA, MEXICO)

The Naica mining district is located in a semi-desertic region (100 km southeast of the city of Chihuahua), on the northwest flank of the Sierra de Naica which, together with Sierra En medio and El Monarca, is elevated above an extensive alluvial floodplain. It is located inside of a hydrological basin (sub basin Tortuguilas) with an extension of approximately 1,300 km<sup>2</sup>. This area is characterized by small “arroyos” which drain run off water originated in the surrounding mountain ranges (Sierra de Naica, En Medio, and El Monarca), towards alluvial plains, which in their lower parts form closed basins. During the raining season these basins host temporary lagoons (e.g., Chancaple, Agua Zoquete, and El Soldado lagoons located at, respectively, the west, southwest, and south of the Naica Mine), and the potential excess of superficial water might feed a shallow phreatic layer. Around these intermittent lagoons, marsh zones are observed subject to floods. These flooding zones have a NW–SE orientation and are parallel to the regional fault systems, thus representing possible recharge sources (Villasuso, 2002).

The materials of the Naica drainage basin, which host the ore deposit, are of Albian–Cenomanian age and form a gentle antiform structure made of a sequence of limestones and marls. This sequence is cut by discontinuous, pre-ore quartz–feldspar dikes (Megaw et al., 1988), which are associated to a relatively shallow subhorizontal igneous intrusion that still generates a broad thermal anomaly in the southwest part of the region. Magnetometric studies have unveiled an igneous source at a depth of between 2.5 and 5 km, some 4 km south of Naica (Villasuso, 2002), while in 2007 a drilling close to the mine shaft met an igneous body about 1,140 m below the surface (Forti and Sanna, 2010).

The ore deposit is made of extensive tabular bodies (Figure 1) and is related to hydrothermal flows induced by Tertiary dykes forming one of the largest chimney-manto (skarn) Ag–Pb–Zn deposits of Mexico (Erwood et al., 1979; Megaw et al., 1988; Palacios et al., 1991; Alva-Valdivia et al., 2003). Its ore mineralogy is represented mainly by early pyrite, galena, sphalerite, chalcopyrite, pyrrhotite, magnetite, rutile, and fluorite. The main ore-forming process was dated at 30.2–26.0 Ma (Alva-Valdivia et al., 2003, and references therein) and the early conditions of ore deposition were estimated to be about 400–500°C and 100–270 MPa (Megaw et al., 1988; Palacios et al., 1991). During a later stage, when the thermal fluids got colder, quartz, anhydrite, and calcite formed veins within the ore bodies (Stone, 1959). Mine activities have reached ca. 890 m below the mine entrance (level

0 at 1,385 masl), and they are some 760 m below the original groundwater level which was at –130 m (1,255 masl). To maintain the mine galleries water free a dewatering of about 1 m<sup>3</sup>/s is required.

As mentioned above, the Naica area is still under a mild thermal anomaly and water springing in the mine galleries has a temperature ranging from 50 to 60°C (Garcia-Ruiz et al., 2007). Two different fault sets are the main structural controls for hydrothermal circulation and therefore for the location of the mineral deposits. The most important of them are the Gibraltar, Naica, and Montaña faults. These structures still control the thermal water flow within the Naica anticline: almost all the water springing in the deep mine galleries comes from fractures related to these faults. Their important role in water circulation is also confirmed by the fact that karst caves have developed in their vicinity. These hypogenic caves (i.e., deep karst cavities that develop from fractured controlled flow of ground water within confined aquifers) formed well after the ore-forming event (Garofalo et al., 2010) and some of them exhibit impressive deposits of very large selenite crystals. For example, along a segment of the Naica fault several such caves have been discovered: Cave of crystals, Ojo de la Reina, and Cueva de las Velas. These caves developed completely isolated from the surface, under hundreds of meters of hydraulic head from the regional aquifer. Partial or effective confinement of this aquifer was achieved by the reduction of rock porosity from the precipitation of the hydrothermal minerals, and by the presence of shale levels (Benevides formation, Figure 1). The most typical cave mineralogy phases are gypsum, celestine, anglesite, jarosite, and goethite.

A detailed study of the geochemical and physicochemical characteristics of the thermal aquifer evidenced a novel formation mechanism of these giant crystals (Garcia-Ruiz et al., 2007) which is based upon the gypsum-anhydrite solubility disequilibrium. At 58°C the gypsum and anhydrite solubilities are the same (Hardie, 1967). At lower temperatures the solubility of gypsum becomes smaller than that of anhydrite. Therefore, below this temperature a solution saturated with respect to anhydrite is automatically super-saturated with respect to gypsum, thus inducing the deposition of gypsum and undersaturation with respect to anhydrite. Hence, the development of a few large crystals instead of many small ones is due to the fact that the temperature drop was extremely slow (data from fluid inclusions indicate that the giant crystals developed in a temperature range between 55 and 58°C (Krueger et al., 2013); which lead to reduced nucleation (Garcia-Ruiz et al., 2007) and a very low growth rate (Van Driessche et al., 2011).

## REFERENCES

- Alva-Valdivia, L. M., Goguitchaichvili, A., and Urrutia-Fucugauchi, J. (2003). Petromagnetic properties in the Naica mining district, Chihuahua, Mexico: searching for source of mineralization. *Earth Planets Space* 55, 19–31.
- Erwood, R. J., Kesler, S. E., and Cloke, P. L. (1979). Compositionally distinct, saline hydrothermal solutions, Naica Mine, Chihuahua, Mexico. *Econ. Geol.* 74, 95–108.
- Forti, P., and Sanna, L. (2010). The Naica project – a multidisciplinary study of the largest gypsum crystal of the world. *Episodes* 33, 23–32.
- Garcia-Ruiz, J. M., Villasuso, R., Ayora, C., Canals, A., and Otalora, F. (2007). Formation of natural gypsum megacrystals in Naica, Mexico. *Geology* 35, 327–330.
- Garofalo, P. S., Fricker, M., Günther, D., Mercuri, A. M., Loretí, M., Forti, P., et al. (2010). A climatic control on the formation of gigantic gypsum crystals within the hypogenic caves of Naica (Mexico)? *Earth Planet Sci. Lett.* 289, 560–569.
- Hardie, L. A. (1967). The gypsum-anhydrite equilibrium at one atmosphere pressure. *Am. Miner.* 52, 171–200.
- Krueger, Y., Garcia-Ruiz, J. M., Canals, A., Martí, D., Frenz, M., and Van Driessche, A. E. S. (2013). Determining gypsum growth temperatures using monophase fluid inclusions – application to the giant gypsum crystals of Naica, Mexico. *Geology*. doi: 10.1130/G33581.1 [Epub ahead of print].
- Megaw, P. K. M., Ruiz, J., and Titley, S. R. (1988). High-temperature, carbonate-hosted Pb–Zn–Ag (Cu)

- deposits of northern Mexico. *Econ. Geol.* 83, 1856–1885.
- Palacios, M. H. A., Querol, S. F., and Lowther, G. K. (1991). “Geology and genesis of the Naica mineral deposits, Chihuahua,” in *Economic Geology of Mexico*, ed. G. P. Salas. (Boulder, CO: Geological Society of America), 259–265.
- Stone, J. G. (1959). Ore genesis in the Naica District, Chihuahua, Mexico. *Econ. Geol.* 54, 1002–1034.
- Van Driessche, A. E., Garcia-Ruiz, J. M., Tsukamoto, K., Patino-Lopez, L. D., and Satoh, H. (2011). Ultraslow growth rates of giant gypsum crystals. *Proc. Natl. Acad. Sci. U.S.A.* 108, 15721–15726.
- Villasuso, M. R. (2002). “Descripción del yacimiento de Naica,” in *Geología Económica de México*, 2nd Edn, eds K. F. Clark, G. A. Salas Piza, and R. C. Estrada (Pachuca: Servicio Geológico Mexicano).



# Presence and diversity of anammox bacteria in cold hydrocarbon-rich seeps and hydrothermal vent sediments of the Guaymas Basin

Lina Russ<sup>1</sup>, Boran Kartal<sup>1</sup>, Huub J. M. op den Camp<sup>1\*</sup>, Martina Sollai<sup>2</sup>, Julie Le Bruchec<sup>3</sup>, Jean-Claude Caprais<sup>3</sup>, Anne Godfroy<sup>4</sup>, Jaap S. Sinninghe Damsté<sup>2</sup> and Mike S. M. Jetten<sup>1</sup>

<sup>1</sup> Department of Ecological Microbiology, Institute for Wetland and Water Research, Radboud University, Nijmegen, Netherlands

<sup>2</sup> Department of Marine Organic Biogeochemistry, NIOZ Royal Netherlands Institute for Sea Research, Den Burg, Texel, Netherlands

<sup>3</sup> Unité Etude des Ecosystèmes Profonds, Laboratoire Environnement Profond, Ifremer, Plouzané, France

<sup>4</sup> Unité Etude des Ecosystèmes Profonds, Laboratoire de Microbiologie des Environnements Extrêmes, Ifremer, UMR6197, CNRS, University of Brest, Plouzané, France

**Edited by:**

Peter Dunfield, University of Calgary, Canada

**Reviewed by:**

Peter Dunfield, University of Calgary, Canada

Takuro Nunoura, Japan Agency for Marine-Earth Science and Technology, Japan

**\*Correspondence:**

Huib J. M. op den Camp,  
Department of Ecological Microbiology, Institute for Wetland and Water Research, Radboud University, Heyendaalseweg 135, 6525AJ Nijmegen, Netherlands  
e-mail: h.opdenCamp@science.ru.nl

Hydrothermally active sediments are highly productive, chemosynthetic areas which are characterized by the rapid turnover of particulate organic matter under extreme conditions in which ammonia is liberated. These systems might be suitable habitats for anaerobic ammonium oxidizing (anammox) bacteria but this has not been investigated in detail. Here we report the diversity and abundance of anammox bacteria in sediments that seep cold hydrocarbon-rich fluids and hydrothermal vent areas of the Guaymas Basin in the Cortés Sea using the unique functional anammox marker gene, hydrazine synthase (*hzsA*). All clones retrieved were closely associated to the "*Candidatus Scalindua*" genus. Phylogenetic analysis revealed two distinct clusters of *hzsA* sequences (*Ca. Scalindua hzsA* cluster I and II). Comparison of individual sequences from both clusters showed that several of these sequences had a similarity as low as 76% on nucleotide level. Based on the analysis of this phylomarker, a very high interspecies diversity within the marine anammox group is apparent. Absolute numbers of anammox bacteria in the sediments samples were determined by amplification of a 257 bp fragment of the *hzsA* gene in a qPCR assay. The results indicate that numbers of anammox bacteria are generally higher in cold hydrocarbon-rich sediments compared to the vent areas and the reference zone. Ladderanes, lipids unique to anammox bacteria were also detected in several of the sediment samples corroborating the *hzsA* analysis. Due to the high concentrations of reduced sulfur compounds and its potential impact on the cycling of nitrogen we aimed to get an indication about the key players in the oxidation of sulfide in the Guaymas Basin sediments using the alpha subunit of the adenosine-5'-phosphosulfate (APS) reductase (*aprA*). Amplification of the *aprA* gene revealed a high number of gammaproteobacterial *aprA* genes covering the two sulfur-oxidizing bacteria *aprA* lineages as well as sulfate-reducers.

**Keywords:** anammox, *hzsA*, *aprA*, hydrothermal vents, cold seep, sulfide

## INTRODUCTION

The Guaymas Basin is a near-shore submarine depression in the central Gulf of California that is characterized by hydrothermally active sediments and hydrocarbon-rich seepages that escape from the sediments at a range of different temperatures (Bazylinski et al., 1988). Geothermally-heated seawater water rises along the ridge segment that is associated with sea floor spreading and escapes via hotspots at high temperatures up to 300°C (Von Damm et al., 1985). Locally, the progressive degradation of organic matter in deeper sediment layers causes the buildup of hydrogen sulfide, methane and other hydrocarbons that seep to the sediment surface at moderate temperatures (cold hydrocarbon-rich seeps) (Vigneron et al., 2013). Due to a high sedimentation rate of the detritus from the productive

surface waters as well as terrestrial input, the crustal fissures are covered with a layer of 100–500 m-thick organic-rich sediments (Calvert, 1966). The hot fluids diffusing upwards lead to accelerated diagenesis by metal sulfide precipitation and thermo-chemical decomposition of organic material within the sediment, leading to a distinct seeping fluid with relatively higher concentrations of ammonium and low molecular weight hydrocarbons and lower concentrations of free sulfides than other lava vent sites (Kawka and Simoneit, 1987; Bazylinski et al., 1988; Von Damm, 1990). This creates an unusual ecosystem at 2000 m depth that is fueled by conversion of reduced inorganic compounds such as hydrogen sulfide or methane by chemoautotrophs. Although the Guaymas Basin sediment is generally well-supplied with ammonium (Von Damm, 1990) and there is sufficient evidence of

nitrate reduction as a potential source for nitrite (Bowles and Joye, 2010; Bowles et al., 2012), anaerobic ammonium oxidation (anammox) has not yet been investigated in Guaymas Basin sediments. It has been assumed that the abundance of reduced carbon and sulfide may favor denitrification and dissimilatory nitrate reduction to ammonium (DNRA) and inhibit anammox (Burgin and Hamilton, 2007; Jensen et al., 2008).

Anammox has been shown to be a key process in the cycling of nitrogen in oxygen-limited systems such as oxygen minimum zones and marine sediments all over the world and molecular surveys could confirm presence of anammox bacteria in very diverse environments such as deep sea sediments, Atlantic hydrothermal vent systems, hot springs, arctic sediments, and petroleum reservoirs (Kuypers et al., 2003, 2005; Trimmer et al., 2003; Byrne et al., 2008; Jaeschke et al., 2009, 2010; Lam et al., 2009; Li et al., 2010; Hong et al., 2011; Harhangi et al., 2012; Borin et al., 2013). So far, anammox bacteria of the genus “*Candidatus Scalindua spp.*” are the major representatives of the order *Brocadiales* in marine ecosystems (van de Vossenberg et al., 2008, 2013; Woebken et al., 2008). Like other anammox bacteria, they derive their energy for growth from the conversion of  $\text{NH}_4^+$  and  $\text{NO}_2^-$  into dinitrogen gas, thereby constituting an important sink for fixed nitrogen under anoxic conditions. In this study we used a combination of specific biomarkers to target anammox bacteria and determine their numbers and diversity within the Guaymas basin. Anammox bacteria are so far the only known bacteria capable of hydrazine production, therefore we used the alpha subunit of the hydrazine synthase (*HzsA*) complex as a molecular marker to detect and quantify anammox (Harhangi et al., 2012). In addition we used ladderane lipids, which are unique to the membranes of anammox bacteria, as biomarkers. (Sinninghe Damsté et al., 2002, 2005).

The importance of the sulfur cycle in the Guaymas Basin sediments has been known already since the discovery of extensive mats of sulfur-oxidizing *Beggiatoa spp.* that were observed at the sediment interface (Jannasch et al., 1989). These organisms thrive on sulfide and nitrate and contribute significantly to the systems primary production (Nelson et al., 1989; McHatton et al., 1996). As the abundance of reduced sulfur compounds might have a substantial impact on the cycling of nitrogen in the Guaymas Basin sediments, we also investigated the diversity of the gene encoding a key enzyme of the dissimilatory sulfate-reduction pathway: dissimilatory adenosine-5'-phosphosulfate (APS) reductase. Homologues of this gene have been found in photo- and chemotrophic sulfur oxidizers, in which it is thought to work in reverse direction, converting sulfite to APS (Frigaard and Dahl, 2009). Two other groups of sulfur oxidizers have been found to be important in marine sediments using different pathways to oxidize reduced sulfur compounds: *Epsilonproteobacteria* using the Sox pathway and *Gammaproteobacteria* related to thiotrophic endosymbionts using the adenosine-5'-phosphosulfate pathway of sulfur oxidation (Hügler et al., 2010). The coupling of the conversion of reduced sulfur compounds to nitrate reduction could have very interesting implications with respect to the formation of complex interactions that would be fueled from the exchange of intermediates.

## MATERIALS AND METHODS

### SAMPLE COLLECTION

Samples were recovered from cold hydrocarbon-rich seeps and hydrothermal vent sediments during the cruise “BIG” (RV L’Atalante, June 2010) on dives 1758-14, 1755-11, 1764-20, and 1766-22 as described by Vigneron et al. (2013). Sets of one location were sampled at about 12 cm distance. A description of the samples can be found in Table 1.

### CHEMICAL ANALYSES

Pore water from the cores was extracted in one (<10 cm) or two centimeters (>10 cm) resolution using Rhizon moisture samplers with a pore size of 0.1  $\mu\text{m}$  (Seeberg-Elverfeldt et al., 2005). Water samples were subsampled by adding either  $\text{ZnCl}_2$  (1:1 vol/vol) for  $\text{H}_2\text{S}$  analysis or freezing at  $-20^\circ\text{C}$  (ammonium) until further analysis. Ammonium was analysed by a manual fluorimetric method (detection limit 1  $\mu\text{M}$ , Holmes et al., 1999). This analysis is sensitive to the presence of hydrogen sulfide ( $\text{H}_2\text{S}$ ) therefore the measurements were corrected for the presence of  $\text{H}_2\text{S}$ . Hydrogen sulfide concentrations were determined by colorimetry according to Fonselius et al. (2007).

### MOLECULAR TECHNIQUES

#### DNA isolation and polymerase chain reaction

Total genomic DNA was isolated from different sediments using the PowerSoil® DNA Isolation Kit (MO BIO Laboratories, Inc.) according to the manufacturer’s protocol. To avoid contamination with our own anammox cultures, isolations were performed in a different department.

All PCR amplifications were performed in a total volume of 25  $\mu\text{l}$  using 12.5  $\mu\text{l}$  PerfeCTa® SYBR® Green FastMix (Quanta), 0.4  $\mu\text{M}$  forward/reverse primer, 2  $\mu\text{l}$  of template and 10.5  $\mu\text{l}$  of DEPC-treated  $\text{H}_2\text{O}$ . Hydrazine synthase amplification was initiated with a denaturation step at  $94^\circ\text{C}$  for 5 min and continued with a standard amplification program of 35 cycles (45 s  $94^\circ\text{C}$ ; 1 min  $56^\circ\text{C}$ ; 45 s  $72^\circ\text{C}$ ). The final elongation step was done at  $72^\circ\text{C}$  for 7 min. Two different primer combinations, targeting the single copy *hzsA* gene, were used on the different samples (Harhangi et al., 2012): I (526F-TAYTTGAAGGDGACTGG; 1857R-AAABGGYGAATCATARTGGC) and V (757F<sub>Scal</sub>-AGT TCNAAYTTGACCC; 1857R-AAABGGYGAATCATARTGGC). The *aprA* fragments of 387 bp were amplified using primers aprA-1-FW-TGGCAGATCATGATYMAYGG and aprA-RV-GGCCGTAACCGCTCTTGAA in the same assay as described for hydrazine synthase (Meyer and Kuever, 2007). The annealing temperature was lowered to  $55^\circ\text{C}$ .

#### Cloning and phylogenetic analysis

The *hzsA* and *aprA* amplicons were cloned in *Escherichia coli* using the pGEM T-easy vector system (Promega) according to the protocol. Clones were randomly selected from overnight-grown LB agar plates containing 100  $\mu\text{M}$  of ampicillin, 200  $\mu\text{M}$  IPTG and 200  $\mu\text{M}$  X-gal. Plasmids were isolated with the GeneJet Plasmid Miniprep Kit (Thermo Fisher Scientific) according to the protocol using 4 ml of overnight bacterial culture. Colony PCR was performed to check cloned plasmids for an insert. Eighty *hza*

**Table 1 | Description of the different samples used in this study.**

| No. | Dive    | Core | (cm)   | Location   | Zone            | Date      | Depth (m) | Latitude     | Longitude     | References                  |
|-----|---------|------|--------|--|-----------------|-----------|-----------|--------------|---------------|-----------------------------|
| 1   | 1758-14 | CT2  | 0–3    | Cold Seep, Vasconcelos active site, white mat        | Sonora Margin   | 6/19/2010 | 1574      | N 27 35.5750 | W 111 28.9840 | Vigneron et al., 2013       |
| 2   | 1758-14 | CT2  | 3–6    |  |                 |           |           |              |               |                             |
| 3   | 1758-14 | CT2  | 6–9    |  |                 |           |           |              |               |                             |
| 4   | 1758-14 | CT2  | 9–12   |  |                 |           |           |              |               |                             |
| 5   | 1758-14 | CT2  | 12–15  |  |                 |           |           |              |               |                             |
| 6   | 1758-14 | CT2  | 15–18  |  |                 |           |           |              |               |                             |
| 7   | 1758-14 | CT2  | 18–21  |  |                 |           |           |              |               |                             |
| 8   | 1758-14 | CT1  |        | Cold Seep, Vasconcelos active site, white mat        | Sonora Margin   | 6/19/2010 | 1574      | N 27 35.5754 | W 111 28.9860 |                             |
| 9   | 1758-14 | CT11 | 0–4    | Cold Seep,   | Sonora Margin   | 6/19/2010 | 1574      | N 27 35.5872 | W 111 28.9859 |                             |
| 10  | 1758-14 | CT11 | 4–6    | Vasconcelos active site, edge of white mat           |                 |           |           |              |               |                             |
| 11  | 1755-11 | CT1  |        | Cold seep, Vasconcelos active site                   | Sonora Margin   | 6/16/2010 | 1573      | N 27 35.5827 | W 111 28.9848 |                             |
| 12  | 1755-11 | CT2  | 1–1.5  | Cold seep, Vasconcelos active site                   | Sonora Margin   | 6/16/2010 | 1573      | N 27 35.5820 | W 111 28.9832 |                             |
| 13  | 1755-11 | CT2  | 6–7    |  |                 |           |           |              |               |                             |
| 14  | 1764-20 | CT3  | 0–2    | Hydrothermal vent, Mat Mound active site, orange mat | Southern Trough | 6/27/2010 | 2005      | N 27 00.3772 | W 111 24.5641 | Callac et al., under review |
| 15  | 1766-22 | CT2  | 0–5    | Hydrothermal vent,                                   | Southern Trough | 6/29/2010 | 2003      | N 27 00.4461 | W 111 24.5243 |                             |
| 16  | 1766-22 | CT2  | 5–10.5 | MegaMat M27 active site, white mat                   |                 |           |           |              |               |                             |
| 17  | 1753-09 | CT4  | 8–11.5 | Reference zone                                       |                 | 6/14/2010 | 1850      | N 27 25.4835 | W 111 30.0779 | Vigneron et al., 2013       |

clones and forty *aprA* clones were selected for Sanger sequencing at the DNA Diagnostics Department of Nijmegen University Medical Center, Nijmegen. Alignments and phylogenetic analysis were performed using the MEGA 5.0 software (Tamura et al., 2011). Related sequences were retrieved via BLAST searches in the Genbank databases. The sequences were submitted to Genbank under the accession numbers KF202916–KF202955 for *aprA* and KF202956–KF203035 for *hzsA* (see Supplementary Tables 1, 2).

#### Quantitative PCR

Primers targeting the *hzsA* gene (1600F<sub>Scal</sub>-GGKTATCARTAT GTAGAAG; 1857R-AAABGGYGAATCATARTGGC) were used in a quantitative PCR assay to assess the absolute number of anammox bacteria in the deep sea samples. Amplifications were again performed in a total volume of 25  $\mu$ l using iQ™ sybr® Green Supermix (Bio Rad) and 1  $\mu$ l template. The amplicon of “*Ca. Scalindua profunda*” with a fragment amplified with the same primers (van de Vossenberg et al., 2013) was diluted in 10-fold steps and used as a standard in the analysis. Amplification was done on a iCycler iQ (Bio Rad) according to the following thermal protocol: The amplification program was started with 3 min at 96°C, followed by 40 cycles of 1 min at 95°C,

1 min 54°C, and 1 min at 72°C and a final elongation step of 5 min at 72°C. A melting curve analysis was performed at the end of the program ranging from 52–90°C in steps of 0.5°C to identify potentially unwanted amplicons. Ten products that were retrieved were cloned into *E. coli* as described above to verify amplification of the correct product. Retrieved plasmids were checked for an insert by colony PCR and sequenced as described before.

#### Lipid analysis

Ladderane fatty acids, including the newly identified short-chain C<sub>14</sub> ladderane fatty acids, were analyzed according to previously described methods (Hopmans et al., 2006; Rush et al., 2012). Briefly, sediments were freeze-dried, homogenized, and extracted using a modified Bligh-Dyer method (Boumann et al., 2006). The extract was saponified by refluxing with aqueous 1 N KOH in 96% methanol for 1 h. The pH of the saponified extract was adjusted to 3 with 2 N HCl in methanol and the fatty acids were extracted with dichloromethane (DCM). The DCM fraction was dried using Na<sub>2</sub>SO<sub>4</sub> and the fatty acids were converted into their corresponding fatty acid methyl esters (FAMEs) by methylation with diazomethane (CH<sub>2</sub>NH<sub>2</sub>). A FAME fraction was

obtained by elution over activated aluminum oxide with DCM. Polyunsaturated fatty acids (PUFAs) were removed by elution over a small AgNO<sub>3</sub> (5%)-impregnated silica column with DCM. The resulting fraction was dissolved in acetone (1 mg/ml) and filtered through a 0.45 µm, 4 mm diameter polytetrafluoroethylene (PTFE) filter and analyzed by high performance liquid chromatography coupled to positive-ion atmospheric pressure chemical ionization tandem mass spectrometry (HPLC/APCI-MS/MS) in selected reaction monitoring (SRM) mode as described by Rush et al. (2012). Ladderane FAMEs were quantified using external calibration curves of isolated methylated ladderane fatty acid standards.

## RESULTS

### BIOGEOCHEMICAL ANALYSIS

Cold hydrocarbon-rich seep (CS) sediments were generally anoxic (Vigneron et al., 2013) and until a depth of 40 cm the temperature was constant at 3°C. As expected, ammonium was present throughout the sediment in concentrations ranging from 10–40 µM. In one core (1758-14 CT11) ammonium levels dropped below the detection limit (1 µM) at 2–3 cm, but increased again with increasing depth (**Figure 1A**). In sediments with hydrothermal activity ammonium concentrations were higher, increasing from 0.5 mM at the interface to 1.8 mM at 4 cm depth. In deeper layers, concentrations varied between 1.4 and 1.8 mM (**Figure 1A**). The temperature at the sediment-water interface was around 20°C and increased linearly to up to 100°C at 40 cm depth. Sulfide was not detected at the sediment interface in any of the samples, but increased rapidly below 1–4 cm sediment depth (**Figure 1B**). In the hydrothermal vent sediment and sediments at the edge of the white mat (1767 CT10 and 1758-14 CT11) concentrations stayed below 10 mM, whereas in sediments visibly covered by mats of sulfur oxidizers (1755-11 CT1 and 1758-14 CT1) sulfide concentrations were higher (**Figure 1B**).

Within the reference zone (REF) core, which was collected outside of the active zone, there was a small peak of ammonium at 2 cm (13 µM). Sulfide was below detection limit throughout the core. Nitrate and nitrite profiles were not available for the sampling sites.

### LADDERANE CORE LIPID ANALYSIS

To confirm the presence and abundance of anammox bacteria in Guaymas Basin sediments we used ladderane fatty acids as an additional, specific biomarker. Selected samples were analyzed for original ladderane lipids (C<sub>18</sub> and C<sub>20</sub> ladderane fatty acids) as well as ladderane oxidation products (C<sub>14</sub> ladderane fatty acids). The concentration of total ladderanes was highest in the cold hydrocarbon-rich seep sediments (up to 310 ng · g sediment<sup>-1</sup>) (**Table 2**). The relative contribution of short chain ladderane fatty acids to the total ladderane lipid pool in cold hydrocarbon-rich seep samples was 66 and 74% at the sediment-water interface (samples 1 and 12, respectively) and increased with sediment depth. The reference zone concentrations of ladderane fatty acids were 60 ng · g sediment<sup>-1</sup> of which 80% were original ladderane lipids. In both hydrothermally active sediments (samples 14 and 15) no ladderane fatty acids could be detected.

**Table 2 | Concentrations of total ladderane fatty acids in different sediment samples and the relative proportion of short chain ladderane fatty acids.**

| Sample number   | 1   | 3   | 6   | 9  | 11 | 12  | 13  | 14 | 15 | 17 |
|---|-----|-----|-----|----|----|-----|-----|----|----|----|
| Ladderane fatty acids<br>(ng · g sediment <sup>-1</sup> ) | 158 | 253 | 234 | 59 | 41 | 157 | 308 | 0  | 0  | 60 |
| % short chain<br>ladderane fatty acids                    | 74  | 84  | 86  | 86 | 45 | 66  | 75  | —  | —  | 20 |

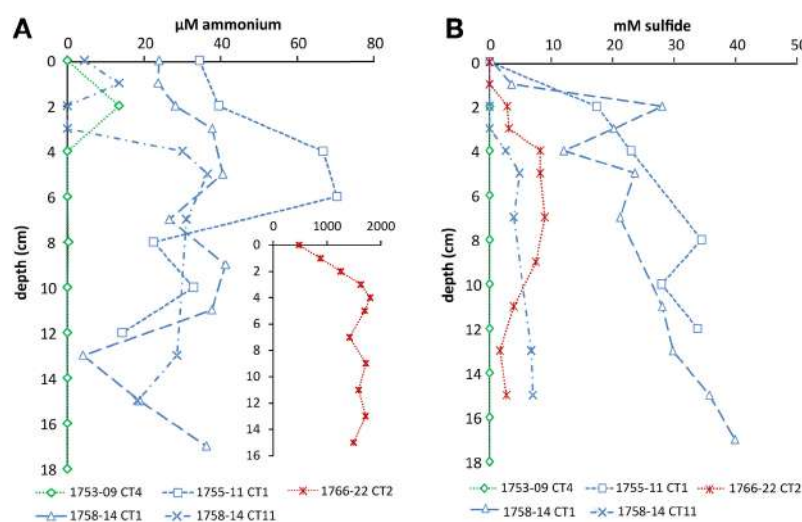


**FIGURE 1 | Depth profiles of (A) ammonium and (B) sulfide in cold seep and hydrothermal sediments.** Sediment cores of the reference zone is depicted in green, cold hydrocarbon-rich seeps in blue and

hydrothermal sites in red. Ammonium in hydrothermal sediments was higher and is therefore shown as an inset (the axes have the corresponding units).

## DIVERSITY OF THE *hzsA* GENE IN GUAYMAS BASIN SEDIMENTS

Amplifying the *hzsA* gene with two different primer sets (757F<sub>Scal</sub>/1857R and 526F/1857R) resulted in 80 clones from Guaymas Basin sediments, all of which were related to the “*Ca. Scalindua*” genus (**Figure 2**). Phylogenetic analysis revealed two distinct clusters of *hzsA* sequences (“*Ca. Scalindua*” *hzsA* cluster I and II). Sequences of cluster II were preferentially amplified using 526F/1857R as primers during amplification. The average similarity within these clusters was 91.6% for cluster I and 88.7% for cluster II. However, comparison of individual sequences revealed that between both clusters several sequences share a similarity as low as 76% at the nucleotide level. Within the “*Ca. Scalindua*” *hzsA* cluster I three subclusters could be identified: BIG I and BIG II consisted mostly of cold hydrocarbon-rich seep sequences. The third cluster consisted of sequences that were related to

the enrichment culture species *S. profunda* (van de Vossenberg et al., 2008) as well as three clones from Northeast Greenland marine sediment (Harhangi et al., 2012). The “*Ca. Scalindua*” *hzsA* cluster II was generally more diverse and composed of two subclusters. The first subcluster containing one sequence from Barents Sea sediment and mostly sequences associated with cold hydrocarbon-rich seeps. The second cluster contained several clones retrieved from the Barents Sea (Harhangi et al., 2012), clones from the Ogasawara Trench in the West Pacific (Nunoura et al., 2013) and clones from cold hydrocarbon-rich seeps, vents and reference zone samples. Generally there seems to be no great correlation between the sample locations and the diversity of anammox bacteria as clones retrieved from cold hydrocarbon-rich seep, reference zone and hydrothermal sediments were found in all clusters.

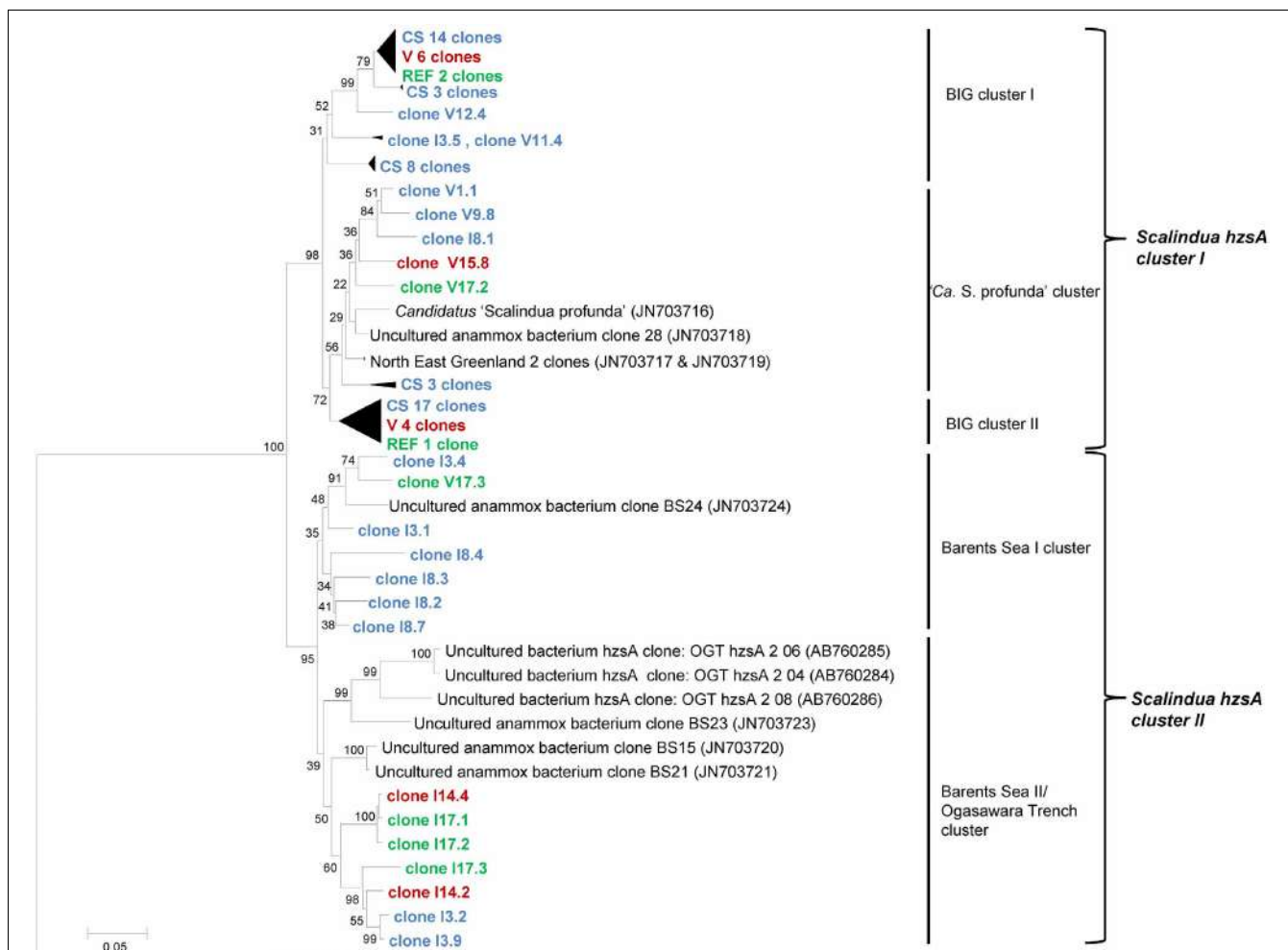


**FIGURE 2 |** Neighbor-joining tree of phylogeny estimated by ClustalW included in the MEGA 5.0 software package, showing >1000 bp fragments of *hzsA* nucleotide sequences retrieved from the Guaymas Basin sediments. Letters (I or V) of the samples indicate the primer set used for amplification and the number refers to the sample. Samples are color-coded and at collapsed nodes abbreviated: reference zone in green

(REF), cold hydrocarbon-rich seeps in blue (CS) and hydrothermal sites in red (V). Values at the internal nodes indicate bootstrap values based on 500 iterations. The bar indicates 5% sequence divergence. The outgroup with other anammox bacteria includes Genbank accession numbers JN703715, JN703714, JN703713, JN703712, AB365070 and CT573071. Accession numbers of individual clones are provided in Supplementary Table 1.

## QUANTIFICATION OF ANAMMOX BACTERIA BY FUNCTIONAL GENE AMPLIFICATION

Based on the *hzsA* biodiversity study (see above) which showed only representatives of the “*Ca. Scalindua*” genus, we determined absolute numbers of anammox bacteria in the sediment samples by amplification of a “*Ca. Scalindua*”-specific 257 bp fragment of the *hzsA* gene in a qPCR assay. The results indicated that numbers of anammox bacteria were generally higher in cold hydrocarbon-rich seep environments compared to the vents (**Figure 3**).

Gene copy numbers of anammox *hzsA* in cold hydrocarbon-rich seep sediments varied between  $1.5 \times 10^6$  to  $1.5 \times 10^7$  copies per gram of sediment. The total number of *hzsA* gene copies was usually highest at the sediment interface and decreased with increasing depth (**Figure 3**, 9/10, 12/13, 15/16). The exception was a whole sediment core (**Figure 3**, 1–7) (0–21 cm), which was analyzed in increments of 3 cm. Here, *hzsA* gene copies increased linearly from the interface peaking at 6–9 cm sediment depth ( $1.47 \times 10^7$  copies · g sediment $^{-1}$ ). In proximity of the hydrothermal vents total numbers of the *hzsA* gene in the sediments were much lower ( $1.9 \times 10^5$  to  $1.3 \times 10^6$  copies · g sediment $^{-1}$ ).

## DIVERSITY OF THE *aprA* GENE

An *aprA* library comprising 39 sequences was generated from selected cold hydrocarbon-rich seep sediments (samples 1, 3, and 9) and the sediment interface of the vents MegaMat M27 (sample 15). The majority of all sequences were affiliated with the *Gamma proteobacteria* (35 sequences), clustering in both *apr* lineages of known sulfur oxidizing bacteria (SOB) (Meyer and Kuever, 2007). Sequences from lineage I were divided into 2 clusters (**Figure 4**). The first cluster consisting of 4 cold hydrocarbon-rich seep clones and 5 from hydrothermal vent sediments were most closely related to gut microflora clones of *Asterechinus*

*elegans* (93%) and endosymbionts of *Olavius ilvae* (86–89%) (Ruehland et al., 2008; Becker et al., 2009). The second cluster was comprised of 11 cold hydrocarbon-rich seep clones and 3 vent clones showing the highest similarity to clones retrieved from hydrothermal vents of the Logatchev field (87–89%) and low temperature hydrothermal oxides at South West Indian ridge (90%) (Hügler et al., 2010). One clone was retrieved within lineage I being most closely related with the uncultured alphaproteobacterial *aprA* genes. The closest hit was a clone retrieved from carbonate sediments at the South West Indian Ridge (88%). Within SOB *apr* lineage II 9 sequences (7 CS and 2 V) grouped within a cluster of endosymbionts and uncultured bacteria of deep-sea environments. Closest hits were obtained with marine sediment clones of the Cascadia margin (94%), gut microflora clones of *Asterechinus elegans* (92%) and endosymbionts of *Riftia pachyptila* (86%) (Meyer and Kuever, 2007; Becker et al., 2009; Blazejak and Schippers, 2011; Brissac et al., 2011; Lenk et al., 2011). Two clones from vent sediments formed a separate cluster in *apr* lineage I, showing a rather low similarity to previously described clones (gut microflora clones of *Asterechinus elegans* 81%). Three of the *aprA* sequences clustered with sulfate-reducing *Delta proteobacteria* of the *Desulfovibrio* and *Desulfobulbus* genus and a single sequence was most closely related with the firmicutes (*Desulfotomaculum* sp. 78%) (Friedrich, 2002; Hügler et al., 2010).

## DISCUSSION

Almost all samples from the cold hydrocarbon-rich seep sediment core that were investigated contained a high relative abundance of short chain ladderane fatty acids (>65%). This high percentage may be explained by degradation of original ladderanes during diagenesis (Rush et al., 2012). Little is known about the biological degradation of ladderanes yet, but it is assumed that it proceeds via the  $\beta$ -oxidation pathway (Beam and Perry, 1974;

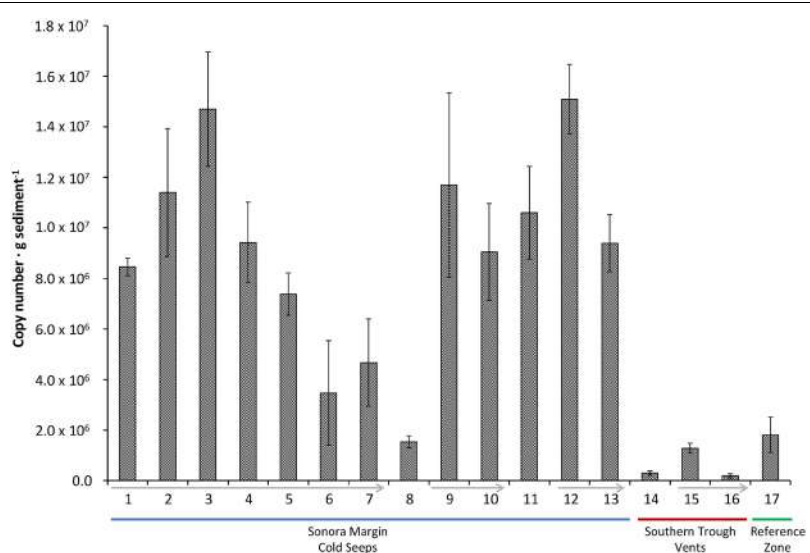
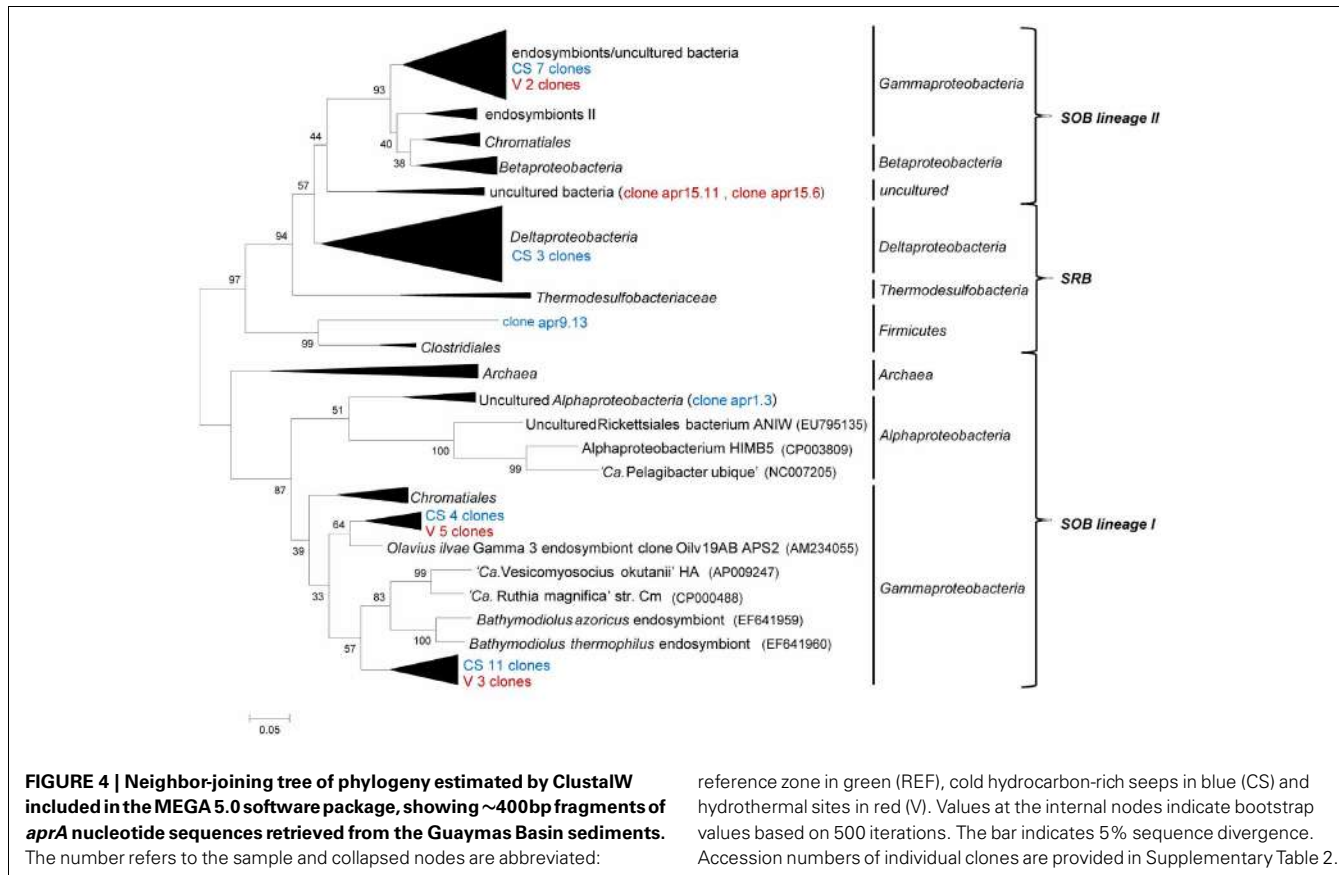


**FIGURE 3 |** *hzsA* copy number in different sediment samples ( $\pm SD$  of technical replicates). Sediment cores of the reference zone is depicted in green, cold hydrocarbon-rich seeps in blue and hydrothermal sites in red. Arrows indicate decreasing sediment depth within a single core.



Dutta and Harayama, 2001). Although the sediments were virtually anoxic, the degradation of original ladderane fatty acids could be the result of periodic exposure to low amounts of oxygen in such a dynamic system. When the concentrations of short and original ladderane fatty acids were compared, a slight increase of original ladderanes and an increase in short chain ladderanes with depth was observed, which corresponded to the acquired qPCR data of core 1758-14 CT2 (Figure 5). This would suggest that on the one hand there was ongoing conversion from long chain fatty acids to the short chain ladderanes in the absence of oxygen, but also that the overall concentration of original ladderanes was higher deeper in the sediment at this specific location. This could be the result of seasonal high burial of anammox biomass and a high ladderane turnover or the *in situ* production of ladderanes in deeper sediment layers. In hydrothermally active sediments no ladderanes could be detected. This could be because ladderanes were unstable at higher temperatures due to their peculiar chemical structure (Jaeschke et al., 2008).

The use of two different primer sets to amplify *hzsA* gene fragments resulted in the retrieval of marine *hzsA* sequences showing a diversity comparable to that reported for 16S rRNA genes of anammox bacteria (Woebken et al., 2008). The functional gene analysis hinted at the high diversity within the “*Ca. Scalindua*” genus, considering that some genera of fresh water anammox shared a higher similarity (*Ca. Jettenia asiatica* and *Ca. Brocadia anammoxidans* 79.4%). This was a first indication using a functional gene that the marine group might consist of more than one

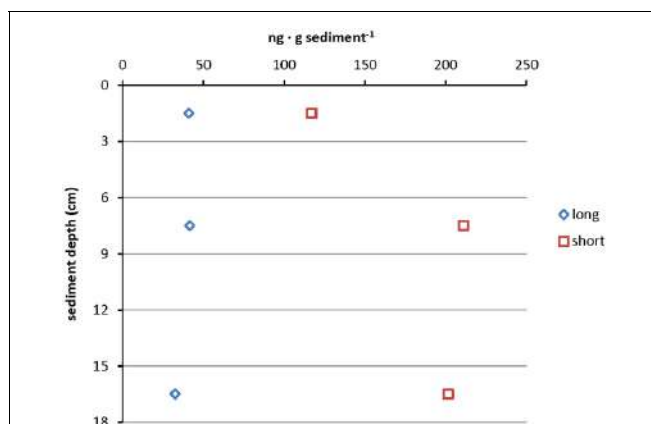


**FIGURE 5 | Depth profile of absolute ladderane lipid concentrations in core 1758-14 CT2 including original ladderanes and short chain ladderane fatty acids.** Data points represent measurements on the sediment sample pooled from 0 to 3 cm, 6 to 9 cm, and 15 to 18 cm sediment depth.

genus or at least showed a very high interspecies diversity within a single genus.

The finding of anammox specific phylomarkers within these sediments was surprising, as the deep sea sediments of the Guaymas Basin were not only rich in organic matter, ammonium and methane, but also contained mM concentrations of

sulfide. Sulfide has been reported to inhibit the anammox process in granular sludge of wastewater treatment plants already at low concentrations (Carvajal-Arroyo et al., 2013; Jin et al., 2013). Although no conclusion can be made with regard to anammox activity in the Guaymas Basin sediments, the results point to the same direction as the highest number of *hzsA* copy numbers usually coincided with the absence of sulfide at the sediment interface and decreased rapidly with depth.

Aerobic ammonium oxidizing Thaumarchaeota were shown to play a role in supplying nitrite for anammox in oxygen minimum zones (OMZ) (Francis et al., 2005; Lam et al., 2009), but in these systems also a cryptic sulfur cycle was reported (Canfield et al., 2010). Since for continental shelf sediments and the Benguela OMZ denitrification was suggested to play a role in nitrite supply (Thamdrup and Dalsgaard, 2002; Kuypers et al., 2005) and the sites of our study are all sulfidic in nature we focused on the possibility of sulfide-driven partial denitrification. Reduced sulfur compounds, such as sulfide, fuel primary production in cold hydrocarbon-rich seeps and are often linked to oxygen and nitrate respiration (Jannasch and Wirsén, 1979; Karl et al., 1980; Lütschlag et al., 2010). The amplification of a key gene in sulfur oxidation revealed a high number of gammaproteobacterial *aprA* genes covering the two SOB *aprA* lineages as well as sulfate-reducers. Previously also *Epsilonproteobacteria* were shown to be abundant in Guaymas Basin sediments likely also gaining energy from growth on sulfide as an electron donor to reduce nitrate (Teske et al., 2002; Bowles et al., 2012). This suggested that reduced sulfur compounds could serve as a link between sulfur and nitrogen cycling in such ecosystems. Although there was no direct evidence for the significance of *Gammaproteobacteria* in sulfur oxidation in the Guaymas Basin sediments the retrieval of such an *aprA* diversity confirmed findings of *Gammaproteobacteria* playing a role in linking the sulfur and nitrogen cycles in marine sediments by coupling sulfide oxidation to nitrate reduction (Mills et al., 2004; Hügler et al., 2010; Lenk et al., 2011). This could have very interesting implications with respect to the formation of

complex interactions that would be driven by the exchange of intermediates (i.e., nitrite). For example, partial denitrification (Błaszczyk, 1992, unpublished data) coupled to sulfide oxidation could supply anammox bacteria with nitrite. Additionally, the oxidation of sulfide might create pockets in which the concentration of free sulfide is low enough so that anammox bacteria remain active. The existence of such an interaction was recently reported (Wenk et al., 2013), but whether this could occur in the sediments or the water column of the Guaymas Basin remains to be determined.

## CONCLUSION

This study shows that anammox bacteria were detected in complex and exotic environments by amplification of the unique functional marker gene *hzsA*, allowing much more specificity than 16S rRNA gene based analysis. The high diversity observed in *hzsA* phylogeny suggested a high interspecies variety within the marine anammox cluster in an essential and highly-conserved gene. Although evidence so far did not favor anammox bacteria in sulfidic sediments (Burgin and Hamilton, 2007) we detected relatively high numbers of anammox gene copies in cold hydrocarbon-rich seep sediments of the Guaymas Basin.

## ACKNOWLEDGMENTS

We would like to thank M LeRoy and the crews of the research vessel L'Atalante and the submersible Nautile of the cruise "BIG" and the scientific team for retrieval of the samples. The cruise was funded by IFREMER (France) and has benefited from a work permit in Mexican waters (DAPA/2/281009/3803, October 28th, 2009). This study was supported by grant 232937 from the European Research Council. B.K. is supported by a Netherlands Organization for Scientific Research grant (VENI 863.11.003).

## SUPPLEMENTARY MATERIAL

The Supplementary Material for this article can be found online at: [http://www.frontiersin.org/Extreme\\_Microbiology/10.3389/fmcb.2013.00219/abstract](http://www.frontiersin.org/Extreme_Microbiology/10.3389/fmcb.2013.00219/abstract)

## REFERENCES

- Bazylinski, D. A., Farrington, J. W., and Jannasch, H. W. (1988). Hydrocarbons in surface sediments from a Guaymas Basin hydrothermal vent site. *Org. Geochem.* 12, 547–558. doi: 10.1016/0146-6380(88)90146-5
- Beam, H. W., and Perry, J. J. (1974). Microbial degradation and assimilation of n-alkyl-substituted cycloparaffins. *J. Bacteriol.* 118, 394–399.
- Becker, P. T., Samadi, S., Zbinden, M., Hoyoux, C., Compère, P., and De Ridder, C. (2009). First insights into the gut microflora associated with an echinoid from wood falls environments. *Cah. Biol. Mar.* 50, 343–352.
- Błaszczyk, M. (1992). Comparison of denitrification by *Paracoccus* *denitrificans*, *Pseudomonas stutzeri* and *Pseudomonas aeruginosa*. *Acta Microbiol. Pol.* 41, 203–210.
- Blazeják, A., and Schippers, A. (2011). Real-time PCR quantification and diversity analysis of the functional genes *aprA* and *dsrA* of sulfate-reducing prokaryotes in marine sediments of the Peru continental margin and the Black Sea. *Front. Microbiol.* 2:253. doi: 10.3389/fmcb.2011.00253
- Borin, S., Mapelli, F., Rolli, E., Song, B., Tobias, C., Schmid, M. C., et al. (2013). Anammox bacterial populations in deep marine hypersaline gradient systems. *Extremophiles* 17, 289–299. doi: 10.1007/s00792-013-0516-x
- Boumann, H. A., Hopmans, E. C., van de Leemput, I., Op den Camp, H. J. M., van de Vossenberg, J., Strous, M., et al. (2006). Ladderane phospholipids in anammox bacteria comprise phosphocholine and phosphoethanolamine head-groups. *FEMS Microbiol. Lett.* 258, 297–304. doi: 10.1111/j.1574-6941.2010.00989.x
- Bowles, M., and Joye, S. (2010). High rates of denitrification and nitrate removal in cold seep sediments. *ISME J.* 5, 565–567. doi: 10.1038/ismej.2010.134
- Bowles, M., Nigro, L., Teske, A., and Joye, S. (2012). Denitrification and environmental factors influencing nitrate removal in Guaymas Basin hydrothermally altered sediments. *Front. Microbiol.* 3:377. doi: 10.3389/fmcb.2012.00377
- Brissac, T., Mercot, H., and Gros, O. (2011). Lucinidae/sulfur-oxidizing bacteria: ancestral heritage or opportunistic association? Further insights from the Bohol Sea (the Philippines). *FEMS Microbiol. Ecol.* 75, 63–76. doi: 10.1111/j.1574-6941.2010.00989.x
- Burgin, A. J., and Hamilton, S. K. (2007). Have we overemphasized the role of denitrification in aquatic ecosystems? A review of nitrate removal pathways. *Front. Ecol. Environ.* 5:89–96. doi: 10.1890/1540-9295(2007)5[89:HWOTRO]2.0.CO2
- Byrne, N., Strous, M., Crepeau, V., Kartal, B., Birrien, J.-L., Schmid, M., et al. (2008). Presence and activity of anaerobic ammonium-oxidizing bacteria at deep-sea hydrothermal vents. *ISME J.* 3, 117–123. doi: 10.1038/ismej.2008.72
- Calvert, S. E. (1966). Origin of diatom-rich, varved sediments from the

- Gulf of California. *J. Geol.* 74, 546–565. doi: 10.1086/627188
- Canfield, D. E., Stewart, F. J., Thamdrup, B., De Brabandere, L., Dalsgaard, T., De Long, E. F., et al. (2010). A cryptic sulfur cycle in oxygen-minimum-zone waters off the Chilean coast. *Science* 330, 1375–1378. doi: 10.1126/science.1196889
- Carvajal-Arroyo, J. M., Sun, W., Sierra-Alvarez, R., and Field, J. A. (2013). Inhibition of anaerobic ammonium oxidizing (anammox) enrichment cultures by substrates, metabolites and common wastewater constituents. *Chemosphere* 91, 22–27. doi: 10.1016/j.chemosphere.2012.11.025
- Dutta, T. K., and Harayama, S. (2001). Biodegradation of n-alkylcycloalkanes and n-alkylbenzenes via new pathways in Alcanivorax sp. strain MBIC 4326. *Appl. Environ. Microbiol.* 67, 1970–1974. doi: 10.1128/AEM.67.4.1970-1974.2001
- Fonselius, S., Dyrssen, D., and Yhlen, B. (2007). *Methods of Seawater Analysis*. Weinheim: Wiley-VCH Verlag GmbH.
- Francis, C. A., Roberts, K. J., Beman, J. M., Santoro, A. E., and Oakley, B. B. (2005). Ubiquity and diversity of ammonia-oxidizing archaea in water columns and sediments of the ocean. *Proc. Natl. Acad. Sci. U.S.A.* 102, 14683–14688. doi: 10.1073/pnas.0506625102
- Friedrich, M. W. (2002). Phylogenetic analysis reveals multiple lateral transfers of adenosine-5'-phosphosulfate reductase genes among sulfate-reducing microorganisms. *J. Bacteriol.* 184, 278–289. doi: 10.1128/JB.184.1.278-289.2002
- Frigaard, N.-U., and Dahl, C. (2009). Sulfur metabolism in phototrophic sulfur bacteria. *Adv. Microb. Physiol.* 54, 103–200. doi: 10.1016/S0065-2911(08)0002-7
- Harhangi, H. R., Le Roy, M., van Aken, T., Hu, B.-L., Groen, J., Kartal, B., et al. (2012). Hydrazine synthase, a unique phylogenarker with which to study the presence and biodiversity of anammox bacteria. *Appl. Environ. Microbiol.* 78, 752–758. doi: 10.1128/AEM.07113-11
- Holmes, R. M., Aminot, A., Kérroué, R., Hooker, B. A., and Peterson, B. J. (1999). A simple and precise method for measuring ammonium in marine and freshwater ecosystems. *Can. J. Fish. Aquat. Sci.* 56, 1801–1808. doi: 10.1139/cjfas-56-10-1801
- Hong, Y.-G., Yin, B., and Zheng, T.-L. (2011). Diversity and abundance of anammox bacterial community in the deep-ocean surface sediment from equatorial Pacific. *Appl. Microbiol. Biotechnol.* 89, 1233–1241. doi: 10.1007/s00253-010-2925-4
- Hopmans, E. C., Kienhuis, M. V. M., Ratray, J. E., Jaeschke, A., Schouten, S., and Damsté, J. S. S. (2006). Improved analysis of ladderane lipids in biomass and sediments using high-performance liquid chromatography/atmospheric pressure chemical ionization tandem mass spectrometry. *Rapid Commun. Mass Spectrom.* 20, 2099–2103. doi: 10.1002/rcm.2572
- Hügler, M., Gärtner, A., and Imhoff, J. F. (2010). Functional genes as markers for sulfur cycling and CO<sub>2</sub> fixation in microbial communities of hydrothermal vents of the Logatchev field. *FEMS Microbiol. Ecol.* 73, 526–537.
- Jaeschke, A., Abbas, B., Zabel, M., Hopmans, E. C., Schouten, S., and Sinninghe Damsté, J. S. (2010). Molecular evidence for anaerobic ammonium-oxidizing (anammox) bacteria in continental shelf and slope sediments off northwest Africa. *Limnol. Oceanogr.* 55, 365.
- Jaeschke, A., Lewan, M. D., Hopmans, E. C., Schouten, S., and Sinninghe Damsté, J. S. (2008). Thermal stability of ladderane lipids as determined by hydrous pyrolysis. *Org. Geochem.* 39, 1735–1741. doi: 10.1016/j.orggeochem.2008.08.006
- Jaeschke, A., Op den Camp, H. J., Harhangi, H., Klimiuk, A., Hopmans, E. C., Jetten, M. S., et al. (2009). 16S rRNA gene and lipid biomarker evidence for anaerobic ammonium-oxidizing bacteria (anammox) in California and Nevada hot springs. *FEMS Microbiol. Ecol.* 67, 343–350. doi: 10.1111/j.1574-6941.2008.00640.x
- Jannasch, H. W., Nelson, D. C., and Wirsén, C. O. (1989). Massive natural occurrence of unusually large bacteria (*Beggiatoa* sp.) at a hydrothermal deep-sea vent site. *Nature* 342, 834–836. doi: 10.1038/342834a0
- Jannasch, H. W., and Wirsén, C. O. (1979). Chemosynthetic primary production at East Pacific sea floor spreading centers. *Bioscience* 29, 592–598. doi: 10.2307/1307765
- Jensen, M. M., Kuypers, M. M., Lavik, G., and Thamdrup, B. (2008). Rates and regulation of anaerobic ammonium oxidation and denitrification in the Black Sea. *Limnol. Oceanogr.* 53, 23–36.
- Jin, R.-C., Yang, G.-F., Zhang, Q.-Q., Ma, C., Yu, J.-J., and Xing, B.-S. (2013). The effect of sulfide inhibition on the ANAMMOX process. *Water Res.* 47, 1459–1469. doi: 10.1016/j.watres.2012.12.018
- Karl, D., Wirsén, C., and Jannasch, H. (1980). Deep-sea primary production at the Galapagos hydrothermal vents. *Science* 207, 1345–1347. doi: 10.1126/science.207.4437.1345
- Kawka, O. E., and Simoneit, B. R. (1987). Survey of hydrothermally-generated petroleums from the Guaymas Basin spreading center. *Org. Geochem.* 11, 311–328. doi: 10.1016/0146-6380(87)90042-8
- Kuypers, M. M., Lavik, G., Woebken, D., Schmid, M., Fuchs, B., Amann, R., et al. (2005). Massive nitrogen loss from the Benguela upwelling system through anaerobic ammonium oxidation. *Proc. Natl. Acad. Sci. U.S.A.* 102, 6478–6483. doi: 10.1073/pnas.0502088102
- Kuypers, M. M., Slikkers, A., Lavik, G., Schmid, M., Jørgensen, B., Kuennen, J., et al. (2003). Anaerobic ammonium oxidation by anammox bacteria in the Black Sea. *Nature* 422, 608–611. doi: 10.1038/nature01472
- Lam, P., Lavik, G., Jensen, M., van de Vossenberg, J., Schmid, M., Woebken, D., et al. (2009). Revising the nitrogen cycle in the Peruvian oxygen minimum zone. *Proc. Natl. Acad. Sci. U.S.A.* 106, 4752–4757. doi: 10.1073/pnas.0812444106
- Lenk, S., Arndt, J., Zerjatke, K., Musat, N., Amann, R., and Mußmann, M. (2011). Novel groups of *Gammaproteobacteria* catalyse sulfur oxidation and carbon fixation in a coastal, intertidal sediment. *Environ. Microbiol.* 13, 758–774. doi: 10.1111/j.1462-2920.2010.02380.x
- Li, H., Chen, S., Mu, B.-Z., and Gu, J.-D. (2010). Molecular detection of anaerobic ammonium-oxidizing (anammox) bacteria in high-temperature petroleum reservoirs. *Microb. Ecol.* 60, 771–783. doi: 10.1007/s00248-010-9733-3
- Lichtschlag, A., Felden, J., Brücher, V., Boetius, A., and De Beer, D. (2010). Geochemical processes and chemosynthetic primary production in different thiotrophic mats of the Håkon Mosby Mud Volcano (Barents Sea). *Limnol. Oceanogr.* 55.
- McHatton, S. C., Barry, J. P., Jannasch, H. W., and Nelson, D. C. (1996). High nitrate concentrations in vacuolate, autotrophic marine *Beggiatoa* spp. *Appl. Environ. Microbiol.* 62, 954–958.
- Meyer, B., and Kuever, J. (2007). Molecular analysis of the diversity of sulfate-reducing and sulfur-oxidizing prokaryotes in the environment, using *aprA* as functional marker gene. *Appl. Environ. Microbiol.* 73, 7664–7679. doi: 10.1128/AEM.01272-07
- Mills, H. J., Martinez, R. J., Story, S., and Sobecky, P. A. (2004). Identification of members of the metabolically active microbial populations associated with *Beggiatoa* species mat communities from Gulf of Mexico cold-seep sediments. *Appl. Environ. Microbiol.* 70, 5447–5458. doi: 10.1128/AEM.70.9.5447-5458.2004
- Nelson, D. C., Wirsén, C. O., and Jannasch, H. W. (1989). Characterization of large, autotrophic *Beggiatoa* spp. abundant at hydrothermal vents of the Guaymas Basin. *Appl. Environ. Microbiol.* 55, 2909–2917.
- Nunoura, T., Nishizawa, M., Kikuchi, T., Tsubouchi, T., Hirai, M., Koide, O., et al. (2013). Molecular biological and isotopic biogeochemical prognoses of the nitrification-driven dynamic microbial nitrogen cycle in hadopelagic sediments. *Environ. Microbiol.* doi: 10.1111/1462-2920.12152. [Epub ahead of print].
- Ruehland, C., Blazejak, A., Lott, C., Loy, A., Erséus, C., and Dubilier, N. (2008). Multiple bacterial symbionts in two species of co-occurring gutless oligochaete worms from Mediterranean sea grass sediments. *Environ. Microbiol.* 10, 3404–3416. doi: 10.1111/j.1462-2920.2008.01728.x
- Rush, D., Hopmans, E. C., Wakeham, S. G., Schouten, S., and Sinninghe Damsté, J. S. (2012). Occurrence and distribution of ladderane oxidation products in different oceanic regimes. *Biogeosciences* 9, 2407–2418. doi: 10.5194/bg-9-2407-2012
- Seeberg-Elverfeldt, J., Schlüter, M., Feseker, T., and Kölling, M. (2005). Rhizon sampling of pore waters near the sediment/water interface of aquatic systems. *Limnol. Oceanogr. Methods* 3, 361–371. doi: 10.4319/lom.2005.3.361
- Sinninghe Damsté, J. S., Rijpstra, W. I. C., Geenevasen, J. A., Strous, M., and Jetten, M. S. (2005). Structural identification of ladderane and other membrane lipids of planctomycetes capable of anaerobic ammonium oxidation (anammox). *FEBS J.* 272, 4270–4283. doi: 10.1111/j.1742-4658.2005.04842.x
- Sinninghe Damsté, J. S., Strous, M., Rijpstra, W. I. C., Hopmans, E. C., Geenevasen, J. A., van Duin, A. C., et al. (2002). Linearly concatenated cyclobutane lipids form a dense

- bacterial membrane. *Nature*. 419, 708–712. doi: 10.1038/nature01128
- Tamura, K., Peterson, D., Peterson, N., Stecher, G., Nei, M., and Kumar, S. (2011). MEGA5: molecular evolutionary genetics analysis using maximum likelihood, evolutionary distance, and maximum parsimony methods. *Mol. Biol. Evol.* 28, 2731–2739. doi: 10.1093/molbev/msr121
- Teske, A., Hinrichs, K.-U., Edgcomb, V., de Vera Gomez, A., Kysela, D., Sylva, S. P., et al. (2002). Microbial diversity of hydrothermal sediments in the Guaymas Basin: evidence for anaerobic methanotrophic communities. *Appl. Environ. Microbiol.* 68, 1994–2007. doi: 10.1128/AEM.68.4.1994-2007.2002
- Thamdrup, B., and Dalsgaard, T. (2002). Production of N<sub>2</sub> through anaerobic ammonium oxidation coupled to nitrate reduction in marine sediments. *Appl. Environ. Microbiol.* 68, 1312–1318. doi: 10.1128/AEM.68.3.1312-1318.2002
- Trimmer, M., Nicholls, J., and Deflandre, B. (2003). Anaerobic ammonium oxidation measured in sediments along the Thames estuary, United Kingdom. *Appl. Environ. Microbiol.* 69, 6447–6454.
- doi: 10.1128/AEM.69.11.6447-6454.2003
- van de Vossenberg, J., Ratray, J. E., Geerts, W., Kartal, B., van Niftrik, L., van Donselaar, E. G., et al. (2008). Enrichment and characterization of marine anammox bacteria associated with global nitrogen gas production. *Environ. Microbiol.* 10, 3120–3129. doi: 10.1111/j.1462-2920.2008.01643.x
- van de Vossenberg, J., Woebken, D., Maalcke, W. J., Wessels, H. J. C. T., Dutilh, B. E., Kartal, B., et al. (2013). The metagenome of the marine anammox bacterium ‘Candidatus Scalindua profunda’ illustrates the versatility of this globally important nitrogen cycle bacterium. *Environ. Microbiol.* 15, 1275–1289. doi: 10.1111/j.1462-2920.2012.02774.x
- Vigneron, A., Cruaud, P., Pignet, P., Caprais, J.-C., Cambon-Bonavita, M.-A., Godfroy, A., et al. (2013). Archaeal and anaerobic methane oxidizer communities in the Sonora Margin cold seeps, Guaymas Basin (Gulf of California). *ISME J.* doi: 10.1038/ismej.2013.18. [Epub ahead of print].
- Von Damm, K. L. (1990). Seafloor hydrothermal activity: black smoker chemistry and chimneys. *Annu. Rev. Earth Planet. Sci.* 18, 173–204. doi: 10.1146/annurev.ea.18.050190.001133
- Von Damm, K. L., Edmond, J. M., Measures, C. I., and Grant, B. (1985). Chemistry of submarine hydrothermal solutions at Guaymas Basin, Gulf of California. *Geochim. Cosmochim. Acta* 49, 2221–2237. doi: 10.1016/0016-7037(85)90223-6
- Wenk, C. B., Blees, J., Zopfi, J., Veronesi, M., Bourbonnais, A., Schubert, C. J., et al. (2013). Anaerobic ammonium oxidation (anammox) bacteria and sulfide-dependent denitrifiers coexist in the water column of a meromictic south-alpine lake. *Limnol. Oceanogr.* 58, 1–12.
- Woebken, D., Lam, P., Kuypers, M. M. M., Naqvi, S. W. A., Kartal, B., Strous, M., et al. (2008). A microdiversity study of anammox bacteria reveals a novel ‘Candidatus Scalindua’ phylotype in marine oxygen minimum zones. *Environ. Microbiol.* 10, 3106–3119. doi: 10.1111/j.1462-2920.2008.01640.x
- Conflict of Interest Statement:** The authors declare that the research was conducted in the absence of any commercial or financial relationships that could be construed as a potential conflict of interest.
- Received: 08 April 2013; accepted: 12 July 2013; published online: 02 August 2013.*
- Citation: Russ L, Kartal B, op den Camp HJM, Sollai M, Le Bruchec J, Caprais J-C, Godfroy A, Sinninghe Damsté JS and Jetten MSM (2013) Presence and diversity of anammox bacteria in cold hydrocarbon-rich seeps and hydrothermal vent sediments of the Guaymas Basin. *Front. Microbiol.* 4:219. doi: 10.3389/fmicb.2013.00219*
- This article was submitted to Frontiers in Extreme Microbiology, a specialty of Frontiers in Microbiology.*
- Copyright © 2013 Russ, Kartal, op den Camp, Sollai, Le Bruchec, Caprais, Godfroy, Sinninghe Damsté and Jetten. This is an open-access article distributed under the terms of the Creative Commons Attribution License (CC BY).*
- The use, distribution or reproduction in other forums is permitted, provided the original author(s) or licensor are credited and that the original publication in this journal is cited, in accordance with accepted academic practice. No use, distribution or reproduction is permitted which does not comply with these terms.*



# Metagenomic insights into the dominant Fe(II) oxidizing *Zetaproteobacteria* from an iron mat at Lō'ihi, Hawai'i

Esther Singer<sup>1</sup>, John F. Heidelberg<sup>2</sup>, Ashita Dhillon<sup>3</sup> and Katrina J. Edwards<sup>1,2\*</sup>

<sup>1</sup> Department of Earth Sciences, University of Southern California, Los Angeles, CA, USA

<sup>2</sup> Department of Biological Sciences, University of Southern California, Los Angeles, CA, USA

<sup>3</sup> Genzyme Corporation, Allston, MA, USA

**Edited by:**

Andreas Teske, University of North Carolina at Chapel Hill, USA

**Reviewed by:**

Craig L. Moyer, Western Washington University, USA

Runar Stokke, University of Bergen, Norway

**\*Correspondence:**

Katrina J. Edwards, Department of Biological Sciences, University of Southern California, 3616 Trousdale Parkway, Los Angeles, CA 90089, USA.

e-mail: kje@usc.edu

*Zetaproteobacteria* are among the most prevalent Fe(II)-oxidizing bacteria (FeOB) at deep-sea hydrothermal vents; however, knowledge about their environmental significance is limited. We provide metagenomic insights into an iron mat at the Lō'ihi Seamount, Hawai'i, revealing novel genomic information of locally dominant *Zetaproteobacteria* lineages. These lineages were previously estimated to account for ~13% of all local *Zetaproteobacteria* based on 16S clone library data. Biogeochemically relevant genes include nitrite reductases, which were previously not identified in *Zetaproteobacteria*, sulfide:quinone oxidases, and ribulose-1,5-bisphosphate carboxylase (RuBisCo). Genes assumed to be involved in Fe(II) oxidation correlate in synteny and share 87% amino acid similarity with those previously identified in the related *Zetaproteobacterium Mariprofundus ferrooxydans* PV-1. Overall, *Zetaproteobacteria* genes appear to originate primarily from within the *Proteobacteria* and the Fe(II)-oxidizing *Leptospirillum* spp. and are predicted to facilitate adaptation to a deep-sea hydrothermal vent environment in addition to microaerophilic Fe(II) and H<sub>2</sub>S oxidation. This dataset represents the first metagenomic study of FeOB from an iron oxide mat at a deep-sea hydrothermal habitat.

**Keywords:** iron oxidation, Lō'ihi Seamount, molybdopterin oxidoreductase, Rubisco, *Zetaproteobacteria*, hydrothermal vents, sulfide oxidation

## INTRODUCTION

Microbial Fe(II) oxidation is widespread in the deep-sea and is thought to play a significant role in rock and mineral weathering (Edwards et al., 2004). The microbial influence on the global iron cycle, and consequently on other linked biogeochemical cycles, such as carbon, has remained poorly understood, although several studies have recently started to investigate key habitats with large potential to host Fe(II)-oxidizing bacteria (FeOB; Edwards et al., 2003, 2004; Rassa et al., 2009; Emerson and Moyer, 2010; Emerson, 2012). Among these habitats are 125,000 seamounts worldwide, which often host extensive hydrothermal vent systems and Fe-rich mats of microbial origin (Wessel et al., 2010; McAllister et al., 2011).

Compared to the most commonly studied marine hydrothermal systems, located at mid-ocean ridge (MOR) spreading centers, the Lō'ihi Seamount hydrothermal system has unique fluid chemistries. For example, vent fluids at Lō'ihi are highly enriched in CO<sub>2</sub>, CH<sub>4</sub>, NH<sub>4</sub>, PO<sub>4</sub>, Fe, and Mn, but depleted in H<sub>2</sub>S (Karl et al., 1988; Sedwick et al., 1992; Wheat et al., 2000; Edwards et al., 2004; Glazer and Rouxel, 2009). The high concentration of dissolved CO<sub>2</sub> buffers the hydrothermal fluids at a lower pH (5.3–5.5) compared to what is most commonly observed at MOR systems (Sedwick et al., 1992; Edwards et al., 2004). The low sulfide concentration results in high hydrothermal Fe concentrations and extensive iron oxide mats by comparison to many MOR systems, where Fe predominately occurs as FeS instead. The summit of Lō'ihi intersects the Oxygen Minimum Zone (OMZ). The low O<sub>2</sub> concentration in bottom seawater at ~1,000 m depth (O<sub>2</sub>

~50 μM) associated with this OMZ and the high Fe concentrations (up to 500 μM) in warm hydrothermal fluids (below 100°C) present beneficial conditions for FeOB, who have to compete with the abiotic oxidation of Fe (Glazer and Rouxel, 2009).

The Lō'ihi Seamount supports abundant FeOB, and is dominated by Fe(II)-oxidizing *Zetaproteobacteria*, as shown in various studies (Emerson and Moyer, 2002; Rassa et al., 2009). The isolation of the first *Zetaproteobacterium Mariprofundus ferrooxydans* PV-1 from an iron mat at a cool (23°C) diffuse vent site at the Lō'ihi Seamount, has initiated evaluation of the ecological significance of this class in biocorrosion (Emerson et al., 2007; Weiss et al., 2007; Singer et al., 2011). Since then *Zetaproteobacteria* have been predominantly found in diverse marine environments and their involvement in microbially mediated Fe(II) oxidation is widely accepted (Handley et al., 2010; Dang et al., 2011; Meyer-Dombard et al., 2012). Continued discoveries of *Zetaproteobacteria* in marine Fe(II) oxidizing niches raise the question whether *Zetaproteobacteria* could be the dominant marine FeOB. However, cultivation of these FeOB present various difficulties to date. Molecular and functional assays to study the biogeochemistry and ecology of Fe(II) oxidation, the molecular mechanism of Fe(II) oxidation, and the cultivation of environmentally representative groups of *Zetaproteobacteria* all have remained elusive and have consequently called for cultivation-independent molecular techniques. Full-length *Zetaproteobacteria* 16S rRNA sequences have so far been published from 11 regions in the world oceans and show that this class appears to follow a strong biogeographic distribution (McAllister et al., 2011). The distribution of operational

taxonomic units (OTUs) appears to be more strongly correlated with geographic occurrence than with environmental parameters, such as temperature, pH, or total Fe concentration (McAllister et al., 2011). The genome of *Mariprofundus ferrooxydans* PV-1 has provided insights into the genomic underlyings of Fe(II)-oxidizing *Zetaproteobacteria* (Singer et al., 2011), but analysis of FeOB-associated iron oxyhydroxide stalks suggests that PV-1 plays a minor role at most sites (Emerson and Moyer, 2010). This study discusses the (meta-)genomic content of new *Zetaproteobacteria* lineages dominant at the Lō'ihi Seamount, Loh clone SPL-4, and Loh clone SPL-7, delivers genomic and proteomic comparisons to PV-1, and attempts to evaluate the environmental potential of *Zetaproteobacteria* at Fe-rich seamounts in the global oceans.

## MATERIALS AND METHODS

### ENVIRONMENTAL SAMPLE SOURCE

Iron oxide-coated microbial biomats were collected by suction sampler using the submersible vehicle *Pisces V* at the Spillway site (Marker 34; 18.91 N, 155.26 W, 1271.95 m,  $T_{\max} = 63^{\circ}\text{C}$ ) at the Lō'ihi Seamount, Hawai'i, in 2003. DNA was extracted using a phenol-chloroform extraction and purified using cesium chloride density gradient centrifugation as described by (Moore and Dowhan, 2002). The extracted and purified DNA was used to construct a library of ~8,000 fosmids (each ~35 kbp) with the Copy Control<sup>TM</sup> Fosmid Library Production kit (Epicentre, Madison, WI, USA) according to the manufacturer's protocol and stored at  $-80^{\circ}\text{C}$ . DNA was extracted at random from 384 fosmids (total library size  $\approx 13.4$  Mbp) with the BACMAX<sup>TM</sup> DNA Purification Kit (Epicentre, Madison, WI, USA) in 2011. The extraction protocol was amended by extending the incubation with the Plasmid DNA Safe mix from 20 min to 24 h under the addition of extra Plasmid-Safe DNase and ATP to minimize contaminating genomic DNA from the *Escherichia coli* fosmid vector.

### SEQUENCING AND ANNOTATION

DNA concentrations from individual fosmids were measured on a Qubit 2.0 Fluorometer and pooled at equal molar amounts. The pooled DNA was sequenced using conventional whole-genome shotgun sequencing on a Roche 454 GS FLX Titanium sequencer at the Core Genomics Center at the University of Pennsylvania and yielded 1,492,332 reads ( $\sim 816$  Mbp). Quality control was performed with Prinseq v0.20.1 (maximum length: 450 bp; minimum quality: 25; maximum homopolymer length: 9 bp; maximum N-tail: 1 bp) (Schmieder and Edwards, 2011) and fosmid vectors were discarded with a custom biopython script (Cock et al., 2009). The remaining metagenome ( $\sim 423$  Mbp) was assembled with Mira using settings: *de novo*, genome, accurate, 454 (Chevreux et al., 1999) and resulted in 3,988 contigs. These 3,988 contigs were further assembled using Geneious Pro v. 5.4.6 (Drummond et al., 2011) leading to 2,865 final contigs with minimum length of 200 bp, average length of 1,956 bp, and average coverage of  $>25\times$ . Annotation of these final 2,865 contigs was performed on the RAST (Rapid Annotation using Subsystem Technology) server version 4.0 (Aziz et al., 2008). Manual curation was performed with the SEED Viewer v. 2.0 (Overbeek, 2005). rRNA sequences were predicted

using BLASTN in CAMERA (Community cyberinfrastructure for Advanced Microbial Ecology Research and Analysis; Sun et al., 2011). Alignment and phylogenetic tree construction of 16S rRNA sequences were performed with the Geneious aligner and PHYML tree builder using the Jukes-Cantor substitution model and 100 bootstraps in Geneious (Guindon and Gascuel, 2003). This Whole-Genome Shotgun project has been deposited at DDBJ/EMBL/GenBank under the accession AMFO00000000. The version described in this paper is the first version, AMFO0-1000000.

### PHYLOGENETIC BINNING

RAST-annotated genes were aligned against the NCBI non-redundant database using the BLASTX algorithm ( $E = 10^{-5}$ ) for community structure analysis. Final contigs of *Zetaproteobacteria* origin were determined by alignment against the genome of *Mariprofundus ferrooxydans* PV-1 (AATS01000000) using the BLASTX algorithm: Genes with best BLASTX matches to the genome of PV-1 average to 62.15% average amino acid identity (AAid) ( $E = 10^{-5}$ ). On this basis we selected all genes with BLASTX hits of  $\geq 60\%$  AAid to PV-1 proteins to be preliminarily binned as *Zetaproteobacteria* genes. Contigs exclusively harboring best BLASTX matches to PV-1 homologs at  $\geq 60\%$  AAid were classified as *Zetaproteobacteria* contigs without further analysis. Contigs including genes homologous to PV-1 genes, but also to other bacterial classes were only included in our *Zeta*-subset if they passed the following requirements: (1) *Zetaproteobacteria* genes dominated in overall number and AAid or (2) remaining non-*Zetaproteobacteria* genes could not be attributed to a single phylogenetic class, which therefore excluded the possibility of chimeras (Treangen et al., 2011). This screening analysis resulted in 853 genes on 86 contigs with 85.57% ANI to PV-1. Ambiguous contigs, which may still belong to the genome of this *Zetaproteobacterium*, but did not pass our screening filters discussed above, were not included in the discussion of this study.

### DNA AND PROTEIN SEQUENCE ANALYSIS

DNA sequence synteny was evaluated with the Artemis Comparison Tool (ACT; Carver et al., 2005). Protein subcellular localization analysis was performed with PSORT (Nakai and Horton, 1999) and Gneg-mPLoc (Shen and Chou, 2010). Signal peptides and distinction between the general export pathway (Sec) and the twin-arginine translocase (Tat) mechanism were predicted on the basis of Hidden Markov Models (HMMs) using PRED-TAT (Bagos et al., 2010). Motif analysis was performed in the Pfam database using MOTIF Search on the GenomeNet network of Kyoto University available at (<http://www.genome.jp>).

## RESULTS

### PHYLOGENY

In total, the dataset harbors five environmental 16S rRNA sequences ( $>500$  bp), two of which are nearly full-length *Zetaproteobacteria* sequences (Table 1; Figure 1). Based on this phylogenetic marker, *Zetaproteobacteria* are well represented at Marker 34, Lō'ihi, which is in line with earlier studies based on polymerase chain reaction (PCR)-dependent 16S rRNA analyses

**Table 1 | Best BLASTN hits of 16S rRNA sequences (>500 bp) in the Lō'ihi iron mat metagenome (retrieved 01/2013).**

| Closest relative in GenBank          | Class               | Accession no. | Contig | Length [bp] |
|--------------------------------------|---------------------|---------------|--------|-------------|
| SPL OTU 1 clone 10                   | Zetaproteobacteria  | JF320745      | 592    | 1,415       |
| Uncultured bacterium clone Poh_5     | Zetaproteobacteria  | JF320730      | 1645   | 1,427       |
| <i>Methylomicrobium alcaliphilum</i> | Gammaproteobacteria | FO082060      | 202    | 1,147       |
| <i>Methylobacter psychrophilus</i>   | Gammaproteobacteria | NR_025016     | 2858   | 770         |
| Uncultured bacterium clone Ld1-14    | Actinobacteria      | GQ246409      | 2406   | 1,485       |

Zetaproteobacteria relatives are marked in bold letters. 16S rRNA sequences from potential fosmid vector contamination (*Escherichia coli*) are not listed here.

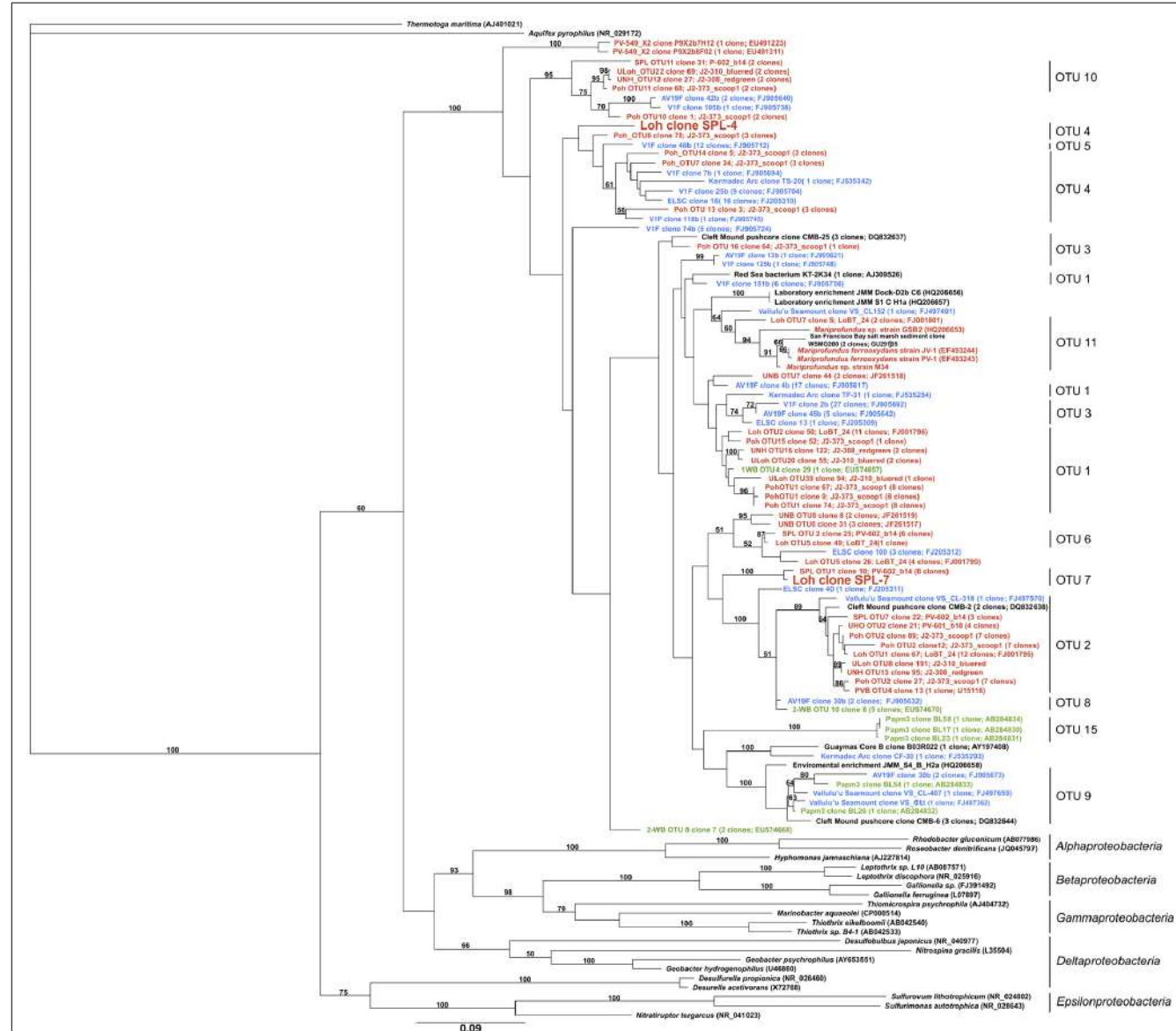


**FIGURE 1 | Maximum-likelihood tree with 100 bootstrap cycles of full-length 16S rRNA gene sequences of all known Zetaproteobacteria species to date and representatives from other *Proteobacteria* classes as stated in (McAllister et al., 2011). Coloring is by geographic origin within the Pacific Ocean: red – Lō'ihi**

Seamount, blue – Vailulu'u Seamount/Tonga Arc/East Lau Spreading Center/Kermadec Arc, green – Southern Mariana Trough. GenBank accession numbers for published sequences are shown in parentheses. The scale bar represents 9 nucleotide substitutions per 100 positions.

(Moyer et al., 1995; Emerson and Moyer, 2002; Rassa et al., 2009). rRNA sequences from other FeOB were not detected. On the basis of their isolation from the Spillway (SPL) site at Lō'ihi, their phylogenetic placement in OTU groups 4 and 7, and because they have not been cultured to date, we named the new *Zetaproteobacteria* lineages Loh clone SPL-4 and Loh clone SPL-7 (**Figure 1**). All *Zetaproteobacteria* genes presented here are assumed to belong to these two lineages.

16S rRNA genes from SPL-4 and SPL-7 are 91% identical to each other, and 90 and 93% identical to the 16S rRNA gene of *Mariprofundus ferrooxydans* PV-1, respectively. Closest relatives from OTUs 4 and 7 have been sampled in the Northern and Southern Pacific, but were previously not considered dominant OTUs at Lō'ihi (McAllister et al., 2011). Clones of OTU 7 have so far only been detected at the Lō'ihi Seamount (Marker 34) representing ~5% of all local *Zetaproteobacteria*; clones from OTU 4 have been isolated from Markers 48 and 57 at Lō'ihi (~8% of local *Zetaproteobacteria*), the Tonga Arc, and the East Lau Spreading Center, and so far show a wider distribution in the Pacific oceans compared to clones from OTU 7 according to (McAllister et al., 2011). Although the biodiversity and biogeography study by McAllister et al. (2011) is the most comprehensive to date, it is important to note that their findings completely rely on results from clone libraries, the results of which are likely to be significantly biased, for instance by *Taq* DNA polymerase errors and PCR template concentrations (Chandler et al., 1997; Acinas et al., 2005). Our findings could hence portray genomic traits that are shared by other Lō'ihi strains and may be applicable to more ubiquitous *Zetaproteobacteria*.

## BIOGEOCHEMICALLY RELEVANT GENES

*Zetaproteobacteria* genes were analyzed with respect to metabolic potential and environmental significance to the iron mat environment at Lō'ihi. We also attempted a broader description of the nature of the *Zetaproteobacteria* by comparative (meta-)genomics with the genome of *Mariprofundus ferrooxydans* PV-1.

## NEW *Zetaproteobacteria* GENE FUNCTIONS

Genes of potential biogeochemical relevance, which have not been described for a *Zetaproteobacterium* before, encode for nitrite reduction (contigs 68 and 2306, **Figure 2**). The nitrite reduction gene cluster on contig 68 is similar in gene content and synteny to those in the genomes of denitrifying *Thiobacillus denitrificans*, *Pseudomonas aeruginosa*, *P. stutzeri*, and *P. denitrificans* (Rinaldo and Cutruzzolà, 2007), e.g., NirS-encoded cytochrome *cd*<sub>1</sub> nitrite

reductase (cd<sub>1</sub>NIR) shares 82% amino acid similarity (AASim) with nitrite reductase from the versatile *Thiobacillus denitrificans* ATCC 25259 (gbAAZ96030.1). Contig 2306 encodes copper-containing nitrite reductase NirK (CuNIR) with 80% and 70% AASim to NirK in the ammonia-oxidizing *Nitrosococcus halophilus* and *Nitrosomonas europaea*, respectively. nirK occurs in a cluster next to genes encoding for cytochromes *c*, which have 68% and 66% AASim to NcgB and NcgC from *Nitrosomonas europaea*, as well as next to two genes encoding for multicopper oxidases type 3, which have 63% and 68% AASim to NcgA.

The two types of dissimilatory NiRs containing either heme cd<sub>1</sub> or two types of Cu centers as prosthetic groups, encoded by *nirS* and *nirK*, respectively, have not been shown to coexist in the same bacterial species, assuming that both encode nitrite reducing activity (Cutruzzolà, 1999; Jones et al., 2008). Hence either nitrite reductases are not conserved among different *Zetaproteobacteria* spp. or *nirK* and *nirS* are rather involved in nitrite detoxification, such as in *Nitrosomonas europaea* (Beaumont et al., 2002). Nevertheless, nitrite reduction may be coupled to Fe(II) oxidation and could render certain *Zetaproteobacteria* spp. facultative anaerobes. This would allow these strains to inhabit a wider range of environments than PV-1, which is known to be a strict microaerophile and can typically acquire energy only at <5% of air-saturated values (Emerson and Merrill Floyd, 2005; Weiss et al., 2007).

It is difficult to infer evolutionary paths of nitrite reductases, because neither *nirS* nor *nirK* are reliable phylogenetic markers (with *nirS* following 16S rRNA phylogenies more congruently). Since both, *nirS* and *nirK* in the *Zetaproteobacteria* genes share most comparable AASim to respective functional genes within the *Gammaproteobacteria*, it remains elusive, which of these types of nitrite reductase is more representative for the *Zetaproteobacteria* and whether one or both types of nitrite reductases were introduced by horizontal gene transfer (HGT).

Nitrate and nitrite reduction are encoded by various other organisms in this Lō'ihi mat environment. Among these organisms are the hydrothermal vent-adapted, thermophilic, strictly aerobic *Marinithermus hydrothermalis*, the sulfur-oxidizing endosymbionts of *Riftia pachyptila* (vent Ph05) and of *Tevnia jerichonana* (vent Tica), which both have very similar physiologies (Gardebrecht et al., 2011), the purple sulfur bacterium *Thiocystis violascens* DSM 198 (Kämpf and Pfennig, 1980), and the widely distributed *Thiobacillus denitrificans*, a facultative anaerobe, which couples inorganic sulfur oxidation as well as anaerobic oxidation of Fe(II) to denitrification at circumneutral pH

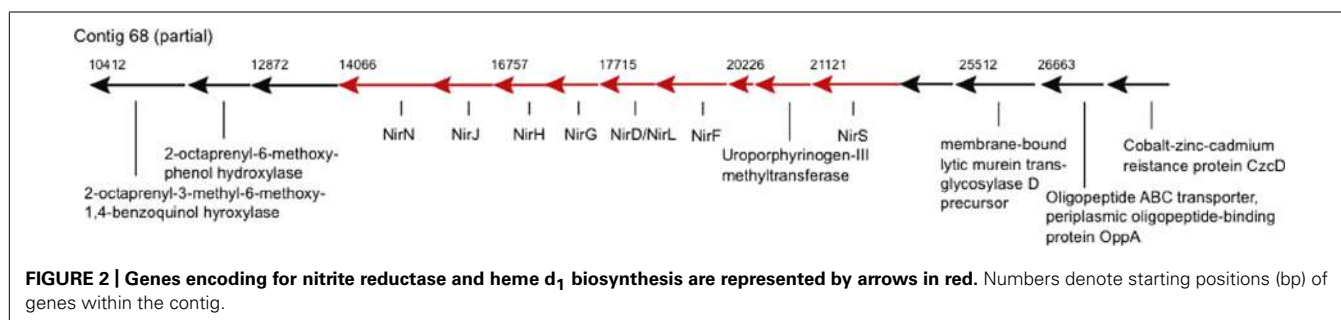


**FIGURE 2 |** Genes encoding for nitrite reductase and heme d<sub>1</sub> biosynthesis are represented by arrows in red. Numbers denote starting positions (bp) of genes within the contig.

(Beller et al., 2006). It appears that most nitrate/nitrite reducing organisms in our dataset are adapted to hydrothermal vent life either following a free-living or endosymbiotic lifestyle and many possess the ability to oxidize a form of sulfur, such as the *Zetaproteobacteria*, as well. Since the iron mat environment provides aerobic and anaerobic niches, the ability to reduce nitrate/nitrite is consequently a beneficial trait that can easily be coupled to the oxidation of inorganic compounds, such as sulfide and iron, and therefore allow survival under dynamic environmental conditions.

Besides nitrite reduction, new *Zetaproteobacteria* gene functions include antibiotic biosynthesis monooxygenase (contig 285), several exodeoxyribonucleases I (contigs 2596, 2709, 280, 68), and three transposases. Otherwise, the genes available from PV-1 and the SPL-strains are fairly comparable in function and abundance. The gene novelty in the *Zetaproteobacteria* genes fit with the lifestyle of facultative anaerobic microorganisms, which inhabit mats at an Fe-rich hydrothermal vent environment and are frequently exposed to contact with other bacteria. Different *Zetaproteobacteria* lineages may adapt to their exact niche via acquisition of diverse survival-enhancing genes, e.g., specific antibiotic biosynthesis or efflux, or more/less heavy metal efflux pumps encoding genes, however, the overall main metabolic potentials appear similar between strains.

## COMPARATIVE GENOMICS WITH *Mariprofundus ferrooxydans* PV-1

### Iron oxidation

The first *Zetaproteobacteria* gene candidates assumed to be involved in neutrophilic microaerophilic Fe(II) oxidation were detected via protein extraction from an Fe(II)-oxidizing PV-1 cell culture (Singer et al., 2011). The extracted molybdopterin oxidoreductase Fe<sub>4</sub>S<sub>4</sub> region (MobB) and most of the surrounding gene cluster (ZP\_01451010- ZP\_01451022) was also identified in our dataset (contigs 12, 296) and shows that gene synteny is well conserved, however, split over two contigs (**Figure 3**). Cytochromes and MobB (contig 296) are more conserved than succinate dehydrogenases (contig 12).

MobB in the SPL-strains shares 82% AASim with MobB in PV-1, while it is 59% and 57% similar to MobB in *Gallionella capsiferriformans* and *Sideroxydans lithotrophicus*, respectively. This indicates that there are sequence and potentially structural differences among MobB within the *Zetaproteobacteria* and in comparison to other FeOB. Both MobB proteins, in PV-1 as well as in the SPL-strains, contain Tat signal sequences and are predicted to harbor transmembrane helices located in the inner membrane. Based on their negative charge at pH 7, the soluble parts of both MobB, including the Fe<sub>4</sub>S<sub>4</sub> region, are predicted to face the periplasm unlike previously described in (Singer et al., 2011). MobB may therefore accept electrons shuttled from the outer membrane to the periplasm during Fe(II) oxidation as depicted in our revised conceptual iron oxidation model (**Figure 4**). Outer membrane cytochromes are likely involved in the import of electrons from ferrous iron into the cells of FeOB, such as in *Acidithiobacillus ferrooxidans* (Bird et al., 2011). Both, PV-1 and the SPL lineages, also harbor genes encoding type IV biogenesis proteins PilAMNOPQ (contigs 592 and 1144), which may aid in the direct contact of Fe-species, such as in *Geobacter* spp. (Mehta et al., 2005).

As neither transcription factors, nor promoters were found in the immediate gene neighborhood vicinity of the MobB gene cluster, it remains unclear if it is in fact actively transcribed in the organism or if transcription is dependent on other genes, which are elsewhere in the genome, for instance involved in redox sensing. Despite the disconnection between contigs 296 and 12 in the SPL-strains, succinate dehydrogenases may still be part of the electron transport chain shuttling electrons during Fe(II) oxidation, however, may not necessarily be transcribed together with the MobB gene cluster.

### Carbon fixation

Genes from our SPL lineages encode for Form IAq ribulose-1,5-biphosphate carboxylase (RuBisCo) large subunit (contig 280) with 77% AASim to *Mariprofundus ferrooxydans* PV-1 (ZP\_01451219) and two RuBisCo activation proteins CbbO and CbbQ (contig 280), which are 72% and 88% similar to respective genes in PV-1 (ZP\_01451217, ZP\_01451218), respectively. Form IAq appears predominantly in obligate chemolithotrophs and functions best in niches with medium to low CO<sub>2</sub> concentrations (0.1–1%) and O<sub>2</sub> present (Badger and Bek, 2007). Form II RuBisCo proteins, which are present in our dataset, could not be unambiguously allocated to the *Zetaproteobacteria* genes, although RuBisCo large and small chain proteins (contig 135) are 87% and 90% similar to respective proteins encoded on the PV-1 genome (ZP\_01453295-96). Associated RuBisCo activation proteins CbbQ and CbbO (contig 135) are 81 and 66% similar to CbbQ (ZP\_01453297) and CbbO (ZP\_01453298) in PV-1. Form II RuBisCo enzymes have a low discrimination threshold against O<sub>2</sub> as an alternative substrate, poor affinity for CO<sub>2</sub>, and therefore potentially take over when the organism moves to a high-CO<sub>2</sub> (1.5%) and low-O<sub>2</sub> environment (Badger and Bek, 2007).

At Marker 34, temperature differences between ambient seawater (2.6°C) and hydrothermal efflux (27°C) may create turbulent eddies in the water column, which would expose cells to oscillating anaerobic and microaerobic conditions, where CO<sub>2</sub> levels are variable (ranging from 2 mM to 20 mM) and dependent on positioning within the chemocline interface (Badger and Bek, 2007; Glazer and Rouxel, 2009). Utilization of both forms of RuBisCo proteins could thus enable SPL-4 and SPL-7 to optimize the acquisition of carbon under a wider range of CO<sub>2</sub> and O<sub>2</sub> concentrations inside and outside the mat in this dynamic system.

### Sulfide oxidation

Sulfide oxidation is encoded by a sulfide-quinone reductase (contig 212), which is 83% AASim to sulfide-quinone reductase in PV-1 (ZP\_01453072). The presence of a transcriptional regulator two genes further upstream (most closely related to ZP\_01451744) suggests that sulfide:quinone oxidoreductase is actively transcribed. Homologs of sulfide-quinone reductases from the SPL-strains are most closely related to genes in *L. ferrooxidans* and other *Leptospirillum* spp., as well as *S. lithotrophicus*. Neither of these organisms was isolated from deep-sea hydrothermal vents, but they are associated with mats dominated by FeOB (Edwards et al., 2000; Emerson et al., 2007; Gotsman et al., 2009).

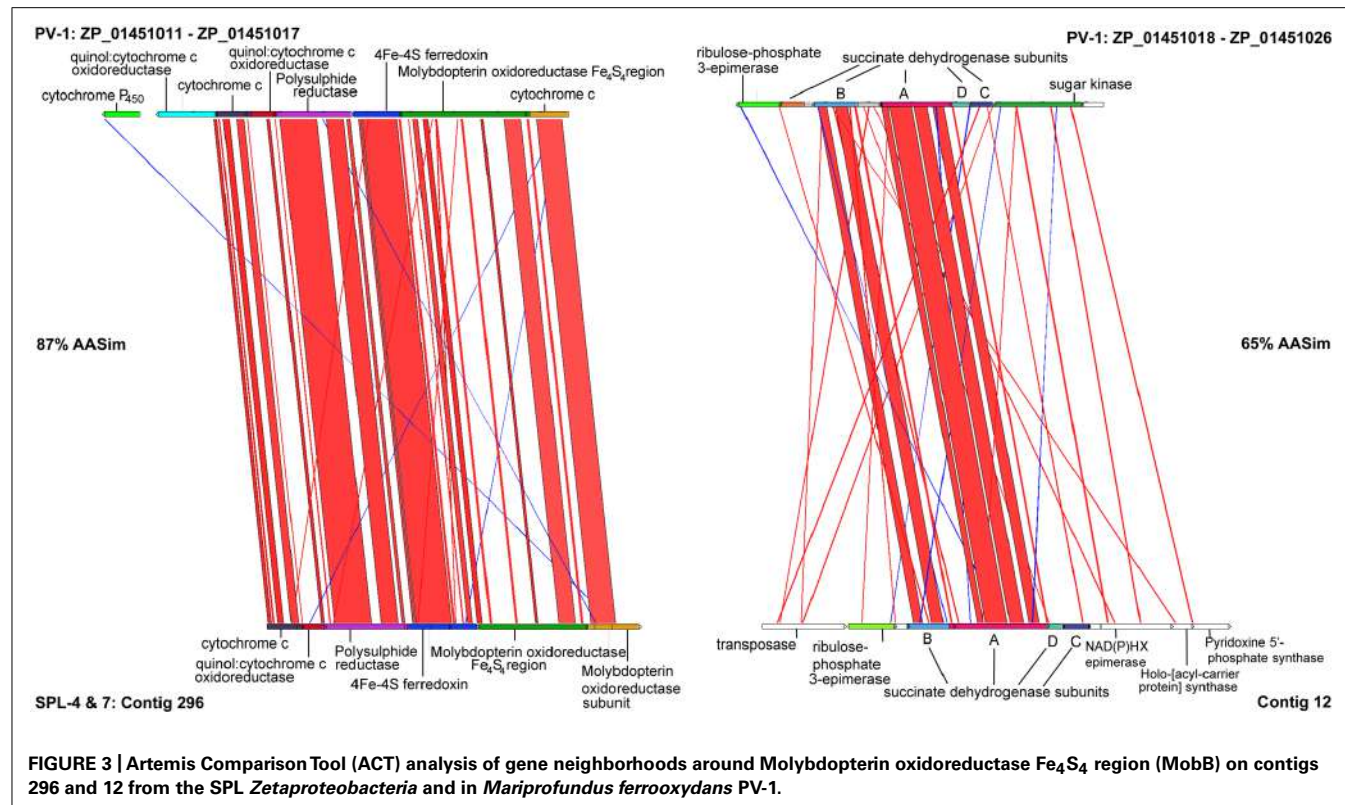


**FIGURE 3 |** Artemis Comparison Tool (ACT) analysis of gene neighborhoods around Molybdopterin oxidoreductase  $\text{Fe}_4\text{S}_4$  region (MobB) on contigs 296 and 12 from the SPL Zetaproteobacteria and in *Mariprofundus ferrooxydans* PV-1.

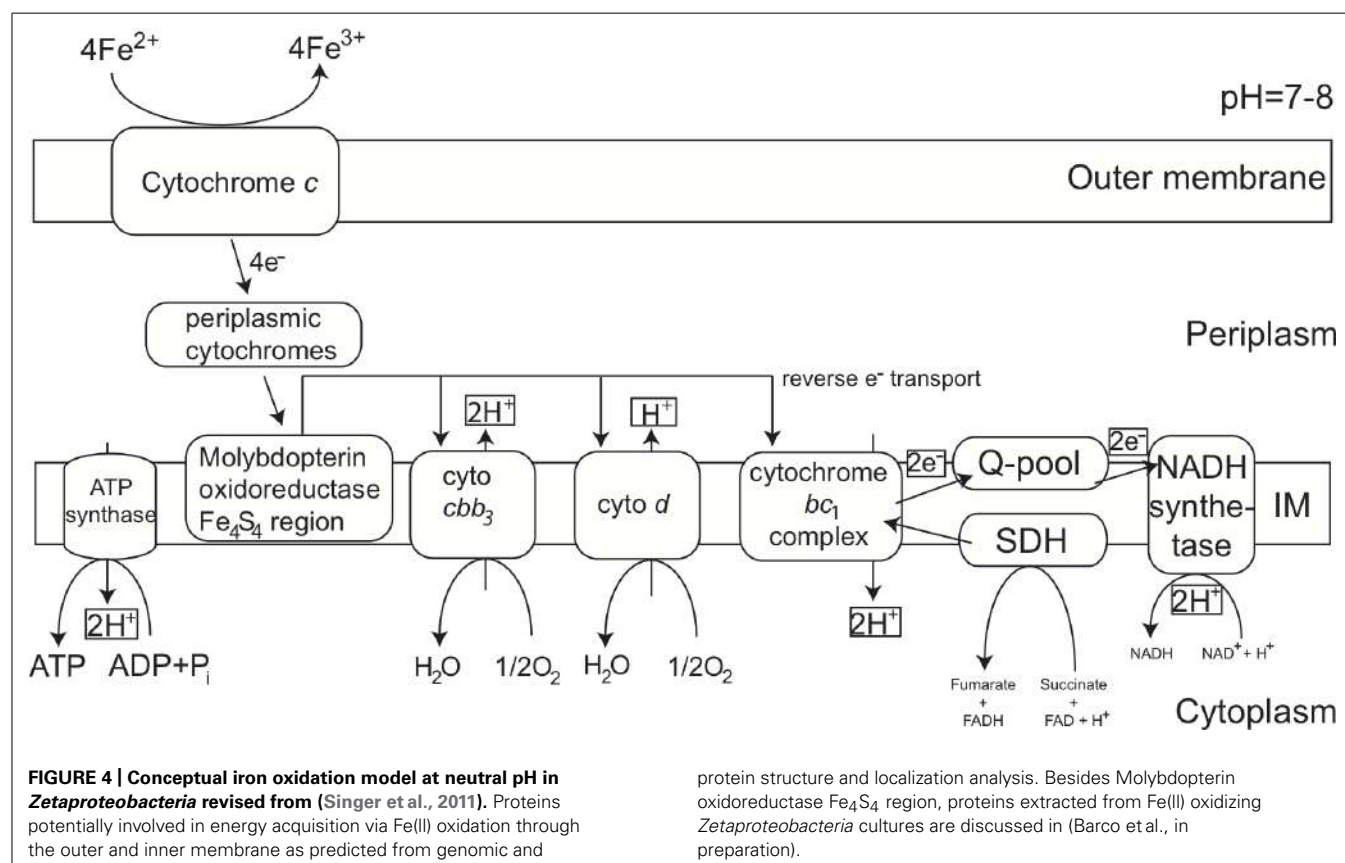


**FIGURE 4 |** Conceptual iron oxidation model at neutral pH in Zetaproteobacteria revised from (Singer et al., 2011). Proteins potentially involved in energy acquisition via Fe(III) oxidation through the outer and inner membrane as predicted from genomic and

protein structure and localization analysis. Besides Molybdopterin oxidoreductase  $\text{Fe}_4\text{S}_4$  region, proteins extracted from Fe(III) oxidizing Zetaproteobacteria cultures are discussed in (Barco et al., in preparation).

The Lō'ihi Seamount is mostly devoid of sulfide (e.g., no sulfur phases were observed in 2006), which is why Fe-oxides are the most common form of Fe(III)-minerals (Glazer and Rouxel, 2009). An elevation in dissolved sulfide concentration has been observed at Lō'ihi during an eruption in 1996 (Davis et al., 2003), however, incidents like that represent the exception rather than the norm. It was recently shown that the distribution of *Zetaproteobacteria* OTUs is more dependent on geographic factors, such as distance than environmental chemistry (McAllister et al., 2011). Because sulfide oxidation is an unfavorable metabolism at Lō'ihi the maintenance of sulfide and sulfite oxidation genes should be an evolutionarily unstable strategy. Hence it remains to be determined if all *Zetaproteobacteria* are capable of sulfide oxidation and if these sulfide-quinone reductases are remainders of ancient *Zetaproteobacteria* or have been introduced along with other genes from FeOB, which may experience high sulfide concentrations more frequently.

## DISCUSSION

### THE *Zetaproteobacteria* IN THE GLOBAL OCEANS

This study has provided novel insights into the physiology, ecology, and genetics of novel *Zetaproteobacteria* strains cycling iron and carbon at a deep-sea hydrothermal vent environment. Loh clones SPL-4 and SPL-7 belong to OTUs 4 and 7, which were previously estimated to account for ~13% of the *Zetaproteobacteria* present at the Lō'ihi Seamount based on 16S clone library data (McAllister et al., 2011). In our metagenomic dataset, which was created from samples of the same environment and not amplified prior to sequencing, these strains were dominant. The discrepancy between PCR- and fosmid-based techniques exemplifies the outcome of barely predictable biases, which should be taken into account, especially when studying microbial diversity in Fe(II) oxidizing environments. In addition, the fosmid kits used in our study were accompanied by major difficulties upon insert retrieval and led to a loss of 50% of the library, primarily due to vector contamination (see Methods section). This loss could have been reduced if whole genome sequencing on environmental DNA had been chosen over the use of fosmid libraries. Thereby a significant amount of genomic content missing from our dataset could have possibly been retrieved and would have potentially revealed further molecular fundamentals of the successful *Zetaproteobacteria* lifestyle beyond those discussed in this study. Annotation of *Zetaproteobacteria* genes was difficult sometimes as current databases are skewed toward *Gammaproteobacteria*, however, the combination of screening filters, including BLAST searches, tetranucleotide patterns and taxonomic classification models based on GLIMMER interpolated context models (ICMs) was tested and enables reliable detection of most *Zetaproteobacteria* genes.

## REFERENCES

- Acinas, S. G., Sarma-Rupavtar, R., Klepac-Ceraj, V., and Polz, M. F. (2005). PCR-induced sequence artifacts and bias: insights from comparison of two 16S rRNA clone libraries constructed from the same sample. *Appl. Environ. Microbiol.* 71, 8966–8969.
- Aziz, R. K., Bartels, D., Best, A. A., Dejongh, M., Disz, T., Edwards, R. A., et al. (2008). The RAST Server: rapid annotations using subsystems technology. *BMC Genomics* 9:75. doi: 10.1186/1471-2164-9-75
- Badger, M. R., and Bek, E. J. (2007). Multiple Rubisco forms in proteobacteria: their functional significance in relation to CO<sub>2</sub> acquisition by the CBB cycle. *J. Exp. Bot.* 59, 1525–1541.
- Bagos, P. G., Nikolaou, E. P., Liakopoulos, T. D., and Tsirigos, K. D. (2010). Combined prediction of Tat and Sec signal peptides with hidden Markov models. *Bioinformatics* 26, 2811–2817.
- Beaumont, H. J. E., Hommes, N. G., Sayavedra-Soto, L. A., Arp, D. J., Arciero, D. M., Hooper, A. B., et al. (2002). Nitrite reductase of *Nitrosomonas europaea* is not essential for production of gaseous nitrogen oxides and confers tolerance to nitrite. *J. Bacteriol.* 184, 2557–2560.

- Beller, H., Chain, P., Letain, T., Chakicherla, A., Larimer, F., Richardson, P., et al. (2006). The genome sequence of the obligately chemolithoautotrophic, facultatively anaerobic bacterium *Thiobacillus denitrificans*. *J. Bacteriol.* 188, 1473–1488.
- Bird, L., Bonnefoy, V., and Newman, D. (2011). Bioenergetic challenges of microbial iron metabolism. *Trends Microbiol.* 19, 330–340.
- Carver, T. J., Rutherford, K. M., Berneman, M., Rajandream, M. A., Barrell, B. G., and Parkhill, J. (2005). ACT: the Artemis comparison tool. *Bioinformatics* 21, 3422–3423.
- Chandler, D., Fredrickson, J., and Brockman, F. (1997). Effect of PCR template concentration on the composition and distribution of total community 16S rDNA clone libraries. *Mol. Ecol.* 6, 475–482.
- Chevreux, B., Wetter, T., and Suhai, S. (1999). “Genome sequence assembly using trace signals and additional sequence information,” in *Computer Science and Biology: Proceedings of the German Conference on Bioinformatics (GCB)*, 45–56.
- Cock, P. J. A., Antao, T., Chang, J. T., Chapman, B. A., Cox, C. J., Dalke, A., et al. (2009). Biopython: freely available Python tools for computational molecular biology and bioinformatics. *Bioinformatics* 25, 1422–1423.
- Cutruzzola, F. (1999). Bacterial nitric oxide synthesis. *Biochim. Biophys. Acta* 1411, 231–249.
- Dang, H., Chen, R., Wang, L., Shao, S., Dai, L., Ye, Y., et al. (2011). Molecular characterization of putative biocorroding microbiota with a novel niche detection of Epsilon- and Zetaproteobacteria in Pacific Ocean coastal seawaters. *Environ. Microbiol.* 13, 3059–3074.
- Davis, A., Clague, D., Zierenberg, R., Wheat, C., and Cousens, B. (2003). Sulfide formation related to changes in the hydrothermal system on Loihi Seamount, Hawai'i, following the seismic event in 1996. *Can. Mineral.* 41, 457–472.
- Drummond, A. J., Ashton, B., Buxton, S., Cheung, M., Cooper, A., Duran, C., et al. (2011). Geneious v. 5.4.6. Available at: <http://www.geneious.com>
- Edwards, K. J., Bach, W., McCollom, T. M., and Rogers, D. R. (2004). Neutrophilic iron-oxidizing bacteria in the ocean: their habitats, diversity, and roles in mineral deposition, rock alteration, and biomass production in the deep-sea. *Geomicrobiol. J.* 21, 393–404.
- Edwards, K. J., Bond, P. L., Druschel, G. K., McGuire, M. M., Hamers, R. J., and Banfield, J. F. (2000). Geochemical and biological aspects of sulfide mineral dissolution: lessons from Iron Mountain, California. *Chem. Geol.* 169, 383–397.
- Edwards, K., Rogers, D., Wirsén, C., and McCollom, T. (2003). Isolation and characterization of novel psychrophilic, neutrophilic, Fe-oxidizing, chemolithoautotrophic  $\alpha$ - and  $\gamma$ -Proteobacteria from the deep sea. *Appl. Environ. Microbiol.* 69, 2906–2913.
- Emerson, D. (2012). Biogeochemistry and microbiology of microaerobic Fe(II) oxidation. *Biochem. Soc. Trans.* 40, 1211–1216.
- Emerson, D., and Merrill Floyd, M. (2005). Enrichment and isolation of iron-oxidizing bacteria at neutral pH. *Methods Enzymol.* 397, 112–123.
- Emerson, D., and Moyer, C. (2002). Neutrophilic Fe-oxidizing bacteria are abundant at the Loihi Seamount hydrothermal vents and play a major role in Fe oxide deposition. *Appl. Environ. Microbiol.* 68, 3085.
- Emerson, D., and Moyer, C. L. (2010). Microbiology of seamounts: common patterns observed in community structure. *Oceanography* 23, 148–163.
- Emerson, D., Rentz, J. A., Lilburn, T. G., Davis, R. E., Aldrich, H., Chan, C., et al. (2007). A novel lineage of proteobacteria involved in formation of marine Fe-oxidizing microbial mat communities. *PLoS ONE* 2:e667. doi: 10.1371/journal.pone.0000667
- Gardebrecht, A., Markert, S., Sievert, S., Felbeck, H., Thürmer, A., Albrecht, D., et al. (2011). Physiological homogeneity among the endosymbionts of *Riftia pachyptila* and *Tevnia jerichonana* revealed by proteogenomics. *ISME J.* 6, 766–776.
- Glazer, B., and Rouxel, O. (2009). Redox speciation and distribution within diverse iron-dominated microbial habitats at Loihi Seamount. *Geomicrobiol. J.* 26, 606–622.
- Goltsman, D. S. A., Denef, V. J., Singer, S. W., Verberkmoes, N. C., Lefsrud, M., Mueller, R. S., et al. (2009). Community genomic and proteomic analyses of chemoautotrophic iron-oxidizing “*Leptospirillum rubarum*” (Group II) and “*Leptospirillum ferrodiazotrophum*” (Group III) bacteria in acid mine drainage biofilms. *Appl. Environ. Microbiol.* 75, 4599–4615.
- Guindon, S., and Gascuel, O. (2003). A simple, fast, and accurate algorithm to estimate large phylogenies by maximum likelihood. *Syst. Biol.* 52, 696–704.
- Handley, K. M., Boothman, C., Mills, R. A., Pancost, R. D., and Lloyd, J. R. (2010). Functional diversity of bacteria in a ferruginous hydrothermal sediment. *ISME J.* 4, 1193–1205.
- Jones, C. M., Stres, B., Rosenquist, M., and Hallin, S. (2008). Phylogenetic analysis of nitrite, nitric oxide, and nitrous oxide respiratory enzymes reveal a complex evolutionary history for denitrification. *Mol. Biol. Evol.* 25, 1955–1966.
- Kämpf, C., and Pfennig, N. (1980). Capacity of Chromatiaceae for chemotrophic growth. Specific respiration rates of *Thiocystis violacea* and *Chromatium vinosum*. *Arch. Microbiol.* 127, 125–135.
- Karl, D., McMurtry, G., Malahoff, A., and Garcia, M. (1988). Loihi Seamount, Hawaii: a mid-plate volcano with a distinctive hydrothermal system. *Nature* 336, 532–535.
- McAllister, S. M., Davis, R. E., McBeth, J. M., Tebo, B. M., Emerson, D., and Moyer, C. L. (2011). Biodiversity and emerging biogeography of the neutrophilic iron-oxidizing Zetaproteobacteria. *Appl. Environ. Microbiol.* 77, 5445–5457.
- Mehta, T., Coppi, M. V., Childers, S. E., and Lovley, D. R. (2005). Outer membrane c-type cytochromes required for Fe(III) and Mn(IV) oxide reduction in *Geobacter sulfurreducens*. *Appl. Environ. Microbiol.* 71, 8634–8641.
- Meyer-Dombard, D. R., Amend, J. P., and Osburn, M. R. (2012). Microbial diversity and potential for arsenic and iron biogeochemical cycling at an arsenic rich, shallow-sea hydrothermal vent (Tutum Bay, Papua New Guinea). *Chem. Geol.* 1–11.
- Moore, D. D., and Dowhan, D. (2002). “Preparation and analysis of DNA”, in *Current Protocols in Molecular Biology* (John Wiley & Sons, Inc) 2.0.1–2.0.3.
- Moyer, C. L., Dobbs, F. C., and Karl, D. M. (1995). Phylogenetic diversity of the bacterial community from a microbial mat at an active, hydrothermal vent system, Loihi Seamount, Hawaii. *Appl. Environ. Microbiol.* 61, 1555–1562.
- Nakai, K., and Horton, P. (1999). PSORT: a program for detecting sorting signals in proteins and predicting their subcellular localization. *Trends Biochem. Sci.* 24, 34–36.
- Overbeek, R. (2005). The subsystems approach to genome annotation and its use in the project to annotate 1000 genomes. *Nucleic Acids Res.* 33, 5691–5702.
- Rassa, A. C., McAllister, S. M., Safran, S. A., and Moyer, C. L. (2009). Zeta-Proteobacteria dominate the colonization and formation of microbial mats in low-temperature hydrothermal vents at Loihi Seamount, Hawaii. *Geomicrobiol. J.* 26, 623–638.
- Rinaldo, S., and Cutruzzola, F. (2007). “Nitrite reductases in denitrification,” in *Biology of the Nitrogen Cycle*, eds H. Bothe, S. J. Ferguson, and W. E. Newton (Amsterdam: Elsevier), 37–54.
- Schmieder, R., and Edwards, R. (2011). Quality control and preprocessing of metagenomic datasets. *Bioinformatics* 27, 863–864.
- Sedwick, P. N., McMurtry, G. M., and Macdougall, J. D. (1992). Chemistry of hydrothermal solutions from Pele's vents, Loihi Seamount, Hawaii. *Geochim. Cosmochim. Acta* 56, 3643–3667.
- Shen, H.-B., and Chou, K.-C. (2010). Gneg-mPLoc: a top-down strategy to enhance the quality of predicting subcellular localization of Gram-negative bacterial proteins. *J. Theor. Biol.* 264, 326–333.
- Singer, E., Emerson, D., Webb, E. A., Barco, R. A., Kuerten, J. G., Nelson, W. C., et al. (2011). *Mariprofundus ferrooxydans* PV-1 the first genome of a marine Fe(II) oxidizing Zetaproteobacterium. *PLoS ONE* 6:e25386. doi: 10.1371/journal.pone.0025386
- Sun, S., Chen, J., Li, W., Altintas, I., Lin, A., Peltier, S., et al. (2011). Community cyberinfrastructure for Advanced Microbial Ecology Research and Analysis: the CAMERA resource. *Nucleic Acids Res.* 39, D546–D551.
- Treangen, T. J., Sommer, D. D., Angly, F. E., Koren, S., and Pop, M. (2011). Next generation sequence assembly with AMOS. *Curr. Protoc. Bioinformatics* Chapter 11:Unit 11.8.
- Weiss, J. V., Rentz, J. A., Plaia, T., Neubauer, S. C., Merrill-Floyd, M., Lilburn, T., et al. (2007). Characterization of neutrophilic Fe(II)-oxidizing bacteria isolated from the rhizosphere of wetland plants and description of *Ferritrophicum radicicola*, nov. sp. nov., and *Sideroxydans paludicola*, nov. sp. *Geomicrobiol. J.* 24, 559–570.
- Wessel, P., Sandwell, D. T., and Kim, S.-S. (2010). The global seamount census. *Oceanography* 23, 24–33.
- Wheat, C., Jannasch, H., Plant, J., Moyer, C., Sansone, F., and McMurtry, G. (2000). Continuous

sampling of hydrothermal fluids from Loihi Seamount after the 1996 event. *J. Geophys. Res.* 105, 19353–19367.

**Conflict of Interest Statement:** The authors declare that the research was conducted in the absence of any commercial or financial relationships

that could be construed as a potential conflict of interest.

*Received:* 05 November 2012; *accepted:* 22 February 2013; *published online:* 19 March 2013.

*Citation:* Singer E, Heidelberg JF, Dhillon A and Edwards KJ (2013) Metagenomic insights into the dominant Fe(II)

oxidizing Zetaproteobacteria from an iron mat at Lō'ihi, Hawai'i. *Front. Microbiol.* 4:52. doi: 10.3389/fmicb.2013.00052

This article was submitted to Frontiers in Extreme Microbiology, a specialty of Frontiers in Microbiology.

Copyright © 2013 Singer, Heidelberg, Dhillon and Edwards. This

is an open-access article distributed under the terms of the Creative Commons Attribution License, which permits use, distribution and reproduction in other forums, provided the original authors and source are credited and subject to any copyright notices concerning any third-party graphics etc.



# Low temperature geomicrobiology follows host rock composition along a geochemical gradient in Lau Basin

Jason B. Sylvan<sup>1</sup>, Tiffany Y. Sia<sup>1</sup>, Amanda G. Haddad<sup>2</sup>, Lindsey J. Briscoe<sup>3</sup>, Brandy M. Toner<sup>3</sup>, Peter R. Girguis<sup>4</sup> and Katrina J. Edwards<sup>1,2\*</sup>

<sup>1</sup> Department of Biological Sciences, University of Southern California, Los Angeles, CA, USA

<sup>2</sup> Department of Earth Sciences, University of Southern California, Los Angeles, CA, USA

<sup>3</sup> Department of Soil, Water, and Climate, University of Minnesota, St. Paul, MN, USA

<sup>4</sup> Department of Organismal and Evolutionary Biology, Harvard University, Cambridge, MA, USA

**Edited by:**

Andreas Teske, University of North Carolina at Chapel Hill, USA

**Reviewed by:**

William D. Orsi, Woods Hole Oceanographic Institution, USA  
Federico Lauro, University of New South Wales, Australia

**\*Correspondence:**

Katrina J. Edwards, Department of Biological Sciences, University of Southern California, 3616 Trousdale Parkway, Los Angeles, CA 90089, USA.

e-mail: kje@usc.edu

The East Lau Spreading Center (ELSC) and Valu Fa Ridge (VFR) comprise a ridge segment in the southwest Pacific Ocean where rapid transitions in the underlying mantle chemistry manifest themselves as gradients in seafloor rock geochemistry. We studied the geology and microbial diversity of three silicate rock samples and three inactive sulfide chimney samples collected, from north to south, at the vent fields Kilo Moana, ABE, Tui Malila, and Mariner. This is the first study of microbial populations on basaltic andesite, which was sampled at Mariner vent field. Silicate rock geochemistry exhibits clear latitudinal trends that are mirrored by changes in bacterial community composition.  $\alpha$ -proteobacteria,  $\epsilon$ -proteobacteria, and Bacteroidetes are most common on a silicate collected from Kilo Moana and their proportions decrease linearly on silicates collected further south. Conversely, a silicate from Mariner vent field hosts high proportions of a unique lineage of Chloroflexi unrelated (<90% sequence similarity) to previously recovered environmental clones or isolates, which decrease at ABE and are absent at Kilo Moana. The exteriors of inactive sulfide structures are dominated by lineages of sulfur oxidizing  $\alpha$ -proteobacteria,  $\gamma$ -proteobacteria, and  $\epsilon$ -proteobacteria, while the interior of one chimney is dominated by putative sulfur-reducing  $\delta$ -proteobacteria. A comparison of bacterial communities on inactive sulfides from this and previous studies reveals the presence of a clade of uncultured Bacteroidetes exclusive to sulfidic environments, and a high degree of heterogeneity in bacterial community composition from one sulfide structure to another. In light of the heterogeneous nature of bacterial communities observed here and in previous studies of both active and inactive hydrothermal sulfide structures, the presence of numerous niches may be detected on these structures in the future by finer scale sampling and analysis.

**Keywords:** geomicrobiology, basalt, inactive sulfides, hydrothermal, bacteroidetes

## INTRODUCTION

The Eastern Lau Spreading Center (ELSC) and Valu Fa Ridge (VFR) comprise the southern portion of the Lau Basin back-arc spreading center, located between the islands of Samoa and Tonga in the southwest Pacific Ocean. Hydrothermal venting was discovered in Lau Basin along the VFR in 1989 (Fouquet et al., 1991) and was subsequently discovered at various other sites along the ELSC and VFR (Langmuir et al., 2004; Ishibashi et al., 2006). The geochemistry of both host rock composition and hydrothermal fluids in Lau Basin changes along the north-south gradient from mid-ocean ridge-like basalt in the north to subduction influenced andesite in the south over the course of <600 km (Escriv et al., 2009; Dunn and Martinez, 2011; Mottl et al., 2011). This is a steeper gradient than seen anywhere else along the global mid-ocean ridge system.

Given the observed gradients in host rock composition and vent fluid geochemistry, Lau Basin is an ideal location to study how geochemistry influences the distribution and composition of biological communities. It has been shown that the gradient in

chemistry influences distributions of megafauna (Podowski et al., 2010) and microbes on active sulfide chimneys (Flores et al., 2012), but no work currently exists examining microbiology on the host rock or inactive hydrothermal sulfides. Seafloor-exposed silicates (thus far basalts are the only seafloor silicates sampled) are known to host diverse microbial communities at mid-ocean ridges (Lysnes et al., 2004; Mason et al., 2009; Santelli et al., 2009), but no samples have been analyzed from back-arc systems, where geochemical controls on silicate microbiology can be tested explicitly. Recent work has also illustrated that microbial communities thrive on inactive hydrothermal sulfides long after venting ceases (Rogers et al., 2003; Suzuki et al., 2004; Kato et al., 2010; Sylvan et al., 2012a). A succession occurs on these sulfides whereby the microbial community present on inactive sulfides is different from that on active structures. This is likely due to a change in mineralogy brought on by the drastic decrease in temperature and disappearance of the reduced substrates in hydrothermal fluids once the vent dies. Similar mineralogical controls are present on other low temperature deep-sea deposits, including basalts, where the microbial

community appears to be selected by substrate type (Toner et al., 2013); bacterial communities collected from seafloor basalts are more similar to each other than to communities on other substrates. The same is true for bacterial communities on inactive sulfides from the East Pacific Rise (EPR), the Okinawa Trough, and Indian Ocean Ridge (Suzuki et al., 2004; Toner et al., 2013). Both seafloor basalts and inactive hydrothermal sulfide structures can be considered extreme environments due to their high metal content and elevated concentrations of elements considered toxic to most life, such as copper.

We examined the geology and microbiology of low temperature deposits collected from four vent fields along the ELSC and VFR during summer 2009. Specifically, we seek to test the hypothesis that bacterial communities are selected by gradients in host rock composition on silicates [basalts and basaltic andesite, classified using total alkalis versus silica (Le Bas and Streckeisen, 1991)] and to determine if bacterial communities on basaltic andesite, for which no data currently exists, differ from those on basalt. We also seek to further understand bacterial communities on inactive sulfides, for which limited data exists.

## MATERIALS AND METHODS

### SAMPLE COLLECTION

Five seafloor rock samples were collected from the ELSC and VFR (Figure 1) during cruise TN-235 on the *R/V Thompson* with ROV Jason II during 16 May–08 June 2009. Silicates located outside areas of diffuse flow and sulfides that appeared inactive on the seafloor were collected from four vent fields (Figure A1 in Appendix; Table 1). Samples were collected using ROV Jason II and then placed in sealed bioboxes on the sampling tray of the ROV for the remainder of the dive, isolating them in seawater from the collection site for the remainder of the dive. Once on deck, the samples were removed from the bioboxes and immediately processed in flame sterilized steel boxes, where they were separated from the seawater in the bioboxes, with a flame sterilized hammer and chisel. Aliquots of rock chips removed from the larger sample for DNA analysis were placed in 5 mL centrifuge tubes and immediately frozen at  $-80^{\circ}\text{C}$ . Subsamples for optical mineralogy (*via* thin section analysis), X-ray diffraction (XRD), and elemental analysis were allowed to air dry on the ship and were subsequently stored at room temperature.

### THIN SECTION ANALYSIS

Standard thin sections (30  $\mu\text{m}$  thick) were made from representative portions of each sample by Spectrum Petrographics, Inc. (Vancouver, WA, USA) and were analyzed using a polarizing petrographic microscope (Zeiss AxioImager.M2m with a Zeiss AxioCam HRc camera) with both reflected and transmitted light.

### X-RAY DIFFRACTION

Approximately 2  $\text{cm}^3$  of each sample was ground to a powder using mortar and pestle and then mounted on a plastic holder using acetone and a disposable wooden stick to ensure random orientation of the particles. After air drying, samples were analyzed on a Siemens d-500 Diffractometer with a cobalt source. The software program JADE (Materials Data, Inc., v9.3.3) was used for phase identification by peak matching.

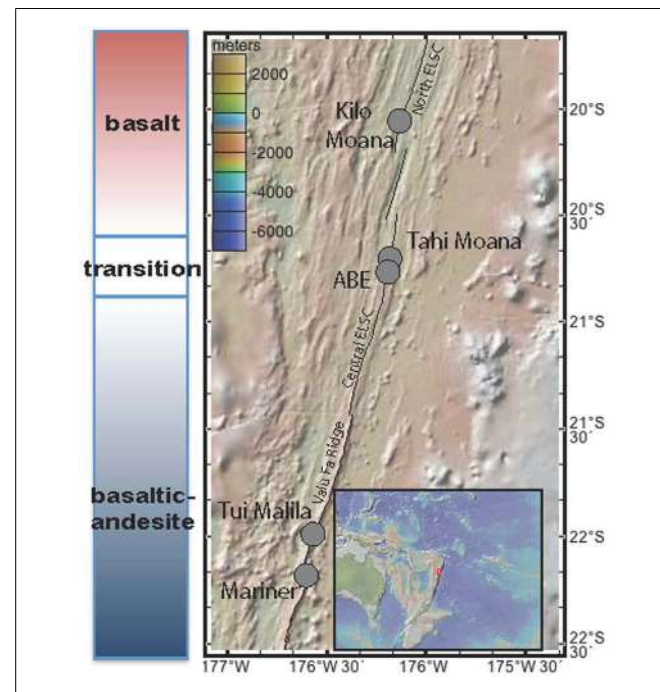


**FIGURE 1 | Map of southern Lau Basin, with the Eastern Lau Spreading Center and Valu Far Ridge.** Samples were collected from Kilo Moana, ABE, Tui Malila, and Mariner vent fields.

### ELEMENTAL ANALYSIS

Major and minor elemental concentrations were determined from the same subsample used for XRD analysis at the University of Minnesota Analytical Geochemistry Lab. Powders were acid digested prior to analysis. Weight percent of major oxides were determined in triplicate on a Thermo Scientific iCAP 6500 dual view Inductively Coupled Plasma – Optical Emission Spectrometer (ICP-OES). Samples were diluted 40-fold prior to analysis with the addition of a Cs matrix modifier and Y as an internal standard and measured using free aspiration of the sample and integrations of five 10 s replicate readings per measurement. Trace elements were determined in duplicate on a Thermo Scientific XSERIES 2 ICP mass spectrometer with an electrospray ionization PC3 Peltier cooled spray chamber, SC-FAST injection loop, and SC-4 autosampler.

### DNA EXTRACTION AND ANALYSIS

DNA was extracted from  $\sim 4 \text{ cm}^3$  of sample using a CTAB phenol/chloroform extraction (Ausubel et al., 1999). qPCR for bacteria was carried out as described previously using primers 338f [5'-ACT CCT ACG GGA GGC AGCAG-3'] and 518r [5'-ATT ACC GCG GCT GCT GG-3' (Einen et al., 2008)]. qPCR for archaea was carried out using primers 806f [5'-ATT AGA TAC CCS BGT AGT-3' (Takai and Horikoshi, 2000)] and 922r [5'-YCC GGC GTT GAN TCC AAT T-3' (DeLong, 1992)]. For both bacterial and archaeal qPCR, 16S rRNA copy numbers  $\text{g}^{-1}$  rock were calculated by multiplying the mean copy number detected from triplicate reactions by the dilution factor (total DNA extraction volume divided by template volume in each qPCR reaction) and divided by the weight

**Table 1 | Samples descriptions and bacterial biomass estimates.**

| Sample  | Vent field | Rock type                         | Rock mineralogy<br>(thin section)  | Rock mineralogy<br>(XRD)   | Bacterial cells g <sup>-1</sup> rock*<br>(% Bacteria versus Archaea) | Archaeal cells<br>g <sup>-1</sup> rock* |
|---------|------------|-----------------------------------|--|--|--|---|
| KiMba   | Kilo Moana | Silicate; basalt                  | Augite (<5%),<br>Plagioclase (5–10%),<br>Aegirine-augite<br><5%), amorphous<br>glass, not porous | Major species: diopside,<br>aegirine-augite<br>Minor species: augite | $4.14 \pm 0.06 \times 10^5$ (93.6%)                                  | $2.82 \pm 0.69 \times 10^4$             |
| ABEbA   | ABE        | Silicate;<br>transitional         | Augite (35%),<br>Plagioclase (20%),<br>moderately altered,<br>not porous                         | Major species:<br>albite, augite<br>Minor species: labradorite       | $5.20 \pm 0.12 \times 10^4$ (99.7%)                                  | $1.49 \pm 0.27 \times 10^2$             |
| Marba   | Mariner    | Silicate;<br>basaltic<br>andesite | Augite (5%),<br>Plagioclase (5–10%),<br>little to no alteration,<br>40% porous                   | Signal too amorphous   | $9.97 \pm 1.12 \times 10^3$ (15.4%)                                  | $5.47 \pm 1.86 \times 10^4$             |
| ABEsO** | ABE        | Outside of an<br>inactive sulfide | Poorly crystalline,<br>pyrite, sphalerite  | Sphalerite, pyrite, barite   | $9.92 \pm 0.34 \times 10^7$ (100%)                                   | Below detection                         |
| ABEsIN  | ABE        | Inside of an<br>inactive sulfide  | nd   | nd   | $1.15 \pm 0.04 \times 10^7$ (99.8%)                                  | $2.87 \pm 0.18 \times 10^4$             |
| TuiMs   | Tui Malila | Inactive sulfide                  | Cinnabar, pyrite,<br>sphalerite, anhydrite   | Barite, sphalerite, pyrite   | $3.65 \pm 0.10 \times 10^7$ (100%)                                   | Below detection                         |

\*As determined by qPCR, ±Standard Error.

\*\*Mineralogical analysis was completed for the bulk sample for ABEs, but DNA analysis was completed on two separate samples from the same chimney, one from the exterior and one from the interior conduit.

of the sample from which DNA was extracted, in grams. The cell number per gram rock was determined by assuming 3.9 16S rRNA gene copies per cell for bacteria and 1.8 16S rRNA gene copies per cell for archaea (Einen et al., 2008). The thermal program employed for both bacterial and archaeal qPCR primer sets was: 10 min at 95°C followed by 45 cycles of 30 s at 95°C, 30 s at 55°C and 25 s at 72°C. Negative controls [polymerase chain reaction (PCR) water included as a template] were included for all qPCR runs, and melt curves for all qPCR products were checked to ensure a single PCR product was generated. Reported values in **Table 1** were all greater than the negative control and no samples yielded multiple PCR products. The reported qPCR reactions were run in triplicate.

Polymerase chain reaction of the 16S rRNA gene and subsequent cloning and sequencing of the product was carried out according to Sylvan et al. (2012b). Briefly, universal bacterial primers 27F (5'-GAG TTT GAT CCT GGC TCA G-3') and 1492R (5'-RGY TAC CTT GTT ACG ACT T-3') were used for PCR. Three reactions were combined and run out on an agarose gel and then excised and extracted using the Zymoclean Gel DNA Recovery Kit (Zymo Research, Irvine, CA, USA). DNA from the extracted PCR band was cloned into the pCR 4 TOPO vector using the TOPO TA Cloning Kit (Invitrogen, Grand Island, NY, USA) and transformants were plated on LB + 100 µg mL<sup>-1</sup>ampicillin according to the manufacturer's instructions. Clones were sequenced at the Beckman Coulter Genomics center in Danvers, MA, USA.

16S rRNA contigs were generated using Geneious v5.6 (Drummond et al., 2011). Edited near full-length 16S rDNA sequences were classified and checked for chimeras using the Bellerophon tool of Greengenes (DeSantis et al., 2006b). The resulting sequences were aligned using the Greengenes NAST server (DeSantis et al., 2006a) and imported into ARB (Ludwig et al., 2004) for selection of sequences to include in phylogenetic trees. Closely related cultured strains to contigs were identified using the "Named Isolates" option with the BLAST function on the Greengenes website ([http://greengenes.lbl.gov/cgi-bin/nphblast\\_interface.cgi](http://greengenes.lbl.gov/cgi-bin/nphblast_interface.cgi)). If no closely related isolate to a contig existed, the nearest neighbor from the ARB database was identified. Closely related isolates and/or sequences were aligned with sequences from this study using MEGA 5 (Tamura et al., 2011). Phylogenetic trees were constructed following manual adjustment of this alignment using both the neighbor-joining method, based on the maximum composite likelihood model and gamma distribution, and maximum likelihood analysis, based on the Jukes–Cantor model with a Gamma distribution. Both types of phylogenies were tested using 1000 bootstrap replicates. Calculation of rarefaction curves and diversity estimates, as well as comparison between clone libraries and those of other studies, was carried out using the software Mothur (Schloss et al., 2009). Pre-clustering (Huse et al., 2010) and the average neighbor clustering algorithm were used to generate distance matrices from which rarefaction curves, estimates of shared richness (*Jclass*, *Jest*), and estimates of shared structure

(theta Yue–Clayton, or  $\Theta$  YC, and Bray–Curtis) were calculated. An operational taxonomic unit (OTU) cutoff of 97% was used for the rarefaction curves and an OTU cutoff of 95% was used for generating a cladogram for inter-sample comparison. In agreement with other prior work (Toner et al., 2013), we found that using a 95% cutoff to build cladograms yielded clearer results than a 97% cutoff. Using a 95% cutoff for OTUs, however, had little impact on the overall number of OTUs and we therefore maintained the commonly accepted value of 97% for OTUs. The cladograms were converted to a circular tree layout in Genious v5.6 (Drummond et al., 2011) and edited in Adobe Illustrator CS6.

DNA sequences generated for this project were deposited in the National Center for Biotechnology Information (NCBI) database under accession numbers KC682512–KC682862. For a few highly represented sequences, where multiple nearly identical clones were generated from a single sample, only one clone was deposited. They are listed here, followed by the number of additional clones they represent: ABEsO\_A7 (25 additional clones), Marba\_A2 (09 additional clones), ABEsIN\_H1 (15 additional clones), ABEsIN\_A1 (47 additional clones), and TuiMs\_A6 (24 additional clones).

## RESULTS

### SAMPLE DESCRIPTIONS, SILICATES

Sample KiMba is a basalt collected from Kilo Moana vent field with a visible glassy rim underlain by ground mass. We sampled the glassy rim. The thin section revealed that KiMba is porphyritic with large phenocrysts in an amorphous glassy matrix that are encroached by spherules. KiMba is not porous, and plagioclase  $[(\text{Na},\text{Ca})(\text{Si},\text{Al})_4\text{O}_8]$ , aegirine-augite  $[(\text{Ca},\text{Na})(\text{Mg},\text{Fe}^{2+},\text{Fe}^{3+})(\text{Si}_2\text{O}_6)]$ , and augite  $[(\text{Ca},\text{Na})(\text{Mg},\text{Fe},\text{Al},\text{Ti})(\text{Si},\text{Al})_2\text{O}_6]$  are represented in the thin section (Figure 2). XRD analysis revealed the presence of diopside  $[\text{CaMg}(\text{Si}_2\text{O}_6)]$  in this sample (Table 1). Sample ABEba is a basalt collected from ABE vent field with an oxidized rim. It was not porous and is rich in augite and plagioclase (Figure 2). The XRD pattern revealed the presence of albite  $(\text{NaAlSi}_3\text{O}_8)$ , augite and labradorite  $[(\text{Na},\text{Ca})(\text{Si},\text{Al})_4\text{O}_8]$ . Sample Marba is basaltic andesite collected from Mariner vent field. It is very porous (Figure 2) with little to no alteration. Plagioclase and augite were detected by thin section analysis, but the XRD signal was too weak to identify specific minerals.

### INACTIVE SULFIDES

Sample ABEs was broken off an inactive sulfide chimney located in ABE vent field. It is poorly crystalline and slightly oxidized. Light microscopy of samples in thin section revealed the presence of pyrite ( $\text{FeS}_2$ ) and sphalerite ( $\text{ZnS}$ ; data not shown); and barite ( $\text{BaSO}_4$ ) was identified in the XRD pattern. A portion of this sample was collected from the outside wall of the chimney (ABEsO) and a separate section was sampled from the inside (ABEsIN) for analysis of the microbial community. Sample TuiMs is a zoned chimney that appeared inactive (no venting or shimmering fluid observed exiting the chimney) on the seafloor at the time of sampling from the Tui Malila vent field. Sulfide minerals are present on the outer rim of the thin section and sulfide and sulfate minerals are present away from the outer rim (Figure 3). On the outer tannish red to deep maroon rim, euhedral cinnabar

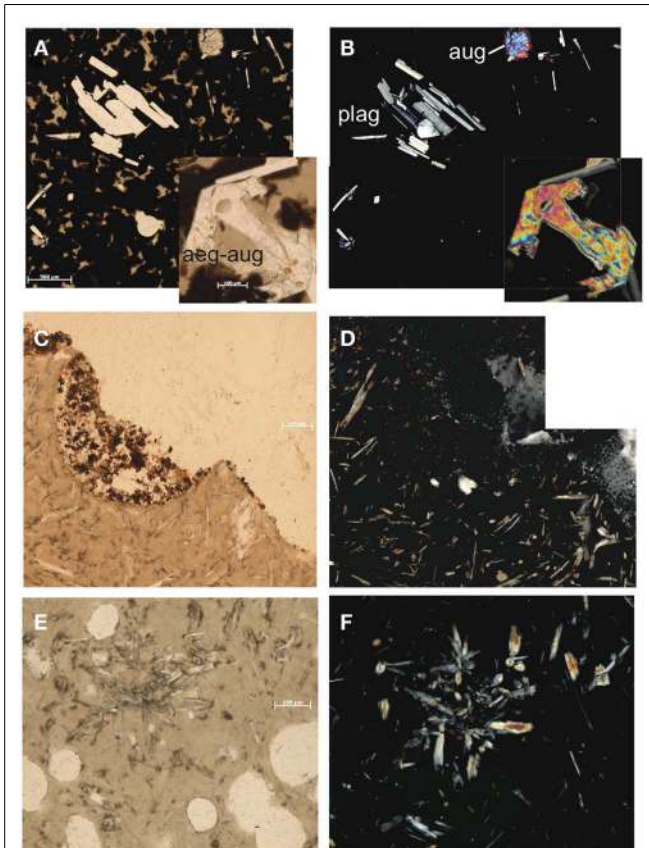


**FIGURE 2 | Thin section photomicrographs of silicate samples.** Plain polar light photomicrograph of basalt KiMba (A) and the same view in crossed polars (B). Plain polar light photomicrograph of basalt ABEba (C) and crossed polars of the same view (D). Plain polar light photomicrograph of sample basaltic andesite Marba (E) and crossed polar image of the same view (F).

( $\text{HgS}$ ) coats and encrusts anhedral pyrite. The interior edge of the thin section is characterized by anhydrite ( $\text{CaSO}_4$ ), sphalerite, and minor anhedral pyrite. XRD analysis reveals the presence of barite, sphalerite, and pyrite.

### GEOCHEMISTRY

Elemental analysis confirms transitions in host rock composition from north to south in the ELSC. Weight percent of Ba, K, P, Si, and Sr oxides and concentrations of V, Cu, Rb, Sr, Ba, La, Ce, Pr, Nd, and Th all increase from north to south in the silicates (Tables 2 and 3). Concentrations of Sc and Co follow the opposite trend. Based on analysis of total alkalis versus silica, KiMba, and ABEba are both sub-alkaline basalts while Marba is sub-alkaline basaltic andesite (data not shown).

Inactive sulfides ABEs and TuiMs were much more elevated in Ba, Cu, Zn, and Sr than the silicate samples (Tables 2 and 3). Sulfide TuiMs had nearly 10-fold more weight percent Ca than ABEs. A significant portion of ABEs and TuiMs was not acid digestible after 2 weeks in acid. This portion was collected and analyzed by XRD, which revealed that is composed of barite for both ABEs and

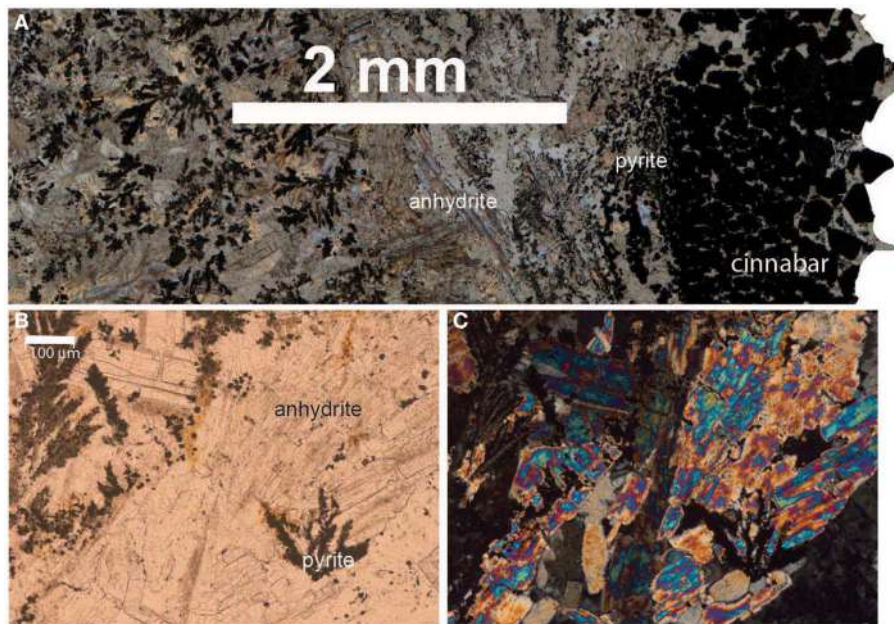


**FIGURE 3 | Thin section photomicrographs of inactive sulfide sample TuiMs.** Plain polar light photomosaic shows transition from cinnabar and pyrite on the rim to anhydrite and pyrite (A). A close up in plain polar light of the anhydrite and pyrite (B) and the same view in crossed polars (C).

**Table 2 | Major oxide composition of the rocks sampled.**

| Oxide                          | KiMba   | ABEba   | Marba   | ABEs   | TuiMs   |
|--------------------------------|---------|---------|---------|--------|---------|
| Al <sub>2</sub> O <sub>3</sub> | 14.76   | 14.5867 | 15.1733 | 0.1282 | 0.15713 |
| BaO                            | 0.0008  | 0.0148  | 0.0203  | 1.8943 | 3.175   |
| CaO                            | 12.0467 | 8.423   | 9.1697  | 0.2079 | 1.7117  |
| Fe <sub>2</sub> O <sub>3</sub> | 11.22   | 12.9633 | 11.9967 | 11.9   | 2.8467  |
| K <sub>2</sub> O               | 0.0366  | 0.2393  | 0.2588  | 0.0455 | 0.0514  |
| MgO                            | 7.7087  | 4.098   | 4.7983  | 0.0414 | 0.047   |
| MnO                            | 0.1839  | 0.3112  | 0.208   | 0.1575 | 0.0134  |
| Na <sub>2</sub> O              | 2.106   | 3.085   | 2.9113  | 0.4025 | 0.1844  |
| P <sub>2</sub> O <sub>5</sub>  | 0.0787  | 0.1402  | 0.15    | 0.0179 | 0.0025  |
| SiO <sub>2</sub>               | 50.88   | 51.8933 | 52.5033 | 8.1507 | 8.1913  |
| SrO                            | 0.0088  | 0.0167  | 0.0183  | 0.3631 | 0.2826  |
| TiO <sub>2</sub>               | 1.0097  | 1.389   | 1.3247  | 0.0105 | 0.0086  |
| ZrO <sub>2</sub>               | 0.0115  | 0.0155  | 0.0139  | 0.0015 | 0.0017  |

Note that totals for ABEs and TuiMs are not 100%; the remaining weight percent is composed primarily of barite for these two sulfides.

TuiMs. With the exception of Sc and Ba, sample ABEs had higher trace element concentrations than sample TuiMs.

## MICROBIOLOGY

Bacterial and archaeal biomass were estimated via qPCR on all samples, including one sample each collected from the outside and inside of ABEs (ABEsO and ABEsIN, respectively). Bacteria accounted for >90% of the combined Bacteria + Archaea on all samples except for Marba and bacterial biomass was higher on the inactive sulfide samples ( $7 \times 10^6$ – $6 \times 10^7$  cells g<sup>-1</sup>) than on the silicates ( $\sim 1 \times 10^4$ – $6 \times 10^5$  cells g<sup>-1</sup>; Table 1). It must be noted,

however, that because the primers used in qPCR are likely biased, this method provides an estimate, and the derived proportions are also estimates.

Given the high proportion of Bacteria versus Archaea, and their presence on all samples, we chose to analyze bacterial diversity. We PCR amplified and cloned near full-length bacterial 16S rRNA from all six samples; 469 total clones were recovered and sequenced, with 48–93 clones per sample (Figure 4). Rarefaction analysis using a 97% cutoff for OTU designation reveals that both basalt samples are more diverse than the other samples (Figure 4). Sample Marba exhibits the lowest diversity.

Further analyses of bacterial OTUs recovered at the phylum level reveals that some phyla exhibit north to south patterns in distribution on the silicates (Figure 4; Figure A2 in Appendix).  $\alpha$ -Proteobacteria decrease in proportion from north to south, as do  $\epsilon$ -proteobacteria and Bacteroidetes. In contrast, Planctomycetes and Chloroflexi increase in proportion from north to south. Because there are only two inactive sulfides, we cannot delineate any conclusions about north to south distributions of bacterial communities on hydrothermally inactive sulfides.

Bacterial populations on the inactive sulfide samples are markedly different from those on the silicates at the phylum level, and each of the three inactive sulfide samples are different from each other. No Chloroflexi were recovered from the sulfides, but given the smaller datasets generated by clone libraries compared to pyrosequencing (e.g., Flores et al., 2012), the absence of taxa must be treated with caution. Sample ABEsO is dominated by  $\gamma$ -proteobacteria, but the inner conduit of the same chimney, ABEsIN, is dominated by  $\delta$ -proteobacteria. Some  $\epsilon$ -proteobacteria and Bacteroidetes are also recovered from ABEsIN, but not from ABEsO. Sample TuiMs harbors a high proportion of

**Table 3 | Trace element compositions of the rocks sampled.**

| Element           | KiMba   | ABEbba  | Marba   | ABEs     | TuiMs   |
|-------------------|---------|---------|---------|----------|---------|
| <sup>7</sup> Li   | 5.13    | 7.51    | 6.14    | 0.74     | 0.33    |
| <sup>31</sup> P   | 271.90  | 504.30  | 535.05  | 70.32    | 18.96   |
| <sup>45</sup> Sc  | 43.61   | 36.56   | 35.80   | 0.03     | 0.04    |
| <sup>51</sup> V   | 340.50  | 417.55  | 428.85  | 6.98     | 3.61    |
| <sup>52</sup> Cr  | 175.50  | 2.45    | 28.76   | 0.89     | 0       |
| <sup>55</sup> Mn  | 1500.50 | 2821.50 | 1685.50 | 1277.50  | 110.50  |
| <sup>59</sup> Co  | 42.91   | 36.95   | 33.30   | 0.05     | 0.01    |
| <sup>60</sup> Ni  | 69.31   | 23.89   | 23.84   | 3.04     | 0.48    |
| <sup>65</sup> Cu  | 77.42   | 77.74   | 80.19   | 2995.00  | 1950.00 |
| <sup>66</sup> Zn  | 86.48   | 133.50  | 84.49   | 102150.0 | 68325.0 |
| <sup>71</sup> Ga  | 15.66   | 18.13   | 17.66   | 2.82     | 11.93   |
| <sup>72</sup> Ge  | 2.49    | 2.73    | 2.63    | 33.32    | 16.25   |
| <sup>85</sup> Rb  | 0.74    | 3.96    | 5.19    | 1.70     | 1.08    |
| <sup>86</sup> Sr  | 75.41   | 143.00  | 155.65  | 3014.00  | 2267.00 |
| <sup>89</sup> Y   | 25.83   | 32.86   | 29.99   | 0        | 0       |
| <sup>91</sup> Zr  | 55.06   | 83.52   | 74.71   | 1.92     | 0.34    |
| <sup>93</sup> Nb  | 0.55    | 1.01    | 0.78    | 0        | 0       |
| <sup>95</sup> Mo  | 0       | 1.39    | 0.46    | 50.80    | 15.08   |
| <sup>111</sup> Cd | 0.07    | 0.17    | 0.07    | 96.67    | 196.80  |
| <sup>118</sup> Sn | 0.52    | 0.81    | 0.65    | 0        | 0       |
| <sup>121</sup> Sb | 0       | 0       | 0       | 42.26    | 68.94   |
| <sup>133</sup> Cs | 0       | 0       | 0       | 0.11     | 0       |
| <sup>137</sup> Ba | 7.73    | 143.05  | 195.60  | 662.55   | 932.90  |
| <sup>139</sup> La | 1.62    | 3.09    | 3.61    | 0.67     | 0.47    |
| <sup>140</sup> Ce | 5.69    | 9.31    | 10.38   | 1.02     | 0.56    |
| <sup>141</sup> Pr | 1.04    | 1.67    | 1.73    | 0.09     | 0.04    |
| <sup>146</sup> Nd | 6.33    | 9.64    | 9.71    | 0.24     | 0.10    |
| <sup>147</sup> Sm | 2.45    | 3.37    | 3.35    | 0.02     | 0.00    |
| <sup>151</sup> Eu | 0.92    | 1.24    | 1.21    | 0.07     | 0.06    |
| <sup>157</sup> Gd | 3.63    | 4.81    | 4.65    | 0.01     | 0.01    |
| <sup>159</sup> Tb | 0.68    | 0.86    | 0.82    | 0.00     | 0.00    |
| <sup>163</sup> Dy | 4.93    | 6.14    | 5.82    | 0        | 0       |
| <sup>165</sup> Ho | 1.07    | 1.31    | 1.23    | 0.00     | 0.00    |
| <sup>166</sup> Er | 3.30    | 4.04    | 3.75    | 0.00     | 0       |
| <sup>169</sup> Tm | 0.48    | 0.59    | 0.55    | 0.00     | 0.00    |
| <sup>172</sup> Yb | 3.23    | 3.94    | 3.65    | 0.00     | 0       |
| <sup>175</sup> Lu | 0.50    | 0.61    | 0.56    | 0.00     | 0.00    |
| <sup>178</sup> Hf | 1.76    | 2.49    | 2.40    | 0.02     | 0       |
| <sup>181</sup> Ta | 0       | 0       | 0       | 0        | 0.01    |
| <sup>182</sup> W  | 0.07    | 0.12    | 0.07    | 0.05     | 0.00    |
| <sup>208</sup> Pb | 0       | 3.07    | 1.41    | 3749.00  | 4972.50 |
| <sup>232</sup> Th | 0.06    | 0.16    | 0.30    | 0.00     | 0       |
| <sup>238</sup> U  | 0       | 0       | 0       | 1.05     | 0.00    |

All concentrations are in ppm.

Proteobacteria in general, and  $\epsilon$ -proteobacteria are the most commonly recovered class.  $\delta$ -Proteobacteria,  $\gamma$ -proteobacteria, and Planctomycetes are the only phyla recovered from all six samples.

Recovered clones that group within the  $\gamma$ -proteobacteria include members of the orders Methylococcales, Thiotrichales, Chromatiales, and Pseudomonadales (Figure 5). Clones classified as Methylococcales are recovered only from sample KiMba.

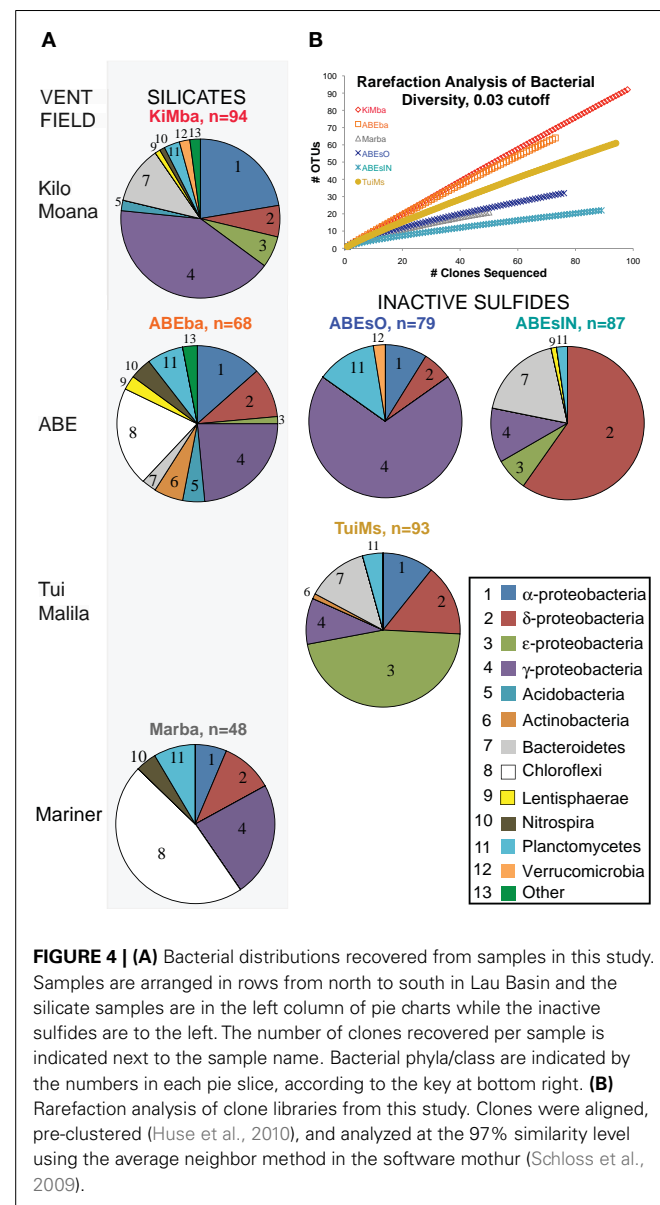
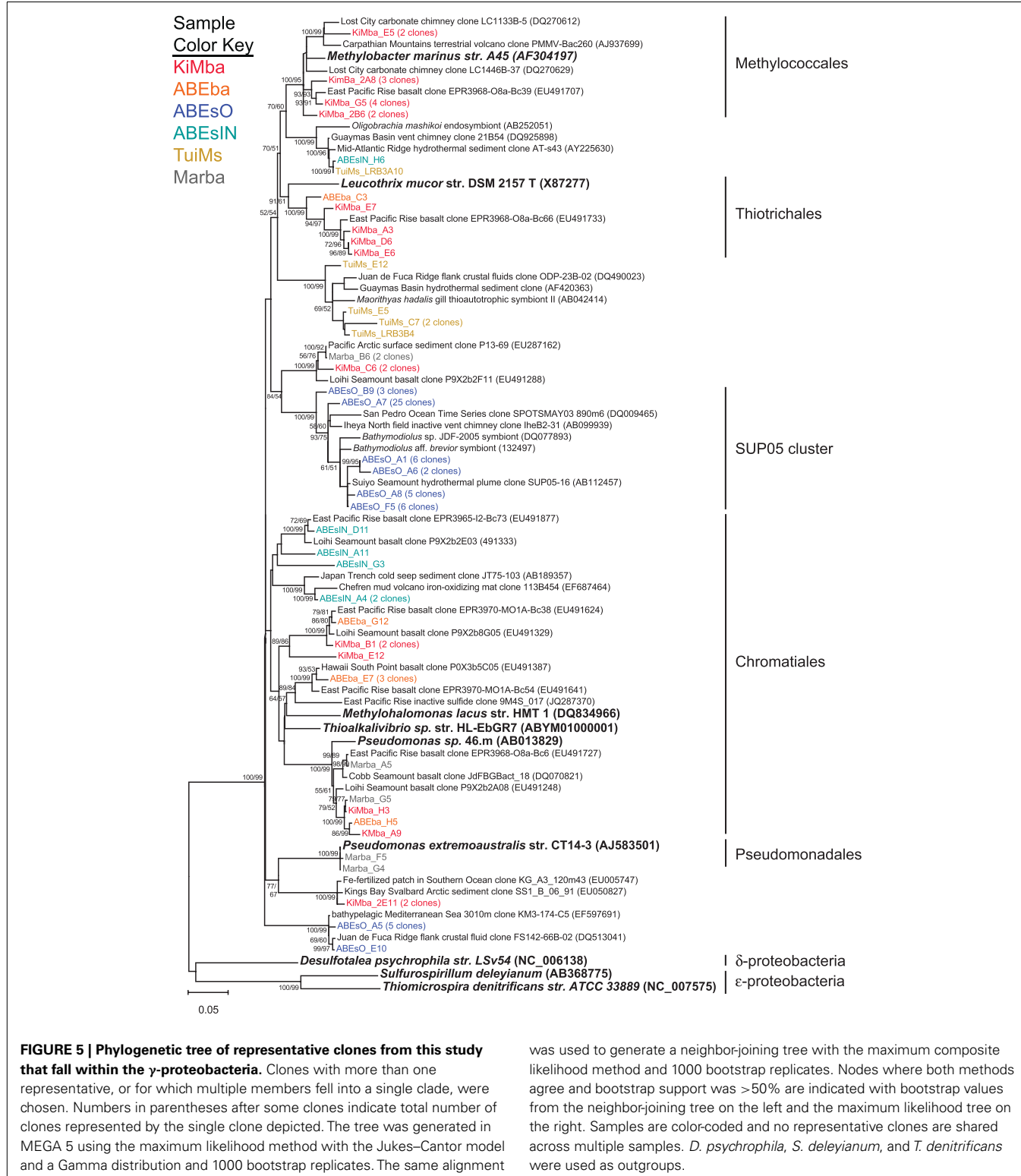


**FIGURE 4 | (A)** Bacterial distributions recovered from samples in this study. Samples are arranged in rows from north to south in Lau Basin and the silicate samples are in the left column of pie charts while the inactive sulfides are to the left. The number of clones recovered per sample is indicated next to the sample name. Bacterial phyla/class are indicated by the numbers in each pie slice, according to the key at bottom right. **(B)** Rarefaction analysis of clone libraries from this study. Clones were aligned, pre-clustered (Huse et al., 2010), and analyzed at the 97% similarity level using the average neighbor method in the software mothur (Schloss et al., 2009).

Those within the Thiotrichales are from the two basalt samples, while clones that fall within the Chromatiales order were recovered from all three silicate samples. Forty-seven clones recovered from ABEsO fall within the SUP05 clade of  $\gamma$ -proteobacteria, but these are exclusive to this sample. Nearly all of the clones that fall within the  $\gamma$ -proteobacteria are most similar to clones or isolates from other mid-ocean ridge or sedimentary settings.

Some of the clones from samples KiMba and TuiMs are closely related to  $\alpha$ -proteobacteria within the Roseobacter clade and the genus *Hyphomicrobium* (Figure 6). Clones that fall within the  $\delta$ -proteobacteria are related to *Nitrospina* and *Desulfocapsa* and uncultured clones from other hydrothermal vent and sedimentary environments. Thirty-three clones recovered from TuiMs and three from ABEsIN are most similar to isolates in the genus *Sulfurimonas* [*Thiomicrospira denitrificans* was recently reclassified into this genus (Takai et al., 2006)].



A diverse group of clones were recovered from our samples that group with phyla outside the Proteobacteria (Figure 7). Among these are a clade of Chloroflexi recovered from the two silicates ABEBa and Marba. None of these clones are closely related to

any cultured isolates, and the most similar environmental clone in the NCBI database is only 95% similar to clone ABEBa\_C8. Eighteen clones recovered from only inactive sulfides TuiMs and ABESIN, represented by clones ABESIN\_H1 and TuiMs\_LRBf3,

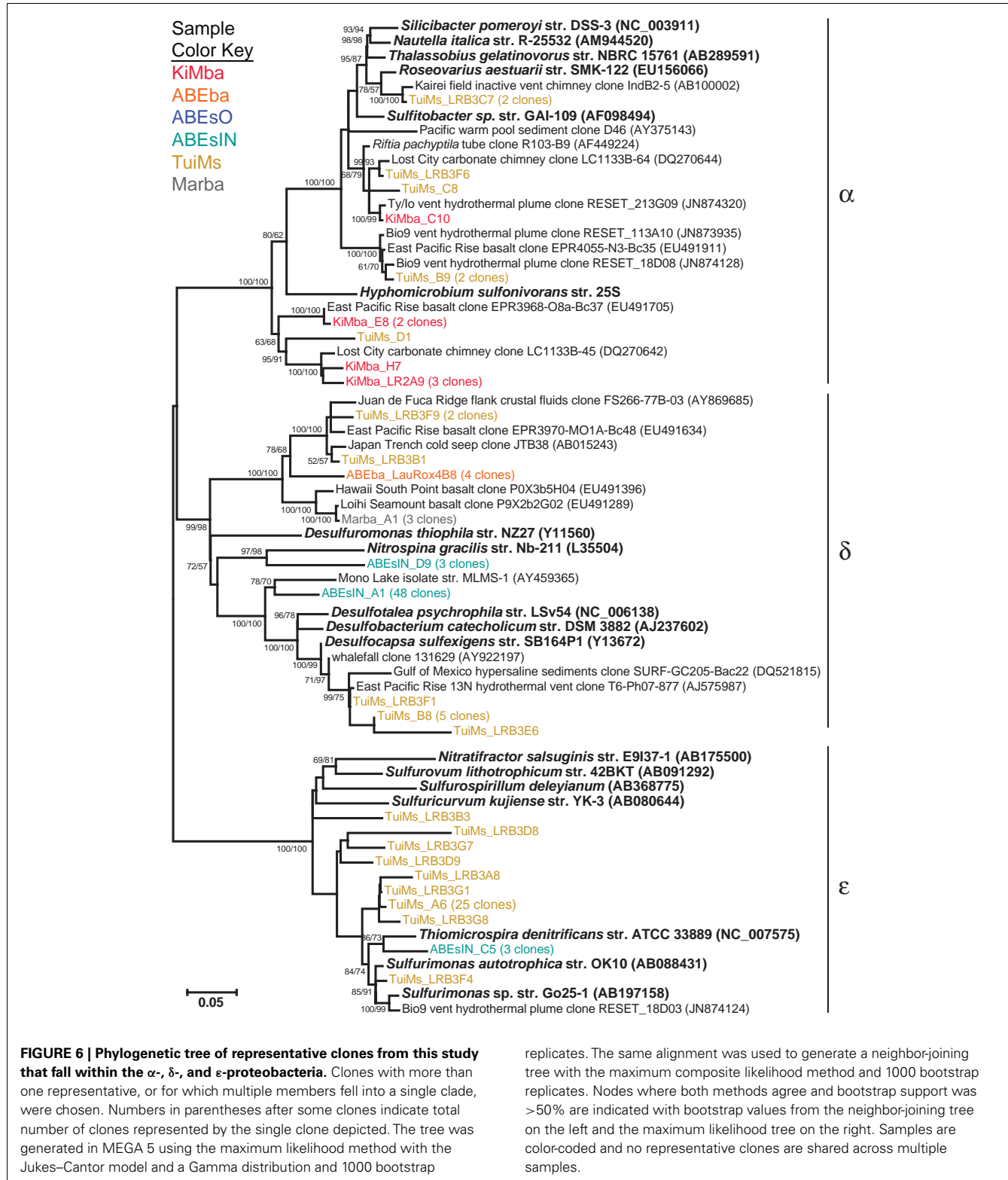


**FIGURE 6 | Phylogenetic tree of representative clones from this study that fall within the  $\alpha$ -,  $\delta$ -, and  $\epsilon$ -proteobacteria.** Clones with more than one representative, or for which multiple members fell into a single clade, were chosen. Numbers in parentheses after some clones indicate total number of clones represented by the single clone depicted. The tree was generated in MEGA 5 using the maximum likelihood method with the Jukes-Cantor model and a Gamma distribution and 1000 bootstrap

group within a cluster of Bacteroidetes clones recovered from other inactive sulfides. This cluster falls within a larger clade, to which clone TuiMs\_LR3E8 belongs, comprised of Bacteroidetes clones recovered exclusively from sulfidic environments.

replicates. The same alignment was used to generate a neighbor-joining tree with the maximum composite likelihood method and 1000 bootstrap replicates. Nodes where both methods agree and bootstrap support was  $>50\%$  are indicated with bootstrap values from the neighbor-joining tree on the left and the maximum likelihood tree on the right. Samples are color-coded and no representative clones are shared across multiple samples.

Nitrospirae were recovered from the three silicates, but not from the sulfides. These clones group most closely with *Nitrospira marina* (Figure 7). Four clones represented by clone ABEba\_C10 are 85% similar to *Ferrimicrobium acidiphilum* str.

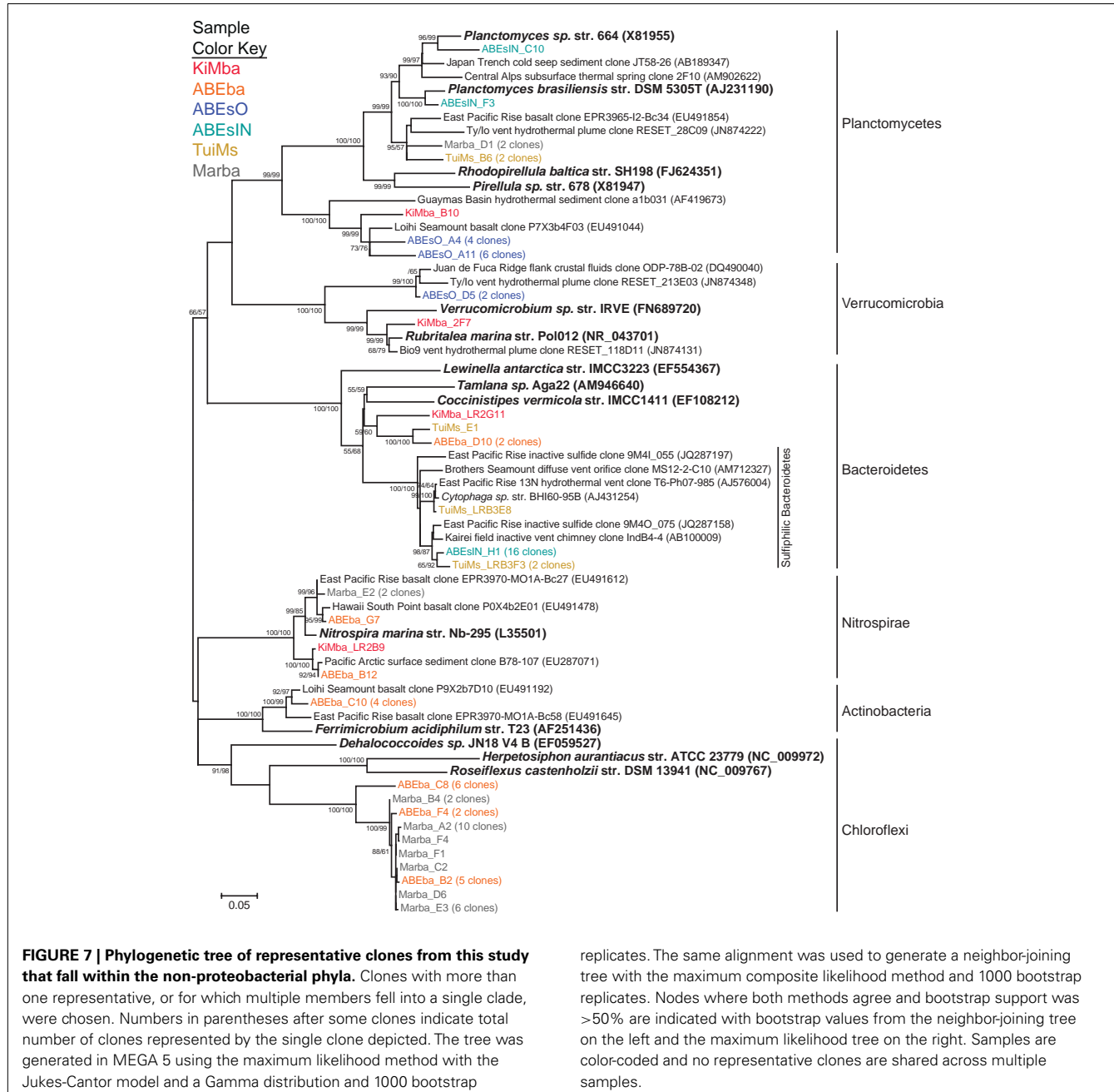


**FIGURE 7 | Phylogenetic tree of representative clones from this study that fall within the non-proteobacterial phyla.** Clones with more than one representative, or for which multiple members fell into a single clade, were chosen. Numbers in parentheses after some clones indicate total number of clones represented by the single clone depicted. The tree was generated in MEGA 5 using the maximum likelihood method with the Jukes-Cantor model and a Gamma distribution and 1000 bootstrap

replicates. The same alignment was used to generate a neighbor-joining tree with the maximum composite likelihood method and 1000 bootstrap replicates. Nodes where both methods agree and bootstrap support was >50% are indicated with bootstrap values from the neighbor-joining tree on the left and the maximum likelihood tree on the right. Samples are color-coded and no representative clones are shared across multiple samples.

T23 and *Acidimicrobium ferrooxidans*, both iron oxidizing acidophiles.

#### CORRELATIONS BETWEEN GEOCHEMISTRY AND MICROBIOLOGY

We used the elemental composition and phylogenetic data to determine correlations between geochemistry and microbiology. For this purpose, the same elemental data was used for ABEsO and ABEsIN because a bulk sample from this sulfide was analyzed for geochemistry. Ideally, one would compare the presence of individual OTUs in a sample with geochemical data to identify correlations between the two. However, using a 97% similarity cutoff for OTUs, only one OTU, comprised by clones TuiMs\_LRB3A10

and ABEsIN\_H6 (Figure 5), has membership from two different samples, and therefore no correlations exist at this cutoff between OTUs and geochemistry. Using a 10% cutoff only resulted in six OTUs with membership from multiple samples. Therefore, we measured correlations between the geochemical data and the abundance of bacterial phyla, as represented by their percentage on each sample. We do not report correlations between elemental variables alone because larger datasets are available for such purposes (e.g., Escrig et al., 2009).

Nitrospirae and Chloroflexi are the only phyla with significant correlations to geochemistry. Both are strongly positively correlated to P, V, La, Ce, Pr, Nd, Th,  $P_2O_5$ , and  $SiO_2$  (Table 4).

**Table 4 | Kendall's  $\tau$  correlations between elemental data and bacterial distributions.**

| Variable 1               | By variable 2  | Kendall $\tau$ | Prob >   $\tau$ |
|--------------------------|--|----------------|-----------------|
| $\gamma$ -Proteobacteria | $\delta$ -Proteobacteria   | -0.9429        | 0.0048          |
| Nitrospirae              | Y, Nb, Sn, Tb, Dy, Ho, Er, Tm, Yb & Lu   | 1              | <0.0001         |
| Nitrospirae              | Li, Mn, Ga, Zr, Sm, Eu, Gd, Hf, W, MnO, Na <sub>2</sub> O, TiO <sub>2</sub> & ZrO <sub>2</sub>   | 0.9549         | 0.0030          |
| Nitrospirae              | P, V, La, Ce, Pr, Nd, Th, P <sub>2</sub> O <sub>5</sub> & SiO <sub>2</sub>                       | 0.8933         | 0.0165          |
| Nitrospirae              | Sb   | -0.8854        | 0.0190          |
| Nitrospirae              | Chloroflexi  | 0.8262         | 0.0427          |
| Bacteroidetes            | $\epsilon$ -Proteobacteria   | 0.9412         | 0.0051          |
| Planctomycetes           | Bacteroidetes  | -0.9276        | 0.0077          |
| Planctomycetes           | $\epsilon$ -Proteobacteria   | -0.8117        | 0.0499          |
| Chloroflexi              | P, V, Rb, La, Ce, Pr, Nd, Th, K <sub>2</sub> O, P <sub>2</sub> O <sub>5</sub> , SiO <sub>2</sub> | 0.8575         | 0.0291          |
| Verrucomicrobia          | $\delta$ -Proteobacteria   | -0.8452        | 0.0341          |
| Verrucomicrobia          | $\gamma$ -Proteobacteria   | 0.8452         | 0.0341          |

Correlations between pairs of variables that are both elemental data are not included here. Only correlations for which  $p < 0.05$  are presented here. When multiple variables are listed in the "by Variable 2" column, this means that both Kendall  $\tau$  and Prob > |  $\tau$  | values are the same between Variable 1 and all variables listed in "by Variable 2" column.

Nitrospirae are additionally positively correlated to the abundance of Y, Nb, Sn, Tb, Dy, Ho, Er, Tm, Yb, Lu, Li, La, Mn, Ga, Zr, Sm, Eu, Gd, Hf, W, MnO, Na<sub>2</sub>O, TiO<sub>2</sub>, and ZrO<sub>2</sub>, and negatively correlated to Sb. A negative correlation exists between abundance of  $\gamma$ -proteobacteria and  $\delta$ -proteobacteria, Planctomycetes and Bacteroidetes, Planctomycetes and  $\epsilon$ -proteobacteria, and Verrucomicrobia and  $\delta$ -proteobacteria. There was a positive correlation between the proportion of Bacteroidetes and  $\epsilon$ -proteobacteria, Nitrospirae and Chloroflexi, and Verrucomicrobia and  $\gamma$ -proteobacteria.

### INACTIVE SULFIDE BIOGEOGRAPHY

We compared the bacterial communities on inactive sulfides recovered during this study with those from previous studies (Suzuki et al., 2004; Kato et al., 2010; Sylvan et al., 2012a; Toner et al., 2013) using an OTU-based approach to determine if the bacterial communities on ABEs and TuiMs are similar to that from any previously analyzed inactive sulfides, and also to determine if any biogeographical patterns could be detected amongst bacterial communities on inactive sulfides (Figure 8). The three silicates from the present study were also included in this analysis. Shared richness of the bacterial communities, as determined using the J<sub>class</sub> and J<sub>est</sub> calculators, and shared structure as determined using the Yue–Clayton and Bray–Curtis calculators, generated similar

results. Sulfide sample TuiMs grouped closely with sulfide rubble collected near K vent at 9°N EPR (3M34 and 3M23), from which a larger proportion of  $\epsilon$ -proteobacteria were recovered than other inactive sulfides. ABEsIN grouped with EPR samples from which  $\delta$ -proteobacteria are prevalent and ABEsO grouped with samples from an inactive sulfide collected from the Okinawa Trough. All three silicates from this study grouped with three samples analyzed from the same inactive sulfide collected from the Mariana Trough.

## DISCUSSION

### NOVELTY OF WORK

Here we investigated microbiology along a geochemical gradient in the ELSC. This back-arc spreading system is of particular interest because it displays clear trends in host rock geochemistry (Escrig et al., 2009; Dunn and Martinez, 2011; Mottl et al., 2011) that are hypothesized to influence microbial communities. We targeted low temperature deposits from four fields along this geochemical gradient and were able to detect patterns in bacterial community composition that correlate with changes in geochemistry. This is also the first study of microbial populations on basaltic andesite. Our sample set is admittedly small compared to pyrosequencing datasets generated by next generation sequencing methods, but the data recovered are informative and we view this work as an initial survey of low temperature geomicrobiology in Lau Basin. It should also be noted that it is unknown if the organisms detected in this study are active, and that DNA may last for some time in the environment, as indicated by the presence of extracellular DNA in deep-sea sediments (Dell'Anno and Danovaro, 2005).

### SILICATES

Our geochemical and mineralogical analysis of the silicates collected reinforces north-south along axis patterns seen for Si, Sr, Ba, La, Ce, Nd, and Th in previous work that looked at fresh lava flows in the ELSC (Escrig et al., 2009; Dunn and Martinez, 2011). It must be pointed out that our samples were not specifically selected for lack of alteration, unlike those in these aforementioned studies. Therefore, deviations from the previous study such as the Ba/Th and Th/La ratios, may be due to oxidative alteration of the collected rocks, or incomplete digestion of Ba-bearing minerals. Accordingly, we use the mineralogical and geochemical data here to better understand the nature of relationships among geochemistry and microbial populations, not to draw larger conclusions about geochemistry in the ELSC.

Bacterial communities on basalts from Lau Basin were more diverse than those on inactive sulfides from this study (Figure 4), in agreement with prior work indicating basalts host extremely diverse bacterial populations (Santelli et al., 2008). Within the sulfide samples, TuiMs is more diverse than both ABEsO and ABEsIN. Inactive sulfide ABEs is ~150% more enriched in Zn than is TuiMs. A recent comparison of inactive sulfides from the EPR found that Zn-rich chimneys harbor fewer OTUs than Fe-rich sulfides (Toner et al., 2013). This is also true here.

North to south patterns in bacterial community composition occur at the phylum level in the ELSC. Kilo Moana (north) is analogous to a mid-ocean ridge vent field, whereas Mariner (south) is strongly influenced by subduction, and ABE exhibits transitional characteristics between the two end-members. As such, patterns

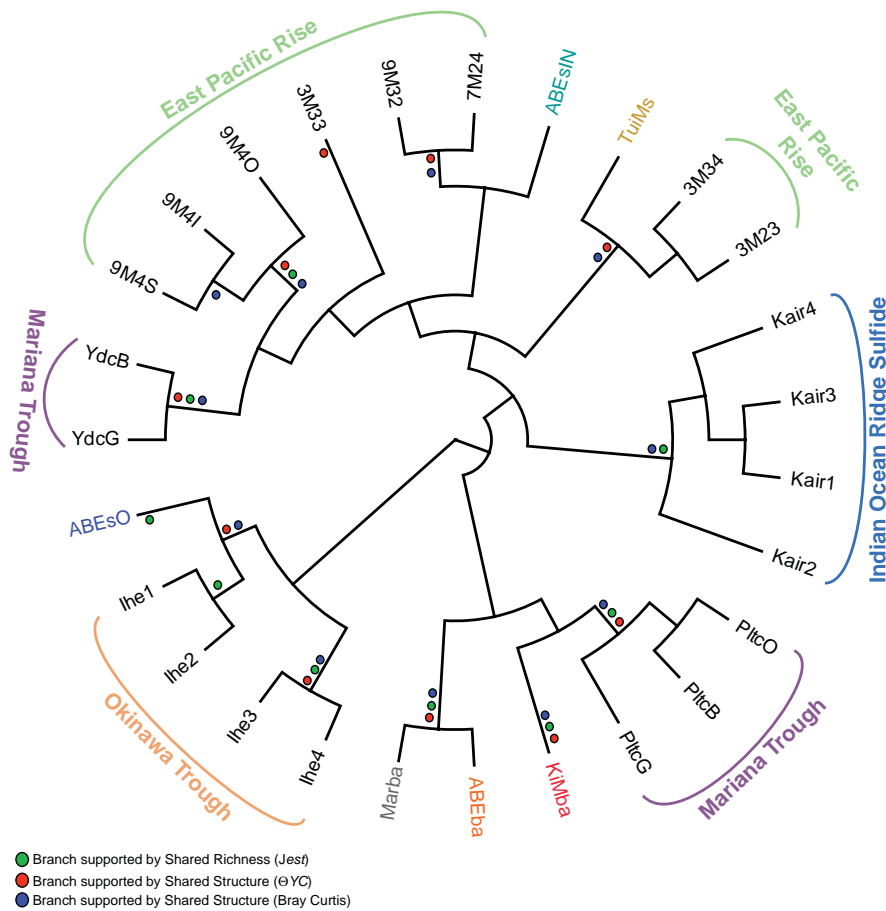


**FIGURE 8 | Cladogram of OTU-based comparison of bacterial communities sampled from inactive sulfides in this and prior studies using the  $J_{\text{class}}$  algorithm.** The three silicate samples from this study are included. Where the  $J_{\text{class}}$  analysis agreed with community comparison using Jest,  $\Theta$ YC, and/or Bray–Curtis algorithms, a dot for the agreeing methods is placed at the node in the cladogram. Overall

agreement is strong between all four methods save for sample 3M33 from the EPR. Sampling location is indicated for samples from prior studies: EPR (Sylvan et al., 2012a), Mariana Trough (Kato et al., 2010), and the Indian Ocean Ridge and Okinawa Trough (Suzuki et al., 2004). Sample color code for samples from this study is the same as in Figures 4–7.

of bacterial membership on the silicate rocks follow this pattern linearly for the  $\alpha$ -proteobacteria,  $\varepsilon$ -proteobacteria, Bacteroidetes, Planctomycetes, and Chloroflexi, where the proportional representation of each phylum on sample ABEba falls between that on samples KiMba and Marba. This is supported in part by the high positive correlation between Bacteroidetes and  $\varepsilon$ -proteobacteria (both decreased from north to south) and the negative correlation between Planctomycetes and Bacteroidetes (opposite north to south patterns). These gradients are likely drivers for absence of shared OTUs between bacterial communities detected on each sample. This is reinforced by Libshuff analysis, which reveals that each silicate harbors a unique bacterial community. Further, when the inactive sulfides are included in this analysis, all six samples in this study are significantly different from each other.

The bacterial community on sample Marba is quite different from what has been observed on previously studied seafloor-exposed basalts (Lysnes et al., 2004; Mason et al., 2009; Santelli et al., 2009), and also from the other basalt samples in this study. The qPCR results indicate that biomass is very low on this sample

compared to mid-ocean ridge basalts, which can host bacterial biomass up to  $10^9$  cells  $\text{g}^{-1}$  (Santelli et al., 2008). Archaea outnumbered Bacteria on sample Marba, whereas all previously measured basalt samples had higher bacterial populations by  $\sim 9:1$  (Einen et al., 2008; Santelli et al., 2008), as did samples KiMba and ABEba.

The high proportion on Marba of clones that fall within the phylum Chloroflexi is also unusual compared to previously analyzed basalts; while this phylum is often represented as a few percent of the total clones on seafloor-exposed basalt samples from mid-ocean ridge settings, the large community membership of a monophyletic clade of Chloroflexi, as seen here, has not previously been observed. Clones from the same clade were also recovered from sample ABEba and all members of this clade are  $<90\%$  similar to the most closely related sequences in the NCBI database. As such, it is impossible to speculate on the ecological niche for the organisms represented by these clones, or whether their presence is or is not affected by substrate geochemistry. The Chloroflexi clones recovered from samples Marba and ABEba fall within the class Anaerolineae, which was also recovered from active hydrothermal

vent sulfides at Mariner (Takai et al., 2008; Flores et al., 2012). However, these studies found low proportions of Anaerolineae, and the clones from active chimneys are distantly related to the clones recovered from samples Marba and ABEba. The classification of the Chloroflexi clones from Marba and ABEba within the same class as those found on active vents indicates that, while unusual, these are not resultant from contamination.

Our finding of a microbial community on a silicate from Mariner vent field that is distinct from those collected at ABE and Kilo Moana mirrors a detailed study of bacterial and archaeal diversity on active sulfide chimneys in the ELS, which also found the microbial communities at Mariner to be distinct (Flores et al., 2012). In that study, the unique geochemistry of the hydrothermal fluids was a driver of the microbial community structure; we believe that the geochemistry of the host rock silicates at Mariner has an equal influence on the microbial communities they support.

Clones classified within the phylum Nitrospirae and the genus *Nitrospira* and the  $\gamma$ -proteobacterial order Chromatiales were recovered from all three silicate samples. The clones related to *Nitrospira* fall within *Nitrospira* sublineage IV, which are known to oxidize nitrite to nitrate mixotrophically (Daims et al., 2001). Members of the Chromatiales are chemolithotrophic sulfur oxidizers that may be capable of autotrophy (Brenner et al., 2005). Clones in both these phyla were closely related to environmental clones recovered from seafloor-exposed basalts from the Juan de Fuca Ridge, Loihi Seamount, and the EPR (Mason et al., 2009; Santelli et al., 2009), indicating that these are widespread lineages on seafloor basalts.

Many of the bacterial clones recovered from silicate samples KiMba and ABEba are closely related to isolates involved in sulfur, methane, and hydrogen biogeochemical cycling. Within the  $\gamma$ -proteobacteria, this includes clones that fall within the order Methylcoccales, aerobic methanotrophs, as well as OTUs allied to the orders Thiotrichales and Chromatiales (Figure 8). Known sulfur oxidizers populate both of these orders. Clones recovered from the basalts classified as  $\epsilon$ -proteobacteria are most closely related to the genera *Sulfurospirillum*, *Nitratirfractor*, and endosymbionts of vent macrofauna (Figure A3 in Appendix). Species within the genus *Sulfurospirillum* heterotrophically oxidize sulfur while those within *Nitratirfractor* chemoautotrophically couple nitrate reduction with H<sub>2</sub> oxidation (Nakagawa et al., 2005; Campbell et al., 2006). The phylum  $\delta$ -proteobacteria is represented by clones from all three silicate samples, indicating that sulfur oxidation and reduction are likely occurring within different niches on the same rocks.

Previous studies have also noted the co-occurrence of sulfur oxidizing and sulfur reducing bacteria on seafloor-exposed basalts (Santelli et al., 2009; Sudek et al., 2009). This indicates that pores within the rocks provide different niches for diverse microbial lifestyles. Fresh basalt is rich in reduced sulfur and therefore sulfur oxidizing lineages are expected (Bach and Edwards, 2003). However, sulfur reducers (both sulfate reducers and bacteria carrying out sulfur disproportionation) may thrive in anaerobic and microaerophilic pockets of these same rocks, where they respire seawater sulfate or oxidized sulfur compounds in the rock substrate, such as elemental sulfur. This is known to occur with iron-respiring microbes on basalts – iron-oxidizers and anaerobic

iron-reducers can be grown on separate incubations of the same basalt rock (Bailey et al., 2009), and therefore, could occur with sulfur respiring bacteria as well.

## INACTIVE SULFIDES

We observed differences between the bacterial communities detected on silicate samples and those detected on the inactive sulfides. This is in agreement with recent work that shows geochemistry strongly influences bacterial community membership on a given substrate, even when temperature and location are similar (Toner et al., 2013), as is the case here for samples ABEba, ABEsO, and ABEsIN, which were all collected from ABE vent field. Further, we found significant differences between bacterial communities detected on the outer chimney wall and inner conduit of the same inactive sulfide chimney, ABEs. Similar zonation was noted in prior studies of both active and inactive sulfide chimneys (Schrenk et al., 2003; Suzuki et al., 2004; Kormas et al., 2006; Sylvan et al., 2012a), likely due to the diverse chemical microenvironments that exist in chimneys, providing many niches for microbes (Kristall et al., 2011).

Sample ABEsO is host to a population of  $\gamma$ -proteobacteria that belongs to the SUP05 clade (Figure 5). The SUP05 clade was originally detected in the hydrothermal plume of the Suiyo Seamount (Sunamura et al., 2004) and has since been detected in hydrothermal plumes in vent fields from Guaymas Basin (Dick and Tebo, 2010), the Mid-Cayman Rise (German et al., 2010), and globally distributed oxygen minimum zones (Walsh et al., 2009). A single clone was also detected on an inactive sulfide collected from the Okinawa Trough (Kato et al., 2010). Metagenomic analysis indicates that these organisms are autotrophic sulfur oxidizers (Walsh et al., 2009). The SUP05 related clones detected in sample ABEsO indicate that these organisms are largely responsible for sulfur oxidation on the outside of this sulfide chimney, but this clade was not detected on the inside of the same sample (ABEsIN). There, a clade that falls within the Chromatiales order, represented by clone ABEsIN\_A4 and three nearby clones (Figure 5), as well as a few  $\epsilon$ -proteobacterial clones, represented by clone ABEsIN\_C5 (Figure 6), likely fulfill the role of sulfur oxidation. These differences are likely due to affinity for different mineralogy between these two clades, or residual community differences inherited from past temperature and geochemical regimes within the active structure.

Clones TuiMs\_LRB3C7, TuiMs\_LRB3F6, TuiMs\_C8, and TuiMs\_B9 (Figure 6) all belong to the  $\alpha$ -proteobacterial family Rhodobacteraceae and are most similar to cultured representatives belonging to the genera *Sulfitobacter* and *Roseovarius*. All the species from these genera whose genome has been sequenced contain the *sox* cluster of genes that imparts the ability to oxidize sulfur (Newton et al., 2010). Therefore, it is likely that inactive sulfide TuiMs harbors at least three different niches for sulfur oxidation to accommodate for S-oxidizing SUP05 bacteria,  $\epsilon$ -proteobacteria, and Rhodobacteraceae.

The clones representative of  $\delta$ -proteobacterial lineages recovered from ABEsIN are only distantly related to their closest cultured relatives; clone ABEsIN\_D9 is 83% similar to *Nitrospina griacilis*, a nitrite oxidizer, and clone ABEsIN\_A1 is 89% similar to both Mono Lake isolate strain MLMS-1 and *Desulfovibrio*

*alkaliphilus* str. AHT2. This former isolate autotrophically couples sulfur oxidation with As-reduction (Hoeft et al., 2004), while the latter oxidizes reduced sulfur compounds (Sorokin et al., 2008). Therefore, it is impossible to assign an ecological role to these clones. As on the silicates studied here, there are also clones representative of  $\delta$ -proteobacteria that are most likely representative of sulfur reducers on the same rocks with sulfur oxidizers (e.g., TuiMs\_B8; Figure 6). This indicates multiple niches within these sulfides, as mentioned above.

Clones TuiMs\_LRB3F3 and ABEsIN\_H1 (Figure 7) group with closely related clones recovered from inactive sulfides collected from the EPR (Sylvan et al., 2012b) and Indian Ocean (Suzuki et al., 2004). In the EPR study, these clones represented 17% of all the clones recovered, and were detected on six of seven samples. Similar clones detected via BlastN (Altschul et al., 1990) in the NCBI database are all from inactive sulfides collected during these previous studies or sulfidic environments such as active hydrothermal vents, oxygen minimum zones, and sediments. Phylogenetic analysis indicates the Bacteroidetes represented by these clones

form their own clade (Figure 9), for which we propose the name of “Sulfophilic Bacteroidetes.” This group includes clones recovered exclusively from sulfidic environments, but no published isolates currently exist. The Sulfophilic Bacteroidetes fall within the Bacteroidales order of the Bacteroidetes; at this broad level of classification, it is impossible to assign an ecological niche to the organisms represented by these clones. It is, however, likely that the Sulfophilic Bacteroidetes require reduced sulfur for growth, given that they are recovered exclusively from sulfidic environments.

Following cessation of venting on a sulfide chimney, a different bacterial assemblage is known to succeed the one present during active venting (Sylvan et al., 2012a). This assemblage is unique from that found on active chimneys (Kato et al., 2010; Sylvan et al., 2012a) and is also different from bacterial communities on other geological substrates in the deep ocean, such as seafloor basalts and sediment (Toner et al., 2013). One of the hallmarks of the succession on hydrothermal sulfide structures is the much lower proportion of  $\epsilon$ -proteobacteria on inactive sulfides (Sylvan et al., 2012a); however,  $\epsilon$ -proteobacteria in the genera *Sulfurimonas*

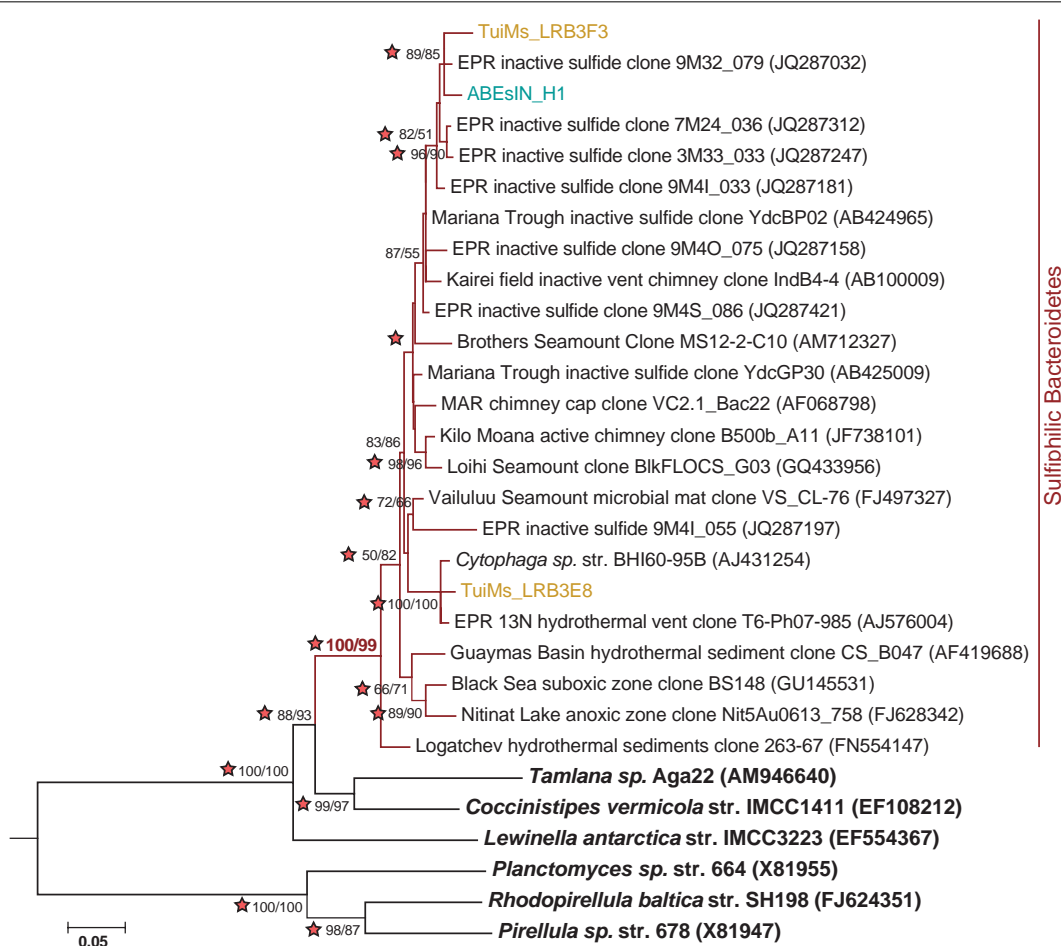


**FIGURE 9 |** Phylogenetic tree of representative clones from this study that fall within the Sulfophilic Bacteroidetes clade (red branches). One representative clone was chosen from each study and from each sample if multiple samples are represented from a study. The tree was generated in MEGA 5 (Tamura et al., 2011) using the maximum likelihood method with the Jukes–Cantor model, Gamma distribution and 1000 bootstrap replicates. The

same alignment was used to generate a neighbor-joining tree with the maximum composite likelihood method and 1000 bootstrap replicates. Nodes where both methods agree and bootstrap support is >50% are indicated with bootstrap values from the neighbor-joining tree on the left and the maximum likelihood tree on the right. Stars indicate nodes supported by Bayesian analysis. *Nitospira marina* was used as an outgroup.

(81% of  $\epsilon$ -proteobacteria on TuiMs) and *Sulfurovum* (9%) represented a surprisingly high proportion on inactive sulfide sample TuiMs. The bacterial community on this sample was most similar to that on two inactive sulfides collected from the EPR, also with higher percentages of  $\epsilon$ -proteobacteria than other inactive sulfides (**Figure 8**). This may indicate that these samples are only recently inactive and calls for dating of inactive sulfide samples in the future. The presence of anhydrite on sample TuiMs supports this argument – anhydrite is a known component of active chimneys but less common on inactive sulfides (Haymon and Kastner, 1981), and it is a major component of active sulfides at the nearby Mariner hydrothermal vent field (Takai et al., 2008). Nearby active chimneys at Tui Malila were dominated by  $\epsilon$ -proteobacteria in the genus *Lebetimonas* and had nearly no *Sulfurimonas* (Flores et al., 2012), therefore it is possible that the bacterial community on chimney TuiMs was in a transition from a thermophilic community similar to those found on active vents at the Tui Malila vent field to the community we detected, which is more indicative of mesophilic microbes. The absence of detectable Archaea on TuiMs also supports the transition away from a microbial community representative of an actively venting sulfide.

The mineralogy of inactive sulfides appears to influence the composition of the extant bacterial communities (Kato et al., 2010; Toner et al., 2013). Indeed, our analysis reveals that there is no biogeographical pattern amongst bacterial communities on inactive sulfides; samples from the Mariana Trough and EPR fall on different branches of **Figure 8**, indicating that populations from the same ocean basin are not always most similarly related to each other. Closer inspection reveals that the composition of bacterial communities is heterogeneous and potentially unique on each structure. In every case where more than one sample was collected from a single sulfide structure (9M4 from the EPR, Kair from the Indian Ocean Ridge, Pltc, and Ydc from the Mariana Trough, and Ihe from the Okinawa Trough), all samples from that sulfide group together on the same branch. The sole exception to this rule is sulfide ABEs, for which the inside conduit harbors a dramatically different bacterial community than the outside wall. This indicates that there is much heterogeneity from one inactive sulfide structure to another, and we still have much to learn about these inactive sulfide ecosystems. Future studies can learn more about the potentially diverse microenvironments within these structures by finely sampling for both mineralogy and microbiology.

### IMPLICATIONS FOR WEATHERING OF SEAFLOOR ROCKS

The noted patterns in microbial communities, both from north to south and between different substrates, have implications for weathering of seafloor rocks. It is known that bacteria incubated with basalt enhance Si, Fe, and Mn release into the aqueous phase (Daughney et al., 2004; Edwards et al., 2004), and it is also likely that differences in substrate composition, which is a known driver of microbial composition (Toner et al., 2013), drive differential weathering rates and products released by endolithic microbes. Microbial biofilms on seafloor incubated hydrothermal sulfides indicate the presence of iron oxyhydroxides (Toner et al., 2009) and a preference by microbes for minerals that are both highly soluble and porous (Edwards et al., 2003). All of these processes interact and result in both bioalteration of seafloor rocks and release of weathering materials into the water column. This is

poorly quantified but likely important for ocean biogeochemistry. It should be noted out that in addition to Bacteria and Archaea, which were analyzed here, there is growing evidence that fungi are also likely important in weathering processes in deep-sea environments (Biddle et al., 2005; Lopez-Garcia et al., 2007; Smith et al., 2011; Ivarsson et al., 2012).

### CONCLUSION

It is likely that the north-south gradients in bacterial community composition are driven by the differences in substrate chemistry between these fields. Many elements display linear transitions from Kilo Moana to Mariner, which makes it difficult to pinpoint which one (or ones) may be driving the observed differences in microbiology, but we were able to detect correlation between the elemental composition of the collected samples and bacterial phyla Nitrospira and Chloroflexi (**Table 4**). Additionally, with the small sample size of this study, it is important to point out that the patterns observed here warrant further investigation and would benefit from additional and more intensive sampling. The samples collected for this study represent an initial foray into the microbiology of low temperature deposits in Lau Basin.

Bacterial communities detected on low temperature silicates and inactive sulfides along the ELSC and VFR in Lau Basin display distinct patterns that are driven by (1) gradients in rock geochemistry from north to south on the silicates, and (2) differences in substrate between the basalts, basaltic andesite, and inactive sulfides. The prevalence of Chloroflexi clones distantly related to any known isolates on basaltic andesite indicates that this substrate may host unique microbial populations. Clones related to organisms involved in multiple facets of sulfur and iron oxidation-reduction processes on the same rocks indicate that multiple micro-niches are present on both silicates and sulfides. Further, multiple niches for the same ecological function, like sulfur oxidation by three different clades of organisms on sulfide ABEs, indicate that fine scale differences in mineralogy likely support similarly nuanced microbial communities. Bacterial communities on inactive sulfides from Lau Basin are not unlike others studied at different sites, but it appears that each structure studied harbors a bacterial community most similar to itself and, therefore, further study of these ecosystems with finer resolution is warranted.

### ACKNOWLEDGMENTS

We thank the captain and crew of the *RV Thomas G. Thompson* and the pilots of *ROV Jason II* for their assistance and expertise in acquiring the samples studied here. Frank Corsetti (USC) kindly allowed the use of his microscopes for the thin section analysis. We thank Linda Sauer and Mike Manno (Characterization Facility, University of Minnesota) for help with XRD and Rick Knurr (Department of Earth Sciences, University of Minnesota) for his expertise running the samples for chemical composition. Parts of this work were carried out in the Characterization Facility, University of Minnesota, which receives partial support from NSF through the MRSEC program. This work was supported by National Science Foundation (NSF) Grant OCE-0732369 to PRG, the NSF funded Center for Dark Energy Biosphere Investigations (Katrina J. Edwards), and a C-DEBI postdoctoral fellowship to JBS. This is C-DEBI contribution number 150.

## REFERENCES

- Altschul, S. F., Gish, W., Miller, W., Myers, E. W., and Lipman, D. J. (1990). Basic local alignment search tool. *J. Mol. Biol.* 215, 403–410.
- Ausubel, F. M., Brent, R., Kingston, R. E., Moore, D. D., Seidman, J. G., Smith, J. A., et al. (1999). *Short Protocols in Molecular Biology*, 4th Edn. New York: Wiley.
- Bach, W., and Edwards, K. J. (2003). Iron and sulfide oxidation within the basaltic ocean crust: implications for chemolithoautotrophic microbial biomass production. *Geochim. Cosmochim. Acta* 67, 3871–3887.
- Bailey, B., Templeton, A., Staudigel, H., and Tebo, B. M. (2009). Utilization of substrate components during basaltic glass colonization by *Pseudomonas* and *Shewanella* isolates. *Geomicrobiol.* J. 26, 648–656.
- Biddle, J. F., House, C. H., and Brenchley, J. E. (2005). Microbial stratification in deeply buried marine sediment reflects changes in sulfate/methane profiles. *Geobiology* 3, 287–295.
- Brenner, D. J., Krieg, N. R., Staley, J. T., Garrity, G. M., Boone, D. R., De Vos, P., et al. (2005). The proteobacteria, Part B, the Gammaproteobacteria, in *Bergey's Manual of Systematic Bacteriology*, 2nd Edn, Ed. G. M. Garrity (East Lansing, MI: Springer).
- Campbell, B. J., Engel, A. S., Porter, M. L., and Takai, K. (2006). The versatile epsilon-proteobacteria: key players in sulphidic habitats. *Nat. Rev. Microbiol.* 4, 458–468.
- Daims, H., Nielsen, J. L., Nielsen, P. H., Schleifer, K. H., and Wagner, M. (2001). In situ characterization of *Nitrospira*-like nitrite oxidizing bacteria active in wastewater treatment plants. *Appl. Environ. Microbiol.* 67, 5273–5284.
- Daughney, C. J., Rioux, J. P., Fortin, D., and Pichler, T. (2004). Laboratory investigation of the role of bacteria in the weathering of basalt near deep sea hydrothermal vents. *Geomicrobiol.* J. 21, 21–31.
- Dell'Anno, A., and Danovaro, R. (2005). Extracellular DNA plays a key role in deep-sea ecosystem functioning. *Science* 309, 2179–2179.
- Delong, E. F. (1992). Archaea in coastal marine environments. *Proc. Natl. Acad. Sci. U.S.A.* 89, 5685–5689.
- DeSantis, T. Z., Hugenholtz, P., Keller, K., Brodie, E. L., Larsen, N., Piceno, Y. M., et al. (2006a). NAST: a multiple sequence alignment server for comparative analysis of 16S rRNA genes. *Nucleic Acids Res.* 34, W394–W399.
- DeSantis, T. Z., Hugenholtz, P., Larsen, N., Rojas, M., Brodie, E. L., Keller, K., et al. (2006b). Greengenes, a chimera-checked 16S rRNA gene database and workbench compatible with ARB. *Appl. Environ. Microbiol.* 72, 5069–5072.
- Dick, G. J., and Tebo, B. M. (2010). Microbial diversity and biogeochemistry of the Guaymas Basin deep-sea hydrothermal plume. *Environ. Microbiol.* 12, 1334–1347.
- Drummond, A. J., Ashton, B., Buxton, S., Cheung, M., Cooper, A., Duran, C., et al. (2011). *Geneious v5.4*. Available at: <http://wwwgeneiouscom>
- Dunn, R. A., and Martinez, F. (2011). Contrasting crustal production and rapid mantle transitions beneath back-arc ridges. *Nature* 469, 198–202.
- Edwards, K. J., Bach, W., McCollom, T. M., and Rogers, D. R. (2004). Neutrophilic iron-oxidizing bacteria in the ocean: their habitats, diversity, and roles in mineral deposition, rock alteration, and biomass production in the deep-sea. *Geomicrobiol.* J. 21, 393–404.
- Edwards, K. J., McCollom, T. M., Konishi, H., and Buseck, P. R. (2003). Seafloor bioalteration of sulfide minerals: results from in situ incubation studies. *Geochim. Cosmochim. Acta* 67, 2843–2856.
- Einen, J., Thorseth, I. H., and Ovreas, L. (2008). Enumeration of Archaea and Bacteria in seafloor basalt using real-time quantitative PCR and fluorescence microscopy. *FEMS Microbiol. Lett.* 282, 182–187.
- Escrivé, S., Bezios, A., Goldstein, S. L., Langmuir, C. H., and Michael, P. J. (2009). Mantle source variations beneath the Eastern Lau Spreading Center and the nature of subduction components in the Lau Basin-Tonga arc system. *Geochem. Geophys. Geosyst.* 10:Q04014. doi:10.1029/2008GC002281
- Flores, G. E., Shakya, M., Meneghin, J., Yang, Z. K., Seewald, J. S., Wheat, C. G., et al. (2012). Inter-field variability in the microbial communities of hydrothermal vent deposits from a back-arc basin. *Geobiology* 10, 333–346.
- Fouquet, Y., Vonstackelberg, U., Charlou, J. L., Donval, J. P., Erzinger, J., Foucher, J. P., et al. (1991). Hydrothermal activity and metallogenesis in the Lau back-arc basin. *Nature* 349, 778–781.
- German, C. R., Bowen, A., Coleman, M. L., Honig, D. L., Huber, J. A., Jakuba, M. V., et al. (2010). Diverse styles of submarine venting on the ultra-slow spreading Mid-Cayman Rise. *Proc. Natl. Acad. Sci. U.S.A.* 107, 14020–14025.
- Haymon, R. M., and Kastner, M. (1981). Hot spring deposits on the East Pacific Rise at 21°N: preliminary description of mineralogy and genesis. *Earth Planet. Sci. Lett.* 53, 363–381.
- Hoeft, S. E., Kulp, T. R., Stolz, J. F., Hollibaugh, J. T., and Oremland, R. S. (2004). Dissimilatory arsenite reduction with sulfide as electron donor: experiments with mono lake water and isolation of strain MLMS-1, a chemoautotrophic arsenate respirer. *Appl. Environ. Microbiol.* 70, 2741–2747.
- Huse, S. M., Welch, D. M., Morrison, H. G., and Sogin, M. L. (2010). Ironing out the wrinkles in the rare biosphere through improved OTU clustering. *Environ. Microbiol.* 12, 1889–1898.
- Ishibashi, J., Lupton, J. E., Yamaguchi, T., Querellou, J., Nunoura, T., and Takai, K. (2006). Expedition reveals changes in Lau Basin hydrothermal system. *Eos (Washington DC)* 87, 13.
- Ivarsson, M., Bengston, S., Belivanova, V., Stamparoni, M., Marone, F., and Tehler, A. (2012). Fossilized fungi in subseafloor Eocene basalts. *Geology* 40, 163–166.
- Kato, S., Takano, Y., Kakegawa, T., Oba, H., Inoue, K., Kobayashi, C., et al. (2010). Biogeography and biodiversity in sulfide structures of active and inactive vents at deep-sea hydrothermal fields of the Southern Mariana Trough. *Appl. Environ. Microbiol.* 76, 2968–2979.
- Kormas, K. A., Tivey, M. K., Von Damm, K., and Teske, A. (2006). Bacterial and archaeal phylotypes associated with distinct mineralogical layers of a white smoker spire from a deep-sea hydrothermal vent site (9 degrees N, East Pacific Rise). *Environ. Microbiol.* 8, 909–920.
- Kristall, B., Nielsen, D., Hannington, M. D., Kelley, D. S., and Delaney, J. R. (2011). Chemical microenvironments within sulfide structures from the Mothra hydrothermal field: evidence from high-resolution zoning of trace elements. *Chem. Geol.* 290, 12–30.
- Langmuir, C. H., German, C. R., Michael, P. J., Yoerger, D. R., Fornari, D. J., Shank, G. C., et al. (2004). Hydrothermal prospecting and petrological sampling in the Lau Basin: background data for the integrated study site. *Eos (Washington DC)* 5, abstr. B13A–0189.
- Le Bas, M. J., and Streckeisen, A. L. (1991). The IUGS systematics of igneous rocks. *J. Geol. Soc. London* 148, 825–833.
- Lopez-Garcia, P., Vereshchaka, A., and Moreira, D. (2007). Eukaryotic diversity associated with carbonates and fluid-seawater interface in Lost City hydrothermal field. *Environ. Microbiol.* 9, 546–554.
- Ludwig, W., Strunk, O., Westram, R., Richter, L., Meier, H., Yadukumar, et al. (2004). ARB: a software environment for sequence data. *Nucleic Acids Res.* 32, 1363–1371.
- Lysnes, K., Thorseth, I. H., Steinsbu, B. O., Ovreas, L., Torsvik, T., and Pedersen, R. B. (2004). Microbial community diversity in seafloor basalt from the Arctic spreading ridges. *FEMS Microbiol. Ecol.* 50, 213–230.
- Mason, O. U., Di Meo-Savoie, C. A., Van Nostrand, J. D., Zhou, J. Z., Fisk, M. R., and Giovannoni, S. J. (2009). Prokaryotic diversity, distribution, and insights into their role in biogeochemical cycling in marine basalts. *ISME J.* 3, 231–242.
- Mottl, M. J., Seewald, J. S., Wheat, C. G., Tivey, M. K., Michael, P. J., Proskurowski, G., et al. (2011). Chemistry of hot springs along the Eastern Lau Spreading Center. *Geochim. Cosmochim. Acta* 75, 1013–1038.
- Nakagawa, S., Takai, K., Inagaki, F., Horikoshi, K., and Sako, Y. (2005). *Nitratiruptor* tergarcus gen. nov., sp. nov. and *Nitratiruptor* *salsuginis* gen. nov., sp. nov., nitrate-reducing chemolithoautotrophs of the epsilon-Proteobacteria isolated from a deep-sea hydrothermal system in the Mid-Okinawa Trough. *Int. J. Syst. Evol. Microbiol.* 55, 925–933.
- Newton, R. J., Griffin, L. E., Bowles, K. M., Meile, C., Gifford, S., Givens, C. E., et al. (2010). Genome characteristics of a generalist marine bacterial lineage. *ISME J.* 4, 784–798.
- Podowski, E. L., Ma, S., Luther, G. W. III, Wardrop, D., and Fisher, C. R. (2010). Biotic and abiotic factors affecting distributions of megafauna in diffuse flow on andesite and basalt along the Eastern Lau Spreading Center, Tonga. *Mar. Ecol. Prog. Ser.* 418, 25–45.
- Rogers, D. R., Santelli, C. M., and Edwards, K. J. (2003). Geomicrobiology of deep-sea deposits: estimating community diversity from low-temperature seafloor rocks and minerals. *Geobiology* 1, 109–117.
- Santelli, C. M., Edgcomb, V. P., Bach, W., and Edwards, K. J. (2009). The diversity and abundance of bacteria inhabiting seafloor lavas positively

- correlate with rock alteration. *Environ. Microbiol.* 11, 86–98.
- Santelli, C. M., Orcutt, B. N., Banning, E., Bach, W., Moyer, C. L., Sogin, M. L., et al. (2008). Abundance and diversity of microbial life in ocean crust. *Nature* 453, 653–657.
- Schloss, P. D., Westcott, S. L., Ryabin, T., Hall, J. R., Hartmann, M., Hollister, E. B., et al. (2009). Introducing mothur: open-source, platform-independent, community-supported software for describing and comparing microbial communities. *Appl. Environ. Microbiol.* 75, 7537–7541.
- Schrenk, M. O., Kelley, D. S., Delaney, J. R., and Baross, J. A. (2003). Incidence and diversity of microorganisms within the walls of an active deep-sea sulfide chimney. *Appl. Environ. Microbiol.* 69, 3580–3592.
- Smith, A., Popa, R., Fisk, M., Nielsen, M., Wheat, C. G., Jannasch, H. W., et al. (2011). In situ enrichment of ocean crust microbes on igneous minerals and glasses using an osmotic flow-through device. *Geochem. Geophys. Geosyst.* 12:Q06007. doi:10.1029/2010GC003424
- Sorokin, D. Y., Tourova, T. P., Mussmann, M., and Muyzer, G. (2008). *Dethiobacter alkaliphilus* gen. nov. sp. nov., and *Desulfurivibrio alkaliphilus* gen. nov. sp. nov.: two novel representatives of reductive sulfur cycle from soda lakes. *Extremophiles* 12, 431–439.
- Sudek, L. A., Templeton, A. S., Tebo, B. M., and Staudigel, H. (2009). Microbial ecology of Fe (hydr)oxide mats and basaltic rock from Vailulu'u Seamount, American Samoa. *Geomicrobiol. J.* 26, 581–596.
- Sunamura, M., Higashi, Y., Miyako, C., Ishibashi, J., and Maruyama, A. (2004). Two bacteria phylotypes are predominant in the Suiyo Seamount hydrothermal plume. *Appl. Environ. Microbiol.* 70, 1190–1198.
- Suzuki, Y., Inagaki, F., Takai, K., Nealson, K. H., and Horikoshi, K. (2004). Microbial diversity in inactive chimney structures from deep-sea hydrothermal systems. *Microb. Ecol.* 47, 186–196.
- Sylvan, J. B., Toner, B. M., and Edwards, K. J. (2012a). Life and death of deep-sea vents: bacterial diversity and ecosystem succession on inactive hydrothermal sulfides. *MBio* 3, e00279–e00211.
- Sylvan, J. B., Pyenson, B. C., Rouxel, O., German, C. R., and Edwards, K. J. (2012b). Time series analysis of two hydrothermal plumes at 9°50'N East Pacific Rise reveals distinct, heterogeneous bacterial populations. *Geobiology* 10, 178–192.
- Takai, K., and Horikoshi, K. (2000). Rapid detection and quantification of members of the archaeal community by quantitative PCR using fluorogenic probes. *Appl. Environ. Microbiol.* 66, 5066–5072.
- Takai, K., Nunoura, T., Ishibashi, J. I., Lupton, J., Suzuki, R., Hamasaki, H., et al. (2008). Variability in the microbial communities and hydrothermal fluid chemistry at the newly discovered Mariner hydrothermal field, southern Lau Basin. *J. Geophys. Res. Biogeosci.* 113:G02031. doi:10.1029/2007JG000636
- Takai, K., Suzuki, M., Nakagawa, S., Miyazaki, M., Suzuki, Y., Inagaki, F., et al. (2006). *Sulfurimonas paralvinellae* sp. nov., a novel mesophilic, hydrogen- and sulfur-oxidizing chemolithoautotroph within the Epsilonproteobacteria isolated from a deep-sea hydrothermal vent polychaete nest, reclassification of *Thiomicrospira denitrificans* as *Sulfurimonas denitrificans* comb. nov. and emended description of the genus *Sulfurimonas*. *Int. J. Syst. Evol. Microbiol.* 56, 1725–1733.
- Tamura, K., Peterson, D., Peterson, N., Stecher, G., Nei, M., and Kumar, S. (2011). MEGA5: molecular evolutionary genetics analysis using maximum likelihood, evolutionary distance and maximum parsimony methods. *Mol. Biol. Evol.* 28, 2731–2739.
- Toner, B. M., Lesniewski, R. A., Marlow, J. J., Briscoe, L. J., Santelli, C. M., Bach, W., et al. (2013). Mineralogy drives bacterial biogeography of hydrothermally inactive seafloor sulfide deposits. *Geomicrobiol. J.* 30, 313–326.
- Toner, B. M., Santelli, C. M., Marcus, M. A., Wirth, R., Chan, C. S., McCollom, T., et al. (2009). Biogenic iron oxyhydroxide formation at mid-ocean ridge hydrothermal vents: Juan de Fuca Ridge. *Geochim. Cosmochim. Acta* 73, 388–403.
- Walsh, D. A., Zaikova, E., Howes, C. G., Song, Y. C., Wright, J. J., Tringe, S. G., et al. (2009). Metagenome of a versatile chemolithoautotroph from expanding oceanic dead zones. *Science* 326, 578–582.
- Conflict of Interest Statement:** The authors declare that the research was conducted in the absence of any commercial or financial relationships that could be construed as a potential conflict of interest.
- Received:** 02 December 2012; **accepted:** 04 March 2013; **published online:** 27 March 2013.
- Citation:** Sylvan JB, Sia TY, Haddad AG, Briscoe LJ, Toner BM, Girguis PR and Edwards KJ (2013) Low temperature geomicrobiology follows host rock composition along a geochemical gradient in Lau Basin. *Front. Microbiol.* 4:61. doi:10.3389/fmicb.2013.00061
- This article was submitted to Frontiers in Extreme Microbiology, a specialty of Frontiers in Microbiology.
- Copyright © 2013 Sylvan, Sia, Haddad, Briscoe, Toner, Girguis and Edwards. This is an open-access article distributed under the terms of the Creative Commons Attribution License, which permits use, distribution and reproduction in other forums, provided the original authors and source are credited and subject to any copyright notices concerning any third-party graphics etc.

## APPENDIX



**FIGURE A1 | Seafloor and shipboard photographs of samples collected during this study.** Sample KiMba as it appeared on the seafloor (**A**) and in the sampling box (**B**). Sample ABEba on the seafloor (**C**) and onboard (**D**). Sample Marba as it appeared on the seafloor (**E**) and on the ship (**F**). Sample ABEs as it was collected by ROV Jason II (**G**) and on the ship (**H**). Sample TuiMs, photographed during collection (**I**) and on the ship (**J**).

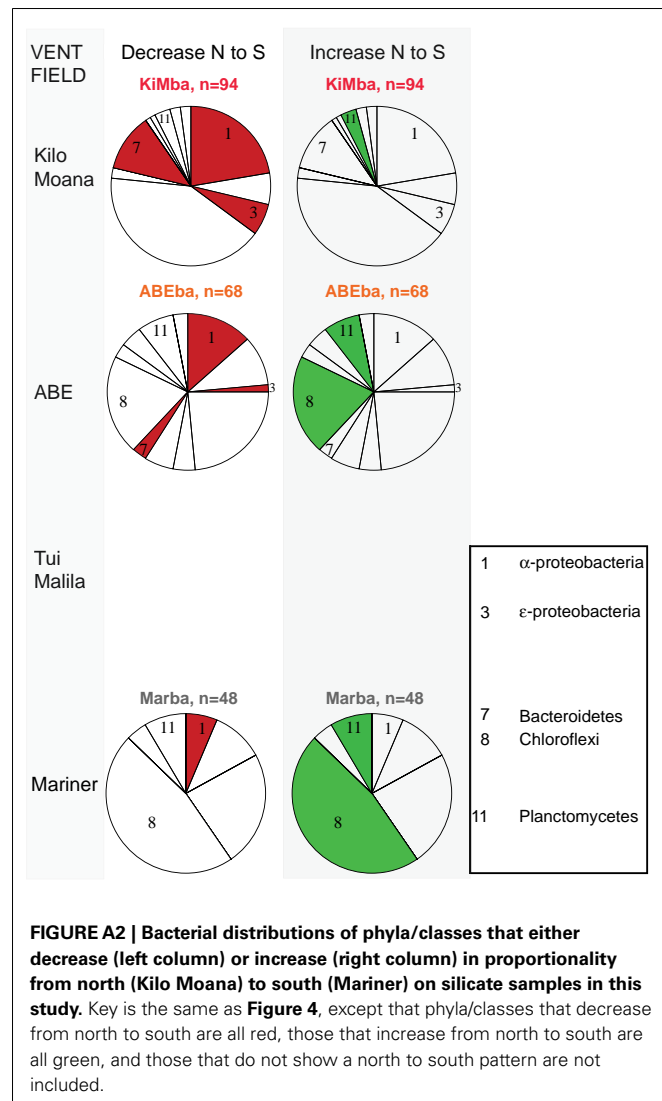


**FIGURE A2 | Bacterial distributions of phyla/classes that either decrease (left column) or increase (right column) in proportionality from north (Kilo Moana) to south (Mariner) on silicate samples in this study.** Key is the same as **Figure 4**, except that phyla/classes that decrease from north to south are all red, those that increase from north to south are all green, and those that do not show a north to south pattern are not included.

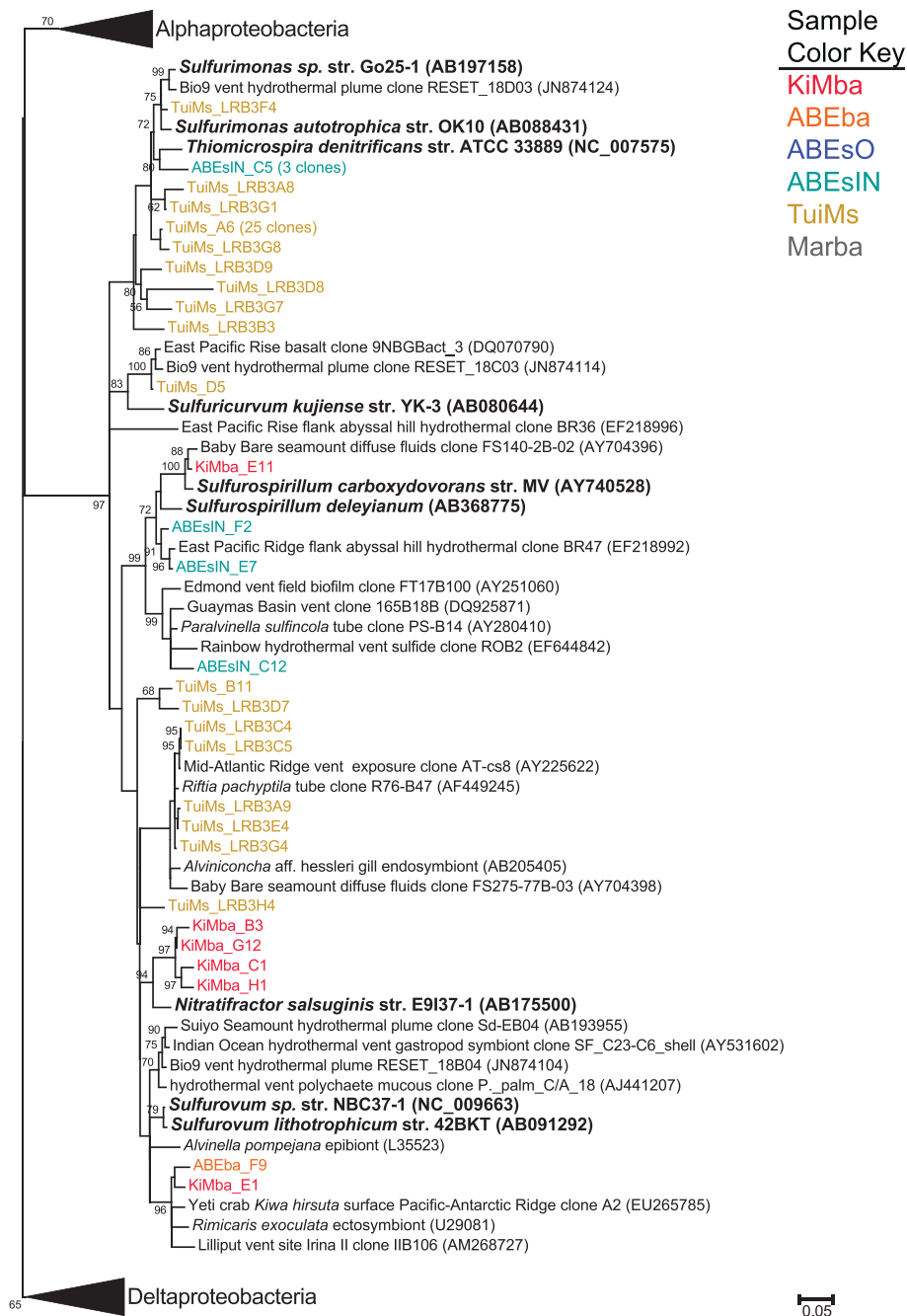


**FIGURE A3 | Phylogenetic tree of all representative clones from this study that fall within the  $\epsilon$ -Proteobacteria.** The tree was generated in MEGA 5 (Tamura et al., 2011) using the maximum likelihood method with the

Jukes–Cantor model and a Gamma distribution and 500 bootstrap replicates. Nodes where bootstrap support is >50% are indicated. Samples are color-coded and no representative clones are shared across multiple samples.



# Widespread occurrence of two carbon fixation pathways in tubeworm endosymbionts: lessons from hydrothermal vent associated tubeworms from the Mediterranean Sea

Vera Thiel<sup>1\*†‡</sup>, Michael Hügler<sup>2‡</sup>, Martina Blümel<sup>1†</sup>, Heike I. Baumann<sup>1</sup>, Andrea Gärtner<sup>1</sup>, Rolf Schmaljohann<sup>1</sup>, Harald Strauss<sup>3</sup>, Dieter Garbe-Schönberg<sup>4</sup>, Sven Petersen<sup>1</sup>, Dominique A. Cowart<sup>5</sup>, Charles R. Fisher<sup>5</sup> and Johannes F. Imhoff<sup>1</sup>

<sup>1</sup> GEOMAR, Helmholtz Centre for Ocean Research Kiel, Kiel, Germany

<sup>2</sup> Water Technology Center Karlsruhe, Karlsruhe, Germany

<sup>3</sup> Institut für Geologie und Paläontologie, Westfälische Wilhelms-Universität Münster, Münster, Germany

<sup>4</sup> Institut für Geowissenschaften, Christian-Albrechts-Universität Kiel, Kiel, Germany

<sup>5</sup> Mueller Laboratory, Department of Biology, The Pennsylvania State University, University Park, PA, USA

**Edited by:**

Andreas Teske, University of North Carolina at Chapel Hill, USA

**Reviewed by:**

John Stoltz, Duquesne University, USA

James F. Holden, University of Massachusetts Amherst, USA

**\*Correspondence:**

Vera Thiel, Biochemistry and Molecular Biology, The Pennsylvania State University, 231 South Frear, University Park, PA 16802, USA.  
e-mail: vut1@psu.edu

**†Present address:**

Vera Thiel, Department of Biochemistry and Molecular Biology, The Pennsylvania State University, University Park, USA;

Martina Blümel, Christian Albrechts Universität Kiel, Institut für Pflanzenzüchtung, Kiel, Germany.

<sup>\*</sup>Vera Thiel and Michael Hügler have contributed equally to this work.

Vestimentiferan tubeworms (siboglinid polychetes) of the genus *Lamellibrachia* are common members of cold seep faunal communities and have also been found at sedimented hydrothermal vent sites in the Pacific. As they lack a digestive system, they are nourished by chemoautotrophic bacterial endosymbionts growing in a specialized tissue called the trophosome. Here we present the results of investigations of tubeworms and endosymbionts from a shallow hydrothermal vent field in the Western Mediterranean Sea. The tubeworms, which are the first reported vent-associated tubeworms outside the Pacific, are identified as *Lamellibrachia anaximandri* using mitochondrial ribosomal and cytochrome oxidase I (COI) gene sequences. They harbor a single gammaproteobacterial endosymbiont. Carbon isotopic data, as well as the analysis of genes involved in carbon and sulfur metabolism indicate a sulfide-oxidizing chemoautotrophic endosymbiont. The detection of a hydrogenase gene fragment suggests the potential for hydrogen oxidation as alternative energy source. Surprisingly, the endosymbiont harbors genes for two different carbon fixation pathways, the Calvin-Benson-Bassham (CBB) cycle as well as the reductive tricarboxylic acid (rTCA) cycle, as has been reported for the endosymbiont of the vent tubeworm *Riftia pachyptila*. In addition to RubisCO genes we detected ATP citrate lyase (ACL – the key enzyme of the rTCA cycle) type II gene sequences using newly designed primer sets. Comparative investigations with additional tubeworm species (*Lamellibrachia luymesi*, *Lamellibrachia* sp. 1, *Lamellibrachia* sp. 2, *Escarpia laminata*, *Seepiophila jonesi*) from multiple cold seep sites in the Gulf of Mexico revealed the presence of *acl* genes in these species as well. Thus, our study suggests that the presence of two different carbon fixation pathways, the CBB cycle and the rTCA cycle, is not restricted to the *Riftia* endosymbiont, but rather might be common in vestimentiferan tubeworm endosymbionts, regardless of the habitat.

**Keywords:** hydrothermal vent, vestimentiferan tubeworm, carbon fixation, endosymbiont, *acl* gene, *cbbM* gene, *Lamellibrachia*, Mediterranean Sea

## INTRODUCTION

Vestimentiferan tubeworms are often dominant members of chemosynthetic communities present at reduced environments such as hydrothermal vents and cold seeps (Vrijenhoek, 2010). So far, hydrothermal vent-associated tubeworms have not been found outside the Pacific. In contrast, seep-associated tubeworms have been found in the Gulf of Mexico (GoM), the Mediterranean Sea, and the margins of the Atlantic Ocean (Cordes et al., 2009; Vrijenhoek, 2010).

The Mediterranean Sea is the world's largest enclosed sea, and represents a hot spot of biodiversity with a considerable number of endemic species (Myers et al., 2000). Its only connection to the

Atlantic Ocean is the narrow and shallow Strait of Gibraltar, which is the sole route for exchange of propagules between these two water bodies. The only vestimentiferan tubeworms documented to date in the Mediterranean Sea belong to the genus *Lamellibrachia* and specimens from several Mediterranean mud volcanoes were recently described as the new species *Lamellibrachia anaximandri* (Southward et al., 2011). The genus *Lamellibrachia* has a worldwide distribution, and occurs in several types of chemosynthetic environments from the shallow to the deep-sea (e.g., Kojima et al., 2002). Within the Mediterranean Sea, *Lamellibrachia* spp. have been discovered in the vicinity of mud volcanoes in the Alboran Sea at 572 m depth (Hilário et al., 2011), from several mud

volcanoes in the Eastern Mediterranean Sea at a depth of about 3,000 m (Olu-Le Roy et al., 2004; Bayon et al., 2009; Duperron et al., 2009; Southward et al., 2011) and also from two sunken ship wrecks in the Eastern and Western Mediterranean (Hughes and Crawford, 2008; Gambi et al., 2011; **Figure 1**).

Hydrocarbon seep communities in the GoM were among the first seep communities to be discovered, are extensively studied, and have a high diversity of tubeworm species (Kennicutt et al., 1985; Miglietta et al., 2010). The Louisiana Slope in the northern GoM area extends from the continental shelf to the salt deformation edge of the Sigsbee Escarpment, and ranges from about 300 to 3,000 m in depth. This area is home to at least six known morphospecies of vestimentiferan tubeworms (Miglietta et al., 2010), including the most commonly studied seep tubeworms, *Lamellibrachia luymesi* (van der Land and Nørrevang, 1975), and *Seepiophila jonesi* (Gardiner et al., 2001).

In contrast to the well-known hydrothermal vent tubeworm *Riftia pachyptila*, which inhabits hard substrate in hot sulfidic environments, members of the genus *Lamellibrachia* live in sedimented areas and are most common in cold seep environments. Seep habitats are generally much less dynamic than vent habitats and may be stable for centuries (Fisher et al., 1997). Compared to vent environments, emanating seep fluids are cooler, often enriched in methane and concentrations of dissolved sulfide may be quite low (Southward et al., 2011). *Lamellibrachia* tubeworms can obtain sulfide from the underlying sediments using the buried, permeable posterior region of the tube termed the “root” (Julian et al., 1999; Freytag et al., 2001). Since *Lamellibrachia*, like other siboglinid polychetes, lack a digestive tract, they are dependent on their endosymbionts for nutrition. Sulfide is transported via hemoglobin molecules in

the blood to the trophosome, a large organ that harbors dense populations of gammaproteobacterial endosymbionts (reviewed by Childress and Fisher, 1992). These endosymbionts oxidize the sulfide to obtain energy and reducing power for autotrophic carbon fixation. A portion of the synthesized organic matter serves in turn as energy source for the host tubeworm (Bright et al., 2000; Stewart and Cavanaugh, 2006). *Lamellibrachia* spp. are not only found at cold seeps, but also at sediment covered hydrothermal sites, e.g., *Lamellibrachia barhami* along the Juan de Fuca Ridge (Juniper et al., 1992), *Lamellibrachia columnata* near hydrothermal vents in the Lau Basin in the southwest Pacific (Southward, 1991) and *Lamellibrachia satsuma* at hydrothermal sites off southern Japan (Miake et al., 2006). Even though the so-called “vent” and “seep” tubeworm genera are clearly specialized for their preferred *in situ* conditions, they have been found at the same site, sometimes occurring only meters apart, e.g., the seep tubeworm *L. barhami* and the vent species *Ridgeia piscesae* at Middle Valley in 2,400 m depth in the northeast Pacific Ocean (McMullin et al., 2003).

Vestimentiferan endosymbionts form a monophyletic cluster within the gammaproteobacteria. They have been shown to cover very large geographic ranges, with nearly identical 16S rRNA in hosts separated by thousands of kilometers. Within the endosymbiont cluster four different groups (one “vent”-group, three “seep”-groups) are distinguishable. So-called “vent” endosymbionts appear to be specific for vent vestimentiferan hosts (e.g., *Riftia*, *Tevnia*, *Ridgeia*, and *Oasisia*), while three different 16S rRNA gene clusters (groups 1–3), possibly representing different strains, were found only in “seep” vestimentiferans (Nelson and Fisher, 2000; McMullin et al., 2003). Site depth has been postulated to be a factor in defining which of the three endosymbiont strains

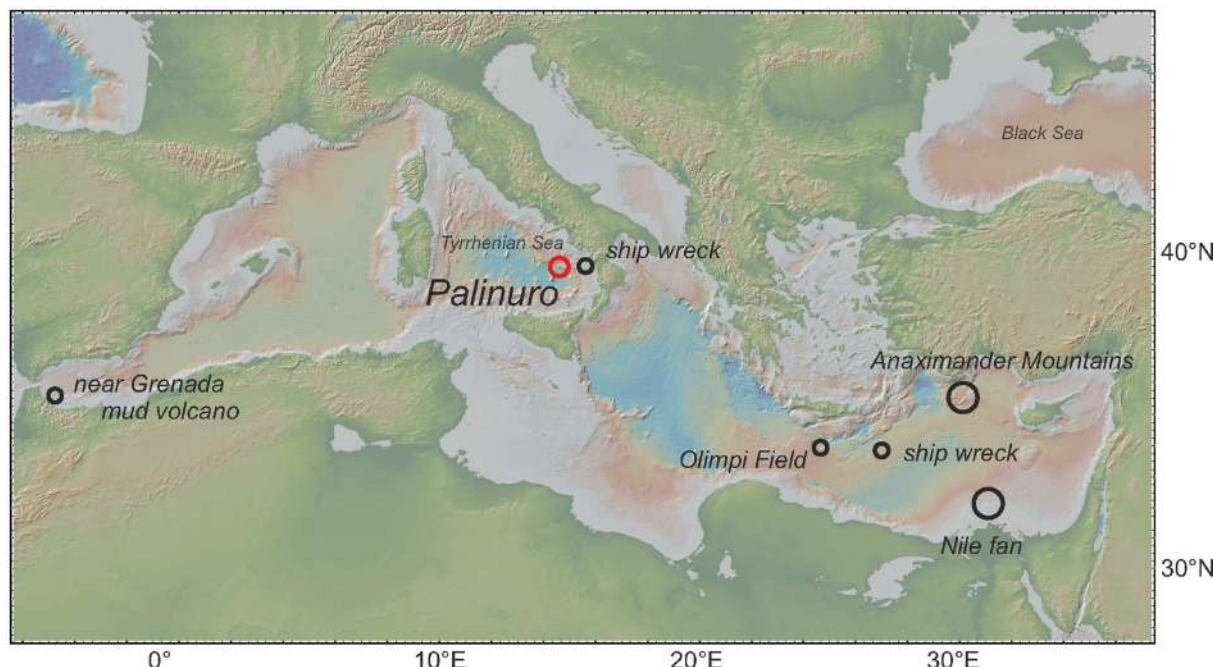


**FIGURE 1 |** Map with locations of vestimentiferan tubeworms of the genus *Lamellibrachia* described from previous studies (black circles) and this study (red circle) within the Mediterranean Sea.

is found in a particular “seep” host, with “group 3” occurring only in shallow water host specimens (McMullin et al., 2003).

The best-studied tubeworm endosymbiont is *Candidatus Endoriftia persephone*, the gammaproteobacterial endosymbiont of the vent-associated tubeworm *Riftia pachyptila*. Its metabolic capacities have been subject of detailed metagenomic, proteomic, and enzymatic studies (Felbeck, 1981; Felbeck et al., 1981; Markert et al., 2007, 2011; Robidart et al., 2008; Gardebrecht et al., 2012). *Candidatus Endoriftia persephone* is a sulfide-oxidizing chemoautotroph. Sulfide is oxidized to sulfate via sulfite and adenosine phosphosulfate (APS). The enzymes involved in the so-called APS pathway are dissimilatory sulfite reductase (DsrAB, working in reverse as sulfide oxidase), APS reductase (AprAB), and ATP sulfurylase (Markert et al., 2007, 2011). Quite surprising is the presence of two alternative carbon fixation pathways in the *Riftia* endosymbiont, the Calvin–Benson–Bassham (CBB) cycle as well as the reductive tricarboxylic acid (rTCA) cycle (Felbeck, 1981; Markert et al., 2007). Both pathways show unique features. The CBB cycle seems more energy-efficient due to modified enzyme equipment (Markert et al., 2011; Gardebrecht et al., 2012; Kleiner et al., 2012) while the rTCA cycle harbors a novel type of ATP citrate lyase (Hügler and Sievert, 2011). In contrast to the *Riftia* endosymbiont there are no genomic, proteomic or metabolomic studies of the endosymbiont(s) of *Lamellibrachia* spp.

This study reports the recovery of vestimentiferan tubeworms from the Palinuro volcanic complex, a submarine volcano in the Tyrrhenian Sea (Western Mediterranean Sea), north of Sicily (Figure 1). The Palinuro complex is part of the active Aeolian Island Arc and consists of several volcanic edifices aligned over a strike length of 55 km (Petersen et al., 2008; Passaro et al., 2010). The volcanic complex is up to 25 km wide at its base and its shallowest portion rises from 3,000 m to a water depth of less than 100 m. Iron and manganese-bearing precipitates were first documented at Palinuro by Kidd and Ármannsson (1979)

providing the first evidence for hydrothermal activity in the area. Hydrothermal sulfides were described by Minniti and Bonavia (1984) and Puchelt and Laschek (1987) within sediment sampled from the most westerly summit of Palinuro. The discovery of living vestimentiferan tubeworm colonies on top of the main volcanic edifices in this western summit in 2006 as well as temperatures of up to 60°C in sediment cores recovered from the seafloor indicated that active hydrothermal venting was taking place at the time although black smoker style venting has not been observed (Petersen et al., 2008; Monecke et al., 2009). Two colonies of these tubeworms were sampled in spring 2011.

We describe the results from detailed analyses of the Palinuro tubeworms and their endosymbionts, which are the first reported vent-associated tubeworms outside the Pacific Ocean. For comparison, several seep tubeworm species from the GoM were also analyzed (Figure 2), providing deeper insights into the geographic dispersal, phylogeny, and metabolic potential of tubeworms and their endosymbionts.

## MATERIALS AND METHODS

### SAMPLING SITE, SAMPLE COLLECTION, AND PROCESSING OF PALINURO TUBEWORMS

Vestimentiferan tubeworm specimens were retrieved from two different colonies termed colony #1 and #2 on the western summit of the Palinuro volcanic complex (Mediterranean Sea, 39°32.44'N, 14°42.38'E, depth: 630 m) during the Pos412 cruise of R/V *Poseidon* in spring 2011. Sampling was conducted using a Mohawk-type remotely operated vehicle (ROV) supplied by Oceaneering Inc. (Aberdeen, UK) fitted with a robotic arm. Locations of the tubeworm collections are given in Table 1.

The ROV was also equipped with a fluid sampling system (Kiel *in situ* pumping system, KIPS, Garbe-Schönberg et al., 2006) capable of acquiring four 550 mL water samples per dive with *in situ* filtration. Parallel to the sampling nozzle was a temperature probe

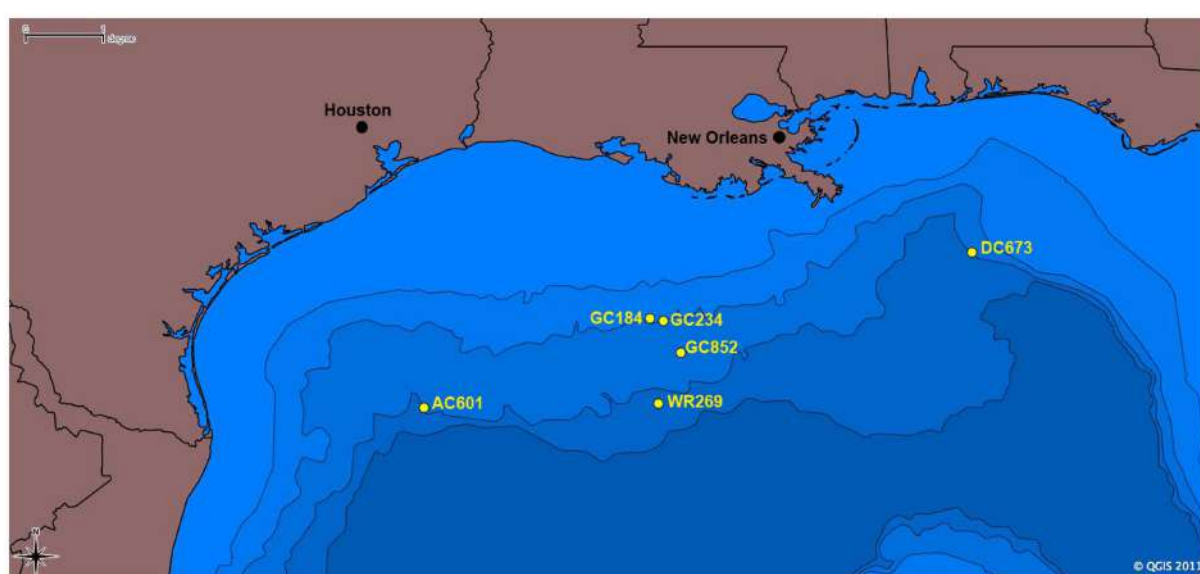


**FIGURE 2 |** Map of sampling locations for tubeworm specimens in the Gulf of Mexico included in this study. Scale is in degrees longitude; 1° = 111.12 km.

**Table 1 | Position of tubeworm colonies sampled during R/V POSEIDON cruise Pos412 at Palinuro volcanic complex, Tyrrhenian Sea and temperatures measured within colonies.**

| Tubeworm colony no. | Station no. | Geographical position (TMS; ROV) | Depth (m) | Temperature (°C) |
|---------------------|-------------|----------------------------------|-----------|------------------|
| Colony #1           | 231-1       | 39°32.45'N/<br>014°42.41'E       | 634       | Top: 14.2        |
|                     |             |                                  |           | Center: 19.4     |
|                     |             |                                  |           | Base: 15.9       |
| Colony #2           | 241-3       | 39°32.427'N/<br>014°42.384'E     | 630       | Top: 15.6        |
|                     |             |                                  |           | Center: 14.7     |
|                     |             |                                  |           | Base: 14.2       |

attached to a data logger. Fluids and temperatures around the colonies were sampled using KIPS and the temperature probe by maneuvering the ROV's robotic arm into the fluid in close proximity to the living tubeworms. Live tubeworms were sampled using the ROV's robotic arm. Immediately after tubeworm sampling, the dive was terminated, and the ROV was recovered. Upon recovery, the tubeworms obtained from colony #1 were put into sterile Petri dishes using sterile tweezers followed by dissection with a sterile scalpel. The animal was then separated from the tube; subsamples were recovered from vestimentum (host tissue free of symbionts) and trophosome (endosymbiont) tissue, and then were stored at  $-20^{\circ}\text{C}$  until further molecular analysis. Samples from colony #2 were immediately stored at  $-20^{\circ}\text{C}$  until further processing in the home laboratory. As the tubeworms from colony #2 exhibited several morphotypes, these were stored in separate vials.

#### GULF OF MEXICO TUBEWORM SAMPLE COLLECTION AND PREPARATION

Gulf of Mexico vestimentiferan tubeworms were sampled from hydrocarbon seep sites during several research cruises between 1997 and 2011 (Table 2; Figure 2). *Lamellibrachia luymesi* and *Seepiophila jonesi* were collected using the Johnson Sea Link submersible from two sites on the Upper Louisiana Slope from about 540 m depth. *Lamellibrachia* sp. 1 and *Lamellibrachia* sp. 2 as well as *Escarapia laminata* were collected from three sites on the Lower Louisiana Slope ranging in depth from 1,975 to 2,604 m. While on board the research vessel, tubeworms were dissected and vestimentum (host tissue free of symbionts) and trophosome (endosymbiont) tissue was preserved at  $-80^{\circ}\text{C}$  or in 95% ethanol solution. All tissue samples were transported to the Pennsylvania State University where whole genomic DNA was obtained using a modified version of the high salt extraction protocol and ethanol precipitation as in Liao et al. (2007). Isolated DNA is currently stored at  $-80^{\circ}\text{C}$  at the Pennsylvania State University.

#### DNA EXTRACTION, PCR AMPLIFICATION, CLONING, AND SEQUENCING

Genomic DNA was extracted from the trophosome and vestimentum tissues of the vestimentiferan tubeworms. The tubeworms were dissected and washed three times in 0.2  $\mu\text{m}$  filtered seawater prior to DNA extraction. DNA of Mediterranean tubeworm samples was isolated using the MoBio Power Biofilm Kit (Mo Bio Laboratories, Carlsbad, CA, USA) according to the protocol

provided. DNA of GoM tubeworm samples was extracted following the protocol of Liao et al. (2007). Cytochrome c oxidase I (COI) genes, mitochondrial and bacterial ribosomal (16S rRNA) genes, as well as *cbbM* and ACL type II genes were analyzed from all individuals. Further functional genes and eukaryotic ribosomal (18S rRNA) genes were analyzed from one individual of colony #1 from the Palinuro volcanic complex.

For all gene amplifications of Mediterranean samples PCR reactions were conducted using Ready-To-Go PCR Beads (GE Healthcare, Munich, Germany) in a total volume of 25  $\mu\text{L}$ . PCR from GoM samples were conducted using 1 U BioBasic TaqPolymerase (BioBasic Inc., Markham, ON, Canada) and 1  $\times$  Thermopol Buffer (NEB Inc., USA) in a total volume of 50  $\mu\text{L}$ . If not stated otherwise 10 pmol of each primer and 100 ng template DNA was used. For all amplifications, initial denaturation was 2 min at  $94^{\circ}\text{C}$ , final annealing was 1 min at annealing temperature, and final elongation 5 min at  $72^{\circ}\text{C}$ . For the cycles denaturation was 40 s at  $94^{\circ}\text{C}$ , annealing duration 40 s at the respective annealing temperature and elongation was 1 min at  $72^{\circ}\text{C}$ . If not stated otherwise, 35 PCR cycles were applied. Fragments of the tubeworms' 18S rRNA and mitochondrial 16S rRNA as well as COI genes were amplified using the (i) primer pairs 5'-start (5'-GGT TGA TCC TGC CAG-3') and 1753rev (5'-GCA GGT TCA CCT ACG G-3') targeting the 18S rRNA gene (30 cycles, 50°C annealing temperature), (ii) primer pair 16Sar/16Sbr (Palumbi et al., 2002) targeting the mitochondrial 16S rRNA gene (30 cycles, 50°C annealing temperature), and (iii) primers LCO 1490 (5'-GGT CAA CAA ATC ATA AAG ATA TTG G-3') and HCO 2198 [5'-TAA ACT TCA GGG TGA CCA AAA AAT CA-3'; 40 cycles, 47°C annealing temperature (Folmer et al., 1994)] using DNA extracted from the symbiont-free vestimentum tissue. Gene fragments of the endosymbiont were amplified using DNA extracted from trophosome tissue as the template. Bacterial 16S rRNA gene fragments were amplified in a 30 cycle PCR at an annealing temperature of 50°C with the general bacterial primer set 27F and 1390R (Palinuro samples; 5'-GAC GGG CRG TGT GTA CAA-3') or 1492R (GoM samples; Lane, 1991). Amplification for fragments of *dsrA* and *aprA* genes was performed using the primer sets *rdsrA240F/rdsrA403R* and *aps1F/aps4R*, respectively (Meyer and Kuever, 2007b; Lavik et al., 2009). Fragments of *soxB* were amplified using the primers *soxB432F/soxB1446B* [10 cycles with 55°C annealing temperature and 25 cycles with 47°C annealing temperature (Petri et al., 2001)]. For the amplification of fragments of the genes coding for the large subunit of RubisCO form I and II, the primer sets *cbbLF/cbbLR* and *cbbMF/cbbMR* were used [both include two initial cycles of 2 min annealing at  $37^{\circ}\text{C}$  and 3 min elongation at  $72^{\circ}\text{C}$ , as well as additional 35 cycles of 53 and 58°C annealing temperature for *cbbL* and *cbbM* respectively (Campbell and Cary, 2004)]. A fragment of the large subunit of the putative type II ATP citrate lyase gene was amplified using the newly designed primer *acl2F1* (5'-CGT CGC CAA GGA AGA GTG GTT C-3') and *acl2R1* (5'-GGC GAT GGC CTC AAA GCC GTT-3') in a 30 cycle PCR with annealing temperatures of 45–56°C (gradient). Fragments of the hydrogen uptake hydrogenase gene *hupL* were amplified with the primer set *HUPLX1/HUPLW2* (Csaki et al., 2001). A fragment of the *norCB* gene for nitric oxide reductase subunits C and B was amplified using the primer set *norC21mF* and *norB6R* (Tank,

**Table 2 | Sample identity, geographic origin, and gene sequences accession numbers of tubeworm specimens and their endosymbionts included in this study.**

| Sample name    | Species                           | Region                               | Site       | Depth (m) | Date collected | Latitude    | Longitude    | Endosymbiont 16S rRNA | Endosymbiont cbbM | Endosymbiont ACL | Host mt16S rRNA | Reference                           |
|----------------|-----------------------------------|--------------------------------------|------------|-----------|----------------|-------------|--------------|-----------------------|-------------------|------------------|-----------------|-------------------------------------|
| Pos412-B1_L1-7 | <i>Lamellibrachia anaximandri</i> | Mediterranean Sea, Palinuro Seamount | Pos412-231 | 634       | 4/27/2011      | 39°32.450'N | 015°42.410'E | HE9833428             | HE978225          | HE978244         | HE974472        | This study                          |
| Pos412-B2_L1-4 | <i>Lamellibrachia anaximandri</i> | Mediterranean Sea, Palinuro Seamount | Pos412-242 | 630       | 4/29/2011      | 39°32.427'N | 015°42.384'E | HE98334952            | HE9782268         | HE9782456        | HE974473        | This study                          |
| DC673_1211     | <i>Lamellibrachia sp. 1</i>       | Gulf of Mexico, DeSoto Canyon        | DC673      | 2604      | 10/30/2006     | 28°18.603'N | 087°18.643'W | HE983327              | HE978212          | HE978229         | HE974464        | This study                          |
| DC673_1209     | <i>Lamellibrachia sp. 2</i>       | Gulf of Mexico, DeSoto Canyon        | DC673      | 2604      | 10/30/2006     | 28°18.603'N | 087°18.643'W | HE983328              | HE978213          | HE978230         | HE974465        | This study                          |
| DC673_1170     | <i>Escarpiá laminata</i>          | Gulf of Mexico, DeSoto Canyon        | DC673      | 2604      | 10/29/2006     | 28°18.603'N | 087°18.643'W | HE983329              | HE978214          | HE978231         | HE974466        | This study                          |
| AC601_E6       | <i>Escarpiá laminata</i>          | Gulf of Mexico, Alaminos Canyon      | AC601      | 2339      | 5/27/2002      | 26°23.365'N | 094°30.880'W | HE983330              | HE978215          | HE978232         | GU068203        | Miglietta et al. (2010), This study |
| AC601_L1       | <i>Escarpiá laminata</i>          | Gulf of Mexico, Alaminos Canyon      | AC601      | 2339      | 5/27/2002      | 26°23.365'N | 094°30.880'W | HE9833312             | HE978216          | HE9782334        | HE974467        | This study                          |
| WR269_E10      | <i>Escarpiá laminata</i>          | Gulf of Mexico, Walker Ridge Canyon  | WR269      | 1975      | 5/25/2002      | 26°40.672'N | 091°39.691'W | HE983333              | HE978217          | HE978235         | HE974468        | This study                          |
| GC852_L4       | <i>Lamellibrachia sp. 1</i>       | Gulf of Mexico, Green Canyon         | GC852      | 1437      | 5/22/2002      | 27°05.768'N | 091°09.897'W | HE983334              | HE978218          | HE978236         | GU068242        | Miglietta et al. (2010), This study |
| GC852_L1       | <i>Lamellibrachia sp. 2</i>       | Gulf of Mexico, Green Canyon         | GC852      | 1437      | 5/22/2002      | 27°05.768'N | 091°09.897'W | HE983335              | HE978219          | HE978237         | HE974469        | This study                          |
| GC852_L5       | <i>Lamellibrachia sp. 1</i>       | Gulf of Mexico, Green Canyon         | GC852      | 1437      | 5/22/2002      | 27°05.768'N | 091°09.897'W | HE983336              | HE978220          | HE978238         | HE983353        | This study                          |
| AC601_L20      | <i>Lamellibrachia sp. 2</i>       | Gulf of Mexico, Alaminos Canyon      | AC601      | 2335      | 5/30/2002      | 26°23.548'N | 094°30.849'W | HE9833378             | HE978221          | HE97823940       | HE974470        | This study                          |
| GC234_4587     | <i>Seepiophila jonesi</i>         | Gulf of Mexico, Green Canyon         | GC234      | 527       | 2003           | 27°26.839'N | 091°08.061'W | HE983339              | HE978222          | HE978241         | HE974471        | This study                          |
| GC184_L9       | <i>Lamellibrachia luymesi</i>     | Gulf of Mexico, Green Canyon         | GC184      | 540       | 1995           | 27°28.171'N | 091°18.265'W | HE983340              | HE978223          | HE978242         | GU068216        | Miglietta et al. (2010), This study |
| GC234_L7       | <i>Lamellibrachia luymesi</i>     | Gulf of Mexico, Green Canyon         | GC234      | 546       | 1995           | 27°26.847'N | 091°07.986'W | HE983341              | HE978224          | HE978243         | GU068238        | Miglietta et al. (2010), This study |

2005) in a 35 cycle PCR using annealing temperatures of 60–50°C (10 touchdown cycles 60°C/–1°C, 25 cycles of 50°C).

Additional primer pairs used in this study include: F2/R5 and 892F/1204R for the two subunits of ATP citrate lyase (Campbell et al., 2003; Hügler et al., 2005); MxaF1003, MxaR1555, MxaR1561 for methanol dehydrogenase gene *mxaF* (Neufeld et al., 2007; Kalyuzhnaya et al., 2008); *mmoXA/mmoXB* for genes encoding the conserved alpha-subunit of the hydroxylase component of the cytoplasmatic soluble methane monooxygenase (sMMO; Auman et al., 2000); and A189F/MB661R for the particulate methane monooxygenase (pMMO) genes present in methanotrophs (Costello and Lidstrom, 1999).

All PCR products were purified via gel extraction using QIAquick gel extraction kit (QIAgen, Hilden, Germany) for Mediterranean samples, and BioBasic EZ-10 spin columns (BioBasic Inc., Markham, ON, Canada) for GoM samples respectively, and either directly sequenced by Sanger sequencing (18S rRNA gene fragments, COI, and functional gene fragments) or cloned into pCR4-TOPO vectors with the TOPO-TA cloning kit (Invitrogen, Carlsbad, CA, USA) as described by the manufacturer before sequencing (16S rRNA gene fragments). Sequencing was conducted using amplification primers and additional internal primers in the case of 16S rRNA genes (342F, 534R; Muyzer et al., 1996); 790F (Thiel et al., 2007). Amplification and sequencing of clones was conducted using vector specific primers M13 forward and M13 reverse (PCR) and T3 and T7 (sequencing), respectively. Sanger sequencing was performed using the BigDye Terminator v1.1 sequencing kit in a 3730xl DNA Analyzer (Applied Biosystems, Carlsbad, CA, USA) as specified by the manufacturer. Sequencing was conducted by the Institut für Klinische Molekularbiologie (IKMB), Universitäts-Klinikum Schleswig-Holstein (UKSH), Kiel, Germany and the sequencing core facility at The Pennsylvania State University, University Park, PA, USA.

#### PHYLOGENETIC ANALYSIS

All sequences were edited with ChromasPro c.c1.33 and compared to the NCBI database using BLAST (Altschul et al., 1997). Functional gene nucleotide sequences were also compared with the non-redundant protein sequence database using the blastx algorithm. The endosymbiont 16S rRNA gene sequences were aligned with the ARB software ([www.arb-home.de](http://www.arb-home.de)) using the ARB FastAligner utility (Ludwig et al., 2004). The sequence alignment was manually refined based on known secondary structures. Sequences of functional genes as well as mitochondrial rRNA genes were aligned using Clustal X (Thompson et al., 1997) and manually adjusted using BioEdit (Hall, 1999). Maximum Likelihood based trees and 100 bootstrap replicates were constructed using PhyML (Guindon and Gascuel, 2003). In order to verify the tree topology, further phylogenetic analyses using Neighbor-Joining and Maximum-Parsimony algorithms were conducted using MEGA5 (Tamura et al., 2011).

#### MICROSCOPY

The morphology of endosymbiotic bacteria in trophosome tissue of the tubeworms was examined using light microscopy and scanning electron microscopy (SEM). Samples for light microscopy were prepared by removing small pieces of tissue from different

parts of the trophosome and subsequent squeezing preparation in a drop of particle-free seawater and examined under 100-fold magnification using a Zeiss Axiohot Epifluorescence Microscope.

Samples for SEM were prepared by disrupting small trophosome samples in 0.2 μm filtered seawater, and then concentrated by filtration on to 0.2 μm polycarbonate membrane filters followed by dehydration through ascending concentrations of ethanol. Subsequently, the samples were critical-point-dried using a Balzers CPD 030 and CO<sub>2</sub> as a transition medium. The filters were sputter-coated with gold-palladium using a Balzers SCD 004 and observed with a Zeiss DSM 940 electron microscope.

#### FLUID CHEMISTRY

After recovery of the ROV Mohawk all KIPS fluid samples were immediately transferred to the onboard ship lab and sub-sampled for subsequent analyses. Both pH and Eh of the fluids were determined immediately after sub-sampling using electrochemical techniques after calibration with certified standards. Dissolved oxygen was determined using standard Winkler titration protocols modified for small volumes. The concentration of dissolved sulfide was determined in 1 mL aliquots using a zinc acetate gelatin solution, which precipitates the dissolved sulfide as colloidal zinc sulfide. Subsequently, the color agent, *N,N*-dimethyl-1,4-phenylenediamine-dihydrochloride, and a catalyst, iron chloride solution, were added to form methylene blue (Cline, 1969). After 1 h, the solutions were measured photometrically at a wavelength of 660 nm using a Genesys Spectra 10 spectrophotometer. The detection limit was 1 μmol/L. Potential oxidation of dissolved hydrogen sulfide during sampling and sample recovery cannot be ruled out, but is likely minimal. Nonetheless, hydrogen sulfide concentration data given in this paper should be considered minimum values. Aliquots for the analysis of nutrients were stored in polypropylene bottles, sealed, and stored in the dark at 4°C until analysis. Aliquots for cation and trace element analysis were pressure-filtrated through 0.2 μm Nucleopore polycarbonate (PC) membrane filters using Sartorius PC filtration units and high purity nitrogen. Samples were acidified with subboiled nitric acid to pH <2 and stored in perfluoralkoxy (PFA) bottles until analysis. Multielement analysis for major ion composition (Cl, B, Si, Na, K, Ca, Mg, Fe, Mn) of the water samples was performed with a SPECTRO Ciros SOP ICP-OES spectrometer after 10-fold dilution and using Y for internal standardization. Trace elements (As, Li, W) were determined by ICP-MS (Agilent 7500 cs at University of Kiel) after 12.5-fold dilution using both In and Re for internal standardization. Certified reference materials NIST1643e, NASS-5, and IAPSO were used for validation and accuracy checks.

#### CARBON ISOTOPE SIGNATURE

The organic carbon isotopic composition of tubeworm tissue ( $\delta^{13}\text{C}_{\text{ORG}}$ ) was determined via continuous flow EA-IRMS using an elemental analyzer interfaced to a ThermoFinnigan Delta Plus isotope ratio mass spectrometer. Briefly, about 40–60 μg of freeze-dried worm tissue was weighed in tin capsules, combusted to CO<sub>2</sub>, and chromatographically purified carbon dioxide was transferred to the mass spectrometer in a He gas stream. Results are reported in the standard delta notation as per mil difference to the Vienna Pee Dee Belemnite. Sample measurements were done in duplicate, and

analytical performance was monitored with international reference materials (USGS 24; USGS 40) and lab standards (anthracite; brown coal) and the reproducibility was generally better than  $\pm 0.15\%$ .

The carbon isotopic composition of dissolved inorganic carbon ( $\delta^{13}\text{CDIC}$ ) from vent fluids was measured using a Thermo Finnigan Gas Bench coupled to a Thermo Finnigan Delta Plus XL. Briefly, 0.5–1.0 mL of hydrothermal fluid was injected into an extainer that contained phosphoric acid, liberating DIC as carbon dioxide. Prior to sample injection, the extainer was flushed with helium.  $\text{CO}_2$  was flushed from the extainer with a stream of helium and injected into the mass spectrometer. Results are reported in the standard delta notation as per mil difference to the Vienna Pee Dee Belemnite. Sample measurements were done in duplicate, and analytical performance was monitored with a sodium carbonate lab standard.

#### NUCLEOTIDE SEQUENCE ACCESSION NUMBERS

The sequence data have been submitted to EMBL/GenBank/DDBJ databases under accession numbers HE9744464–85, HE978212–46, and HE983327–53.

## RESULTS

### BIOGEOCHEMICAL CHARACTERIZATION OF THE TUBEWORM HABITAT AT PALINURO

For the present study, two colonies of vestimentiferan tubeworms as well as their biogeochemical environment were sampled by means of a ROV. The tubeworms occurred within a sediment-filled depression at the western summit of the Palinuro volcanic complex in water depths of around 630 m and formed small bushes, up to 1 m<sup>2</sup> in diameter, mainly on sedimented surfaces but some patches also occurred in areas where volcanic rocks were present at the seafloor. Frequently, shimmering water was observed rising above the tubeworm colonies suggesting active fluid emanation. The first colony (colony #1) appeared to be comprised mainly of equally sized animals. The second colony (colony #2), however, consisted of animals of different sizes, indicating different ages, or variation in exposure to hydrothermal fluid at different places within the colony.

Remotely operated vehicle assisted measurements of water temperature across and within the tubeworm colonies revealed a maximum recorded temperature of 19.4°C, about 5°C above ambient seawater temperatures of 14°C (Table 1). Diffusely venting warm hydrothermal fluids reached a maximum temperature of 58.4°C within small depressions in close proximity to the tubeworms. Chloride concentrations in these fluids were significantly higher than in ambient seawater indicating influx of hydrothermal brine eventually leading to the formation of small stratified brine pools in these depressions. Chemical analyses of vent and pore fluids sampled from sediment cores collected in the same area revealed that local hydrothermal fluids were anoxic,  $\text{H}_2\text{S}$ -rich, acidic and displayed an elevated salinity. Concentrations of dissolved alkali and alkali earth elements (potassium, calcium, lithium, cesium), silica, arsenic, and tungsten (“Fluid end-member” in Table 3) were significantly higher when compared to normal bottom seawater. Fluid samples confirmed that this hydrothermal fluid was highly diluted with ambient seawater

**Table 3 | Composition of seawater-hydrothermal fluid mixtures inside tubeworm colonies #1 and #2.**

|                      |               | Fluid endmember | Colony #1,<br>232 ROV-2 | Colony #2,<br>237 ROV-1 | Seawater<br>221 CTD |
|----------------------|---------------|-----------------|-------------------------|-------------------------|---------------------|
| T                    | °C            |                 | 14.7                    | 15.9                    | 14.4                |
| pH                   |               |                 | 6.9                     | 6.7                     | 8.2                 |
| Diss. $\text{O}_2$   | $\mu\text{M}$ | –               | 230                     | 139                     |                     |
| $\text{H}_2\text{S}$ | $\mu\text{M}$ |                 | 72                      | 32                      | –                   |
| Cl                   | $\text{mM}$   | 984             | 640                     | 634                     | 626                 |
| B                    | $\text{mM}$   | 11              | 0.52                    | 0.52                    | 0.47                |
| Si                   | $\text{mM}$   | 1.7             | 0.02                    | 0.02                    | 0.01                |
| Na                   | $\text{mM}$   | 681             | 528                     | 526                     | 520                 |
| K                    | $\text{mM}$   | 65              | 12                      | 11.9                    | 11.5                |
| Ca                   | $\text{mM}$   | 78              | 12.4                    | 12.3                    | 11.8                |
| Li                   | $\mu\text{M}$ | 7.7             | 0.06                    | 0.06                    | 0.03                |
| Mn                   | $\mu\text{M}$ |                 | 3                       | <1                      | <1                  |
| Fe                   | $\mu\text{M}$ |                 | <2                      | <2                      | <2                  |
| As                   | $\mu\text{M}$ | 222             | 9.6                     | 10                      | <5                  |
| W                    | $\text{nM}$   | 224             | 1.6                     | –                       | <0.3                |

as it passed through the two tubeworm colonies leading to partly oxygenated waters (139 and 227  $\mu\text{mol/L}$  dissolved  $\text{O}_2$ , Table 3) and reduced levels of sulfide. Still, dissolved sulfide concentrations of 32 and 72  $\mu\text{mol/L}$  were measured in water samples from among the tubes in the tubeworm colonies. In contrast, a maximum concentration of dissolved sulfide of 5,172  $\mu\text{mol/L}$  was measured for the “hottest” hydrothermal fluids (58°C) sampled at Palinuro.

### CHARACTERIZATION OF THE TUBEWORMS

#### Characterization of Palinuro tubeworms

A wide range of sizes of vestimentiferan tubeworms were collected from the Palinuro volcanic complex (Figure 3). The tubes of the collected animals ranged up to 15 cm in length with a maximum exterior diameter of 3 mm at the anterior end, decreasing slightly to the posterior end. The anterior region was banded reddish brown and white, whereas the posterior region was a more uniform brownish color. The tube walls were thick and rigid in the anterior region, becoming thinner and more flexible in the posterior regions. The vestimentiferan tubeworm hosts were identified by molecular analyses of the 18S rRNA gene as well as the mitochondrial genes for ribosomal 16S rRNA and the cytochrome c oxidase I (COI). All three genes were amplified from DNA extracted from tubeworm vestimentum, which is free of endosymbionts. Based on COI and mitochondrial 16S rRNA nucleotide analyses, all individuals analyzed from tubeworm colony #1 and the four individuals exhibiting different morphologies from tubeworm colony #2 obtained from the Palinuro volcanic complex belonged to the same species. The maximum difference between the COI gene fragments sequences was two bases (total investigated length 650 bp) and one base for the mitochondrial 16S rRNA gene (total investigated length 529 bp). In accordance with 18S rRNA gene, mitochondrial 16S rRNA gene and COI sequence the tubeworm could be identified as the newly described species *Lamellibrachia anaximandri* (Southward et al., 2011).

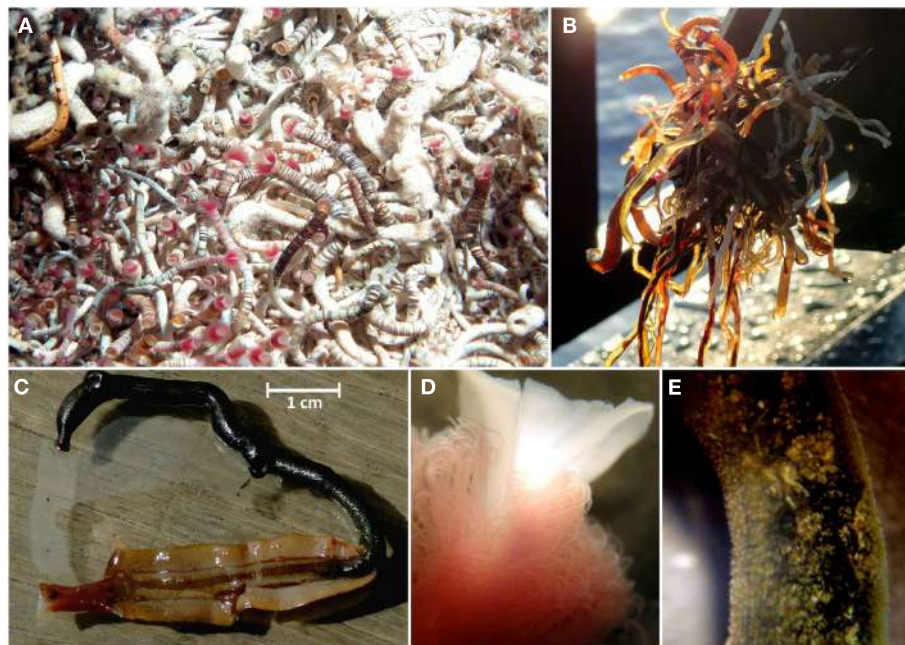


**FIGURE 3 |** *Lamellibrachia* sp. tubeworms recovered from the Palinuro volcanic complex (Mediterranean Sea). **(A)** in their natural habitat (photo obtained at Palinuro during cruise Pos340), **(B)** directly after ROV Mohawk

recovery (Pos412) onboard, **(C)** individual from colony #1 dissected from its tube (not used for further analysis), **(D)** stereo-micrograph of plume region, **(E)** stereo-micrograph of trophosome region.

### Characterization of Gulf of Mexico tubeworms

Gulf of Mexico tubeworm samples were identified using mitochondrial 16S rRNA genes amplified from DNA extracted from the endosymbiont free vestimentum tissue. Phylogenetic results confirmed the initial morphological characterizations of *Lamellibrachia luyimesi*/*Lamellibrachia* sp. 1 (van der Land and Nørrevang, 1975), *Lamellibrachia* sp. 2, *Escarapia laminata* (Jones, 1985), and *Seepiophila jonesi* (Gardiner et al., 2001; Table 2; Figure 4).

### CHARACTERIZATION OF THE TUBEWORM ENDOSYMBIONTS

#### Endosymbionts of *L. anaximandri* from Palinuro

Microscopic studies on the Palinuro *L. anaximandri* revealed high numbers of coccoid bacterial cells in broken trophosome tissue. These endosymbiotic bacterial cells varied considerably in size (2–10 µm diameter) and shape (spherical to irregularly coccoid). The color in the light microscope ranged from light to dark brown. Different modes of cell division were observed: equal division, unequal division, and budding (Figure 5). The cell surface of many endosymbionts showed a characteristic pattern of small invaginations (0.2–0.5 µm diameter), while others had a completely smooth surface. Frequently it was observed that cells in the process of budding or unequal cell division had a structured surface in the larger (older) part of the cell, while the bud was smooth (Figure 5).

The bacterial endosymbionts of the tubeworms were identified by constructing 16S rRNA gene clone libraries from DNA extracted from the trophosome tissue of 11 tubeworm individuals. For each specimen at least 20 clones were sequenced and analyzed. The bacterial 16S rRNA gene sequences of each specimen had >99% sequence identity, thus representing a single OTU. The

consensus sequences (OTUs) from the different individuals were identical (100% sequence identity over a total length of 1,387 bp), indicating that only one bacterial endosymbiont phylotype was present in the Palinuro tubeworms. BLAST analysis revealed the gammaproteobacterial sulfide-oxidizing “phylotype 2” bacterial endosymbiont of *L. anaximandri* from the Eastern Mediterranean mud volcanoes as the closest relative (FM165438, 99.7% sequence identity, five nucleotides differences over a total length of 1,387 bp (Duperron et al., 2009). Other closely related sequences originate from other *Lamellibrachia* spp. and seep vestimentiferan endosymbionts from outside the Mediterranean (Figure 6). The endosymbionts of hydrothermal vent tubeworms *Riftia pachyptila* and *Tevnia jerichonana* were more distantly related and clustered on a separate branch within the 16S rRNA gene tree (Figure 6).

#### Phylogeny of seep vestimentiferan endosymbionts from the Gulf of Mexico

Bacterial endosymbionts from GoM tubeworm specimen were identified by amplification and direct sequencing of 16S rRNA genes from DNA extracted from the trophosome tissue.

The GoM vestimentiferan tubeworm’s endosymbionts were affiliated with the three monophyletic groups of seep vestimentiferan tubeworm endosymbiont sequences described by McMullin et al. (2003). Three specimens from GoM site DC673 (*Lamellibrachia* sp. 1, *Lamellibrachia* sp. 2, and *E. laminata* (DC673\_1211, DC673\_1209, DC673\_1170) shared the identical (100% 16S rRNA gene sequence) “group 2” endosymbiont, very closely related to the sequences from *Lamellibrachia* sp. 1 and sp. 2 endosymbionts at site GC852 (GC852\_L4, GC852\_L1, GC852\_L5) and *E. laminata* endosymbiont sequence from WR269

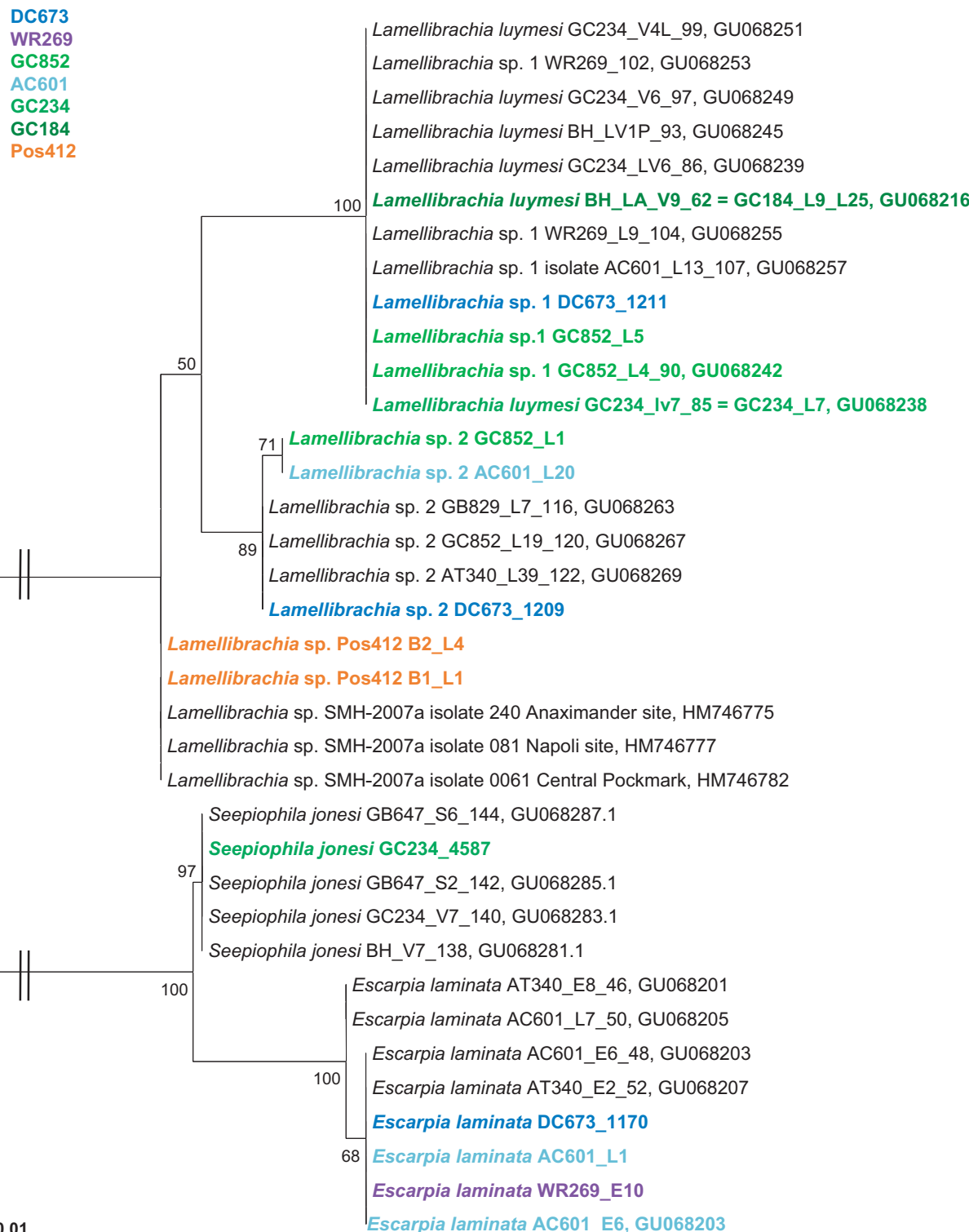


**FIGURE 4 | Phylogenetic relationship of vestimentiferan tubeworms based on mitochondrial 16S rRNA gene sequences.**  
The Maximum Likelihood tree was calculated using the GTR model.

Numbers at the nodes indicate the proportion of occurrences in 100 bootstrap replicates. The scale represents 0.01 substitutions per nucleotide site.

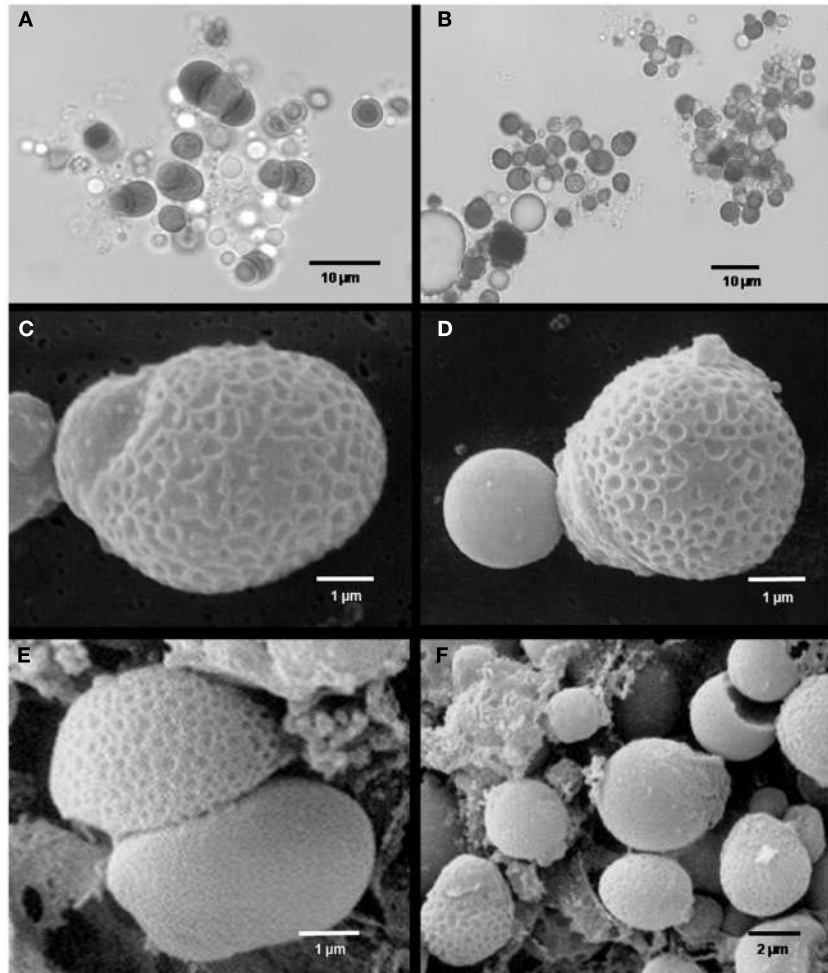


**FIGURE 5 | Microscopic images of Palinuro *Lamellibrachia anaximandri* specimen endosymbionts. (A,B)** Light micrographs showing trophosome content with large spherical prokaryotic cells (dark) of different size and shape. Various stages of equal and unequal

cell division as well as budding can be recognized. **(C–F)** Scanning electron micrographs showing endosymbionts with characteristically structured cell surface. Probable budding stages **(C,D)** and unequal cell division **(E,F)**.

(WR269\_E10). However, the endosymbiont sequence derived from an *E. laminata* specimen at site AC601 (AC601\_E6) differed and clustered with “group 1” sequences. In two other tube-worm specimens (*E. laminata* and *Lamellibrachia* sp. 2) from site AC601 (AC601\_L1, AC601\_L20) we detected two different endosymbionts, one clustering with “group 1” (AC601\_L1-PT1, AC601\_L20-PT1) and the other with “group 2” (AC601\_L1-PT2, AC601\_L20-PT2). Endosymbiont sequences derived from *S. jonesi* and *L. luymesi* tubeworms from the shallower sites GC234 (GC234\_4587, GC234\_L7), and GC184 (GC184\_L9) clustered with “group 3” sequences (Figure 6).

#### Genes involved in endosymbiont energy metabolism

In order to determine the potential energy-generating pathways for chemoautotrophic growth of the endosymbiont from the Palinuro *L. anaximandri*, we tried to amplify fragments of genes coding for key enzymes involved in the oxidation of sulfur compounds, hydrogen and methane.

The genetic potential for sulfur oxidation of the endosymbiont was analyzed by amplifying gene fragments coding for dissimilatory sulfite reductase (*dsrAB*), APS reductase (*aprA*) – both enzymes of the APS pathway – and sulfate thiohydrolase (*soxB*), an essential component of the Sox multienzyme complex (Friedrich et al., 2001). Fragments of all three genes (*dsrAB*, *aprA*, *soxB*) were recovered supporting a sulfide-oxidizing chemotrophic energy metabolism of the endosymbiont. Sequence similarities as well as phylogenetic analysis showed them to be very similar to the endosymbionts of other *L. anaximandri* (*apr* within symbiont cluster) and the vestimentiferans *Riftia pachyptila* and *Tevnia jerichonana* from hydrothermal vents on the East Pacific Rise (*dsrAB*, *soxB*; Figure 7). The 397 bp *aprA* sequence showed highest similarity (97% nucleotide similarity, 100% amino acid similarity) to *L. anaximandri* endosymbiont “phylotype 1” described from seep specimens at the Amon mud volcano in the Eastern Mediterranean (Duperron et al., 2009). Phylogenetic analysis places the *Lamellibrachia* *aprA* sequences in a cluster of oxidizing

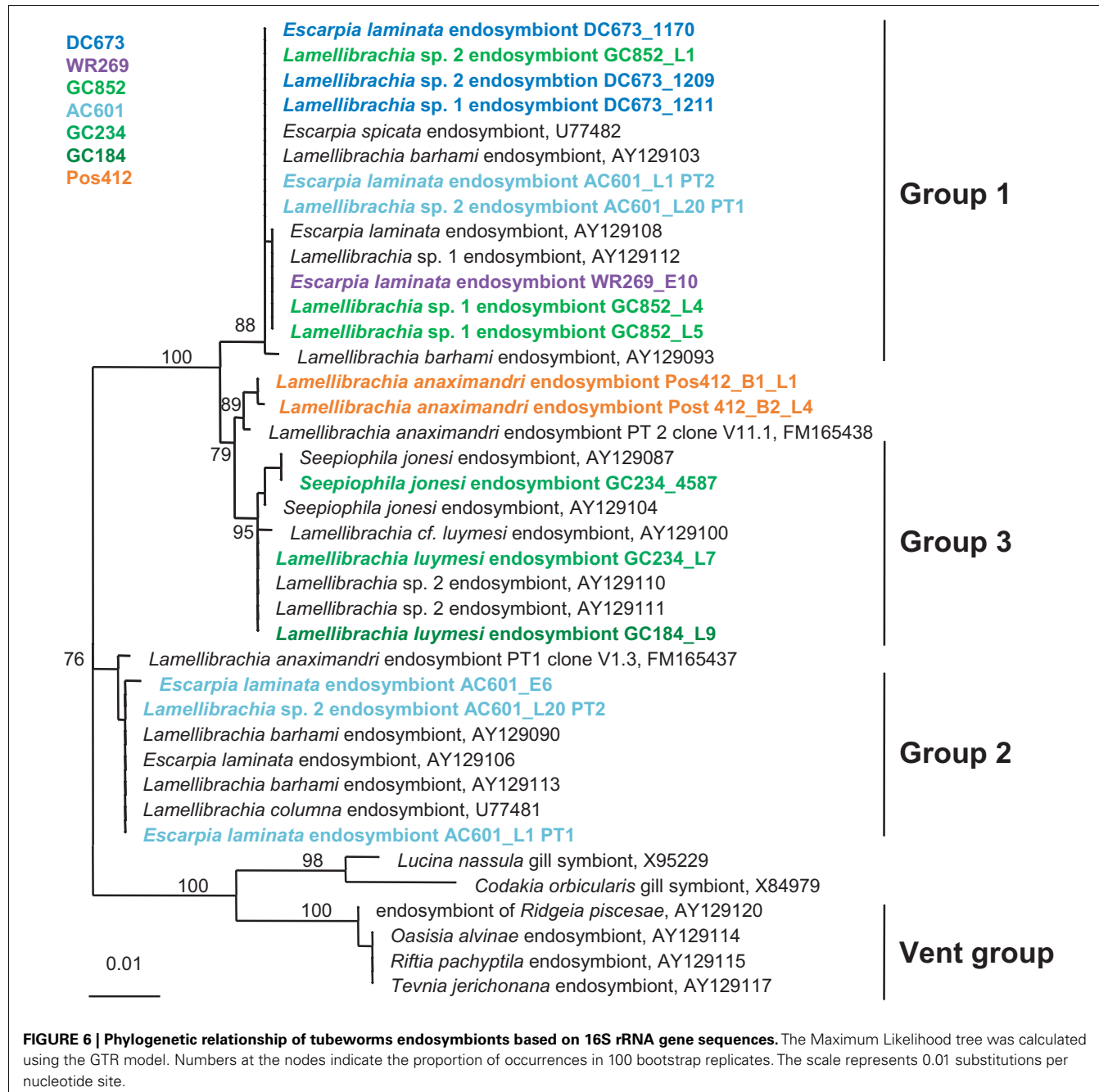


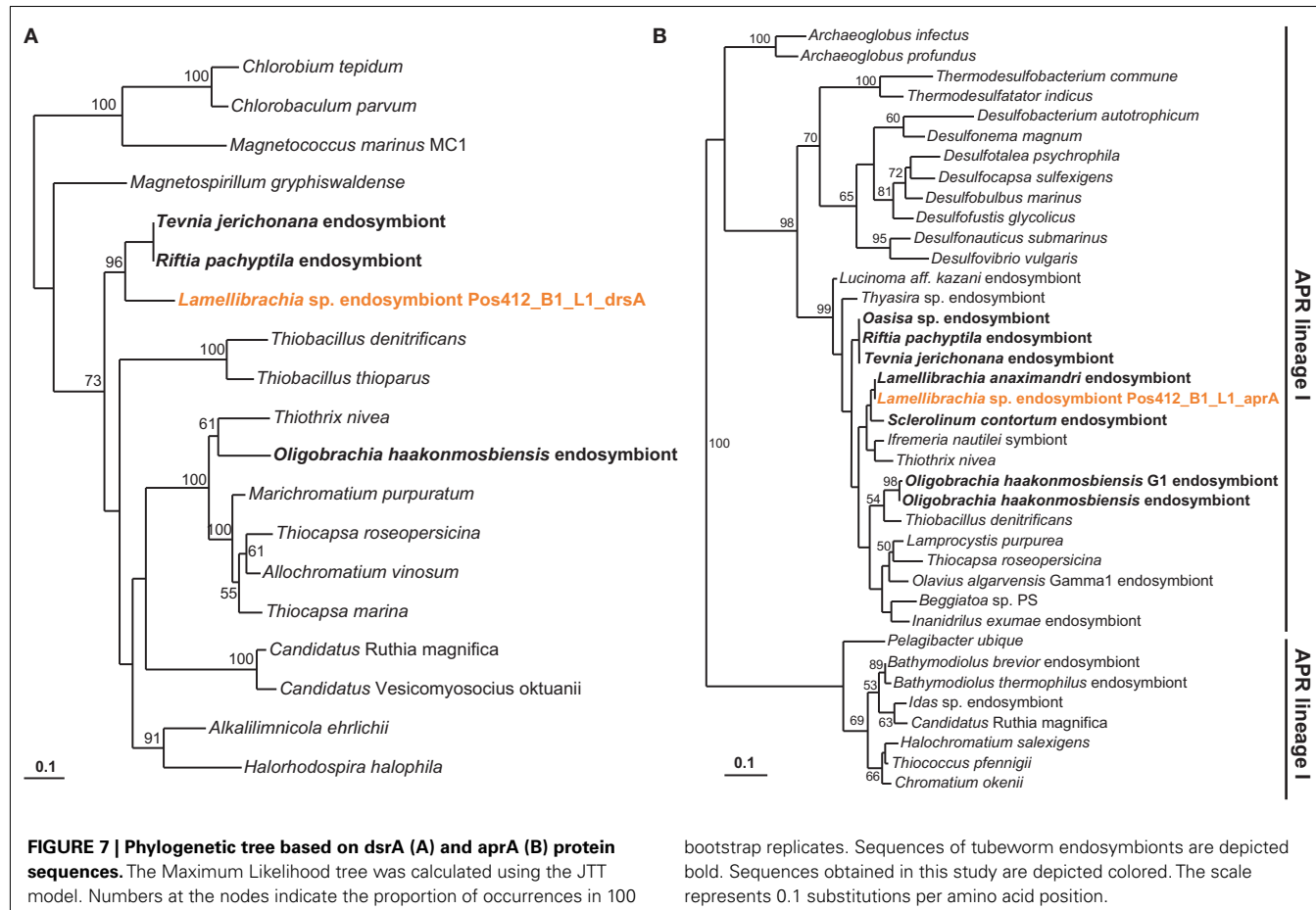
**FIGURE 6 | Phylogenetic relationship of tubeworms endosymbionts based on 16S rRNA gene sequences.** The Maximum Likelihood tree was calculated using the GTR model. Numbers at the nodes indicate the proportion of occurrences in 100 bootstrap replicates. The scale represents 0.01 substitutions per nucleotide site.

lineage II APS reductase gene sequences of endosymbiotic and free-living beta- and gammaproteobacteria including endosymbionts of *Riftia* and *Tevnia* (Meyer and Kuever, 2007a; Markert et al., 2011; Gardebrecht et al., 2012). The *dsrAB* gene fragment (987 bp) was most closely related to dissimilatory sulfite reductase genes from the *Riftia/Tevnia* endosymbiont (NZ\_AFZB01000023, EGW53672, and EGV52261, 80% nucleotide and 84% amino acid sequence similarity, Figure 7).

Likewise, the 986 bp *soxB* fragment from *L. anaximandri* from Palinuro showed highest similarities to *soxB* from *Candidatus*

*Endoriftia persephone* (EF618617, EGV50931, and EGW54296, 84% nucleotide similarity, 90% amino acid similarity).

A fragment of the *hupL* gene, encoding the large subunit of a [NiFe] uptake hydrogenase was amplified using the primer set W1 and Wxy. BLAST search as well as phylogenetic analysis demonstrated highest similarity with reference sequences from the *Riftia/Tevnia* endosymbiont (EGV51840, EGW53439, 82% nucleotide identity, 93% amino acid identity). This enzyme has been shown to be involved in the oxidation of molecular hydrogen for energy generation (Petersen et al., 2011; Kleiner et al., 2012).



Key genes for enzymes of methane oxidation (*mxaF*, *mmoX*, *pmoA*) were not successfully amplified with the different primer sets (MxaF1003, MxaR1555, MxaR1561, *mmoXA*, *mmoXB*, A189F, MB661R; Costello and Lidstrom, 1999; Auman et al., 2000; Neufeld et al., 2007; Kalyuzhnaya et al., 2008) used in this study.

#### Genes involved in nitrate reduction

A nitric oxide reductase (*norCB*) gene sequence was successfully amplified and sequenced from the Palinuro *L. anaximandri* endosymbiont indicating the potential to reduce nitrate. The closest relative was again the endosymbiont of *Riftia/Tevnia* (EMBL entry ZP\_08818090) with 95% amino acid sequence similarity. In the metagenomes of the *Riftia* and *Tevnia* endosymbionts, all genes needed for a complete respiration of nitrate to dinitrogen gas have been detected, and it has been suggested that the endosymbionts of these species could possibly use nitrate as alternative electron acceptor (Gardebrecht et al., 2012).

#### Genes involved in carbon fixation

To investigate the autotrophic potential of the endosymbionts, we tried to amplify key genes of two carbon fixation pathways, the CBB cycle and the reductive tricarboxylic acid (rTCA) cycle.

The CO<sub>2</sub> fixing enzyme ribulose 1,5-bisphosphate carboxylase/oxygenase (RubisCO) is the key enzyme of the CBB cycle. In proteobacteria, two different types are known, form I, encoded

by the *cbbL* gene, and form II encoded by *cbbM*. In accordance with other studies on *Lamellibrachia* spp. endosymbionts (Elsaied and Naganuma, 2001; Elsaied et al., 2002), we failed to amplify *cbbL* from the Palinuro tubeworm endosymbiont. In contrast, a fragment of the *cbbM* gene was detected supporting the usage of the CBB cycle for carbon fixation by the endosymbiont as was also previously demonstrated for other *Lamellibrachia* spp. endosymbionts (Elsaied and Naganuma, 2001; Elsaied et al., 2002; Vrijenhoek et al., 2007). The *cbbM* sequence displayed high similarity (96% nucleotide similarity, 100% amino acid similarity) to the bacterial endosymbiont of *L. anaximandri* from the Eastern Mediterranean (FM165442 and CAQ63473, Duperron et al., 2009), but was quite different from *cbbM* sequences of *Riftia/Tevnia* endosymbionts (AF047688, 78% nucleotide similarity, 75% amino acid similarity).

Based on genomic, proteomic, enzymatic as well as isotopic data, the *Riftia pachyptila* endosymbiont uses the rTCA cycle in addition to the CBB cycle for autotrophic carbon fixation (Markert et al., 2007, 2011; Gardebrecht et al., 2012). Yet a novel type of ATP citrate lyase (type II ACL) might be active in this case (Hügler and Sievert, 2011).

Newly designed primers were used to amplify a putative type II ACL from the endosymbionts of the Palinuro tubeworms. Unexpectedly, amplified fragments of this type II ACL gene indicate additional use of the rTCA cycle for carbon fixation

in the Palinuro *L. anaximandri* endosymbiont as well. BLAST results with sequence similarities of 78% amino acid identities, as well as the phylogenetic analysis indicate the gene to be most closely related to the *Riftia* and *Tevnia* endosymbiont (NCBI entry ZP\_08829917 and ZP\_08817421). In contrast genes coding for a conventional ACL could not be detected using previously published primers for either sub-units (*aclA* or *aclB*, Campbell et al., 2003; Hügler et al., 2005).

#### **Carbon fixation genes in seep vestimentiferan endosymbionts from the Gulf of Mexico**

The discovery of ACL genes in the *L. anaximandri* endosymbiont from the Palinuro volcanic complex raised the question about the further distribution of these genes in tubeworm endosymbionts, especially seep species. Thus we analyzed endosymbionts from 13 tubeworms from six different sites in the GoM. We discovered the type II ACL genes in all tubeworm endosymbionts investigated, regardless of their host species identity or site in the GoM (Table 2). Sequence analysis revealed the type II ACL gene to be highly conserved between the different GoM tubeworm endosymbionts. Three different phylotypes were found to be present in the 13 tubeworm samples in the GoM, and all three differed from the sequences found in the Palinuro *L. anaximandri* endosymbionts (Figure 8A). All GoM endosymbionts of host specimens from the sites DC673, WR269, and GC852 (DC673\_1211, DC673\_1209, DC673\_1170, WR269\_E10, GC852\_L4, GC852\_L1, GC852\_L5) shared identical (100% AA similarity) type II ACL gene sequences (cluster 2) regardless of host species identity. Endosymbionts of GoM host specimens from the shallower Green Canyon sites GC234 and GC184 (GC234\_4587, GC184\_L9, GC234\_L7) also bear one single type II ACL gene sequence (cluster 3; 100% AA similarity), which differed from the deep water site sequence in 14 AA. The third sequence type (cluster 1) was retrieved from endosymbionts of Alaminos Canyon site AC601 (AC601\_E6, AC601\_L1, AC601\_L20). Within AC601\_L1 and AC601\_L20 a second ACL sequence type identical to the sequences of cluster 2 was also retrieved. In phylogenetic analysis, the GoM tubeworm endosymbiont ACL type II sequences formed a cluster together with the Mediterranean *L. anaximandri* endosymbiont sequences, and were clearly separated from the *Riftia/Tevnia* sequences (Figure 8A).

In addition to the *acl* genes, we also amplified the *cbbM* gene of the GoM tubeworm endosymbionts. As expected, all endosymbionts harbored a *cbbM* gene in addition to the *acl* gene. Similar to the 16S rRNA and *acl* genes, the *cbbM* genes from the GoM endosymbionts formed three different clusters (Figure 8B). Cluster 1 comprises the sequences of Alaminos Canyon site AC601 specimens, AC601\_E6, AC601\_L1, and AC601\_L20. The *cbbM* sequences of DeSoto Canyon, Walker Ridge, and Green Canyon specimens DC673\_1211, DC673\_1209, WR269\_E10, GC852\_L4, GC852\_L1, GC852\_L5 form a second cluster (cluster 2), while the *cbbM* sequence of sample DC673\_1170 falls in between these two clusters. Cluster 3 (Green Canyon samples GC234\_4587, GC184\_L9, GC234\_L7) is clearly separated from the others. The *cbbM* sequences from the Mediterranean tubeworm endosymbionts form a separate cluster. Quite interestingly, the *cbbM*

sequences of the *Riftia/Tevnia* endosymbionts are only distantly related (Figure 8B).

#### **ISOTOPIC SIGNATURE**

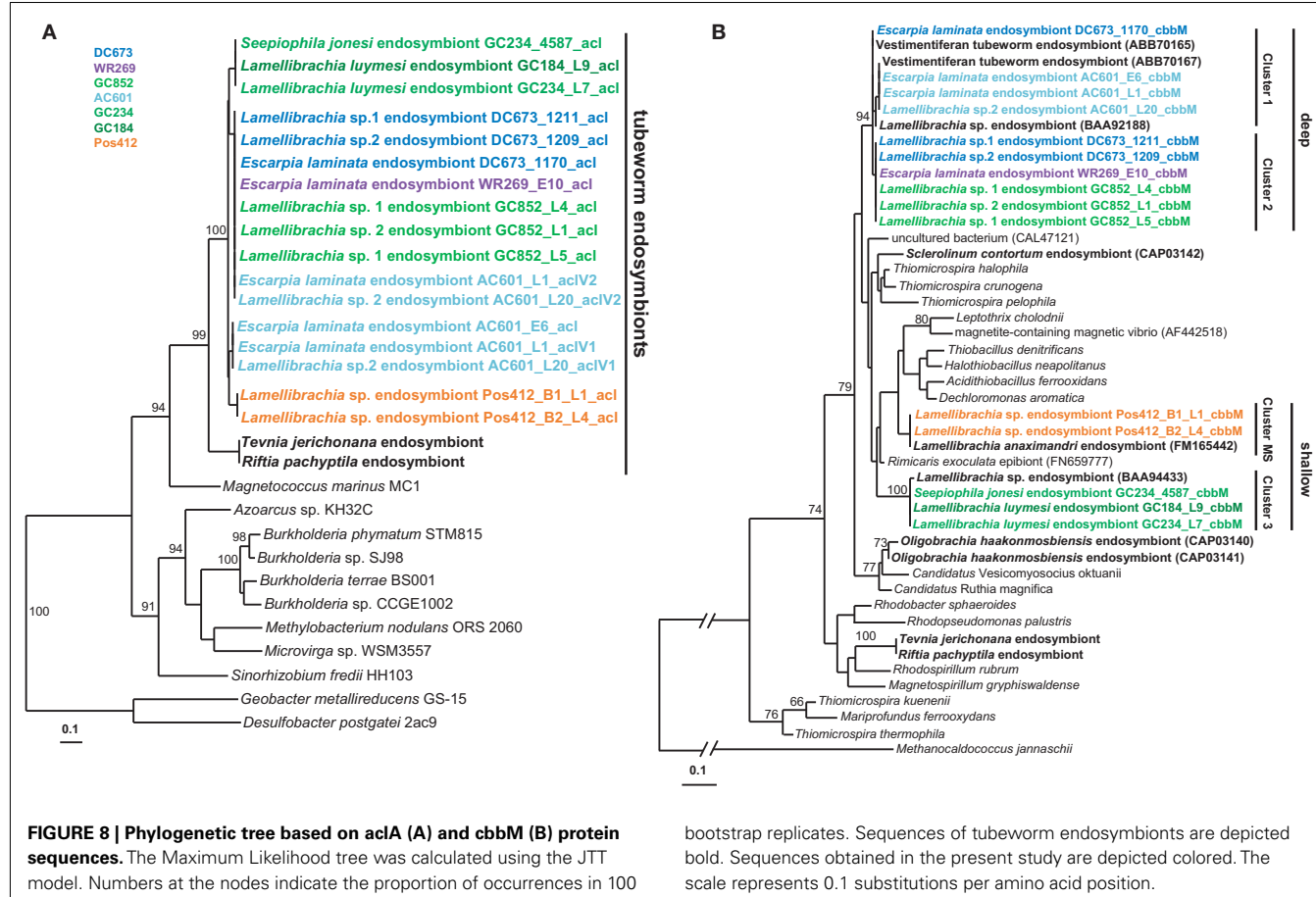
Bulk organic carbon isotopes analyses of gill tissue from two Palinuro tubeworms resulted in  $\delta^{13}\text{C}$  values of  $-22.5$  and  $-23.4\text{\textperthousand}$ , which are in accordance to previous measurements of Mediterranean *Lamellibrachia* spp. (Olu-Le Roy et al., 2004; Carrier et al., 2010) but more positive than most *Lamellibrachia* spp. from non-Mediterranean hydrocarbon seeps (Becker et al., 2011). The carbon isotopic composition of dissolved inorganic carbon in emanating diffuse fluids sampled at the tubeworm colonies display  $\delta^{13}\text{C}$  values of  $-0.39$  and  $-0.68\text{\textperthousand}$ . The  $\delta^{13}\text{CDIC}$  values of additional samples of shimmering water in the area range from  $-1.62$  to  $+1.76\text{\textperthousand}$ .

## **DISCUSSION**

### **PHYLOGENY AND BIOGEOGRAPHY OF THE MEDITERRANEAN TUBEWORMS**

The discovery of living vestimentiferan tubeworm colonies associated with active hydrothermal venting during a seafloor survey of the Palinuro volcanic complex (Mediterranean Sea) in July 2006 (Petersen et al., 2008; Monecke et al., 2009) came as a surprise, as until then, vent-associated tubeworms were only known from the Pacific Ocean. Living individuals of the tubeworms were sampled during a research cruise in 2011 and this communication is the first description of the worms and their endosymbionts. Phylogenetic analyses of 18S rRNA, COI and mitochondrial 16S rRNA genes showed that the tubeworms from Palinuro are *Lamellibrachia anaximandri* recently described from mud volcanoes of the Eastern Mediterranean (Southward et al., 2011). The highest *in vivo* temperatures measured among the tubes in tubeworm aggregations at the Palinuro hydrothermal vent field were  $15.6$ – $19.4^\circ\text{C}$ , elevated by as much as  $5.4^\circ\text{C}$  from the surrounding Mediterranean Seawater ( $14^\circ\text{C}$ ) and the previously published tubeworm-bearing locations in the Eastern Mediterranean ( $13$ – $14^\circ\text{C}$ ), extending the previously described temperature range of the species (Southward et al., 2011). *L. anaximandri* has also been detected in a mud volcano field in the Western Mediterranean (Hilário et al., 2011), as well as on two ship wrecks in the Eastern Mediterranean ( $110$  km southeast of Crete, Hughes and Crawford, 2008) and the Southern Tyrrhenian Sea (Gambi et al., 2011; Figure 1). Even though this species has not been detected in the Northeastern Atlantic it has been hypothesized to occur at the West African and Lusitanian margins as well (Hilário et al., 2011).

The high diversity of habitats for the Mediterranean *Lamellibrachia* species is in accordance with *Escarpia* spp. and other *Lamellibrachia* spp. Originally regarded as seep species, they were subsequently found in several non-seep habitats, i.e., at sediment covered hydrothermal sites in the Pacific (Juniper et al., 1992; Fujikura et al., 2006; Miake et al., 2006; Miura and Kojima, 2006), as well as ship wrecks (Dando et al., 1992), and whale falls (Feldman et al., 1998). Considering the high diversity of so-called “seep” tubeworm habitats a high site-flexibility of these organisms becomes apparent and supports the importance of different non-seep habitats in their geographic distribution and the stepping



stone hypothesis (Kimura and Weiss, 1964; Smith and Kukert, 1989; Black et al., 1994; Olu et al., 2010). Larval survival of at least three weeks and about five weeks has been demonstrated for the vestimentiferans *Riftia pachyptila* and *Lamellibrachia luymesi* respectively, suggesting potential dispersal distances on the order of 100 km for seep and vent vestimentiferans (Young et al., 1996; Marsh et al., 2001; Tyler and Young, 2003). A variety of reducing habitats, functioning as dispersal stepping-stones separated by days or weeks and connected by currents or shared water masses could facilitate the large species ranges described for many vestimentiferans, including the seep species *L. barhami*, which has been found in seep and low activity vent sites spanning at least 4,000–6,000 km of geographical distance (McMullin et al., 2003).

## PHYLOGENY OF ENDOSYMBIOTS

The trophosome of the *L. anaximandri* specimens from Palinuro analyzed in this study harbored a single gammaproteobacterial phylotype regardless of collection site or morphotype. The endosymbiont was closely related (99.7%) to the phylotype 2 found in *L. anaximandri* from the Amon mud volcano east of the Nile deep-sea fan (Duperron et al., 2009). The dominating endosymbiont (phylotype 1) of the seep specimen from the Amon mud volcano was not found in the tubeworms at the Palinuro hydrothermal vents.

This study is the first to characterize vestimentiferan tube-worm endosymbionts of shallow hydrothermal vents in the Mediterranean Sea. The gammaproteobacterial endosymbiont clusters with endosymbionts of other seep-associated tubeworms and are clearly distinct from the endosymbionts of vent tubeworms like *Riftia* and *Tevnia* (Fisher et al., 1997; Nelson and Fisher, 2000; McMullin et al., 2003; Vrijenhoek et al., 2007). The phylogenetic affiliation of the Palinuro *L. anaximandri* endosymbiont with “group 3” endosymbiont 16S rRNA gene sequences, as well as the affiliation of the dominating phylotype of *L. anaximandri* specimen obtained from 1,157 m depth at Amon mud volcano with “group 1,” may indicate separation by depth, as suggested for other seep vestimentiferan endosymbionts (McMullin et al., 2003). However, both Mediterranean phylotype sequences show considerable differences to the “group 1” and “group 3” cluster sequences in signature nucleotide positions (Table A1 in Appendix) and Mediterranean and GoM tubeworms do not share identical endosymbiont phylotypes. Further, in the Amon mud volcano specimen, phylotypes of “group 1” and “group 3” are present, yet in assumed different abundances (deduced from the numbers of sequences in the clone libraries; Duperron et al., 2009). Endosymbionts of different groups are also present in individuals of *Lamellibrachia* sp. 2 (AC601\_L20) and *E. lamnata* (AC601\_L1) tubeworms from the GoM site AC601 (this study). Thus separation by depth alone cannot explain these

observations and further studies are needed in order to reveal the question how endosymbionts are selected by their vestimentiferan hosts.

### METABOLIC CHARACTERISTICS OF THE ENDOSYMBIONT

Based on the functional gene analyses of this study, the endosymbiont of *Lamellibrachia anaximandri* from Palinuro is a sulfide-oxidizing chemoautotroph.  $\delta^{13}\text{C}$  values measured in this study are in consistence with previous studies of *L. anaximandri* from Eastern Mediterranean mud volcano fields (Olu-Le Roy et al., 2004; Carlier et al., 2010), and together with delta  $\delta^{15}\text{N}$  and  $\delta^{34}\text{S}$  from previous studies support a chemoautotrophic endosymbiont based nutrition for the host tubeworm (Carlier et al., 2010). Due to the presence of *dsrAB* and *aprA* genes, sulfide oxidation most likely is carried out via the APS pathway with sulfite and adenosine phosphosulfate as intermediates. As in the *Riftia pachyptila* endosymbiont, *soxB* is also present in the endosymbiont of *L. anaximandri* from Palinuro. In thiosulfate-utilizing bacteria, *SoxB* functions as sulfate thiohydrolase. However, since tubeworm endosymbiont carbon fixation is not stimulated by thiosulfate, its function in the tubeworm endosymbionts remains uncertain (Fisher et al., 1989; Markert et al., 2011).

Although high methane fluxes were noted in the habitat of *L. anaximandri* in mud volcano habitats (Olu-Le Roy et al., 2004), genes of methane oxidation were not successfully amplified with the primer sets used in this study. In contrast, the potential to use hydrogen as an energy source was suggested by the detection of the key gene for hydrogen oxidation, *hupL* in the endosymbiont from the Palinuro *L. anaximandri*. The *hupL* gene was most similar to the respective genes of the *Riftia* and *Tevnia* endosymbionts, where it is even expressed *in situ* (Markert et al., 2011; Petersen et al., 2011). Hydrogen concentrations have not been measured in the hydrothermal fluids from Palinuro volcano complex. However, hydrogen is present in the fluids at many hydrothermal vents, and elevated hydrogen contents are present at vent systems associated with ultramafic (mantle) rocks, or, e.g., following a volcanic eruption (Wetzel and Shock, 2000; Allen and Seyfried, 2003; Kumagai et al., 2008; Petersen et al., 2011). Such H<sub>2</sub>-rich fluids found at vent systems associated with ultramafic rocks have recently been shown to be used as an energy source by the endosymbionts of a mussel, *Bathymodiolus puteoserpentis* (Petersen et al., 2011). The endosymbionts in *Bathymodiolus* spp. mussels are located on the external edge of the cells of gill filaments that are themselves only two cells thick. As a result, passive diffusion of the energy source (hydrogen, sulfide, and/or methane in different species) is sufficient to fuel the chemoautotrophic life style of these animals (Childress and Fisher, 1992). In contrast, the endosymbionts in tube-worms are deep in an interior tissue and must rely on the host blood to supply the electron donor for chemoautotrophy. Sulfide is transported in millimolar concentrations to the trophosome, bound to hemoglobin molecules in vestimentiferan tubeworms. Transport molecules for hydrogen or methane have not been found in these animals and thus both hydrogen and methane are unlikely to contribute significantly to the metabolism of the intact symbiosis in most environments (Childress and Fisher, 1992). However, the gammaproteobacterial endosymbiont might use hydrogen as potential energy source in its free-living stage. Thus,

the potential for use of hydrogen by tubeworm endosymbionts deserves additional study.

Detection of *cbbM* sequences coding for a form II RubisCO in all vestimentiferan tubeworms reviewed in this study indicates that the potential to fix CO<sub>2</sub> via the CBB cycle is widespread in vestimentiferan tubeworms (Elsaied and Naganuma, 2001; Elsaied et al., 2002; Naganuma et al., 2005; Vrijenhoek et al., 2007; Dupertren et al., 2009) and the detection of all genes of this cycle in the metagenome of the *Riftia* endosymbiont suggest this pathway is fully functional in vestimentiferans (see Markert et al., 2011 for further details). Enzyme activity measurements of RubisCO and phosphoribulokinase add further evidence to the usage of the CBB cycle in *Riftia* and *Lamellibrachia* endosymbionts (Felbeck, 1981; Felbeck et al., 1981). Up to now, there is no evidence for the presence of RubisCO form I (*cbbL*) in either the *Riftia/Tevnia* or any *Lamellibrachia* endosymbiont (this study; Elsaied and Naganuma, 2001; Elsaied et al., 2002; Naganuma et al., 2005; Dupertren et al., 2009).

In addition, *acl* genes, coding for ATP citrate lyase, the key enzyme of the rTCA cycle were recovered from the Palinuro *L. anaximandri* endosymbiont using newly designed primers, suggesting the presence of the rTCA cycle as alternate carbon fixation pathway. The operation of the rTCA cycle in addition to the CBB cycle was first shown for the *Riftia* and *Tevnia* endosymbiont using a combination of metagenomic, proteomic and enzymatic approaches (Markert et al., 2007; Robidart et al., 2008; Gardebrecht et al., 2012). In the case of the *Riftia/Tevnia* endosymbiont, citrate cleavage is accomplished by an unusual type of ATP citrate lyase, tentatively named ACL type II (Hügler and Sievert, 2011). The recovered *acl* sequence from the Mediterranean Palinuro *L. anaximandri* endosymbiont showed high similarities to the sequence of the *Riftia/Tevnia* endosymbiont (Figure 8A). Subsequent analyses of seep vestimentiferan (*Escarpiella*, *Seepiophila*, and *Lamellibrachia*) endosymbionts from different sites at the Gulf of Mexico showed the presence of type II ACL genes there as well. This implicates a wider distribution of these genes than previously thought. The presence of two different carbon fixation pathways – the CBB cycle and the rTCA cycle – in a single bacterium seems not restricted to the *Riftia/Tevnia* endosymbiont, but rather seems to be a common feature of vestimentiferan tubeworm endosymbionts, regardless of genus or habitat.

Despite the still rather scarce dataset of type II ACL gene sequences, these sequences appear to be monophyletic in tubeworm endosymbionts (Figure 8A). Similarly, ribosomal genes as well as *aprA* genes support a monophyletic origin for the tubeworm endosymbionts (Figures 6 and 7). In contrast, a monophyletic origin of the *cbbM* gene of tubeworm endosymbionts is not clearly supported by the phylogenetic analyses performed here (Figure 8B). This could mean that the rTCA cycle is the evolutionary older CO<sub>2</sub> fixation pathway in the endosymbionts, and the *cbbM* gene is acquired afterward, e.g., via lateral gene transfer. This evolutionary aspect clearly requires further studies.

The presence of two different carbon fixation pathways increases the metabolic versatility of the tubeworm endosymbionts. In case of the *Riftia/Tevnia* endosymbiont proteomic data suggest the usage of both pathways simultaneously (Markert et al., 2007, 2011; Gardebrecht et al., 2012). This is also supported by the isotopic signature of the *Riftia* tubeworms (Markert et al.,

2007). The carbon isotopic fractionation associated with the rTCA cycle is generally smaller than the one observed for the CBB cycle (House et al., 2003). Considering the carbon isotopic composition of ca.  $-23\text{\textperthousand}$  measured for plume tissue of two *L. anaximandri* tubeworms from Palinuro low temperature diffuse vent sites and a respective carbon isotopic composition of dissolved inorganic carbon ( $\delta^{13}\text{C}_{\text{DIC}}$  between  $-0.7$  and  $-0.4\text{\textperthousand}$ ), the isotopic difference would be consistent with the operation of the CBB cycle for autotrophic carbon fixation. Neither a greatly attenuated isotopic fractionation characteristic for the rTCA cycle nor an isotopic signature reflecting a substantial contribution from methane-derived carbon is discernible at the site studied here. Yet, one has to keep in mind, that the isotopic signature provides only indirect evidence and neither the actual fractionation by the enzymes involved in the rTCA cycle present in tubeworm endosymbionts, nor fractionation during uptake and transport of DIC to the endosymbionts are known. Thus future studies are needed in order to determine the conditions for the usage, as well as the regulation of the two different carbon fixation pathways in vestimentiferan tubeworm endosymbionts (Hügler and Sievert, 2011).

## CONCLUSION

In this study we characterize vestimentiferan tubeworms and their endosymbionts from the Mediterranean Sea and the GoM. The tubeworms retrieved from a shallow water hydrothermal vent field in the Western Mediterranean – Palinuro volcanic complex – represent the first vestimentiferan tubeworms found associated with hydrothermal venting outside the Pacific Ocean. Our molecular studies of marker genes (18S rRNA, mitochondrial 16S rRNA, and COI) identify the tubeworms as the recently described species *L. anaximandri*, the only vestimentiferan species described from the Mediterranean Sea to date.

Based on 16S rRNA gene surveys we conclude that the Palinuro *L. anaximandri* harbor a single gammaproteobacterial endosymbiont, closely related to endosymbionts of other *Lamellibrachia* spp. (Figure 6). Carbon isotopic data and the analysis of functional genes suggest a sulfide-oxidizing chemoautotrophic lifestyle. Energy can be generated by oxidizing reduced sulfur compounds via the APS pathway involving dissimilatory sulfite reductase and APS reductase. Due to the presence of a *hupL* gene one can speculate that the endosymbiont has the potential to use hydrogen as a supplemental energy source. Nitrate could potentially serve as alternative electron acceptor for the endosymbiont, as we detected a nitric oxide reductase gene sequence (*norCB*) and it was shown, that the metagenome of the *Riftia/Tevnia* endosymbiont includes all genes needed for the complete reduction of nitrate to dinitrogen gas (Gardebrecht et al., 2012).

Surprisingly, we were able to detect the key genes of two alternative carbon fixation pathways, namely *cbbM*, encoding RubisCO form II, the key enzyme of the CBB cycle, and a gene

coding for ATP citrate lyase type II, the key enzyme of the rTCA cycle. Newly designed primers were used to amplify a gene sequence of the type II ACL. The presence of the rTCA cycle in addition to the CBB cycle for carbon fixation was previously shown for the endosymbiont of the vent-associated tubeworms *Riftia pachyptila* and *Tevnia jerichonana* (Markert et al., 2007; Gardebrecht et al., 2012). However, before this study, only the CBB cycle was documented as a carbon fixation pathway for *Lamellibrachia* spp. (Felbeck, 1981; Felbeck et al., 1981; Elsaied and Naganuma, 2001; Elsaied et al., 2002; Vrijenhoek et al., 2007). We also demonstrate the presence of the key genes of both carbon cycles in the endosymbionts from *Lamellibrachia luymesi*, *Lamellibrachia* sp. 1, *Lamellibrachia* sp. 2, *Escarapia laminata*, and *Seepiophila jonesi* from the Gulf of Mexico. These results suggest that the occurrence of two carbon fixation pathways in one bacterium may be a common feature of vestimentiferan tubeworm endosymbionts, which in turn indicates that this feature is more widely distributed than previously considered. It has already been shown, that carbon fixation through the rTCA cycle is important at deep-sea hydrothermal vent sites (cf. Hügler and Sievert, 2011 and references therein). Our study indicates that the rTCA cycle could play an important role at seep sites as well.

## ACKNOWLEDGMENTS

The authors would like to thank the captain and crew of R/V *Poseidon* for their support during cruise Pos412. We also gratefully acknowledge the support of ROV pilots Jamie Norman and Paul Hastings during sampling as well as Peter Buchanan (Oceaneering Inc., Aberdeen, UK) for good cooperation during ROV Mohawk negotiations and adaptation for research purposes. We further thank Katrin Kleinschmidt (GEOMAR, Kiel, Germany) for onboard support. We also thank the captains and crews of the R/V *Seward Johnson* and NOAA ship *Ronald Brown* as well as the pilots and support personnel for the Johnson Sea Link submersible and ROV Jason II for assistance with the collection of GoM Tubeworms. For Sanger sequencing, we would like to thank the teams from the IKMB at the UK-SH, Kiel, Germany and from the sequencing facility at the Pennsylvania State University, PA, USA. Artur Fugmann and Ben Hindersmann (WWU Münster, Germany) are thanked for their assistance during stable isotope measurements, and Ulrike Westernströer and Karen Bremer (CAU Kiel, Germany) for help with elemental analysis. Further, we thank Chunya Huang (Pennsylvania State University, PA, USA) for assistance during COI gene analysis and Costantino Vetriani (Rutgers University, NJ, USA) for fruitful discussion. JFI, SP, DGS, and HS acknowledge support through the German Science Foundation (IM12/18). CRF acknowledges the support of the US NSF, the US Bureau of Ocean Energy Management and US NOAA Office of Ocean Exploration for many years of support for the study of GoM seep communities.

## REFERENCES

- Allen, D. E., and Seyfried, W. E. (2003). Compositional controls on vent fluids from ultramafic-hosted hydrothermal systems at mid-ocean ridges: an experimental study at 400°C, 500 bars. *Geochim. Cosmochim. Acta* 67, 1531–1542.
- Altschul, S. F., Madden, T. L., Schäffer, A. A., Zhang, J., Zhang, Z., Miller, W., et al. (1997). Gapped BLAST and PSI-BLAST: a new generation of protein database search programs. *Nucleic Acids Res.* 25, 3389–3402.
- Auman, A. J., Stolyar, S., Costello, A. M., and Lidstrom, M. E. (2000). Molecular characterization of methanotrophic isolates from freshwater lake sediment. *Appl. Environ. Microbiol.* 66, 5259–5266.
- Bayon, G., Loncke, L., Dupré, S., Caprais, J. C., Ducassou, E., Duperron, S., et al. (2009). Multi-disciplinary investigation

- of fluid seepage on an unstable margin: the case of the Central Nile deep sea fan. *Mar. Geol.* 261, 92–104.
- Becker, E. L., Macko, S. A., Lee, R. W., and Fisher, C. R. (2011). Stable isotopes provide new insights into physiological ecology at Gulf of Mexico cold seeps. *Naturwissenschaften* 98, 169–174.
- Black, M. B., Lutz, R. A., and Vrijenhoek, R. C. (1994). Gene flow among vestimentiferan tube worm (*Riftia pachyptila*) populations from hydrothermal vents of the eastern Pacific. *Mar. Biol.* 120, 33–39.
- Bright, M., Keckeis, H., and Fisher, C. R. (2000). An autoradiographic examination of carbon fixation, transfer and utilization in the *Riftia pachyptila* symbiosis. *Mar. Biol.* 136, 621–632.
- Campbell, B. J., and Cary, S. C. (2004). Abundance of reverse tricarboxylic acid cycle genes in free-living microorganisms at deep-sea hydrothermal vents. *Appl. Environ. Microbiol.* 70, 6282–6289.
- Campbell, B. J., Stein, J. L., and Cary, S. C. (2003). Evidence of chemolithoautotrophy in the bacterial community associated with *Alvinella pompejana*, a hydrothermal vent polychaete. *Appl. Environ. Microbiol.* 69, 5070–5078.
- Carlier, A., Ritt, B., Rodrigues, C. F., Sarrazin, J., Olu, K., Grall, J., et al. (2010). Heterogeneous energetic pathways and carbon sources on deep eastern Mediterranean cold seep communities. *Mar. Biol.* 157, 2545–2565.
- Childress, J. J., and Fisher, C. R. (1992). The biology of hydrothermal vent animals: physiology, biochemistry, and autotrophic symbioses. *Oceanogr. Mar. Biol. Ann. Rev.* 30, 337–441.
- Cline, J. D. (1969). Spectrophotometric determination of hydrogen sulfide in natural waters. *Limnol. Oceanogr.* 454–458.
- Cordes, E. E., Bergquist, D. C., and Fisher, C. R. (2009). Macro-ecology of Gulf of Mexico cold seeps. *Ann. Rev. Mar. Sci.* 1, 143–168.
- Costello, A. M., and Lidstrom, M. E. (1999). Molecular characterization of functional and phylogenetic genes from natural populations of methanotrophs in lake sediments. *Appl. Environ. Microbiol.* 65, 5066–5074.
- Csaki, R., Hanczar, T., Bodrossy, L., Murrell, J. C., and Kovacs, K. L. (2001). Molecular characterization of structural genes coding for a membrane bound hydrogenase in *Methylococcus capsulatus* (Bath). *FEMS Microbiol. Lett.* 205, 203–207.
- Dando, P. R., Southward, A. F., Southward, E. C., Dixon, D. R., and Crawford, A. (1992). Shipwrecked tube worms. *Nature* 356, 667–667.
- Duperron, S., De Beer, D., Zbinden, M., Boetius, A., Schipani, V., Kahil, N., et al. (2009). Molecular characterization of bacteria associated with the trophosome and the tube of *Lamellibrachia* sp., a siboglinid annelid from cold seeps in the Eastern Mediterranean. *FEMS Microbiol. Ecol.* 69, 395–409.
- Elsaied, H., Kimura, H., and Naganuma, T. (2002). Molecular characterization and endosymbiotic localization of the gene encoding D-ribulose 1,5-bisphosphate carboxylase/oxygenase (RuBisCO) form II in the deep-sea vestimentiferan trophosome. *Microbiology* 148, 1947–1957.
- Elsaied, H., and Naganuma, T. (2001). Phylogenetic diversity of ribulose-1, 5-bisphosphate carboxylase/oxygenase large-subunit genes from deep-sea microorganisms. *Appl. Environ. Microbiol.* 67, 1751–1765.
- Felbeck, H. (1981). Chemoautotrophic potential of the hydrothermal vent tube worm, *Riftia pachyptila* Jones (Vestimentifera). *Science* 213, 336–338.
- Felbeck, H., Childress, J. J., and Somero, G. N. (1981). Calvin-Benson cycle and sulphide oxidation enzymes in animals from sulphide-rich habitats. *Nature* 293, 291–293.
- Feldman, R. A., Shank, T. M., Black, M. B., Baco, A. R., Smith, C. R., and Vrijenhoek, R. C. (1998). Vestimentiferan on a whale fall. *Biol. Bull.* 194, 116–119.
- Fisher, C. R., Childress, J. J., and Minchin, E. (1989). Autotrophic carbon fixation by the chemoautotrophic symbionts of *Riftia pachyptila*. *Biol. Bull.* 177, 372–385.
- Fisher, C. R., Urcuyo, I. A., Simpkins, M. A., and Nix, E. (1997). Life in the slow lane: growth and longevity of cold-seep vestimentiferans. *Mar. Ecol.* 18, 83–94.
- Folmer, O., Black, M., Hoeh, W., Lutz, R., and Vrijenhoek, R. (1994). DNA primers for amplification of mitochondrial cytochrome c oxidase subunit I from diverse metazoan invertebrates. *Mol. Marine Biol. Biotechnol.* 3, 294–299.
- Freytag, J. K., Girguis, P. R., Bergquist, D. C., Andras, J. P., Childress, J. J., and Fisher, C. R. (2001). A paradox resolved: sulfide acquisition by roots of seep tubeworms sustains net chemoautotrophy. *Proc. Natl. Acad. Sci. U.S.A.* 98, 13408–134013.
- Friedrich, C. G., Rother, D., Bardischewsky, F., Quentmeier, A., and Fischer, J. (2001). Oxidation of reduced inorganic sulfur compounds by bacteria: emergence of a common mechanism? *Appl. Environ. Microbiol.* 67, 2873–2882.
- Fujikura, K., Fujiwara, Y., and Kawato, M. (2006). A new species of *Osedax* (Annelida: Siboglinidae) associated with whale carcasses off Kyushu, Japan. *Zool. Sci.* 23, 733–740.
- Gambi, M. C., Schulze, A., and Amato, E. (2011). Record of *Lamellibrachia* sp. (Annelida: Siboglinidae: Vestimentifera) from a deep shipwreck in the western Mediterranean Sea (Italy). *Mar. Biodivers. Rec.* 4, e24.
- Garbe-Schönberg, D., Koschinsky, A., Ratmeyer, V., Jähnlich, H., and Westernströer, U. (2006). KIPS – a new multiport valve-based all-Teflon fluid sampling system for ROVs. *Geophys. Res. Abstr.* 8, 07032.
- Gardebrecht, A., Markert, S., Sievert, S. M., Felbeck, H., Thürmer, A., Albrecht, D., et al. (2012). Physiological homogeneity among the endosymbionts of *Riftia pachyptila* and *Tevnia jerichonana* revealed by proteogenomics. *ISMEJ* 6, 766–776.
- Gardiner, S. L., McMullin, E., and Fisher, C. R. (2001). *Seepiophila jonesi*, a new genus and species of vestimentiferan tube worm (Annelida: Pogonophora) from hydrocarbon seep communities in the Gulf of Mexico. *Proc. Biol. Soc. Wash.* 114, 694–707.
- Guindon, S., and Gascuel, O. (2003). A simple, fast, and accurate algorithm to estimate large phylogenies by maximum likelihood. *Syst. Biol.* 52, 696–704.
- Hall, T. A. (1999). BioEdit: a user-friendly biological sequence alignment editor and analysis program for Windows 95/98/NT. *Nucleic Acids Symp. Ser.* 41, 95–98.
- Hilário, A., Comas, M. C., Azevedo, L., Pinheiro, L., Ivanov, M. K., and Cunha, M. R. (2011). First record of a Vestimentifera (Polychaeta: Siboglinidae) from chemosynthetic habitats in the western Mediterranean Sea—Biogeographical implications and future exploration. *Deep Sea Res. Part I Oceanogr. Res. Pap.* 58, 200–207.
- House, C. H., Schopf, J. W., and Stetter, K. O. (2003). Carbon isotopic fractionation by Archaeans and other thermophilic prokaryotes. *Org. Geochem.* 34, 345–356.
- Hughes, D. J., and Crawford, M. (2008). A new record of the vestimentiferan *Lamellibrachia* sp. (Polychaeta: Siboglinidae) from a deep shipwreck in the eastern Mediterranean. *Mar. Biodivers. Rec.* 1, e21.
- Hügler, M., and Sievert, S. M. (2011). Beyond the calvin cycle: autotrophic carbon fixation in the ocean. *Ann. Rev. Mar. Sci.* 3, 261–289.
- Hügler, M., Wirsen, C. O., Fuchs, G., Taylor, C. D., and Sievert, S. M. (2005). Evidence for autotrophic CO<sub>2</sub> fixation via the reductive tricarboxylic acid cycle by members of the Epsilon-subdivision of proteobacteria. *J. Bacteriol.* 187, 3020–3027.
- Jones, M. L. (1985). On the Vestimentifera, new phylum: six new species, and other taxa, from hydrothermal vents and elsewhere. *Bull. Biol. Soc. Wash.* 117–158.
- Julian, D., Gaill, F., Wood, E., Arp, A. J., and Fisher, C. R. (1999). Roots as a site of hydrogen sulfide uptake in the hydrocarbon seep vestimentiferan *Lamellibrachia* sp. *J. Exp. Biol.* 202, 2245–2257.
- Juniper, S. K., Tunnicliffe, V., and Southward, E. C. (1992). Hydrothermal vents in turbidite sediments on a Northeast Pacific spreading centre: organisms and substratum at an ocean drilling site. *Can. J. Zool.* 70, 1792–1809.
- Kalyuzhnaya, M. G., Hristova, K. R., Lidstrom, M. E., and Chistoserdova, L. (2008). Characterization of a novel methanol dehydrogenase in representatives of *Burkholderiales*: implications for environmental detection of methylotrophy and evidence for convergent evolution. *J. Bacteriol.* 190, 3817–3823.
- Kennicutt, M. C., Brooks, J. M., Bidigare, R. R., Fay, R. R., Wade, T. L., and McDonald, T. J. (1985). Vent-type taxa in a hydrocarbon seep region on the Louisiana slope. *Nature* 317, 351–353.
- Kidd, R. B., and Ármannsson, H. (1979). Manganese and iron micronodules from a volcanic seamount in the Tyrrhenian Sea. *J. Geol. Soc. London* 136, 71–76.
- Kimura, M., and Weiss, G. H. (1964). The stepping stone model of population structure and the decrease of genetic correlation with distance. *Genetics* 49, 561–576.
- Kleiner, M., Wentrup, C., Lott, C., Teeling, H., Wetzel, S., Young, J., et al. (2012). Metaproteomics of a gutless marine worm and its symbiotic microbial community reveal unusual pathways

- for carbon and energy use. *Proc. Natl. Acad. Sci. U.S.A.* 109, E1173–E1182.
- Kojima, S., Ohta, S., Yamamoto, T., Miura, T., Fujiwara, Y., Fujikura, K., et al. (2002). Molecular taxonomy of vestimentiferans of the western Pacific and their phylogenetic relationship to species of the eastern Pacific. *Mar. Biol.* 141, 57–64.
- Kumagai, H., Nakamura, K., Toki, T., Morishita, T., Okino, K., Ishibashi, J. I., et al. (2008). Geological background of the Kairei and Edmond hydrothermal fields along the Central Indian Ridge: implications of their vent fluids' distinct chemistry. *GeoFluids* 8, 239–251.
- Lane, D. (1991) "16S/23S rRNA sequencing," in *Nucleic Acid Techniques in Bacterial Systematics*, eds E. Stackebrandt and M. Goodfellow (Chichester: John Wiley & Sons), 115–175.
- Lavik, G., Stührmann, T., Brüchert, V., Van der Plas, A., Mohrholz, V., Lam, P., et al. (2009). Detoxification of sulphidic African shelf waters by blooming chemolithotrophs. *Nature* 457, 581–584.
- Liao, X., Wang, D., Yu, X., Li, W., Cheng, L., Wang, J., et al. (2007). Characterization of novel microsatellite loci in rare minnow (*Gobiocypris rarus*) and amplification in closely related species in Gobioninae. *Conserv. Genet.* 8, 1003–1007.
- Ludwig, W., Strunk, O., Westram, R., Richter, L., Meier, H., Yadukumar, et al. (2004). ARB: a software environment for sequence data. *Nucleic Acids Res.* 32, 1363–1371.
- Markert, S., Arndt, C., Felbeck, H., Becher, D., Sievert, S. M., Hügler, M., et al. (2007). Physiological proteomics of the uncultured endosymbiont of *Riftia pachyptila*. *Science* 315, 247–250.
- Markert, S., Gardebrecht, A., Felbeck, H., Sievert, S. M., Klose, J., Becher, D., et al. (2011). Status quo in physiological proteomics of the uncultured *Riftia pachyptila* endosymbiont. *Proteomics* 11, 3106–3117.
- Marsh, A. G., Mullineaux, L. S., Young, C. M., and Manahan, D. T. (2001). Larval dispersal potential of the tubeworm *Riftia pachyptila* at deep-sea hydrothermal vents. *Nature* 411, 77–80.
- McMullin, E. R., Hourdez, S., Schaeffer, S. W., and Fisher, C. R. (2003). Phylogeny and biogeography of deep sea vestimentiferan tubeworms and their bacterial symbionts. *Symbiosis* 34, 1–41.
- Meyer, B., and Kuever, J. (2007a). Molecular analysis of the distribution and phylogeny of dissimilatory adenosine-5-phosphosulfate reductase-encoding genes (aprBA) among sulfur-oxidizing prokaryotes. *Microbiology* 153, 3478–3498.
- Meyer, B., and Kuever, J. (2007b). Phylogeny of the alpha and beta subunits of the dissimilatory adenosine-5-phosphosulfate (APS) reductase from sulfate-reducing prokaryotes—origin and evolution of the dissimilatory sulfate-reduction pathway. *Microbiology* 153, 2026–2044.
- Miake, H., Tsukahara, J., Hashimoto, J., Uematsu, K., and Maruyama, T. (2006). Rearing and observation methods of vestimentiferan tubeworm and its early development at atmospheric pressure. *Cah. Biol. Mar.* 47, 471–475.
- Miglietta, P. M., Hourdez, S., Cowart, D. A., Schaeffer, S. W., and Fisher, C. (2010). Species boundaries of Gulf of Mexico vestimentiferans (Polychaeta: Siboglinidae) inferred from mitochondrial genes. *Deep Sea Res. Part II Top. Stud. Oceanogr.* 57, 1916–1925.
- Minniti, M., and Bonavia, F. F. (1984). Copper-ore grade hydrothermal mineralization discovered in a seamount in the Tyrrhenian Sea (Mediterranean): is the mineralization related to porphyry-coppers or to base metal lodes? *Mar. Geol.* 59, 271–282.
- Miura, T., and Kojima, S. (2006). Two new species of vestimentiferan tubeworm (Polychaeta: Siboglinidae aka Pogonophora) from the Brothers Caldera, Kermadec Arc, South Pacific Ocean. *Species Divers.* 11, 209–224.
- Monecke, T., Petersen, S., Lackschewitz, K., Hügler, M., and Hannington, M. D. (2009). Shallow submarine hydrothermal systems in the Aeolian volcanic arc, Italy. *Eos (Washington DC)* 90, 110–111.
- Muyzer, G., Hottentrager, S., Teske, A., and Wawer, C. (1996). "Denaturing gradient gel electrophoresis of PCR-amplified 16S rDNA. A new molecular approach to analyze the genetic diversity of mixed microbial communities," in *Molecular Microbial Ecology Manual*, eds A. D. L. Akkermans, J. D. van Elsas, and F. J. A. de Brujin (Dordrecht: Kluwer Academic Publishing), 3.4.4.1–3.4.4.22.
- Myers, N., Mittermeier, R. A., Mittermeier, C. G., Da Fonseca, G. A. B., and Kent, J. (2000). Biodiversity hotspots for conservation priorities. *Nature* 403, 853–858.
- Naganuma, T., Elsaied, H. E., Hoshii, D., and Kimura, H. (2005). Bacterial endosymbioses of gutless tube-dwelling worms in nonhydrothermal vent habitats. *Mar. Biotechnol.* 7, 416–428.
- Nelson, K., and Fisher, C. R. (2000). Absence of cospeciation in deep-sea vestimentiferan tube worms and their bacterial endosymbionts. *Symbiosis* 28, 1–15.
- Neufeld, J. D., Schäfer, H., Cox, M. J., Boden, R., McDonald, I. R., and Murrell, J. C. (2007). Stable-isotope probing implicates Methylophaga spp. and novel Gammaproteobacteria in marine methanol and methylamine metabolism. *ISME J.* 1, 480–491.
- Olu, K., Cordes, E. E., Fisher, C. R., Brooks, J. M., Sibuet, M., and Desbruyères, D. (2010). Biogeography and potential exchanges among the Atlantic Equatorial Belt cold-seep faunas. *PLoS ONE* 5:e11967. doi:10.1371/journal.pone.0011967
- Olu-Le Roy, K., Sibuet, M., Fiala-Médioni, A., Gofas, S., Salas, C., Mariotti, A., et al. (2004). Cold seep communities in the deep eastern Mediterranean Sea: composition, symbiosis and spatial distribution on mud volcanoes. *Deep Sea Res. Part 1 Oceanogr. Res. Pap.* 51, 1915–1936.
- Palumbi, S. R., Martin, A., Romano, S., McMillan, W. O., Stice, L., and Grabowski, G. (2002). *The Simple Fool's Guide to PCR*. Department of Zoology and Kewalo Marine Laboratory, University of Hawaii, Honolulu.
- Passaro, S., Milano, G., D'Isanto, C., Ruggieri, S., Tonielli, R., Bruno, P. P., et al. (2010). DTM-based morphometry of the Palinuro seamount (Eastern Tyrrhenian Sea): geomorphological and volcanological implications. *Geomorphology* 115, 129–140.
- Petersen, J. M., Zielinski, F. U., Pape, T., Seifert, R., Moraru, C., Amann, R., et al. (2011). Hydrogen is an energy source for hydrothermal vent symbioses. *Nature* 476, 176–180.
- Petersen, S., Monecke, T., Augustin, N., De Benedetti, A. A., Esposito, A., Gärtner, A., et al. (2008). Drilling submarine hydrothermal systems in the Tyrrhenian Sea, Italy. *Interridge News* 17, 21–23.
- Petri, R., Podgorsek, L., and Imhoff, J. F. (2001). Phylogeny and distribution of the soxB gene among thiosulfate-oxidizing bacteria. *FEMS Microbiol. Lett.* 197, 171–178.
- Puchelt, H., and Laschek, D. (1987). Massive sulphide ores in the Tyrrhenian sea from Sonne cruise 41. *Terra Cognita* 7, 188.
- Robidart, J. C., Bench, S. R., Feldman, R. A., Novoradovsky, A., Podell, S. B., Gaasterland, T., et al. (2008). Metabolic versatility of the *Riftia pachyptila* endosymbiont revealed through metagenomics. *Environ. Microbiol.* 10, 727–737.
- Smith, C. R., and Kukert, H. (1989). Vent fauna on whale remains. *Nature* 341, 27–28.
- Southward, E. C. (1991). Three new species of Pogonophora, including two vestimentiferans, from hydrothermal sites in the Lau Back-arc Basin (Southwest Pacific Ocean). *J. Nat. Hist.* 25, 859–881.
- Southward, E. C., Andersen, A. C., and Hourdez, S. (2011). *Lamellibrachia anaximandri* n. sp., a new vestimentiferan tubeworm (Annelida) from the Mediterranean, with notes on frenulate tubeworms from the same habitat. *Zoosystema* 33, 245–279.
- Stewart, F. J., and Cavanaugh, C. M. (2006). "Symbiosis of thioautotrophic bacteria with *Riftia pachyptila*," in *Molecular Basis of Symbiosis*, ed. J. Overmann (Berlin: Springer), 197–225.
- Tamura, K., Peterson, D., Peterson, N., Stecher, G., Nei, M., and Kumar, S. (2011). MEGA5: molecular evolutionary genetics analysis using maximum likelihood, evolutionary distance, and maximum parsimony methods. *Mol. Biol. Evol.* 28, 2731–2739.
- Tank, M. (2005). *Vorkommen von Genen des dissimilatorischen Stickstoff-Stoffwechsels im Atlantischen Ozean*. Christian-Albrechts-Universität Kiel, Kiel.
- Thiel, V., Neulinger, S. C., Staufenberger, T., Schmaljohann, R., and Imhoff, J. F. (2007). Spatial distribution of sponge-associated bacteria in the Mediterranean sponge *Tethya aurantium*. *FEMS Microbiol. Ecol.* 59, 47–63.
- Thompson, J. D., Gibson, T. J., Plewniak, F., Jeanmougin, F., and Higgins, D. G. (1997). The CLUSTAL\_X windows interface: flexible strategies for multiple sequence alignment aided by quality analysis tools. *Nucleic Acids Res.* 25, 4876–4882.

- Tyler, P. A., and Young, C. M. (2003). Dispersal at hydrothermal vents: a summary of recent progress. *Hydrobiologia* 503, 9–19.
- van der Land, J., and Nørrevang, A. (1975). The systematic position of *Lamellibrachia* (Annelida, Vestimentifera). *J. Zool. Syst. Evol. Res.* 1, 86–101.
- Vrijenhoek, R. C. (2010). Genetic diversity and connectivity of deep-sea hydrothermal vent metapopulations. *Mol. Ecol.* 19, 4391–4411.
- Vrijenhoek, R. C., Duhaime, M., and Jones, W. J. (2007). Subtype variation among bacterial endosymbionts of tubeworms (Annelida: Siboglinidae) from the Gulf of California. *Biol. Bull.* 212, 180–184.
- Wetzel, L. R., and Shock, E. L. (2000). Distinguishing ultramafic-from basalt-hosted submarine hydrothermal systems by comparing calculated vent fluid compositions. *J. Geophys. Res.* 105, 8319–8340.
- Young, C. M., Vázquez, E., Metaxas, A., and Tyler, P. A. (1996). Embryology of vestimentiferan tube worms from deep-sea methane/sulphide seeps. *Nature* 381, 514–516.
- commercial or financial relationships that could be construed as a potential conflict of interest.
- Received: 04 October 2012; paper pending published: 05 November 2012; accepted: 26 November 2012; published online: 14 December 2012.*
- Citation: Thiel V, Hügler M, Blümel M, Baumann HI, Gärtner A, Schmaljohann R, Strauss H, Garbe-Schönberg D, Petersen S, Cowart DA, Fisher CR and Imhoff JF (2012) Widespread occurrence of two carbon fixation pathways in tubeworm endosymbionts: lessons from hydrothermal vent associated tubeworms from the Mediterranean Sea. *Front. Microbiol.* 3:423. doi: 10.3389/fmicb.2012.00423*
- This article was submitted to Frontiers in Extreme Microbiology, a specialty of Frontiers in Microbiology.*
- Copyright © 2012 Thiel, Hügler, Blümel, Baumann, Gärtner, Schmaljohann, Strauss, Garbe-Schönberg, Petersen, Cowart, Fisher and Imhoff. This is an open-access article distributed under the terms of the Creative Commons Attribution License, which permits use, distribution and reproduction in other forums, provided the original authors and source are credited and subject to any copyright notices concerning any third-party graphics etc.*

## APPENDIX

**Table A1 | Signature nucleotide of tubeworm endosymbiont 16S rRNA gene sequences from vent- and seep vestimentiferan tubeworms.**

| <i>E. coli</i> pos. | 75   | 77   | 79   | 80   | 90   | 92   | 137  | 231  | 250  | 258  | 268  | 286  | 301  | 381  |
|---------------------|------|------|------|------|------|------|------|------|------|------|------|------|------|------|
| Vent                | c    | g    | a    | g    | t    | t    | c    | t    | a    | g    | c    | a    | g/a  | a/c  |
| Seep-1              | a    | t    | g    | a    | c    | a    | t    | c    | t    | a    | t    | g    | g    | c    |
| Seep-2              | a    | t    | g    | a    | c    | a    | t    | c    | t    | a    | t    | g    | g    | c    |
| Seep-3              | a    | t    | g    | a    | c    | a    | t    | c    | t    | a    | t    | g    | g    | c    |
| PT-1                | a    | t    | g    | a    | c    | a    | t    | c    | a    | a    | c    | g    | g    | c    |
| PT-2                | a    | t    | g    | a    | c    | a    | t    | c    | t    | a    | t    | g    | g    | a    |
| Pos412              | a    | t    | g    | a    | c    | a    | t    | c    | t    | a    | t    | g    | g    | c    |
| <i>E. coli</i> pos. | 441  | 446  | 457  | 459  | 460  | 461  | 463  | 469  | 488  | 646  | 648  | 650  | 658  | 831  |
| Vent                | a    | g    | c    | g    | a    | g    | a    | c    | c    | g    | a    | g    | a    | c    |
| Seep-1              | a    | t    | c    | a    | g    | a    | t    | g    | a    | c    | t    | a    | g    | t    |
| Seep-2              | a    | t    | t    | a    | g    | a    | t    | g    | a    | c    | t    | a    | g    | t    |
| Seep-3              | g    | t    | c    | a    | g    | g    | t    | a    | a    | c    | t    | a    | g    | t    |
| PT-1                | a    | t    | c    | a    | g    | g    | t    | a    | a    | c    | t    | a    | g    | t    |
| PT-2                | a    | t    | c    | a    | g    | a    | t    | a    | a    | c    | t    | a    | g    | t    |
| Pos412              | a    | t    | c    | a    | g    | a    | t    | a    | a    | c    | t    | a    | g    | t    |
| <i>E. coli</i> pos. | 849  | 859  | 986  | 987  | 998  | 999  | 1000 | 1002 | 1006 | 1007 | 1008 | 1009 | 1010 | 1011 |
| Vent                | c    | c    | a    | g    | c    | c    | t    | g    | c    | t    | t    | t    | c    | t    |
| Seep-1              | t    | a    | t    | a    | c    | c    | t    | a    | c    | t    | t    | g    | t    | t    |
| Seep-2              | t    | a    | t    | a    | t    | g    | a    | a    | t    | c    | c    | t    | g    | t    |
| Seep-3              | t    | a    | t    | a    | t    | g    | a    | a    | t    | c    | c    | a    | g    | t    |
| PT-1                | t    | a    | t    | a    | c    | c    | t    | a    | c    | t    | t    | g    | t    | t    |
| PT-2                | t    | a    | t    | a    | t    | g    | a    | a    | t    | c    | c    | a    | g    | c    |
| Pos412              | t    | a    | t    | a    | t    | g    | a    | a    | t    | c    | c    | a    | g    | c    |
| <i>E. coli</i> pos. | 1019 | 1020 | 1021 | 1022 | 1023 | 1036 | 1037 | 1040 | 1041 | 1042 | 1043 | 1121 | 1135 | 1152 |
| Vent                | g    | a    | t    | t    | g    | g    | c    | a    | g    | t    | g    | t    | g    | a    |
| Seep-1              | a    | c    | t    | t    | g    | a    | t    | a    | g    | t    | g    | a    | g    | t    |
| Seep-2              | c    | g    | g    | g    | a    | —    | c    | g    | a    | a    | a    | t    | a    | a    |
| Seep-3              | c    | a    | g    | g    | a    | —    | c    | g    | a    | a    | a    | a    | g    | t    |
| PT-1                | a    | c    | t    | t    | g    | a    | t    | a    | g    | t    | g    | a    | g    | t    |
| PT-2                | c    | a    | g    | g    | a    | —    | c    | g    | a    | a    | a    | a    | g    | t    |
| Pos412              | c    | a    | g    | g    | a    | —    | c    | g    | a    | a    | a    | a    | g    | t    |
| <i>E. coli</i> pos. | 1155 | 1219 | 1243 | 1257 | 1278 |      |      |      |      |      |      |      |      |      |
| Vent                | g    | t    | c    | t    | c    |      |      |      |      |      |      |      |      |      |
| Seep-1              | a    | a    | c    | c    | t    |      |      |      |      |      |      |      |      |      |
| Seep-2              | a    | a    | a/c  | t    | t    |      |      |      |      |      |      |      |      |      |
| Seep-3              | a    | a    | c    | c    | t    |      |      |      |      |      |      |      |      |      |
| PT-1                | a    | a    | c    | c    | t    |      |      |      |      |      |      |      |      |      |
| PT-2                | a    | a    | c    | c    | t    |      |      |      |      |      |      |      |      |      |
| Pos412              | a    | a    | c    | c    | t    |      |      |      |      |      |      |      |      |      |

"Vent" vestimentiferan group includes endosymbiont rRNA gene sequences of *Riftia pachyptila*, *Tevnia jerichonana*, and *Osásia alvinae*. "Seep" vestimentiferan tubeworm endosymbiont cluster "seep-(1–3)" refer to grouping according to McMullin et al. (2003). PT1 and PT2 refer to *Lamellibrachia anaximandri* endosymbionts, phylotype 1 and phylotype 2 according to Duperron et al. (2009). Pos412 refers to the *Lamellibrachia anaximandri* endosymbiont rRNA gene sequence phylotype obtained from the Palinuro volcanic complex during cruise Pos412 of R/V Poseidon in this study. The position numbers refer to *E. coli* gene sequence positions.



# Multilocus sequence analysis of *Thermoanaerobacter* isolates reveals recombining, but differentiated, populations from geothermal springs of the Uzon Caldera, Kamchatka, Russia

Isaac D. Wagner<sup>1†</sup>, Litty B. Varghese<sup>1</sup>, Christopher L. Hemme<sup>2,3</sup> and Juergen Wiegel<sup>1\*</sup>

<sup>1</sup> Department of Microbiology, University of Georgia, Athens, GA, USA

<sup>2</sup> Department of Botany and Microbiology, University of Oklahoma, Norman, OK, USA

<sup>3</sup> Institute for Environmental Genomics, University of Oklahoma, Norman, OK, USA

## Edited by:

Andreas Teske, University of North Carolina at Chapel Hill, USA

## Reviewed by:

Patricia L. Siering, Humboldt State University, USA

Antonio Ventosa, University of Sevilla, Spain

## \*Correspondence:

Juergen Wiegel, Department of Microbiology, University of Georgia, 1000 Cedar Street, Athens, GA 30602-2605, USA  
e-mail: juergenwiegel@gmail.com

## †Present address:

Isaac D. Wagner, Denver, USA  
e-mail: isaacwagner56@gmail.com

Thermal environments have island-like characteristics and provide a unique opportunity to study population structure and diversity patterns of microbial taxa inhabiting these sites. Strains having ≥98% 16S rRNA gene sequence similarity to the obligately anaerobic *Firmicutes Thermoanaerobacter uzonensis* were isolated from seven geothermal springs, separated by up to 1600 m, within the Uzon Caldera (Kamchatka, Russian Far East). The intraspecies variation and spatial patterns of diversity for this taxon were assessed by multilocus sequence analysis (MLSA) of 106 strains. Analysis of eight protein-coding loci (*gyrB*, *lepA*, *leuS*, *pyrG*, *recA*, *recG*, *rplB*, and *rpoB*) revealed that all loci were polymorphic and that nucleotide substitutions were mostly synonymous. There were 148 variable nucleotide sites across 8003 bp concatenates of the protein-coding loci. While pairwise  $F_{ST}$  values indicated a small but significant level of genetic differentiation between most subpopulations, there was a negligible relationship between genetic divergence and spatial separation. Strains with the same allelic profile were only isolated from the same hot spring, occasionally from consecutive years, and single locus variant (SLV) sequence types were usually derived from the same spring. While recombination occurred, there was an “epidemic” population structure in which a particular *T. uzonensis* sequence type rose in frequency relative to the rest of the population. These results demonstrate spatial diversity patterns for an anaerobic bacterial species in a relatively small geographic location and reinforce the view that terrestrial geothermal springs are excellent places to look for biogeographic diversity patterns regardless of the involved distances.

**Keywords:** multilocus sequence analysis, *Thermoanaerobacter*, microbial biogeography, Uzon Caldera, Kamchatka, hot springs

## INTRODUCTION

The Kamchatka Peninsula is located on the northern side of the Kurile-Kamchatka arc and is considered one of the outstanding volcanic regions in the world. The peninsula contains many active volcanoes and numerous related geothermal features including terrestrial geothermal springs, fumaroles, and geysers (Karpov and Naboko, 1990). The Uzon Caldera in Kamchatka is the result of a giant explosion of a stratovolcano during the mid-Pleistocene and the region now contains an array of geothermal features in close proximity (Karpov and Naboko, 1990). A variety of novel thermophilic microorganisms have been isolated from geothermal springs of Kamchatka including *Thermoanaerobacter* taxa. Three of the 14 species presently classified within the *Thermoanaerobacter* genus (May 2013, <http://www.bacterio.cict.fr/t/thermoanaerobacter.html>) were isolated from hot springs of Kamchatka: *Thermoanaerobacter uzonensis* (Wagner et al., 2008), *Thermoanaerobacter siderophilus* (Slobodkin et al., 1999), and *Thermoanaerobacter sulfurophilus* (Bonch-Osmolovskaya et al.,

1997). Furthermore, diverse and unique microbial communities within geothermal springs of the Uzon Caldera have been revealed through 16S rRNA gene clone libraries (Burgess et al., 2011), and high-throughput sequencing of the 16S rRNA gene V6 hypervariable region (D. E. Crowe, pers. communication).

Terrestrial hot springs are frequently regarded as having insular characteristics: they are often well-defined and can be geographically isolated. In addition, geothermal springs in close proximity may have markedly different geochemical properties. For these reasons the comparison of microorganisms from different hot springs provides the opportunity to investigate the spatial patterns of biodiversity. Island-like environments also provide an excellent opportunity to assess gene flow between locations. Understanding characteristics such as genetic variation and gene migration within microbial communities then provides insight into how variations develop and are maintained in natural populations. Biogeographic diversity patterns have been observed for some microorganisms

inhabiting terrestrial hot springs, including cyanobacteria (Papke et al., 2003), *Rhodothermus* (Petursdottir et al., 2000), *Thermus* (Hreggvidsson et al., 2006), *Sulfurihydrogenibium* (Takacs-Vesbach et al., 2008), and *Sulfolobus* (Whitaker et al., 2003). Since the 16S rRNA gene sequence is slowly evolving and therefore of little use in intraspecies comparisons (Cooper and Feil, 2004), reports that describe biogeographic patterns within a microbial species have often focused on sequencing and analysis of more rapidly evolving non-coding or protein-coding loci (Whitaker, 2006). In some studies multilocus sequence analysis (MLSA), a technique that utilizes the sequencing of multiple gene fragments to assess the phylogeny and population structure of a group of related strains (Gevers et al., 2005), has been utilized to analyze the spatial diversity patterns of a microbial group (Whitaker et al., 2003; Papke et al., 2007).

Gene flow between sites is significant because of the ensuing potential for recombination within a population. While homologous recombination is reported to occur at varying rates within microbial populations, it has attracted attention because of its importance to fields such as microbial systematics, ecology, population genetics, and evolution (Achtman and Wagner, 2008). As Papke et al. (2007) state, there are potentially two contrasting effects of homologous recombination within a population. Homologous recombination acts as a diversifying force when a pair of strains have strikingly different alleles with one gene, while the remaining genes are identical. Conversely, homologous recombination is a cohesive force when divergent strains share a single identical allele. Considering taxa from terrestrial hot springs, the moderately thermophilic cyanobacterium *Mastigocladus laminosus* was found to be recombining (Miller et al., 2007), as was the population of the aerobic archaeum *Sulfolobus* from the Mutnovsky region of Kamchatka (Whitaker et al., 2005). However, multilocus enzyme electrophoresis of *Rhodothermus marinus* isolates from Iceland indicated that the species is clonal and that recombination occurs rarely (Petursdottir et al., 2000).

Strains of *T. uzonensis*, an obligately anaerobic species within the *Firmicutes* phylum, were repeatedly isolated from geothermal spring samples collected from the Uzon Caldera region of Kamchatka, Far East Russia. The isolation of these microorganisms prompted an initial question of whether spatial patterns of diversity would be observed for this species within this relatively narrow geographical location. To address this question MLSA was performed with 106 strains of *T. uzonensis* from seven pools separated by 140–1600 m within the Uzon Caldera region of Kamchatka, Far East Russia. Because the occurrence and frequency of recombination within and between subpopulation can strongly affect whether biogeographic patterns are observed, we also assessed the influence of homologous recombination on this taxon in this region.

## MATERIALS AND METHODS

### SAMPLE COLLECTION AND ISOLATION OF *TERMOANAEROBACTER* STRAINS

During August 2005 and August 2006, mixed water and sediment samples were collected from geothermal springs within the Uzon Caldera during the Kamchatka Microbial Observatory

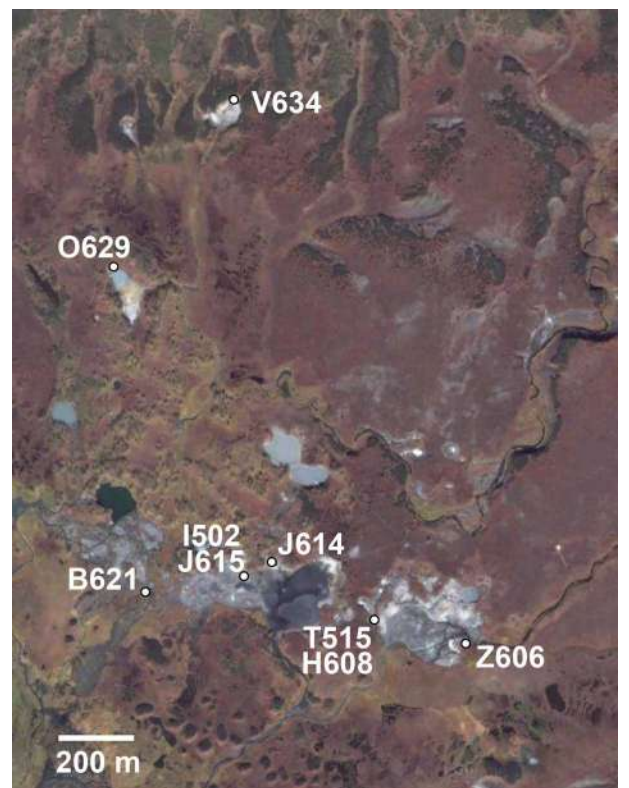


**FIGURE 1 | Location of sample sites in the Uzon Caldera for 106 *T. uzonensis* strains used in this study.** Hot spring positions and abbreviations (Table 1) were overlaid on the satellite image. Image © 2009 Google—Imagery © 2009 DigitalGlobe, GeoEye, Map data © 2009 Geocentre Consulting.

field seasons (Figure 1). The samples collected had temperature between 49–75°C and pH 5–7.5 (Table 1). Water and sediment samples were transferred to sterilized 100 ml bottles, filled to the brim, sealed with butyl rubber stoppers, transferred to Athens, GA, USA, and stored at 4°C. In the laboratory, 1 ml of mixed water/sediment was transferred to 50 ml Wheaton serum bottles containing 20 ml of an anaerobic mineral medium (Wagner et al., 2008) supplemented with 1 g·l<sup>-1</sup> glucose, 0.5 g·l<sup>-1</sup> yeast extract, and 50 mM thiosulfate. Enrichment cultures were incubated at 62°C for 48 h. A 10<sup>-1</sup> dilution was prepared, streaked onto a 2.15% (w/v) agar plate of the same medium composition, and then incubated anaerobically at 62°C for 48 h. A single colony was selected and re-streaked for isolation on a new agar plate a minimum of two times. Each isolate was derived from its own enrichment culture. To assess culture purity following the repeated single colony isolations, electropherograms of the protein coding loci and 16S rRNA gene were manually examined for correct base calling. Sequences with ambiguous sites were re-sequenced or colonies were isolated anew and loci re-sequenced. Within this study the entire set of isolates was considered the population while the collection of strains derived from a single hot spring was regarded as a subpopulation.

**Table 1 | Geothermal springs of the Uzon Caldera from which *T. uzonensis* strains were isolated.**

| Geothermal spring (abbreviation) | Year | Temperature (°C) | pH      | Number of isolates genotyped |
|----------------------------------|------|------------------|---------|------------------------------|
| Arkashin Shaft (I502)            | 2005 | 72               | 5       | 8                            |
| Arkashin Shaft (A615)            | 2006 | 60–63            | 5.5     | 7                            |
| Thermophilny (T515)              | 2005 | 62–65            | 7.0–7.5 | 7                            |
| Thermophilny (H608)              | 2006 | 53–72            | 6.0–6.5 | 19                           |
| Burlyashi outflow (B621)         | 2006 | 65               | 7       | 18                           |
| Pulsating Spring (J614)          | 2006 | 72               | 5.2     | 7                            |
| ON1 (O629)                       | 2006 | 65–72            | 5.5     | 12                           |
| Vent 1 North (V634)              | 2006 | 67               | 6       | 18                           |
| Zavarzin (Z606)                  | 2006 | 49–55            | 5.5     | 10                           |

Sample sites, sampling year, environmental factors, and number of isolates genotyped.

#### PCR AMPLIFICATION OF THE 16S rRNA GENE AND PROTEIN CODING LOCI

Genomic DNA was isolated with the UltraClean Microbial DNA Isolation kit (Mo Bio). The 16S rRNA gene sequence was amplified with the 27F and 1492R primers (Lane, 1991) using PrimeSTAR HS DNA Polymerase (Takara). The thermal cycler conditions for amplification were: 30 cycles of 98°C for 10 s, 58°C for 5 s, and then 72°C for 90 s. Purification of the amplification product and the subsequent sequencing reaction was performed by Macrogen USA (Rockville, MD).

The universally conserved protein coding genes analyzed in this study were selected from those suggested by Santos and Ochman (2004); *gyrB*, *lepA*, *leuS*, *pyrG*, *recA*, *recG*, *rplB*, and *rpoB*. Primers for the amplification of universally conserved protein coding genes from *Thermoanaerobacter* isolates (Table 2) were designed from the genes of representatives of the family *Thermoanaerobacteraceae* with sequenced genomes; *Thermoanaerobacter pseudethanolicus* strain 39E (Refseq: NC\_010321), *Caldanaerobacter subterraneus* subsp. *tengcongensis* strain MB4 (Refseq: NC\_003869), *Thermoanaerobacter* sp. X514 (Refseq: NC\_010320), and *Carboxydotothermus hydrogenoformans* Z-2901 (Refseq: NC\_007503).

The universally conserved protein coding genes were amplified with Phusion High-Fidelity polymerase PCR Master Mix with HF Buffer (New England Biolabs). Amplification was performed in a Mastercycler ep Gradient thermal cycler (Eppendorf). Conditions for the amplification of the *gyrB*, *lepA*, *leuS*, *pyrG*, *recG*, and *rpoB* loci were: 98°C for 10 s; then 30 cycles of 98°C for 1 s, 56°C for 5 s, and 72°C for 20 s; and then 72°C for 1 min. Conditions for the amplification of the *recA* and *rplB* loci were: 98°C for 10 s; then 30 cycles of 98°C for 1 s, 56°C for 5 s, and 72°C for 12 s; and then 72°C for 1 min. Purification of the amplification product and the subsequent sequencing reaction was performed by Macrogen USA (Rockville, MD). All nucleotide sequences were deposited to GenBank and are available through the Entrez PopSet database; accession numbers for the different loci from *T. uzonensis* are: 16S rRNA gene, 30113600; *pyrG*, 306992496; *gyrB*, 310780896; *rplB*,

**Table 2 | Oligonucleotide primers for the amplification of universally conserved protein coding genes from *Thermoanaerobacter uzonensis* isolates.**

| Locus       | Primer name | Oligonucleotide sequence (5'-3') |
|-------------|-------------|----------------------------------|
| <i>pyrG</i> | pyrG-F      | AAGYCGCGCMTATCAGTTGCWRRT         |
|             | pyrG-R      | TGGRTGRAYTGGAYGCYACAAA           |
| <i>leuS</i> | leuS-F      | GTYGYCAAACGTGTTGCAAACGARC        |
|             | leuS-R      | TCATTCTGCTKCCATCAGGKCCCA         |
| <i>gyrB</i> | gyrB-F      | AGCSGTAAGAAARAGGCCAGGAAT         |
|             | gyrB-R      | TYCCTCGKAGTGGAAAGTATCGCTT        |
| <i>recA</i> | recA-F      | AGYCARATAGAGAGRCAGTTGGC          |
|             | recA-R      | CTCCATAGGAATACCAAGCACAC          |
| <i>rplB</i> | rplB-R      | GTGTCTTATARCCYAAATGCAGGCT        |
|             | rplB-F      | ATCTCCCGGCAGACGTCAAAT            |
| <i>rpoB</i> | rpoB-R      | TCTCTAATGGCTGCWACAACYGGR         |
|             | rpoB-F      | TACGTCCTGTACAAGTGGGCAACA         |
| <i>recG</i> | recG-R      | AAATTCTGACCTGCCAACTCTRCC         |
|             | recG-F      | ACAGGYGYAGTAGARTTAGTSTGG         |
| <i>lepA</i> | lepA-R      | YTTCACCCTGTCATGCGCTT             |
|             | lepA-F      | TTGAGGCGCAAACCCTTGCTAATG         |

304564022; *recG*, 306992180; *recA*, 304564400; *rpoB*, 304561479; *lepA*, 302120473; and *leuS*, 301133848.

#### ANALYSIS OF SEQUENCE DIVERSITY

The 16S rRNA gene sequences were aligned and initially analyzed with Sequencher 4.1 (Gene Codes). Multiple sequence alignments were prepared with NAST (Desantis et al., 2006) through the GreenGenes web application (<http://greengenes.lbl.gov/>). Multiple sequence alignments of the protein coding gene sequences were prepared with ClustalW (Larkin et al., 2007). Protein-coding loci sequences were initially aligned with the homologous gene sequences from the related *Thermoanaerobacteraceae* with sequenced genomes and then checked for spurious insertion or deletions. For every 96-well plate sequenced the locus from one isolate was sequenced multiple times to check that the DNA sequencing was accurate.

Sequence heterogeneity was determined using DnaSP (Rozas and Rozas, 1999) or MEGA 4.1 (Tamura et al., 2007). Characteristics assessed included the total number of polymorphic nucleotide sites, S; the number of alleles for the gene sequence loci, n<sub>a</sub>; and the average number of nucleotide substitutions per site, P<sub>i</sub>. Taking into account the deduced primary protein sequence, the number of variable amino acid sites was determined for each locus. Genetic diversity, H, was calculated as described by Haubold and Hudson (2000), using the LIAN 3.5 web server (<http://adenine.biz.fl-weiheinstephan.de/cgi-bin/lian/lian.cgi.pl>). This metric was calculated for each protein-coding locus taking into consideration all 106 *T. uzonensis* isolates and for the set of isolates from each hot spring.

A phylogenetic tree based on concatenates of the eight protein coding loci was prepared considering the 49 unique genotypes observed among the set of 106 *T. uzonensis* strains. The phylogenetic analysis was performed in MEGA 5 (Tamura et al., 2011). A concatenated sequence with the same protein coding gene sequences from *Thermoanaerobacter italicus* Ab9<sup>T</sup> (Hemme et al., 2010) was included in the analysis as an out-group. Nucleotide substitution models were evaluated and the model having the lowest goodness-of-fit Bayesian Information Criterion value was used to construct a tree using the maximum likelihood method. The initial tree for the maximum likelihood analysis was constructed automatically and the Nearest-Neighbor-Interchange heuristic search method was used to search for topologies that fit the data better. Reliability of the tree topology was assessed with the bootstrap method using 100 replications.

### CALCULATING $F_{ST}$ VALUES AND ASSESSING THE RELATIONSHIP BETWEEN DIVERGENCE AND SPATIAL SEPARATION

Pairwise  $F_{ST}$  values between *T. uzonensis* subpopulations from different hot springs were calculated with Arlequin 3.5 (Excoffier and Lischer, 2010), using concatenates of the eight protein-coding loci.  $F_{ST}$  values were tested for significance against 1000 randomized bootstrap resamplings. The relationship between the genetic divergence, based on nucleotide p-distance from concatenates of the eight protein-coding loci, and spatial separation was examined by calculating Spearman's rho rank correlation value, and the significance level of the Spearman's rho statistic, using the RELATE subprogram within Primer v6 (PRIMER-E Ltd).

### ASSESSING RECOMBINATION WITHIN THE *T. uzonensis* POPULATION

For a protein-coding locus, each different allele was assigned a number and the eight-loci sequence type for each isolate was tabulated. The influence of recombination on the population was first assessed by calculating the standardized index of association,  $I_A^S$ , to determine the randomness of the distribution of alleles (Haubold and Hudson, 2000).  $I_A^S$  values were calculated considering all 106 isolates and considering only the 91 strains isolated from samples collected in 2006.  $I_A^S$  values were also calculated considering the 49 unique sequence types from 2005 and 2006, as well as the 45 unique genotypes from 2006. Lastly,  $I_A^S$  values were calculated for each hot spring subpopulation taking into account all isolates and unique genotypes. Recombination in the *T. uzonensis* population was also assessed by examination of single locus variant (SLV) genotypes as described by Feil et al. (2000). Here, SLV genotypes were compiled and the sequence diversity for the variable loci were tabulated. If the variant allele differed by only single nt it was considered a point mutation. The allele was considered to have been the result of homologous recombination if it differed by multiple nt substitutions, or was observed multiple times in the dataset.

## RESULTS

### ISOLATION OF *Thermoanaerobacter* STRAINS

Anaerobic thermophilic strains were isolated from mixed water and sediment samples collected at seven different geothermal springs in the Uzon Caldera. In total, 106 isolates, between seven

and 19 from each hot spring sampled, were analyzed by MLSA (Table 1). From 101 strains, the near full-length 16S rRNA gene sequence ( $\geq 1337$  bp) was obtained and a comparison of the 16S rRNA gene sequence from these isolates revealed  $\geq 98\%$  16S rRNA gene sequence similarity to each other and to the *Thermoanaerobacter uzonensis* type strain JW/IW010<sup>T</sup> (Wagner et al., 2008). The geothermal springs from which strains were obtained were separated by at most 1600 m (Figure 1). Each isolate was derived from its own enrichment culture. Hot springs yielding *T. uzonensis* isolates had temperatures of 49–75°C, measured at the location sampled, and circumneutral pH values (Table 1). Attempts to obtain isolates from two additional springs within the Uzon Caldera, “Oil Pool” (75°C, pH 4) and “K4 Well” (60°C; above 100°C in the 16 m deep well shaft, pH 7), were unsuccessful even though 12 or more enrichments were prepared from each sample. The type strain of *T. uzonensis*, JW/IW010<sup>T</sup>, was not included in the MLSA study since it was isolated from a hot spring which at the time of this study had disappeared.

### PROTEIN-CODING LOCI HETEROGENEITY

The protein coding genes used in this study were among those recommended by Santos and Ochman (2004): DNA gyrase subunit B (*gyrB*), GTP-binding protein LepA (*lepA*), leucyl-tRNA synthetase (*leuS*), CTP synthase (*pyrG*), bacterial DNA recombination protein RecA (*recA*), ATP-dependent DNA helicase RecG (*recG*), 50S ribosomal protein L2 (*rplB*), and RNA polymerase subunit B (*rpoB*). The genes are distributed throughout the sequenced genomes of the *Thermoanaerobacteraceae* (Hemme et al., 2010; detailed data not shown). To minimize the inclusion of apparent sequence heterogeneity due to DNA sequencing errors the protein-coding loci were amplified with Phusion High-Fidelity DNA Polymerase in HF Buffer (New England BioLabs, Inc).

There were 148 variable sites from a total of 8003 bp in common across the eight protein-coding loci. All loci were polymorphic, however, the amount of variation at each locus differed (Table 3). For example, the number of variable nucleotide sites (S) observed for a locus varied from 3 for the *rplB* locus, to 42 for the *recG* locus. The deduced primary protein sequence revealed that most nucleotide substitutions were synonymous (Table 3).

### GENETIC DIFFERENTIATION OF *T. uzonensis* SUBPOPULATIONS

Genetic differentiation of the subpopulations from different hot spring was assessed by calculation of the pairwise  $F_{ST}$  values (Table 4). The  $F_{ST}$  values ranged from 0.082 to 0.706, and most values were found to be significant based on a bootstrap resampling test. Two of the five comparisons that were found to not be significantly different were the comparisons between Arkashin over multiple years and Thermophilny over multiple years.

Hot springs from which *T. uzonensis* isolates were derived were separated by distances that varied from about 140–1600 m (Figure 1), measured using a QuickBird (DigitalGlobe) satellite image (D. E. Crowe, personal communication). The relationship between the spatial separation of the hot springs and the genetic divergence of the *T. uzonensis* isolates was assessed by

**Table 3 | Characteristics of eight protein coding loci examined from the set of 106 *T. uzonensis* strains isolated from hot springs of the Uzon Caldera.**

|   | <i>gyrB</i> | <i>lepA</i> | <i>leuS</i> | <i>pyrG</i> | <i>recA</i> | <i>recG</i> | <i>rplB</i> | <i>rpoB</i> |
|---|-------------|-------------|-------------|-------------|-------------|-------------|-------------|-------------|
| Length (nt)   | 1111        | 1264        | 1040        | 1204        | 739         | 1227        | 507         | 911         |
| Number of alleles ( $n_a$ )                             | 4           | 13          | 10          | 25          | 7           | 16          | 4           | 8           |
| Genetic diversity, $H$                                  | 0.32        | 0.62        | 0.75        | 0.93        | 0.36        | 0.89        | 0.49        | 0.57        |
| Variable nt sites (S)                                   | 16          | 14          | 24          | 30          | 6           | 42          | 3           | 13          |
| Average nucleotide diversity ( $P_i$ ) per 100 nt sites | 0.185       | 0.095       | 0.269       | 0.654       | 0.052       | 0.95        | 0.11        | 0.363       |
| Variable amino acid residues                            | 8           | 4           | 13          | 12          | 2           | 22          | 1           | 3           |

Characteristics calculated for each protein coding locus were: nucleotide sequence length, nt; number of alleles,  $n_a$ ; total number of polymorphic nucleotide sites, S; average number of nucleotide substitutions per site,  $P_i$ ; and the variable amino acid residues.

**Table 4 | *T. uzonensis* hot spring subpopulation pairwise  $F_{ST}$  values.**

|             | A615   | I502  | B621   | H608   | T515   | J614  | O629  | V634  |
|-------------|--------|-------|--------|--------|--------|-------|-------|-------|
| <b>I502</b> | 0.347* |       |        |        |        |       |       |       |
| <b>B621</b> | 0.175  | 0.521 |        |        |        |       |       |       |
| <b>H608</b> | 0.374  | 0.657 | 0.147  |        |        |       |       |       |
| <b>T515</b> | 0.287  | 0.706 | 0.082* | 0.093* |        |       |       |       |
| <b>J614</b> | 0.301  | 0.643 | 0.280  | 0.441  | 0.268* |       |       |       |
| <b>O629</b> | 0.336  | 0.619 | 0.198  | 0.331  | 0.304  | 0.359 |       |       |
| <b>V634</b> | 0.430  | 0.698 | 0.182  | 0.381  | 0.333  | 0.426 | 0.214 |       |
| <b>Z606</b> | 0.238* | 0.565 | 0.217  | 0.407  | 0.311  | 0.364 | 0.367 | 0.382 |

Hot spring abbreviations given in **Table 1**.  $F_{ST}$  values were tested for significance against 1000 randomized bootstrap resamplings; \*indicates  $P > 0.01$ .

calculation of the Spearman's rank correlation coefficient: rho = 0.086, significance level of sample statistic: 0.83%.

## DISTRIBUTION OF ALLELES AND GENOTYPES

In the *T. uzonensis* population, the number of alleles at a particular protein-coding locus varied from 4 (*rplB* and *gyrB*) to 25 (*pyrG*). The genetic diversity,  $H$ , varied from 0.32 for *gyrB* to 0.93 for *pyrG* for the individual protein-coding loci (**Table 3**) and the average was 0.62. Correspondingly, some alleles were found in a high proportion of the *T. uzonensis* population, e.g., *gyrB* allele 1, 82.1%; *recA* allele 1, 79.2%; and *rplB* allele 3, 67.9% (detailed data not shown). The distribution of alleles within a hot spring subpopulation was also examined. The seven isolates from Arkashin Shaft 2006 shared the same *gyrB*, *lepA*, and *recA* allele, but had comparatively high variation at the *leuS*, *pyrG*, and *recG* loci (**Table 5**). Among the 18 *T. uzonensis* isolates from Thermophilny 2006, there was a single *gyrB* locus allele, while the other seven loci were variable. All of the isolates from Arkashin Shaft 2005 had the same protein-coding loci sequence type, whereas considerable variation was found at all loci from the set of the Burlyashi outflow isolates (**Table 5**). Occasionally a particular allele was only observed within the *T. uzonensis* subpopulation from one hot spring and this was especially evident at the *pyrG* locus (**Figure 2**). For example, *pyrG* alleles 24 and 25 were only found in isolates from Vent 1 North (closest spring analyzed was ON1, approximately 530 m away), *pyrG* alleles 15 and 16 were only in strains from Thermophilny isolated in 2005 and 2006 (closest spring

examined was Zavarzin, about 210 m distant), and *pyrG* allele 1 was only found in *T. uzonensis* strains from Arkashin in both 2005 and 2006 (closest spring analyzed, Pulsating Spring about 140 m away).

Among the 106 *T. uzonensis* strains there were 49 unique sequence types (STs, **Table 6**). A majority of the STs, 35 of the 49, were unique to a single isolate and at most a sequence type was held by 11 isolates (STs 23 and 36; **Table 6**). Within the Uzon Caldera, isolates with identical genotypes were, in all instances, derived from the same hot springs. *T. uzonensis* isolates were obtained from samples collected at the Arkashin and Thermophilny springs in 2005 and 2006 and for both springs, strains with the same allelic profile were obtained over the 2 years. There were 11 pairs of SLVs among the 49 genotypes. Of these SLVs pairs, 10 were of genotypes held by isolates from the same hot spring (**Table 7**). The phylogenetic tree inferred from concatenates of the protein coding loci showed that genotypes of strains isolated from the same geothermal spring occasionally clustered together (**Figure 3**). Most bootstrap values were below 50%, which indicated minimal reliability in the tree topology.

## ASSESSING THE INFLUENCE OF RECOMBINATION ON THE *T. uzonensis* POPULATION OF THE UZON CALDERA

The influence of recombination on the *T. uzonensis* population structure was assessed by calculating the standardized index of association,  $I_A^S$ , to determine the randomness of the distribution of alleles (Haubold and Hudson, 2000). This statistic is expected to be zero in populations that are freely recombining and greater than zero if there is linkage disequilibrium.  $I_A^S$  was estimated to be 0.086 when all 106 isolates were analyzed and this value was significantly different from zero ( $P < 0.001$ ). However, when  $I_A^S$  is calculated using only the 49 unique STs the value decreases to 0.028 ( $P = 0.028$ ). Similar values were obtained when the analysis was restricted to the strains isolated in 2006 (**Table 8**). The  $I_A^S$  statistic was also calculated for the set of isolates from each spring separately and the  $I_A^S$  values were higher when the calculation was restricted to the subpopulations (**Table 8**).

As stated above, there were 11 SLVs pairs among the *T. uzonensis* genotypes. Following the method of binning recombination and mutation events (Feil et al., 2000), SLVs are considered to be the result of mutation if they are single nucleotide changes and are unique in the dataset, whereas recombination events can have

**Table 5 | Characteristics of protein coding loci examined from *T. uzonensis* subpopulations from different hot springs in the Uzon Caldera.**

| Hot Spring (year)        |                      | <i>gyrB</i> | <i>lepA</i> | <i>leuS</i> | <i>pyrG</i> | <i>recA</i> | <i>recG</i> | <i>rplB</i> | <i>rpoB</i> |
|--------------------------|----------------------|-------------|-------------|-------------|-------------|-------------|-------------|-------------|-------------|
| Arkashin Shaft (2006)    | <i>n<sub>a</sub></i> | 1           | 1           | 4           | 4           | 1           | 3           | 3           | 2           |
|                          | <i>H</i>             | 0           | 0           | 0.71        | 0.81        | 0           | 0.71        | 0.67        | 0.48        |
|                          | <i>S</i>             | 0           | 0           | 16          | 16          | 0           | 19          | 2           | 3           |
| Burlyashi Outflow (2006) | <i>n<sub>a</sub></i> | 3           | 4           | 6           | 11          | 4           | 6           | 3           | 5           |
|                          | <i>H</i>             | 0.52        | 0.40        | 0.76        | 0.91        | 0.54        | 0.76        | 0.31        | 0.48        |
|                          | <i>S</i>             | 4           | 4           | 22          | 22          | 3           | 33          | 2           | 11          |
| Thermophilny (2006)      | <i>n<sub>a</sub></i> | 1           | 3           | 5           | 6           | 3           | 6           | 3           | 2           |
|                          | <i>H</i>             | 0           | 0.20        | 0.65        | 0.68        | 0.57        | 0.68        | 0.11        | 0.20        |
|                          | <i>S</i>             | 0           | 3           | 15          | 22          | 2           | 16          | 2           | 5           |
| Thermophilny (2005)      | <i>n<sub>a</sub></i> | 2           | 4           | 4           | 4           | 3           | 4           | 1           | 1           |
|                          | <i>H</i>             | 0.48        | 0.71        | 0.86        | 0.86        | 0.52        | 0.86        | 0           | 0           |
|                          | <i>S</i>             | 12          | 8           | 3           | 17          | 2           | 9           | 0           | 0           |
| Pulsating Spring (2006)  | <i>n<sub>a</sub></i> | 2           | 3           | 2           | 2           | 1           | 2           | 2           | 1           |
|                          | <i>H</i>             | 0.57        | 0.71        | 0.57        | 0.57        | 0           | 0.57        | 0.57        | 0           |
|                          | <i>S</i>             | 15          | 2           | 1           | 6           | 0           | 13          | 1           | 0           |
| ON1 (2006)               | <i>n<sub>a</sub></i> | 2           | 4           | 2           | 2           | 1           | 4           | 3           | 4           |
|                          | <i>H</i>             | 0.17        | 0.77        | 0.41        | 0.41        | 0           | 0.56        | 0.53        | 0.64        |
|                          | <i>S</i>             | 3           | 3           | 1           | 17          | 0           | 24          | 2           | 10          |
| Vent 1 North (2006)      | <i>n<sub>a</sub></i> | 2           | 5           | 3           | 3           | 1           | 3           | 2           | 2           |
|                          | <i>H</i>             | 0.11        | 0.71        | 0.57        | 0.57        | 0           | 0.57        | 0.11        | 0.11        |
|                          | <i>S</i>             | 12          | 4           | 2           | 8           | 0           | 28          | 1           | 5           |
| Zavarzin (2006)          | <i>n<sub>a</sub></i> | 2           | 3           | 3           | 2           | 2           | 4           | 2           | 3           |
|                          | <i>H</i>             | 0.36        | 0.60        | 0.60        | 0.20        | 0.47        | 0.71        | 0.47        | 0.62        |
|                          | <i>S</i>             | 3           | 2           | 2           | 8           | 1           | 20          | 1           | 9           |

The eight isolates from Arkashin 2005 had the same genotype. Characteristics calculated for each protein coding locus were: number of alleles, *n<sub>a</sub>*; genetic diversity, *H*; and number of polymorphic nucleotide sites, *S*.

single or multiple nucleotide changes and are encountered several times independently. Of the 11 SLVs, seven appear to be due to recombination events while four are due to mutation (**Table 7**).

## DISCUSSION

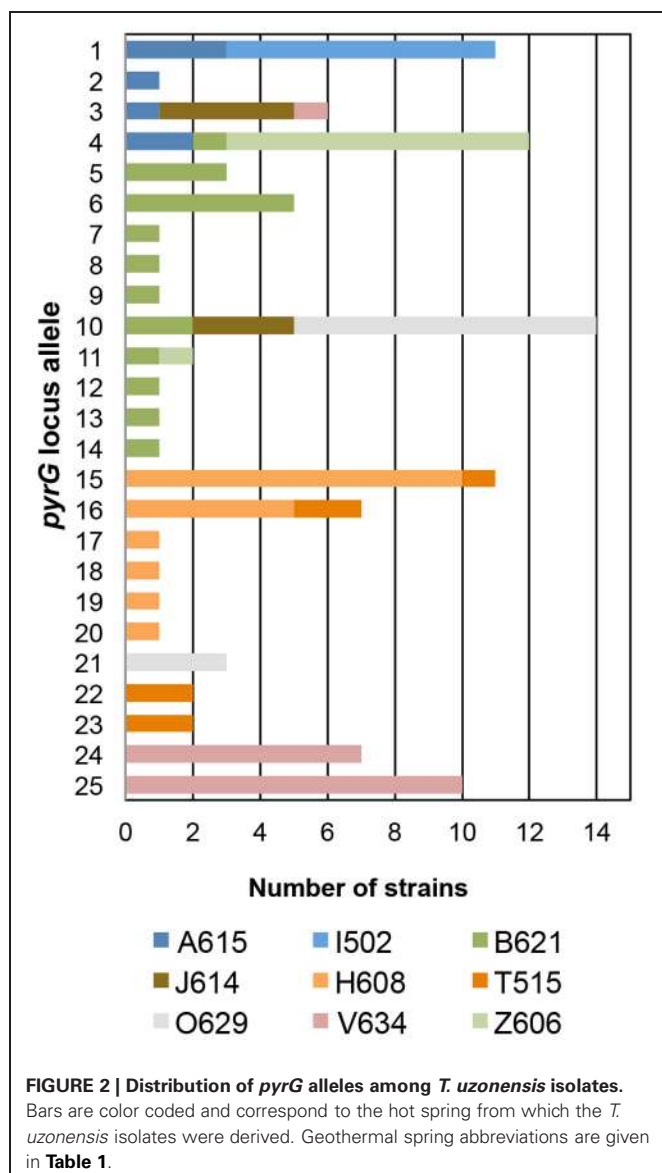
The study of variability in natural populations is important because it can provide insight into the evolutionary forces through which variation develops and is maintained (Smith, 1995). The diversity of 106 *T. uzonensis* strains, isolated from seven hot springs within one region, was assessed through the sequencing and analysis of eight protein coding loci. This MLSA revealed that while recombination occurs, the subpopulations from different springs in this region are genetically differentiated. The results presented here are based on an initial culture-dependent step where the focus was to obtain similar strains under identical isolation conditions. As such, we acknowledge that this set of *T. uzonensis* strains may not necessarily reflect the full diversity of *T. uzonensis* in this environment.

A 16S rRNA gene sequence similarity of  $\geq 97\%$  between strains is evidence that the isolates may belong within the same

species (Stackebrandt and Goebel, 1994). Therefore the high ( $\geq 98\%$ ) 16S rRNA gene sequence similarity to each other and to *Thermoanaerobacter uzonensis* strain JW/IW010<sup>T</sup> (Wagner et al., 2008) supported the view that these isolates belong to the same species. This idea was further bolstered by the MLSA results, in particular the relatively low amount of nucleotide sequence variation at the protein coding loci.

The eight protein coding loci examined within the *T. uzonensis* population were polymorphic and a range of variation was observed across the different loci (**Table 3**). Comparable levels of sequence diversity have been observed in other MLSA-based studies of the population structure of a microbial species within a region. The number of polymorphic sites per locus varied from 2 to 12 for six protein-coding loci from 60 *Sulfolobus* isolates from the Mutnovsky region of Kamchatka, Far East Russia (Whitaker et al., 2005), and among 36 *Halorubrum* isolates from two solar salterns at Santa Pola near Alicante, Spain, four protein-coding loci had 30–61 polymorphic sites per locus (Papke et al., 2004).

The spatial scale of microbial diversity studies are important to consider. Previous authors have noted that environmental factors

**FIGURE 2 |** Distribution of *pyrG* alleles among *T. uzonensis* isolates.

Bars are color coded and correspond to the hot spring from which the *T. uzonensis* isolates were derived. Geothermal spring abbreviations are given in Table 1.

or historical contingencies are thought to influence patterns of genetic variation on smaller scales, while isolation distance is believed to supersede environmental effects at intercontinental scales (Takacs-Vesbach et al., 2008). For example, greater divergence among the protein-coding loci was reported for both *Sulfobolus* (Whitaker et al., 2003) and *Halorubrum* (Papke et al., 2007) when the isolates analyzed were from regions separated by  $\geq 250$  km. While the focus of this report is the diversity of *T. uzonensis* within Uzon Caldera hot springs, similar strains were also isolated from two hot springs within the Geyser Valley region, 10 km east of the Uzon Caldera, and one hot spring from the Mutnovsky volcano region, located 250 km south of the Uzon Caldera and Geyser Valley. Analyses with the protein-coding loci from these strains revealed, with few exceptions, an increase in genetic divergence with an increase in geographic distance (data not shown).

**Table 6 | Summary of *T. uzonensis* sequence types.**

| Sequence type | Allelic profile    | No. of isolates | Spring                  |
|---------------|--------------------|-----------------|-------------------------|
| 1             | 1;1;2;2;1;2;2;1    | 1               | Arkashin 2006           |
| 2             | 1;1;1;3;1;3;2      | 1               | Arkashin 2006           |
| 3             | 1;1;3;4;1;2;1;1    | 1               | Arkashin 2006           |
| 4             | 1;1;4;4;1;2;3;2    | 1               | Arkashin 2006           |
| 23            | 1;1;1;1;1;1;1;1    | 11              | Arkashin 2005, 2006     |
| 24            | 4;1;9;3;1;10;2;2   | 3               | Pulsating Spring 2006   |
| 25            | 4;7;9;3;1;10;2;2   | 1               | Pulsating Spring 2006   |
| 26            | 3;6;5;10;1;2;3;5   | 3               | Pulsating Spring 2006   |
| 27            | 1;8;5;10;1;11;1;7  | 1               | ON1 2006                |
| 28            | 1;7;1;21;1;12;3;8  | 1               | ON1 2006                |
| 29            | 1;1;1;21;1;9;3;8   | 1               | ON1 2006                |
| 30            | 1;7;1;21;1;9;3;8   | 1               | ON1 2006                |
| 31            | 1;8;5;10;1;11;1;3  | 3               | ON1 2006                |
| 32            | 3;7;5;10;1;3;2;2   | 1               | ON1 2006                |
| 33            | 1;4;5;10;1;11;1;3  | 4               | ON1 2006                |
| 40            | 4;4;9;3;1;6;2;2    | 1               | Vent 1 North 2006       |
| 41            | 1;12;1;25;1;11;3;3 | 2               | Vent 1 North 2006       |
| 42            | 1;13;5;24;1;3;3;3  | 1               | Vent 1 North 2006       |
| 43            | 1;11;1;25;1;11;3;3 | 8               | Vent 1 North 2006       |
| 44            | 1;1;5;24;1;3;3;3   | 6               | Vent 1 North 2006       |
| 45            | 1;1;5;4;7;2;3;2    | 1               | Zavarzin 2006           |
| 46            | 1;4;1;4;1;15;3;3   | 1               | Zavarzin 2006           |
| 47            | 3;1;5;4;7;2;2;6    | 2               | Zavarzin 2006           |
| 48            | 1;11;9;11;1;16;2;2 | 1               | Zavarzin 2006           |
| 49            | 1;4;1;4;1;14;3;3   | 5               | Zavarzin 2006           |
| 5             | 1;1;5;6;1;4;2;4    | 1               | Burylashi 2006          |
| 6             | 1;1;6;7;3;5;4;2    | 1               | Burylashi 2006          |
| 7             | 1;1;1;8;1;3;3;3    | 1               | Burylashi 2006          |
| 8             | 1;1;5;9;1;2;3;3    | 1               | Burylashi 2006          |
| 9             | 3;2;5;10;1;6;3;5   | 1               | Burylashi 2006          |
| 10            | 1;1;5;4;1;3;3;2    | 1               | Burylashi 2006          |
| 11            | 1;3;5;11;1;4;2;6   | 1               | Burylashi 2006          |
| 12            | 1;1;5;5;2;2;3;3    | 3               | Burylashi 2006          |
| 13            | 3;1;1;12;1;2;3;3   | 1               | Burylashi 2006          |
| 14            | 1;4;1;13;1;7;3;3   | 1               | Burylashi 2006          |
| 15            | 2;1;7;10;4;4;3;3   | 1               | Burylashi 2006          |
| 16            | 2;1;4;6;1;2;3;3    | 3               | Burylashi 2006          |
| 17            | 1;1;8;6;4;4;3;3    | 1               | Burylashi 2006          |
| 18            | 1;4;1;14;1;7;3;3   | 1               | Burylashi 2006          |
| 19            | 1;5;9;17;1;8;3;3   | 1               | Thermophilny 2006       |
| 20            | 1;1;10;18;1;3;2;2  | 1               | Thermophilny 2006       |
| 21            | 1;1;1;19;5;9;3;2   | 1               | Thermophilny 2006       |
| 22            | 1;4;5;20;1;2;3;3   | 1               | Thermophilny 2006       |
| 34            | 4;1;1;22;6;13;3;3  | 1               | Thermophilny 2005       |
| 35            | 4;7;1;22;1;13;3;3  | 1               | Thermophilny 2005       |
| 36            | 1;1;8;15;4;4;3;3   | 11              | Thermophilny 2005, 2006 |
| 37            | 1;9;5;23;1;2;3;3   | 1               | Thermophilny 2005       |
| 38            | 1;1;9;16;1;5;3;3   | 7               | Thermophilny 2005, 2006 |
| 39            | 1;10;5;23;1;2;3;3  | 1               | Thermophilny 2005       |

Allelic profile protein-coding loci order: *gyrB*, *lexA*, *leuS*, *pyrG*, *recA*, *recG*, *rplB*, and *rpoB*.

**Table 7 | Examination of single locus variants among the *T. uzonensis* population.**

| Sequence type 1 |                        | Sequence type 2 |                          | Locus, bp differences | SLV analysis |
|-----------------|------------------------|-----------------|--------------------------|-----------------------|--------------|
| ST              | Spring, year           | ST              | Spring, year             |                       |              |
| 14              | Burylashi, 2006        | 18              | Burylashi, 2006          | <i>pyrG</i> , 10      | R            |
| 17              | Burylashi, 2006        | 36              | Thermophilny, 2005, 2006 | <i>pyrG</i> , 13      | R            |
| 24              | Pulsating Spring, 2006 | 25              | Pulsating Spring, 2006   | <i>lepA</i> , 1       | R            |
| 27              | ON1, 2006              | 31              | ON1, 2006                | <i>rpoB</i> , 2       | R            |
| 28              | ON1, 2006              | 30              | ON1, 2006                | <i>recG</i> , 1       | M            |
| 29              | ON1, 2006              | 30              | ON1, 2006                | <i>lepA</i> , 1       | R            |
| 31              | ON1, 2006              | 33              | ON1, 2006                | <i>lepA</i> , 1       | R            |
| 37              | Thermophilny, 2005     | 39              | Thermophilny, 2005       | <i>lepA</i> , 6       | R            |
| 41              | Vent 1 North, 2006     | 43              | Vent 1 North, 2006       | <i>lepA</i> , 1       | M            |
| 42              | Vent 1 North, 2006     | 44              | Vent 1 North, 2006       | <i>lepA</i> , 1       | M            |
| 46              | Zavarzin, 2006         | 49              | Zavarzin, 2006           | <i>recG</i> , 1       | M            |

Each row lists the SLV sequence types, the differing protein coding locus and number of polymorphic nucleotide sites, and whether the locus was deemed to be the result of recombination, R; or mutation, M, according to the SLV analysis.

The genetic diversity values,  $H$ , calculated for the *gyrB*, *recA* and *rplB* loci were relatively low (**Table 3**), and for these three genes a particular allele was found held by a high percentage of the *T. uzonensis* strains. A similar observation was made for a set of *Halorubrum* isolates where a single *bop* allele was found in >85% of the strains and this was interpreted as being in part the result of selection, which drove the allele to high frequency (Papke, 2009). This explanation is compatible with some of the genes examined within the *T. uzonensis* population. The most notable exceptions were the *pyrG* and *recG* loci. Balancing selection may, in part, explain the diverse set of *recG* alleles observed within the population. Interestingly, for the *pyrG* locus a particular allele was often only found among the strains from a single hot spring (**Figure 2**). This could be the result of genetic drift within subpopulations, a neutral force, or positive selection of the particular allele within the hot spring subpopulation. One potential observation from a MLSA study would be the clustering of genotypes according to origin in a phylogenetic tree prepared from concatenates of the different loci. Only limited clustering was sequence types was observed (**Figure 3**), but this was not an unexpected result. The genes included in this study may have been influenced by different evolutionary processes, which potentially complicates phylogenetic analyses, and moreover there was evidence for homologous recombination in this population.

The investigated hot springs were separated by distances of 140–1600 m (**Figure 1**), and therefore *T. uzonensis* strains that developed in one pool could be distributed among the springs of the Uzon Caldera by wind, water, and local fauna (e.g., birds and brown bears). Moreover, there was evidence that gene flow between regions occurs as the same *rplB* allele was found in isolates from the Uzon Caldera, Geyser Valley, and Mutnovsky volcano regions (data not shown). Many of the described *Thermoanaerobacter* taxa, including *T. uzonensis* JW/IW010<sup>T</sup>, are known to form spores or contain sporulation-specific genes (Brill and Wiegel, 1997; Onyenwoke et al., 2004; Wagner et al., 2008). Sporulation would undoubtedly contribute to the ability of *T.*

*uzonensis* to survive transport between geothermal springs within and between regions, a form of passive dispersal as discussed by Martiny et al. (2006). Despite the close spatial proximity of the hot springs in this study, the pairwise  $F_{ST}$  values indicated that there was a small but significant level of genetic differentiation between most subpopulations (**Table 4**). There was a negligible association between the genetic divergence of *T. uzonensis* isolates and the geographic separation of the corresponding hot springs. This observation supports the concept mentioned earlier: that on smaller scales, as mainly investigated in this study, environmental factors or historical contingencies are believed to be of primary importance in determining whether patterns of genetic variation exist (Takacs-Vesbach et al., 2008).

Although the different geothermal springs sampled had approximately the same temperature and pH where the sample was collected (**Table 1**), there were other physicochemical differences. For example, the Arkashin Shaft spring is geochemically distinct in that it has a high arsenic concentration (4252 mg kg<sup>-1</sup> measured within Arkashin Shaft in 2006; Burgess et al., 2011). The hot springs in this study also differed in size and physical setting. Previous studies have revealed that at the community level microbial richness increases with habitat volume (Bell et al., 2005; Van Der Gast et al., 2005). The Burlyashi spring was the largest hot spring sampled (personal observation) and this property may, in part, explain the high diversity observed among the 18 strains from the Burlyashi spring outflow (**Table 5**).

Analyses of microbial populations have revealed that while homologous recombination occurs at widely varying rates, it has been observed among most taxa (Papke et al., 2007). The genomes of *Thermoanaerobacter* strains isolated from the Piceance Basin, Colorado, USA, revealed considerable recombination (C. L. Hemme, unpublished results). Our results show that the *T. uzonensis* population in the Uzon Caldera was influenced by frequent recombination. However, the difference in  $F_A^S$  values calculated from all 106 isolates and the 49 unique STs (**Table 8**) provides evidence of an “epidemic” population structure, in which recombination occurs while particular clones also

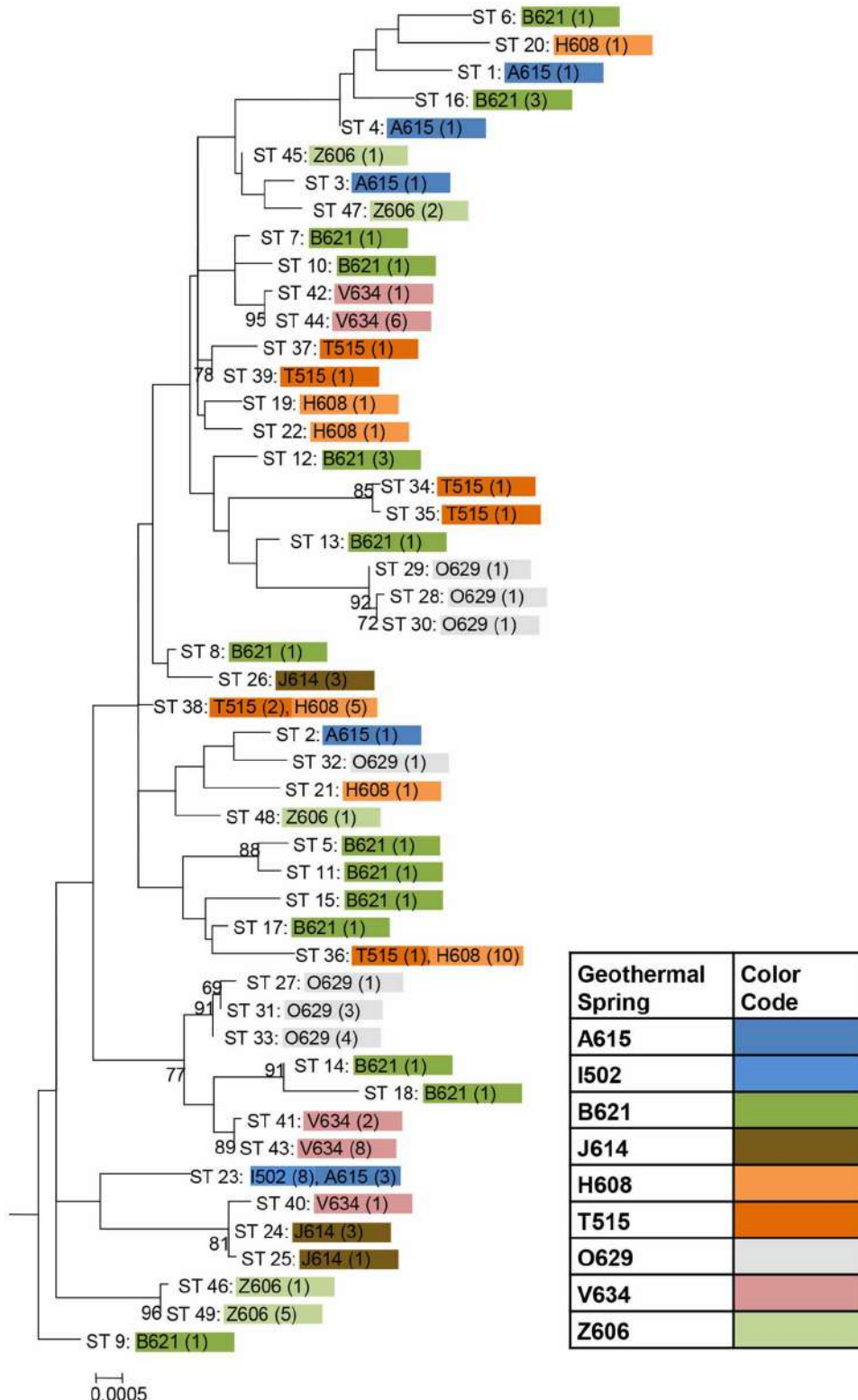


**FIGURE 3 | Phylogenetic tree based on concatenates of the eight protein coding loci from the 49 unique sequence types among 106 *T. uzonensis* strains.** ST designations match those given in Table 6 and are color coded according to hot spring origin. The number of strains having the particular ST is given in parentheses. Hot spring abbreviations are given in Table 1. The

maximum likelihood tree was constructed using the Hasegawa-Kishino-Yano model with a rates among sites setting of gamma distributed with invariant sites. Only bootstrap proportions of 50 or higher are included on the tree. The tree is drawn to scale, with branch lengths measured in the number of substitutions per site.

**Table 8 | Standardized index of association values calculated with the *T. uzonensis* MLSA dataset.**

| Set of <i>T. uzonensis</i> strains analyzed | All isolates                                | Unique genotypes                        |
|---|---|---|
| Uzon Caldera isolates from 2005 and 2006    | 106 isolates<br>$I_A^S = 0.086 (P < 0.001)$ | 49 ST<br>$I_{AS}^S = 0.028 (P = 0.028)$ |
| Uzon Caldera isolates from 2006             | 91 isolates<br>$I_A^S = 0.090 (P < 0.001)$  | 45 ST<br>$I_{AS}^S = 0.030 (P = 0.021)$ |
| Arkashin Shaft 2006                         | 7 isolates<br>$I_A^S = 0.209 (P < 0.001)$   | 4 ST<br>$I_{AS}^S = 0.041 (P = 0.286)$  |
| Burlyashi outflow (2006)                    | 18 isolates<br>$I_A^S = 0.071 (P = 0.012)$  | 14 ST<br>$I_{AS}^S = 0.018 (P = 0.293)$ |
| Thermophilny (2005)                         | 7 isolates<br>$I_A^S = 0.179 (P < 0.001)$   | 6 ST<br>$I_{AS}^S = 0.141 (P = 0.028)$  |
| Thermophilny (2006)                         | 19 isolates<br>$I_A^S = 0.390 (P < 0.001)$  | 4 ST<br>$I_{AS}^S = -0.027 (P = 0.537)$ |
| Pulsating Spring (2006)                     | 7 isolates<br>$I_A^S = 0.841 (P < 0.001)$   | 3 ST<br>NA                              |
| ON1 (2006)                                  | 12 isolates<br>$I_A^S = 0.463 (P < 0.001)$  | 7 ST<br>$I_{AS}^S = 0.346 (P < 0.001)$  |
| Vent 1 North (2006)                         | 18 isolates<br>$I_A^S = 0.478 (P < 0.001)$  | 5 ST<br>$I_{AS}^S = 0.524 (P < 0.001)$  |
| Zavarzin (2006)                             | 10 isolates<br>$I_A^S = 0.545 (P < 0.001)$  | 5 ST<br>$I_{AS}^S = 0.211 (P = 0.007)$  |

rise in frequency. *Sulfolobus* isolates from two hot springs in the Mutnovsky region of Kamchatka, similarly had an epidemic population structure (Whitaker et al., 2005), and this population structure has been proposed as indicating that certain clonal types may have increased fitness. Within the *T. uzonensis* population the view that a sequence type held by multiple isolates has increased fitness is particularly intriguing considering the sequence types found over consecutive years within the Arkashin and Thermophilny springs.

## REFERENCES

- Achtman, M., and Wagner, M. (2008). Microbial diversity and the genetic nature of microbial species. *Nat. Rev. Microbiol.* 6, 431–440.
- Bell, T., Ager, D., Song, J.-I., Newman, J. A., Thompson, I. P., Lilley, A. K., et al. (2005). Larger islands house more bacterial taxa. *Science* 308, 1884. doi: 10.1126/science.1111318
- Bonch-Osmolovskaya, E., Miroshnichenko, M., Chernykh, N., Kostrikina, N., Pikuta, E., and Rainey, E. (1997). Reduction of elemental sulfur by moderately thermophilic organotrophic bacteria and the description of *Thermoanaerobacter sulfurophilus* sp. nov. *Mikrobiologiya* 66, 581–587.
- Brill, J. A., and Wiegel, J. (1997). Differentiation between spore-forming and asporogenous bacteria using a PCR and Southern hybridization based method. *J. Microbiol. Methods* 31, 29–36. doi: 10.1016/S0167-7012(97)00091-2
- Burgess, E. A., Unrine, J. M., Mills, G. L., Romanek, C. S., and Wiegel, J. (2011). Comparative geochemical and microbiological characterization of two thermal pools in the Uzon Caldera, Kamchatka, Russia. *Microb. Ecol.* 63, 471–489. doi: 10.1007/s00248-011-9979-4
- Cooper, J. E., and Feil, E. J. (2004). Multilocus sequence typing—what is resolved? *Trends Microbiol.* 12, 373–377. doi: 10.1016/j.tim.2004.06.003
- Desantis, T. Z., Hugenholtz, P., Larsen, N., Rojas, M., Brodie, E. L., Keller, K., et al. (2006). Greengenes, a chimera-checked 16S rRNA gene database and workbench compatible with ARB. *Appl. Environ. Microbiol.* 72, 5069–5072. doi: 10.1128/AEM.03006-05
- Excoffier, L., and Lischer, H. E. L. (2010). Arlequin suite ver 3.5: a new series of programs to perform population genetics analyses under Linux and Windows. *Mol. Ecol. Resour.* 10, 564–567. doi: 10.1111/j.1755-0998.2010.02847.x
- Feil, E. J., Smith, J. M., Enright, M. C., and Spratt, B. G. (2000). Estimating recombination parameters in *Streptococcus pneumoniae* from multilocus

While there is great potential for *T. uzonensis* strains to be transferred between hot springs within the Uzon Caldera, isolates with identical sequence types were always derived from the same spring and SLV sequence types were usually isolated from a single site. This observation, along with the pairwise  $F_{ST}$  values, suggests that the *T. uzonensis* subpopulations within different hot springs are ecologically distinct and future studies could be performed to further examine the genetic and physiological differences between strains. Moreover, the genetic differentiation of subpopulations is likely influenced by the physicochemical differences between the geothermal springs. While there was strong evidence for frequent recombination within the *T. uzonensis* population, the observation that subpopulations were genetically differentiated is not unexpected. Simulations performed by Hanage et al. (2006) demonstrated that distinct clusters of similar genotypes can emerge in populations with a range of mutation and recombination rates. This MLSA additionally suggests that there are interesting genome dynamics within the *T. uzonensis* taxon with some alleles approaching fixation throughout the entire population. Other alleles were only seen within particular subpopulations, potentially the result of positive selection within the hot spring or genetic drift. Comparing the genomes of strains from different springs would provide insight into the genomic context of the protein-coding loci herein examined and would provide information concerning the variation in gene content among strains. While physical isolation of subpopulations is an important factor that influences the genetic divergence between sites, this work shows that differentiated populations can emerge within a region.

## ACKNOWLEDGMENTS

This research was supported by NSF grants MCB 0238407 (Kamchatka Microbial Observatory). We thank D. E. Crowe, P. A. Schroeder, C. S. Romanek, C. L. Zhang, E. A. Burgess, E. A. Bonch-Osmolovskaya, and the other members of the Kamchatka Microbial Observatory for assistance in the field. We thank E. Yokoyama, and A. Torrens for their preliminary work with the sequencing of protein coding gene loci.

## SUPPLEMENTARY MATERIAL

The Supplementary Material for this article can be found online at: [http://www.frontiersin.org/Frontiers\\_in\\_Extreme\\_Microbiology/10.3389/fmicb.2013.00169/abstract](http://www.frontiersin.org/Frontiers_in_Extreme_Microbiology/10.3389/fmicb.2013.00169/abstract)

- sequence typing data. *Genetics* 154, 1439–1450.
- Gevers, D., Cohan, F. M., Lawrence, J. G., Spratt, B. G., Coenye, T., Feil, E. J., et al. (2005). Re-evaluating prokaryotic species. *Nat. Rev. Microbiol.* 3, 733–739. doi: 10.1038/nrmicro1236
- Hanage, W. P., Spratt, B. G., Turner, K. M. E., and Fraser, C. (2006). Modelling bacterial speciation. *Philos. Trans. R. Soc. B Biol. Sci.* 361, 2039–2044. doi: 10.1098/rstb.2006.1926
- Haubold, B., and Hudson, R. R. (2000). LIAN 3.0: detecting linkage disequilibrium in multilocus data. *Bioinformatics* 16, 847–849. doi: 10.1093/bioinformatics/16.9.847
- Hemme, C. L., Mouttaki, H., Lee, Y.-J., Zhang, G., Goodwin, L., Lucas, S., et al. (2010). Sequencing of multiple clostridial genomes related to biomass conversion and biofuel production. *J. Bacteriol.* 192, 6494–6496. doi: 10.1128/JB.01064-10
- Hreggvidsson, G. O., Skirnisdottir, S., Smit, B., Hjorleifsdottir, S., Marteinsson, V. T., Petursdottir, S., et al. (2006). Polyphasic analysis of *Thermus* isolates from geothermal areas in Iceland. *Extremophiles* 10, 563–575. doi: 10.1007/s00792-006-0530-3
- Karpov, G. A., and Naboko, S. I. (1990). Metal contents of recent thermal waters, mineral precipitates and hydrothermal alteration in active geothermal fields, Kamchatka. *J. Geochim. Explor.* 36, 57–71. doi: 10.1016/0375-6742(90)90051-B
- Lane, D. J. (1991). “16S/23S rRNA sequencing,” in *Nucleic Acid Techniques in Bacterial Systematics*, eds E. Stackebrandt and M. Goodfellow (Chichester: Wiley), 115–175.
- Larkin, M. A., Blackshields, G., Brown, N. P., Chenna, R., Mcgettigan, P. A., Mcwilliam, H., et al. (2007). Clustal W and Clustal X version 2.0. *Bioinformatics* 23, 2947–2948. doi: 10.1093/bioinformatics/btm404
- Martiny, J. B. H., Bohannan, B. J. M., Brown, J. H., Colwell, R. K., Fuhrman, J. A., Green, J. L., et al. (2006). Microbial biogeography: putting microorganisms on the map. *Nat. Rev. Microbiol.* 4, 102–112. doi: 10.1038/nrmicro1341
- Miller, S. R., Castenholz, R. W., and Pedersen, D. (2007). Phylogeography of the thermophilic cyanobacterium *Mastigocladus laminosus*. *Appl. Environ. Microbiol.* 73, 4751–4759. doi: 10.1128/AEM.02945-06
- Onyenwoke, R. U., Brill, J. A., Farahi, K., and Wiegel, J. (2004). Sporulation genes in members of the low G+ C Gram-type-positive phylogenetic branch (*Firmicutes*). *Arch. Microbiol.* 182, 182–192. doi: 10.1007/s00203-004-0696-y
- Papke, R. T. (2009). A critique of prokaryotic species concepts. *Methods Mol. Biol.* 532, 379–395. doi: 10.1007/978-1-60327-853-9\_22
- Papke, R. T., Koenig, J. E., Rodríguez-Valera, F., and Doolittle, W. F. (2004). Frequent recombination in a saltern population of *Halorubrum*. *Science* 306, 1928–1929.
- Papke, R. T., Ramsing, N. B., Bateson, M. M., and Ward, D. M. (2003). Geographical isolation in hot spring cyanobacteria. *Environ. Microbiol.* 5, 650–659. doi: 10.1046/j.1462-2920.2003.00460.x
- Papke, R. T., Zhaxybayeva, O., Feil, E. J., Sommerfeld, K., Muise, D., and Doolittle, W. F. (2007). Searching for species in haloarchaea. *Proc. Natl. Acad. Sci. U.S.A.* 104, 14092–14097. doi: 10.1073/pnas.0706358104
- Petursdottir, S. K., Hreggvidsson, G. O., Da Costa, M. S., and Kristjansson, J. K. (2000). Genetic diversity analysis of *Rhodothermus* reflects geographical origin of the isolates. *Extremophiles* 4, 267–274. doi: 10.1007/s007920070012
- Rozas, J., and Rozas, R. (1999). DnaSP version 3: an integrated program for molecular population genetics and molecular evolution analysis. *Bioinformatics* 15, 174–175. doi: 10.1093/bioinformatics/15.2.174
- Santos, S. R., and Ochman, H. (2004). Identification and phylogenetic sorting of bacterial lineages with universally conserved genes and proteins. *Environ. Microbiol.* 6, 754–759. doi: 10.1111/j.1462-2920.2004.00617.x
- Slobodkin, A. I., Tourova, T. P., Kuznetsov, B. B., Kostrukina, N. A., Chernyh, N. A., and Bonch-Osmolovskaya, E. A. (1999). *Thermoanaerobacter siderophilus* sp. nov., a novel dissimilatory Fe (III)-reducing, anaerobic, thermophilic bacterium. *Int. J. Syst. Bacteriol.* 49, 1471–1478. doi: 10.1099/00207713-49-4-1471
- Smith, J. M. (1995). “Do bacteria have population genetics,” in *SGM Symposium 52: Population Genetics of Bacteria*, eds S. Baumberg, J. P. W. Young, E. M. H. Wellington, and J. R. Saunders (New York, NY: Cambridge University Press), 1–12.
- Stackebrandt, E., and Goebel, B. M. (1994). Taxonomic note: a place for DNA-DNA reassociation and 16S rRNA sequence analysis in the present species definition in bacteriology. *Int. J. Syst. Bacteriol.* 44, 846–849. doi: 10.1099/00207713-44-4-846
- Takacs-Vesbach, C., Mitchell, K., Jackson-Weaver, O., and Reysenbach, A. L. (2008). Volcanic calderas delineate biogeographic provinces among Yellowstone thermophiles. *Environ. Microbiol.* 10, 1681–1689. doi: 10.1111/j.1462-2920.2008.01584.x
- Tamura, K., Dudley, J., Nei, M., and Kumar, S. (2007). MEGA4: molecular genetic evolutionary analysis (MEGA) software. Version 4.0. *Mol. Biol. Evol.* 24, 1596–1599. doi: 10.1093/molbev/msm092
- Tamura, K., Peterson, D., Peterson, N., Stecher, G., Nei, M., and Kumar, S. (2011). MEGA5: molecular evolutionary genetics analysis using maximum likelihood, evolutionary distance, and maximum parsimony methods. *Mol. Biol. Evol.* 28, 2731–2739. doi: 10.1093/molbev/msr121
- Van Der Gast, C. J., Lilley, A. K., Ager, D., and Thompson, I. P. (2005). Island size and bacterial diversity in an archipelago of engineering machines. *Environ. Microbiol.* 7, 1220–1226. doi: 10.1111/j.1462-2920.2005.00802.x
- Wagner, I. D., Zhao, W., Zhang, C. L., Romanek, C. S., Rohde, M., and Wiegel, J. (2008). *Thermoanaerobacter uzonensis* sp. nov., an anaerobic thermophilic bacterium isolated from a hot spring within the Uzon Caldera, Kamchatka, Far East Russia. *Int. J. Syst. Evol. Microbiol.* 58, 2565–2573. doi: 10.1099/ijss.0.65343-0
- Whitaker, R. J. (2006). Allopatric origins of microbial species. *Philos. Trans. R. Soc. Lond. B Biol. Sci.* 361, 1975–1984. doi: 10.1098/rstb.2006.1927
- Whitaker, R. J., Grogan, D. W., and Taylor, J. W. (2003). Geographic barriers isolate endemic populations of hyperthermophilic archaea. *Science* 301, 976–978. doi: 10.1126/science.1086909
- Whitaker, R. J., Grogan, D. W., and Taylor, J. W. (2005). Recombination shapes the natural population structure of the hyperthermophilic archaeon *Sulfolobus islandicus*. *Mol. Biol. Evol.* 22, 2354–2361. doi: 10.1093/molbev/msi233

**Conflict of Interest Statement:** The authors declare that the research was conducted in the absence of any commercial or financial relationships that could be construed as a potential conflict of interest.

Received: 24 January 2013; accepted: 04 June 2013; published online: 21 June 2013.

Citation: Wagner ID, Varghese LB, Hemme CL and Wiegel J (2013) Multilocus sequence analysis of *Thermoanaerobacter* isolates reveals recombining, but differentiated, populations from geothermal springs of the Uzon Caldera, Kamchatka, Russia. *Front. Microbiol.* 4:169. doi: 10.3389/fmicb.2013.00169

This article was submitted to Frontiers in Extreme Microbiology, a specialty of Frontiers in Microbiology.

Copyright © 2013 Wagner, Varghese, Hemme and Wiegel. This is an open-access article distributed under the terms of the Creative Commons Attribution License, which permits use, distribution and reproduction in other forums, provided the original authors and source are credited and subject to any copyright notices concerning any third-party graphics etc.

## ADVANTAGES OF PUBLISHING IN FRONTIERS



### FAST PUBLICATION

Average 90 days  
from submission  
to publication



### COLLABORATIVE PEER-REVIEW

Designed to be rigorous –  
yet also collaborative, fair and  
constructive



### RESEARCH NETWORK

Our network  
increases readership  
for your article



### OPEN ACCESS

Articles are free to read,  
for greatest visibility



### TRANSPARENT

Editors and reviewers  
acknowledged by name  
on published articles



### GLOBAL SPREAD

Six million monthly  
page views worldwide



### COPYRIGHT TO AUTHORS

No limit to  
article distribution  
and re-use



### IMPACT METRICS

Advanced metrics  
track your  
article's impact



### SUPPORT

By our Swiss-based  
editorial team